Binding Position of Ibuprofen with Bovine Serum Albumin Determined by Measuring Nuclear Magnetic Resonance Relaxation Time[1)]

Masami TANAKA,*[,a] Yutaka ASAHI,[a] Seizo MASUDA[b] and Tadatoshi OTA[c]

Faculty of Pharmaceutical Sciences, Tokushima Bunri University,[a] Yamashiro-cho, Tokushima 770, Japan and Technical College[b] and Faculty of Engineering,[c] Tokushima University, Minamijosanjima-cho, Tokushima 770, Japan. *Received June 8, 1990*

The binding of ibuprofen (IB) to bovine serum albumin (BSA) was predominantly attributed to a hydrophobic interaction based on the thermodynamic parameters obtained by equilibrium dialysis. Little variation in the proton chemical shift of IB was observed when concentrations of the IB were changed (1—10 mM), or with the addition of BSA (7.25×10^{-5} M). The spin–lattice relaxation time (T_1) of IB was almost concentration-independent, but decreased in the presence of BSA to 36—45% for the phenyl group and its neighborhood, and to 70—97% for the other positions. The spin–spin relaxation rate ($1/T_2$) of IB was also almost concentration-independent, but significantly increased *ca.* 37 times for the phenyl group and 12—24 times for the alkyl group in the presence of BSA. The ratio of the spin–spin relaxation rate of the free IB to the bound IB ($(1/T_2)_b/(1/T_2)_f$) of the phenyl group was 2—3 times larger than that of the alkyl group as shown by a contour plot (Chart 1). The binding of IB to BSA was considered to involve mainly the phenyl group of IB.

Keywords hydrophobic interaction; ibuprofen; bovine serum albumin; nuclear magnetic resonance; spin–lattice relaxation time; spin–spin relaxation time; spin–spin relaxation rate; equilibrium dialysis

In part I[2)] of this series involving interaction between drugs and water-soluble polymers, the interaction between warfarin and polyvinylpyrrolidone (PVP) was studied, and it was concluded that hydrophobic binding played an important role. In part II,[3)] the binding position of phenylbutazone (PB) with bovine serum albumin (BSA) was elucidated by means of nuclear magnetic resonance (NMR) to be the phenyl group of PB, and it was concluded that the ratio of the spin–spin relaxation rate ($1/T_2$) of the free drug to that of the bound drug was the most useful parameter for this study.

Recently, Oida[4)] attempted to classify the binding site on human serum albumin (HSA) by difference NMR spectroscopy. Sudlow *et al.*[5)] proposed the existence of two kinds of binding sites (I, II) on HSA, and classified the drugs into two groups: site I drugs such as PB, and site II drugs such as ibuprofen (IB), according to the binding site.

In the present paper, the interaction between the site II drug (IB) and BSA was investigated by NMR relaxation rate to compare the rate of the site I drug (PB) to BSA as in the previous paper. It was concluded that the binding position of IB to BSA in mainly at the phenyl group, the same as PB.

Experimental

Materials The IB was of special reagent grade from Sigma, and was used without further purification. The BSA was from Wako and its average molecular weight was 6.9×10^4. Other reagents were from commercial sources and were used without further purification.

Equilibrium Dialysis The equilibrium dialysis method was the same as described previously.[3)] The drug concentration was determined by ultraviolet (UV) absorbance on a Simadzu UV-180 spectrometer. UV λ_{max}^{pH7} nm (ε): IB, 222 (17900).

NMR Spectroscopy The NMR spectrum was observed by the same method described previously.[3)] The spin–lattice relaxation time (T_1) was obtained by the inversion recovery method[6)] according to Eq. 1:

$$\ln(M_0 - M_t) = -\frac{t}{T_1} + \ln(2M_0) \quad (1)$$

where t is the interval between the π pulse and $\pi/2$ pulse, M_0 is the equilibrium magnetization at $t=0$, and M_t is the macroscopic magnetization at t. The spin–spin relaxation time (T_2) was obtained by the Carr–Purcell–Meiboom–Gill (CPMG)[7)] method according to Eq. 2:

$$\ln(M_{t2}) = \ln(M_{t1}) - \frac{\tau}{T_2} \quad (2)$$

where t_1 and t_2 are the times when a free induction decay (FID) is observed after the $\pi/2$ pulse, M_{t1} and M_{t2} are the macroscopic magnetizations at t_1 and t_2, respectively, and τ is the interval between t_1 and t_2.

Results and Discussion

The Binding Constant of IB to BSA Determined by Equilibrium Dialysis The binding of the drug (IB) to the polymer (BSA) was examined by equilibrium dialysis at 20—40° C. The free drug concentration (Df) was determined from the residual drug concentration, and the number of mol of drug binding to 1 mol of the polymer (r) was estimated from the decrease in drug concentration. The plot of r *vs.* r/Df produced a linear relationship, as shown in Fig. 1, and satisfied Eq. 3 proposed by Scatchard[8)]:

$$\frac{r}{Df} = Kn - Kr \quad (3)$$

where n is the number of binding sites per mol of the polymer and K is the binding constant between the drug and the polymer. The n- and K-values were calculated from the intercept on the abscissa and the slope of the line. Kuchar *et al.*[9)] reported that the interaction between IB and BSA involved two classes of binding sites ($K_1 = 1.7 \times 10^5\ M^{-1}$ as the binding constant of the primary site). However, as shown in the linear relationship in Fig. 1, it seemed sufficient to consider only one class of binding site in this work. Furthermore, since the binding constant of this work (Table I) was smaller than that of Kuchar *et al.*,[9)] it is considered that binding to the secondary site was observed in this work. The number of binding sites ($n=3$) was independent of temperature (20—40 °C). The thermodynamic parameters were calculated from the linear relationship between ln K and the reciprocal absolute temperature ($1/T$) (Table I). The values of the standard increases of enthalpy (ΔH°) and free energy (ΔG°) were negative and large, and the value of the standard increase

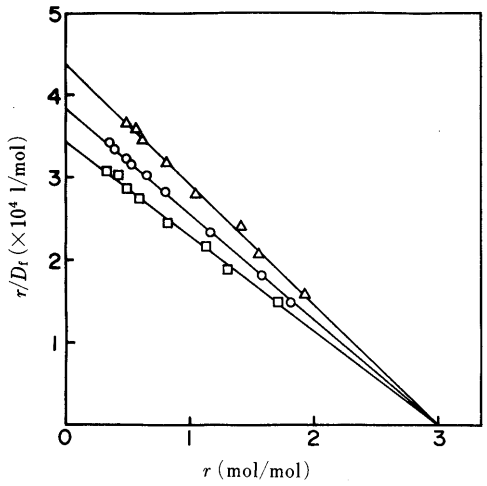

Fig. 1. Scatchard Plots for the Binding of IB to BSA (7.25×10^{-5} M) in 0.1 M Phosphate Buffer (pH 7) at 20 °C (△), 30 °C (○) and 40 °C (□)

TABLE I. Thermodynamic Parameters for the Binding of IB to BSA

Temp. (°C)	K ($\times 10^4$ M^{-1})	$\Delta G°$ (kJ/mol)	$\Delta H°$ (kJ/mol)	$\Delta S°$ (J/mol/K)
20	1.45	−23.34	−9.20	48.26
30	1.28	−23.80		48.18
40	1.14	−24.30		48.22
				(Av.) 48.22

[BSA] = 7.25×10^{-5} M, pH = 7, [phos. buf.] = 0.1 M.

of entropy ($\Delta S°$) was positive. From these results, it can be explained that the decrease of energy is due to the hydrophobic interaction between IB and BSA, and that the increase of entropy is based on the destruction of the iceberg structure. Additionally, since the binding constant increased with ion strength (Table II), it was also considered that the interaction between IB and BSA was hydrophobic.

The Chemical Shift of IB The chemical shifts of IB under typical conditions were shown in Table III (in 0.1 M phosphate buffer solution at pH 7). The variation of chemical shift was less than 0.001 ppm at diluting the solution of IB from 10 to 1 mM. Furthermore, the variation of chemical shift was less than 0.026 ppm in the presence of BSA (7.25×10^{-5} M). Therefore, it is difficult to determine the binding position from the change of chemical shift of IB.

Spin–Lattice Relaxation Time The spin–lattice relaxation time (T_1) of IB under typical conditions was measured by the inversion recovery method (Table IV). Little variation of T_1 was observed by diluting the solution of IB from 10 to 1 mM. The T_1-values of each proton in the presence of BSA (7.25×10^{-5} M) decreased to 70.3% (1-CH_3), 96.6% (2-CH_3), 38.4% (3-CH), 80.9% (4-CH_2), 36.5% (5-CH), 44.5% (6-CH), 42.0% (7-CH), respectively. From these results, it is predicted that the phenyl group and the adjacent methine group mainly interact with BSA.

Spin–Spin Relaxation Rate The spin–spin relaxation time (T_2) of IB was measured by the CPMG method and a series of spectra were shown in Fig. 2. The spin–spin relaxation rate ($1/T_2$) was used instead of T_2 (Table V). Little variation of $1/T_2$ was observed by diluting the solution of IB from 10 to 1 mM. In the presence of BSA (7.25×10^{-5} M), the $1/T_2$-values of the phenyl group and other protons increased *ca.* 37 and 12—24 times, respectively. Therefore, it is considered again that the binding position of IB to BSA in mainly at the phenyl group. The increase of $1/T_2$-values (12—37 times) was far larger than those of the $1/T_1$-values (1.03—2.74 times). Therefore, it is considered that the $1/T_2$-value is sensitive to small

TABLE II. Dependence of the Binding Constant on the Buffer Concentration

[phos. buf.] (M)	K ($\times 10^4$ M^{-1})
0.05	1.07
0.1	1.28
0.2	1.37

pH = 7, 30 °C.

TABLE III. Chemical Shifts ($\delta^{a)}$) of IB

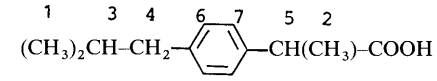

Concentration	1-CH_3	2-CH_3	3-CH	4-CH_2	5-CH	6-CH	7-CH
	d	d	m	d	q	d	d
10 mM IB	0.809	1.321	1.776	2.413	3.542	7.143	7.206
1 mM IB	0.808	1.320	1.776	2.413	3.541	7.143	7.205
10 mM IB/ 7.25×10^{-5} M BSA	0.791	1.314	1.757	2.387	3.530	7.124	7.191

a) From tetramethylsilane (external reference), pH = 7, [phos. buf.] = 0.1 M, 40 °C.

TABLE IV. Spin–Lattice Relaxation Time (T_1, s) of IB

Concentration	1-CH_3	2-CH_3	3-CH	4-CH_2	5-CH	6-CH	7-CH
10 mM IB	1.28	0.89	2.50	1.15	3.15	2.54	2.74
1 mM IB	1.41	1.02	2.75	1.22	3.43	2.73	2.88
10 mM IB/ 7.25×10^{-5} M BSA	0.90	0.86	0.96	0.93	1.15	1.13	1.15

pH = 7, [phos. buf.] = 0.1 M, 40 °C.

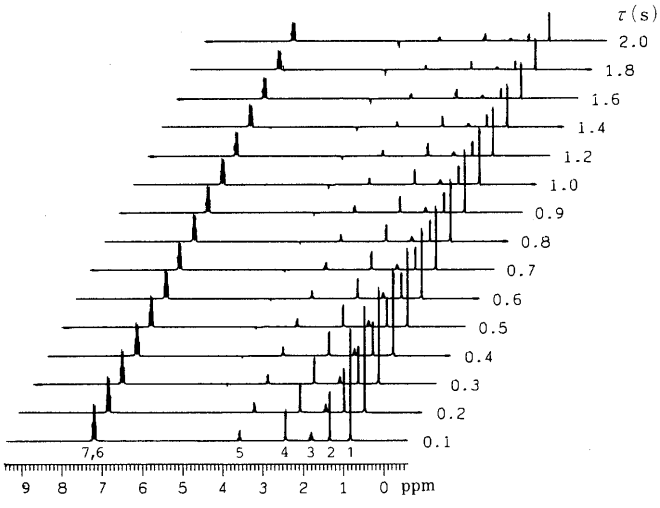

Fig. 2. Spin–Spin Relaxation Traces Obtained by the Carr–Purcell–Meiboom–Gill Method for Protons of IB

TABLE V. Spin–Spin Relaxation Rates ($1/T_2$) of IB

Peak	$1/T_2$ (s^{-1})	$(1/T_2)_{f1}$ (s^{-1})	$(1/T_2)_{f2}$ (s^{-1})	n/B ($\times 10^2$)	$n=3$ (dialysis) $(1/T_2)_b$ ($\times 10^2 s^{-1}$)	$n=3$ (dialysis) $(1/T_2)_b/(1/T_2)_{f1}$ ($\times 10^2$)	$n=100$ (assumed) $(1/T_2)_b$ ($\times 10\,s^{-1}$)	$n=100$ (assumed) $(1/T_2)_b/(1/T_2)_{f1}$ ($\times 10$)
1-CH_3	12.3	0.917	0.943	2.20	8.39	9.14	2.61	2.84
2-CH_3	15.4	1.220	1.493	2.65	12.52	10.27	3.88	3.18
3-CH	13.5	0.725	1.020	2.31	9.85	13.60	3.03	4.18
4-CH_2	16.9	0.787	0.870	2.84	15.31	19.44	4.67	5.93
5-CH	12.5	0.521	0.735	2.10	8.39	16.11	2.57	4.93
6-CH	14.9	0.412	0.505	2.48	12.00	29.17	3.64	8.85
7-CH	15.9	0.424	0.430	2.72	14.01	33.07	4.24	10.02

$1/T_2$, overall observed (10 mM IB/7.25×10^{-5} M BSA); $(1/T_2)_{f1}$, free IB (10 mM) observed; $(1/T_2)_{f2}$, free IB (1 mM) observed; $(1/T_2)_b$, IB bound to BSA calculated; n, number of binding sites on BSA; B, ratio of IB bound to BSA.

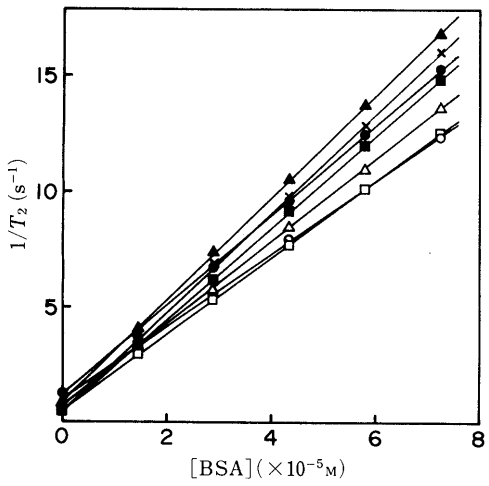

Fig. 3. Effect of BSA on the Proton Relaxation Rate ($1/T_2$) of IB
[IB] = 10 mM, pH = 7, at 40 °C. ○, 1-CH_3; ●, 2-CH_3; △, 3-CH; ▲, 4-CH_2; □, 5-CH; ■, 6-CH; ×, 7-CH.

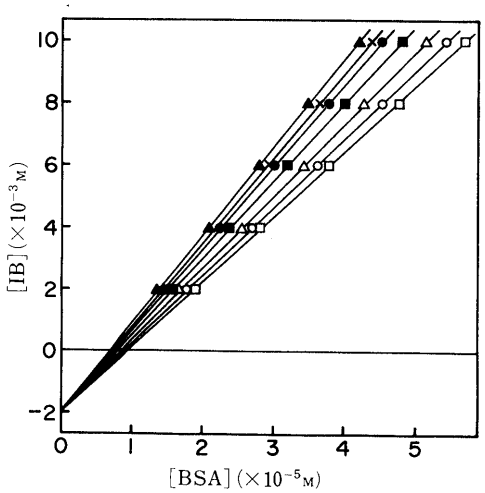

Fig. 4. Linear Relationships (Eq. 5) between Concentrations of Free IB and BSA Estimated from the Proton Relaxation Rate ($1/T_2$) of IB
○, 1-CH_3; ●, 2-CH_3; △, 3-CH; ▲, 4-CH_2; □, 5-CH; ■, 6-CH; ×, 7-CH.

changes in the molecular environment.

Effect of Concentration of BSA on the Spin–Spin Relaxation Rate The linear relationship between the spin–spin relaxation rates ($1/T_2$) for all the protons and the concentration of BSA was obtained in the range of 0 to 7.25×10^{-5} M (Fig. 3). The slopes decreased in the order of 4-CH_2, 7-CH, 6-CH, 2-CH_3, 3-CH, 5-CH, 1-CH_3. However, the binding position of IB to BSA could not be clearly determined because of a small difference in the slope and also because of different spin–spin relaxation rates of the free drug ($(1/T_2)_f$).

Spin–Spin Relaxation Rate of the Bound Drug In order to measure the spin–spin relaxation rate of the bound drug ($(1/T_2)_b$), we modified the method proposed by Jardetzky[10] as mentioned in the previous paper, based on the following equation:

$$\frac{1}{T_2}=\left(\frac{1}{T_2}\right)_f+B\left[\left(\frac{1}{T_2}\right)_b-\left(\frac{1}{T_2}\right)_f\right] \quad (4)$$

where $(1/T_2)_f$ is the spin–spin relaxation rate of the free drug and B is the proportion of the drug (IB) bound to the protein (BSA). As the proportion of the drug bound to BSA is small ($B\ll1$), Eq. 5 is valid:

$$[IB]=-\frac{1}{K}+\frac{n}{B}[BSA] \quad (5)$$

where [IB] and [BSA] are the concentrations of free IB and BSA, respectively, K is the binding constant, and n is the number of binding sites on BSA. Therefore, in the linear plot of [IB] *vs.* [BSA], the slope and the intercept on the ordinate correspond to n/B and $-1/K$, respectively. As the n-value is obtainable through equilibrium dialysis, the B-value can be calculated. When the calculated value of B and the values of $1/T_2$ and $(1/T_2)_f$ are substituted into Eq. 4, $(1/T_2)_b$ can be evaluated.

The plot between $1/T_2$ *vs.* [BSA] for all the protons of IB showed a linear relationship under the conditions of ([IB] = 10 mM, and [BSA] = 0—7.25×10^{-1} M) (Fig. 3). Similar experiments were carried out at various concentrations of IB (2—10 mM). Based on a series of experiments, an arbitrary value ($10\,s^{-1}$) near the minimum of $1/T_2$ was chosen. Pairs of [IB] and [BSA] providing a constant value of $1/T_2$ ($10\,s^{-1}$) were obtained from the linear relationship between $1/T_2$ and [BSA]. Equation 5 could be applied because a linear relationship between [IB] and [BSA] was observed in Fig. 4. Thus, the values of $(1/T_2)_b$ were calculated by means of Eqs. 5 and 4 (Table V).

It is considered that all n/B values are almost the same ($2.47\pm0.28\times10^2$) in Table V. The $(1/T_2)_b/(1/T_2)_{f1}$ value of the phenyl group (6-CH, 7-CH) is 2—3 times as large as those of the other alkyl protons. The ratio of 1-CH_3 furthest from the phenyl group was smallest. The ratio of 4-CH_2

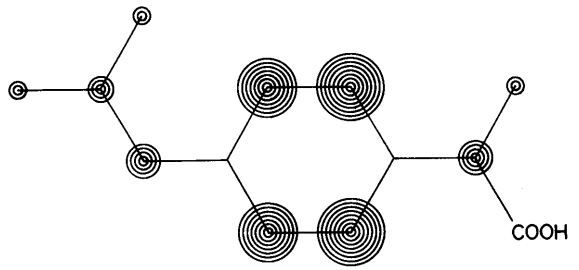

Chart 1. Contour Plot of the Ratio of the Spin–Spin Relaxation Rate of Free IB to Bound IB

adjacent to the phenyl group had the largest value of alkyl protons. On the other hand, the ratio of 5-CH was smaller than that of 4-CH_2 although both groups are adjacent to the phenyl group, due to the presence of a hydrophilic carboxyl group adjacent to 5-CH. The contour plot of the ratio $(1/T_2)_b/(1/T_2)_{f1}$ is clearly illustrated in Chart 1. It can be understood that the phenyl group is the main binding position and that the effect of binding decreases according to increased distance from the phenyl group. The binding constant determined from the NMR relaxation rate (*ca.* $5.26 \times 10^2\ M^{-1}$) was somewhat smaller than that obtained by the equilibrium dialysis method. Since the drug (IB) concentration for the NMR measurement (2—10 mM) was higher than that in the equilibrium dialysis method (0.05—0.5 mM) and the drug/protein ratio was of the order of one hundred, it is considered that the binding site examined by NMR was secondary (in other words, nonspecific) compared to the equilibrium dialysis method. If the number of nonspecific sites (n) was assumed to be 100, the relative values of $(1/T_2)_b/(1/T_2)_{f1}$ did not vary, although the absolute values decreased as shown in Table V. Therefore, the conclusion mentioned above stands even if the binding was nonspecific.

Gambhir *et al.*[11] and Fehske *et al.*[12] reported that the binding site of HSA to IB involved His-146, Lys-195 and Tyr-411 according to the chemical modification method. Oida[4] also reported the involvement of His-146, Lys-195, and Arg-145 by difference NMR spectroscopy. A similar binding site is also predicted for the IB–BSA system in this work. However, the binding of IB to nonspecific sites on BSA should be considered because the drug/protein ratio was vary large in this work. IB belongs to the site II drug classification reported by Sudlow *et al.*[5] The conclusion obtained in this work is that binding of IB to BSA is mainly at the phenyl group, the same as PB, a site I drug.

References

1) This report constitutes Part III of the series entitled "Interaction between Drugs and Water-Soluble Polymers." This work was presented at the 108th Annual Meeting of the Pharmaceutical Society of Japan, Hiroshima, 1988.
2) M. Tanaka, Y. Asahi, S. Masuda and T. Ota, *Chem. Pharm. Bull.*, **36**, 4645 (1988).
3) M. Tanaka, Y. Asahi, S. Masuda and T. Ota, *Chem. Pharm. Bull.*, **37**, 3177 (1989).
4) T. Oida, *J. Biochem.* (Tokyo), **100**, 99 (1986).
5) G. Sudlow, D. J. Birkett and D. N. Wade, *Mol. Pharmacol.*, **11**, 824 (1975).
6) R. L. Vold, J. S. Waugh, M. P. Klein and D. E. Phelps, *J. Chem. Phys.*, **48**, 3831 (1968).
7) S. Meiboom and D. Gill, *Rev. Sci. Instrum.*, **29**, 688 (1958).
8) G. F. Scatchard, *Ann. N. Y. Acad. Sci.*, **51**, 660 (1949).
9) M. Kuchar, B. Brenova, V. Rejholec, P. Verner and O. Numecek, *Pharmazie*, **38**, 744 (1983).
10) O. Jardetzky, *Advan. Chem. Phys.*, **7**, 499 (1964).
11) K. K. Gambhir, R. H. McMenamy and F. Watson, *J. Biol. Chem.*, **250**, 6711 (1975).
12) K. J. Fehske, W. E. Muller and U. Wollert, *Arch. Biochem. Biophys.*, **205**, 217 (1980).

Interaction of 8-Anilinonaphthalene-1-sulfonate with α-Cyclodextrin

Juziro NISHIJO,* Masako YASUDA, and Mayumi NAGAI

Kobe Women's College of Pharmacy, Motoyama-kitamachi, Higashinada-ku, Kobe 658, Japan. *Received June 18, 1990*

The interaction of 8-anilinonaphthalene-1-sulfonate (ANS) with α-cyclodextrin was investigated in a 0.1 M phosphate buffer at pH 7.4 by fluorescence spectrophotometry. Utilizing the fact that the fluorescence intensity of ANS increases in the presence of α-cyclodextrin, the thermodynamic parameters for inclusion complex formation were determined as follows; $\Delta G° = -1.25$ kcal/mol at 25 °C, $\Delta H° = -3.0$ kcal/mol, $\Delta S° = -5.8$ e.u. The driving force for the inclusion complex formation was cosidered to be the van der Waals–London dispersion force and hydrogen bonding between $-SO_3^-$ of ANS and the secondary hydroxyl groups of α-cyclodextrin.

Also, from the measurements of proton nuclear magnetic resonance spectra and studies with Corey Pauling Koltun models, the probable structure was determined.

Keywords 8-anilinonaphthalene-1-sulfonate; α-cyclodextrin; fluorescence; inclusion complex; thermodynamic parameter; ^{1}H-NMR

8-Anilinonaphthalene-1-sulfonate (ANS) is known to be a fluorescent probe for exploring hydrophobic regions.[1] The fluorescence of this agent is quenched in water, but in hydrophobic environments it is augmented substantially with shifts of the emission toward shorter wavelengths.[2] In addition, biological substances such as proteins, having intramolecular hydrophobic regions can interact with ANS to result in changes in the fluorescence spectra of ANS. Taking advantage of this property, ANS has been used to study the structures and functions of biological substances.[3]

It has been reported that the fluorescence emitted by ANS increases markedly when cyclodextrins such as β- or γ-cyclodextrin, related to biological substances, were added to an aqueous solution.[4,5] The fluorescence intensity has been considered to originate with presence of ANS in the cavity of the cyclodextrin molecule. Consequently, changes in the fluorescence spectra offer one means of demonstrating the hydrophobicity of a cavity. Thus, the hydrophobic bond is suggested as an important force in the formation of the inclusion complex between ANS and cyclodextrin. However, it was reported that the enthalpy term contributes more than the entropy term to the formation of the inclusion complex between ANS and β-cyclodextrin.[6] Further, we have reported similar results for the interaction of ANS with β-cyclodextrin.[7]

In the present study, the authors investigated the interaction between ANS and α-cyclodextrin by measuring the changes of fluorescence spectra in a phosphate buffer, to compare it with the same relationship between ANS and β-cyclodextrin already reported. α-Cyclodextrin was selected because its cavity is smallest in the cyclodextrin family, and therefore the structure of the inclusion complex is easiest to investigate in the present study. The changes in enthalpy and entropy due to the formation of the inclusion complex were determined so that the driving forces acting between the various components of the complex could be clarified. Further, the probable structure of the inclusion complex was studied by using Corey Pauling Koltun (CPK) models and by considering proton nuclear magnetic resonance (^{1}H-NMR) data.

Experimental

Materials Reagent-grade α-cyclodextrin supplied by Nakarai Chemicals, Ltd. was recrystallized twice from water and dried over P_2O_5 for 5 h at 110 °C in a vacuum before use. Two kinds of ANS were supplied by Nakarai Chemicals, Ltd. For ^{1}H-NMR spectroscopy, ammonium salt recrystallized twice from water was used, and for other experiments, its mangesium salt purified by crystallization twice from water was used.

^{1}H-NMR Spectra ^{1}H-NMR spectra were recorded in deuterium oxide on a Varian XL-200 (200 MHz) spectrometer with tetramethylsilane (TMS) as an external reference. The conditions for Fourier transfer measurements were: acquisition time, 3 s; pulse angle, 90°; delay time, 2 s; number of transients, 96.

Fluorescence Spectra Fluorescence spectra were measured with a Shimadzu RF-503A recording fluorescence spectrophotometer at 5, 15, 25, and 40 °C. To obtain a given temperature, water maintained at a constant temperature with a thermostat was circulated through the cell holder. The change of temperature during the measurements was within ±0.1 °C. The lamp emission intensity changed only slightly during measurements. But, in order to obtain reliable data, the spectra were corrected by repeating the measurement of the standard sample after that of each sample.

Absorption Spectra Absorption spectra were taken on a Shimadzu UV 300 spectrophotometer at 25 °C. The measurements were carried out in a 0.1 M sodium phosphate buffer of pH 7.4.

Results and Discussion

Figure 1 shows the effects of α-cyclodextrin on the absorption spectra of ANS. These spectra were measured, using a buffer solution containing the same concentrations of α-cyclodextrin as the sample, as reference. The absorption spectra varied by addition of α-cyclodextrin, although the

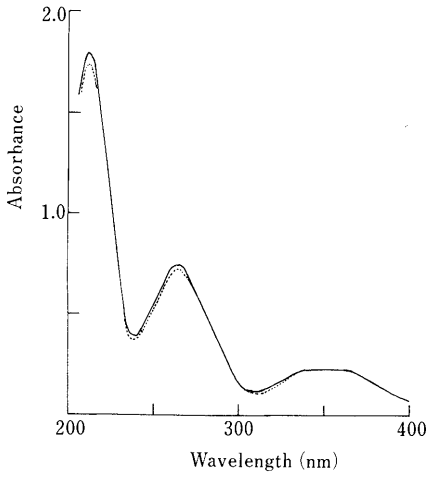

Fig. 1. Absorption Spectra of ANS in the Presence of α-Cyclodextrin in 0.1 M Sodium Phosphate Buffer of pH 7.4 at 25 °C

—: ANS alone (4.0×10^{-5} M), ---: ANS (4.5×10^{-5} M) + α-cyclodextrin (3.5×10^{-2} M).

changes were only slight. The hypochromic effect at the wavelength of 215 nm assigned to B_b[8] was most remarkable.

Figure 2 shows part of the fluorescence spectra of 1.0×10^{-4} M of ANS measured in the presence of α-cyclodextrin at different concentrations in a 0.1 M phosphate buffer (pH 7.4) at 25 °C. The concentrations of α-cyclodextrin ranged from 10 to 100 times higher than that of ANS. Fluorescence intensity increased as the concentration of the α-cyclodextrin increased, with the shift of fluorescence maximizing at shorter wavelengths. Changes in the fluorescence and absorption spectra were not seen when D-glucose or D-maltose was added in place of α-cyclodextrin. Therefore, it is clear that the interaction of ANS with α-cyclodextrin is closely related to the cavity of the oligosaccharide.

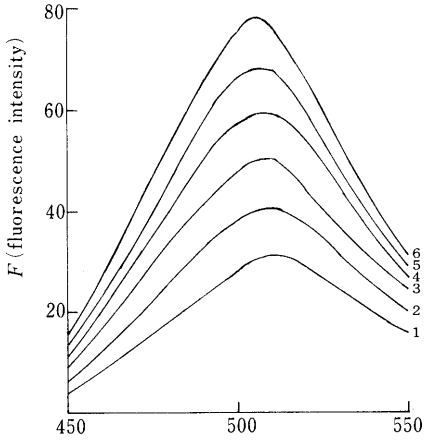

Fig. 2. Fluorescence Spectra of 1.0×10^{-4} M ANS in the Presence of α-Cyclodextrin in 0.1 M Phosphate Buffer of pH 7.4 at 25 °C

The concentrations of α-cyclodextrin are: 1, 0; 2, 2.0×10^{-3} M; 3, 4.0×10^{-3} M; 4, 6.0×10^{-3} M; 5, 8.0×10^{-3} M; 6, 1.0×10^{-2} M. The excitation wavelength is 365 nm.

^{1}H-NMR spectra and a CPK model were used to estimate the structure of the inclusion complex between ANS and α-cyclodextrin. In Fig. 3a, a ^{1}H-NMR spectrum of 3.0×10^{-2} M ANS in deuterium oxide at 30 °C is shown. The assignments of the proton signals of ANS were undertaken on the basis of homonuclear decoupling, as well as a comparison with the ^{1}H-NMR spectra of analogous compounds.[9,10] The proton signals of ANS shifted with the addition of α-cyclodextrin. In the presence of 3.0×10^{-2} M α-cyclodextrin, for example, as shown in Fig. 3b, the protons of benzene and naphthalene rings shifted downfield except for the signals due to 4′-H and 7-H, respectively. The downfield shifts of the signals due to 3′-H, 5′-H, 2′-H, and 6′-H of the benzene ring and those due to 2-H and 3-H of naphthalene ring were prominent. The downfield shift of the signal due to 2-H was particularly prominent. The magnitudes of the shifts of the proton signals due to ANS in the presence of α-cyclodextrin at various concentrations are shown in Fig. 5a.

A ^{1}H-NMR spectrum of 3.0×10^{-2} M α-cyclodextrin solution is shown in Fig. 4a. The spectrum is different from that (Fig. 4b) in the presence of 3.0×10^{-2} M ANS. The comparison of these two spectra revealed that the signals due to protons of all types in the α-cyclodextrin molecule were shifted in the presence of ANS. The shift of the signals

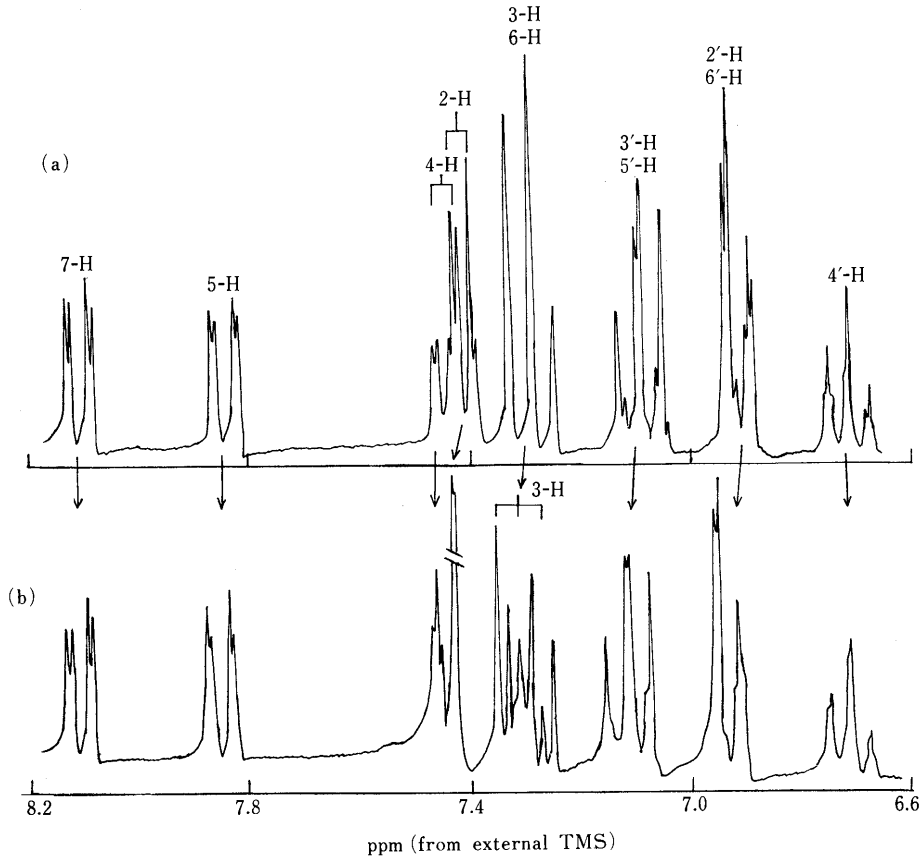

Fig. 3. ^{1}H-NMR Spectra of ANS in the Presence of α-Cyclodextrin in Deuterium Oxide at 30 °C

(a) ANS alone (3.0×10^{-2} M), (b) ANS (3.0×10^{-2} M) + α-cyclodextrin (3.0×10^{-2} M).

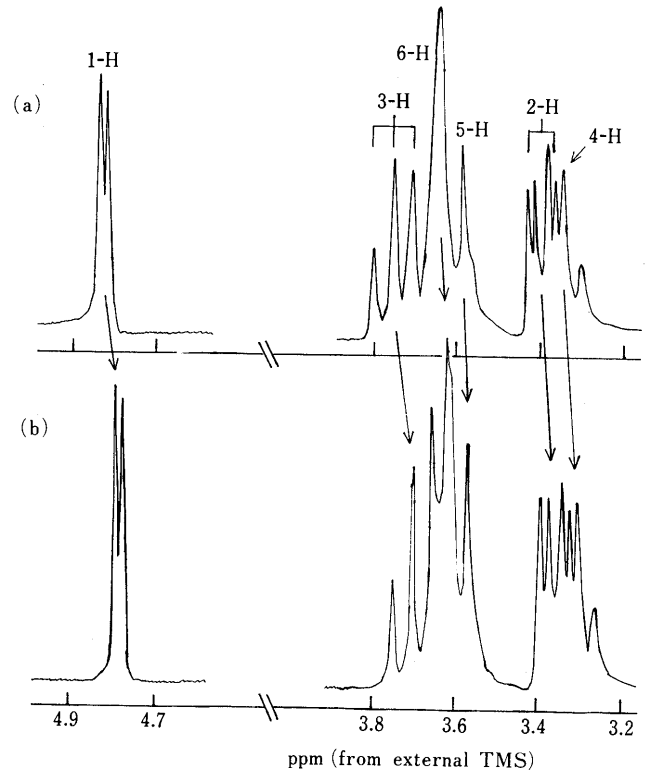

Fig. 4. ^{1}H-NMR Spectra of α-Cyclodextrin in the Presence of ANS in Deuterium Oxide at 30 °C

(a) α-cyclodextrin alone (3.0×10^{-2} M), (b) α-cyclodextrin (3.0×10^{-2} M) + ANS (3.0×10^{-2} M).

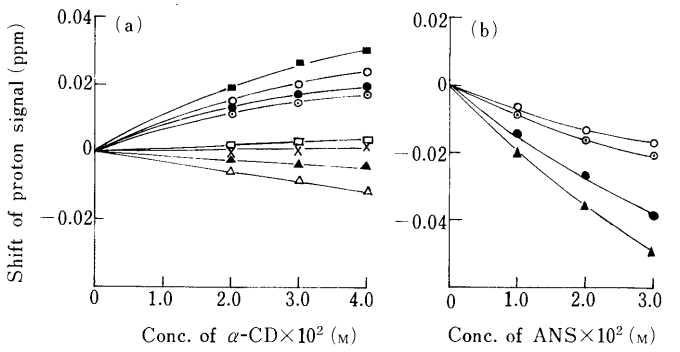

Fig. 5. (a) Induced ^{1}H-NMR Chemical Shifts of ANS (3.0×10^{-2} M) in the presence of α-Cyclodextrin

■, 2-H; ○, 2′-H, 6′-H; ●, 3′-H, 5′-H; ⊙, 3-H; □, 5-H, 4-H; ×, 6-H; ▲, 7-H; △, 4-H.

(b) Induced ^{1}H-NMR Chemical Shifts of α-Cyclodextrin (3.0×10^{-2} M) in the Presence of ANS

○, 6-H; ⊙, 5-H; ●, 1-H, 2-H, 4-H; ▲, 3-H.

due to 3-H on the inner surface of the cavity was most prominent, followed by the signals due to 1-H, 2-H, and 4-H, which lie on the outer surface of the cavity at the secondary hydroxyl group side and show a similar magnitude of shift. On the other hand, the upfield shifts of the signals due to 5-H and 6-H lying on the inner surface of the primary hydroxyl group side were not so prominent as those due to the other protons of α-cyclodextrin. The magnitudes of the shifts of the proton signals due to α-cyclodextrin in the presence of ANS at various concentrations are shown in Fig. 5b.

As possible structures for the inclusion complex, judging from the investigation by using CPK model, three kinds of structures described next are considered (Fig. 6), (a): the benzene ring of ANS is enclosed in the cavity of α-cyclodextrin from the side of the secondary hydroxyl group at a considerable depth, the naphthalene ring being almost outside the cavity, (b): the naphthalene ring enters only shallowly into the cavity from the side of the secondary hydroxyl group, a great part of the naphthalene ring and the benzene ring remaining outside the cavity; (c): the benzene ring is enclosed in the cavity at a considerable depth from the primary hydroxyl group, and the naphthalene ring is almost entirely outside of the cavity. It is considered that the upfield shifts of the proton signals lying on the inner surface of α-cyclodextrin result mainly from the magnetic anisotropy of the benzene or naphthalene rings of the ANS molecule. Therefore, since the magnitudes of the upfield signal shifts caused by protons on the inner surface of α-cyclodextrin are in the order 3-H > 5-H > 6-H, this suggests that the structure in Fig. 6c cannot occur. The structure described in Fig. 6b cannot be expected to produce upfield shifts of both signals due to the 5-H and 6-H of α-cyclodextrin, although the values found are high. Therefore, it was assumed that the inclusion complex does not have the structure described in Fig. 6b. If the complex had the structure described in Fig. 6a, it would not be surprising that the upfield shift of the 3-H signal is greater than that of 5-H, and that of 5-H is greater than that of 6-H. Consequently, ANS is estimated to be enclosed in α-cyclodextrin in the manner illustrated in Fig. 6a.

A more detailed structure containing hydrogen bonding between ANS and α-cyclodextrin will be discussed hereafter. If the complex has the structure shown in Fig. 6a, the shifts of the signals due to the protons of ANS can be explained as follows. The signals due to 2′-H, 6′-H, 3′-H and 5′-H of benzene ring shifted downfield as mentioned above. These shifts are considered to have occured mainly because these

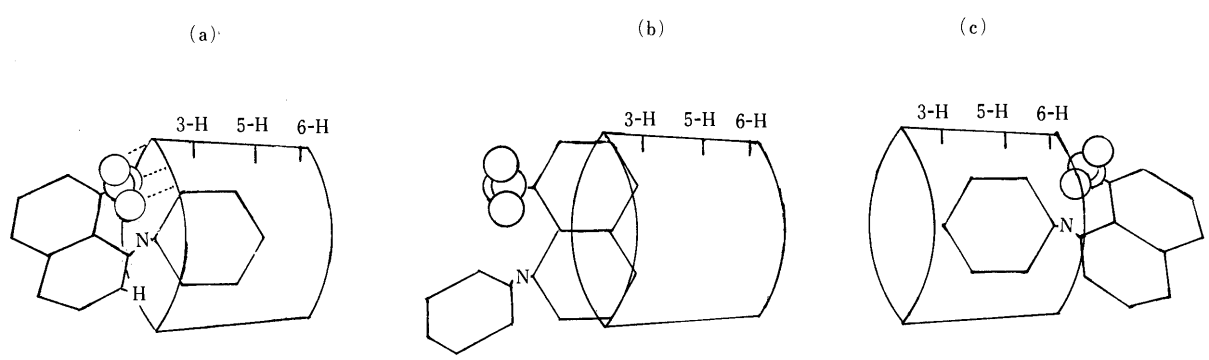

Fig. 6. Possible Structures of the Inclusion Complex of ANS with α-Cyclodextrin in Aqueous Solution Based on CPK Space-Filling Models

hydrogen atoms contacted strongly with the atoms lying on the inner surface of the cavity of ANS, namely by the steric compression effect. The signal due to 4′-H shifted upfield, though only slightly. This is because 4-H scarcely had contact with the atoms of α-cyclodextrin, and the slight upfield shift is attributed to the C–C bond anisotropy of α-cyclodextrin and so on.[11] Also, the signals due to 2-H, 3-H, 4-H, 5-H, and 6-H of the naphthalene ring shifted downfield as mentioned above. Especially, the signals due to 2-H showed a prominent downfield shift. It is reasonable to consider that the shift is caused by the hydrogen bonding between $-SO_3^-$ of ANS and the secondary hydroxyl groups of α-cyclodextrin, because the secondary hydroxyl group of cyclodextrin has the property of a proton donor ($pK_a = 12$)[12]. Therefore, the electron density of 2-H decreases remarkably and the signal due to 2-H shows a remarkable downfield shift. Secondly, the downfield shift of 3-H was prominent. It can be presumed that the downfield shift occurs from a decrease of electron density of 3-H resulting from the hydrogen bonding mentioned above.

On the other hand, the signals due to 1-H, 2-H and 4-H lying on outer surface of α-cyclodextrin shifted upfield significantly in the presence of ANS. If it is assumed that the strong hydrogen bonding is formed between the $-SO_3^-$ group and the secondary hydroxyl groups of α-cyclodextrin, that would explain the significant upfield shifts. Therefore, the structure of the inclusion complex of ANS with α-cyclodextrin shown in Fig. 6a was furthermore supported. Also, as mentioned above, the upfield shift of the 3-H signal was much more prominent than that of the 5-H signal. It is clear that in addition to the magnetic anisotropy of benzene ring, the increase of electron density of 3-H resulting from the hydrogen bonding contributes significantly to the upfield shift of the 3-H signal. Therefore, it is considered that there is no large difference between the 3-H and 5-H signals concerning the magnitudes of the upfield shift due to magnetic anisotropy, and the benzene ring of ANS is included at a considerable depth.

Further considerations on the complexation shifts of the proton signals were then carried out. When the benzene ring is included in the cavity of cyclodextrin, the signals due to 3′-H and 5′-H are expected to shift more downfield than those of 2′-H and 6′-H because the former reacts more to steric compression effects than the latter. However, the experiment reported that the signals due to 2′-H and 6′-H shift more downfield than those of 3′-H and 5′-H, though only slightly. It is estimated that these downfield shifts can occur because the formation of the inclusion complex makes the benzene and naphthalene rings more coplanar. But, there is a conflict. If this occured, the signals due to 7-H would be expected to shift downfield, but they actually resulted in an upfield shift, though only slightly. However, the conflict is now resolved because the 7-H could lie within the boundaries of the cavity and receive C–C bond anisotropy of α-cyclodextrin and so on.

Thus, it is clear that the most probable structure of the inclusion complex of ANS with α-cyclodextrin is that shown in Fig. 6a. This structure was different from that of the inclusion complex of ANS with β-cyclodextrin reported.[7] The most probable structure of the latter was as follows; an entire benzene ring is contained in the cavity from the side of the primary hydroxyl groups of β-cyclodextrin to a considerable depth in the cavity, and a part of the naphthalene ring is enveloped. Also, the hydrogen bonding in which $-SO_3^-$ takes part was not detected. In this way, it is very interesting that ANS is enclosed in a different mode in the cavity of cyclodextrin, depending on the size of the cavity.

As described above, the fluorescence intensity of ANS increases significantly in the presence of α-cyclodextrin. By taking advantage of this effect of α-cyclodextrin, the formation constant K was estimated. Assuming a 1 : 1 complex, when a large excess of α-cyclodextrin is added to ANS, Eq. 2 applies.

$$\mathrm{CD} + \mathrm{ANS} \leftrightarrows \mathrm{CD\text{–}ANS} \tag{1}$$

$$K = \frac{X}{C_0(A_0 - X)} \tag{2}$$

$$\Delta F = \Delta F_a + \Delta F_c \tag{3}$$

$$\Delta F = \frac{1}{1 + C_0 K}\Delta F_A - \frac{1}{1 + C_0 K}\Delta F_{\infty 1:1} + \Delta F_{\infty 1:1} \tag{4}$$

Here, C_0, A_0, and X represent the total concentration of α-cyclodextrin, the total concentration of ANS, and the concentration of the ANS–α-cyclodextrin complex, respectively. Also, CD represents α-cyclodextrin. The fluorescence intensity (ΔF) observed is a sum of those of free ANS (ΔF_a) and complex ANS (ΔF_c) (Eq. 3). Equation 4 is valid where ΔF_A and $\Delta F_{\infty 1:1}$ denote the fluorescence intensities which should be observed when all ANS is free and when it has formed the ANS–α-cyclodextrin complex, respectively. Formation constant K can be estimated from Eq. 4 using the nonlinear squares program MULTI.[13] The values obtained at 5, 15, 25, and 40 °C are shown in Table I. Also, Fig. 7 shows the binding curves for α-cyclodextrin with ANS together with the theoretical curves obtained using the calculated parameters. The van't Hoff plots obtained by plotting log K against the absolute temperature are shown in Fig. 8. The changes in enthalpy ($\Delta H°$) and entropy ($\Delta S°$) accompanying the complexation were determined in the usual way. Each value obtained is shown in Table I.

In the case of complexation in an aqueous solution, van der Waals–London dispersion force, hydrogen bonding, hydrophobic interaction, release of high-energy water molecules from the cavity of cyclodextrin, and the release of strain energy in a macromolecular ring of cyclodextrin

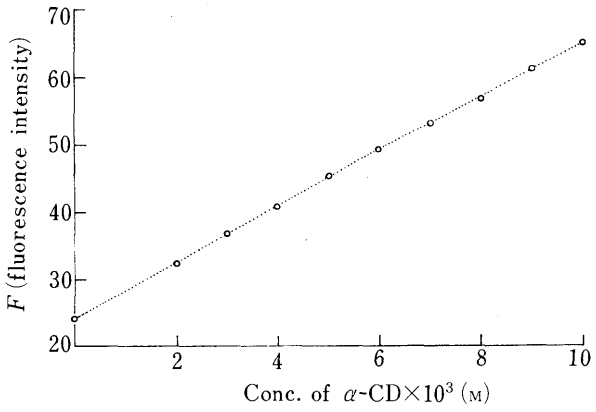

Fig. 7. Binding Curve of α-Cyclodextrin with ANS

○, observed fluorescence intensity; - - -, theoretical curve, which was obtained from Eq. 4, using the calculated parameters.

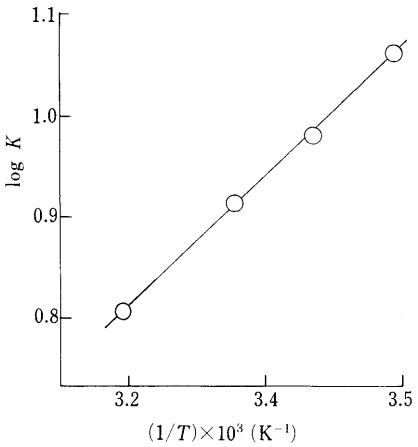

Fig. 8. The Van't Hoff Plot of the Data in Table I

TABLE I. Thermodynamic Parameters for Inclusion Complex Formation of ANS with α-Cyclodextrin

Temp. (°C)	$K^{a)}$ (M^{-1})	$\Delta G°$ (kcal/mol)	$\Delta H°$ (kcal/mol)	$\Delta S°$ (e.u.)
5	11.6	−1.35		
15	9.5	−1.29		
25	8.2	−1.25	−3.0±0.3	−5.8±0.6
40	6.4	−1.16		

a) These values are averages, which were obtained from 5 repetitive runs. Average probable errors are ±7% for *K*.

have all been reported to play a big part in the interaction.[14] However, according to Tabushi *et al.*[15] the van der Waals–London dispersion force and hydrophobic interaction are major driving forces for inclusion complexation between cyclodextrin and a guest molecule. In the present study, it was found that the complexation is accompanied by negative changes in both enthalpy and entropy, suggesting that the van der Waals–London dispersion force and hydrogen bonding are mainly responsible for the inclusion complex formation.

Now, the thermodynamic parameters for complex formation of ANS with β-cyclodextrin were determined according to the procedure of Hanna and Ashbaugh assuming a 1 : 1 complex, the reciprocals of the increases of the fluorescence intensities being plotted to the those of β-cyclodextrin concentrations added excessively.[7] The thermodynamic parameters were determined as follows: $K=70.9\,M^{-1}$ at 25 °C, $\Delta H°=-1.92$ kcal/mol, $\Delta S°=2.1$ e.u. The two primary driving forces for the complex formation of ANS with β-cyclodextrin were considered to be the van der Waals–London dispersion force and hydrophobic interaction. In the inclusion complex of ANS with β-cyclodextrin, the ANS moiety is rather loosely packed in the cavity. Therefore, it seemed reasonable that the change in enthalpy ($\Delta H°$) would take a small negative value and the change in entropy ($\Delta S°$) a small positive one.

In the present study, as a possible structure of the inclusion complex between ANS and α-cyclodextrin, the structure shown in Fig. 6a was estimated. When this structure was examined again using the CPK model, it was found that the benzene ring moiety of ANS is tightly packed and naphthalene ring moiety is tightly fixed by hydrogen bonding mentioned above. Consequently, it seems reasonable that the change in enthalpy ($\Delta H°$) is more negative and the change in entropy ($\Delta S°$) is negative, different from the case of β-cyclodextrin. Also, the formation constant of the complex of ANS with α-cyclodextrin is smaller than that of ANS with β-cyclodextrin. From the discussions mentioned above, this is attributable to the prominent negative entropy change accompanying the complex formation of ANS with α-cyclodextrin, resulting from the narrow cavity of α-cyclodextrin and the hydrogen bonding between $-SO_3^-$ and secondary hydroxyl group, in spite of the facts that they contribute to a considerable decrease in enthalpy.

It has been reported[2] that there are also two cases in which the fluorescence intensity of ANS increases. In the first case, observed in a non-aqueous solvent, the coplanarity of the aromatic rings increased more than in an aqueous solution. In the second conducted in a viscous solution the motion of the ANS molecule was restricted more strongly than in an aqueous solution. It has become apparent that the coplolanarity of the aromatic rings of ANS increases more in the inclusion complex than in an uncomplex form from the ^{1}H-NMR spectra. Also, it is easily considered that the motion of the ANS molecule may be resticted more strongly in the inclusion complex than in the uncomplex form. Therefore, the increase in fluorescence intensity can be attributed to both cases.

Acknowledgement We are grateful to Prof. S. Asada for direction of the working program, MULTI, and to Miss E. Ohno for the measurements of the fluorescence spectra.

References

1) D. C. Turner and L. Brand, *Biochemistry*, **7**, 3381 (1968).
2) G. R. Penzer, *Eur. J. Biochem.*, **25**, 218 (1972).
3) N. Kamo, T. Aiuchi, K. Kurihara, and Kobatake, *Colloid & Polymer Sci.*, **256**, 31 (1978).
4) H. Kondo, H. Nakatani, and K. Hiromi, *J. Biochem.* (Tokyo), **79**, 393 (1976).
5) K. Miyazima, M. Sawada, T. Ueda, and M. Nakagaki, *Nippon Kagaku Kaishi*, **1984**, 527.
6) G. C. Cafena and F. V. Bright, *Anal. Chem.*, **61**, 905 (1989).
7) J. Nishijo and M. Nagai, *J. Pharm. Sci.*, in press.
8) F. C. Greene, *Biochemistry*, **14**, 747 (1975).
9) G. O. Dudek, *Spectrochim. Acta*, **19**, 691 (1963).
10) D. C. F. Garbutt, K. G. R. Pachler, and J. R. Parrich, *J. Chem. Soc.*, **1965**, 2324.
11) R. J. Bergeron and R. Rowan, *Bioorg. Chem.*, **5**, 425 (1976).
12) R. L. VanEttem, G. A. Clowes, J. F. Sebastian, and M. L. Bende, *J. Am. Chem. Soc.*, **89**, 3253 (1967).
13) K. Yamaoka and T. Nakagawa, *J. Pharmacobio-Dyn.*, **6**, 595 (1983).
14) M. Komiyama and M. L. Bender, *J. Am. Chem. Soc.*, **100**, 2259 (1978).
15) I. Tabushi, Y. Kiyosuke, T. Sugimoto, and K. Yamamura, *J. Am. Chem. Soc.*, **100**, 916 (1978).

Reaction of Aromatic *N*-Oxides with Dipolarophiles. XV. Formation of the 1,5-Sigmatropy Products and Their Double Ene Reaction Products

Toshikazu MATSUOKA, Kikuma ONO, Kazunobu HARANO and Takuzo HISANO*

Faculty of Pharmaceutical Sciences, Kumamoto University, 5–1 Oe-honmachi, Kumamoto 862, Japan. *Received May 14, 1990*

In connection with the pericyclic reaction of 3,5-dimethylpyridine *N*-oxide with *N*-substituted maleimides, the structure of a 1,5-sigmatropy product was determined by the X-ray crystallographic method. In the reaction of 2-alkylpyridine *N*-oxides with *N*-substituted maleimides, we have isolated a series of 1:3 ene reaction products of a new type.

The primary *exo* cycloadducts readily transform into the *endo* 1,5-sigmatropic rearrangement products, which again react with two molecules of *N*-substituted maleimide to give the 1:3 ene reaction products. The observed reaction behavior and plausible reaction pathways are discussed in terms of frontier molecular orbital considerations.

Keywords pericyclic reaction; MNDO frontier molecular orbital; charge transfer complex; X-ray analysis; pyridine *N*-oxide; *N*-phenylmaleimide; 1:3 ene reaction product; ene reaction

Cycloaddition reactions have figured prominently in both synthetic and mechanistic chemistry. In the past decade, we have examined the 1,3-dipolar cycloadditions of aromatic *N*-oxides (I) with aryl isocyanates and clarified several controlling factors in the 1,3-dipolar reaction based on kinetic data and molecular orbital calculation.[1] In the reaction, the stereochemistry of the cycloaddition could not be established, because the isocyanates have a linear structure and both *exo* and *endo* addition give the same product.

Recently, we reported the 1,3-dipolar cycloaddition of 3,5-dimethylpyridine *N*-oxide (Ia) with *N*-substituted maleimides (II), and discussed the stereochemistry of the transition state. The cycloaddition afforded the *endo* 2,3-dihydrofuro[3,2-*b*]pyridine-type cycloadducts (III) arising from 1,5-sigmatropic rearrangement of primary *exo* cycloadducts.[2] This makes a striking contrast to the results obtained in the cycloadditions of some nitrones such as *N*,α-diphenylnitrone with II, wherein the *endo* cycloadditions were mainly observed.[3a]

In this connection, we have reported an X-ray analysis[4] of the 1,5-sigmatropic rearrangement product derived from the cycloadduct of 3,5-dimethylpyridine *N*-oxide and *N*-butylmaleimide. In this paper, we describe the 1,3-dipolar cycloaddition of various alkylpyridine *N*-oxides (Ia—h) with *N*-substituted maleimides (IIa—i). The results are discussed here in detail in comparison with the previous work and additional data that we have obtained.

Results

Cycloaddition of 3,5-Dimethylpyridine *N*-Oxide (Ia) with *N*-Substituted Maleimides (II) To Examine the generality of the *exo* cycloaddition, the 1,3-dipolar cycloadditions of Ia with II were performed. The yields and spectral data for the products are summarized in Tables I and II.

As can be seen in Table I, the mass spectra (MS) of the products (III) showed molecular peaks corresponding to the 1:1 adducts. The infrared (IR) spectra of III exhibited characteristic absorptions of a cyclic imido carbonyl group in the vicinity of 1715 cm^{-1}. The proton nuclear magnetic resonance (^{1}H-NMR) spectra showed two methyl signals as a singlet and a weakly split singlet due to allylic coupling. Three angular methine protons appeared as an ABX pattern. Inspection of the coupling constants indicates that the three protons are oriented in *cis* disposition. This suggests that the primary cycloadditions proceed *via exo* transition states (see Chart 1).

X-Ray Analysis of the 1,5-Sigmatropic Rearrangement Product In general, 1,3-dipolar cycloadditions of nitrones and azomethine imines involving the phenanthridine skeleton give mainly *endo* primary cycloadducts.[3a,b] Stereoselective *exo*-cycloaddition has scarcely been observed in the field of cycloaddition. So far as we know, there are only a few examples of the *exo*-cycloaddition of pyridine *N*-oxides.

Therefore, we performed a single crystal X-ray analysis. Suitable single crystals could be obtained only in the case

TABLE I. Cycloadducts (IIIa—k) from the 1,3-Dipolar Reaction of 3,5-Dimethylpyridine *N*-Oxide (Ia) with *N*-Substituted Maleimides (IIa—k)[a]

Adduct[b]	R	Yield (%)	mp (°C)	Formula	High-resolution MS Calcd (Found)	IR (cm^{-1}) C=O
IIIaa	Ph	40.2	172.5—173.5	$C_{17}H_{16}N_2O_3$[c]		1715
IIIab	*p*-ClC_6H_4	25.2	209	$C_{17}H_{15}ClN_2O_3$[c]		1710
IIIac	*p*-MeC_6H_4	40.2	187—188	$C_{18}H_{18}N_2O_3$[c]		1715
IIIad	*p*-FC_6H_4	42.5	187—188	$C_{17}H_{15}FN_2O_3$	314.1067 (314.1096)	1716
IIIae	*m*-FC_6H_4	41.8	135—137	$C_{17}H_{15}FN_2O_3$	314.1067 (314.1113)	1714
IIIaf	*o*-FC_6H_4	43.1	152—153	$C_{17}H_{15}FN_2O_3$	314.1067 (314.1096)	1724
IIIag	*p*-Cl, *o*-FC_6H_3	26.7	187—188	$C_{17}H_{14}ClFN_2O_3$	348.0667 (348.0656)	1724
IIIah	*m*-Cl, *p*-FC_6H_3	10.3	153—154	$C_{17}H_{14}ClFN_2O_3$	348.0667 (348.0666)	1722
IIIai	*o*-Cl, *p*-FC_6H_3	25.3	187—190	$C_{17}H_{14}ClFN_2O_3$	348.0667 (348.0661)	1724

a) Refluxed for 10 h in toluene. IIIaa, IIIab and IIIac: see ref. 2*b*. *b*) Colorless needles, recrystallized from C_6H_6. *c*) Analyzed for C, H and N; the results were within ±0.3% of theoretical values.

TABLE II. ^{1}H-NMR Spectral Data for the Cycloadducts (III)

Comp. No.	^{1}H-NMR δ (400 MHz, in $CDCl_3$)
IIIad	1.35 (3H, s, C_{8a}-Me), 1.87 (3H, d, J=1.8 Hz, C_7-Me), 4.10 (1H, dd, J=9.3, 8.0 Hz, C_{4a}-H), 4.35 (1H, dd, J=9.3, 2.2 Hz, C_{4b}-H), 4.93 (1H, d, J=8.0 Hz, C_{1a}-H), 5.93 (1H, dd, J=2.2, 2.2 Hz, C_8-H), 7.10—7.42 (4H, m, aromatic CH), 7.82 (1H, dd, J=2.2, 2.2 Hz, C_6-H)
IIIae	1.34 (3H, s, C_{8a}-Me), 1.87 (3H, d, J=2.2 Hz, C_7-Me), 4.11 (1H, dd, J=9.5, 8.0 Hz, C_{4a}-H), 4.35 (1H, dd, J=9.5, 2.2 Hz, C_{4b}-H), 4.93 (1H, d, J=8.0 Hz, C_{1a}-H), 5.93 (1H, dd, J=2.2, 2.2 Hz, C_8-H), 7.10—7.35 (4H, m, aromatic CH), 7.81 (1H, dd, J=2.2, 2.2 Hz, C_6-H)
IIIaf	1.35 (3H, br s, C_{8a}-Me), 1.79 and 1.88 (3H, br s, C_7-Me),[a] 4.15 (1H, br s, C_{4a}-H), 4.37 (1H, br s, C_{4b}-H), 4.97 (1H, br s, C_{1a}-H), 5.93 (1H, br s, C_8-H), 7.13—7.42 (4H, m, aromatic CH), 7.83 (1H, br s, C_6-H)
IIIag	1.34 (3H, s, C_{8a}-Me), 1.87 (3H, d, J=1.8 Hz, C_7-Me), 4.16 (1H, br s, C_{4a}-H), 4.35 (1H, br s, C_{4b}-H), 4.97 (1H, br s, C_{1a}-H), 5.92 (1H, d, J=1.8 Hz, C_8-H), 7.09—7.27 (3H, m, aromatic CH), 7.82 (1H, br s, C_6-H)
IIIah	1.36 (3H, s, C_{8a}-Me), 1.89 (3H, d, J=1.8 Hz, C_7-Me), 4.13 (1H, dd, J=9.0, 8.0 Hz, C_{4a}-H), 4.34 (1H, dd, J=9.0, 2.6 Hz, C_{4b}-H), 4.93 (1H, d, J=8.0 Hz, C_{1a}-H), 5.94 (1H, dd, J=1.8, 1.5 Hz, C_8-H), 7.14—7.36 (3H, m, aromatic CH), 7.83 (1H, dd, J=1.5, 2.6 Hz, C_6-H)
IIIai	1.36 (3H, s, C_{8a}-Me), 1.92 (3H, d, J=1.8 Hz, C_7-Me), 4.18 (1H, dd, J=9.0, 8.0 Hz, C_{4a}-H), 4.31 (1H, dd, J=9.0, 2.6 Hz, C_{4b}-H), 4.99 (1H, d, J=8.0 Hz, C_{1a}-H), 5.98 (1H, dd, J=1.8, 1.5 Hz, C_8-H), 7.06—7.26 (3H, m, aromatic CH), 7.86 (1H, dd, J=1.5, 2.6 Hz, C_6-H)

a) Split due to restricted rotation about o-FC_6H_4 group.

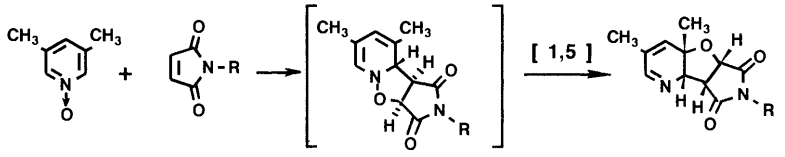

Ia II III

R

IIa: Ph
IIb: p-ClC_6H_4
IIc: p-MeC_6H_4
IId: p-FC_6H_4
IIe: m-FC_6H_4
IIf: o-FC_6H_4
IIg: p-Cl,o-FC_6H_3
IIh: m-Cl,p-FC_6H_3
IIi: o-Cl,p-FC_6H_3
IIj: n-butyl

Chart 1

of the *N*-butyl derivative (IIIaj).[4]

The crystal structure was solved by the direct method using the MULTAN78 series of programs.[5] Refinement to an *R* factor of 6.11% was obtained by the least-squares method on 2099 nonzero structure factors. As can be seen in the computer-generated drawing, IIIaj was confirmed to be an *endo* cycloadduct, providing definitive evidence of *exo* primary cycloaddition.

The torsion angles of H7–C7–C11–H11 and H11–C11–C12–H12 are 9.0° and 29.0°, respectively. These values are consistent with those calculated based on the coupling constants using the Karplus equation.[6] The torsion angle of N1–C2–C3–C4 is 12.4°, indicating that the 1-azadiene moiety is not planar. The C5–O6 bond length, 1.460 Å is greater than the O6–C7 bond length (1.423 Å). This elongation might be caused by steric repulsion between the *N*-substituted succinimide ring and the dihydropyridine moiety.

Cycloaddition of 2-Alkylpyridine *N*-Oxide with *N*-Substituted Maleimides Next, as an extension of the cycloaddition mentioned above, we carried out the reaction using 2-alkylpyridine *N*-oxides as 1,3-dipoles. In the reaction of 2,3-dimethylpyridine *N*-oxide (Ib), 2,5-dimethylpyridine *N*-oxide (Ic) and 5-ethyl-2-methylpyridine *N*-oxide (Id) with *N*-substituted maleimides (II), the reaction behaviors were different from the case of 3,5-dimethylpyridine *N*-oxide (Ia). The products obtained were revealed to be a series of cycloadducts of a new type (IV).

The high-resolution MS of IVba showed the molecular peak (M^+) at *m/z* 642.2087, which is consistent with the 1 : 3 adduct of Ib and IIa (calcd for $C_{37}H_{30}N_4O_7$: 642.2114).

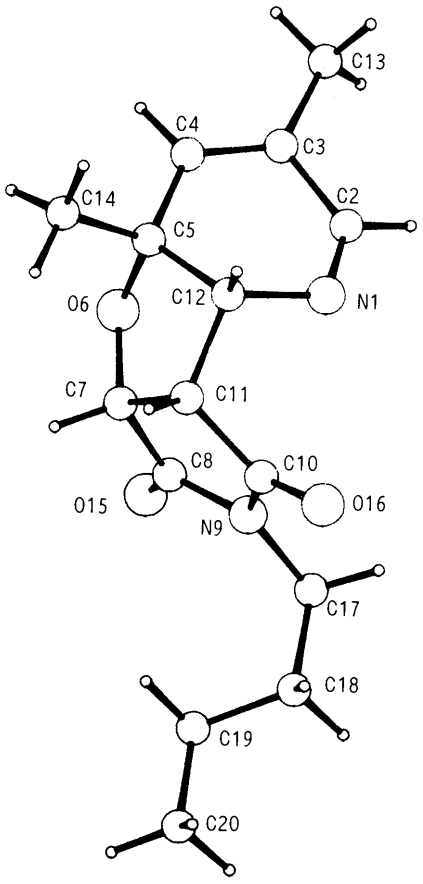

Fig. 1. Ortep Drawing of IIIaj

The IR spectrum of IVba showed a characteristic imido-carbonyl group absorption at 1720 cm^{-1}. The ^{13}C-nuclear magnetic resonance (^{13}C-NMR) spectrum of IVba exhibited ten sp^3 carbon signals from 18.3 to 75.7 ppm.[7] The ^1H-NMR spectrum of VIba exhibited one methyl signal at δ 1.60, one olefinic proton signal at δ 6.32 and four *cis*-oriented angular methine protons at δ 4.05—4.94. The details of the spectrum are depicted in Fig. 2. Inspection of the *J*-value between C_{4a}-H and C_{4b}-H indicates that IVba should be assigned as the *endo* product. The assignment was supported by the spectral behavior of the products (III) derived from the reaction of 3,5-

TABLE III. Fractional Atomic Coordinates[a] and Isotropic Temperature Factors (*B*) of IIIaj with Their Estimated Standard Deviations in Parentheses

Atom	*x/a*	*y/b*	*z/c*	*B*[b]
N1	−1647 (1)	6816 (2)	−2529 (3)	3.47 (5)
C2	−1165 (1)	7573 (3)	−2131 (4)	3.93 (7)
C3	−517 (1)	7096 (3)	−2103 (4)	3.91 (7)
C4	−410 (1)	5703 (4)	−2195 (4)	3.86 (7)
C5	−927 (1)	4637 (3)	−2393 (4)	3.35 (6)
O6	−1024 (1)	4164 (2)	−551 (3)	3.70 (4)
C7	−1646 (1)	3662 (3)	−614 (4)	3.17 (6)
C8	−1939 (1)	4270 (3)	991 (4)	3.45 (6)
N9	−2462 (1)	5029 (2)	319 (3)	3.49 (5)
C10	−2556 (1)	5061 (3)	−1572 (4)	3.32 (6)
C11	−2019 (1)	4304 (3)	−2299 (3)	3.02 (5)
C12	−1552 (1)	5316 (3)	−3095 (3)	3.17 (6)
C13	−19 (2)	8232 (4)	−1925 (6)	5.83 (10)
C14	−780 (1)	3337 (4)	−3532 (5)	4.97 (9)
O15	−1759 (1)	4133 (3)	2585 (3)	5.06 (6)
O16	−2999 (1)	5606 (2)	−2438 (3)	4.54 (5)
C17	−2878 (2)	5737 (4)	1490 (5)	4.77 (8)
C18	−3486 (2)	4936 (4)	1551 (5)	5.16 (9)
C19	−3422 (2)	3432 (4)	2309 (5)	5.15 (9)
C20	−4039 (2)	2675 (5)	2346 (5)	5.81 (10)
H2	−1233 (13)	8556 (31)	−1805 (38)	4.41 (65)
H4	4 (12)	5321 (30)	−2064 (36)	3.84 (60)
H7	−1669 (11)	2605 (28)	−574 (34)	3.09 (53)
H11	−2155 (12)	3548 (28)	−3102 (34)	3.25 (55)
H12	−1634 (11)	5317 (28)	−4367 (33)	3.00 (53)
H131	399 (16)	7815 (39)	−1890 (46)	6.72 (86)
H132	−73 (16)	8795 (40)	−972 (47)	6.85 (89)
H133	−28 (16)	8892 (39)	−2919 (47)	6.60 (86)
H141	−1126 (15)	2597 (36)	−3596 (43)	5.72 (76)
H142	−434 (14)	2852 (34)	−2938 (40)	4.92 (69)
H143	−721 (14)	3644 (34)	−4778 (41)	5.17 (72)
H171	−2651 (14)	5813 (33)	2614 (42)	5.14 (72)
H172	−2968 (14)	6698 (35)	938 (42)	5.42 (74)
H181	−3739 (15)	5542 (36)	2379 (44)	5.72 (77)
H182	−3700 (14)	4847 (34)	249 (40)	4.95 (70)
H191	−3156 (15)	2872 (36)	1521 (42)	5.52 (75)
H192	−3182 (16)	3585 (39)	3618 (48)	6.83 (88)
H201	−3990 (16)	1681 (39)	2907 (47)	6.85 (88)
H202	−4240 (15)	2653 (37)	1207 (44)	6.14 (81)
H203	−4312 (15)	3280 (36)	3019 (43)	5.78 (77)

a) Positional parameters are multiplied by 10^4. *b*) Thermal parameters are given as the equivalent temperature factors ($Å^2$).

TABLE IV. Bond Distances (Å) of IIIaj for Non-hydrogen Atoms with Their Estimated Standard Deviations in Parentheses

	Distance (Å)		Distance (Å)
N1–C2	1.265 (4)	N1–C12	1.468 (4)
C2–C3	1.471 (4)	C3–C4	1.311 (5)
C3–C13	1.502 (5)	C4–C5	1.489 (4)
C5–O6	1.460 (3)	C5–C12	1.531 (4)
C5–C14	1.518 (5)	O6–C7	1.423 (3)
C7–C8	1.509 (4)	C7–C11	1.525 (4)
C8–N9	1.379 (4)	C8–O15	1.201 (4)
N9–C10	1.384 (4)	N9–C17	1.467 (4)
C10–C11	1.506 (4)	C10–O16	1.203 (4)
C11–C12	1.541 (4)	C17–C18	1.518 (5)
C18–C19	1.498 (5)	C19–C20	1.513 (6)

TABLE V. Bond Angles (°) of IIIaj for Non-hydrogen Atoms with Their Estimated Standard Deviations in Parenthesis

	Angle (°)		Angle (°)
C2–N1–C12	116.7 (2)	N1–C1–C3	127.0 (3)
C2–C3–C4	118.0 (3)	C2–C3–C13	118.0 (3)
C4–C3–C13	124.0 (3)	C3–C4–C5	121.2 (3)
C4–C5–O6	106.9 (2)	C4–C5–C12	113.1 (2)
C4–C5–C14	112.1 (3)	O6–C5–C12	103.0 (2)
O6–C5–C14	109.6 (2)	C12–C5–C14	111.7 (2)
C5–O6–C7	107.4 (2)	O6–C7–C8	109.4 (2)
O6–C7–C11	108.5 (2)	C8–C7–C11	105.0 (2)
C7–C8–N9	108.0 (2)	C7–C8–O15	127.2 (3)
N9–C8–O15	124.8 (3)	C8–N9–C10	113.4 (2)
C8–N9–C17	123.4 (2)	C10–N9–C17	123.2 (3)
N9–C10–C11	108.2 (2)	N9–C10–O16	124.3 (3)
C11–C10–O16	127.6 (3)	C7–C11–C10	104.8 (2)
C7–C11–C12	103.4 (2)	C10–C11–C12	114.8 (2)
N1–C12–C5	116.0 (2)	N1–C12–C11	110.2 (2)
C5–C12–C11	102.6 (2)	N9–C17–C18	113.1 (3)
C17–C18–C19	114.7 (3)	C18–C19–C20	113.0 (3)

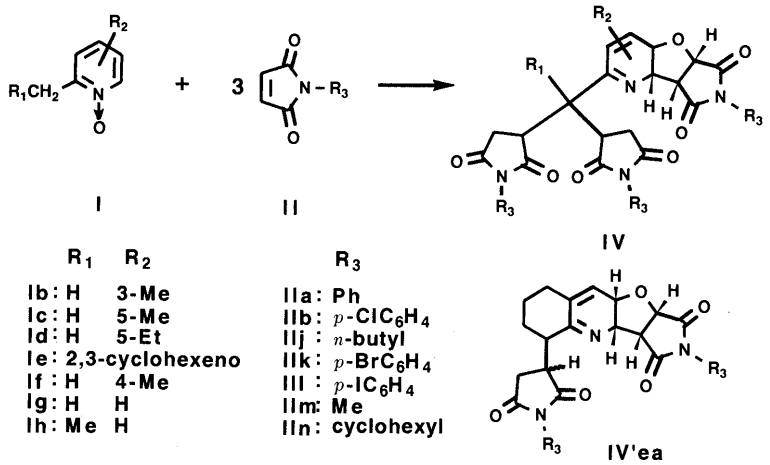

Chart 2

TABLE VI. Ene Reaction Products (IV) from the 1,3-Dipolar Reaction of 2-Alkylpyridine *N*-Oxide (Ia) with *N*-Substituted Maleimides (IIa—g)[a]

Product[b]	R	Yield (%)	mp (°C)	Formula	High-resolution MS Calcd (Found)	IR (cm^{-1}) C=O
IVba	Ph	18.3	254—255	$C_{37}H_{30}N_4O_7$	642.2114 (642.2087)	1720
IVbb	*p*-ClC_6H_4	24.1	250—251	$C_{37}H_{27}Cl_3N_4O_7$[c]		1712
IVbj	*n*-Butyl	20.0	175—177	$C_{31}H_{42}N_4O_7$	582.3053 (582.3029)	1698
IVbk	*p*-BrC_6H_4	22.2	259—261	$C_{37}H_{27}Br_3N_4O_7$[c]		1712
IVbl	*p*-IC_6H_4	17.1	239—241	$C_{37}H_{27}I_3N_4O_7$[c]		1712
IVbm	Me	25.7	248—249	$C_{22}H_{24}N_4O_7$	456.1645 (456.1633)	1692
IVbn	Cyclohexyl	20.5	254—255	$C_{37}H_{48}N_4O_7$	660.3523 (660.3522)	1704
IVca	Ph	32.7	226—227	$C_{37}H_{40}N_4O_7$	642.2114 (642.2144)	1704
IVcb	*p*-ClC_6H_4	24.1	234—236	$C_{37}H_{27}Cl_3N_4O_7$[c]		1710
IVcj	*n*-Butyl	41.5	141—142	$C_{31}H_{42}N_4O_7$	582.3053 (582.3035)	1694
IVck	*p*-BrC_6H_4	17.1	191—193	$C_{37}H_{27}Br_3N_4O_7$	876.9508 (876.9500)	1712
IVcl	*p*-IC_6H_4	14.7	190—192	$C_{37}H_{27}I_3N_4O_7$	1020.9090 (1020.8940)	1712
IVda	Ph	25.2	235—237	$C_{38}H_{32}N_4O_7$	656.2271 (656.2253)	1708

a) Refluxed for 10 h in toluene. *b*) Colorless needles, recrystallized from *n*-hexane–Me_2CO. *c*) Analyzed for C, H and N; the results were within ±0.3% of theoretical values.

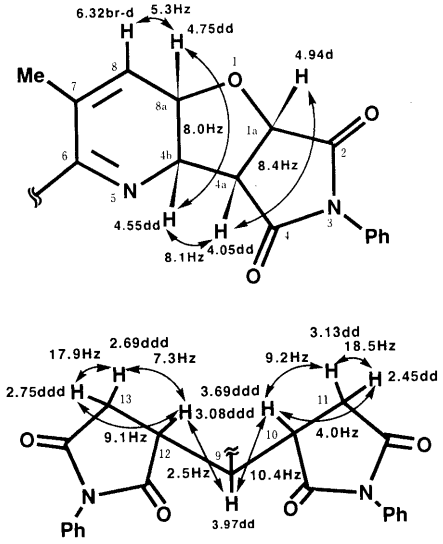

Fig. 2. ^{1}H-NMR Spectrum of IVba

dimethylpyridine *N*-oxide (Ia) with *N*-substituted maleimides (II), whose structures were confirmed by X-ray analysis.

As shown in Fig. 2, the two succinimide moieties exhibited ABX patterns. The spectral data for IVbb—da can be similarly assigned to the corresponding 1 : 3 ene reaction products (Tables VI and VII).

Attempts to isolate 1 : 1 cycloadducts by changing the I/II ratios were unsuccessful, giving rise only to the 1 : 3 ene reaction products (IV).

On the other hand, in the reaction of 2,3-cyclohexenopyridine *N*-oxide (Ie) with IIa, the 1 : 3 ene reaction product could not be obtained, but the 1 : 2 ene reaction product (IV'ea) was isolated as colorless needles (mp 179—182 °C) in 36.3% yield. The adduct (IV'ea) showed strong carbonyl absorption at 1714 cm^{-1} in the IR spectrum. The high-resolution MS spectrum of IV'ea showed M^+ at *m/z* 495.1794, which corresponds to the 1 : 2 ene reaction product of Ie and IIa. In the ^{1}H-NMR spectrum of IV'ea, digital integration showed the existence of twenty-five protons. The spectrum showed complex signals, presumably due to the existence of conformational isomers. As the temperature

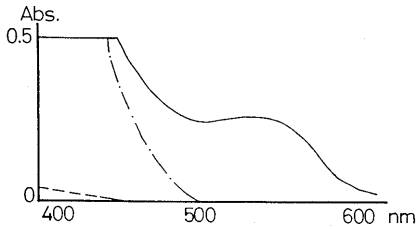

Fig. 3. Charge-Transfer Complex Formation in the Reaction of Ii with IIa

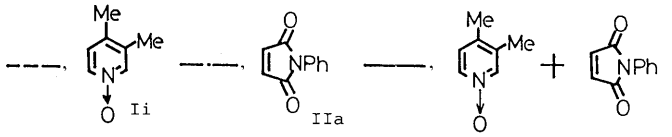

was raised, the signals became sharper but a completely averaged spectrum could not be obtained even at 100 °C. However, each of the proton signals was observed at a magnetic field consistent with the structure of IV'ea depicted in Chart 2. The ^{13}C-NMR spectrum of IV'ea also exhibited similar behavior (see Experimental). In the MS of IV'ea, the peak at *m/z* 477 ($M^+ - H_2O$) probably results from cleavage of an ether linkage followed by hydrogen rearrangement and elimination of water, leading to aromatization of the dihydropyridine ring. The fragmentation pattern is common in the adducts IV.

Charge Transfer Complex Formation In contrast, 2,4-dimethylpyridine *N*-oxide (If), 2-methylpyridine *N*-oxide (Ig), 2-ethylpyridine *N*-oxide (Ih) and 3,4-dimethylpyridine *N*-oxide (Ii) did not afford cycloadducts. In these cases, coloration due to charge-transfer (CT) complex formation was observed. When IIa was added to I in toluene solution, there was a marked intensification of the red color and the visible absorption spectrum of the mixture was different from the spectra of pure samples of the two solutes. This observation indicates that the reactions of I with II proceed *via* CT complex formation, which might play an important role in stabilizing the ground state.[8] In the cases of If—i, the reactions were stalled as a result of CT complex formation.[9]

Herbicidal Activity In the preliminary study, we found that the product (III) bearing the chloro substituent showed moderate herbicidal activity. So, we examined the herbicidal

TABLE VII. ^{1}H-NMR Spectral Data for the Ene Reaction Products (IV)[a]

Comp. No.	^{1}H-NMR δ (400 MHz)
IVba[b]	1.60 (3H, br s, C_7-Me), 2.45 (1H, dd, J=4.0, 18.5 Hz, C_{11}-H), 2.75 (1H, dd, J=7.3, 17.9 Hz, C_{13}-H), 2.69 (1H, dd, J=9.1, 17.9 Hz, C_{13}-H), 3.08 (1H, ddd, J=2.5, 7.3, 9.1 Hz, C_{12}-H), 3.13 (1H, dd, J=9.2, 18.5 Hz, C_{11}-H), 3.69 (1H, ddd, J=4.0, 9.2, 10.4 Hz, C_{10}-H), 3.97 (1H, dd, J=2.5, 10.4 Hz, C_9-H), 4.05 (1H, dd, J=8.1, 8.4 Hz, C_{4a}-H), 4.55 (1H, dd, J=8.1, 8.0 Hz, C_{4b}-H), 4.75 (1H, dd, J=8.0, 5.3 Hz, C_{8a}-H), 4.94 (1H, d, J=8.4 Hz, C_{1a}-H), 6.32 (1H, br d, J=5.3 Hz, C_8-H), 7.18—7.50 (15H, m, aromatic CH)
IVbb[c]	2.03 (3H, br s, C_7-Me), 2.26 (1H, dd, J=4.5, 17.9 Hz, C_{11}-H), 2.38 (1H, dd, J=8.4, 17.9 Hz, C_{11}-H), 2.73 (1H, dd, J=6.8, 17.6 Hz, C_{13}-H), 2.89 (1H, dd, J=9.5, 17.6 Hz, C_{13}-H), 3.17—3.23 (1H, m, C_{10}-H), 3.62 (1H, ddd, J=4.5, 8.4, 10.3 Hz, C_{12}-H), 3.99 (1H, br d, J=10.4 Hz, C_9-H), 4.19 (1H, dd, J=8.1, 8.4 Hz, C_{4a}-H), 4.39—4.43 (2H, m, C_{4b}-H, C_{8a}-H), 4.93 (1H, d, J=8.1 Hz, C_{1a}-H), 6.40 (1H, br d, J=4.4 Hz, C_8-H), 7.14—7.58 (12H, m, aromatic CH)
IVbj[c]	0.89—0.95 (9H, m, $-CH_2CH_2CH_2CH_3$), 1.23—1.39 (6H, m, three $-CH_2CH_2CH_2CH_3$), 1.44—1.63 (6H, m, three $-CH_2CH_2CH_2CH_3$), 2.00 (3H, br s, C_7-Me), 2.28 (1H, dd, J=18.3, 4.8 Hz, C_{11}-H), 2.44 (1H, dd, J=17.6, 9.2 Hz, C_{13}-H), 2.53 (1H, dd, J=17.6, 6.6 Hz, C_{13}-H), 2.81 (1H, dd, J=18.3, 9.5 Hz, C_{11}-H), 2.81 (1H, ddd, J=10.3, 9.2, 6.6 Hz, C_{12}-H), 3.29 (1H, ddd, J=9.5, 9.5, 4.8 Hz, C_{10}-H), 3.38—3.57 (6H, m, three $-CH_2CH_2CH_2CH_3$), 3.75 (1H, m, C_9-H), 3.90 (1H, dd, J=8.4, 8.4 Hz, C_{4a}-H), 4.30 (1H, dd, J=8.4, 8.4 Hz, C_{4b}-H), 4.35 (1H, dd, J=5.5, 8.4 Hz, C_{8a}-H), 4.75 (1H, d, J=8.4 Hz, C_{1a}-H), 6.26 (1H, dd, J=1.5, 5.5 Hz, C_8-H)
IVbk[c]	2.03 (3H, br s, C_7-Me), 2.27 (1H, dd, J=6.8, 17.5 Hz, C_{11}-H), 2.38 (1H, dd, J=9.3, 17.5 Hz, C_{11}-H), 2.73 (1H, dd, J=5.1, 18.0 Hz, C_{13}-H), 2.89 (1H, dd, J=8.9, 18.0 Hz, C_{13}-H), 3.18—3.21 (1H, m, C_{10}-H), 3.61 (1H, ddd, J=5.1, 8.9, 8.9 Hz, C_{12}-H), 3.99 (1H, br d, J=8.9 Hz, C_9-H), 4.19 (1H, dd, J=8.1, 8.4 Hz, C_{4a}-H), 4.38—4.43 (2H, m, C_{4b}-H, C_{8a}-H), 4.93 (1H, d, J=8.4 Hz, C_{1a}-H), 6.40 (1H, br d, J=5.1 Hz, C_8-H), 7.14—7.58 (12H, m, aromatic CH)
IVbl[b]	2.02 (3H, br s, C_7-Me), 2.26 (1H, dd, J=4.8, 17.4 Hz, C_{11}-H), 2.40 (1H, dd, J=8.6, 17.4 Hz, C_{11}-H), 2.72 (1H, dd, J=6.8, 17.9 Hz, C_{13}-H), 2.87 (1H, dd, J=9.3, 17.9 Hz, C_{13}-H), 3.16—3.22 (1H, m, C_{10}-H), 3.55—3.62 (1H, m, C_{12}-H), 3.97 (1H, br d, J=9.9 Hz, C_9-H), 4.17 (1H, dd, J=8.1, 8.4 Hz, C_{4a}-H), 4.37—4.43 (2H, m, C_{4b}-H, C_{8a}-H), 4.91 (1H, d, J=8.4 Hz, C_{1a}-H), 6.37 (1H, br d, J=3.7 Hz, C_8-H), 6.92—7.88 (12H, m, aromatic CH)
IVbm[b]	1.97 (3H, br s, C_7-Me), 2.17 (1H, dd, J=17.6, 9.2 Hz, C_{13}-H), 2.28 (1H, dd, J=17.6, 6.2 Hz, C_{13}-H), 2.56 (2H, d, J=6.8, 17.9 Hz, C_{11}-H), 2.72 (3H, s, *N*-Me), 2.80 (3H, s, *N*-Me), 2.82 (3H, s, *N*-Me), 2.93 (1H, ddd, J=6.2, 9.2, 9.9 Hz, C_{12}-H), 3.20 (1H, d, J=16.5, 6.8 Hz, C_{10}-H), 3.74 (1H, br d, J=9.9 Hz, C_9-H), 3.99 (1H, dd, J=8.1, 8.4 Hz, C_{4a}-H), 4.18—4.25 (2H, m, C_{4b}-H, C_{8a}-H), 4.69 (1H, d, J=8.4 Hz, C_{1a}-H), 6.30 (1H, br d, J=5.5 Hz, C_8-H)
IVbn[c]	1.12—2.17 (30H, m, methylene protons of cyclohexyl), 1.95 (3H, s, C_7-Me), 2.45 (1H, dd, J=18.0, 4.4 Hz, C_{13}-H), 2.63—2.77 (3H, m, C_{13}-H, C_{11}-H), 2.92 (1H, ddd, J=7.0, 3.7, 9.2 Hz, C_{10}-H), 3.27 (1H, ddd, J=4.4, 4.4, 8.8 Hz, C_{12}-H), 3.66—3.71 (1H, m, C_9-H), 3.68 (1H, dd, J=8.1, 9.2 Hz, C_{4a}-H), 3.84—4.00 (3H, m, methine protons of cyclohexyl), 4.41 (1H, m, C_{4b}-H), 4.46 (1H, m, C_{8a}-H), 4.64 (1H, d, J=8.1 Hz, C_{1a}-H), 6.06 (1H, dd, J=4.4, 1.7 Hz, C_8-H)
IVca[c]	1.33 (3H, s, C_{8a}-Me), 2.62 (1H, dd, J=4.8, 18.8 Hz, C_{11}-H), 2.96 (1H, dd, J=11.7, 20.2 Hz, C_{13}-H), 3.12 (1H, dd, J=9.4, 18.8 Hz, C_{11}-H), 3.18 (1H, m, C_{12}-H), 3.21 (1H, m, C_{13}-H), 3.58 (1H, ddd, J=2.5, 4.8, 9.4 Hz, C_{10}-H), 3.74 (1H, dd, J=2.5, 6.2 Hz, C_9-H), 3.86 (1H, dd, J=7.7, 9.9 Hz, C_{4a}-H), 4.52 (1H, d, J=9.9 Hz, C_{4b}-H), 4.89 (1H, d, J=7.7 Hz, C_{1a}-H), 5.87 (1H, d, J=9.9 Hz, C_7-H), 6.35 (1H, d, J=9.9 Hz, C_8-H), 7.12—7.46 (15H, m, aromatic CH)
IVcb[b]	1.23 (3H, s, C_{8a}-Me), 2.73—2.95 (4H, m, C_{11}-H, C_{13}-H), 3.51 (1H, br s, C_{10}-H), 3.59—3.63 (2H, m, C_9-H, C_{12}-H), 4.05 (1H, dd, J=7.9, 9.7 Hz, C_{4a}-H), 4.50 (1H, d, J=9.7 Hz, C_{4b}-H), 4.91 (1H, d, J=7.9 Hz, C_{1a}-H), 6.08 (1H, d, J=9.7 Hz, C_7-H), 6.39 (1H, d, J=9.7 Hz, C_8-H), 7.24—7.58 (12H, m, aromatic CH)
IVcj[c]	0.89—0.95 (9H, m, three $-CH_2CH_2CH_2CH_3$), 1.24 (3H, s, C_{8a}-Me), 1.25—1.62 (12H, m, three $-CH_2CH_2CH_2CH_3$), 2.47 (1H, dd, J=18.0, 5.1 Hz, C_{13}-H), 2.85—2.95 (1H, m, C_{11}-H), 2.88 (1H, dd, J=18.0, 8.5 Hz, C_{13}-H), 3.01—3.07 (1H, m, C_{11}-H), 3.09 (1H, dd, J=3.3, 5.9 Hz, C_{10}-H), 3.26—3.36 (1H, m, C_{12}-H), 3.32—3.51 (6H, m, three $-CH_2CH_2CH_2CH_3$), 3.58 (1H, dd, J=5.9, 2.9 Hz, C_9-H), 3.68 (1H, dd, J=7.7, 9.9 Hz, C_{4a}-H), 4.31 (1H, d, J=9.9 Hz, C_{4b}-H), 4.74 (1H, d, J=7.7 Hz, C_{1a}-H), 5.66 (1H, J=9.9 Hz, C_7-H), 6.12 (1H, J=9.9 Hz, C_8-H)
IVck[b]	1.22 (3H, s, C_{8a}-Me), 2.72—2.93 (4H, m, C_{11}-H, C_{13}-H), 3.48—3.53 (1H, m, C_{10}-H), 3.58—3.65 (2H, m, C_9-H, C_{12}-H), 4.04 (1H, dd, J=7.7, 9.9 Hz, C_{4a}-H), 4.49 (1H, d, J=9.9 Hz, C_{4b}-H), 4.89 (1H, d, J=7.7 Hz, C_{1a}-H), 6.06 (1H, d, J=9.9 Hz, C_7-H), 6.39 (1H, d, J=9.9 Hz, C_8-H), 7.16—7.71 (12H, m, aromatic CH)
IVcl[b]	1.22 (3H, s, C_{8a}-Me), 2.75—2.88 (4H, m, C_{11}-H, C_{13}-H), 3.44—3.52 (1H, m, C_{10}-H), 3.55—3.63 (2H, m, C_9-H, C_{12}-H), 4.03 (1H, dd, J=7.7, 9.9 Hz, C_{4a}-H), 4.48 (1H, d, J=9.9 Hz, C_{4b}-H), 4.88 (1H, d, J=7.7 Hz, C_{1a}-H), 6.04 (1H, d, J=9.9 Hz, C_7-H), 6.36 (1H, d, J=9.9 Hz, C_8-H), 7.16—7.71 (12H, m, aromatic CH)
IVda[b]	0.78 (3H, t, J=7.5 Hz, C_{8a}-CH_2CH_3), 1.50—1.62 (2H, m, C_{8a}-CH_2CH_3), 2.71 (1H, dd, J=9.2, 17.8 Hz, C_{13}-H), 2.80—2.86 (3H, m, C_{13}-H, C_{11}-H), 3.54—3.60 (2H, m, C_{10}-H, C_{12}-H), 3.67—3.70 (1H, m, C_9-H), 4.08 (1H, dd, J=7.5, 10.4 Hz, C_{4a}-H), 4.58 (1H, d, J=10.4 Hz, C_{4b}-H), 4.91 (1H, d, J=7.5 Hz, C_{1a}-H), 6.20 (1H, d, J=10.1 Hz, C_7-H), 6.39 (1H, d, J=10.1 Hz, C_8-H), 7.18—7.50 (15H, m, aromatic CH)

a) Numbering sequence: see Fig. 2. *b*) In DMSO-d_6. *c*) In $CDCl_3$.

activities of other cycloadducts in the series.

The *N*-(*p*-chlorophenyl) derivative (IIIab) showed herbicidal activity against Green Amaranth, with 100% blighting at 4 ppm. Furthermore, the *N*-(*p*-tolyl) derivative (IIIac) was effective against monocotyledons (43% blighting) and against Foxtail green (85% blighting) at 4 ppm.

The biological activities of IV could not be examined in aqueous solution, because the compounds are not soluble in water. The biological activities of IV in non-aqueous solutions are under investigation, and the results will be published in the near future.

Discussion

As hitherto mentioned, in the case of 3,5-dimethylpyridine *N*-oxide (Ia), the pericyclic reaction afforded 2,3-dihydrofuro[3,2-*b*]pyridines (III) as final products. On the other hand, 2-alkylpyridine *N*-oxides (Ib—e) gave 1 : 3 (or 1 : 2) ene reaction products (IV). The difference in the pericyclic reaction behavior can be ascribed to the existence of the α-methyl group on the pyridine nucleus.

Next, mention should be made of the formation mechanism of the 1 : 3 ene reaction product, taking into consideration previously reported mechanistic aspects of analogous reactions.[10] The formation mechanism of the 1 : 3 ene reaction products can be analyzed by dividing the whole reaction into four steps from the frontier molecular orbital (FMO) theoretical point of view[11] (Chart 3). The first step of the reaction is the concerted 1,3-cycloaddition

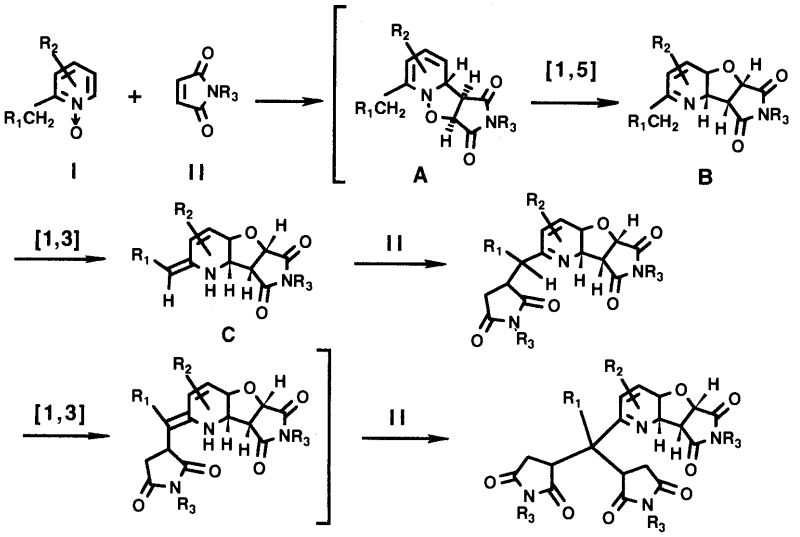

Chart 3

of I with II. Molecular orbital calculations based on the modified neglect of diatomic overlap (MNDO) approximation[12] were performed and the results are summarized in Fig. 4. Sustmann[13] has classified 1,3-dipolar cycloadditions into three general types according to the highest occupied molecular orbital (HOMO)–lowest unoccupied molecular orbital (LUMO) arrangement of the 1,3-dipole and dipolarophile. They are the normal electron demand, the inverse electron demand, and the neutral electron demand types. The normal electron demand reaction is dominated by the interaction of the HOMO of the 1,3-dipole and the LUMO of the dipolarophile. As can be seen in Fig. 4, the first step of the reaction of I with II falls into the category of a normal electron demand reaction in Sustmann's classification, wherein the dominant interaction occurs between the HOMO of I and the LUMO of II.

In the 2,3-dihydrofuro[3,2-*b*]pyridine skeleton of the 1 : 3 ene reaction product, four *cis* oriented angular methine protons were observed. This suggests that the primary cycloaddition of I with II proceeds *via* the *exo* transition state, in which unfavorable secondary orbital interactions[2b,4] do not occur.

The second step of the reaction can be explained by the sigmatropic 1,5-shift of the primary cycloadduct (A) to the rearrangement product (B). Based on the structure optimization data for simple model compounds (type A and type B), the latter is considered to be more stable by about 30 kcal/mol than the former in terms of the heat of formation.[14]

The third step of the reaction is 1,3-sigmatropic hydrogen shift of the rearrangement product (B) to the enamine-type compound (C). Though the suprafacial 1,3-sigmatropy is a forbidden process under thermal conditions, the lone pair

The fourth step of the reaction is the attack of the second molecule of the maleimide on the enamine-type compound (C), commonly referred to as the "ene reaction". From the MNDO calculations on the heterodiene-type model compound (D) and enamine-type model compound (E) shown in Fig. 5, the HOMO orbital of E lies 1.28 eV higher than that of D, indicating that ene reaction of E with II is more advantageous than hetero-Diels–Alder reaction of D with II.[11b] It can be suggested that the marked increase of

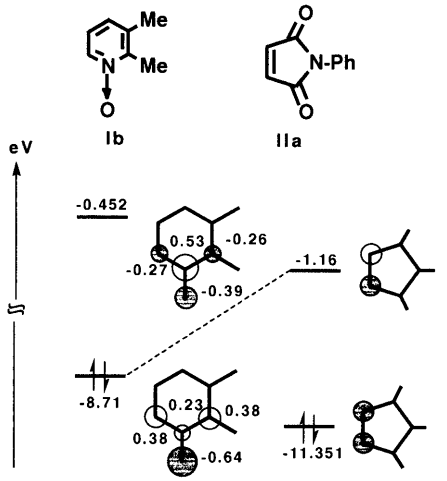

Fig. 4. MNDO Calculation of 2,3-Dimethylpyridine *N*-Oxide (Ib) and *N*-Phenylmaleimide (IIa)

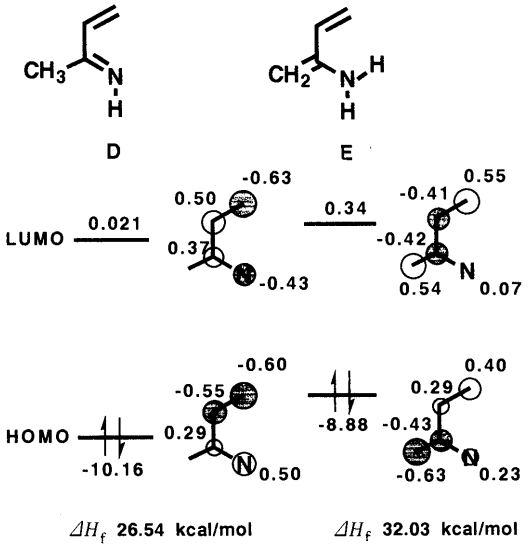

Fig. 5. MNDO Calculation of Model Compounds (D and E)

on the ring nitrogen is in phase with the lobe of the hydrogen on the α-Me group, which makes it possible for the proton to migrate to the ring nitrogen.

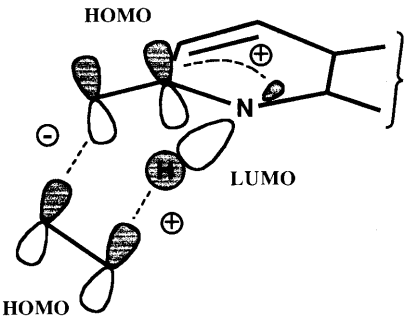

Fig. 6. Three System Interaction in the Third Step of the Reaction

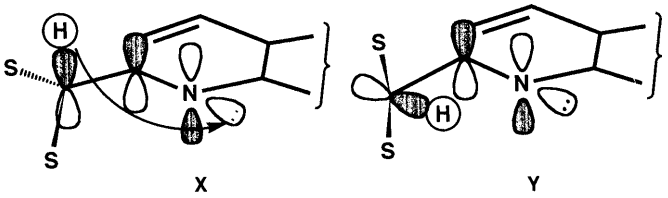

S: 3-(*N*-substituted)-succinimido

Fig. 7. Plausible Conformations for 1,3-Hydrogen Shift

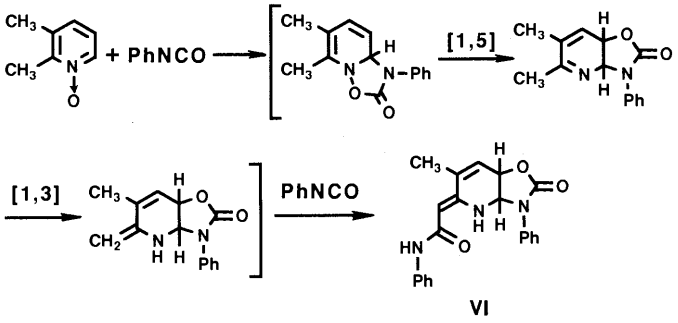

Chart 4

the HOMO level increases the perturbation energy and compensates for the 5.49 kcal/mol $\{\Delta H_f(E) - \Delta H_f(D)\}$ disadvantage in heat of formation.[11a] The magnitude of the HOMO coefficients of the enamine-type model compound (E) is greatest upon the exocyclic terminal methylene carbon, and therefore the second molecule of the maleimide attacks the methylene carbon.

The mode of this step can be rationalized in terms of a three system interaction[15] as depicted in Fig. 6. In this case, the exocyclic methylene moiety (π-HOMO) and double bond (π-HOMO) of maleimides participate in the reaction as donors, and the N–H σ-bond works as an acceptor (σ-LUMO). In the same manner, 1,3-sigmatropic hydrogen shift might be repeated when the third molecule of maleimide attacks the exocyclic methylene moiety.

In this step, the migrating hydrogen atom has to take a conformation (X) in which the C–H σ-bond lies in parallel with the lobe of the *Pz* orbital. In the case of the disubstituted compounds (Y), the steric interference between the *N*-substituted succinimide rings and the 2,3-dihydropyridine moiety prevents the parallel arrangement. Therefore, a fourth molecule of II could not participate in the reaction. Similarly, for the reaction of Ig, only the 1 : 2 adduct (IV'ea) could be obtained.

In connection with this reaction, the reaction of 2,3-dimethylpyridine with IIa was examined and afforded 2-[3-(*N*-phenylsuccinimido)methyl]-3-methylpyridine (V) in 34% yield.

As mentioned in the previous papers,[9] the cycloaddition of 2-alkylpyridine *N*-oxides (Ib, c) with phenyl isocyanates resulted in the formation of 1 : 2 cycloadducts (VI) and the pathway for the formation of the 1 : 2 cycloadducts may be explained in the same manner as mentioned above.

Experimental

All melting points are uncorrected. ^{1}H-NMR spectra were taken with Hitachi R-600 (60 MHz) and JEOL GX-400 (400 MHz) spectrometers for *ca.* 10% (w/v) solution with tetramethylsilane (TMS) as an internal standard; chemical shifts are expressed in δ values. IR spectra were recorded on a Hitachi 270-30 infrared spectrophotometer equipped with a double-blade grating. Visible absorption spectra were taken with a Hitachi 150-20 spectrometer. MS were taken with a JEOL JMS-DX303HF double-focussing spectrometer operating at an ionization potential of 75 eV. Molecular orbital calculations were performed on a FACOM M-360 computer at the Information Processing Center of Kumamoto University. Graphic analysis of the MO calculation and X-ray data were performed on a FACOM G-150 work station and a Fujitsu FM R-60HD personal computer.

Materials 3,5-Dimethylpyridine *N*-oxide (Ia), 2,3-dimethylpyridine *N*-oxide (Ib), 2,5-dimethylpyridine *N*-oxide (Ic), 5-ethyl-2-methylpyridine *N*-oxide (Id), 2,3-cyclohexenopyridine *N*-oxide (Ie), 2,4-dimethylpyridine *N*-oxide (If), 2-methylpyridine *N*-oxide (Ig), 2-ethylpyridine *N*-oxide (Ih) and 3,4-dimethylpyridine *N*-oxide (Ii) were prepared according to the established methods.[16] *N*-Substituted maleimides (IIa—n) were also prepared according to the established methods.[17]

Reaction of 3,5-Dimethylpyridine *N*-Oxides (Ia) with *N*-Substituted Maleimides (II). General Procedures A solution of Ia (0.01 mol) and II (0.02 mol) in 10 ml of absolute toluene was refluxed for 10 h. After cooling, the solution was concentrated *in vacuo*. The residue was purified by column chromatography on silica gel using AcOEt as an eluent to give III, which was purified by recrystallization (see Tables I and II).

Reaction of 2-Alkyl Substituted Pyridine *N*-Oxides (Ib—i) with *N*-Substituted Maleimides (II). General Procedures A solution of I (0.01 mol) and II (0.03 mol) in 10 ml of absolute toluene was refluxed for 10 h. After cooling, the solution was concentrated *in vacuo*. The residue was purified by column chromatography on silica gel using AcOEt as an eluent to give IV, which was purified by recrystallization (see Tables VI and VII).

According to the general procedure, Ie was allowed to react with IIa to give IV'ea in 36.4% yield, mp 184—186 °C (Me_2CO, colorless powder). IR (KBr): 1714 (C=O) cm^{-1}. MS *m/z*: 495 (M^+), 477 ($M^+ - H_2O$). High-resolution MS *m/z*: 495.179 (M^+, Calcd for $C_{29}H_{25}N_3O_5$: 495.180). ^{1}H-NMR (in DMSO-d_6 at 100 °C) δ: 1.56—1.79 (2H, m, C_{10}-H), 2.02—2.24 (2H, m, C_{14}-H), 2.49—3.06 (4H, m, C_{11}-H, C_{12}-H), 3.47—3.50 (1H, m, C_{13}-H), 3.66—3.70 (1H, m, C_9-H), 4.01—4.03 (1H, m, C_{4a}-H), 4.43—4.47 (1H, m, C_{4b}-H), 4.58 (1H, br s, C_{8a}-H), 4.80 (1H, d, J=8.1 Hz, C_{1a}-H), 6.01 (1H, br s, C_8-H), 7.14—7.47 (10H, m, aromatic CH). ^{13}C-NMR (in DMSO-d_6 at 100 °C) δ: 29.69, 30.89 (br s), 31.36, 32.21 (br s), 44.84, 45.72, 48.40, 49.36, 73.3, 75.7, 132.33, 132.76 (br s), 132.97, 167.18, 172.59 (br s), 174.56 (br s), 176.56 (br s). Phenyl carbons were observed in the range of δ 126.17—128.99.

Reaction of 2,3-Dimethylpyridine with *N*-Phenylmaleimide (IIa) A solution of IIa (0.01 mol) in 5 ml of 2,3-dimethylpyridine was heated at 120 °C for 6 h. After cooling, the excess 2,3-dimethylpyridine was removed under reduced pressure. The residue was purified by column chromatography on silica gel using C_6H_6–AcOEt (1 : 1) as an eluent to give crude V, which was purified by recrystallization from AcOEt to give V as colorless prisms (34% yield), mp 124—126 °C. IR (KBr): 1708 cm^{-1}. ^{1}H-NMR ($CDCl_3$) δ: 2.30 (3H, s, C_3-Me), 2.78 (1H, dd, J=4.8, 17.4 Hz, methylene proton of succinimide), 3.03 (1H, dd, J=9.4, 17.4 Hz, methylene proton of succinimide), 3.28—3.34 (1H, m, methine proton of succinimide), 3.41—3.50 (2H, m, C_2-CH_2), 7.04—7.07 (1H, m, C_4-H), 7.25—7.50 (6H, m, C_5-H and phenyl CH), 8.27—8.29 (1H, m, C_6-H). High-resolution MS *m/z*: 280.1193 (M^+, Calcd $C_{17}H_{16}N_2O_2$: 280.1212).

X-Ray Crystallography Crystal data. $C_{15}H_{20}N_2O_3$ (IIIaj): monoclinic $P2_1/n$, a=21.691 (11) Å, b=9.240 (4) Å, c=7.356 (4) Å, β=96.27 (4)°, V=1465.5 (12) Å^3, D_m=1.238 g cm^{-3} (aq. KI), D_c=1.253 g cm^{-3}, Z=4, Mo K_α radiation (40 kV, 20 mA), λ=0.7107 Å.

The cell constants were determined by a least-squares procedure using the value of the Bragg angles of 17 reflections measured on a Rigaku AFC-6 four-circle autodiffractometer equipped with a graphite-monochromated Mo K_α source, and interfaced to a PANAFACOM U-1200 minicomputer.

The space group $P2_1/n$ was selected from the number of molecules per unit cell ($Z=4$) and was later confirmed in the course of the structure refinement. Intensity data were collected in the range $2\theta<60°$ using the θ–2θ scan technique. A variable scan rate was adopted. Two reflections were monitored after measurement of every 100 reflections. Of the 3174 independent reflections, 2467 were treated as observed ($F_O>3\sigma F$). The intensities were corrected for Lorentz and polarization effects, but no correction was applied for absorption.

Structure Solution and Refinement An overall temperature factor obtained from a Wilson plot did not give the correct solution. Therefore, the value of 5.0 Å^2 was used to calculate normalized structure factor. The structure was solved by the direct method using the MULTAN78 series of programs. An E map calculated with 390 signed E's ($E>1.2$), which gave a combined figure of merit of 2.255, revealed the positions of all the expected nonhydrogen atoms. Refinements were carried out by the block-diagonal least-squares method. Six cycles of isotropic refinement and 6 cycles of anisotropic refinement led to an R index of 0.106. All the hydrogens were located at calculated positions. After adding the hydrogens and isotropic refinement for hydrogens, we obtained a final R of 0.061. Thermal parameters of the hydrogens were refined with calculated shifts damped by a factor of 0.1. In final refinements, 2099 reflections with $2\theta<55°$ were used and the following weights were applied to the observed reflections: $w=1.0$ for $F_O<20.0$, $w=400/F_O^2$ for $F_O>20.0$.

All structure-solving programs were from the Information Processing Center of Kumamoto University (Universal Crystallographic Computation Program System, UNICS III).[18]

Measurement of Visible Absorption Spectra Solutions of Ii (1 mmol/l) and IIa (1 mmol/l) in dry C_6H_6 were used for the measurement at 25 °C. The results are shown in Fig. 3.

Acknowledgement The authors wish to express their thanks to the members of the Analytical Department of the Faculty of Pharmaceutical Sciences, Kumamoto University. They are also grateful to Mr. Nakatomi, President of Hisamitsu Pharmaceutical Co., Inc., for partial financial support.

References and Notes

1) *a*) T. Matsuoka, M. Shinada, F. Suematsu, K. Harano and T. Hisano, *Chem. Pharm. Bull.*, **32**, 2077 (1984) and references cited therein; *b*) K. Harano, R. Kondo, M. Murase, T. Matsuoka and T. Hisano, *ibid.*, **34**, 966 (1986); *c*) K. Harano, F. Suematsu, T. Matsuoka and T. Hisano, *ibid.*, **32**, 543 (1984).
2) *a*) T. Matsuoka, K. Harano and T. Hisano, *Chem. Pharm. Bull.*, **31**, 2948 (1983); *b*) T. Hisano, K. Harano, T. Matsuoka, H. Yamada and M. Kurihara, *ibid.*, **35**, 1049 (1987).
3) *a*) T. Hisano, K. Harano, T. Matsuoka, S. Watanabe and T. Matsuzaki, *Chem. Pharm. Bull.*, **37**, 907 (1989); *b*) Y. Tamura, Y. Miki and M. Ikeda, *J. Chem. Soc., Perkin Trans. 1*, **1976**, 1702.
4) K. Harano, T. Matsuoka, M. Eto, T. Matsuzaki and T. Hisano, *Heterocycles*, **29**, 1029 (1989).
5) P. Main, S. E. Hull, L. Lessinger, G. Germain, J. P. Declercq and M. M. Moolfson, "MULTAN78, A System of Computer Programs for the Automatic Solution of Crystal Structure from X-Ray Diffraction Data," Univ. of York, England, 1978.
6) M. Karplus, *J. Chem. Phys.*, **30**, 11 (1959).
7) Chemical shifts of sp^3 carbons (in dimethyl sulfoxide-d_6 (DMSO-d_6), ppm): 18.3, 30.3, 34.4, 38.2, 41.2, 42.1, 50.9, 61.2, 73.1, 75.7.
8) K. Mok and M. J. Nye, *J. Chem. Soc., Perkin Trans. 1*, **1975**, 1810.
9) Concerning with the CT-complex formation, Mok and Nye[8] suggested that whether the cycloaddition does occur or not depends upon the relative stabilities of the ground state and transition state. We obtained some results which support their suggestion experimentally, *i.e.* the cycloaddition of pyridine *N*-oxides with phenyl isocyanates or *N*-phenylmaleimides proceeds, whereas that with 4-phenyl-1,2,4-triazoline-3,5-dione or tetracyanoethylene does not. In the latter cases, charge transfer might be sufficiently great that the reaction course might be altered to result in a stepwise reaction (substitution reaction) or formation of a stable CT-complex which could not transform into the corresponding cycloadduct.[1b]
10) *a*) T. Hisano, M. Ichikawa, T. Matsuoka, K. Muraoka and M. Hamana, *Org. Prep. Proced. Int.*, **13**, 409 (1981); *b*) T. Matsuoka, K. Harano, H. Kubo and T. Hisano, *Chem. Pharm. Bull.*, **34**, 572 (1986).
11) *a*) K. Fukui, "Kagaku Hanno To Densi No Kido (Chemical Reactions and Electron Orbitals)," Maruzen, Tokyo, 1976; *b*) I. Fleming, "Frontier Orbitals and Organic Chemical Reactions," John Wiley & Sons, Ltd., London, 1976, pp. 106—109.
12) M. J. S. Dewar and W. Thiel, *J. Am. Chem. Soc.*, **99**, 4899, 4907 (1977); M. J. S. Dewar and J. J. P. Stewart, "Quantum Chemistry Program Exchange (QCPE), Program No. 464," Indiana University, 1984.
13) R. Sustmann, *Tetrahedron Lett.*, **1971**, 2717, 2721.
14) Calculations on a model cycloadduct of pyridine *N*-oxide with ethylene indicate that the heat of formation (ΔH) of the 1,5-sigmatropy product is 26.7 kcal/mol smaller than that of the primary one, suggesting the primary adduct to be thermodynamically less stable.[2]
15) S. Inagaki, H. Fujimoto and K. Fukui, *J. Am. Chem. Soc.*, **98**, 4693 (1976).
16) E. Ochiai, "Aromatic Amine Oxides," Elsevier Publishing Co., Amsterdam, 1967.
17) M. P. Cava, A. A. Deana, K. Muth and M. J. Mitchell, *Org. Syn. Coll. Vol.*, **5**, 944 (1973).
18) T. Sakurai and K. Kobayashi, *Rikagaku Kenkyusho Hokoku*, **55**, 69 (1979); S. Kawano, *Koho, Comput. Center Kyushu Univ.*, **16**, 113 (1983).

Synthesis of Malabaricones, Diarylnonanoids Occurring in Myristicaceous Plants

Yoshisuke TSUDA,* Shinzo HOSOI, and Yorii GOTO

Faculty of Pharmaceutical Sciences, Kanazawa University, 13–1 Takara-machi, Kanazawa 920, Japan. *Received June 4, 1990*

Naturally occurring diarylnonanoids, malabaricones A, B, C, D, and 1-(2-hydroxy-6-methoxyphenyl)-9-(3,4-methylenedioxyphenyl)-nonan-1-one were synthesized from a common intermediate, 6-benzyloxyhexyltriphenyl phosphonium bromide, by use of the Wittig reaction and crossed aldol reaction as key steps.

Keywords malabaricone; diarylnonanoid; Myristicaceae; synthesis; 6-benzyloxyhexyltriphenyl phosphonium bromide; Wittig reaction; crossed aldol reaction; dehydration

The plants of Myristicaceae characteristically contain a group of compounds classified as diarylnonanoids (Table I), all of which are derivatives of 2,6-dihydroxyacetophenone and are considered to be biosynthesized from a phenylpropanoid and six C_2 units. Malabaricones A—D are the typical examples,[1a] and one of them (malabaricone C) was recently suggested to have significant biological activities (such as nematocidal,[1c] bacteriocidal,[2] and antioxidant[3] activities). So far, only one report on the synthesis of malabaricone A has appeared.[4] This paper describes our synthesis of the above diarylnonanoids.

Our synthetic scheme is indicated in Chart 1. We chose a hexane unit differently substituted at the two termini, *e.g.* 6-benzyloxyhexylphosphonium salt, as a common intermediate. The C–C bond formations at ① and ② followed by additional manipulations were expected to lead to the desired diarylnonanoids.

Results and Discussion

Syntheses of the Common Intermediate 5 and 7-Arylheptanols 7 Based on the results of preliminary experiments, we chose a benzyl group for protection of one terminus of hexanediol. Acetals such as an ethoxyethyl or an acetyl group were not appropriate because of their susceptibility to bromination or low selectivity in monoprotection.

1,6-Hexanediol mono-benzyl ether **2**[5] was obtained in 46% yield on mono-benzylation of 1,6-hexanediol and converted to the bromide **3** in 88% yield by *N*-bromosuccinimide and triphenylphosphine according to a known procedure[6] with some modifications. Heating of **3** with triphenylphosphine at 140 °C without solvent gave the expected phosphonium salt **4** in 75% yield.

The phosphonium salt **4** was converted to the ylide with potassium *tert*-butoxide (*tert*-BuOK) in tetrahydrofuran

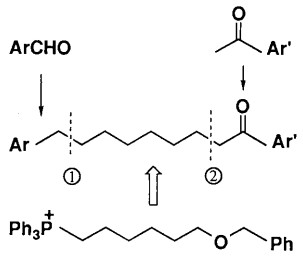

Chart 1

TABLE I. Naturally Occurring Diarylnonanoids

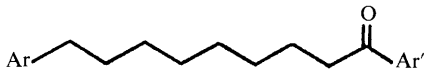

Compd.	Name	Botanical sources	References
1a	Malabaricone A	*Myristica malabarica* LAM.	1*a*)
		M. dactyloides GAERTN.	1*b*, *c*)
1b	Malabaricone B	*M. malabarica* LAM.	1*a*)
		M. dactyloides GAERTN.	1*b*, *c*)
1c	Malabaricone C	*M. malabarica* LAM.	1*a*)
		M. dactyloides GAERTN.	1*b*)
		M. fragrans HOUTT.	1*d*)
1d	Malabaricone D	*M. malabarica* LAM.	1*a*)
		M. dactyloides GAERTN.	1*b*, *c*)
1e	No name	*M. dactyloides* GAERTN.	1*b*)
1f	No name	*M. dactyloides* GAERTN.	1*c*)
1g	No name	*M. dactyloides* GAERTN.	1*c*)
1h	No name	*M. glabla* BL. (*Horsfieldia glabla* WARB.)	1*c*)

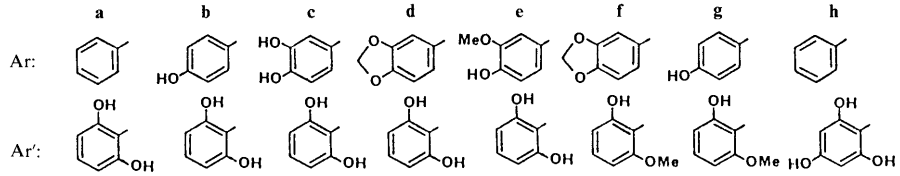

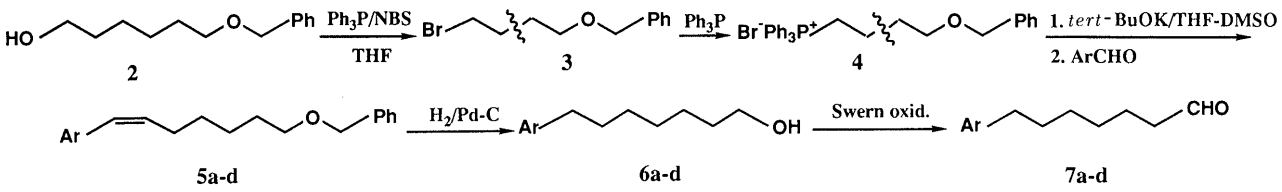

Chart 2

for **a**—**d**, see Table II

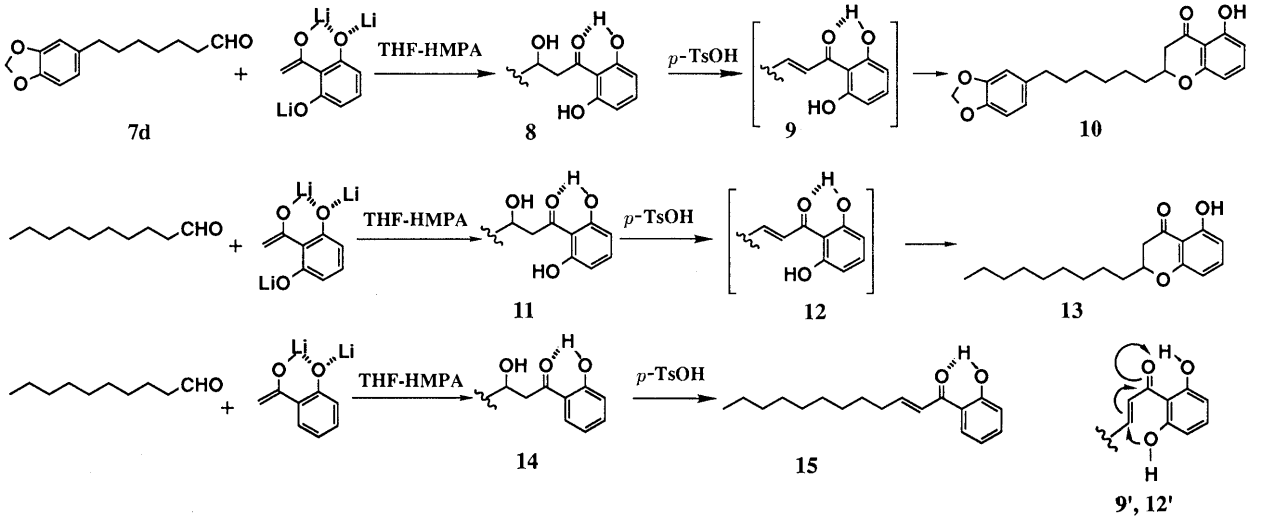

Chart 3

TABLE II. Yields in the Conversions of **4**→**5**→**6**→**7** (see Chart 2)

Ar	Yield (%)		
	4→5	5→6	6→7
a	49	93	98
b	69	85	95
c	71	83	98
d	75	92	98

Ar: for **5**—**7**

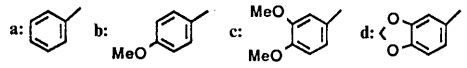

(THF)–dimethyl sulfoxide (DMSO) and allowed to react with various aromatic aldehydes to yield 7-arylheptenol benzyl ethers **5** in 50—75% yield (Table II). Sonication during the formation of the ylide increased the yields of **5**. The configurations of the olefinic moiety in **5** are mainly *Z* as evidenced from the coupling constant of $J = 11.5$ Hz[7] for the two olefinic protons in the proton nuclear magnetic resonance (^{1}H-NMR) spectra.

Hydrogenation of **5** in ethanol over 10% Pd–C gave, with concomitant hydrogenolysis of the benzyl group, the 7-arylheptanols **6** in high yields.

Synthesis of Malabaricones The 7-arylheptanol **6d** was subjected to Swern oxidation and the resulting aldehyde **7d** was coupled with the tri-anion derived from 2,6-dihydroxyacetophenone and 3 mol eq of lithium diisopropylamide (LDA) in THF–hexamethylphosphoric triamide (HMPA) to give the aldol product **8** in 38% yield. Without HMPA no aldol product was obtained.

Treatment of **8** with a catalytic amount of *p*-toluenesulfonic acid (TsOH) gave the chromanone derivative **10** (66% yield), instead of the expected conjugated ketone **9**. Model experiments of this dehydration reaction on the 2-hydroxy and 2,6-dihydroxy derivatives, **14** and **11**, revealed that the mono-phenolic compound **14** gave the expected conjugated ketone **15** smoothly, while the di-phenolic compound **11** gave the chromanone **13** exclusively on the same treatment. This indicated that one of the *ortho*-phenolic group is strongly hydrogen bonded to the carbonyl group, and therefore, although the conjugated ketones are formed by dehydration, the free phenolic hydroxy group in the 2,6-dihydroxy compounds (*e.g.* **9'** and **12'**) rapidly adds in a Michael fashion to the conjugated enone, while the hydroxy group in 2-hydroxy compounds is masked by hydrogen bonding and does not add to the conjugated enone.

Therefore the 7-arylheptanals **7** prepared by Swern oxidation of **6** were subjected to aldol condensation with the di-anion derived from 2-benzyloxy-6-hydroxyacetophenone as described above. Addition of HMPA was again necessary to obtain the products in these reactions. The resulting aldol products **16** were smoothly dehydrated to the conjugated ketones **17** as expected.

Hydrogenation of **17** in acetone (for preventing over-reduction of the carbonyl group) over 10% Pd–C gave, with concomitant hydrogenolysis of the benzyl group, the saturated 2,6-dihydroxyacetophenone derivatives **18**. Compounds **18a**, mp 78—80 °C, and **18d**, mp 91—92 °C, were identical with malabaricone A (**1a**) and malabaricone D (**1d**), respectively.

Compounds **18b** and **18c** were demethylated with boron tribromide in dichloromethane to give the phenols of mp 102—104 °C and mp 119—121 °C, which were identical with malabaricones B (**1b**) and C (**1c**), respectively.

In a similar manner, 1-(2-hydroxy-6-methoxyphenyl)-9-(3,4-methylenedioxyphenyl)nonan-1-one **18e**, mp 52—53 °C, was synthesized starting from **7d** and 2-hydroxy-6-

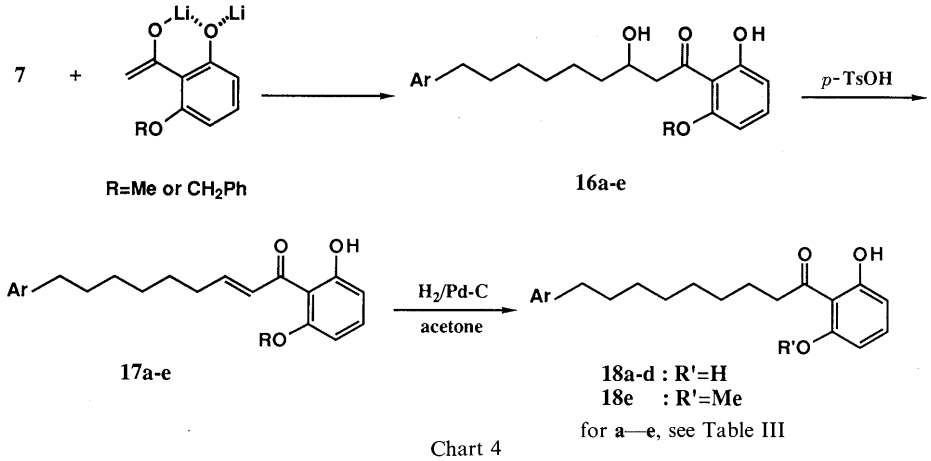

Chart 4

TABLE III. Yields in the Conversion of **7→16→17→18** (see Chart 4)

Ar	Yield (%) 7→16	16→17	17→18
a	71	86	89 (R′=H)
b	74	88	88 (R′=H)
c	73	91	88 (R′=H)
d	77	85	71 (R′=H)
e	100	90	91 (R′=Me)

	a	b	c	d	e
Ar		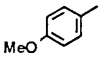	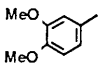		
R or R′	$PhCH_2$	$PhCH_2$	$PhCH_2$	$PhCH_2$	Me

methoxyacetophenone and was shown to be identical with a natural diarylnonanoid **1e** found in *Myristica dactyloides*.[1d]

The identities of the above synthesized diarylnonanoids with the natural compounds were confirmed by comparisons of their physical and spectral data with those reported.

Experimental

Unless otherwise stated, the following procedures were adopted. Melting points were taken on a Yanagimoto micro hot-stage melting point apparatus and are uncorrected. Infrared (IR) spectra were taken for the $CHCl_3$ solutions on a JASCO A-202 spectrometer and are given in cm^{-1}. ^{1}H-NMR spectra were taken for the $CDCl_3$ solutions on a JEOL JNM-FX100 (FT-NMR; 100 MHz) spectrometer and are given in δ (s, singlet; d, doublet; t, triplet; q, quartet; m, multiplet; br, broad). Aromatic protons indicated by ranges appeared as multiplets. Mass spectra (MS) were measured with a Hitachi H-80 mass spectrometer at an ionization voltage of 20 eV and major peaks are indicated by *m/z* (%). Ultraviolet (UV) spectra were measured in ethanol with a Hitachi 323 spectrometer and λ_{max} are given in nm (ε). Organic extracts were washed with brine, dried over anhydrous Na_2SO_4, and concentrated *in vacuo*. Column chromatography was performed on silica gel (Fuji-Davison BW-820MH).

6-Benzyloxyhexyl Bromide (3) *N*-Bromosuccinimide (9.9 g, 56 mmol) and PPh_3 (14.59 g, 56 mmol) were added to a stirred solution of 1,6-hexanediol mono-benzyl ether **2**[5] (5.78 g, 28 mmol) in THF (200 ml) in several portions at room temperature. After 2 h, the reaction mixture was concentrated to half the initial volume and diluted with hexane. The precipitate was removed by filtration and the filtrate was concentrated to leave a residue, which was chromatographed to give **3** (6.63 g, 88%) as a colorless oil. ^{1}H-NMR: 1.20—2.00 (8H), 3.35 (2H, dd, J=15, 7 Hz, $-CH_2Br$), 3.50 (2H, dd, J=15, 6 Hz, $-CH_2O-$), 4.49 (2H, s, $PhCH_2O-$), 7.32 (5H, br s, Ph-H). MS: 272 and 270 (1 : 1, each 1%) (M^+ for ^{81}Br and ^{79}Br), 92 (100).

6-Benzyloxyhexyltriphenylphosphonium Bromide (4) Compound **3** (947 mg, 3.5 mmol) and PPh_3 (917 mg, 3.5 mmol) were heated at 140 °C for 2 h. The mixture was crystallized from acetone–ether to give **4** (1.39 g, 75%) as colorless prisms, mp 125—127.5 °C. ^{1}H-NMR: 1.24—1.80 (8H), 3.42 (2H, t, J=6.5 Hz, $-OCH_2-$), 3.74 (2H, m, $-P^+CH_2-$), 4.44 (2H, s, $-OCH_2Ph$), 7.49 (5H, s, Ph-H), 7.60—7.96 (15H, Ph-H). MS: 453 ($Ph_3PP^+(CH_2)_6OCH_2Ph$, 1), 262 (100). *Anal.* Calcd for $C_{31}H_{34}BrOP$: C, 69.54; H, 6.46. Found: C, 69.79; H, 6.42.

(*Z*)-1-Benzyloxy-7-arylhept-6-enes (5) (General Procedure) An aromatic aldehyde (10.5 mmol) in THF (5 ml) was added dropwise to a stirred solution of the ylide [9.5 mmol, prepared from *tert*-BuOK and **4** in THF–DMSO (25 : 1, 165 ml)] under an Ar atmosphere and the mixture was stirred for an additional 50 min with occasional sonication at room temperature. The reaction mixture was poured into ice-water, acidified with HCl and extracted with $CHCl_3$. Chromatography of the residue from the $CHCl_3$ extract gave the corresponding arylheptenol benzyl ether **5** in the yield indicated in Table II. The products were used directly for hydrogenation. The spectral data are as follows.

(*Z*)-1-Benzyloxy-7-phenylhept-6-ene (**5a**): This was prepared from **4** and benzaldehyde as a yellow oil. ^{1}H-NMR: 1.20—1.80 (6H), 2.19 (2H, m, $=CHCH_2-$), 3.45 (2H, t, J=6.3 Hz, $-CH_2O-$), 4.49 (2H, s, $-OCH_2Ph$), 5.59 (1H, dt, J=11.5, 7 Hz, $PhCH=CH-$), 6.38 (1H, d, J=11.5 Hz, $PhCH=CH-$), 7.08—7.38 (10H, Ph-H). MS: 280 (M^+, 2), 91 (100).

(*Z*)-1-Benzyloxy-7-(4-methoxyphenyl)hept-6-ene (**5b**): This was prepared from **4** and 4-methoxybenzaldehyde as a yellow oil. ^{1}H-NMR: 1.20—1.80 (6H), 2.28 (2H, m, $=CHCH_2-$), 3.45 (2H, t, J=6.3 Hz, $-CH_2O-$), 3.78 (3H, s, OCH_3), 4.47 (2H, s, $PhCH_2O-$), 5.55 (1H, dt, J=11.5, 7.5 Hz, $ArCH=CH-$), 6.34 (1H, br d, J=11.5 Hz, $ArCH=CH-$), 6.82, 7.18 (each 2H, d, J=8 Hz, ArH), 7.30 (5H, br s, Ph-H). MS: 310 (M^+, 37), 121 (100).

(*Z*)-1-Benzyloxy-7-(3,4-dimethoxyphenyl)hept-6-ene (**5c**): This was prepared from **4** and 3,4-dimethoxybenzaldehyde as a yellow oil. ^{1}H-NMR: 1.29—1.76 (6H), 2.30 (2H, m, $=CHCH_2-$), 3.45 (2H, t, J=6.3 Hz, $-CH_2O-$), 3.86 (6H, s, $2\times OCH_3$), 4.48 (2H, s, $PhCH_2O-$), 5.55 (1H, dt, J=11.5, 7.5 Hz, $ArCH=CH-$), 6.33 (1H, br d, J=11.5 Hz, $ArCH=CH-$), 7.25 (3H, br s, ArH), 7.31 (5H, br s, Ph-H). MS: 340 (M^+, 60), 151 (100).

(*Z*)-1-Benzyloxy-7-(3,4-methylenedioxyphenyl)hept-6-ene (**5d**): This was prepared from **4** and piperonal as a yellow oil. ^{1}H-NMR: 1.12—1.80 (6H), 1.92—2.45 (2H, m, $=CHCH_2-$), 3.45 (2H, t, J=6.3 Hz, $-CH_2O-$), 4.48 (2H, s, $-OCH_2Ph$), 5.52 (1H, dt, J=11.5, 6.5 Hz, $ArCH=CH-$), 5.93 (2H, s, $-OCH_2O-$), 6.28 (1H, dt, J=11.5, 2 Hz, $ArCH=CH-$), 6.58—6.86 (3H, ArH), 7.30 (5H, br s, Ph-H). MS: 324 (M^+, 29), 135 (100).

7-Arylheptanols 6 (General Procedure) One of compounds **5** (6.5 mmol) in ethanol (50 ml) was hydrogenated over 10% Pd–C (0.8 g) at room temperature under hydrogen pressure of 4 kg/cm^2 for 24 h. Removal of the catalyst and the solvent from the mixtue left an oil which was purified by chromatography to give the corresponding arylheptanol **6** in the yield indicated in Table II.

7-Phenylheptanol (**6a**): Colorless oil. IR: 3620. ^{1}H-NMR: 1.18—1.76 (10H), 2.60 (2H, t, J=7.8 Hz, $PhCH_2-$), 3.62 (2H, t, J=6.3 Hz, $-CH_2OH$), 7.04—7.36 (5H, Ph-H). MS: 192 (M^+, 26), 104 (100). High resolution mass spectra (HRMS) *m/z* (M^+): Calcd for $C_{13}H_{20}O$: 192.1513. Found: 192.1522.

7-(4-Methoxyphenyl)heptanol (**6b**): Colorless solid, mp <30 °C. IR: 3620. ^{1}H-NMR: 1.12—1.76 (10H), 2.54 (2H, t, J=7.8 Hz, $ArCH_2-$), 3.60 (2H, br s, $-CH_2OH$), 6.75, 7.08 (each 2H, d, J=8.5 Hz, ArH). MS: 222 (M^+, 91), 121 (100). HRMS *m/z* (M^+): Calcd for $C_{14}H_{22}O_2$: 222.1619.

Found: 222.1610.

7-(3,4-Dimethoxyphenyl)heptanol (**6c**): Colorless oil. IR: 3620. ^{1}H-NMR: 1.20—1.76 (10H), 2.56 (2H, t, J=7.8 Hz, $ArCH_2$–), 3.64 (2H, t, J=6.3 Hz, –C$\underline{H}_2$OH), 3.86 (6H, s, 2 × OCH_3), 6.60—6.84 (3H, ArH). MS: 252 (M^+, 46), 151 (100). HRMS m/z (M^+): Calcd for $C_{15}H_{24}O_3$: 252.1727. Found: 252.1719.

7-(3,4-Methylenedioxyphenyl)heptanol (**6d**): Colorless oil. IR: 3620. ^{1}H-NMR: 1.08—1.76 (10H), 2.52 (2H, t, J=7.8 Hz, $ArCH_2$–), 3.60 (2H, t, J=6.3 Hz, –C$\underline{H}_2$OH), 5.93 (2H, s, –OCH_2O–), 6.48—6.80 (3H, ArH). MS: 236 (M^+, 55), 135 (100). HRMS m/z (M^+): Calcd for $C_{14}H_{20}O_3$: 236.1411. Found: 236.1405.

7-Arylheptanals 7 (General Procedure) A 7-arylheptanol (0.79 mmol) in CH_2Cl_2 (3 ml) was added to a stirred solution of DMSO (0.15 ml) and oxalyl chloride (0.16 ml) in CH_2Cl_2 (2 ml) at −78 °C. After 15 min, Et_3N (0.45 ml) was added and stirring was continued at −78 °C for 5 min, then at room temperature for 20 min. The reaction mixture was diluted with CH_2Cl_2, washed with 1 N HCl, and concentrated. Chromatography of the product gave the corresponding 7-arylheptanal **7** in the yield indicated in Table II. These compounds gave the following spectral data, and were used for the next step without further characterization.

7-Phenylheptanal (**7a**): Colorless oil. IR: 1720. ^{1}H-NMR: 1.05—1.81 (8H), 2.39 (2H, td, J=7.5, 2 Hz, –CH_2CHO), 2.59 (2H, t, J=7.5 Hz, $PhCH_2$–), 6.85—7.35 (5H, Ph-H), 9.70 (1H, t, J=2 Hz, –CHO). MS: 190 (M^+, 100).

7-(4-Methoxyphenyl)heptanal (**7b**): Colorless oil. IR: 1720. ^{1}H-NMR: 1.14—1.78 (8H), 2.40 (2H, td, J=7.5, 2 Hz, –C$\underline{H}_2$CHO), 2.54 (2H, t, J=7.5 Hz, $ArCH_2$–), 3.78 (3H, s, OCH_3), 6.78, 7.06 (each 2H, d, J=8 Hz, ArH), 9.75 (1H, t, J=2 Hz, –CHO). MS: 220 (M^+, 27), 121 (100).

7-(3,4-Dimethoxyphenyl)heptanal (**7c**): Colorless oil. IR: 1717. ^{1}H-NMR: 1.18—1.86 (8H), 2.40 (2H, td, J=7.5, 2 Hz, –C$\underline{H}_2$CHO), 2.54 (2H, t, J=7.5 Hz, $ArCH_2$–), 3.85, 3.87 (each 3H, s, 2 × OCH_3), 6.50—6.82 (3H, ArH), 9.74 (1H, t, J=2 Hz, –CHO). MS: 250 (M^+, 36), 151 (100).

7-(3,4-Methylenedioxyphenyl)heptanal (**7d**): Colorless oil. IR: 1722. ^{1}H-NMR: 1.04—1.80 (8H), 2.43 (2H, td, J=7.5, 2 Hz, –C$\underline{H}_2$CHO), 2.52 (2H, t, J=7.5 Hz, $ArCH_2$–), 5.90 (2H, s, –OCH_2O–), 6.55—6.76 (3H, ArH), 9.75 (1H, t, J=2 Hz, –CHO). MS: 234 (M^+, 80), 135 (100).

Benzylation of 2,6-Dihydroxyacetophenone 2,6-Dihydroxyacetophenone (0.5 g, 3.3 mmol) and NaH (131 mg, 3.3 mmol) in DMSO (10 ml) were stirred at room temperature for 10 min. Benzyl bromide (0.4 ml, 3.4 mmol) was added and stirring was continued for 1 h. The reaction mixture was poured into cold 1 N HCl and extracted with CH_2Cl_2. Chromatography of the product gave 2-benzyloxy-6-hydroxyacetophenone (610 mg, 76%), mp 109—110 °C, as yellow needles from benzene–ether. ^{1}H-NMR: 2.59 (3H, s, CH_3), 5.09 (2H, s, –OCH_2Ph), 6.44 (1H, d, J=8 Hz, ArH), 6.56 (1H, d, J=8 Hz, ArH), 7.30 (1H, t, J=8 Hz, ArH), 7.39 (5H, br s, Ph-H), 13.25 (1H, s, OH). MS: 242 (M^+). 2,6-Dibenzyloxyacetophenone (130 mg, 12%) was also obtained as a yellow gum. ^{1}H-NMR: 2.49 (3H, s, CH_3), 5.07 (4H, s, –OCH_2Ph × 2), 6.59 (2H, d, J=8 Hz, ArH), 7.10—7.35 (11H, Ph-H and ArH). MS: 332 (M^+), 91 (100).

Condensation of 2,6-Dihydroxyacetophenone with Decanal and Dehydration of the Product [8-Hydroxy-2-nonylchroman-4-one (13)] 2,6-Dihydroxyacetophenone (0.5 g, 3.19 mmol) in THF (6 ml) was added dropwise to a solution of LDA (10 mmol) in THF (5 ml) over 5 min at −78 °C under an Ar atmosphere and the mixture was stirred for 15 min. A solution of n-decanal (0.66 ml, 3.5 mmol) and HMPA (1.8 ml, 10 mmol) in THF (6 ml) was added, and the reaction mixture was stirred at −78 °C for 50 min, and at 0 °C for 1 h, then poured into cold 10% HCl and extracted with AcOEt. Work-up of the extract gave an aldol (**11**, 263 mg). A solution of the aldol **11** and p-TsOH (134 mg, 0.7 mmol) in benzene (10 ml) was heated under reflux for 45 min. The cooled mixture was washed with saturated aqueous $NaHCO_3$, and concentrated. Chromatography of the residue gave the chromanone **13** (270 mg, 28% from 2,6-dihydroxyacetophenone) as a yellow oil. IR: 1641, 1626, 1573. ^{1}H-NMR: 0.88 (3H, br t, J=7 Hz, CH_3), 1.28 (16H, br s), 2.72 (2H, m, –CH_2CO–), 4.34 (1H, m, >CHO–), 6.36 (1H, dd, J=8, 1 Hz, ArH), 6.44 (1H, dd, J=8, 1 Hz, ArH), 7.32 (1H, t, J=8 Hz, ArH). MS: 290 (M^+, 12), 137 (100). HRMS m/z (M^+): Calcd for $C_{18}H_{26}O_3$: 290.1883. Found: 290.1889.

Condensation of o-Hydroxyacetophenone with Decanal and Dehydration of the Product [1-(2-Hydroxyphenyl)-2-dodecen-1-one (15)] o-Hydroxyacetophenone (1.13 g, 8.3 mmol) in THF (5 ml) was added dropwise to a solution of LDA (17.6 mmol) in THF (10 ml) over 5 min at −78 °C under an Ar atmosphere, and the mixture was stirred for 30 min. n-Decanal (1.7 ml, 9 mmol) in THF (8 ml) and HMPA (3.2 ml, 18.4 mmol) was added to this solution and the mixture was stirred for a further 1 h. Work-up of the reaction mixture as described above gave an aldol (**14**, 203 mg). The aldol **14** and p-TsOH (158 mg, 0.83 mmol) in benzene (20 ml) was heated under reflux for 4 h. Work-up of the mixture gave, after chromatography, the enone **15** (2 g, 88% from o-hydroxyacetophenone) as a yellow oil. IR: 1643, 1615, 1585. ^{1}H-NMR: 0.88 (3H, br t, J=7 Hz, CH_3), 1.00—1.50 (14H), 2.31 (2H, dt, J=6, 6.6 Hz, =$CHCH_2$–), 6.86 (1H, t, J=8 Hz, ArH), 6.96 (1H, d, J=8 Hz, ArH), 6.96 (1H, d, J=15 Hz, –COC$\underline{H}$=CH–), 7.20 (1H, dt, J=15, 6 Hz, –COCH=C$\underline{H}$–), 7.43 (1H, t, J=8 Hz, ArH), 7.76 (1H, d, J=8 Hz, ArH), 12.74 (1H, s, OH). MS: 274 (M^+, 6), 140 (100). HRMS m/z (M^+): Calcd for $C_{18}H_{26}O_2$: 274.1934. Found: 274.1934.

Condensation of 7-Arylheptanals (7) with 2-Benzyloxy-6-hydroxyacetophenone (General Procedure) 2-Benzyloxy-6-hydroxyacetophenone (0.58 mmol) in THF (4 ml) was added dropwise to a solution of LDA (2 mmol) in THF (3 ml) over 5 min at −78 °C under an Ar atmosphere and the mixture was stirred for 2 h. After addition of HMPA (0.5 ml), a 7-arylheptanal **7** (0.58 mmol) in THF (4 ml) was added dropwise to the above mixture over 5 min. The whole was stirred at −78 °C for 1 h, and at −15 °C for 30 min, then poured into cold 1 N HCl and extracted with $CHCl_3$. Work-up of the extract gave, on chromatography the corresponding aldol **16** in the yield indicated in Table III.

1-(2-Benzyloxy-6-hydroxyphenyl)-3-hydroxy-9-phenylnonan-1-one (**16a**): Pale yellow prisms (from hexane–ether), mp 59—60 °C. IR: 1619, 1594. ^{1}H-NMR: 0.96—1.80 (10H), 2.60 (2H, t, J=8 Hz, $PhCH_2$–), 2.93 (1H, dd, J=18, 9 Hz) and 3.18 (1H, dd, J=18, 3 Hz) (–CH_2CO–), 4.02 (1H, m, >C$\underline{H}$OH), 5.07 (2H, s, $PhCH_2O$–), 6.42 (1H, d, J=8 Hz, ArH), 6.56 (1H, d, J=8 Hz, ArH). 7.00—7.48 (11H, ArH and Ph-H). MS: 432 (M^+, 6), 91 (100). HRMS m/z (M^+): Calcd for $C_{28}H_{32}O_4$: 432.2302. Found: 432.2292.

1-(2-Benzyloxy-6-hydroxyphenyl)-3-hydroxy-9-(4-methoxyphenyl)-nonan-1-one (**16b**): Pale yellow prisms (from hexane–ether), mp 40—41 °C. IR: 1618, 1593. ^{1}H-NMR: 0.92—1.60 (10H), 2.46 (2H, t, J=8 Hz, $ArCH_2$–), 2.87 (1H, dd, J=14, 8.5 Hz) and 3.13 (1H, dd, J=14, 3 Hz) (–CH_2CO–), 3.69 (3H, s, OCH_3), 3.96 (1H, m, >C$\underline{H}$OH), 4.99 (2H, s, $PhCH_2O$–), 6.38 (1H, dd, J=8, 1 Hz, ArH), 6.50 (1H, dd, J=8, 1 Hz, ArH), 6.73, 7.01 (each 2H, d, J=9.5 Hz, ArH), 7.10—7.42 (6H, Ph-H and ArH). MS: 462 (M^+, 2), 121 (100). HRMS m/z (M^+): Calcd for $C_{29}H_{34}O_5$: 462.2407. Found: 462.2386.

1-(2-Benzyloxy-6-hydroxyphenyl)-3-hydroxy-9-(3,4-dimethoxyphenyl)nonan-1-one (**16c**): Pale yellow prisms (from hexane–ether), mp 73—75 °C. IR: 1625, 1600. ^{1}H-NMR: 1.00—1.76 (10H), 2.55 (2H, t, J=8 Hz, $ArCH_2$–), 2.95 (1H, dd, J=18, 8 Hz) and 3.18 (1H, dd, J=18, 3 Hz) (–CH_2CO–), 3.84, 3.86 (each 3H, s, 2 × OCH_3), 4.04 (1H, m, >C$\underline{H}$OH), 5.07 (2H, s, $PhCH_2O$–), 6.43 (1H, dd, J=8, 1 Hz, ArH), 6.56 (1H, dd, J=8, 1 Hz, ArH), 6.60—6.80 (3H, ArH), 7.16—7.44 (6H, Ph-H and ArH). MS: 492 (M^+, 4), 91 (100). HRMS m/z (M^+): Calcd for $C_{30}H_{36}O_6$: 492.2513. Found: 492.2517.

1-(2-Benzyloxy-6-hydroxyphenyl)-3-hydroxy-9-(3,4-methylenedioxyphenyl)nonan-1-one (**16d**): Pale yellow prisms (from benzene–ether), mp 89—90 °C. IR: 1619, 1594. ^{1}H-NMR: 1.00—1.88 (10H), 2.51 (2H, t, J=7.8 Hz, $ArCH_2$–), 2.90 (1H, br s, OH), 2.97 (1H, dd, J=18.5, 8.5 Hz) and 3.22 (1H, dd, J=18.5, 3 Hz) (–CH_2CO–), 4.02 (1H, m, >C$\underline{H}$OH), 5.08 (2H, s, –OCH_2Ph), 5.89 (2H, s, –OCH_2O–), 6.42—6.77 (5H, ArH), 7.27—7.43 (6H, ArH and Ph-H), 13.03 (1H, s, OH). MS: 476 (M^+, 13), 91 (100). HRMS m/z (M^+): Calcd for $C_{29}H_{32}O_6$: 476.2200. Found: 476.2220.

1-(2-Hydroxy-6-methoxyphenyl)-3-hydroxy-9-(3,4-methylenedioxyphenyl)nonan-1-one (**16e**): Compound **16e** (100%) was prepared from **7d** and 6-hydroxy-2-methoxyacetophenone, as described for the corresponding benzyl ether, as pale yellow prisms (from hexane–ether), mp 85—86 °C. IR: 1619, 1595. ^{1}H-NMR: 1.16—1.80 (10H), 2.52 (2H, t, J=7.5 Hz, $PhCH_2$–), 3.05 (1H, dd, J=18, 8 Hz) and 3.29 (1H, dd, J=18, 4 Hz) (–CH_2CO–), 3.88 (3H, s, OCH_3), 4.12 (1H, m, C$\underline{H}$OH), 5.89 (2H, s, –OCH_2O–), 6.39 (1H, d, J=8 Hz, ArH), 6.52—6.80 (3H, ArH), 6.54 (1H, d, J=8 Hz, ArH), 7.28 (1H, t, J=8 Hz, ArH). MS: 400 (M^+, 23), 135 (100). HRMS m/z (M^+): Calcd for $C_{23}H_{28}O_6$: 400.1886. Found: 400.1891.

1-(2,6-Dihydroxyphenyl)-3-hydroxy-9-(3,4-methylenedioxyphenyl)nonan-1-one (8) Compound **8** was prepared from **7d** and 2,6-dihydroxyacetophenone in the manner described for the preparation of the monobenzyl derivative with the use of 4 mol eq of LDA, in the yield of 38%, as a yellow oil. IR: 3350, 1641, 1625. ^{1}H-NMR: 1.12—1.80 (10H), 2.51 (2H, t, J=7.8 Hz, $ArCH_2$–), 3.06 (1H, dd, J=12, 4 Hz) and 3.40 (1H, dd, J=12, 9 Hz) (–CH_2CO–), 4.22 (1H, m, >C$\underline{H}$OH), 5.90 (2H, s, –OCH_2O–), 6.40 (2H, d, J=8 Hz, ArH), 6.48—6.76 (3H, ArH), 7.30 (1H, t, J=8 Hz, ArH). MS: 386 (M^+, 1), 135 (100). HRMS m/z (M^+): Calcd for $C_{22}H_{26}O_6$: 386.1730. Found: 386.1723.

Dehydration of the Aldol 8 The aldol **8** (90 mg, 0.23 mmol) and p-TsOH

(5 mg, 0.02 mmol) in benzene (10 ml) were heated under reflux for 3.5 h, and the mixture was worked up as described below to give the chromanone **10** (58 mg, 66%) as a yellow oil. IR: 3200, 1627, 1600. ^{1}H-NMR: 1.12—1.92 (10H), 2.53 (2H, t, J=7.6 Hz, $ArCH_2$–), 2.68 (2H, m, –CH_2CO–), 4.28 (1H, m, >CHO–), 5.90 (2H, s, –OCH_2O–), 6.32—6.46 (2H, ArH), 6.48—6.78 (3H, ArH), 7.38 (1H, d, J=8 Hz, ArH). MS: 368 (M^+, 90), 163 (100). HRMS m/z (M^+): Calcd for $C_{22}H_{24}O_5$: 368.1624. Found: 368.1627.

Dehydration of the Aldols 16 (General Procedure) One of the aldols **16** (0.65 mmol) and *p*-TsOH (0.11 mmol) in benzene (10 ml) were heated under reflux for 1 h. The mixture was cooled, washed with saturated aqueous $NaHCO_3$, and concentrated. Chromatography of the residue gave the corresponding enone **17** in the yield indicated in Table III.

1-(2-Benzyloxy-6-hydroxyphenyl)-9-phenyl-2-nonen-1-one (**17a**): Yellow oil. IR: 1637, 1611, 1575. ^{1}H-NMR: 1.06—1.74 (8H), 2.02 (2H, m, –CH_2CH=), 2.59 (2H, t, J=7.5 Hz, $PhCH_2$–), 5.08 (2H, s, $PhCH_2O$–), 6.52 (1H, dd, J=8, 1 Hz, ArH), 6.60 (1H, dd, J=8, 1 Hz, ArH), 6.78—7.46 (11H, ArH, Ph-H, and –CH=CHCO–). MS: 414 (M^+, 5), 91 (100). HRMS m/z (M^+): Calcd for $C_{28}H_{30}O_3$: 414.2196. Found: 414.2219.

1-(2-Benzyloxy-6-hydroxyphenyl)-9-(4-methoxyphenyl)-2-nonen-1-one (**17b**): Yellow oil. IR: 1637, 1609, 1575. ^{1}H-NMR: 0.98—1.62 (8H), 1.96 (2H, m, –CH_2CH=), 2.45 (2H, t, J=8 Hz, $ArCH_2$–), 3.69 (3H, s, OCH_3), 5.01 (2H, s, $PhCH_2O$–), 6.39 (1H, dd, J=8, 1 Hz, ArH), 6.52 (1H, dd, J=8, 1 Hz, ArH), 6.73, 6.99 (each 2H, d, J=8 Hz, ArH), 7.00—7.42 (8H, ArH, Ph-H, and –CH=CHCO–). MS: 444 (M^+, 13), 91 (100). HRMS m/z (M^+): Calcd for $C_{29}H_{32}O_4$: 444.2266. Found: 444.2273.

1-(2-Benzyloxy-6-hydroxyphenyl)-9-(3,4-dimethoxyphenyl)-2-nonen-1-one (**17c**): Yellow prisms (from hexane–ether), mp 50—53 °C. IR : 1640, 1615, 1580. ^{1}H-NMR: 1.04—1.72 (8H), 2.04 (2H, m, –CH_2CH–), 2.52 (2H, t, J=8 Hz, $ArCH_2$–), 3.84, 3.86 (each 3H, s, 2×OCH_3), 5.09 (2H, s, $PhCH_2$–), 6.44 (1H, d, J=8 Hz, ArH), 6.56 (1H, d, J=8 Hz, ArH), 6.62—6.88 (3H, ArH), 6.88—7.52 (8H, –CH=CHCO–, ArH, and Ph-H). MS: 474 (M^+, 38), 91 (100). HRMS m/z (M^+): Calcd for $C_{30}H_{34}O_5$: 474.2407. Found: 474.2401.

1-(2-Benzyloxy-6-hydroxyphenyl)-9-(3,4-methylenedioxyphenyl)-2-nonen-1-one (**17d**): Yellow oil. IR: 1639, 1611, 1576. ^{1}H-NMR: 1.12—1.72 (8H), 2.04 (2H, m, –CH_2CH=), 2.51 (2H, t, J=7.8 Hz, $ArCH_2$–), 5.10 (2H, s, $PhCH_2O$–), 5.90 (2H, s, –OCH_2O–), 6.44 (1H, dd, J=8, 1 Hz, ArH), 6.56 (1H, dd, J=8, 1 Hz, ArH), 6.58—6.74 (3H, ArH), 6.80—7.50 (8H, ArH, Ph-H, and –CH=CHCO–). MS: 458 (M^+, 3), 91 (100). HRMS m/z (M^+): Calcd for $C_{29}H_{30}O_5$: 458.2029. Found: 458.2082.

1-(2-Hydroxy-6-methoxyphenyl)-9-(3,4-methylenedioxyphenyl)-2-nonen-1-one (**17e**): Yellow oil. IR: 1637, 1611, 1577. ^{1}H-NMR: 1.20—1.76 (8H), 2.28 (2H, m, –CH_2CH=), 2.52 (2H, t, J=7.5 Hz, $ArCH_2$–), 3.88 (3H, s, OCH_3), 5.90 (2H, s, –OCH_2O–), 6.52 (1H, dd, J=8, 1 Hz, ArH), 6.56 (1H, dd, J=8, 1 Hz, ArH), 6.56—6.74 (3H, ArH), 7.00 (1H, dt, J=15, 6 Hz, –CH=CHCO–), 7.16 (1H, d, J=15 Hz, –CH=CHCO–), 7.30 (1H, t, J=8 Hz, ArH). MS: 382 (M^+, 19), 177 (100). HRMS m/z (M^+): Calcd for $C_{23}H_{26}O_5$: 382.1781. Found: 382.1754.

Hydrogenation of the Enones 17 (General Procedure) A solution of an enone **17** (0.11 mmol) in acetone (20 ml) was hydrogenated over 10% Pd–C (50 mg) at room temperature under a hydrogen atmosphere at a pressure of 3.5 kg/cm^2 for 6 h. Removal of the catalyst and the solvent from the reaction mixture provided a residue, which was purified by chromatography to give **18** in the yield indicated in Table III.

1-(2,6-Dihydroxyphenyl)-9-phenylnonan-1-one (Malabaricone A) [**18a** (=**1a**)]: Pale yellow prisms (from hexane–ether), mp 78—80 °C (lit. 81—82 °C).[1a] IR: 3350, 1626, 1599. ^{1}H-NMR: 1.06—1.82 (12H), 2.60 (2H, t, J=7.5 Hz, $PhCH_2$–), 3.12 (2H, d, J=7.5 Hz, –CH_2CO–), 6.37 (2H, d, J=8 Hz, ArH), 6.98—7.36 (6H, ArH and Ph-H), 9.78 (1H, br s, OH). MS: 326 (M^+, 21), 137 (100). *Anal.* Calcd for $C_{21}H_{26}O_3$: C, 77.27; H, 8.03. Found: C, 77.13; H, 8.27. The data were identical with these reported for malabaricone A.[1a]

1-(2,6-Dihydroxyphenyl)-9-(4-methoxyphenyl)nonan-1-one (**18b**): Yellow prisms (from hexane–ether), mp 78—80 °C. IR: 3300, 1626, 1605. ^{1}H-NMR: 1.08—1.80 (12H), 2.52 (2H, t, J=7.5 Hz, $ArCH_2$–), 3.10 (2H, t, J=8 Hz, –CH_2CO–), 3.76 (3H, s, OCH_3), 6.34 (2H, d, J=8 Hz, ArH), 6.78, 7.04 (each 2H, d, J=8 Hz, ArH), 7.20 (1H, t, J=8 Hz, ArH). MS: 356 (M^+, 46), 121 (100). HRMS m/z (M^+): Calcd for $C_{22}H_{28}O_4$: 356.1988. Found: 356.1986.

1-(2,6-Dihydroxyphenyl)-9-(3,4-dimethoxyphenyl)nonan-1-one (**18c**): Pale yellow prisms (from benzene), mp 128—130 °C. IR: 3300, 1635, 1605. ^{1}H-NMR: 1.12—1.88 (12H), 2.55 (2H, t, J=7.5 Hz, $ArCH_2$–), 3.15 (2H, t, J=7.5 Hz, –CH_2CO–), 3.83, 3.85 (each 3H, s, 2×OCH_3), 6.38 (2H, d, J=8 Hz, ArH), 6.56—6.86 (3H, ArH), 7.16 (1H, t, J=8 Hz, ArH). MS: 386 (M^+, 79), 151 (100). HRMS m/z (M^+): Calcd for $C_{23}H_{30}O_5$: 386.2094. Found: 386.2096.

1-(2,6-Dihydroxyphenyl)-9-(3,4-methylenedioxyphenyl)nonan-1-one (Malabaricone D) [**18d** (=**1d**)]: Yellow prisms (from benzene–hexane), mp 90.5—92 °C (lit. 90—91 °C).[1a] UV: 225 (16300), 274 (13300), 345 (2600). IR ($CDCl_4$): 3591, 1633, 1605. ^{1}H-NMR: 1.08—1.88 (12H), 2.52 (2H, t, J=7.6 Hz, $ArCH_2$–), 3.12 (2H, t, J=7.6 Hz, –CH_2CO–), 5.90 (2H, s, –OCH_2O–), 6.37 (2H, d, J=8 Hz, ArH), 6.56—6.78 (3H, ArH), 7.21 (1H, t, J=8 Hz, ArH), 9.50 (2H, s, OH). MS: 370 (M^+, 100). *Anal.* Calcd for $C_{22}H_{26}O_5$: C, 71.35; H, 7.00. Found: C, 71.08; H, 7.17. The data were identical with those reported for malabaricone D.[1a]

1-(2-Hydroxy-6-methoxyphenyl)-9-(3,4-methylenedioxyphenyl)-nonan-1-one [(**18e** (=**1f**)]: Pale yellow prisms (from chloroform–methanol), mp 52—53 °C (lit. 51—52 °C).[1c] IR: 1619, 1595. ^{1}H-NMR: 1.12—1.88 (12H), 2.52 (2H, t, J=7.5 Hz, $ArCH_2$–), 3.03 (2H, t, J=7.5 Hz, –CH_2CO–), 3.88 (3H, s, OCH_3), 5.90 (2H, s, –OCH_2O–), 6.38 (1H, dd, J=8, 1 Hz, ArH), 6.58 (1H, dd, J=8, 1 Hz, ArH), 6.56—6.80 (3H, ArH), 7.32 (1H, t, J=8 Hz, ArH). MS: 384 (M^+, 63), 151 (100). *Anal.* Calcd for $C_{23}H_{29}O_5$: C, 71.85; H, 7.34. Found: C, 71.41; H, 7.59. The data were identical with those reported for the corresponding natural product by Kumar *et al.*[1c]

1-(2,6-Dihydroxyphenyl)-9-(4-hydroxyphenyl)nonan-1-one (Malabaricone B) (1b) Boron tribromide (110 mg, 0.44 mmol) was added to a stirred solution of **18b** (27 mg, 0.078 mmol) in CH_2Cl_2 (8 ml) at 0 °C, and the mixture was allowed to warm to room temperature, then stirred for 20 min, poured into ice-water and extracted with AcOEt. Chromatography of the residue obtained by evaporation of the extract gave **1b** (25 mg, 96%) as pale yellow prisms (from benzene), mp 102—104 °C (lit. 102 °C).[1a] IR: 3300 br, 1626, 1604. ^{1}H-NMR: 1.00—1.88 (12H), 2.51 (2H, t, J=7 Hz, $ArCH_2$–), 3.15 (2H, t, J=7 Hz, –$COCH_2$–), 6.36 (2H, d, J=8 Hz, ArH), 6.68, 7.00 (each 2H, d, J=8 Hz, ArH), 7.19 (1H, t, J=8 Hz, ArH). MS: 342 (M^+, 40), 137 (100). *Anal.* Calcd for $C_{21}H_{26}O_4$: C, 73.66; H, 7.65. Found: C, 73.48; H, 7.75. The data were identical with those reported for malabaricone B.[1a]

1-(2,6-Dihydroxyphenyl)-9-(3,4-dihydroxyphenyl)nonan-1-one (Malabaricone C) (1c) Boron tribromide (93 mg, 0.37 mmol) was added to a stirred solution of **18c** (20 mg, 0.052 mmol) in CH_2Cl_2 (7 ml), at 0 °C, and the mixture was allowed to warm to room temperature, then stirred for 10 min, poured into ice-water and extracted with AcOEt. The organic layer was washed, dried, and passed through a column of polyamide (Woelm, for thin layer chromatography), then the column was washed with the same solvent. Elution of the column with methanol yielded a crude product which was purified by chromatography on a Sephadex LH-20 (Pharmacia Fine Chemical) column with methanol to give **1c** (18 mg, 97%) as pale yellow prisms from benzene, mp 119—121 °C (lit. 125—126 °C).[1d] IR: 1631, 1607. ^{1}H-NMR ($CDCl_3$+CD_3OD): 1.08—1.88 (12H), 2.46 (2H, t, J=7.5 Hz, $ArCH_2$–), 3.13 (2H, t, J=7.5 Hz, –$COCH_2$–), 6.35 (2H, d, J=8 Hz, ArH), 6.46 (1H, dd, J=8, 1.5 Hz, ArH), 6.60 (1H, d, J=1.5 Hz, ArH), 6.66 (1H, d, J=8 Hz, ArH), 7.16 (1H, t, J=8 Hz, ArH). MS: 358 (M^+, 66), 137 (100). *Anal.* Calcd for $C_{21}H_{26}O_5$: C, 70.37; H, 7.31. Found: C, 70.54; H, 7.54. This was identical with malabaricone C as confirmed by direct comparisons with an authentic sample.[1d]

References and Notes

1) *a*) K. K. Purushothaman, A. Sarada, and J. D. Connolly, *J. Chem. Soc., Perkin Trans. 1*, **1977**, 587; *b*) N. F. Cooray, E. R. Jansz, S. Wimalasena, J. P. Wijesekera, and B. M. Nair, *Phytochemistry*, **26**, 3369 (1987); *c*) N. S. Kumar, H. M. T. B. Herath, and V. Karunaratne, *ibid.*, **27**, 465 (1988); *d*) N. Nakamura, F. Kiuchi, Y. Tsuda, and K. Kondo, *Chem. Pharm. Bull.*, **36**, 2685 (1988); *e*) M. M. M. Pinto, A. Kijjoa, B. Tantisewie, M. Yoshida, and O. R. Gottlieb, *Phytochemistry*, **27**, 3988 (1988).

2) Private communication from Prof. M. Hattori, Toyama Medical and Pharmaceutical University.

3) Private communication from Prof. N. Nakatani, Osaka City University.

4) M. R. Parthasarathy and S. Gupta, *Indian J. Chem., Sect. B*, **24B**, 965 (1985).

5) P. M. Collins and H. Hansjorg, *J. Chem. Soc., Perkin Trans. 1*, **1984**, 1525.

6) A. K. Bose and B. La, *Tetrahedron Lett.*, **1973**, 3937.

7) I. Yasuda, K. Takeya, and H. Itokawa, *Chem. Pharm. Bull.*, **29**, 564 (1981). The *trans*-isomers should give a coupling constant of J=14—16 Hz [see also, F. Kiuchi, N. Nakamura, Y. Tsuda, K. Kondo, and H. Yoshimura, *ibid.*, **36**, 2452 (1988)].

Photocyclization of Enamides. XXXIII.[1] Total Syntheses of (±)-Agroclavines, (±)-Fumigaclavine B, and (±)-Lysergene[2]

Ichiya NINOMIYA,* Toshiko KIGUCHI, Chiyomi HASHIMOTO, and Takeaki NAITO

Kobe Women's College of Pharmacy, Motoyamakita, Higashinada, Kobe 658, Japan. *Received June 11, 1990*

Total syntheses of several ergoline-type alkaloids, (±)-agroclavine (21), (±)-agroclavine I (24), (±)-fumigaclavine B (28), and (±)-lysergene (33), were accomplished *via* a route involving reductive photocyclization of the enamide 5 followed by oxidative cleavage of the dihydrofuran ring.

Keywords enamide; reductive photocyclization; ergot alkaloid; agroclavine; agroclavine I; fumigaclavine B; lysergene; total syntheses

In Parts XXIV[3] and XXIX,[4] we reported the total syntheses of four ergoline alkaloids having an oxygen function in a substituent at the 8-position *via* a route involving reductive photocyclization of the enamide A as shown in Chart 1. Our synthetic route consisted of oxidative cleavage of a dihydrofuran ring and lithium aluminum hydride reduction of the photocylized lactam B to furnish 9-hydroxy derivatives C as the common key intermediates. However, when a benzoyl group was employed as the protective group for the indolinic nitrogen as reported previously,[3,4] it was necessary to carry out the highly selective reduction of the lactam carbonyl group in the presence of the *N*-benzoyl group or to reintroduce a protective group onto the nitrogen after deprotection caused by the reductive process involved.

In order to avoid the above inconvenience caused by the use of benzoyl as a protective group, we employed the enamide **5** bearing a *p*-methoxyphenylsulfonyl group on nitrogen of the indoline moiety in place of the benzoyl group in A, hoping to develop an improved synthesis of ergoline-type alkaloids, and succeeded in straightforward total syntheses of four ergoline alkaloids including fumigaclavine B and lysergene, which had eluded synthetic attack,[5] according to the route developed for depyrrole analogs[6] and a new procedure for the conversion of indolines to indoles.[4]

Preparation of the Key Intermediates 9, 11, 12, and 14 The tricyclic ketone **4**, which carries a *p*-methoxyphenylsulfonyl group on nitrogen, was prepared as follows in four steps from the known compound **1**[7] in 73% overall yield. Replacement of the *N*-benzoyl group by a *p*-methoxyphenylsulfonyl group was performed by acid hydrolysis of **1** followed by sulfonylation with *p*-methoxyphenylsulfonyl chloride to give **2** in 87% yield. Compound **2** was oxidized with *m*-chloroperbenzoic acid to give the epoxide **3** in 90% yield. Then the conversion of the epoxide **3** to the ketone **4** was investigated in order to avoid a tedious step involving the use of very hygroscopic magnesium dibromide in the conversion employed previously.[7] The conversion was achieved in 93% yield by adding the epoxide **3** dropwise to refluxing toluene in the presence of *p*-toluenesulfonic acid.[8] The ketone **4** showed a strong infrared (IR) absorption at 1712 cm^{-1} (CO). The tricyclic ketone **4** thus obtained was converted to the enamine by treatment with methylamine, and acylation of this enamine with furan-3-carbonyl chloride in the presence of triethylamine afforded the enamide **5** in 90% yield. The enamide **5** showed the proton nuclear magnetic resonance (^{1}H-NMR) signal of an olefinic proton at δ 6.41 as a doublet (J=2 Hz) and a strong IR absorption at 1630 cm^{-1} (NCO). Irradiation of the enamide **5** by the procedure established previously,[3] namely, in the presence of sodium borohydride in benzene and methanol (8 : 1, v/v) at 5 °C by using a high pressure mercury lamp through a Pyrex filter, afforded a complex mixture of products which had lost the *p*-methoxyphenylsulfonyl group. This is in agreement with the known result[9] on the cleavage of the sulfonamide group by irradiation under almost the same conditions. On the other hand, irradiation of the enamide **5** under the same condition described above except for the use of a uranyl glass filter in place of a Pyrex filter gave the desired product in good yield. This photocyclized product was found to be a mixture of three isomeric lactams **6**, **7**, and **8**, which were separated by repeated chromatography on a medium-pressure column in 53%, 21%, and 6% isolated yields, respectively. The structures of **6**—**8** were established to be as expected from their mass spectra (MS), which exhibited a molecular ion peak at m/z 452, two mass units larger than that of the enamide **5**, and from their IR absorptions at 1640—1636 cm^{-1} (NCO). Their stereochemistries were established by comparison of their ^{1}H-NMR spectra with those of the *N*-benzoyl derivatives.[3] That is, the D/E-*cis*-fusion and the *trans* relationship between 11b- and 11c-H for the three lactams **6**—**8**, and the C/D-*trans* structure for **6** and **8** and *cis* structure for **7** were determined. Furthermore, the relative configuration between 5a- and 6a-H was also deduced as being *cis* for **6** and **7** and *trans* for **8**. The ratio of the three stereoisomeric products **6**—**8**

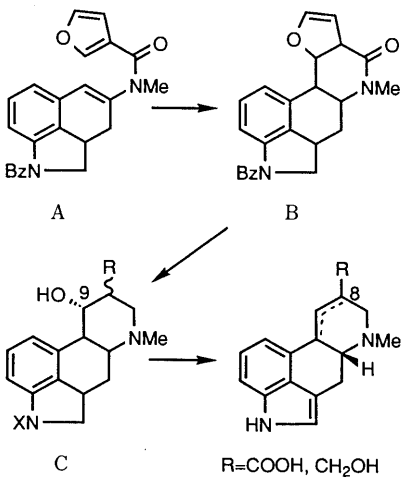

Chart 1

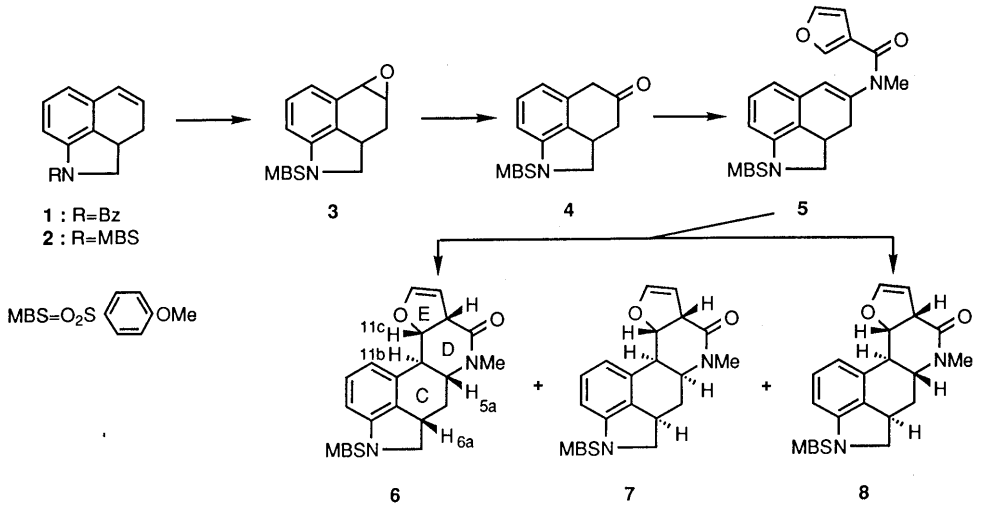

Chart 2

was almost identical with that of the three *N*-benzoyl lactams B which were previously obtained by the reductive photocyclization of the *N*-benzoyl enamide A,[3] and was not influenced by the solvent used.

Of the cyclized lactams **6**—**8**, the 5a,6a-*cis*-lactams **6** and **7** were used for the total syntheses of agroclavines, fumigaclavine B and lysergene. Ring opening of the dihydrofuran ring of the photocyclized lactams **6** and **7** was accomplished according to the procedure described previously.[4] Ozonolysis of the *trans*-lactam **6** in methylene dichloride at $-30\,^{\circ}C$ followed by reduction with lithium aluminum hydride afforded the diol **9** in 45% yield. The diol **9** was treated with mesyl chloride in pyridine at $0\,^{\circ}C$ to give the monomesylate **10** in 89% yield, and this product was reduced with sodium borohydride in dimethyl sulfoxide (DMSO)[10] at $80\,^{\circ}C$ to give the 8-methyl-9-ol **11** in 74% yield. By the same procedure, the *cis*-lactam **7** was converted to the diol **12** in 58% yield and then the epimeric 8-methyl-9-ol **14** was obtained from **12** *via* the corresponding mesylate **13** in 46% yield. The stereochemistries of these products **9**, **11**, **12**, and **14** were established from the ^{1}H-NMR spectra, particularly the coupling constants between the two hydrogens at the 9- and 10-positions (8—11 Hz) and between those at 8- and 9-positions (5—6 Hz). The 1,3-diaxial relationship of 3- and 5-H was deduced from the signal pattern of 4-Hax which appears as a quartet ($J=11.5$—12 Hz) at δ 1.44—1.21. These data were consistent with a stable chair conformation of ring D with the 9-hydroxy group in the equatorial orientation, as shown by the structures D for **9** and **11**, and E for **12** and **14** in Chart 3.

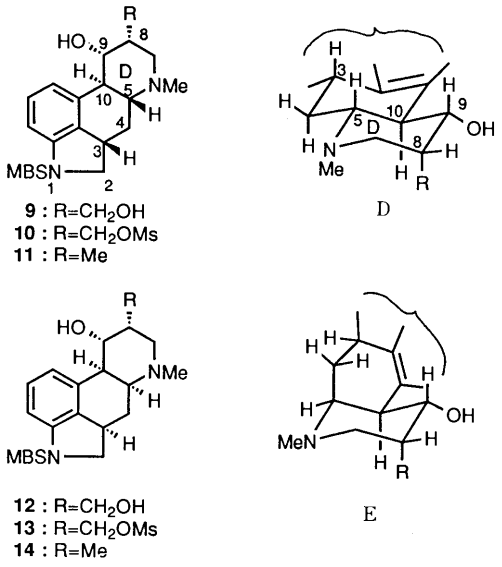

Chart 3

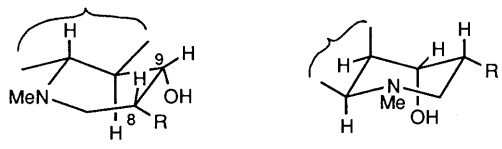

Chart 4

These compounds **9**, **11**, **12** and **14** bear all the necessary functional groups for their conversions to ergot alkaloids having an ergoline skeleton.

Total Synthesis of (±)-Agroclavine (21) and (±)-Agroclavine I (24) Agroclavine (**21**), having a C/D-*trans*-8,9-didehydroergoline structure, occupies an important position in the biosynthetic pathway[5] of ergot alkaloids. Its isomer, agroclavine I (**24**), was isolated from a *Penicillium kapuscinski* strain in 1984 and proposed to have a C/D-*cis*-8,9-didehydroergoline structure.[11] It was later synthesized by two groups.[12,13] For the synthesis of these two alkaloids, the regioselective introduction of a double bond into the 8,9-position from both the C/D-*trans*- **11** and *cis*-alcohols **14** was investigated. In the case of the C/D-*trans*-alcohol, we had previously investigated various methods of the depyrrole analogs.[6] However, the desired product was obtained only as a minor product with thionyl chloride. This result was explained as follows: the reactive intermediate would exist mostly in the stable chair form D (Chart 3) in equilibrium with the less favored boat form F (Chart 4), and the small amount of the latter form F would account for the poor formation of the desired compound having the 8,9-double bond as a result of *trans*-diaxial elimination of the 9-hydroxy group and 8-hydrogen. This suggests that the C/D-*cis*-alcohol **14** may give stereoselec-

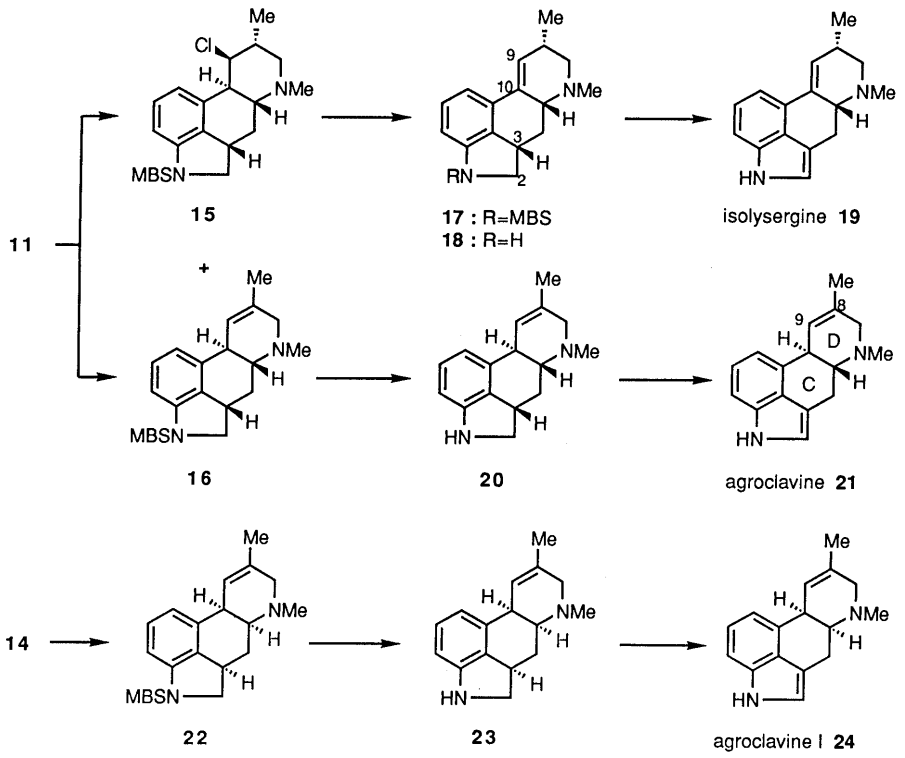

Chart 5

tively the desired compound having the 8,9-double bond since the existence of another conformation G having the 9α-axial hydroxy group and 8β-axial hydrogen in the reactive intermediate would become possible due to the C/D-*cis*-structure in **14**.

Treatment of the C/D-*trans*-9α-alcohol **11** with thionyl chloride in benzene under reflux afforded the inverted 9β-chloride **15** in 64% yield together with the 8,9-dehydrated product **16** in 24% yield, the result being in agreement with the case of the depyrrole analogs.[6] The structures of these products were firmly established from their ^{1}H-NMR signals at δ 4.71 (br s, 9-H) and 1.32 (d, J=8 Hz, 8-Me) for **15** and δ 5.97 (br s, 9-H) and 1.74 (br s, 8-Me) for **16**. On the other hand, under the same conditions, the C/D-*cis*-9α-alcohol **14** was smoothly converted in 64% yield into the dehydrated product **22**, which showed ^{1}H-NMR signals at δ 5.28 (br s, 9-H) and 1.60 (br s, 8-Me). Treatment of the 9β-chloride **15** with 1,8-diazabicyclo[5.4.0]undec-7-ene (DBU) in benzene under reflux afforded in 89% yield the unsaturated amine **17**, which was characterized as having a double bond at the 9,10-position by the ^{1}H-NMR signals at δ 6.39 (br dd, J=5, 2 Hz, 9-H) and 1.18 (d, J=7 Hz, 8-Me).

Reductive cleavage of the protecting group of indoline in **17** was achieved by treatment with lithium aluminum hydride in dimethoxyethane (DME) under reflux to give 2,3-dihydroisolysergine (**18**) in 93% yield. Removal of the protecting group of indoline in **16** and **22** was also performed smoothly with sodium in liquid ammonia to afford **20** and **23** in quantitative yields. Finally, the conversion of the indolines **18**, **20**, and **23** into the corresponding indoles was carried out by applying the new procedure reported previously.[4] Treatment of the indolines **18**, **20**, and **23** with 0.5 mol eq of phenylseleninic anhydride in the presence of 3 mol eq of indole at 40 °C in tetrahydrofuran (THF) gave (±)-isolysergine (**19**), (±)-agroclavine (**21**), and (±)-agroclavine I (**24**) in good yields respectively. The product **19** was identical with an authentic sample of unnatural isolysergine, which was prepared by the known procedure[14] from natural lysergene given by Professor Yamatodani, by direct comparison. The product **21** was found to be identical with natural agroclavine by direct comparison and the ^{1}H-NMR of the product **24** was found to be identical with that reported for natural agroclavine I.[11] Thus, we have completed total syntheses of both (±)-agroclavine (**21**) and (±)-agroclavine I (**24**).

Total Synthesis of (±)-Fumigaclavine B (28) Fumigaclavine B (**28**) was isolated in 1961 by Spilsbury and Wilkinson,[15] who proposed the structure having an 8β-methyl configuration on the basis of its conversion into lysergine (9,10-didehydro-6,8β-dimethylergoline) upon soda-lime distillation. In 1974,[16] this proposed structure was revised by Bach *et al.*, based on ^{1}H-NMR analysis, to that having α-axial 8-methyl group and a β-axial 9-hydroxy group with a C/D-*trans* ring juncture. Polonsky *et al.*[17] supported this structure, showing that hydroboration of agroclavine gave fumigaclavine B along with isofumigaclavine B, but the stereochemical structure remained unestablished.

Thus, we planned the synthesis of this compound having the proposed structure by inverting the 9α-hydroxy group in **11**. Inversion of the 9α-hydroxy group to its epimeric β-orientation was performed according to the procedure applied to the depyrrole analog.[6] Treatment of **11** with mesyl chloride in pyridine at room temperature gave the mesylate **25** in quantitative yield. When the mesylate **25**, without purification, was treated with potassium superoxide[18] in DMSO in the presence of 18-crown-6-ether at room temperature, the 9β-hydroxy derivative **26** and dehydro derivative **17** were obtained in 54% and 10% yields, respectively. The minor product **17** was identical with the

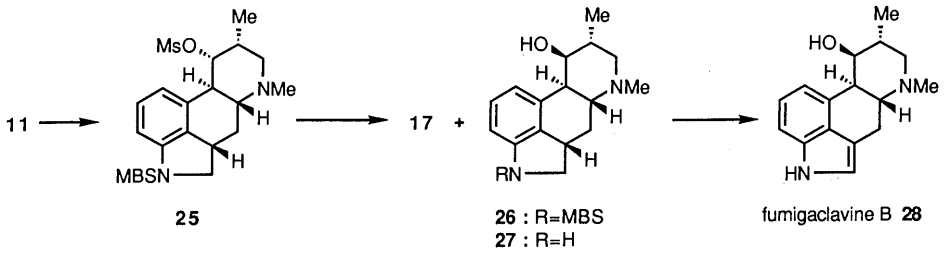

Chart 6

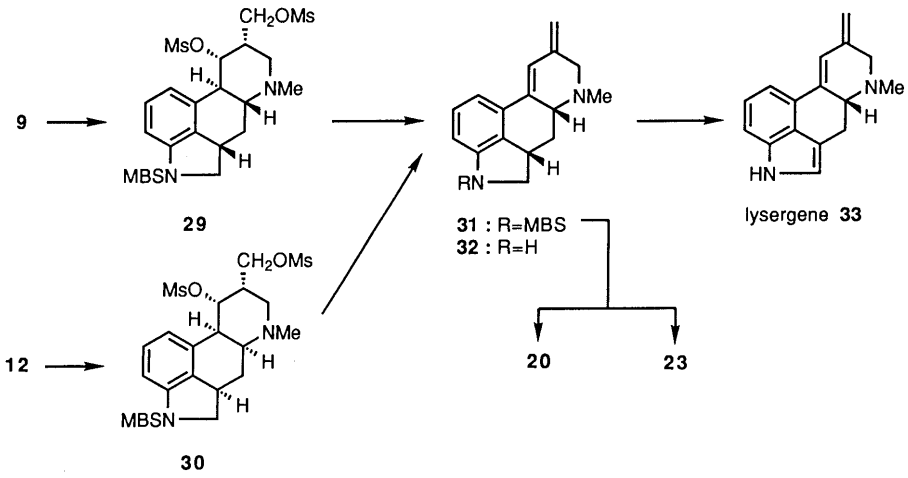

Chart 7

product which had been prepared by dehydrohalogenation of the chloride **15**. The ^{1}H-NMR spectrum of **26** showed signals at δ 4.32 (br s, 9-H), 2.95 (br d, $J=10$ Hz, 10-H), and 1.20 (d, $J=7$ Hz, 8-Me), thus confirming its stereochemistry. Treatment of **26** with sodium in liquid ammonia removed the protective group on nitrogen of the indoline moiety to afford 2,3-dihydrofumigaclavine B (**27**) and subsequent treatment with phenylseleninic anhydride in the presence of indole gave (±)-fumigaclavine B (**28**) in 76% yield from **26**. This was found to be identical with natural fumigaclavine B upon comparison of their spectral data, thus firmly establishing the proposed stereostructure of fumigaclavine B (**28**) and completing its first total synthesis.

Having thus synthesized (±)-fumigaclavine B (**28**), we rechecked its ^{1}H-NMR assignment by using the decoupling technique and nuclear Overhauser effect (NOE) measurement, and found that the previous assignment[16] for the hydrogens at the 4-, 5-, 7-, and 10-positions must be revised.

Total Synthesis of (±)-Lysergene (33) Lysergene (**33**) has a diene structure,[19] and total synthesis of this alkaloid was achieved by double elimination of two hydroxy groups in the diols **9** and **12**. The C/D-*trans*-diol **9** and the C/D-*cis*-diol **12** were mesylated with mesyl chloride in pyridine at room temperature to give the dimesylate **29** in 85% yield from **9** and the dimesylate **30** in 81% yield from **12**, respectively. Treatment of the dimesylates **29** and **30** with potassium *tert*-butoxide in DMSO at room temperature brought about smooth double elimination of the two mesyloxy groups to afford the same diene **31** in 52% yield from **29** and 51% yield from **30**, respectively. The ^{1}H-NMR spectrum of **31** showed three broad singlets due to two olefinic protons at δ 6.79, 4.99 and 4.88. Reductive cleavage of the protecting group of **31** was achieved with lithium aluminum hydride in DME under reflux to give 2,3-dihydrolysergene (**32**). Without purification, **32** was then converted into (±)-lysergene (**33**), upon dehydrogenation with phenylseleninic anhydride in the presence of indole, in 58% yield from **31**. The final product **33** was found to be identical with natural lysergene[19] by direct comparison, thus completing its first total synthesis.

Alternatively, treatment of the diene **31** with sodium in liquid ammonia brought about reductive cleavage of the protecting group and concomitant reduction of the diene structure to afford a mixture of the C/D-*trans*- **20** and *cis*-amines **23** in the ratio of 2 : 1. Dehydrogenation with phenylseleninic anhydride in the presence of indole afforded (±)-agroclavine (**21**) and (±)-agroclavine I (**24**) in 45% and 23% isolated yields from **31**, respectively. These products **21** and **24** were identical with the samples prepared from **16** and **22**.

Experimental

The ^{1}H-NMR spectra were measured with JEOL PMX-60 (60 MHz) and Varian XL-200 (200 MHz) instruments for solutions in deuteriochloroform unless otherwise stated (with tetramethylsilane as an internal reference), and the IR spectra were measured with a Hitachi 215 machine for solutions in chloroform unless otherwise stated. MS were taken with a Hitachi 80 spectrometer. All melting points were determined with a Kofler-type hot-stage apparatus and are uncorrected. Reactions were performed under a nitrogen atmosphere. Extracts from the reaction mixture were washed with water, dried over anhydrous sodium sulfate, and evaporated under reduced pressure. Thin layer chromatography (TLC) was performed on pre-coated Silica gel 60F-254 plates (0.25 mm thick, Merck) and preparative-TLC (p-TLC) on pre-coated Silica gel 60F-254 plates (0.5 mm thick, Merck), and spots were detected by ultraviolet (UV) irradiation of the plate at 254 and 300 nm. Medium-pressure column chromatography was undertaken on a 530-4-10V apparatus (Yamazen) using Lobar grosse B (310-25, Lichroprep Si60,

Merck) column. For flash column chromatography, Merck Kiesel gel 60 (230—400 mesh) was used. Ether refers to diethyl ether.

1-[(4-Methoxyphenyl)sulfonyl]-1,2,2a,3-tetrahydrobenz[*cd*]indole (2) A solution of 1-benzoyl-1,2,2a,3-tetrahydrobenz[*cd*]indole (**1**)[7] (6.54 g) in methanol (275 ml) containing concentrated hydrochloric acid (25 ml) was refluxed for 8 h. The reaction mixture was concentrated to a small volume and then diluted with water, and washed with benzene. The aqueous layer was made alkaline with 10% aqueous sodium carbonate and extracted with benzene. The extract was washed, dried, and evaporated to give a brown oil which was, without further purification, treated in benzene (100 ml) under reflux with 4-(methoxyphenyl)sulfonyl chloride (5.16 g) in the presence of triethylamine (3 g). After 5 h, the reaction mixture was cooled and washed with aqueous sodium bicarbonate and water. The organic layer was dried, and evaporated. The residue was crystallized from ether to give the sulfonamide **2** (7.13 g, 87%), mp 134—138 °C (colorless crystals from ethyl acetate–ether). IR: 1354, 1162 (NSO_2) cm^{-1}. ^{1}H-NMR (200 MHz) δ:7.91 (2H, br d, J=9 Hz, ArH), 7.43 (1H, d, J=8 Hz, 8-H), 7.18 (1H, t, J=8 Hz, 7-H), 6.96 (2H, br d, J=9 Hz, ArH), 6.76 (1H, d, J=8 Hz, 6-H), 6.49 (1H, dd, J=9, 3 Hz, 5-H), 5.96 (1H, ddd, J=9, 6, 2 Hz, 4-H), 4.38 (1H, m, 2-H), 3.84 (3H, s, OMe), 3.45—3.16 (2H, m, 2- and 2a-H), 2.50 (1H, m, 3-H_{eq}), 1.99 (1H, m, 3-H_{ax}). *Anal.* Calcd for $C_{18}H_{17}NO_3S$: C, 66.03; H, 5.23; N, 4.28. Found: C, 65.91; H, 5.11; N, 4.31.

4,5-Epoxy-1,2,2a,3,4,5-hexahydro-1-[(4-methoxyphenyl)sulfonyl]benz[*cd*]indole (3) *m*-Chloroperbenzoic acid (80%, 3.04 g) was added all at once to a solution of the sulfonamide **2** (4 g) in chloroform (100 ml). The solution was swirled until all the peracid was dissolved and then kept at 5°C for 3 h. The reaction mixture was washed with aquous sodium thiosulfate, 5% aqueous sodium hydroxide, and water. The organic layer was dried and evaporated, and the residue was crystallized from ethyl acetate–hexane to give the epoxide **3** (3.7 g, 90%), mp 165—168 °C (colorless crystals from benzene–hexane). IR: 1356, 1160 (NSO_2) cm^{-1}. ^{1}H-NMR (200 MHz) δ: 7.75 (2H, br d, J=9 Hz, ArH), 7.55 (1H, d, J=8 Hz, 8-H), 7.22 (1H, t, J=8 Hz, 7-H), 7.11 (1H, d, J=8 Hz, 6-H), 6.92 (2H, br d, J=9 Hz, ArH), 4.31 (1H, dd, J=11, 9 Hz, 2-H), 3.81 (3H, s, OMe), 3.79 (1H, d, J=4 Hz, 5-H), 3.65 (1H, dd, J=4, 3 Hz, 4-H), 3.32 (1H, dd, J=11, 10 Hz, 2-H), 3.06 (1H, m, 2a-H), 2.61 (1H, ddd, J=14, 7, 3 Hz, 3-H_{eq}), 1.32 (1H, dd, J=14, 11 Hz, 3-H_{ax}). *Anal.* Calcd for $C_{18}H_{17}NO_4S$: C, 62.96; H, 4.99; N, 4.08. Found: C, 63.20; H, 4.91; N, 4.19.

1-[(4-Methoxyphenyl)sulfonyl]-1,2,2a-3-tetrahydrobenz[*cd*]-indol-4(5*H*)-one (4) A toluene solution (220 ml) of *p*-toluenesulfonic acid (1.23 g) was refluxed for 0.5 h with a Dean-Stark apparatus to remove water, and then a solution of the epoxide **3** (2 g) in toluene (15 ml) was added dropwise to the resulting stirred solution under reflux. After being refluxed for 1 h, the mixture was ice-cooled and washed with aqueous saturated sodium bicarbonate and water. The organic layer was dried and evaporated. The residue was crystallized from benzene to give the ketone **4** (1.86 g, 93%), mp 149—151 °C (colorless needles from benzene–hexane). IR: 1712 (CO), 1358, 1160 (NSO_2) cm^{-1}. ^{1}H-NMR (200 MHz) δ: 7.78 (2H, br d, J=9 Hz, ArH), 7.49 (1H, d, J=8 Hz, 8-H), 7.24 (1H, t, J=8 Hz, 7-H), 6.94 (2H, br d, J=9 Hz, ArH), 6.83 (1H, d, J=8 Hz, 6-H), 4.41 (1H, dd, J=9, 8 Hz, 2-H), 3.83 (3H, s, OMe), 3.50 (1H, m, 2a-H), 3.46 (2H, s, 5-H_2), 3.38 (1H, dd, J=11, 9 Hz, 2-H), 2.96 (1H, dd, J=16, 5 Hz, 3-H_{eq}), 2.13 (1H, dd, J=16, 12 Hz, 3-H_{ax}). *Anal.* Calcd for $C_{18}H_{17}NO_4S \cdot 1/5C_6H_6$: C, 64.23; H, 5.11; N, 3.90. Found: C, 64.30; H, 5.06; N, 3.75.

***N*-[1-[(4-Methoxyphenyl)sulfonyl]-1,2,2a,3-tetrahydrobenz[*cd*]indol-4-yl]-*N*-methyl-3-furancarboxamide (5)** Anhydrous methylamine gas was bubbled into a boiling solution of the ketone **4** (2.1 g) in toluene (300 ml) under a nitrogen stream for 6 h; water was removed as it was formed. The mixture was refluxed further to remove the excess of methylamine by bubbling nitrogen. Triethylamine (1 g) was added to the resulting ice-cooled, stirred solution and then a solution of freshly prepared furan-3-carbonyl chloride (0.8 g) in anhydrous benzene (50 ml) was added dropwise. After being refluxed for 2 h the mixture was cooled, diluted with benzene, and washed. The organic layer was dried and evaporated. Flash chromatography (methylene dichloride) of the residue gave the enamide **5** (2.48 g, 90%) as a pale yellow glass. IR: 1630 (NCO), 1355, 1160 (NSO_2) cm^{-1}. ^{1}H-NMR (200 MHz) δ: 7.82—7.70 (3H, m, 2′-H and ArH), 7.42 (1H, d, J=7 Hz, 8-H), 7.32 (1H, t, J=2 Hz, 5′-H), 7.17 (1H, t, J=7 Hz, 7-H), 6.95 (2H, br d, J=9 Hz, ArH), 6.73 (1H, d, J=7 Hz, 6-H), 6.58 (1H, dd, J=2, 1 Hz, 4′-H), 6.41 (1H, d, J=2 Hz, 5-H), 4.31 (1H, m, 2a-H), 3.84 (3H, s, OMe), 3.30—3.25 (2H, m, 2-H_2), 3.21 (3H, s, NMe), 2.52—2.22 (2H, m, 3-H_2). High-resolution MS m/z: Calcd for $C_{24}H_{22}N_2O_5S$ (M^+) 450.1247. Found: 450.1246.

Reductive Photocyclization of the Enamide 5 A solution of a mixture of the enamide **5** (1.3 g) and sodium borohydride (1.3 g) in benzene–methanol (8 : 1, 900 ml) was irradiated with a high-pressure (300 W) mercury lamp through an uranyl glass filter (Eikosha, Osaka, Japan, PIH-300) at 5°C for 2 h. The reaction mixture was washed and the organic layer was dried and evaporated to afford a crystalline residue, which was chromatographed on a medium-pressure column (acetonitrile: methylene dichloride = 1 : 4). (3aβ,5aβ,6aβ,11bα,11cβ)-5,5a,6,6a,7,8,11b,11c-Octahydro-8-[(4-methoxyphenyl)sulfonyl]-5-methylfuro[4,3-*fg*]quinolin-4(3a*H*)-one (**6**) (694 mg, 53%) was obtained from the first fraction. The residue obtained from the second fraction was rechromatographed on a medium-pressure column (benzene : methanol = 98.5 : 1.5) to give (3aβ,5aα,6aα,11bα,11cβ)-5,5a,6,6a,7,8,11b,11c-octahydro-8-[(4-methoxyphenyl)sulfonyl]-5-methylfuro[4,3-*fg*]quinolin-4(3a*H*)-one (**7**) (275 mg, 21%) and (3aβ,5aβ,6aα,11bα,11cβ)-5,5a,6,6a,7,8,11b,11c-octahydro-8-[(4-methoxyphenyl)sulfonyl]-5-methylfuro[4,3-*fg*]quinolin-4(3a*H*)-one (**8**) (79 mg, 6%). The lactam **6**: mp 222—224 °C (colorless crystals from methylene dichloride–ethyl acetate). IR: 1640 (NCO), 1355, 1160 (NSO_2) cm^{-1}. ^{1}H-NMR (200 MHz) δ: 7.80 (2H, br d, J=8 Hz, ArH), 7.45 (1H, d, J=8 Hz, 9-H), 7.39 (1H, d, J=8 Hz, 11-H), 7.22 (1H, t, J=8 Hz, 10-H), 6.96 (2H, br d, J=8 Hz, ArH), 6.44 (1H, t, J=2.5 Hz, 2-H), 5.34 (1H, t, J=2.5 Hz, 3-H), 4.84 (1H, dd, J=12, 10 Hz, 11c-H), 4.31 (1H, m, 7-Hβ), 3.84 (3H, s, OMe), 3.82 (1H, dt, J=12, 2.5 Hz, 3a-H), 3.52 (1H, ddd, J=12, 10, 3 Hz, 5a-H), 3.31—3.10 (2H, m, 6a-H and 7-Hα), 3.02 (3H, s, NMe), 2.91 (1H, t, J=10 Hz, 11b-H), 2.58 (1H, dt, J=12, 4 Hz, 6-H_{eq}), 1.51 (1H, br q, J=12 Hz, 6-H_{ax}). MS m/z: 452 (M^+). *Anal.* Calcd for $C_{24}H_{24}N_2O_5S$: C, 63.70; H, 5.35; N, 6.19. Found: C, 63.69; H, 5.10; N, 6.03. The lactam **7**: mp 237—239 °C (dec.) (colorless crystals from methylene dichloride–ethyl acetate). IR: 1638 (NCO), 1358, 1162 (NSO_2) cm^{-1}. ^{1}H-NMR (200 MHz) δ: 7.80 (2H, br d, J=8 Hz, ArH), 7.48 (1H, d, J=8 Hz, 9-H), 7.23 (1H, t, J=8 Hz, 10-H), 7.10 (1H, d, J=8 Hz, 11-H), 6.97 (2H, br d, J=8 Hz, ArH), 6.38 (1H, t, J=2.5 Hz, 2-H), 5.30 (1H, t, J=2.5 Hz, 3-H), 4.46 (1H, dd, J=11, 10 Hz, 11c-H), 4.27 (1H, m, 7-Hβ), 3.86 (3H, s, OMe), 3.78 (1H, dt, J=11, 2.5 Hz, 3a-H), 3.56 (1H, ddd, J=12.5, 5, 3 Hz, 5a-H), 3.34—3.10 (3H, m, 11b-H, 7-Hα, and 6a-H), 3.08 (3H, s, NMe), 2.32 (1H, dt, J=12, 3 Hz, 6-H_{eq}), 1.39 (1H, br q, J=12 Hz, 6-H_{ax}). MS m/z: 452 (M^+). *Anal.* Calcd for $C_{24}H_{24}N_2O_5S \cdot 1/10CH_2Cl_2$: C, 62.79; H, 5.29; N, 6.08. Found: C, 62.69; H, 5.37; N, 6.12. The lactam **8**: mp 231—233 °C (colorless crystals from methylene dichloride–ethyl acetate). IR: 1636 (NCO), 1358, 1162 (NSO_2) cm^{-1}. ^{1}H-NMR (200 MHz) δ: 7.80 (2H, br d, J=8 Hz, ArH), 7.51 (1H, d, J=8 Hz, 9-H), 7.38—7.20 (2H, m, 10- and 11-H), 6.96 (2H, br d, J=8 Hz, ArH), 6.38 (1H, t, J=2.5 Hz, 2-H), 5.32 (1H, t, J=2.5 Hz, 3-H), 5.06 (1H, t, J=10 Hz, 11c-H), 4.42 (1H, m, 7-Hβ), 4.04 (1H, td, J=10, 2.5 Hz, 3a-H), 3.85 (3H, s, OMe), 3.40—3.08 (3H, m, 5a-H, 6a-H, and 7-Hα), 2.98 (3H, s, NMe), 2.86 (1H, t, J=10 Hz, 11b-H), 2.14 (1H, m, 6-H_{eq}), 1.98 (1H, m, 6-H_{ax}). MS m/z: 452 (M^+). *Anal.* Calcd for $C_{24}H_{24}N_2O_5S \cdot 1/5CH_2Cl_2$: C, 61.91; H, 5.24; N, 5.97. Found: C, 61.94; H, 5.26; N, 6.27.

(3β,8α,9α)-2,3-Dihydro-8-hydroxymethyl-1-[(4-methoxyphenyl)sulfonyl]-6-methylergolin-9-ol (9) Ozone gas was slowly bubbled at −30 °C into a solution of the *trans*-lactam **6** (900 mg) in methylene dichloride (70 ml) in the presence of oil violet until the violet color disappeared (10 min). Removal of the solvent gave the residue, which was dissolved in anhydrous THF (200 ml), and this solution was added dropwise to a solution of lithium aluminum hydride (300 mg) in anhydrous ether (200 ml) under reflux. The mixture was refluxed for an additional 2 h, and treatment in the usual way gave a crystalline residue, which was recrystallized from methanol to give the diol **9** (400 mg, 45%) as colorless needles, mp 200—201.5 °C. IR (Nujol): 3500—3150 (OH), 1355, 1160 (NSO_2) cm^{-1}. ^{1}H-NMR (200 MHz) δ ($CDCl_3$–CD_3OD): 7.82—7.72 (3H, m, 12-H, and ArH), 7.36 (1H, d, J=8 Hz, 14-H), 7.14 (1H, t, J=8 Hz, 13-H), 6.98 (2H, br d, J=8 Hz, ArH), 4.22 (1H, m, 2-Hβ), 4.15 (1H, dd, J=11, 7 Hz, C$\underline{H}_2$OH), 4.02 (1H, m, 2-Hα), 3.98 (1H, dd, J=11, 5 Hz, 9-H), 3.89 (1H, dd, J=11, 5 Hz, C$\underline{H}_2$OH), 3.86 (3H, s, OMe), 3.14 (1H, m, 3-H), 3.02 (1H, dd, J=12, 3 Hz, 7-H_{eq}), 2.93 (1H, t, J=11 Hz, 10-H), 2.50—2.32 (2H, m, 4-H_{eq} and 7-H_{ax}), 2.31 (3H, s, NMe), 2.19 (1H, m, 8-H), 2.02 (1H, br t, J=11 Hz, 5-H), 1.21 (1H, br q, J=12 Hz, 4-H_{ax}). *Anal.* Calcd for $C_{23}H_{28}N_2O_5S$: C, 62.14; H, 6.35; N, 6.30. Found: C, 62.21; H, 6.39; N, 6.29.

(3β,8α,9α)-2,3-Dihydro-8-methanesulfonyloxymethyl-1-[(4-methoxyphenyl)sulfonyl]-6-methylergolin-9-ol (10) Mesyl chloride (0.1 ml) was added dropwise to a stirred solution of the diol **6** (115 mg) in pyridine (2 ml) under ice-cooling, and the mixture was stirred at 0 °C for an additional 3.5 h. Then 10% aqueous ammonium hydroxide was added to the reaction mixture, which was then extracted with methylene dichloride. The extract was washed, dried, and evaporated to give a crystalline residue which was recrystallized from ether to afford the monomesylate **10** (120 mg, 89%) as colorless crystals, mp 233—235 °C (dec.). IR: 1360, 1160 (NSO_2

and OSO_2) cm^{-1}. ^{1}H-NMR (60 MHz) δ: 4.82—4.56 (2H, m, 8-C$\underline{H}_2$OMs), 4.22 (1H, m, 2-Hβ), 4.06 (1H, m, 9-H), 3.85 (3H, s, OMe), 3.06 (3H, s, OMs), 2.42 (3H, s, NMe). *Anal.* Calcd for $C_{24}H_{30}N_2O_7S_2$: C, 55.15; H, 5.79; N, 5.36. Found: C, 55.13; H, 5.86; N, 5.29.

(3β,8α,9α)-2,3-Dihydro-1-[(4-methoxyphenyl)sulfonyl]-6,8-dimethylergolin-9-ol (11) Sodium borohydride (108 mg) was added to a stirred solution of the monomesylate **10** (140 mg) in DMSO (1 ml) at 10 °C, and the mixture was heated at 80°C for 8 h. Water was added to the cooled reaction mixture and the whole was extracted with ethyl acetate. The extract was washed, dried, and evaporated. The residue was purified by p-TLC (methylene dichloride : methanol = 9 : 1) to afford the alcohol **11** (85 mg, 74%), mp 199—200 °C (colorless needles from chloroform–ether). IR: 3608 (OH), 1354, 1162 (NSO_2) cm^{-1}. ^{1}H-NMR (200 MHz) δ: 7.81 (2H, br d, J = 8 Hz, ArH), 7.67 (1H, d, J = 8 Hz, 12-H), 7.42 (1H, d, J = 8 Hz, 14-H), 7.16 (1H, t, J = 8 Hz, 13-H), 6.95 (2H, br d, J = 8 Hz, ArH), 4.23 (1H, m, 2-Hβ), 3.89 (1H, dd, J = 11, 5 Hz, 9-H), 3.84 (3H, s, OMe), 3.20—2.96 (2H, m, 2-Hα and 3-H), 2.94—2.78 (2H, m, 7-H_{eq} and 10-H), 2.45—2.30 (2H, m, 4-H_{eq} and 7-H_{ax}), 2.32 (3H, s, NMe), 2.14 (1H, m, 8-H), 1.95 (1H, br t, J = 11 Hz, 5-H), 1.22 (1H, br q, J = 12 Hz, 4-H_{ax}), 1.19 (3H, d, J = 7 Hz, 8-Me). *Anal.* Calcd for $C_{23}H_{28}N_2O_4S$: C, 64.46; H, 6.59; N, 6.54. Found: C, 64.55; H, 6.47; N, 6.23.

(3α,8α,9α,10α)-2,3-Dihydro-8-hydroxymethyl-1-[(4-methoxyphenyl)-sulfonyl]-6-methylergolin-9-ol (12) According to the procedure given for the preparation of **9**, ozonolysis of the *cis*-lactam **7** (1.08 g) in methylene dichloride (75 ml) in the presence of oil violet followed by reduction with lithium aluminum hydride (1.5 g) in anhydrous ether–THF (1 : 1, 300 ml) gave a crystalline residue, which was recrystallized from methylene dichloride–ether to afford the diol **12** (620 mg, 58%) as pale yellow crystals, mp 172—174 °C. IR: 3500—3150 (OH), 1355, 1160 (NSO_2) cm^{-1}. ^{1}H-NMR (200 MHz) δ: 7.78 (2H, br d, J = 8 Hz, ArH), 7.40 (1H, d, J = 8 Hz, 14-H), 7.16 (1H, t, J = 8 Hz, 13-H), 7.03 (1H, d, J = 8 Hz, 12-H), 6.93 (2H, br d, J = 8 Hz, ArH), 4.25 (1H, br dd, J = 9, 8 Hz, 2-Hβ), 4.10—3.96 (2H, m, C$\underline{H}_2$OH), 3.84 (3H, s, OMe), 3.71 (1H, dd, J = 9, 5 Hz, 9-H), 3.34 (1H, dd, J = 9, 5 Hz, 10-H), 3.26 (1H, m, 5-H), 3.22 (1H, dd, J = 12, 9 Hz, 2-Hα), 3.01 (1H, m, 3-H), 2.79 (2H, m, 7-H_2), 2.41 (3H, s, NMe), 2.11 (1H, m, 4-H_{eq}), 1.93 (1H, m, 8-H), 1.44 (1H, br q, J = 11.5 Hz, 4-H_{ax}). *Anal.* Calcd for $C_{23}H_{28}N_2O_5S$: C, 62.14; H, 6.35; N, 6.30. Found: C, 62.01; H, 6.29; N, 6.28.

(3α,8α,9α,10α)-2,3-Dihydro-1-[(4-methoxyphenyl)sulfonyl]-6,8-dimethylergolin-9-ol (14) According to the mesylation procedure described for **9**, treatment of the diol **12** (460 mg) in pyridine (2 ml) with mesyl chloride (0.4 ml) followed by flash chromatography (methylene dichloride : methanol = 98 : 2) gave the monomesylate **13** (430 mg, 81%) as a pale yellow glass. IR: 1360, 1160 (NSO_2 and OSO_2) cm^{-1}. ^{1}H-NMR (60 MHz) δ: 3.85 (3H, s, OMe), 3.07 (3H, s, Ms), 2.47 (3H, s, NMe). Sodium borohydride (450 mg) was added to a stirred solution of the above mesylate **13** (300 mg) in DMSO (6 ml) at 10 °C and the mixture was heated at 80 °C for 2 h. The same work-up as described for the preparation of **11** followed by a flash chromatography (methylene dichloride : methanol = 95 : 5) gave the alcohol **14** (139 mg, 57%) as a colorless glass. IR: 3432 (OH), 1356, 1162 (NSO_2) cm^{-1}. ^{1}H-NMR (200 MHz) δ: 7.74 (2H, br d, J = 8 Hz, ArH), 7.35 (1H, d, J = 8 Hz, 14-H), 7.11 (1H, t, J = 8 Hz, 13-H), 6.95—6.84 (3H, m, 12-H and ArH), 4.19 (1H, br dd, J = 9, 8 Hz, 2-Hβ), 3.79 (3H, s, OMe), 3.60 (1H, dd, J = 8, 5 Hz, 9-H), 3.18 (1H, dd, J = 12, 9 Hz, 2-Hα), 3.12 (1H, m, 5-H), 2.98 (1H, br dd, J = 8, 6 Hz, 10-H), 2.92 (1H, m, 3-H), 2.61 (1H, dd, J = 12, 4 Hz, 7-H_{eq}), 2.36 (1H, dd, J = 12, 4 Hz, 7-H_{ax}), 2.33 (3H, s, NMe), 2.08 (1H, m, 4-H_{eq}), 1.98 (1H, m, 8-H), 1.30 (1H, br q, J = 12 Hz, 4-H_{ax}), 1.07 (3H, d, J = 7 Hz, 8-Me). High-resolution MS m/z: Calcd for $C_{23}H_{28}N_2O_4S$ (M^+) 428.1768. Found: 428.1777.

Reaction of the Alcohol 11 with Thionyl Chloride Thionyl chloride (17.2 ml) was added dropwise to a stirred, ice-cooled solution of the alcohol **11** (259 mg) in benzene (80 ml), and the mixture was gently refluxed for 1.5 h. The excess of thionyl chloride and the solvent were removed. Then 10% aqueous sodium carbonate was added to the residue, and the resulting solution was extracted with methylene dichloride. The extract was washed, dried and evaporated. Flash chromatography (methylene dichloride : methanol = 97 : 3) of the residue gave (3β,8α,9β)-9-chloro-2,3-dihydro-1-[(4-methoxyphenyl)sulfonyl]-6,8-dimethylergoline (**15**) (180 mg, 64%) and (3β,8α,9β)-8,9-didehydro-2,3-dihydro-1-[(4-methoxyphenyl)-sulfonyl]-6,8-dimethylergoline (**16**) (60 mg, 24%). The chloride **15**: mp 161.5—164 °C (colorless needles from methanol). IR: 1370, 1180 (NSO_2) cm^{-1}. ^{1}H-NMR (200 MHz) δ: 7.80 (2H, br d, J = 8 Hz, ArH), 7.42 (1H, d, J = 8 Hz, 14-H), 7.23 (1H, t, J = 8 Hz, 13-H), 6.96 (2H, br d, J = 8 Hz, ArH), 6.88 (1H, d, J = 8 Hz, 12-H), 4.71 (1H, br s, 9-H), 4.25 (1H, m, 2-Hβ), 3.84 (3H, s, OMe), 3.32—3.04 (3H, m, 2-Hα, 3-H, and 10-H), 2.89 (1H, dd, J = 12, 4 Hz, 7-H_{ax}), 2.63 (1H, br d, J = 12 Hz, 7-H_{eq}), 2.60—2.25 (3H, m, 4-Heq, 5-H, and 8-H), 2.37 (3H, s, NMe), 1.32 (3H, d, J = 8 Hz, 8-Me), 1.28 (1H, m, 4-H_{ax}). *Anal.* Calcd for $C_{23}H_{27}ClN_2O_3S$: C, 61.80; H, 6.09; N, 6.27. Found: C, 61.53; H, 6.06; N, 6.33. The unsaturated amine **16**: a pale brown glass. IR: 1360, 1170 (NSO_2) cm^{-1}. ^{1}H-NMR (200 MHz) δ: 7.81 (2H, br d, J = 8 Hz, ArH), 7.42 (1H, d, J = 8 Hz, 14-H), 7.22 (1H, t, J = 8 Hz, 13-H), 7.05—6.90 (3H, m, 12-H and ArH), 5.97 (1H, br s, 9-H), 4.25 (1H, m, 2-Hβ), 3.85 (3H, s, OMe), 3.43 (1H, m, 10-H), 3.36—2.96 (4H, m, 2-Hα, 3-H, and 7-H_2), 2.62—2.35 (2H, m, 4-H_{eq} and 5-H), 2.44 (3H, s, NMe), 1.74 (3H, br s, 8-Me), 1.40 (1H, q, J = 11.5 Hz, 4-H_{ax}). High-resolution MS m/z: Calcd for $C_{23}H_{26}N_2O_3S$ (M^+) 410.1663. Found: 410.1682.

(3β,8α)-9,10-Didehydro-2,3-dihydro-1-[(4-methoxyphenyl)sulfonyl]-6,8-dimethylergoline (17) A solution of the chloride **15** (67 mg) and DBU (1.6 ml) in benzene (50 ml) was heated under reflux for 40 h. The reaction mixture was cooled and washed, and the organic layer was dried and evaporated. The residue was purified by p-TLC (methylene dichloride : methanol = 96 : 4) to afford **17** (53 mg, 89%), mp159—160 °C (colorless crystals from methanol). IR: 1356, 1162 (NSO_2) cm^{-1}. ^{1}H-NMR (200 MHz) δ: 7.82 (2H, br d, J = 8 Hz, ArH), 7.43 (1H, dd, J = 8, 1.5 Hz, 14-H), 7.28—7.14 (2H, m, 12- and 13-H), 6.96 (2H, br d, J = 8 Hz, ArH), 6.39 (1H, br dd, J = 5, 2 Hz, 9-H), 4.29 (1H, m, 2-Hβ), 3.86 (3H, s, OMe), 3.32—3.06 (2H, m, 2-Hα and 3-H), 2.90—2.44 (3H, m, 4-H_{eq} and 7-H_2), 2.48 (3H, s, NMe), 2.42—2.31 (2H, m, 5- and 8-H), 1.21 (1H, m, 4-H_{ax}), 1.18 (3H, d, J = 7 Hz, 8-Me). *Anal.* Calcd for $C_{23}H_{26}N_2O_3S$: C, 67.29; H, 6.38; N, 6.82. Found: C, 67.16; H, 6.48; N, 6.71.

(3β)-2,3-Dihydroisolysergine (18) Lithium aluminum hydride (30 mg) was added in small portions to a solution of the unsaturated amine **17** (20 mg) in anhydrous DME (6 ml) at room temperature, and the mixture was refluxed for 5 h. Treatment in the usual way gave a residue, which was purified by p-TLC (chloroform : methanol = 9 : 1) to afford **18** (11 mg, 93%) as a colorless powder. ^{1}H-NMR (200 MHz) δ: 7.10—6.92 (2H, m, 12- and 13-H), 6.53 (1H, dd, J = 7, 1.5 Hz, 14-H), 6.38 (1H, br d, J = 4 Hz, 9-H), 3.73 (1H, m, 2-Hβ), 3.38—3.08 (2H, m, 3-H and 2-Hα), 2.94 (1H, m, 5-H), 2.80—2.30 (4H, m, 4-H_{eq}, 7-H_2, and 8-H), 2.54 (3H, s, NMe), 1.44 (1H, br q, J = 11 Hz, 4-H_{ax}), 1.23 (3H, d, J = 7 Hz, 8-Me). High-resolution MS m/z: Calcd for $C_{16}H_{20}N_2$ (M^+) 240.1625. Found: 240.1626.

(±)-Isolysergine (19) A solution of the amine **18** (9 mg), phenylseleninic anhydride (6.7 mg), and indole (13 mg) in THF (2 ml) was heated at 40°C for 2 h. The solvent was partly evaporated off, and 10% aqueous sodium carbonate was added to the residue. The mixture was extracted with methylene dichloride. The extract was washed, dried, and evaporated to give a residue, which was purified by p-TLC (chloroform : methanol = 92 : 8) to afford (±)-isolysergine (**19**), mp 112—114 °C (from acetone–hexane). IR: 3500 (NH) cm^{-1}. ^{1}H-NMR (200 MHz) δ: 7.98 (1H, br s, NH), 7.28—7.14 (3H, m, 12—14-H), 6.94 (1H, br s, 2-H), 6.43 (1H, br dd, J = 5, 2 Hz, 9-H), 3.47 (1H, dd, J = 14, 6 Hz, 4-H_{eq}), 3.30 (1H, m, 5-H), 2.78 (1H, ddd, J = 14, 11, 2 Hz, 4-H_{ax}), 2.83—2.60 (2H, m, 7-H_2), 2.60 (3H, s, NMe), 2.54 (1H, m, 8-H), 1.21 (3H, d, J = 7 Hz, 8-Me). The IR and ^{1}H-NMR spectra and Rf value of (±)-(**19**) were found to be identical with those of a sample prepared by the reported procedure[14] from natural lysergene[19] provided by Professor Yamatodani. High-resolution MS m/z: Calcd for $C_{16}H_{18}N_2$ (M^+) 238.1468. Found: 238.1461.

(3β)-2,3-Dihydroagroclavine (20) Sodium (10 mg) was added in small portions over 10 min to liquid ammonia (*ca.* 100 ml), and a solution of the amine **16** (55 mg) in THF (1 ml) was added dropwise to the resulting solution. The mixture was stirred for a further 1 h before excess of ammonium chloride was added to stop the reaction. Ammonia was evaporated off, the residue was treated with water and the mixture was extracted with methylene dichloride. The extract was dried and evaporated to give a crystalline residue, which was recrystallized from ether to give **20** (30 mg, 94%) as colorless crystals, mp 139—141 °C. IR: 3400 (NH) cm^{-1}. ^{1}H-NMR (200 MHz) δ: 7.09 (1H, t, J = 8 Hz, 13-H), 6.79 (1H, d, J = 8 Hz, 12-H), 6.57 (1H, d, J = 8 Hz, 14-H), 6.02 (1H, br s, 9-H), 3.69 (1H, m, 2-Hβ), 3.60 (1H, m, 2-Hα), 3.50 (1H, m, 10-H), 3.40—3.00 (4H, m, 1-H, 3-H, and 7-H_2), 2.57 (1H, ddd, J = 11, 9.5, 2 Hz, 5-H), 2.49 (1H, m, 4-H_{eq}), 2.45 (3H, s, NMe), 1.74 (3H, br s, 8-Me), 1.54 (1H, q, J = 11 Hz, 4-H_{ax}). High-resolution MS m/z: Calcd for $C_{16}H_{20}N_2$ (M^+) 240.1626. Found: 240.1630.

(±)-Agroclavine (21) A mixture of **20** (15 mg), phenylseleninic anhydride (10.5 mg) and indole (20.6 mg) in THF (4.5 ml) was heated at 40°C for 1.5 h. Following work-up as described for the preparation of **19**, (±)-agroclavine (**21**) (13.2 mg, 89%) was obtained, mp 182—184 °C (dec.)

(from ether) (lit.[20] mp 189—191 °C (dec.)). ^{1}H-NMR (200 MHz) δ: 7.98 (1H, br s, NH), 7.20—7.03 (3H, m, 12—14-H), 6.94 (1H, br s, 2-H), 6.20 (1H, br s, 9-H), 3.76 (1H, br, $W_{1/2}$ = 18 Hz, 10-H), 3.34 (1H, dd, J = 14, 4 Hz, 4-H$_{eq}$), 3.26 (1H, br d, J = 15 Hz, 7-H$_{eq}$), 2.96 (1H, br d, J = 15 Hz, 7-H$_{ax}$), 2.80 (1H, ddd, J = 14, 12, 1.5 Hz, 4-H$_{ax}$), 2.56 (1H, ddd, J = 12, 9, 4 Hz, 5-H), 2.52 (3H, s, NMe), 1.79 (3H, br s, 8-Me). The IR and ^{1}H-NMR spectra and *Rf* value of (±)-(**21**) were found to be identical with those of natural agroclavine provided by Professor Yamatodani. High-resolution MS *m/z*: Calcd for $C_{16}H_{18}N_2$ (M^+) 238.1468. Found: 238.1476.

(3α,10α)-8,9-Didehydro-2,3-dihydro-1-[(4-methoxyphenyl)sulfonyl]-6,8-dimethylergoline (22) According to the dehydration procedure described for **11**, treatment of **14** (115 mg) and thionyl chloride (5 ml) in benzene (25 ml) followed by purification by p-TLC (methylene dichloride: methanol = 95 : 5) gave **22** (70 mg, 64%) as a colorless glass. IR: 1354, 1160 (NSO_2) cm^{-1}. ^{1}H-NMR (200 MHz) δ: 7.80 (2H, br d, J = 8 Hz, ArH), 7.37 (1H, d, J = 8 Hz, 14-H), 7.20 (1H, t, J = 8 Hz, 13-H), 7.00—6.90 (3H, m, 12-H and ArH), 5.28 (1H, br s, 9-H), 4.25 (1H, dd, J = 10, 8 Hz, 2-Hβ), 3.85 (3H, s, OMe), 3.73 (1H, br, $W_{1/2}$ = 13 Hz, 10-H), 3.25 (1H, dd, J = 12.5, 10 Hz, 2-Hα), 3.19 (1H, m, 5-H), 3.01 (1H, m, 3-H), 2.92 (2H, br s, 7-H$_2$), 2.56 (3H, s, NMe), 2.07 (1H, m, 4-H$_{eq}$), 1.60 (3H, br s, 8-Me), 1.20 (1H, q, J = 12 Hz, 4-H$_{ax}$). High-resolution MS *m/z*: Calcd for $C_{23}H_{26}N_2O_3S$ (M^+) 410.1663. Found: 410.1677.

(±)-Agroclavine I (24) According to the deprotection procedure described for **16**, deprotection of **22** (41 mg) in liquid ammonia (*ca.* 50 ml) with sodium (8 mg) gave (3β)-2,3-dihydroagroclavine I (**23**) as a colorless glass. ^{1}H-NMR (200 MHz) δ: 7.08 (1H, t, J = 8 Hz, 13-H), 6.70 (1H, d, J = 8 Hz, 12-H), 6.52 (1H, d, J = 8 Hz, 14-H), 5.40 (1H, br s, 9-H), 3.76 (1H, br, $W_{1/2}$ = 12 Hz, 10-H), 3.68 (1H, m, 2-Hβ), 3.30 (1H, ddd, J = 12, 5.5, 3 Hz, 5-H), 3.20—3.04 (2H, m, 2-Hα and 3-H), 2.96 (2H, br s, 7-H$_2$), 2.60 (3H, s, NMe), 2.16 (1H, ddd, J = 12, 4, 3 Hz, 4-H$_{eq}$), 1.63 (3H, br s, 8-Me), 1.38 (1H, m, 4-H$_{ax}$). Without purification, a mixture of **23**, phenylseleninic anhydride (17 mg) and indole (33 mg) in THF (6 ml) was heated at 40 °C for 2 h. Following work-up as described for the preparation of **19**, (±)-agroclavine I (**24**) (17 mg, 71% from **22**) was obtained, mp 152—154 °C (from ether) (lit.[13] mp 157—158 °C). ^{1}H-NMR (200 MHz) δ: 7.98 (1H, br s, NH), 7.26—6.98 (3H, m, 12—14-H), 6.90 (1H, br s, 2-H), 5.57 (1H, br s, 9-H), 4.03 (1H, br, 10-H), 3.46 (1H, dt, J = 10, 5 Hz, 5-H), 3.18 (2H, br s, 7-H$_2$), 3.04 (1H, dd, J = 15, 5 Hz, 4-H$_{eq}$), 2.87 (1H, br dd, J = 15, 10 Hz, 4-H$_{ax}$), 2.64 (3H, s, NMe), 1.67 (3H, br s, 8-Me). The ^{1}H-NMR data for (±)-(**24**) were found to be identical with those reported for natural agroclavine I.[11] High-resolution MS *m/z*: Calcd for $C_{16}H_{18}N_2$ (M^+) 238.1468. Found: 238.1451.

(3β,8α,9β)-2,3-Dihydro-1-[(4-methoxyphenyl)sulfonyl]-6,8-dimethylergolin-9-ol (26) According to the mesylation procedure described for **9**, treatment of the alcohol **11** (50 mg) in pyridine (1 ml) with mesyl chloride (0.4 ml) at room temperature for 5 h gave the mesylate **25**. ^{1}H-NMR (60 MHz) δ: 4.70 (1H, dd, J = 11, 5 Hz, 9-H), 3.80 (3H, s, OMe), 2.96 (3H, s, OMs), 2.27 (3H, s, NMe), 1.33 (3H, d, J = 7 Hz, 8-Me). Without purification, the mesylate **25** was dissolved in DMSO (1.85 ml) containing 18-crown-6-ether (150 mg). Potassium superoxide (50 mg) was added to the resulting solution, and the mixture was stirred vigorously at room temperature for 1 h. Then water was added to the reaction mixture, and the whole was extracted repeatedly with ethyl acetate. The combined extracts were washed with brine, dried, and evaporated. The residue was purified by p-TLC (chloroform : methanol = 92 : 8) to afford the alcohol **26** (27 mg, 54%) and the unsaturated amine **17** (5 mg, 10%), which was identical with the sample prepared from **15** upon comparison of their *Rf* values and IR and ^{1}H-NMR spectra. **26**: mp 149—152 °C (colorless crystals from ether–methylene dichloride). IR: 1355, 1160 (NSO_2) cm^{-1}. ^{1}H-NMR (200 MHz) δ: 7.83 (2H, br d, J = 8 Hz, ArH), 7.43 (1H, d, J = 8 Hz, 14-H), 7.24 (1H, t, J = 8 Hz, 13-H), 7.02—6.91 (3H, m, 12-H and ArH), 4.32 (1H, br s, 9-H), 4.25 (1H, m, 2-Hβ), 3.86 (3H, s, OMe), 3.28—3.10 (2H, m, 2-Hα and 3-H), 2.95 (1H, br d, J = 10 Hz, 10-H), 2.73 (1H, br dd, J = 10, 4 Hz, 7-H$_{ax}$), 2.60 (1H, br d, J = 10 Hz, 7-H$_{eq}$), 2.50 (1H, br t, J = 10 Hz, 5-H), 2.47 (1H, br d, J = 10 Hz, 4-H$_{eq}$), 2.36 (3H, s, NMe), 2.06 (1H, m, 8-H), 1.25 (1H, m, 4-H$_{ax}$), 1.20 (3H, d, J = 7 Hz, 8-Me). High-resolution MS *m/z*: Calcd for $C_{23}H_{28}N_2O_4S$ (M^+) 428.1774. Found; 428.1768.

(±)-Fumigaclavine B (28) According to the deprotection procedure described for **16**, deprotection of **26** (29 mg) in liquid ammonia (*ca.* 50 ml) with sodium (5 mg) gave (3β)-2,3-dihydrofumigaclavine B (**27**) as a colorless powder. ^{1}H-NMR (200 MHz) δ ($CDCl_3$–CD_3OD): 7.06 (1H, t, J = 8 Hz, 13-H), 6.74 (1H, d, J = 8 Hz, 12-H), 6.58 (1H, d, J = 8 Hz, 14-H), 4.36 (1H, br s, 9-H), 3.64 (1H, m, 2-Hβ), 3.22—3.03 (2H, m, 2-Hα and 3-H), 2.96 (1H, br d, J = 10 Hz, 10-H), 2.81 (1H, dd, J = 12, 4 Hz, 7-H$_{ax}$), 2.74—2.44 (3H, m, 4-H$_{eq}$, 5-H, and 7-H$_{eq}$), 2.40 (3H, s, NMe), 2.05 (1H, m, 8-H), 1.34 (1H, m, 4-H$_{ax}$), 1.23 (3H, d, J = 7 Hz, 8-Me). Without purification, a mixture of **27**, phenylseleninic anhydride (12 mg) and indole (22 mg) in THF (6 ml) was heated at 40 °C for 2 h. Following work-up as described for the preparation of **19**, (±)-fumigaclavine (**28**) (13 mg, 76% from **26**) was obtained, mp 198—200 °C (dec.) (from 95% ethanol). ^{1}H-NMR (200 MHz) δ: 8.02 (1H, br s, NH), 7.18—6.96 (3H, m, 12—14-H), 6.86 (1H, br s, 2-H), 4.50 (1H, br s, 9-H: 10% intensity increase upon irradiation at δ 1.26 and 11% intensity increase upon irradiation at δ 2.12), 3.34 (1H, d, J = 11 Hz, 4-H$_{eq}$), 3.29 (1H, br d, J = 9 Hz, 10-H: 16% intensity increase upon irradiation at δ 1.26), 2.81 (1H, dd, J = 11, 4 Hz, 7-H$_{ax}$: 4% intensity increase upon irradiation at δ 2.12), 2.68 (1H, td, J = 11, 1.5 Hz, 4-H$_{ax}$), 2.58 (1H, dd, J = 11, 2 Hz, 7-H$_{eq}$: 5% intensity increase upon irradiation at δ 1.26), 2.58 (1H, m, 5-H), 2.41 (3H, s, NMe), 2.12 (1H, m, 8-H: 14% intensity increase upon irradiation at δ 1.26), 1.26 (3H, d, J = 7 Hz, 8-Me). The IR and ^{1}H-NMR spectra of (±)-(**28**) were found to be identical with those of natural fumigaclavine B provided by Dr. Polonsky. High-resolution MS *m/z*: Calcd for $C_{16}H_{20}N_2O$ (M^+) 256.1574. Found: 256.1568.

(3β,8α,9α)-2,3-Dihydro-9-methanesulfonyloxy-8-methanesulfonyloxymethyl-1-[(4-methoxyphenyl)sulfonyl]-6-methylergoline (29) Mesyl chloride (0.2 ml) was added to a solution of the *trans*-diol **8** (120 mg) in pyridine (3 ml) at 0 °C, and the solution was stirred at room temperature for 5 h. The resulting solution was worked up in the same manner as described for the preparation of **10**, and the residue was recrystallized from methylene dichloride–methanol to give the dimesylate **29** (144 mg, 85%) as colorless needles, mp 162—163 °C (dec.). IR: 1360, 1175, 1160 (NSO_2 and OSO_2) cm^{-1}. ^{1}H-NMR (60 MHz) δ: 4.90 (1H, m, 9-H), 4.61 (2H, m, 8-C$\underline{H}_2$OMs), 3.80 (3H, s, OMe), 3.03 and 3.00 (each 3H, s, Ms × 2), 3.26 (3H, s, NMe). *Anal.* Calcd for $C_{25}H_{32}N_2O_9S_3 \cdot 1/5CH_2Cl_2$: C, 49.00; H, 5.29; N, 4.54. Found: C, 49.14; H, 5.27; N, 4.56.

(3α,8α,9α,10α)-2,3-Dihydro-9-methanesulfonyloxy-8-methanesulfonyloxymethyl-1-[(4-methoxyphenyl)sulfonyl]-6-methylerogoline (30) According to the mesylation procedure described above, treatment of the *cis*-diol **12** (120 mg) in pyridine (3 ml) with mesyl chloride (0.2 ml) gave the dimesylate **30** (138 mg, 81%), mp 182—184 °C (dec.) (colorless crystals from methylene dichloride–methanol). IR: 1360, 1180, 1160 (NSO_2 and OSO_2) cm^{-1}. ^{1}H-NMR (60 MHz) δ: 4.82 and 4.59 (each 1H, m, 8-C$\underline{H}_2$OMs), 4.54 (1H, m, 9-H), 4.27 (1H, m, 3-H), 3.85 (3H, s, OMe), 3.09 and 2.60 (each 3H, s, Ms × 2), 2.46 (3H, s, NMe). *Anal.* Calcd for $C_{25}H_{32}N_2O_9S_3$: C, 49.99; H, 5.37; N, 4.66. Found: C, 49.72; H, 5.42; N, 4.67.

(3β)-9,10-Didehydro-2,3-dihydro-1-[(4-methoxyphenyl)sulfonyl]-6-methyl-8-methyleneergoline (31) From the *trans*-dimesylate **29**: Potassium *tert*-butoxide (120 mg) was added to a solution of the dimesylate **29** (144 mg) in DMSO (3 ml) at 10 °C, and the resulting solution was stirred at room temperature for 2 h. Water was added to the reaction mixture and the whole was extracted with ethyl acetate. The extract was washed, dried and evaporated. The residue was purified by p-TLC (ethyl acetate) to give the diene **31** (48 mg, 52%), mp 147—149 °C (dec.) (pale yellow needles from ethyl acetate). IR: 1600 (diene), 1360, 1160 (NSO_2) cm^{-1}. ^{1}H-NMR (200 MHz) δ: 7.71 (2H, br d, J = 8 Hz, ArH), 7.35 (1H, d, J = 8 Hz, 14-H), 7.22 (1H, d, J = 8 Hz, 12-H), 7.14 (1H, t, J = 8 Hz, 13-H), 6.86 (2H, br d, J = 8 Hz, ArH), 6.79 (1H, br s, 9-H), 4.99 and 4.88 (each 1H, br s, C=C$\underline{H}_2$), 4.22 (1H, br t, J = 7 Hz, 2-Hβ), 3.78 (3H, s, OMe), 3.40 (1H, d, J = 14 Hz, 7-H$_{eq}$), 3.30—3.04 (4H, m, 2-Hα, 3-H, 5-H, and 7-H$_{ax}$), 2.38 (1H, dt, J = 12, 4 Hz, 4-H$_{eq}$), 2.34 (3H, s, NMe), 1.21 (1H, q, J = 12 Hz, 4-H$_{ax}$). *Anal.* Calcd for $C_{23}H_{24}N_2O_3S \cdot 1/3H_2O$: C, 66.64; H, 6.00; N, 6.75. Found; C, 66.49; H, 5.73; N, 6.60. From the *cis*-dimesylate **30**: According to the procedure described above, treatment of a solution of the *cis*-dimesylate **30** (138 mg) in DMSO (3 ml) with potassium *tert*-butoxide (120 mg) gave the diene **31** (45 mg, 51%), which was identical with the sample prepared from the *trans*-dimesylate **30** upon comparison of their *Rf* values and IR and ^{1}H-NMR spectra.

(±)-Lysergene (33) According to the deprotection procedure described for **17**, deprotection of **31** (24 mg) in DME (5 ml) with lithium aluminum hydride (30 mg) gave (3β)-2,3-dihydrolysergene (**32**) as a yellow powder. IR: 3400 (NH), 1620 (diene) cm^{-1}. ^{1}H-NMR (60 MHz) δ: 6.77 (1H, br s, 9-H), 4.98 and 4.86 (each 1H, br s, C=C$\underline{H}_2$), 2.43 (3H, s, NMe). Without purification, a mixture of **32**, phenylseleninic anhydride (6.5 mg) and indole (14.5 mg) in THF (4 ml) was heated at 40 °C for 2 h. Following work-up as described for the preparation of **19**, (±)-lysergene (**33**) (8 mg, 58% from **31**) was obtained, mp 210—212 °C (dec.) (from acetone). ^{1}H-NMR (200 MHz) δ ($CDCl_3$–CD_3OD): 7.34—7.26 (3H, m, 12—14-H), 7.02 and 6.98 (each 1H, br s, 2- and 9-H), 5.12 and 5.01 (each 1H, br s, C=C$\underline{H}_2$), 3.60—3.20 (4H, m, 4-H$_{eq}$, 5-H, and 7-H$_2$), 2.77 (1H, ddd, J = 14, 11, 2 Hz, 4-H$_{ax}$), 2.58 (3H, s, NMe). The IR and ^{1}H-NMR spectra and *Rf* value of

(±)-(**33**) were found to be identical with those of natural lysergene.[19] High-resolution MS *m/z*: Calcd for $C_{16}H_{16}N_2$ (M^+) 236.1312. Found: 236.1322.

Reaction of the Diene 31 with Sodium in Liquid Ammonia According to the deprotection procedure given for **16**, treatment of the diene **30** (28 mg) in liquid ammonia (*ca.* 15 ml) with sodium (5 mg) gave a mixture of **20** and **23** in the ratio of 2:1, which was, without purification, dehydrogenated with phenylseleninic anhydride (10 mg) and indole (22 mg) in THF (6 ml) at 40 °C for 2 h. Usual work-up followed by purification by p-TLC (methylene dichloride : methanol = 92 : 8) afforded (±)-agroclavine (**21**) (6.5 mg, 45%) and (±)-agroclavine I (**24**) (3.1 mg, 23%). These products were identical with the sample prepared from **16** and **22** upon comparison of their *Rf* values and IR and ^{1}H-NMR spectra, respectively.

Acknowledgements We thank Professor S. Yamatodani of Kobe Women's University, Japan, for samples of natural agroclavine and lysergene, and Dr. J. Polonsky of I. C. S. N., Gif-sur-Yvette, France, for the specimen of natural fumigaclavine B. We are grateful to Misses H. Kamioka and Y. Shinohara for technical assistance.

References

1) Part XXXII: T. Naito, O. Miyata, N. Kida, K. Namoto, and I. Ninomiya, *Chem. Pharm. Bull.*, **38**, 2419 (1990).
2) Preliminary communications: T. Kiguchi, C. Hashimoto, and I. Ninomiya, *Heterocycles*, **22**, 43 (1984); *idem*, *ibid.*, **23**, 1925 (1985); *idem*, *ibid.*, **23**, 2891 (1985).
3) I. Ninomiya, C. Hashimoto, T. Kiguchi, and T. Naito, *J. Chem. Soc., Perkin Trans. 1.* **1985**, 941.
4) I. Ninomiya, C. Hashimoto, T. Kiguchi, T. Naito, D. H. R. Barton, X. Lusinchi, and P. Milliet, *J. Chem. Soc., Perkin Trans. 1*, **1990**, 707.
5) I. Ninomiya and T. Kiguchi, "The Alkaloids," Vol. 38, ed. A. Brossi, Academic Press, New York, 1990, Chapter 1.
6) I. Ninomiya, C. Hashimoto, T. Kiguchi, and T. Naito, *Chem. Pharm. Bull.*, **34**, 2799 (1986).
7) D. E. Nichols, J. M. Robinson, G. S. Li, J. M. Cassady, and H. G. Floss, *Org. Prep. Proced. Int.*, **9**, 277 (1977).
8) M. Braun and C. Bernard, *Justus Liebigs Ann. Chem.*,**1985**, 435.
9) B. Umezawa, O. Hoshino, and S. Sawaki, *Chem. Pharm. Bull.*, **17**, 1115 and 1120 (1969).
10) H. M. Bell, C. W. Vanderslice, and A. Spehar, *J. Org. Chem.*, **34**, 3923 (1969).
11) V. G. Sakharovsky and A. G. Kozlovsky, *Tetrahedron Lett.*, **25**, 109 (1984).
12) A. P. Kozikowski and P. D. Stein, *J. Am. Chem. Soc.*, **107**, 2569 (1985).
13) M. Somei, F. Yamada, and Y. Makita, *Heterocycles*, **26**, 895 (1987).
14) Y. Nakahara, T. Niwaguchi, and H. Ishii, *Chem. Pharm. Bull.*, **25**, 1756 (1977).
15) J. F. Spilsbury and S. Wilkinson, *J. Chem. Soc.*, **1961**, 2085.
16) N. J. Bach, H. E. Boaz, E. C. Kornfeld, C. J. Chang, H. G. Floss, E. W. Hagaman, and E. Wenkert, *J. Org. Chem.*, **39**, 1272 (1974).
17) B. Arnoux, M. A. Merrien, C. Pascard, J. Polonsky, and P. M. Scott, *J. Chem. Res. (S)*,**1978**, 210.
18) E. J. Corey, K. C. Nicolaou, M. Shibasaki, Y. Machida, and C. S. Shiner, *Tetrahedron Lett.*, **1975**, 3183.
19) S. Yamatodani and M. Abe, *Nippon Nogei Kagaku Kaishi*, **34**, 424 (1960).
20) M. Somei, Y. Makita, and F. Yamada, *Chem. Pharm. Bull.*, **34**, 948 (1986).

Electroreductive Synthesis of Bicyclic Ketones Mediated by Cobalt or Nickel Complexes

Shigeko OZAKI,* Toshikazu NAKANISHI, Mari SUGIYAMA, Chie MIYAMOTO, and Hidenobu OHMORI

Faculty of Pharmaceutical Sciences, Osaka University 1-6, Yamadaoka, Suita, Osaka 565, Japan. *Received June 14, 1990*

Fused and spiro carbocyclic compounds were synthesized by electrochemical reductions of bromoalkylcyclohexenones using cobalt or nickel complexes as mediators.

Keywords electrochemical reduction; mediator; cobalt complex; nickel complex; bromoalkylcyclohexenone; bicyclic ketone; conjugated addition

The conjugated addition reactions of organometallic nucleophile to α,β-enones are useful synthetic methods for the formation of fused[1] and spiro[1,2] carbocyclic rings. These addition reactions often require the rigid control of temperature and protection from moisture or oxygen owing to the high sensitivity of the reagents used. The construction of carbocyclic rings by VB_{12} mediated electrochemical reduction of bromoalkylcyclohexenones[3] could be a potential synthetic replacement for the usual methods using organometallic reagents, owing to the fact that the reaction can conveniently be performed at ambient temperature without any protection from moisture. In such carbocyclic rings formation, the alkyl–cobalt(III) complexes, which are formed as intermediates[3,4] by the reaction of alkyl bromide with electrogenerated Co(I) complexes, have been shown to exhibit the nucleophilic reactivity on further reduction in the same way as in many other electrochemical reductions catalyzed by VB_{12}.[5,6] Recently the transient alkyl–Ni(III)complex was reported to be formed also in the electrochemical reduction of $Br(CH_2)_4CN$ mediated by Ni(II) macrocycle, (*R,R,S,S*)-Ni(tmc),[7] as well as in the reaction of CH_3I with Ni(I) (OEiBC),[8] a model compound of the co-factor of F-430. These studies suggest the possibility that electroreductively generated Co(I) or Ni(I) complexes with ligands which do not so closely resemble those of VB_{12} or the co-factor of F 430 may also work in the electrochemical reduction of bromoalkanes as well as VB_{12} or Ni(II) (OEiBC). Little is yet known about the electrochemical and structural features which make VB_{12} and its close analogues so effective as catalysts in electrochemical and chemical reductions, though there are many useful reactions which employ them.

In this paper we report the electroreductive synthesis of bicyclic ketones by intramolecular conjugated addition of alkyl bromides to 2-cyclohexen-1-ones using the square-planar cobalt or nickel complexes as mediators and we explore the structural demands for the cobalt or nickel complexes to function effectively as mediators in the reaction.

Results and Discussion

Preparation and Electrochemical Behavior of the Cobalt and Nickel Complexes The cobalt(III) and nickel(II) complexes and a cobalt(II) complex (Co(bae)) reported here were prepared according to the literature methods (see Experimental). All of the complexes involve coordination of tetradentated neutral or dianionic ligands in a square-planar manner (Chart 1). Except for cyclam, (*trans*-[14]aneN$_4$) and CR, (Me_2[14]py-dieneN$_4$), the ligands of the complexes are open-chain and have different degrees and positions of unsaturation.

Measurements of the proton nuclear magnetic resonance (^{1}H-NMR) spectra of these complexes were performed except for Co (cyclam)$ClO_4 \cdot Cl_2$,[9] Ni (cyclam) $(ClO_4)_2$,[10] and Ni (CR) $(ClO_4)_2$[10] which showed insufficient solubility in various solvents. The ^{1}H-NMR signals of two Co(III) complexes with neutral ligands, Co(III) (bpmp) I_3 and Co(III) (bpep) $I_2 \cdot OH$, appear in the range from -19.4 to 34.9 ppm and from 2.4 to 31.0 ppm, respectively (see Experimental). These unusually large variations in the shielding of the hydrogen nuclei indicate that the complexes are paramagnetic in the solvents used for the measurements.[11] Measurements of the magnetic moments of these two Co(III) complexes by Evans method,[12] however, were not successful owing to insufficient solubility of the complexes in every solvent examined. The ^{1}H-NMR signals

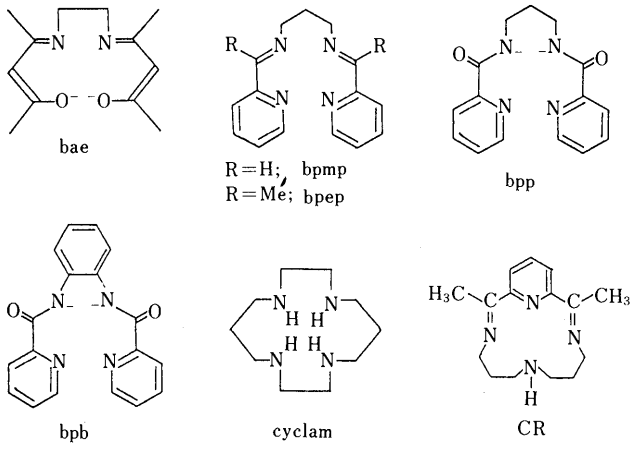

Chart 1

Abbreviations are given in the Experimental section.

TABLE I. The Potentials of Redox Couples Observed by Cyclic Voltammetry[a]

Complex	M(III)/M(II)	M(II)/M(I)	
Co (bae)		−1.91/−1.81	
Ni (bae)		−2.24/−1.96	
Co (bpmp) I_3	−0.78/−0.70	−1.08/−0.93	−1.52/−1.26
Co (bpep) $I_2 \cdot OH$	−0.77/−0.60	−1.20/−1.13	−1.65/−1.57
Co (bpp) AcO	−0.48/−0.29	−1.50/−1.24	−2.12/−1.80
Ni (bpp)		−1.59/−1.53	−2.20/−2.10
Co (bpb) Cl	−0.25/−0.15	−1.37/−1.30	−2.12/−2.04
Ni (bpb)		−1.58/−1.49	−2.03/−1.92
Co (cyclam) Cl_2	−0.49/−0.39		−2.05[b]
Ni (cyclam) $(ClO_4)_2$		−1.59/−1.48	
Ni (CR) $(ClO_4)_2$		−0.75/−0.67	−1.25/−1.15

a) Volt *vs.* SCE, measured using 3 mM complex in DMF containing 0.1 M TEAP at a scan rate of 0.1 V/s under inert gas. *b*) Irreversible.

of Co(III) and Ni(II) complexes with dianionic ligands, Co (bae), Ni (bae), Co (bpp) AcO, Ni (bpp), Co (bpb) Cl, and Ni (bpb) are in the ordinary range, 0 to 10 ppm, which would suggest that these complexes are diamagnetic.

As a preliminary to the electrochemical reduction of bromoalkylcyclohexenones using these complexes as mediators, the electrochemical properties of the complexes were examined by cyclic voltammetry. As shown in Table I, all complexes showed at least one well-defined reversible or quasi-reversible peak in the potential range of -0.25 to -2.20 V *vs.* SCE.

The tentative assignment of peaks was performed on the basis of comparisons with those cited in the literatures.[9,10] The potentials of the redox couples corresponding to Co(II)/Co(I) and Ni(II)/Ni(I) are much less negative than those of the substrates, 2- or 3-bromoalkyl-2-cyclohexenones ($E_p < -2.28$ V *vs.* SCE). The potentials of the redox couples with dianionic ligands are a little more negative than those of complexes with neutral ligands. It was examined by cyclic voltammetry if the electroreductively generated transient intermediates, Co(I) or Ni(I) complexes, react as nucleophiles with the 2- or 3-bromoalkyl-2-cyclohexenones. A one-electron or a two-electron nucleophilic transfer from Ni(I) (bpb) to 2-(4-bromobutyl)-2-cyclohexen-1-one was, in fact, indicated by the comparison of the cyclic voltammogram of Ni (bpb) alone with that of Ni (bpb) including 2-(4-bromobutyl)-2-cyclohexen-1-one, (Fig. 1A), in which the reversible wave which corresponds to the Ni(II)/Ni(I) couple became irreversible with an increase of the peak height corresponding to reduction of Ni(II) (bpb). The use of excess amount of NH_4Br, which would be added in preparative electrolysis of the bromoalkylcyclohexenones as a proton source, reduced the reversibility of the redox couple of Ni (bpb), namely the peak height of reduction of Ni(II) (bpb) was increased and that of oxidation of Ni(I) (bpb) was reduced to less than one-half (Fig. 1B). As shown in cyclic voltammetry of Co(III) (bpep) (Fig. 1C), a redox couple corresponding to Co(II)/Co(I) at $-1.20/-1.13$ V became irreversible on saturation with molecular oxygen, while that corresponding to Co(III)/Co(II) remained, though its reversibility was reduced. These cyclic voltammetric properties of the Co or Ni complexes indicate that the proton donor, NH_4Br and molecular oxygen react with the active intermediates, Co(I) or Ni(I) complexes, as well as the substrate. Other complexes listed in Table I also showed similar behavior to Ni (bpb) or Co (bpep) in cyclic voltammetry.

We could not assign the peak corresponding to reduction of the postulated intermediate, alkyl–Ni(I) or alkyl–Co(I) complexes.[4]

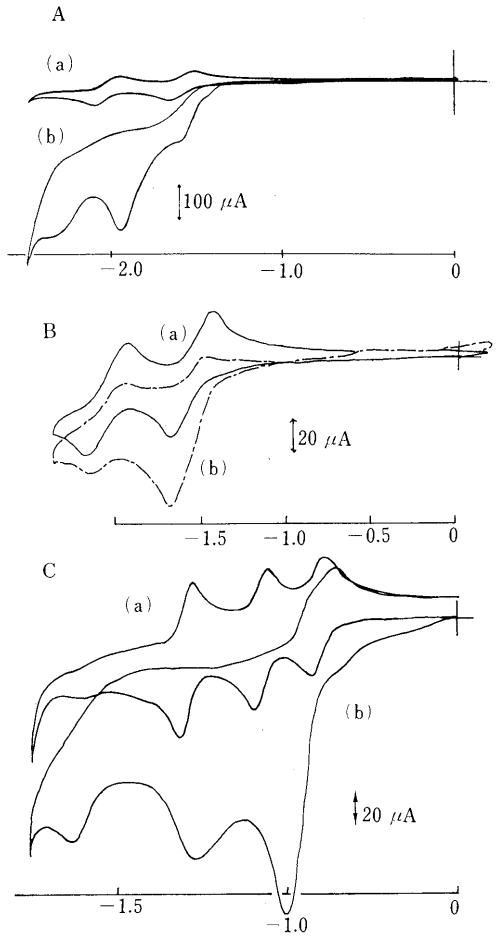

Fig. 1A. Cyclic Voltammograms of Ni(bpb) (3 mM) in DMF, 0.1 M TEAP, at a Scan Rate of 0.10 V/s

(a) Ni(bpb) alone. (b) Ni(bpb) with 2-(4-bromobutyl)-2-cyclohexen-1-one (20 mM) and NH_4Br (40 mM).

Fig. 1B. Cyclic Voltammograms of Ni(bpb) (3 mM) in DMF, 0.1 M TEAP, at a Scan Rate of 0.10 V/s

(a) Ni(bpb) alone. (b) Ni(bpb) with NH_4Br (5 mM).

Fig. 1C. Cyclic Voltammograms of Co(bpep) (3 mM) in DMF, 0.1 M TEAP at a Scan Rate of 0.10 V/s

(a) Co(bpep) alone. (b) Co(bpep) after saturation of O_2.

Controlled Potential Electrolysis of 2-, or 3-Bromoalkyl-2-cyclohexen-1-ones Mediated by Cobalt or Nickel Complexes Based on the results of cyclic voltammetry, electrolysis of 2-, or 3-bromoalkyl-2-cyclohexen-1-one was performed in *N*,*N*-dimethylformamide (DMF) containing a substrate (10 mM), the cobalt or nickel complex (3 mM), NH_4Br or NH_4ClO_4 (20 mM) as a proton source, and a supporting electrolyte, Et_4NClO_4 (0.1 M) at a potential about 0.4 V more negative than the redox couple corresponding to Co(II)/Co(I) or Ni(II)/Ni(I),[4] except for the case of using Co (bae) or Ni (bae) (Table I), under an atmosphere of inert gas in the dark. The electrolysis of **1** and **4** leads to two types of products, *i.e.*, bicyclic ketones **2** and **5**, respectively, which are formed by 1,4-addition, and alkylcyclohexenones **3** and **6** formed by reductive protolysis (Chart 2).

Results of the electrolysis of bromoalkylcyclohexenones **1** and **4** are summarized in Tables II and III.

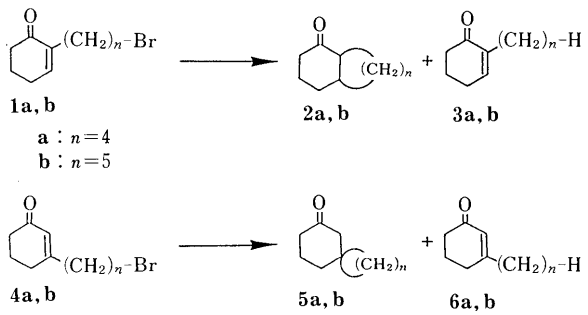

Chart 2

The total yields of bicyclic ketones and alkylcyclohexenones ranged from 23% to 86% depending on the structure of the complexes. The complexes with macrocyclic ligands, *i.e.*, cyclam and CR, seem to be somewhat more effective than those with open-chain ligands. Co(bpmp) which has hydrogens sensitive to dehydrogenation is a less effective catalyst than Co(bpep) of which ligand has the same structure as Co(bpmp), except for that the hydrogens are substituted by methyl groups. The applied potentials (−1.2 to −2.0 V) seem to have no distinct effect on the yields. On changing the length of the side-chain in the bromocyclohexenones from 4 to 5, the yields of bicyclic ketones decreased and those of alkylcyclohexanones increased with the exception of the electrolysis of **4** using Ni (cyclam) as a mediator. The formation of bicyclic ketones **2** was not stereospecific. No products which would be formed by 1,2-addition were detected by gas liquid chromatography (GLC). Nearly the same yields and distribution of products were obtained in either electrolysis performed under visible light or in the dark when Co (bpb), Ni (bpb), or Ni (cyclam) were used as mediator. In the electolyses performed without any complex, only a small amount of an alkylcyclohexenone, **3a** or **6a**, was formed. When Co(cyclam), which shows a redox couple Co(II)/Co(I) at −0.49/−0.39 V was used as a mediator, electrolysis of the substrates did not proceed. In some electrolyses, the electrolyte which was originally colored by the complex used, became turbid, then the electric current decreased rapidly. This could be caused partly by irreversible oxygenation of the transient low valent Co(I), Co(II), Ni(I) complexes by molecular oxygen remaining in the electrolytes.[13] The differences in the yields of products among complexes seem to depend partly on how effectively molecular oxygen is removed from the electrolytes.

No distinct difference in catalytic behavior was found between cobalt and nickel complexes. Reaction schemes are proposed for the specific case of 3-(4-bromobutyl)-2-cyclohexen-1-one as a substrate and a Co(III) complex as a mediator, though the postulated intermediate has not been isolated yet.

The electroreductively generated Co(I) complex B would react with 3-(4-bromobutyl)-2-cyclohexen-1-one through a two-electron nucleophilic pathway to give an intermediate, alkyl cobalt(III) complex C. On further reduction of the alkyl cobalt(III) complex C, the carbon–cobalt bond in C acts as a carbanionic nucleophile in the internal carbon–

TABLE II. Electroreduction of 2-Bromoalkyl-2-cyclohexen-1-ones (**1**) Mediated by Ni or Co Complex[a]

Complex	$E_{app.}$ V *vs.* SCE	Products and yield (%)[b] **2**[c]		**3**	
		$n=4$	$n=5$	$n=4$	$n=5$
Co (bae)	−1.7	19	6	12	17
Ni (bae)	−2.0	52	26	2	13
Co (bpmp) I_3	−1.5	15	14	10	13
Co (bpep) I_2·OH	−1.7	41	18	16	17
Co (bpp) AcO	−1.7	52	28	5	21
Ni (bpp)	−1.8	53	30	2	7
Co (bpb) Cl	−1.7	53	19	1	18
Ni (bpb)	−1.6	48	42	0	15
Ni (cyclam) $(ClO_4)_2$	−1.8	70	33	6	18
Ni (CR) $(ClO_4)_2$	−1.2	60	42	1	14
Blank	−1.7	0	0	29	0

a) Electrolysis using 10 mM substrate, 3 mM complex, and 20 mM NH_4Br or NH_4ClO_4 in DMF containing 0.1 M TEAP under an inert gas in the dark unless otherwise stated. *b*) Based on the substrate; determined by GLC. *c*) Mixture of *cis* and *trans* (1 : 1.4—1 : 2).

TABLE III. Electroreduction of 3-Bromoalkyl-2-cyclohexen-1-ones (**4**) Mediated by Ni or Co Complex[a]

Complex	$E_{app.}$ V *vs.* SCE	Products and yield (%)[b] **5**		**6**	
		$n=4$	$n=5$	$n=4$	$n=5$
Co (bae)	−1.7	22	9	11	16
Ni (bae)	−2.0	40	33	7	27
Co (bpmp) I_3	−1.5	12	11	5	15
Co (bpep) I_2·OH	−1.7	31	17	6	12
Co (bpp) AcO	−1.8	47	40	11	13
Ni (bpp)	−1.8	43	44	18	17
Co (bpb) Cl	−1.7	45	12	1	18
Ni (bpb)	−1.9	45	20	3	18
Ni (cyclam) $(ClO_4)_2$	−1.8	30	65	4	21
Ni (CR) $(ClO_4)_2$	−1.2	42	16	4	19
Blank	−1.7	0	0	33	0

a) Under the same condition as stated in Table II. *b*) Based on a substrate; determined by GLC.

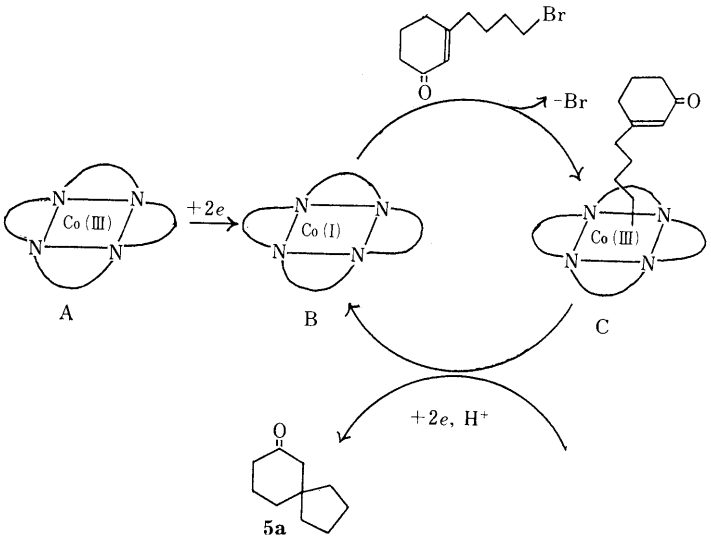

Fig. 2

carbon bond formation to give the Co(I) complex B and a spirocycle **5a** *via* a conjugated addition. It has been shown that the cleavage reaction of the alkyl–cobalt bond has to be much faster than the rate of Co(I) alkylation in a cobalt complex mediated electroreduction of bromoalkanes.[4] That study seemed to suggest that excessively stable intermediates (alkyl–metal complexes) and insufficient applied potential for reductive cleavage of the alkyl–metal bond are not desirable. It is not certain if the applied potentials used in the present electrolyses, which were decided based on the cyclic voltammetric behavior of the complexes, are sufficient so that reductive cleavage of alkyl–cobalt or alkyl–nickel bonds can proceed quickly enough that a photolytic cleavage of the alkyl–metal bond[3] becomes negligible, though the products which would be formed through coupling of radical species were not observed in the electrolyses carried out under visible light. As shown by the cyclic voltammograms of Ni (bpb) with excess NH_4Br (Fig. 1B), unfavorable protonation of Ni(I) (bpb) will occur competitively with the electrophilic attack of a substrate, a bromoalkane, on Ni(I) (bpb) when an excess amount of NH_4Br is present. This may indicate that the effective mediator in electroreductions of bromoalkanes should combine the properties of being a very strong nucleophile toward the substrates with being a weak base toward proton.[8] The acid-promoted dissociation of complexes, which results in the metal loss from complexes, has been shown to be much slower for cyclic tetraamine complexes than for open-chain ones.[14] The observed differences in catalytic behavior between complexes with macrocyclic ligands and those with open-chain ligands may be partly attributed to the difference in rate between these processes.

Further investigations to improve the conditions of electrolysis and the structure of complexes so as to obtain efficient catalysts for electrochemical reductions leading to carbon–carbon bond formations are in progress.

Experimental

Instrumentation GLC were performed on a JEOL JGC-20K chromatograph with a PEG 20M glass column (2 m long, 3 mm diameter). GLC integrations were done with a Takeda Riken TR-2215A integrator. NMR spectra were taken on a JEOL FX-90Q, or a Hitachi R-600 instrument. Chemical shifts are reported relative to Me_4Si or residual protons of deuterated NMR solvents. Visible and UV spectra were taken on a Hitachi 124 spectrophotometer. Infrared (IR) spectra were taken on a JASCO A 202 instrument.

Synthesis All complexes were synthesized according to the literature with slight modifications and purified repeatedly by recrystallizations until the complexes gave well defined reversible or quasi-reversible couples in cyclic voltammetry. The synthesized complexes gave appropriate elemental analyses. ^{1}H-NMR spectra were taken for all compounds except for Co (cyclam), Ni (cyclam) and Ni (CR), which showed poor solubility in deuterated NMR solvents. Co (bae), bisacetylacetone–ethylenediiminocobalt(II),[15] orange needles, mp > 155 °C (dec.) ^{1}H-NMR (90 MHz, $CDCl_3$) δ: mixture of tautomers, 5.06 and 4.99 (2H, s, CH), 3.80—2.73 (4H, m, CH_2CH_2), 2.01 and 1.88 (12H, s, CH_3). Ni (bae),[16] reddish brown plates, mp 199—200 °C. ^{1}H-NMR (90 MHz, $CDCl_3$) δ: 4.90 (2H, s, CH), 3.04 (4H, s, CH_2CH_2), 1.86 (12H, s, CH_3). Co (cyclam), [Co(III) [14]ane N_4 Cl_2 ClO_4],[17] pale green amorphous solid, mp > 280 °C. Ni(II) (cyclam) $(ClO_4)_2$,[10] orange needles, mp > 280 °C (dec.). Co (bpb), *N,N'*-bis(2'-pyridinecarboxamide)-1,2-benzenediaminocobalt(III) chloride hydrate,[18] yellowish brown amorphous solid, mp > 280 °C (dec.). ^{1}H-NMR (90 MHz, methanol-d_4) δ: 9.13 (2H, d, J = 6 Hz, Ph), 8.83—8.32 (2H, m, pyridines), 8.22—7.95 (6H, m, pyridines), 7.26—6.80 (2H, m, Ph). Ni(II) (bpb),[18] dark red amorphous solid, mp > 280°C. ^{1}H-NMR (90 MHz, DMSO-d_6) δ: 8.18 (2H, d, J = 5 Hz, Ph), 8.10—7.82 (4H, m, pyridines), 7.40—7.66 (4H, m, pyridines), 6.75—7.14 (2H, m, Ph). Co(bpp), *N,N'*-bis(2'-pyridinecarboxamide)-1,3-propanediaminocobalt(III) monoacetate,[18] dark brown amorphous solid. mp > 280°C (dec.). ^{1}H-NMR (90 MHz, $CDCl_3$) δ: 7.28—8.36 (8H, m, pyridines), 3.36—4.10 (2H, m, $CH_2C\underline{H}_2CH_2$), 1.83 (3H, s, CH_3CO), 1.16—1.43 (4H, m, $C\underline{H}_2CH_2C\underline{H}_2$). Ni(II) (bpp),[18] reddish brown amorphous solid, mp > 280 °C (dec.). ^{1}H-NMR (90 MHz, $CDCl_3$) δ: 8.19—7.79 (6H, m, pyridines), 7.65 (2H, s, pyridines), 1.65 (6H, s, $CH_2CH_2CH_2$). Co (bpmp), *N,N'*-bis(2'-pyridylmethylidene-1,3-propanediaminocobalt(III) triiodide,[19] dark brown amorphous solid, mp > 280 °C (dec.). ^{1}H-MNR (90 MHz, MeOH-d_4) δ: 34.9 (4H, s, pyridines), 17.7 (4H, s, pyridines), 8.68—6.00 (2H, m, $CH_2C\underline{H}_2CH_2$), 1.1—0.1 (4H, m, $C\underline{H}_2CH_2C\underline{H}_2$), −19.4 (2H, s, =CH). Co (bpep), *N,N'*-bis(2'-pyridylethylidene)-1,3-propanediaminocobalt(III) diiodide hydroxide,[20] brown amorphous solid, mp > 280 °C (dec.). ^{1}H-NMR (90 MHz, D_2O) δ: 31.0 (4H, s, pyridines), 16.9 (4H, s, pyridines), 16.5 (6H, s, CH_3), 9.3—7.1 (2H, m, $CH_2C\underline{H}_2CH_2$), 2.7—2.2 (4H, m, $C\underline{H}_2CH_2C\underline{H}_2$). Ni (CR), Ni(II) ($Me_2$[14]py-dieneN$_4$) $(ClO_4)_2$,[21] reddish brown needles, mp 272—274 °C (dec.).

2-(4-Bromobutyl)-2-cyclohexen-1-one, **1a**, 2-(5-bromopentyl)-2-cyclohexen-1-one, **1b**,[22] 3-(4-bromobutyl)-2-cyclohexen-1-one, **4a**,[23,24] and 3-(5-bromopentyl)-2-cyclohexen-1-one, **4b**, were prepared according to the cited references. **1a** was obtained as a pale yellow oil by silica gel column chromatography with *n*-hexane–AcOEt (20 : 1) as the eluent. ^{1}H-NMR (90 MHz, $CDCl_3$) δ: 6.68 (1H, t, J = 4 Hz, C=CH–), 3.41 (2H, t, J = 7 Hz, $-CH_2Br$), 2.41—1.70 (12H, m, methylenes). **1b** was obtained as colorless oil by silica gel column chromatography with *n*-hexane–AcOEt (20 : 1) as the eluent. ^{1}H-NMR (60 MHz, $CDCl_3$) δ: 6.72 (1H, s, C=CH–), 3.40 (2H, t, J = 6 Hz, $-CH_2Br$), 2.53—1.31 (14H, m, methylenes). IR (neat): 2920, 1670 (C=O) cm^{-1}. **4a** was obtained as a pale yellow liquid (bp. 122 °C/1.5 mmHg). ^{1}H-NMR (60 MHz, $CDCl_3$) δ: 5.89 (1H, s, C=CH–), 3.43 (2H, t, J = 6 Hz, $-CH_2Br$), 2.47—1.65 (12H, m, methylenes). IR (neat): 2900, 1650 (C=O), 1625 (C=C) cm^{-1}. **4b** was obtained as a colorless liquid (bp 122 °C/1.5 mmHg). ^{1}H-NMR (60 MHz, $CDCl_3$) δ: 5.73 (1H, s, C=CH–), 3.32 (2H, t, J = 6Hz, $-CH_2Br$), 2.40—1.33 (14H, m, methylenes). IR (film): 1670 (C=O), 1625 (C=C) cm^{-1}. 2-Butyl-2-cyclohexen-1-one, **3a**, and 2-pentyl-2-cyclohexen-1-one, **3b**, were prepared by the same method as that used for preparation of 2-(4-bromobutyl)-2-cyclohexen-1-one but using bromobutane and bromopentane, respectively, in place of 1,4-dibromobutane and 1,5-dibromopentane. **3a** was obtained as a colorless liquid (bp 52—54 °C/1 mmHg). ^{1}H-NMR (60 MHz, $CDCl_3$) δ: 6.63 (1H, br, C=CH–), 2.48—0.90 (15H, m, $-CH_3$ and methylenes). IR (film): 2950, 1670 (C=O) cm^{-1}. **3b** was obtained as a colorless liquid (bp 73—76 °C/1 mmHg). ^{1}H-NMR (60 MHz, $CDCl_3$) δ: 6.58 (1H, br, C=CH–), 2.46—0.88 (17H, m, $-CH_3$ and methylenes). IR (film): 2950, 1670 (C=O) cm^{-1}. 3-Butyl-2-cyclohexen-1-one, **6a**, and 3-pentyl-2-cyclohexene-1-one, **6b**, were prepared by the same method as that used for preparation of 3-(4-bromobutyl)-2-cyclohexen-1-one using chlorobutane and chloropentane, respectively, instead of 4-chloro-2-butoxy-2-tetrahydropyran and 5-chloro-2-pentoxy-2-tetrahydropyran. **6a** was obtained as a colorless liquid (bp 83—89 °C/3 mmHg). ^{1}H-NMR (60 MHz, $CDCl_3$) δ: 5.89 (1H, s, C=CH–), 2.46—0.92 (15H, m, $-CH_3$ and methylenes). IR (film): 1670 (C=O), 1620 (C=C) cm^{-1}. **6b** was obtained as a colorless liquid (bp 119 °C/10 mmHg). ^{1}H-NMR (60 MHz, $CDCl_3$) δ: 5.79 (1H, s, C=CH–), 2.42—1.05 (14H, m, methylenes), 0.90 (3H, t, J = 4 Hz, $-CH_2CH_3$). IR (film): 2930, 1665 (C=O), 1620 (C=C) cm^{-1}.

Spiro(4,5)decan-7-one was prepared according to the literature.[2] The crude compound was purified after being transformed into a bisulfite compound using sodium bisulfite.

Colorless oil, ^{1}H-NMR (60 MHz, $CDCl_3$) δ: 2.25 (4H, s), 2.0—0.80 (12H, m). IR (film): 2900, 1710 (C=O), 1450, 1230 cm^{-1}. Spiro(5,5)undecan-8-one was prepared and purified by the same method as used for spiro(4,5)decan-7-one but with 1,5-dibromopentane instead of 1,4-dibromobutane. ^{1}H-NMR (60 MHz, $CDCl_3$) δ: 2.5—2.0, 2.18 (4H, m, s), 2.0—1.5 (4H, m), 1.35 (4H, s), 1.21 (6H, s). IR (film): 2900, 1715 (C=O), 1455 cm^{-1}. Perhydrobenzocyclohepten-1-one, **2b** was prepared and purified according to the literature.[23] Colorless oil, ^{1}H-NMR (60 MHz, $CDCl_3$) δ: 2.6—2.1 (3H, m), 2.1—1.0 (15H, m). DMF was purified by distillation under reduced pressure (70 °C/39 mmHg) after desiccation over $MgSO_4$.

Tetraethylammonium perchlorate (TEAP) was prepared by adding an aqueous solution of tetraethylammonium bromide to perchloric acid (70%) and recrystallized successively from hot water and ethanol. All other chemicals were used without purification.

Cyclic Voltammetry Cyclic voltammetry was performed with a three electrode system employing a linear scanning unit (Huso Electrochemical

System, model HECS 321B) equipped with a potentiostat (Hokuto Denko Ltd., model HR 101B). The electrode system consisted of a glassy-carbon indicator electrode, a glassy-carbon counter electrode and a SCE. Measurements were carried out with a substrate concentration of 3 mM and a sweep rate of 0.1 V s^{-1}.

Controlled Potential Electrolysis Controlled potential electrolysis was carried out with a potentiostat (Hokuto Denko Ltd., model HA 101 or HA 105S) and the quantity of consumed electricity was measured with a coulombmeter (Hokuto Denko Ltd., model HF 201 or HF 102). The electrolyses were generally performed with 10 mM substrate, 3 mM catalyst and 20 mM NH_4Br or NH_4ClO_4 in 10 ml of DMF containing 0.1 M TEAP using an H-type divided cell with a glassy-carbon plate electrode and mechanical stirring under a stream of nitrogen or argon in the dark or under visible light. The products from electroreduction were isolated by column chromatography and identified by comparison of their spectroscopic (IR and ^{1}H-NMR) data with those of authentic samples.

References

1) T. L. Macdonald and S. Mahalingam, *J. Am. Chem. Soc.*, **102**, 2113 (1980).
2) P. A. Wender and A. W. White, *J. Am. Chem. Soc.*, **110**, 2218 (1988) and references cited therein.
3) R. Scheffold, M. Dike, S. Dike, T. Herold, and L. Welder, *J. Am. Chem. Soc.*, **102**, 3642 (1980).
4) D. Lexa, *J. Electroanal. Chem.*, **100**, 159 (1979).
5) L. Walder, G. Lytz, K. Meier, and R. Scheffold, *Helv. Chim. Acta*, **61**, 3013 (1978).
6) *a*) A. Fischli, *Helv. Chim. Acta*, **61**, 2560 and 3028 (1978); *b*) *Idem*, *ibid.*, **62**, 882 (1979); *c*) A. Fischli and D. Suss, *ibid.*, **62**, 48 and 2361 (1979); *d*) A. Fischli and P. Müller, *ibid.*, **63**, 529 (1980); *e*) R. Scheffold and E. Amble, *Angew. Chem. Int. Ed. Engl.*, **19**, 629 (1980).
7) A. Bakac and J. H. Espenson, *J. Am. Chem. Soc.*, **108**, 5353 (1986).
8) A. M. Stolzenberg and M. T. Stershic, *J. Am. Chem. Soc.*, **110**, 5397 (1988).
9) *a*) A. M. Tait, F. V. Lovecchio, and D. H. Busch, *Inorg. Chem.*, **16**, 2206 (1977); *b*) D. H. Busch, *Acc. Chem. Res.*, **11**, 392 (1978).
10) *a*) F. V. Lovecchio, E. S. Gore, and D. H. Busch, *J. Am. Chem. Soc.*, **96**, 3109 (1974); *b*) L. Fabbirizzi, A. Perotti, A. Profumo, and T. Soldi, *Inorg. Chem.*, **25**, 4256 (1986).
11) J. W. Emsley, J. Feeney and L. H. Sutcliffe, "High Resolution Nuclear Magnetic Resonance Spectroscopy," Vol. 2, Pergamon Press, New York, 1966, p. 826.
12) D. F. Evans, *J. Chem. Soc.*, **1959**, 2003.
13) *a*) B. Durham, T. J. Anderson, J. A. Switzer, J. F. Endicott, and M. D. Glick, *Inorg. Chem.*, **16**, 271 (1977); *b*) C.-L. Wong, J. A. Switzer, K. D. Balakrishnan, and J. F. Endicott, *J. Am. Chem. Soc.*, **102**, 5511 (1980); *c*) A. Bakac and J. H. Espenson, *ibid.*, **112**, 2273 (1990).
14) L.-H. Chen and C.-S. Chung, *Inorg. Chem.*, **27**, 1880 (1988).
15) G. Schwarzenbach and K. Litz, *Helv. Chim. Acta*, **23**, 1139 (1940).
16) P. J. MaCcarthy, R. J. Hovey, K. Ueno, and A. E. Martell, *J. Am. Chem. Soc.*, **77**, 5820 (1955).
17) B. Bosnich, C. K. Doon, and M. L. Tobe, *Inorg. Chem.*, **4**, 1102 (1965).
18) R. L. Chapman and R. V. Vagg, *Inorg. Chim. Acta*, **33**, 27 (1979).
19) T. G. Campbell and F. L. Urbach, *Inorg. Chem.*, **12**, 1836 (1973).
20) D. A. Stotter and J. Trotten, *J. Chem. Soc., Dalton Trans.*, **1977**, 868.
21) J. L. Kahn and D. H. Busch, *Inorg. Chem.*, **8**, 1149 (1969).
22) *a*) D. F. Taber, *J. Org. Chem.*, **41**, 2649 (1976); *b*) M. A. Guaciaro, P. M. Wovkulich, and A. B. Smith, *Tetrahedron Lett.*, **47**, 4661 (1978); *c*) C. Shih, E. L. Fritzen, and J. S. Swenton, *J. Org. Chem.*, **45**, 4462 (1980).
23) J. M. Conia and F. Rouessac, *Tetrahedron*, **16**, 45 (1961).
24) R. D. Rieke and S. E. Bales, *J. Am. Chem. Soc.*, **96**, 1775 (1974).

Conjugated-Triene Intermediates in the Sommelet–Hauser Rearrangement of Cyclic 1-Methyl-2-phenylammonium 1-Methylides

Fumihiko SUMIYA, Naohiro SHIRAI, and Yoshiro SATO*

Faculty of Pharmaceutical Sciences, Nagoya City University, Tanabe-dori, Mizuho-ku, Nagoya 467, Japan. *Received June 22, 1990*

Fluoride ion-induced desilylation of 1-methyl-1-(trimethylsilyl)methyl-2-(2-substituted phenyl)pyrrolidinium (3a), -piperidinium (3b and 3c), and -perhydroazepinium iodides (3d and 3e) gave high yields of eight- (5a), nine- (5b and 5c), and ten-membered cyclic amines (5d, 5e, 6d and 6e), containing conjugated-triene bond systems. These triene products are intermediates in the Sommelet–Hauser rearrangement of cyclic 1-methyl-2-phenylammonium 1-methylides (4), and were isomerized to the corresponding Sommelet–Hauser rearrangement products (7) in the presence of a strong base or an acid (except for 5b). Heating of these trienes in xylene yielded mixtures of the Stevens rearrangement products (8) and ring-opened amines (9). Selective formation of 8 was achieved by ultraviolet irradiation of the trienes (5) in hexane. The reaction mechanisms are discussed.

Keywords ylide; Sommelet–Hauser rearrangement; desilylation; ring expansion; conjugated triene; fluoride; sigmatropic rearrangement; cyclic amine

We previously reported that the reaction of 1-methyl-1-(trimethylsilyl)methyl-2-(2-substituted phenyl)piperidinium iodides (**3b** and **3c**, $n=2$) with cesium fluoride in *N,N*-dimethylformamide (DMF) gave good yields of 2-methyl-1,3,4,5,6,11a-hexahydro-2*H*-2-benzazonines (**5b** and **5c**, $n=2$, nine-membered cyclic amines), which were regarded as unstable intermediates in the Sommelet–Hauser rearrangement of 1-methyl-2-(2-substituted phenyl)piperidinium 1-methylides (**4b** and **4c**, $n=2$) to 2-methyl-2,3,4,5,6,7-hexahydro-1*H*-2-benzazonines (**7b** and **7c**, $n=2$).[1] As a further extension of this work, we tried to obtain eight- and ten-membered cyclic amines by the desilylation reaction of 1-methyl-1-(trimethylsilyl)methyl-2-phenylpyrrolidinium (**3a**, $n=1$) and 1-methyl-1-(trimethylsilyl)methyl-2-(2-substituted phenyl)perhydroazepinium iodides (**3d** and **3e**, $n=3$), and compared the chemical properties of the eight-, nine- and ten-membered cyclic amines, which contain conjugated triene bonds.

Results and Discussion

Three starting amines, 2-phenyl-1-[(trimethylsilyl)methyl]pyrrolidine (**2a**) and 2-(2-substituted phenyl)-1-[(trimethylsilyl)methyl]perhydroazepines (**2d** and **2e**) were prepared by reaction of 2-phenylpyrrolidine (**1a**) and 2-(2-substituted phenyl)perhydroazepines (**1d** and **1e**) with (halogenomethyl)trimethylsilane.

Quaternization of **2** with iodomethane proceeded in refluxing acetonitrile to give the cyclic ammonium iodides (**3**); however, they were obtained as hygroscopic oils and were difficult to crystallize. The desilylation reaction of **3** with cesium fluoride, therefore, was carried out *in situ* at room temperature after the quaternization in DMF at 60 °C.

The reaction of **2a** gave 2-methyl-1,2,3,4,5,10a-hexahydro-2-benzazocine (**5a**) as a sole product in 68% yield, similar to the formation of **5b**, **c** from **2b**, **c**[1] (entries 1—3 in Table I). However, **2d** and **2e** afforded mixtures of geometrical isomers of 2-methyl-1,2,3,4,5,6,7,12a-octahydro-2-benzazecine (**5d** and **6d**) and the 9-methyl substituted analogs (**5e** and **6e**) (entries 4 and 5). The structures of these products were confirmed by H–H correlation spectroscopy (COSY) nuclear magnetic resonance (NMR) analyses at 400 MHz. The major isomer from **2e** was assigned as **5e** (*E*-form) from observation of nuclear Overhauser effect (NOE) enhancements of the two vinylic protons (8-H and

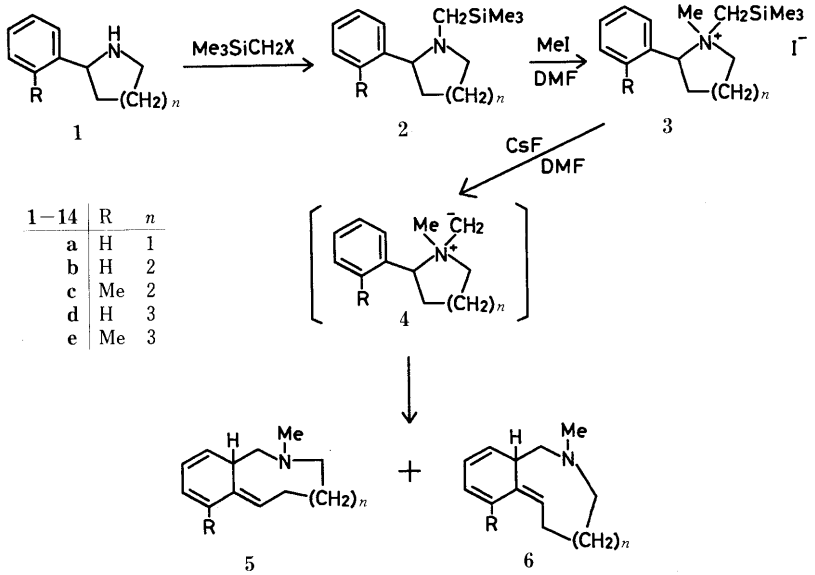

Chart 1

10-H) upon irradiation of the 9-methyl resonance. A similar NOE on **5c** was reported previously.[1] The major product from **2d** was also assigned as **5d** from a comparison of the chemical shifts in the ^{1}H-NMR spectra with those of **5e**. The minor products from **2d** and **2e** were assigned as **6d** and **6e**, respectively.

Compounds **5b—d** could be stored as hexane solutions without appreciable decomposition for more than a month in a refrigerator(−20 °C), though the neat oils decomposed slowly at room temperature. Compounds **5a**, **5e**, **6d** and **6e** slowly decomposed even in dilute solutions at low temperature.

Thus, the ylides **4** were exclusively converted into the conjugated-triene compounds **5** and **6** by ring expansion, but not into the Sommelet–Hauser rearrangement products **7** under non-basic conditions. The ylide **4a** or **4b** produced by the reaction of 1,1-dimethyl-2-phenylpyrrolidinium or 1,1-dimethyl-2-phenylpiperidinium salts with sodium amide in liquid ammonia, contrary to the above, gave only the Sommelet–Hauser rearrangement products, 2-methyl-1,2,3,4,5,6-hexahydro-2-benzazocine (**7a**)[2] and 2-methyl-2,3,4,5,6,7-hexahydro-1*H*-2-benzazonine (**7b**).[3]

It seems that the formation of the Sommelet–Hauser rearrangement products **7** requires the presence of a strong base. When **5a**, **b** and **6d** were dissolved in a solution of 10% potassium hydroxide in ethanol, they were exclusively isomerized to **7a**, **7b** and 2-methyl-1,2,3,4,5,6,7,8-octahydro-2-benzazecine (**7d**), respectively, at room temperature (entries 1, 2, and 4 in Table II). The solution of **5d** was heated at 60 °C, because the conversion to **7d** was slow at room temperature (entry 3).

Thus, [1,3] hydrogen shift in the aromatization of **5** and **6** to **7** proceeds by the proton elimination–addition process assisted by bases. The rearrangement process can also be accelerated by strong acid. The addition of hydrogen chloride to a solution of **5a**, **d** or **6d** in hexane selectively gave **7a** or **7d** (entries 5, 7, and 8 in Table II). However, **5b** predominantly afforded *N*-methyl-5-phenylpentylamine (**13b**) as reported previously (entry 6).[1] When deuteriochloric acid was used in the reaction of **5a** or **5b**, a deuterium atom was found on the carbon at the 6-position of **7a** or at the benzylic position of **13b**, respectively (Chart 3).

This result indicates that the acid has two promotion routes; the addition of a proton (or deuterium) on the conjugated-triene bonds is followed by elimination of a proton from the angular carbon to give **7a** and **7d** (route

Table I. Reaction of Cesium Fluoride with Cyclic 1-Methyl-2-(2-substituted phenyl)-1-(trimethylsilyl)methylammonium Iodides (**3**) Prepared from Cyclic 2-(2-Substituted phenyl)-1-(trimethylsilyl)methylamines (**2**) with MeI

Entry	Starting compound	Reaction time (h) with MeI at 60 °C	Products, **5** and **6** Total yield (%)	Ratio **5**:**6**	UV absorption[a] λ_{max}, nm (log ε)
1	**2a**	7	68	100:0	315 (3.8)
2[b]	**2b**	6	74	100:0	318 (3.8)
3[b]	**2c**	6	69	100:0	319 (3.8)
4	**2d**	50	72	75:25	**5d**, 308 (3.8), **6d**, 313[d]
5	**2e**	50	24[c]	86:14	**5e**, 305,[d] **6e**, 302[d]

a) In *n*-hexane. *b*) Reference 1. *c*) Quaternization was not completed. *d*) Molar absorption coefficient was not determined due to the instability of the product.

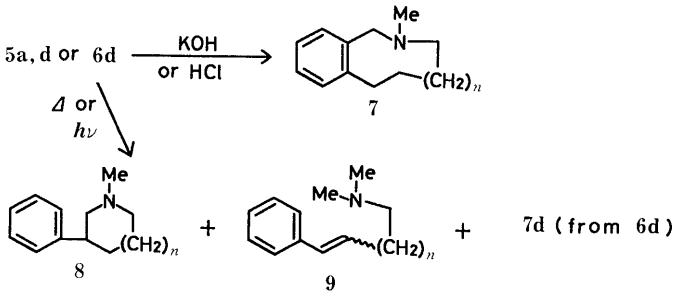

Chart 2

Table II. Isomerizations of **5** and **6** in the Presence of Acid or Base

Entry	Starting compound	*n*	Conditions: Base or acid	Temp. (°C)	Time (h)	Yield of **7** (%)
1	**5a**	1	KOH	rt	20	82
2[a]	**5b**	2	KOH	rt	24	78
3	**5d**	3	KOH	60	6	88
4	**6d**	3	KOH	rt	15	89
5	**5a**	1	HCl	rt	70	87
6	**5b**	2	HCl	rt	70	0[b]
7	**5d**	3	HCl	rt	70	87
8	**6d**	3	HCl	rt	70	82

a) Reference 1. *b*) *N*-Methyl-5-phenylpentylamine (**13b**) was obtained in 88% yield.[1]

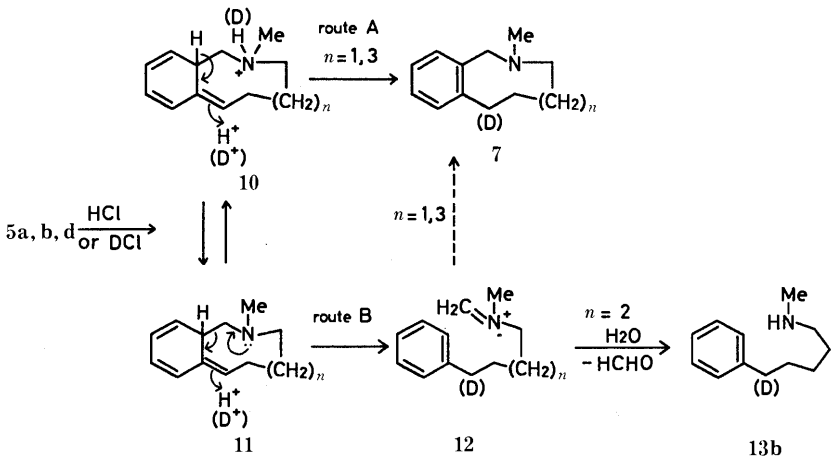

Chart 3

TABLE III. Isomerizations of **5** and **6** by Heating or UV Irradiation

Entry	Starting compound	*n*	Reaction conditions[a]	Products **8**, **9**, and **7** Total yield (%)	Ratio **8**:**9**:**7**
1	**5a**	1	Heat	86	71:29: 0
2[b]	**5b**	2	Heat	90	13:87: 0
3	**5d**	3	Heat	83	54:46: 0
4	**6d**	3	Heat	85	77:13:10
5	**5a**	1	*hv*	93	93: 7: 0
6	**5b**	2	*hv*	95	90:10: 0
7	**5b**	2	*hv*[c]	86	95: 5: 0
8	**5d**	3	*hv*	92	100: 0: 0

a) Heat: xylene solution was heated at reflux for 2 h; *hv*: hexane solution was irradiated at 10 °C with a 100 W medium-pressure mercury lamp for 2 h. *b*) Reference 1. *c*) Methanol solution.

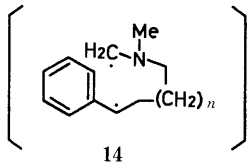

14

Fig. 1. Diradical Intermediate

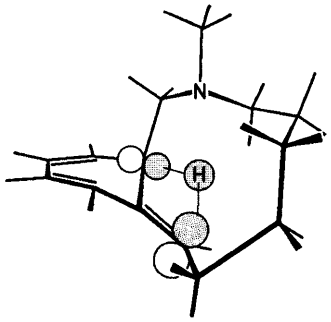

Fig. 2. A [1,3] Antarafacial Hydrogen Migration of **6d**

A in Chart 3), or is followed by ring-opening to give an iminium compound (**12**) which is hydrolyzed to **13b** during the aqueous work-up (route B). Compound **5b** showed an unusually large *Rf* value (0.73) on a thin layer chromatography (TLC) plate (Merck alumina, type E, 5% ether in hexane) in contrast to the small values of **5a** (*Rf* 0.17) and **5d** (*Rf* 0.50). This result suggests that the polarity (which may be regarded as basicity in this case) of **5b** is lower than those of the others. Although it is still unclear what is really inducing the low polarity, the low basicity of **5b** may permit the formation of **13b** *via* route B. There would be no remarkable difference of chemical behavior between **5a**, **5d** and **5b**, if **7a** and **7d** were produced from **12a** and **12d** by the Pictet–Spengler ring closure.

We previously reported that **5b** was converted smoothly in refluxing toluene into two isomers: 1-methyl-3-phenylperhydroazepine (**8b**) and (*E*)-*N*,*N*-dimethyl-5-phenyl-4-pentenylamine (**9b**).[1] Heating of **5a**, **d** or **6d** in refluxing xylene also gave mixtures of **8a**, **d** and **9a**, **d** (entries 1, 3, and 4 in Table III). These compounds may be produced by homolyses of the C–C bonds in **5** or **6**, giving diradical intermediates (**14**), followed by recombination or hydrogen transfer similar to that discussed previously for **5b**.[1] Formation of small amounts of **7d** was observed only from **6d** (entry 4). Although the isomerization from **5** to **7** by a thermal [1,3] hydrogen sigmatropic rearrangement is symmetry-forbidden, the conformation of **6d** may permit a [1,3] antarafacial migration.[4]

A [1,3] migration of carbon is allowed under photochemical conditions, and indeed, ultraviolet (UV) irradiation of **5a**, **5b** or **5d** in hexane (or methanol) resulted in selective formation of **8** (entries 5—8 in Table III).

Experimental

All reactions were carried out under a nitrogen or argon atmosphere. DMF was distilled under reduced pressure from barium oxide. Cesium fluoride was dried over phosphorus pentoxide at 180 °C under reduced pressure. ^{1}H-NMR spectra were recorded on a JEOL JNM MH-100, a FX-100, or a GSX-400 spectrometer using Me_4Si as an internal standard. Chemical shifts are reported in ppm (δ), and signals are described as s (singlet), d (doublet), t (triplet), m (multiplet) or br (broad). Infrared (IR) spectra were recorded on a Jasco IRA-2 spectrometer. Mass spectra (MS) were measured on a JEOL JMS-DX 300 GC-MS system (electron ionization (EI) or chemical ionization (CI)). Gas liquid chromatographic (GLC) analyses were performed on a Hitachi 263-30 gas chromatograph with a flame ionization detector using a 2 m column of 5% polyethylene glycol 20M on Uniport HP. Preparative and analytical high-performance liquid chromatography (HPLC) were carried out on a Tosoh CCP 8000 system. UV spectra were recorded on a Shimadzu UV-240 spectrophotometer. Melting points and boiling points are uncorrected. Distillation was performed in a Büchi Kugelrohr distillation apparatus.

2-Phenyl-1-[(trimethylsilyl)methyl]pyrrolidine (2a) A solution of 2-phenylpyrrolidine[5] (**1a**, 5.43 g, 36.7 mmol) and (chloromethyl)trimethylsilane (2.15 g, 17.6 mmol) in dimethyl sulfoxide (DMSO, 40 ml) was heated at 80 °C for 20 h. The reaction mixture was poured into water and extracted with diethyl ether (about 42% of **1a** was recovered from the aqueous layer). The ether layer was washed with 1% Na_2CO_3, dried ($MgSO_4$), and concentrated under reduced pressure. Acetic anhydride (4 ml) was added to the residue at room temperature to remove unreacted **1a**, and the mixture was stirred overnight. Then 10% hydrochloric acid was added and the whole was extracted with ether. The acid layer was made alkaline with sodium hydroxide and extracted with ether. The ethereal extract was dried ($MgSO_4$), concentrated, and distilled to give **2a** (3.58 g, 88%), bp 146 °C (15 mmHg, oven temperature). ^{1}H-NMR ($CDCl_3$): 0.00 (9H, s, Me_3Si), 1.45 and 2.09 (2H, AB q, J=14.1 Hz, CH_2Si), 1.55—1.65 (1H, m), 1.71—1.82 (1H, m), 1.82—1.94 (1H, m), 2.04—2.12 (1H, m), 2.18 (1H, apparent q, J=8.8 Hz, 5-H), 3.06 (1H, t, J=8.0 Hz, 2-H), 3.28 (1H, m, 5-H), 7.19—7.25 (1H, m), 7.27—7.35 (4H, m). *Anal.* Calcd for $C_{14}H_{23}NSi$: C, 72.04; H, 9.95; N, 6.00. Found: C, 71.97; H, 10.02; N, 5.85.

2-Phenyl-1-[(trimethylsilyl)methyl]perhydroazepine (2d) A solution of 2-phenylperhydroazepine[6] (**1d**, 2.58 g, 14.7 mmol) and (iodomethyl)-trimethylsilane (1.58 g, 7.37 mmol) in DMSO (20 ml) was heated at 80 °C for 20 h. The reaction mixture was worked up in a similar manner to that described above. Distillation of the extract gave **2d** (1.33 g, 63%), bp 150 °C (6 mmHg, oven temperature). ^{1}H-NMR ($CDCl_3$): −0.04 (9H, s, Me_3Si), 1.42—1.93 (8H, m), 1.94 (2H, s, CH_2Si), 2.78 (1H, ddd, J=1.9, 8.8, 14.4 Hz, 7-H), 2.92 (1H, ddd, J=2.4, 7.1, 14.4 Hz, 7-H), 3.50 (1H, t, J=6.0 Hz, 2-H), 7.15—7.19 (1H, m), 7.25—7.29 (2H, m), 7.35—7.38 (2H, m). *Anal.* Calcd for $C_{16}H_{27}NSi$: C, 73.51; H, 10.43; N, 5.36. Found: C, 73.62; H, 10.23; N, 5.51.

2-(2-Methylphenyl)-1-[(trimethylsilyl)methyl]perhydroazepine (2e) *O*-Methylcaprolactim was treated with 2-methylphenyllithium to give 2-(2-methylphenyl)-3,4,5,6-tetrahydro-2*H*-azepine according to the reported method.[7] Reduction of the crude product with lithium aluminum hydride was carried out in ether overnight at room temperature to give 2-(2-methylphenyl)perhydroazepine (**1e**, total yield 6%), bp 155 °C (10 mmHg, oven temperature). ^{1}H-NMR ($CDCl_3$): 1.55—1.95 (9H, m), 2.35 (3H, s, CH_3Ar), 2.85 (1H, m, 7-H), 3.18 (1H, m, 7-H), 3.93 (1H, dd, J=3.3, 9.9 Hz, 2-H), 7.08—7.13 (2H, m), 7.14—7.20 (1H, m), 7.45 (1H, d, J=7.5 Hz). *Anal.* Calcd for $C_{13}H_{19}N$: C, 82.48; H, 10.12; N, 7.40. Found: C, 82.58; H, 10.29; N, 7.17.

A solution of **1e** (1.293 g, 6.8 mmol) and (iodomethyl)trimethylsilane (745 mg, 3.5 mmol) in DMSO (5 ml) was heated at 100 °C for 14 h. The reaction mixture was poured into water and extracted with ether. The extract was dried ($MgSO_4$) and concentrated under reduced pressure. The residual oil was chromatographed on an alumina column (hexane) to give

2e (420 mg, 44%), bp 140 °C (1.5 mmHg, oven temperature). ^{1}H-NMR ($CDCl_3$): −0.05 (9H, s, Me_3Si), 1.38—1.80 (8H, m), 1.85 and 1.89 (2H, AB q, J=14.6 Hz, CH_2Si), 2.31 (3H, s, CH_3Ar), 2.82 (1H, ddd, J=2.0, 8.8, 14.5 Hz, 7-H), 2.92 (1H, ddd, J=2.6, 6.7, 14.5 Hz, 7-H), 3.66 (1H, dd, J=2.0, 6.2 Hz, 2-H), 7.07—7.10 (2H, m), 7.13—7.17 (1H, m), 7.60 (1H, d, J=7.5 Hz). *Anal.* Calcd for $C_{17}H_{29}NSi$: C, 74.11; H, 10.61; N, 5.08. Found: C, 74.49; H, 11.05; N, 4.87.

Ylide Formation Reaction A solution of **2** (2 mmol) and iodomethane (1.7 g, 12 mmol) in DMF (10 ml) was heated at 60 °C for the time listed in Table I. Then the excess of iodomethane and 3 ml of DMF were distilled off under reduced pressure. Cesium fluoride (1.52 g, 10 mmol) was added, and the mixture was stirred at room temperature for 20 h. The reaction mixture was poured into 1% Na_2CO_3 (200 ml) and extracted with ether (4 × 100 ml). The ether layer was washed with 1% Na_2CO_3 (3 × 100 ml), dried ($MgSO_4$), and concentrated under reduced pressure to give **5** and **6**. The results are listed in Table I. Compounds **5** and **6** were isolated on an HPLC column (Merck Hibar LiChrosorb NH_2, 250 mm × 10 mm). The eluates were monitored at 235 nm with a UV detector. The mobile phases at 5 ml/min were programed as follows. For **5a**, hexane for 2 min then linearly to a mixture of 20% ether in hexane for 5 min. A fraction of retention time 7.5 min was collected and concentrated. For **5d** and **6d**, from 0 to 20% ether in hexane linearly for 20 min. Fractions of 4.6 min (**5d**) and 5.9 min (**6d**) were collected. For **5e** and **6e**, from 0 to 20% ether in hexane linearly for 10 min. Fractions of 4.4 min (**5e**) and 5.9 min (**6e**) were collected.

2-Methyl-1,2,3,4,5,10a-hexahydro-2-benzazocine (5a) An undistillable oil (the purity was judged to be >98% by HPLC). ^{1}H-NMR ($CDCl_3$): 1.45—1.54 (1H, m, 4-H), 1.84—1.93 (1H, m, 4-H), 2.00—2.10 (1H, m, 1-H), 2.17—2.27 (1H, m, 5-H), 2.44 (3H, s, CH_3N), 2.47—2.58 (3H, m, 1-H, 3-H), 2.59—2.70 (1H, m, 5-H), 3.52 (1H, br s, 10a-H), 5.69—5.78 (3H, m, 6-H, 8-H, 10-H), 5.97 (1H, dd, J=5.0, 10.0 Hz, 9-H), 6.07 (1H, d, J=9.5 Hz, 7-H).

(*Z*)-2-Methyl-1,2,3,4,5,6,7,12a-octahydro-2-benzazecine (5d)[8] An undistillable oil (the purity was judged to be >98% by HPLC). ^{1}H-NMR ($CDCl_3$): 1.23—1.34 (2H, m, 5-H), 1.56—1.86 (4H, m, 4-H, 6-H), 1.93—1.99 (1H, m, 3-H), 2.12 (3H, s, CH_3N), 2.14—2.17 (1H, m, 7-H), 2.23—2.27 (1H, m, 1-H), 2.31—2.37 (1H, m, 1-H), 2.44—2.54 (1H, m, 7-H), 2.82—2.89 (1H, m, 3-H), 3.56—3.62 (1H, m, 12a-H), 5.54 (1H, dd, J=4.4, 12.3 Hz, 8-H), 5.70 (1H, dd, J=5.3, 9.4 Hz, 10-H), 5.80 (1H, dd, J=5.8, 9.4 Hz, 12-H), 5.97 (1H, dd, J=5.3, 9.4 Hz, 11-H), 6.06 (1H, d, J=9.4 Hz, 9-H).

(*E*)-2-Methyl-1,2,3,4,5,6,7,12a-octahydro-2-benzazecine (6d)[8] An undistillable oil (the purity was judged to be >98% by HPLC). ^{1}H-NMR ($CDCl_3$): 1.12—1.19 (1H, m, 4-H), 1.34—1.46 (2H, m, 5-H, 6-H), 1.47—1.54 (2H, m, 3-H, 5-H), 1.61—1.70 (2H, m, 4-H, 6-H), 1.94 (1H, dd, J=9.5, 13.2 Hz, 1-H), 1.99—2.12 (2H, m, 3-H, 7-H), 2.30 (3H, s, CH_3N), 2.41 (1H, dd, J=5.1, 13.2 Hz, 1-H), 2.45—2.54 (1H, m, 7-H), 2.90—2.93 (1H, m, 12a-H), 5.55—5.60 (1H, m, 8-H), 5.84—5.91 (2H, m, 10-H, 12-H), 6.00 (1H, dd, J=5.3, 9.5 Hz, 11-H), 6.41 (1H, d, J=9.5 Hz, 9-H).

(*E*)2,9-Dimethyl-1,2,3,4,5,6,7,12a-octahydro-2-benzazecine (5e)[8] An undistillable oil (the purity was judged to be >98% by HPLC). ^{1}H-NMR (benzene-d_6): 1.12—1.27 (2H, m, 4-H, 5-H), 1.47—1.56 (1H, m, 6-H), 1.60—1.78 (2H, m, 4-H, 6-H), 1.79—1.84 (1H, m, 3-H), 1.91 (3H, s, CH_3C), 2.00 (3H, s, CH_3N), 2.00—2.10 (2H, m, 5-H, 7-H), 2.15—2.20 (1H, m, 1-H), 2.33—2.44 (2H, m, 1-H, 7-H), 2.60—2.68 (1H, m, 3-H), 3.47—3.52 (1H, m, 12a-H), 5.63 (1H, d, J=5.4 Hz, 10-H), 5.66—5.75 (2H, m, 8-H, 12-H), 5.95 (1H, dd, J=5.4, 9.3 Hz, 11-H).

The NMR spectrum of the stereoisomer **6e** was not obtained because **6e** was insufficiently stable.

Isomerization of 5a, 5d and 6d in the Presence of a Base Compound **5a**, **5d** or **6d** (0.1 mmol) was dissolved in a solution of 10% potassium hydroxide in ethanol (3 ml). The solution was mixed with saturated aqueous sodium chloride solution (20 ml) after stirring under the conditions listed in Table II, and the whole was extracted with ether (2 × 20 ml). The ether layer was washed with saturated aqueous sodium chloride solution, dried ($MgSO_4$), and concentrated under reduced pressure to give **7a** or **7d**. The yields are listed in Table II.

2-Methyl-1,2,3,4,5,6-hexahydro-2-benzazocine (7a) bp 137 °C (17 mmHg, oven temperature, lit.[2] bp 120—122 °C (9 mmHg)); NMR data for this compound were not reported.[2] ^{1}H-NMR ($CDCl_3$, 100 MHz): 1.54—1.78 (4H, m, 4-H, 5-H), 2.39 (3H, s, CH_3N), 2.46 (2H, t, J=6 Hz, 3-H), 2.76—2.92 (2H, m, 6-H), 3.78 (2H, s, 1-H), 7.12—7.28 (4H, m).

2-Methyl-1,2,3,4,5,6,7,8-octahydro-2-benzazecine (7d) bp 152 °C (12 mmHg, oven temperature). ^{1}H-NMR ($CDCl_3$): 1.05—1.13 (2H, m), 1.33—1.40 (2H, m), 1.47—1.53 (2H, m), 1.75 (2H, m), 2.27 (3H, s, CH_3N), 2.29 (2H, t, J=5.8 Hz, 3-H), 3.00 (2H, br s, 8-H), 3.63 (2H, s, 1-H), 7.07—7.10 (2H, m), 7.20—7.22 (2H, m). *Anal.* Calcd for $C_{14}H_{21}N$: C, 82.70; H, 10.41; N, 6.89. Found: C, 82.42; H, 10.26; N, 6.89.

Isomerization of 5a, 5d and 6d in the Presence of Acid A saturated solution of hydrogen chloride in ether (15 ml) was added to a solution of **5a**, **5d** or **6d** (0.18 mmol) in hexane (15 ml), and the mixture was stirred at room temperature for 70 h. The mixture was made alkaline with sodium hydroxide and extracted with ether (4 × 40 ml). The extract was dried ($MgSO_4$) and concentrated under reduced pressure to give **7a** or **7d**. The yields are listed in Table II.

A 10% solution of deuterium chloride in deuterium oxide (3 ml) was added to a solution of **5a** (18 mg, 0.1 mmol) in hexane (10 ml). The mixture was stirred and worked up in the manner described above to give 6-deutero-2-methyl-1,2,3,4,5,6-hexahydro-2-benzazocine (**7a**-*d*, 15 mg, 83%), an oil (the purity was judged to be >98% by ^{1}H-NMR). ^{1}H-NMR ($CDCl_3$): 1.57—1.62 (2H, m, 4-H), 1.69 (2H, q, J=6.4 Hz, 5-H), 2.38 (3H, s, CH_3N), 2.45 (2H, t, J=5.0 Hz, 3-H), 2.83 (1H, t, J=6.1 Hz, 6-H), 3.77 (2H, s, 1-H), 7.13—7.26 (4H, m). MS (EI, 70 eV) *m/z* (%): 176 (M^+, 89), 147 (98), 105 (100).

Thermal Isomerization of 5a, 5b and 6d A solution of **5** or **6** (0.15 mmol) in xylene (7 ml) was heated at reflux for 2 h and then extracted with 0.5 N hydrochloric acid (4 × 30 ml). The acid layer was washed with ether, made alkaline with sodium hydroxide, and then again extracted with ether. The ethereal extract was dried ($MgSO_4$) and concentrated under reduced pressure to give a mixture of **8a, d** and **9a, d** (and **7d** from **6d**). The mixture was separated on an HPLC column (Merck LiChrosorb NH_2, 250 mm × 10 mm). The eluates were monitored at 235 nm with a UV detector. The mobile phases at 5 ml/min were programed as follows. For **8a** and **9a**, from 20 to 40% ether in hexane linearly for 10 min. Fractions of 5.3 min (**8a**) and 7.5 min (**9a**) were collected. For **8d** and **9d**, from 10 to 30% ether in hexane for 10 min. Fractions of 4.4 min (**8d**) and 10.0 min (**9d**) were collected. The yields are summarized in Table III. The ratios were determined from the integrated values of GLC analyses.

1-Methyl-3-phenylpiperidine (8a) bp 126 °C (14 mmHg, oven temperature). ^{1}H-NMR ($CDCl_3$): 1.37—1.48 (1H, m), 1.70—1.82 (2H, m), 1.89—1.98 (3H, m), 2.30 (3H, s, CH_3N), 2.83 (1H, m), 2.93 (2H, m), 7.18—7.32 (5H, m). *Anal.* Calcd for $C_{12}H_{17}N$: C, 82.23; H, 9.78; N, 7.99. Found: C, 82.45; H, 9.98; N, 7.94.

1-Methyl-3-phenylperhydroazocine (8d) bp 153 °C (12 mmHg, oven temperature). ^{1}H-NMR ($CDCl_3$): 1.60—1.97 (8H, m), 2.33 (3H, s, CH_3N), 2.51—2.64 (3H, m, 2-H, 8-H), 2.70 (1H, dd, J=10.2, 13.2 Hz, 2-H), 2.83—2.89 (1H, m, 3-H), 7.14—7.20 (3H, m), 7.25—7.29 (2H, m). *Anal.* Calcd for $C_{14}H_{21}N$: C, 82.70; H, 10.41; N, 6.89. Found: C, 82.74; H, 10.55; N, 6.95.

(*E*)-*N*,*N*-Dimethyl-4-phenyl-3-butenylamine (9a) bp 140 °C (12 mmHg, oven temperature); the boiling point and NMR data for this compound were not reported.[9] ^{1}H-NMR ($CDCl_3$): 2.27 (6H, s, CH_3N), 2.38—2.45 (4H, m, 1-H, 2-H), 6.18—6.25 (1H, m, 3-H), 6.43 (1H, d, J=16 Hz, 4-H), 7.17—7.24 (1H, m), 7.28—7.35 (4H, m). MS (EI, 70 eV) *m/z* (%): 115 (2), 58 (100); (CI, CH_4) *m/z* (%): 176 (M^++H, 100), 58 (79).

(*E*)-*N*,*N*-Dimethyl-6-phenyl-5-hexenylamine (9d) bp 167 °C (12 mmHg, oven temperature, lit.[10] bp 147—148 °C (10 mmHg)); NMR data for this compound were not reported.[10] ^{1}H-NMR ($CDCl_3$): 1.47—1.54 (4H, m, 2-H, 3-H), 2.22 (6H, s, CH_3N), 2.24—2.29 (4H, m, 1-H, 4-H), 6.18—6.25 (1H, m, 5-H), 6.39 (1H, d, J=15.8 Hz, 6-H), 7.16—7.20 (1H, m), 7.26—7.34 (4H, m). MS (EI, 70 eV) *m/z* (%): 203 (M^+, 18), 84 (56), 58 (100).

Photochemical Isomerization of 5a, 5b and 5d A solution of **5a**, **5b** or **5d** (0.1 mmol) in hexane or methanol (7 ml) was irradiated at 10 °C with a 100 W medium-pressure mercury lamp for 2 h. After evaporation of the solvent under reduced pressure, the residual oil was analyzed by GLC. The main products were identified by comparison of the retention times on GLC with those of authentic samples of **8a**, **b**, **d** and two minor products were assigned as geometrical isomers of **9a**, **b**, respectively. The results are shown in Table III.

Acknowledgment We are grateful to the Ministry of Education, Science, and Culture, Japan, for a Grant-in-Aid (No. 01571160).

References and Notes

1) N. Shirai, F. Sumiya, Y. Sato, and M. Hori, *J. Chem. Soc., Chem. Commun.*, **1988**, 370; *idem, J. Org. Chem.*, **54**, 836 (1989).
2) G. C. Jones and C. R. Hauser, *J. Org. Chem.*, **27**, 3572 (1962).
3) D. Lednicer and C. R. Hauser, *J. Am. Chem. Soc.*, **79**, 4449 (1957).
4) J. March, "Advanced Organic Chemistry," 3rd ed., John Wiley and

Sons, Inc., New York, 1985, pp. 1014—1017.
5) L. C. Craig, H. Bulbrook, and R. M. Hixon, *J. Am. Chem. Soc.*, **53**, 1831 (1931).
6) O. Cervinka and L. Hub, *Collect. Czech. Chem. Commun.*, **30**, 3111 (1965).
7) C. A. Zezza, M. B. Smith, B. A. Ross, A. Arhin, and P. L. E. Cronin, *J. Org. Chem.*, **49**, 4397 (1984).
8) The *E* and *Z* nomenclature of **5d**, **6d**, and **5e** is dependent on the presence of the methyl group at C-9.
9) B. E. Maryanoff, A. B. Reitz, and B. A. Duhl-Emswiler, *J. Am. Chem. Soc.*, **107**, 217 (1985).
10) C. Glacet, B. Hasiak, and A. Benattar, *C. R. Hebd. Seances Acad. Sci., Ser. C*, **282**, 1085 (1976) [*Chem. Abstr.*, **86**, 29232*p* (1977)].

A Facile Synthesis of Benzo[*b*]furan Derivatives Including Naturally Occurring Neolignans *via* Regioselective Lithiation of *ortho*-Cresols Using the Bis(dimethylamino)phosphoryl Group as a Directing Group[1)]

Mitsuaki WATANABE,*[,a] Mutsuhiro DATE,[b] Kenji KAWANISHI,[b] Takako HORI,[b] and Sunao FURUKAWA[b]

Center for Instrumental Analysis,[a] Faculty of Pharmaceutical Sciences,[b] Nagasaki University, 1–14 Bunkyo-machi, Nagasaki 852, Japan.
Received June 25, 1990

A facile synthesis of 2-arylbenzo[*b*]furans *via* directed lithiation of *ortho*-tolyl tetramethylphosphorodiamidates as the key step is described. Lithiation of *ortho*-tolyl tetramethylphosphorodiamidates at −105 °C followed by reaction with aromatic esters and then acidic treatment led to 2-arylbenzo[*b*]furans in modest overall yields. The utility of this strategy has been demonstrated in regioselective and short syntheses of the naturally occurring neolignans carinatin, eupomatenoid-1, and eupomatenoid-13.

Keywords lithiation; *ortho*-cresol; bis(dimethylamino)phosphoryl group; 2-arylbenzo[*b*]furan; carinatin; eupomatenoid-1; eupomatenoid-13; *ortho*-tolyl tetramethylphosphorodiamidate

Since benzo[*b*]furan was first synthesized by Perkin in 1870,[2)] benzofuran derivatives have been the subject of much research because of their physiological, pharmacological, therapeutic, or toxic properties.[3)] 2-Arylbenzo[*b*]furan derivatives are well known as components of a large number of natural products such as phytoalexins and neoliganans.[3,4)] Although numerous synthetic methods for the benzo[*b*]furan ring have appeared,[3a,d)] procedures for the syntheses of substituted benzo[*b*]furans *via* the formation of 2′-hydroxydeoxybenzoin derivatives as a key step[5)] are more effective routes than cyclodehydration of aryloxy derivatives such as aryloxyaldehydes because of the regioselectivity in the ring closure step.[3a,d)] However, the preparation of 2′-hydroxydeoxybenzoin derivatives having substituents on the aromatic ring is difficult in the previously reported method.[3a,d,5)]

In cases where a methyl group is located in an *ortho*-position to certain directed lithiation groups on an aromatic compound, the acidifying and chelation effects of directed lithiation groups promote facile deprotonation from the *ortho*-methyl group to form the corresponding benzylic anions, which can react with electrophiles.[6)] These reactions were used for chain extension and applied in syntheses of fused aromatic ring systems.[6)] Typically, *ortho*-toluamide anions or *ortho*-toluate anions have been used in a number of synthetic studies as useful reaction intermediates.[6,7)] In this connection, if the benzylic anions are generated from *ortho*-cresol derivatives, quenching with electrophiles followed by cyclization may provide a new synthetic route to benzo[*b*]furan derivatives.[3)]

Metalation of *ortho*-cresol derivatives as shown in Chart 1 has been investigated.[8)] In general, the metalations are complicated by competing ring and *ortho*-methyl deprotonations. In 1986, Bates and Siahaan reported that the *ortho*-cresol (**1**) was metalated under harsh conditions (*n*-BuLi–*tert*-BuOK in refluxing heptane for 3 h).[8f)] The dianions were reacted with a variety of alkyl halides to give the alkylated cresols. Lithiation of 2-methylanisole (**2**) with *tert*-BuLi in refluxing cyclohexane for 10 h followed by addition of electrophiles afforded two products, resulting from ring and benzylic metalations.[8b)] On the other hand, in the lithiation of 2-(methoxymethoxy)toluene (**3**) with *tert*-BuLi in hexane at 0 °C for 1 h, ring metalation was exclusively observed in high yield.[8c,d)] Furthermore, Sibi and Snieckus reported that aromatic *vs. ortho*-methyl proton abstraction selectivity was influenced by the metalation conditions such as the base employed for the metalation of (2-methylphenyl)carbamate (**4**).[8e)] In this context, we thought that for the synthesis of benzo[*b*]-furans from *ortho*-cresol derivatives *via* the metalation route, a new directing group for the regioselective benzylic lithiation is necessary.[1)]

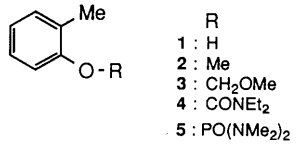

R
1 : H
2 : Me
3 : CH_2OMe
4 : $CONEt_2$
5 : $PO(NMe_2)_2$

Chart 1

In this paper, we describe the successful benzylic lithiation of *ortho*-cresol derivatives (**5**)[1)] using the bis(dimethylamino)phosphoryl group as a directing group[9)] and the application of the new methodology to a facile synthesis of benzo[*b*]furans including the naturally occurring neolignans carinatin,[10)] eupomatenoid-1,[11)] and eupomatenoid-13.[11d)]

The required *ortho*-tolyl *N*,*N*,*N*′,*N*′-tetramethylphosphorodiamidates (**5a—f**) were prepared by two different routes. Compounds **5a** and **5e** were prepared in 96% and 90% yields by the reaction of *ortho*-cresol (**1**) and 2,6-dimethylphenol, respectively, with bis(dimethylamino)-phosphoryl chloride in the presence of sodium hydride in tetrahydrofuran (THF).[9)] The methoxy-substituted **5b—d, f** were regioselectively synthesized in 87—95% yields

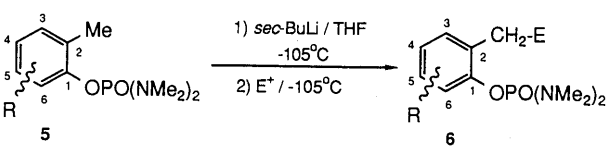

5

	R
5a :	H
5b :	6-MeO

6

	R	E	yield (%)
6a :	H	Me	81 (31)[a)]
6b :	6-MeO	Me	73
6c :	H	Me_3Si	55 (69)[a)]
6d :	H	C_6H_5-CH(OH)	43
6e :	H	4′-(MeO)-C_6H_4-CH(OH)	54
6f :	H	HOOC	48
6g :	H	MeOC	90 (40)[a)]

a) LDA was used as a base

Chart 2

TABLE I. Physical Properties and Spectral Data of *ortho*-Tolyl Tetramethylphosphorodiamidate Derivatives (**6**)

Compd. No.	Formula (MS, *m/z*, M^+)	bp (mp) (°C) (Recryst. solvent)	Analysis (%) Calcd (Found) C	H	N	UV λ_{max}^{EtOH} nm (log ε)	IR $\nu_{cm^{-1}}^{KBr}$	^{1}H-NMR δ ($CDCl_3$)
6a	$C_{12}H_{21}N_2O_2P$ (256)	130/0.5	56.23 (55.85	8.26 8.19	10.93 10.65)	265.4(2.71), 272(2.69)	3470, 2940, 1590, 1490, 1460, 1310, 1240, 1180, 990, 920	1.19 (3H, t, J=7.2 Hz), 2.15—2.50 (2H, m), 2.70 (12H, d, J=10.2 Hz), 6.92—7.28 (4H, m)
6b	$C_{13}H_{23}N_2O_3P$ (286)	140/0.5	54.53 (54.47	8.10 8.18	9.79 9.62)	273(s, 3.05), 278(3.09)	3450, 2940, 1580, 1475, 1305, 1285, 1230, 1175, 1085, 990, 910	1.21 (3H, t, J=7.6 Hz), 2.57—2.74 (2H, m), 2.75 (12H, d, J=10.2 Hz), 3.84 (3H, s), 6.66—7.05 (3H, m)
6c	$C_{14}H_{27}N_2O_2PSi$ (314)	110/0.2	53.48 (53.22	8.66 8.61	8.91 8.78)	270.5(2.96), 277(2.94)	3450, 2950, 2900, 1580, 1490, 1316, 1240, 1180, 1000, 930	0.16 (9H, s), 2.27 (2H, s), 2.87 (12H, d, J=9.6 Hz), 7.09—7.43 (4H, m)
6d	$C_{18}H_{25}N_2O_3P$ (348)	61—61.5 (Ether–pentane)	62.05 (62.09	7.23 7.23	8.04 8.07)	253(s, 2.47), 259(s, 2.87), 266(3.02), 272.5(2.87)	3390, 2940, 1490, 1455, 1310, 1230, 1210, 1170, 1000, 990, 920	2.67 (12H, d, J=10.8 Hz), 2.97—3.28 (2H, m), 3.94 (1H, br s), 4.78—5.03 (1H, m), 7.12—7.43 (9H, m)
6e	$C_{19}H_{27}N_2O_4P$ (378)	95 (CH_2Cl_2–hexane)	60.30 (60.17	7.19 7.14	7.40 7.31)	273.5(3.29), 283(3.12)	3400, 2930, 1620, 1520, 1490, 1310, 1210, 1170, 1000, 920	2.70 (12H, d, J=10.2 Hz), 2.98—3.12 (2H, m), 3.69 (1H, br s), 3.74 (3H, s), 4.77—4.96 (1H, m), 6.79 (2H, d, J=9.0 Hz), 7.00—7.25 (4H, m), 7.25 (2H, d, J=9.0 Hz)
6f	$C_{12}H_{19}N_2O_4P$ (286)	120—130 (Ether–CH_2Cl_2)	50.32 (50.08	6.69 6.57	9.83 9.67)	266(2.65), 272(2.62)	3450, 2930, 2880, 2850, 1725, 1605, 1585, 1495, 1460, 1305, 1220, 1180, 1160, 1000, 945, 920	2.76 (12H, d, J=10.3 Hz), 3.74 (2H, s), 6.97 (1H, d, J=8.1 Hz), 7.16—7.28 (3H, m), 7.50 (1H, d, J=7.7 Hz)
6g	$C_{13}H_{21}N_2O_3P$ (284)	154/1.6	54.92 (55.13	7.45 7.39	9.85 9.89)	266.5(2.82), 273(2.77)	3460, 2900, 1720, 1590, 1495, 1460, 1310, 1220, 1180, 990, 920	2.14 (3H, s), 2.72 (12H, d, J=10.2 Hz), 3.76 (2H, s), 7.08—7.37 (4H, m)

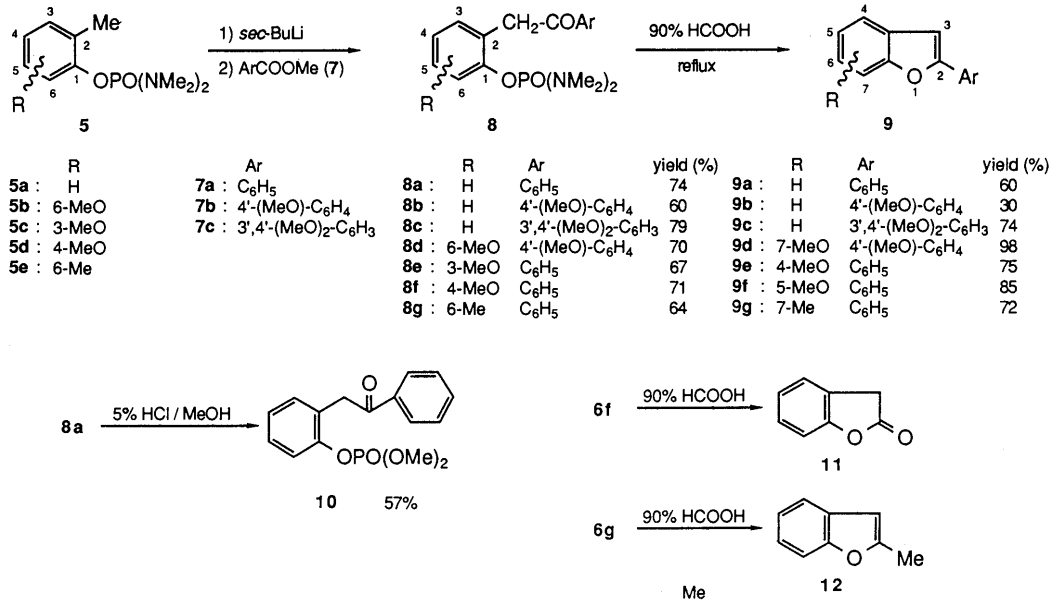

Chart 3

by the *ortho*-lithiation of methoxy-substituted phenols using the bis(dimethylamino)phosphoryl group as a directing group, followed by methylation as already reported by us.[9c,d]

Lithiation of the phosphorodiamidate **5a** with 1.2 eq of *sec*-BuLi in THF at −105 °C for 1 h resulted in the formation of the bright yellow benzylic anion, which, upon treatment with MeI at −105 °C and quenching with saturated NH_4Cl solution at −90 °C, gave 2-ethylphenyl tetramethylphosphorodiamidate (**6a**) in 81% yield.[1] Using trimethylsilyl chloride and aromatic aldehydes as electrophiles, the corresponding condensed products (**6c—e**) were synthesized in moderate yields (Chart 2). When the benzylic anion of **5a** generated with *sec*-BuLi was quenched with carbon dioxide or *N*-methoxy-*N*-methylacetamide,[12] the phenylacetic acid derivative **6f** or phenylacetone derivative **6g** was obtained in 48% or 90% yield, respectively. The 6-methoxy-substituted tolyl phosphorodiamidate (**5b**) behaved in a similar manner and the corresponding ethyl compound **6b** was obtained in 73% yield after treatment with MeI. Lithium diisopropylamide (LDA) could also be used for the generation of benzylic

TABLE II. Physical and Spectral Data for Deoxybenzoin Derivatives (**8**)

Compd. No.	Formula (MS, m/z, M^+)	bp (mp) (°C) (Recryst. solvent)	Analysis (%) Calcd (Found) C	H	N	UV λ_{max}^{EtOH} nm (log ε)	IR $\nu_{cm^{-1}}^{KBr}$	^{1}H-NMR δ ($CDCl_3$)
8a	$C_{18}H_{23}N_2O_3P$ (346)	105—106 (CH_2Cl_2–hexane)	62.41 (62.44	6.69 6.71	8.09 8.04)	244(4.16), 273(s, 3.34)	3425, 2930, 1690, 1490, 1470, 1350, 1310, 1220, 1175, 1000, 980, 920	2.61 (12H, d, J=9.6 Hz), 4.36 (2H, s), 7.12—7.50 (7H, m), 7.93—8.15 (2H, m)
8b	$C_{19}H_{25}N_2O_4P$ (376)	77—78 (Ether)	60.63 (60.52	6.70 6.69	7.44 7.44)	274(4.26)	3430, 2950, 1680, 1600, 1490, 1460, 1350, 1310, 1260, 1220, 1170, 1000, 975, 920	2.65 (12H, d, J=9.6 Hz), 3.85 (3H, s), 4.31 (2H, s), 6.89 (2H, d, J=9.0 Hz), 7.11—7.32 (4H, m), 7.99 (2H, d, J=9.0 Hz)
8c	$C_{20}H_{27}N_2O_5P$ (406)	114—115 (CH_2Cl_2–hexane)	59.10 (59.10	6.70 6.63	6.89 6.68)	229(4.22), 275(4.05), 305.5(3.91)	3430, 2930, 1670, 1590, 1510, 1490, 1460, 1420, 1350, 1310, 1260, 1240, 1220, 1160, 1020, 990, 920	2.65 (12H, d, J=9.6 Hz), 3.89 (3H, s), 3.92 (3H, s), 4.33 (2H, s), 6.87 (1H, d, J=8.0 Hz), 7.10—7.33 (4H, m), 7.55 (1H, s), 7.68 (1H, d, J=8.0 Hz)
8d	$C_{20}H_{27}N_2O_5P$ (406)	148—150 (Ether)	59.10 (59.24	6.70 6.63	6.89 6.92)	218(4.30), 277(4.29)	3420, 2940, 1685, 1605, 1480, 1460, 1310, 1220, 1180, 1165, 1080, 1005, 990, 900	2.65 (12H, d, J=9.6 Hz), 3.85 (6H, s), 4.52 (2H, s), 6.80—7.00 (5H, m), 8.08 (2H, d, J=9.6 Hz)
8e	$C_{19}H_{25}N_2O_4P$ (376)	Oil	60.63 (60.82	6.70 6.97	7.44 7.33)	242(3.90), 272(3.42), 278(3.41)	3450, 2930, 2900, 1695, 1595, 1470, 1310, 1275, 1220, 1180, 1110, 1090, 1000, 990, 945	2.58 (12H, d, J=10.8 Hz), 3.70 (3H, s), 4.38 (2H, s), 6.57—7.48 (7H, m), 7.92—8.09 (1H, m)
8f	$C_{19}H_{25}N_2O_4P$ (376)	124—126 (Ether)	60.63 (60.48	6.70 6.66	7.44 7.46)	229(4.12), 244(4.11), 283(3.53)	3430, 2940, 2900, 1675, 1580, 1495, 1460, 1445, 1335, 1310, 1280, 1215, 1200, 1160, 1030, 1000, 970, 925	2.64 (12H, d, J=9.6 Hz), 3.73 (3H, s), 4.38 (2H, s), 6.73—6.89 (2H, m), 7.19—7.58 (4H, m), 8.01—8.17 (2H, m)
8g	$C_{19}H_{25}N_2O_3P$ (360)	123—124 (Ether)	63.32 (63.13	6.99 6.90	7.77 7.74)	244(4.17), 289(s, 2.85)	2920, 2900, 1690, 1600, 1470, 1350, 1300, 1220, 1210, 1165, 1090, 1000, 990, 915	2.33 (3H, s), 2.61 (12H, d, J=10.8 Hz), 4.56 (2H, s), 6.89—7.10 (3H, m), 7.38—7.61 (3H, m), 7.87—8.18 (2H, m)

TABLE III. Physical and Spectral Data for 2-Arylbenzo[*b*]furan Derivatives (**9**)

Compd. No.	Formula (MS, m/z, M^+)	mp (bp) (°C) (Recryst. solvent)	Analysis (%) Calcd (Found) C	H	UV λ_{max}^{EtOH} nm (log ε)	IR $\nu_{cm^{-1}}^{KBr}$	^{1}H-NMR δ ($CDCl_3$)
9a	$C_{14}H_{19}O$ (194)	118—119 (Ether–CH_2Cl_2)	86.57 (86.27	5.19 5.42)	225(s, 4.07), 230(s, 4.06), 242(s, 3.85), 304(4.50), 315(s, 4.34)	3050, 1560, 1490, 1470, 1450, 1440, 1260, 1200, 1170, 1020, 920, 810	6.99 (1H, s), 7.13—7.92 (9H, m)
9b	$C_{15}H_{12}O_2$ (224)	145—146 (Ether–hexane)	80.33 (80.11	5.39 5.48)	309.5(4.56), 323(s, 4.37)	2960, 2840, 1615, 1500, 1460, 1250, 1180, 1020, 840	3.76 (3H, s), 6.97 (1H, s), 6.87 (2H, d, J=9.0 Hz), 7.02—7.46 (4H, m), 7.70 (2H, d, J=9.0 Hz)
9c	$C_{16}H_{14}O_3$ (254)	116—118 (Ether–CH_2Cl_2)	75.57 (75.56	5.55 5.64)	300(s, 4.26), 314.5(4.35), 328(s, 4.23)	2940, 2840, 1610, 1510, 1440, 1450, 1340, 1250, 1230, 1140, 1020, 940, 860	3.80 (3H, s). 3.87 (3H, s), 6.77 (1H, d, J=9.0 Hz), 6.77 (1H, s), 7.06—7.54 (6H, m)
9d	$C_{16}H_{14}O_3$ (254)	80—81 (Ether–pentane)	75.57 (75.33	5.55 5.64)	250.5(4.03), 257.5(s, 3.91), 300(4.55), 306(4.39), 320(4.29)	3000, 2955, 2945, 2840, 1620, 1596, 1505, 1495, 1435, 1300, 1255, 1220, 1180, 1100, 1040, 915, 840	3.79 (3H, s), 4.00 (3H, s), 6.65—7.86 (8H, m)
9e	$C_{15}H_{12}O_2$ (224)	56—58 (Ether–pentane)	80.33 (80.18	5.39 5.67)	236.5(4.16), 244.5(s, 4.12), 298.5(4.40), 309(s, 4.39), 325(s, 4.14)	3000, 2950, 2900, 2840, 1600, 1500, 1480, 1430, 1360, 1250, 1160, 1090, 1020, 920, 840	4.14 (3H, s), 6.72—6.90 (1H, m), 7.35—8.21 (9H, m)
9f	$C_{15}H_{12}O_2$ (224)	121—123 (Ether)	80.33 (80.19	5.39 5.48)	290(s, 3.35), 300(3.40), 314(3.40)	3000, 2830, 1610, 1595, 1470, 1445, 1430, 1205, 1140, 1030, 1020, 915, 845	3.81 (3H, s), 6.76—7.06 (3H, m), 7.25—7.46 (4H, m), 7.35—8.21 (2H, m)
9g	$C_{15}H_{12}O$ (208)	130/0.4	86.51 (86.62	5.81 6.04)	234.5(4.06), 245(3.96), 292(s, 4.39), 298.5(s, 4.42), 303.5(4.45), 317(4.30)	3050, 2920, 1610, 1560, 1480, 1450, 1420, 1300, 1290, 1210, 1180, 1020, 920, 860	2.51 (3H, s), 6.86 (1H, s), 6.98—7.87 (8H, m)

anions from **5** (Chart 2; **6a**, **6c**, and **6g**). The structures of all compounds were established by infrared (IR), ultraviolet (UV), proton nuclear magnetic resonance (^{1}H-NMR),[9d] mass spectral (MS) data and elemental analyses as summarized in Table I.

As shown in Chart 3, when **5a** was lithiated with *sec*-BuLi at $-105\,^\circ$C for 1 h and subsequently treated with methyl benzoate (**7a**) at $-105\,^\circ$C, the deoxybenzoin derivative **8a** was obtained in 74% yield after usual work-up and chromatographic purification. The same compound (**8a**) was also obtained in 64% yield by using benzonitrile instead of **7a**. When various methoxy- or methyl-substituted tolyl phosphorodiamidates (**5b—e**) and methoxy-substituted benzoates (**7b**, **c**) were used, methoxy-substituted deoxybenzoins (**8b—g**), which were difficult to prepare by using the previous methods,[5] were regioselectively synthesized in 60—79% yields. Acidic treatment of **8a** in refluxing 90% formic acid[9b,c,d] for 1 h gave 2-phenylbenzo[*b*]furan (**9a**)[5,13] in 60% yield, resulting from dephosphorylation and subsequent cyclodehydration. However, when **8a** was refluxed in 5% HCl in dry methanol for 4 h, 2-(phenacyl)phenyl dimethylphosphate (**10**) was obtained in 57% yield and no **9a** was detected. On the other hand, refluxing of **8a** with 90% acetic acid for 12 h gave **9a** in 81% yield. Although compound **9a** was synthesized by the treatment of **8a** with either 90% formic acid or 90% acetic acid, acidic cyclization with acetic acid requires a longer reaction time than that with formic acid. A variety of methoxy- or methyl-substituted 2-arylbenzo[*b*]furan derivatives (**9b—g**)[14] were synthesized in the same way from **8b—g**, using formic acid, in moderate to high yields. Similarly, 2(3*H*)-benzo[*b*]furanone (**11**)[15] and 2-methylbenzo[*b*]furan (**12**)[13] were obtained in 54% and 90% yields from **6f** and **6g**, respectively, by the treatment with formic acid. Since **5b—d** are easily and regioselectively accessible by the directed lithiation of the corresponding phosphorodiamidates followed by methylation,[9c,d] the above sequences provide a general and efficient route to benzo[*b*]furan derivatives. Physical and spectral data for deoxybenzoins and benzo[*b*]furan derivatives thus obtained are summarized in Tables II and III, respectively.

For the application of this benzo[*b*]furan synthesis to the total synthesis of naturally occurring 3-methyl-2-arylbenzo[*b*]furan derivatives,[4] it is necessary to establish the scope and limitations of this reaction as regards the position of deprotonation on benzenoid rings having a variety of substituents. We chose **5f**, **6a**, and **6b** as test cases for aromatic *vs. ortho*-methyl or *ortho*-ethyl proton abstraction under the lithiation conditions (Chart 4). Lithiation of **5f** with *sec*-BuLi followed by addition of MeI gave **13** in 32% yield and none of the ethyl compound was isolated. When **6a** was lithiated with *sec*-BuLi and subsequently reacted with MeI, compound **14** (resulting from ring deprotonation) was obtained in 90% yield. The same compound (**14**) was alternatively prepared in 96% yield by the lithiation of **5e** followed by treatment with MeI. On the other hand, lithiation of **6b** followed by reaction with methyl piperonylate (**7d**) gave the deoxybenzoin derivative **8h** in 37% yield. Acidic treatment of **8h** gave the desired 3-methy-2-arylbenzo[*b*]furan (**9h**) in 38% yield. The above results clearly suggest the following lithiation bahavior: i) although the *ortho*-methyl group of **5a—e** was easily deprotonated to generate the corresponding benzylic anion as shown in Charts 2 and 3, when a methoxy group is located at the *meta*-position of the phosphorodiamidate group, such as in **5f**, lithiation occurred at the position between the two functions presumably due to dual directing ability of the two groups; ii) in the case where an ethyl group is attached to the *ortho*-position of the phosphorodiamidate group, such as in **6a**, exclusive ring lithiation was effected; iii) when the *ortho*-position was substituted with a methoxy group, such as in **6b**, deprotonation from the side chain occurred to generate the benzylic anion and electrophiles could be regioselectively introduced at the benzylic position.

On the basis of the above results, the utility of the benzofuran synthesis was demonstrated for the total synthesis of the neolignans carinatin, eupomatenoid-1, and eupomatenoid-13 (Chart 5). Carinatin (**20**) is a 2-arylbenzofuran natural product isolated from the bark

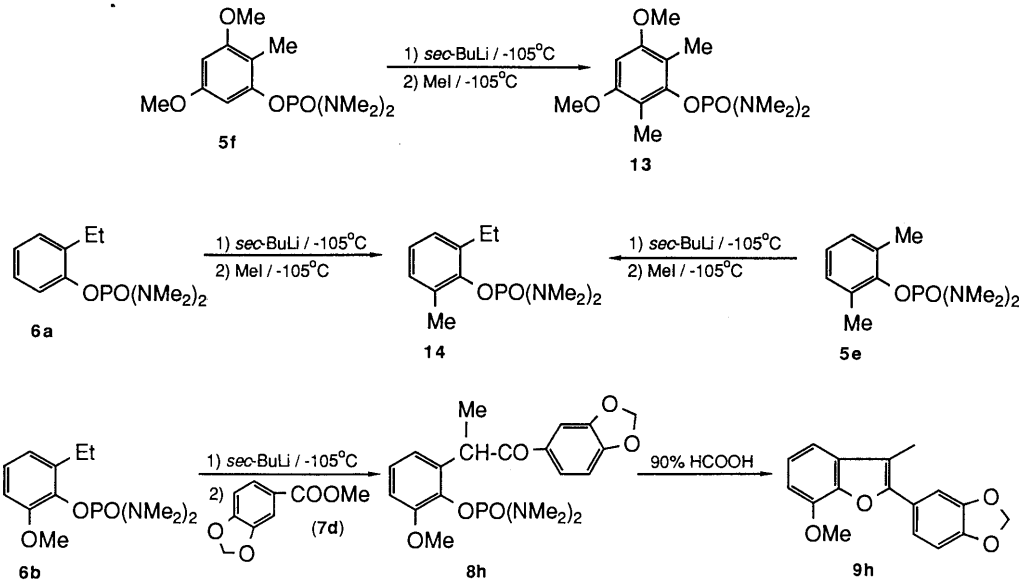

Chart 4

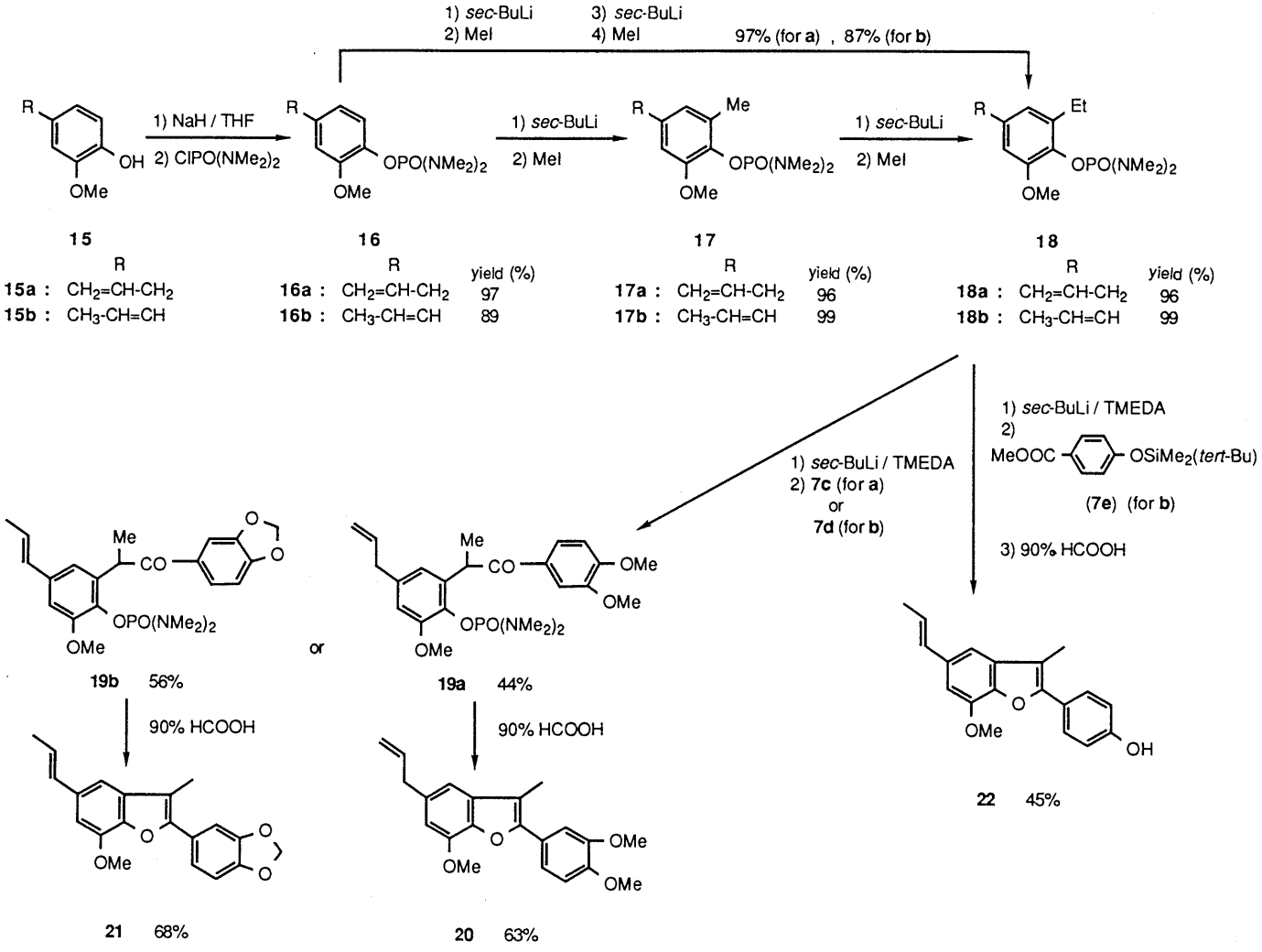

Chart 5

of *Virola carinata* (BENTH.) Warburg in 1982 and was identified as 5-allyl-2-(3,4-dimethoxyphenyl)-7-methoxy-3-methylbenzo[*b*]furan by spectroscopic analysis and partial synthesis from carinatone, which was isolated together with **20**, by Kawanishi *et al.*[10] Various eupomatenoids have been shown to possess basic structures belonging to the 2-aryl-3-methyl-5-(*E*)-propenylbenzofuran system.[4] Eupomatenoids-1 (**21**) and -13 (**22**) were isolated from the bark of *Eupomatia laurina* R. Br. in 1969 and in 1979, respectively.[11] The structures of eupomatenoids-1 and -13 were elucidated as 7-methoxy-3-methyl-2-(3,4-methylenedioxyphenyl)-5-[(*E*)-prop-1-enyl]benzo[*b*]furan and 2-(4-hydroxyphenyl)-7-methoxy-3-methyl-5-[(*E*)-prop-1-enyl]-benzo[*b*]furan, respectively.[11] The first total synthesis of eupomatenoid-1 (**21**) was reported in 1969 by Taylor *et al.* using oxidative ring contraction of the flavylium salt to form the benzo[*b*]furan ring as a key step.[11a] In 1983, McKittrick and Stevenson reported the total syntheses of eupomatenoids-1 (**21**) and -13 (**22**) using an intramolecular Wittig reaction[14b,16] of *ortho*-aroyloxy benzyl triphenylphosphonium bromides.[11e] However, each of these syntheses suffers from the disadvantages of many reaction steps and low overall yields. We report here a new procedure for the syntheses of carinatin, eupomatenoids-1, and -13.

Eugenol (**15a**) and isoeugenol (**15b**) were phosphorylated under the conditions described for **5** to give the requisite **16a** and **16b** in 97% and 87% yields, respectively. *O*-Bis(dimethylamino)phosphorylated eugenol (**16a**) was lithiated with *sec*-BuLi at −105 °C followed by treatment with MeI to give **17a** in quantitative yield. Compound **17a** was again lithiated and subsequently methylated to afford the ethyl compound **18a** quantitatively. Similarly, the ethyl compound **18b** was synthesized from **16b** *via* **17b** in quantitative yield. Compounds **18a** and **18b** were alternatively prepared in 97% and 87% yields, in a one-pot procedure[17] without isolation of **17a** and **17b**, starting from **16a** and **16b**, respectively. When a THF solution of methyl veratrate (**7c**) was injected into a solution of lithiated **18a** generated with 1.3 eq of *sec*-BuLi at −105 °C, the condensation product **19a** was obtained in 11% yield. On the other hand, inverse addition of a THF solution of lithiated **18a** into a solution of **7c** at −105 °C afforded **19a** in 31% yield. Finally, lithiation of **18a** with *sec*-BuLi in the presence of *N,N,N',N'*-tetramethylethylenediamine (TMEDA) at −105 °C gave, after inverse addition to **7c**, compound **19a** in satisfactory yield (44% yield). Acidic treatment of **19a** furnished **20** in 64% yield after standard work-up and chromatographic purification. The synthetic **20** was shown to be identical with an authentic sample[10] of carinatin on the basis of melting point, spectroscopic, and

thin layer chromatographic comparisons. For the synthesis of eupomatenoid-1, a THF solution of methyl piperonylate (**7d**) was injected into a solution of lithiated **18b** generated with 1.3 eq of *sec*-BuLi in the presence of 1.3 eq of TMEDA at −105 °C, giving the condensation product **19b** in 56% yield. This product (**19b**) was converted into **21** in 68% yield by treatment with formic acid. Similarly, **18b** was lithiated and subsequently reacted with methyl *p*-(*tert*-butyldimethylsilyloxy)benzoate (**7e**) to give the condensation product, which, without isolation, was treated with 90% formic acid to give **22** in 45% overall yield. Synthetic **21** and **22** were shown to be identical with eupomatenoid-1 and -13, respectively, on the basis of the reported melting points and spectroscopic comparisons.[11] The naturally occurring neolignans, eupomatenoids-1 (**21**) and -13 (**22**), have previously been synthesized in 1.6% and *ca.* 5.5% overall yields, respectively.[11e] Our approach provided carinatin (**20**) in 26%, **21** in 33%, and **22** in 39% overall yields.

In conclusion, we have shown that lithiation of *ortho*-cresol derivatives having a bis(dimethylamino)phosphoryl group as a directing group gave the corresponding benzylic anions which could be trapped with various electrophiles. The benzylic anions were condensed with benzoates to give various deoxybenzoin derivatives which were treated with formic acid to afford 2-arylbenzo[*b*]furan derivatives in moderate to good overall yields. The developed methodology was demonstrated to be applicable for the efficient synthesis of naturally occurring neolignans, *i.e.*, carinatin, eupomatenoid-1, and -13.

Experimental

All melting points are uncorrected. The IR spectra were obtained in KBr disk using a JASCO 810 spectrophotometer. The UV spectra were recorded in 95% ethanol on a Hitachi 323 spectrophotometer. The ^{1}H-NMR spectra were obtained with JEOL FX 90Q, JEOL JNM-PMX 60, and JEOL JNM GX-400 spectrometers using $CDCl_3$ as a solvent and tetramethylsilane as an internal reference. Elemental analyses were performed at the Microanalytical Laboratory of the Center for Instrumental Analysis in Nagasaki University. All solvents used for lithiation reaction were freshly distilled from sodium benzophenone ketyl before use. Chromatography was carried out by flash chromatography on a column of Kieselgel 60 (230—400 mesh).

***ortho*-Tolyl Tetramethylphosphorodiamidates (5a—e)** Compounds **5a**—**d** are known.[9c,d] Compound **5e** was prepared by the reaction of 2,6-dimethylphenol with bis(dimethylamino)phosphoryl chloride in the presence of NaH in THF according to the literature method.[9c,d] 2,6-Dimethylphenyl *N,N,N',N'*-tetramethylphosphorodiamidate (**5e**), 90% yield, bp 115 °C/2 mmHg. MS *m/z*: 256 (M^+). IR (neat): 3450, 2930, 2800, 1480, 1310, 1270, 1230, 1180, 1100, 1070, 1000 cm^{-1}. UV nm (log ε): 263 (2.50). ^{1}H-NMR δ: 2.35 (6H, s), 2.75 (12H, d, J=9.5 Hz), 6.90—7.00 (3H, m). *Anal.* Calcd for $C_{12}H_{21}N_2O_2P$: C, 56.23; H, 8.26; N, 10.93. Found: C, 56.30; H, 8.23; N, 10.79.

Lithiation Reaction of 5a, b with Electrophiles: Synthesis of 6a—g[1] The following procedure for the synthesis of 2-ethylphenyl *N,N,N',N'*-tetramethylphosphorodiamidate (**6a**) is representative; the other compounds (**6b—g**) were obtained similarly.

2-Ethylphenyl *N,N,N',N'*-Tetramethylphosphorodiamidate (**6a**): A solution of *sec*-BuLi (1.00 M in cyclohexane, 6.0 ml, 6.0 mmol) was injected into a stirred solution of *ortho*-tolyl tetramethylphosphorodiamidate (**5a**, 1.2 g, 5.0 mmol) in THF (50 ml) at −150 °C (liquid nitrogen–ethanol bath) under a nitrogen atmosphere. The mixture was stirred at −105 °C for 1 h, and then a solution of MeI (1.0 g, 7.0 mmol) in THF (20 ml) was injected into the yellow lithiated solution at −105 °C. The yellow color gradually disappeared during the addition of electrophiles. Stirring was continued for an additional 1 h at −105 °C. The reaction mixture was quenched with saturated NH_4Cl solution at −90 °C and the solution was allowed to warm to room temperature. THF was removed under reduced pressure. The residue was extracted with CH_2Cl_2 and the CH_2Cl_2 layer was washed with 5% $Na_2S_2O_3$ solution, dried over Na_2SO_4, and then evaporated to give 2-ethylphenyl tetramethylphosphorodiamidate (**6a**) as an oil, which was distilled to give pure **6a** (1.04 g, 81%), bp 130 °C/0.5 mmHg (see Table I). Use of LDA, generated with *n*-BuLi and diisopropylamine at 0 °C, as a base in the above reaction instead of *sec*-BuLi gave **6a** in 31% yield.

General Procedure for the Synthesis of Deoxybenzoin Derivatives (8a—g) The following procedure for the synthesis of 2-(phenacyl)phenyl *N,N,N',N'*-tetramethylphosphorodiamidate (**8a**) is representative; the other deoxybenzoins (**8b—g**) were obtained similarly.

2-(Phenacyl)phenyl *N,N,N',N'*-Tetramethylphosphorodiamidate (**8a**): A solution of methyl benzoate (**7a**, 0.87 g, 7.0 mmol) in THF (10 ml) was injected into a lithiated solution of **5a** (1.2 g, 6.0 mmol), generated as above, at −150 °C. Stirring was continued for an additional 1 h at −105 °C. The reaction mixture was quenched with saturated NH_4Cl solution at −90 °C and the solution was allowed to warm to room temperature. After usual work-up and chromatographic purification using CH_2Cl_2 as an eluent gave **8a** (1.28 g, 74%), mp 105—106 °C (CH_2Cl_2–hexane) (see Table II). Compound **8a** was also prepared in 64% yield employing benzonitrile as an electrophile instead of benzoate (**7a**) in the above reaction.

General Procedure for the Synthesis of 2-Arylbenzo[*b*]furans (9a—g) The following procedure for the synthesis of 2-phenylbenzo[*b*]furan (**9a**) is representative; the other 2-arylbenzo[*b*]furan derivatives (**9b—g**) were obtained similarly.

2-Phenylbenzo[*b*]furan (**9a**): A solution of **8a** (1.73 g, 5.0 mmol) in 90% HCOOH (6 ml) was refluxed for 1 h. After removal of HCOOH under reduced pressure, 5% $NaHCO_3$ solution was added to the residue and the mixture was extracted with CH_2Cl_2. The organic layer was separated, dried over Na_2SO_4, and evaporated to give a residue, which was chromatographed with benzene as an eluent to give 2-phenylbenzo[*b*]furan (**9a**). Further purification by recrystallization from ether–CH_2Cl_2 gave pure **9a** (mp 118—119 °C, 0.58 g, 60%) (lit.[5a] mp 119.5—121 °C; lit.[5b] mp 120—121 °C; lit.[13] mp 119—121 °C; lit.[16] mp 120—121 °C) (see Table III). Alternatively, compound **9a** (0.12 g, 81%) was obtained by the treatment of **8a** (0.25 g, 0.76 mmol) with refluxing 90% acetic acid (10 ml) for 12 h.

2-(Phenacyl)phenyl Dimethylphosphate (10) A solution of **8a** (0.69 g, 2.0 mmol) in 5% HCl–MeOH (30 ml) was refluxed for 4 h. After removal of MeOH, the residue was chromatographed with CH_2Cl_2–acetone (9 : 1) as an eluent to give 2-(phenacyl)phenyl dimethylphosphate (**10**) as a viscous oil (0.36 g, 57%). MS *m/z*: 320 (M^+). IR (neat): 2955, 1690, 1595, 1580, 1495, 1450, 1335, 1285, 1220, 1180, 1040, 960 cm^{-1}. UV nm (log ε): 244 (3.18). ^{1}H-NMR δ: 3.70 (6H, d, J=10.9 Hz), 4.36 (2H, s), 7.15—7.57 (7H, m), 7.94—8.10 (2H, m). *Anal.* Calcd for $C_{16}H_{17}O_5P$: C, 57.14; H, 5.10. Found: C, 57.36; H, 5.43.

2(3*H*)-Benzo[*b*]furanone (11) A solution of **6f** (0.86 g, 3.0 mmol) in 90% HCOOH (3 ml) was refluxed for 1 h. Standard work-up and purification by chromatography using CH_2Cl_2 as an eluent gave **11** (0.22 g, 54%), bp 130 °C/20 mmHg (lit.[15] mp 44—47 °C). MS *m/z*: 134 (M^+). ^{1}H-NMR δ: 3.70 (2H, s), 6.92—7.29 (4H, m). IR (Nujol): 3350, 2900, 1710, 1600, 1500, 1450, 1410, 1350, 1265, 1210, 1190, 1100 cm^{-1}.

2-Methylbenzo[*b*]furan (12) A solution of **6g** (0.85 g, 3.0 mmol) in 90% HCOOH (5 ml) was refluxed for 1 h. Standard work-up and distillation gave **12** (0.36 g, 90%), bp 197—198 °C (lit.[13] bp 50 °C/0.2 mmHg). MS *m/z*: 132 (M^+). ^{1}H-NMR δ: 2.30 (3H, s), 6.19 (1H, br s), 6.95—7.42 (4H, s). IR (neat): 3010, 2900, 1605, 1590, 1460, 1440, 1380, 1310, 1270, 1250, 1180, 1100, 1005, 940 cm^{-1}.

3,5-Dimethoxy-2,6-dimethylphenyl *N,N,N',N'*-Tetramethylphosphorodiamidate (13) A solution of MeI (0.86 g, 6.0 mmol) in THF (10 ml) was injected into a lithiated solution of **5f** (1.2 g, 4.0 mmol) in THF (80 ml), generated with *sec*-BuLi (5.2 ml, 5.2 mmol) at −105 °C for 1 h, with stirring at −105 °C. Stirring was continued for an additional 1 h at −105 °C. Standard work-up and purification by chromatography using CH_2Cl_2–acetone (9 : 1) gave **13** (0.4 g, 32%), mp 87—90 °C (ether–pentane). MS *m/z*: 316 (M^+). IR (KBr): 2920, 1620, 1595, 1500, 1460, 1430, 1410, 1310, 1220, 1200, 1120, 1000, 940 cm^{-1}. UV nm (log ε): 223 (3.96), 280 (3.45). ^{1}H-NMR δ: 2.12 (6H, s), 2.72 (12H, d, J=9.6 Hz), 3.76 (6H, s), 6.28 (1H, s). *Anal.* Calcd for $C_{14}H_{25}N_2O_4P$: C, 53.19; H, 7.97; N, 8.86. Found: C, 52.92; H, 7.79; N, 8.90.

2-Ethyl-6-methylphenyl *N,N,N',N'*-Tetramethylphosphorodiamidate (14) A solution of MeI (0.72 g, 5.1 mmol) in THF (10 ml) was injected into a lithiated THF solution (80 ml) of **6a** (1.0 g, 4.0 mmol), generated with *sec*-BuLi (5.1 ml, 5.1 mmol) at −105 °C for 1 h, with stirring at −105 °C. The reaction mixture was stirred for an additional 1 h at −105 °C. Standard work-up and distillation gave **14** (1.0 g, 93%), bp 120 °C/0.2 mmHg. MS

m/z: 270 (M^+). IR (neat): 2920, 2800, 1460, 1300, 1230, 1170, 1100, 1060, 1000, 910 cm^{-1}. UV nm (log ε): 265 (2.41). ^{1}H-NMR δ: 1.17 (3H, t, J=7.8 Hz), 2.33 (3H, s), 2.52—2.70 (2H, m), 2.69 (12H, d, J=9.0 Hz), 6.99 (3H, s). *Anal.* Calcd for $C_{13}H_{23}N_2O_2P$: C, 57.76; H, 8.58; N, 10.36. Found: C, 57.53; H, 8.63; N, 10.29. Compound **14** was also prepared in 96% yield by a similar lithiation of **5e** followed by addition of MeI.

7-Methoxy-3-methyl-2-(3,4-methylenedioxyphenyl)benzo[*b*]furan (9h) A solution of methyl piperonylate (**7d**, 0.72 g, 4.0 mmol) was injected into a lithiated solution of **6b** (0.57 g, 2.0 mmol) in THF (80 ml), generated with *sec*-BuLi (3.2 ml, 3.0 mmol) at −105 °C for 1 h, with stirring at −105 °C. Standard work-up and chromatographic purification using CH_2Cl_2–acetone (7:3) as an eluent gave the deoxybenzoin derivative **8h** (0.32 g, 37%), mp 117—118 °C (ether–pentane). MS *m/z*: 434 (M^+). IR (KBr): 2900, 1680, 1610, 1580, 1510, 1480, 1440, 1350, 1300, 1280, 1260, 1220, 1170, 1100, 1050, 990, 920 cm^{-1}. UV nm (log ε): 227.2 (4.33), 277 (3.88), 312.5 (3.88). ^{1}H-NMR δ: 1.46 (3H, d, J=6.6 Hz), 2.73 (6H, d, J=8.4 Hz), 2.78 (6H, d, J=9.6 Hz), 3.77 (3H, s), 5.16 (1H, q, J=6.6 Hz), 5.86 (2H, s), 6.54—6.95 (4H, m), 7.63—7.85 (2H, m). *Anal.* Calcd for $C_{21}H_{27}N_2O_6P$: C, 58.06; H, 6.26; N, 6.45. Found: C, 57.77; H, 6.28; N, 6.49. A solution of **8h** (0.16 g, 0.35 mmol) in 90% HCOOH (5 ml) was refluxed for 1 h. Standard work-up and purification by chromatography using CH_2Cl_2 as an eluent gave **9h** (0.04 g, 38%), mp 86—90 °C (ether–pentane). MS *m/z*: 282 (M^+). IR (KBr): 2900, 1620, 1580, 1500, 1485, 1460, 1375, 1275, 1250, 1240, 1095, 1050, 1040, 930 cm^{-1}. UV nm (log ε): 214 (4.46), 301.5 (s) (4.30), 315.5 (4.31). ^{1}H-NMR δ: 1.25 (3H, s), 4.02 (3H, s), 5.99 (2H, s), 6.70—7.36 (6H, m). *Anal.* Calcd for $C_{17}H_{14}O_4$: C, 72.33; H, 5.00. Found: C, 72.50; H, 5.31.

4-Allyl-2-methoxyphenyl *N,N,N′,N′*-Tetramethylphosphorodiamidate (16a) This was prepared in 97% yield by the reaction of eugenol (**15a**) with bis(dimethylamino)phosphoryl chloride under the conditions described for **5**, bp 160 °C/0.8 mmHg. MS *m/z*: 298 (M^+). IR (neat): 2930, 2890, 1635, 1590, 1510, 1460, 1300, 1270, 1235, 1210, 1190, 1150, 1130, 990, 920 cm^{-1}. UV nm (log ε): 277 (3.84), 282 (3.79). ^{1}H-NMR (400 MHz) δ: 2.73 (12H, dd, J=9.9, 1.1 Hz), 3.33 (2H, d, J=6.6 Hz), 3.83 (3H, d, J=1.5 Hz), 5.05—5.10 (2H, m), 5.88—5.99 (1H, m), 6.70 (1H, d, J=8.1 Hz), 6.72 (1H, d, J=1.1 Hz), 7.15 (1H, dd, J=8.1, 1.1 Hz). *Anal.* Calcd for $C_{14}H_{23}N_2O_3P$: C, 56.36; H, 7.77; N, 9.39. Found: C, 56.06; H, 7.76; N, 9.59.

2-Methoxy-4-[(*E*)-prop-1-enyl]phenyl *N,N,N′,N′*-Tetramethylphosphorodiamidate (16b) This was prepared in 89% yield by the reaction of isoeugenol (**15b**) with bis(dimethylamino)phosphoryl chloride under the conditions described for **5**, bp 167 °C/0.8 mmHg. MS *m/z*: 298 (M^+). IR (neat): 2930, 1585, 1510, 1460, 1415, 1300, 1270, 1210, 1155, 1125, 1035, 995 cm^{-1}. UV nm (log ε): 255 (4.25), 292 (s) (3.66), 297 (3.67), 308 (3.46). ^{1}H-NMR δ: 1.82 (3H, d, J=4.8 Hz), 2.69 (12H, d, J=10.2 Hz), 3.82 (3H, s), 6.02—6.24 (2H, m), 6.73—6.87 (2H, m), 7.10—7.26 (1H, m). *Anal.* Calcd for $C_{14}H_{23}N_2O_3P$: C, 56.36; H, 7.77; N, 9.39. Found: C, 56.32; H, 7.70; N, 9.44.

4-Allyl-2-methoxy-6-methylphenyl *N,N,N′,N′*-Tetramethylphosphorodiamidate (17a) This was obtained in 96% yield by the lithiation of **16a** followed by addition of MeI, bp 140 °C/0.5 mmHg. MS *m/z*: 312 (M^+). IR (neat): 2920, 2900, 2850, 1635, 1590, 1495, 1460, 1425, 1330, 1300, 1235, 1205, 1190, 1145, 1100, 990, 900 cm^{-1}. UV nm (log ε): 273 (3.20), 281 (3.22). ^{1}H-NMR (400 MHz) δ: 2.33 (3H, s), 2.75 (12H, dd, J=9.9, 0.7 Hz), 3.29 (2H, d, J=6.6 Hz), 3.82 (3H, s), 5.05 (1H, dd, J=9.9, 0.7 Hz), 5.09 (1H, dd, J=16.9, 1.1 Hz), 5.88—5.98 (1H, m), 6.57 (1H, s), 6.58 (1H, s). *Anal.* Calcd for $C_{15}H_{25}N_2O_3P$: C, 57.65; H, 8.06; N, 9.01. Found: C, 57.93; H, 8.16; N, 8.87.

2-Methoxy-6-methyl-4-[(*E*)-prop-1-enyl]phenyl *N,N,N′,N′*-Tetramethylphosphorodiamidate (17b) This was obtained in 99% yield by the lithiation of **16b** followed by addition of MeI, bp 155 °C/0.7 mmHg. MS *m/z*: 312 (M^+). IR (neat): 2930, 2900, 2850, 1590, 1500, 1465, 1420, 1340, 1310, 1235, 1210, 1150, 1105, 1000, 900 cm^{-1}. UV nm (log ε): 258 (4.21), 295 (3.52), 307 (s) (3.33). ^{1}H-NMR δ: 1.80 (3H, d, J=4.8 Hz), 2.31 (3H, s), 2.70 (12H, d, J=9.0 Hz), 3.80 (3H, s), 6.00—6.20 (2H, m), 6.69 (2H, s). *Anal.* Calcd for $C_{15}H_{25}N_2O_3P$: C, 57.65; H, 8.06; N, 9.01. Found: C, 57.91; H, 8.05; N, 8.96.

4-Allyl-2-ethyl-6-methoxyphenyl *N,N,N′,N′*-Tetramethylphosphorodiamidate (18a) This was obtained in 96% yield by the lithiation of **17a** followed by addition of MeI, bp 130 °C/0.3 mmHg. MS *m/z*: 326 (M^+). IR (neat): 2930, 2900, 2850, 1620, 1590, 1485, 1460, 1430, 1340, 1305, 1235, 1205, 1190, 1150, 1000, 905 cm^{-1}. UV nm (log ε): 272 (3.01), 281 (3.02). ^{1}H-NMR (400 MHz) δ: 1.21 (3H, t, J=7.4 Hz), 2.73 (2H, q, J=7.4 Hz), 2.57 (12H, d, J=9.9 Hz), 3.32 (2H, d, J=6.6 Hz), 3.83 (3H, s), 5.06 (1H, dd, J=10.6 Hz, 1.8 Hz), 5.09 (1H, dd, J=16.9, 1.8 Hz), 5.89—5.99 (1H, m), 6.58 (1H, d, J=1.6 Hz), 6.62 (1H, d, J=1.6 Hz). *Anal.* Calcd for $C_{16}H_{27}N_2O_3P$: C, 58.88; H, 8.33; N, 8.58. Found: C, 58.67; H, 8.30; N, 8.66. Compound **18a** was alternatively prepared in 97% yield by the following tandem lithiation[17] starting from **16a**. A solution of *sec*-BuLi (1.0 M in cyclohexane, 6.0 ml, 6.0 mmol) was injected into a stirred solution of **16a** (1.5 g, 5.0 mmol) in THF (50 ml) at −105 °C under a nitrogen atmosphere. The mixture was stirred at −105 °C for 1 h, and then a solution of MeI (1.0 g, 7.0 mmol) in THF (20 ml) was injected into the lithiated solution at −105 °C. Stirring was continued for an additional 1 h at −80 °C. The reaction mixture was again cooled at −105 °C. A solution of *sec*-BuLi (7.0 ml, 7.0 mmol) was then injected into the stirred solution at −105 °C. The mixture was stirred at −105 °C for 1 h, and a solution of MeI (1.0 g, 7.0 mmol) in THF (10 ml) was injected into the lithiated solution at −105 °C. Standard work-up and purification by distillation gave **18a** (1.58 g, 97%).

2-Ethyl-6-methoxy-4-[(*E*)-prop-1-enyl]phenyl *N,N,N′,N′*-Tetramethylphosphorodiamidate (18b) This was obtained in 99% yield or in 87% yield by the lithiation of **17b** followed by addition of MeI, or by tandem lithiation[17] starting from **16b**, respectively, under the conditions described above, bp 155 °C/0.7 mmHg. MS *m/z*: 326 (M^+). IR (neat): 2930, 2890, 1585, 1490, 1460, 1305, 1235, 1205, 1145, 995 cm^{-1}. UV nm (log ε): 258 (4.21), 295 (3.53), 307 (3.33). ^{1}H-NMR δ: 1.17 (3H, t, J=7.2 Hz), 1.82 (3H, d, J=4.8 Hz), 2.70 (12H, d, J=9.0 Hz), 2.76 (2H, q, J=7.2 Hz), 3.82 (3H, s), 6.12—6.22 (2H, m), 6.71 (2H, s). *Anal.* Calcd for $C_{16}H_{27}N_2O_3P$: C, 58.88, H, 8.33; N, 8.58. Found: C, 58.58; H, 8.17; H, 8.50.

5-Allyl-2-(3,4-dimethoxyphenyl)-7-methoxy-3-methylbenzo[*b*]furan: Carinatin (20) A solution of *sec*-BuLi (1.0 M in cyclohexane, 5.2 ml, 5.2 mmol) was injected into a solution of **18a** (1.3 g, 4.0 mmol) and TMEDA (0.78 ml, 5.2 mmol) in THF (30 ml) at −105 °C under a nitrogen atmosphere. The mixture was stirred at −105 °C for 1 h, and this lithiated solution was injected into a stirred solution of methyl veratrate (**7c**, 1.57 g, 8.0 mmol) in THF (50 ml) at −105 °C. Stirring was continued for an additional 1 h at −105 °C, then standard work-up and chromatographic purification with CH_2Cl_2 as an eluent gave the deoxybenzoin derivative **19a** (0.86 g, 44%) as a viscous oil. MS *m/z*: 490 (M^+). IR (neat): 2930, 1670, 1585, 1510, 1485, 1460, 1420, 1300, 1265, 1205, 1145, 995 cm^{-1}. UV nm (log ε): 227 (3.69), 278 (3.35), 308 (3.22). ^{1}H-NMR (400 MHz) δ: 1.50 (3H, d, J=6.6 Hz), 2.77 (6H, d, J=9.9 Hz), 2.80 (6H, d, J=9.9 Hz), 3.21 (2H, d, J=6.6 Hz), 3.84 (3H, s), 3.88 (3H, s), 3.90 (3H, s), 4.94—5.00 (2H, m), 5.11 (1H, q, J=6.6 Hz), 5.77—5.87 (1H, m), 6.46 (1H, d, J=1.8 Hz), 6.59 (1H, d, J=1.8 Hz), 6.83 (1H, d, J=8.4 Hz), 7.62 (1H, d, J=2.2 Hz), 7.83 (1H, dd, J=8.4, 2.2 Hz). *Anal.* Calcd for $C_{25}H_{35}N_2O_6P \cdot 1/2H_2O$: C, 60.09; H, 7.26; N, 5.64. Found: C, 59.79; H, 7.13; N, 5.79. A solution of **19a** (0.24 g, 0.48 mmol) in 90% HCOOH (5 ml) was refluxed for 30 min. Standard work-up and chromatographic purification with benzene as an eluent gave carinatin (**20**, 0.1 g, 63%), mp 87—88 °C (EtOH) (lit.[10] mp 88—91 °C). MS *m/z*: 338 (M^+). IR (KBr): 2930, 2820, 1620, 1600, 1580, 1510, 1480, 1460, 1380, 1260, 1220, 1140, 1100, 1050, 1020, 915 cm^{-1}. UV nm (log ε): 248 (s) (3.52), 311 (3.88). ^{1}H-NMR (400 MHz) δ: 2.42 (3H, s), 3.48 (2H, d, J=6.6 Hz), 3.93 (3H, s), 3.97 (3H, s), 4.03 (3H, s), 5.09 (1H, dd, J=11.2, 1.8 Hz), 5.13 (1H, dd, J=18.1, 1.8 Hz), 6.04 (1H, ddt, J=18.1, 11.2, 6.6 Hz), 6.64 (1H, d, J=1.5 Hz), 6.92 (1H, d, J=1.5 Hz), 6.95 (1H, d, J=8.8 Hz), 7.34 (1H, dd, J=8.8, 2.2 Hz), 7.34 (1H, d, J=2.2 Hz).

7-Methoxy-3-methyl-2-(3,4-methylenedioxyphenyl)-5-[(*E*)-prop-1-enyl]-benzo[*b*]furan: Eupomatenoid-1 (21) A solution of *sec*-BuLi (4.5 ml, 4.5 mmol) was injected into a stirred solution of **18b** (0.98 g, 3.0 mmol) and TMEDA (0.7 ml, 4.5 mmol) in THF (50 ml) at −105 °C under a nitrogen atmosphere. The mixture was stirred at −105 °C for 1 h, and a solution of methyl piperonylated (**7d**, 1.0 g, 6.0 mmol) in THF (10 ml) was injected into the lithiated solution at −105 °C. Standard work-up and purification by chromatography using CH_2Cl_2 as an eluent gave the deoxybenzoin derivative **19b** (0.8 g, 56%) as a viscous oil. MS *m/z*: 474 (M^+). IR (neat): 2930, 2900, 1705, 1675, 1605, 1580, 1485, 1445, 1355, 1300, 1250, 1220, 1145, 1050, 1035, 995 cm^{-1}. UV nm (log ε): 224 (4.45), 258 (4.16), 310 (3.96). ^{1}H-NMR (400 MHz) δ: 1.48 (3H, d, J=6.6 Hz), 1.79 (3H, d, J=6.6 Hz), 2.77 (6H, d, J=9.9 Hz), 2.79 (6H, d, J=9.5 Hz), 3.86 (3H, s), 5.08 (1H, q, J=6.6 Hz), 5.96 (2H, s), 6.04 (1H, dq, J=15.8, 6.6 Hz), 6.20 (1H, d, J=15.8 Hz), 6.55 (1H, d, J=1.5 Hz), 6.75 (1H, d, J=1.5 Hz), 6.76 (1H, d, J=8.4 Hz), 7.62 (1H, d, J=1.5 Hz), 7.78 (1H, dd, J=8.4, 1.5 Hz). *Anal.* Calcd for $C_{24}H_{31}N_2O_6P \cdot H_2O$: C, 58.52; H, 6.75; N, 5.69. Found: C, 58.59; H, 6.79; N, 5.33. A solution of **19b** (0.27 g, 0.57 mmol) in 90% HCOOH (5 ml) was refluxed for 30 min. Standard work-up and purification by chromatography using benzene as an eluent gave eupomatenoid-1 (**21**, 0.13 g, 68%), mp 147 °C (EtOH) (lit.[11e] mp

154—156 °C). MS *m/z*: 338 (M^+). IR (KBr): 960 cm^{-1}. UV nm (log ε): 236 (3.54), 267 (3.56), 313 (3.47). ^{1}H-NMR (400 MHz) δ: 1.90 (3H, dd, *J*=6.6, 1.46 Hz), 2.39 (3H, s), 4.04 (3H, s), 6.01 (2H, s), 6.21 (1H, dq, *J*=15.7, 6.6 Hz), 6.49 (1H, dq, *J*=15.7, 1.46 Hz), 6.82 (1H, d, *J*=1.46 Hz), 6.90 (1H, d, *J*=8.43 Hz), 7.03 (1H, d, *J*=1.1 Hz), 7.28 (1H, d, *J*=1.1 Hz), 7.29 (1H, dd, *J*=8.43, 1.46 Hz). *Anal.* Calcd for $C_{20}H_{18}O_4$: C, 74.52; H, 5.63. Found: C, 74.22; H, 5.69.

2-(4-Hydroxyphenyl)-7-methoxy-3-methyl-5-[(*E*)-prop-1-enyl]benzo[*b*]-furan: Eupomatenoid-13 (22) The reaction of **18b** (0.98 g, 3.0 mmol) with methyl *p*-(*tert*-butyldimethylsilyloxy)benzoate (**7e**, 1.6 g, 6.0 mmol) under the conditions described above gave a crude deoxybenzoin derivative (0.96 g). A solution of this crude product (0.96 g) in 90% HCOOH (8 ml) was refluxed for 1 h. Standard work-up and chromatographic purification using CH_2Cl_2–acetone (19:1) as an eluent gave eupomatenoid-13 (**22**, 0.4 g, 45%), mp 194—196 °C (benzene) (lit.[11e] mp 194—196 °C). MS *m/z*: 294 (M^+). IR (KBr): 3395, 1610, 1590, 1510, 1265, 1175, 1140, 1085, 1050, 965, 830 cm^{-1}. UV nm (log ε): 225 (s) (4.24), 267 (4.54), 292 (4.44), 302 (s) (4.42), 320 (s) (4.19). ^{1}H-NMR (400 MHz) δ: 1.90 (3H, d, *J*=4.9 Hz), 2.40 (3H, s), 4.04 (3H, s), 4.95 (1H, br s), 6.22 (1H, dq, *J*=16.2, 4.9 Hz), 6.53 (1H, d, *J*=16.2 Hz), 6.82 (1H, d, *J*=1.2 Hz), 6.92 (2H, d, *J*=6.0 Hz), 7.04 (1H, d, *J*=1.2 Hz), 7.69 (2H, d, *J*=6.0 Hz). *Anal.* Calcd for $C_{19}H_{18}O_3$: C, 74.52; H, 5.63. Found: C, 74.22; H, 5.69.

Acknowledgement We are greatful to Professor K. Kawanishi, Kobe Women's College of Pharmacy, for providing an authentic sample of carinatin. We are indebted to the staff of the Center for Instrumental Analysis is Nagasaki University for IR, UV, MS and NMR measurements and elemental analysis. Thanks are due to Mr. R. Akiyoshi and Miss Y. Honda for assistance in the experimental work.

References

1) A part of this work has appeared in a preliminary form: M. Date, K. Kawanishi, T. Hori, M. Watanabe, and S. Furukawa, *Chem. Pharm. Bull.*, **37**, 2884 (1989).
2) W. H. Perkin, *J. Chem. Soc.*, **23**, 368 (1870).
3) *a*) P. Cagnlant and D. Cagnlant, "Advances in Heterocyclic Chemistry," Vol. 18, Academic Press, New York, 1975, p. 337; *b*) A. Katritzky and C. W. Rees, "Comprehensive Heterocyclic Chemistry," Vol. 4, Pergamon Press, New York, 1984, p. 531; *c*) *Idem*, *ibid.*, Vol. 4, p. 599; *d*) *Idem*, *ibid.*, Vol. 4, p. 657.
4) D. A. Whiting, *Natural Product Report*, **1985**, 191; Y. Shizuri, *Yuki Gosei Kagaku Kyokai Shi*, **42**, 889 (1984); S. Yamamura, *ibid.*, **43**, 583 (1985).
5) *a*) J. W. Schulenberg and S. Archer, *J. Am. Chem. Soc.*, **82**, 2035 (1960); *b*) R. E. Koenigkramer and H. Zimmer, *J. Org. Chem.*, **45**, 3994 (1980); *c*) R. Beugelmans and H. Ginsburg, *J. Chem. Soc., Chem. Commun.*, **1980**, 508; *d*) B. Ledoussal, A. Gorgues, and A. Lecog, *ibid.*, **1986**, 171.
6) For recent reviews of lithiation reactions, see: *a*) H. W. Gschwend and H. R. Rodriguez, *Org. React.*, **26**, 1 (1979); *b*) V. Snieckus, *Heterocycles*, **14**, 1649 (1980); *c*) P. Beak and V. Snieckus, *Acc. Chem. Res.*, **15**, 306 (1982); *d*) M. Watanabe, *Yuki Gosei Kagaku Kyokai Shi*, **41**, 728 (1983); *e*) N. S. Narashimhan and R. S. Mali, *Synthesis*, **1983**, 957; *f*) *Idem*, *Top. in Curr. Chem.*, **138**, 63 (1987); *g*) V. Snieckus, *Bull. Soc. Chim. Fr.*, **1988**, 67.
7) *a*) M. Watanabe, M. Sahara, S. Furukawa, R. Billedeau, and V. Snieckus, *Tetrahedron Lett.*, **23**, 1647 (1982); *b*) M. Watanabe, M. Sahara, M. Kubo, S. Furukawa, R. J. Billedeau, and V. Snieckus, *J. Org. Chem.*, **49**, 742 (1984); *c*) M. Watanabe, M. Date, and S. Furukawa, *Chem. Pharm. Bull.*, **37**, 292 (1989); *d*) M. Date, M. Watanabe, and S. Furukawa, *ibid.*, **38**, 902 (1990), and references cited therein.
8) *a*) R. L. Letsinger and A. W. Schnizer, *J. Org. Chem.*, **16**, 869 (1951); *b*) T. E. Harmon and D. A. Shirley, *ibid.*, **39**, 3164 (1974); *c*) H. Christensen, *Synthetic Commun.*, **5**, 65 (1975); *d*) M. R. Winkle and R. C. Ronald, *J. Org. Chem.*, **47**, 2101 (1982); R. C. Ronald and M. R. Winkle, *Tetrahedron*, **39**, 2031 (1983); *e*) M. P. Sibi and V. Snieckus, *J. Org. Chem.*, **48**, 1935 (1983); *f*) R. B. Bates and T. J. Siahaan, *ibid.*, **51**, 1432 (1986).
9) *a*) D. Seebach, J-J. Lohman, M. A. Syfring, and M. Yoshifuji, *Tetrahedron*, **39**, 1963 (1983); *b*) J. H. Näsman, N, Kopola, and G. Pensar, *Tetrahedron Lett.*, **27**, 1391 (1986); *c*) M. Watanabe, M. Date, K. Kawanishi, M. Tsukazaki, and S. Furukawa, *Chem. Pharm. Bull.*, **37**, 2564 (1989); *d*) M. Watanabe, M. Date, K. Kawanishi, T. Hori, and S. Furukawa, *ibid.*, **38**, 2637 (1990).
10) K. Kawanishi, Y. Uhara, and Y. Hashimoto, *Phytochemistry*, **21**, 929 (1982); *idem*, *ibid.*, **21**, 2725 (1982); *idem*, *ibid.*, **22**, 2277 (1983).
11) *a*) R. S. McCredie, E. Ritchie, and W. C. Taylor, *Aust. J. Chem.*, **22**, 1011 (1969); *b*) B. F. Bowden, E. Ritchie, and W. C. Taylor, *ibid.*, **25**, 2659 (1972); *c*) R. Ahmed and R. Stevenson, *Phytochemistry*, **14**, 2710 (1975); *d*) R. W. Read and W. C. Taylor, *Aust. J. Chem.*, **32**, 2317 (1979); *e*) B. A. McKittrick and R. Stevenson, *J. Chem. Soc., Perkin Trans. 1*, **1983**, 475.
12) S. Nahm and S. M. Weinreb, *Tetrahedron Lett.*, **22**, 3851 (1981); T. A. Oster and T. M. Harris, *ibid.*, **24**, 1851 (1983).
13) D. R. Buckle and C. T. M. Rockell, *J. Chem. Soc., Perkin Trans. 1*, **1985**, 2443.
14) *a*) C. Deschamps-Vallet, J-B. Ilotse, M. Meyer-Dayan, and D. Molho, *Tetrahedron Lett.*, **13**, 1109 (1979); *b*) A. Hercouet and M. Le Corre, *Tetrahedron*, **37**, 2867 (1981); *c*) J. Grimshaw and N. Thompson, *J. Chem. Soc., Chem. Commun.*, **1987**, 240.
15) C.-S. Chien, T. Kawasaki, and M. Sakamoto, *Chem. Pharm. Bull.*, **33**, 5071 (1985).
16) A. Hercouet and M. Le Corre, *Tetrahedron Lett.*, **1979**, 2145.
17) M. Watanabe and V. Snieckus, *J. Am. Chem. Soc.*, **102**, 1457 (1980).

Heterophylliins A, B, C, D and E, Ellagitannin Monomers and Dimers from *Corylus heterophylla* FISCH.

Takashi YOSHIDA,[a] Zhe-Xiong JIN,[b] and Takuo OKUDA*,[a]

Faculty of Pharmaceutical Sciences, Okayama University,[a] Tsushima, Okayama 700, Japan and Department of Chinese Medicine, Heilongjiang Commercial College,[b] 50 Togda Street, Harbin, China. *Received June 26, 1990*

Two new ellagitannin monomers, heterophylliins A (12) and E (13), and three dimers, heterophylliins B (17), C (18) and D (19), were isolated from leaf extract of *Corylus heterophylla* (Betulaceae), and their structures were elucidated based on spectral and chemical evidence. Seven known tannins, 1,2,3,6-tetra-*O*-galloyl-β-D-glucose, tellimagrandin II, casuarictin, casuarinin, rugosin C, rugosin F, and degalloylrugosin F, were also isolated.

Keywords *Corylus heterophylla*; Betulaceae; ellagitannin; dimeric ellagitannin; heterophylliin A; heterophylliin B; heterophylliin C; heterophylliin D; heterophylliin E; C-glycosidic tannin

Corylus heterophylla FISCH. (Betulaceae) is a tree widely grown in Japan, Korea and the northern part of China. The nut of this tree is used as an appetite stimulator and a digestive,[1] and also as a food in these countries. During a survey of the distribution of tannins in the betulaceous plants, we found that leaf extract of this plant collected in China is rich in tannins, and we isolated thirteen polyphenolic constituents including new ellagitannin monomers and dimers, named heterophylliins A, B, C, D and E. This paper presents a detailed account of their isolation and structural characterization.

The aqueous acetone homogenate of dried leaves of *C. heterophylla* was fractionated by a combination of column chromatographies over Diaion HP-20, Toyopearl HW-40 and MCI-gel CHP-20P, as described in the experimental section, to yield new monomers, heterophylliins A (**12**) and E (**13**), and dimers, heterophylliins B (**17**), C (**18**) and D (**19**). Eight polyphenolics, which were identified as quercetin 3-*O*-β-D-glucuronide,[2] 1,2,3,6-tetra-*O*-galloyl-β-D-glucose (**1**),[3] tellimagrandin II (**2**),[4,5a] casuarictin (**5**),[5a] rugosin C (**7**),[6] casuarinin (**8**),[5] rugosin F (**10**)[7] and degalloylrugosin F (**11**),[8,9] were also isolated.

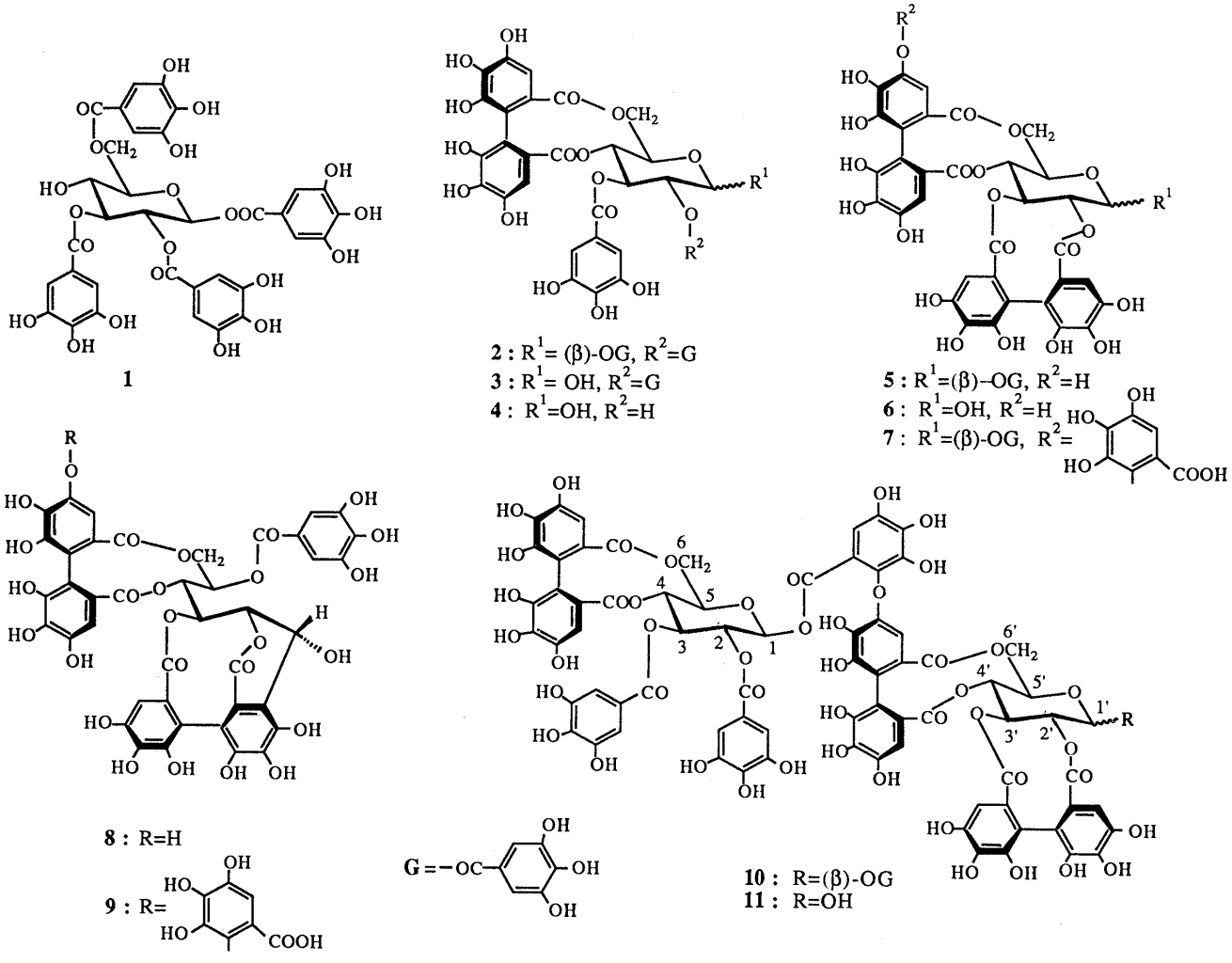

Chart 1

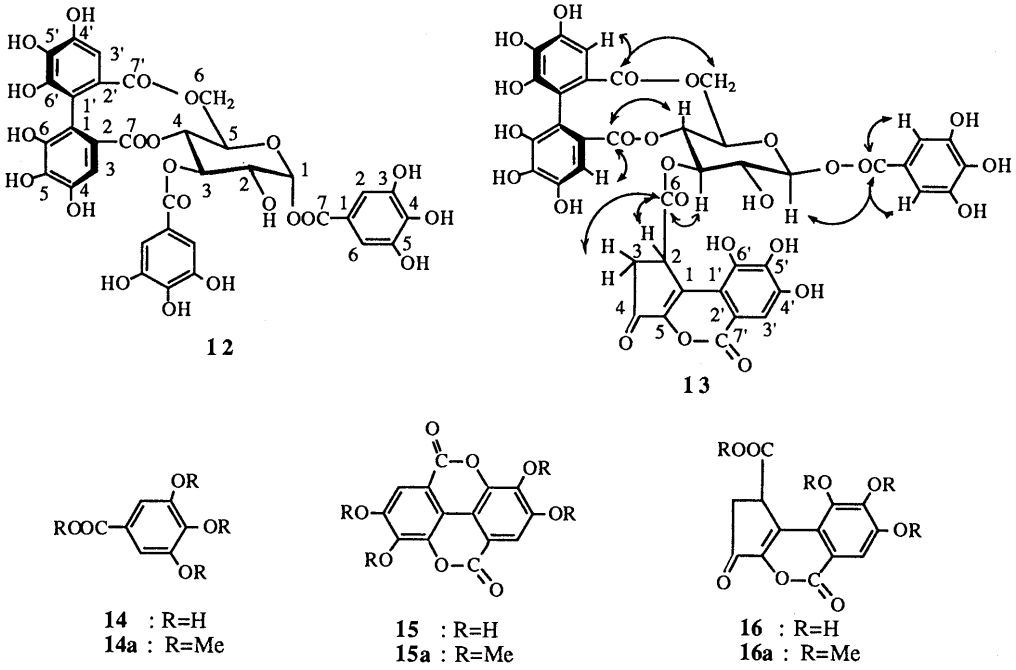

12

13

14 : R=H
14a : R=Me

15 : R=H
15a : R=Me

16 : R=H
16a : R=Me

Chart 2

Heterophylliin A (**12**), $[\alpha]_D$ +117° (MeOH), gave, upon acid hydrolysis, glucose, gallic acid (**14**) and ellagic acid (**15**). Its fast atom bombardment mass spectrum (FAB-MS) showed an $(M+Na)^+$ peak at *m/z* 809, indicating its molecular formula to be $C_{34}H_{26}O_{22}$. The presence of two galloyl groups and a hexahydroxydiphenoyl (HHDP) group in **12** was indicated by two 2H singlets at δ 7.03 and 7.24, and two 1H singlets at δ 6.48 and 6.62 in the proton nuclear magnetic resonance (^{1}H-NMR) spectrum. The (*S*)-configuration of the chiral HHDP group was shown by a positive Cotton effect at 238 nm in the circular dichroism (CD) spectrum.[10] The ^{1}H-NMR spectrum (acetone-d_6) also showed the presence of an α-oriented acyloxy group at the anomeric center of the glucose core with $^4C_1$ conformation, as revealed by a doublet (J=4 Hz) at δ 6.43 assignable to H-1. The presence of a free hydroxyl group at C-2 of glucose was also demonstrated by the coupling of the H-2 signal with a hydroxyl proton [δ 4.22 (ddd, J=7,4,10 Hz), 5.01 (d, J=7 Hz, OH)] which was collapsed to a double doublet (J=4, 10 Hz) upon addition of D_2O. The chemical shifts of the C-6 methylene protons (δ5.26 and 3.75) suggested the presence of the HHDP group at O-4—O-6.[4] Based on these data, heterophylliin A was characterized as 1,3-di-*O*-galloyl-4,6-*O*-(*S*)-hexahydroxydiphenoyl-α-D-glucose (**12**), which was confirmed by its enzymatic degalloylation, yielding gemin D (**4**).[11]

Heterophylliin E (**13**), $[\alpha]_D$ −36° (MeOH), was isolated as an off-white amorphous powder. Methylation of **13** followed by methanolysis yielded methyl tri-*O*-methylgallate (**14a**), dimethyl hexamethoxydiphenate, and methyl tri-*O*-methylbrevifolin-carboxylate (**16a**).[12] A sugar component liberated upon acid hydrolysis of **13** was identified as glucose. The ^{1}H-NMR spectrum of **13** exhibited a signals due to a galloyl group at δ 7.07, two 1H singlets ascribable to an HHDP group at δ 6.57 and 6.60, and clear signals of $^4C_1$ glucopyranose residue. This spectrum also showed a 1H singlet at δ 7.34, and a methine [δ 4.51 (dd, J=2,8 Hz)] and methylene proton signals [δ 2.89 (dd, J=8, 18 Hz) and 2.52 (dd, J=2, 18 Hz)] assignable to the protons of a brevifolin-carboxyl group. These data, coupled with six carbonyl carbon signals (δ 193.7, 172.5, 168.5, 168.3, 165.4 and 161.3) in the ^{13}C-nuclear magnetic resonance (^{13}C-NMR) spectrum, indicated that heterophylliin E is a hydrolyzable tannin consisting of a galloyl group, an HHDP moiety, a brevifolin-carboxyl group and a glucose core. These data and an $(M+Na)^+$ ion peak at *m/z* 931 in FAB-MS indicate the molecular formula of heterophyllin E to be $C_{40}H_{28}O_{25}$. The ^{1}H–^{1}H shift correlation spectrum (COSY) of **13** showed that the acyl groups are at O-1, O-3, O-4 and O-6 of the glucose core, and the coupling constant (J=8.5 Hz) of H-1 (δ-5.74) indicated β-configuration of the anomeric acyloxy group. The location of each acyl group on the glucose core was determined by the ^{1}H–^{13}C long-range COSY spectrum (J=7 Hz): The proton signal (δ 7.07) of a galloyl group was correlated through its ester carbonyl carbon (δ 165.4) with the anomeric proton (δ 5.74), by three-bond long-range couplings, permitting the assignment of the galloyl group to O-1 of glucose. The ester carbonyl carbon resonance at δ-168.5 gave cross peaks with the HHDP proton signal at δ 6.60 and the H-4 signal at δ 4.89. Similarly, the signal at δ 168.3 was correlated with the other HHDP proton (δ 6.57) and H-6 signal (δ 3.75). Finally, the carbon signal at δ 172.5, which was correlated with H-3 (δ 5.22) of glucose, showed cross peaks with the methine (δ 4.51) and one of the methylene protons (δ 2.89) in the brevifolin-carboxyl moiety (Chart 2). Based on these data and CD spectral data which exhibited a Cotton effect ($[\theta]_{236}+10.4\times10^4$), ($[\theta]_{265}$ -4.0×10^4) characteristic of the (*S*)-HHDP group,[10] the structure of heterophylliin E was established to be **13**.

Heterophylliin B (**17**), $[\alpha]_D$ +141° (MeOH), was isolated as an off-white amorphous powder. Based on the assignment of each signal by ^{1}H–^{1}H COSY (Table I), it was shown to be a dimeric hydrolyzable tannin composed of a $^4C_1$

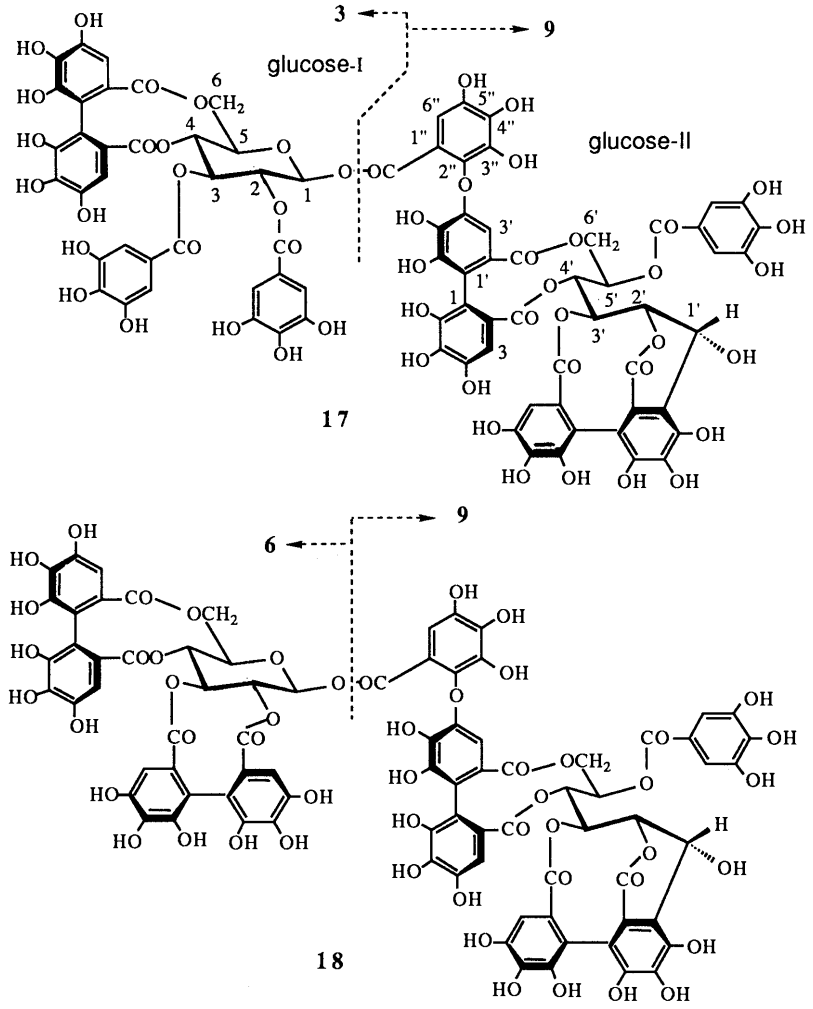

Chart 3

glucopyranose (glucose-I), and an open-chain glucose core (glucose-II), analogous to that in the C-glucosidic tannins.[5] The proton signals of glucose-I showed a typical pattern of an ellagitannin possessing a fully acylated glucose core. The signals of glucose-II protons were analogous to those of casuarinin (**8**),[5] as shown in Table I. The presence of the C-glucosidic monomer unit in **17** was further supported by the ^{13}C-NMR spectrum which exhibited only one hemiacetal carbon (δ 93.1) in the 90—100 ppm region. Among eleven glucose carbon resonances in the 80—60 ppm region, six (δ 76.7, 74.2, 71.2, 69.8, 67.6, 64.6) were again analogous to those of **8**.[13] Three 2H singlets and six 1H singlets in the aromatic region of the ^{1}H-NMR spectrum of **17** suggested the presence of three galloyl groups, a valoneoyl group, and two HHDP groups, one of which participates in the glucosidic linkage. These constituent units and ten ester carbonyl carbons were confirmed by the ^{13}C resonances described in the experimental section. The chemical shifts of the glucose-I signals were similar to those of tellimagrandin II (**2**) (Tables I and II). These data and FAB-MS data [m/z 1895 $(M+Na)^+$] indicate that heterophylliin B is a dimer, produced biogenetically by intermolecular C–O oxidative coupling[14] between **2** and **8**, forming a valoneoyl group. The structure (**17**) thus proposed was verified by partial hydrolysis of **17** with hot water, to yield tellimagrandin I (**3**) and hippophaenin B (**9**).[5b,15]

Heterophylliin C (**18**), $[\alpha]_D$ +101° (MeOH), showed an $(M+Na)^+$ ion peak at m/z 1893 in FAB-MS, which is two mass units lower than that of heterophylliin B (**17**), indicating the molecular formula $C_{82}H_{54}O_{52}$. The ^{1}H-NMR spectrum of **18** exhibited a 2H singlet at δ 7.04 and eight 1H singlets at δ 7.12, 6.79, 6.64, 6.51, 6.47, 6,43, 6.34 and 6.15. The presence of a $^4C_1$ glucopyranose and an open-chain glucose core in **18**, as in the case of **17**, was revealed by the ^{1}H–^{1}H COSY spectrum. The chemical shifts of the open-chain glucose signals were in good agreement with those of glucose-II in **17** (Table I). These spectral data clearly indicate that heterophylliin C is a C-glucosidic hydrolyzable tannin dimer in which two galloyl groups in glucose-I of **17** are replaced by an HHDP group. This assignment was further substantiated by the ^{13}C-NMR spectrum of **18**, in which the glucose carbon resonance are closely similar to those of casuarictin (**5**) and casuarinin (**8**), as shown in Table II. The structure (**18**) for heterophylliin C was finally confirmed by its partial hydrolysis with hot water to yield pedunculagin (**6**) and hippophaenin B (**9**).

Heterophylliin D (**19**), $[\alpha]_D$ +78° (MeOH), was isolated as an off-white amorphous powder, and showed a pseudomolecular ion peak [m/z 1893 $(M+Na)^+$] in FAB-MS, like that of heterophylliin C (**18**). However, the ^{1}H-

TABLE I. ^{1}H-NMR Data for the Glucose Moieties of Heterophylliins B (**17**) and C (**18**), and Their Reference Compounds (**2**, **5** and **8**) (500 MHz, Acetone-d_6, J in Hz)

	17[a]	**2**	**8**	**5**	**18**[a]
Glucose-I					
H-1	6.04 d (J=8)	6.20 d (J=8)		6.19 d (J=9)	6.06 d (J=9)
H-2	5.51 dd (J=8, 9.5)	5.58 dd (J=8, 9.5)		5.16 t (J=9)	5.09 t (J=9)
H-3	5.75 t (J=9.5)	5,83 t (J=9.5)		5.42 dd (J=9, 10)	5.36 dd (J=9, 10)
H-4	5.14 t (J=9.5)	5.20 t (J=9.5)		5.14 t (J=10)	5.08 t (J=10)
H-5	4.41 dd (J=5.5, 9.5)	4.54 dd (J=6, 9.5)		4.48 dd (J=7, 10)	4.40 dd (J=7, 10)
H-6	5.23 dd (J=5.5, 13.5)	5.36 dd (J=6, 13)		5.33 dd (J=7, 13)	5.25 dd (J=7, 13)
	3.81 d (J=13.5)	3.87 d (J=13)		3.85 d (J=13)	3.80 d (J=13)
Glucose-II					
H-1′	5.60 d (J=5)		5.60 d (J=5)		5.60 d (J=5)
H-2′	4.65 dd (J=1.5, 5)		4.64 dd (J=2, 5)		4.63 dd (J=2, 5)
H-3′	5.42 br s		5.41 dd (J=2, 2.5)		5.42 br s
H-4′	5.41 br d (J=8)		5.42 dd (J=2.5, 8)		5.40 br d (J=8)
H-5′	5.27 dd (J=3, 8)		5.31 dd (J=3, 8)		5.36 dd (J=3, 8)
H-6′	4.79 dd (J=3, 13.5)		4.82 dd (J=3, 13)		4.79 dd (J=3, 13)
	4.01 d (J=13.5)		4.04 d (J=13)		4.00 d (J=13)

a) Measured in acetone-d_6–D_2O.

TABLE II. ^{13}C-NMR Data for the Glucose Moieties of Heterophylliins B (**17**) and C (**18**), and Their Reference Compounds (**2**, **5** and **8**) (126 MHz, Acetone-d_6)

	17[a]	**2**	**8**	**18**[a]	**5**
Glucose-I					
C-1	93.1	93.8		91.8	92.4
C-2	71.7	71.8		75.9	76.0
C-3	73.2	73.3		77.2	77.3
C-4	70.5	70.8		69.0	69.3
C-5	72.8	73.1		73.3	73.5
C-6	62.9	63.1		62.9	63.1
Glucose-II					
C-1′	67.6		67.1	67.1	
C-2′	76.7		76.9	76.9	
C-3′	69.8		69.9	69.6	
C-4′	74.2		74.0	74.0	
C-5′	71.2		70.9	70.9	
C-6′	64.6		64.5	64.5	

a) Measured in acetone-d_6–D_2O.

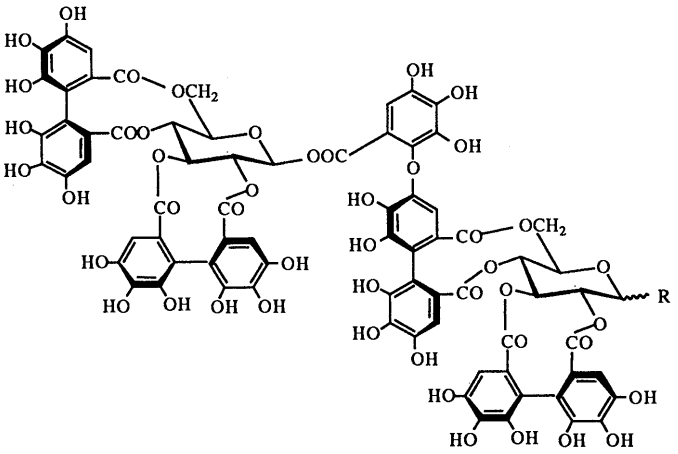

19 : R=(β)-OG
20 : R=OH

Chart 4

NMR spectrum of **19** showed the sugar proton signals characteristic of two fully acylated $^4C_1$ glucopyranose residues,[13] unlike those of **17** and **18**. Twelve glucose carbon signals in the ^{13}C-NMR spectrum were exhibited as six pair-like signals (1 : 1), resonating within 0.1 ppm for each pair, indicating analogy of the substituents on each glucose core. A 2H singlet and nine 1H singlets in the aromatic region of the ^{1}H-NMR spectrum (see Experimental) are attributable to a galloyl, a valoneoyl and three HHDP groups. Ten ester carbonyl carbon resonances in the ^{13}C-NMR spectrum were consistent with the presence of these groups. The absolute configuration of each HHDP and valoneoyl group in **19** was determined to be (*S*), by the strong positive Cotton effect at 236 nm in the CD spectrum.[10] Based on these spectral data, heterophylliin D was presumed to be a dimer formed biogenetically by C–O oxidative coupling between two moles of casuarictin (**5**). The structure (**19**) of heterophylliin D thus assigned was confirmed by its chemical conversion into a known dimer, roxbin A (**20**),[16] by enzymatic degalloylation.

This is the first report of the isolation of dimeric hydrolyzable tannins from a plant of Betulaceae. Heterophylliins B and C, which are C-glucosidic analogues of rugosin-type dimers, may be characteristic metabolites in betulaceous plants, which are taxonomically close to fagaceous plants, known to be rich in C-glucosidic tannins.[17]

Experimental

Optical rotations were measured on a JASCO DIP-4 digital polarimeter at room temperature. ^{1}H-NMR (500 MHz) and ^{13}C-NMR (126 MHz) spectra were recorded on a Varian VXR-500 instrument and FAB-MS on a VG 70-SE instrument with a 3-nitrobenzyl alcohol matrix. CD spectra were measured on a JASCO JIP-500A. Diaion HP-20, MCI-gel CHP-20P (Mitsubishi Kasei), Toyopearl HW-40 (coarse, fine grades) (Tosoh), and Sephadex LH-20 (Pharmacia Fine Chemicals) were used for column chromatography. Normal phase high performance liquid chromatography (HPLC) was carried out on a Shimadzu LC-6A with a column of Superspher Si60 (Merck) using *n*-hexane–MeOH–tetrahydrofuran (THF)–HCOOH (60 : 45 : 15 : 1) containing oxalic acid (500 mg/1.2 l). Reversed-phase HPLC was performed on a column of LiChrospher RP-18 (ODS) (Merck) in a oven at 40 °C, using the following solvent systems, (A) 0.05 M KH_2PO_4–0.05 M H_3PO_4–EtOH–EtOAc (42.5 : 42.5 : 10 : 5), (B) 0.05 M KH_2PO_4–0.05 M H_3PO_4–EtOH–EtOAc (43 : 43 : 10 : 5).

Isolation of Tannins Dried leaves (3 kg) of *C. heterophylla* collected at

Harbin, China, in May, were homogenized in acetone–H_2O (7:3) (10 l×3), and the homogenate was filtered. The filtrate was concentrated to *ca.* 2 l, and submitted to column chromatography over Diaion HP-20 (14 cm i.d. × 55 cm) developing with H_2O→10% MeOH→30% MeOH→40% MeOH→50% MeOH→MeOH→70% aqueous acetone. A part (22 g) of the 40% MeOH eluate (45.6 g) was further chromatographed on Toyopearl HW-40 (coarse) (5 cm i.d. × 51 cm) developing with 60% MeOH→70% MeOH→MeOH–H_2O–acetone (7:2:1)→MeOH–H_2O–acetone (6:2:2). From the 60% MeOH eluate, quercetin 3-*O*-*β*-D-glucuronide (querciturone) (2 g) was obtained. The 70% MeOH eluate, showing a main peak at t_R 2.8 min in HPLC (normal phase), was purified by column chromatography on MCI-gel CHP-20P (30% MeOH), to give heterophylliin E (**13**) (70 mg). The fractions containing peaks of t_R 3.0—4.5 min in normal phase HPLC were similarly chromatographed repeatedly over MCI-gel CHP-20P (20% MeOH→30% MeOH), Sephadex LH-20 (70% EtOH) and Toyopearl HW-40 (fine) (50% MeOH), to yield heterophylliin A (**12**) (24 mg), tellimagrandin II (**2**) (25 mg), 1,2,3,6-tetra-*O*-galloyl-*β*-D-glucose (**1**) (15 mg), casuarictin (**6**) (45 mg), casuarinin (**8**) (7 mg) and rugosin C (**7**) (25 mg). The eluate with MeOH–H_2O–acetone (6:2:2) from the Toyopearl HW-40 (coarse) column chromatography were divided into eight fractions (fr.I—VIII), according to the peaks in HPLC. Fraction VI gave rugosin F (**10**) (546 mg). Repeated chromatography of fr. III (662 mg) over Toyopearl HW-40 (fine) with 70% MeOH MeOH–H_2O–acetone (7:2:1) afforded degalloylrugosin F (**11**) (80 mg) and heterophylliin B (**17**) (53 mg). Fraction IV (756 mg) was further purified by column chromatography over MCI-gel CHP-20P with 20% MeOH→30% MeOH to give a further crop of heterophylliin B (**17**) (117 mg). Fraction V (346 mg) was similarly purified by repeated chromatography over MCI gel CHP-20P with the same solvent system to give heterophylliin C (**18**) (41 mg). Fraction VIII gave heterophylliin D (**19**) (59 mg), after rechromatography on MCI-gel CHP-20P with 40% MeOH.

Quercetin 3-*O*-*β*-D-Glucuronide Pale yellow needles, mp 200—202 °C (dec.), $[\alpha]_D$ −22° (*c*=1.0 , MeOH). FAB-MS *m/z*: 479 $(M+H)^+$, 501 $(M+Na)^+$. ^{1}H-NMR(acetone-d_6–D_2O) δ: 12.6 (1H, s, 5-OH), 10.90, 9.78, 9.25 (each 1H, s, 7-, 3′-, 4′-OH), 7.55 (1H, dd, *J*=2, 9 Hz, H-6′), 7.52 (1H, d, *J*=2 Hz, H-2′), 6.82 (1H, d, *J*=9 Hz, H-5′), 6.39 (1H, d, *J*=2 Hz, H-8), 6.19 (1H, d, *J*=2 Hz, H-6), 5.48 [1H, d, *J*=7.4 Hz, glucuronyl(gluc) H-1], 3.55 (1H, d, *J*=10 Hz, gluc H-5), 3.2—3.4 (gluc H-2, 3, 4, overlapped with H_2O signals). ^{13}C-NMR(DMSO-d_4) δ: 156.2 (C-2), 133.1 (C-3), 177.2 (C-4), 161.2 (C-5), 98.8 (C-6), 164.2 (C-7), 93.6 (C-8), 156.2 (C-8a), 103.9 (C-4a), 120.8 (C-1′), 116.0 (C-2′), 144.9 (C-3′), 148.6 (C-4′), 115.2 (C-5′), 121.7 (C-6′), 101.1 (gluc C-1), 71.3 (gluc C-2), 73.8 (gluc C-3), 75.8, 76.0 (gluc C-4, 5), 169.8 (gluc C-6).

Degalloylrugosin F (11) A pale brown amorphous powder, $[\alpha]_D$ +96° (*c*=1.0, MeOH). FAB-MS *m/z*: 1743 $(M+Na)^+$. ^{1}H-NMR (acetone-d_6–D_2O) δ: 7.00 (2H, s), 6.95, 6.96 (2H in total), [galloyl (G)], 7.13, 7.12 (1H in total), 6.64, 6.63 (1H in total), 6.59, 6.58 (1H in total), 6.53, 6.48 (1H in total), 6.46, 6.45 (1H in total), 6.36, 6.35 (1H in total), 6.21, 6.19 (1H in total), [HHDP and valoneoyl (Val)], 6.10, 6.11 (each d, *J*=8 Hz, H-1), 5.53 (dd, *J*=8, 9.5 Hz, H-2), 5.79 (t, *J*=9.5 Hz, H-3), 5.16 (t, *J*=9.5 Hz, H-4), 4.47 (dd, *J*=9.5, 6.5 Hz, H-5), 5.30 (dd, *J*=6.5, 13.5 Hz, H-6), 3.80 (d, *J*=13.5 Hz, H-6), 5.39 (d, *J*=4 Hz, H-1′, *α*-anomer), 5.02 (d, *J*=8.5 Hz, H-1′, *β*-anomer), 5.03 (dd, *J*=4, 9.5 Hz, H-2′, *α*-anomer), 4.83 (dd, *J*=8.5, 9.5 Hz, H-2′, *β*-anomer), 5.43 (t, *J*=9.5 Hz, H-3′, *α*-anomer), 5.20 (t, *J*=9.5 Hz, H-3′, *β*-anomer), 4.98 (t, *J*=9.5 Hz, H-4′, *α*,*β*-anomer), 4.53, 4.15 (each dd, *J*=6, 9.5 Hz, H-5′, *α*,*β*-anomer), 5.20, 5.17 (each dd, *J*=6, 13.5 Hz, H-6′, *α*,*β*-anomer), 3.71, 3.63 (each d, *J*=13.5 Hz, H-6′, *α*,*β*-anomer). ^{13}C-NMR (acetone-d_6–D_2O) δ: glucose carbons: 93.1 (C-1), 75.0 (C-2), 73.2 (C-3), 70.6 (C-4), 73.1 (C-5), 63.5, 63.0 (C-6, 6′), 91.7, 95.3 (C-1′), 75.5, 78.2 (C-2′), 75.6, 77.4 (C-3′), 69.8, 69.6 (C-4′), 67.3, 72.9 (C-5′).

An aqueous solution of rugosin F (**10**) (2 mg) was incubated with tannase[18] at 37°C for 3 h, and the reaction mixture was analyzed by HPLC (reversed-phase, solvent A), revealing the formation of **11** (t_R 6.0 and 6.5 min) and gallic acid (**14**) (t_R 3.1 min).

Heterophylliin A (12) An off-white amorphous powder, $[\alpha]_D$ +117° (*c*=0.6, MeOH). *Anal.* Calcd for $C_{34}H_{26}O_{22}\cdot 6H_2O$: C, 45.60; H, 4.20. Found: C, 45.90; H, 3.81. FAB-MS *m/z*: 809 $(M+Na)^+$ CD (MeOH) [*θ*] (nm): $+9.2\times10^4$ (238), -2.8×10^4 (265), $+1.4\times10^4$ (290). ^{1}H-NMR (acetone-d_6–D_2O) δ: 7.03, 7.24 (each 2H, s, G), 6.62, 6.48 (each 1H, s, HHDP), 6.43 (1H, d, *J*=4 Hz, H-1), 4.22 (1H, dd, *J*=4, 10 Hz, H-2), 5.65 (1H, t, *J*=10 Hz, H-3), 5.06 (1H, t, *J*=10 Hz, H-4), 4.57 (1H, dd, *J*=6.5, 10 Hz, H-5), 5.26 (1H, dd, *J*=6.5, 13.5 Hz, H-6), 3.75 (1H, d, *J*=13.5 Hz, H-6). ^{13}C-NMR (acetone-d_6–D_2O) δ: 92.9 [glucose(glu) C-1], 70.3 (glu C-2), 74.3 (glu C-3), 70.6 (glu C-4), 70.5 (glu C-5), 63.3 (glu C-6), 110.1, 110.18 [each 2C, G C-2, 6], 120.5, 126.3 (G C-1), 138.9, 139.4 (G C-4), 145.7, 146.1 (each 2C, G C-3,4), 107.7, 107.8 (HHDP C-3, 3′), 115.7, 115.8 (HHDP C-1, 1′), 125.7, 126.3 (HHDP C-2, 2′), 136.2, 136.4 (HHDP C-5, 5′), 144.3 (2C), 145.1, 145.2 (HHDP C-4, 4′, 6, 6′), 165.4, 167.2, 167.8 168.3 (ester carbonyl).

Acid Hydrolysis of 12 A solution of **12** (1 mg) in 5% H_2SO_4 (1 ml) was heated on a boiling-water bath for 6 h. The reaction mixture was extracted with EtOAc, and the EtOAc layer was analyzed by reversed-phase HPLC (solvent **B**), revealing the formation of gallic acid (**14**) (t_R 3.12 min) and ellagic acid (**15**) (t_R 10.5 min). A sugar component was identified as glucose by gas liquid chromatography (GLC) (2% OV-1, column temperature 170°C), after neutralization of the aqueous layer with ion exchange resin (Amberlite IRC 400), followed by evaporation and trimethylsilylation.

Degalloylation of 12 with Tannase A few drops of tannase were added to a solution of **12** (1 mg) in H_2O (1 ml), and the reaction mixture was left standing at 37 °C for 5 h. The formation of gemin D (**4**) and gallic acid was confirmed by HPLC (normal and reversed-phase) of the reaction mixture, using the solvent systems A, B and C.

Heterophylliin B (17) An off-white amorphous powder, $[\alpha]_D$ +141° (*c*=1.0, MeOH). *Anal.* Calcd for $C_{82}H_{56}O_{52}\cdot 12H_2O$: C, 47.10; H, 3.83. Found: C, 46.98; H, 3.63. FAB-MS *m/z*: 1895 $(M+Na)^+$. CD (MeOH) [*θ*] (nm): 19×10^4 (230), -4.4×10^4 (260), $+3.1\times10^4$ (284). ^{1}H-NMR (acetone-d_6–D_2O) δ: 7.05, 6.99, 6.95 (each 2H, s, G), 7.08, 6.82, 6.63, 6.48, 6.46, 6.13, (each 1H, s, HHDP and Val), glucose protons, see Table I. ^{13}C-NMR (acetone-d_6–D_2O) δ: 104.0, 105.3, 107.7, 108.0, 109.7, 109.9, 117.3 [HHDP C-3, 3′, Val C-3, 3′, 6″), 110.0 [6C, G C-2, 6], 112.6, 115.4, 115.7, 115.9, 116.2, 116.3, 117.1 (HHDP C-1, 1′, Val C-1, 1′, 1″), 119.8, 120.0 (2C) (G C-1), 120.7, 124.4, 125.5, 126.2, 126.5, 127.3 (HHDP C-2, 2′, Val C-2, 2′), 134.9, 136.2, 136.5, 136.6, 136.8, 138.0, 138.6 (HHDP C-5, 5′, Val C-5, 5′, 2″), 139.2, 139.3, 139.5 (G C-4), 140.3, 141.2 (Val C-3″, 4″), 143.0, 143.5, 143.6, 144.3 (2C), 145.0, 145.1 (2C), 145.3, 145.9, 146.0, 146.1, 146.6 (HHDP C-4, 4′, 6, 6′, Val C-4, 4′, 6, 6′, 5″), 145.7 (2C), 145.8 (2C), 145.9 (2C) (G C-3, 5), 169.6, 168.8, 168.7, 168.2, 167.8, 166.6, 166.1, 166.0, 165.1, 162.4 (ester carbonyl), glucose carbons, see Table II.

Partial Hydrolysis of Heterophylliin B (17) A solution of **17** (30 mg) in H_2O (10 ml) was heated on a boiling-water bath for 2 h. After concentration, the reaction mixture was chromatographed over MCI-gel CHP-20P developing with water containing stepwise-increasing amounts of MeOH. The 30% MeOH eluate gave tellimagrandin I (**3**) (2 mg) and hippophaenin B (**9**) (1.5 mg), which were identified by direct comparison of physical data with those of authentic samples.

Heterophylliin C (18) A light brown amorphous powder, $[\alpha]_D$ +101° (*c*=1.0, MeOH). *Anal.* Calcd for $C_{82}H_{54}O_{52}\cdot 15H_2O$: C, 45.98; H, 3.92. Found: C, 45.65; H, 3.52. FAB-MS *m/z*: 1893 $(M+Na)^+$. UV λ_{max}^{MeOH} nm (log *ε*): 215 (5.40), 255 (4.87). CD (MeOH) [*θ*] (nm): $+25\times10^4$ (233), -9.4×10^4 (260), $+5.0\times10^4$ (283). ^{1}H-NMR (acetone-d_6–D_2O) δ: 7.04 (2H, s, G) , 7.12, 6.79. 6.64, 6.51, 6.47, 6.43, 6.34, 6.15 (each 1H, s, HHDP and Val), glucose protons, see Table I. ^{13}C-NMR (acetone-d_6–D_2O) δ: 104.1, 105.3, 107.2, 107.4, 107.5, 108.0, 108.3, 109.7, 117.2 (HHDP C-3, 3′, Val C-3, 3′, 6″), 110.0 (2C) (G C-2, 6), 112.9, 114.5, 114.9, 115.4, 115.7, 116.1, 116.2, 116.3, 116.9 (HHDP C-1, 1′, Val C-1, 1′, 1″), 120.7 (G C-1), 120.0, 124.3, 125.5, 125.6, 126.0, 126.1, 126.6, 127.3 (HHDP C-2, 2′, Val C-2, 2′), 134.9, 136.2, 136.3, 136.4, 136.5, 136.6, 136.8, 137.8, 138.6 (HHDP C-5, 5′, Val C-5, 5′, 2″), 139.2 (G C-4), 140.4, 141.2 (Val C-3″, 4″), 145.1 (2C, G C-3, 5), 143.2, 143.5, 143.6, 144.2 (2C), 144.3, 144.4, 144.8, 144.9, 145.0, 145.1 (2C), 145.7, 145.9 (2C), 146.1, 146.8 (HHDP C-4, 4′, 6, 6′, Val C-4, 4′, 6, 6′, 5″), 169.6, 169.3, 169.0, 168.8, 168.6, 168.1, 168.0, 166.0, 165.0, 162.8 (ester carbonyl), glucose carbons, see Table II.

Partial Hydrolysis of Heterophylliin C (18) A solution of **18** (2 mg) in water (2 ml) was heated on a boiling-water bath for 2 h. The reaction mixture was analyzed by HPLC (reversed-phase, solvents B and C), which indicated the formation of pedunculagin (**6**) and hippophanenin B (**9**).

Heterophylliin D (19) An off-white amorphous powder, $[\alpha]_D$ +78° (*c*=1.0, MeOH). FAB-MS *m/z*: 1893 $(M+Na)^+$. UV λ_{max}^{MeOH} nm (log *ε*): 215 (5.27), 255 (4.88). CD (MeOH) [*θ*] (nm): $+29.3\times10^4$ (236), -10.3×10^4 (261), $+3.1\times10^4$ (282). ^{1}H-NMR (acetone-d_6–D_2O) δ: 7.13 (2H, s, G), 7.16, 6.64, 6.52, 6.49, 6.43, 6.39, 6.38, 6.34, 6.20 (each 1H, s, HHDP and Val), 6.08, 6.13 (each d, *J*=8.5 Hz, glu H-1, 1′), 5.35, 5.38 (each dd, *J*=9.5, 10 Hz, glu H-3, 3′), 5.26, 5.20 (each dd, *J*=7, 13 Hz, glu H-6, 6′), 5.13, 5.17 (each dd, *J*=8.5, 9.5 Hz, glu H-2, 2′), 5.07, 5.05 (each t, *J*=10 Hz, glu H-4, 4′), 4.40 (m, glu H-5, 5′), 3.74, 3.79 (each d, *J*=13 Hz, glu H-6, 6′). ^{13}C-NMR (acetone-d_6–D_2O) δ: 92.0, 91.9 (glu C-1, 1′), 75.8, 75.7 (glu C-2, 2′), 77.1 (glu C-3, 3′), 69.0 (glu C-4, 4′), 73.4, 73.3 (glu C-5, 5′), 63.0, 62.9 (glu C-6, 6′), 104.8, 107.1 (2C), 107.3, 107.4, 107.5, 107.7, 108.1, 109.7 (HHDP C-3, 3′, Val C-3, 3′, 6″), 110.1

(2C) (G C-2, 6), 113.3, 114.3, 114.6, 114.8, 114.9, 115.4, 115.7, 116.0, 117.1 (HHDP C-1, 1′, Val C-1, 1′, 1″), 119.6 (G C-1), 125.2, 125.5, 125.6, 125.8, 125.9, 126.0, 126.1, 126.2 (HHDP C-2, 2′, Val C-2, 2′), 136.1, 136.3, 136.4, 136.45 (2C), 136.54 (2C), 136.9, 137.5 (HHDP C-5, 5′, Val C-5, 5′, 2″), 139.9 (G C-4), 140.5, 141.2 (Val C-3″, 4″), 145.0 (2C) (G C-3, 5), 143.4, 144.1, 144.2, 144.3 (2C), 144.4 (2C), 144.6, 144.9, 145.1, 145.2, 146.1, 146.8 (HHDP C-4, 4′, 6, 6′, Val C-4, 4′, 6, 6′, 5″), 169.23, 169.20, 169.17, 168.7, 168.1, 167.9 (2C), 167.6, 165.0, 163.0 (ester carbonyl).

Degalloylation of Heterophylliin D (19) A mixture of **19** (30 mg) and tannase in water (3 ml) was left standing at 37°C for 5 h. The reaction mixture, after addition of dilute HCl, was concentrated, and the residue was subjected to column chromatography over MCI-gel CHP-20P developing with $H_2O \rightarrow 10\%$ MeOH $\rightarrow 30\%$ MeOH $\rightarrow 40\%$ MeOH in a stepwise gradient mode, to give gallic acid (**14**) (10% MeOH eluate), and roxbin A (**20**) (2.5 mg) (40% MeOH eluate), which was identified by ^{1}H-NMR spectral comparison with an authentic sample.

Heterophylliin E (13) An off-white amorphous powder, $[\alpha]_D$ −36° ($c=1.0$, MeOH). *Anal.* Calcd for $C_{40}H_{28}O_{25}\cdot 7H_2O$: C, 46.42; H, 4.10. Found: C, 46.42; H, 4.65. FAB-MS m/z: 931 $(M+Na)^+$. UV λ_{max}^{MeOH} nm (log ε): 222 (5.01), 275 (4.86), 340 (4.16). CD (MeOH) $[\theta]$ (nm): $+10.4\times10^4$ (236), -4.0×10^4 (265), $+1.4\times10^4$ (286), -0.6×10^4 (313). ^{1}H-NMR (acetone-d_6–D_2O) δ: 7.07 (2H, s, galloyl), 6.60, 6.57 (each 1H, s, HHDP), 7.34 [1H, s, brevifolin carboxyl (brev) H-3′], 4.51 (1H, dd, $J=2$, 8 Hz, brev H-2), 2.89 (1H, dd, $J=8$, 18 Hz, brev H-3), 2.52 (1H, dd, $J=2$, 18 Hz, brev H-3), 5.74 (1H, d, $J=8.5$ Hz, H-1), 3.70 (1H, dd, $J=8.5$, 9.5 Hz, H-2), 5.22 (1H, t, $J=9.5$ Hz, H-3), 4.89 (1H, t, $J=9.5$ Hz, H-4), 4.25 (1H, dd, $J=9.5$, 6.5 Hz, H-5), 5.22 (1H, dd, $J=6.5$, 13.5 Hz, H-6), 3.75 (1H, d, $J=13.5$ Hz, H-6). ^{13}C-NMR (acetone-d_6–D_2O) δ: 95.4 (gluc C-1), 71.7 (gluc C-2), 76.6 (gluc C-3), 70.6 (gluc C-4), 72.5 (gluc C-5), 63.2 (gluc C-6), 42.2 (brev C-2), 37.6 (brev C-3), 107.9, 108.0 (HHDP C-3, 3′), 109.3 (brev C-3′), 110.1 (2C) (G C-2, 6), 114.6 (brev C-1′), 115.7, 115.8 (HHDP C-1, 1′), 116.2 (brev C-2′), 119.9 (G C-1), 125.7, 126.2 (HHDP C-2, 2′), 136.3, 136.5 (HHDP C-5, 5′), 138.6 (brev C-1), 139.6 (G C-4), 140.6 (brev C-5′), 143.6, 144.3, 145.1, 145.2, 145.9 (HHDP C-4, 4′, 6, 6′, brev C-6′), 146.0 (2C) (G C-3, 5), 147.3 (brev C-5), 149.9 (brev C-4′), 193.7 (brev C-4), 172.5 (brev C-6), 168.5 (HHDP C-7), 168.3 (HHDP C-7′), 165.4 (G C-7), 161.3 (brev C-7′).

Methylation of Heterophylliin E (13) Followed by Methanolysis A mixture of **13** (7 mg), anhydrous K_2CO_3 (40 mg) and Me_2SO_4 (5 μl) in dry acetone (3 ml) was refluxed for 4 h. After filtering inorganic materials off, the reaction mixture was evaporated, and was directly methanolyzed with 1% NaOMe in MeOH to give methyl tri-*O*-methylgallate (**14a**) (1 mg), dimethyl hexamethoxydiphenate (0.5 mg) and methyl tri-*O*-methylbrevifolin-carboxylate (**16a**) (0.8 mg), which were identified by co-chromatography with authentic samples (thin layer chromatography) and by ^{1}H-NMR spectral comparisons.

Acid Hydrolysis of Heterophylliin E (13) A solution of **13** (3 mg) in 1% H_2SO_4 (1 ml) was heated in a boiling-water bath for 5 h. After cooling, the reaction mixture was extracted with EtOAc. The sugar component in the aqueous layer was identified as glucose by GLC (2% OV-1, column temperature 170 °C) after trimethylsilylation. The EtOAc soluble portion gave gallic acid (**14**), ellagic acid (**15**) and brevifolin-carboxylic acid (**16**), which were identified by co-chromatography with the authentic samples in HPLC (reversed-phase, solvent B).

Acknowledgements The authors are grateful to Dr. N. Toh, Faculty of Engineering, Kyushu Kyoritsu University, for the CD measurements, and Mr. S. Iwadow, Faculty of Pharmaceutical Sciences, Okayama University, for recording the FAB mass spectra. A Varian VXR-500 instrument of the SC-NMR Laboratory of Okayama University was used for the ^{1}H- and ^{13}C-NMR spectral measurements.

References and Notes

1) L. M. Perry, "Medicinal Plants of East and Southeast Asia," MIT Press, Cambridge, Massachusetts, 1980, p. 57.
2) *a*) I. A. Pearl and S. F. Parling, *J. Org. Chem.*, **28**, 1442 (1963); *b*) K. R. Markham and L. J. Porter, *Phytochemistry*, **12**, 2007 (1973).
3) E. A. Haddock, R. K. Gupta, S. M. K. Al-Shafi, E. Haslam, and D. Magnolato, *J. Chem. Soc. Perkin Trans. 1*, **1982**, 2515.
4) K. Wilkins and B. A. Bohm, *Phytochemistry*, **15**, 211 (1976).
5) *a*) T. Okuda, T. Yoshida, M. Ashida, and K. Yazaki, *J. Chem. Soc., Perkin Trans. 1*, **1983**, 1765; *b*) T. Sakai, T. Tanaka, G. Nonaka, I. Nishioka, and K. Mitsuhashi, Abstracts of Papers, The 110th Annual Meeting of The Pharmaceutical Society of Japan, Sapporo, August 1990, Vol. 2, p. 165.
6) T. Okuda, T. Hatano, K. Yazaki, and N. Ogawa, *Chem. Pharm. Bull.*, **30** 4230 (1982).
7) T. Okuda, T. Hatano, and N. Ogawa, *Chem. Pharm. Bull.*, **30** 4234 (1982).
8) T. Hayashi, M. Nishizawa, T. Yamagishi, G. Nonaka, and I. Nishioka, Abstracts of Papers, The 31st Annual Meeting of The Japanese Society of Pharmacognosy, Tokyo, 1984, p. 42.
9) The orientation of the valoneoyl group in **11**, which had remained unsolved, has been established to be the same as that of **10** by chemical correlation between **11** and **10** (see Experimental).
10) T. Okuda, T. Yoshida, T. Hatano, T. Koga, N. Toh, and K. Kuriyama, *Tetrahedron Lett.*, **23**, 3931 (1982).
11) T. Yoshida, T. Maruyama, M. U. Memon, T. Shingu, and T. Okuda, *Phytochemistry*, **24**, 1941 (1985).
12) O. T. Schmidt and K. Bernauer, *Justus Liebigs Ann. Chem.*, **588**, 211 (1954).
13) T. Hatano, T. Yoshida, T. Shingu, and T. Okuda, *Chem. Pharm. Bull.*, **36**, 3849 (1988).
14) T. Okuda, T. Yoshida, and T. Hatano, *Heterocycles*, **39**, 1195 (1990).
15) T. Yoshida, K. Tanaka, X.-M. Chen, and T. Okuda, *Phytochemistry*, in press.
16) T. Yoshida, X.-M. Chen, T. Hatano, M. Fukushima, and T. Okuda, *Chem. Pharm. Bull.*, **35**, 1817 (1987).
17) E. Haslam, "Plant Polyphenols. Vegitable Tannins Revisited," Cambridge University Press, Cambridge, 1989, p. 90.
18) T. Yoshida, K. Tanaka, X.-M. Chen, and T. Okuda, *Chem. Pharm. Bull.*, **37**, 920 (1989).

Chemical and Chemotaxonomical Studies of Ferns. LXXX.[1] Proanthocyanidins of *Arachniodes sporadosora* NAKAIKE and *A. exilis* CHING

Nobutoshi TANAKA,*[,a] Ryoki ORII,[a] Kazuo OGASA,[a] Hiroshi WADA,[a] Takao MURAKAMI,[b] Yasuhisa SAIKI[c] and Chiu-Ming CHEN[d]

Faculty of Pharmaceutical Sciences, Science University of Tokyo,[a] Funakawara-machi, Ichigaya, Shinjuku-ku, Tokyo 162, Japan, Faculty of Industrial Science and Technology, Science University of Tokyo,[b] Yamasaki 2641, Noda, Chiba 278, Japan, Department of Pharmaceutical Sciences, Kobe Gakuin University,[c] Arise, Igawatani-machi, Nishi-ku, Kobe 673, Japan and Department of Chemistry, National Tsing Hua University,[d] Kuang Fu Road, Hsinchu, Taiwan, China. *Received July 3, 1990*

Three new trimeric proanthocyanidins were isolated in lactone form (1L, 2L and 3L) and acid form (1A, 2A and 3A) from the fronds of both *Arachniodes sporadosora* NAKAIKE and *A. exilis* CHING. Their structures were determined by spectroscopic methods and thiolytic degradation.

Keywords *Arachniodes sporadosora*; *Arachniodes exilis*; Aspidiaceae; fern; proanthocyanidin; sweet substance; ^{13}C-NMR

There has been considerable progress in the chemistry of proanthocyanidins in the last two decades. Recently, Nishioka and his co-workers, who have made an important contribution in this field, reported the presence of many proanthocyanidins in several ferns.[2] Hori *et al.* have also isolated new proanthocyanidins from a Pteridaceous fern, *Dennstaedtia distenta*.[3] In a continuation of our chemical studies of ferns, three more new proanthocyanidins were isolated not only as their lactone forms, **1L**, **2L** and **3L**, but also as acid forms, **1A**, **2A** and **3A**, from *Arachniodes sporadosora* (KUNZ.) NAKAIKE and *A. exilis* CHING. In this paper, we describe the structure determination of these compounds.

A. sporadosora and *A. exilis* are Aspidiaceous ferns found in the region from south of the Kanto district, Japan, to Taiwan, China. They frequently grow in the same area, and hybridize readily with each other. Their methanol extracts showed similar chromatographic patterns on silica gel, suggesting a closs relationship between them. From the methanol extract of the air-dried fronds of either *A. sporadosora* or *A. exilis*, the above-mentioned six compounds were isolated by repeated chromatography on Sephadex LH-20.

Compound **1L**, a pale brown amorphous solid, $[\alpha]_D^{20}$ +65° (c=1.0, MeOH), was positive to the ferric chloride reagent and gave a red color with HCl in EtOH, suggesting it to be a proanthocyanidin. In the secondary ion mass spectrum (SI-MS), **1L** gave the $[M+H]^+$ ion peak at m/z 905. In the carbon-13 nuclear magnetic resonance (^{13}C-NMR) spectrum, **1L** showed thirty-six signals assignable to the A- and B-ring carbons of three epicatechin-type units, indicating that **1L** is a trimeric proanthocyanidin (Table I). The remaining eleven signals included a ketal carbon signal at δ 104.9, suggesting that **1L** possesses a proanthocyanidin A-type unit (**8**) in the molecule.[4] A typical trimer **9** containing a proanthocyanidin A-type unit has been isolated from the root bark of *Cinnamomum zeylanicum*.[5] The ^{13}C-NMR spectral data of **9** (in Chart 2) were in good agreement with those of **1L** except that the C-2 and C-3 signals of the bottom unit of **1L** showed an upfield shift (−4.3 ppm) and a downfield shift (+3.6 ppm), respectively, and the signal of C-4 of the bottom unit of **9** (δ 29.2) was replaced by three signals at δ 36.1 (CH), 39.9 (CH_2) and 176.3 (COO). These spectral data indicated that the bottom unit of **1L** possesses a carboxymethylene unit at C-4. Considering its molecular weight and the fact that **1L** gave a tridecaacetate [field desorption mass spectrum (FD-MS) m/z: 1450 (M^+)] with acetic anhydride in pyridine, this carboxymethylene unit was expected to form a lactone ring with the hydroxyl group at C-5.[6] A compound similar to this putative bottom unit has been isolated from an Aspidiaceous fern, *Dryopteris filix-mas*, and named dryopterin (**6**).[7] The ^{13}C-NMR data of the C-ring of **6** are in good agreement with those of the bottom unit of **1L**.

On degradation with acid in the presence of benzylmercaptan, **1L** gave a dimeric proanthocyanidin thioether **4** and the bottom unit **6**. Their properties and spectral data were the same as those of proanthocyanidin A-2 4′-benzylthio-

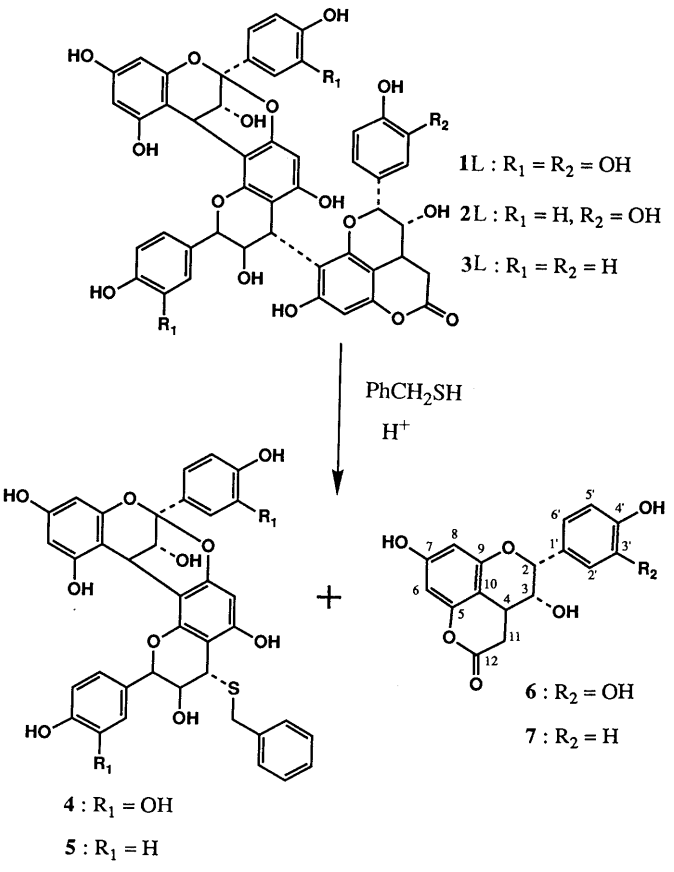

Chart 1

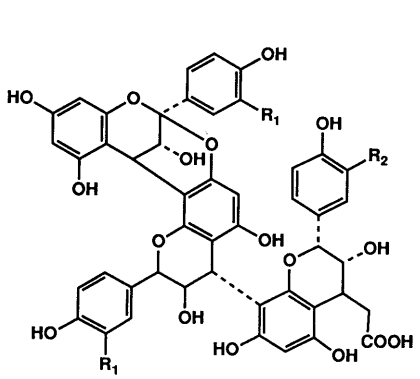

1A : $R_1 = R_2 = OH$
2A : $R_1 = H, R_2 = OH$
3A : $R_1 = R_2 = H$

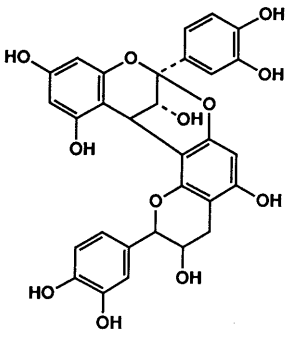

8

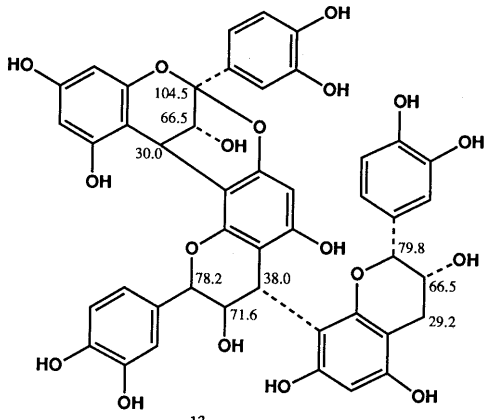

9 (^{13}C-NMR data in D_2O - acetone-d_6)

Chart 2

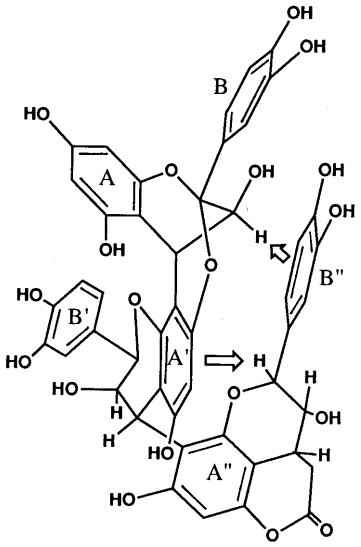

Fig. 1

ether (**4**)[5] and dryopterin (**6**).[8] Therefore, **1L** was determined to be a coupling product of proanthocyanidin A-2 (**8**) and dryopterin (**6**) with the position of the interflavonoid linkage remaining to be confirmed as either (4β-6) or (4β-8).[9] In the proton nuclear magnetic resonance (^{1}H-NMR) spectrum of **1L**, the signals corresponding to those of C-3-H (δ 4.06) of **4** and C-2-H (δ 4.80) of **6** appeared at δ 3.28 and 4.38, respectively. These remarkable upfield shifts are attributable to the magnetic anisotropic effects of the B″-ring and the A′-ring which can be located just in front of the protons only when **1L** possesses a (4′β-8) linkage (see Fig. 1). Therefore, the structure of **1L** was determined as epicatechin-(4β→8,2β→O→7)-epicatechin-(4β→8)-dryopterin.[10]

Compound **2L**, a pale brown amorphous solid, $[\alpha]_D^{20}$ + 62° (c = 1.2, MeOH), showed the $[M+H]^+$ ion peak at m/z 873 in the SI-MS, indicating that **2L** possesses a molecular formula smaller than that of **1L** by two oxygen atoms. The ^{1}H- and ^{13}C-NMR data of **2L** were almost the same as those of **1L** except that the signals corresponding to two of the three catechol-type B-rings of **1L** were replaced by those of two *p*-hydroxyphenyl groups (Tables I and II).

On thiolytic degradation, **2L** gave a dimeric proanthocyanidin thioether **5**, a pale brown amorphous solid, $[\alpha]_D^{20}$ + 64° (c = 0.7, acetone), and dryopterin (**6**). The structure of **5** was confirmed as epiafzelechin-(4β→8,2β→O→7)-epiafzelechin 4′-benzylthioether by comparison of its ^{1}H- and ^{13}C-NMR data with those of **4** (Table II). Therefore, the structure of **2L** was determined as epiafzelechin-(4β→8, 2β→O→7)-epiafzelechin-(4β→8)-dryopterin.

Compound **3L**, a pale brown amorphous solid, $[\alpha]_D^{20}$ + 71° (c = 1.5, MeOH), was found to have a molecular formula with one less oxygen atom than **2L** basing on the $[M+H]^+$ ion peak at m/z 857 in the SI-MS. The ^{1}H- and ^{13}C-NMR data were almost the same as those of **2L** except that the catechol-type B-ring of the bottom unit of **2L** was displaced by a *p*-hydroxyphenyl group. On thiolytic degradation, **3L** gave the dimeric proanthocyanidin thioether **5** and a bottom unit **7**, a colorless amorphous powder, $[\alpha]_D^{20}$ − 30° (c = 0.2, MeOH). The structure of **7** was confirmed as 3′-deoxydryopterin by comparison of its ^{1}H- and ^{13}C-NMR data with those of dryopterin **6** (Table II). Therefore, the structure of **3L** was determined as epiafzelechin-(4β→8,2β→O→7)-epiafzelechin-(4β→8)-3′-deoxydryopterin.

Compounds **1A**, **2A** and **3A** gave $[M+H]^+$ ion peaks at m/z 923, 891 and 875 in the SI-MS, indicating that they have larger molecular weights by 18 mass units than **1L**, **2L** and **3L**, respectively. Compound **1A** showed almost the same ^{1}H- and ^{13}C-NMR spectra as those of **1L** except for the signals due to H-11α, C-11 and C-12 (Tables I and II). The differences in the chemical shifts suggested that the lactone group of **1L** had been hydrolyzed in the case of **1A**. This suggestion was supported by the fact that **1A** gave an undecamethylate with methyl iodide and K_2CO_3 in acetone, FD-MS m/z: 1090 [M^+]. On thiolytic degradation, **1A** gave the same products, **4** and **6**, as those of **1L**, forming the lactone ring under these reaction conditions. Thus, the structure of **1A** was assigned as the free acid form of **1L**.[12] Similarly, the structures of **2A** and **3A** were assigned as the free acid forms of **2L** and **3L**, respectively.

Compounds **1L**, **2L** and **3L** (alternatively, **1A**, **2A** and **3A**) are examples of a new type of proanthocyanidin which possesses a terminal two-carbon unit, probably originating from malonyl coenzyme A. Compounds **1L** and **1A** have a sweet taste, similarly to compound **9**.[13] However,

TABLE I. ^{13}C-NMR Data in D_2O–Acetone-d_6 (1 : 1)

C	1L	1A	2L	2A	3L	3A
2	104.9	104.8	105.0	105.0	104.9	104.6
	78.0	77.9	78.1	78.2	78.3	77.9
	75.5	75.4	75.7	75.7	75.7	75.4
3	71.4	71.3	71.5	71.6	71.8	71.5
	70.1	70.2	70.2	70.7	70.5	70.6
	66.5	66.4	66.6	66.6	66.6	66.3
4	38.2	38.1	38.3	38.4	38.4	38.1
	36.1	36.2	36.2	36.6	36.5	36.5
	28.2	28.1	28.4	28.4	28.4	28.1
5,7,9	156.9	156.8	157.0	157.0	156.8	156.4
	155.9	155.8	156.1	156.1	156.1	155.8
	155.5	155.4	155.6	155.7	155.7	155.4
	155.1	155.0	155.2	155.3	155.3	155.0
	155.1	155.0	155.2	155.1	155.2	154.7
	155.0	154.8	155.1	154.9	155.0	154.5
	153.7	153.6	153.8	153.8	153.8	153.5
	151.4	151.2	151.5	151.4	151.2	151.1
	150.5	150.4	150.6	150.6	150.4	150.3
6,8,10	108.2	108.1	108.3	108.3	108.3	108.0
	106.4	106.3	106.5	106.6	106.5	106.3
	105.9	105.8	106.0	106.0	105.8	105.6
	102.8	103.2	102.9	104.1	103.7	104.3
	99.5	99.4	99.8	99.8	99.8	99.5
	98.2	98.1	98.3	98.3	98.4	98.1
	96.8	96.9	96.9	97.2	97.2	96.9
	96.7	96.6	96.8	96.8	96.8	96.5
	95.8	95.8	95.9	96.1	96.0	95.7
11	39.9	41.3[a]	40.1	43.4[a]	39.8	44.6[a]
12	176.3	177.4[a]	176.3	179.1[a]	176.2	180.2[a]
3,4-Dihydroxyphenyl						
1′	132.3	132.3	132.5	132.7		
	131.9	131.8				
	131.3	131.2				
2′	116.8	116.6	115.3	115.3		
	115.6	115.5				
	115.3	115.2				
3′,4′	145.9	145.8	145.3	145.2		
	145.6	145.4	144.8	144.7		
	145.3	145.1				
	145.0	144.9				
	144.8	144.7				
	144.7	144.5				
5′	116.6	116.4	115.9	116.0		
	116.2	116.1				
	116.1	116.0				
6′	121.3	121.2	119.4	119.5		
	119.8	119.8				
	119.5	119.4				
p-Hydroxyphenyl						
1′			131.4	131.4	131.7	131.8
			130.8	130.8	131.1	131.4
					130.6	130.8
2′,6′			130.7	130.7	130.4	130.7
			129.2	129.2	128.9	129.2
					128.8	129.1
3′,5′			116.6	116.2	116.0	116.6
			115.9	115.9	115.5	115.8
					115.3	115.6
4′			157.8	157.8	157.5	157.9
			157.4	157.4	157.1	157.5
					156.7	157.1

The numbering system for the flavane skeleton is adopted. The numbers 11 and 12 represent an additional carboxymethylene unit. *a*) The chemical shifts changed with concentration.[11]

compounds **2L**, **2A**, **3L** and **3A** have an astringent taste.

Experimental

Melting points were determined with a Yanagimoto micromelting apparatus and are uncorrected. Optical rotations were taken with a JASCO DIP-360 automatic polarimeter. The ^{1}H-NMR and ^{13}C-NMR spectra were measured with a JEOL GSX-500 spectrometer. Ultraviolet (UV) spectra were recorded on a Hitachi 323 spectrometer and infrared (IR) spectra on a Shimadzu IR-460 spectrometer. Circular dichroism (CD) spectra were recorded on a JASCO J-600 spectrometer. Mass spectra (MS) were measured with Hitachi M-80A and JEOL SX-102 spectrometers.

Isolation Procedure The air-dried fronds (800 g) of *Arachniodes sporadosora* NAKAIKE, collected in October at Uchiurayama, Chiba Prefecture, were extracted twice with 3 l of MeOH under reflux for 6 h. The combined extracts (6 l) and then 10 l of MeOH were passed over activated charcoal (100 g) packed in a column of 7 cm diameter. The resulting solution was concentrated to about 500 ml under reduced pressure and 1 l of acetone was added. The gummy precipitates were removed and the remaining solution was evaporated. The residue (11 g) was repeatedly chromatographed on Sephadex LH-20 using acetone–water, EtOH and EtOH–water as eluents to yield compounds **1L** (1.1 g), **1A** (0.2 g), **2L** (0.5 g), **2A** (0.5 g), **3L** (0.3 g) and **3A** (0.2 g).

The air-dried fronds (650 g) of *A. exilis* CHING, collected in October at Uchiurayama, Chiba Prefecture, were extracted and separated in a similar manner as above to yield compounds **1L** (0.9 g), **1A** (0.3 g), **2L** (0.4 g), **2A** (0.1 g), **3L** (0.2 g) and **3A** (0.1 g).

Compound 1L A pale brown amorphous powder, $[\alpha]_D^{20}$ +65° (c=1.0, MeOH). UV λ_{max}^{MeOH} nm (log ε): 284 (4.10). IR ν_{max}^{KBr} cm^{-1}: 3370, 1700, 1605, 1520, 1210, 1110, 1060, 1005, 820, 780. SI-MS m/z: 905 $[M+H]^+$.

Compound 1A A pale brown amorphous powder, $[\alpha]_D^{20}$ +79° (c=1.0, MeOH). UV λ_{max}^{MeOH} nm (log ε): 284 (4.04). IR ν_{max}^{KBr} cm^{-1}: 3370, 1700, 1610, 1510, 1210, 1110, 1060, 1005, 820, 780. SI-MS m/z: 923 $[M+H]^+$.

Compound 2L A pale brown amorphous powder, $[\alpha]_D^{20}$ +62° (c=1.2, MeOH). UV λ_{max}^{MeOH} nm (log ε): 224 (4.86), 279 (3.72). IR ν_{max}^{KBr} cm^{-1}: 3380, 1700, 1610, 1515, 1210, 1140, 1115, 1090, 1065, 1005, 830. SI-MS m/z: 873 $[M+H]^+$.

Compound 2A A pale brown amorphous powder, $[\alpha]_D^{20}$ +78° (c=1.0, MeOH). UV λ_{max}^{MeOH} nm (log ε): 225 (4.91), 280 (3.90). IR ν_{max}^{KBr} cm^{-1}: 3400, 1695, 1605, 1505, 1210, 1140, 1115, 1090, 1065, 1005, 830. SI-MS m/z: 891 $[M+H]^+$.

Compound 3L A pale brown amorphous powder, $[\alpha]_D^{20}$ +71° (c=1.5, MeOH). UV λ_{max}^{MeOH} nm (log ε): 225 (4.92), 277 (3.78). IR ν_{max}^{KBr} cm^{-1}: 3380, 1700, 1610, 1510, 1210, 1115, 1090, 1065, 1005, 830. SI-MS m/z: 857 $[M+H]^+$.

Compound 3A A pale brown amorphous powder, $[\alpha]_D^{20}$ +84° (c=1.1, MeOH), UV λ_{max}^{MeOH} nm (log ε): 224 (4.97), 277 (3.94). IR ν_{max}^{KBr} cm^{-1}: 3400, 1700, 1610, 1510, 1210, 1115, 1090, 1060, 1000, 835. SI-MS m/z: 875 $[M+H]^+$.

The Tridecaacetate of 1L A mixture of **1L** (50 mg), pyridine (2 ml) and acetic anhydride (2 ml) was allowed to stand for 19 h at room temperature, then poured into ice-water. The products were extracted with EtOAc. The extract was washed with 10% Na_2CO_3 solution, 10% HCl solution and water, then dried over anhydrous Na_2SO_4 and concentrated under reduced pressure. The residue was chromatographed on Sephadex LH-20 using 10% MeOH in benzene as an eluent to yield the tridecaacetate (38 mg). A colorless amorphous powder, $[\alpha]_D^{20}$ +37° (c=0.3, $CHCl_3$). UV λ_{max}^{MeOH} nm (log ε): 278 (3.90). IR ν_{max}^{KBr} cm^{-1}: 2940, 1770, 1615, 1600, 1500, 1440, 1370, 1210, 1110, 1060, 1015, 900, 840. FD-MS m/z: 1450 $[M^+]$.

The Undecamethylate of 1A Compound **1A** (40 mg) was dissolved in dry acetone (20 ml) and then methyl iodide (8 ml) and anhydrous K_2CO_3 (6 g) were added. The mixture was stirred under reflux for 8 h and poured into ice-water. The products were extracted with EtOAc. The extract was washed with water, dried over anhydrous Na_2SO_4 and evaporated. The residue was chromatographed on silica gel using 20% acetone in $CHCl_3$ as an eluent to yield 38 mg of the undecamethylate of **1A**. A colorless amorphous powder, $[\alpha]_D^{20}$ +25° (c=1.6, $CHCl_3$). UV λ_{max}^{MeOH} nm (log ε): 281 (4.32). IR ν_{max}^{KBr} cm^{-1}: 3450, 3000, 2950, 2850, 1720, 1600, 1505, 1450, 1260, 1120, 1020, 810, 760. FD-MS m/z: 1090 $[M^+]$.

Degradation of 1L Compound **1L** (520 mg) was dissolved in EtOH (17 ml) containing benzylmercaptan (7 ml) and glacial acetic acid (5 ml), and the solution was refluxed under argon for 20 h. After removal of the volatile solvent, the residual oil was chromatographed on Sephadex LH-20 using EtOH as an eluent to yield **4** (27 mg) and **6** (8 mg).

4: A pale brown amorphous powder, $[\alpha]_D^{20}$ +87° (c=1.3, acetone). UV λ_{max}^{MeOH} nm (log ε): 282 (4.17). IR ν_{max}^{KBr} cm^{-1}: 3350, 1610, 1510, 1435, 1280, 1140, 1060. SI-MS m/z: 699 $[M+H]^+$.

6: A colorless amorphous powder, $[\alpha]_D^{20}$ −59° (c=0.6, MeOH). UV λ_{max}^{MeOH} nm (log ε): 282 (3.88). IR ν_{max}^{KBr} cm^{-1}: 3370, 1700, 1600, 1510, 1455, 1270, 1140, 1100, 1020, 820. CD : $[\theta]_{282}$ −1270° (c=0.01, MeOH).

TABLE II. ^{1}H-NMR Data in D_2O–Acetone-d_6 (1 : 1)

	1L	1A	4	6		2L	2A		3L	3A	5	7
Top unit												
H-3	3.28 d (3)	3.26 d (3)	4.06 d (3)		H-3	3.30 d (4)	3.29 d (4)	H-3	3.19 d (4)	3.18 d (3)	4.05 d (3)	
H-4	4.12 d (3)	4.10 d (3)	4.36 d (3)		H-4	4.12 d (4)	4.10 d (4)	H-4	4.00 d (4)	3.99 d (3)	4.35 d (3)	
H-6	5.92 d (2)	5.91 d (2)	5.98 d (2)		H-6	5.91 d (2)	5.91 d (2)	H-6	5.91 d (2)	5.90 d (2)	5.97 d (2)	
H-8	6.03 d (2)	6.02 d (2)	6.07 d (2)		H-8	6.02 d (2)	6.02 d (2)	H-8	6.01 d (2)	6.00 d (2)	6.05 d (2)	
H-2′	7.01 d (2)	7.00 d (2)	7.12 d (2)		H-2′6′	7.30 d (9)	7.30 d (9)	H-2′6′	7.28 d (9)	7.27 d (9)	7.42 d (9)	
H-5′	6.87 d (8)	6.86 d (9)	6.84 d (8)		H-3′5′	6.86 d (9)	6.86 d (9)	H-3′5′	6.85 d (9)	6.85 d (9)	6.84 d (9)	
H-6′	6.80 dd (8, 2)	6.80 dd (9, 2)	6.89 dd (8, 2)									
Middle unit												
H-2	5.59 br s	5.56 br s	5.23 br s		H-2	5.63 br s	5.61 br s	H-2	5.62 br s	5.59 br s	5.28 br s	
H-3	4.14 br s	4.14 br s	3.95 d (2)		H-3	4.15 br s	4.16 br s	H-3	4.12 br s	4.12 br s	3.94 d (3)	
H-4	4.42 br s	4.39 br s	4.04 d (2)		H-4	4.42 br s	4.39 br s	H-4	4.41 br s	4.38 br s	4.06 d (3)	
H-6	6.14 s	6.11 s	6.11 s		H-6	6.13 s	6.10 s	H-6	6.11 s	6.07 s	6.11 s	
H-2′	7.34 d (2)	7.31 d (2)	7.19 d (2)		H-2′6′	7.65 d (9)	7.64 d (9)	H-2′6′	7.61 d (9)	7.60 d (9)	7.45 d (9)	
H-5′	6.88 d (9)	6.86 d (9)	6.84 d (8)		H-3′5′	6.88 d (9)	6.87 d (9)	H-3′5′	6.87 d (9)	6.86 d (9)	6.84 d (9)	
H-6′	7.15 dd (9, 2)	7.14 dd (9, 2)	6.98 dd (8, 2)									
Bottom unit												
H-2	4.38 br s	4.37 br s	Benzyl CH_2	4.80 br s	H-2	4.37 br s	4.38 br s	H-2	4.45 br s	4.87 br s	Benzyl CH_2	4.87 br s
H-3	3.59 br s	3.58 br s	3.93 s	3.86 br s	H-3	3.58 br s	3.59 br s	H-3	3.58 br s	3.58 br s	3.94 s	3.86 br s
H-4	3.29 m	3.26 m	H-4 7.16 br t (8)	3.30 ddd (10, 4, 2)	H-4	3.30 m	3.26 m	H-4	3.27 m	3.23 m	H-4 7.18 br t (7)	3.31 ddd (11, 4, 2)
H-6	5.79 s	5.78 s	H-3,5 7.24 br t (8)	5.90 d (2)	H-6	5.73 s	5.79 s	H-6	5.79 s	5.79 s	H-3,5 (2)	5.89 d (2)
H-8				5.98 d (2)				H-8			7.25 br t (7)	5.98 d (2)
H-11α	2.92 dd (17, 3)	2.80 dd (16, 4)	H-2,6 7.32 d	2.89 dd (16, 4)	H-11α	2.89 dd (16, 4)	2.71 dd (16, 4)	H-11α	2.75 dd (16, 4)	2.57 dd (11, 4)	H-2,6 7.33 d	2.90 dd (16, 4)
H-11β	2.22 dd (17, 12)	2.20 dd (16, 10)	(7)	2.38 dd (16, 10)	H-11β	2.21 dd (16, 12)	2.19 dd (16, 9)	H-11β	2.22 dd (16, 9)	2.18 dd (11, 8)	(7)	2.39 dd (16, 11)
H-2′	6.80 d (2)	6.79 d (2)		6.79 br s	H-2′	6.79 d (2)	6.81 d (2)	H-2′6′	7.19 d (9)	7.20 d (8)		7.29 d (8)
H-5′	6.84 d (8)	6.86 d (9)		6.79 br s	H-5′	6.80 d (8)	6.80 d (9)	H-3′5′	6.77 d (9)	6.76 d (8)		6.80 d (8)
H-6′	6.74 dd (8, 2)	6.74 dd (9, 2)		6.96 br s	H-6′	6.73 dd (8, 2)	6.75 dd (9, 2)					

Chemical shifts: ppm. Multiplicity: s, singlet; d, doublet; br s, broad singlet; br t, broad triplet; m, multiplet. Coupling constants (in parentheses): Hz.

MS *m/z*: 330 [M^+].

Degradation of 2L Compound **2L** (150 mg) was degraded in the same way as compound **1L** to yield **5** (11 mg) and **6** (3 mg).

5: A pale brown amorphous powder, $[\alpha]_D^{20}$ +64° (*c*=0.7, acetone). UV λ_{max}^{MeOH} nm (log ε): 225 (4.84), 278 (4.00). IR ν_{max}^{KBr} cm^{-1}: 3350, 1610, 1505, 1440, 1220, 1140, 1110, 1060, 830. SI-MS *m/z*: 667 [M+H]$^+$.

Degradation of 3L Compound **3L** (150 mg) was degraded in the same way as compound **1L** to yield **5** (8 mg) and **7** (3 mg).

7: A colorless amorphous powder, $[\alpha]_D^{20}$ −30° (*c*=0.2, MeOH). UV λ_{max}^{MeOH} nm (log ε): 278 (3.67). IR ν_{max}^{KBr} cm^{-1}: 3400, 1700, 1610, 1505, 1460, 1250, 1145, 1095. CD: $[\theta]_{282}$ −1900° (*c*=0.01, MeOH). MS *m/z*: 314 [M^+].

Degradation of 1A Compound **1A** (150 mg) was degraded in the same way as compound **1L** to yield **4** (17 mg) and **6** (3 mg).

References and Notes

1) Part LXXIX: K. Hori, T. Satake, Y. Saiki and T. Murakami, *Yakugaku Zasshi*, **110**, 315 (1990).
2) T.-H. Hwang, Y. Kashiwada, G. Nonaka and I. Nishioka, *Phytochemistry*, **29**, 279 (1990); Y. Kashiwada, M. Morita, G. Nonaka and I. Nishioka, *Chem. Pharm. Bull.*, **38**, 856 (1990).
3) K. Hori, T. Satake, Y. Saiki, T. Murakami and C.-M. Chen, *Chem. Pharm. Bull.*, **36**, 4301 (1988).
4) D. Jacques, E. Haslam, G. R. Bedford and D. Greatbanks, *J. Chem. Soc., Perkin Trans. 1*, **1974**, 2263.
5) G. Nonaka, S. Morimoto and I. Nishioka, *J. Chem. Soc., Perkin Trans. 1*, **1983**, 2139.
6) As the H-3 signal of the bottom unit appears at δ 3.59 in the ^{1}H-NMR spectrum of **1L**, C-3-OH is not considered to form the lactone ring.
7) C. Karl, P. Alsted and G. Muller, *Z. Naturforsch.*, **36C**, 607 (1981).
8) The absolute configuration of dryopterin (**6**) had not been determined.[7] We determined it as (2*R*), (3*R*) and (4*S*) by comparing the circular dichroism (CD) spectrum of **6**, $[\theta]_{282}$ −1280° (MeOH), with that of (−)-epicatechin, $[\theta]_{282}$ −2320° (MeOH).
9) Usual epicatechin-type proanthocyanidins possess 4β-configuration, avoiding steric interaction between the oxygen substituents at C-3 and C-5 and those in the *ortho*-positions on the A-ring of the linked

unit. The possibility of 4α-configuration is ruled out by the evidence described below and also the nuclear Overhauser effect (NOE) correlation two-dimensional NMR spectrum (NOESY) of **1**L where NOE between C-2-H of the middle unit and C-2-H of the bottom unit was observed.

10) Nomenclature of proanthocyanidins: R. W. Hemingway, L. Y. Foo and L. J. Porter, *J. Chem. Soc., Perkin Trans. 1,* **1982**, 1209.

11) The chemical shifts of C-11 and C-12 changed with concentration in this solvent system in the range of several ppm. This phenomenon is considered to be related to the equilibrium between the dimeric form of carboxylic acid and the hydrogen-bonded comlex of carboxylic acid with solvent. See: G. E. Maciel and D. D. Traficante, *J. Am. Chem. Soc.*, **88**, 220 (1966).

12) Recently, I. Nishioka and his co-workers isolated compound **1**A from an Aspidiaceous fern, *Polysticum polyblepharum*; M. Morita, Y. Kashiwada, G. Nonaka and I. Nishioka, Abstracts of Papeprs, The 36th Annual Meeting of the Japanese Society of Pharmacognosy, Kumamoto. Oct. 1989, p. 170. We also isolated **1**A from *P. tsus-simense* and a Polypodiaceous fern, *Loxogramma saziran.*

13) I. Nishioka, *Kagaku To Seibutsu*, **24**, 428 (1986).

Tannins and Related Compounds. CIII.[1] Isolation and Characterization of New Monomeric, Dimeric and Trimeric Ellagitannins, Calamansanin and Calamanins A, B and C, from *Terminalia calamansanai* (BLANCO) ROLFE

Takashi TANAKA,[a] Akemi MORITA,[a] Gen-ichiro NONAKA,[a] Ta-chen LIN,[a] Itsuo NISHIOKA*,[a] and Feng-chi HO[b]

Faculty of Pharmaceutical Sciences, Kyushu University 62,[a] 3-1-1 Maidashi, Higashi-ku, Fukuoka 812, Japan and Taiwan Forestry Research Institute, Heng-chun Branch,[b] Heng-chun, Taiwan, Republic of China. *Received July 6, 1990*

Continuing chemical examination on tannins of Combretaceous Plants has led to the isolation of four new ellagitannins, calamansanin and calamanins A, B, and C, together with ten structurally known tannins and related compounds, from the leaves of *Terminalia calamansanai* (BLANCO) ROLFE. On the basis of chemical and spectroscopic evidence, the structures of calamansanin and calamanin A were established as 1,6-di-*O*-galloyl-2,3-*O*-(*S*)-hexahydroxydiphenoyl-4-*O*-(*S*)-flavogallonyl-α-D-glucose (11) and 1-*O*-galloyl-2,3-*O*-(*S*)-hexahydroxydiphenoyl-4,6-*O*-(*S*)-valoneoyl-α-D-glucose (14), respectively, while calamanin B and calamanin C were characterized as dimeric and trimeric ellagitannins 15 and 16, respectively, in which the glucose units are linked through valoneoyl group(s).

Keywords *Terminalia calamansanai*; Combretaceae; ellagitannin; calamansanin; calamanin; flavogallonic acid; valoneic acid; gallagic acid; tannin; oxidative phenol coupling

In previous papers, we demonstrated that tannins in *Terminalia catappa* L.[2] and *T. chebula* L.[1] (Combretaceae) consist of esters of various phenolcarboxylic acids which are biosynthetically derived by oxidative carbon–carbon and/or carbon–oxygen couplin(s) of galloyl groups attached to the glucose core. These acids include so-called gallic acid dimers [4,4′,5,5′,6,6′-hexahydroxydiphenic acid, dehydrohexahydroxydiphenic acid, chebulic acid], trimers (flavogallonic acid, tergallic acid), and tetramers (gallagic acid, terchebulic acid). These structural variations in the tannins of the genus *Terminalia* thus prompted us to examine other *Terminalia* species. The present paper describes the results of the examination of *T. calamansanai* (BLANCO) ROLFE, which grows in the Philippine Islands and is used medicinally as a lithontriptic.

The aqueous acetone extract of the fresh leaves was repeatedly chromatographed over Sephadex LH-20 (H_2O–MeOH and EtOH–H_2O–acetone), MCI-gel CHP 20P (H_2O–MeOH), Fuji-gel ODS G3 (H_2O–MeOH) and cellulose (2% AcOH) to yield four new ellagitannins named calamansanin (**11**) and calamanins A (**14**), B (**15**) and C (**16**), together with ten known tannins [2,3-*O*-(*S*)-4,4′,5,5′,6,6′-hexahydroxydiphenoyl (HHDP)-D-glucose (**1**),[3] sanguiins H-4 (**2**)[4] and H-1 (**3**),[5] 1-desgalloyleugeniin

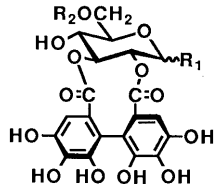

	R_1	R_2
1 :	OH	H
2 :	(α)OG	H
3 :	(α)OG	G

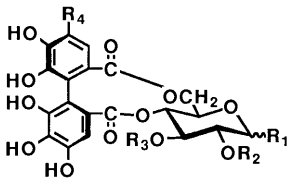

	R_1	R_2	R_3	R_4
4 :	OH	G	G	OH
5 :	(β)OG	G	G	OH
6 :	(β)OG	G	G	A
7 :	(α)OG	HHDP		OH
8 :	OH	HHDP		A

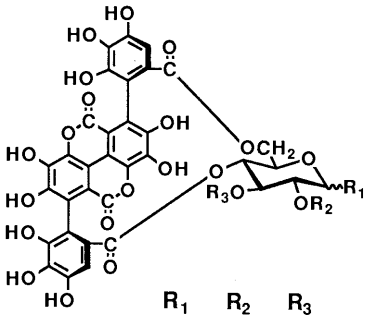

	R_1	R_2	R_3
9 :	OH	H	H
10 :	(α)OG	HHDP	

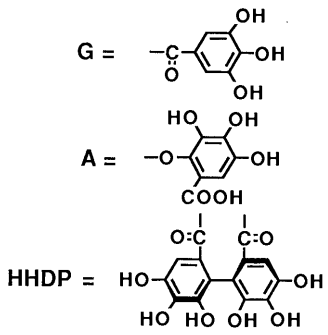

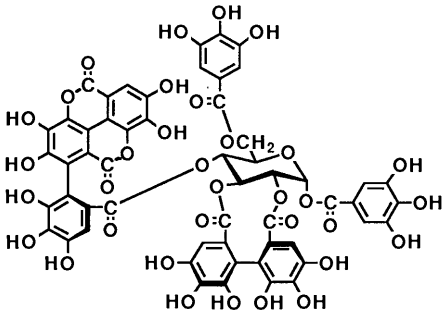

11

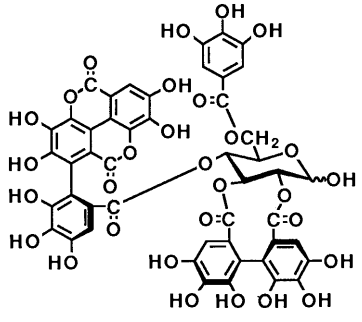

12

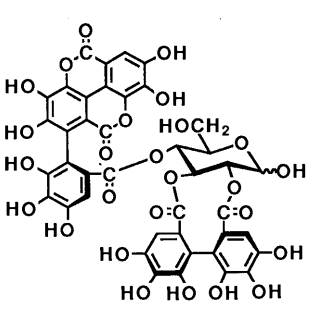

13

(**4**),[6] eugeniin (**5**),[7] rugosin A (**6**),[8] 1(α)-*O*-galloylpedunculagin (**7**),[9] praecoxin A (**8**),[8] punicalin (**9**)[10] and 1(α)-*O*-galloylpunicalagin(**10**)[11]].

Calamansanin (**11**) showed four one-proton singlet signals (δ 7.49, 7.25, 6.48 and 6.44) and two two-proton singlets (δ 7.25 and 6.73) in the proton nuclear magnetic resonance (^{1}H-NMR) spectrum. The latter signals suggested the presence of two galloyl groups. The observation of seven aliphatic proton signals [δ 6.55 (d, J=4 Hz), 5.69 (t, J=10 Hz), 5.59 (t, J=10 Hz), 5.27 (dd, J=4, 10 Hz), 4.75 (dd, J=2, 13 Hz), 4.48 (br d, J=10 Hz) and 4.08 (dd, J=3, 13 Hz)] indicated the presence of a hexopyranose core and their chemical shifts showed all the hydroxyl groups to be acylated. Furthermore, the coupling constants implied that the hexose moiety is an α-glucopyranose with a $^4C_1$ conformation. The carbon-13 nuclear magnetic resonance (^{13}C-NMR) spectrum more clearly showed the presence of the galloyl groups, the α-glucopyranose moiety and one HHDP group (δ 108.0, 108.8, 114.5 and 126.3). The aromatic carbon signals appearing at δ 110.8, 111.3, 118.2 and 123.7 and two signals at δ 158.5 and 159.8 due to δ-lactones were characteristic of a flavogallonyl group. These findings suggested that **11** possesses phenol carboxylic acid moieties analogous to those of terflavin A (**12**),[2] except for the presence of one extra galloyl group.

When calamansanin (**11**) was subjected to partial hydrolysis with tannase, a hydrolysate (**13**) was obtained, along with gallic acid, and this product was found to be identical with 2,3-*O*-(*S*)-HHDP-4-*O*-(*S*)-flavogallonyl-D-glucose (terflavin C).[2] On the basis of these spectral and chemical data, calamansanin was characterized as 1,6-di-*O*-galloyl-2,3-*O*-(*S*)-HHDP-4-*O*-(*S*)-flavogallonyl-α-D-glucopyranose (**11**).

Calamanin A (**14**) was shown by ^{1}H-NMR spectral analysis to possess a galloyl (δ 7.22, 2H, s), an HHDP (δ 6.61 and 6.41, each 1H, s) and a valoneoyl group (δ 7.16, 6.48 and 6.28, each 1H, s) in the molecule. The chemical shifts and coupling patterns of the aliphatic signals, which were analogous to those observed in the spectrum of **11**, suggested the occurrence of an α-glucopyranose core with $^4C_1$ conformation. However, the chemical shift of one of the glucose C-6 proton signals, appearing at relatively lower field (δ 5.24), was different from that of **11**, and this observation was consistent with the presence of the HHDP or valoneoyl group at the glucose 4,6-positions.[9]

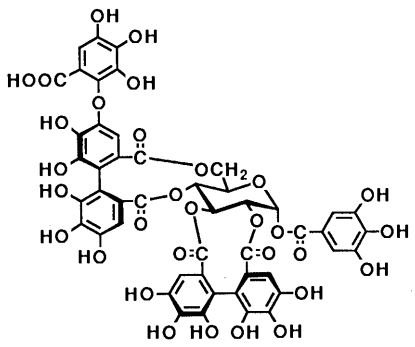

14

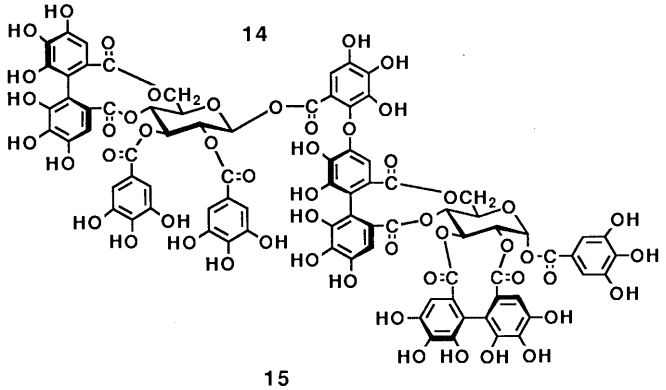

15

On enzymatic hydrolysis with tannase, **14** furnished gallic acid and a hydrolysate, whose ^{1}H-NMR spectrum and physical data were found to be identical with those of praecoxin A (**8**).[8] Since the anomeric signal was observed at lower field (δ 6.55, d, J=4 Hz), the galloyl group was determined to be located at the C-1 position. Thus, the structure of calamanin A was established to be 1-*O*-galloyl-2,3-*O*-(*S*)-HHDP-4,6-*O*-(*S*)-valoneoyl-α-D-glucopyranose (**14**).

Calamanin B (**15**) showed, in the negative fast atom bombardment mass spectrum (FAB-MS), the $[M-H]^-$ ion peak at m/z 1871, suggesting that **15** is a dimeric hydrolyzable tannin. The ^{1}H-NMR spectrum exhibited signals arising from α- and β-glucopyranose moieties, and their chemical shifts and coupling constants were closely related to those of 1(α)-*O*-galloylpedunculagin (**7**) plus eugeniin (**5**). The presence of three galloyl groups in the molecule was apparent from three two-proton singlet signals at δ 7.34, 7.16 and 6.98. The seven aromatic one-proton resonances suggested the presence of two HHDP groups and one valoneoyl ester. The ^{13}C-NMR spectrum showed signals due to α- and β-glucopyranose rings, whose chemical shifts agreed fairly well with those of **7** plus **5**. These spectral findings implied that **15** has a dimeric structure consisting of 1(α)-*O*-galloylpedunculagin and eugeniin moieties linked through a valoneoyl group.

The structure of **15** was conclusively established on the basis of the result of partial hydrolysis of **15** with hot H_2O (80 °C), which yielded almost equimolar amounts of 1-desgalloyleugeniin (**4**) and calamanin A (**14**). Accordingly, the structure of calamanin B was determined to be as shown by the formula **15**.

Calamanin C (**16**) was strongly adsorbed on Sephadex LH-20 dextran gels, and was only elutable with 50% aqueous acetone. The ^{1}H-NMR spectrum was somewhat analogous to that of calamanin B (**15**), but showed more complex signal patterns. In the aromatic region, five two-proton singlets observed between δ 6.99—7.25 indicated the presence of five galloyl groups, while ten one-proton singlets, of which two (δ 7.17 and 7.13) were assignable to the valoneoyl aromatic protons, implied the presence of two valoneoyl and two HHDP groups. Furthermore, the appearance of three anomeric doublets [δ 6.58 (J=4 Hz), 6.10 (J=8 Hz) and 6.06 (J=8 Hz)], together with sugar signals all possessing large coupling constants (J=8—10 Hz), suggested that **16** has one α- and two β-glucopyranose moieties.

Methylation of **16** with dimethyl sulfate and potassium carbonate in dry acetone yielded the tritetracontamethyl ether. Successive methanolysis with sodium methoxide in MeOH gave methyl 3,4,5-trimethoxybenzoate, dimethyl hexamethoxydiphenoate (**17**) and trimethyl octa-*O*-methylvaloneate (**18**). The negative sign of the specific optical

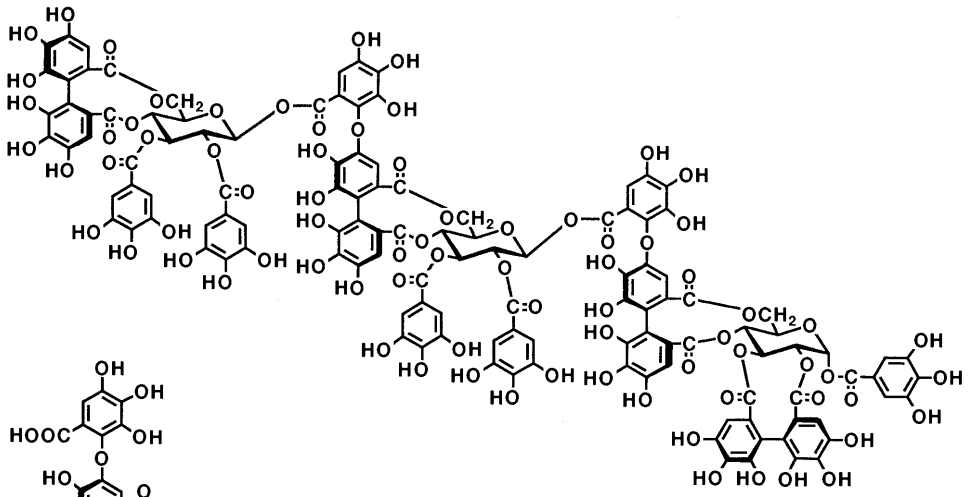

16

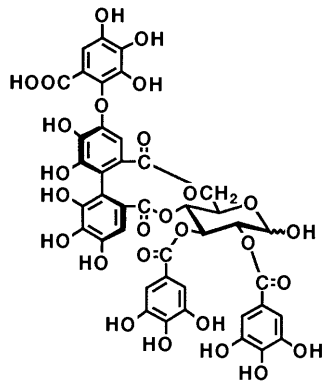

19

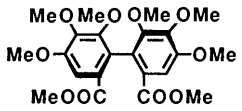

17

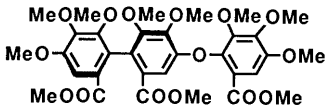

18

rotations of the latter two compounds established the atropisomerism to be in the *S*-series.

In contrast to the case of **15**, partial hydrolysis of **16** with hot H_2O gave a complex mixture of products, which was analyzed by reversed-phase high-performance liquid chromatography (HPLC), and peaks corresponding to those of 1-desgalloyleugeniin (**4**), 2,3-di-*O*-galloyl-4,6-*O*-(*S*)-valoneoyl-D-glucose [rugosin B (**19**)][8] and calamanin A (**14**) were observed. These results, in combination with the above-mentioned spectral data, established the structure of calamanin C to be as represented by the formula **16**.

Calamanins B (**15**) and C (**16**) are the first examples of dimeric and trimeric ellagitannins to be isolated from Combretaceous plants. Apart from the tannins in other Combretaceous species, the major tannin (0.4% of fresh weight) of *T. calamansanai* was found to be 1(α)-*O*-galloylpunicalagin (**10**), which possesses a gallagyl ester group at the 4,6-positions of the glucopyranose moiety. The isolation of calamansanin (**11**) in this study thus indicates that the gallagyl group is formed biosynthetically by an oxidative carbon–carbon coupling between the flavogallonyl and the galloyl groups. Further examination of other Combretaceous plants is in progress.

Experimental

Details of the instruments and chromatographic conditions used throughout this work are the same as described in the previous paper,[1] except for the following. HPLC was conducted on a Toyo Soda apparatus equipped with an SP-8700 solvent delivery system and a UV-8 model II spectrophotometer.

Isolation of Tannins The fresh leaves (5.0 kg) of *T. calamansanai* collected in Taiwan (May, 1987) were extracted three times with 80% aqueous acetone at room temperature. The acetone was removed by evaporation under reduced pressure (*ca.* 40 °C), and the resulting precipitates, consisting mainly of chlorophylls, were removed by filtration. The filtrate was further concentrated and applied to a column of Sephadex LH-20. Elution with H_2O containing increasing amounts of MeOH and finally with 50% aqueous acetone gave five fractions; I (30.6 g), II (11.0 g), III (100.7 g), IV (18.0 g) and V (25.0 g). Fraction I was further chromatographed over Sephadex LH-20 with H_2O to afford 2,3-*O*-(*S*)-HHDP-D-glucose (**1**) (320 mg). Fraction II was rechromatographed over MCI-gel CHP 20P (H_2O–MeOH) and Sephadex LH-20 (EtOH) to give punicalin (**9**) (43 mg). Fraction III consisted mainly of 1(α)-*O*-galloylpunicalagin (**10**), and was chromatographed on MCI-gel CHP 20P (H_2O–MeOH) and Avicel cellulose (2% AcOH) to give **10** (20.1 g), sanguiin H-4 (**2**) (44 mg) and praecoxin A (**8**) (124 mg). Repeated chromatographies of fraction IV on MCI-gel CHP 20P (H_2O–MeOH), Sephadex LH-20 (60—80% aqueous MeOH), Bondapak C_{18}/Porasil B (H_2O–MeOH) and Avicel cellulose (2% AcOH) yielded sanguiin H-1 (**3**) (213 mg), 1-desgalloyleugeniin (**4**) (2.5 g), rugosin A (**6**) (54 mg) and calamansanin (**11**) (186 mg). On similar chromatographies, fraction V gave eugeniin (**5**) (159 mg), 1(α)-*O*-galloylpedunculagin (**7**) (370 mg) and calamanins A (**14**) (523 mg), B (**15**) (385 mg) and C (**16**) (150 mg).

Calamansanin (11) A yellow powder (H_2O), mp 240 °C (dec.), $[\alpha]_D^{23}$ +243.0° (c=1.1, MeOH). *Anal.* Calcd for $C_{55}H_{34}O_{34}$: C, 53.32; H, 2.77. Found: C, 53.61; H, 2.57. Negative FAB-MS *m/z*: 1237 $(M-H)^-$. ^{1}H-NMR (acetone-d_6 + D_2O, 270 MHz) δ: 7.49 [1H, s, flavogallonyl (FL)-H], 7.25 (3H, s, galloyl-H and FL-H), 6.73 (2H, s, galloyl-H), 6.55 (1H, d, J=4 Hz, H-1), 6.48, 6.44 (each 1H, s, HHDP-H), 5.67 (1H, t, J=10 Hz, H-3), 5.59 (1H, t, J=10 Hz, H-4), 5.27 (1H, dd, J=4, 10 Hz, H-2), 4.75 (1H, dd, J=2, 13 Hz, H-6), 4.48 (1H, br d, J=10 Hz, H-5), 4.08 (1H, dd, J=3, 13 Hz, H-6). ^{13}C-NMR (acetone-d_6 + D_2O, 25.05 MHz) δ: 61.9 (C-6), 67.1, 71.5, 73.7, 75.4 (C-2, 3, 4, 5), 90.6 (C-1), 108.0, 108.8 (HHDP C-3, 3'), 109.8, 110.5 (galloyl C-2, 6), 110.8, 111.3 (FL C-3, 3''), 114.5 (HHDP C-1, 1'), 118.2, 120.4, 120.9, 121.3 (galloyl C-1, FL-C), 123.7, 126.3 (HHDP C-2, 2', FL-C), 136.4, 136.6, 138.7, 139.9 (galloyl C-4, HHDP C-5, 5', FL-C), 144.3, 144.4, 145.0, 145.2, 145.4, 146.3, 146.7, 148.2 (galloyl C-3,5, HHDP C-4, 4', 6, 6', FL-C), 158.5, 159.8 (δ-lactone), 164.9, 165.2, 166.2, 168.4, 169.1 (COO).

Partial Hydrolysis of 11 with Tannase A solution of **11** (100 mg) in H_2O (5 ml) was incubated with tannase at 35°C for 24 h. The reaction mixture was concentrated and the residue was treated with EtOH. The EtOH soluble portion was subjected to Sephadex LH-20 chromatography with EtOH to yield 2,3-*O*-(*S*)-HHDP-4-*O*-(*S*)-flavogallonyl-D-glucose (terflavin C) (**13**) (20 mg), as a yellow amorphous powder, $[\alpha]_D^{23}$ +32.6° (c=1.2, MeOH). ^{1}H-NMR (acetone-d_6 + D_2O, 100 MHz) δ: 7.59, 7.32, 7.31 (FL-H), 6.54, 6.40, 6.39 (HHDP-H).

Calamanin A (14) A tan amorphous powder, $[\alpha]_D^{25}$ +123.0° (c=0.5, MeOH). *Anal.* Calcd for $C_{48}H_{32}O_{31}\cdot H_2O$: C, 47.53; H, 3.57. Found: C,

47.49; H, 3.44. Negative FAB-MS *m/z*: 1103 $(M-H)^-$. ^{1}H-NMR (acetone-d_6+D_2O, 100 MHz) δ: 7.22 (2H, s, galloyl-H), 7.16, 6.61, 6.48, 6.41, 6.28 (each 1H, s, HHDP-H, valoneoyl-H), 6.55 (1H, d, $J=4$ Hz, H-1), 5.60 (1H, t, $J=10$ Hz, H-3), 5.37 (1H, dd, $J=4$, 10 Hz, H-2), 5.24 (1H, dd, $J=7$, 13 Hz, H-6), 5.14 (1H, t, $J=10$ Hz, H-4), 4.61 (1H, dd, $J=7$, 10 Hz, H-5), 3.74 (1H, d, $J=13$ Hz, H-6). ^{13}C-NMR (acetone-d_6+D_2O, 67.80 MHz) δ: 63.3, 69.2, 70.9, 74.1, 75.9, 90.6 (glucose), 165.1, 167.2, 168.1, 168.2, 168.7, 169.6 (COO).

Partial Hydrolysis of 14 with Tannase **14** (30 mg) was hydrolyzed with tannase in a manner similar to that described for **11** to yield praecoxin A (**8**)(13 mg), as a tan amorphous powder, $[\alpha]_D^{25}$ +83.9° ($c=1.1$, acetone). ^{1}H-NMR (acetone-d_6+D_2O) δ: 7.17, 6.60, 6.56, 6.51, 6.37, 6.32, 6.30 (5H, in total, each s, HHDP-H, valoneoyl-H).

Calamanin B (15) A tan amorphous powder, $[\alpha]_D^{25}$ +132.0° ($c=1.0$, MeOH). *Anal.* Calcd for $C_{82}H_{56}O_{52}\cdot 1/2H_2O$: C, 52.32; H, 3.05. Found: C, 52.20; H, 2.88. Negative FAB-MS *m/z*: 1871 $(M-H)^-$. ^{1}H-NMR (acetone-d_6+D_2O, 270 MHz) δ: 7.24, 7.16 (each 2H, s, galloyl-H), 7.04 (1H, s, valoneoyl-H), 6.98 (2H, s, galloyl-H), 6.64, 6.61, 6.51, 6.49, 6.43, 6.22 (each 1H, s, HHDP-H, valoneoyl-H), 6.57 (1H, d, $J=4$ Hz, H-1), 6.11 (1H, d, $J=8$ Hz, H-1′), 5.81 (1H, t, $J=10$ Hz, H-3′), 5.59 (1H, dd, $J=9$, 10 Hz, H-3), 5.58 (1H, dd, $J=8$, 10 Hz, H-2′), 5.39 (1H, dd, $J=4$, 9 Hz, H-2), 5.30 (1H, dd, $J=7$, 13 Hz, H-6′), 5.22 (1H, dd, $J=7$, 12 Hz, H-6), 5.18, 5.16 (each 1H, t, $J=10$ Hz, H-4, 4′), 4.64 (1H, dd, $J=7$, 10 Hz, H-5), 4.86 (1H, dd, $J=7$, 10 Hz, H-5′), 3.84 (1H, d, $J=13$ Hz, H-6′), 3.74 (1H, d, $J=12$ Hz, H-6). ^{13}C-NMR (acetone-d_6+D_2O, 67.80 MHz) δ: 63.1, 63.3, 69.1, 70.6, 70.8, 71.7, 72.8, 73.4, 74.0, 75.8, 90.6, 93.1 (glucose), 162.5, 165.3, 166.4, 166.8, 167.9, 168.2 (2C), 168.5, 168.7, 169.7 (COO).

Partial Hydrolysis of 15 with Hot H_2O A solution of **15** (200 mg) in H_2O (20 ml) was heated at 80 °C for 4 h. After cooling, the resulting precipitates were collected by filtration, and identified as ellagic acid by infrared (IR) spectral comparison. The filtrate was concentrated and subjected to column chromatography on Sephadex LH-20 with 80% aqueous MeOH to yield 1-desgalloyleugeniin (**4**) (25.8 mg) and calamanin A (**14**) (25.3 mg).

Calamanin C (16) A tan amorphous powder, $[\alpha]_D^{25}$ +131.0° ($c=1.1$, MeOH). *Anal.* Calcd for $C_{123}H_{84}O_{77}$: C, 52.88; H, 3.03. Found: C, 52.88; H, 2.73. ^{1}H-NMR (acetone-d_6+D_2O, 270 MHz) δ: 7.25 (2H, s, galloyl-H), 7.17, 7.13 (each 1H, s, valoneoyl-H), 7.05, 7.04, 7.02, 6.99 (each 2H, s, galloyl-H), 6.67, 6.64, 6.52, 6.51, 6.50, 6.45, 6.22, 6.17 (each 1H, s, HHDP-H, valoneoyl-H), 6.58 (1H, d, $J=4$ Hz, H-1), 6.10, 6.06 (each 1H, d, $J=8$ Hz, H-1′, 1″), 5.82, 5.79 (each 1H, t, $J=10$ Hz, H-3′, 3″), 5.65—5.54 (3H in total, m, H-3, 2′, 2″), 5.04 (1H, dd, $J=4$, 10 Hz, H-2), 5.30—5.16 (3H in total, m, H-6, 6′, 6″), 5.16 (3H, br t, $J=10$ Hz, H-4, 4′, 4″), 4.66 (1H, dd, $J=6$, 10 Hz, H-5), 4.51—4.44 (2H, m, H-5′, 5″), 3.82, 3.79, 3.76 (each 1H, d, $J=13$ Hz, H-6, 6′, 6″). ^{13}C-NMR (acetone-d_6+D_2O, 67.80 MHz) δ: 63.1, 63.2, 63.3, 69.2, 70.6, 70.7, 70.8, 71.7 (2C), 72.8, 72.9, 73.4 (2C), 74.1, 75.9, 90.7, 93.1 (2C) (glucose), 162.4, 162.5, 165.4, 166.3, 166.4, 166.8, 166.9, 167.9, 168.0, 168.1, 168.2 (2C), 168.5, 168.8, 169.7 (COO).

Methylation of 16, Followed by Alkaline Methanolysis A mixture of **16** (72 mg), dimethyl sulfate (1 ml) and anhydrous potassium carbonate (1.2 g) in dry acetone (20 ml) was heated under reflux with stirring for 4 h. After removal of inorganic salts by filtration, the filtrate was concentrated to a syrup, which was chromatographed over silica gel. Elution with benzene–acetone (9 : 1) gave the tritetracontamethyl ether (46 mg), as a white amorphous powder. IR (KBr): 2930, 1750 (CO), 1588, 1460, 1392, 1332 cm^{-1}. A solution of the tritetracontamethyl ether (39 mg) in 2% methanolic sodium methoxide (4 ml) was left standing at room temperature for 20 h, then neutralized with Amberlite IR-120B (H^+ form) resin and concentrated *in vacuo*. The residue was separated by silica gel chromatography with benzene–acetone (97 : 3—95 : 5) to give methyl 3,4,5-trimethoxybenzoate (2 mg), colorless needles, mp 80—81 °C, dimethyl (*S*)-4,4′,5,5′,6, 6′-hexamethoxydiphenoate (**17**) (1.7 mg), a colorless syrup, $[\alpha]_D^{25}$ −24.0° ($c=0.1$, $CHCl_3$), and trimethyl octa-*O*-methylvaloneate (**18**) (10 mg), a colorless syrup, $[\alpha]_D^{25}$ −19.2° ($c=1.0$, $CHCl_3$). IR ($CHCl_3$): 2950, 1725 (CO), 1595 cm^{-1}.

Partial Hydrolysis of 16 with Hot H_2O A solution of **16** (10 mg) in H_2O (2 ml) was heated at 80° for 8 h. The reaction mixture was analyzed by HPLC to detect 1-desgalloyleugeniin (**4**), rugosin B (**19**) and calamanin A (**14**). HPLC: column, Zorbax SIL (4.6 mm i.d. × 250 mm); solvent, hexane–MeOH–tetrahydrofuran-formic acid (45 : 27 : 9 : 1) containing oxalic acid (250 mg/l); flow rate, 1.0 ml/min; t_R 11.7 and 12.5 min for **4**, t_R 13.9 and 14.5 min for **19** and t_R 15.6 min for **14**.

Acknowledgements The authors thank Dr. M. Kanaoka (Sankyo Co., Ltd). for providing tannase, Mr. Y. Tanaka and Miss Y. Soeda for ^{1}H- and ^{13}C-NMR measurements, and Mr. R. Isobe for FAB-MS measurements. They are also indebted to the staff of the Central Analysis Room of this university for elemental analysis.

References

1) Part CII: T.-C. Lin, G. Nonaka and I. Nishioka, *Chem. Pharm. Bull.*, **38**, 3004 (1990).
2) T. Tanaka, G. Nonaka and I. Nishioka, *Chem. Pharm. Bull.*, **34**, 1039 (1986).
3) M. Seikel and W. E. Hillis, *Phytochemistry*, **9**, 1115 (1970).
4) T. Tanaka, G. Nonaka and I. Nishioka, *J. Chem. Research*, (*S*), **1985**, 176; (*M*), **1985**, 2001.
5) G. Nonaka, T. Tanaka and I. Nishioka, *J. Chem. Soc., Perkin Trans. 1*, **1982**, 1067.
6) S.-H. Lee, T. Tanaka, G. Nonaka and I. Nishioka, *Phytochemistry*, **29**, 3621 (1990).
7) G. Nonaka, M. Harada and I. Nishioka, *Chem. Pharm. Bull.*, **28**, 685 (1980).
8) T. Okuda, T. Hatano, K. Yazaki and N. Ogawa, *Chem. Pharm. Bull.*, **30**, 4230 (1982).
9) R. K. Gupta, S. M. K. Al-Shafi, K. Layden and E. Haslam, *J. Chem. Soc., Perkin Trans. 1*, **1982**, 2525.
10) T. Tanaka, G. Nonaka and I. Nishioka, *Chem. Pharm. Bull.*, **34**, 650 (1986).
11) T. Okuda, T. Hatano, M. Matsuda, P. B. English, L. J. Filippich and G. R. Cao, Abstracts of Papers, The 106th Annual Meeting of the Pharmaceutical Society of Japan, Chiba, April 1986, p. 214.

Facile Total Synthesis of Carbonolides by Wittig–Horner Macro-Cyclization and Stereoselective Epoxidation[1)]

Noriyuki NAKAJIMA,[a] Kouichi UOTO,[a] Osamu YONEMITSU,*,[a] and Tadashi HATA[b]

Faculty of Pharmaceutical Sciences, Hokkaido University,[a] Kita-12, Nishi-6, Kita-ku, Sapporo 060, Japan and Analytical and Metabolic Research Laboratories, Sankyo Co., Ltd.,[b] 1-2-58, Hiromachi, Shinagawa-ku, Tokyo 140, Japan. *Received July 16, 1990*

Sixteen-membered dienone type macrolide aglycons, carbonolide B (1), niddanolide (5), and platenolide W_1 (6), were synthesized highly stereoselectively from D-glucose *via* Yamaguchi's esterification of two fragments, 8 (C1—C10) and 9 (C11—C16), followed by Wittig–Horner cyclization. Stereoselective epoxidation of the 16-membered dienones (34, 35) gave epoxy-enone-type macrolide aglycons, carbonolide A (2) and EOP aglycon (7).

Keywords macrolide aglycon; carbonolide; total synthesis; Yamaguchi's esterification; Wittig–Horner cyclization; stereoselective epoxidation; conformation; NOE

Carbonolide B (**1**) and A (**2**), leuconolide A_3 (**3**), and maridonolide II (**4**) are four representative 16-membered aglycones, differing in oxidation levels, in the largest group of macrolide antibiotics.[2)] For the synthesis of these aglycons (**1**—**4**), it seems reasonable to synthesize **1** first, and then to convert **1** to **2**—**4** by stereoselective epoxidation and reduction, because a facile common methodology for the synthesis of enone and dienone type aglycons has been established through the stereoselective synthesis of 12-membered methynolide,[3)] 14-membered pikronolide,[4)] and 16-membered tylonolide[5)] by virtue of some stereoselective reactions, MPM (4-methoxybenzyl) protection,[6)] and Wittig–Horner cyclization.[3-5,7)] We report here the synthesis of carbonolide B (**1**),[8)] niddanolide (**5**)[9)] and platenolide W_1 (**6**),[10)] and their stereoselective epoxidation to carbonolide A (**2**)[11)] and its homolog, EOP aglycon (**7**).[12,13)]

Results and Discussion

Synthesis of Niddanolide (5), Carbonolide B (1) and Platenolide W_1 (6) According to the established methodology,[3-5)] our retro-synthesis can be depicted as shown in Chart 1; the esterification between two stereoselectively synthesized fragments, **8** and **9**, and subsequent Wittig–Horner cyclization are the most important steps.

The small C11—C16 fragment (**9**)[14)] has only one chiral center and was easily synthesized from L(−)-malic acid *via* the known allylic alcohol (**11**).[15)] The primary alcohol of **11** was first protected with an MPM group,[6)] and the ketal group was removed to give the diol, whose primary alcohol was selectively tosylated and then reduced to give **12**. Deprotection of the MPM group with 2,3-dichloro-5,6-dicyanobenzoquinone (DDQ),[6)] followed by oxidation with manganese dioxide gave **9**.

The large C1—C10 fragment (**8**) is quite similar to the C1—C10 fragment used in the synthesis of tylonolide,[5)] the only difference being in the C4-substituent, and hence the methodology employed in the synthesis of tylonolide was directly applicable to the synthesis of **8**. The alcohol (**13**),[5b)]

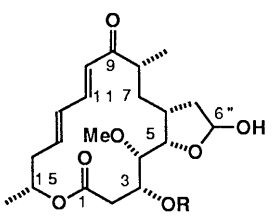

5: R=H niddanolide
1: R=COMe carbonolide B
6: R=COEt platenolide W_1

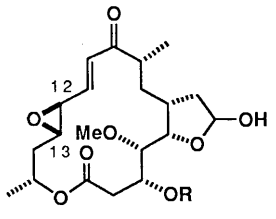

2: R=COMe carbonolide A
7: R=COEt EOP aglycon

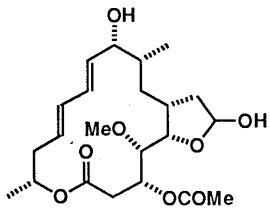

3: leuconolide A_3 (josanolide)

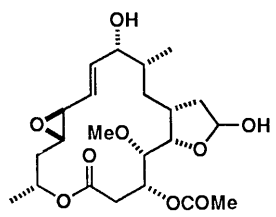

4: maridonolide II

Fig. 1

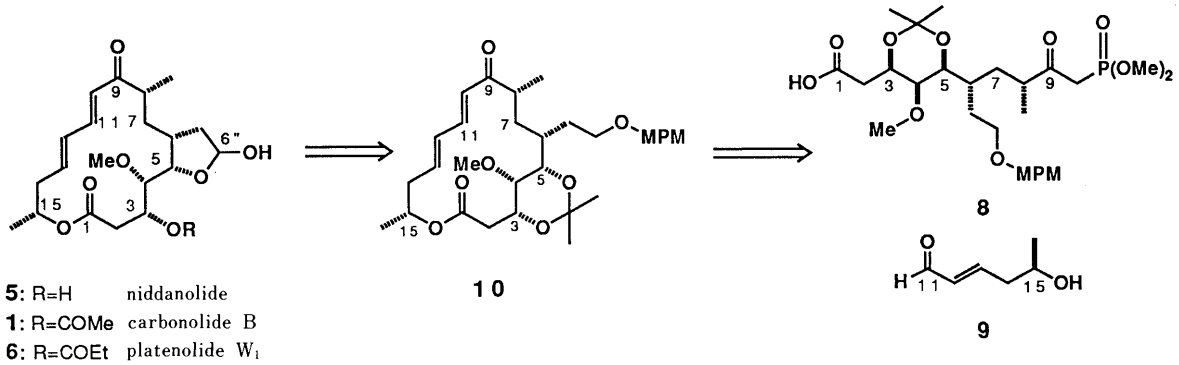

5: R=H niddanolide
1: R=COMe carbonolide B
6: R=COEt platenolide W_1

10

8

9

Chart 1

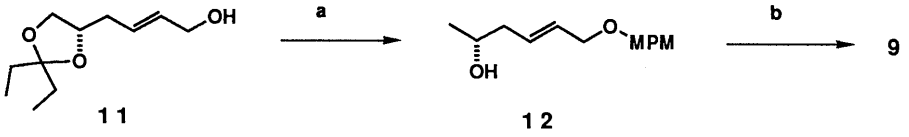

(a) 1) MPMCl, NaH, DMSO-THF (4:3) (94%); 2) 1% H_2SO_4-MeOH; TsCl, Py., CH_2Cl_2 (2 steps 70%). 3) $LiAlH_4$, ether, (92%); (b) 1) DDQ, CH_2Cl_2-H_2O; 2) MnO_2, CH_2Cl_2 (2 steps, 86%).

Chart 2

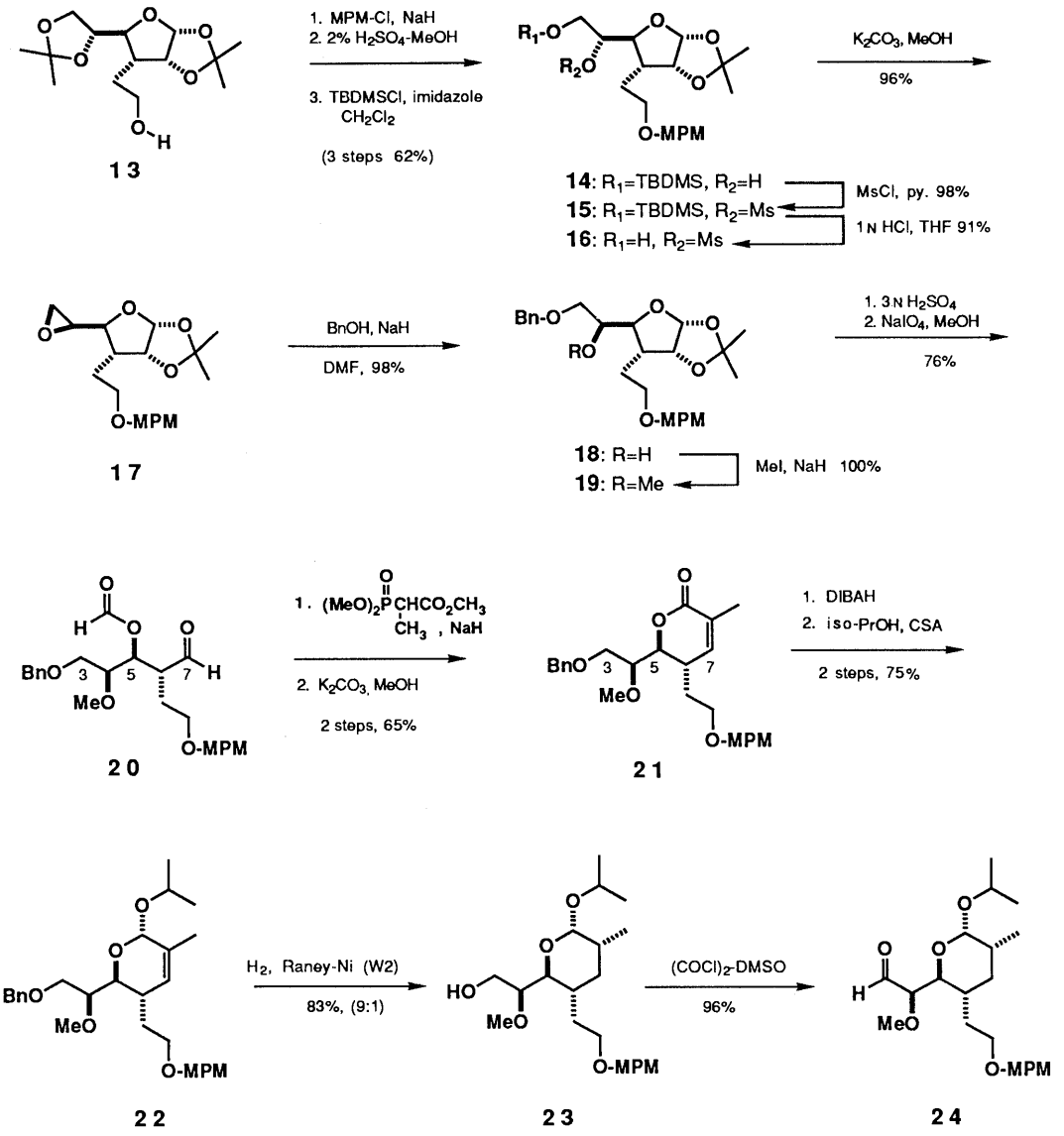

Chart 3

easily available from D-glucose, was selected as a suitable starting material, although inversion at the C5-position[16] was required. The MPM protection of **13** and then hydrolysis of the ketal group gave the diol, whose primary alcohol was protected with a *tert*-butyldimethylsilyl (TBDMS) group to give **14**. Mesylation of the remaining secondary alcohol to **15** and subsequent removal of the TBDMS protection gave **16**, which was readily converted to the epoxide (**17**). The epoxide ring was opened with sodium benzyl alcoholate, and the resulting alcohol (**18**) was converted to the desired methoxy compound (**19**), which has three consecutive chiral centers corresponding to the C4—C6 portion of **1**—**7**.

The fourth chiral center at C8 was introduced by hydrogenation of the unsaturated lactolide (**22**) as follows. After removal of the isopropylidene group of **19** with 3 N sulfuric acid in dioxane, the resulting diol was cleaved with sodium periodate to obtain the aldehyde (**20**), which was treated with the sodium salt of trimethyl 1-phosphonopropionate at $-90\,^{\circ}C$ and then potassium carbonate in methanol to yield the α,β-unsaturated lactone (**21**). Reduction of **21** with diisobutylaluminum hydride (DIBAH)

followed by treatment with isopropanol in the presence of camphorsulfonic acid (CSA) gave the anomerically pure α-lactolide (**22**) in good yield. Finally selective removal of the benzyl protection[6d] and reduction of the double bond were accomplished by catalytic hydrogenation in the presence of Raney nickel (W_2) to give **23** with 9.0:1 selectivity at C8.[17] The Swern oxidation of **23** readily gave the aldehyde (**24**).

The final chiral center at C3 was constructed by a chelation-controlled addition of allylmetal compounds to the α-alkoxyaldehyde (**24**). When **24** was treated with allyltrimethylsilane in the presence of titanium tetrachloride,[18] the expected product (**25**) was obtained with high stereoselectivity (60:1), but the yield was only 22% because of unavoidable loss of the MPM group. The Grignard reaction with allymagnesium bromide at −90 °C also proceeded smoothly to give **25**, but the 3,4-*syn* selectivity was unsatisfactory (4:1). An excellent result, however, was obtained under Yamamoto's conditions.[19] When **24** was treated with allyltributyltin in the presence of magnesium bromide at −60 °C, the chelation-controlled addition took place almost completely stereoselectively to give **25** with 76:1 selectivity. The structure of **25** was confirmed after conversion to **27**. The acetal of **25** was hydrolyzed with 1 N hydrochloric acid in tetrahydrofuran (THF), and the resulting hemiacetal was reduced with calcium borohydride to give the open-chain triol (**26**). The 1,3-diol group of **26** was protected as an acetonide by treatment with 2,2-dimethoxypropane in the presence of CSA to give **27**. In the nuclear magnetic resonance (NMR) spectrum of **27**, nuclear Overhauser enhancement (NOE) of H_a and H_b from the axial methyl of isopropylidene group was observed to be 12.4 and 8.3%, respectively. Thus, the introduction of all the chiral centers required for the C1—C10 fragment (**8**) was completed.

Compound **27** was finally converted to the C1—C10 fragment (**8**) in essentially the same way as described for the synthesis of tylonolide.[5] Oxidation of the primary alcohol of **27** under Swern's conditions readily gave the aldehyde (**28**), which was treated with the lithio derivative of dimethyl methylphosphonate at −80 °C and then oxidized with pyridinium dichromate (PDC) in *N*,*N*-dimethylformamide (DMF) to give the ketophosphonate (**29**). Finally oxidation of the terminal olefin of **29** under Lemieux–von Rudloff's conditions[20] gave the carboxylic acid (C1—C10 fragment, **8**) in good yield.

Coupling between the C1—C10 (**8**) and C11—C16 (**9**) fragments proceeded smoothly under the conditions of Yamaguchi's esterification method,[21] and the resulting ester (**30**) was subjected to the Wittig–Horner cyclization under Aristoff–Nicolaou's conditions.[7] When **30** was heated with powdered potassium carbonate and 18-crown-6 in toluene at 80 °C, the cyclization was completed within 3 h to give the expected 16-membered dienone (**10**), but in modest yield (30—40%), probably because β-elimination at C2—C3 occurred concomitantly. The yield of **10** was improved to 57% by carrying out the cyclization at room temperature for a longer reaction time (15—20 h).

Removal of the MPM group by DDQ oxidation[6] proceeded smoothly and gave the primary alcohol (**31**), which was oxidized under Swern's conditions to give the aldehyde (**32**). The remaining isopropylidene group was

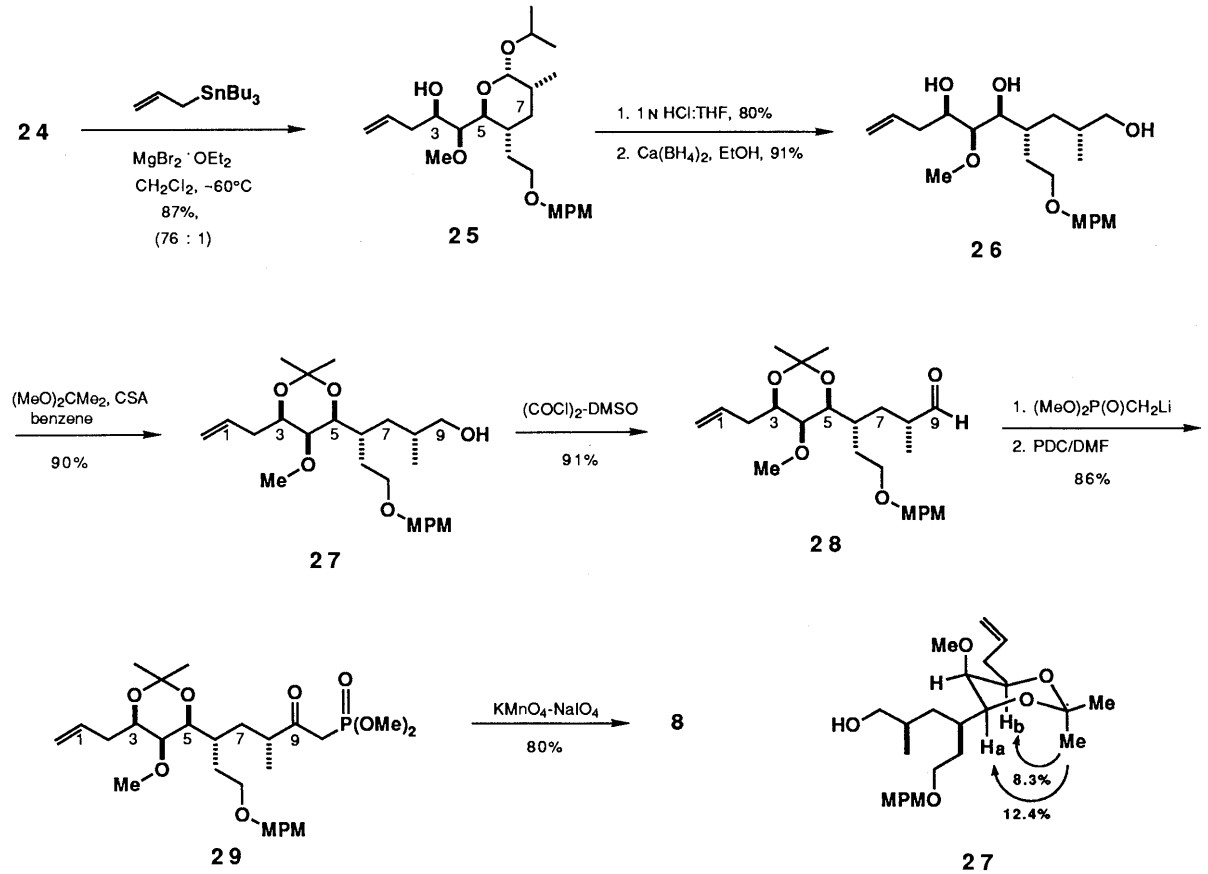

Chart 4

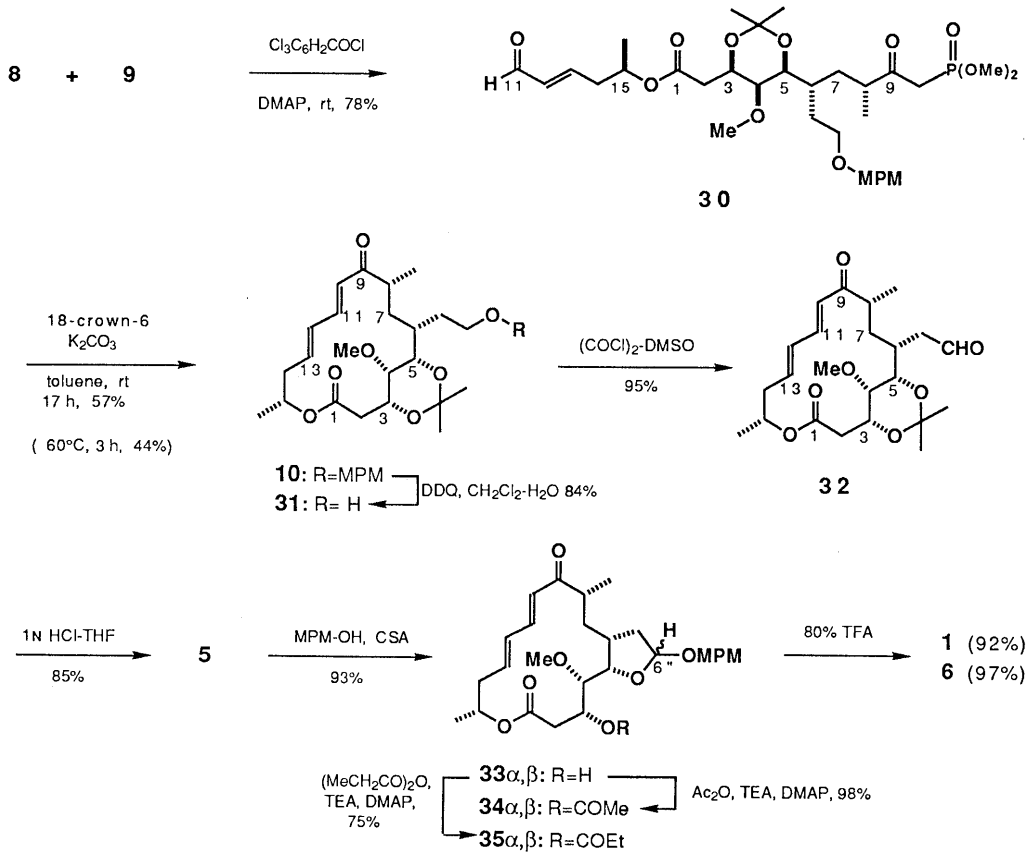

Chart 5

TABLE I. The Matrix of ^{1}H-NOE Obtained for **33** in $CDCl_3$

NOE observed (%)

Signal irradiated \ ^{1}H	2a	2b	3	4	5	6	7a	7b	8	8Me	10	11	12	13	14a	14b	15
2a		38															
2b	NOE			NOE													
3				5.5	3.5	3.2	4.3						2.7	1.9		2.4	
4		4.9	5.9		2.7		5.4										
5				2.2													
6			3.2		8.1				4.9								
7a			3.2	8.6						4.4		8.1					
7b																	
8				1.6		8.1				2.7		1.6					
8Me							4.3		3.8			1.9					
10				4.3			3.2			0.9			10.8				
11														10.8			2.2
12											7.0						3.8
13											1.9	11.9					NOESY
14a														3.5		32	7.0
14b													NOE		NOE		
15														NOESY			

immediately removed with 1 N hydrochloric acid in THF to give niddanolide (**5**).[9,22] Treatment of **5** with 4-methoxybenzyl alcohol (MPMOH) in the presence of CSA gave the 4-methoxybenzyl furanoside (**33**) as a mixture of 6″-epimers (**33**α, **33**β). Acetylation of the C3 secondary alcohol followed by removal of the MPM protecting group with trifluoroacetic acid gave carbonolide B (**1**)[22] in excellent yield. Platenolide W_1 (**6**) was similarly obtained by *O*-propionylation of **33**.[22]

Synthesis of Carbonolide A (2) and EOP Aglycon (7) Double bonds in macro-ring compounds tend to be situated perpendicular to the plane of the rings in order to minimize transannular interactions. The two faces of a double bond are effectively differentiated and a reagent usually attacks at the less hindered peripheral face. Accordingly, formation of a stereoselective product is expected,[23] although it is quite difficult to predict which face of the double bond is peripheral.

For the synthesis of **2** and **7** from carbonolide B type compounds (such as **10**, **33**—**35**) by regio- and stereoselective epoxidation of the C12–C13 double bond,[24,25] it was essential to know the 16-membered ring conformations.

In order to analyze the conformation of **33**, all the proton signals in its 500 MHz ^{1}H-NMR spectrum were first assigned with the aid of two dimensional proton correlated spectroscopy (2D ^{1}H-COSY) experiments, and then NOE and NOE correlation spectroscopy (NOESY) spectra were taken.[26] From the results summarized in Table I, we concluded that the most probable conformation of **33** is as shown in Fig. 2, in which the C12–C13 double bond fortunately lies favorably for the selective epoxidation.[27] This conformation was confirmed by a single-crystal X-ray analysis of **34** (Fig. 3) which revealed that the conformation in the solid state is almost the same as that in solution.

When **34** and **35** were treated with *m*-chloroperbenzoic acid (MCPBA) in the presence of sodium hydrogen carbonate at room temperature, the expected epoxides, **36** and **37**, were obtained with complete stereoselectivity in 90 and 73% yields, respectively. The MPM protecting groups of **36** and **37** were removed by DDQ oxidation[6] to readily give carbonolide A (**2**) and EOP aglycon (**7**).[28]

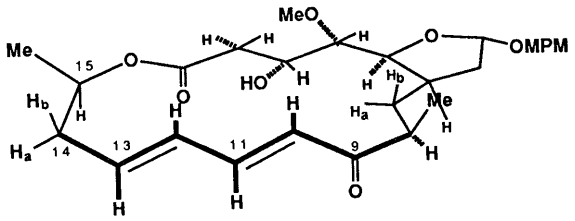

33

Fig. 2

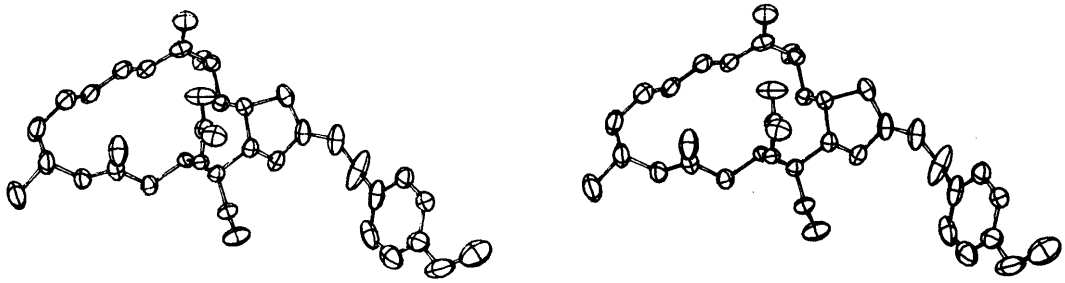

Fig. 3

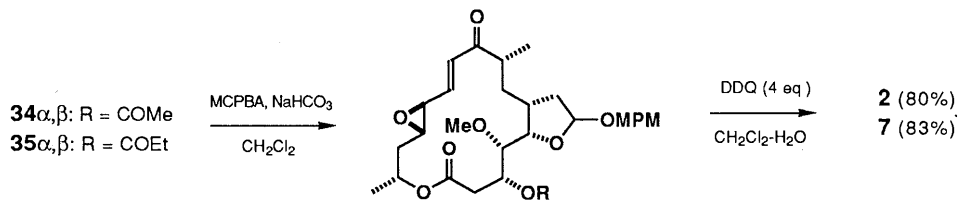

36α,β: R = COMe (90%)
37α,β: R = COEt (73%)

Chart 6

Experimental

All melting points were measured with a Yanaco hot-stage micro melting point apparatus and are uncorrected. Optical rotations were measured with a JASCO DIP-4 digital polarimeter. Infrared (IR) spectra were recorded in $CHCl_3$ or neat on a JASCO IRA-2 spectrometer. ^{1}H-NMR spectra were recorded in $CDCl_3$ on a JEOL FX-100, JEOL JMX GX-270, or JEOL JMS GX-500 instrument. Low- and high-resolution mass spectra (MS) were taken on a JEOL JMS HX-110 or JEOL JMS DX-303 spectrometer. Ultraviolet (UV) spectra were obtained on a Varian Cary 219 spectrophotometer using ethanol as a solvent.

6-(4-Methoxybenzyloxy)hex-4(*E*)-en-2(*R*)-ol (12) A solution of **11** (5.40 g, 18 mmol) in THF (20 ml) was added dropwise to a stirred suspension of NaH (1.0 g, 25 mmol: 60% oil suspension) in dimethyl sulfoxide (DMSO)–THF (4:3) solution (140 ml) under an argon atmosphere at room temperature. After 1 h, MPM chloride (3.9 g, 25 mmol) was added, and stirring was continued for 10 h. The reaction mixture was poured into cold aqueous NH_4Cl solution, and extracted with CH_2Cl_2. The extract was washed with brine, dried over anhydrous $MgSO_4$, and evaporated *in vacuo* to leave an oil, which was chromatographed on a silica gel column using EtOAc–hexane (1:5) as the eluant to give the MPM ether as a colorless oil (5.4 g, 94%). $[\alpha]_D^{16}$ +1.7° (c=2.80, MeOH). ^{1}H-NMR δ: 0.89 (6H, t, J=7.1 Hz), 1.61 (2H, q, J=7.6 Hz), 1.65 (2H, q, J=7.3 Hz), 2.20—2.40 (2H, m), 3.52 (1H, t, J=7.0 Hz), 3.77—4.09 (4H, m), 3.80 (3H, s), 4.43 (2H, s), 5.65—5.69 (2H, m), 6.87 (2H, d, J=8.4 Hz), 7.26 (2H, d, J=8.5 Hz). MS m/z (relative intensity): 320 (M^+, 0.6%), 291 (8.5), 135 (5.2), 129 (21.9), 121 (100), 91 (4.8), 57 (25).

A stirred ice-cold MeOH solution (80 ml) of the MPM ether (2.0 g,

6.2 mol) was treated with 2% H_2SO_4 (20 ml) and the solution was stirred for 4 h at room temperature. After neutralization with $NaHCO_3$, the reaction mixture was evaporated *in vacuo*, and the residue was extracted with CH_2Cl_2. The extract was washed with brine, dried over anhydrous $MgSO_4$, and evaporated to leave a diol as a colorless oil (1.5 g, 97%). $[\alpha]_D^{16}$ −9.1° (c = 1.94, MeOH). ^{1}H-NMR δ: 2.11—2.23 (4H, m), 3.42—3.72 (3H, m), 3.80 (3H, s), 3.96 (2H, dd, J = 2.7, 1.0 Hz), 4.44 (2H, s), 5.66—5.76 (2H, m), 6.87 (2H, d, J = 8.8 Hz). MS m/z (relative intensity): 252 (M^+, 0.64%), 251 (0.22), 221 (0.37), 176 (2.2), 137 (13.7), 121 (100), 109 (12.5), 91 (13.7), 77 (38.6). Exact MS m/z Calcd for $C_{14}H_{20}O_4$ (M^+): 252.1361. Found: 252.1366. IR ν (neat) cm^{-1}: 3550 (OH), 1650.

A solution of the diol (0.5 g, 5.19 mmol), tosyl chloride (392 mg, 1.96 mmol) and pyridine (0.24 ml, 2.94 mmol) in CH_2Cl_2 (5 ml) was stirred for 10 h at room temperature. The reaction mixture was poured into cold aqueous NH_4Cl solution, and extracted with CH_2Cl_2. The extract was successively washed with 10% HCl, saturated aqueous $NaHCO_3$, and brine, and dried over anhydrous $MgSO_4$. Concentration of the solvent gave an oil, which was chromatographed on a silica gel short column with EtOAc–hexane (1 : 2) as the eluant to give the tosylate as a colorless oil (574 mg, 72%). $[\alpha]_D^{15}$ +8.6° (c = 1.30, MeOH). ^{1}H-NMR δ: 2.10—2.30 (3H, m), 2.44 (2H, s), 3.80 (3H, s), 3.87—4.08 (4H, m), 4.41 (2H, s), 5.60—5.69 (2H, m), 6.87 (2H, d, J = 8.5 Hz), 7.21—7.38 (4H, m), 7.79 (2H, d, J = 8.3 Hz). MS m/z (relative intensity): 406 (M^+, 2.5%), 405 ($M^+ - 1$, 4.9), 375 (2.36), 348 (0.84), 269 (0.69), 256 (1.0), 176 (9.3), 155 (31.5), 137 (99), 121 (100), 109 (14.6), 91 (59.3). Exact MS m/z Calcd for $C_{21}H_{26}O_6S$ (M^+): 406.1450. Found: 406.1473. IR ν (neat) cm^{-1}: 3400 (OH), 1610, 1510, 1450, 1350, 1300, 1240, 1190.

A solution of the tosylate (314 mg, 0.072 mmol) in ether (3 ml) was added to a stirred solution of $LiAlH_4$ (36 mg, 0.95 mmol) in ether (5 ml) at 0 °C under an argon atmosphere. After 40 min, H_2O (37 μl), 15% NaOH (37 μl), and H_2O (110 μl) were successively added, and the resulting precipitates were removed by filtration. After evaporation of the solvent, the residue was purified through a short silica gel column with hexane–EtOAc (3 : 1) to afford **12** as a colorless oil (167 mg, 92%). $[\alpha]_D^{15}$ −2.3° (c = 1.12, MeOH). ^{1}H-NMR δ: 1.20 (3H, d, J = 6.4 Hz), 1.52 (1H, s), 2.10—2.25 (2H, d, J = 4.4 Hz), 3.80 (3H, s), 4.44 (2H, s), 5.66—5.76 (2H, m), 6.87 (2H, d, J = 8.6 Hz), 7.27 (2H, d, J = 8.5 Hz). MS m/z (relative intensity): 236 (M^+, 2.2%), 213 (0.67), 205 (0.9), 176 (7.5), 137 (29.2), 121 (100), 109 (10.4), 77 (11.4). Exact MS m/z Calcd for $C_{14}H_{20}O_3$ (M^+): 236.1413. Found: 236.1399. IR ν (neat) cm^{-1}: 3350 (OH), 1650, 1520.

5(*R*)-Hydroxy-2(*E*)-hexenal (9) DDQ (237 mg, 1.0 mmol) was added to a stirred solution of **12** (206 mg, 0.87 mmol) in CH_2Cl_2 (10 ml) and H_2O (0.5 ml). After being stirred for 40 min, the reaction mixture was quenched by addition of saturated $NaHCO_3$, and extracted with EtOAc. The extract was dried ($MgSO_4$) and concentrated to leave an oil, which was chromatographed on a silica gel column (hexane : EtOAc = 2 : 1) to give the diol (90 mg, 90%) as a colorless oil.

A mixture of the above diol (90 mg, 0.9 mmol) in CH_2Cl_2 (2 ml) and active MnO_2 (740 mg) was stirred for 1 h. After filtration to remove the MnO_2, the filtrate was concentrated *in vacuo*, and the residue was chromatographed on a silica gel column (EtOAc–hexane, 1 : 1) to give **9** as a colorless oil (86 mg, 90%). $[\alpha]_D^{15}$ −15.0° (c = 1.46, MeOH). ^{1}H-NMR δ: 1.27 (3H, d, J = 6.2 Hz), 1.65 (1H, s), 2.45—2.53 (2H, m), 4.04 (1H, sex, J = 6.2 Hz), 6.19 (1H, ddt, J = 16.0, 8.1, 1.1 Hz), 6.90 (1H, dt, J = 16.0, 7.3 Hz), 9.53 (1H, d, J = 8.1 Hz). IR ν (neat) cm^{-1}: 3350 (OH), 1680 (CO).

6-*O*-(*tert*-Butyldimethylsilyl)-3-deoxy-1,2-*O*-isopropylidene-3-*C*-[2-(4-methoxybenzyloxy)ethyl]-α-D-allofuranose (14) A solution of **13** (2.07 g, 7.18 mmol) in THF (12 ml) was added dropwise to a stirred suspension of NaH (560 mg, 14 mmol: 60% oil suspension) in DMF (8 ml) under an argon atmosphere at room temperature. After 2 h, MPM chloride (1.6 g, 10 mmol) was added, and stirring was continued for 2.5 h. The reaction mixture was poured into cold aqueous NH_4Cl solution, and extracted with CH_2Cl_2. The extract was washed with brine, dried over anhydrous $MgSO_4$, and evaporated *in vacuo* to leave an oil, which was chromatographed on a silica gel column using EtOAc–hexane (1 : 5) as the eluant to give the MPM ether as a colorless oil (2.83 g, 96.5%). $[\alpha]_D^{19}$ +52° (c = 3.06, $CHCl_3$). ^{1}H-NMR δ: 1.30 (3H, s), 1.34 (3H, s), 1.41 (3H, s), 1.50 (3H, s), 1.85—1.97 (1H, m), 1.99—2.05 (2H, m), 3.56—3.61 (2H, m), 3.75—3.78 (1H, m), 3.81 (3H, s), 3.90—4.10 (3H, m), 4.46 (2H, ABq, J = 4.4 Hz), 4.57 (1H, t, J = 4.0 Hz), 5.72 (1H, d, J = 3.5 Hz), 6.88 (2H, d, J = 8.5 Hz), 7.27 (2H, d, J = 8.5 Hz).

A stirred ice-cold MeOH solution (400 ml) of the MPM ether (53 g, 0.13 mol) was treated with 2% H_2SO_4 (100 ml) and the solution was stirred for 5 h at room temperature. After neutralization with $NaHCO_3$, the reaction mixture was evaporated *in vacuo*, and the residue was extracted with CH_2Cl_2. The extract was washed with H_2O, dried over anhydrous $MgSO_4$, and evaporated to leave an oil, which was dissolved in CH_2Cl_2 (200 ml) containing imidazole (13.0 g, 191 mmol). The solution was cooled in an ice-bath, and a CH_2Cl_2 solution (50 ml) of TBDMS chloride (14 g, 93 mmol) was added dropwise. After 1 h, the reaction mixture was washed with saturated aqueous NH_4Cl solution, dried over anhydrous $MgSO_4$, and evaporated *in vacuo* to leave a colorless oil, which was chromatographed on a silica gel column with EtOAc–hexane (1 : 10) as the eluent to give the recovered MPM ether (9 g, 17%) and **14** as a colorless oil (40 g, 64%). $[\alpha]_D^{16}$ +44° (c = 2.54, $CHCl_3$). ^{1}H-NMR δ: 0.07 (6H, s), 0.89 (9H, s), 1.30 (3H, s), 1.48 (3H, s), 1.89 (1H, ddt, J = 14.0, 11.5, 5.5 Hz), 2.04—2.13 (2H, m), 2.63 (1H, d, J = 4.0 Hz), 3.50—3.67 (1H, m), 3.75—3.82 (2H, m), 3.80 (3H, s), 4.46 (1H, d, J = 14.5 Hz), 4.50 (1H, d, J = 14.5 Hz), 4.58 (1H, t, J = 3.5 Hz), 5.72 (1H, d, J = 3.5 Hz), 6.87 (2H, d, J = 8.5 Hz), 7.27 (2H, d, J = 8.5 Hz). IR ν (neat) cm^{-1}: 3450 (OH).

6-*O*-(*tert*-Butyldimethylsilyl)-3-deoxy-1,2-*O*-isopropylidene-5-*O*-methanesulfonyl-3-*C*-[2-(4-methoxybenzyloxy)ethyl]-α-D-allofuranose (15) A solution of **14** (2.46 g, 5.19 mmol) and mesyl chloride (1.18 g, 10.3 mmol) in pyridine (12 ml) was stirred for 6 h at room temperature. The reaction mixture was poured into cold aqueous NH_4Cl solution, and extracted with CH_2Cl_2. The extract was successively washed with 10% HCl, saturated aqueous $NaHCO_3$, and brine, and dried over anhydrous $MgSO_4$. Concentration of the solvent gave an oil, which was chromatographed on a silica gel short column with EtOAc–hexane (1 : 5) as the eluant to give **15** as a colorless oil (2.80 g, 97.9%). $[\alpha]_D^{15}$ +40° (c = 2.30, $CHCl_3$). ^{1}H-NMR δ: 0.07 (6H, s), 0.89 (9H, s), 1.30 (3H, s), 1.49 (3H, s), 1.92 (1H, q, J = 6.5 Hz), 2.25 (1H, ddt, J = 10.0, 4.5, 6.0 Hz), 3.07 (3H, s), 3.59 (2H, t, J = 6.0 Hz), 3.80 (3H, s), 3.86 (2H, d, J = 6.0 Hz), 4.10 (1H, dd, J = 10.0, 4.0 Hz), 4.42 (1H, d, J = 11.5 Hz), 4.48 (1H, d, J = 11.5 Hz), 4.60 (1H, t, J = 4.0 Hz), 4.71 (1H, dt, J = 4.4, 5.5 Hz), 5.72 (1H, d, J = 4.0 Hz), 6.87 (2H, d, J = 8.5 Hz), 7.27 (2H, d, J = 8.5 Hz).

3-Deoxy-1,2-*O*-isopropylidene-5-*O*-methanesulfonyl-3-*C*-[2-(4-methoxybenzyloxy)ethyl]-α-D-allofuranose (16) A solution of **15** (130 g, 0.239 mmol) in THF (500 ml) and 1 N HCl (100 ml) was stirred for 1 h at room temperature. After neutralization with $NaHCO_3$, the solution was evaporated *in vacuo*, and the residue was extracted with CH_2Cl_2. The extract was washed with brine, dried over anhydrous $MgSO_4$, and evaporated *in vacuo* to leave **16** as a colorless oil (97 g, 91%). $[\alpha]_D^{15}$ +40° (c = 2.10, $CHCl_3$). ^{1}H-NMR δ: 1.30 (3H, s), 1.49 (3H, s), 1.85 (1H, ddt, J = 14.0, 3.0, 5.5 Hz), 1.93 (1H, dd, J = 14.0, 5.5 Hz), 2.21 (1H, dd, J = 10.0, 4.5 Hz), 2.40 (1H, t, J = 6.0 Hz), 3.10 (3H, s), 3.56 (1H, ddd, J = 14.0, 5.0, 3.0 Hz), 3.61 (1H, ddd, J = 14.0, 5.5, 3.0 Hz), 3.81 (3H, s), 3.89 (2H, dd, J = 6.0, 5.0 Hz), 4.11 (1H, dd, J = 10.0, 4.0 Hz), 4.42 (1H, d, J = 11.5 Hz), 4.47 (1H, d, J = 11.5 Hz), 4.58 (1H, dd, J = 6.0, 5.0 Hz), 4.77 (1H, dt, J = 4.0, 5.0 Hz), 5.74 (1H, d, J = 4.0 Hz), 6.88 (2H, d, J = 8.5 Hz), 7.27 (2H, d, J = 8.5 Hz). MS m/z (relative intensity): 348 (M^+, 0.9%), 311 (3), 228 (19), 197 (7), 121 (23), 43 (100). IR ν (neat) cm^{-1}: 3450 (OH).

6-*O*-Benzyl-3-deoxy-1,2-*O*-isopropylidene-3-*C*-[2-(4-methoxybenzyloxy)ethyl]-β-L-talofuranose (18) A stirred MeOH solution of **16** (20 g, 44.8 mmol) was treated with K_2CO_3 (7.3 g, 52.8 mmol) at room temperature. After 2 h, NH_4Cl was added to quench the reaction. The MeOH was concentrated to dryness, and the residue was dissolved in CH_2Cl_2, washed with brine, dried over anhydrous $MgSO_4$, and concentrated *in vacuo* to leave an oil, which was chromatographed on a silica gel column with EtOAc–hexane (1 : 3) as the eluant to give the epoxide (**17**) as an oil (15 g, 96%).

A DMF (5 ml) solution of benzyl alcohol (491 mg, 4.54 mmol) was added to a stirred suspension of NaH (182 mg, 4.55 mmol; 60% activity) in DMF (5 ml) under argon at room temperature. After 30 min, **17** (318 mg, 0.91 mmol) was added, and the stirring was continued for 90 min at 60 °C. The reaction mixture was cooled, poured into cooled aqueous NH_4Cl solution, and extracted with ether. The extract was washed with brine, dried over anhydrous $MgSO_4$, and evaporated *in vacuo* to leave an oil, which was chromatographed on a silica gel column with EtOAc–hexane (1 : 3) as the eluant to give **18** as a colorless oil (408 mg, 98%). $[\alpha]_D^{15}$ +42° (c = 3.10, $CHCl_3$). ^{1}H-NMR δ: 1.30 (3H, s), 1.48 (3H, s), 1.67 (1H, ddt, J = 14.0, 10.0, 4.5 Hz), 1.88 (1H, ddt, J = 14.0, 10.0, 6.5 Hz), 2.30 (1H, d, J = 6.5 Hz), 2.34 (1H, tt, J = 10.5, 4.5 Hz), 3.56 (1H, dd, J = 10.0, 5.0 Hz), 3.58 (1H, ddd, J = 14.0, 10.5, 4.5 Hz), 3.59 (1H, ddd, J = 14.0, 7.0, 6.5 Hz), 3.64 (1H, dd, J = 10.0, 7.5 Hz), 3.79 (3H, s), 3.77—3.87 (1H, m), 3.86 (1H, dd, J = 10.0, 1.0 Hz), 4.42 (1H, d, J = 11.5 Hz), 4.47 (1H, d, J = 11.5 Hz), 4.54 (1H, d, J = 11.5 Hz), 4.58 (1H, dd, J = 4.5, 3.5 Hz), 4.59 (1H, d, J = 11.5 Hz), 5.77 (1H, d, J = 4.0 Hz), 6.87 (2H, d, J = 8.5 Hz), 7.24—7.34 (7H, m). MS m/z (relative intensity): 458 (M^+, 0.5%), 309 (1.5), 279 (1.3), 173 (5), 121 (100), 91 (27.5). Exact MS m/z Calcd for $C_{26}H_{34}O_7$ (M^+):

458.2304. Found: 458.2303. IR ν (neat) cm^{-1}: 3450 (OH).

6-*O*-Benzyl-3-deoxy-1,2-*O*-isopropylidene-3-*C*-[2-(4-methoxybenzyloxy)ethyl]-5-*O*-methyl-β-L-talofuranose (19) A solution of **18** (65 g, 0.14 mol) in THF (200 ml) was added dropwise to a stirred suspension of NaH (8.5 g, 0.21 mol; 60% oil suspension) in DMSO (100 ml) and THF (100 ml) under argon at room temperature. After 2 h, iodomethane (30 g, 0.20 mol) was added, and the stirring was continued for 12 h. The reaction mixture was poured into cold aqueous NH_4Cl solution, and extracted with CH_2Cl_2. The extract was washed with brine, dried over anhydrous $MgSO_4$, and evaporated *in vacuo* to leave an oil, which was chromatographed on a silica gel short column using EtOAc–hexane (1 : 2) as the eluant to give **19** as a colorless oil (66.2 g, 100%). $[\alpha]_D^{15}$ +45° (c = 2.0, $CHCl_3$). ^{1}H-NMR δ: 1.30 (3H, s), 1.47 (3H, s), 1.68 (1H, ddt, J = 14.0, 4.0, 7.0 Hz), 1.89 (1H, ddt, J = 14.0, 10.5, 5.5 Hz), 2.31 (1H, tt, J = 10.5, 4.0 Hz), 3.45 (1H, ddd, J = 7.0, 5.0, 1.5 Hz), 3.50 (3H, s), 3.57 (1H, ddd, J = 14.0, 7.0, 5.5 Hz), 3.64 (1H, ddd, J = 14.0, 7.0, 5.5 Hz), 3.68 (1H, dd, J = 10.0, 5.0 Hz), 3.75 (1H, dd, J = 10.0, 7.0 Hz), 3.80 (3H, s), 3.91 (1H, dd, J = 10.5, 1.5 Hz), 4.42 (1H, d, J = 11.5 Hz), 4.48 (1H, d, J = 11.5 Hz), 4.56 (1H, dd, J = 4.0, 3.5 Hz), 4.55 (2H, s), 5.77 (1H, d, J = 3.5 Hz), 6.87 (2H, d, J = 8.5 Hz), 7.24—7.34 (7H, m). MS m/z (relative intensity): 472 (M^+, 0.5%), 323 (1.0), 278 (1.6), 219 (4.3), 121 (100), 91 (29). Exact MS m/z Calcd for $C_{27}H_{36}O_7$ (M^+): 472.2462. Found: 472.2482.

(2*R*,3*R*,4*S*)-5-Benzyloxy-3-formyloxy-4-methoxy-2-[2-(4-methoxybenzyloxy)ethyl]pentanal (20) A solution of **19** in dioxane (300 ml) and 3 N H_2SO_4 (100 ml) was stirred for 48 h at room temperature. The reaction mixture was neutralized with $NaHCO_3$ and evaporated *in vacuo*. The residue was extracted with CH_2Cl_2, washed with brine, dried over anhydrous $MgSO_4$, and evaporated to leave an oil, which was chromatographed on a silica gel column using EtOAc–hexane (1 : 2) as the eluant to give recovered **19** (13.5 g, 64%) and the diol as a viscous oil (6.8 g, 36%).

An aqueous solution of $NaIO_4$ (6.8 g, 0.03 mol in 85 ml of H_2O) was added to a MeOH solution (200 ml) of the above diol at 5 °C. After 2 h, the precipitate was filtered off, and then the filtrate was concentrated *in vacuo*, and extracted with CH_2Cl_2. The extract was dried over anhydrous $MgSO_4$, and evaporated to leave **20** as a colorless oil (6.7 g, 99%), which was used for the next reaction without further purification. $[\alpha]_D^{18}$ +14° (c = 2.7, $CHCl_3$). ^{1}H-NMR δ: 1.80 (1H, dq, J = 17.5, 7.0 Hz), 1.97 (1H, ddt, J = 17.5, 10.0, 7.5 Hz), 2.76 (1H, dddd, J = 7.5, 7.0, 4.0, 3.5 Hz), 3.38 (3H, m), 3.43—3.59 (5H, m), 3.38 (3H, s), 3.79 (3H, s), 4.37 (2H, s), 4.48 (2H, s), 5.47 (1H, t, J = 3.3 Hz), 7.22 (2H, d, J = 8.8 Hz), 7.28—7.35 (5H, m), 8.12 (2H, s), 9.65 (1H, d, J = 4.0 Hz). MS m/z (relative intensity): 430 (M^+, 0.2%), 321 (0.5), 157 (6), 121 (100), 91 (46). Exact MS m/z Calcd for $C_{24}H_{30}O_7$ (M^+): 430.1992. Found: 430.2011. IR ν (neat) cm^{-1}: 1720, 1710 (CO).

(2*Z*,4*S*,5*S*,6*S*)-7-Benzyloxy-5-hydroxy-6-methoxy-4-[2-(4-methoxybenzyloxy)ethyl]-2-methylhept-2-enoic Acid δ-Lactone (21) A THF (100 ml) solution of trimethyl α-phosphonopropionate (16.2 g, 82.6 mmol) was added dropwise to a stirred suspension of NaH (8.5 g, 0.21 mol; 60% oil suspension) in THF (100 ml) under argon at 0 °C. After evolution of hydrogen had ceased, the solution was cooled to −90 °C, and a THF solution (100 ml) of **20** (11.0 g, 25.5 mmol) was added dropwise within 1 h. The reaction mixture was allowed to warm to −20 °C for 2 h, and then aqueous NH_4Cl was added in order to quench the reaction. The whole mixture was extracted with ether, and the extract was washed with brine, dried over anhydrous $MgSO_4$, and evaporated *in vacuo* to leave an oil, which was dissolved in MeOH. This solution was stirred and K_2CO_3 (3.5 g, 25 mmol) was added at 0 °C, then after 4 h, NH_4Cl was added. The reaction mixture was concentrated to dryness, and the residue was extracted with CH_2Cl_2. The extract was washed with brine, dried over anhydrous $MgSO_4$, and concentrated *in vacuo* to leave a colorless oil, which was chromatographed on a silica gel column with EtOAc–hexane (1 : 4) as the eluant to give **21** as a colorless oil (6.5 g, 58%). $[\alpha]_D^{18}$ +43° (c = 2.15, $CHCl_3$). ^{1}H-NMR δ: 1.66 (1H, ddt, J = 14.0, 8.5, 6.0 Hz), 1.87 (3H, t, J = 1.5 Hz), 1.89 (1H, ddd, J = 14.0, 6.0, 5.0 Hz), 2.91 (1H, dddd, J = 9.0, 8.5, 5.0, 1.5 Hz), 3.46 (3H, s), 3.53 (2H, t, J = 6.0 Hz), 3.57 (1H, ddd, J = 6.0, 5.5, 3.0 Hz), 3.70 (1H, dd, J = 10.0, 5.5 Hz), 3.75 (1H, dd, J = 10.0, 6.0 Hz), 3.79 (3H, s), 4.34 (1H, dd, J = 9.0, 3.0 Hz), 4.39 (1H, d, J = 11.5 Hz), 4.44 (1H, d, J = 11.5 Hz), 4.50 (1H, d, J = 11.5 Hz), 4.55 (1H, d, J = 11.5 Hz), 6.47 (1H, sex, J = 1.5 Hz), 6.86 (2H, d, J = 8.8 Hz), 7.23 (7H, d, J = 8.8 Hz). MS m/z (relative intensity): 440 (M^+, 0.9%), 349 (4), 319 (1.8), 275 (1.6), 213 (7), 121 (100), 91 (43). Exact MS m/z Calcd for $C_{26}H_{32}O_6$ (M^+): 440.2199. Found: 440.2202. IR ν (neat) cm^{-1}: 1710 (CO).

(2*S*,5*S*,6*S*)-6-[2-Benzyloxy-1(*S*)-methoxyethyl]-5,6-dihydro-2-isopropyloxy-5-[2-(4-methoxybenzyloxy)ethyl]-3-methylpyran (22) A 1 M hexane solution of DIBAH (28 ml) was added to a CH_2Cl_2 (100 ml) solution of **21** (6.2 g, 14 mmol) under argon at −80 °C. After 1 h, MeOH was added to decompose the reagent, and the reaction mixture was washed with 0.5 N HCl, 10% $NaHCO_3$ and brine, dried over $MgSO_4$, then evaporated to afford a colorless oil. This oil was dissolved in iso-PrOH (100 ml), and after addition of CSA (310 mg) the mixture was stirred for 1 h at room temperature. After addition of triethylamine (TEA) (1 ml), the reaction mixture was evaporated *in vacuo*, and the residue was chromatographed on a silica gel column with EtOAc–hexane (1 : 5) as the eluant to give **22** as a colorless oil (5.1 g, 75%). $[\alpha]_D^{19}$ +43° (c = 1.2, $CHCl_3$). ^{1}H-NMR δ: 1.14 (3H, d, J = 6.5 Hz), 1.16 (3H, d, J = 6.5 Hz), 1.48 (1H, ddt, J = 14.0, 9.0, 7.0 Hz), 1.66 (3H, t, J = 1.8 Hz), 1.79 (1H, ddt, J = 14.0, 3.5, 7.0 Hz), 2.63 (1H, t, J = 9.0 Hz), 3.50 (3H, s), 3.54 (2H, t, J = 7.0 Hz), 3.64 (1H, ddd, J = 5.5, 4.5, 1.0 Hz), 3.67 (1H, dd, J = 8.5, 4.5 Hz), 3.73 (1H, dd, J = 9.0, 1.0 Hz), 3.78 (3H, s), 3.79 (1H, dd, J = 8.5, 5.5 Hz), 3.94 (1H, heptet, J = 6.5 Hz), 4.40 (1H, d, J = 11.5 Hz), 4.45 (1H, d, J = 11.5 Hz), 4.52 (1H, d, J = 11.5 Hz), 4.56 (1H, d, J = 11.5 Hz), 4.82 (1H, s), 5.54 (1H, s), 6.86 (2H, d, J = 8.8 Hz), 7.23—7.34 (7H, m). MS m/z (relative intensity) 484 (M^+, 0.5%), 424 (0.5), 319 (1.5), 353 (1.3), 259 (10), 121 (100), 91 (28). Exact MS m/z Calcd for $C_{29}H_{40}O_6$ (M^+): 484.2824. Found: 484.2813.

2(*S*)-{2(*S*)-Isopropyloxy-5(*R*)-[2-(4-methoxybenzyloxy)ethyl-3(*R*)-methyl-6(*S*)-tetrahydropyranyl}-2-methoxyethanol (23) An EtOH solution of **22** (4.6 g, 9.4 mmol) was hydrogenated in the presence of Raney Ni W-2 (12 ml of EtOH suspension) at ordinary temperature and pressure. After 9 h, the catalyst was filtered off, and the filtrate was chromatographed on silica gel column with EtOAc–hexane (1 : 5) as the eluant to give recovered **22** (0.75 g, 6.1%) and **23** as a colorless oil (2.9 g, 77.8%). ^{1}H-NMR δ: 0.81 (3H, d, J = 7.0 Hz), 1.10 (3H, d, J = 6.2 Hz), 1.20 (3H, d, J = 6.2 Hz), 1.31—1.50 (3H, m), 1.68—1.79 (2H, m), 1.94—2.07 (1H, m), 2.80 (1H, s), 3.40—3.51 (3H, m), 3.47 (3H, s), 3.71—3.92 (4H, m), 3.80 (3H, s), 4.42 (2H, ABq, J = 5.5 Hz), 4.69 (1H, d, J = 3.3 Hz), 6.87 (2H, d, J = 8.8 Hz), 7.26 (2H, d, J = 8.8 Hz). MS m/z (relative intensity): 336 (M^+ − 60, 0.9%), 305 (1.8), 215 (1.5), 121 (100). Exact MS m/z Calcd for $C_{19}H_{28}O_5$ (M^+ − 60): 336.1937. Found: 336.1956. IR ν (neat) cm^{-1}: 3450 (OH).

2(*S*)-{2(*S*)-Isopropyloxy-5(*R*)-[2-(4-methoxybenzyloxy)ethyl]-3(*R*)-methyl-6(*S*)-tetrahydropyranyl}-2-methoxyethanal (24) Dry Me_2SO (0.75 ml, 5.26 mmol) in CH_2Cl_2 (15 ml) was added dropwise during 15 min to an efficiency stirred solution of oxalyl chloride (0.69 ml, 7.90 mmol) in dry CH_2Cl_2 (40 ml) at −90 °C, and a solution of **23** (2.08 g, 5.26 mmol) in CH_2Cl_2 (4 ml) was added to the mixture within 10 min. Stirring was continued at −90 °C for 30 min, then Et_3N (2.9 ml, 20.8 mmol) was added dropwise. The reaction mixture was allowed to warm to −70 °C (over *ca.* 1 h), and then quenched with H_2O (20 ml). The organic layer was separated, and the aqueous layer was extracted with ether (100 ml × 2). The combined extracts were washed with brine, dried over $MgSO_4$, and evaporated *in vacuo*. The residue was chromatographed on a silica gel column with hexane–EtOAc (3 : 1) as the eluant to give the aldehyde (**24**) as a colorless oil (1.99 g, 96%). ^{1}H-NMR δ: 0.79 (3H, d, J = 6.8 Hz), 1.04 (3H, d, J = 6.0 Hz), 1.12 (3H, d, J = 6.1 Hz), 1.26—2.25 (6H, m), 3.43—3.59 (2H, m), 3.51 (3H, s), 3.71—3.78 (2H, m), 3.80 (3H, s), 4.00 (2H, dd, J = 10.8, 2.9 Hz), 4.43 (2H, s), 4.60 (1H, d, J = 3.2 Hz), 6.87 (2H, d, J = 8.8 Hz), 7.25 (2H, d, J = 8.8 Hz), 9.78 (1H, d, J = 1.2 Hz). MS m/z (relative intensity): 394 (M^+, 0.5%), 334 (28.3), 225 (4.6), 213 (30.2), 199 (100), 185 (15.6), 169 (6.7), 157 (35.8), 137 (30.4), 122 (100), 121 (99), 95 (66.6). Exact m/z Calcd for $C_{22}H_{34}O_5$ (M^+): 394.2356. Found: 394.2349. Calcd for $C_{19}H_{26}O_5$ (M^+ − 60): 334.1781. Found: 334.1768. IR ν (neat) cm^{-1}: 1730 (CO).

5(*S*)-{2(*S*)-Isopropyloxy-5(*R*)-[2-(4-methoxybenzyloxy)ethyl]-3(*R*)-methyl-6(*S*)-tetrahydropyranyl}-4(*R*)-hydroxy-5-methoxypentene (25) A stirred solution of the above aldehyde **24** (1.72 g, 4.3 mmol) in dry CH_2Cl_2 (100 ml), cooled at −50 °C under nitrogen, was treated with a 1 M solution of $MgBr_2 \cdot OEt_2$ (8.6 ml, 8.6 mmol) in ether. After 10 min, allyltri-*n*-butyltin (2.76 g, 8.6 mmol) in CH_2Cl_2 (100 ml) was added. The mixture was stirred below −60 °C for 15 min, and the reaction was quenched with saturated aqueous NH_4Cl (10 ml). The cooling bath was then removed and the reaction mixture was allowed to warm to room temperature. The whole was extracted with CH_2Cl_2, and the extract was washed with brine, and dried over anhydrous $MgSO_4$. After evaporation of the solvent, the residue was chromatographed on a silica gel column with hexane–EtOAc (2 : 1) as the eluant to afford the 3,4-*anti* isomer of **25** (20 mg, 1%) and **25** as a colorless oil (1.43 g, 76%). ^{1}H-NMR δ: 0.81 (3H, d, J = 7.0 Hz), 1.09 (3H, d, J = 6.0 Hz), 1.18 (3H, d, J = 6.2 Hz), 1.28—1.42 (1H, m), 1.51 (1H, dt, J = 12.5, 4.0 Hz), 1.75—1.88 (2H, m), 1.94—2.04 (1H, m), 2.25 (1H, dt, J = 14.0, 7.0 Hz), 2.35 (1H, ddd, J = 14.0, 7.0, 5.0 Hz), 3.14 (1H, s), 3.39

(1H, dd, J=5.0, 0.5 Hz), 3.46—3.54 (2H, m), 3.59 (3H, s), 3.65 (2H, dd, J=10.0, 0.5 Hz), 3.80 (3H, s), 3.80 (1H, heptet, J=6.0 Hz), 4.40 (1H, d, J=11.5 Hz), 4.45 (1H, d, J=11.5 Hz), 4.69 (1H, d, J=3.5 Hz), 5.09 (1H, dd, J=16.0, 2.0 Hz), 5.11 (1H, ddd, J=10.0, 3.5, 1.5 Hz), 5.87 (1H, ddt, J=16.0, 10.0, 7.0 Hz), 6.87 (2H, d, J=8.8 Hz), 7.25 (2H, d, J=8.8 Hz). MS m/z (relative intensity) 436 (M^+, 0.2%), 376 (2.4), 303 (0.6), 261 (1.8), 153 (0.5), 121 (100). Exact MS m/z Calcd for $C_{22}H_{32}O_5$ (M^+): 376.2249. Found: 376.2252. IR ν (neat) cm^{-1}: 3400 (OH).

(2*R*,4*R*,5*S*,6*S*,7*R*)-6-Methoxy-4-[2-(4-methoxybenzyloxy)ethyl]-2-methyl-9-decene-1,5,7-triol (26) A solution of **25** (1.2 g, 2.76 mmol) in 1 N HCl (40 ml) and THF (120 ml) was stirred at 50 °C for 6 h. After neutralization with solid $NaHCO_3$, the reaction mixture was evaporated to dryness. CH_2Cl_2 and water were added to the residue, and the CH_2Cl_2 layer was separated. The aqueous layer was extracted with CH_2Cl_2 (30 ml × 2), and the organic layers were combined and dried over $MgSO_4$. After evaporation of the solvent, purification of the residue on a silica gel column with hexane–EtOAc (1 : 1) as the eluant afforded recovered **25** (63 mg, 5%) and a lactol as a colorless oil (857 mg, 80%).

A solution of $CaCl_2$ (726 mg, 6.54 mmol) in EtOH (50 ml) was cooled at −40 °C, and $NaBH_4$ (424 mg, 10.9 mmol) in EtOH (30 ml) was added dropwise. NaCl separated out at once as a fine solid. After 30 min, an EtOH (10 ml) solution of the above lactol (726 mg) was added to the resulting $Ca(BH_4)_2$ solution at −20 °C. The reaction mixture was stirred for 3 h at room temperature, then excess $Ca(BH_4)_2$ was decomposed by addition of 1 N HCl, and the mixture was neutralized with Na_2CO_3. After removal of the precipitates by filtration, the filtrate was concentrated *in vacuo*. The residue was extracted with CH_2Cl_2, dried over $MgSO_4$, and evaporated *in vacuo* to leave **26** as a colorless oil (783 mg, 91%). $[\alpha]_D^{22}$ +6.4° (c=5.10, $CHCl_3$). ^{1}H-NMR δ: 0.92 (3H, d, J=6.4 Hz), 1.26—1.92 (6H, m), 2.30—2.38 (2H, m), 3.20—3.70 (7H, m), 3.54 (3H, s), 3.79 (3H, s), 4.42 (2H, s), 5.05—5.18 (2H, m), 5.69—6.04 (1H, m), 6.86 (2H, d, J=8.8 Hz), 7.24 (2H, d, J=8.8 Hz). MS m/z (relative intensity): 396 (M^+, 0.57), 346 (0.36), 323 (0.63), 305 (1.0), 280 (6.7), 262 (6.7), 224 (8.3), 171 (18.3), 155 (33.9), 137 (42.7), 121 (100), 98 (36.4). Exact MS m/z Calcd for $C_{22}H_{36}O_6$ (M^+): 396.2512. Found: 396.2531. IR ν cm^{-1}: 3400 (OH).

(2*R*,4*R*,5*S*,6*S*,7*R*)-5,7-Isopropylidenedioxy-6-methoxy-4-[2-(4-methoxybenzyloxy)ethyl]-2-methyl-9-decenol (27) A benzene solution (30 ml) of 2,2-dimethoxypropane (2.4 ml), **26** (775 mg, 1.96 mmol) and CSA (23 mg) was stirred at room temperature for 2 h. Et_3N (1 ml) was added to quench the reaction and after evaporation of the solvent, the residue was chromatographed on a silica gel column (hexane–AcOEt, 2 : 1) to give the acetal **27** as a colorless oil (766 mg, 90%). $[\alpha]_D^{12}$ +10° (c=2.70, $CHCl_3$). ^{1}H-NMR δ: 0.88 (3H, d, J=6.2 Hz), 1.06—1.11 (1H, m), 1.40 (3H, s), 1.43 (3H, s), 1.46—1.61 (2H, m), 1.75—1.87 (1H, m), 1.95—2.10 (1H, m), 2.35 (1H, ddd, J=14.0, 7.5, 7.0 Hz), 2.42 (1H, ddd, J=14.0, 7.0, 6.5 Hz), 3.10 (1H, s), 3.37 (1H, dd, J=11.5, 4.5 Hz), 3.48 (1H, dd, J=7.5, 1.5 Hz), 3.53 (1H, dd, J=13.5, 7.5 Hz), 3.59 (1H, dd, J=11.5, 4.0 Hz), 3.73 (1H, dt, J=1.5, 7.0 Hz), 3.80 (3H, s), 4.42 (2H, s), 5.01 (1H, ddd, J=17.0, 3.0, 1.5 Hz), 5.07 (1H, ddd, J=10.0, 1.5, 1.0 Hz), 5.81 (1H, dddd, J=17.0, 10.0, 7.5, 6.5 Hz), 6.87 (2H, d, J=8.5 Hz), 7.24 (2H, d, J=8.5 Hz). MS m/z (relative intensity) 421 (M^+ − 15, 0.1%), 280 (1.4), 262 (1.8), 137 (11), 121 (99), 98 (100). IR ν (neat) cm^{-1}: 3350 (OH).

(2*R*,4*R*,5*S*,6*S*,7*R*)-5,7-Isopropylidenedioxy-6-methoxy-4-[2-(4-methoxybenzyloxy)ethyl]-2-methyl-9-decenal (28) A solution of DMSO (0.37 ml, 5.22 mmol) in dry CH_2Cl_2 (10 ml) was added to a stirred solution of oxalyl chloride (0.3 ml, 3.44 mmol) in dry CH_2Cl_2 (20 ml) at −70 °C. After 15 min, a CH_2Cl_2 (30 ml) solution of **27** (765 mg, 1.74 mmol) was added to the reaction mixture. Stirring was continued for 30 min at −65 °C, and then Et_3N (1.2 ml, 8.6 mmol) was added. After 30 min at −65 °C, the reaction mixture was warmed to −30 °C and then quenched with saturated aqueous NH_4Cl. After dilution with CH_2Cl_2, the CH_2Cl_2 solution was washed with brine, and dried over $MgSO_4$. After evaporation of the solvent, the residue was purified on a silica gel column with hexane–EtOAc (2 : 1) as the eluant to afford **28** as a viscous oil (684 mg, 91%). $[\alpha]_D^{15}$ +10° (c=2.07, $CHCl_3$). ^{1}H-NMR δ: 1.05 (3H, d, J=6.8 Hz), 1.37 (6H, s), 1.26—2.65 (8H, m), 3.45—3.72 (5H, m), 3.52 (3H, s), 3.80 (3H, s), 4.41 (2H, s), 5.02—5.19 (2H, m), 5.68—6.00 (1H, m), 6.86 (2H, d, J=8.8 Hz), 7.24 (2H, d, J=8.8 Hz), 9.57 (1H, d, J=2.0 Hz). IR ν (neat) cm^{-1}: 1715 (CO).

Dimethyl (3*R*,5*R*,6*S*,7*S*,8*R*)-6,8-Isopropylidenedioxy-7-methoxy-5-[2-(4-methoxybenzyloxy)ethyl]-3-methyl-2-oxo-10-undecenylphophonate (29) A 1.5 M *n*-BuLi solution in hexane (3.28 ml, 4.8 mmol) was added to a stirred solution of dimethyl methylphosphonate (0.68 ml, 6.27 mmol) in THF (30 ml) at −80 °C. After 30 min, a solution of **28** (0.68 g, 1.57 mmol) in THF (30 ml) was added dropwise, and the reaction mixture was gradually warmed to −40 °C during 6 h. After the reaction had been quenched with saturated NH_4Cl solution, the whole mixture was extracted with ether, and the extract was washed with brine, dried over $MgSO_4$, and evaporated *in vacuo* to give the β-hydroxyphosphonate as a colorless oil (0.87 g, 99%).

Pyridinium dichromate (PDC) (3.5 g, 9.4 mmol) was added to a stirred solution of the β-hydroxyphosphonate (0.87 g, 1.56 mmol) in DMF (35 ml) at room temperature. After 7 h, the reaction mixture was poured into H_2O and then extracted with ether. The extract was washed with brine, dried over $MgSO_4$, and concentrated *in vacuo*, and the residue was chromatographed on a silica gel column with EtOAc to give the β-ketophosphonate (**29**) as a colorless oil (693 mg, 86.5%). $[\alpha]_D^{18}$ −6.6° (c=1.31, $CHCl_3$). ^{1}H-NMR δ: 1.07 (3H, d, J=6.6 Hz), 1.17 (1H, ddd, J=14.0, 8.5, 3.5 Hz), 1.40 (3H, s), 1.44 (3H, s), 1.75 (1H, ddd, J=14.0, 7.0, 3.0 Hz), 1.84 (1H, ddd, J=14.0, 7.0, 3.0 Hz), 1.95—2.05 (2H, m), 2.35—2.41 (2H, m), 3.06 (1H, t, J=1.0 Hz), 3.15 (2H, d, J=22.0 Hz), 3.45—3.55 (2H, m), 3.57 (1H, dd, J=9.5, 1.0 Hz), 3.52 (3H, s), 3.76 (3H, d, J=11.0 Hz), 3.78 (3H, d, J=11.0 Hz), 3.80 (3H, s), 4.40 (2H, s), 5.08 (1H, dd, J=10.0, 1.5 Hz), 5.13 (1H, ddd, J=17.5, 3.0, 1.5 Hz), 5.81 (1H, ddd, J=17.0, 10.0, 7.2 Hz), 6.86 (2H, d, J=8.4 Hz), 7.23 (2H, d, J=8.4 Hz). MS m/z (relative intensity): 556 (M^+, 0.2%), 541 (0.2), 396 (0.8), 378 (2), 275 (3), 202 (16), 180 (23), 121 (100). Exact MS m/z Calcd for $C_{28}H_{45}O_9$ (M^+): 556.2801. Found: 556.2815. IR ν (neat) cm^{-1}: 1720, 1705 (CO).

(3*R*,4*S*,5*S*,6*R*,8*R*)-10-Dimethoxyphosphono-3,5-isopropylidenedioxy-4-methoxy-6-[2-(4-methoxybenzyloxy)ethyl]-8-methyl-9-oxodecanoic Acid (8) A solution of **29** in acetone (30 ml), 10% aqueous $NaHCO_3$ (1.9 ml) and a 0.1 M solution of $KMnO_4$ in H_2O (1.86 ml) were added succesively to a stirred aqueous solution of $NaIO_4$ (2.0 g in 18 ml H_2O) at room temperature. After 1 h, the reaction mixture was filtered, then the filtrate was mixed with CH_2Cl_2, and the mixture was washed with aqueous NH_4Cl and brine, dried over anhydrous $MgSO_4$, and evaporated *in vacuo* to leave the carboxylic acid **8** as a colorless oil (425 mg, 80%). $[\alpha]_D^{18}$ +16° (c=3.60, $CHCl_3$). ^{1}H-NMR δ: 1.06 (3H, d, J=6.6 Hz), 1.17 (1H, ddd, J=14.0, 8.5, 3.5 Hz), 1.42 (3H, s), 1.43 (3H, s), 1.76 (1H, ddd, J=14.0, 7.0, 3.0 Hz), 1.86 (1H, ddd, J=14.0, 6.5, 5.0 Hz), 1.97—2.03 (1H, m), 2.68 (2H, d, J=6.6 Hz), 2.90—2.97 (1H, m), 3.15 (2H, d, J=22.0 Hz), 3.18 (1H, t, J=1.0 Hz), 3.50 (3H, s), 3.41—3.57 (2H, m), 3.64 (3H, d, J=9.2 Hz), 3.76 (3H, d, J=11.0 Hz), 3.78 (3H, d, J=11.0 Hz), 3.80 (3H, s), 4.20 (1H, dt, J=6.6, 1.0 Hz), 4.40 (2H, s), 5.07—5.30 (2H, m), 6.86 (2H, d, J=8.4 Hz), 7.22 (2H, d, J=8.4 Hz). MS m/z (relative intensity): 556 (M^+ − 18, 0.3%), 395 (1.7), 377 (1.8), 202 (13), 180 (21.5), 121 (100). Exact MS m/z Calcd for $C_{27}H_{41}O_{10}$ (M^+ − 18): 556.2438. Found: 556.2422. IR ν (neat) cm^{-1}: 3450 (OH), 1720, 1705 (CO).

4-Formyl-1(*R*)-methyl-3(*Z*)-butenyl (3*R*,4*S*,5*S*,6*R*,8*R*)-10-Dimethoxyphosphono-3,5-isopropylidenedioxy-4-methoxy-6-[2-(4-methoxybenzyloxy)ethyl]-8-methyl-9-oxodecanoate (30) 2,4,6-Trichlorobenzoyl chloride (185 mg, 0.76 mmol) was added dropwise to a stirred solution of **8** (425 mg, 0.74 mmol) and Et_3N (0.105 ml, 0.76 mmol) in THF (10 ml) at room temperature. After 1 h, precipitated Et_3N·HCl was filtered off and the filtrate was evaporated *in vacuo* to leave an oil, which was dissolved in toluene (10 ml). To this stirred solution, a mixture of **9** (100 mg, 0.88 mmol) and DMAP (93 mg, 0.76 mmol) in toluene (10 ml) was added. After 1.5 h, the reaction mixture was diluted with ether, washed with brine and saturated $NaHCO_3$, dried ($MgSO_4$), and evaporated *in vacuo*. The residue was chromatographed on a silica gel column with hexane–EtOAc (1 : 2) to give **30** as a colorless oil (388 mg, 78%). $[\alpha]_D^{17}$ −4.8° (c=2.92, $CHCl_3$). ^{1}H-NMR δ: 1.06 (3H, d, J=7.0 Hz), 1.18 (1H, ddd, J=14.0, 8.5, 3.5 Hz), 1.29 (3H, d, J=6.5 Hz), 1.41 (6H, s), 1.67—1.91 (2H, m), 1.95—2.05 (1H, m), 2.57—2.65 (4H, m), 2.88—3.01 (1H, m), 3.14 (2H, d, J=22.5 Hz), 3.14 (1H, t, J=0.5 Hz), 3.44—3.53 (3H, m), 3.47 (3H, s), 3.63 (1H, dd, J=9.2, 0.5 Hz), 3.76 (3H, d, J=11.5 Hz), 3.77 (3H, d, J=11.5 Hz), 3.80 (3H, s), 4.22 (1H, ddd, J=7.5, 6.5, 1.5 Hz), 4.40 (2H, s), 5.13 (1H, sextet, J=6.5 Hz), 6.16 (1H, ddt, J=16.0, 7.5, 1.2 Hz), 6.77 (1H, dt, J=16.0, 7.5 Hz), 6.86 (1H, d, J=8.4 Hz), 7.23 (1H, d, J=8.4 Hz), 9.51 (1H, d, J=7.5 Hz). FI-MS m/z 671 (M^+ + 1, 84%), 670 (M^+, 100), 121 (70.9). IR ν (neat) cm^{-1}: 1730, 1710, 1695 (CO).

6″-Dihydro-6″-*O*-(4-methoxybenzyl)-3,5-*O*-isopropylideneniddanolide (10) K_2CO_3 (47 mg, 0.34 mmol) was added to the solution of **30** (38.0 mg, 0.056 mmol) and 18-crown-6 (180 mg, 0.684 mmol) in toluene (57 ml), and the reaction mixture was stirred vigorously at room temperature. After 17 h, the reaction mixture was quenched by addition of saturated NH_4Cl (10 ml), and the mixture was poured into ether (20 ml). The organic layer was washed with saturated KCl, dried over $MgSO_4$, and concentrated *in vacuo*. The residue was chromatographed on a silica gel column with hexane–EtOAc (3 : 1) to give **10** as a colorless oil (17.6 mg, 57%). $[\alpha]_D^{19}$ +1.8° (c=2.19, $CHCl_3$). ^{1}H-NMR δ: 1.15 (3H, d, J=7.0 Hz), 1.31 (3H,

d, J=6.2 Hz), 1.36 (3H, s), 1.37—1.50 (2H, m), 1.40 (3H, s), 1.62—1.73 (1H, m), 2.00 (1H, dt, J=14.3, 8.3 Hz), 2.15 (1H, ddt, J=14.0, 5.5, 7.0 Hz), 2.31 (1H, ddd, J=14.0, 10.5, 9.5 Hz), 2.46 (1H, dd, J=14.5, 4.5 Hz), 2.50 (1H, ddd, J=14.5, 4.5, 2.8 Hz), 2.60—2.70 (1H, m), 2.71 (1H, dd, J=14.5, 8.5 Hz), 2.92 (1H, dd, J=1.5, 1.0 Hz), 3.427 (1H, ddd, J=13.5, 6.0, 2.0 Hz), 3.431 (1H, ddd, J=13.5, 6.0, 2.0 Hz), 3.56 (3H, s), 3.76 (1H, dd, J=4.0, 1.0 Hz), 3.81 (3H, s), 4.11 (1H, ddd, J=8.5, 4.5, 1.5 Hz), 4.40 (2H, s), 5.16 (1H, ddq, J=10.5, 2.8, 6.2 Hz), 6.04 (1H, ddd, J=15.0, 6.3, 4.5 Hz), 6.18 (1H, dd, J=15.5, 10.0 Hz), 6.35 (1H, d, J=15.5 Hz), 6.88 (2H, d, J=8.8 Hz), 6.96 (1H, dd, J=15.5, 10.0 Hz), 7.24 (2H, d, J=8.8 Hz). MS m/z (relative intensity): 544 (M^+, 0.2%), 408 (0.3), 318 (4), 249 (4), 234 (4), 150 (11), 121 (100). Exact MS m/z Calcd for $C_{31}H_{44}O_8$ (M^+): 544.3037. Found: 544.3053. IR ν (neat) cm^{-1}: 1720, 1675 (CO).

(6″-Dihydro-3,5-*O*-isopropylidene)niddanolide (31) DDQ (33 mg, 0.15 mmol) was added to a stirred solution of **10** (39.6 mg, 0.073 mmol) in CH_2Cl_2 (1 ml) and H_2O (0.05 ml). Stirring was continued for 1 h, then the reaction mixture was quenched by addition of saturated $NaHCO_3$, and the mixture was extracted with EtOAc. The extract was dried ($MgSO_4$) and concentrated to leave an oil, which was purified on a silica gel column with hexane–EtOAc (1 : 1) to give **31** as a colorless oil (26 mg, 84%). $[\alpha]_D^{21}$ +14.4° (c=1.38, $CHCl_3$). ^{1}H-NMR δ: 1.19 (3H, d, J=7.0 Hz), 1.32 (3H, d, J=6.2 Hz), 1.43 (6H, s), 1.35—1.79 (4H, m), 1.98—2.10 (3H, m), 2.23—2.38 (1H, m), 2.44—2.55 (3H, m), 2.64—2.75 (2H, m), 3.53—3.61 (1H, m), 3.57 (3H, s), 3.66—3.72 (1H, m), 3.79 (1H, dd, J=4.0, 1.1 Hz), 4.12 (1H, dq, J=4.4, 1.5 Hz), 5.10—5.21 (1H, m), 6.04 (1H, ddd, J=15.0, 6.3, 4.5 Hz), 6.18 (1H, dd, J=15.5, 10.0 Hz), 6.35 (1H, d, J=15.5 Hz), 7.03 (1H, dd, J=15.5, 10.0 Hz). MS m/z (relative intensity): 424 (M^+, 0.4%), 409 (5), 334 (5), 250 (24), 233 (55), 150 (79), 121 (100). Exact MS m/z Calcd for $C_{23}H_{36}O_7$ (M^+): 424.2461. Found: 424.2466. IR ν (neat) cm^{-1}: 3400 (OH), 1720, 1670 (CO).

(3,5-*O*-Isopropylidene)niddanolide (32) Dry Me_2SO (0.24 ml, 3.39 mmol) in dry CH_2Cl_2 (1 ml) was added dropwise during 15 min to an efficiently stirred solution of oxalyl chloride (0.15 ml, 1.7 mmol) in dry CH_2Cl_2 (1 ml), cooled to below −78 °C under an argon atmosphere. After 15 min at −78 °C, a solution of **31** (0.36 g, 0.85 mmol) was added to the mixture during 10 min. Stirring was continued at −78 °C for 30 min, then Et_3N (0.7 ml, 5 mmol) was added dropwise, and after removal of the cooling bath, the reaction mixture was allowed to warm to room temperature (over *ca.* 1 h). Then H_2O (20 ml) was added, the organic layer was separated, and the aqueous layer was extracted with ether (30 ml × 2). The combined extracts were washed with brine, dried over $MgSO_4$, and evaporated *in vacuo*. The residue was chromatographed on a silica gel column with hexane–EtOAc (2 : 1) as the eluant to give the aldehyde **32** (0.34 g, 95%) as a colorless oil. $[\alpha]_D^{17.5}$ −1.6° (c=1.50, $CHCl_3$). ^{1}H-NMR δ: 1.19 (3H, d, J=6.8 Hz), 1.32 (3H, d, J=6.3 Hz), 1.33 (3H, s), 1.37 (1H, ddd, J=15.0, 9.8, 3.4 Hz), 1.39 (3H, s), 1.87 (1H, ddd, J=14.6, 10.3, 6.8 Hz), 2.24 (1H, ddd, J=17.1, 7.8, 2.0 Hz), 2.32 (1H, dt, J=14.6, 4.4 Hz), 2.39—2.47 (1H, m), 2.49 (1H, dd, J=14.6, 3.9 Hz), 2.4 (1H, ddd, J=14.6, 4.9, 2.9 Hz), 2.72 (1H, dd, J=15.1, 7.8 Hz), 2.74 (1H, m), 2.91 (1H, s), 3.07 (1H, ddd, J=17.6, 5.4, 1.5 Hz), 3.52 (3H, s), 3.87 (1H, dd, J=4.9, 0.5 Hz), 4.15 (1H, ddd, J=7.8, 3.9, 1.5 Hz), 5.22 (1H, ddq, J=9.3, 2.9, 6.3 Hz), 6.10 (1H, ddd, J=15.6, 10.3, 4.9 Hz), 6.19 (1H, dd, J=15.6, 10.3 Hz), 6.26 (1H, d, J=15.6 Hz), 7.01 (1H, dd, J=15.6, 10.3 Hz), 9.70 (1H, dd, J=2.0, 1.7 Hz). MS m/z (relative intensity): 407 (M^+ − 15, 8.6%), 364 (5.5), 248 (24), 150 (93), 121 (100), 71 (84.5). Exact MS m/z Calcd for $C_{22}H_{31}O_7$ (M^+ − 15): 407.2070. Found: 407.2080. IR ν ($CHCl_3$) cm^{-1}: 1740 (shoulder), 1720, 1680 (CO).

Niddanolide Hemiacetal (5) A solution of **31** (0.34 g, 0.80 mmol) in 1 N HCl (2 ml) and THF (10 ml) was stirred at room temperature for 6 h. After neutralization with solid $NaHCO_3$, the reaction mixture was evaporated to dryness. CH_2Cl_2 (20 ml) and water (10 ml) were added to the residue, and the CH_2Cl_2 layer was separated. The aqueous layer was extracted with CH_2Cl_2, and the combined extracts were dried over $MgSO_4$. After evaporation of the solvent, purification of the residue on a silica gel column with hexane–EtOAc (1 : 1) as the eluant afforded **5** as colorless fine needles (256 mg, 85%), mp 188—189 °C. $[\alpha]_D^{16.5}$ +13.3° (c=1.07, $CHCl_3$). ^{1}H-NMR δ: 1.20 (0.34H, d, J=7.0 Hz), 1.21 (0.66H, d, J=7.0 Hz), 1.30 (3H, s), 1.33 (3H, s), 1.50—1.75 (2H, m), 1.80—2.00 (1H, m), 2.10 (1H, dd, J=13.0, 6.0 Hz), 2.18 (1H, dd, J=16.0, 1.5 Hz), 2.20—2.70 (2H, m), 2.80 (0.66H, dd, J=16.0, 8.5 Hz), 2.84 (0.34H, dd, J=16.0, 11.0 Hz), 3.31 (0.34H, dd, J=6.5, 1.0 Hz), 3.47—3.59 (1H, m), 3.52 (2H, s), 3.55 (1H, s), 3.65 (0.66H, dt, J=11.5, 1.5 Hz), 3.89 (0.66H, s), 3.95 (0.34H, s), 4.13 (1H, dd, J=7.0, 5.5 Hz), 4.40 (1H, dd, J=9.0, 3.5 Hz), 5.24 (1H, ddq, J=18.0, 3.0, 7.0 Hz), 5.46 (0.34H, dt, J=6.5, 2.0 Hz), 5.57 (0.66H, t, J=4.5 Hz), 6.00—6.20 (2H, m), 6.30 (0.34H, d, J=15.5 Hz), 6.34 (0.66H, d, J=15.5 Hz), 7.08 (0.34H, dd, J=15.5, 9.5 Hz), 7.16 (0.66H, dd, J=15.5, 9.5 Hz). MS m/z (relative intensity): 382 (M^+, 6%), 364 (10), 231 (16.5), 150 (94), 121 (100). Exact MS m/z Calcd for $C_{20}H_{30}O_7$ (M^+): 382.1992. Found: 382.1999. *Anal.* Calcd for $C_{20}H_{30}O_7$: C, 62.81; H, 7.91. Found: C, 62.65; H, 7.91. IR ν (neat) cm^{-1}: 3500 (OH), 1705, 1675 (CO). UV $\lambda_{max}^{ethanol}$ nm (log ε): 274 (4.28).

Niddanolide 4-Methoxybenzylacetal (33α, β) A solution of **5** (120 mg, 0.314 mmol) in CH_2Cl_2 (2 ml) was treated with 4-methoxybenzyl (MPM) alcohol (164 mg, 1.19 mmol) and CSA (7.3 mg, 10 mol%) at room temperature for 3 h. After neutralization with TEA (0.1 ml), the reaction mixture was concentrated *in vacuo*, and the residue was purified on a silica gel column with hexane–EtOAc (2 : 1) as the eluant to give **33β** as colorless prisms (97.5 mg, 62%), mp 161.5—163 °C. $[\alpha]_D^{24}$ +57.8° (c=0.95, $CHCl_3$). ^{1}H-NMR δ: 1.19 (3H, d, J=6.8 Hz), 1.32 (3H, d, J=6.2 Hz), 1.56 (1H, dd, J=14.5, 11.5 Hz), 1.90—2.05 (3H, m), 2.07 (1H, dd, J=16.2, 2.0 Hz), 2.16 (1H, ddd, J=14.2, 13.0, 9.5 Hz), 2.44 (1H, ddq, J=9.5, 2.5, 6.8 Hz), 2.54 (1H, ddd, J=13.0, 4.0, 2.5 Hz), 2.87 (1H, dd, J=16.5, 11.0 Hz), 3.06 (1H, dd, J=9.0, 1.0 Hz), 3.58 (3H, s), 3.67 (1H, dt, J=10.5, 1.5 Hz), 3.79 (3H, s), 4.34 (1H, dd, J=9.0, 3.0 Hz), 4.42 (1H, d, J=11.5 Hz), 4.70 (1H, d, J=11.5 Hz), 5.23 (1H, ddq, J=13.0, 2.5, 6.2 Hz), 5.24 (1H, dd, J=5.5, 3.5 Hz), 6.07 (1H, ddd, J=15.0, 9.5, 4.0 Hz), 6.15 (1H, dd, J=15.0, 9.5 Hz), 6.34 (1H, d, J=15.0 Hz), 6.84—6.89 (2H, m), 7.16 (1H, dd, J=15.0, 9.5 Hz), 7.24—7.29 (2H, m). MS m/z (relative intensity): 502 (M^+, 0.4%), 470 (0.2), 381 (1.4), 366 (2.5), 249 (4.2), 231 (11.2), 187 (2.2), 150 (5.0), 121 (100), 109 (6.0). Exact MS m/z Calcd for $C_{28}H_{38}O_8$ (M^+): 502.2567. Found: 502.2605. *Anal.* Calcd for $C_{28}H_{38}O_8$: C, 66.91; H, 7.62. Found: C, 66.78; H, 7.82. IR ν (neat) cm^{-1}: 3600 (OH), 1735, 1710, 1665 (CO), 1615, 1580, 1450, 1290, 1200, 1140. UV $\lambda_{max}^{ethanol}$ nm (log ε): 274 (4.34).

Continued elution provided **33α** as colorless prisms (49.5 mg, 31%), mp 141—142 °C. $[\alpha]_D^{27}$ +8.5° (c=1.3, $CHCl_3$). ^{1}H-NMR δ: 1.21 (3H, d, J=7.0 Hz), 1.32 (3H, d, J=6.5 Hz), 1.54 (1H, dd, J=12.0, 2.5 Hz), 1.77 (1H, ddd, J=12.0, 7.0, 5.0 Hz), 1.85 (1H, d, J=13.5 Hz), 1.91 (1H, ddd, J=13.0, 12.0, 2.5 Hz), 2.06—2.24 (1H, m), 2.16 (1H, dd, J=16.1, 1.5 Hz), 2.44 (1H, ddq, J=13.5, 2.5, 7.0 Hz), 2.53 (1H, dt, J=12.5, 3.0 Hz), 2.86 (1H, dd, J=16.1, 11.0 Hz), 3.08 (1H, d, J=9.5 Hz), 3.57 (3H, s), 3.65 (1H, d, J=11.0 Hz), 3.81 (3H, s), 4.13 (1H, dd, J=9.5, 4.0 Hz), 4.42 (1H, d, J=11.5 Hz), 4.72 (1H, d, J=11.5 Hz), 5.19 (1H, d, J=6.0 Hz), 5.21 (1H, m), 6.05 (1H, ddd, J=15.0, 10.0, 4.5 Hz), 6.14 (1H, dd, J=15.0, 10.0 Hz), 6.38 (1H, d, J=15.0 Hz), 6.84—6.90 (2H, m), 7.15 (1H, dd, J=15.0, 9.5 Hz), 7.21—7.28 (2H, m). MS m/z (relative intensity): 502 (M^+, 0.04%), 470 (0.1), 381 (0.8), 366 (5.2), 316 (2.3), 231 (7.7), 187 (2.7), 150 (8.1), 121 (100), 109 (7.7). Exact MS m/z Calcd for $C_{28}H_{38}O_8$ (M^+): 502.2567. Found: 502.2541. *Anal.* Calcd for $C_{28}H_{38}O_8$: C, 66.91; H, 7.62. Found: C, 66.72; H, 7.81. IR ν (neat) cm^{-1}: 3450 (OH), 1700, 1680 (CO), 1635 (C=C).

Carbonolide B 4-Methoxybenzylacetal (34α, β) A solution of **33β** (31 mg, 0.062 mmol) in a mixture of acetic anhydride (18 μl), Et_3N (77 μl), DMAP (1 mg), and CH_2Cl_2 (2 ml) was allowed to stand at room temperature for 3 h. The reaction mixture was diluted with CH_2Cl_2 and washed with saturated aqueous NH_4Cl, and brine, and dried over $MgSO_4$. The solvent was removed *in vacuo* and the residue was chromatographed on a silica gel column with AcOEt–hexane (1 : 2) as the eluant to give **34β** as colorless prisms (33.0 mg, 98%), mp 148.5—149 °C. **34β**: $[\alpha]_D^{24}$ +93.8° (c=0.82, $CHCl_3$). ^{1}H-NMR δ: 1.19 (3H, d, J=7.0 Hz), 1.28 (3H, d, J=6.5 Hz), 1.88—1.96 (1H, m), 2.03 (3H, ddd, J=11.0, 10.0, 5.2 Hz), 2.07 (3H, s), 2.19 (1H, ddd, J=13.2, 10.0, 5.2 Hz), 2.20 (1H, dd, J=14.5, 1.5 Hz), 2.51 (1H, dt, J=13.0, 3.7 Hz), 2.55 (1H, ddq, J=9.5, 2.8, 6.5 Hz), 2.97 (1H, dd, J=14.5, 11.5 Hz), 3.21 (1H, dd, J=9.0, 1.5 Hz), 3.61 (3H, s), 3.80 (3H, s), 3.96 (1H, dd, J=9.2, 3.5 Hz), 4.42 (1H, d, J=11.5 Hz), 4.68 (1H, d, J=11.5 Hz), 5.01 (1H, ddq, J=9.5, 2.8, 6.5 Hz), 5.06 (1H, dt, J=11.5, 1.5 Hz), 5.32 (1H, dd, J=6.0, 4.0 Hz), 6.07 (1H, ddd, J=15.0, 10.0, 4.0 Hz), 6.08 (1H, dd, J=15.0, 10.0 Hz), 6.31 (1H, d, J=15.5 Hz), 6.85—6.88 (2H, m), 7.25—7.28 (2H, m), 7.29 (1H, dd, J=15.5, 10.0 Hz). MS m/z (relative intensity): 544 (M^+, 0.2%), 423 (4.0), 408 (5.6), 249 (4.8), 231 (8.8), 121 (100). Exact MS m/z Calcd for $C_{30}H_{40}O_9$ (M^+): 544.2673. Found: 544.2661.

Similarly, **33α** (21 mg, 0.042 mmol) gave **34α** as a colorless oil (22.5 mg, 99%). **34α**: $[\alpha]_D^{24}$ +18.2° (c=0.85, $CHCl_3$). ^{1}H-NMR δ: 1.20 (3H, d, J=7.0 Hz), 1.27 (3H, d, J=6.5 Hz), 1.57 (1H, t, J=10.5 Hz), 1.83—1.86 (1H, m), 1.91 (1H, d, J=13.5 Hz), 1.99—2.10 (2H, m), 2.05 (3H, s), 2.185 (1H, ddd, J=13.5, 11.5, 8.5 Hz), 2.193 (1H, dd, J=15.0, 1.5 Hz), 2.52 (1H, dt, J=13.5, 3.8 Hz), 2.47—2.60 (1H, m), 2.97 (1H, dd, J=15.0, 11.0 Hz), 3.22 (1H, dd, J=9.5, 1.0 Hz), 3.59 (3H, s), 3.74 (1H, dd, J=9.7, 3.3 Hz), 3.81 (3H, s), 4.41 (1H, d, J=11.5 Hz), 4.69 (1H, d, J=11.5 Hz), 5.00 (1H, ddq, J=9.5, 3.0, 6.5 Hz), 5.03 (1H, dt, J=11.0, 1.0 Hz), 5.15 (1H, d,

J=6.0 Hz), 6.05 (1H, ddd, J=15.5, 10.5, 4.5 Hz), 6.18 (1H, dd, J=15.0, 10.0 Hz), 6.36 (1H, d, J=15.0 Hz), 6.85—6.88 (2H, m), 7.22—7.25 (2H, m), 7.26 (1H, dd, J=15.5, 10.0 Hz). MS m/z (relative intensity): 502 (M^+-32, 0.1%), 423 (1.0), 408 (4.0), 231 (6.7), 121 (100). IR ν (neat) cm^{-1}: 1740, 1730, 1680 (CO), 1630, 1600 (C=C).

Platenolide W_1 4-Methoxybenzylacetal (35α, β) A solution of **33β** (11 mg, 0.022 mmol) in a mixture of propionic anhydride (16 μl), Et_3N (46 μl) and CH_2Cl_2 (2 ml) was allowed to stand at room temperature for 3 h. The reaction mixture was diluted with CH_2Cl_2 and washed with saturated aqueous NH_4Cl, and brine, and dried over $MgSO_4$. The solvent was removed *in vacuo* and the residue was chromatographed on a silica gel column with AcOEt–hexane (1 : 2) as the eluant to give **35β** as a colorless oil (9.5 mg, 78%). **35β**: $[\alpha]_D^{21.5}$ +80.5° (c=0.38, $CHCl_3$). ^{1}H-NMR δ: 1.12 (3H, d, J=7.5 Hz), 1.18 (3H, d, J=7.0 Hz), 1.28 (3H, d, J=6.0 Hz), 1.60 (1H, dd, J=14.0, 9.0 Hz), 1.85—2.00 (1H, m), 2.07 (1H, dd, J=13.0, 6.0 Hz), 2.20 (1H, ddd, J=13.0, 10.5, 9.5 Hz), 2.21 (1H, dd, J=15.0, 1.5 Hz), 2.35 (1H, q, J=7.5 Hz), 2.36 (1H, q, J=7.5 Hz), 2.53—2.66 (1H, m), 2.96 (1H, dd, J=15.0, 11.0 Hz), 3.21 (1H, dd, J=9.5, 1.0 Hz), 3.581 (1H, m), 3.60 (3H, s), 3.80 (3H, s), 3.96 (1H, dd, J=9.5, 3.5 Hz), 4.42 (1H, d, J=11.5 Hz), 4.68 (1H, d, J=11.5 Hz), 4.99 (1H, m), 5.08 (1H, d, J=11.0 Hz), 5.21 (1H, dd, J=5.5, 4.2 Hz), 6.07 (1H, ddd, J=15.0, 9.5, 4.0 Hz), 6.19 (1H, dd, J=15.0, 10.0 Hz), 6.30 (1H, d, J=15.5 Hz), 6.86—6.88 (2H, m), 7.22—7.24 (2H, m), 7.29 (1H, dd, J=15.5, 10.0 Hz). MS m/z (relative intensity): 558 (M^+, 0.4%), 442 (4.7), 231 (10), 189 (5.7), 121 (100), 57 (12.8). Exact MS m/z Calcd for $C_{31}H_{42}O_6$ (M^+): 558.2829. Found: 558.2839. IR ν (neat) cm^{-1}: 1735, 1720, 1685 (CO), 1635 (C=C).

Similarly, **33α** (12.3 mg, 0.024 mmol) gave **35α** as a colorless oil (10.3 mg, 75%). **35α**: $[\alpha]_D^{21.5}$ +15.6° (c=0.41, $CHCl_3$). ^{1}H-NMR δ: 1.11 (3H, d, J=7.5 Hz), 1.20 (3H, d, J=7.5 Hz), 1.28 (3H, d, J=6.5 Hz), 1.55—1.64 (1H, m), 1.65—1.75 (1H, m), 1.82—1.88 (1H, m), 1.92 (1H, d, J=13.6 Hz), 2.04 (1H, m), 2.19 (1H, dd, J=15.0, 1.0 Hz), 2.32 (1H, q, J=7.5 Hz), 2.33 (1H, q, J=7.5 Hz), 2.51 (1H, dt, J=13.0, 3.5 Hz), 2.47—2.60 (1H, m), 2.97 (1H, dd, J=15.0, 11.5 Hz), 3.21 (1H, dd, J=9.5, 1.0 Hz), 3.581 (1H, dd, J=8.5, 2.5 Hz), 3.584 (3H, s), 3.73 (1H, dd, J=9.5, 3.0 Hz), 3.80 (3H, s), 4.40 (1H, d, J=11.5 Hz), 4.68 (1H, d, J=11.5 Hz), 4.97 (1H, m), 5.04 (1H, d, J=11.0 Hz), 5.14 (1H, d, J=6.0 Hz), 6.06 (1H, ddd, J=15.5, 9.5, 4.5 Hz), 6.18 (1H, dd, J=15.0, 10.0 Hz), 6.36 (1H, d, J=15.5 Hz), 6.86—6.88 (2H, m), 7.22—7.24 (2H, m), 7.27 (1H, dd, J=15.5, 10.0 Hz). MS m/z (relative intensity): 558 (M^+, 0.4%), 526 (0.42), 442 (0.42), 437 (6.0), 396 (5.3), 348 (14.9), 231 (44.2), 189 (36), 121 (100), 57 (99). Exact MS m/z Calcd for $C_{31}H_{42}O_6$ (M^+): 558.2829. Found: 558.2848. IR ν (neat) cm^{-1}: 1730, 1680 (CO), 1635 (C=C).

Carbonolide B Hemiacetal (1) A solution of **34α, β** (18.8 mg, 0.035 mmol) in trifluoroacetic acid (0.8 ml) and water (0.2 ml) was stirred at 0 °C for 15 min. After neutralization with saturated aqueous $NaHCO_3$, the reaction mixture was extracted with AcOEt three times, and the combined extracts were washed with brine, and dried over $MgSO_4$. After evaporation of the solvent, purification of the residue on a silica gel column with hexane–EtOAc (1 : 2) as the eluant afforded **1** as an amorphous solid (13.5 mg, 92%), mp 86—87.5 °C. $[\alpha]_D^{19}$ +44° (c=0.8, $CHCl_3$). ^{1}H-NMR δ: 1.21 (0.75H, d, J=7.0 Hz), 1.27 (0.25H, d, J=7.0 Hz), 1.29 (1H, d, J=6.5 Hz), 1.87 (1H, dd, J=13.0, 5.5 Hz), 1.94—2.03 (1H, m), 2.06 (0.25H, s), 2.08 (0.75H, s), 2.09—2.15 (1H, m), 2.20 (2H, d, J=14.0 Hz), 2.25—2.35 (1H, m), 2.51 (1H, ddd, J=14.0, 3.5, 2.8 Hz), 2.53—2.65 (1H, m), 2.89 (0.25H, dd, J=15.0, 11.0 Hz), 2.95 (0.75H, dd, J=15.0, 11.0 Hz), 3.17 (0.75H, d, J=9.5 Hz), 3.24 (0.25H, dd, J=8.0, 1.0 Hz), 3.55 (0.7H, s), 3.57 (0.3H, s), 3.78 (0.3H, dd, J=7.5, 4.5 Hz), 4.03 (0.67H, dd, J=9.5, 3.2 Hz), 4.55—5.09 (1H, m), 5.04 (0.7H, d, J=10.5 Hz), 5.15 (0.3H, ddd, J=10.5, 2.5, 1.0 Hz), 5.44 (0.3H, dd, J=6.2, 1.8 Hz), 5.57 (0.7H, t, J=5.0 Hz), 6.10 (1H, d, J=15.0 Hz), 6.18 (1H, d, J=15.0 Hz), 6.33 (1H, d, J=15.5 Hz), 7.22 (0.3H, dd, J=15.5, 10.0 Hz), 7.28 (0.7H, dd, J=15.5, 10.0 Hz). MS m/z (relative intensity): 424 (M^+, 3%), 406 (3.4), 248 (6.4), 231 (8.5), 175 (6.4), 150 (20), 121 (56), 98 (30), 71 (43), 43 (100). Exact MS m/z Calcd for $C_{22}H_{32}O_8$ (M^+): 424.2088. Found: 424.2098. IR ν (neat) cm^{-1}: 3425, 1740, 1730, 1680, 1640, 1600, 1450, 1370, 1310, 1240, 1120.

Platenolide W_1 Hemiacetal (6) A solution of **35α, β** (9.1 mg, 0.016 mmol) in trifluoroacetic acid (0.8 ml) and water (0.2 ml) was stirred at 0°C for 15 min. After neutralization with saturated aqueous $NaHCO_3$, the reaction mixture was extracted with AcOEt three times, and the combined extracts were washed with brine and dried over $MgSO_4$. After evaporation of the solvent, purification of the residue on a silica gel column with hexane–EtOAc (1 : 2) as the eluant afforded **6** as an amorphous solid (6.8 mg, 97%), mp 84.5—86 °C. $[\alpha]_D^{19}$ +41.5° (c=0.68, $CHCl_3$). ^{1}H-NMR δ: 1.12 (0.9H, d, J=7.5 Hz), 1.13 (2.1H, d, J=7.5 Hz), 1.20 (3H, d, J=7.0 Hz), 1.26 (0.9H, d, J=6.0 Hz), 1.28 (2.1H, d, J=6.0 Hz), 1.55—1.75 (2H, m), 1.80—1.89 (1H, m), 1.95—2.05 (1H, m), 2.10—2.16 (0.3H, m), 2.21 (1H, dd, J=13.5, 2.0 Hz), 2.45 (2H, dq, J=2.5, 7.5 Hz), 2.51 (1H, ddd, J=13.5, 4.7, 3.0 Hz), 2.60 (0.7H, dt, J=6.5, 2.5 Hz), 2.63 (0.3H, t, J=6.2 Hz), 2.88 (0.3H, dd, J=15.5, 9.5 Hz), 2.94 (0.7H, dd, J=15.0, 11.5 Hz), 3.18 (0.7H, dd, J=9.5, 1.2 Hz), 3.27 (0.3H, dd, J=7.5, 3.0 Hz), 3.55 (2H, s), 3.57 (1H, s), 3.79 (0.3H, dd, J=7.5, 5.0 Hz), 4.02 (0.7H, dd, J=9.5, 3.5 Hz), 4.93—5.06 (1H, m), 5.05 (0.7H, dt, J=11.2, 1.8 Hz), 5.18 (0.3H, ddd, J=9.5, 3.5, 2.0 Hz), 5.43 (0.3H, dd, J=6.5, 1.5 Hz), 5.56 (0.7H, t, J=5.0 Hz), 6.08 (1H, ddd, J=15.5, 10.0, 4.5 Hz), 6.19 (1H, dd, J=15.5, 9.5 Hz), 6.31 (1H, d, J=15.5 Hz), 7.21 (0.3H, dd, J=15.5, 10.0 Hz), 7.35 (0.7H, dd, J=15.5, 10.0 Hz). MS m/z (relative intensity): 438 (M^+, 6.4%), 420 (10), 248 (11), 231 (19), 189 (10.6), 150 (35), 121 (72), 57 (100). Exact MS m/z Calcd for $C_{23}H_{32}O_8$ (M^+): 438.2254. Found: 438.2229. IR ν (neat) cm^{-1}: 1735, 1680, 1640.

Carbonolide A 4-Methoxybenzylacetal (36) MCPBA (27 mg, 0.16 mmol; 85% purity) and $NaHCO_3$ (10 mg) were added to a stirred solution of **34β** (24 mg, 0.044 mmol) in CH_2Cl_2 (2 ml) at room temperature. After 8 h, the reaction mixture was poured into saturated aqueous NH_4Cl solution and extracted with CH_2Cl_2. The extract was washed with brine, dried over $MgSO_4$, and evaporated *in vacuo* to leave an oil, which was chromatographed on a silica gel column with EtOAc–hexane (1 : 2) as the eluant to give the epoxide (**36β**) as a colorless viscous oil (22.2 mg, 90%). **36β**: $[\alpha]_D^{1.2}$ +52.1° (c=1.12, $CHCl_3$). ^{1}H-NMR δ: 1.23 (3H, d, J=7.0 Hz), 1.28 (3H, d, J=6.2 Hz), 1.35 (1H, dd, J=10.7, 6.9 Hz), 1.38 (1H, ddd, J=14.3, 12.1, 9.0 Hz), 1.54 (1H, t, J=12.2 Hz), 1.71 (1H, m), 1.88 (1H, m), 1.91 (1H, ddd, J=6.2, 4.6, 0.7 Hz), 2.01 (3H, s), 2.03 (1H, m), 2.29 (1H, dt, J=14.0, 2.3 Hz), 2.30 (1H, dd, J=13.0, 2.7 Hz), 2.48 (1H, ddq, J=11.3, 3.5, 7.0 Hz), 2.98 (1H, dd, J=13.0, 12.0 Hz), 3.14 (1H, dt, J=9.8, 1.8 Hz), 3.20 (1H, dd, J=9.2, 1.8 Hz), 3.22 (1H, dd, J=9.8, 1.4 Hz), 3.63 (3H, s), 3.80 (3H, s), 4.02 (1H, dd, J=9.3, 3.7 Hz), 4.44 (1H, d, J=11.5 Hz), 4.69 (1H, d, J=11.5 Hz), 4.93 (1H, ddq, J=12.1, 2.7, 6.1 Hz), 4.98 (1H, ddd, J=11.7, 2.2, 1.7 Hz), 5.23 (1H, dd, J=5.5, 4.5 Hz), 6.61 (1H, dd, J=16.0, 9.5 Hz), 6.74 (1H, d, J=16.0 Hz), 6.86—6.89 (2H, m), 7.25—7.28 (2H, m). MS m/z (relative intensity): 560 (M^+, 0.56%), 528 (0.43), 439 (3.6), 424 (0.7), 248 (1.9), 175 (16), 163 (5.2), 143 (5.2), 121 (100), 109 (7.3). Exact MS m/z Calcd for $C_{30}H_{40}O_{10}$ (M^+): 560.2621. Found: 560.2602. IR ν (neat) cm^{-1}: 1730, 1690, 1630, 1615.

Similarly, **34α** (14 mg, 0.02 mmol) gave **36α** as a colorless viscous oil (12.0 mg, 83%). **36α**: ^{1}H-NMR δ: 1.23 (3H, d, J=7.0 Hz), 1.28 (3H, d, J=6.2 Hz), 1.40 (1H, dt, J=12.5, 2.5 Hz), 1.46 (1H, t, J=12.5 Hz), 1.89—2.10 (3H, m), 1.99 (3H, s), 2.30 (1H, m), 2.31 (1H, dd, J=13.0, 2.2 Hz), 2.50 (1H, m), 2.97 (1H, dd, J=12.5, 12.0 Hz), 3.16 (1H, dt, J=9.8, 1.8 Hz), 3.21 (1H, dd, J=9.2, 1.8 Hz), 3.24 (1H, dd, J=9.8, 0.5 Hz), 3.61 (3H, s), 3.81 (1H, dd, J=9.0, 4.0 Hz), 3.81 (3H, s), 4.42 (1H, d, J=11.5 Hz), 4.70 (1H, d, J=11.5 Hz), 4.93 (1H, ddq, J=12.0, 3.0, 6.5 Hz), 4.99 (1H, dt, J=11.7, 2.2, 1.7 Hz), 5.16 (1H, d, J=5.5 Hz), 6.58 (1H, dd, J=15.5, 8.8 Hz), 6.77 (1H, d, J=15.5 Hz), 6.86—6.89 (2H, m), 7.22—7.25 (2H, m). MS m/z (relative intensity): 560 (M^+, 4.4%), 528 (1.6), 439 (15), 423 (5.2), 175 (19), 121 (100). Exact MS m/z Calcd for $C_{30}H_{40}O_{10}$ (M^+): 560.2621. Found: 560.2629. UV $\lambda_{max}^{ethanol}$ nm ($\log\varepsilon$): 224 (4.08).

EOP Aglycon 4-Methoxybenzylacetal (37β) MCPBA (10.7 mg, 0.06 mmol; 85% purity) and $NaHCO_3$ (6 mg) were added to a stirred solution of **35β** (8 mg, 0.014 mmol) in CH_2Cl_2 (1 ml) at room temperature. After 9 h, the reaction mixture was diluted with CH_2Cl_2, washed with saturated aqueous $NaHCO_3$ and brine, and dried over $MgSO_4$. The solvent was removed *in vacuo* to leave an oil, which was chromatographed on a silica gel column with AcOEt–hexane (1 : 2) as the eluant to give the epoxide (**37β**) as an oil (6.0 mg, 73%). **37β**: $[\alpha]_D^{21.5}$ +52.0° (c=0.70, $CHCl_3$). ^{1}H-NMR δ: 1.06 (3H, t, J=7.2 Hz), 1.22 (3H, d, J=7.0 Hz), 1.27 (3H, d, J=6.5 Hz), 1.34 (1H, dd, J=11.5, 7.0 Hz), 1.40 (1H, ddd, J=14.2, 12.0, 10.0 Hz), 1.63—1.74 (1H, m), 1.85—1.95 (1H, m), 2.06 (1H, dd, J=14.0, 6.0 Hz), 2.28 (1H, q, J=7.2 Hz), 2.29 (1H, q, J=7.2 Hz), 2.31 (1H, dd, J=12.5, 2.3 Hz), 2.31—2.42 (1H, m), 2.97 (1H, dd, J=12.5, 11.5 Hz), 3.19 (1H, dd, J=9.0, 2.0 Hz), 3.22 (1H, dd, J=9.2, 2.0 Hz), 3.24 (1H, dd, J=9.5, 1.4 Hz), 3.63 (3H, s), 3.80 (3H, s), 4.02 (1H, dd, J=9.5, 3.5 Hz), 4.43 (1H, d, J=11.0 Hz), 4.68 (1H, d, J=11.0 Hz), 4.90 (1H, ddq, J=12.5, 3.0, 6.5 Hz), 5.02 (1H, ddd, J=10.5, 3.0, 1.5 Hz), 5.25 (1H, dd, J=6.0, 4.5 Hz), 6.61 (1H, dd, J=15.5, 8.5 Hz), 6.74 (1H, d, J=15.5 Hz), 6.86—6.89 (2H, m), 7.24—7.28 (2H, m). MS m/z (relative intensity): 574 (M^+, 0.35%) 542 (0.21), 500 (0.15), 453 (3.3), 437 (1.5), 420 (0.72), 247 (2.7), 189 (15.6), 157 (4.6), 137 (6.7), 121 (100), 109 (10.4), 57 (19). Exact MS m/z Calcd for $C_{31}H_{42}O_{10}$ (M^+): 574.2778. Found: 574.2766. IR ν (neat) cm^{-1}: 1740, 1730, 1695 (CO), 1635, 1620 (C=C).

Carbonolide A Hemiacetal (2) DDQ (37 mg, 0.156 mmol) was added to a stirred solution of **36α, β** (22.6 mg, 0.04 mmol) in a mixture of CH_2Cl_2

and H_2O (20 : 1, 1.0 ml) at room temperature. After 1 h, the reaction mixture was poured into aqueous $NaHCO_3$ solution and extracted with CH_2Cl_2. The extract was washed with brine, dried over anhydrous $MgSO_4$, and evaporated *in vacuo* to leave an oil, which was chromatograhed on a silica gel column using EtOAc–hexane (1 : 1) as the eluant to give **2** as an amorphous solid (14.0 mg, 80%), mp 82.5—84 °C. $[\alpha]_D^{19}$ +15° (c=0.81, $CHCl_3$). ^{1}H-NMR δ: 1.25 (3H, d, J=7.0 Hz), 1.28 (3H, d, J=7.3 Hz), 1.36—1.43 (1H, m), 1.70—1.76 (0.7H, m), 1.77—1.84 (0.7H, m), 1.82 (1H, dd, J=6.0, 4.5 Hz), 1.83 (0.3H, dd, J=6.0, 4.5 Hz), 1.87 (0.3H, dd, J=6.0, 4.5 Hz), 2.00 (0.3H, s), 2.02 (0.7H, s), 2.12 (0.3H, dd, J=13.5, 5.5 Hz), 2.13 (0.7H, dd, J=13.5, 5.5 Hz), 2.30 (0.7H, dd, J=13.0, 2.8 Hz), 2.37 (0.3H, dd, J=8.0, 3.5 Hz), 2.45—2.63 (1H, m), 2.93 (0.3H, dd, J=13.0, 10.5 Hz), 2.94 (0.7H, dd, J=12.5, 11.7 Hz), 3.14 (0.3H, dt, J=13.0, 10.5 Hz), 3.20 (0.7H, dd, J=9.0, 1.5 Hz), 3.22 (0.7H, dd, J=9.0, 2.0 Hz), 3.27 (0.3H, dd, J=9.0, 2.0 Hz), 3.57 (0.7H, s), 3.60 (0.3H, s), 3.74 (0.3H, dd, J=9.0, 4.5 Hz), 3.78 (0.7H, dd, J=9.0, 4.5 Hz), 4.09 (0.7H, dd, J=9.5, 4.0 Hz), 4.11 (0.3H, t, J=7.0 Hz), 4.90—5.05 (1H, m), 4.98 (1H, ddd, J=10.5, 2.5, 1.5 Hz), 5.48 (0.3H, dd, J=6.0, 1.5 Hz), 5.59 (0.7H, dd, J=6.0, 4.0 Hz), 6.58 (0.3H, dd, J=16.0, 9.0 Hz), 6.60 (0.7H, dd, J=16.0, 9.0 Hz), 6.75 (0.3H, d, J=16.0 Hz), 6.76 (0.7H, d, J=16.0 Hz). MS m/z (relative intensity): 440 (M^+, 2.6%), 422 (4.5), 380 (5.2), 368 (4.2), 256 (24), 236 (21), 216 (99), 171 (32), 149 (61), 57 (100). Exact MS m/z Calcd for $C_{22}H_{32}O_9$ (M^+): 440.2047. Found: 440.2069. IR ν (neat) cm^{-1}: 1735, 1705, 1680.

EOP Aglycon Hemiacetal (7) DDQ (7 mg, 0.03 mmol) was added to a stirred solution of **37**α,β (6.0 mg, 0.01 mmol) in a mixture of CH_2Cl_2 and H_2O (20 : 1, 0.5 ml) at room temperature. After 50 min, the reaction mixture was poured into aqueous $NaHCO_3$ solution, and extracted with CH_2Cl_2. The extract was washed with brine, dried over anhydrous $MgSO_4$, and evaporated *in vacuo* to leave an oil, which was chromatographed on a silica gel column using EtOAc–hexane (2 : 1) as the eluant to give **7** as an amorphous solid (3.9 mg, 83%), mp 75—76 °C. $[\alpha]_D^{18.5}$ +12.6° (c=0.31, $CHCl_3$). ^{1}H-NMR δ: 1.07 (2.1H, t, J=7.0 Hz), 1.16 (0.9H, t, J=7.0 Hz), 1.25 (3H, d, J=7.3 Hz), 1.27 (3H, d, J=6.3 Hz), 1.40 (1H, dt, J=11.5, 2.0 Hz), 1.52 (1H, t, J=13.0 Hz), 1.61—1.74 (1H, m), 1.79—1.91 (1H, m), 2.13 (1H, dd, J=13.0, 6.0 Hz), 2.29 (1H, q, J=7.0 Hz), 2.30 (1H, q, J=7.0 Hz), 2.47—2.66 (1H, m), 2.91 (0.3H, dd, J=13.2, 11.2 Hz), 2.95 (0.7H, t, J=13.2 Hz), 3.11—3.27 (2H, m), 3.56 (2.1H, s), 3.59 (0.9H, s), 3.78 (0.3H, dd, J=9.0, 5.0 Hz), 4.10 (1H, dd, J=10.0, 4.0 Hz), 4.20—4.30 (0.3H, m), 4.47 (0.3H, J=9.5, 8.5 Hz), 4.86—4.98 (1H, m), 4.99 (0.7H, ddd, J=11.5, 3.0, 1.5 Hz), 5.06 (0.3H, ddd, J=11.5, 3.0, 2.5 Hz), 5.48 (0.3H, dd, J=5.5, 0.5 Hz), 5.58 (0.7H, dd, J=5.5, 4.0 Hz), 6.59 (0.3H, dd, J=15.5, 8.5 Hz), 6.62 (0.7H, dd, J=15.5, 8.5 Hz), 6.69 (0.7H, d, J=15.5 Hz), 6.70 (0.3H, d, J=15.5 Hz). MS m/z (relative intensity): 436 (M^+, 3.1%), 380 (3.5), 265 (1.7), 253 (2.3), 247 (4.4), 203 (4.4), 189 (8.5), 177 (4.6), 161 (8.3), 149 (11), 139 (8.3), 121 (21), 108 (73), 98 (72), 95 (31), 81 (31), 71 (57), 57 (100), 44 (85). Exact MS m/z Calcd for $C_{23}H_{32}O_8$: 436.2097. Found: 436.2079. IR ν (neat) cm^{-1}: 1740, 1705, 1680, 1625.

Crystal Structure of 34β Colorless prisms of **34**β were mounted on a Rigaku AFC-5 diffractometer and exposed to graphite monochromated Cu K_α radiation. The unit cell parameters are a=19.259(5)A, b=15.370(5)A, and c=10.022(3)A in space group $p2_12_12_1$ (z=4). Of the 2821 reflections measured with a $2\theta/\omega$ scan, 2274 were independently observed at the level of $F \geq 3(F)$. The structure was solved by MULTAN78[29] and refined by using the block-diagonal least-squares method with anisotropic temperature factors for non-hydrogen atoms. All hydrogen atoms were located from the difference Fourier map and refined with isotropic temperature factors. The final R factor was 0.056. Calculations were carried out with the DIRECT-SEARCH program system.[30] Four tables consisting of atomic fractional coordinates, bond lengths, and bond angles have been deposited as supplementary materials.

References and Notes

1) Chiral Synthesis of Polyketide-Derived Natural Products. XXXIV. For part XXXIII. see: I. Noda, K. Horita, Y. Oikawa and O. Yonemitsu, *Tetrahedron Lett.*, **31**, 6035 (1990).
2) S. Omura, "Macrolide Antibiotics," Academic Press, Orlando, Florida, 1984.
3) *a*) Y. Oikawa, T. Tanaka, and O. Yonemitsu, *Tetrahedron Lett.*, **27**, 3647 (1986); *b*) T. Tanaka, N. Nakajima, T. Hamada, and O. Yonemitsu, *Chem. Pharm. Bull.*, **35**, 2203 (1987).
4) *a*) N. Nakajima, T. Hamada, T. Tanaka, Y. Oikawa, and O. Yonemitsu, *J. Am. Chem. Soc.*, **108**, 4645 (1986); *b*) N. Nakajima, T. Hamada, Y. Oikawa, and O. Yonemitsu, *Chem. Pharm. Bull.*, **35**, 2228 (1987).
5) *a*) T. Tanaka, Y. Oikawa, T. Hamada, and O. Yonemitsu, *Tetrahedron Lett.*, **27**, 3651 (1986); *b*) *Idem*, *Chem. Pharm. Bull.*, **35**, 2209, 2219 (1987).
6) *a*) Y. Oikawa, T. Yoshioka, and O. Yonemitsu, *Tetrahedron Lett.*, **33**, 885, 889 (1982); *b*) Y. Oikawa, T. Tanaka, and O. Yonemitsu, *ibid.*, **25**, 5393 (1984); *c*) Y. Oikawa, T. Tanaka, K. Horita, and O. Yonemistu, *ibid.*, **25**, 5397 (1984); *d*) K. Horita, T. Yoshioka, T. Tanaka, Y. Oikawa, and O. Yonemitsu, *Tetrahedron*, **42**, 3021 (1986); *e*) N. Nakajima, R. Abe, K. Horita, and O. Yonemitsu, *Tetrahedron Lett.*, **29**, 4139 (1988).
7) *a*) K. C. Nicolaou, S. P. Seitz, and M. R. Pavia, *J. Am. Chem. Soc.*, **104**, 2030 (1982); *b*) W. C. Still and V. J. Novack, *ibid.*, **106**, 1148 (1984); *c*) P. A. Aristoff, *J. Org. Chem.*, **46**, 1954 (1981).
8) *a*) K. Tatsuta, Y. Amemiya, S. Maniwa, and M. Kinoshita, *Tetrahedron Lett.*, **21**, 2837 (1980); *b*) K. C. Nicolaou, S. P. Seitz, and M. P. Pavia, *J. Am. Chem. Soc.*, **103**, 1222 (1981).
9) Niddamycin: G. Huber, K. Wallhausser, L. Fries, A. Steigler, and H. Weidenmuller, *Arzneim.-Forsch.*, **12**, 1191 (1962).
10) Platenomycin W_1: A. Kinumaki, I. Takamori, Y. Sugawara, Y. Seki, M. Suzuki, and T. Okuda, *J. Antibiot.*, **27**, 117 (1974).
11) Carbomycin A: R. B. Woodward, L. S. Weiler, and P. C. Dutta, *J. Am. Chem. Soc.*, **87**, 4662 (1965).
12) EOP: M. Suzuki, T. Furumaki, K. Takeda, and T. Setoguchi, Japan. Kokai 48-10, 288 (1973) [*Chem. Abstr.*, **78**, 134495*j* (1973)].
13) The first syntheses of **2**, **5**, **6**, and **7** have been completed in this work.
14) Unless otherwise noted, the numberings are based on those of **1**—**7**.
15) *a*) S. Masamune, H. P. Ma, J. W. Ellingboe, and Y. Ito, *J. Org. Chem.*, **49**, 2873 (1984); *b*) *Cf.* Y. Guindon, Y. C. Yoakim, M. A. Bernstein, and H. E. Monton, *Tetrahedron Lett.*, **26**, 1185 (1985).
16) Based on the numbering of D-glucose.
17) In an attempt to increase the stereoselectivity of the catalytic hydrogenation of the C7–C8 double bond, the lactone (**21**) was converted to the lactolide (**23**), but the result was still unsatisfactory.
18) *a*) H. Sakurai, *Pure Appl. Chem.*, **54**, 1 (1982); *b*) A. Hosomi and H. Sakurai, *Tetrahedron Lett.*, **17**, 1295 (1976).
19) *a*) Y. Yamamoto, H. Yatagai, Y. Naruta, and K. Maruyama, *J. Am. Chem. Soc.*, **102**, 7107 (1980); *b*) Y. Yamamoto, H. Yatagai, Y. Ishihara, N. Maeda, and K. Maruyama, *Tetrahedron*, **40**, 2239 (1984); *c*) G. E. Keck and D. E. Abbot, *Tetrahedron Lett.*, **25**, 1879 (1984).
20) R. U. Lemieux and E. von Rudloff, *Can. J. Chem.*, **30**, 1701, 1710 (1955).
21) J. Inanaga, K. Hirata, H. Saeki, T. Katsuki, and M. Yamaguchi, *Bull. Chem. Soc. Jpn.*, **52**, 1989 (1979).
22) Niddanolide (**5**), carbonolide B (**1**), and platenolide W_1 (**6**) are 2 : 1, 3 : 1, and 2.3 : 1 isomeric mixtures, respectively, with respect to the hemiacetal position.
23) W. C. Still, *J. Am. Chem. Soc.*, **101**, 2493 (1979); *b*) T. Takahashi, H. Nemoto, Y. Kanda, and J. Tuji, *Tetrahedron*, **43**, 5520 (1987).
24) There are two precedents for the epoxidation of similar 16-membered dienones. 3-Deoxyrosaranolide[25a] and rosaranolide[25b] were stereoselectively synthesized from the corresponding dienones by MCPBA oxidation.
25) *a*) W. C. Still and V. J. Novack, *J. Am. Chem. Soc.*, **106**, 1148 (1984); *b*) R. H. Schlessinger, M. A. Poss, and S. Richardson, *ibid.*, **108**, 3112 (1986).
26) For solution conformation studies in macrocyclic systems: *a*) A. B. Smith, III, J. L. Wood, C. J. Rizzo, G. T. Furst, P. J. Carroll, J. Donhue, and S. Omura, *J. Org. Chem.*, **55**, 1133 (1990); *b*) J. R. Everrett and J. W. Tyler, *J. Chem. Soc., Perkin Trans. 2*, **1987**, 1659; *c*) S. K. Arora and A. M. Kook, *J. Org. Chem.*, **52**, 1530 (1987); *d*) L. Cellai, S. Cerrini, A. Serge, M. Brufani, W. Fedli, and A. Vaciago, *ibid.*, **47**, 2652 (1982).
27) The structure of the C9—C13 dienone is 9,10-*s-cis*, 10,11-*trans*, 11,12-*s-trans*, and 12,13-*trans*.
28) Both carbonolide A (**2**) and EOP aglycon (**7**) are 2.5 : 1 isomeric mixtures with respect to the hemiacetal position.
29) P. Main, S. E. Hull, L. Lessinger, G. Germain, J.-P. Declercq, and M. M. Woolfson, MULTAN-78, A System of Computer Programs for the Automatic Solution of Crystal Structures from X-ray Diffraction Data, University of York, England and Louvain, Belgium, 1978.
30) Y. Koyama and K. Okada, *Acta Crystallogr., Sect. A*, **31**, S18 (1975).

Quinolizidines. XXVIII.[1] Racemic and Chiral Syntheses of Ochromianine, an Indoloquinolizidine Alkaloid from *Neisosperma miana*

Tozo FUJII,* Masashi OHBA, Takeshi TACHINAMI, and Takako OHASHI

Faculty of Pharmaceutical Sciences, Kanazawa University, Takara-machi, Kanazawa 920, Japan. *Received July 17, 1990*

A full account is given of the first racemic and chiral syntheses of 11-methoxydihydrocorynantheol [(−)-1], a candidate structure for the *Neisosperma* alkaloid ochromianine. Coupling of (±)-*trans*-6-ethoxy-3-ethyl-2,3,4,5-tetrahydro-4-pyridineacetic acid ethyl ester [(±)-6] with 2-chloro-1-(6-methoxy-1*H*-indol-3-yl)ethanone (4) in the presence of KBr produced the lactam ketone (±)-7, which was then converted into the lactam (±)-9 through the oxazolium salt (±)-8. Bischler–Napieralski cyclization of (±)-9 followed by catalytic hydrogenation gave the tetracyclic ester (±)-11. On reduction with $LiAlH_4$, (±)-11 yielded the racemic target (±)-1. A parallel synthetic route starting from (+)-6 and 4 afforded the chiral target (−)-1 *via* (+)-7, 8, (+)-9, and (−)-11. Identity of synthetic (−)-1 with ochromianine unequivocally established the structure and absolute stereochemistry of this alkaloid.

Keywords *Neisosperma* alkaloid; ochromianine; 11-methoxydihydrocorynantheol; indoloquinolizidine alkaloid synthesis; chiral synthesis; lactim ether alkylation; keto amide cyclization; oxazolium salt reduction; Bischler–Napieralski cyclization; hydride reduction

In 1974, Koch and co-workers[2] reported the isolation of (−)-ochromianine, a new *Corynanthe*-type indoloquinolizidine alkaloid, from the bark of a New Caledonian plant named *Ochrosia miana* H. BN. ex GUILL. (family Apocynaceae) at that time. The name of the plant was later revised to *Neisosperma miana* (BAILLON ex-WHITE) BOITEAU.[3] The French group deduced the structure and absolute configuration of (−)-ochromianine to be (−)-**1**[4] on the basis of spectral analysis as well as chiroptical and biosynthetic rationales.[2] Now the correctness of this structure assignment has been confirmed by us as a result of the following racemic and chiral syntheses of the candidate structure **1**. A brief account of the results reported here has been published in a preliminary form.[3b]

In designing synthetic routes to (±)-**1** and (−)-**1**, our recent racemic and chiral syntheses of ochropposinine (**2**),[1,5] a structurally analogous alkaloid from *Neisosperma* and *Ochrosia* plants,[6] through the "lactim ether route"[7-9] were reliable guides, generating 10-demethoxy versions as shown in Chart 1. Thus, 3-chloroacetyl-6-methoxyindole (**4**), a precursor of rings A, B, and C in **1**, was first prepared from 6-methoxyindole (**3**)[10] in 50% yield according to a general 3-chloroacetylation procedure[11] using chloroacetyl chloride and pyridine in toluene (55—60 °C, 2 h). This

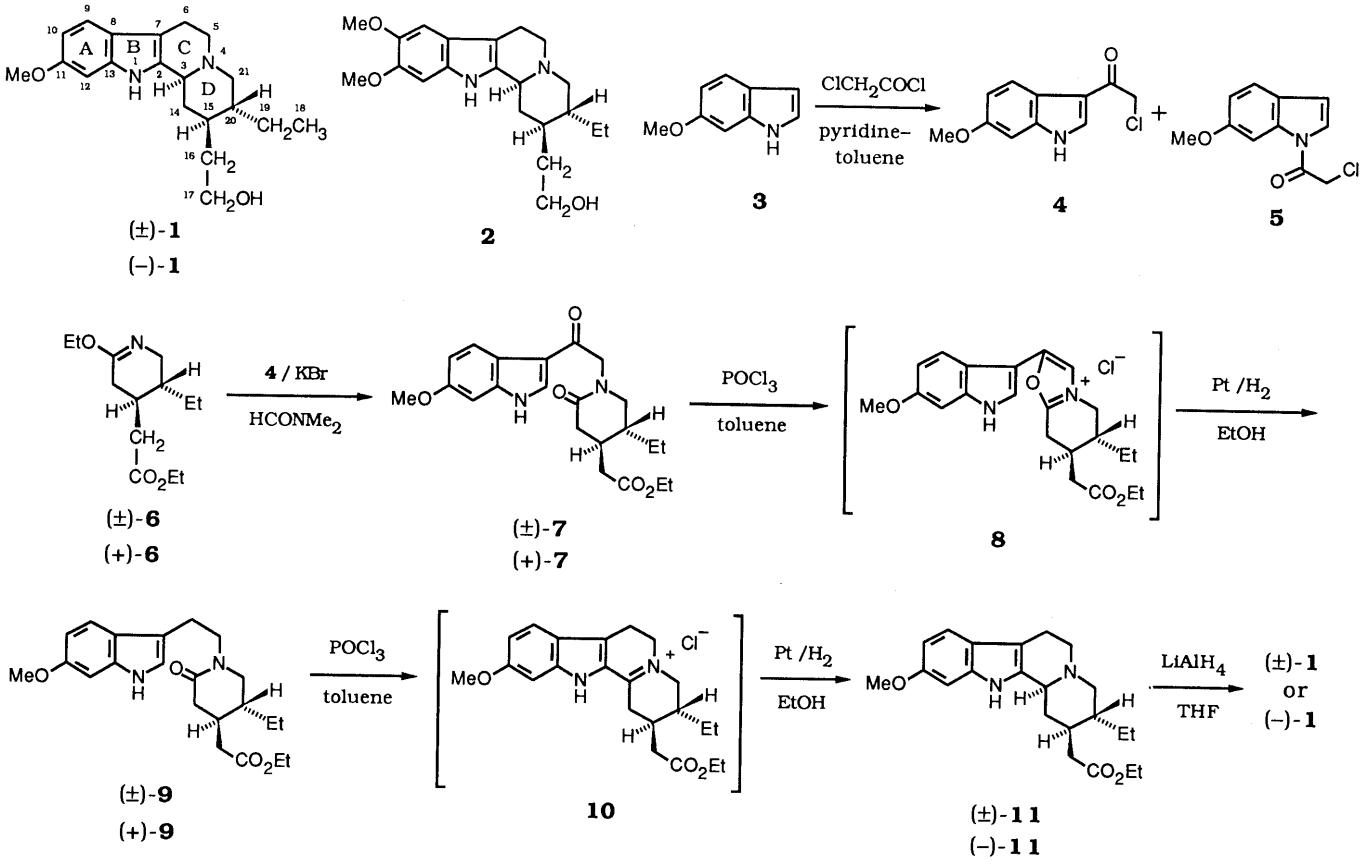

Chart 1

3-acylation was accompanied with the formation of a small amount (2% yield) of the 1-acylated derivative **5**, as anticipated.[1,5,11]

The racemic synthesis of the candidate structure **1** started with coupling of the lactim ether (±)-**6**[12] (a precursor of ring D) with **4** in $HCONMe_2$ in the presence of KBr at 58 °C for 48 h, which produced the lactam ketone (±)-**7** in 61% yield. For reduction of the ketonic group of (±)-**7** to the corresponding methylene group, we followed the lead of the oxazole method that had been successfully applied to analogous structures.[1,5,13] Thus, (±)-**7** was treated with $POCl_3$ in boiling toluene for 2 h, and the crude product, presumed to be the oxazolium salt (±)-**8**, was reduced by catalytic hydrogenation (Pt/H_2, EtOH, 1 atm, room temperature, 2 h) to give the lactam (±)-**9** in 55% overall yield [from (±)-**7**]. Conversion of (±)-**9** into the tetracyclic ester (±)-**11** through the quaternary iminium salt (±)-**10** was effected in 87% overall yield by means of Bischler–Napieralski cyclization ($POCl_3$, boiling toluene, 2 h) followed by catalytic hydrogenation (Pt/H_2, EtOH, 1 atm, room temperature, 4 h). The hydrogen at C(3) was assigned the α configuration by analogy with catalytic hydrogenation of similar systems,[14] and the correctness of this assignment was supported by the appearance of absorption bands assignable to a *trans*-quinolizidine ring[15] in the infrared (IR) spectrum of (±)-**11** in $CHCl_3$. On reduction with $LiAlH_4$ in tetrahydrofuran (THF) at room temperature for 1 h, (±)-**11** afforded the target alcohol (±)-**1** in 90% yield. Although no sample of natural (−)-ochromianine was available for a direct comparison, the ultraviolet (UV) (in EtOH), IR (in $CHCl_3$), proton nuclear magnetic resonance (^{1}H-NMR) (in $CDCl_3$), and mass spectra (MS) of (±)-**1** were found to be virtually identical with those obtained previously with a natural sample. Accordingly, the structure and relative stereochemistry of this alkaloid have been unequivocally established as **1** or its mirror image.

For the chiral synthesis of (−)-**1**, a parallel sequence of conversions starting with the lactim ether (+)-**6**[8b,16] was followed (Chart 1). Treatment of (+)-**6** with **4** in $HCONMe_2$ in the presence of KBr at 60 °C for 72 h provided the lactam ketone (+)-**7** in 75% yield. Cyclization of (+)-**7** with $POCl_3$ and catalytic hydrogenation of the resulting crude oxazolium salt **8** gave the lactam (+)-**9** in 67% yield [from (+)-**7**]. On Bischler–Napieralski cyclization followed by catalytic hydrogenation, (+)-**9** afforded the tetracyclic ester (−)-**11** *via* the iminium salt **10** in 91% overall yield. Finally, $LiAlH_4$ reduction of (−)-**11** in THF produced the desired alcohol (−)-**1** in 87% yield. The UV, IR, and ^{1}H-NMR spectra and MS of the synthetic (−)-**1** were virtually identical with those of natural (−)-ochromianine, and the chiral identity of (−)-**1** with the alkaloid was shown by the same sign of their specific rotations and by their virtually identical circular dichroism (CD) spectra.

In conclusion, the structure of the *Neisosperma* alkaloid (−)-ochromianine has now been established as 11-methoxydihydrocorynantheol [(−)-**1**] as a result of the above racemic and chiral syntheses of **1**. These syntheses represent new additions to the range[9] of the synthesis of indoloquinolizidine alkaloids by the "lactim ether route",[7,8] which remains the best available vehicle for unified racemic and chiral syntheses of the benzo[*a*]quinolizidine-type *Alangium* alkaloids.[7]

Experimental

General Notes All melting points were taken on a Yamato MP-1 capillary melting point apparatus and are corrected. Unless otherwise stated, the organic solutions obtained after extraction were dried over anhydrous Na_2SO_4 and concentrated under reduced pressure. Thin-layer chromatography (TLC) was developed on Merck silica gel 60 F_{254} plates (0.25-mm thickness) or Merck aluminum oxide F_{254} (type E) plates (0.25 mm), and spots were detected by means of UV absorbance measurement (at 254 nm) and/or by spraying with the standard $KMnO_4$ or I_2–KI reagent. Flash chromatography[17] was carried out by using Merck silica gel 60 (No. 9385). See ref. 1 for details of instrumentation and measurements. Elemental analyses were performed by Mr. Y. Itatani and his associates at Kanazawa University. The following abbreviations are used: br = broad, d = doublet, dd = doublet-of-doublets, m = multiplet, q = quartet, s = singlet, sh = shoulder, t = triplet.

2-Chloro-1-(6-methoxy-1*H*-indol-3-yl)ethanone (4) and 1-(Chloroacetyl)-6-methoxy-1*H*-indole (5) A stirred mixture of 6-methoxyindole (**3**)[10] (3.97 g, 27 mmol) and pyridine (4.27 g, 54 mmol) in dry toluene (60 ml) was kept at 55—60 °C in an atmosphere of N_2, and a solution of chloroacetyl chloride (6.10 g, 54 mmol) in dry toluene (12 ml) was added dropwise over a period of 40 min. The resulting mixture was stirred at the same temperature for 2 h and then cooled to deposit a dark oil. The oil was separated from the toluene layer, washed with three 5-ml portions of toluene, and triturated with MeOH. The precipitate that resulted was filtered off to give **4** (3.02 g, 50%) as a brown solid, mp 224.5—225.5 °C (dec.). Recrystallization from $CHCl_3$–EtOH (1 : 1, v/v) yielded an analytical sample of **4** as colorless prisms, mp 250—252 °C (dec.); MS *m/z*: 225, 223 (M^+); UV λ_{max}^{EtOH} 242 nm (ε 12500), 281 (12600), 309 (9170); IR ν_{max}^{Nujol} cm^{-1}: 3180 (NH), 1628 (CO); ^{1}H-NMR (Me_2SO-d_6) δ: 3.79 (3H, s, OMe), 4.82 (2H, s, $COCH_2Cl$), 6.85 [1H, dd, *J* = 8.5, 2 Hz, C(5′)-H], 6.97 [1H, d, *J* = 2 Hz, C(7′)-H], 8.00 [1H, d, *J* = 8.5 Hz, C(4′)-H], 8.30 [1H, d, *J* = 3 Hz, C(2′)-H], 11.91 (1H, br, NH).[18] *Anal.* Calcd for $C_{11}H_{10}ClNO_2$: C, 59.07; H, 4.51; N, 6.26. Found: C, 59.00; H, 4.47; N, 6.26.

The above toluene layer, obtained from the reaction mixture by decantation, was concentrated *in vacuo*, and the residue was dissolved in $CHCl_3$–EtOH (10 : 1, v/v) (120 ml). The resulting solution was washed successively with H_2O, saturated aqueous $NaHCO_3$, and saturated aqueous NaCl, dried, and concentrated to leave a brown oil. Purification of the oil by flash chromatography[17] using CH_2Cl_2 as the eluent gave **5** (105 mg, 2%) as a yellowish solid, mp 98—100.5 °C. Recrystallization from MeOH produced an analytical sample of **5** as a colorless fluff, mp 111—111.5 °C; MS *m/z*: 225, 223 (M^+); UV λ_{max}^{EtOH} 252 nm (ε 21800), 275 (sh) (8720); IR ν_{max}^{Nujol} 1722 cm^{-1} (CO); ^{1}H-NMR (Me_2SO-d_6) δ: 3.81 (3H, s, OMe), 5.08 (2H, s, $COCH_2Cl$), 6.71 [1H, d, *J* = 4 Hz, C(3)-H], 6.93 [1H, dd, *J* = 8.5, 2 Hz, C(5)-H], 7.52 [1H, d, *J* = 8.5 Hz, C(4)-H], 7.71 [1H, d, *J* = 4 Hz, C(2)-H], 7.91 [1H, d, *J* = 2 Hz, C(7)-H]. *Anal.* Calcd for $C_{11}H_{10}ClNO_2$: C, 59.07; H, 4.51; N, 6.26. Found: C, 58.92; H, 4.51; N, 6.38.

(±)-*trans*-1-[2-(6-Methoxy-1*H*-indol-3-yl)-2-oxoethyl]-5-ethyl-2-oxo-4-piperidineacetic Acid Ethyl Ester [(±)-7] A mixture of (±)-**6**[12] (1.25 g, 5.2 mmol), **4** (1.23 g, 5.5 mmol), and KBr (1.62 g, 13.6 mmol) in $HCONMe_2$ (8 ml) was stirred at 58 °C for 48 h. After cooling, the reaction mixture was diluted with H_2O (40 ml) and extracted with CH_2Cl_2. The CH_2Cl_2 extracts were combined and washed successively with saturated aqueous $NaHCO_3$ and H_2O, then dried, and concentrated to leave an orange oil. The oil was dissolved in AcOEt (15 ml), and the resulting solution was kept at 4 °C for 2 h. The precipitate that resulted was filtered off to give a first crop (1.06 g) of (±)-**7** as a pale yellowish solid, mp 141—143 °C. The filtrate was concentrated *in vacuo*, and the residual oil was purified by column chromatography (silica gel, AcOEt) to yield a second crop (0.21 g) of (±)-**7**, mp 145—147 °C. The total yield of (±)-**7** was 1.27 g (61%). Recrystallization of the crude (±)-**7** from AcOEt furnished an analytical sample as a colorless solid, mp 147.5—149 °C; MS *m/z*: 400 (M^+); UV λ_{max}^{EtOH} 241 nm (ε 15600), 280 (13300), 370 (sh) (9260); IR ν_{max}^{Nujol} cm^{-1}: 3170 (NH), 1722 (ester CO), 1656 (ArCO), 1610 (lactam CO); ^{1}H-NMR ($CDCl_3$) δ: 0.93 (3H, t, *J* = 7.5 Hz, $CCH_2\underline{Me}$), 1.27 (3H, t, *J* = 7 Hz, $OCH_2\underline{Me}$), 3.80 (3H, s, OMe), 4.15 (2H, q, *J* = 7 Hz, $O\underline{CH_2}Me$), 4.43 (2H, s, $ArCO\underline{CH_2}N$), 6.83 [1H, d, *J* = 2.5 Hz, C(7′)-H], 6.86 [1H, dd, *J* = 9, 2.5 Hz, C(5′)-H], 7.62 [1H, d, *J* = 3 Hz, C(2′)-H], 8.08 [1H, d, *J* = 9 Hz, C(4′)-H], 9.80 (1H, br, NH).[18] *Anal.* Calcd for $C_{22}H_{28}N_2O_5$: C, 65.98; H, 7.05; N, 7.00. Found: C, 65.82; H, 7.11; N, 6.85.

(4*R*,5*R*)-1-[2-(6-Methoxy-1*H*-indol-3-yl)-2-oxoethyl]-5-ethyl-2-oxo-4-piperidineacetic Acid Ethyl Ester [(+)-7] A mixture of (+)-**6**[8b,16]

(1.13 g, 4.7 mmol), **4** (1.10 g, 4.9 mmol), and KBr (1.44 g, 12.1 mmol) in $HCONMe_2$ (9 ml) was stirred at 60 °C in an atmosphere of N_2 for 72 h. Work-up of the reaction mixture was similar to the first half of that described above for (±)-**7**, giving a reddish brown oil (1.98 g). Purification of the oil by flash chromatography[17] (AcOEt) gave (+)-**7** (1.41 g, 75%) as a reddish brown glass, which crystallized from AcOEt–hexane (1 : 1, v/v). Recrystallization from the same solvent system yielded an analytical sample as colorless prisms, mp 98.5—100.5 °C; $[\alpha]_D^{21}$ +34.5° (*c* = 0.50, EtOH); MS *m/z*: 400 (M^+); IR $\nu_{max}^{CHCl_3}$ cm^{-1}: 3460 (free NH), 3215 (associated NH), 1728 (ester CO), 1660 (ArCO), 1628 (lactam CO). *Anal.* Calcd for $C_{22}H_{28}N_2O_5$: C, 65.98; H, 7.05; N, 7.00. Found: C, 66.13; H, 7.14; N, 6.80. The IR ($CHCl_3$), UV (EtOH), and ^{1}H-NMR ($CDCl_3$) spectra and TLC mobility of this sample were idential with those of (±)-**7**.

(±)-*trans*-1-[2-(6-Methoxy-1*H*-indol-3-yl)ethyl]-5-ethyl-2-oxo-4-piperidineacetic Acid Ethyl Ester [(±)-9] A mixture of (±)-**7** (443 mg, 1.1 mmol) and $POCl_3$ (3.40 g, 22.2 mmol) in dry toluene (30 ml) was heated under reflux in an atmosphere of N_2 for 2 h. After cooling, the precipitate that resulted was filtered off, washed successively with hexane (10 ml) and ether (10 ml), and dried to afford a grayish solid (486 mg), presumed to be (±)-**8**. The solid was dissolved in EtOH (40 ml), and the ethanolic solution was hydrogenated over Adams catalyst (90 mg) at atmospheric pressure and room temperature for 2 h. The catalyst was removed by filtration, and the filtrate was concentrated *in vacuo*. The residue was then partitioned by extraction with a mixture of aqueous $NaHCO_3$ and CH_2Cl_2. The CH_2Cl_2 extracts were washed successively with H_2O and saturated aqueous NaCl, dried, and concentrated to leave a brown oil (323 mg). Purification of the oil by flash chromatography[17] [AcOEt–hexane (5 : 1, v/v)] furnished (±)-**9** [235 mg, 55% overall yield from (±)-**7**] as a brown solid. Recrystallization from AcOEt–hexane (1 : 1, v/v) gave an analytical sample as faintly brownish pillars, mp 98—99.5 °C; MS *m/z*: 386 (M^+); UV λ_{max}^{EtOH} 225 nm (ε 34900), 266 (sh) (3550), 275 (4180), 294 (4920); IR $\nu_{max}^{CHCl_3}$ cm^{-1}: 3490 (free NH), 3295 (associated NH), 1728 (ester CO), 1628 (lactam CO); ^{1}H-NMR ($CDCl_3$) δ: 0.77 (3H, t, *J* = 7 Hz, $CCH_2\underline{Me}$), 1.26 (3H, t, *J* = 7 Hz, $OCH_2\underline{Me}$), 3.84 (3H, s, OMe), 4.13 (2H, q, *J* = 7 Hz, $OC\underline{H}_2Me$), 6.79 [1H, dd, *J* = 8.5, 2 Hz, C(5′)-H], 6.85 [1H, d, *J* = 2 Hz, C(7′)-H], 6.93 [1H, d, *J* = 2 Hz, C(2′)-H], 7.52 [1H, d, *J* = 8.5 Hz, C(4′)-H], 7.89 (1H, br, NH).[18] *Anal.* Calcd for $C_{22}H_{30}N_2O_4$: C, 68.37; H, 7.82; N, 7.25. Found: C, 68.38; H, 7.96; N, 7.37.

(4*R*,5*R*)-1-[2-(6-Methoxy-1*H*-indol-3-yl)ethyl]-5-ethyl-2-oxo-4-piperidineacetic Acid Ethyl Ester [(+)-9] A mixture of (+)-**7** (1.69 g, 4.2 mmol) and $POCl_3$ (12.9 g, 84.1 mmol) in dry toluene (105 ml) was heated under reflux in an atmosphere of N_2 for 2 h. Work-up of the reaction mixture, catalytic hydrogenation [Adams catalyst (330 mg), 1 atm, room temperature, 3 h] of the resulting crude **10** (2.28 g) in EtOH (170 ml), and flash chromatography[17] [AcOEt–hexane (5 : 1, v/v)] of the hydrogenated product were carried out in a manner similar to that described above for (±)-**9**, giving (+)-**9** [1.09 g, 67% overall yield from (+)-**7**] as a reddish brown solid. Recrystallization from AcOEt–hexane (1 : 2, v/v) provided an analytical sample as faintly brownish pillars, mp 81.5—82.5 °C; $[\alpha]_D^{19}$ +77.6° (*c* = 0.50, EtOH); MS *m/z*: 386 (M^+). *Anal.* Calcd for $C_{22}H_{30}N_2O_4$: C, 68.37; H, 7.82; N, 7.25. Found: C, 68.41; H, 8.03; N, 7.48. The IR ($CHCl_3$), UV (EtOH), and ^{1}H-NMR ($CDCl_3$) spectra and TLC behavior of this sample were identical with those of (±)-**9**.

(±)-11-Methoxycorynan-17-oic Acid Ethyl Ester [(±)-11] A mixture of (±)-**9** (485 mg, 1.25 mmol) and $POCl_3$ (1.15 g, 7.5 mmol) in dry toluene (7 ml) was heated under reflux in an atmosphere of N_2 for 2 h. After cooling, the reaction mixture was concentrated *in vacuo*, and the residue was partitioned by extraction with a mixture of $CHCl_3$ and H_2O. The $CHCl_3$ extracts were washed with saturated aqueous NaCl, dried, and concentrated to leave crude (±)-**10** (516 mg) as a yellow glass. The glass was dissolved in EtOH (60 ml), and the solution was hydrogenated over Adams catalyst (60 mg) at atmospheric pressure and room temperature for 4 h. The catalyst was removed by filtration, and the filtrate was concentrated *in vacuo* to leave a solid, which was dissolved in H_2O (120 ml). The resulting aqueous solution was made alkaline with 10% aqueous Na_2CO_3 and then extracted with benzene. The benzene extracts were combined, washed with H_2O, dried, and concentrated to leave a brown oil (444 mg). Purification of the oil by flash chromatography[17] [AcOEt–hexane (1 : 1, v/v)] gave (±)-**11** [403 mg, 87% overall yield from (±)-**9**] as a yellow solid. Recrystallization from AcOEt–hexane (1 : 4, v/v) furnished an analytical sample as colorless needles, mp 120—124 °C; MS *m/z*: 370 (M^+); UV λ_{max}^{EtOH} 228 nm (ε 35300), 270 (4790), 298 (6170); IR $\nu_{max}^{CHCl_3}$ cm^{-1}: 3490 (free NH), 3390 (associated NH), 2840, 2810, 2760 (*trans*-quinolizidine ring[15]), 1725 (ester CO); ^{1}H-NMR ($CDCl_3$) δ: 0.92 (3H, t, *J* = 6.5 Hz, $CCH_2\underline{Me}$), 1.29 (3H, t, *J* = 7 Hz, $OCH_2\underline{Me}$), 3.83 (3H, s, OMe), 4.18 (2H, q, *J* = 7 Hz, $OC\underline{H}_2Me$), 6.74 [1H, dd, *J* = 8.5, 2 Hz, C(10)-H], 6.81 [1H, d, *J* = 2 Hz, C(12)-H], 7.33 [1H, d, *J* = 8.5 Hz, C(9)-H], 7.65 (1H, br, NH). *Anal.* Calcd for $C_{22}H_{30}N_2O_3$: C, 71.32; H, 8.16; N, 7.56. Found: C, 71.07; H, 8.24; N, 7.78.

11-Methoxycorynan-17-oic Acid Ethyl Ester [(−)-11] Cyclization of (+)-**9** (1.07 g, 2.8 mmol) was carried out [$POCl_3$ (2.55 g, 16.6 mmol), dry toluene (15 ml), 1 h] as described above for (±)-**11**, affording **10** (1.20 g) as a yellowish brown solid. Catalytic hydrogenation of the total amount of **10** in EtOH (130 ml) [Adams catalyst (130 mg), 1 atm, room temperature, 1 h] and work-up of the reaction mixture were also effected as described above for (±)-**11**, giving (−)-**11** [930 mg, 91% overall yield from (+)-**9**] as a yellowish solid, mp 106.5—107.5 °C. Recrystallization of the solid from AcOEt–hexane (1 : 4, v/v) produced an analytical sample as colorless needles, mp 106.5—108.5 °C; $[\alpha]_D^{22}$ −22.1° (*c* = 0.50, EtOH); MS *m/z*: 370 (M^+). *Anal.* Calcd for $C_{22}H_{30}N_2O_3$: C, 71.32; H, 8.16; N, 7.56. Found: C, 71.22; H, 8.31; N, 7.61. The IR ($CHCl_3$), UV (EtOH), and ^{1}H-NMR ($CDCl_3$) spectra and TLC mobility of this sample were identical with those of (±)-**11**.

(±)-11-Methoxycorynan-17-ol [(±)-11-Methoxydihydrocorynantheol] [(±)-1] A solution of (±)-**11** (111 mg, 0.3 mmol) in dry tetrahydrofuran (THF) (2 ml) was added dropwise to a stirred, ice-cooled suspension of $LiAlH_4$ (34.4 mg, 0.91 mmol) in THF (3 ml) over a period of 15 min. After the resulting mixture had been stirred at room temperature for 1 h, THF (2 ml), H_2O (0.08 ml), 10% aqueous NaOH (0.08 ml), and H_2O (0.16 ml) were added in that order under ice-cooling. Stirring was continued at room temperature for 30 min, and the insoluble material that resulted was filtered off and washed with THF (20 ml). The filtrate and washings were combined, dried over anhydrous K_2CO_3, and concentrated to leave a yellow glass. Purification of the glass by flash chromatography[17] [AcOEt–EtOH (20 : 1, v/v)] yielded (±)-**1** (88.8 mg, 90%) as a yellowish solid. Recrystallization from AcOEt gave an analytical sample as colorless needles, mp 174—176 °C (dec.); MS *m/z* (relative intensity): 329 ($M^+ + 1$) (39), 328 (M^+) (100), 327 (100), 326 (8), 299 (9), 283 (17), 281 (7), 255 (31), 214 (11), 201 (9), 200 (44), 199 (23), 186 (16), 174 (8); UV λ_{max}^{EtOH} 228 nm (ε 37100), 270 (4840), 298 (6180); IR ν_{max}^{KBr} cm^{-1}: 3430 (NH), 3245 (NH, OH), 2860, 2810, 2760 (*trans*-quinolizidine ring[15]); $\nu_{max}^{CHCl_3}$ cm^{-1}: 3635 (free OH), 3490 (free NH), 3285 (associated NH and OH), 2810, 2760 (*trans*-quinolizidine ring[15]); ^{1}H-NMR ($CDCl_3$) δ: 0.90 (3H, t, *J* = 6.5 Hz, $CCH_2\underline{Me}$), 1.95 (1H, br, $CH_2O\underline{H}$), 3.65—3.85 (2H, m, $C\underline{H}_2OH$), 3.82 (3H, s, OMe), 6.74 [1H, dd, *J* = 8.5, 2 Hz, C(10)-H], 6.82 [1H, d, *J* = 2 Hz, C(12)-H], 7.32 [1H, d, *J* = 8.5 Hz, C(9)-H], 7.92 (1H, br, NH). *Anal.* Calcd for $C_{20}H_{28}N_2O_2$: C, 73.14; H, 8.59; N, 8.53. Found: C, 73.02; H, 8.81; N, 8.53. The IR ($CHCl_3$), UV (EtOH), and ^{1}H-NMR ($CDCl_3$) spectra and MS of this sample were virtually identical with those[19] of natural (−)-ochromianine.[2]

11-Methoxycorynan-17-ol (11-Methoxydihydrocorynantheol) [(−)-1] Reduction of the tetracyclic ester (−)-**11** (371 mg, 1 mmol) with $LiAlH_4$ (113 mg, 3 mmol) [THF (16 ml), room temperature, 1 h], work-up of the reaction mixture, and purification of the crude product were effected as described above for the racemic series, yielding (−)-**1** (287 mg, 87%) as a yellow solid. Recrystallization of the solid from AcOEt gave an analytical sample as yellowish needles, mp 162—169 °C (dec.); MS *m/z*: 328 (M^+); $[\alpha]_D^{25}$ −28.0° (*c* = 1.00, EtOH); $[\alpha]_{577}^{25}$ −29.8° (*c* = 1.00, EtOH); CD (*c* = 1.22 × 10^{-4} M, EtOH) [θ]^{23} (nm): +2620 (304) (pos. max.), +660 (285) (neg. max.), +3770 (273) (pos. max.), +1640 (254) (neg. max.), +16500 (238) (pos. max.). *Anal.* Calcd for $C_{20}H_{28}N_2O_2$: C, 73.14; H, 8.59; N, 8.53. Found: C, 72.94; H, 8.80; N, 8.45. The MS, IR ($CHCl_3$), UV (EtOH), and ^{1}H-NMR ($CDCl_3$) spectra and TLC mobility of this sample were identical with those of (±)-**1**. The synthetic (−)-**1** was virtually identical (by comparison of the above spectra, CD spectrum, and specific rotation) with natural (−)-ochromianine [$[\alpha]_{578}^{20}$ −15° (*c* = 1, EtOH)].[2,19,20]

Acknowledgment This work was sponsored in part by the Ministry of Education, Science and Culture, Japan, under a Grant-in-Aid for Scientific Research (C) (No. 58570869) and by the Japan Research Foundation for Optically Active Compounds. We also wish to express our appreciation to Professor Michel Koch (Université René Descartes) for his invaluable help in making a comparison between the natural and synthetic alkaloids.

References and Notes

1) Paper XXVII in this series, T. Fujii, M. Ohba, T. Tachinami, and H. Miyajima, *Chem. Pharm. Bull.*, **38**, 1200 (1990).
2) *a*) N. Preaux, M. Koch, and M. Plat, *Phytochemistry*, **13**, 2607 (1974); *b*) N. Preaux, Ph. D. Thesis, Université Pierre et Marie Curie–Paris

VI, June 1976.
3) *a*) F. R. Forsberg, P. Boiteau, and M.-H. Sachet, *Adansonia Ser. 2*, **17**, 23 (1977); *b*) T. Fujii, M. Ohba, T. Tachinami, T. Ohashi, M. Koch, and E. Seguin, *Heterocycles*, **29**, 1037 (1989).
4) Unless otherwise noted, the structural formulas of optically active compounds in this paper represent their absolute configurations.
5) T. Fujii, M. Ohba, T. Tachinami, H. Miyajima, M. Koch, and E. Seguin, *Heterocycles*, **24**, 1215 (1986).
6) *a*) N. Peube-Locou, M. Koch, M. Plat, and P. Potier, *Ann. Pharm. Fr.*, **30**, 821 (1972); *b*) *Idem, Phytochemistry*, **11**, 2109 (1972); *c*) A. S. Amarasekera and L. S. R. Arambewela, *Fitoterapia*, **57**, 55 (1986); *d*) A. A. L. Gunatilaka, H. C. Fernando, Atta-ur-Rahman, M. M. Qureshi, and S. Balasubramaniam, *Heterocycles*, **28**, 999 (1989); *e*) E. Seguin, M. Koch, and T. Sevenet, *J. Nat. Prod.*, **45**, 738 (1982); *f*) E. Seguin, F. Hotellier, M. Koch, and T. Sevenet, *ibid.*, **47**, 687 (1984); *g*) J. Bruneton, T. Sevenet, and A. Cavé, *Phytochemistry*, **11**, 3073 (1972); *h*) A. Ahond, H. Fernandez, M. Julia-Moore, C. Poupat, V. Sánchez, P. Potier, S. K. Kan, and T. Sévenet, *J. Nat. Prod.*, **44**, 193 (1981).
7) For reviews, see *a*) T. Fujii and M. Ohba, "The Alkaloids," Vol. XXII, ed. by A. Brossi, Academic Press, New York, 1983, Chapter 1; *b*) T. Fujii, *Yakugaku Zasshi*, **103**, 257 (1983); *c*) T. Fujii, M. Ohba, and S. Yoshifuji, *Heterocycles*, **27**, 1009 (1988).
8) *a*) T. Fujii, M. Ohba, K. Yoneyama, H. Kizu, and S. Yoshifuji, *Chem. Pharm. Bull.*, **34**, 669 (1986); *b*) T. Fujii, M. Ohba, K. Shimohata, and S. Yoshifuji, *Heterocycles*, **26**, 2949 (1987).
9) For the "lactim ether route" leading to the indolo[2,3-*a*]quinolizidine system, see *a*) T. Fujii, S. Yoshifuji, and H. Ito, *Heterocycles*, **7**, 149 (1977); *b*) *Idem, Chem. Pharm. Bull.*, **36**, 3348 (1988); *c*) T. R. Govindachari and S. Rajeswari, *Indian J. Chem.*, **22B**, 531 (1983); *d*) Refs. 1 and 5.
10) *a*) R. B. Woodward, F. E. Bader, H. Bickel, A. J. Frey, and R. W. Kierstead, *Tetrahedron*, **2**, 1 (1958); *b*) S. Raucher and G. A. Koolpe, *J. Org. Chem.*, **48**, 2066 (1983); *c*) P. L. Feldman and H. Rapoport, *Synthesis*, **1986**, 735.
11) J. Bergman, J.-E. Bäckvall, and J.-O. Lindström, *Tetrahedron*, **29**, 971 (1973).
12) *a*) T. Fujii and S. Yoshifuji, *Chem. Pharm. Bull.*, **27**, 1486 (1979); *b*) J. Gutzwiller, G. Pizzolato, and M. R. Uskoković, *Helv. Chim. Acta*, **64**, 1663 (1981).
13) *a*) P. C. Young and R. Robinson, *J. Chem. Soc.*, **1933**, 275; *b*) A. P. Kozikowski and A. Ames, *J. Org. Chem.*, **45**, 2548 (1980).
14) E. E. van Tamelen and J. B. Hester, Jr., *J. Am. Chem. Soc.*, **91**, 7342 (1969).
15) *a*) E. Wenkert and D. K. Roychaudhuri, *J. Am. Chem. Soc.*, **78**, 6417 (1956); *b*) F. Bohlmann, *Chem. Ber.*, **91**, 2157 (1958).
16) T. Fujii, M. Ohba, K. Yoneyama, and H. Kizu, *Chem. Pharm. Bull.*, **33**, 358 (1985).
17) W. C. Still, M. Kahn, and A. Mitra, *J. Org. Chem.*, **43**, 2923 (1978).
18) For convenience, each position of the indole ring is indicated by a primed number.
19) The log ε value (2.65) at λ_{max} 268 nm reported in ref. 2*a* for the UV spectrum of natural (−)-ochromianine in EtOH is apparently too small. For a correct value, see Fig. 28 in ref. 2*b*, p. 93.
20) The previously published values[2)] for $\Delta\varepsilon$ in the CD spectrum of natural (−)-ochromianine are apparently about 5 times as large as those of the synthetic (−)-**1**. According to a personal communication from Professor M. Koch (Université René Descartes) in February 1989, their published values were incorrect, most probably due to a transcription or calculation error.

Synthesis of Mutagenic Amino-α-carbolines AαC and MeAαC by the Thermal Electrocyclic Reaction of 2-Azahexa-1,3,5-triene Intermediates

Satoshi HIBINO,* Eiichi SUGINO, Takeshi KUWADA, Naoki OGURA, Yohko SHINTANI and Kohichi SATOH

Faculty of Pharmacy & Pharmaceutical Sciences, Fukuyama University, 985 Higashimura, Fukuyama, Hiroshima 729–02, Japan. *Received August 13, 1990*

The potent mutagens, 2-amino-9*H*-pyrido[2,3-*b*]indole (AαC) and 2-amino-3-methyl-9*H*-pyrido[2,3-*b*]indole (MeAαC) were synthesized by the thermal electrocyclic reaction of 2-azahexa-1,3,5-triene intermediates.

Keywords mutagen; α-carboline; synthesis; AαC; MeAαC; iminophosphorane; aza-Wittig reaction; electrocyclic reaction; 2-azahexa-1,3,5-triene

The potent mutagens, 2-amino-9*H*-pyrido[2,3-*b*]indole (**1a**: AαC) and 2-amino-3-methyl-9*H*-pyrido[2,3-*b*]indole (**1b**: MeAαC) were isolated from pyrolysates of protein and of tryptophan as a result of extensive research on environmental mutagens and carcinogens, and their structures were determined by X-ray analysis.[1] Syntheses of these α-carbolines have been reported by Matsumoto and co-workers.[2]

We are currently interested in the synthesis of condensed heteroaromatic compounds, especially fused pyridine ring systems, by the thermal electrocyclic reaction of monoazahexa-1,3,5-triene systems including one double bond of the aromatic or heteroaromatic.[3] We describe here the synthesis of AαC (**1a**) and MeAαC (**1b**) as an application of this methodology to the α-carboline framework.

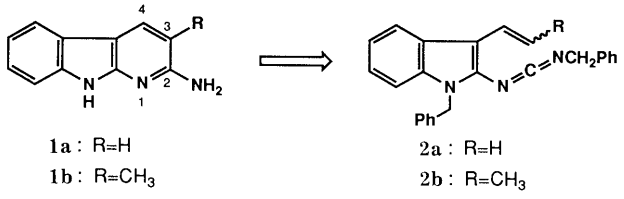

Chart 1

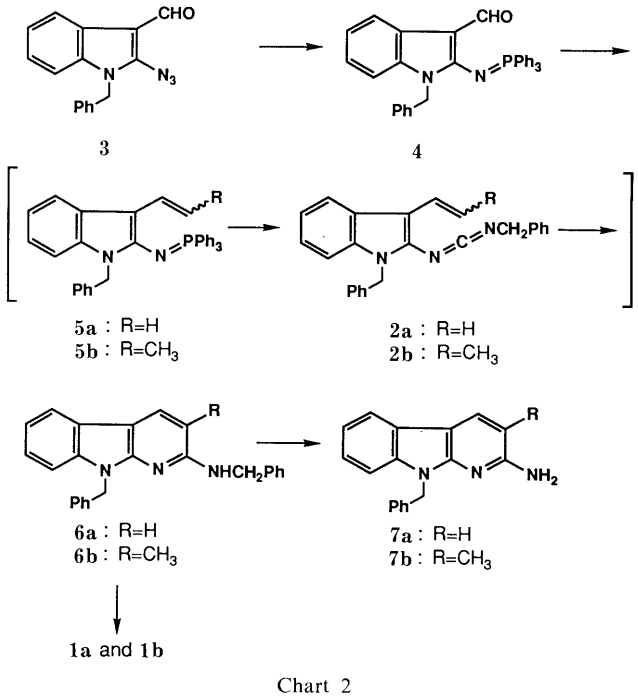

Chart 2

As shown in the retrosynthetic pathway (Chart 1), 3-alkenylindole-2-carbodiimide derivatives (**2**) derived from the cleavage of the 2,3-bond of **1**, that is, a 2-azahexa-1,3,5-triene system, were chosen as the key intermediates in this study.

We started from the readily available 2-azido-1-benzylindole-3-carboxaldehyde (**3**)[4] as follows (Chart 2). Treatment of the azide (**3**) with triphenylphosphine at room temperature gave the iminophosphorane (**4**) in 76.2% yield. Wittig reaction of the iminophosphorane (**4**) with methylenetriphenylphosphorane or ethylenetriphenylphosphorane in tetrahydrofuran (THF) at 0 °C led to the corresponding 3-alkenylindole-iminophosphoranes (**5**). After the solvent had been changed to toluene, the addition of benzylisocyanate followed by heating at 120 °C (external) gave the desired α-carbolines (**6**) in 77.5% (**6a**) and 71.3% (**6b**) yields from **4**, respectively. It seems that the conversion of **4** into **6** involves initial Witting reaction followed by aza-Wittig reaction[5] to give a carbodiimide (**2**) as a highly reactive 2-azahexa-1,3,5-triene intermediate, which readily undergoes electrocyclic ring closure followed by 1,3-hydrogen shift to give the α-carboline (**6**) as expected.

The protected α-carboline (**6**) was submitted to hydrogenolysis over 10% Pd–C/H_2 or 5% Pt–C/H_2 in acetic acid at room temperature. However, the desired AαC (**1a**) and MeAαC (**1b**) were not obtained, but instead the monodebenzylated compounds (**7a**) and (**7b**) were obtained in good yields, respectively. It was found that selective cleavage of the benzyl group occurred at the amino group at the 2-position. This was confirmed by the disappearance of the broad singlet (2H) at δ 4.55 or δ 4.77 due to methylene protons of the benzylamino group at the 2-position in the nuclear magnetic resonance (NMR) spectra of the dibenzyl compounds (**6a** and **6b**) and the appearance of a D_2O exchangeable signal (2H) at δ 4.50 or δ 4.17 due to the amino group at the 2-position in the NMR spectra of the monobenzyl compounds (**7a** and **7b**), respectively.

Our attention was then turned to the Lewis acid-catalyzed debenzylation of *N*-benzylindoles developed by Murakami and co-workers.[6] Treatment of the dibenzyl AαC (**6a**) with anhydrous aluminum chloride in benzene at room temperature gave AαC (**1a**) in 71.4% yield. In a similar way, treatment of dibenzyl MeAαC (**6b**) with anhydrous aluminum chloride cleanly gave MeAαC (**1b**) in 81.1% yield. The physical data of both compounds were identical with those reported for **1a** and **1b**.[2]

Thus, the syntheses of AαC (**1a**) and MeAαC (**1b**) were achieved *via* the thermal electrocyclic reaction of the

2-azahexa-1,3,5-triene intermediated (**2**) in 46.2% and 44.1% overall yields, respectively, in a three-step sequence from **3**. These overall yields are fairly better than those reported by Matsumoto and co-workers.[2)]

Experimental

Melting points were determined with a Yanagimoto micro melting point apparatus and are uncorrected. ^{1}H-NMR spectra were taken with JEOL JNM FX-100 and JEOL PMX 60Si instruments using tetramethylsilane as an internal standard. The following abbreviations are used: singlet (s), doublet (d), quartet (q) and multiplet (m). Mass spectra (MS) were measured with Shimadzu GC-MS 6020 and 9020DF instruments at 70 eV chamber voltage on a direct inlet system. Silica gel (60—100 mesh, Merck Art 7734) was used for column chromatography. Anhydrous $AlCl_3$ was ground down before use. All reactions were carried out under an N_2 atmosphere unless otherwise stated.

1-Benzyl-2-(triphenylphosphoranylidenamino)indole-3-carboxaldehyde (4) A solution of the azide (**3**)[3)] (1 g, 3.62 mmol) and triphenylphosphine (0.99 g, 3.78 mmol) in dry CH_2Cl_2 (20 ml) was stirred at room temperature for 4 h. After removal of the solvent, the resulting residue was washed with 20% Et_2O–hexane, and recrystallized from benzene–hexane to give the iminophosphorane (**4**) (1.3 g, 76.2%), mp 194—196 °C. This compound should be used as quickly as possible. ^{1}H-NMR ($CDCl_3$): δ 5.39 (2H, s, C$\underline{H}_2$), 6.74—8.28 (24H, m, aromatic protons), 9.38 (1H, s, C$\underline{H}$O). MS *m/z*: 510 (M^+). *Anal.* Calcd for $C_{37}H_{27}N_2OP$: C, 79.98; H, 5.33; N, 5.49. Found: C, 80.15; H, 5.55; N, 5.43.

2-Benzylamino-9-benzylpyrido[2,3-*b*]indole (6a) A solution of the aldehyde (**4**) (200 mg, 0.39 mmol) in anhydrous THF (2 ml) was added dropwise to a stirred solution of methylenetriphenylphosphorane [prepared from methyl triphenylphosphonium bromide (195 mg, 0.546 mmol) and *n*-BuLi (1.5 M hexane solution; 0.36 ml, 0.54 mmol) in anhydrous THF (3 ml)] under cooling with ice. The mixture was stirred at room temperature for 12 h, then the solvent was changed to toluene (8 ml), and a solution of benzylisocyanate (67 mg, 0.51 mmol) in toluene (2 ml) was added. The mixture was refluxed at 120 °C (external) for 12 h, then allowed to cool to room temperature. An aqueous saturated solution of NH_4Cl (50 ml) was added. The mixture was extracted with $CHCl_3$ (30 ml × 3 times) and the combined $CHCl_3$ extracts were washed with brine, dried over Na_2SO_4 and concentrated to dryness. The residue was purified by column chromatography (silica gel, 30 g) using EtOAc–hexane (2 : 98, v/v) as an eluent to give the dibenzyl α-carboline (**6a**) (110.3 mg, 75.5%), mp 93—94 °C (from benzene–hexane). ^{1}H-NMR ($CDCl_3$) δ: 4.55 (2H, br s, NHC$\underline{H}_2$Ph), 4.83 (1H, br s, N$\underline{H}$, exchangeable with D_2O), 5.43 (2H, s, NC$\underline{H}_2$Ph), 6.17 (1H, d, J=7 Hz, C_3-H), 6.95—7.83 (14H, m, aromatic protons), 8.01 (1H, d, J=7 Hz, C_4-H). MS *m/z*: 363 (M^+). *Anal.* Calcd for $C_{25}H_{21}N_3$: C, 82.61; H, 5.82; N, 11.56. Found: C, 82.75; H, 5.95; N, 11.49.

2-Benzylamino-9-benzyl-3-methylpyrido[2,3-*b*]indole (6b) A solution of the aldehyde (**4**) (200 mg, 0.39 mmol) in anhydrous THF (2 ml) was added dropwise to a stirred solution of ethylenetriphenylphosphorane [prepared from ethylphenylphosphonium bromide (195 mg, 0.546 mmol) and *n*-BuLi (1.5 M hexane solution, 0.36 ml, 0.54 mmol) in anhydrous THF (3 ml)] under cooling with ice. The mixture was stirred at room temperature for 12 h, then the solvent was changed to toluene (8 ml), and a solution of benzylisocyanate (67 mg, 0.51 mmol) in toluene (2 ml) was added. The mixture was refluxed at 120 °C (external) for 12 h, then allowed to cool to room temperature. An aqueous saturated solution of NH_4Cl (50 ml) was added. The mixture was extracted with $CHCl_3$ (30 ml × 3 times) and the combined $CHCl_3$ extracts were washed with brine, dried over Na_2SO_4 and concentrated to dryness. The residue was purified by column chromatography (silica gel, 30 g) using EtOAc–hexane (2 : 98, v/v) as an eluent to give the dibenzyl α-carboline (**6b**) (105.4 mg, 71.3%), mp 153—155 °C. ^{1}H-NMR ($CDCl_3$), 2.33: (3H, s, C$\underline{H}_3$), 4.77 (2H, br s NHC$\underline{H}_2$Ph), 5.50 (2H, s, NC$\underline{H}_2$Ph), 7.10—7.78 (14H, m, aromatic protons), 7.82 (1H, br s, C_4-H). MS *m/z*: 377 (M^+). *Anal.* Calcd for $C_{26}H_{23}N_3$: C, 82.72; H, 6.14; N, 11.13. Found: C, 82.88; H, 6.30; N, 11.02.

2-Amino-9-benzylpyrido[2,3-*b*]indole (7a) A solution of dibenzyl α-carboline (**6a**) (100 mg, 0.275 mmol) and 10% Pd–C (100 mg) (or 5% Pt–C, 200 mg) in AcOH (20 ml) was stirred under an H_2 atmosphere at room temperature. After 12 h, the mixture was filtered and the filtrate was evaporated under reduced pressure. The residue was purified by column chromatography (silica gel, 15 g) using EtOAc–benzene (10 : 90, v/v) as an eluent to give the monobenzyl α-carboline (**7a**) (62 mg, 82.4%), mp 128—130 °C (from benzene–hexane). ^{1}H-NMR ($CDCl_3$) δ: 4.50 (2H, br s, N$\underline{H}_2$, exchangeable with D_2O), 5.50 (2H, s, NC$\underline{H}_2$Ph), 6.32 (1H, d, J=8 Hz, C_3-H), 7.05—7.32 (9H, m, aromatic protons), 7.97 (1H, d, J=8 Hz, C_4-H). MS *m/z*: 261 (M^+). *Anal.* Calcd for $C_{18}H_{15}N_3$: C, 79.09; H, 5.53; N, 15.38. Found: C, 79.21; H, 5.68; N, 15.35.

2-Amino-9-benzyl-3-methylpyrido[2,3-*b*]indole (7b) A solution of dibenzyl α-carboline (**6b**) (52.7 mg, 0.14 mmol) and 10% Pd–C (50 mg) (or 5% Pt–C, 100 mg) in AcOH (20 ml) was stirred under an H_2 atmosphere. After 12 h, the mixture was filtered and the filtrate was evaporated under reduced pressure. The residue was purified by column chromatography (silica gel, 10 g) using benzene–hexane (50 : 50, v/v) as an eluent to give the monobenzyl α-carboline (**7b**) (34.1 mg, 85.0%), mp 191—192 °C (from benzene–hexane). ^{1}H-NMR ($CDCl_3$) δ: 2.25 (3H, s, C$\underline{H}_3$), 4.17 (2H, br s, N$\underline{H}_2$, exchangeable with D_2O), 5.50 (2H, s, NC$\underline{H}_2$Ph), 6.80—6.90 (9H, m, aromatic protons), 7.85 (1H, s, C_4-H). MS *m/z*: 287 (M^+). *Anal.* Calcd for $C_{19}H_{17}N_3$: C, 79.41; H, 5.96; N, 14.62. Found: C, 79.50; H, 6.13; N, 14.55.

2-Amino-9*H*-pyrido[2,3-*b*]indole (AαC) (1a) Anhydrous $AlCl_3$ (305 mg, 2.28 mmol) was added to a stirred solution of dibenzyl α-carboline (**6a**) (103.5 mg, 0.285 mmol) in dry benzene (5 ml). The mixture was stirred at room temperature for 14 h, then poured into water (100 ml) and extracted with $CHCl_3$ (80 ml × 2 times). The combined $CHCl_3$ layer was washed with aqueous saturated $KHCO_3$ (50 ml) and brine (50 ml), dried over Na_2SO_4 and evaporated under reduced pressure. The residue was purified by column chromatography (silica gel, 20 g) using EtOAc–benzene (20 : 80, v/v) as an eluent to give AαC (**1a**) (36 mg, 71.4%), mp 201—202 °C (from $CHCl_3$–hexane) (lit.,[2a)] mp 202 °C). ^{1}H-NMR (DMSO-d_6) δ: 6.10 (2H, s, N$\underline{H}_2$), 6.40 (1H, d, J=8.2 Hz, C_3-H), 7.00—7.82 (4H, m, aromatic protons), 8.04 (1H, d, J=8.2 Hz, C_4-H), 11.18 (1H, br s, ind-N$\underline{H}$). MS *m/z*: 183 (M^+).

2-Amino-3-methyl-9*H*-pyrido[2,3-*b*]indole (MeAαC) (1b) Anhydrous $AlCl_3$ (530 mg, 3.98 mmol) was added to a solution of dibenzyl α-carboline (**6b**) (250 mg, 0.663 mmol) in dry benzene (20 ml). The mixture was stirred for 14 h, then poured into water (100 ml), and extracted with $CHCl_3$ (80 ml × 2 times). The combined $CHCl_3$ layer was washed with aqueous saturated $KHCO_3$ (50 ml) and brine (50 ml), dried over Na_2SO_4 and evaporated under reduced pressure. The residue was purified by column chromatography (silica gel, 50 g) using EtOAc–benzene (20 : 80, v/v) to give MeAαC (**1b**) (106 mg, 81.1%), mp 215—218 °C (from $CHCl_3$–hexane) (lit.,[2b)] mp 215—218 °C). ^{1}H-NMR (DMSO-d_6) δ: 2.21 (3H, s, CH_3), 5.85 (2H, br s, N$\underline{H}_2$), 7.00—7.85 (4H, m, aromatic protons), 7.90 (1H, s, C_4-H), 11.04 (1H, br s, ind-N$\underline{H}$). MS *m/z*: 197 (M^+).

References

1) *a*) D. Yoshida, T. Matsumoto, R. Yoshimura and T. Matsuzaki, *Biochem. Biophys. Res. Commun.*, **83**, 915 (1978); *b*) D. Yoshida, H. Nishigata and T. Matsumoto, *Agric. Biol. Chem.*, **43**, 1769 (1979); *c*) R. Kato and Y. Yamazoe, *Jpn. J. Cancer Res.* (*Gann*), **78**, 297 (1987).
2) *a*) T. Matsumoto, D. Yoshida, H. Tomita and H. Matsushita, *Agric. Biol. Chem.*, **43**, 675 (1979); *b*) T. Matsumoto, D. Yoshida and H. Tomita, *ibid.*, **45**, 2031 (1981).
3) *a*) S. Hibino, E. Sugino, N. Ogura, Y. Shintani and K. Sato, *Heterocycles*, **30**, 271 (1990); *b*) S. Hibino, E. Sugino, Y. Adachi, K. Nomi and K. Sato, *ibid.*, **28**, 275 (1989) and references cited therein.
4) J. Becher, K. Pluta, N. Krake, K. Blöndum, N. J. Christensen and M. V. Vinander, *Synthesis*, **1989**, 530.
5) *a*) E. Rossi, G. Celentano, R. Stradi and A. Strada, *Tetrahedron Lett.*, **31**, 903 (1990); *b*) P. Molina, A. Tárraga and M. José Lidón, *J. Chem. Soc., Perkin Trans. 1*, **1990**, 1727; *c*) A. W. Johnson, "Ylid Chemistry," Academic Press, New York and London, 1966, Chap. 6; *d*) H. J. Bestmann and K. Zimmerman, "Organic Phosphorus Compounds," ed. by G. M. Kosolapoff and L. Mair, Wiley Interscience, New York, 1972, Vol. 3.
6) Y. Murakami, T. Watanabe, A. Kobayashi and Y. Yokoyama, *Synthesis*, **1984**, 738.

Synthesis and Salidiuretic Activity of 2,3-Dihydro-8-(1-pyrrolyl)-1,2,4-triazolo[4,3-*a*]pyridines and 5,6-Dihydro-4*H*-pyrido[2,3-*c*]pyrrolo[1,2-*e*]-1,2,5-triazepines

Brigitte BOUTEAU,[a] Jean-Louis IMBS,[b] Jean-Charles LANCELOT,[a] Mariette BARTHELMEBS,[b] and Max ROBBA*,[a]

Laboratoire de Chimie Thérapeutique, U.F.R des Sciences Pharmaceutiques, Université de Caen,[a] 1, rue Vaubénard, 14032-caen, Cedex, France and Institut de Pharmacologie et de Medecine Expérimentale URA CNRS 0589, Faculté de Medecine, Université Louis Pasteur,[b] 11, rue Humann, 67000-Strasbourg, France. *Received May 28, 1990*

Starting from 2-hydrazino-3-(1-pyrrolyl)pyridine 3 a series of 2,3-dihydro-8-(1-pyrrolyl)-1,2,4-triazolo[4,3-*a*]-pyridines 49—50 and 5,6-dihydro-4*H*-pyrido[2,3-*c*]pyrrolo[1,2-*e*]-1,2,5-triazepines 32—42 were synthesized and tested *p.o.* in rats for salidiuretic and renal vasodilator activity.

Keywords pyrrole; pyridine; triazolopyridine; triazepine; intramolecular cyclization; ^{1}H-NMR

In connection with our program on new heterocyclic compounds[1-4] with diuretic and antihypertensive activity, we were interested in the synthesis of triazolopyridines and analogues of 5-amino-8-(2-ethoxyethyl)-7-phenyl-5-triazolo[1,5-*c*]pyrimidine (bemitradine)[5-13] and we now report the synthesis and preliminary diuretic activity of 2,3-dihydro-8-(1-pyrrolyl)-1,2,4-triazolo[4,3-*a*]pyridines and 5,6-dihydro-4*H*-pyrido[2,3-*c*]pyrrolo[1,2-*e*]-1,2,5-triazepines.

Chemistry We have previously reported[1] the synthesis of new structures such as 8-(1-pyrrolyl)-1,2,4-triazolo[4,3-*a*]pyridines **6** and 6*H*-pyrido[2,3-*c*]pyrrolo[1,2-*e*]-1,2,5-triazepine **5** from 2-chloro-3-(1-pyrrolyl)pyridine **2** and from 2-hydrazino-3-(1-pyrrolyl)pyridine **3** as previously described.

The present study revealed that, when cyclization reactions were initiated from 2-hydrazino-3-(1-pyrrolyl)pyridine (**3**), they led either to dihydro-8-(1-pyrrolyl)triazolopyridines **8** or to a tricyclic dihydropyridopyrrolotriazepine system **9** and we have attempted to increase our knowledge about the parameters affecting the site of cyclization in order to obtain dihydropyrrolyltriazolopyridines or dihydropyridopyrrolotriazepines regiospecifically. Thus, treatment of 2-hydrazino-3-(1-pyrrolyl)pyridine (**3**) in hot EtOH with various alicyclic carbonyl derivatives afforded intermediate hydrazones **10**—**24**. In the same way, treatment of **3** with aromatic carbonyl derivatives led to hydrazones **25**—**31**. Hydrazones **10**—**31**, being very unstable, were immediately involved without isolation in cyclization reactions. Two experimental procedures were used: treatment of a solution of hydrazone in EtOH by a slight excess of 30% hydrobromic acid, in acetic acid, or treatment of a solution in diethyl ether by gaseous hy-

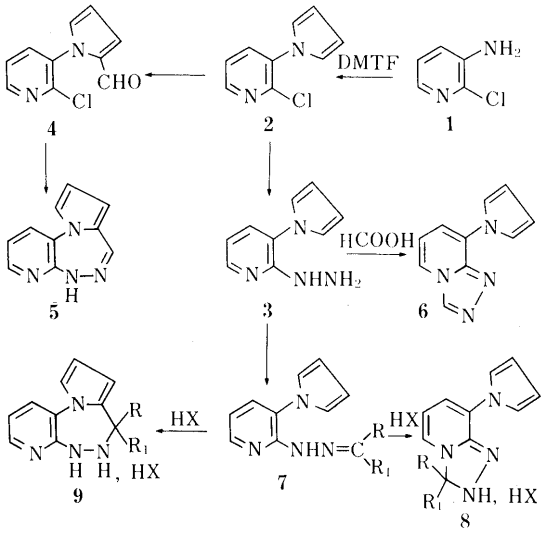

Chart 1

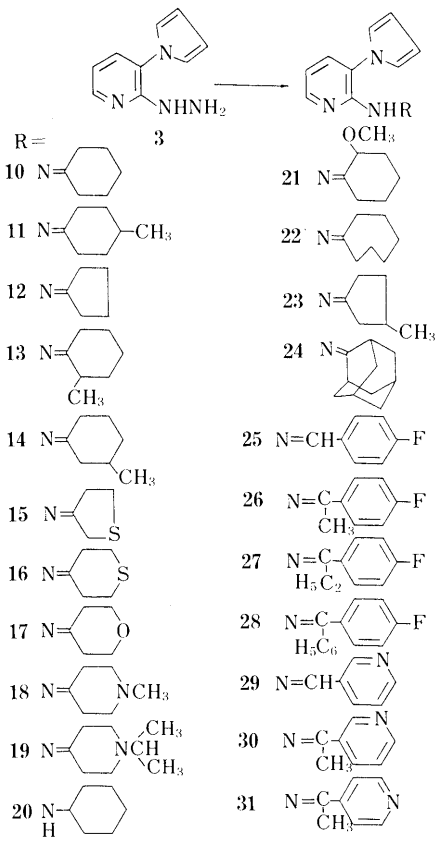

Chart 2

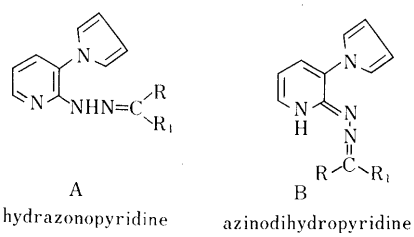

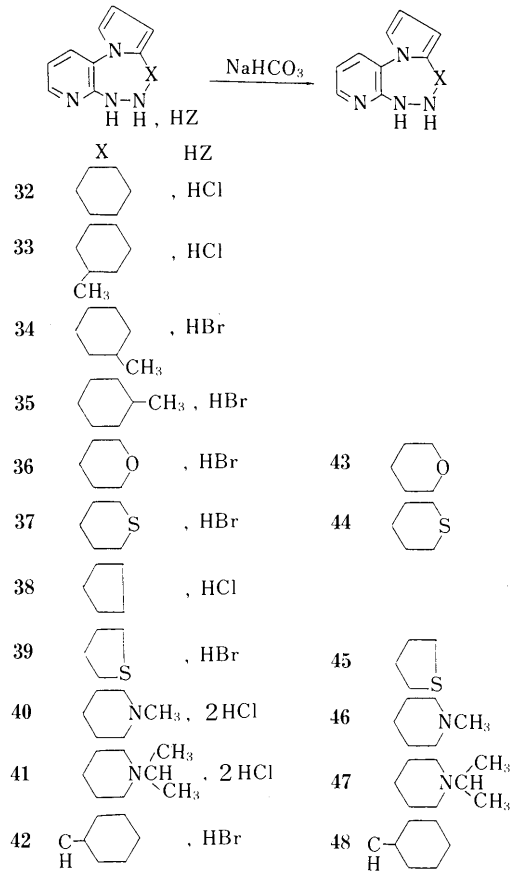

Chart 3

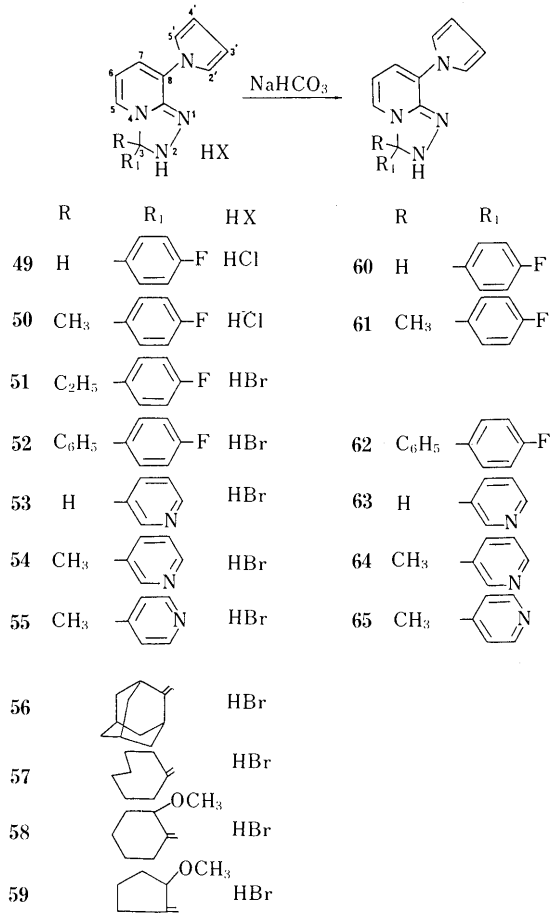

Chart 4

TABLE I

No.	Dose mg/kg *p.o.*	Test of diuresis	Lipschitz natriuresis	Renal blood flow	Mean arterial pressure
32	100	0.92	1.50	Increase	Slight decrease
32	1	0.28	0.48	No effect	No effect
34	100	0.45	0.66	No effect	Decrease
45	100	0.47	0.13	No effect	No effect
46	100	0.17	0.88	No effect	Slight decrease
46	10	0.54	0.79	Not measured	Not measured
47	100	0.69	1.06	No effect	No effect
47	10	0.56	0.72	Not measured	Not measured
63	100	0.48	0.66	Not measured	Not measured
60	100	0.44	0.33	No effect	No effect
61	100	0.70	0.50	No effect	No effect

The figure under diuresis is the ratio between the mean volume of urine eliminated during the 5 h following gavage with the product to be tested and that for the 5 h following gavage with 1 g/kg of urea.

The figure under natriuresis is the ratio between the mean quantity of Na^+ eliminated during the 5 h following forcible feeding with the product to be tested and that for the 5 h following forcible feeding with 1 g/kg of urea.

TABLE II. ^{1}H-NMR(DMSO-d_6) Spectral Data for 5,6-Dihydro-4*H*-pyrido[2,3-*c*]pyrrolo[1,2-*e*]-1,2,5-triazepines **32**—**42**

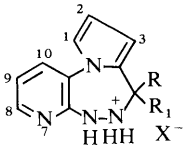

Compound	H1	H2	H3	H8	H9	H10
32	7.26	6.20	6.10	8.16	6.76	7.96
33	7.30	6.18	6.03	8.23	6.96	8.00
34	7.30	6.23	6.16	8.23	6.96	7.93
35	7.30	6.15	6.03	8.20	6.90	7.93
36	7.33	6.18	6.08	8.23	7.00	8.02
37	7.32	6.18	6.12	8.23	7.00	7.97
38	7.26	6.22	6.22	8.13	7.11	8.13
39	7.37	6.23	6.23	8.30	7.07	8.02
40	7.37	6.23	6.13	8.27	7.03	8.03
41	7.35	6.23	6.15	8.25	7.00	8.02
42	7.33	6.28	6.28	8.18	7.20	8.18

drogen chloride.

There are two possible sites for cyclization, either the α-pyrrolic carbon or the pyridinic nitrogen, and the reaction orientation appears to be dependent on both the hydrazone–azine tautomerism and the size of the hydrazone substituents. Hydrazonopyridine tautomeric form A favors cyclization on the α-pyrrolic carbon probably because of the possibility of two free-rotating bonds pyridine C_2–NH and NH–N=, which causes the system to be in favor of keeping the hydrazone group next to pyrrole ring.

On the other hand, in the azinodihydropyridine form B, the structure is much more rigid and allows only one free rotating bond (=N–N=) which favors cyclization in dihydrotriazolopyridine.

This assumption is confirmed when hydrazone and azine structures were built with molecular models. Thus hydrazones **10**—**21**, which carry small size aliphatic substituents, led to isolation of dihydropyridopyrrolotriaze-

TABLE III. ^{1}H-NMR(DMSO-d_6) Spectral Data for 5,6-Dihydro-4*H*-pyrido[2,3-*a*]pyrrolo[1,2-*c*]-1,2,5-triazepines **43**—**48**

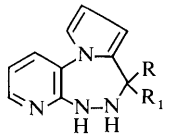

Compound	H1	H2	H3	H8	H9	H10
43[a]	7.17	6.15	6.07	7.90	6.77	7.83
44	7.17	6.15	6.07	7.90	6.80	7.83
45	7.20	6.20	6.20	7.92	6.87	7.82
46	7.13	6.10	6.00	7.82	6.77	7.82
47	7.10	6.10	6.00	7.83	6.75	7.78
48	7.15	6.07	5.90	7.70	7.83	6.65

a) $J_{1,2}=3.30$ Hz, $J_{1,3}=1.5$ Hz, $J_{2,3}=3.60$ Hz, $J_{9,10}=7.80$ Hz, $J_{8,10}=1.80$ Hz, $J_{8,9}=4.80$ Hz.

TABLE IV. ^{1}H-NMR(DMSO-d_6) Spectral Data for 2,3-Dihydro-3-(3-pyridyl)-8-(1-pyrrolyl)-1,2,4-triazolo[4,5-*a*]pyridines **49**—**59**

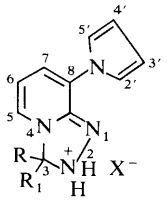

Compound	H2′ H5′	H3′ H4′	H5	H6	H7
49	7.10	6.33	8.33	7.20	8.03
50	7.26	6.40	8.28	8.25	8.25
51	7.20	6.38	8.27	7.30	8.27
52	6.90	6.13	8.37	7.42	8.17
53	7.04	6.30	8.61	7.60	8.31
54	7.17	6.31	8.70	7.70	8.41
55	7.10	6.30	8.61	7.60	8.31
56	7.16	6.31	8.00	7.16	8.00
57	7.11	6.31	8.08	7.11	8.00
58	7.10	6.25	8.03	7.00	8.03
59	7.13	6.33	8.08	7.13	7.93

pine hydrochlorides **32**, **33**, **38**, **40**, dihydrochlorides **41** or hydrobromides **34**—**37**, **39** and **42**. On the other hand hydrazones with bulky substituents such as adamantane **24**, cycloheptane **22**, 2-methoxycyclohexane **21**, 3-methylcyclopentane **23**, or with aromatic substituents **25**—**31**, afforded dihydropyrrolyltriazolopyridine hydrochlorides **49**—**50** or hydrobromides **51**—**59**. Some free bases **60**—**65** were also obtained from the corresponding salts. The structures of these compounds were confirmed on the basis of the ^{1}H-nuclear magnetic resonance ^{1}H-NMR spectral analysis.

Biological Evaluation These molecules were studied in the Wistar rat (Sexal strain, males weighing about 250 g) from two points of view: existence of salidiuretic activity associated with a renal vasodilatory effect, or not associated with H.

1. Methods Salidiuretic Activity: The test of Lipschitz[14] modified according to Rupp[15] enables the evaluation, in the conscious rat, of the effect of a product to be tested, administered by gavage on the volume of urine and the renal elimination of sodium, compared with the effects of an oral loading of 1 g/kg of urea. For each dose

TABLE V. ^{1}H-NMR(DMSO-d_6) Spectral Data for 2,3-Dihydro-3-(3-pyridyl)-8-(1-pyrrolyl)-1,2,4-triazolo[4,5-*a*]pyridines **60**—**65**

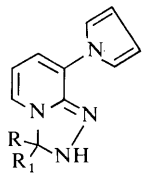

Compound	H2′ H5′	H3′ H4′	H5	H6	H7
60	6.93	6.25	8.25	6.93	7.60
61	7.00	6.27	8.23	7.00	7.53
62	6.68	6.00	8.30	6.93	7.93
63	6.90	6.20	8.40	7.27	8.17
64	6.98	6.20	8.47	7.27	8.20
65	6.80	6.40	8.58	6.80	7.47

and each product, mean diuresis and natriuresis were measured (in a metabolism cage for 5 h, 8 rats) and the ratio between the effects of the product tested and those of the urea loading are calculated. If this ratio is above 0.81 for urine volume, it means that a diuretic effect can be assumed; similarly, a significant natriuretic effect can be assumed if the natriuresis ratio is above 0.72.[16]

By way of comparison, under the same experimental conditions, the diuresis ratio was 11.5 ($n=8$) for furosemide (100 mg/kg, *p.o.*), 1.27 ($n=16$) for amiloride (100 mg/kg, *p.o.*) and 2.39 ($n=16$) for triamterene (100 mg/kg, *p.o.*).

Renal Vasodilator Action: Under Inactin-induced anesthesia (100 mg/kg, i.p.), the renal blood flow was measured with an electromagnetic probe (Skalar transflow 601) placed on the left renal artery. Blood pressure was measured at the level of the carotid artery (Statham P23 Db transducer). These parameters were recorded for 30 min prior to and 240 min after the intragastric gavage of the drug tested (in suspension at a volume of 0.3 ml of an aqueous solution of 10% gumarabic).

2. Results Pyridopyrrolotriazepines **32**, **46** and **47** had weak but significant natriuretic effects. These were scarcely detectable with doses of 10 mg/kg, *p.o.*, and disappeared with a dose of 1 mg/kg. The salidiuretic effect of **32** was accompanied by renal vasodilatation and a slight decrease in peripheral vascular resistance with a dose of 100 mg/kg *p.o.*

This data suggests that the pyridopyrrolotriazepine tricyclic structure derivative **32** comprises a pharmacophore for the salidiuretic and vasodilator effects which is not encountered with the dihydropyrrolyltriazolopyridine bicyclic structure.

Experimental

Melting points were determined with a Kofler Heizbank apparatus and are uncorrected. Infrared (IR) spectra were recorded as KBr pellets on a Perkin-Elmer 257 G spectrophotometer, and ^{1}H-NMR spectra were obtained on a VARIAN EM 90 spectrometer for solution in dimethyl sulfoxide-d_6 (DMSO-d_6). Chemical shifts are expressed in ppm downfield from Me_4Si as an internal standard, and the *J* values are given in Hertz.

General Procedure for the Preparation of Hydrobromides and Hydrochlorides of 5,6-Dihydro-4*H*-pyrido[2,3-*c*]pyrrolo[1,2-*e*]-1,2,5-triazepines 32—42 and 2,3-Dihydro-8-(1-pyrrolyl)-1,2,4-triazolo[4,3-*a*]pyridines 49—59 Method a: Preparation of Hydrobromides: *x* g (*x*′ mol) of 2-hydrazino-3-(1-pyrrolyl)pyridine (**3**) were added to an absolute EtOH (100 ml) solution containing a 1.1 eq of carbonyl derivative. The reaction

mixture was refluxed for 2 h and the solvent was evaporated off. The obtained residual oil was dissolved in an absolute EtOH (5 ml), then 30% of hydrobromic acid in acetic acid (3 ml) was added. After being stirred at room temperature for 1 h, the precipitate was isolated, washed with diethyl ether (20 ml), dried and recrystallized from an appropriate solvent.

Method b: Preparation of Hydrochloride: Gaseous hydrogen chloride was bubbled through the obtained residual oil dissolved in anhydrous diethyl ether (80 ml) for 2 min. The precipitate was collected by filtration, washed with diethyl ether (20 ml), dried and recrystallized from an appropriate solvent.

5,6-Dihydro-4*H*-pyrido[2,3-*c*]pyrrolo[1,2-*e*]-1,2,5-triazepine-4-spiro-cyclohexane Hydrochloride (32) **3** (2 g, 11.5 mol) and cyclohexanone (1.1 g, 12.6 mmol) afforded **32** (2.12 g, 55%), mp 230 °C (MeCN). IR ν_{max}^{KBr} cm^{-1}: 3200, 2660, 1640 (NH, NH_2^+). *Anal.* Calcd for $C_{15}H_{19}ClN_4$: C, 61.95; H, 6.58; Cl, 12.19; N, 19.26. Found: C, 62.00; H, 6.60; Cl, 12.20; N, 19.30.

5,6-Dihydro-4*H*-pyrido[2,3-*c*]pyrrolo[1,2-*e*]-1,2,5-triazepine-4-spiro-1′-(2′-methyl cyclohexane) Hydrochloride (33) **3** (2 g, 11 mmol) and 2-methylcyclohexanone (1.3 g, 12.6 mmol) afforded **33** (0.059 g, 17%), mp 170 °C (MeCN). IR ν_{max}^{KBr} cm^{-1}: 3220, 3195, 2600 (NH, NH_2^+). *Anal.* Calcd for $C_{16}H_{21}ClN_4$: C, 63.04; H, 6.94; Cl, 11.63; N, 18.38. Found: C, 63.30; H, 6.85; Cl, 11.87; N, 18.54.

5,6-Dihydro-4*H*-pyrido[2,3-*c*]pyrrolo[1,2-*e*]-1,2,5-triazepine-4-spiro-1′-(3′-methyl cyclohexane) Hydrobromide (34) **3** (2 g, 11.5 mmol) and 3-methylcyclohexanone (1.29 g, 12.6 mmol) afforded **34** (2.33 g, 58%), mp 238 °C (EtOH). IR ν_{max}^{KBr} cm^{-1}: 3200, 3160, 2670, 1640 (NH, NH_2^+). *Anal.* Calcd for $C_{16}H_{21}BrN_4$: C, 55.02; H, 6.06; Br, 22.80; N, 16.04. Found: C, 54.89; H, 5.97; Br, 23.00; N, 16.06.

5,6-Dihydro-4*H*-pyrido[2,3-*c*]pyrrolo[1,2-*e*]-1,2,5-triazepine-4-spiro-1′-(4′-methyl cyclohexane) Hydrobromide (35) **3** (2 g, 11.5 mmol) and 4-methylcyclohexanone (1.29 g, 12.6 mmol) afforded **35** (2.30 g, 57%), mp 236 °C (MeCN). IR ν_{max}^{KBr} cm^{-1}: 3200, 3160, 2670, 1640 (NH, NH_2^+). *Anal.* Calcd for $C_{16}H_{21}BrN_4$: C, 55.02; H, 6.06; Br, 22.88; N, 16.04. Found: C, 55.03; H, 6.12; Br, 22.79; N, 16.20.

5,6-Dihydro-4*H*-pyrido[2,3-*c*]pyrrolo[1,2-*e*]-1,2,5-triazepine-4-spiro-4′-(tetrahydropyrane) Hydrobromide (36) **3** (2 g, 11,5 mmol) and 4*H*-tetrahydropyran-4-one (11.26 g, 12.6 mmol) afforded **36** (1.3 g, 34%), mp 238 °C (MeCN). IR ν_{max}^{KBr} cm^{-1}: 3200, 3060, 3010, 2950, 2860, 1625 (NH, NH_2^+). *Anal.* Calcd for $C_{14}H_{17}BrN_4O$: C, 49.87; H, 5.08; Br, 23.70; N, 16.61. Found: C, 49.78; H, 5.18; Br, 23.82; N, 16.67.

5,6-Dihydro-4*H*-pyrido[2,3-*c*]pyrrolo[1,2-*e*]-1,2,5-triazepine-4-spiro-4′-tetrahydrothiopyrane Hydrobromide (37) **3** (2 g, 11.5 mmol) and tetrahydrothiopyran-4-one (1.46 g, 12.6 mmol) afforded **37** (2.8 g, 69%), mp 244 °C (MeCN). IR ν_{max}^{KBr} cm^{-1}: 3200, 3150, 3100, 3040, 2960, 2900, 2790 (NH, NH_2^+). *Anal.* Calcd for $C_{14}H_{17}BrN_4S$: C, 47.60; H, 4.85; Br, 22.62; S, 9.07. Found: C, 47.77; H, 4.97; Br, 22.41; S, 8.94.

5,6-Dihydro-4*H*-pyrido[2,3-*c*]pyrrolo[1,2-*e*]-1,2,5-triazepine-4-spiro-cyclopentane Hydrochloride (38) **3** (2 g, 11.5 mmol) and cyclopentanone (0.97 g, 12.6 mmol) afforded **38** (2 g, 63%), mp 238 °C (EtOH). IR ν_{max}^{KBr} cm^{-1}: 3200, 3190, 2650, 1630 (NH, NH_2^+). *Anal.* Calcd for $C_{14}H_{17}ClN_4$: C, 60.75; H, 6.19; Cl, 12.81; N, 20.24. Found: C, 60.79; H, 6.18; Cl, 12.71; N, 20.44.

5,6-Dihydro-4*H*-pyrido[2,3-*c*]pyrrolo[1,2-*e*]-1,2,5-triazepine-4-spiro-3′-(tetrahydrothiophene) Hydrobromide (39) **3** (2 g, 11.5 mmol) and tetrahydrothiophen-3-one (1.29 g, 12.6 mmol) afforded **39** (1.7 g, 45%), mp 246 °C (MeCN). IR ν_{max}^{KBr} cm^{-1}: 3180, 3100, 3020, 2960, 2770, 2700, 1640 (NH, NH_2^+). *Anal.* Calcd for $C_{13}H_{15}BrN_4S$: C, 46.03; H, 4.46; Br, 23.55; N, 16.51. Found: C, 46.09; H, 4.36; Br, 23.75; N, 16.45.

5,6-Dihydro-4*H*-[2,3-*c*]pyrrolo[1,2-*e*]-1,2,5-triazepine-4-spiro-4′-1′-methylpiperidine Hydrochloride (40) **3** (2 g, 11.5 mmol) and 1-methylpiperidine-4-one (1.43 g, 12.6 mmol) afforded **40** (1.65 g, 42%), mp 225 °C (MeOH). IR ν_{max}^{KBr} cm^{-1}: 3200, 3075, 2940, 2700, 1630 (NH, NH_2^+). *Anal.* Calcd for $C_{15}H_{21}Cl_2N_5$: C, 52.64; H, 6.18; Cl, 20.72; N, 20.46. Found: C, 52.56; H, 6.12; Cl, 21.00; N, 20.48.

5,6-Dihydro-4*H*-pyrido[2,3-*c*]pyrrolo[1,2-*e*]-1,2,5-triazepine-4-spiro-4′-(1′-isopropylpiperidine) Dihydrochloride (41) **3** (2 g, 11.5 mmol) and 1-isopropylpiperidine-4-one (1.8 g, 12.6 mmol) afforded **41** (2.73 g, 64%), mp 265 °C (iso-PrOH). IR ν_{max}^{KBr} cm^{-1}: 3180, 3120, 2960, 2940, 2530, 1605 (NH, NH_2^+). *Anal.* Calcd for $C_{17}H_{25}Cl_2N_5$: C, 55.14; H, 6.80; Cl, 18.91; N, 19.15. Found: C, 54.94; H, 6.71; Cl, 18.61; N, 19.31.

4-Cyclohexyl-5,6-dihydro-4*H*-pyrido[2,3-*c*]pyrrolo[1,2-*e*]-1,2,5-triazepine Hydrobromide (42) **3** (1.7 g, 9.7 mmol) and cyclohexane-4-carboxaldehyde (1.2 g, 10.6 mmol) afforded **42** (2.50 g, 73%), mp 234 °C (MeCN). IR ν_{max}^{KBr} cm^{-1}: 3180, 3090, 2930, 2850, 1630 (NH, NH_2^+). *Anal.* Calcd for $C_{16}H_{21}BrN_4$: C, 55.02; H, 6.06; Br, 22.88; N, 16.04. Found: C, 54.84; H, 5.96; Br, 23.00; N, 15.96.

2,3-Dihydro-3*H*-3-(4-fluorophenyl)-8-(1-pyrrolyl)-1,2,4-triazolo[4,3-*a*]pyridine Hydrochloride Monohydrate (49) **3** (2.5 g, 14.7 mmol) and 4-fluorobenzaldehyde (2.01 g, 16.1 mmol) afforded **49** (2.6 g, 53%), mp 210 °C (iso-PrOH). IR ν_{max}^{KBr} cm^{-1}: 3440, 3320, 1635 (NH, NH_2^+). *Anal.* Calcd for $C_{16}H_{16}ClFN_4O$: C, 54.74; H, 4.21; N, 10.78. Found: C, 57.68; H, 4.25; N, 10.60.

2,3-Dihydro-3-(4-fluorophenyl)-3-methyl-8-(1-pyrrolyl)-1,2,4-triazolo-[4,3-*a*]pyridine Hydrochloride (50) **3** (2.1 g, 12 mmol) and 4-fluoroacetophenone (1.83 g, 13.2 mmol) afforded **50** (2.2 g, 55%), mp 220 °C (iso-PrOH). IR ν_{max}^{KBr} cm^{-1}: 3320, 3260, 2800, 2700, 1630 (NH_2^+). *Anal.* Calcd for $C_{17}H_{16}ClFN_4$: C, 61.66; H, 4.84; F, 5.74; N, 16.93. Found: C, 61.84; H, 4.85; F, 5.80; N, 17.00.

2,3-Dihydro-3-ethyl-3-(4′-fluorophenyl)-8-(1-pyrrolyl)-1,2,4-triazolo-[4,3-*a*]pyridine Hydrobromide (51) **3** (2 g, 11.5 mmol) and 4-fluoropropiophenone (1.92 g, 12.6 mmol) afforded **51** (3.1 g, 70%), mp 240 °C (MeCN). IR ν_{max}^{KBr} cm^{-1}: 3440, 3340, 3320, 2960, 2860, 1630 (NH_2^+). *Anal.* Calcd for $C_{18}H_{18}BrFN_4$: C, 55.34; H, 4.66; F, 4.88; N, 14.39. Found: C, 55.70, H, 4.67; F, 5.00; N, 14.41.

2,3-Dihydro-3-(4-fluorophenyl)-3-phenyl-8-(1-pyrrolyl)-1,2,4-triazolo-[4,3-*a*]pyridine (52) **3** (2.5 g, 14.4 mmol) and 4-fluorobenzophenone (2.87 g, 15.8 mmol) afforded **52** (2.8 g, 45%), mp 265 °C (MeCN). IR ν_{max}^{KBr} cm^{-1}: 3300, 2820, 2720, 1630 (NH_2^+). *Anal.* Calcd for $C_{22}H_{18}BrFN_4$: C, 60.41; H, 4.12; Br, 18.27. Found: C, 60.48; H, 4.15; Br, 18.47.

2,3-Dihydro-3*H*-3-(3-pyridyl)-8-(1-pyrrolyl)-1,2,4-triazolo[4,3-*a*]pyridine Hydrobromide (53) **3** (2 g, 11.5 mmol) and pyridine-3-carboxaldehyde (1.35 g, 12.6 mmol) afforded **53** (2.2 g, 56%), mp 240 °C (MeCN). IR ν_{max}^{KBr} cm^{-1}: 3300, 2800, 1640 (NH_2^+). *Anal.* Calcd for $C_{15}H_{14}BrN_5$: C, 52.34; H, 4.10; Br, 23.21; N, 20.35. Found: C, 52.26; H, 4.19; Br, 23.35; N, 20.14.

2,3-Dihydro-3-methyl-3-(3-pyridyl)-8-(1-pyrrolyl)-1,2,4-triazolo[4,3-*a*]-pyridine Hydrobromide (54) **3** (2 g, 11.5 mmol) and 3-acetylpyridine (1.53 g, 12.6 mmol) afforded **54** (1..3 g, 32%), mp 236 °C (MeCN). IR ν_{max}^{KBr} cm^{-1}: 3100, 3030, 2900, 1630 (NH_2^+). *Anal.* Calcd for $C_{16}H_{16}BrN_5$: C, 53.64; H, 4.50; N, 19.55. Found: C, 53.64; H, 4.45; N, 19.43.

2,3-Dihydro-3-methyl-3-(4-pyridyl)-8-(1-pyrrolyl)-1,2,4-triazolo[4,3-*a*]-pyridine Hydrobromide (55) **3** (2 g, 11.5 mmol) and 4-acetylpyridine (1.39 g, 12.6 mmol) afforded **55** (1.8 g, 36%), mp 270 °C (MeCN). IR ν_{max}^{KBr} cm^{-1}: 3200, 3230, 2780 (NH_2^+). *Anal.* Calcd for $C_{16}H_{16}BrN_5$: C, 53.63; H, 4.50; Br, 22.30; N, 19.55. Found: C, 53.33; H, 4.52; Br, 22.15; N, 19.49.

2,3-Dihydro-8-(1-pyrrolyl)-1,2,4-triazolo[4,3-*a*]pyridine-3-spiro-2′-adamantane Hydrobromide (56) **3** (2 g, 11.5 mmol) and adamantan-2-one (1.73 g, 12.6 mmol) afforded (**56**) (1.73 g, 22%), mp 260 °C (MeOH). IR ν_{max}^{KBr} cm^{-1}: 3100, 2920, 2800, 1625 (NH_2^+). *Anal.* Calcd for $C_{19}H_{21}BrN_4$: C, 59.21; H, 5.49; N, 14.54. Found: C, 59.44; H, 5.50; N, 14.54.

2,3-Dihydro-8-(1-pyrrolyl)-1,2,4-triazolo[4,3-*a*]pyridine-3-spirocycloheptane Hydrobromide (57) **3** (2 g, 11.5 mmol) and cycloheptanone (1.29 g, 12.6 mmol) afforded **57** (1.1 g, 27%) mp 226 °C (EtOH). IR ν_{max}^{KBr} cm^{-1}: 3100, 2910, 2830 (NH_2^+). *Anal.* Calcd for $C_{16}H_{21}BrN_4$: C, 55.02; H, 6.06; N, 16.04. Found: C, 55.21; H, 6.10; N, 16.12.

2,3-Dihydro-8-(1-pyrrolyl)-1,2,4-triazolo[4,3-*a*]pyridine-3-spiro-(2′-methoxycyclohexane) Hydrobromide (58) **3** (2 g, 11.5 mmol) and 2-methoxycyclohexanone (1.47 g, 12.6 mmol) afforded **58** (0.9 g, 21%), mp 140 °C (acetone). IR ν_{max}^{KBr} cm^{-1}: 3500, 3350, 2940, 1640 (NH_2^+). *Anal.* Calcd for $C_{16}H_{21}BrN_4O$: C, 52.61; H, 5.79; N, 15.35. Found: C, 52.45; H, 5.80; N, 15.25.

2,3-Dihydro-8-(1-pyrrolyl)-1,2,4-triazolo[4,3-*a*]pyridine-3-spiro-(3′-methoxycyclopentane) Hydrobromide (59) **3** (2 g, 11.5 mmol) and 3-methoxycyclopentanone (1.13 g, 12.6 mmol) afforded **59** (2 g, 52%), mp 180 °C (EtOH). IR ν_{max}^{KBr} cm^{-1}: 3350, 2950, 1640 (NH_2^+). *Anal.* Calcd for $C_{15}H_{19}BrN_4$: C, 53.74; H, 5.71; N, 16.71. Found: C, 53.60; H, 5.69; N, 16.69.

General Procedure for the Preparation of 5,6-Dihydro-4*H*-pyrido[2,3-*c*]-pyrrolo[1,2-*e*]-1,2,5-triazepines and 2,3-Dihydro-8-(1-pyrrolyl)-1,2,4-triazolo[4,3-*a*]pyridines x g of hydrobromide or hydrochloride (x' mmol) were added to a 100 ml aqueous solution of saturated sodium hydrogen carbonate. After stirring at room temperature for 1 h, the obtained precipitate was collected by filtration, washed with 50 ml H_2O, dried and recrystallized in an appropriate solvent.

5,6-Dihydro-4*H*-pyrido[2,3-*c*]pyrrolo[1,2-*e*]-1,2,5-triazepine-4-spiro-4′-tetrahydropyran (43) **36** (2 g, 5.9 mmol). Yield (0.62 g, 41%), mp 210 °C. (Et_2O). IR ν_{max}^{KBr} cm^{-1}: 3260, 3220 (NH). *Anal.* Calcd for $C_{14}H_{16}N_4O$: C, 65.61; H, 6.29; N, 21.86. Found: C, 65.48; H, 6.29; N, 21.82.

5,6-Dihydro-4*H*-pyrido[2,3-*c*]pyrrolo[1,2-*e*]-1,2,5-triazepine-4-spiro-4′-

tetrahydrothiopyran (44) **37** (1.4 g, 3.9 mmol). Yield (0.55 g, 51%) mp 170 °C (Et_2O). IR ν_{max}^{KBr} cm^{-1}: 3270, 3215 (NH). *Anal.* Calcd for $C_{14}H_{16}N_4S$: C, 61.74; H, 5.92; N, 20.57; S, 11.27. Found: C, 61.76; H, 5.94; N, 20.58; S, 11.43.

5,6-Dihydro-4*H*-pyrido[2,3-*c*]pyrrolo[1,2-*e*]-1,2,5-triazepine-4-spiro-3′-tetrahydrothiophene (45) **39** (1.7 g, 5 mmol). Yield (0.5 g, 38%), mp 178 °C (Et_2O). IR ν_{max}^{KBr} cm^{-1}: 3260, 3220 (NH). *Anal.* Calcd for $C_{13}H_{14}N_4S$: C, 60.44; H, 5.46; N, 21.69; S, 12.41. Found: C, 60.20; H, 5.49; N, 21.63; S, 12.33.

5,6-Dihydro-4*H*-pyrido[2,3-*c*]pyrrolo[1,2-*e*]-1,2,5-triazepine-4-spiro-4′-*N*-methylpiperidine (46) **40** (1.65 g, 4.7 mmol). Yield (0.8 g, 62%), mp 190 °C (CH_3CN). IR ν_{max}^{KBr} cm^{-1}: 3220, 3100 (NH). *Anal.* Calcd for $C_{15}H_{19}N_5$: C, 66.89; H, 7.11; N, 26.00. Found: C, 67.00; H, 7.14; N, 26.01.

5,6-Dihydro-4*H*-pyrido[2,3-*c*]pyrrolo[1,2-*e*]-1,2,5-triazepine-4-spiro-4′-*N*-isopropylpiperidine (47) **41** (1.6 g, 4.3 mmol). Yield (0.5 g, 40%), mp 164 °C (Et_2O). IR ν_{max}^{KBr} cm^{-1}: 3260, 3230 (NH). *Anal.* Calcd for $C_{17}H_{23}N_5$: C, 68.66; H, 7.79; N, 23.55. Found: C, 68.68; H, 7.70; N, 23.60.

4-Cyclohexyl-5,6-dihydro-4*H*-pyrido[2,3-*c*]pyrrolo[1,2-*e*]-1,2,5-triazepine (48) **42** (1.65 g, 4.7 mmol). Yield (0.7 g, 55%), mp 116 °C (Et_2O). IR ν_{max}^{KBr} cm^{-1}: 3280, 3220 (NH). *Anal.* Calcd for $C_{16}H_{20}N_4$: C, 71.61; H, 7.51; N, 20.88. Found: C, 71.77; H, 7.54; N, 20.70.

2,3-Dihydro-3-(4-fluorophenyl)-8-(1-pyrrolyl)-1,2,4-triazolo[4,5-*a*]pyridine (60) **49** (0.2 g, 0.6 mmol). Yield (0.1 g, 57%), mp 90 °C (Et_2O). IR ν_{max}^{KBr} cm^{-1}: 3330 (NH). *Anal.* Calcd for $C_{16}H_{13}FN_4$: C, 68.56; H, 4.67; F, 6.78; N, 19.99. Found: C, 68.52; H, 4.68; F, 6.62; N, 19.78.

2,3-Dihydro-3-(4-fluorophenyl)-3-methyl-8-(1-pyrrolyl)-4-1,2,4-triazolo-[4,5-*a*]pyridine (61) **50** (2.2 g, 6.7 mmol). Yield (0.69 g, 35%), mp 120 °C (Et_2O). IR ν_{max}^{KBr} cm^{-1}: 3360 (NH). *Anal.* Calcd for $C_{17}H_{15}FN_4$: C, 69.37; H, 5.14; F, 6.45; N, 19.04. Found: C, 69.24; H, 5.16; F, 6.33; N, 19.05.

2,3-Dihydro-3-(4-fluorophenyl)-3-phenyl-8-(1-pyrrolyl)-1,2,4-triazolo-[4,5-*a*]pyridine (62) **52** (1.5 g, 3.4 mmol). Yield (0.5 g, 42%), mp 160 °C (Et_2O). IR ν_{max}^{KBr} cm^{-1}: 3320 (NH). *Anal.* Calcd for $C_{22}H_{17}FN_4$: C, 74.14; H, 4.81; F, 5.33; N, 15.72. Found: C, 74.20; H, 4.92; F, 5.28; N, 15.72.

2,3-Dihydro-3-(3-pyridyl)-8-(1′-pyrrolyl)-1,2,4-triazolo[4,5-*a*]pyridine (63) **53** (1 g, 2.9 mmol). Yield (0.35 g, 46%), mp 151 °C (Et_2O). IR ν_{max}^{KBr} cm^{-1}: 3120 (NH). *Anal.* Calcd for $C_{15}H_{13}N_5$: C, 68.43; H, 4.98; N, 26.60. Found: C, 68.43; H, 5.02; N, 26.51.

2,3-Dihydro-3-(3-pyridyl)-8-(1′-pyrrolyl)-1,2,4-triazolo[4,5-*a*]pyridine pyridine (64) **54** (0.8 g, 2.2 mmol). Yield (0.3 g, 48%), mp 140 °C (Et_2O). IR ν_{max}^{KBr} cm^{-1}: 3280 (NH), 1550, 1445, 1380, 1370, 660. *Anal.* Calcd for $C_{16}H_{15}N_5$: C, 69.30; H, 5.45; N, 25.25. Found: C, 69.22; H, 5.42; N, 25.28.

2,3-Dihydro-3-methyl-3-(4-pyridyl)-8-(1-pyrrolyl)-1,2,4-triazolo[4,5-*a*]-pyridine (65) **55** (1.5 g, 4.1 mmol). Yield (0.2 g, 17%), mp 126 °C. IR ν_{max}^{KBr} cm^{-1}: 3335 (NH). *Anal.* Calcd for $C_{15}H_{15}N_5$: C, 69.30; H, 5.45; N, 25.25. Found: C, 69.29; H, 5.50; N, 25.28.

References and Notes

1) *a*) J. C. Lancelot, D. Laduree, and M. Robba, *Chem. Pharm. Bull.*, **20**, 4242 (1985); *b*) J. C. Lancelot, H. El Kashef, and M. Robba, *Heterocycles*, **23**, 909 (1985).
2) *a*) J. C. Lancelot, S, Rault, J. M. Gazengel, and M. Robba, *Chem. Pharm. Bull.*, **30**, 1674 (1982); *ibid.*, **31**, 45 (1983); *idem, ibid.*, **31**, 4447 (1984).
3) J. C. Lancelot, S. Rault, N. H. Dung, and M. Robba, *Chem. Pharm. Bull.*, **31**, 3160 (1983).
4) M. Cugnon de Sevricourt, H. El Kashef, S. Rault, and M. Robba, *Synthesis*, **9**, 710 (1981).
5) H. J. Petersen, C. K. Nielsen, and E. Arrigoni-Martelli, *J. Med. Chem.*, **21**, 773 (1978).
6) I. Moriguchi, K. Komatsu, and Y. Matsushita, *J. Med. Chem.*, **23**, 20 (1980).
7) H. J. Petersen, Ger. Patent, 2557438.
8) C. K. Nielsen and E. Arrigoni-Martelli, *Act. Pharmacol. Toxicol.*, **49**, 427, (1981).
9) E. Eilersten, J. W. Hart, M. P. Magnussen, H. Soerensen, and E. Arrigoni-Martelli, *Xenobiotica*, **12**, 177 (1982).
10) E. Mikkelsen and O. L. Pedersen, *Acta Pharmacol. Toxicol.*, **51**, 407 (1982).
11) U. B. Olsen and E. Arrigoni-Martelli, *Eur. J. Pharmacol.*, **88**, 389 (1983).
12) P. Bellemann, A. Schade, and R. Towart, *Proc. Natl. Acad. Sci. U.S.A.*, **80**, 2356 (1983).
13) J. C. A. Van Meel, W. M. Timmermans, and P. A. Van Zwieten, *Eur. J. Pharmacol.*, **92**, 27 (1983).
14) W. L. Lipschitz, Z. Hadidian, and A. Kerpcsar, *J. Pharmacol, Exp. Ther.*, **79**, 97 (1943).
15) W. Rupp, *Arzneim.-Fosrch.*, **27**, 289 (1977).
16) C. M. Kagawa and M. J. Kaim, *Arch. Int. Pharmacodyn.*, **137**, 241 (1962).

Studies on Cardiotonic Agents. V.[1] Synthesis of 1-(6,7-Dimethoxy-4-quinazolinyl)piperidine Derivatives Carrying Various 5-Membered Heterocyclic Rings at the 4-Position

Yuji NOMOTO,*,[a] Haruki TAKAI,[a] Tadashi HIRATA,[b] Masayuki TERANISHI,[b] Tetsuji OHNO,[a] and Kazuhiro KUBO[a]

Pharmaceutical Research Laboratories, Fuji, Kyowa Hakko Kogyo Co., Ltd.,[a] Shimotogari 1188, Nagaizumicho, Shizuoka 411, Japan and Tokyo Research Laboratories, Kyowa Hakko Kogyo Co., Ltd.,[b] Asahimachi 3-6-6, Machidashi, Tokyo 194, Japan. *Received June 6, 1990*

A series of 1-(6,7-dimethoxy-4-quinazolinyl)piperidines carrying various 5-membered heterocycles at the 4-position was synthesized and examined for cardiotonic activity in anesthesized dogs. The (4-oxo-2-thioxo-3-imidazolidinyl)amino derivatives showed the most potent inotropic activity. Marked loss of activity was observed in the 2,4-dihydro-3-thioxo-3*H*-1,2,4-triazolyl, the 2,4-dihydro-3-oxo-3*H*-pyrazolyl and the (2,3-dihydro-2-thioxo-3*H*-1,3,4-thiadiazol-5-yl)amino derivatives. The synthesis and structure–activity relationships are discussed.

Keywords cardiotonic agent; structure–activity relationship; piperidine; quinazoline; 3-amino-4-oxo-2-thioxoimidazolidine; 2,4-dihydro-3-thioxo-3*H*-1,2,4-triazole; 2,4-dihydro-3-oxo-3*H*-pyrazole; 5-amino-2,3-dihydro-2-thioxo-3*H*-1,3,4-thiadiazole

The extensive search to find a non-glycoside, non-catecholamine replacement for digitalis led to the discovery of several new cardiotonic drugs.[2] In a previous paper,[1] we described the synthesis and the cardiotonic activities of a series of 1-(6,7-dimethoxy-4-quinazolinyl)piperidine derivatives carrying 5-substituted 2,4-dioxo- and 4-oxo-2-thioxoimidazolidine ring (**1**, **2**) (Chart 1). These structure–activity relationship studies demonstrated the beneficial effects of the isopropyl and the *sec*-butyl substituents at the 5-position of the imidazolidine ring. These findings prompted us to carry out the structural modification of **1** and **2** with other 5-membered heterocyclic rings. The present paper describe the synthesis and the pharmacological evaluation of 1-(6,7-dimethoxy-4-quinazolinyl)piperidine derivatives carrying 3-amino-4-oxo-2-thioxoimidazolidine, 2,4-dihydro-3-thioxo-3*H*-1,2,4-triazole, 2,4-dihydro-3-oxo-3*H*-pyrazole and 5-amino-2,3-dihydro-2-thioxo-3*H*-1,3,4-thiadiazole rings at the 4-position, as summarized in Table I.

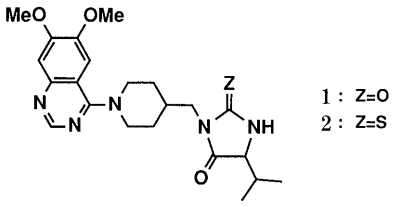

Chart 1

Chemistry The synthetic sequences leading to the 2,3-dihydro-2-thioxo-3*H*-1,3,4-thiadiazoles are outlined in Chart 2. The thiosemicarbazides (**4**, **7**) prepared from the isothiocyanates (**3**, **6**)[1] with hydrazine hydrate were treated with 2 eq of CS_2 in the presence of Et_3N in dimethylformamide (DMF) to afford the thiadiazoles **5** and **8**, respectively (method A, Chart 2). The structure of **5** was assigned mainly on the basis of its proton nuclear magnetic resonance (^{1}H-NMR) spectrum which exhibited a signal of the NH proton at the 5-position of the thiadiazole ring at δ 7.68 ppm as a broad triplet.

The 2,4-dihydro-3-thioxo-3*H*-1,2,4-triazol-4-yl derivatives (**9**, **10**) were obtained by ring closure reaction of **7** with appropriate carboxylic acid (method B). Compound **9** was converted to the methylthiotriazole (**11**) by alkylation with MeI in the presence of NaH in DMF (method C, Chart 3).

We also investigated the synthesis of the 2,4-dihydro-3-thioxo-3*H*-1,2,4-triazol-2-yl derivatives. In order to synthesize the ring system, we attempted to prepare the hydrazine (**15**) as intermediate. The 4-piperidone (**12**)[3] was condensed with *tert*-butyl carbazate to give the hydrazone (**13**) which was reduced with $NaCNBH_3$[4] to afford the Boc-hydrazine

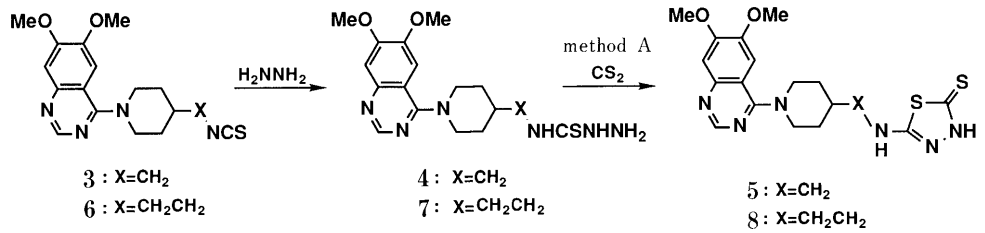

Chart 2

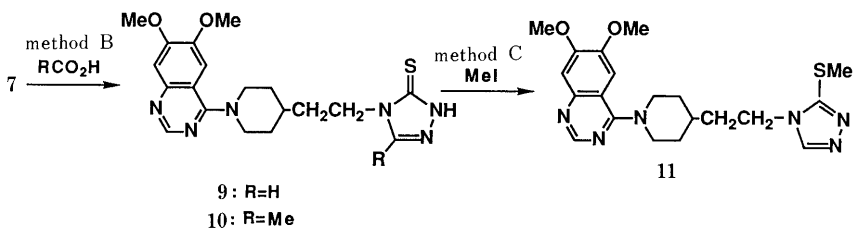

Chart 3

TABLE I

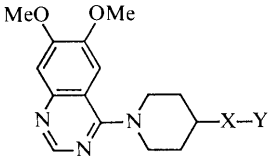

Compd. No.	X	Y	Method yield (%)	mp (°C) (Crystn. solv.)	Formula	Analysis (%) Calcd (Found)		
						C	H	N
5	CH_2	(2,3-Dihydro-2-thioxo-3*H*-1,3,4-thiadiazol-5-yl)amino	A 58	220—225 (DMF–H_2O)	$C_{18}H_{22}N_6O_2S_2 \cdot 1/4H_2O$	51.11 (50.91)	5.36 5.70	19.87 19.46)
8	CH_2CH_2	(2,3-Dihydro-2-thioxo-3*H*-1,3,4-thiadiazol-5-yl)amino	A 47	142—145 (DMF–H_2O)	$C_{19}H_{24}N_6O_2S_2 \cdot 1/2H_2O$	51.68 (51.91)	5.72 5.87	19.02 18.77)
9	CH_2CH_2	2,4-Dihydro-3-thioxo-3*H*-1,2,4-triazol-4-yl	B 74	188—190 (DMF–H_2O)	$C_{19}H_{24}N_6O_2S$	56.98 (56.81)	6.04 6.13	20.98 20.75)
10	CH_2CH_2	5-Methyl-2,4-dihydro-3-thioxo-3*H*-1,2,4-triazol-4-yl	B 85	256—258 (DMF–H_2O)	$C_{20}H_{26}N_6O_2S$	57.95 (57.83)	6.32 6.51	20.27 20.29)
11	CH_2CH_2	3-Methylthio-4*H*-1,2,4-triazol-4-yl	C 46	148—150 (DMF–H_2O)	$C_{20}H_{26}N_6O_2S$	57.95 (57.68	6.32 6.41	20.27 19.91)
17	—	5-Isopropyl-2,4-dihydro-3-thioxo-3*H*-1,2,4-triazol-2-yl	D 33	269—271 (DMF–H_2O)	$C_{20}H_{26}N_6O_2S$	57.95 (57.83	6.32 6.00	20.27 20.34)
19[a]	—	5-*sec*-Butyl-2,4-dihydro-3-thioxo-3*H*-1,2,4-triazol-2-yl	D 30	208—211 (MeOH–Et_2O)	$C_{21}H_{28}N_6O_2S \cdot HCl \cdot 1/2H_2O$	53.21 (53.18	6.38 6.46	17.73 17.68)
20	—	5-Methyl-2,4-dihydro-3-oxo-3*H*-pyrazol-2-yl	E 76	228—232 (DMF–H_2O)	$C_{19}H_{23}N_5O_3$	61.77 (61.80	6.28 6.22	18.96 18.71)
21	—	5-Isopropyl-2,4-dihydro-3-oxo-3*H*-pyrazol-2-yl	E 83	182 (DMF–H_2O)	$C_{21}H_{27}N_5O_3$	63.45 (63.33	6.86 7.05	17.61 17.26)
22	—	4,5-Dimethyl-2,4-dihydro-3-oxo-3*H*-pyrazol-2-yl	E Quant.	254—256 (DMF–H_2O)	$C_{20}H_{25}N_5O_3$	62.65 (62.38	6.57 6.73	18.26 18.51)
23	—	4-Butyl-5-methyl-2,4-dihydro-3-oxo-3*H*-pyrazol-2-yl	E 87	120—123 (DMF–H_2O)	$C_{23}H_{31}N_5O_3 \cdot 1/2H_2O$	63.57 (63.21	7.42 7.64	16.12 15.84)
24	—	3,4,5,6,7,8-Hexahydro-3-oxo-2*H*-indazol-2-yl	E 37	214—216 (DMF–H_2O)	$C_{22}H_{27}N_5O_3$	64.53 (64.32	6.65 6.70	17.10 16.83)
28	—	(5-Isopropyl-4-oxo-2-thioxo-3-imidazolidinyl)amino	F 52	240—244 (DMF–H_2O)	$C_{21}H_{28}N_6O_3S \cdot 1/2H_2O$	55.61 (55.43	6.44 6.61	18.53 18.21)
29	—	(5-*sec*-Butyl-4-oxo-2-thioxo-3-imidazolidinyl)amino	F 42	228—231 (DMF–H_2O)	$C_{22}H_{30}N_6O_3S$	57.62 (57.66	6.59 6.82	18.33 17.93)
30	—	(5-Isopropyl-2,4-dioxo-3-imidazolidinyl)amino	G 34	130—133 (DMF–H_2O)	$C_{21}H_{28}N_6O_4 \cdot H_2O$	56.49 (56.65	6.77 6.44	18.82 19.13)

a) As HCl salt.

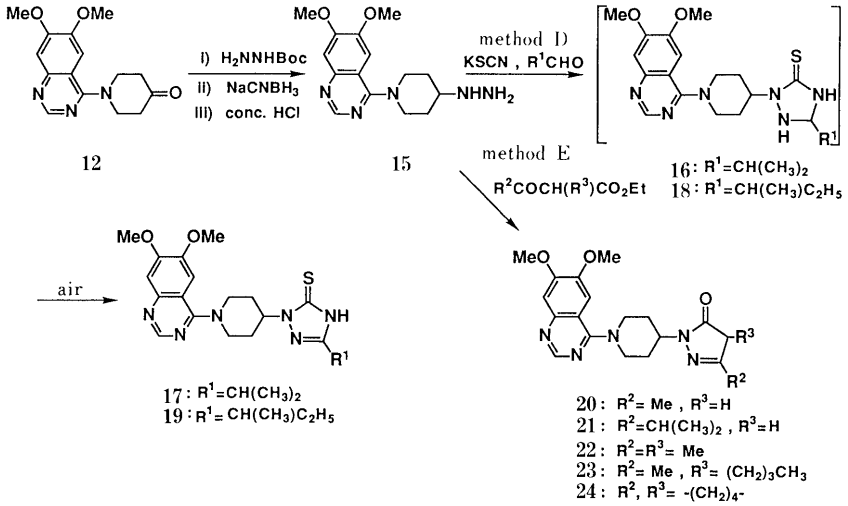

Chart 4

(**14**). Deprotection of **14** gave the hydrazine (**15**) as HCl salt in good yield. An attempt to get the free base of **15** failed because of instability of the compound under alkaline condition. Reaction of **15** with isobutylaldehyde and KSCN in 1 N HCl for 15 h afforded the 5-isopropyl-2-thioxo-1,2,4-triazoline (**16**)[5] which was not isolated because of instability under aerobic conditions, followed by air oxidation of **16** under alkaline conditions to afford the triazole **17**. The

5-isobutyl derivative (**19**) was similarly obtained (method D, Chart 4).

Compound **15** was also converted to the 2,4-dihydro-3-oxo-3*H*-pyrazole derivatives (**20**—**24**) by treatment with some β-ketocarboxylic acid esters in the presence of Et_3N in 50% AcOH (method E, Chart 4). The reaction did not proceed in the absence of Et_3N.

The synthesis of the (4-oxo-2-thioxoimidazolidinyl)amino derivatives (**28**, **29**) was achieved as follows. Treatment of **12** with methyl hydrazinocarbodithioate[6] afforded the hydrazonecarbodithioate (**25**), and subsequent reduction of **25** with $NaBH_4$ gave the 4-piperidylhydrazinocarbodithioate (**26**). In ^{1}H-NMR spectra, **25** showed a broad singlet due to NH at δ 10.80 ppm, and **26** showed two broad singlets due to NH protons at δ 10.63 ppm (assignable to CSNH) and δ 5.58 ppm (assignable to NHNHCS). Condensation of **26** with DL-valine methyl ester gave no triazinyl derivative (**27**) but the (4-oxo-2-thioxo-3-imidazolidinyl)amino derivative (**28**) (method F, Chart 5). The structure of **28** was confirmed mainly on the basis of the ^{1}H-NMR spectrum. The resonances of two NH protons appeared at δ 7.70 ppm as broad singlet and δ 4.95 ppm as doublet (J=3 Hz). Considering the effects of the neighboring group, the signal at δ 7.70 ppm was assignable to CSNH proton, and that at

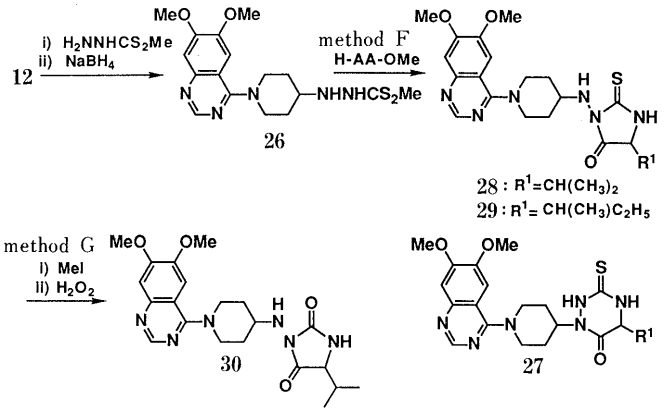

Chart 5

TABLE II. Cardiotonic Activity of Some Quinazoline Derivatives in Anesthetized Dogs

Compd. No.	Cardiotonic activity			
	LV$dP/dt$ max[a] (Δ%)		Relative[b] potency	Duration (min)
5	2.4	(2)	—	—
8	5.9	(2)	0.14	10
9	30.4±8.6		0.81	15
10	27.1±3.7		0.74	10
11	34.8±7.7		0.99	15
17	19.2	(2)	0.60	10
19	22.1	(2)	0.69	10
20	10.1	(2)	0.26	3
21	7.8	(2)	0.24	3
22	−9.2	(2)	—	—
23	12.1	(2)	0.26	5
28	43.7±5.3		1.03	>60
29	44.1±1.5		1.04	60

a) Each value represents the mean±standard error of triplicate experiments except where otherwise noted in parentheses. b) Compared to the percent increase in LV$dP/dt$ max observed with milrinone (0.05 mg/kg) in the same dog.

δ 4.95 ppm to CHNHN proton, suggesting the 5-membered structure. S-Alkylation of **28** with MeI in alkaline condition and subsequent oxidation with 30% H_2O_2 in 50% AcOH at 0—5 °C gave the hydrolyzed product, the (2,4-dioxo-3-imidazolidinyl)amino derivative (**30**) in 35% yield (method G, Chart 5). Compound **30** showed the signal of NH proton at δ 4.43 ppm as doublet (J=3 Hz), also suggesting the 5-membered structure.

Biological Results Cardiotonic activities of the compounds listed in Table I were evaluated in anesthetized open chest dogs using procedures previously described.[7] The results of the test are shown in Table II. The positive cardiotonic activity of the compounds was determined by measuring percent increase in maximum dP/dt left ventricular pressure (LVdP/dt max, Δ%) after i.v. administration (0.15 mg/kg) in anesthetized mogrel dogs of either sex (8—15 kg). The potency of cardiotonic activity of the test compounds was compared with milrinone[8] (0.05 mg/kg i.v.). Relative potency was calculated as the LVdP/dt max of each compound to that of milrinone (milrinone=1) in the same dog.

With regard to the effect of the substituents of the piperidine ring at the 4-position, it appeared that the introduction of the thiadiazole (**5**, **8**) and the pyrazole (**20**—**23**) rings resulted in diminished cardiotonic activity. The triazoles (**9**—**11**, **17**, **19**) showed moderate activity of short duration. The imidazolidinyl amino derivatives (**28**, **29**) showed potent and long-lasting activity. In a previous paper,[1] we reported that 2,4-dioxo- and 4-oxo-2-thioxoimidazolidine derivatives (**1**, **2**) exhibited potent and long-lasting cardiotonic activity. These findings suggested that presence of the 2,4-dioxo- or 4-oxo-2-thioxoimidazolidine ring at the 4-position of the piperidine was essential for improved cardiotonic activity, and replacement of the methylene group between the piperidine and the imidazolidine rings with an amino group retained the activity. Compound **28** showed potent oral activity comparable to that of milrinone[8] with longer duration of action (data not shown).

Experimental

All melting points were determined on a Büchi 510 micro melting point apparatus and are uncorrected. Infrared (IR) spectra were measured on a JASCO IR810 spectrophotometer. ^{1}H-NMR spectra were measured on a Hitachi R-90H and a JEOL JNM-GX-270 spectrometer using tetramethylsilane (TMS) as an internal standard.

[1-(6,7-Dimethoxy-4-quinazolinyl)-4-piperidyl]methylthiosemicarbazide (4) A solution of **3** (29.0 g, 82 mmol) in MeOH (300 ml) was added dropwise to a solution of hydrazine hydrate (100 ml) in MeOH (200 ml) over a 15 min period at room temperature. The reaction mixture was concentrated in reduced pressure and the residue was partitioned between $CHCl_3$ and water. The organic layer was dried over $MgSO_4$ and evaporated. Crystallization of the residue from MeOH–diisopropyl ether afforded **4** (28.3 g, 89%) which was used in the next reaction without further purification. An analytical sample was recrystallized from MeOH–diisopropyl ether, mp 194—195 °C. *Anal.* Calcd for $C_{17}H_{24}N_6O_2S$: C, 54.23; H, 6.44; N, 22.31. Found: C, 54.51; H, 6.40; N, 22.03. IR (KBr): 1620, 1580, 1540 cm^{-1}. ^{1}H-NMR (DMSO-d_6) δ: 8.57 (1H, br, NH), 8.51 (1H, s, Ar-H), 7.86 (1H, br, NH), 7.20 (1H, s, Ar-H), 7.11 (1H, s, Ar-H), 4.50 (2H, br, NH_2), 4.13 (2H, br, piperidine), 3.92, 3.90 (each 3H, s, CH_3O), 3.60—2.80 (7H, m, piperidine, $-CH_2-$), 1.80 (m, 2H, piperidine).

Method A. 5-[1-(6,7-Dimethoxy-4-quinazolinyl)-4-piperidyl]methylamino-2,3-dihydro-2-thioxo-3*H*-1,3,4-thiadiazole (5) A mixture of **4** (3.0 g, 8.0 mmol), Et_3N (2.2 ml, 16 mmol) and CS_2 (0.96 ml, 16 mmol) in DMF (20 ml) was stirred for 30 min at room temperature, then at 100 °C for 1.5 h. The reaction mixture was concentrated under reduced pressure, and

the residue was partitioned between $CHCl_3$ and water. The organic layer was washed with water, dried with $MgSO_4$ and evaporated. The residue was crystallized from MeOH to afford crude **5** as crystals which were recrystallized from DMF–water to give pure **5** (1.7 g, 58%). IR (KBr): 1620, 1570, 1500 cm^{-1}. ^{1}H-NMR (DMSO-d_6) δ: 13.30 (1H, br, NH), 8.52 (1H, s, Ar-H), 7.68 (1H, br, NH), 7.21 (1H, s, Ar-H), 7.12 (1H, s, Ar-H), 4.17 (2H, d, J=13 Hz, piperidine), 3.93, 3.91 (each 3H, s, CH_3O), 3.42—3.00 (7H, m, piperidine, $-CH_2-$), 1.85 (2H, m, piperidine). Compound **8** was obtained by a procedure similar to that described above except that **7** was used as starting material.

Method B. 4-[2-{1-(6,7-Dimethoxy-4-quinazolinyl)-4-piperidyl}ethyl]-2,4-dihydro-3-thioxo-3*H*-1,2,4-triazole (9) Compound **7** (10.0 g, 26 mmol) was dissolved in formic acid (300 ml) and the resulting solution was stirred for 4 h at 100 °C, then concentrated. The residue was neutralized with 2 N NaOH and partitioned between $CHCl_3$ and water. The organic layer was dried over $MgSO_4$, then evaporated. The residual crystals were recrystallized from DMF–water to give **9** (7.6 g, 74%). IR (KBr): 1600, 1570, 1500 cm^{-1}. ^{1}H-NMR (DMSO-d_6) δ: 8.63 (1H, s, Ar-H), 8.39 (1H, s, Ar-H), 7.25 (1H, s, Ar-H), 7.08 (1H, s, Ar-H), 6.20 (1H, br, NH), 4.18 (2H, d, J=13 Hz, piperidine), 4.00, 3.98 (each 3H, s, CH_3O), 3.50—1.42 (11, m, piperidine, $-CH_2CH_2-$). Compound **10** was obtained by a similar procedure to that described above except that acetic acid was used instead of formic acid.

Method C. 4-[2-{1-(6,7-Dimethoxy-4-quinazolinyl)-4-piperidyl}ethyl]-3-methylthio-4*H*-1,2,4-triazole (11) A mixture of **9** (4.0 g, 10 mmol) and NaH (60% oil suspension) (0.60 g, 15 mmol) in DMF was stirred for 15 min at room temperature and MeI (0.63 ml, 10 mmol) was added. The reaction mixture was stirred for 15 min and poured into water and neutralized with 1 N HCl, then extracted with $CHCl_3$. The organic layer was washed with water, dried and evaporated. The residue was purified by column chromatography (SiO_2, 100 g, 4% MeOH–$CHCl_3$) to afford residual **11** as crystals which were recrystallized from DMF–water to give pure **11** (1.9 g, 46%). IR (KBr): 1620, 1580 cm^{-1}. ^{1}H-NMR (DMSO-d_6) δ: 8.65 (1H, s, Ar-H), 8.40 (1H, s, Ar-H), 7.23 (1H, s, Ar-H), 7.08 (1H, s, Ar-H), 4.17 (2H, d, J=13 Hz, piperidine), 4.02, 4.00 (each 3H, s, CH_3O), 3.62—1.45 (11H, m, piperidine, $-CH_2CH_2-$), 3.17 (3H, s, CH_3S).

1-(6,7-Dimethoxy-4-quinazolinyl)-4-piperidinone *tert*-Butoxycarbonylhydrazone (13) A solution of **12** (2.6 g, 8.9 mmol) and *tert*-butyl carbazate (1.2 g, 9.1 mmol) in MeOH (30 ml) was stirred for 30 min at room temperature. The reaction mixture was evaporated and the residue was crystallized from Et_2O to give crude crystals of **13** (3.1 g, 86%). The crystals were used in the next reaction without further purification. An analytical sample was recrystallized from DMF–water to give pure **13**, mp 194—195 °C. *Anal.* Calcd for $C_{20}H_{27}N_5O_4 \cdot H_2O$: C, 57.27; H, 6.97; N, 16.70. Found: C, 57.58; H, 6.81; N, 16.53. IR (KBr); 1725, 1620 cm^{-1}. ^{1}H-NMR ($CDCl_3$) δ: 8.66 (1H, s, Ar-H), 7.64 (1H, br. NH), 7.27 (1H, s, Ar-H), 7.13 (1H, s, Ar-H), 4.02, 4.00 (each 3H, s, CH_3O), 3.90 (4H, m, piperidine), 2.65 (4H, m, piperidine), 1.58 (9H, s, *tert*-butyl).

***N*-[1-(6,7-Dimethoxy-4-quinazolinyl)-4-piperidyl]-*N'*-*tert*-butoxycarbonylhydrazine (14)** A solution of **13** (3.0 g, 7.5 mmol) and $NaCNBH_3$ (0.47 g, 7.5 mmol) in 50% AcOH (20 ml) was stirred for 15 min at room temperature, then concentrated. The residue was neutralized with 1 N NaOH and extracted with $CHCl_3$. The organic layer was washed with water, dried over $MgSO_4$ and evaporated to dryness. The residual crystals were recrystallized from DMF–water to give **14** (2.9 g, 95%), mp 192—193 °C. *Anal.* Calcd for $C_{20}H_{29}N_5O_4$: C, 59.54; H, 7.24; N, 17.36. Found: C, 59.22; H, 7.24; N, 17.48. IR (KBr): 1720, 1620 cm^{-1}. ^{1}H-NMR ($CDCl_3$) δ: 8.62 (1H, s, Ar-H), 7.20 (1H, s, Ar-H), 7.08 (1H, s, Ar-H), 6.18 (1H, br, NH), 4.22 (2H, m, piperidine), 4.02, 4.00 (each 3H, s, CH_3O), 3.60—1.63 (7H, m, piperidine), 1.52 (9H, s, *tert*-butyl).

1-(6,7-Dimethoxy-4-quinazolinyl)-4-piperidylhydrazine·2HCl (15·2HCl) A solution of **14** (4.0 g, 10.0 mmol) in conc. HCl (4 ml) was stirred for 30 min at room temperature. MeOH (15 ml) was added to the mixture and the precipitated crystals were collected by filtration and recrystallized from MeOH–Et_2O to afford **15**·2HCl (3.6 g, 96%), mp 245 °C (dec.). *Anal.* Calcd for $C_{15}H_{21}N_5O_2 \cdot 2HCl$: C, 47.88; H, 6.16; N, 18.61. Found: C, 47.93; H, 6.00; N, 18.50. IR (KBr): 1620, 1590 cm^{-1}. ^{1}H-NMR (DMSO-d_6–D_2O) δ: 8.61 (1H, s, Ar-H), 7.28 (1H, s, Ar-H), 7.19 (1H, s, Ar-H), 4.65 (2H, m, piperidine), 4.00, 3.96 (each 3H, s, CH_3O), 3.65 (2H, m, piperidine), 2.55—1.58 (5H, m, piperidine).

Method D. 2-[1-(6,7-Dimethoxy-4-quinazolinyl)-4-piperidyl]-2,4-dihydro-5-isopropyl-3-thioxo-3*H*-1,2,4-triazole (17) A mixture of **15**·2HCl (3.0 g, 8.0 mmol), KSCN (1.0 g, 10 mmol) and isobutyraldehyde (1.0 ml, 11 mmol) in 1 N HCl (30 ml) was stirred for 10 min at room temperature. MeOH (50 ml) was added to the mixture, then stirred for 15 h. The solvent was removed by decantation, the residual **16** was dissolved in a mixture of MeOH (20 ml) and $CHCl_3$ (10 ml), and the solution was adjusted to pH 9 with 2 N NaOH. Air was passed through the solution for 3 h at room temperature, then the reaction mixture was evaporated. The resultant residue was purified by column chromatography (SiO_2, 100 g, 3.5% MeOH–$CHCl_3$) to give crude **17** which was recrystallized from DMF–water to give pure **17** (1.1 g, 33%). IR (KBr): 1620, 1580 cm^{-1}. ^{1}H-NMR ($CDCl_3$) δ: 12.50 (1H, br, NH), 8.70 (1H, s, Ar-H), 7.42 (1H, s, Ar-H), 7.13 (1H, s, Ar-H), 5.00 (1H, m, piperidine), 4.43 (2H, m, piperidine), 4.04, 4.00 (each 3H, s, CH_3O), 3.35—2.13 (7H, m, piperidine, CH), 1.37, 1.35 (each 3H, d, J=7 Hz, CH_3). A similar procedure as that described above was carried out except that 2-methylbutyraldehyde was used instead of isobutyraldehyde to give compound **19**.

Method E. 2-[1-(6,7-Dimethoxy-4-quinazolinyl)-4-piperidyl]-2,4-dihydro-5-isopropyl-3-oxo-3*H*-pyrazole (21) A solution of **15**·2HCl (3.0 g, 8.0 mmol), Et_3N (4.2 ml, 30 mmol) and ethyl isobutyrylacetate (1.3 ml, 8.0 mmol) in 50% AcOH (30 ml) was stirred for 6 h at room temperature. The reaction mixture was neutralized with 2 N NaOH and extracted with $CHCl_3$. The organic layer was washed with water, dried and evaporated to dryness, and the crystalline residue was recrystallized from DMF–water to give **21** (2.4 g, 76%). IR (KBr): 1620, 1570 cm^{-1}. ^{1}H-NMR ($CDCl_3$) δ: 8.68 (1H, s, Ar-H), 7.27 (1H, s, Ar-H), 7.13 (1H, s, Ar-H), 4.40—1.90 (10H, m, piperidine, CH), 4.03, 4.00 (each 3H, s, CH_3O), 3.24 (2H, s, CH_2), 1.20, 1.18 (each 3H, d, J=7 Hz, CH_3). Compounds **20**, **22**—**24** were obtained by a similar procedure as that described above except that ethyl acetoacetate, ethyl 2-methylacetoacetate, ethyl 2-butylacetoacetate and ethyl 2-oxocyclohexanecarboxylate were used, respectively, instead of ethyl isobutyrylacetate.

Methyl 1-(6,7-Dimethoxy-4-quinazolinyl)-4-piperidylidenehydrazinocarbodithioate (25) A mixture of **12** (8.0 g, 28 mmol) and methyl hydrazinecarbodithioate[6] (3.4 g, 28 mmol) in MeOH (100 ml) was stirred for 1 h at room temperature. The precipitated crystals were collected by filtration, washed with MeOH and dried to afford crude **25** (8.0 g, 74%). The crystals were used without further purification in the next reaction. An analytical sample was recrystallized from DMF–water, mp 189—190 °C. *Anal.* Calcd for $C_{17}H_{21}N_5O_2S_2$: C, 52.15; H, 5.42; N, 17.88. Found: C, 52.03; H, 5.71; N, 17.63. IR (KBr): 1620 cm^{-1}. ^{1}H-NMR ($CDCl_3$) δ: 10.80 (1H, br, NH), 8.58 (1H, s, Ar-H), 7.23 (2H, s, Ar-H), 3.96 (6H, s, CH_3O), 3.90—2.55 (8H, m, piperidine), 2.46 (3H, s, SCH_3).

Methyl *N'*-[1-(6,7-Dimethoxy-4-quinazolinyl)-4-piperidyl]hydrazinocarbodithioate (26) A solution of **25** (8.0 g, 20 mmol) and $NaBH_4$ (1.2 g, 32 mmol) in MeOH (20 ml) was stirred for 40 min at room temperature, and neutralized with 1 N HCl. The resulting mixture was extracted with $CHCl_3$, then the organic layer was washed with water, dried and concentrated under reduced pressure. The residue was crystallized with Et_2O to give crude **26** (5.9 g, 73%). The crystals were used in the next reaction without further purification. An analytical sample was recrystallized from DMF–water, mp 145—146 °C. *Anal.* Calcd for $C_{17}H_{23}N_5O_2S_2$: C, 51.88; H, 5.90; N, 17.79. Found: C, 51.80; H, 5.63; N, 17.58. IR (KBr): 1620 cm^{-1}. ^{1}H-NMR ($CDCl_3$) δ: 10.63 (1H, br, NH), 8.47 (1H, s, Ar-H), 7.15 (1H, s, Ar-H), 7.06 (1H, s, Ar-H), 5.58 (1H, br, NH), 4.08 (2H, m, piperidine), 3.93 (6H, s, CH_3O), 3.20—1.43 (7H, m, piperidine), 2.33 (3H, s, SCH_3).

Method F. 3-[1-(6,7-Dimethoxy-4-quinazolinyl)-4-piperidyl]amino-5-isopropyl-4-oxo-2-thioxoimidazolidine (28) A mixture of **26** (3.1 g, 7.8 mmol), DL-valine methyl ester·HCl (2.6 g, 16 mmol) and Et_3N (2.2 ml, 16 mmol) in DMF (30 ml) was stirred for 5 h at 110 °C. The reaction mixture was concentrated under reduced pressure, then the residue was mixed with water and extracted with $CHCl_3$. The organic layer was dried and evaporated to dryness, and the residue was purified by column chromatography (SiO_2, 150 g, 5% MeOH–$CHCl_3$) to give **28** (1.8 g, 52%) as crystals. An analytical sample was recrystallized from DMF–water. IR (KBr): 1760, 1580 cm^{-1}. ^{1}H-NMR ($CDCl_3$) δ: 8.54 (1H, s, Ar-H), 7.70 (1H, br, NH), 7.31 (1H, s, Ar-H), 7.08 (1H, s, Ar-H), 4.95 (1H, d, J=3 Hz, NH), 4.15 (2H, m, piperidine), 4.03, 3.97 (each 3H, s, CH_3O), 3.50—1.75 (9H, m, piperidine, CH, CH), 1.12, 0.98 (each 3H, d, J=7 Hz, CH_3). Compound **29** was obtained by a similar procedure as that described above except that DL-isoleucine methyl ester·HCl was used instead of DL-valine methyl ester·HCl.

Method G. 3-[1-(6,7-Dimethoxy-4-quinazolinyl)-4-piperidyl]-amino-5-isopropyl-2,4-dioxoimidazolidine (30) MeI (1.1 ml, 18 mmol) was added to a mixture of **28** (4.5 g, 9.4 mmol) and K_2CO_3 (2.7 g, 20 mmol) in a mixture of MeOH (20 ml) and $CHCl_3$ (20 ml), then the whole was stirred for 1 h at room temperature. The precipitated salts were removed by filtration and the filtrate was concentrated. The resulting oil was dissolved in 50%

AcOH (30 ml), then 30% H_2O_2 (1.0 ml) was added to the solution with ice-cooling. After stirring for 1 h at 0—5 °C, the solution was adjusted to pH 10 with 2 N NaOH and extracted with $CHCl_3$. The organic layer was washed with saturated $NaHSO_3$ and water, then concentrated under reduced pressure. The resulting residue was purified by column chromatography (SiO_2, 100 g, 5% MeOH–$CHCl_3$) to give crystalline **30** which was recrystallized from DMF–water to give pure **30** (1.4 g, 34%). IR (KBr): 1780, 1720, 1620 cm^{-1}. ^{1}H-NMR ($CDCl_3$) δ: 8.65 (1H, s, Ar-H), 7.37 (1H, s, Ar-H), 7.08 (1H, s, Ar-H), 6.12 (1H, s, NH), 4.43 (1H, d, J=3 Hz, NH), 4.20 (2H, m, piperidine), 4.03, 3.98 (each 3H, s, CH_3O), 3.42—1.70 (9H, m, piperidine, CH, CH), 1.08, 0.95 (each 3H, d, J=7 Hz, CH_3).

References and Notes

1) Part IV: Y. Nomoto, H. Obase, H. Takai, H. Hirata, M. Teranishi, T. Ohno and K. Kubo, *Chem. Pharm. Bull.*, **38**, 3014 (1990).
2) For a recent review; M. D. Taylor, I. Sircar and R. P. Steffen, *Annu. Rep. Med. Chem.*, **22**, 85 (1987).
3) J. C. Danilewicz, A. G. Evans, A. L. Ham and C. Thomson, Ger. Patent 0485 (1979) [*Chem. Abstr.*, **92**, 41948*h* (1980)].
4) H. E. Baumgarten, P. Y-N. Chen, H. W. Taylor and D-R. Hwang, *J. Org. Chem.*, **41**, 3805 (1976).
5) I. Arai, *Bull. Chem. Soc. Jpn.*, **46**, 2215 (1973).
6) D. L. Klayman, J. P. Scovill, J. Bruce and J. F. Bartosevich, *J. Med. Chem.*, **27**, 84 (1984).
7) Part I: Y. Nomoto, H. Obase, H. Takai, H. Hirata, M. Teranishi, J. Nakamura and K. Kubo, *Chem. Pharm. Bull.*, **38**, 1591 (1990).
8) A. A. Alousi, J. M. Canter, M. J. Montenaro. D. J. Fort and R. A. Ferrari, *Fed. Proc., Fed. Am. Soc. Exp. Biol.*, **410**, 663 (1981).

Novel 1,4-Dihydropyridine Calcium Antagonists. II. Synthesis and Antihypertensive Activity of 3-[4-(Substituted Amino)phenylalkyl]ester Derivatives

Atsuyuki ASHIMORI, Taizo ONO, Yoshihisa INOUE, Satoshi MORIMOTO, Masahiro EDA, Takeshi UCHIDA, Yutaka OHTAKI, Yoshiyuki FUJINO, Hideaki KIDO, Yasushi OGURA, Chikara FUKAYA,* Masahiro WATANABE, and Kazumasa YOKOYAMA

Research Division, The Green Cross Corporation, 1180–1, Shodaiotani 2-chome, Hirakata-shi, Osaka 573, Japan. *Received June 11, 1990*

Novel 1,4-dihydropyridine derivatives bearing 3-[4-(substituted amino)phenylalkyl]ester side chains were prepared and tested for their antihypertensive activity in spontaneously hypertensive rats. Most compounds showed a more potent antihypertensive effect and a longer duration of action than nicardipine. The derivatives with a benzhydrylpiperazinyl and a benzhydrylpiperidinyl group were distinctive. 2-[4-(4-Benzhydryl-1-piperazinyl)phenyl]ethyl methyl 1,4-dihydro-2,6-dimethyl-4-(3-nitrophenyl)-3,5-pyridinedicarboxylate (4e), its 4-(4-cyano-2-pyridyl) analogue (4f), its 3-[4-(4-benzhydryl-1-piperazinyl)phenyl]propyl ester analogue (4h), its 2-[4-(4-benzhydryl-1-piperidinyl)phenyl]ethyl ester analogue (4j), and its 2-[4-(1-benzhydryl-4-piperidinyl)phenyl]ethyl ester analogue (4k) were selected as candidates for further pharmacological investigations.

Keywords 1,4-dihydropyridine-3-[4-(substituted amino)phenylalkyl]ester; calcium antagonist; antihypertensive effect; benzhydrylpiperazinyl group; benzhydrylpiperidinyl group; spontaneously hypertensive rat

Introduction

In a previous paper,[1] we reported the syntheses and hypotensive effects of 4-(substituted pyridyl)-1,4-dihydropyridine derivatives, and three compounds (**1**, **2**, and **3**) were selected as candidates for further elaboration of their structures (Fig. 1).

We prepared 1,4-dihydropyridine calcium antagonists which have a novel ester side chain containing one or more amine functions and a benzene ring placed between the amine and the alkylene groups, expecting that the metabolism could be delayed to some extent by introducing such functions. We are interested in how the lipophilic benzene ring interacts with a receptor and influence its pharmacological properties. Although there are a few reports[2] on such derivatives bearing alkyl-, alkoxy-, or halo-substituted phenylalkyl ester side chains, their pharmacological profiles have never been reported in detail. Alkylamino and aralkylamino, in particular, either piperidinyl or piperazinyl with a benzhydryl group were selected as functional groups for the substituent on the benzene ring, because this type of moiety has been employed in some vasodilating drugs (*e.g.*, cinnarizine[3] and flunarizine[3]) and a dihydropyridine calcium antagonist CV-4093 (manidipine).[4]

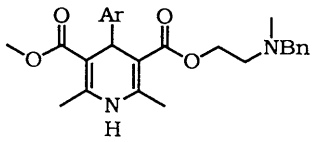

1 : Ar= 4-CN-2-Py

2 : Ar= 3-CF_3-2-Py

3 : Ar= 2-CF_3-3-Py

Fig. 1

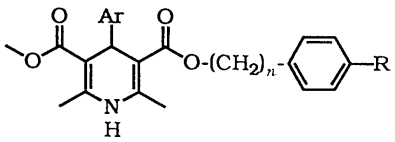

4

Ar : 3-NO_2-Ph, 4-CN-2-Py, and 3-CF_3-2-Py

R : dimethylamino, dibenzylamino, benzhydrylpiperazino, and benzhydrylpiperidinyl

n = 2 or 3

Fig. 2

Thus, we synthesized the series of compounds shown in Fig. 2 and some related compounds and tested for their antihypertensive effects in spontaneously hypertensive rats (SHR); the results are described in this paper.

Chemistry Methods for the Construction of 1,4-Dihydropyridine Skeleton Prepared compounds (**4a—m**) are listed in Table I. For the substituent at the 4-position of the 1,4-dihydropyridine ring, we employed 4-cyano-2-pyridyl and 2-trifluoromethyl-3-pyridyl groups, which were originally developed in our laboratory,[1] in addition to the most popular 3-nitrophenyl group. They were synthesized either *via* the Hantzsch reaction (method A),[5] its modified reaction (method B), or through the esterification reaction of 1,4-dihydropyridine monocarboxylic acid (**9**) with alcohols (**10**) (method C)[6] (Chart 1).

Method for the Synthesis of Side Chains Alcohols employed in the preparation of the ester side chians of each derivatives were synthesized as shown in Charts 2, 3 and 4.

Preparation of Side Chains of 4c—g, 4i, 4j and 4l (Charts 2 and 3) Compound **10b**, the side chain of **4c** and **4d**, were obtained by direct dibenzylation of *p*-aminophenethyl alcohol (**12**). Compounds **10c** and **10d**, the side chains of **4e—g** and **4i**, were easily derived from **12** by treatment with bis(2-chloroethyl)amine hydrochloride in refluxing BuOH,[7] and the following benzhydrylation with benzhydryl bromide and 4,4′-difluorobenzhydryl bromide, respectively. Compound **10e**, the side chain of **4l**, was also synthesized from **12** *via* **15**. The reductive amination of **14** with **12** using $NaBH_3CN$ as a reducing agent gave **15** in moderate yield.[8] Compound **15** was then methylated by reductive alkylation

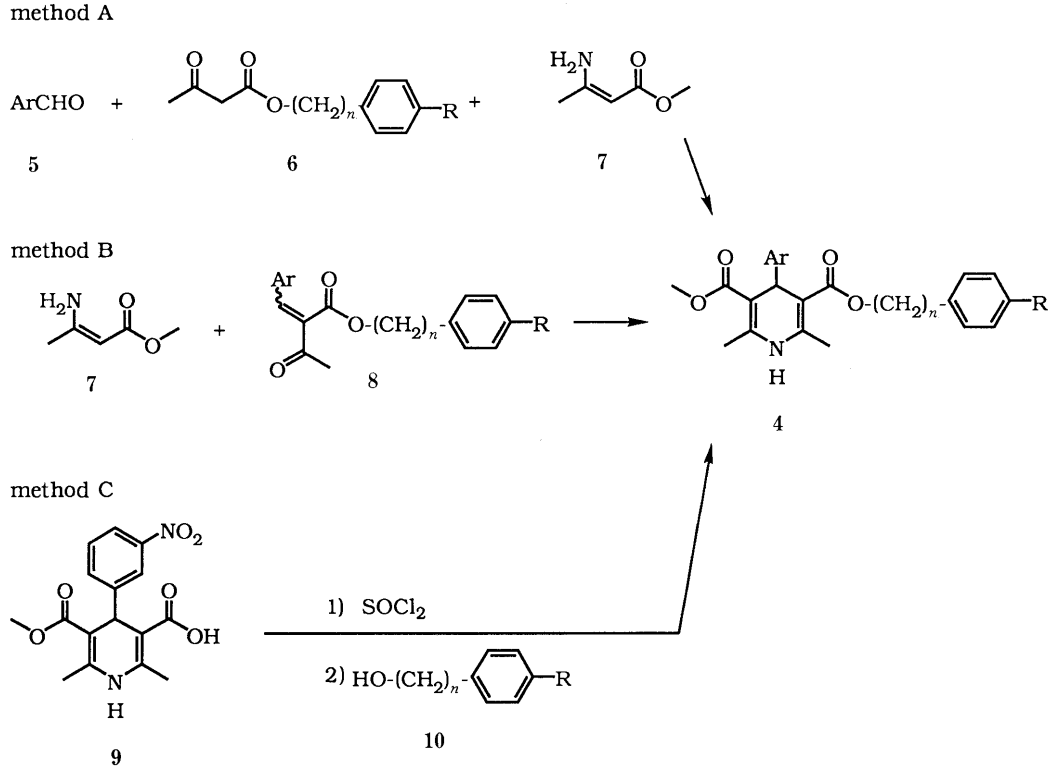

Chart 1

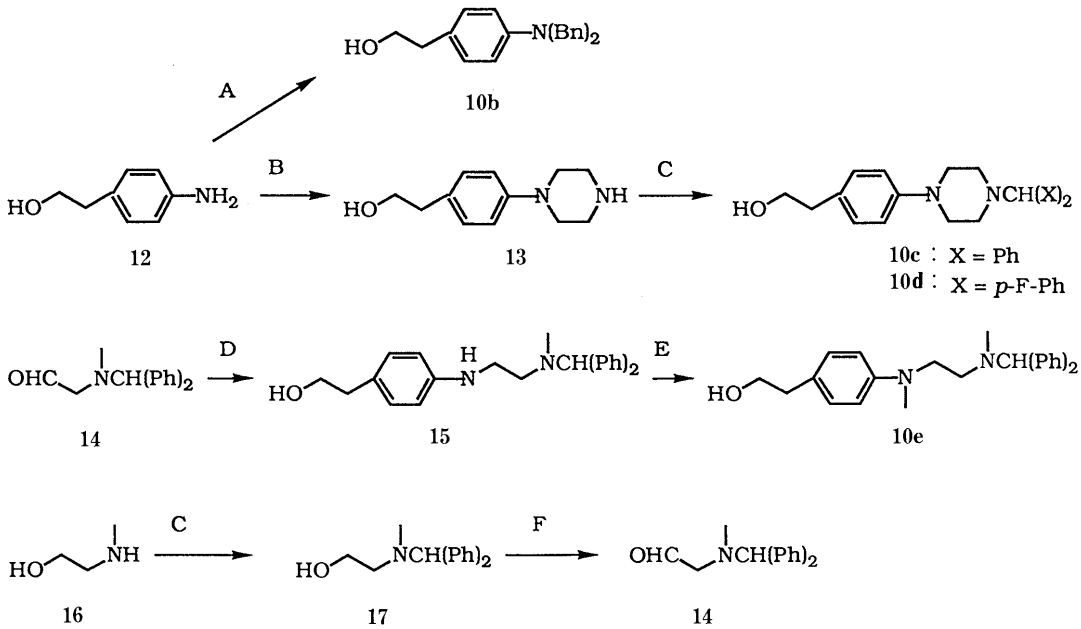

A) BnBr, K_2CO_3/DMF, r.t. (94%) B) $(ClCH_2CH_2)_2NH \cdot HCl$/BuOH, refl. (79%) C) $(Ph)_2CHBr$ or $(p\text{-F-Ph})_2CHBr$, K_2CO_3/DMF, r.t. (**10c**, 57%; **10d**, 50%; **17**, 59%) D) 12, $NaBH_3CN$/MeOH, r.t. (51%) E) 37% aq. HCHO, $NaBH_3CN$/MeOH, r.t. (66%) F) DMSO, DCC, H_3PO_4, r.t. (30%)

Chart 2

with HCHO. Aldehyde **14** was derived from aminoalcohol **16** by *N*-benzhydrylation, followed by oxidation of the obtained intermediate **17**. The method for the synthesis of **10f**, the side chain of **4j**, was as follows: Compound **18** derived from **12** by known methods[9] was reduced with $NaBH_4$ to give the corresponding alcohol **19**, which was treated with *p*-toluenesulfonyl chloride in pyridine. The tosyloxy leaving group of **20** was replaced by a cyano group by the method of Henbest and Jackson,[10] namely, **20** was treated with NaCN in *N*-methyl-2-pyrrolidone and *tert*-BuOH at 80—90 °C to give **21** in moderate yield. After the protecting group of the primary alcohol of **21** was changed into a tetrahydropyranyl (THP) group, **22** was treated with phenylmagnesium bromide twice to afford **24** in good yield. Dehydration and a concomitant exchange of THP for acetyl (Ac) was performed by treatment of **24** with H_2SO_4–AcOH

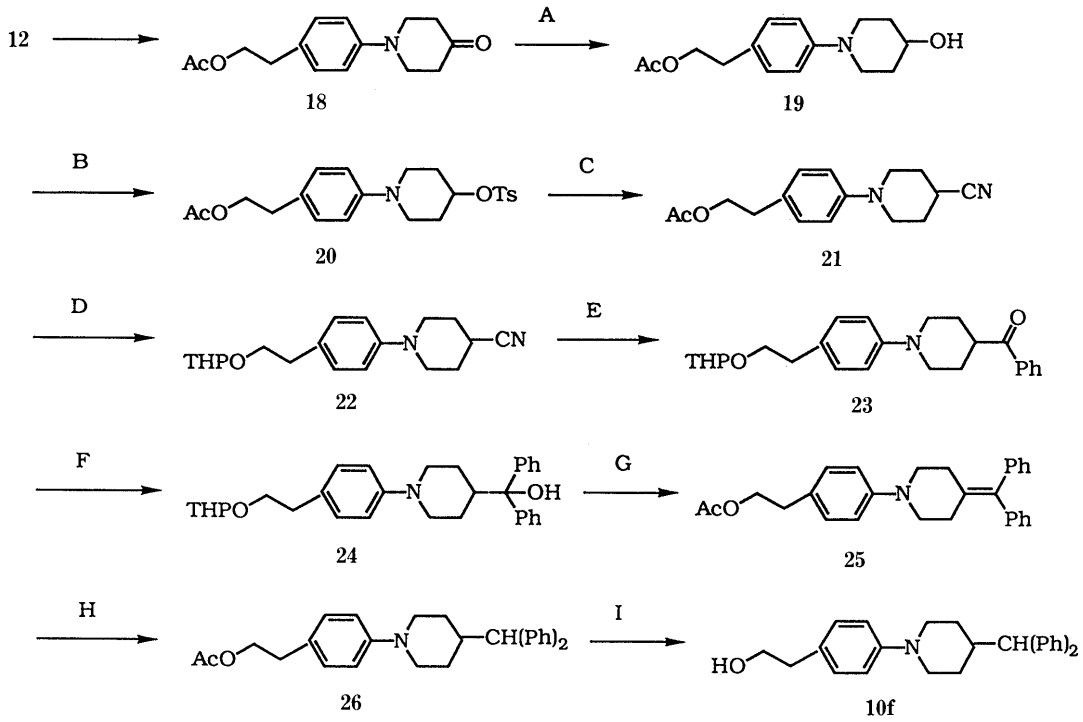

A) $NaBH_4$/MeOH, r.t. (96%) B) TsCl/pyridine, r.t. (81%) C) NaCN/*N*-methyl-2-pyrrolidone and *tert*-BuOH, 80—90 °C (45%) D) i) K_2CO_3/MeOH, r.t.; ii) DHP, TsOH/CH_2Cl_2, r.t. (80%) E) i) PhMgBr/Et_2O, r.t.; ii) 12 N H_2SO_4, ice-water cooling (66%) F) i) PhMgBr/Et_2O–THF, r.t; ii) 25% NH_4Cl (96%) G) H_2SO_4–AcOH (2:8), r.t. (66%) H) H_2, 10% Pd on charcoal/AcOH–$HClO_4$, 65—70 °C (79%) I) K_2CO_3/MeOH, r.t. (91%)

Chart 3

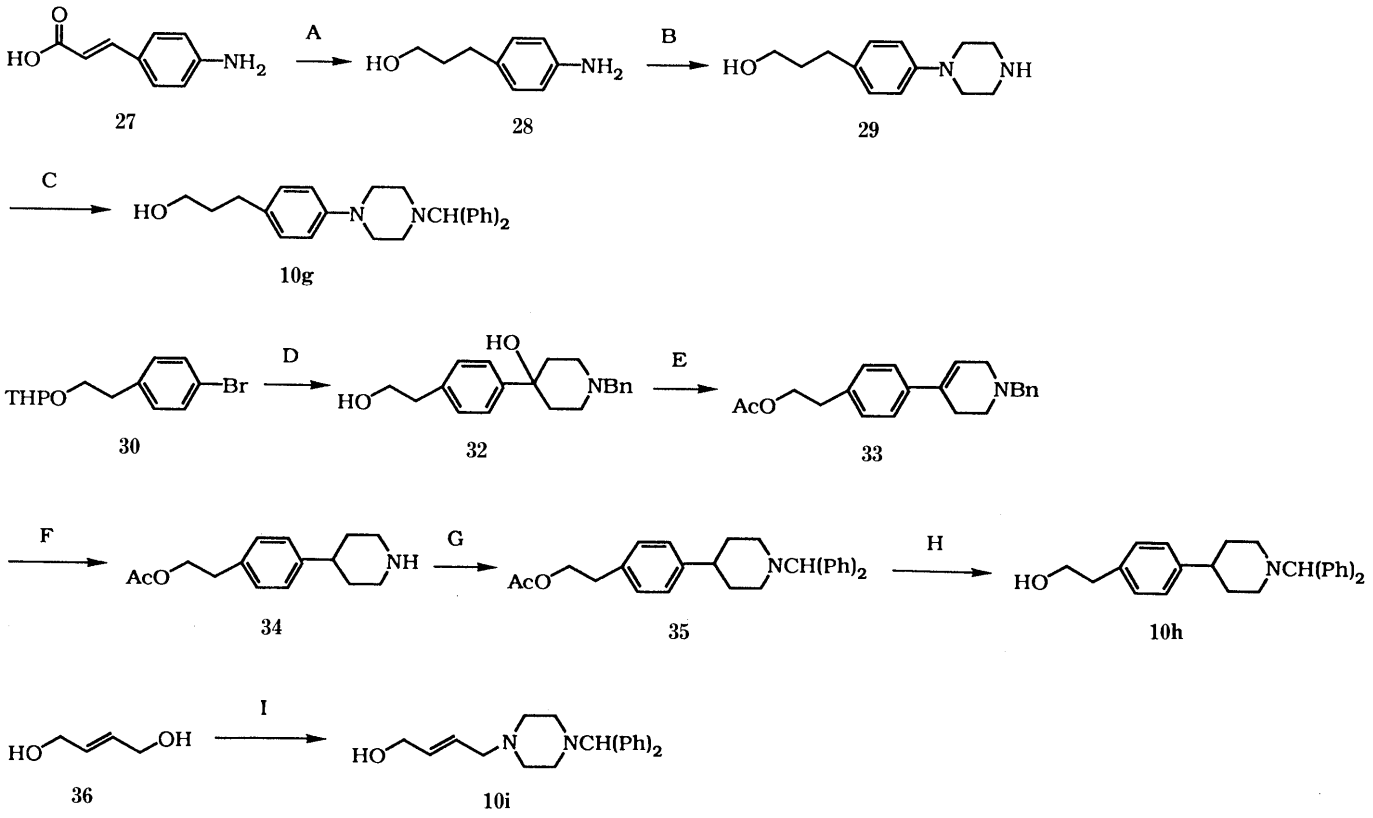

A) i) H_2, 5% Pd on charcoal/MeOH, r.t.; ii) HCl/MeOH, refl.; iii) $LiAlH_4$/THF, 22—23 °C (91%) B) $(ClCH_2CH_2)_2NH \cdot HCl$/BuOH, refl. (62%) C) $(Ph)_2CHBr$, K_2CO_3/DMF, r.t. (60%) D) i) BuLi/THF, < −60 °C; ii) 1-benzyl-4-piperidone (**31**), −60—−40 °C; iii) 10% HCl/MeOH, r.t. (76%) E) H_2SO_4–AcOH (2:8), r.t. (51%) F) H_2, 10% Pd on charcoal/AcOH–$HClO_4$, 65—70 °C (96%) G) $(Ph)_2CHBr$, K_2CO_3/DMF, r.t. (73%) H) K_2CO_3/MeOH, r.t. (89%) I) i) MsCl, NEt_3/THF–CH_2Cl_2, r.t.; ii) 1-benzhydrylpiperazine, K_2CO_3/DMF, r.t. (30%)

Chart 4

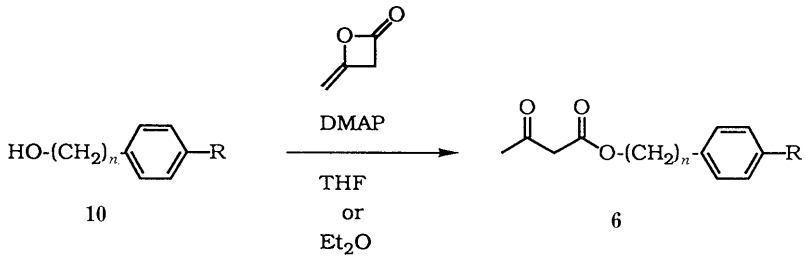

Chart 5

TABLE I. Physical and Biological Data of 1,4-Dihydropyridines (**4**)

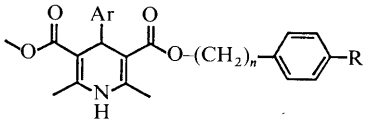

4

Compd. No.	Ar[a]	Method	R	*n*	Yield (%)	mp (°C)	Recrystn. solvent[b]	HR-SIMS[c] Found (Calcd)	Max. reduction of SBP (%)	Duration (h)
4a	4-CN-2-Py	A	NMe_2	2	45	184—186	M	461.2255 (461.2187)	4	—
4b	2-CF_3-3-Py	A	NMe_2	2	43	199—204	M	504.2131 (504.2109)	19	5
4c	4-CN-2-Py	A	NBn_2	2	40	194.5—197	M–C	613.2842 (613.2813)	20	11
4d	2-CF_3-3-Py	A	NBn_2	2	37	141—142	IPE–M–C	656.2703 (656.2733)	13	—
4e	3-NO_2-Ph	A, B, C		2	92[d]	Amorph.	—	—[g]	35	13
4f	4-CN-2-Py	A, B		2	48[e]	218—220	IPE–C	668.3168 (668.3234)	29	9
4g	2-CF_3-3-Py	A		2	13	Amorph.	—	711.3196 (711.3156)	29	16
4h	3-NO_2-Ph	C		3	73	Amorph.	—	637.2994 (637.3023)	46	22
4i	3-NO_2-Ph	C		2	94	Amorph.	—	701.3385 (701.3337)	34	16
4j	3-NO_2-Ph	C		2	75	Amorph.	—	723.3027 (723.2992)	42	20
4k	3-NO_2-Ph	C		2	48	Amorph.	—	686.3263 (686.3228)	42	>24
4l	3-NO_2-Ph	C	$NMeCH_2CH_2NMeCH(Ph)_2$	2	53	Amorph.	—	686.3204 (686.3228)	38	4
4m	3-NO_2-Ph	A	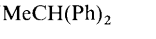		27	Amorph.	—	689.3358 (689.3337)	12	—
Nicardipine·HCl									10	—
Manidipine·2HCl									42	6

a) 4-CN-2-Py, 4-cyano-2-pyridyl; 2-CF_3-3-Py, 2-trifluoromethyl-3-pyridyl; 3-NO_2-Ph, 3-nitrophenyl. *b*) C, $CHCl_3$; IPE, isopropyl ether; M, MeOH. *c*) Compounds were converted to corresponding hydrochlorides and then analyzed. The method of conversion was described in Experimental section. *d*) The yield by method C. *e*) The yield by method B. *f*) Whole ester group. *g*) Compound **4e** was converted to dihydrochloride and used for elemental analysis. The data are shown in Experimental section. Amorph. = amorphous.

(2 : 8, v/v) to afford **25**, which was hydrogenated in AcOH using 10% Pd on charcoal in the presence of $HClO_4$ to yield **26**. Compound **26** was hydrolyzed in a methanolic base to afford **10f** in high yield.

Preparation of Side Chain of 4h, 4k and 4m (Chart 4) Successive treatment of **27** with H_2 over 5% Pd on charcoal in MeOH, dry HCl in MeOH, and $LiAlH_4$ in tetrahydrofuran (THF) gave **28** in high yield. Compound **10g**, the side chain of **4h**, was derived from **28** as in the case of **12**. Compound **10h**, the side chain of **4k**, was obtained in the following manner: Lithiated **30**[11] was treated with *N*-benzyl-4-piperidone (**31**), and the following deprotection of the primary alcohol gave **32**, which was dehydrated and acetylated at the same time by treatment with H_2SO_4–AcOH (2 : 8, v/v) to give **33**. Treatment of **33** with H_2 over 10% of Pd on charcoal in AcOH–$HClO_4$ was followed by benzhydrylation of the secondary amine to give **35**. Compound **10h** was obtained by hydrolysis of **35** with K_2CO_3 in MeOH. Compound **10i**, the side chain of **4m**, was obtained by one pot reaction of (*E*)-2-butene-1,4-diol (**36**) with methanesulfonyl chloride in THF followed by an amination with 1-benzhydrylpiperazine. 2-(4-Dimethylaminophenyl)ethyl alcohol (**10a**) is commercially available.

In cases where 1,4-dihydropyridine derivatives were

prepared by method A or B, the corresponding alcohols obtained above were converted to acetoacetic acid esters **6** by treatment with diketene in the presence of a catalytic amount of 4-dimethylaminopyridine (DMAP) in THF or Et_2O as shown in Chart 5.[12]

Results and Discussion

Antihypertensive activity and duration of action of the 1,4-dihydropyridine derivatives (**4a—m**) are shown in Table I.

Most of the compounds synthesized except **4a** have more potent antihypertensive activity than nicardipine which was used as a control compound.

Concerning the substituent at the 4-position of the 1,4-dihydropyridine ring, the derivatives with 2-trifluoromethyl-3-pyridyl group showed longer duration than those with a 4-cyano-2-pyridyl or a 3-nitrophenyl group (*e.g.*, **4a** < **4b**, **4c** < **4d**, and **4e**, **4f** < **4g**) like the previous examples (*e.g.*, **1** < **3**).[1] However, there seemed to be no distinct relationship between the potency of antihypertensive effect and the substituents used at 4-position.

The derivatives which have a piperazine moiety with a benzhydryl group (**4e—g**) showed more potent and longer lasting antihypertensive activity than the compounds without such a group (**4a—d**), and when the alkylene was lengthened from ethylene to trimethylene ($n=2 \rightarrow n=3$, *i.e.*, **4e**→**4h**) the antihypertensive effect and duration were increased. However, the introduction of a fluorine atom into the 4-position on each benzene ring of the benzhydryl moiety had little influence on the antihypertensive action (**4e** *vs.* **4i**).

Interestingly, replacement of either nitrogen atom of the piperizine ring in **4e** by a carbon atom gave rise to increased antihypertensive effect and, in particular, prolongation of the duration of action (**4j** and **4k**). From these results, neither nitrogen atom of the piperazine ring is necessarily required for the antihypertensive activity. In addition, the fact that the straight chain analogue **4l** preserves activity suggests the structural flexibility of this portion of the molecule to show the antihypertensive activity.

Although manidipine (Fig. 3),[4] which will soon come onto the market, showed a potent antihypertensive activity, the duration of action was not as long (*ca.* 6 h; see Table I). It is remarkable to note that compound **4e**, in which a benzene ring is introduced between the alkylene and the piperazine ring of manidipine, has somewhat less antihypertensive activity and yet the duration of action is more than twice as long as manidipine. This would be due, at least in part, to a tardiness of the metabolism or an increase of the affinity to a drug receptor caused by the introduced benzene ring.

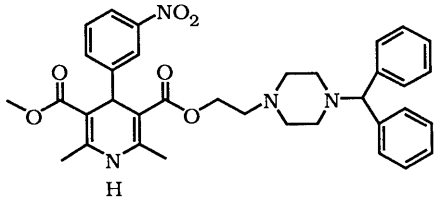

CV-4093 (manidipine)

Fig. 3

Among the compounds described above, **4e** (AE0047), **4f**, **4h**, **4i** and **4k** were selected as candidates for further pharmacological investigations. One of the investigations indicated that AE0047 had a potent and selective vasodilating action to canine vertebral artery, and this property is thought to be an additional benefit to an antihypertensive drug.

Experimental

Melting points were determined on a Yanagimoto micromelting point apparatus and are uncorrected. Infrared (IR) spectra were recorded on a Shimadzu IR-420 spectrometer. ^{1}H-Nuclear magnetic resonance (^{1}H-NMR) spectra were determined on a Hitachi R-24 (60 Mc) or a BRUKER AC-200 spectrometer with tetramethylsilane (TMS) as an internal standard. Secondary ion mass spectra (SIMS) were measured on a Hitachi M-2000 instrument, and precise mass analysis were performed by high resolution SIMS (HR-SIMS). Extraction solvents were dried over anhydrous $MgSO_4$. Silica gel 60, 230—400 mesh (Nacalai Tesque) was used for flash column chromatography, and Kieselgel 60, F_{254} (Merck) plates were used for thin layer chromatography (TLC).

2-(4-Dibenzylaminophenyl)ethyl Alcohol (10b) To a solution of **12** (1.04 g, 7.6 mmol) in *N*,*N*-dimethylformamide (DMF) (9 ml), K_2CO_3 (4.20 g, 30 mmol) and benzyl bromide (2.99 g, 18 mmol) were added successively at room temperature, and the mixture was stirred at the same temperature for 2.5 h. After addition of H_2O, the resulting mixture was extracted with Et_2O. The extract was washed with brine, dried, and the solvent was removed. The residue was chromatographed on silica gel with $CHCl_3$–MeOH (98 : 2, v/v) to give the product (**10b**) as a pale yellow oil (2.28 g, 94%). IR (film): 3350, 3025, 1620, 1520, 1495, 1450 cm^{-1}. ^{1}H-NMR ($CDCl_3$) δ: 1.48 (1H, s), 2.69 (2H, t, J=6 Hz), 3.71 (2H, t, J=6 Hz), 4.56 (4H, s), 6.62, 6.92 (4H, A_2B_2-q, J=8.5 Hz), 7.18 (10H, s).

2-[4-(1-Piperazinyl)phenyl]ethyl Alcohol (13) A mixture of **12** (10.15 g, 74 mmol), bis(2-chloroethyl)amine hydrochloride (6.61 g, 37 mmol) and BuOH (66 ml) was refluxed for 23.5 h. After cooling to room temperature, the resulting solution was poured into H_2O, which was made alkaline with 15% NaOH to pH 10—11 with ice-water cooling. The resulting mixture was extracted with $CHCl_3$, the extract was washed with brine, dried, and the solvent was removed. The residue was chromatographed on silica gel with $CHCl_3$–MeOH (1 : 1, v/v) to yield the product (**13**) as a pale yellow solid (6.00 g, 79%). IR (KBr): 3300, 1615, 1515, 1450 cm^{-1}. ^{1}H-NMR ($CDCl_3$) δ: 2.10 (2H, s), 2.75 (2H, t, J=6 Hz), 2.8—3.2 (8H, m), 3.77 (2H, t, J=6 Hz), 6.7—6.95 (2H, m), 6.95—7.15 (2H, m).

2-[4-(4-Benzhydryl-1-piperazinyl)phenyl]ethyl Alcohol (10c) To a solution of **13** (6.00 g, 29 mmol) in DMF (33 ml) were added successively, K_2CO_3 (8.03 g, 58 mmol) and benzhydryl bromide (7.54 g, 31 mmol) at room temperature, and the mixture was stirred at the same temperature for 2 h. The resulting mixture was poured into H_2O, and then extracted with Et_2O. The extract was washed with brine, dried, and the solvent was removed. The product (**10c**) was isolated by chromatography on silica gel with AcOEt–hexane (1 : 1, v/v) to give a colorless oil (6.19 g, 57%). IR ($CHCl_3$): 3600, 2950, 1615, 1490, 1430 cm^{-1}. ^{1}H-NMR ($CDCl_3$) δ: 1.71 (1H, s), 2.35—2.65 (4H, m), 2.71 (2H, t, J=6 Hz), 2.95—3.3 (4H, m), 3.72 (2H, t, J=6 Hz), 4.23 (1H, s), 6.65—6.9 (2H, m), 6.9—7.55 (12H, m).

2-[4-{4-(4,4′-Difluorobenzhydryl)-1-piperazinyl}phenyl]ethyl alcohol (**10d**) was obtained by similar treatment of **13** with 4,4′-difluorobenzhydryl bromide as a colorless solid (yield 50%). IR (KBr): 3300, 2850, 1605, 1505, 1455 cm^{-1}. ^{1}H-NMR ($CDCl_3$) δ: 1.50 (1H, br s), 2.72 (2H, t, J=6 Hz), 2.4—2.6 (4H, m), 3.0—3.2 (2H, m), 3.75 (2H, t, J=6 Hz), 4.20 (1H, s), 6.7—7.5 (12H, m).

2-(*N*-Benzhydryl-*N*-methylamino)ethyl alcohol (**17**) was obtained by similar treatment of *N*-methylethanolamine (**16**) with benzhydryl bromide as a colorless oil (yield 59%). IR (film): 3300, 2950, 2750, 1590, 1490, 1450 cm^{-1}. ^{1}H-NMR ($CDCl_3$) δ: 2.18 (3H, s), 2.70 (2H, t, J=7 Hz), 3.48 (2H, t, J=7 Hz), 4.37 (1H, s), 7.0—7.5 (10H, br).

2-[4-{2-(*N*-Benzhydryl-*N*-methylamino)ethylamino}phenyl]ethyl Alcohol (15) To a solution of **17** (5.00 g, 21 mmol) and *N*,*N*-dicyclohexylcarbodiimide (16.50 g, 80 mmol) in dimethyl sulfoxide (DMSO) (100 ml) was added, 1.0 M H_3PO_4 in DMSO (10 ml) at room temperature, and the mixture was stirred at the same temperature for 2.5 h. After removing the precipitated dicyclohexylurea by filtration, 1 M K_2CO_3 was added to the filtrate, and the resulting mixture was extracted with CH_2Cl_2. The extract was washed with brine, dried, and the solvent was removed. The obtained residue was chromatographed on silica gel with AcOEt–hexane (1 : 5, v/v)

to give aldehyde **14** (1.54 g, 30%), which was used immediately in the next reaction. To a solution of aldehyde **14** (780 mg, 3.3 mmol) and **12** (1.34 g, 9.8 mmol) in MeOH (50 ml), $NaBH_3CN$ (163 mg, 2.6 mmol) was added at room temperature, and the mixture was stirred at the same temperature for 2.5 h. After the solvent was removed, the residue was purified by chromatography on silica gel with AcOEt–hexane (1 : 1, v/v). The product (**15**) was obtained as a pale yellow oil (600 mg, 51%). IR (film): 3300, 2875, 1610, 1495, 1450 cm^{-1}. ^{1}H-NMR ($CDCl_3$) δ: 2.18 (3H, s), 2.61 (2H, t, J=6 Hz), 2.74 (2H, t, J=6.5 Hz), 3.17 (2H, t, J=6 Hz), 3.77 (2H, t, J=6.5 Hz), 4.44 (1H, s), 6.56, 7.01 (4H, A_2B_2-q, J=8.5 Hz), 7.15—7.40 (10H, m).

2-[4-[*N*-{2-(*N*-Benzhydryl-*N*-methylamino)ethyl}-*N*-methylamino]-phenyl]ethyl Alcohol (10e) To a solution of **15** (44 mg, 0.12 mmol) in CH_3CN (10 ml) were added successively, 37% aqueous HCHO (10 mg, 0.12 mmol) and $NaBH_3CN$ (8 mg, 0.10 mmol) at room temperature. After the resulting mixture was stirred at the same temperature for 2 h, the solvent was removed. H_2O was added to the mixture, and then the mixture was extracted with Et_2O. The extract was washed with brine and dried. After evaporation of the solvent, the residue was chromatographed on silica gel with AcOEt–hexane (1 : 1, v/v) to give the product (**10e**) as a pale yellow oil (30 mg, 66%). IR (film): 3300, 2850, 1610, 1500, 1455 cm^{-1}. ^{1}H-NMR ($CDCl_3$) δ: 1.54 (1H, br s), 2.25 (3H, s), 2.55 (2H, t, J=7 Hz), 2.73 (2H, t, J=6.5 Hz), 2.84 (3H, s), 3.44 (2H, t, J=7 Hz), 3.76 (2H, t, J=6.5 Hz), 4.39 (1H, s), 6.49, 6.98 (4H, A_2B_2-q, J=8.5 Hz), 7.0—7.4 (10H, m).

2-[4-(4-Hydroxy-1-piperidinyl)phenyl]ethyl Acetate (19) To a solution of **18** (2.17 g, 8.9 mmol) in MeOH (22 ml), $NaBH_4$ (168 mg, 4.4 mmol) was added with ice-water cooling. After the reaction mixture was stirred at the same temperature for 30 min, the resulting solution was poured into H_2O, and extracted with CH_2Cl_2. The extract was washed with brine, dried, and the solvent was removed. Purification by chromatography on silica gel with AcOEt–hexane (2 : 1, v/v) gave the product (**19**) as a pale yellow oil (2.10 g, 96%). IR (film): 3400, 2975, 1740, 1620, 1520, 1470, 1245 cm^{-1}. ^{1}H-NMR ($CDCl_3$) δ: 1.6—1.8 (2H, m), 1.9—2.05 (2H, m), 2.03 (3H, s), 2.67 (1H, br s), 2.84 (2H, t, J=7 Hz), 2.8—2.95 (2H, m), 3.51 (2H, dt, J=13, 4 Hz), 3.7—3.9 (1H, m), 4.22 (2H, t, J=7 Hz), 6.8—6.95 (2H, m), 7.05—7.2 (2H, m).

2-[4-{4-(*p*-Toluenesulfonyloxy)-1-piperidinyl}phenyl]ethyl Acetate (20) To a solution of **19** (100 mg, 0.38 mmol) in pyridine (1 ml), *p*-toluenesulfonyl chloride (109 mg, 0.57 mmol) was added with ice-water cooling. The reaction mixture was stirred at room temperature for 17 h under N_2 atmosphere. After addition of H_2O to the mixture and acidification with 5 N AcOH to *ca.* pH 4, the resulting mixture was extracted with Et_2O. The extract was washed with brine, dried, and the solvent was removed. The residue was chromatographed on silica gel with AcOEt–hexane (1 : 2, v/v) to give the product (**20**) as a pale yellow oil (115 mg, 81%). IR (film): 2950, 1735, 1615, 1515, 1360, 1240, 1180 cm^{-1}. ^{1}H-NMR ($CDCl_3$) δ: 1.85—2.0 (4H, m), 2.03 (3H, s), 2.7—2.85 (1H, m), 2.86 (2H, t, J=7 Hz), 3.0—3.15 (2H, m), 3.35—3.45 (2H, m), 4.23 (2H, t, J=7 Hz), 6.85—6.95 (2H, m), 7.1—7.2 (2H, m).

2-[4-(4-Cyano-1-piperidinyl)phenyl]ethyl Acetate (21) To a solution of **20** (2.47 g, 5.9 mmol) in *N*-methyl-2-pyrrolidone (161 ml) and *tert*-BuOH (8.5 ml), NaCN (3.48 g, 71 mmol) was added at room temperature and stirred at 80—90 °C for 15 h under N_2 atmosphere. The resulting solution was poured into crushed ice and the mixture was extracted with Et_2O. The extracts was washed with brine, dried, and the solvent was removed. The product was isolated by chromatography on silica gel with AcOEt–hexane (1 : 2, v/v) to afford **21** as a pale yellow oil (731 mg, 45%). IR (film): 2975, 2250, 1740, 1615, 1520, 1425, 1240 cm^{-1}. ^{1}H-NMR ($CDCl_3$) δ: 1.95—2.1 (4H, m), 2.03 (3H, s), 2.7—2.85 (1H, m), 2.86 (2H, t, J=7 Hz), 3.0—3.15 (2H, m), 3.35—3.45 (2H, m), 4.23 (2H, t, J=7 Hz), 6.85—6.95 (2H, m), 7.1—7.2 (2H, m).

4-Cyano-1-[4-{2-(tetrahydropyran-2-yloxy)ethyl}phenyl]piperidine (22) To a solution of **21** (719 mg, 2.6 mmol) in MeOH (10 ml), a catalytic amount of K_2CO_3 (*ca.* 3 mol%) was added at room temperature, and the mixture was stirred at the same temperature for 1 h. The reaction mixture was poured into 10% K_2CO_3, and then extracted with CH_2Cl_2. The extract was washed with brine, dried, and the solvent was removed. After the obtained residue (600 mg) was dissolved in CH_2Cl_2 (10 ml), 3,4-dihydro-2*H*-pyran (DHP) (328 mg, 4.6 mmol), *p*-toluenesulfonic acid (644 mg, 3.4 mmol), and pulverized molecular sieves 3A (350 mg) were added successively to the solution, and then the mixture was stirred at room temperature for 1.5 h. Molecular sieves were filtered off and the filtrate was poured into 10% K_2CO_3. The organic layer was separated, and the aqueous layer was further extracted with CH_2Cl_2. The combined extracts were washed with brine, dried, and the solvent was removed. The residue was chromatographed on silica gel with AcOEt–hexane (1 : 2, v/v) to give the product (**22**) as a pale yellow oil (663 mg, 80%). IR (film): 2950, 2225, 1615, 1515, 1445, 1140, 1120 cm^{-1}. ^{1}H-NMR ($CDCl_3$) δ: 1.45—1.9 (6H, m), 1.9—2.1 (4H, m), 2.2—2.4 (1H, m), 2.87 (2H, t, J=7 Hz), 2.95—3.1 (2H, m), 3.35—3.5 (2H, m), 3.4—3.8 (2H, m), 3.5—4.0 (2H, m), 4.59 (1H, t, J=3 Hz), 6.8—6.9 (2H, m), 7.1—7.2 (2H, m).

4-Benzoyl-1-[4-{2-(tetrahydropyran-2-yloxy)ethyl}phenyl]piperidine (23) To a solution of PhMgBr in Et_2O (1.37 N, 0.90 ml, 1.2 mmol) was added, a solution of **22** (175 mg, 0.56 mmol) in Et_2O (2 ml) with ice-water cooling under N_2 atmosphere. After stirring at room temperature for 1.5 h, H_2O was added to the mixture, and then 12 N H_2SO_4 was added with ice-water cooling until the colorless solid precipitate had disappeared. The organic layer was separated, and after the aqueous layer was made alkaline with K_2CO_3 to pH 11, the solution was extracted with AcOEt. The combined extracts were washed with brine, dried, and the solvent was removed. Purification of the residue by chromatography on silica gel with AcOEt–hexane (1 : 3, v/v) gave the product (**23**) as a colorless solid (145 mg, 66%). IR (KBr): 2950, 2850, 1665, 1615, 1595, 1580, 1520, 1455, 1140 cm^{-1}. ^{1}H-NMR ($CDCl_3$) δ: 1.45—1.9 (6H, m), 1.9—2.05 (4H, m), 2.75—2.9 (4H, m), 3.3—3.55 (2H, m), 3.5—3.95 (5H, m), 4.60 (1H, t, J=3 Hz), 6.85—6.95 (2H, m), 7.1—7.2 (2H, m), 7.4—7.55 (3H, m), 7.95—8.05 (2H, m).

4-(1-Hydroxy-1,1-diphenyl)methyl-1-[4-{2-(tetrahydropyran-2-yloxy)-ethyl}phenyl]piperidine (24) To a solution of PhMgBr in Et_2O (1.37 N, 3.5 ml, 4.8 mmol) was added dropwise, a solution of **23** in THF (8 ml) with ice-water cooling, following this addition, the reaction mixture was stirred at room temperature for 40 min. To the resulting mixture were added successively, 25% NH_4Cl and H_2O, and then the resulting mixture was extracted with CH_2Cl_2. The extract was washed with brine, dried, and the solvent was removed. The residue was chromatographed on silica gel with AcOEt–hexane (2 : 7, v/v) to give the product (**24**) as a pale yellow oil (1.04 g, 96%). IR (film): 3400, 2950, 1610, 1515, 1445, 1120 cm^{-1}. ^{1}H-NMR ($CDCl_3$) δ: 1.45—1.85 (11H, m), 2.5—2.8 (3H, m), 2.82 (2H, t, J=7.5 Hz), 3.4—3.9 (6H, m), 4.59 (1H, t, J=3 Hz), 6.8—6.9 (2H, m), 7.05—7.15 (2H, m), 7.15—7.45 (6H, m), 7.45—7.55 (4H, m).

2-[4-(Benzhydrylidene-1-piperidinyl)phenyl]ethyl Acetate (25) A mixture of **24** (1.04 g, 2.2 mmol) and H_2SO_4–AcOH (2 : 8, v/v) (10 ml) was stirred at room temperature for 1 h. After the reaction mixture was poured into H_2O and made alkaline with K_2CO_3 to pH 11, the resulting mixture was extracted with CH_2Cl_2. The extract was washed with brine, dried, and the solvent was removed. The product was isolated by chromatography on silica gel with AcOEt–hexane (1 : 6, v/v) to give **25** as a pale yellow oil (603 mg, 66%). IR (film): 2950, 1740, 1615, 1515, 1490, 1460, 1440, 1240 cm^{-1}. ^{1}H-NMR ($CDCl_3$) δ: 2.02 (3H, s), 2.50 (4H, t, J=6 Hz), 2.84 (2H, t, J=7 Hz), 3.24 (4H, t, J=6 Hz), 4.23 (2H, t, J=7 Hz), 6.8—6.9 (2H, m), 7.05—7.35 (12H, m).

2-[4-(4-Benzhydryl-1-piperidinyl)phenyl]ethyl Acetate (26) To a solution of **25** (600 mg, 1.5 mmol) in AcOH (10 ml), 70% $HClO_4$ (0.3 ml) was added. After 10% Pd on charcoal (600 mg) was added to the solution under N_2 atmosphere, N_2 was replaced by H_2, and then the mixture was stirred at 65—70 °C for 3 h. The catalyst was filtered off, and the filter was washed with MeOH and CH_2Cl_2. After evaporation of the solvent, 10% K_2CO_3 was added to the residue, and the resulting mixture was extracted with AcOEt. The extract was washed with brine, dried, and the solvent was removed. The residue was chromatographed on silica gel with AcOEt–hexane (1 : 7, v/v) to afford the product (**26**) as a pale yellow oil (476 mg, 79%). IR (film): 2925, 1735, 1615, 1515, 1490, 1450, 1240 cm^{-1}. ^{1}H-NMR ($CDCl_3$) δ: 1.3—1.45 (2H, m), 1.67 (2H, d, J=13 Hz), 2.02 (3H, s), 2.24 (1H, dt, J=11, 3.5 Hz), 2.65 (2H, td, J=12, 2.5 Hz), 2.83 (2H, t, J=7 Hz), 3.53 (1H, d, J=11 Hz), 3.55—3.65 (2H, m), 4.22 (2H, t, J=7 Hz), 6.8—6.9 (2H, m), 7.05—7.15 (2H, m), 7.15—7.4 (10H, m).

2-[4-(4-Benzhydryl-1-piperidinyl)phenyl]ethyl Alcohol (10f) To a solution of **26** (469 mg, 1.1 mmol) in MeOH (5 ml) was added, a catalytic amount of K_2CO_3 (*ca.* 3 mol%) at room temperature, and the obtained mixture was stirred at the same temperature for 1 h. After the reaction mixture was poured into 10% K_2CO_3, the resulting mixture was extracted with CH_2Cl_2. The extract was washed with brine, dried, and the solvent was removed. Purification of the residue by chromatography on silica gel with AcOEt–hexane (2 : 5, v/v) gave the product (**10f**) as a colorless solid (387 mg, 91%). IR (KBr): 3325, 2900, 1610, 1515, 1490, 1450 cm^{-1}. ^{1}H-NMR ($CDCl_3$) δ: 1.25—1.45 (3H, m), 1.6—1.7 (2H, m), 2.25 (1H, dt, J=11, 3.5 Hz), 2.66 (2H, td, J=12, 2.5 Hz), 2.77 (2H, t, J=6.5 Hz), 3.56 (1H, d, J=11 Hz), 3.55—3.65 (2H, m), 3.80 (2H, br s), 6.8—6.9 (2H, m), 7.05—7.15 (2H, m), 7.15—7.4 (10H, m).

3-(4-Aminophenyl)propyl Alcohol (28) To a solution of **27** (8.04 g, 40 mmol) in MeOH (340 ml), 5% Pd on charcoal (870 mg) was added under N_2 atmosphere. After N_2 was replaced by H_2, the mixture was stirred at room temperature for 55 min. The catalyst was filtered off, and the filter was rinsed with MeOH. The filtrate was evaporated to dryness to give a colorless solid (8.03 g). A mixture of the solid (8.03 g) and 10% dry HCl in MeOH (126 ml) was refluxed for 1.5 h. After cooling in an ice-water bath, the reaction mixture was poured into ice-water and made alkaline with K_2CO_3 to pH 9—10. The resulting solution was extracted with $CHCl_3$, and then the extract was washed with brine, dried, and the solvent was evaporated to dryness to yield a colorless solid (7.17 g). To a suspension of $LiAlH_4$ (2.73 g, 72 mmol) in THF (87 ml), a solution of the solid (7.17 g) obtained above in THF (95 ml) was added dropwise at 8—15 °C with ice-water cooling. After the addition was completed, the reaction mixture was stirred at 22—23 °C for 1.5 h. The resulting mixture was worked up as usual to give a crude mixture, which was purified by chromatography on silica gel with $CHCl_3$–MeOH (94:6, v/v) to afford the product (**28**) as a colorless oil (5.54 g, 91%). IR (film): 3300, 2925, 1620, 1515, 1450 cm^{-1}. ^{1}H-NMR ($CDCl_3$) δ: 1.5—2.05 (2H, m), 2.4—2.7 (2H, m), 2.91 (3H, br s), 3.54 (2H, t, J=6.5 Hz), 6.4—6.7 (2H, m), 6.75—7.05 (2H, m).

3-[4-(1-Piperazinyl)phenyl]propyl Alcohol (29) Compound **29** was obtained as a pale yellow solid (yield 62%) by the same method as used for the synthesis of **13**. IR (KBr): 3250, 2900, 2825, 1615, 1520, 1445 cm^{-1}. ^{1}H-NMR ($CDCl_3$) δ: 1.65—2.1 (2H, m), 2.13 (2H, s), 2.45—2.8 (2H, m), 2.8—3.25 (8H, m), 3.57 (2H, t, J=6.5 Hz), 6.65—6.9 (2H, m), 6.9—7.15 (2H, m).

3-[4-(4-Benzhydryl-1-piperazinyl)phenyl]propyl Alcohol (10g) Compound **10g** was obtained as a slightly yellow oil (yield 60%) by the same method as used for the synthesis of **10c**. IR ($CHCl_3$): 3600, 2950, 2825, 1615, 1510, 1490, 1455 cm^{-1}. ^{1}H-NMR ($CDCl_3$) δ: 1.45—2.05 (2H, m), 2.35—2.75 (6H, m), 2.95—3.25 (4H, m), 3.55 (2H, t, J=6 Hz), 4.19 (1H, s), 6.6—6.85 (2H, m), 6.85—7.05 (2H, m).

2-[4-(1-Benzyl-4-piperidinyl)phenyl]ethyl Alcohol (32) To a solution of **30** (7.53 g, 26 mmol) in THF (70 ml), BuLi in hexane (10 w/v%, 16.9 ml, 26 mmol) was added dropwise at below −60 °C under N_2 atmosphere. After the addition was completed, the solution was stirred at the same temperature for 30 min. Keeping the temperature below −60 °C, a solution of **31** (5.00 g, 26 mmol) in THF (30 ml) was added dropwise to the reaction mixture, and stirred for 2.5 h. After the solution was allowed to warm to *ca.* −40 °C, H_2O was added and then the resulting mixture was extracted with CH_2Cl_2. The extract was washed with brine, dried, and the solvent was removed to give a pale yellow oil (10.95 g). To a solution of the oil (10.95 g) in MeOH (120 ml), 10% HCl (60 ml) was added at room temperature. After the reaction mixture was stirred at the same temperature for 1 h, the solution was poured into H_2O, which was made alkaline with K_2CO_3. After extraction of the resulting mixture with CH_2Cl_2, the extract was washed with brine, dried, and the solvent was removed. The product (**32**) was obtained by chromatography on silica gel with $CHCl_3$–MeOH (86:14, v/v) as a pale yellow oil (6.21 g, 76%). IR ($CHCl_3$): 3625, 3450, 2975, 2850, 1515, 1500, 1480 cm^{-1}. ^{1}H-NMR ($CDCl_3$) δ: 1.69 (2H, d, J=12 Hz), 2.15 (2H, td, J=13, 4.5 Hz), 2.53 (2H, td, J=12, 2 Hz), 2.3—2.7 (2H, br), 2.7—2.8 (2H, br), 2.81 (2H, t, J=6.5 Hz), 3.62 (2H, s), 3.80 (2H, t, J=6.5 Hz), 7.1—7.5 (9H, m).

2-[4-(1-Benzyl-1,2,5,6-tetrahydro-4-pyridyl)phenyl]ethyl Acetate (33) Compound **33** was obtained as a pale yellow oil (yield 51%) by the same method as used for the synthesis of **25**. IR (film): 2900, 2800, 1740, 1515, 1495, 1240 cm^{-1}. ^{1}H-NMR ($CDCl_3$) δ: 2.02 (3H, s), 2.5—2.6 (2H, br), 2.65—2.75 (2H, m), 2.91 (2H, t, J=7 Hz), 3.15, 3.18 (2H, A_2B_2-q, J=3 Hz), 3.63 (2H, s), 4.26 (2H, t, J=7 Hz), 6.0—6.1 (1H, m), 7.1—7.4 (9H, m).

2-[4-(4-Piperidinyl)phenyl]ethyl Acetate (34) Compound **34** was obtained as a slightly yellow oil (yield 96%) by the same method as used for the synthesis of **26**. IR (film): 2925, 2825, 1735, 1510, 1440, 1240 cm^{-1}. ^{1}H-NMR ($CDCl_3$) δ: 1.6—1.95 (4H, m), 2.04 (3H, s), 2.59 (1H, dt, J=12, 4 Hz), 2.78 (2H, dt, J=12, 2.5 Hz), 2.90 (2H, t, J=7 Hz), 3.26 (2H, d, J=12 Hz), 3.66 (1H, br s), 4.26 (2H, t, J=7 Hz), 7.16 (4H, s).

2-[4-(1-Benzhydryl-4-piperidinyl)phenyl]ethyl Acetate (35) Compound **35** was obtained as a slightly yellow oil (yield 73%) by the same method as used for the synthesis of **10c**. IR (film): 2950, 2800, 1740, 1600, 1520, 1495, 1460, 1240 cm^{-1}. ^{1}H-NMR ($CDCl_3$) δ: 1.7—2.0 (6H, m), 2.03 (3H, s), 2.3—2.6 (1H, m), 2.89 (2H, t, J=7 Hz), 3.00 (2H, d, J=10.5 Hz), 4.26 (2H, t, J=7 Hz), 4.29 (1H, s), 7.1—7.5 (14H, m).

2-[4-(1-Benzhydryl-4-piperidinyl)phenyl]ethyl Alcohol (10h) Compound **10h** was obtained as a slightly yellow oil (yield 89%) by the same method as used for the synthesis of **10f**. IR (film): 3325, 2925, 2800, 1600, 1515, 1490, 1450 cm^{-1}. ^{1}H-NMR ($CDCl_3$) δ: 1.5—2.0 (7H, m), 2.4—2.6 (1H, m), 2.81 (2H, t, J=6.5 Hz), 3.00 (2H, d, J=10.5 Hz), 3.82 (2H, t, J=6.5 Hz), 4.29 (1H, s), 7.1—7.5 (14H, m).

4-(4-Benzhydryl-1-piperazinyl)-(*E*)-2-buten-1-ol (10i) To a solution of **36** (3.04 g, 35 mmol, E:Z=3:1) and NEt_3 (2.32 g, 23 mmol) in CH_2Cl_2 (5 ml) and THF (6 ml), methanesulfonyl chloride (2.63 g, 23 mmol) in THF (8 ml) was added dropwise at room temperature. After the addition was completed, the mixture was stirred at the same temperature for 1.5 h. After the precipitated Et_3N·HCl was filtered off, the filtrate was evaporated to dryness to give a pale yellow oil. To a solution of 1-benzhydrylpiperazine (5.87 g, 23 mmol) in DMF (20 ml), K_2CO_3 (3.18 g, 23 mmol) and a solution of the oil in DMF (10 ml) were added successively at room temperature. After stirring at 65—70 °C for 1 h under N_2 atmosphere, the resulting mixture was poured into H_2O, and then extracted with Et_2O. The extract was washed with brine, dried, and the solvent was removed. The residue was chromatographed on silica gel with $CHCl_3$–MeOH (10:1, v/v) to give the product (**10i**) as a colorless oil (2.12 g, 30%). IR (film): 3400, 2950, 2800, 1600, 1495, 1460 cm^{-1}. ^{1}H-NMR ($CDCl_3$) δ: 2.45 (8H, s), 2.59 (1H, s), 2.9—3.1 (2H, m), 4.0—4.15 (2H, m), 4.22 (1H, s), 5.55—5.95 (2H, m), 7.05—7.55 (10H, m).

General Method for the Synthesis of Acetoacetic Acid Esters (6) To a THF or Et_2O solution of **10**, diketene (1.2 eq of **10**) and a catalytic amount of DMAP were added with ice-salt cooling. After the addition of the reagents, the reaction mixture was stirred at the same temperature for 30 min and at room temperature for 3—16 h. To the mixture, 0.1% NaOH

Table II. Yields and Spectral Data of Acetoacetic Acid Esters (**6**)

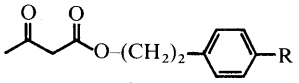

6

Compd. No.	R	Yield (%)	IR ν_{max} (cm^{-1})	^{1}H-NMR ($CDCl_3$) δ (ppm)
6a	NMe_2	76	2925, 2800, 1740, 1710, 1615, 1520, 1450 (KBr)	2.20 (3H, s), 2.84 (2H, t, J=7 Hz), 2.89 (6H, s), 3.38 (2H, s), 4.27 (2H, t, J=7 Hz), 6.63, 7.02 (2H, A_2B_2q, J=9 Hz)
6b	NBn_2	82	3025, 2925, 1740, 1720, 1620, 1520, 1495, 1455 (film)	2.15 (3H, s), 2.81 (2H, t, J=6 Hz), 3.36 (2H, s), 4.25 (2H, t, J=6 Hz), 4.57 (4H, s), 6.5—6.75 (2H, m), 6.8—7.1 (2H, m), 7.19 (10H, s)
6c	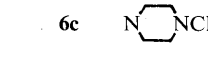	100	3025, 2975, 2800, 1740, 1720, 1620, 1520, 1495, 1450 (film)	2.18 (3H, s), 2.4—2.7 (4H, m), 2.85 (2H, t, J=6.5 Hz), 3.0—3.35 (4H, m), 3.39 (2H, s), 4.24 (1H, s), 4.29 (2H, t, J=6.5 Hz), 6.65—6.9 (2H, m), 6.9—7.6 (2H, m)
6d	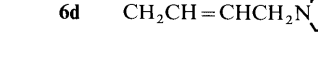 [a]	75	2925, 2800, 1740, 1720, 1600, 1495, 1450 (film)	2.20 (3H, s), 2.44 (8H, br s), 5.64 (2H, d, J=5.5 Hz), 3.41 (2H, s), 4.22 (1H, s), 4.59 (2H, d, J=5.5 Hz), 5.69 (1H, ddd, J=15.5, 6, 5.5 Hz), 5.83 (1H, ddd, J=15.5, 6, 5.5 Hz), 7.1—7.4 (10H, m)

a) Whole ester group.

was added and then the resulting mixture was extracted with Et_2O or CH_2Cl_2. The extract was washed with 0.1% NaOH (twice) and brine, dried, and the solvent was evaporated to dryness to give the acetoacetic acid ester (**6**), which was used in the next reaction either without further purification or after purification by chromatography on silica gel. Yields and spectral data are shown in Table II.

Typical Procedure for Method A 2-(4-Dimethylaminophenyl)ethyl Methyl 4-(4-Cyano-2-pyridyl)-1,4-dihydro-2,6-dimethyl-3,5-pyridinedicarboxylate (**4a**): A solution of 4-cyano-2-pyridinecarboxaldehyde (1.01 g, 7.6 mmol), 2-(4-dimethylaminophenyl)ethyl acetoacetate (**6a**, 1.90 g, 7.6 mmol), and methyl 3-aminocrotonate (**7**, 903 mg, 7.6 mmol) in 2-propanol (10 ml) was stirred at 40—45 °C for 26 h. The solvent was removed and the residue was chromatographed on silica gel with AcOEt–hexane (9 : 1, v/v). The product (**4a**) was recrystallized from MeOH to give a colorless powder (1.58 g, 45%).

The other compounds were similarly prepared, except **4e** for which refluxing temperature was necessary.

Typical Procedure for Method B 2-[4-(4-Benzhydryl-1-piperazinyl)phenyl]ethyl Methyl 4-(4-Cyano-2-pyridyl)-1,4-dihydro-2,6-dimethyl-3,5-pyridinedicarboxylate (**4f**): A solution of 4-cyano-2-pyridinecarboxaldehyde (828 mg, 6.3 mmol) and 2-[4-(4-benzhydryl-1-piperazinyl)phenyl]ethyl acetoacetate (**6c**, 2.86 g, 6.3 mmol) in benzene (14 ml) containing piperidine (107 mg, 1.3 mmol) and AcOH (376 mg, 6.3 mmol) was refluxed for 1 h with azeotropic removal of H_2O using a Dean–Stark trap. After cooling to room temperature, the reaction mixture was washed with H_2O, aqueous saturated $NaHCO_3$, and brine. After drying, the solvent was evaporated to dryness, and the residue was chromatographed on silica gel with AcOEt–hexane (2 : 3, v/v) to give 2-[4-(4-benzhydryl-1-piperazinyl)-phenyl]ethyl 2-(4-cyano-2-pyridylmethylidene)acetoacetate (2.36 g) as an amorphous solid. A solution of the amorphous solid and methyl 3-aminocrotonate (**7**, 447 mg, 3.9 mmol) in 2-propanol (18 ml) was refluxed for 4 h. The solvent was distilled off and the residue was chromatographed on silica gel with AcOEt–hexane (3 : 1, v/v). The product (**4f**) was recrystallized from isopropyl ether–$CHCl_3$ to give a slightly yellow powder (2.35 g, 59%).

Compound **4e** was prepared similarly by method B.

Typical Procedure for Method C 2-[4-(4-Benzhydryl-1-piperazinyl)phenyl]ethyl Methyl 1,4-Dihydro-2,6-dimethyl-4-(3-nitrophenyl)-3,5-pyridinedicarboxylate (**4e**): To a suspension of carboxylic acid (**9**, 3.00 g, 9.0 mmol) in $CHCl_3$ (24 ml) and DMF (6 ml) was added $SOCl_2$ (1.18 g, 9.9 mmol) at 4—5 °C with ice-water cooling and this was then stirred for 2 h at the same temperature. The solution of **10c** (3.36 g, 9.0 mmol) in $CHCl_3$ (6 ml) was added to the reaction mixture at 5—7 °C and stirred for 1 h at 4—5 °C. The reaction mixture was diluted with $CHCl_3$ (30 ml), washed with 1 N NaOH and brine, dried, and the solvent was removed. The residue was purified by chromatography on silica gel with AcOEt–hexane (2 : 3, v/v) to give the product (**4e**) as a yellow amorphous powder (5.70 g, 92%). *Anal.*[13] Calcd for $C_{41}H_{42}N_4O_6 \cdot 2HCl$: C, 62.77; H, 6.01; N, 7.14; Cl, 9.04. Found: C, 63.01; H, 6.08; N, 7.05; Cl, 8.76.

The other compounds were prepared similarly by method C.

Spectral data of **4** are shown in Table III.

Method for the Preparation of Hydrochlorides of 4 To a solution of **4** (2.30 mmol) in CH_2Cl_2 (30 ml), a solution of HCl in dioxane (the same equivalent of HCl with **4**)[14] was added at room temperature. After the solution was stirred at the same temperature for 2.5 h, the solvent was removed. The residue was dissolved in EtOH (25 ml) and then the solvent

TABLE III. Spectral Data of 1,4-Dihydropyridines (**4**) Listed in Table I

Compd. No.	IR (KBr) ν_{max} (cm^{-1})	^{1}H-NMR ($CDCl_3$) δ (ppm)
4a	3200, 3100, 2950, 2225, 1705, 1665, 1620, 1600, 1520, 1500, 1440	2.25 (6H, s), 2.80 (2H, t, J=6 Hz), 2.91 (6H, s), 3.63 (3H, s), 4.24 (2H, t, J=6 Hz), 5.14 (1H, s), 6.62, 7.00 (4H, A_2B_2q, J=8 Hz), 7.05 (1H, s), 7.15—7.4 (2H, m), 8.52 (1H, d, J=5 Hz)
4b	3300, 3200, 3100, 2950, 1710, 1700, 1650, 1620, 1520, 1500, 1455, 1430, 1120	2.27, 2.30 (each 3H, s), 2.75 (2H, t, J=7 Hz), 2.89 (6H, s), 3.58 (3H, s), 4.16 (2H, t, J=7 Hz), 5.63 (1H, s), 6.01 (1H, s), 6.5—6.75 (2H, m), 6.9—7.15 (2H, m), 7.33 (1H, dd, J=7.5, 5 Hz), 7.84 (1H, d, J=7.5 Hz), 8.43 (1H, d, J=5 Hz)
4c	3325, 3200, 3075, 2950, 2225, 1700, 1660, 1620, 1600, 1545, 1495, 1450, 1430	2.19, 2.24 (each 3H, s), 2.74 (2H, t, J=6 Hz), 3.55 (3H, s), 4.18 (2H, t, J=6 Hz), 4.58 (4H, s), 5.17 (1H, s), 6.5—6.75 (2H, m), 6.8–7.05 (3H, m), 7.05—7.45 (12H, m), 8.50 (1H, d, J=5 Hz)
4d	3275, 3200, 3100, 2950, 1695, 1650, 1620, 1520, 1495, 1455, 1435	2.21, 2.27 (each 3H, s), 2.67 (2H, t, J=6.5 Hz), 3.56 (3H, s), 4.15 (2H, t, J=6.5 Hz), 4.59 (4H, s), 5.60 (1H, s), 5.91 (1H, s), 6.5—6.7 (2H, m), 6.75—7.0 (2H, m), 7.1—7.4 (11H, m), 7.86 (1H, d, J=7.5 Hz), 8.51 (1H, d, J=5 Hz)
4e	3325, 2950, 2800, 1680, 1615, 1520, 1480, 1450, 1430, 1345	2.30, 2.35 (each 3H, s), 2.45—2.65 (4H, m), 2.82 (2H, t, J=7 Hz), 3.05—3.25 (4H, m), 3.64 (3H, s), 4.23 (2H, t, J=7 Hz), 4.26 (1H, s), 5.07 (1H, s), 5.73 (1H, s), 6.80, 7.04 (4H, A_2B_2q, J=8.5 Hz), 7.1—7.6 (12H, m), 7.97 (1H, ddd, J=8, 2.5, 1 Hz), 8.06 (1H, t, J=2.5 Hz)
4f	3300, 3050, 2950, 2800, 2225, 1700, 1660, 1615, 1595, 1545, 1485, 1450, 1430	2.23, 2.27 (each 3H, s), 2.45—2.6 (4H, m), 2.80 (2H, t, J=6.5 Hz), 3.05—3.2 (4H, m), 3.62 (3H, s), 4.1—4.4 (2H, m), 4.26 (1H, s), 5.14 (1H, s), 6.79 (1H, s), 6.82, 7.05 (4H, A_2B_2q, J=8.5 Hz), 7.1—7.5 (12H, m), 8.60 (1H, dd, J=5, 0.5 Hz)
4g	3325, 2950, 2800, 1700, 1650, 1615, 1515, 1490, 1450, 1430, 1120	2.24, 2.28 (each 3H, s), 2.6—2.95 (6H, m), 2.95—3.3 (4H, m), 3.57 (3H, s), 3.95—4.45 (2H, m), 4.28 (1H, s), 5.59 (1H, s), 5.86 (1H, s), 6.6—7.0 (4H, m), 7.0—7.55 (11H, m), 7.89 (1H, d, J=7.5 Hz), 8.46 (1H, d, J=5 Hz)
4h	3375, 2950, 2800, 1690, 1650, 1615, 1530, 1490, 1455, 1435, 1350	1.75—2.1 (2H, m), 2.34, 2.36 (each 3H, s), 2.4—2.6 (4H, m), 3.05—3.2 (4H, m), 3.65 (3H, s), 3.9—4.15 (2H, m), 4.26 (1H, s), 5.12 (1H, s), 5.93 (1H, s), 6.80, 6.89 (4H, A_2B_2q, J=9 Hz), 7.1—7.5 (11H, m), 7.65 (1H, dt, J=8, 1.5 Hz), 7.98 (1H, ddd, J=8, 2.5, 2.5 Hz), 8.11 (1H, t, J=2.5 Hz)
4i	3350, 2950, 2800, 1680, 1650, 1610, 1520, 1480, 1430, 1345	2.31, 2.36 (each 3H, s), 2.45—2.6 (4H, m), 2.82 (2H, t, J=7 Hz), 3.1—3.25 (4H, m), 3.64 (3H, s), 4.22 (2H, t, J=7 Hz), 4.26 (1H, s), 5.07 (1H, s), 5.82 (1H, s), 6.78, 6.97 (4H, A_2B_2q, J=8.5 Hz), 7.0—7.55 (12H, m), 7.98 (1H, ddd, J=8.5, 2.5, 2.5 Hz), 8.06 (1H, t, J=2.5 Hz)
4j	3325, 2925, 1685, 1610, 1520, 1480, 1430, 1345	1.1—1.45 (2H, m), 1.70 (2H, br s), 2.1—2.35 (1H, m), 2.30, 2.35 (each 3H, s), 2.64 (2H, td, J=12, 2.5 Hz), 2.81 (2H, t, J=7 Hz), 3.5—3.65 (3H, m), 3.64 (3H, s), 4.22 (2H, t, J=7 Hz), 5.07 (1H, s), 5.77 (1H, s), 6.80, 7.02 (4H, A_2B_2q, J=8.5 Hz), 7.1—7.35 (11H, m), 7.51 (1H, dt, J=8, 1.5 Hz), 7.97 (1H, ddd, J=8, 2, 2 Hz), 8.06 (1H, t, J=2 Hz)
4k	3350, 3050, 2975, 1690, 1620, 1535, 1490, 1460, 1440, 1355	1.65—2.05 (6H, m), 2.28, 2.34 (each 3H, s), 2.4—2.6 (1H, m), 2.87 (2H, t, J=7 Hz), 3.00 (2H, t, J=10.5 Hz), 3.64 (3H, s), 4.26 (2H, t, J=7 Hz), 4.29 (1H, s), 5.07 (1H, s), 5.88 (1H, s), 7.05—7.55 (16H, m), 7.97 (1H, ddd, J=8, 2.5, 2.5 Hz), 8.07 (1H, t, J=2.5 Hz)
4l	3300, 2900, 1680, 1520, 1490, 1460, 1440, 1320	2.25 (3H, s), 2.31, 2.35 (each 3H, s), 2.54 (2H, t, J=7.5 Hz), 2.77 (2H, t, J=7 Hz), 2.82 (3H, s), 3.43 (2H, t, J=7.5 Hz), 3.64 (3H, s), 4.20 (2H, t, J=7 Hz), 4.39 (1H, s), 5.09 (1H, s), 5.80 (1H, s), 6.45, 6.93 (4H, A_2B_2q, J=8.5 Hz), 7.1—7.6 (11H, m), 7.54 (1H, dt, J=8, 1.5 Hz), 7.97 (1H, ddd, J=8, 2, 2 Hz), 8.08 (1H, t, J=2 Hz)
4m	3325, 2950, 2800, 1695, 1620, 1530, 1485, 1450, 1430, 1350	2.33, 2.34 (each 3H, s), 2.43 (8H, br s), 2.98 (2H, d, J=5.5 Hz), 3.60 (3H, s), 4.22 (1H, s), 4.52 (2H, d, J=5.5 Hz), 5.08 (1H, s), 5.6—5.85 (2H, m), 5.87 (1H, s), 7.15—7.45 (11H, m), 7.59 (1H, dt, J=8, 2 Hz), 7.94 (1H, ddd, J=8, 2, 2 Hz), 8.07 (1H, t, J=2 Hz)

was evaporated to dryness to give the hydrochloride of **4**. All hydrochlorides of **4** were obtained as amorphous solids and subjected to pharmacological testing.

Biological Test[15] The experiments were performed in groups of 3—6 male SHR (10 to 11 weeks old). Systolic blood pressure (SBP) was measured in a conscious state by a tail cuff plethysmographic method with an electrosphygmomanometer (PE-300, Narco Bio-System) at 0, 1, 2, 4, 7 and 24 h after administration. The test compounds were converted to hydrochlorides and were prepared as a solution or a suspension in aqueous 0.3% Tween 80 solution and orally administered at a dose of 3 mg/kg (10 ml/kg). Antihypertensive effects are shown as maximum reductions in SBP (%) from 0 h values. Duration of antihypertensive effects, carefully estimated by time course curves of SBP, is shown in hours by which SBP recovered to half maximum reductions.

References and Notes

1) Part I: A. Ashimori, T. Ono, T. Uchida, Y. Ohtaki, C. Fukaya, M. Watanabe, and K. Yokoyama, *Chem. Pharm. Bull.*, **38**, 2446 (1990).
2) F. Bossert, E. Wehinger, K. Stoepel, W. Vater, and S. Kazda, Ger. Patent 2508181 (1976) [*Chem. Abstr.*, **86**, 29638*a* (1977)].
3) J. M. Van Nueten and P. A. J. Janssen, *Arch. Int. Pharmacodyn. Ther.*, **204**, 37 (1973); L. K. C. Desmedt, C. J. E. Niemegeers, and P. A. J. Janssen, *Arzneim.-Forsch.*, **25**, 1408 (1975).
4) K. Meguro, M. Aizawa, T. Sohda, Y. Kawamatsu, and A. Nagaoka, *Chem. Pharm. Bull.*, **33**, 3787 (1985).
5) A. Hantzsch, *Justus Liebigs Ann. Chem.*, **215**, 1 (1982); F. Bossert, H. Meyer, and E. Wehinger, *Angew. Chem. Int. Ed. Engl.*, **20**, 762 (1981) and references cited therein.
6) K. Tamazawa, H. Arima, T. Kojima, Y. Isomura, M. Okada, S. Fujita, T. Furuya, T. Takenaka, O. Inagaki, and M. Terai, *J. Med. Chem.*, **29**, 2504 (1986).
7) R. F. Parcell, U.S. Patent 3028390 (1962) [*Chem. Abstr.*, **57**, 8590*c* (1962)].
8) C. F. Lane, *Synthesis*, **1975**, 135 and references cited therein.
9) J. T. Braunholtz and F. G. Mann, *J. Chem. Soc.*, **1957**, 4166; N. Itoh, *Chem. Pharm. Bull.*, **10**, 55 (1962).
10) H. B. Henbest and W. R. Jackson, *J. Chem. Soc.*, **1962**, 954.
11) Compound **30** was prepared from **12** by the usual Sandmeyer reaction, followed by protection of hydroxy group by THP group. See, *e.g.* B. L. Zenitz and W. H. Hartung, *J. Org. Chem.*, **11**, 444 (1966); K. F. Bernady, M. B. Floyd, J. F. Poletto, and M. J. Weiss, *ibid.*, **44**, 1438 (1979).
12) S. R. Wilson and M. F. Price, *J. Org. Chem.*, **49**, 722 (1984).
13) Dihydrochloride of **4e** was prepared in the following manner: **4e** (7.0 mmol) was dissolved in CH_2Cl_2 (20 ml) and HCl gas was bubbled into the solution at its reflux temperature for 30 min and then with ice-salt cooling for 20 min to give a precipitated solid. The mixture was allowed to warm to room temperature and then the precipitate was collected by filtration to afford **4e**·2HCl (4.5 g) as a pale yellow powder. Dihydrochloride of **4e** was elementally analyzed. Calculated values were made assuming 3.19% water content determined by Karl Fisher method.
14) Concentration of HCl was determined by titration with 1 N NaOH using phenolphthalein as an indicator.
15) D. Pruneau and F. Roy, *Arzneim.-Forsch.*, **37**, 416 (1987).

Synthesis of Lanosterol Derivatives with a Functional Group at C-32, Including an Antineoplastic Sterol, 3β-Hydroxylanost-7-en-32-oic Acid

Yoshiko SONODA,[a] Kimiko ICHINOSE,[a] Tomoko YOSHIMURA,[a] Yoshihiro SATO,*[,a] and Takuma SASAKI[b]

Kyoritsu College of Pharmacy,[a] Shibakoen 1-chome, Minato-ku, Tokyo 105, Japan and Cancer Research Institute, Kanazawa University,[b] Takaramachi, Kanazawa 920, Japan. *Received June 13, 1990*

Lanosterol derivatives with a functional group at C-32 have been synthesized from 3β-acetoxylanostan-7α-ol. The key reaction of the synthesis is the hypoiodite reaction of 3β-acetoxylanostan-7α-ol. *In vitro* antitumor activity testing of the lanosterol derivatives revealed that 3β-hydroxylanost-7-en-32-oic acid has antineoplastic activity.

Keywords antitumor activity; lanosterol derivative; 32-functional group; hypoiodite reaction; cholesterol biosynthesis; inhibitor

The biosynthesis of cholesterol from lanosterol requires the removal of the methyl group at carbons 4 and 14.[1] The initial step in the removal of these methyl groups has been considered to be the 14-methyl demethylation,[1] which is catalyzed by cytochrome P-450$_{14DM}$ (lanosterol 14-demethylase). Probable intermediates are 32-hydroxy and 32-oxo lanosterol derivatives.[2] The 14-methyl group (at C-32) of lanosterol is removed as formic acid,[3] resulting in the formation of the demethylated product (8,14,24-triene) (Fig. 1). 24,25-Dihydrolanosterol is also demethylated like lanosterol and converted to the demethylated product (8,14-diene). Mammalian and yeast cytochrome P-450$_{14DM}$ have been purified by Gaylor *et al.*[4] and Yoshida and Aoyama.[5] Aoyama *et al.*[6] reported that 32-hydroxy- and 32-oxo-24,25-dihydrolanosterol were converted to the corresponding 8,14-diene by purified cytochrome P-450$_{14DM}$ from yeast. Also, we reported that the 32-hydroxy and 32-oxo derivatives of lanosterol were converted to the 8,14-diene by partially purified cytochrome P-450$_{14DM}$ from rat liver.[7] On the other hand, lanosterol derivatives with a 32-oxo group have been shown to inhibit sterol biosynthesis in animal cells in culture.[8] Such naturally occurring oxygenated steroids may important in regulating sterol biosynthesis. Recently, (24*Z*)-3-oxolanosta-8,24-dien-26-oic acid,[9] a lanosterol derivative with a 26-carboxyl group, with potent inhibitory activity on cholesterol biosynthesis, has been isolated from *Kadsura heteroclita* and *K. longipedunculata*. We have reported that 7-oxo-24,25-dihydrolanosterol is a potent inhibitor of cytochrome P-450$_{14DM}$ from rat liver.[7] Inhibitors of cytochrome P-450$_{14DM}$ are candidates for cholesterol-lowering agents and antimycotics. Further, panasterol,[10] a lanosterol derivative with a 32-carboxyl group, having potent antileukemic activity (IC_{50} value of 3.6 μg/ml against L1210 cells), has been isolated from the Okinawa marine sponge *Penares* sp. With the intention of investigating the antineoplastic activity and the effect on cytochrome

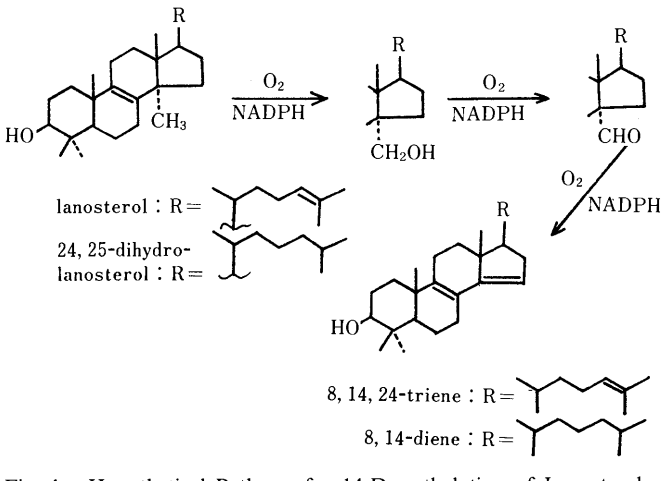

Fig. 1. Hypothetical Pathway for 14-Demethylation of Lanosterol or 24,25-Dihydrolanosterol

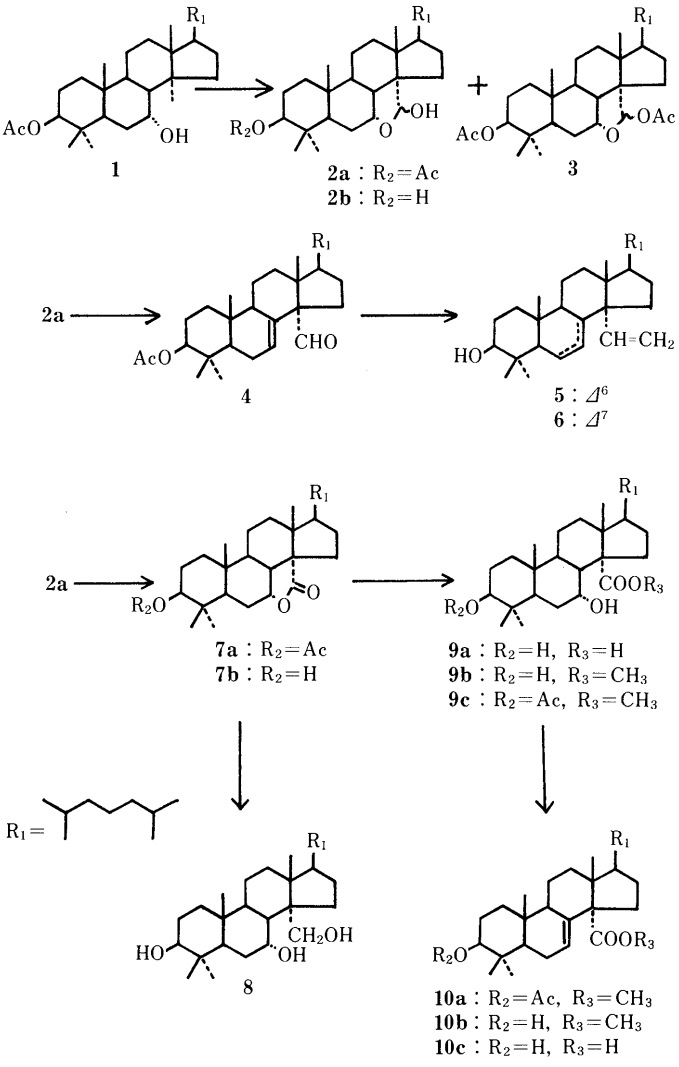

Chart 1

P-450$_{14DM}$ of lanosterol derivatives, we studied the synthesis of such compounds with a 32-functional group, as shown in Chart 1.

This report describes a simplified synthesis of 32-functionalized lanosterol derivatives possessing a formyl, a vinyl, or a carboxyl group. Since we reported previously a simplified synthesis of 3β-acetoxylanostan-7α-ol (**1**),[11] **1** was used as the starting material for the synthesis of 32-functionalized lanosterol derivatives. As previously reported, **1** was prepared by catalytic hydrogenation of 3β-acetoxylanost-8-en-7-one. Hypoiodite reaction[12] of **1** afforded the 32-hydroxy-7,32-oxide (**2a**) in 50% yield together with a small amount of the 32-acetoxy-7,32-oxide (**3**). Hydrolysis of **3** gave the same product (**2b**) as the hydrolysis of **2a**.

Reaction of **2a** with pyridinium hydrogen chloride in acetic anhydride afforded 3β-acetoxylanost-7-en-32-al (**4**) in 20% yield; this product was identical with a sample prepared previously.[11] Treatment of **4** with methyl triphenylphosphonium bromide in the presence of *n*-butyl lithium gave the vinyl compounds (**5** and **6**, 1 : 1). It is assumed that **5** was formed by isomerization during the Wittig reaction. Interestingly, the vinyl compound (**6**) was reported to be an inhibitor of lanosterol 14-methyl demethylase.[13] Jones' oxidation of **2a** gave the lactone (**7a**) in good yield. The lactone (**7a**) has been synthesized by Barton and his coworkers,[14] but they did not synthesize lanosterol 32-carboxylic acid. Treatment with aqueous alkali failed to convert **7a** to the carboxylic acid. In an alternative approach, **7a** was treated with NaOEt in EtOH, giving the desired carboxylic acid (**9a**) in high yield. On the other hand, treatment of **7a** with Na in EtOH gave the hydroxymethyl compound (**8**). In the next step, we prepared the methyl ester (**9b**) of **9a** by esterification with diazomethane. Controlled acetylation of **9b** provided methyl 3β-acetoxy-7α-hydroxylanostan-32-oate (**9c**). Next, the methyl ester (**9c**) was transformed to the dehydrated compound (**10a**) with phosphoryl chloride in pyridine. In order to obtain 3β-hydroxylanost-7-en-32-oic acid (**10c**), the acetoxy ester (**10a**) was treated with 10% or 20% potassium hydroxide. However, the product was the methyl ester (**10b**), indicating failure of the hydrolysis of the methyl ester.

In an alternative approach, we examined halogenolysis[15] with lithium iodide, which is used for conversion of the sterically hindered methyl ester into the corresponding acid. Thus, the methyl ester (**10b**) was heated with lithium iodide in 2,4,6-collidine to give the carboxylic acid (**10c**) in good yield.

The carboxylic acid (**10c**) thus synthesized in the present investigation was expected to have an antileukemic activity. Therefore, the *in vitro* antitumor activity of lanosterol derivatives synthesized in our laboratory on murine leukemia L1210 and human epidermoid carcinoma KB cells was tested, and it was found that 3β-hydroxylanost-7-en-32-oic acid (**10c**) showed the strongest activity against the test cells (Table I). It is interesting that the Δ^7-COOH compound (**10c**) showed almost the same level of antitumor activity as that of panasterol.[10] The effects of lanosterol derivatives synthesized in this study on cytochrome P-450$_{14DM}$ will be reported elsewhere.

TABLE I. *In Vitro* Antitumor Activity of Lanosterol Derivatives on L1210 and KB Cells

Test compound[a]	IC_{50} (μg/ml)	
	L1210	KB
Δ^7-COOH (**10c**)	2.3	7.2
Δ^7-COOMe (**10b**)	(−2.3)[b]	(8.0)
7α-OH,COOMe (**9b**)	(41.2)	(42.6)
7α-OH,COOH (**9a**)	(7.2)	(27.6)
7α-OH,CH_2OH (**8**)	(36.9)	(40.8)
Δ^7-CH_2OH[c]	(7.2)	(0.3)
26-OH[c]	29.0	(31.7)
25-OH[c]	(45.7)	(41.4)
24*R*-Epoxy[c]	2.7	7.6
24*S*-Epoxy[c]	28.0	29.0
24-OH[c]	(37.1)	6.2
22*R*-OH[c]	27.0	12.6
24-Oxo[c]	4.0	8.0
7-Oxo[c]	(30.5)	(3.0)
7,11-Dioxo[c]	13.5	16.5
11-Oxo[c]	15.5	15.0
24-Ethylidene[c]	(−2.5)	(22.0)
Lanosterol	16.0	28.0
24,25-Dihydrolanosterol	(−1.6)	(47.0)

a) Each test compound was dissolved or suspended in DMSO. *b*) Figures in parentheses are values of percentage inhibition at the concentration of 50 μg/ml. *c*) Abbreviations: Δ^7-CH_2OH, lanost-7-ene-3β,32-diol[16]; 26-OH, lanosta-8,24-diene-3β,26-diol[17]; 25-OH, lanost-8-ene-3β,25-diol[17]; 24*R*-epoxy, (24*R*)-24,25-epoxylanost-8-en-3β-ol[17]; 24*S*-epoxy, (24*S*)-24,25-epoxylanost-8-en-3β-ol[17]; 24-OH, lanost-8-ene-3β,24-diol[17]; 22*R*-OH, (22*R*)-22-hydroxylanosta-8,24-dien-3β-ol[18]; 24-oxo, 24-oxolanost-8-en-3β-ol[17]; 7-oxo, 7-oxolanost-8-en-3β-ol[17]; 7,11-dioxo, 7,11-dioxolanost-8-en-3β-ol[19]; 11-oxo, 11-oxolanost-8-en-3β-ol[19]; 24-ethylidene, 24-ethylidenelanost-8-en-3β-ol.[20]

Experimental

All melting points were obtained on a micro-melting point determination apparatus and are uncorrected. Proton nuclear magnetic resonance (^{1}H-NMR) spectra were obtained on a JEOL FX-200 NMR spectrometer in deuteriochloroform. Abbreviations used: s = singlet, d = doublet, br s = broad singlet, dd = double doublet, m = multiplet. Mass spectra (MS) were recorded on a JEOL D-100 spectrometer at 75 eV ionizing potential. "The usual work-up" refers to dilution of the reaction mixture with water, extraction with CH_2Cl_2, washing of the extract with water, drying over Na_2SO_4, and concentration under reduced pressure.

Hypoiodite Reaction of 3β-Acetoxylanostan-7α-ol (1) A suspension of lead tetraacetate (1.77 g, 4 mmol) and calcium carbonate (600 mg, 6 mmol) in benzene (200 ml) was mixed with iodine (252 mg, 1 mmol) and 3β-acetoxylanostan-7α-ol (**1**, 488 mg, 1 mmol). The mixture was irradiated with a 450 W high-pressure mercury-vapor lamp (Ushio type MM2) until decolorization in an atmosphere of nitrogen. After the reaction mixture had cooled to room temperature, insoluble lead salts were filtered off. The filtrate was washed with 10% $Na_2S_2O_3$ solution and water, and dried over Na_2SO_4. The benzene was evaporated off under reduced pressure. The residue was chromatographed over silica gel (50 g). Elution with benzene afforded 7α,32-epoxylanostane-3β,32-diol diacetate (**3**, 150 mg). Further elution with methylene chloride afforded 7α,32-epoxylanostane-3β,32-diol 3-acetate (**2a**, 300 mg), which was recrystallized from MeOH to give **2a** as colorless needles, mp 185—186 °C. *Anal.* Calcd for $C_{32}H_{54}O_4$: C, 76.44; H, 10.83. Found: C, 76.75; H, 10.76. MS *m/z*: 484 ($M^+ - H_2O$), 457 (base peak). ^{1}H-NMR δ (ppm): 0.79 (3H, s, 18-CH_3), 0.85 (6H, d, J=6.6 Hz, 26 and 27-CH_3), 0.82 (3H, s, 30-CH_3), 0.84 (3H, s, 31-CH_3), 0.91 (3H, s, 19-CH_3), 2.05 (3H, s, 3-$OCOCH_3$), 4.32 (1H, br s, 7-H), 4.50 (1H, m, 3-H), 5.61 (1H, br s, 32-H).

The diacetate (**3**) was characterized by hydrolysis to give **2b**. Compound **3** was dissolved in 10% ethanolic potassium hydroxide and refluxed for 1 h. After usual work-up, the residue was recrystallized from MeOH to give **2b** as colorless needles, mp 189—190 °C. *Anal.* Calcd for $C_{30}H_{52}O_3$: C, 78.20; H, 11.38. Found: C, 77.94; H, 10.90. MS *m/z*: 442 ($M^+ - H_2O$), 414 (base peak). ^{1}H-NMR δ (ppm): 0.77 (3H, s, 18-CH_3), 0.854 (3H, d, J=6.6 Hz, 26 or 27-CH_3), 0.864 (3H, d, J=6.6 Hz, 26 or 27-CH_3), 0.856 (3H, s, 31-CH_3), 0.90 (3H, s, 19-CH_3), 0.94 (3H, s, 30-CH_3), 4.32 (1H, br s, 7-H), 3.23 (1H, m, 3-H), 5.62 (1H, br s, 32-H).

3β-Acetoxylanost-7-en-32-al (4) A mixture of 7α,32-epoxylanostane-

3β,32-diol 3-acetate (**2a**, 0.1 g) and pyridinium hydrogen chloride (0.2 g) in acetic anhydride (10 ml) was refluxed for 15 h. After usual work-up, the residue was chromatographed on silica gel (10 g). Elution with benzene gave **4** (20 mg). Further elution with methylene chloride gave the starting material (**2a**, 70 mg).

Wittig Reaction of 3β-Acetoxylanost-7-en-32-al (4) *n*-Butyl lithium (14%, 0.3 ml) was added to a suspension of methyl triphenylphosphonium bromide (0.3 g) in anhydrous benzene (5 ml) and the mixture was stirred at room temperature for 10 min. Then, a solution of **4** (0.1 g) in anhydrous benzene (2.5 ml) was added, and the mixture was stirred at room temperature for 5 h. The reaction mixture was poured into water and extracted with benzene. The residue from the extract was column-chromatographed on 10% $AgNO_3$-impregnated silica gel (10 g). Elution with benzene (frs. 4 and 5) gave a solid (20 mg), which was recrystallized from MeOH to give 14-vinyl-4,4-dimethylcholest-6-en-3β-ol (**5**) as colorless needles. mp 99—100 °C. *Anal.* Calcd for $C_{31}H_{52}O$: C, 84.48; H, 11.89. Found: C, 84.36; H, 11.52. MS *m/z*: 440 (M^+, base peak), 425 ($M^+ - CH_3$). ^{1}H-NMR δ (ppm): 0.80 (3H, s, 18-CH_3), 0.86 (3H, d, J=6.6 Hz, 26 or 27-CH_3), 0.87 (3H, d, J=6.6 Hz, 26 or 27-CH_3), 0.86, 0.89, 1.00 (each 3H, each s, 30-, 19-, 31-CH_3), 3.23 (1H, m, 3-H), 5.00 (1H, dd, J=2.5, 18 Hz, $_{H}^{}>C=C<^{H}_{H}$), 5.08 (1H, dd, J=2.5, 9 Hz, $_{H}^{}>C=C<^{H}_{H}$), 5.46 (1H, d, J=8 Hz, 6- or 7-H), 6.30 (1H, dd, J=9, 18 Hz, C<u>H</u>=CH_2). Further elution with benzene (frs. 7 and 8) gave a solid (20 mg), which was recrystallized from MeOH to give 14-vinyl-4,4-dimethylcholest-7-en-3β-ol (**6**) as colorless needles, mp 106—107 °C (ref.[13] 106.5—107.0 °C). MS *m/z*: 440 (M^+, base peak), 425 ($M^+ - CH_3$). ^{1}H-NMR δ (ppm): 0.69 (3H, s, 18-CH_3), 0.861 (3H, d, J=6.6 Hz, 26 or 27-CH_3), 0.87 (3H, d, J=6.6 Hz, 26 or 27-CH_3), 0.862, 0.89, 0.99 (each 3H, each s, 30-, or 19- or 31-CH_3), 3.23 (1H, m, 3-H), 4.95 (1H, dd, J=2.5, 9 Hz, $_{H}^{}>C=C<^{H}_{H}$), 5.01 (1H, dd, J=2.5, 18 Hz, $_{H}^{}>C=C<^{H}_{H}$), 5.31 (1H, br s, 7-H), 6.28 (1H, dd, J=9, 18 Hz, C<u>H</u>=CH_2).

Oxidation of 7α,32-Epoxylanostane-3β,32-diol 3-Acetate (2a) Jones' reagent (1.5 ml) was added slowly (over 10 min) to a stirred solution of **2a** (0.3 g) in acetone (100 ml) and stirring was continued for 2 h at room temperature. After usual work-up, the extracted product was recrystallized from MeOH to give 3β-acetoxylanostano-32,7α-lactone (**7a**, 0.28 g) as colorless needles, mp 285—287 °C (ref.[14] 287—290 °C). MS *m/z*: 500 (M^+, base peak), 485 ($M^+ - CH_3$), 457. ^{1}H-NMR δ (ppm): 0.81 (3H, s, 18-CH_3), 0.83 (3H, s, 30-CH_3), 0.845 (3H, s, 31-CH_3), 0.850 (6H, d, J=6.6 Hz, 26 and 27-CH_3), 0.852 (3H, s, 19-CH_3), 0.91 (3H, d, J=6.6 Hz, 21-CH_3), 4.45 (1H, m, 3-H), 4.50 (1H, br s, 7-H).

The lactone (**7a**) was hydrolyzed with 10% methanolic KOH under reflux for 1 h. After usual work-up, the residue was recrystallized from MeOH to give **7b** as colorless needles, mp 255—257 °C. *Anal.* Calcd for $C_{30}H_{50}O_3$: C, 78.55; H, 10.99. Found: C, 79.03; H, 11.09. MS *m/z*: 458 (M^+, base peak), 443 ($M^+ - CH_3$), 430. ^{1}H-NMR δ (ppm): 0.80 (3H, s, 18-CH_3), 0.85 (3H, s, 31-CH_3), 0.87 (6H, d, J=6.6 Hz, 26 and 27-CH_3), 0.89 (3H, s, 19-CH_3), 0.95 (3H, s, 30-CH_3), 3.23 (1H, m, 3-H), 4.54 (1H, br s, 7-H).

Lanostane-3β,7α,32-triol (8) Na (2 g) was added to a solution (100 ml) of 3β-acetoxylanostano-32,7α-lactone (**7a**, 0.2 g) and the reaction mixture was refluxed for 2 d, then poured into ice-water and neutralized with dilute HCl. The usual work-up afforded a yellow residue, which was column-chromatographed on Sephadex LH-20 (1 cm × 20 cm). Elution with CH_2Cl_2 (fr. 1) gave a solid (0.05 g) which was identified as **7b**. Further elution with CH_2Cl_2 (frs. 4 and 5) gave a solid (0.13 g), which was recrystallized from MeOH to give **8** as colorless needles, mp 240—241 °C. *Anal.* Calcd for $C_{30}H_{54}O_3$: C, 77.86; H, 11.76. Found: C, 77.48; H, 11.42. MS *m/z*: 414 ($M^+ - H_2O$, CH_2O, base peak), 399. ^{1}H-NMR δ (ppm): 0.81 (6H, s, 18 and 31-CH_3), 0.87 (6H, d, J=6.6 Hz, 26 and 27-CH_3), 0.95 (3H, s, 30-CH_3), 0.98 (3H, s, 19-CH_3), 3.30 (1H, m, 3-H), 3.49 (1H, d, J=11.2 Hz, 32-H), 3.90 (1H, d, J=11.2 Hz, 32-H), 4.00 (1H, br s, 7-H).

3β,7α-Dihydroxylanostan-32-oic Acid (9a) A solution of 3β-acetoxylanostano-32,7α-lactone (**7a**, 0.2 g) in EtOH (5 ml) was added to a solution of 2% NaOEt in EtOH (100 ml) and the reaction mixture was refluxed for 1 week, then poured into ice-water and neutralized with dilute HCl. The usual work-up afforded a yellow residue, which was column-chromatographed on Sephadex LH-20 (1 cm × 20 cm). Elution with methylene chloride (fr. 1) gave a solid (0.1 g) which was identified as **7b**. Further elution with methylene chloride (frs. 6 and 7) gave a solid (0.1 g), which was recrystallized from MeOH to give **9a** as colorless needles, mp 275—276 °C. *Anal.* Calcd for $C_{30}H_{52}O_4$: C, 75.58; H, 11.00. Found: C, 75.23; H, 10.92. MS *m/z*: 458 ($M^+ - H_2O$), 413 (base peak). ^{1}H-NMR δ (ppm): 0.78 (3H, s, 18-CH_3), 0.86 (6H, d, J=6.6 Hz, 26 and 27-CH_3), 0.85 (3H, s, 31-CH_3), 0.90 (3H, s, 30-CH_3), 0.94 (3H, s, 19-CH_3), 3.28 (1H, m, 3-H), 4.00 (1H, br s, 7-H).

Methyl 3β,7α-Dihydroxylanostan-32-oate (9b) 3β,7α-Dihydroxylanostan-32-oic acid (**9a**) was methylated by diazomethane in ether to give **9b**. Recrystallization from MeOH gave colorless needles of mp 178—180 °C. *Anal.* Calcd for $C_{31}H_{54}O_4$: C, 75.87; H, 11.09. Found: C, 75.62; H, 11.05. MS *m/z*: 490 (M^+), 458, 413 (base peak), 395. ^{1}H-NMR δ (ppm): 0.79 (3H, s, 18-CH_3), 0.85 (3H, s, 31-CH_3), 0.86 (6H, d, J=6.6 Hz, 26 and 27-CH_3), 0.89 (3H, s, 30-CH_3), 0.93 (3H, s, 19-CH_3), 3.25 (1H, m, 3-H), 3.61 (3H, s, $COOCH_3$), 4.95 (1H, br s, 7-H).

Methyl 3β-Hydroxylanost-7-en-32-oate (10b) Methyl 3β,7α-dihydroxylanostan-32-oate (**9b**, 0.1 g) was acetylated with Ac_2O–pyridine for 2 h at room temperature to give the 3β-acetate (**9c**). The crude product was dissolved in pyridine (1 ml), $POCl_3$ (0.5 ml) was added, and the mixture was refluxed for 1 h. The usual work-up afforded the residue, which was confirmed by ^{1}H-NMR to be methyl 3β-acetoxylanost-7-en-32-oate (**10a**). The crude product (**10a**) was hydrolyzed with 10% methanolic KOH under reflux for 1 h. After the usual work-up, the residue was recrystallized from MeOH to give **10b** as colorless needles, mp 144—145 °C. *Anal.* Calcd for $C_{31}H_{52}O_3$: C, 78.76; H, 11.09. Found: C, 78.86; H, 11.08. MS *m/z*: 472 (M^+), 413 (base peak), 395. ^{1}H-NMR δ (ppm): 0.69 (3H, s, 18-CH_3), 0.859 (3H, d, J=6.6 Hz, 26 or 27-CH_3), 0.864 (3H, d, J=6.6 Hz, 26 or 27-CH_3), 0.89 (6H, 30 and 31-CH_3), 0.98 (3H, s, 19-CH_3), 3.25 (1H, m, 3-H), 3.61 (3H, s, 14-$COOCH_3$), 5.42 (1H, br s, 7-H).

3β-Hydroxylanost-7-en-32-oic Acid (10c) The ester (50 mg) in 2,4,6-collidine (10 ml) was heated under reflux with lithium iodide (0.25 g) for 3 h. The reaction mixture was cooled, poured into water, acidified with dilute HCl, and extracted with CH_2Cl_2. The extract was washed with water, dried, and evaporated to give a solid, which was column-chromatographed on silica gel. Elution with CH_2Cl_2 gave **10c** (40 mg), which was recrystallized from AcOEt–*n*-hexane to give colorless needles of mp 212—214 °C. *Anal.* Calcd for $C_{30}H_{50}O_3$: C, 78.55; H, 10.99. Found: C, 78.12; H, 10.65. MS *m/z*: 458 (M^+), 413 (base peak). ^{1}H-NMR δ (ppm): 0.71 (3H, s, 18-CH_3), 0.86 (6H, d, J=6.6 Hz, 26 and 27-CH_3), 0.89 (6H, s, 30 and 31-CH_3), 0.91 (3H, d, J=6.6 Hz, 20-CH_3), 0.99 (3H, s, 19-CH_3), 3.25 (1H, m, 3-H), 5.52 (1H, br s, 7-H).

Assay of *in Vitro* Antitumor Activity *In vitro* antitumor activity was determined by using murine leukemia L1210 and human epidermoid carcinoma KB cells. Roswell Park Memorial Institute Medium 1610 supplemented with 10% heat-inactivated fetal bovine serum and 50 μg/ml of kanamycin was used as the cell culture medium. Tumor cells (2×10^3 cells/ml) were cultured in a CO_2 gas incubator at 37 °C for 72 h in 1 ml of medium containing various concentrations of test compound. Their viability, estimated by use of a modified colorimetric [3-(4,5-dimethylthiazol-2-yl)-2,5-diphenyl-tetrazolium bromide] (MTT) assay,[21] was compared to that of control cells incubated in the identical medium without the compound. The antitumor activity was evaluated in terms of IC_{50} (the concentration in μg/ml required for 50% inhibition of cell growth). The IC_{50} value was obtained by plotting the logarithm of concentration of the test compound *vs.* the growth rate (percentage of control) of the treated cells.

References

1) N. B. Myant, "The Biology of Cholesterol and Related Steroids," William Heinemann, Medical Books Ltd., London, 1981, pp. 163—213; G. J. Schroepfer, Jr., *Annu. Rev. Biochem.*, **51**, 603 (1982).
2) G. F. Gibbons, C. R. Pullinger, and K. A. Mitropoulos, *Biochem. J.*, **183**, 309 (1979).
3) K. Alexander, M. Akhtar, R. B. Boar, J. F. McGhie, and D. H. R. Barton, *J. Chem. Soc., Chem. Commun.*, **1972**, 383; M. Akhtar, K. Alexander, R. B. Boar, J. F. McGhie, and D. H. R. Barton, *Biochem. J.*, **169**, 449 (1978).
4) J. Trzaskos, S. Kawata, and J. L. Gaylor, *J. Biol. Chem.*, **261**, 14651 (1986).
5) Y. Yoshida and Y. Aoyama, *J. Biol. Chem.*, **259**, 1655 (1984).
6) Y. Aoyama, Y. Yoshida, Y. Sonoda, and Y. Sato, *J. Biol. Chem.*, **262**, 1239 (1987); *idem, ibid.*, **264**, 18502 (1989).
7) Y. Sekigawa, Y. Sonoda, and Y. Sato, *Chem. Pharm. Bull.*, **36**, 3049 (1988); Y. Sonoda, Y. Sekigawa, and Y. Sato, *ibid.*, **37**, 2762 (1989).
8) G. F. Gibbons, C. R. Pullinger, H. W. Chen, W. K. Cavenee, and A. A. Kandutsch, *J. Biol. Chem.*, **255**, 395 (1980).
9) K. Kangouri, T. Miyoshi, A. Ikeda, S. Omura, L.-N. Li, and H. Xue, *Agric. Biol. Chem.*, **54**, 993 (1990).

10) J. F. Cheng, J. Kobayashi, H. Nakamura, and Y. Ohizumi, Y. Hirata, and T. Sasaki, *J. Chem. Soc., Perkin Trans. 1*, **1988**, 2403.
11) Y. Sonoda, Y. Tanoue, M. Yamaguchi, and Y. Sato, *Chem. Pharm. Bull.*, **35**, 394 (1987).
12) K. Heusler, J. Kalvoda, P. Wieland, G. Anner, and A. Wettstein, *Helv. Chim. Acta*, **45**, 2575 (1962).
13) L. L. Frye and C. H. Robinson, *J. Chem. Soc., Chem. Commun.*, **1988**, 129.
14) P. L. Batten, T. J. Bentley, R. B. Boar, R. W. Draperand, J. F. McGhie, and D. H. Barton, *J. Chem. Soc., Perkin Trans. 1*, **1972**, 739.
15) F. Elisinger, J. Schreiber, and A. Eschenmoser, *Helv. Chim. Acta*, **43**, 113 (1960).
16) Y. Sonoda and Y. Sato, *Chem. Pharm. Bull.*, **35**, 394 (1987).
17) Y. Sonoda and Y. Sato, *Chem. Pharm. Bull.*, **31**, 1698 (1983).
18) Y. Sonoda and Y. Sato, *Chem. Pharm. Bull.*, **31**, 907 (1983).
19) Y. Sonoda, Y. Sekigawa, and Y. Sato, *Chem. Pharm. Bull.*, **36**, 966 (1988).
20) Y. Sato and Y. Sonoda, *Chem. Pharm. Bull.*, **29**, 356 (1981).
21) J. Carmichael, W. G. DeGraff, A. F. Gazdar, J. D. Minna, and J. B. Mitchell, *Cancer Res.*, **47**, 936 (1987).

Characterization of Technetium-99m Complexes of Pentane-2,4-dione Bis(*N*-methylthiosemicarbazone)

Yasushi ARANO,[a] Masashi YABUKI,[a] Alun G. JONES,[b] and Akira YOKOYAMA*,[a]

Department of Radiopharmaceutical Chemistry, Faculty of Pharmaceutical Sciences, Kyoto University,[a] Sakyo-ku, Kyoto 606, Japan and Department of Radiology, Harvard Medical School,[b] Boston, 02115, MA, U.S.A. *Received June 19, 1990*

Further characterization of the two neutral technetium-99m (^{99m}Tc) complexes of pentane-2,4-dione bis(*N*-methylthiosemicarbazone) (PETS) was carried out using a new dianionic PETS derivative, 3,3-dimethyl-pentane-2,4-dione bis(*N*-methylthiosemicarbazone) (DM-PETS), and the well characterized ^{99m}Tc complex of 2,2,9,9-tetramethyl-4,7-diaza-1,10-decanedithiol (DADT) as references. While PETS generated two neutral ^{99m}Tc complexes, ^{99m}Tc-PETS-L_1 and ^{99m}Tc-PETS-L_2, by both the stannous reduction method and the ligand exchange reaction with six-coordinated ^{99m}Tc(V) complex of *N,N'*-ethylenebis(acetylacetone imine), DM-PETS formed only one neutral ^{99m}Tc complex. ^{99m}Tc-PETS-L_2, the more lipophilic complex of the two ^{99m}Tc-PETS, was obtained with a much higher yield than ^{99m}Tc-PETS-L_1 by the ligand exchange reaction of PETS with the five-coordinated ^{99m}Tc(V) complex of glucoheptonate. In addition, while ^{99m}Tc-PETS-L_2 and ^{99m}Tc-DADT remained unchanged in the presence of CN^- anions, a breakdown of the original complexes was observed in ^{99m}Tc-PETS-L_1 and ^{99m}Tc-DM-PETS. All four ^{99m}Tc complexes exhibited similar brain, heart and pancreas extraction when injected into mice. These cummulative results imply that ^{99m}Tc-PETS-L_1 and ^{99m}Tc-DM-PETS are six-coordinated mononuclear ^{99m}Tc(V) complexes and that ^{99m}Tc-PETS-L_2 is a five-coordinated mononuclear ^{99m}Tc(V) complex. These results also suggest that while the chelate ring structure of the ^{99m}Tc-dithiosemicarbazone (DTS) chelate played a singificant role in its stability, ionization of the third proton of the PETS molecule and the subsequent resonating structure afforded further stability to the ^{99m}Tc-PETS complex. Markedly high lipophilicity of the ^{99m}Tc-PETS-L_2 may also be explained by assuming that ^{99m}Tc-PETS-L_2 is the five-coordinated resonating structure.

Keywords Technetium-99m; radiopharmaceutical; dithiosemicarbazone; octahedral; square-pyramidal; stability; lipophilicity

Introduction

We previously reported that a new dithiosemicarbazone (DTS) ligand, pentane-2,4-dione bis(*N*-methylthiosemicarbazone) (PETS), holding a 5–6–5 membered chelate ring structure, yielded two neutral technetium-99m (^{99m}Tc) complexes of different lipophilicity. Both complexes exhibited much higher stability and lipophilicity than those of the 5–5–5 membered ^{99m}Tc–DTS chelate, as well as rapid extraction in the brain and heart, when injected into mice.[1]

In the present study, the PETS derivative, 3,3-dimethyl-pentane-2,4-dione bis(*N*-methylthiosemicarbazone) (DM-PETS) was synthesized. While PETS can ionize up to three protons upon technetium coordination due to its diverse resonating structure, DM-PETS was designed to release only two protons in spite of having the same coordination geometry as that of PETS. DM-PETS also differs from diacetyl bis(*N*-methylthiosemicarbazone) (DA-α-DTS) in its chelate ring size, although it has the same number of ionized protons upon technetium coordination. Typical resonating structures of the three ligands are shown in Fig. 1. After the ^{99m}Tc labeling of PETS and DM-PETS, *in vitro* characteristics and *in vivo* behaviors of the ^{99m}Tc complexes were investigated using the well characterized ^{99m}Tc complex of 2,2,9,9-tetramethyl-4,7-diaza-1,10-decanedithiol (DADT) (Fig. 2) as a reference. Factors influencing the stability of ^{99m}Tc–DTS complexes and the relation between the two ^{99m}Tc–PETS complexes were discussed.

Materials and Methods

Experimental Chemistry All chemicals were of reagent grade and were used as received. Organic compounds were characterized by their melting point, proton nuclear magnetic resonance (^{1}H-NMR) and elemental analysis. Nuclear magnetic resonance (NMR) spectra were taken by Bruker AC-300 using tetramethylsilane as an internal standard. DADT was synthesized according to the procedure of Chiotellis *et al.*,[2] Glucoscan kits, containing glucoheptonate (200 mg) and Sn^{2+} (0.06 mg), were purchased from NEN/DuPont. Analysis of ^{99m}Tc labeling reactions was performed using high performance liquid chromatography (HPLC) utilizing a reverse phase column (Cosmosil C_{18}, 4.6 × 150 mm, Nacalai Tesque, Japan) and an inflow system comprised of a radiodetector.

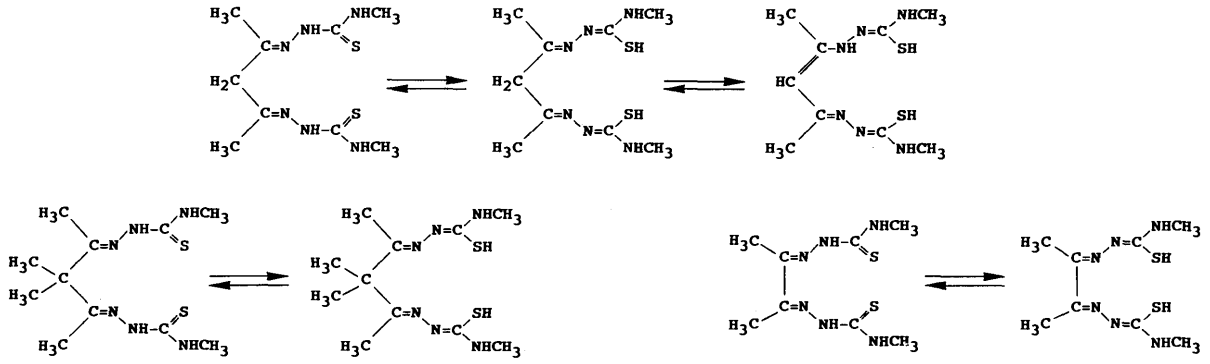

Fig. 1. Typical Resonating Structures of PETS (Top), DM-PETS (Bottom, Left) and DA-α-DTS (Bottom, Right)

While PETS can liberate up to three protons, DM-PETS and DA-α-DTS can ionize two protons. PETS and DM-PETS form a 5–6–5 membered chelate and DA-α-DTS forms a 5–5–5 membered chelate with technetium.

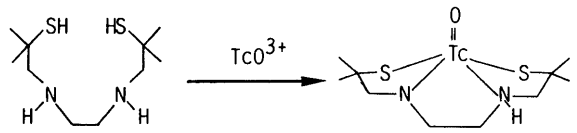

Fig. 2. Chemical Structure of DADT and Its Technetium Complex

Elution was carried out with a mixture of CH_3CN and 5 mM NH_4OAc (1 : 1) at a flow rate of 1 ml/min.

Synthesis of 3,3-Dimethyl-pentane-2,4-dione Bis(*N*-methylthiosemicarbazone) (DM-PETS) The precursor, 3,3-dimethyl-pentane-2,4-dione was synthesized according to the procedure of Bloomfield in a 41% yield (bp 168—172 °C).[3] 3,3-Dimethyl-pentane-2,4-dione (0.64 g, 5 mmol) in ethanol (80 ml) was added dropwise to a solution of *N*-methylthiosemicarbazide (1.16 g, 11 mmol) in 0.1 N HCl (80 ml) at room temperature then kept stirring overnight. The precipitated crystals were collected and washed with H_2O and cold ethanol. The product (0.15 g) was obtained as a white crystal (9.9% yield). mp 163—165 °C. *Anal.* Calcd for $C_{11}H_{22}N_6S_2$: C, 43.68; H, 7.33; N, 27.79. Found: C, 43.52; H, 7.45; N, 27.59. ^{1}H-NMR (DMSO-d_6) ppm: 1.06 (6H, d, CH_3), 1.34 (3H, s, CH_3), 1.93 (3H, s, CH_3), 2.94 (6H, d, $NHCH_3$), 5.78 (1H, s, NH), 7.88 (1H, s, NH), 8.38 (2H, d, $NHCH_3$).

Preparation of ^{99m}Tc Complexes ^{99m}Tc–PETS complexes were synthesized by the stannous reduction method according to the procedure as previously described.[1] Two isolated ^{99m}Tc–PETS complexes with HPLC retention times of 9.7 and 11.6 min were abbreviated as ^{99m}Tc–PETS-L_1 and ^{99m}Tc–PETS-L_2, respectively.

^{99m}Tc–DM-PETS was synthesized by the stannous reduction method as follows: to a 1 ml solution of DM-PETS (10^{-3} M) prepared in 0.1 M phosphate buffer (pH 8.0) was added 0.5 ml of $^{99m}TcO_4^-$ (18.5—37 MBq) and 10 μl of freshly prepared stannous chloride (2.2×10^{-2} M in 0.1 N HCl). The reaction mixture was heated at 85 °C for 100 min. The product was then separated by HPLC, followed by extraction with 3 ml of ethyl acetate. After evaporating the organic solvent under a stream of N_2, the residue was dissolved in saline to give a DM-PETS concentration of 2.4×10^{-4} M.

^{99m}Tc–DADT was synthesized according to the procedure of Lever *et al.*[4] as follows: to DADT ligand (2 mg) dissolved in 1 ml of 0.1 M phosphate buffer (pH 7.0) was added 0.5 ml of $^{99m}TcO_4^-$ (12.1—18.5 MBq), followed by the addition of 10 μl of $SnCl_2$ (1.33×10^{-4} M) in ethanol. After stirring at room temperature for 10 min, the reaction mixture was extracted with 5 ml of $CHCl_3$, and the $CHCl_3$ layer was dried over anhydrous sodium sulfate. The filtered solution was condensed to dryness under a stream of N_2. The residue was then dissolved in saline to give a DADT concentration of 2.4×10^{-4} M.

Ligand Exchange Reaction To a 1 ml solution of PETS, DM-PETS (1×10^{-3} M in 0.1 M phosphate buffer, pH 8.0) or DADT (3×10^{-3} M in the same buffer), was added a 1 ml solution of ^{99m}Tc complex of *N,N'*-ethylenebis(acetylacetone imine) (^{99m}Tc–(en)) in CH_2Cl_2, prepared according to the procedure of Deutsch *et al.*[5] After evaporating CH_2Cl_2 under a stream of N_2, the reaction mixture was heated at 85 °C for 15 min, extracted with hexane, then analyzed by HPLC.

The glucoscan kit was reconstituted by adding 5 ml of $^{99m}TcO_4^-$ to give a final glucoheptonate (GH) concentration of 40 mg/ml. To a 1 ml solution of PETS, DM-PETS (1×10^{-3} M in 0.1 M acetate buffer, pH 5.0) was added 1 ml solution of ^{99m}Tc–GH. The reaction mixture was heated at 85 °C for 2 h, extracted with hexane, then analyzed by HPLC.

Electrophoresis Cellulose acetate electrophoresis was carried out in phosphate buffer (0.1 M, pH 7.0) at an electrostatic field of 0.8 mA/cm for 30 min, using presoaked strips (1 × 11 cm). Under these conditions, $^{99m}TcO_4^-$ migrates 2.5 to 3 cm towards the anode.

Stability Measurement A 1 ml solution of ^{99m}Tc–DM-PETS was mixed with 3 ml of mouse plasma and incubated at 37 °C. At appropriate times after incubation, 500 μl of each sample was withdrawn, deproteinized by ultrafiltration at 1500*g* for 30 min, and the filtrate analyzed by HPLC.

To each 0.5 ml solution of ^{99m}Tc–PETS-L_1, ^{99m}Tc–PETS-L_2, ^{99m}Tc–DM-PETS and ^{99m}Tc–DADT containing 2.4×10^{-4} M ligand, a 0.5 ml solution of 10 mM of KCN in 0.1 M of acetate buffer (pH 6.0) was added and incubated at 37 °C. At appropriate times after incubation, 50 μl of each sample was withdrawn and analyzed by HPLC.

Partition Coefficient (PC) The PC of the ^{99m}Tc complexes was determined according to the procedure as described before[1]: 100 μl of each ^{99m}Tc complex was mixed with 3 ml each of octanol and buffer (0.1 M phosphate buffer, pH 7.0, 7.4, 8.0). Samples were vortexed for 30 s at room temperature then centrifuged at 500*g* for 5 min. A 50 μl portion of each fraction was collected and counted. The PC was determined by calculating the ratio of counts per minute of 50 μl of octanol to that of the buffer. Samples from the octanol layer were repartitioned with the same volume of buffer until consistent partition coefficient values were obtained (three to four times).

Protein Binding The relative plasma protein binding of ^{99m}Tc–PETS-L_1, ^{99m}Tc–PETS-L_2, ^{99m}Tc–DM-PETS and ^{99m}Tc–DADT was compared by the trichloroacetic acid (TCA) precipitation method. Fifty microliters solutions of ^{99m}Tc complexes were added to 500 μl of mouse plasma, and incubated at 37 °C for 10 min, after which 1 ml of saline and 1 ml of 5% TCA were added. After centrifugation at 3000*g* for 15 min, supernatant was aspirated, and the residue was washed with 1 ml of saline and 1 ml of 5% TCA, then centrifuged. The relative plasma protein binding of each ^{99m}Tc complex was determined by calculating the ratio of counts per minute of precipitate to that of total radioactivity.

Mice Distribution Studies Biodistribution of ^{99m}Tc–PETS-L_1 and ^{99m}Tc–PETS-L_2 in mice was compared with that of ^{99m}Tc–DM-PETS and ^{99m}Tc–DADT. Fifty microliters of ^{99m}Tc complexes were injected into ddY male mice (5 weeks old) from the lateral tail vein. At appropriate times after injection, the mice were decapitated and blood samples were collected. The organs of interest were excised, weighed, and the radioactivity was counted.

Results

Preparation of DM-PETS DM-PETS was synthesized by the alkylation of the precursor, pentane-2,4-dione, in the presence of sodium hydride, followed by the condensation reaction of the resulting 3,3-dimethylpentane-2,4-dione with *N*-methylthiosemicarbazide in the presence of an acid catalyst.

Preparation of ^{99m}Tc Complexes Radiochemical purities of ^{99m}Tc–PETS-L_1, ^{99m}Tc–PETS-L_2, ^{99m}Tc–DM-PETS and ^{99m}Tc–DADT were determined to be over 98% by HPLC analysis. The HPLC retention time of the four ^{99m}Tc complexes is shown in Table I.

***In Vitro* Studies** Cellulose acetate electrophoresis of ^{99m}Tc–PETS-L_1, ^{99m}Tc–PETS-L_2, ^{99m}Tc–DM-PETS and ^{99m}Tc–DADT showed a single peak at the origin, and no further ^{99m}Tc radioactivity was observed.

The stability of ^{99m}Tc–DM-PETS in mouse plasma is shown in Fig. 3. HPLC analysis of the 5 min incubation sample showed a slight decrease of the original radioactivity. After this, however, ^{99m}Tc–DM-PETS remained unchanged during the following 3 h incubation as well as after the addition of fresh plasma.

In Fig. 4, HPLC radioactivity profiles of the ligand exchange reactions of PETS with ^{99m}Tc–(en) and ^{99m}Tc–GH are shown. When PETS was reacted with ^{99m}Tc–(en), two radioactive peaks with the same retention time as those of ^{99m}Tc–PETS-L_1 and ^{99m}Tc–PETS-L_2 were observed with almost the same radiochemical yields. On the other hand, when ^{99m}Tc–GH was reacted with PETS, radioactivity corresponding to that of ^{99m}Tc–PETS-L_2 was obtained as a major component and that of ^{99m}Tc–PETS-L_1 was observed as only a minor peak (Fig. 4). Radioactivity peaks corresponding to those of the stannous reduction method were also observed by the exchange reaction of DM-PETS and DADT with both ^{99m}Tc–(en) and ^{99m}Tc–GH.

HPLC profiles of the four ^{99m}Tc complexes in the presence of CN^- anions are shown in Fig. 5. The monodentate ligand, CN^-, altered the HPLC radioactivity traces of ^{99m}Tc–PETS-L_1 and ^{99m}Tc–DM-PETS. On the other hand, HPLC radioactivity traces of ^{99m}Tc–PETS-L_2 and ^{99m}Tc–

TABLE I. Comparative Lipophilicity of the Four ^{99m}Tc Complexes

	PC[a]			Protein binding[b]	HPLC retention time (min)
	7.0	7.4	8.0		
^{99m}Tc–PETS-L_1	284.4 (41.9)	259.1 (32.5)	269.3 (49.9)	24.3 (1.5)	9.7
^{99m}Tc–PETS-L_2	841.2 (82.0)	820.0 (63.1)	791.7 (79.5)	40.9 (1.2)	11.6
^{99m}Tc–DM-PETS	321.6 (19.1)	327.2 (16.4)	321.7 (7.9)	17.6 (1.3)	11.8
^{99m}Tc–DADT	82.1 (3.5)	81.2 (3.2)	82.6 (5.6)	6.7 (0.3)	8.8

a) Partition coefficient: octanol/0.1 M phosphate buffer. Mean (S.D.) for three experiments. *b*) % serum protein binding. Mean (S.D.) for three experiments.

TABLE II. Biodistribution of the Four ^{99m}Tc Complexes in Mice[a]

Time (min)	^{99m}Tc–PETS-L_1			^{99m}Tc–PETS-L_2			^{99m}Tc–DM-PETS			^{99m}Tc–DADT		
	2	5	15	2	5	15	2	5	15	2	5	15
Brain	3.44	2.07	0.84	4.92	3.29	1.39	2.25	1.69	0.73	2.90	2.20	0.58
	(0.45)	(0.26)	(0.09)	(0.35)	(0.58)	(0.08)	(0.58)	(0.26)	(0.12)	(0.28)	(0.22)	(0.03)
Heart	5.32	3.43	1.80	6.35	3.69	2.36	6.43	4.37	2.39	4.27	2.82	1.18
	(0.66)	(0.34)	(0.49)	(0.62)	(0.98)	(0.24)	(1.24)	(0.57)	(0.34)	(0.34)	(0.26)	(0.08)
Pancreas	6.35	3.69	1.96	7.93	5.03	2.97	4.36	4.00	2.38	5.73	3.47	1.26
	(0.63)	(1.15)	(0.24)	(0.82)	(0.72)	(0.61)	(1.12)	(0.61)	(0.28)	(0.30)	(0.33)	(0.07)
Blood	2.57	1.98	1.52	3.22	2.70	2.44	1.63	1.40	1.12	2.40	1.86	1.23
	(0.29)	(0.16)	(0.21)	(0.31)	(0.11)	(0.19)	(0.48)	(0.29)	(0.14)	(0.22)	(0.12)	(0.10)

a) % injected dose per gram tissue. Mean (S.D.) for five mice.

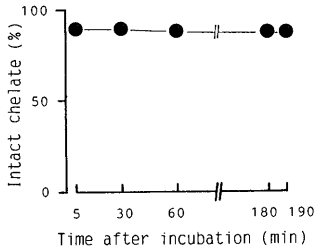

Fig. 3. Plasma Stability of ^{99m}Tc–DM-PETS

^{99m}Tc–DM-PETS was incubated at 37 °C in murine plasma. At various intervals, a plasma sample was withdrawn and deproteinized. The percent of radioactivity remaining as intact chelate was determined by HPLC.

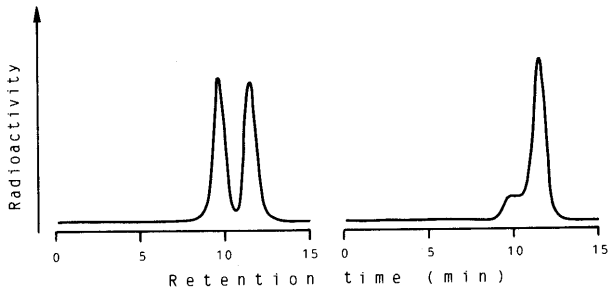

Fig. 4. HPLC Elution Profiles of Radioactivity

The profile after hexane extraction of the reaction mixture of PETS and ^{99m}Tc–(en) (left), and PETS and ^{99m}Tc–GH (right). Formation of ^{99m}TC–PETS-L_1 and ^{99m}Tc–PETS-L_2 was demonstrated by HPLC analysis.

DADT remained unchanged under the same reaction conditions.

The PC value, relative plasma protein binding and HPLC retention time of the four ^{99m}Tc complexes are summarized in Table I. PCs between pH 7.0 and pH 8.0 were essentially the same for all four ^{99m}Tc complexes. ^{99m}Tc–PETS-L_2 showed extremely high lipophilicity; the PC value of this complex was 3 times higher than that of ^{99m}Tc–PETS-L_1 and ^{99m}Tc–DM-PETS, and 10 times higher than that of ^{99m}Tc–DADT. The plasma protein binding of these complexes was proportional to their PC values.

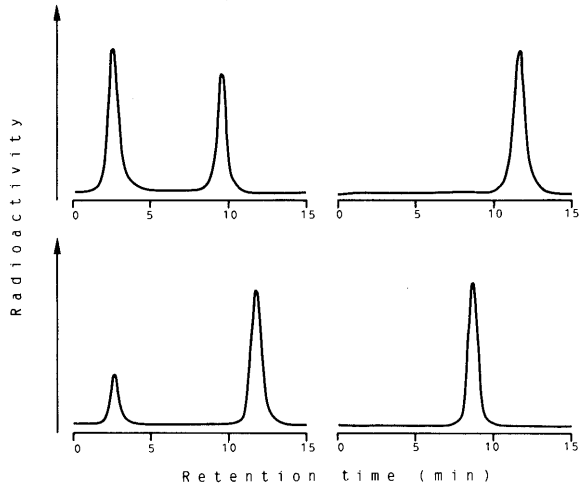

Fig. 5. HPLC Elution Profiles of Radioactivity

The radioactivity profile of ^{99m}Tc–PETS-L_1 (top, left), ^{99m}Tc–PETS-L_2 (top, right), ^{99m}Tc–DM-PETS (bottom, left) and ^{99m}Tc–DADT (bottom, right) in the presence of 5 mM of KCN and subsequent incubation at 37 °C for 2 h.

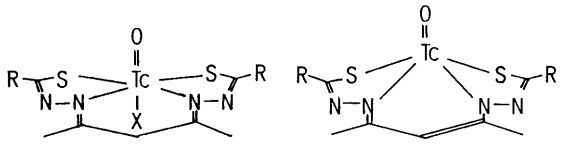

Fig. 6. Proposed Structure of ^{99m}Tc–PETS-L_1 (Left) and ^{99m}Tc–PETS-L_2 (Right)

Biodistribution in Mice In Table II, biodistribution of the four ^{99m}Tc complexes in mice is shown. All ^{99m}Tc complexes exhibited rapid radioactivity accumulation in

the brain, heart and pancreas with gradual clearance over time. The amount of radioactivity accumulated in these organs was virtually proportional to the levels found in the blood.

Discussion

Since our development of a ^{99m}Tc complex that crosses the intact blood-brain-barrier (BBB),[6] synthesis and characterization of technetium complexes reflecting cerebral blood flow have been carried out by many research groups.[2,7-9] All characterized technetium complexes that cross the BBB are neutral, lipophilic and relatively small (< 500 daltons) mononuclear complexes with a pentavalent TcO^{3+} core.[7,8] The ^{99m}Tc–DADT complex, used as a reference in this study, is in this category (Fig. 2).[7,9] Technetium complexes of N_2S_2 ligands other than DADT have also been characterized; they are also pentavalent mononuclear complexes containing a TcO^{3+} core.[10-12] Both PETS and DM-PETS have N_2S_2 donors for technetium coordination (Fig. 1) and the formation of ^{99m}Tc–PETS-L_1, ^{99m}Tc–PETS-L_2 and ^{99m}Tc–DM-PETS was indicated by the reaction of PETS or DM-PETS with the pentavalent ^{99m}Tc complexes of ^{99m}Tc–(en) and ^{99m}Tc–GH (Fig. 4).[5,13] It is, therefore, most likely that ^{99m}Tc–PETS-L_1, ^{99m}Tc–PETS-L_2 and ^{99m}Tc–DM-PETS are pentavalent mononuclear technetium complexes. This is supported by the similar *in vivo* behavior of ^{99m}Tc–PETS-L_1, ^{99m}Tc–PETS-L_2 and ^{99m}Tc–DM-PETS to that of ^{99m}Tc–DADT (Table II).

DM-PETS generated one neutral ^{99m}Tc complex with high stability (Fig. 3) and lipophilicity (Table I). ^{99m}Tc–DM-PETS also exhibited brain extraction when injected into mice (Table II). While DM-PETS and PETS form a 5–6–5 membered chelate with ^{99m}Tc, DM-PETS acts, as DA-α-DTS does, as a dianionic tetradentate ligand (Fig. 1). These results clearly indicate that the increased chelate ring structure from 5–5–5 to 5–6–5 played a significant role in the improved stability of the ^{99m}Tc–DTS chelate. Formation of only one neutral ^{99m}Tc complex of DM-PETS implies the presence of the third ionizable proton in the PETS molecule to be responsible for the two neutral ^{99m}Tc complex formations.

Two different structures have been reported as being mononuclear pentavalent technetium complexes of N_2S_2 ligands; a five-coordinated square-pyramidal structure (Fig. 2)[7,10,12] and a six-coordinated octahedral structure.[11] As shown in Fig. 4, the six-coordinated ^{99m}Tc–(en) and the five-coordinated ^{99m}Tc–GH afforded ^{99m}Tc–PETS-L_1 and ^{99m}Tc–PETS-L_2 with different radiochemical yields.[5,13] A difference between ^{99m}Tc–PETS-L_1 and ^{99m}Tc–PETS-L_2 was also observed in their liphophilicity and the reactivity toward CN^- anions, as shown in Table I and Fig. 5. These results imply a structural difference between ^{99m}Tc–PETS-L_1 and ^{99m}Tc–PETS-L_2 and suggest ^{99m}Tc–PETS-L_2 is the five-coordinated square-pyramidal structure.

Since DM-PETS acts as a dianionic ligand, coordination of an additional monodentate anion to the $^{99m}TcO^{3+}$ core is necessary for the neutral complex formation (Fig. 1). Present studies of ^{99m}Tc–DM-PETS as well as a report of the technetium complex of pentane-2,4-dione bis(*S*-methyldithiocarbazate) support the hypothesis that ^{99m}Tc–DM-PETS is the six-coordinated octahedral structure.[11] An altered HPLC ^{99m}Tc–DM-PETS profile by the presence of CN^- anions, when compared with the unchanged HPLC profile of the five-coordinated square-pyramidal structure of ^{99m}Tc–DADT, also implies a structural difference between ^{99m}Tc–DM-PETS and ^{99m}Tc–DADT. Comparative *in vitro* studies indicate the resemblance of ^{99m}Tc–DM-PETS to ^{99m}Tc–PETS-L_1 rather than to ^{99m}Tc–PETS-L_2 (Table I, Fig. 5).

The data imply that the structure of ^{99m}Tc–PETS-L_1 is a six-coordinated pentavalent mononuclear ^{99m}Tc complex and that ^{99m}Tc–PETS-L_2 is a five-coordinated pentavalent mononuclear ^{99m}Tc complex with a resonating structure, resulting from the deprotonation of the third proton from the PETS molecule.[14] In other words, while the chelate ring structure plays a significant role in the stability of the ^{99m}Tc–DTS chelate, ionization of the third proton of the PETS molecule and subsequent resonating of the five-coordinated structure affords further stability to the ^{99m}Tc–PETS complex. Extremely high lipophilicity of ^{99m}Tc–PETS-L_2 may be well explained by assuming that ^{99m}Tc–PETS-L_2 is the five-coordinated resonating structure. Further characterization of technetium–PETS complexes is also under way using technetium-99.

References

1) Y. Arano, M. Yabuki, T. Yahata, K. Horiuchi, and A. Yokoyama, *Chem. Pharm. Bull.*, **38**, 3099 (1990).
2) E. Chiotellis, A. D. Varvarigou, TH. Maina, and C. I. Stassinopoulou, *Nucl. Med. Biol.*, **15**, 215 (1988).
3) J. J. Bloomfield, *J. Org. Chem.*, **26**, 4112 (1961).
4) S. Z. Lever, H. D. Burns, T. M. Kervitsky, H. W. Goldfarb, D. V. Woo, D. F. Wong, L. A. Epps, A. V. Kramer, and H. N. Wagner, Jr., *J. Nucl. Med.*, **26**, 1287 (1985).
5) S. S. Jurisson, K. Dancey, M. McPartin, P. A. Tasker, and E. Deutsch, *Inorg. Chem.*, **23**, 4743 (1984); E. Deutsch, J. Vanderheyden, P. Gerundini, K. Libson, W. Hirth, F. Colombo, A. Savi, and F. J. Fazio, *Nucl. Med.*, **28**, 1870 (1987).
6) A. Yokoyama, Y. Arano, T. Hosotani, A. Yamada, K. Horiuchi, K. Yamamoto, K. Torizuka, N. Ueda, and M. Hazue, "Proceeding of the Third World Congress of Nuclear Medicine and Biology," Pergamon Press, Paris, 1982, pp. 1097—1100; A. Yokoyama, A. Yamada, Y. Arano, K. Horiuchi, K. Yamamoto, and K. Torizuka "Technetium in Chemistry and Nuclear Medicine," ed. by E. Deutsch, M. Nicolini, and H. N. Wagner Jr. Raven Press, New York, 1983, pp. 109—111.
7) L. A. Epps, H. D. Burns, S. Z. Lever, H. W. Goldfarb, and H. N. Wagner, Jr., *Appl. Radiat. Isot.*, **38**, 661 (1987); H. F. Kung, Y.-Z. Guo, C.-C. Yu, J. Billings, V. Subramanyam, and J. C. Calabrese, *J. Med. Chem.*, **32**, 433 (1989); R. H. Mach, H. F. Kung, Y.-Z. Guo, C.-C. Yu, V. Subramanyam, and J. C. Calabrese, *Nucl. Med. Biol.*, **16**, 829 (1989).
8) S. S. Jurisson, K. Aston, C. K. Fair, E. O. Schlemper, P. R. Sharp, and D. E. Troutner, *Inorg. Chem.*, **26**, 3576 (1987); C. K. Fair, D. E. Troutner, E. O. Schlemper, R. K. Murmann, and M. L. Hoppe, *Acta Cryst.*, **C40**, 1544 (1984).
9) H. F. Kung, M. Molnar, J. B. Billings, R. Wicks, and M. Blau, *J. Nucl. Med.*, **25**, 326 (1984).
10) A. Davison, A. G. Jones, C. Orvig, and M. Sohn, *Inorg. Chem.*, **20**, 1629 (1981); A. G. Jones, A. Davison, M. LaTegola, J. M. Brodack, C. Orvig, M. Sohn, A. K. Toothaker, C. J. L. Lock, K. J. Franklin, C. E. Costello, S. A. Carr, K. Biemann, and M. L. Kaplan, *J. Nucl. Med.*, **23**, 801 (1982).
11) J. G. H. DuPreez, T. I. A. Ferber, and O. Knoesen, *Inorg. Chim. Acta*, **133**, 3 (1987).
12) R. Faggiani and C. J. Lock, *Acta Cryst.*, **C44**, 777 (1988); S. Truffer, E. Ianoz, and P. Lerch, *Inorg. Chim. Acta*, **149**, 217 (1988).
13) W. De Kieviet, *J. Nucl. Med.*, **22**, 703 (1981); L. L-Y Hwang, N. Ronca, N. A. Solomon, and J. Steigman, *Int. J. Appl. Radiat. Isot.*, **36**, 475 (1984).
14) E. Bayed and E. Bretmaier, *Chem. Ber.*, **101**, 1579 (1968).

Synthesis and Pharmacological Effects of Optically Active 2-[4-(4-Benzhydryl-1-piperazinyl)phenyl]-ethyl Methyl 1,4-Dihydro-2,6-dimethyl-4-(3-nitrophenyl)-3,5-pyridinedicarboxylate Hydrochloride

Atsuyuki ASHIMORI, Takeshi UCHIDA, Yutaka OHTAKI, Mikio TANAKA, Kazuhito OHE, Chikara FUKAYA,* Masahiro WATANABE, Masao KAGITANI, and Kazumasa YOKOYAMA

Research Division, The Green Cross Corporation, 1180–1, Shodaiotani 2-chome, Hirakata-shi, Osaka 573, Japan. *Received June 21, 1990*

Optically active 2-[4-(4-benzhydryl-1-piperazinyl)phenyl]ethyl methyl 1,4-dihydro-2,6-dimethyl-4-(3-nitrophenyl)-3,5-pyridinedicarboxylate [(*S*)-(+)-1 and (*R*)-(−)-1] hydrochlorides were synthesized with high optical purities from (*R*)-(−)- and (*S*)-(+)-1,4-dihydro-5-methoxycarbonyl-2,6-dimethyl-4-(3-nitrophenyl)-3-pyridinecarboxylic acids [(*R*)-(−)-6 and (*S*)-(+)-6], which are available from (±)-6 by optical resolution using quinidine and cinchonidine, respectively. From pharmacological investigations of (*S*)-(+)-1 and (*R*)-(−)-1 such as the antihypertensive effect on spontaneously hypertensive rats and inhibition of [^{3}H]nimodipine binding to rat cardiac membrane homogenate, the active form of 1 was defined to be the (4*S*)-(+)-enantiomer of 1.

Keywords 1,4-dihydropyridine; calcium antagonist; antihypertensive effect; receptor binding assay; optically active compound; AE0047

Introduction

In a previous paper,[1] we reported the synthesis and antihypertensive activity of 1,4-dihydropyridine derivatives with 3-[4-(substituted amino)phenylalkyl] ester, and that among them, 2-[4-(4-benzhydryl-1-piperazinyl)phenyl]ethyl methyl 1,4-dihydro-2,6-dimethyl-4-(3-nitrophenyl)-3,5-pyridinedicarboxylate dihydrochloride (**1**·2HCl, AE0047) had long lasting antihypertensive activity and selective vasodilating activity on canine vertebral artery. AE0047 has been selected as a promising candidate from other pharmacological investigations also. Since **1** has an asymmetric center at C-4 of the dihydropyridine ring, it is a racemic mixture (Fig. 1). We have been interested in biological activities of each enantiomer of **1** because a number of reports described that one optical isomer of 1,4-dihydropyridine derivatives showed much more potent biological activities than the other.[2–8] Therefore, we synthesized each enantiomer of **1**, and investigated the difference of *in vivo* and *in vitro* biological activities, namely antihypertensive activity on spontaneously hypertensive rats (SHR) and the effect on the binding of [^{3}H]nimodipine to rat cardiac membranes.

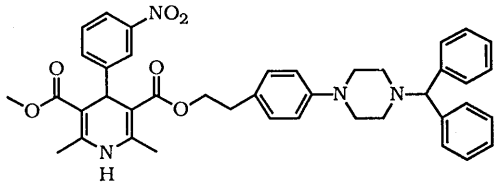

1

Fig. 1

In this paper, we report the synthesis of each enantiomer of **1** and their biological activities.

Synthesis Method for synthesis of each enantiomer of **1** is shown in Charts 1 and 2.

Optically active nicardipine[3] and other such 1,4-dihydropyridine derivatives[6–8] were synthesized from (+)- and (−)-**6** which were obtained by an optical resolution of 1-ethoxymethylated (±)-**6** and subsequent removal of the ethoxymethyl group. Tamazawa *et al.*[6] and Kajino *et al.*[8] independently determined the absolute configuration of **6** by X-ray crystallographic analysis of its derivatives to assign unambiguously that (+)-**6** and (−)-**6** have *S* and *R* configurations at C-4, respectively.

We tried to ascertain the utility of the direct optical resolution of (±)-**6** reported by Genain.[9] Several hundreds of grams of (±)-**6** was easily prepared from ethylene

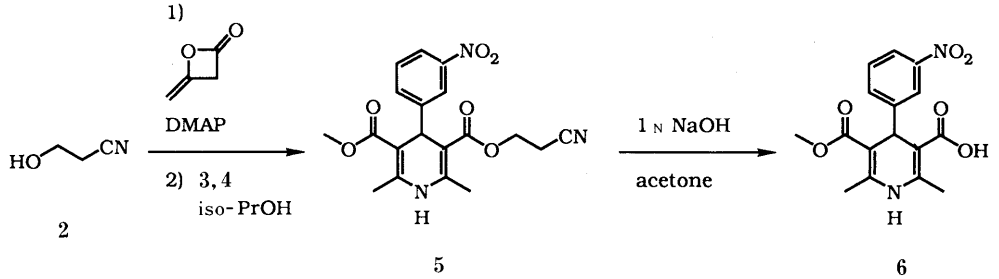

2 5 6

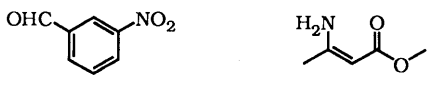

3 4

Chart 1

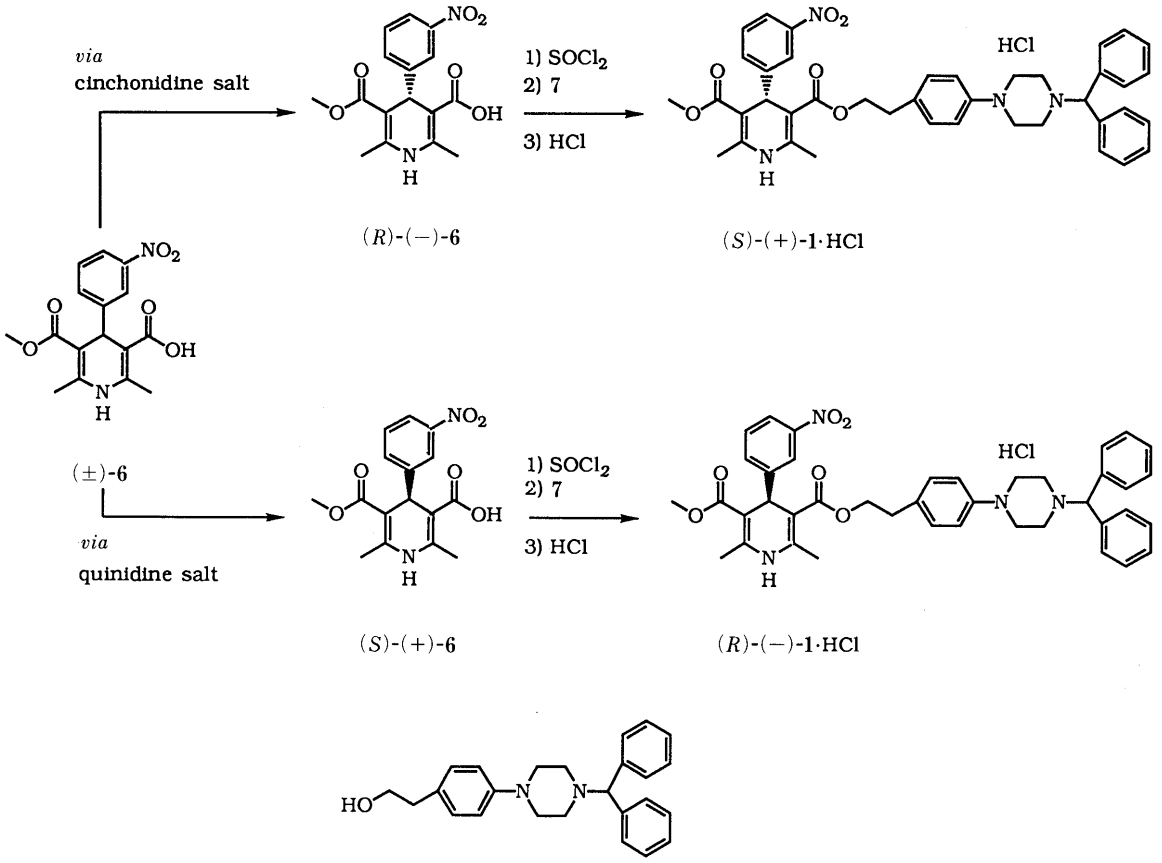

Chart 2

cyanohydrin (**2**) *via* 1,4-dihydropyridine **5** in a *ca.* 60% overall yield without chromatographical purification (Chart 1).[10] The compound (*S*)-(+)-**6** was obtained in a 46% yield from a quinidine salt of **6** in pure form by recrystallizing it to a constant optical rotation. On the other hand, **6** recovered from the mother liquor gave (*R*)-(−)-**6** by recrystallizing it as cinchonidine salt (yield 48%). Treatment of (*R*)-(−)-**6** and (*S*)-(+)-**6** with $SOCl_2$, and a subsequent reaction with **7** gave (*S*)-(+)-**1** and (*R*)-(−)-**1**, respectively. They were treated with a solution of hydrogen chloride in 1,2-dimethoxyethane (DME) in Et_2O–CH_2Cl_2 (90 : 10, v/v) to afford monohydrochlorides, (*S*)-(+)-**1**·HCl, 62%, mp 143.5—147 °C, $[\alpha]_D^{20}$ +31.0° (c=0.50, acetone) and (*R*)-(−)-**1**·HCl, 59%, mp 145—149 °C, $[\alpha]_D^{20}$ −31.4° (c=0.50, acetone) (Chart 2).

Determination of Optical Purities of (*S*)-(+)-1 and (*R*)-(−)-1 The optical purities of (*S*)-(+)-**1**·HCl and (*R*)-(−)-**1**·HCl were determined by high performance liquid chromatography (HPLC) analyses using chiral stationary phase columns, Chiralcel OF® (4.6 mm i.d. × 250 mm) [column temperature, 50 °C; mobile phase, hexane–2-propanol–trifluoroacetic acid (50 : 50 : 0.05, v/v); flow rate, 1.0 ml/min; detection, ultraviolet (UV) at 254 nm] and Chiralpak AD® (4.6 mm i.d. × 250 mm) [column temperature, 40 °C; mobile phase, hexane–ethanol (9 : 1, v/v); flow rate, 1.0 ml/min; detection, UV at 254 nm] purchased from Daicel Chemical Industries, Tokyo, Japan. Retention times of the compounds are as follows: in Chiralcel OF®, (*S*)-(+)-**1**, 22.5 min; (*R*)-(−)-**1**, 50.3 min; in Chiralpak AD®, (*S*)-(+)-**1**, 23.1 min; (*R*)-(−)-**1**, 27.0 min. Since in both cases the peaks of antipodal compounds were not detected at all, the optical purities of each compound were concluded to be almost 100% ee.

TABLE I. Effects of (±)-**1**, (*S*)-(+)-**1**, and (*R*)-(−)-**1** on SBP in SHR (*p.o.* Administration)

Drug and dose (mg/kg)	*n*	Reduction of SBP (%) (mean ± S.E.)				
		Before	1 h[b]	2 h[b]	4 h[b]	7 h[b]
Vehicle[a]	6	0	0±2	1±2	0±1	3±2
(±)-**1**						
1	6	0	10±3	14±2	16±2	12±2
3	6	0	31±1	36±3	35±1	26±1
10	6	0	41±2	43±2	41±2	38±1
(*S*)-(+)-**1**						
0.3	6	0	1±3	11±2	5±3	8±3
1	6	0	19±3	21±2	17±2	15±2
3	3	0	43±4	51±2	41±1	33±4
(*R*)-(−)-**1**						
30	6	0	4±2	11±2	11±3	11±3

a) 0.3% Tween 80 solution. *b*) Time after administration.

Pharmacological Results and Discussion The antihypertensive effects of (±)-AE0047 and each enantiomer of AE0047 on SHR are shown in Table I. The compound (*S*)-(+)-**1** showed a dose dependent potent antihypertensive effect, particularly at doses of 1 and 3 mg/kg, and the duration was estimated to be over 7 h, whereas at a dose of 30 mg/kg the antihypertensive effect of (*R*)-(−)-**1** was barely comparable to the effect of (*S*)-(+)-**1** at a dose of 0.3 mg/kg. Although the antihypertensive effect of (±)-**1**

Table II. Inhibition of [^{3}H]Nimodipine Binding to Rat Cardiac Membrane Homogenate

Drug	Concentrations required for 50% inhibition (nM)
(±)-**1**	0.26
(*S*)-(+)-**1**	0.13
(*R*)-(−)-**1**	18.2
(±)-Nicardipine	0.48

was less than (*S*)-(+)-**1**, it had enough potency at doses 3 and 10 mg/kg. The doses necessary for a 30% reduction of systolic blood pressure (SBP) (ED_{30}) obtained from the dose–response curves were 1.1 mg/kg in (*S*)-(+)-**1** and 2.6 mg/kg in (±)-**1**, respectively. These results indicate that the antihypertensive effect of (±)-**1** depends mostly on (*S*)-(+)-**1**, which is supported by the fact that the ED_{30} value of (*S*)-(+)-**1** is about a half of the value of (±)-**1**.

We performed a receptor binding assay to evaluate phamacological profiles of these compounds *in vitro*. Drug concentrations required for 50% inhibition of [^{3}H]nimodipine binding to rat cardiac membrane homogenate (IC_{50}) of these compounds and (±)-nicardipine are shown in Table II. The compound (*S*)-(+)-**1** shows the highest affinity to the receptor, and the affinity was decreased in the following order; (±)-**1** (0.26 nM) > (±)-nicardipine (0.48 nM) > (*R*)-(−)-**1** (18.2 nM). The affinity of (*S*)-(+)-**1** was found to be 140-fold higher than (*R*)-(−)-**1** and to be 2-fold higher than (±)-**1**. This result is consistent with the potency of the antihypertensive effects obtained in the *in vivo* study.

Conclusion

We synthesized the compounds (*S*)-(+)-**1** and (*R*)-(−)-**1** with high optical purities from (*R*)-(−)-**6** and (*S*)-(+)-**6**, respectively, which were obtained by the direct optical resolution of (±)-**6** through its quinidine and cinchonidine salts. From pharmacological investigations *in vivo* and *in vitro*, the active form of **1** was defined to be the (4*S*)-(+)-enantiomer of **1**. The 4*S* configuration of **1** was found to be important for interaction with the 1,4-dihydropyridine receptor, as is found in other 1,4-dihydropyridine enantiomers.

Experimental

Melting points were determined on a Yanagimoto micromelting point apparatus and were uncorrected. Infrared (IR) spectra were recorded on a Shimadzu IR-420 spectrophotometer. ^{1}H-Nuclear magnetic resonance (^{1}H-NMR) spectra were determined on a BRUKER AC-200 spectrometer with tetramethylsilane (TMS) as an internal standard. Optical rotations were measured on a JASCO DIP-181 digital polarimeter. Extraction solvents were dried over anhydrous $MgSO_4$. Silica gel 60, 230—400 mesh (Nacalai Tesque) was used for flash column chromatography, and Kieselgel 60, F_{254} (Merck) plates were used for thin layer chromatography (TLC).

(±)-1,4-Dihydro-5-methoxycarbonyl-2,6-dimethyl-4-(3-nitrophenyl)-3-pyridinecarboxylic Acid [(±)-6] Diketene (106 ml, 1.36 mol) was added dropwise to ethylene cyanohydrin (**2**, 96.5 g, 1.36 mmol) preheated at about 80 °C at temperatures between 75 and 100 °C over 1.5 h. After the addition was completed, the mixture was stirred at 70—80 °C for 2.5 h. After dissolving the resulting mixture in 2-propanol (450 ml), *m*-nitrobenzaldehyde (**3**, 205.2 g, 1.36 mmol), methyl 3-aminocrotonate (**4**, 156.3 g, 1.36 mmol) and 2-propanol (510 ml) were added to the solution, and then refluxed for 7 h, stirred at room temperature for 11 h, and with ice-water cooling for 3 h. A precipitated solid was collected by filtration, and rinsed with 2-propanol. After drying *in vacuo* at 50 °C overnight, the compound **5** was obtained as a yellow powder (332.4 g). To a solution of **5** obtained above in acetone (1300 ml) was added 1 N NaOH (2600 ml at a time) with water cooling. After the mixture was stirred at 28 °C for 1 h, the resulting solution was diluted with water (2600 ml) and then washed with CH_2Cl_2 (three times). With ice-water cooling, the aqueous layer was acidified with 35% HCl to pH 1—2, and stirred for 3 h to afford a precipitated solid. The solid collected by filtration was rinsed with water and then dried *in vacuo* at 50 °C for 4 d to give the product [(±)-**6**] as a slightly yellow powder (268.9 g, 60%), mp 199—200 °C. IR (KBr): 3325, 2925, 2700, 2600, 1670, 1655, 1605, 1525, 1480, 1435, 1350 cm^{-1}. ^{1}H-NMR [DMSO-d_6 + $CDCl_3$ (10 : 1, v/v)] δ: 2.29, 2.30 (each 3H, s), 3.56 (3H, s), 5.00 (1H, s), 7.45—7.65 (2H, m), 7.9—8.05 (2H, m), 8.94 (1H, s), 11.82 (1H, br s). *Anal.* Calcd for $C_{16}H_{16}N_2O_6$: C, 57.83; H, 4.85; N, 8.43. Found: C, 57.74; H, 4.67; N, 8.33.

Optical Resolution of (±)-1,4-Dihydro-5-methoxycarbonyl-2,6-dimethyl-4-(3-nitrophenyl)-3-pyridinecarboxylic Acid [(±)-6] Quinidine (293.66 g, 0.91 mol) was added portionwise to a suspension of (±)-**6** (300.81 g, 0.91 mol) in *N*,*N*-dimethylformamide (DMF) (500 ml) with warming. After the addition was completed, further DMF (370 ml) was added to the mixture, and the remaining solid was completely dissolved at about 85 °C. Hot water (*ca.* 60—70 °C, 580 ml) was added portionwise to the solution, and then kept at room temperature for 53 h. The crystals formed were collected by filtration and recrystallized from DMF–water (3 : 2, v/v) to give the (*R*)-(−)-**6**-quinidine salt (151.4 g) as yellow needles, mp 199—200 °C, $[\alpha]_D^{20}$ +96.4° (*c* = 0.50, acetone). IR (KBr): 3350, 3225, 2950, 1645, 1620, 1590, 1570, 1530, 1510, 1485, 1440, 1330 cm^{-1}. *Anal.* Calcd for $C_{36}H_{40}N_4O_8$: C, 65.84; H, 6.14; N, 8.53. Found: C, 65.85; H, 6.17; N, 8.46. The obtained (*R*)-(−)-**6**-quinidine salt was suspended in 0.47 N NaOH (507 ml, containing 1.03 eq of NaOH), and then washed with CH_2Cl_2 (three times). With ice-water cooling, the aqueous layer was acidified with 35% HCl to pH 1—2, and then stirred for 1.5 h. A precipitated solid was collected by filtration, and dried *in vacuo* at about 60 °C to afford (*R*)-(−)-**6** (72.11 g, 48%) as a slightly yellow powder, mp 169—170 °C, $[\alpha]_D^{20}$ −24.6° (*c* = 0.50, acetone) [lit.[3] $[\alpha]_D^{20}$ −19.6° (*c* = 0.542, acetone)]. *Anal.* Calcd for $C_{16}H_{16}N_2O_6$: C, 57.83; H, 4.85; N, 8.43. Found: C, 57.98; H, 4.79; N, 8.34. The mother liquor obtained after the first recrystallization was concentrated and the residue was worked up in the same way used in the case of (*R*)-(−)-**6**-quinidine salt. The obtained (*S*)-(+)-**6** (141.3 g, 0.43 mol) was treated with cinchonidine (125.2 g, 0.43 mol) in a similar manner used for the preparation of (±)-**6**-quinidine salt to give (*S*)-(+)-**6**-cinchonidine salt (144.2 g) as pale yellow fine needles, mp 188—189 °C, $[\alpha]_D^{20}$ −45.0° (*c* = 0.50, MeOH). IR (KBr): 3350, 3075, 2950, 1670, 1640, 1610, 1590, 1525, 1490, 1440, 1345 cm^{-1}. *Anal.* Calcd for $C_{35}H_{38}N_4O_7$: C, 67.08; H, 6.11; N, 8.94. Found: C, 67.23; H, 6.21; N, 8.72. By the same work up described above, (*S*)-(+)-**6** was obtained as a slightly yellow powder (69.46 g, 46%), mp 168.5—170 °C, $[\alpha]_D^{20}$ +24.4° (*c* = 0.50, acetone) [lit.[3] $[\alpha]_D^{20}$ +19.1° (*c* = 0.556, acetone)]. *Anal.* Calcd for $C_{16}H_{16}N_2O_6$: C, 57.83; H, 4.85; N, 8.43. Found: C, 58.04; H, 4.85; N, 8.25.

(4*S*)-(+)-2-[4-(4-Benzhydryl-1-piperazinyl)phenyl]ethyl Methyl 1,4-Dihydro-2,6-dimethyl-4-(3-nitrophenyl)-3,5-pyridinedicarboxylate [(*S*)-(+)-1] Hydrochloride To a suspension of (*R*)-(−)-**6** (62.32 g, 0.188 mol) in CH_2Cl_2 (400 ml) and DMF (100 ml) was added $SOCl_2$ (22.31 g, 0.188 mol) at 5—9 °C with ice-water cooling under N_2 atmosphere, and then stirred for 2.5 h at the same temperature. The solution of **7** (67.76 g, 0.182 mol) in CH_2Cl_2 (120 ml) was added to the reaction mixture and stirred for 16 h at about 5 °C. The resulting mixture was diluted with CH_2Cl_2 (500 ml) and then washed with water and brine, dried, and removed. After the addition of AcOEt to the residue, the mixture was washed with 5% K_2CO_3 and brine, and then dried. Concentration of the solvent following chromatography on silica gel with C_6H_6–AcOEt (4 : 1, v/v) afforded (*S*)-(+)-**1** as a yellow powder (107.45 g, 83%). IR (KBr). 3325, 3025, 2950, 2800, 1680, 1645, 1610, 1520, 1485, 1450, 1430, 1345 cm^{-1}. ^{1}H-NMR ($CDCl_3$) δ: 2.30, 2.35 (each 3H, s), 2.55 (4H, br t, *J* = 5 Hz), 2.82 (2H, t, *J* = 7 Hz), 3.15 (4H, br t, *J* = 5 Hz), 3.64 (3H, s), 4.23 (2H, t, *J* = 7 Hz), 4.26 (1H, s), 5.07 (1H, s), 5.80 (1H, s), 6.80, 7.04 (4H, A_2B_2q, *J* = 8.5 Hz), 7.1—7.6 (12H, m), 7.97 (1H, ddd, *J* = 8, 2.5, 1 Hz), 8.06 (1H, t, *J* = 2.5 Hz). To a solution of (*S*)-(+)-**1** (105.45 g) obtained above in Et_2O–CH_2Cl_2 (9 : 1, v/v) (2000 ml) was added dropwise a solution of hydrogen chloride in DME (2.45 N, 69 ml) at room temperature. After the addition was completed, the mixture was stirred at room temperature for 40 min. A precipitated solid was collected by filtration, which was

rinsed with Et_2O, and then dried *in vacuo* to give (*S*)-(+)-**1**·HCl (83.69 g, 75%) as a yellow powder, mp 143.5—147 °C, $[\alpha]_D^{20}$ +31.0° (*c*=0.50, acetone). IR (KBr): 3375, 3050, 2925, 2550, 1690, 1610, 1520, 1485, 1455, 1435, 1350 cm^{-1}. ^{1}H-NMR ($CDCl_3$) δ: 2.25, 2.36 (each 3H, s), 2.82 (2H, t, *J*=6.5 Hz), 3.0—3.2 (2H, br), 3.35—3.6 (4H, br), 3.64 (3H, s), 3.75—4.05 (2H, br), 4.24 (2H, t, *J*=6.5 Hz), 4.88 (1H, br d, *J*=7 Hz), 5.06 (1H, s), 6.42 (1H, s), 6.76, 7.00 (4H, A_2B_2q, *J*=8 Hz), 7.2—7.65 (8H, m), 7.8—8.1 (6H, m), 13.10 (1H, br s). *Anal.* Calcd for $C_{41}H_{42}N_4O_6$·HCl: C, 68.09; H, 5.99; N, 7.75. Found: C, 68.43; H, 5.83; N, 7.65.

(4*R*)-(−)-2-[4-(4-Benzhydryl-1-piperazinyl)phenyl]ethyl Methyl 1,4-Dihydro-2,6-dimethyl-4-(3-nitrophenyl)-3,5-pyridinedicarboxylate [(*R*)-(−)-1] Hydrochloride The compound (*R*)-(−)-**1**·HCl was prepared from (*S*)-(+)-**6** by the same method employed for the synthesis of (*S*)-(+)-**1**·HCl; yield 59%, mp 145—149 °C, $[\alpha]_D^{20}$ −31.4° (*c*=0.50, acetone). *Anal.* Calcd for $C_{41}H_{42}N_4O_6$·HCl: C, 68.09; H, 5.99; N, 7.75. Found: C, 68.07; H, 5.85; N, 7.74.

Biological Tests Antihypertensive Activity[11]: The experiments were performed in groups of 3—6 male SHR. SBP was measured in a conscious state by a tail cuff plethysmographic method with an electrosphygmomanometer (PS-200A, Riken-Kaihatsu) at 0, 1, 2, 4 and 7 h after oral administration. The test compounds were prepared as follows: A compound was dissolved in EtOH (0.3 ml) and Tween 80 (0.1 ml) and then diluted with distilled water for the volume of administration to be 10 ml/kg. Antihypertensive effects are shown as reductions in SBP (%) from 0 h values.

Receptor Binding Assay Rat cardiac membrane for the assay was prepared by the same method reported by Ishii *et al.*[12]

To a solution of a test compound in 0.5 ml of 50 mM Tris buffer (pH 7.4) containing 0.1% albumin was added 0.05 ml of [^{3}H]nimodipine (4.729 TBq/mmol) in 10% EtOH (160000 dpm) and 0.5 ml of cardiac membrane homogenate. After incubation at 25 °C for 3 h in the dark, the incubation mixture was filtered under vacuum through a glass fiber filter (Whatman GF/F), and washed twice with 1 ml of 50 mM Tris buffer (pH 7.4) which was used for washing the test tube, and three times with another 5 ml of Tris buffer (pH 7.4). After the addition of 2 ml of Soluene-350 (Packard) to the cardiac membrane homogenate, and standing overnight, 13 ml of Hionic-Fluor was added to the mixture, and kept in a cool and dark place for 24 h. Subsequently, the radio activity was measured by liquid scintillation counter (Tri-carb Model 4640CD, Packard). Non-specific binding was determined by the result of measurement in the presence of 100 ng/ml of (±)-**1**.

References and Notes

1) A. Ashimori, T. Ono, Y. Inoue, S. Morimoto, M. Eda, T. Uchida, Y. Ohtaki, Y. Fujino, H. Kido, Y. Ogura, C. Fukaya, M. Watanabe, and K. Yokoyama, *Chem. Pharm. Bull.*, **39**, 91 (1991).
2) R. Towart, E. Wehinger, and H. Meyer, *Naunyn-Schmiedeberg's Arch. Pharmacol.*, **317**, 183 (1981).
3) T. Shibanuma, M. Iwanami, K. Okuda, T. Takenaka, and M. Murakami, *Chem. Pharm. Bull.*, **28**, 2809 (1980).
4) T. Takenaka, I. Miyazaki, M. Asano, S. Higuchi, and H. Maeno, *Jpn. J. Pharmacol.*, **32**, 665 (1982).
5) R. Towart, E. Wehinger, H. Meyer, and S. Kazda, *Arzneim.-Forsch.*, **32**, 338 (1982).
6) T. Tamazawa, H. Arima, T. Kojima, Y. Isomura, M. Okada, S. Fujita, T. Furuya, T. Takenaka, O. Inagaki, and M. Terai, *J. Med. Chem.*, **29**, 2504 (1986).
7) K. Muto, T. Kuroda, H. Kawato, A. Karasawa, K. Kubo, and N. Nakamizo, *Arzneim.-Forsch.*, **38**, 1662 (1988).
8) M. Kajino, T. Wada, Y. Nagai, A. Nagaoka, and K. Meguro, *Chem. Pharm. Bull.*, **37**, 2225 (1989).
9) G. Genain, Eur. Patent 273349 (1988) [*Chem. Abstr.*, **109**, 190260z (1988)].
10) E. Wehinger and F. Bossert, Ger. Patent 2847237 (1980) [*Chem. Abstr.*, **93**, 150124c (1980)].
11) D. Pruneau and F. Roy, *Arzneim.-Forsch.*, **37**, 416 (1987).
12) A. Ishii, K. Nishida, T. Oka, and N. Nakamizo, *Arzneim.-Forsch.*, **38**, 1733 (1988).

Antiviral Activities of Glycyrrhizin and Its Modified Compounds against Human Immunodeficiency Virus Type 1 (HIV-1) and Herpes Simplex Virus Type 1 (HSV-1) *in Vitro*

Kazuhiro HIRABAYASHI,[a,b] Susumu IWATA,[a] Hiroatsu MATSUMOTO,[a] Takeo MORI,[a] Shoji SHIBATA,*[,c] Masanori BABA,[b] Masahiko ITO,[b] Shiro SHIGETA,[b] Hideki NAKASHIMA[d] and Naoki YAMAMOTO[d]

Research Laboratory, Minophagen Pharmaceutical Co.,[a] Komatsubara, Zama, Kanagawa 228, Japan, Department of Bacteriology, Fukushima Medical College,[b] Fukushima 960–12, Japan, Shibata Laboratory of Natural Medicinal Materials,[c] c/o Minophagen Pharmaceutical Co., Yotsuya 3–2–7, Shinjuku-ku, Tokyo 160, Japan, and Department of Virology and Parasitology, Yamaguchi University School of Medicine,[d] Ube, Yamaguchi 755, Japan.
Received July 11, 1990

Chemically modified compounds of glycyrrhizin have been synthesized and evaluated for their inhibitory effect on the replication of human immunodeficiency virus type 1 (HIV-1) and herpes simplex virus type 1 (HSV-1). Among them, the 11-deoxo compound having a heteroannular diene structure at the C and D rings proved as active against HIV-1 as glycyrrhizin in MT-4 and MOLT-4 cells. It completely inhibited HIV-1-induced cytopathogenicity in both cell lines at a concentration of 0.16 mM. The compound was also effective against HSV-1 with a 50% inhibitory concentration of 0.5 μM.

Keywords glycyrrhizin analog; HIV-1; HSV-1; antiviral activity

It has been reported that glycyrrhizin, the major saponin isolated from licorice root (*Glycyrrhiza* spp.), is inhibitory to the replication of human immunodeficiency virus type 1 (HIV-1) *in vitro*, the etiologic agent of the acquired immune deficiency syndrome (AIDS).[1] This finding has been developed to the clinical use of a glycyrrhizin preparation, Stronger Neominophagen C (SNMC), to protect HIV-1 carriers from the crisis of AIDS.[2] In addition, it was demonstrated that glycyrrhizin inhibited the *in vitro* growth and cytopathogenicity of several deoxyribonucleic acid (DNA) and ribonucleic acid (RNA) viruses including herpes simplex virus type 1 (HSV-1), Newcastle disease virus, vesicular stomatitis virus, and poliovirus type 1.[3] Baba and Shigeta, two of the present authors, reported the antiviral activity of glycyrrhizin against varicella–zoster virus (VZV) in cell culture.[4]

On the basis of these results, some chemically modified compounds of glycyrrhizin were investigated for their inhibitory effect on the replication of HIV-1 and HSV-1. The functional groups of glycyrrhetinic acid, the aglycone part of glycyrrhizin, at the 11 and 20 positions, and the carboxyl at the 5′ position of the sugar portion were modified. The αβ-unsaturated carbonyl system of the C-ring of the glycyrrhetinic acid part was converted into a heteroannular diene system at the C and D rings. By the above modifications, the following compounds (**3**—**7**) were prepared starting from glycyrrhizin (**1**) to test their antiviral activity.

Materials and Methods

Apparatus Melting points were taken on a Yanaco micro melting point apparatus and are uncorrected. Optical rotations were determined in MeOH with a JASCO model JZO ORD/CD polarimeter. Infrared (IR) spectra were recorded with a JASCO IR-700 spectrophotometer and ultraviolet (UV) spectra with a Hitachi 2-20 spectrometer. Nuclear magnetic resonance (NMR) spectra were recorded on a JEOL GX-400 NMR spectrometer using 10—20 mg/0.45 ml dimethyl sulfoxide (DMSO-d_6) as a solvent and tetramethylsilane (TMS) as an internal standard. Chemical shifts were reported in ppm downfield from this standard. Fast atom bombardment (FAB) mass spectral analysis was performed with a JEOL DX-300 spectrometer. A high performance liquid chromatograph (HPLC) consisting of a Spectra-Physics SP-8700 solvent pumping system with bellows damper (NBD-III), ERC-7520 (refraction index-detector) or SSC-Y-1000 (UV- detector) and a Rheodyne model 7125 injection value was used. Chromatograms were recorded on an SIC-7000B (System Instruments) integrator. Experiments were performed on a column (25 cm × 10 mm i.d.) (Senshu Scientific) packed with Nucleosil 100-5 C_{18} (octadecyl silica, 5 μm) (Macherey, Nagel and Co., Duren, G. F. R.). Column chromatography was performed using a Kieselgel 60 column (70—230 mesh, Merck). Thin layer chromatography (TLC) was conducted on precoated Kieselgel 60 F_{254} plated (0.20 mm thick, Merck) with $CHCl_3$–MeOH–H_2O (65 : 35 : 10, lower layer). The molecular composition of the compound given by the chemical formula was determined by elemental analysis.

Preparation of Test Compounds Commercially available glycyrrhizin (**1**) isolated from licorice root was used as the starting material for chemical modification.

18β-Olean-12-ene-3β,11β-diol-30-oic Acid 3-*O*-β-D-Glucuronopyranosyl-(1→2)β-D-glucuronopyranoside (11β-Hydroglycyrrhizin) (2) To a mixture of $NaBH_4$ (7.56 g, 0.2 mol) dissolved in aq 1N NaOH (50 ml) and tetrahydrofuran (THF) (100 ml) at 80 °C, glycyrrhizin (**1**) (8.23 g, 0.01 mol) dissolved in THF (100 ml) was added dropwise and allowed to react for 24 h under reflux in a H_2O bath. The reaction mixture was stirred with acetone (50 ml) at room temperature (r.t.), and dil. HCl was added to adjust to pH 9—10. The filtrate of the reaction mixture was concentrated to 100 ml, and then precipitated by the addition of acetone (700 ml) and MeOH (300 ml). The crude product was refluxed with boiling 75% EtOH (200 ml) to remove insoluble substances. From the filtrate 11β-hydroglycyrrhizin Na salt (7.6 g) was separated (yield 85%). 11β-Hydroglycyrrhizin (**2**) was obtained by treating the Na-salt with Dowex 50 W-X2 Type II in H_2O. mp 271—277 °C (dec.), $[\alpha]_D$ +80.0° (MeOH), $C_{42}H_{64}O_{16}\cdot 2H_2O$. IR ν_{max}^{KBr} cm^{-1}: 1050 (C–OH), 1080 (C–O–C), 1710 (COOH), 2950 (CH_3), 3450 (OH). (−)FAB MS *m/z*: 823 $(M-1)^+$. ^{13}C-NMR δ: 179.0 (s, C-30), 170.5 (s), 170.0 (s, C′-6, C″-6), 148.5 (s, C-13), 121.5 (d, C-12), 104.1 (d), 103.3 (d, C′-1, C″-1), 61.2 (d, C-11).

Olean-11,13(18)-diene-3β-ol-30-oic Acid 3-*O*-β-D-Glucuronopyranosyl-(1→2)β-D-glucuronopyranoside (3) 11β-Hydroglycyrrhizin Na salt (5 g) dissolved in H_2O (100 ml) was treated with dil. HCl to adjust to pH 7—8. The solution was heated at 100 °C for 6 h. After cooling, the reaction mixture was acidified to pH 2—3 and then extracted twice with *n*-BuOH (100 ml). On evaporation, compound **3** was obtained. Yield: 4.2 g (92.7%); mp 247—250 °C (dec.), $[\alpha]_D$ −120.0° (MeOH), $C_{42}H_{62}O_{15}\cdot 2H_2O$. UV λ_{max}^{MeOH} nm: 243, 251, 260. IR ν_{max}^{KBr} cm^{-1}: 1040 (C–OH), 1080 (C–O–C), 1640 (C=C–C=C), 1720 (COOH), 2930 (CH_3), 3400 (OH). (−)FAB MS *m/z*: 805 $(M-1)^+$. ^{1}H-NMR (in CD_3OD) δ (TMS): 6.35 (1H, dd J=16 Hz, vinyl-H), 5.59 (1H, d, J=12 Hz, vinyl-H). ^{13}C-NMR δ: 178.9 (s, C-30), 170.2 (s), 169.9 (s, C′6. C″-6), 135.1 (s, C-30), 134.4 (s) (C-13, C-18), 127.8 (d), 126.3 (d, C-11, C-12), 104.6 (d), 103.5 (d, C′-1, C″-2), 88.5 (d, C-3). Kitagawa *et al.*[5] isolated compound **3**, mp 249—251 °C, $[\alpha]_D$ −120.0° (MeOH), from Dong-bei licorice (Glycyrrhiza uralensis root) as one of the minor saponins and called licorice saponin C-2.

Olean-11,13(18)-diene-3β,30-diol-3-*O*-β-D-glucopyranosyl(1→2)β-D-glucopyranoside (4) Trimethyl ester penta-acetate of compound **3** (500 mg) dissolved in dry THF (20 ml) was added to a solution of $NaAlH_2(OCH_2CH_2OCH_3)_2$ (70% in toluene) (2.9 ml) in dry THF (20 ml) under vigorous stirring at 60 °C in an N_2 atmosphere. The reaction was

continued for 1 h, and after cooling, the reaction mixture was decomposed with 10% HCl to adjust pH 3—4 and added with aq. *n*-BuOH. The organic layer of the filtered solution was washed with H_2O 3 times. The solvent was evaporated to obtain a residue which was chromatographed on a silica gel (solvent: $CHCl_3$–MeOH (9 : 1)) to give a main fraction. The fraction was separated on HPLC using MeOH–H_2O (8 : 2) to afford compound **4**. Yield: 273 mg; mp 267—270 °C, $[\alpha]_D$ −41.6° (MeOH), $C_{42}H_{68}O_{12}\cdot 4H_2O$. UV λ_{max}^{MeOH} nm: 243, 252, 260. IR ν_{max}^{KBr} cm^{-1}: 1030 (C–OH), 1080 (C–O–C), 1640 (C=C–C=C), 2920 (CH_3), 3400 (O–H). (−)FAB MS *m/z*: 763 $(M-1)^+$. ^{13}C-NMR δ: 135.2 (s), 134.6 (s, C-13, C-18 or reversed), 127.5 (d), 127.0 (d, C-11, C-12), 104.7 (d), 103.5 (d, C′-1, C″-1), 64.2 (t, C-30), 61.0 (t), 60.8 (t, C′-6, C″-6).

18β-Olean-12-ene-11-oxo-3β,30-diol-3-*O*-β-D-glucuronopyranosyl(1→2)β-D-glucuronopyranoside (5) Penta-acetate of glycyrrhizin dimethyl ester at the di-glucuronide moiety was prepared according to the method of Sasaki *et al.*[6] The selective reduction of glycyrrizin 30-COOH was performed according to Yamada's method.[7] A solution of ethyl chloroformate (0.55 g) in THF (2.5 ml) was added to a solution of dimethyl ester pentaacetate of glycyrrhizin (5.3 g) and triethylamine (0.51 g) in THF (25 ml) during the course of 30 min at −5 °C, and the mixture was stirred for 30 min at the same temperature. The precipitate was filtered off and washed with THF, and the combined filtrate and washings were added during 30 min to a solution of $NaBH_4$ (0.47 g) in H_2O (5 ml) at 10—15 °C on cooling. Then the reaction mixture was stirred at r.t. for 4 h and made acidic with HCl, when the reaction mixture was separated into two layers. The organic layer washed with 10% aq. NaOH and H_2O was dried over anhydr. Na_2SO_4. The solvent was evaporated to obtain a residue which was chromatographed on a silica gel (solvent: $CHCl_3$–MeOH (100 : 1)) to give a main product (1.25 g). One percent aq. KOH solution (14 ml) was added to the solution of the main product (200 mg), and the mixture was stirred at r.t. for 20 min. After deionization by treatment with Amberlite IRA-120B, the product was purified by HPLC (solvent: CH_3CN–3% aq. AcOH (4 : 6)) to afford compound **5**. Yield: 133 mg; mp 241—245 °C, $[\alpha]_D$ +54.0° (MeOH), $C_{42}H_{64}O_{15}\cdot 3H_2O$. UV λ_{max}^{MeOH} nm: 248. IR ν_{max}^{KBr} cm^{-1}: 1050 (C–OH), 1090 (C–O–C), 1650 (C=O), 1720 (COOH), 2920 (CH_3), 3420 (O-H). (+)FAB MS *m/z*: 809 $(M+1)^+$. ^{13}C-NMR δ: 199.5 (s, C-11), 170.6 (s), 170.4 (s, C′-6, C″-6), 170.2 (s, C-13), 127.5 (d, C-12), 104.8 (d), 103.6 (d, C′-1, C″-1), 64.3 (t, C-30).

18β-Olean-12-ene-3β,11ξ,30-triol-3-*O*-β-D-glucopyranosyl(1→2)β-D-glucopyranoside (6) Treatment of glycyrrhizin (500 mg) with diazomethane in MeOH at r.t. for 4 h yielded trimethyl ester. On acetylation glycyrrhizin trimethyl ester gave pentaacetate. Penta-acetylglycyrrhizin trimethyl ester dissolved in dry THF (20 ml) was added to a solution of $NaAlH_2(OCH_2CH_2OCH_3)_2$ (70% in toluene) (2.9 ml) in dry THF (20 ml) under vigorous stirring at 60 °C in an N_2 atmosphere. The reaction was continued for 1 h. After cooling, the reaction mixture was decomposed with 10% HCl to adjust to pH 3—4 and extracted with aq. *n*-BuOH (50 ml). The organic layer was washed with H_2O 3 times. The solvent was evaporated to obtain a residue which was chromatographed on silica gel (solvent: $CHCl_3$–MeOH–H_2O (40 : 10 : 1)) to give a main fraction. The fraction was separated on HPLC using a solvent system MeOH–H_2O (8 : 2) to afford compound **6**. Yield: 208 mg; mp 216—218 °C, $[\alpha]_D$ +51.2° (MeOH), $C_{42}H_{70}O_{13}\cdot 4H_2O$. IR ν_{max}^{KBr} cm^{-1}: 1030 (C–OH), 1080 (C–O–C), 2940 (CH_3), 3400 (O–H). (−)FAB MS *m/z*: 781 $(M-1)^+$. ^{13}C-NMR δ: 144.7 (s, C-13), 127.4 (d, C-12), 103.8 (d), 103.6 (d, C′-1, C″-1), 64.3 (d, C-11), 64.3 (t, C-30), 61.0 (t), 60.9 (t, C′-6, C″6).

18β-Olean-12-ene-3β,30-diol-3-*O*-β-D-glucopyranosyl(1→2)β-D-glucopyranoside (7) A solution of compound **6** (300 mg) in dry EtOH (30 ml) was stirred with Pd/C (10%, 1 g) for 12 h under an H_2 stream. The reaction mixture was filtered and evaporated *in vacuo* to obtain compound **7**. Yield: 164 mg; mp 222—224 °C, $[\alpha]_D$ +36.8° (MeOH), $C_{42}H_{70}O_{12}\cdot 3H_2O$. IR ν_{max}^{KBr} cm^{-1}: 1030 (C–OH), 1080 (C–O–C), 2940 (CH_3), 3380 (O–H). (−)FAB MS *m/z*: 765 $(M-1)^+$. ^{13}C-NMR δ: 144.4 (s, C-13), 121.6 (d, C-12), 103.8 (d), 103.6 (d, C′-1, C″-1), 64.3 (t, C-30), 61.0 (t), 60.9 (t, C′-6, C″-6), 23.0 (t, C-11).

Biological Experiments A. Cells and Viruses MT-4[8] and MOLT-4 (clone 8)[9] were used for anti-HIV-1 assays. The cells were cultured and maintained in RPMI-1640 medium supplemented with 10% heat-inactivated fetal calf serum, 100 IU/ml of penicillin G, and 100 μg/ml streptomycin. The HIV-1 was obtained from the culture supernatant of MOLT-4/HTLV-III_B cells.[10] For anti-HSV-1 test, we employed a KOS strain of HSV-1 and human embryonic fibroblast (HEF) cells growing in Eagle's minimum essential medium (MEM) supplemented with 10% heat-inactivated newborn calf serum (NCS) and antibiotics.

B. Anti-HIV-1 Assay The activity of the compounds against HIV-1 replication in MT-4 was based on the inhibition of virus-induced cytopathogenicity, as previously described.[11] Briefly, MT-4 cells were suspended at 2×10^5 cells per ml and infected with HIV-1 at 1000 50% cell culture infective doses per ml. Immediately after infection, 100 μl of the cell suspension was put into each well of a flat-bottomed microtiter tray containing various concentrations of the test compounds. After 5 d of incubation at 37 °C, the number of viable cells was determined by the 3-(4,5-dimethylthiazol-2-yl)-2,5-diphenyl-tetrazolium bromide (MTT) method, as previously described.[12]

The activity was also monitored by the viability and HIV-1 antigen expression in MOLT-4 (clone 8) cells infected with HIV-1 in the absence or presence of the test compounds. In this experiment, MOLT-4 (clone 8) cells were infected with HIV-1 at a multiplicity of infection of 0.002 and incubated at 37 °C. On day 3 after infection, viral antigen expression was measured by indirect immunofluorescence using a polyclonal antibody. For the viability test, half of the culture medium was replaced by fresh culture medium containing appropriate concentrations of the compounds. The cells were incubated for another 2 d, and the number of viable cells was counted microscopically in a hematocytometer by the trypan blue exclusion method. The cytotoxicity of the compounds was determined by measuring the viability of mock-infected MT-4 and MOLT-4 (clone 8) cells in parallel with the virus-infected cells.

C. Reverse Transcriptase (RT) Assay The effect of the compounds on HIV-1 RT activity was evaluated with the enzyme obtained from disrupted virions which had been partially purified and concentrated from the supernatant of MOLT-4/HTLV-III_B cells. The assay was performed at 37 °C for 30 min in a 50 μl reaction mixture containing 50 mM Tris–HCl (pH 8.4), 2 mM dithiothreitol, 100 mM KCl, 10 mM $MgCl_2$, 0.1% Triton X-100, 1 μCi of [methyl-^{3}H]-dTTP (30 Ci/mmol), 0.01 OD unit of poly(rA). oligo (dT), test compound and *ca.* 0.1 U of enzyme. The reaction was stopped with 200 μl of 5% trichloroacetic acid, and the precipitated material was analyzed for radioactivity.

D. Anti-HSV-1 Assay Assay of the compound for HSV-1 replication was carried out in confluent HEF monolayer cells in a flat-bottomed microtiter tray. The HEF cells were infected with 50 plaque forming units (PFU) of HSV-1 and incubated at 37 °C in the presence of various concentrations of the test compounds. After 5—7 d, HSV-1-induced cytopathogenicity was recorded microscopically.

Results and Discussion

When the inhibitory effect of glycyrrhizin (**1**) and its derivatives (**3**—**7**) was examined for HIV-1 replication in MT-4 cells, glycyrrhizin (**1**) and compound **3** were found to have achieved more than 80% protection of the cells from the virus-induced destruction at a concentration of 0.62 and 0.16 mM, respectively (Table I). In particular, compound **3** almost completely suppressed HIV-1-induced cytopathogenicity at this concentration. Compounds **4** and **5** were slightly inhibitory to HIV-1 replication at subtoxic concentrations (Table I), yet other compounds (**6** and **7**) did not show any activity at their non-toxic concentrations (data not shown).

In MOLT-4 (clone 8) cells, compound **3** also exhibited the selective inhibition at a concentration between 0.16 and 0.31 mM (Fig. 1). The compound slightly reduced the number of viable mock-infected cells at a concentration of 1.24 mM. The HIV-1 antigen expression in MOLT-4 (clone 8) was suppressed by compounds **1** and **3** at concentrations higher than 0.16 mM (Fig. 2). In contrast, compounds **4** and **5** were totally inactive against the antigen expression. When we examined the effect of compound **3** on HIV-1 RT activity, no inhibition was observed at the concentrations active against HIV-1 induced cytopathogenicity in MOLT-4 cells.

In the next experiment, we investigated the inhibitory effect of glycyrrhizin and its homologs on HSV-1 replication in HEF cells. As shown in Table III, glycyrrhizin and compound **3** proved inhibitory to HSV-1 replication, their 50% inhibitory concentrations (IC_{50}) for HSV-1 cytopatho-

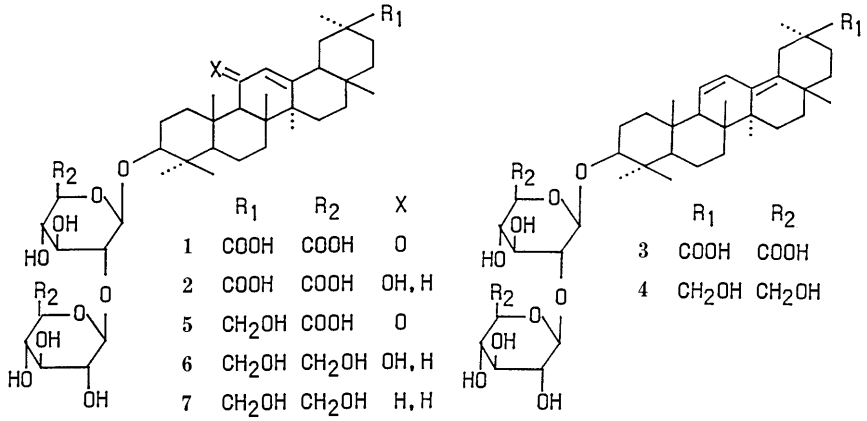

Chart 1

TABLE I. Inhibitory Effect of Glycyrrhizin and its Modified Compounds on HIV-1 Replication in MT-4 Cells

Concentration (mM)	Number of viable cells[a] (%)			
	1	3	4	5
2.48	0	0	N.D.	N.D.
1.24	30.7	0	N.D.	N.D.
0.62	81.9	0	N.D.	N.D.
0.31	39.1	60.9	N.D.	17.5
0.16	8.4	92.8	56.7	57.4
0.08	8.1	11.6	20.4	7.0
0.04	4.5	1.7	9.6	10.2

a) Number of viable cells is determined by the MTT method and expressed as the percentage of mock-infected control. N.D., not determined.

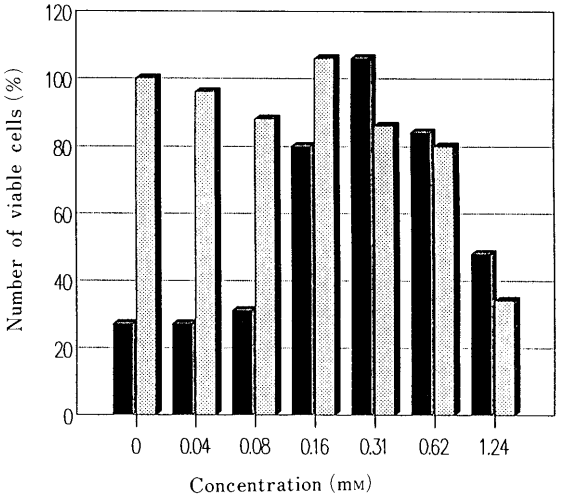

Fig. 1. Inhibitory Effect of Compound **3** on HIV-1 Replication in MOLT-4 Cells

The viability of HIV-1-infected cells (■) and mock-infected cells (▨) was assessed by the trypan blue exclusion method. The number of viable cells is expressed as the percentage of the mock-infected control.

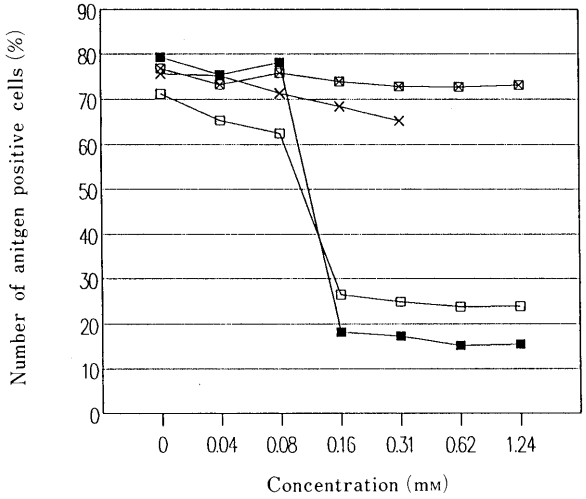

Fig. 2. Inhibitory Effect of Glycyrrhizin (■) and Compounds **3** (□), **4** (⊠) and **5** (×) on HIV-1 Antigen Expression in MOLT-4 Cells

HIV-1 antigen positive cells were detected by indirect immunofluorescence using polyclonal antibody on day 3 after infection.

genicity being 3.6 and 0.5μM, respectively. Other compounds (**4**—**7**) did not affect the replication of HSV-1 nor the cell morphology of mock-infected HEF cells (data not shown).

Based on the anti-HIV-1 activity of glycyrrhizin *in vitro*,[1] the glycyrrhizin preparation, SNMC has been clinically applied to HIV-1 carriers by i.v. administration, and indeed, their immunological parameters have been improved.[2] The present study indicates that a glycyrrhizin analog compound **3** also seems applicable to the treatment of AIDS. Furthermore, compound **3** might be safer than glycyrrhizin in long-term administration because, it is less capable of exerting pseudoaldosteronism, as suggested by our earlier investigations.[13]

The RT assay suggests that, like glycyrrhizin,[1] the anti-HIV-1 activity of compound **3** is not due to the inhibition of RT activity. The mechanism of action of the compound remains to be elucidated. It has been demonstrated that glycyrrhizin partially prevents the adsorption of HIV-1 particles to $CD4^+$ cells.[14] Inhibition of protein kinase C (PKC) activity by glycyrrhizin has also been discussed in relation to its anti-HIV-1 effect.[15] However, it is still not known whether the inhibition of virus adsorption and the inhibition of PKC activity are definitely related, though the binding of HIV-1 to $CD4^+$ lymphocytes induces rapid phosphorylation of CD4 receptors which involve PKC.[15] On the other hand, comparative study with other glycyrrhizin analogs (**4**—**7**) has revealed that the presence of a carboxyl group at the 20-position in compound **3** is essential for the anti-HIV-1 activity, while the hetero-annular diene C/D ring system in compound **3** is convertible with the $\alpha\beta$-unsaturated carbonyl structure in C-ring of glycyrrhizin. These results suggest

that the carboxyl group at 20-position may play a crucial role in inhibiting the virus adsorption.

Considering the current extreme prevalence of AIDS, the finding of effective chemotherapeutic agents is highly desired. In this regard, compound **3** should be further pursued for its potential as an anti-AIDS agent.

Acknowledgements The authors thank Dr. A. Sato, Mr. S. Mori and Mr. K. Konno, Fukushima Medical College, for their excellent technical assistance, and Messrs. T. Takeuchi, N. Nagata, T. Okai and M. Abe of Minophagen Pharmaceutical Co. for their useful support. Their appreciation is also extended to Prof. I. Nishioka, Kyushu University, and members of the Central Analytical Laboratory, Meiji College of Pharmacy, for FAB-MS, NMR, IR and UV spectral analyses.

References

1) M. Ito, H. Nakajima, M. Baba, R. Pauwels, E. De Clercq, S. Shigeta, and N. Yamamoto, *Antiviral Res.*, **7**, 127 (1987).
2) T. Hattori, S. Ikematsu, A. Koito, S. Matsushita, Y. Maeda, M. Hada, M. Fujimaki, and K. Takatsuki, *Antiviral Res.*, **11**, 255 (1989).
3) R. Pompei, O. Flore, M. A. Marcialis, A. Pani, and B. Loddo, *Nature* (London), **281**, 689 (1979).
4) M. Baba and S. Shigeta, *Antiviral Res.*, **7**, 99 (1987).
5) I. Kitagawa, J. L. Zhou, M. Sakagami, T. Taniyama, and M. Yoshikawa, *Chem. Pharm. Bull.*, **36**, 3710 (1988).
6) U. Sasaki, K. Mizutani, R. Kasai, and O. Tanaka, *Chem. Pharm. Bull.*, **36**, 3491 (1988).
7) K. Ishizumi, K. Koga, and S. Yamada, *Chem. Pharm. Bull.*, **16**, 492 (1968).
8) S. Harada, Y. Koyanagi, and N. Yamamoto, *Science*, **229**, 563 (1985).
9) R. Kikukawa, Y. Koyanagi, S. Harada, N. Kobayashi, M. Hatanaka, and N. Yamamoto, *J. Virology*, **57**, 1159 (1986).
10) S. Harada, Y. Koyanagi, and N. Yamamoto, *Virology*, **146**, 272 (1985).
11) R. Pauwels, E. De Clercq, J. Desmyter, J. Balzarini, P. Gaubau, P. Herdewijn, H. Vanderhaeghe, and M. Vandeputte, *J. Virol. Methods*, **16**, 171 (1987).
12) R. Pauwels, J. Balzarini, M. Baba, R. Snoeck, D. Schols, P. Herdewijn. J. Desmyster, and E. De Clercq, *J. Virol. Methods*, **20**, 309 (1988).
13) S. Shibata, K. Takahashi, S. Yano, M. Harada, H. Saito, Y. Tamura, A. Kumagai, K. Hirabayashi, M. Yamamoto, and N. Nagata, *Chem. Pharm. Bull.*, **35**, 1910 (1987).
14) M. Ito, A. Sato, K. Hirabayashi, F. Tanabe, S. Shigeta, M. Baba, E. De Clercq, H. Nakashima, and N. Yamamoto, *Antiviral Res.*, **10**, 289 (1988).
15) A. P. Fields, D. P. Bednarik, A. Hess, and W. S. May, *Nature* (London), **333**, 278 (1988).

A New Sapogenol and Other Constituents in Abri Semen, the Seeds of *Abrus precatorius* L. I[1)]

Junei KINJO, Kumiko MATSUMOTO, Mutsumi INOUE, Takashi TAKESHITA and Toshihiro NOHARA*

Faculty of Pharmaceutical Sciences, Kumamoto University, 5–1 Oe-honmachi, Kumamoto 862, Japan. *Received June 27, 1990*

Further study on the chemical constituents of the *Abrus* species resulted in the isolation of a new sapogenol, abrisapogenol J (1), from the methanolysate of the seeds for *Abrus precatorius* L., together with sophoradiol (4), its 22-*O*-acetate (2) and hederagenin methyl ester (5). The structure of 1 has been elucidated to be 3β,22β-dihydroxy-11-oxoolean-13(18)-ene by the use of hetero nuclear multiple bonds correlation (HMBC) spectroscopy. In addition, various compounds, trimethyl tryptophan dipolar ion (3), kaikasaponin III methyl ester (6), abrine (7), abrusin (8) and its 2″-*O*-apioside (9) were obtained from the methanolic extract.

Keywords Abri Semen; *Abrus precatorius*; Leguminosae; oleanene sapogenol; abrisapogenol J; sophoradiol 22-*O*-acetate; sophoradiol; hederagenin; kaikasaponin III; trimethyl tryptophan dipolar ion

In the course of the our studies on the chemical constituents of Abri Herba, the whole plants of *Abrus cantoniensis* HANCE (Leguminosae), it was found that the crude saponin fraction of this plant was effective for a hepatic injury induced by CCl_4.[2)] We elucidated the structures of seven new sapogenols, abrisapogenol A—G, from the methanolysate of this fraction.[3)] In connection with these studies, we tried to clarify the components of Abri Semen, the seeds of *Abrus precatorius* L. Now we have obtained a novel sapogenol, named abrisapogenol J (**1**), together with three sapogenols, sophoradiol (**4**),[4)] its 22-*O*-acetate (**2**), and hederagenin methyl ester (**5**)[5)] from the methanolysate of the crude saponin fraction of the seeds as shown in Chart 1. Moreover, we have isolated

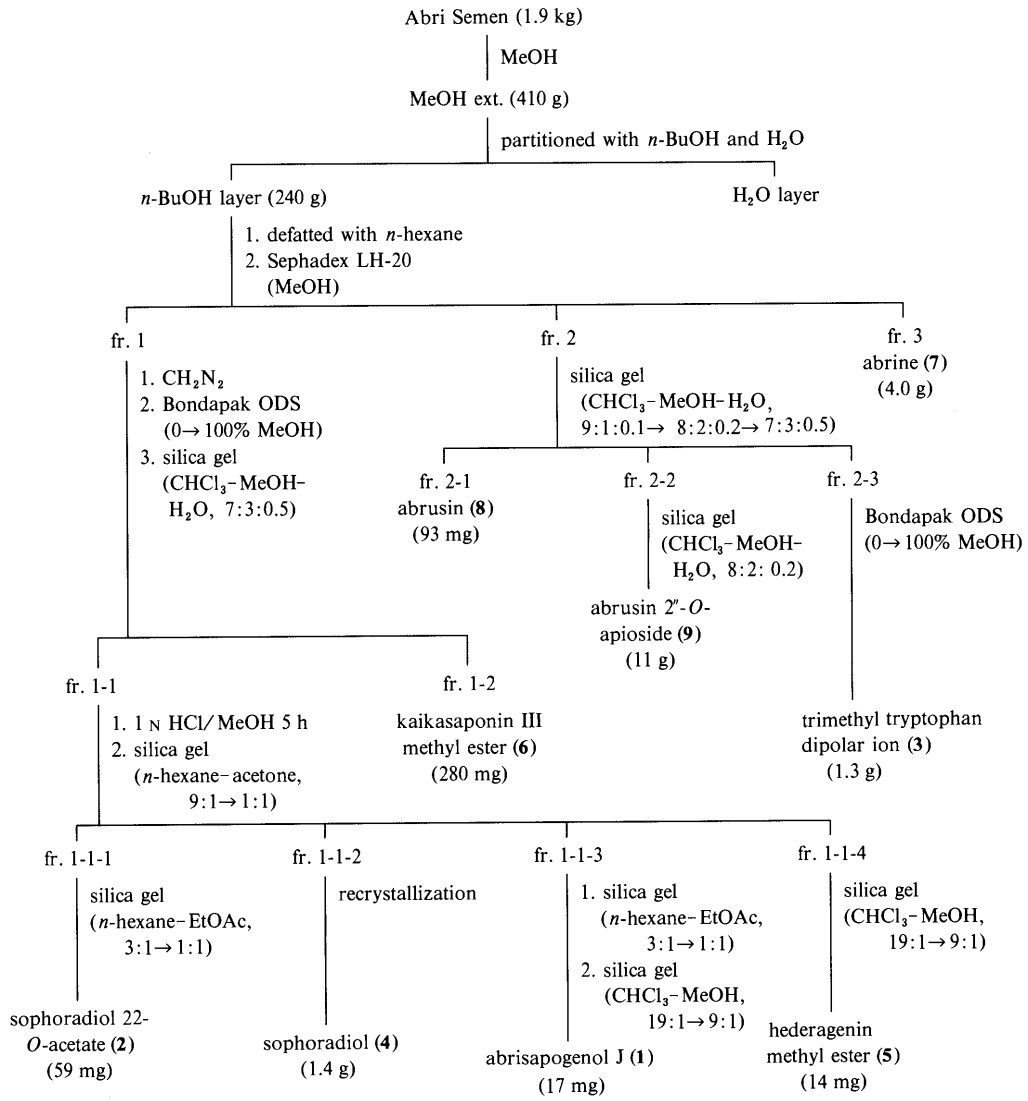

Chart 1. Isolation of Compd. **1**—**9** from Abri Semen

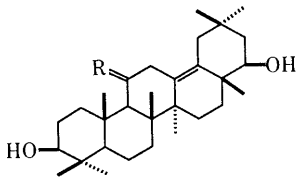

	R
abrisapogenol J (1)	O
abrisapogenol G (10)	H_2

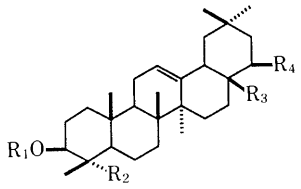

	R_1	R_2	R_3	R_4
sophoradiol 22-*O*-acetate (2)	H	CH_3	CH_3	$OCOCH_3$
sophoradiol (4)	H	CH_3	CH_3	OH
hederagenin methyl ester (5)	H	CH_2OH	$COOCH_3$	H
kaikasaponin III methyl ester (6)	glc UAMe^2-gal^2-rha	CH_3	CH_3	OH

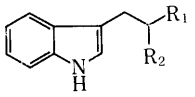

	R_1	R_2
trimethyl tryptophan dipolar ion (3)	$N^+(CH_3)_3$	COO^-
abrine (7)	$NHCH_3$	COOH

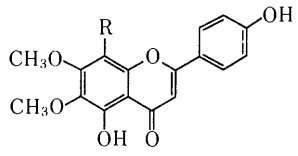

	R
abrusin (8)	glc
abrusin 2″-*O*-apioside (9)	glc^2-api

five compounds from the MeOH extract. This paper deals with the structural determination of **1**—**3** and identification of the other compounds.

Abrisapogenol J (**1**) was obtained as colorless needles, mp 223—224 °C and showed signals due to eight *tert*-methyl groups in the ^{1}H-nuclear magnetic resonance (^{1}H-NMR) spectrum (Table I), which was reminiscent of the oleanan type triterpene. However, since the proton at C-12 was not observed, it seemed to be an olean-13(18)-ene such as abrisapogenol G (**10**).[3a] Also, signals adjacent to the hydroxy groups, 3α-H and 22α-H, were fundamentally identical with those of **10** [3.23 (1H, dd, J=11.0, 5.1 Hz, H-3); 3.35 (1H, dd, J=10.4, 6.5 Hz, H-22)]. In the ^{13}C-NMR spectrum, **1** had thirty carbon signals including two olefinic signals (δ 132.8 and 133.5) as singlet which supported the location of the double bond. On the other hand, comparing with that of **10**, a carbonyl group (δ 209.2) was observed instead of the disappearance of a triplet signal. The electron impact-mass spectrum (EI-MS) of **1** showed the molecular ion at *m/z* 456, which increased 14 mass units that of **10**. In order to confirm the location of the carbonyl group, we measured the heteronuclear multiple bonds correlation (HMBC) spectrum[6] of **1**. The ^{13}C–^{1}H (methyl group) long range correlation by HMBC spectrum gave the partial structure of **1** as shown in Fig. 1 and twenty-six carbons in **1** were assignable. The carbonyl signal and three triplet signals (δ 18.0, 27.2 and 45.1), which correspond to C-2, 6, 11 and 12, remained unassignable. The ^{13}C–^{1}H correlation spectroscopy (COSY) and the ^{1}H–^{1}H COSY of **1** suggested that the location of the carbonyl group should be at C-11, because the proton signal at C-9 (δ 63.4) was observed at δ 2.32 as singlet. Consequently, the above-mentioned triplet carbon signals (δ 18.0, 27.2 and 45.1) were assigned at C-6, C-2 and C-12, respectively. Therefore, the structure of **1** was determined to be 3β,22β-dihydroxy-11-oxoolean-13(18)-ene.

Since the hydrolytic change from olean-12(13)-ene to 13(18)-ene was assumed, compound **4** (sophoradiol) was

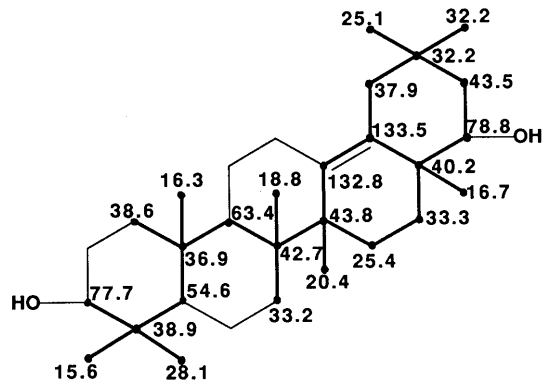

Fig. 1. Partial Structure of **1** with the Assignable Carbons (●) by HMBC Spectrum

subjected to hydrolysis under the same conditions to give **1**. After 12 h, some hydrolytic cleavage, possibly dehydration, was observed. However no transformation from **4** to **10** occurred. In a similar manner as above, glycyrrhetic acid produced only a spot which showed the same fluorescence as glycyrrhetic acid itself on thin layer chromatography (TLC) under a ultraviolet (UV) lamp. It meant that no cleavage of the α,β-unsaturated ketone group in glycyrrhetic acid occurred under acid hydrolysis. Hence, **1** couldn't be an artifact by acid hydrolysis.

Compound **2** showed a hydroxy (3500 cm^{-1}) and a carbonyl group (1700 cm^{-1}) in the infrared (IR) spectrum. The ^{1}H-NMR of **2** gave signals due to not only eight *tert*-methyl groups but also an acetyl group. In the low field region, an olefinic proton (δ 5.26), a proton adjacent to the acetyl group, and another proton (δ 3.22) next to the hydroxy group were observed. As compared with those of 3,22-diacetate for **4**,[7] **2** was suggested to be the 22-monoacetate of **4**, since the other signals could be assigned except for the proton at C-3. In addition, the EI-MS of **2** which exhibited peaks due to the characteristic fragmentation at *m/z* 276 (D/E ring) and 208 (A/B ring) by *retro*

TABLE I. ^{1}H-NMR Data of **1** and **2** (δ: ppm, in $CDCl_3$)

	1	2
H-1_{eq}	2.86 (dt, J=13.2, 3.7 Hz)	
H-3	3.21 (dd, J=10.6, 5.5 Hz)	3.22 (dd, J=10.5, 4.0 Hz)
H-5	0.64 (d, J=11.7 Hz)	
H-9	2.32 (s)	
H-12_{eq}	3.34 (d, J=17.6 Hz)	H-12 5.26 (t, J=3.4 Hz)
H-12_{ax}	2.79 (dd, J=17.6, 2.2 Hz)	
H-19_{eq}	2.17 (d, J=13.9 Hz)	
H-22	3.39 (dd, J=11.0, 5.9 Hz)	4.64 (t, J=3.7 Hz)
Methyl	0.74 (C_{30}), 0.80 (C_{24}), 0.81 (C_{26}), 0.97 (C_{29}), 0.98 (C_{28}), 1.00 (C_{23}), 1.16 (C_{25}), 1.30 (C_{27})	0.79, 0.82, 0.89, 0.94, 0.98, 1.00×2, 1.15
Acetyl		2.03

TABLE II. ^{13}C-NMR Data of **1**, **5** and **6** (δ: ppm, Pyridine-d_5)

	1	5		6	
C-1	38.6	38.1	38.9	Glc UA C-1	105.3
C-2	27.2	27.7	21.1	C-2	79.0
C-3	77.7	76.9	90.0	C-3	76.1
C-4	38.9	41.8	39.6	C-4	73.1
C-5	54.6	51.5	55.9	C-5	76.5
C-6	18.0	18.5	18.5	C-6	170.6
C-7	33.2	32.4	33.2	COOMe	52.0
C-8	42.7	39.2	40.0		
C-9	63.4	47.6	47.9	Gal C-1	101.9
C-10	36.9	36.9	38.9	C-2	78.4
C-11	209.2	23.6	23.8	C-3	76.7
C-12	45.1	122.3	122.5	C-4	70.4
C-13	132.8	143.7	144.8	C-5	76.3
C-14	43.8	41.6	42.4	C-6	61.9
C-15	25.4	26.8	26.4		
C-16	33.3	23.0	28.7	Rha C-1	102.7
C-17	40.2	46.7	38.0	C-2	72.6
C-18	133.5	41.3	45.3	C-3	72.3
C-19	37.9	45.8	46.8	C-4	74.3
C-20	32.2	30.7	30.9	C-5	69.4
C-21	43.5	33.8	42.3	C-6	18.9
C-22	78.8	32.4	75.6		
C-23	28.1	72.2	28.4		
C-24	15.6	11.4	15.7		
C-25	16.3	15.7	16.8		
C-26	18.8	16.8	17.2		
C-27	20.4	25.9	25.7		
C-28	16.7	178.3	28.2		
C-29	32.2	33.1	33.2		
C-30	25.1	23.4	21.1		
COOMe		49.8			

Diels–Alder fission supported this structure unambigously. Therefore, **2** was determined to be 3β-hydroxy-22β-acetoxyolean-12-ene. Compound **2** is its first example of isolation in nature.

Compound **3** was obtained as an amorphous powder and did not react with CH_2N_2–ether solution. The positive fast atom bombardment (FAB)-MS of **3** showed the molecular ion peak (M^++H) at m/z 247, but negative FAB-MS of **3** did not give a clear fragment peak. In the ^{1}H-NMR spectrum of **3**, an overlapped methyl group (δ 3.20, 9H, s) was observed along with the signals of an indolyl group. The ^{13}C-NMR of **3** showed a strong peak at δ 53.0 which was assignable to the methyl group connected with an ammonium group.[8] Since the IR spectrum gave a carboxylate absorption at 1640 cm^{-1} and the postive FAB-MS showed the characteristic fragmentation peaks at m/z 188 [M^++H−N(Me)$_3$] and m/z 144 [M^++H−N(Me)$_3$−CO_2], the structure of **3** was determined to be 2-trimethylammonio-3-(3-indolyl)propionate, *i.e.*, trimethyl tryptophan dipolar ion. The methyl ester form of **3** has already been reported,[9] but the anion form is the first example.

Compound **4**—**9** was identified with sophoradiol, hederagenin methyl ester, kaikasaponin III methyl ester,[10] abrine,[11] abrusin, abrusin 2″-*O*-apioside[12] respectively, by various spectral data and physical data.

Experimental

All melting points were determined on a Yanagimoto micro-melting point apparatus and are uncorrected. The optical rotations were measured with a JASCO DIP-360 automatic digital polarimeter. The IR spectra were recorded with a Hitachi IR spectrometer, model 270-30. The ^{1}H- and ^{13}C-NMR spectra were measured with a JEOL JNM-GX 400NMR spectrometer and chemical shifts are given on a δ (ppm) scale with tetramethylsilane as an internal standard. The EI- and FAB-MS were measured with a JEOL DX-300 spectrometer. TLC was performed on precoated Kieselgel 60 F_{254} plates (Merck). Column chromatography was carried out on Kieselgel 60 (70—230 mesh, and 230—400 mesh, Merck), Sephadex LH-20 (Pharmacia) and Bondapak C_{18} (Waters).

Extraction and Isolation Abri Semen was purchased from Uchida Wakanyaku Co., Ltd., Tokyo. The crushed Abri Semen (1.9 kg) were extracted with MeOH three times under reflux. The combined extract was concentrated and partitioned with *n*-BuOH and H_2O. The *n*-BuOH extract (240 g) was separated by various chromatography to give compound **3**, **7**—**9** and crude saponin fraction (fr. 1) (Chart 1). After methylation by CH_2N_2, the methylated saponin fraction (fr. 1-1) was subjected to acid methanolysis with 1 N HCl/MeOH. The methanolysate was chromatographed by silica gel column to afford compound **1**, **2**, **4** and **5**.

Compound **1** (Abrisapogenol J): Colorless needles, mp 223—224 °C, $[\alpha]_D$ −67.0° (c=0.11, $CHCl_3$). EI-MS m/z: 456 (M^+), 235, 225, 205. IR (KBr): 3465 (ν_{O-H}), 2950, 1710 ($\nu_{C=O}$) cm^{-1}. ^{1}H-NMR: Table I. ^{13}C-NMR: Table II.

Compound **2** (Sophoradiol 22-*O*-Acetate): An amorphous powder $[\alpha]_D$ +65.5° (c=0.25, MeOH). EI-MS m/z: 484 (M^+), 276, 216, 208. IR (KBr): 3500 (ν_{O-H}), 2900, 1700 ($\nu_{C=O}$). ^{1}H-NMR : Table I.

Compound **3** (Trimethyl Tryptophan Dipolar Ion): An amorphous powder, $[\alpha]_D$ +81.5° (c=0.29, MeOH). Positive FAB-MS m/z: 274 (M^++H), 188, 144, 136. IR (KBr): 3450 (ν_{O-H}), 1640 (ν_{COO^-}) cm^{-1}. ^{1}H-NMR (DMSO-d_6) δ: 7.21 (1H, s, H-2), 7.62 (1H, d, J=8 Hz, H-4), 7.12 (1H, t, J=8 Hz, H-5), 7.19 (1H, t, J=8 Hz, H-6), 7.44 (1H, d, J=8 Hz, H-7), 3.29 (2H, m, H_2-10), 3.81 (1H, dd, J=9, 2 Hz, H-11), 3.20 (9H, s, N(Me)$_3$). ^{13}C-NMR (DMSO-d_6) δ: 125.3, 108.8, 119.5, 120.5, 123.0, 113.1, 128.0, 137.1, 24.0, 80.0, 171.0, 53.0 (C-2—12, N(Me)$_3$).

Compound **4** (Sophoradiol): Colorless needles, mp 220—222 °C, $[\alpha]_D$ +87.5° (c=0.25, $CHCl_3$–MeOH). IR (KBr): 3350 (ν_{O-H}), 2900, 1380, 1020 cm^{-1}. EI-MS m/z: 442 (M^+), 234 (D/E ring), 219, 208 (A/B ring). ^{13}C-NMR ($CDCl_3$) δ: 38.7, 27.3, 79.0, 38.8, 55.3, 18.4, 32.8, 39.7, 47.7, 37.0, 23.5, 122.5, 143.9, 41.5, 25.4, 28.1, 37.4, 44.8, 46.2, 30.5, 42.1, 76.6, 28.2, 15.6, 15.6, 17.0, 25.9, 28.1, 32.9, 20.0 (C-1—30).

Solvolysis of 4 A solution of **4** (10 mg) in 1 N HCl/MeOH was heated under reflux for 12 h and the reaction mixture was neutralized by 3% KOH/MeOH. After filtration and evaporation *in vacuo*, the residue taken in a small amount of $CHCl_3$–MeOH was analyzed by TLC ($CHCl_3$–MeOH, 19:1, *n*-hexane–acetone, 3:1). None was shown to be identical with the authentic sample of **10**.

Solvolysis of Glycyrrhetic Acid A solution of glycyrrhetic acid (1 mg) in 1 N HCl/MeOH was treated the same way as the above. After neutralization, the mixture was analyzed by TLC (*n*-hexane–acetone, 2:1). Except for the spot of glycyrrhetic acid (Rf, 0.28), only one other spot (Rf, 0.42) was observed. The latter spot showed fluorescence such as glycyrrhetic acid under the UV lamp.

Compound **5** (Hederagenin Methyl Ester): An amorphous powder $[\alpha]_D$ +63.1° (c=0.11, $CHCl_3$). IR (KBr): 3485 (ν_{O-H}), 2945, 1735 ($\nu_{C=O}$) cm^{-1}. EI-MS m/z: 486 (M^+), 427, 262 (D/E ring), 224 (A/B ring), 203. ^{1}H-NMR ($CDCl_3$) δ: 0.72, 0.89, 0.90, 0.92, 0.95, 1.12 (each 3H, s, *tert*-Me×6), 3.62 (3H, s, COOMe), 3.43, 3.73 (each 1H, ABq, J=10.3 Hz, H_2-23), 5.28 (1H, br t, J=3.5 Hz, H-12). ^{13}C-NMR ($CDCl_3$) δ: 38.1, 27.7, 76.9, 41.8, 51.5, 18.5, 32.4, 39.2, 47.6, 36.9, 23.6, 122.3, 143.7, 41.6, 26.8, 23.0, 46.7, 41.3, 45.8, 30.7, 33.8, 32.4, 72.2, 11.4, 15.7, 16.8, 25.9, 178.3,

33.1, 23.4, 49.8 (C-1—30, COOMe).

Compound **6** (Kaikasaponin III Methyl Ester): An amorphous powder, $[\alpha]_D$ −4.4° (c=0.56, MeOH). ^{1}H-NMR (pyridine-d_5) δ: 0.87, 1.00×2, 1.16, 1.22, 1.26, 1.29, 1.39 (each 3H, s, *tert*-Me×8), 2.39 (1H, d, J=12.8 Hz, H-18), 3.29 (1H, br d, J=7.3 Hz, H-3), 3.72 (3H, s, OMe), 5.01, 5.66, 6.27 (each 1H, anomeric protons). ^{13}C-NMR: Table II.

Compound **7** (Abrine): An amorphous powder, $[\alpha]_D$ +61.6° (c=0.51, 1 N NaOH). EI-MS m/z: 218 (M^+), 173, 130. ^{13}C-NMR (DMSO-d_6) δ: 126.4, 109.2, 120.1, 121.1, 123.7, 113.4, 128.7, 138.5, 27.6, 65.8, 174.5, 33.9 (C-2—12, N-Me).

Compound **8** (Abrusin): An amorphous powder, $[\alpha]_D$ −7.1° (c=0.13, MeOH). ^{13}C-NMR (DMSO-d_6) δ: 167.3, 100.6, 182.4, 153.1, 136.1, 157.4, 107.5, 150.6, 111.2, 117.9, 129.3×2, 117.5×2, 165.7 (C-2—10, 1′—4′), 62.0, 60.4 (C-6,7-OMe), 74.7, 70.7, 78.8, 70.8, 82.2, 61.6 (glc C-1—6).

Compound **9** (Abrusin 2″-*O*-Apioside): An amorphous powder, $[\alpha]_D$ +105.1° (c=0.5, MeOH). FAB-MS m/z: 608 (M^+). ^{1}H-NMR (DMSO-d_6) δ: 3.83, 3.92 (OMe×2), 6.88 (1H, s, H-3), 6.98 (2H, d, J=8.8 Hz, H-3′), 8.07 (2H, d, J=8.8 Hz, H-2′). ^{13}C-NMR (DMSO-d_6) δ: 164.7, 100.6, 182.8, 152.9, 135.9, 157.4, 107.3, 150.5, 110.8, 121.1, 129.2, 116.3, 161.5 (C-2—10, 1′—4′), 61.1, 60.4 (OMe×4), 72.9, 74.8, 79.0, 70.7, 81.9, 61.8 (glc C-1—6), 108.8, 76.3, 79.0, 72.6, 62.0 (api C-1—6).

Solvolysis of 9 A solution of **9** (100 mg) in HCl/MeOH was heated under reflux for 4 h and the reaction mixture was neutralized by 3% KOH/MeOH. After filtration and evaporation *in vacuo*, the residue was subjected to Sephadex LH-20 column chromatography to afford **8** (30 mg).

Acknowledgement We thank Mr. M. Sawada, JEOL Ltd., for the measurement of HMBC spectrum.

References

1) Part XIX in the series of the studies on leguminous plants.
2) *a*) T. C. Chiang and H. M. Chang, *Planta Medica*, **46**, 52 (1982); *b*) T. Takeshita, J. Kinjo, T. Nohara, H. Itoh, Y. Niiho and T. Yamazaki, Abstracts of Papers, 34th Annual Meeting of the Japanese Society of Pharmacognosy, Osaka, 1985, p. 65.
3) *a*) T. Takeshita, S. Hamada and T. Nohara, *Chem. Pharm. Bull.*, **37**, 846 (1989); *b*) Y. Sakai, T. Takeshita, J. Kinjo, Y. Ito and T. Nohara, *ibid.*, **38**, 824 (1990).
4) *a*) M. Takahashi, S. Ishimasa and Y. Koyama, *Yakugaku Zasshi*, **80**, 698 (1960); *b*) T. C. Chiang and H. M. Chang, *J. Chem. Soc., Chem. Commun.*, **1982**, 785.
5) O. Texier, A. Ahond, F. Regerat and H. Pourrat, *Phytochemistry*, **23**, 2903 (1984).
6) A. Bax and M. F. Summers, *J. Am. Chem. Soc.*, **108**, 2093 (1986).
7) J. Kinjo, I. Miyamoto, K. Murakami, K. Kida, T. Tomimatsu, M. Yamasaki and T. Nohara, *Chem. Pharm. Bull.*, **33**, 1293 (1985).
8) K. Tsuzuki, T. Sunazuka, S. Murai, H. Toyoda, S. Omura, N. Inatomi and Z. Itoh, *Chem. Pharm. Bull.*, **37**, 2687 (1989).
9) S. Ghosal and K. S. Dutta, *Phytochemistry*, **10**, 195 (1971).
10) J. Kinjo, T. Takeshita, Y. Abe, N. Terada, H. Yamashita, M. Yamasaki, K. Takeuchi, K. Murakami, T. Tomimatsu and T. Nohara, *Chem. Pharm. Bull.*, **36**, 1174 (1988).
11) E. J. Miller and W. Robson, *J. Chem. Soc.*, **1938**, 1910.
12) K. R. Markham, J. W. Wallace, Y. N. Babu, V. K. Murty and M. G. Rao, *Phytochemistry*, **28**, 299 (1989).

Constituents of Zingiberaceae. I. Diarylheptanoids from the Rhizomes of Ginger (*Zingiber officinale* ROSCOE)

Hiroe KIKUZAKI, Junko USUGUCHI and Nobuji NAKATANI*

Department of Food and Nutrition, Faculty of Science of Living, Osaka City University, Sugimoto, Sumiyoshi-ku, Osaka 558, Japan. *Received July 4, 1990*

Two new diarylheptanoids, *meso*-3,5-diacetoxy-1,7-bis(4-hydroxy-3-methoxyphenyl)heptane (3a) and 3,5-diacetoxy-1-(4-hydroxy-3,5-dimethoxyphenyl)-7-(4-hydroxy-3-methoxyphenyl)heptane (4a) were isolated from the rhizomes of ginger (*Zingiber officinale* ROSCOE), together with dehydroxytetrahydrocurcumin (gingerenone A, 1) and hexahydrocurcumin (2). Their structures were elucidated on the basis of chemical and spectroscopic evidence.

Keywords ginger; *Zingiber officinale*; Zingiberaceae; diarylheptanoid; curcuminoid; spice

Ginger, the rhizome of *Zingiber officinale* ROSCOE, is one of the most popular spices and is also used as an oriental folk medicine. Its chemical constituents reportedly include a large number of terpenoids such as zingiberene and geraniol[1] and pungent components, *e.g.* shogaol and gingerol.[2] Many diarylheptanoids were isolated from the plants belonging to Zingiberaceae,[3] however, only a few were obtained from *Z. officinale* ROSCOE.[4] In this paper, we describe the isolation and structural elucidation of four diarylheptanoids including two new ones from ginger.

Dried rhizomes of ginger were extracted with dichloromethane and the extract was stream-distilled. The non-volatile components were subjected to chromatography on a silica gel column using benzene–acetone as an eluent to afford eleven fractions. The sixth and seventh fractions were successively chromatographed on a Sephadex LH-20 column and a silica gel column to give compound **1**. Compounds **2**, **3a** and **4a** were isolated from the eighth fraction in a similar way.

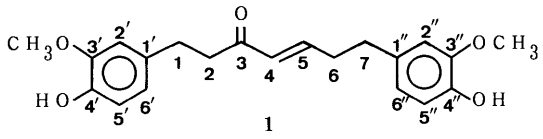

1

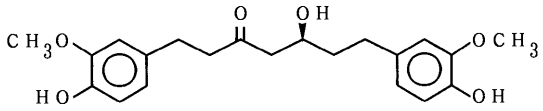

2

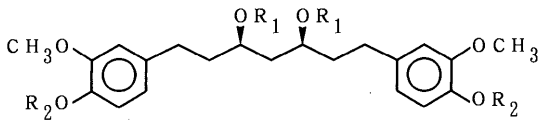

3a : R_1 = Ac, R_2 = H
3b : R_1 = R_2 = Ac

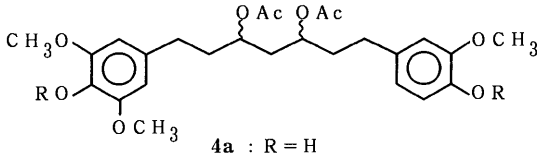

4a : R = H
4b : R = Ac

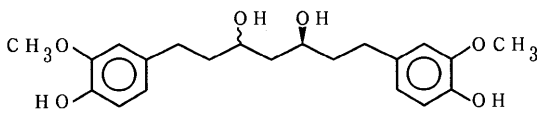

5a : 3*R*
5b : 3*S*

Chart 1

Compound **1** was obtained as an oil, and gave a molecular ion peak in the high-resolution mass spectrum (HRMS) at *m/z* 356.1578, which indicated the molecular formula of $C_{21}H_{24}O_5$. On the basis of the spectral and physical data, compound **1** was identified as gingerenone A [1,7-bis(4-hydroxy-3-methoxyphenyl)hept-4-en-3-one], which has recently been isolated from the same source.[4b]

Compound **2** was colorless needles, mp 87 °C, and identified as hexahydrocurcumin [5-hydroxy-1,7-bis(4-hydroxy-3-methoxyphenyl)heptan-3-one]. It is known that authentic hexahydrocurcumin has the specific rotation of +9.0° and the stereochemistry at the 5-position is of S configuration.[3b,4a] The specific rotation of this compound was +6.0°, so the configuration at the 5-position of **2** must be *S*.

Compound **3a** was obtained as an oil and gave a molecular ion peak in the HRMS at *m/z* 460.2091, which indicated the molecular formula of $C_{25}H_{32}O_8$. The infrared (IR) spectrum showed the presence of a hydroxyl group at 3420 cm^{-1} and an ester at 1720 cm^{-1}. In the proton nuclear magnetic resonance (^{1}H-NMR) spectrum, the signal at δ 2.01 (6H, s) showed the presence of two acetyl groups. This fact was supported by the mass fragments of *m/z* 400 and 340 in the mass spectrum (MS), the former being yielded by deacetoxylation from the molecular ion of *m/z* 460 and the latter from the ion of *m/z* 400. A set of a two proton double triplet at δ 2.50 (J=7.9, 14.0 Hz) and 2.56 (J=7.9, 14.0 Hz) was attributed to the geminal protons of the benzylic methylene (H-1, 7), which were coupled with two methylene protons at C-2 and 6, observed as an apparent quartet at δ 1.84 (4H, J=7.9 Hz). When the signal at δ 1.84 (H-2, 6) was irradiated, the apparent quintet at δ 4.94 (2H, J=6.1 Hz) assignable to acetoxymethine protons, changed into a double doublet (J=6.1, 7.3 Hz), which coupled with geminal methylene protons at δ 1.75 (1H, dt, J=6.1, 14.0 Hz), and 1.95 (1H, dt, J=7.3, 14.0 Hz). Furthermore, when the signal at δ 4.94 was irradiated, the quartet at δ 1.84 was collapsed into a triplet (J=7.9 Hz), and the double triplets at δ 1.75 and 1.95 into two doublets with a coupling constant of 14.0 Hz each. This fact indicated that both C-3 and 5 are substituted by acetoxyl groups. Six aromatic protons [δ 6.63 (2H, br d, J=7.9 Hz), 6.65 (2H, br s), 6.81 (2H, d, J=7.9 Hz)] accompanied by two arylic methoxyl ones [δ 3.87 (6H, s)] in the ^{1}H-NMR and six

TABLE I. ^{13}C-NMR Spectral Data for Compounds **3a**—**5b**

Carbon No.	3a	3b	4a	4b	5a	5b
1	31.25	31.60	31.79	32.25	31.98	32.40
2	35.99	35.67	36.02[a)]	35.65[c)]	41.13	41.02
3	70.73	70.65	70.63[b)]	70.64	71.66	68.40
4	38.51	38.69	38.59	38.73	44.37	44.88
5	70.73	70.65	70.68[b)]	70.64	71.66	68.40
6	35.99	35.67	35.97[a)]	35.68[c)]	41.13	41.02
7	31.25	31.60	31.25	31.61	31.98	32.40
1′	133.12	140.20	132.99	139.72	134.74	134.86
2′	114.29	112.61	105.04	105.01	112.82	112.86
3′	146.43	150.90	147.00	151.99	148.12	148.12
4′	143.86	137.97	132.27	120.35	145.39	145.39
5′	110.98	122.60	147.00	151.99	115.78	115.58
6′	120.89	120.39	105.04	105.01	121.47	121.50
1″	133.12	140.20	133.11	140.18	134.74	134.86
2″	114.29	112.61	114.29	112.61	112.82	112.86
3″	146.43	150.90	146.45	150.90	148.12	148.12
4″	143.86	137.97	143.86	137.97	145.39	145.39
5″	110.98	122.60	110.98	122.60	115.78	115.58
6″	120.89	120.39	120.87	120.39	121.47	121.50
3′OMe	55.90	55.87	56.29	56.13	56.16	56.19
5′OMe			56.29	56.13		
3″OMe	55.90	55.87	55.90	55.87	56.16	56.19
3,5OAc	170.64	170.69	170.64	170.70		
	21.16	21.15	21.14	21.13		
4′OAc		169.20		168.90		
		20.68		20.47		
4″OAc		169.20		169.20		
		20.68		20.68		

a—*c*) Assignments interchangeable. The measurements were made in $CDCl_3$ (**3a**, **3b**, **4a** and **4b**) and acetone-d_6 (**5a** and **5b**) with TMS as internal standard.

TABLE II. ^{1}H-NMR Spectral Data for Compounds **3a**—**5b**

Proton No.	3a	3b	4a	4b	5a	5b
H-1a	2.50 dt	2.56 dt	2.49 dt	2.50—2.60 m	2.57 dt	2.57 ddd
H-1b	2.56 dt	2.62 dt	2.57 dt	2.61 dt	2.68 dt	2.69 ddd
H-2	1.84 q	1.88 q	1.84 q	1.88 q	1.71 q	1.72 m
H-3	4.94 quint	4.97 quint	4.94 quint	4.97 quint	3.78—3.84 m	3.90 m
H-4a	1.75 dt	1.76 dt	1.75 dt	1.76 dt	1.52 dt	1.58 t
H-4b	1.95 dt	1.97 dt	1.95 dt	1.97 dt	1.65 dt	1.58 t
H-5	4.94 quint	4.97 quint	4.94 quint	4.97 quint	3.78—3.84 m	3.90 m
H-6	1.84 q	1.88 q	1.84 q	1.88 q	1.71 q	1.72 m
H-7a	2.50 dt	2.56 dt	2.50 dt	2.50—2.60 m	2.57 dt	2.57 ddd
H-7b	2.56 dt	2.62 dt	2.57 dt	2.61 dt	2.68 dt	2.70 ddd
H-2′	6.65 br s	6.76 d	6.37 s	6.40 s	6.81 d	6.81 d
H-5′	6.81 d	6.92 d			6.72 d	6.72 d
H-6′	6.63 br d	6.72 dd	6.37 s	6.40 s	6.64 dd	6.64 dd
H-2″	6.65 br s	6.76 d	6.64 br s	6.76 d	6.81 d	6.81 d
H-5″	6.81 d	6.92 d	6.81 d	6.92 d	6.72 d	6.72 d
H-6″	6.63 br d	6.72 dd	6.63 br d	6.72 dd	6.64 dd	6.64 dd
3′OMe	3.87 s	3.82 s	3.87 s	3.80 s	3.81 s	3.82 s
5′OMe			3.87 s	3.80 s		
3″OMe	3.87 s	3.82 s	3.87 s	3.82 s	3.81 s	3.82 s
3OAc	2.01 s	2.01 s	2.02 s[a)]	2.02 s[b)]		
5OAc	2.01 s	2.01 s	2.01 s[a)]	2.01 s[b)]		
4′OAc		2.30 s		2.32 s		
4″OAc		2.30 s		2.30 s		

a, *b*) Assignments interchangeable. The measurements were made in $CDCl_3$ (**3a**, **3b**, **4a** and **4b**) and acetone-d_6 (**5a** and **5b**) with TMS as internal standard. Multiplicities come from observed spectra (400 MHz). *J* (Hz) **3a**, **3b**, **4a**, **4b** and **5a**: 1a, 1b = 7a, 7b = 14.0; 1, 2 = 7, 6 = 7.9; 4a, 4b = 14.0. **5b**: 1a, 1b = 7a, 7b = 14.0; 1a, 2a = 7a, 6a = 6.7; 1a, 2b = 7a, 6b = 9.2; 1b, 2a = 7b, 6a = 6.1; 1b, 2b = 7b, 6b = 9.2. **3a**: 5′, 6′ = 5″, 6″ = 7.9. **3b**, **5a** and **5b**: 2′, 6′ = 2″, 6″ = 1.8; 5′, 6′ = 5″, 6″ = 7.9. **4a**: 5″, 6″ = 7.9. **4b**: 2″, 6″ = 1.8; 5″, 6″ = 7.9.

aromatic carbons (δ 133.12, 114.29, 146.43, 143.86, 110.98, 120.89) in the carbon-13 nuclear magnetic resonance (^{13}C-NMR) suggested the presence of two 4-hydroxy-3-methoxyphenyl groups, which was supported by the stable fragment ion at *m/z* 137 as a base peak in the MS. The ^{13}C-NMR spectrum revealed only thirteen peaks in spite of the molecular formula of $C_{25}H_{32}O_8$. This fact and a specific rotation of 0° suggested that this compound (**3a**) had a symmetrical skeleton and that the structure was 3,5-diacetoxy-1,7-bis(4-hydroxy-3-methoxyphenyl)heptane.

Acetylation of **3a** with acetic anhydride and pyridine introduced two more acetyl groups on the structure of **3a**, exhibiting a molecular ion peak at *m/z* 544. The IR spectrum of this compound (**3b**) showed a new absorption band of acetate at 1755 cm^{-1} with the disappearance of the hydroxyl peak at 3240 cm^{-1} in the spectrum of **3a**. The signal of two phenolic acetates was observed at δ 2.30 in the ^{1}H-NMR.

In order to determine the stereochemistry at C-3 and 5, compound **2** (5*S* configuration) was reduced with $NaBH_4$ to afford **5a** and **5b**, and separated by silica gel column chromatography. Compound **5a** was a colorless oil and showed the molecular ion peak at *m/z* 376 in the MS. The absorption band of a carbonyl group at 1702 cm^{-1} in the IR spectrum of **2** disappeared. The ^{13}C-NMR spectrum revealed a new signal of oxymethine carbon at δ 71.66 instead of that of the carbonyl one at δ 211.35 of **2**. The specific rotation ($[\alpha]_D^{25}$ 0°) together with the results of ^{13}C-NMR data[3c)] indicated that this compound was *meso* type, namely (3*R*,5*S*)-1,7-bis(4-hydroxy-3-methoxyphenyl)-heptan-3,5-diol. Compound **5b** was obtained as colorless needles, mp 136 °C. A comparison of **5b** with **5a** in the ^{13}C-NMR spectrum showed upfield shifts of C-2, 6 (0.1 ppm) and C-3, 5 (3.3 ppm), and downfield shifts of C-1, 7 (0.4 ppm) and C-4 (0.5 ppm).[3c,5)] The specific rotation ($[\alpha]_D^{25}$ −7.4°) confirmed the configuration of **5b** to be (3*S*, 5*S*). Alkaline hydrolysis of compound **3a** gave 3,5-dihydroxyl compound. The behavior of thin layer chromatography (TLC) and spectral data of this compound was identical with those of **5a**. Furthermore, the spectral data of **3b** was identical with those of acetyl derivative of compound **5a**. Thus, the structure of compound **3a** was concluded to be *meso*-3,5-diacetoxy-1,7-bis(4-hydroxy-3-methoxyphenyl)heptane.

Compound **4a** was obtained as an oil and gave a molecular ion peak at *m/z* 490.2202 in the HRMS, corresponding to the molecular formula of $C_{26}H_{34}O_9$. Spectral characteristics of this compound indicated that **4a** had a similar structure to **3a**. In the IR spectrum, absorption bands of a hydroxyl group and an ester were observed at 3480 and 1725 cm^{-1}, respectively. The presence of two acetyl groups was supported by the signals at *m/z* 430 and 370 in the MS, which were produced stepwise by deacetoxylation from the molecular ion (*m/z* 490). In the ^{1}H-NMR, the signal of a nine proton singlet at δ 3.87 showed the presence of three methoxyl groups, which suggested that compound **4a** was a methoxylated derivative of **3a**, considering that the molecular size of **4a** was 30 mass (OCH_2) larger than that of **3a**. Three aromatic protons [δ 6.63 (br d, *J* = 7.9 Hz), 6.64 (br s), 6.81 (d, *J* = 7.9 Hz)] and ^{13}C-NMR data suggested the presence of a 4-hydroxy-3-methoxyphenyl group. Other aromatic protons were observed at δ 6.37 as a two proton singlet. It is deduced from this fact that **4a** had a symmetrical tetrasubstituted benzene ring in place of the 1,3,4-trisubstituted one of **3a**. The typical mass fragment

ion peak at m/z 167 indicated the presence of dimethoxy-monohydroxyphenyl group. The substitution pattern of the aromatic ring was determined to be two methoxyl groups at C-3′ and 5′ and a hydroxyl one at C-4′, by the chemical shifts of ^{13}C-NMR data based on the results of calculations.

Acetylation of **4a** gave compound **4b** as a colorless oil. The IR spectrum showed a new absorption band of acetate at 1760 cm^{-1}, with disappearance of the hydroxyl peak at 3420 cm^{-1} in the spectrum of **4a**. The signals of two phenolic acetates were observed at δ 2.30 and 2.32. Other spectral data (^{1}H-NMR, ^{13}C-NMR) supported the structure of compound **4b**.

On the basis of all the above data, **4a** was concluded to be 3,5-diacetoxy-1-(4-hydroxy-3,5-dimethoxyphenyl)-7-(4-hydroxy-3-methoxyphenyl)heptane. The absolute configuration of the acetoxy groups is now under investigation.

Experimental

Melting points were taken on a Yanagimoto micro melting point apparatus and are uncorrected. Ultraviolet (UV) absorption spectra were determined on a Hitachi 220 spectrophotometer and IR spectra were recorded with a Perkin Elmer 1720X. ^{1}H-NMR (400 MHz) and ^{13}C-NMR (100 MHz) spectra were run on a JEOL GX-400 using tetramethylsilane (TMS) as an internal standard. MS were obtained on a Hitachi M-2000. Optical rotation was measured with a Union PM-101. Column chromatographies were performed using Merck silica gel 60 (70—230 mesh) and Pharmacia Sephadex LH-20, and TLC was done using silica gel GF-254.

Extraction and Isolation Dried ground rhizomes of ginger (955 g) from China were extracted five times with dichloromethane (CH_2Cl_2, 2 l each) at room temperature. The combined CH_2Cl_2 extract was concentrated on a rotary evaporator to yield a brown viscous residue (62.8 g). This extract was steam-distilled to give the non-volatile fraction (29.5 g), which was subjected to chromatography on a silica gel column eluted stepwise with benzene–acetone to give eleven fractions. The sixth and seventh fractions eluted with benzene–acetone (97 : 3) were rechromatographed on a Sephadex LH-20 column using isopropyl alcohol as an eluent to separate six fractions, the fifth of which was purified by column chromatography on silica gel using *n*-hexane–acetone (4 : 1) as an eluent to give compound **1** (130 mg). The eighth fraction eluted with benzene–acetone (97 : 3) was subjected to column chromatography on silica gel eluted with *n*-hexane–acetone (2 : 1) to separate six fractions. The fourth fraction was rechromatographed on a silica gel column with *n*-hexane–acetone (2 : 1) as an eluent to give compound **3a** (39 mg) and **4a** (29 mg). The fifth fraction was purified by column chromatography on silica gel using benzene–methanol (95 : 5) as an eluent to afford compound **2** (24 mg).

Compound **1** (Gingerenone A): MS m/z (%): 356 (M^+, 25), 205 (5), 179 (3), 151 (5), 137 (100). HRMS m/z: 356.1578 (M^+, Calcd for $C_{21}H_{24}O_5$: 356.1621). UV λ_{max}^{EtOH} nm (log ε): 230.0 (4.27), 281.5 (3.85). IR ν_{max}^{film} cm^{-1}: 3435, 1696, 1615, 1516, 1034, 975. ^{1}H-NMR ($CDCl_3$) δ: 2.49 (2H, q, J=7.3 Hz, H-6), 2.70 (2H, t, J=7.3 Hz, H-7), 2.83 (4H, m, H-1, 2), 3.858 (3H, s, OCH_3), 3.864 (3H, s, OCH_3), 5.50 (1H, s, OH), 5.51 (1H, s, OH), 6.10 (1H, d, J=16.1 Hz, H-4), 6.65 (1H, br s, H-2′ or 2″), 6.69 (1H, br s, H-2′ or 2″), 6.65—6.70 (2H, m, H-6′, 6″), 6.82 (1H, d, J=7.8 Hz, H-5′ or 5″), 6.83 (1H, d, J=8.5 Hz, H-5′ or 5″). ^{13}C-NMR ($CDCl_3$) δ: 29.87, 34.16, 34.44, 42.13, 55.91, 110.95, 111.15, 114.34, 114.38, 120.83, 120.93, 130.74, 132.61, 133.19, 143.95, 144.05, 146.37, 146.43, 146.60, 199.60.

Compound **2** (Hexahydrocurcumin): mp 87 °C (benzene). $[\alpha]_D^{20}$: +6.0° (c=1.68, $CHCl_3$). MS m/z (%): 374 (M^+, 3), 356 (5), 194 (27), 180 (21), 151 (10), 137 (100). HRMS m/z: 374.1763 (M^+, Calcd for $C_{21}H_{26}O_6$: 374.1728). UV λ_{max}^{EtOH} nm (log ε): 227.0 (4.36), 281.0 (4.05). IR ν_{max}^{film} cm^{-1}: 3435, 1702, 1603, 1516, 1033. ^{1}H-NMR ($CDCl_3$) δ: 1.63 (1H, dddd, J=4.3, 6.7, 10.1, 14.0 Hz, H-6), 1.77 (1H, dddd, J=5.5, 9.2, 9.2, 14.0 Hz, H-6), 2.51 (1H, dd, J=7.9, 17.4 Hz, H-4), 2.57 (1H, dd, J=3.1, 17.4 Hz, H-4), 2.59 (1H, ddd, J=6.7, 9.2, 12.9 Hz, H-7), 2.71 (2H, t, J=7.3 Hz, H-2), 2.72 (1H, ddd, J=5.5, 10.1, 12.9 Hz, H-7), 2.82 (2H, t, J=7.3 Hz, H-1), 3.85 (3H, s, OCH_3), 3.86 (3H, s, OCH_3), 4.03 (1H, dddd, J=3.1, 4.3, 7.9, 9.2 Hz, H-5), 5.53 (1H, s, OH), 5.55 (1H, s, OH), 6.64 (1H, dd, J=1.8, 7.9 Hz, H-6′ or 6″), 6.66 (1H, d, J=1.8 Hz, H-2′ or 2″), 6.67 (1H, dd, J=1.8, 7.9 Hz, H-6′ or 6″), 6.70 (1H, d, J=1.8 Hz, H-2′ or 2″), 6.81 (2H, d, J=7.9 Hz, H-5′, 5″). ^{13}C-NMR ($CDCl_3$) δ: 29.27, 31.40, 38.34, 45.39, 49.35, 55.88, 66.92, 111.01, 111.12, 114.29, 114.44, 120.74, 120.92, 132.55, 133.69, 143.76, 144.02, 146.45, 146.49, 211.35.

Compound **3a**: $[\alpha]_D^{20}$: 0° (c=0.95, $CHCl_3$). MS m/z (%): 460 (M^+, 22), 400 (4), 340 (3), 204 (8), 190 (25), 175 (11), 163 (14), 150 (11), 137 (100). HRMS m/z: 460.2091 (M^+, Calcd for $C_{25}H_{32}O_8$: 460.2094). UV λ_{max}^{EtOH} nm (log ε): 227.5 (sh, 3.72), 281.0 (3.40). IR ν_{max}^{film} cm^1: 3420, 1720, 1600, 1025.

Acetyl Derivative of **3a**: To a solution of 6 mg of compound **3a** in pyridine (0.5 ml), acetic anhydride (0.5 ml) was added, and the mixture was allowed to stand overnight at room temperature. The reaction mixture was poured into cold 2 N HCl and then extracted with CH_2Cl_2. The organic layer was washed with water, dried over anhydrous $CaCl_2$ and evaporated to dryness. The crude product was purified by column chromatography on silica gel using *n*-hexane–acetone (2 : 1) as an eluent to give a colorless oil (**3b**). MS m/z (%): 544 (M^+, 2), 502 (31), 484 (1), 460 (11), 442 (12), 400 (13), 340 (15), 204 (10), 190 (26), 175 (8), 163 (12), 150 (11), 137 (100). IR ν_{max}^{film} cm^{-1}: 1763, 1735, 1605, 1509.

Compound **4a**: $[\alpha]_D^{20}$: −1.4° (c=0.72, $CHCl_3$), MS m/z (%): 490 (M^+, 34), 430 (3), 370 (3), 234 (5), 220 (11), 205 (2), 204 (7), 193 (14), 190 (11), 180 (7), 175 (7), 167 (53), 163 (21), 150 (13), 137 (100), HRMS m/z: 490.2202 (M^+, Calcd for $C_{26}H_{34}O_9$: 490.2201). UV λ_{max}^{EtOH} nm (log ε): 230.0 (sh, 4.05), 280.0 (3.56). IR ν_{max}^{film} cm^{-1}: 3480, 1725, 1600, 1030.

Acetyl Derivative of **4a**: Acetylation of **4a** (6 mg) was carried out as described above. Compound **4b**: IR ν_{max}^{film} cm^{-1}: 1763, 1734, 1604, 1510.

Hydrogenation of **2**: To a solution of compound **2** (16.8 mg) in EtOH (5 ml), 3.5 mg of $NaBH_4$ was added at room temperature, and the mixture was allowed to stand for 1 h. After removing the solvent *in vacuo*, the reaction mixture was poured into cold 0.2 N HCl, and then extracted with CH_2Cl_2. The organic layer was washed with water, dried over anhydrous $CaCl_2$ and concentrated. The product was chromatographed on a silica gel column with CH_2Cl_2–methanol (97 : 3) as an eluent to give compounds **5a** and **5b**. Compound **5a**: $[\alpha]_D^{25}$: 0° (c=0.68, EtOH). MS m/z (%): 376 (M^+, 13), 358 (9), 340 (1), 190 (9), 163 (6), 151 (6), 150 (13), 138 (36), 137 (100). HRMS m/z: 376.1875 (M^+, Calcd for $C_{21}H_{28}O_6$: 376.1884). UV λ_{max}^{EtOH} nm (log ε): 227.5 (3.81), 281.0 (3.48). IR ν_{max}^{film} cm^{-1}: 3391, 1603, 1516, 1034. Compound **5b**: mp 136 °C (benzene–chloroform). $[\alpha]_D^{25}$: −7.4° (c=0.27, EtOH). MS m/z (%): 376 (M^+, 17), 358 (12), 340 (1), 190 (9), 163 (7), 151 (10), 150 (7), 138 (37), 137 (100). HRMS m/z: 376.1871 (M^+, Calcd for $C_{21}H_{28}O_6$: 376.1884). IR ν_{max}^{film} cm^{-1}: 3368, 1602, 1516, 1033.

Acetyl Derivative of Compound **5a**: Spectral data from MS, IR, ^{1}H- and ^{13}C-NMR of this compound were identical in all respects with those of compound **3b**.

Alkaline Hydrolysis of Compound **3a**: Compound **3a** (6.6 mg) was dissolved in 0.5 ml of 2% methanolic KOH, and the mixture was left overnight at room temperature. After removing the solvent *in vacuo*, the reaction mixture was poured into cold 0.1 N HCl, and subsequently extracted with CH_2Cl_2. The organic layer was washed with water, dried over anhydrous $CaCl_2$ and evaporated to dryness (5.3 mg). The residue was chromatographed on a silica gel column with a mixture of CH_2Cl_2–methanol as an eluent to give a colorless oil. Spectral data from MS, IR, ^{1}H- and ^{13}C-NMR of this compound was identical in all respects with those of compound **5a**.

References

1) M. Miyazawa and H. Kameoka, *Agric. Biol. Chem.*, **52**, 2961 (1988).
2) D. W. Connell and M. D. Sutherland, *Aus. J. Chem.*, **2**, 1033 (1969); A. Lapworth and F. N. Wykes, *J. Chromatogr. Sci.*, **111**, 790 (1917); L. K. Peason and R. A. Royle, *Pharm. J.*, **103**, 78 (1919); D. J. Harvey, *J. Chromatogr.*, **212**, 75 (1981).
3) *a*) M. Kuroyanagi, T. Noro, S. Fukushima, R. Aiyama, A. Ikuta, H. Itokawa and M. Morita, *Chem. Pharm. Bull.*, **31**, 1544 (1983); *b*) H. Itokawa, H. Morita, I. Midorikawa, R. Aiyama and M. Morita, *ibid.*, **33**, 4889 (1985); *c*) S. Uehara, I. Yasuda, K. Akiyama, H. Morita, K. Takeya and H. Itokawa, *ibid.*, **35**, 3298 (1987).
4) *a*) T. Murata, M. Shinohara and M. Miyamoto, *Chem. Pharm. Bull.*, **20**, 2291 (1972); *b*) K. Endo, E. Kanno and Y. Oshima, *Phytochemistry*, **29**, 797 (1990).
5) T. Hashimoto, M. Tori and Y. Asakawa, *Chem. Pharm. Bull.*, **34**, 1846 (1986).

Determination of Gallopamil in Human Plasma by Selected Ion Monitoring

Jun KOKATSU,* Shigeji JINGU, and Toshio SUWA

Research Laboratory, Taisho Pharmaceutical Co., Ltd., 1–403, Yoshino-cho, Omiya, Saitama 330, Japan. *Received May 22, 1990*

A gas chromatographic mass spectrometric procedure using selected ion monitoring is described for the quantification of gallopamil in human plasma. Gas chromatographic separation of gallopamil from phenolic metabolite isomers is made possible by treatment with ethyl chloroformate. The detection limit for the quantitation by the present method is 0.09 ng/ml of plasma. The method has sufficient sensitivity to permit pharmacokinetic studies with human subjects following the oral administration of gallopamil hydrochloride.

Keywords gallopamil; gas chromatography-selected ion monitoring; extraction–derivatization; oral administration; human plasma

Gallopamil, DL-5-[(3,4-dimethoxyphenylethyl)methylamino]-2-isopropyl-2-(3,4,5-trimethoxyphenyl)valeronitrile (a) (Chart 1), is a calcium channel antagonist, about three to five times more potent than verapamil in its cardiovascular parameters.[1)]

High-performance liquid chromatographic methods were reported for the determination of gallopamil in biological fluids with detection limits of 0.2[2)] and 0.9 ng/ml.[3)] With these methods, it should thus be possible to clarify the pharmacokinetics at a dose of 50 mg in humans. However, a more sensitive means is necessary to determine the pharmacokinetics of gallopamil even at the low dosage of 12.5 mg which might be the lowest clinical dosage for Japanese. This paper describes a selective and sensitive gas chromatographic mass spectrometry selected ion monitoring (GC/MS-SIM) method for the analysis of gallopamil in human plasma. The sample preparation involves extraction-derivatization with ethyl chloroformate and purification by a Sep-pak silica cartridge.

Experimental

Materials and Reagents Gallopamil (a), DL-2-isopropyl-2-(3,4,5-trimethoxyphenyl)-5-[(3,4,5-trimethoxyphenylethyl)methylamino]valeronitrile (b), used as an internal standard (I.S.), DL-5-[(4-hydroxy-3-methoxyphenylethyl)methylamino]-2-isopropyl-2-(3,4,5-trimethoxyphenyl)valeronitrile (c), and DL-5-[(3-hydroxy-4-methoxyphenylethyl)methylamino]-2-isopropyl-2-(3,4,5-trimethoxyphenyl)valeronitrile (d) were kindly supplied by Knoll AG (Ludwigs-hafen, G.F.R.). All these compounds were characterized by GC/MS. Ethyl chloroformate was purchased from Tokyo Kasei Kogyo (Tokyo, Japan). The Sep-pak silica cartridge was obtained from Waters Assoc., (Milford, MA, U.S.A.). All other reagents and solvents were of the highest quality available.

Instrumentation A JEOL JMS-DX303 GC/MS instrument equipped with a JMA-DA5000 data processing system was used to determine gallopamil in human plasma. The GC column was a cross-linked methylsilicone fused silica DB-1 megabore column (15 m × 0.53 mm i.d.; coating thickness 1.5 μm, J&W Scientific Inc.). The GC oven temperature was 270 °C. The mass spectrometer was operated at an ionization energy of 70 eV with an emission current of 300 μA in the electron impact (EI) mode. The interfacial region between the chromatograph and mass spectrometer was maintained at 270 °C. Quantitation was performed by selected ion monitoring, focusing on the common fragment ion at *m/z* 333 for gallopamil and I.S. Mass spectra were measured with a Shimadzu QP-1000 mass spectrometer by EI and chemical ionization (CI) with isobutane as the reagent gas at a pressure of 4×10^{-5} Torr. The ionization energy and trap current were 200 eV and 150 μA, respectively.

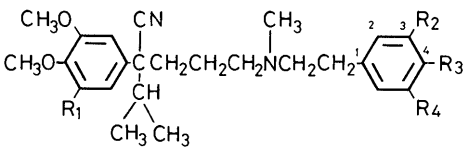

gallopamil	(a):	$R_1=R_2=R_3=OCH_3$, $R_4=H$
internal standard	(b):	$R_1=R_2=R_3=R_4=OCH_3$
metabolite	(c):	$R_1=R_2=OCH_3$, $R_3=OH$, $R_4=H$
metabolite	(d):	$R_1=R_3=OCH_3$, $R_2=OH$, $R_4=H$
verapamil	:	$R_1=R_4=H$, $R_2=R_3=OCH_3$

Chart 1

Extraction and Derivatization To 1.0 ml of plasma in a round bottom test tube were added 2.5 ng of a methanolic solution of I.S. and 150 μl of a hydrochloric solution (4 N) along with 5 ml of chloroform, and the mixture was then shaken for 15 min at room temperature. After centrifugation at 4000 rpm for 10 min at 18 °C, the lower layer was transferred to another identical tube. The extract was vigorously shaken with 450 μl of ethyl chloroformate and 1 ml of sodium hydroxide (1 N) for 15 min at room temperature. After centrifugation at 4000 rpm for 10 min at 18 °C, the whole of the chloroform extracts was applied onto the Sep-pak silica cartridge column. After being rinsed with 4 ml of chloroform followed by 4 ml of chloroform–methanol (99 : 1), the cartridge was eluted with 4 ml of chloroform–methanol (4 : 1). The solvent was evaporated at 40 °C using a centrifugal evaporator (Yamato Kagaku Co., Tokyo). To completely remove trace amounts of ethyl chloroformate, the tube was evaporated to dryness under a stream of nitrogen. The dried residue was dissolved in 15 μl of methanol and 1 μl of this solution was subjected to GC/MS.

Calibration Curve The calibration curve for the determination of gallopamil by GC/MS-SIM was obtained by plotting the ratio of the peak area of gallopamil to that of I.S. (2.5 ng/ml of plasma) against concentration. Standard solutions containing 0.09, 0.19, 0.47, 2.35, 7.04 and 14.08 ng/ml of plasma were prepared.

Results and Discussion

GC/MS Conditions Since gallopamil has the same mass spectrometric properties as verapamil[4)] due to its methoxy analogue structure, the EI mass spectrum of gallopamil showed only one major fragment at *m/z* 333 (Fig. 1), formed by loss of the dimethoxybenzyl moiety. The situation was the same with the similarly structured I.S., having the same extraction and chromatographic characteristics as gallopamil: it showed a very dominant fragment at *m/z* 333 due to the loss of the trimethoxybenzyl moiety. The common fragment ion at *m/z* 333 for gallopamil and I.S. was used for mass chromatography and SIM analysis.

Gallopamil is extensively metabolized in the liver to produce a secondary amine as the main metabolite by N-dealkylation. However, the drug is also susceptible to O-demethylation, yielding the corresponding phenolic metabolite isomers.[1)] Figure 2A shows a typical mass chromatographic separation of gallopamil and two kinds of O-demethylated metabolites without derivatization reaction. Monitoring the characteristic ion of *m/z* 333, it is evident that these phenolic metabolites interfered with the measurement of the unchanged drug. Since the metabolites

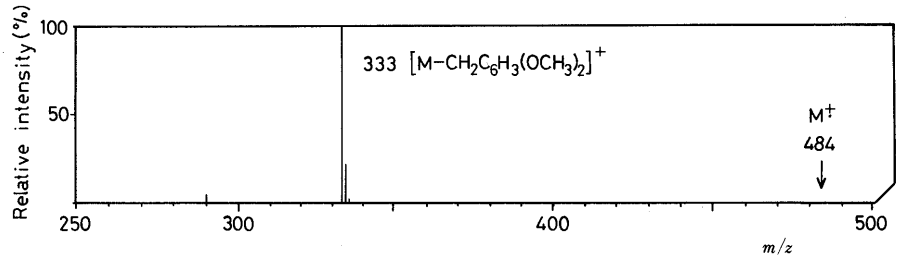

Fig. 1. Mass Spectra of Gallopamil

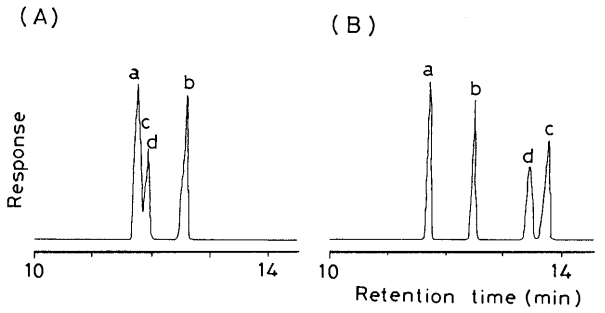

Fig. 2. Mass Chromatograms of (A) Untreated and (B) Treated Standard Mixture with Ethyl Chloroformate

Peaks: a, gallopamil; b, internal standard; c, 4-demethylated metabolite; d, 3-demethylated metabolite.

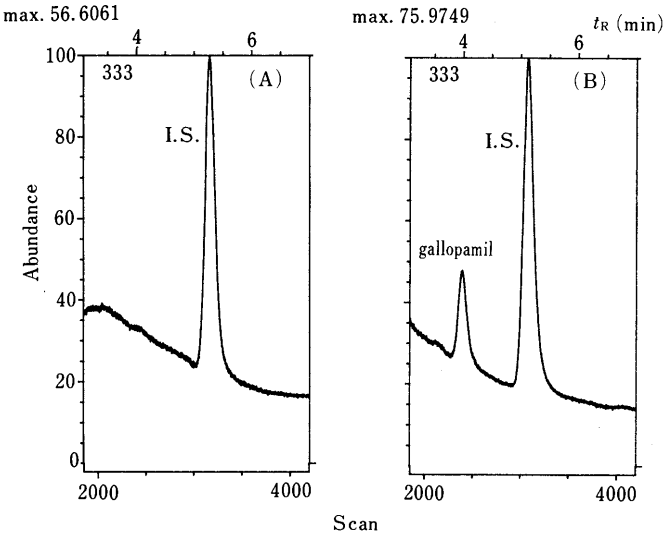

Fig. 3. Selected-Ion Recordings of (A) Blank Human Plasma and (B) Human Plasma Spiked with 0.5 ng/ml of Gallopamil Base and 2.5 ng/ml of Internal Standard

TABLE I. Precision and Accuracy of the Present Method for the Determining Gallopamil in Samples of Spiked Plasma

Concentration added (ng/ml)	Concentration found (mean ± S.D.) (ng/ml, $n=5$)	Coefficient variation (%)	Accuracy (%)
0.09	0.098 ± 0.004	3.6	108.9
0.19	0.189 ± 0.002	1.0	99.5
0.47	0.468 ± 0.013	2.8	99.6
2.35	2.333 ± 0.031	1.3	99.3
7.04	7.071 ± 0.217	3.1	100.4
14.08	14.087 ± 0.163	1.2	100.0

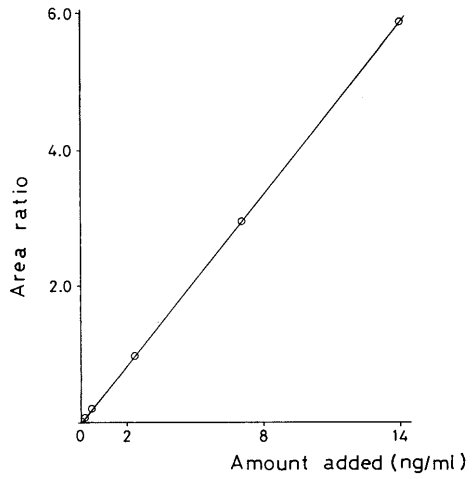

Fig. 4. Calibration Curve for the Determination of Gallopamil Base in Plasma

$r=0.9998$.

have been reported present as minor metabolites in subjects dosed with gallopamil,[5] we separated gallopamil from them by selective derivatization of the phenolic hydroxy function. However, ordinary derivatization methods such as acetylation, trifluoroacetylation and silylation were found unsuitable for the determination of gallopamil, due either to inadequate reactivity or instability of the products. The selective conversion of phenolic metabolites to O-carbamates was carried out according to the method of Makita *et al.*[6,7] with a minor modification; this was reported as an alternative method for analyzing simple phenols and phenolic acids as their O-isobutylcarbonyl derivatives. As shown in Fig. 2B, use of this O-ethoxycarbamate conversion reaction made it possible to completely separate the unchanged drug from the interfering phenolic metabolites, without decreasing the peak area of gallopamil. The formation of these O-carbamate derivatives was confirmed by the presence of quasi-molecular ions at m/z 543 in CI mass spectrometry and the characteristic ion at m/z 333 in EI mass spectrometry (data not shown).

Plasma Determination The purification of a plasma sample has been achieved by a combination of the extraction from human plasma at acidic pH using chloroform[8] and purification with the Sep-pak silica cartridge following extraction–derivatization using ethyl chloroformate. These procedures make it possible to maintain chromatographic efficiency and eliminate any side-reactions with remaining ethyl chloroformate,[9] so that continuous analysis of plasma samples could be conducted at 15 min intervals. Figure 3 shows typical GC/MS selected-ion recordings (SIR) obtained from extracted blank plasma and a spiked plasma

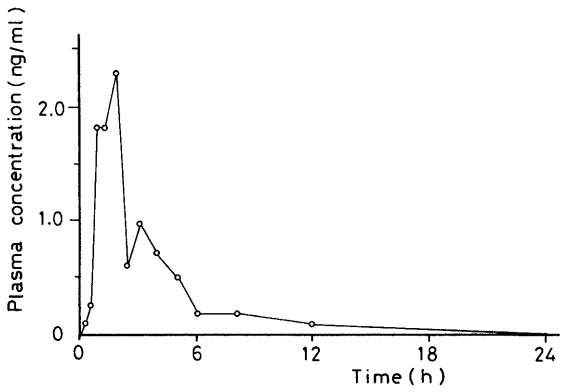

Fig. 5. Plasma Concentration of Gallopamil *versus* Time in One Subject after the Oral Administration of Gallopamil Hydrochloride at a Dose of 12.5 mg

standard. Although the baseline in the SIR is relatively high, the peak intensities were sufficient to determine gallopamil, since the drug-free control plasma gave no interfering peaks. The retention times for gallopamil and I.S. were approximately 4.0 and 5.2 min, respectively.

The detection limit was approximately 0.05 ng (as free base)/ml of plasma and the calibration curve was obtained by spiking a sample of plasma with a gallopamil range of over 0.09 to 14.08 ng per ml. As shown in Fig. 4 and Table I, the calibration curve was linear with correlation coefficients of 0.9998 ($n=6$), and coefficients of variation ($n=5$) of 2.2% on average.

Monitoring of Plasma Concentration It was possible to determine gallopamil at a level as low as 0.09 ng/ml of plasma by the above method without interference from the metabolites. The applicability of this method was confirmed by determination of plasma concentration following the oral administration of 12.5 mg of gallopamil hydrochloride to healthy subjects. A representative plasma concentration level is shown in Fig. 5. At 12 h, the level of gallopamil was 0.1 ng/ml. The sensitivity of this technique is sufficiently high to permit pharmacokinetic studies on man.

Conclusions

The chromatographic separation of gallopamil from phenolic metabolites was effected through the formation of O-ethoxycarbamate using GC/MS-SIM, without any interference. The results of determinations of plasma concentration following the oral administration of the drug at a dose as low as 12.5 mg confirms the usefulness of this method for human subjects.

References

1) B. Stieren, V. Bühler, H. G. Hege, M. Hollmann, H. Neuss, M. Schlepper, and J. Weymann, "Gallopamil, Pharmacological and Clinical Profile of a Calcium Antagonist," M. Kaltenbach and R. Hopf (ed.), Springer-Verlag, New York, 1984, pp. 88—93.
2) M. Nieder and H. Jaeger, *J. Chromatogr.*, **414**, 492 (1987).
3) A. M. McLean, E. B. Atkinson, K. Rein, D. A. Ruggirello, M. A. Gonzalez, and P. K. Noonan, *Pharmaceut. Res.*, **4**, 327 (1987).
4) B. Spiegelhalder and M. Eichelbaum, *Arzneim.-Forsch./Drug Res.*, **27**, 94 (1977).
5) J. Weymann, V. Bühler, H. G. Hege, H. Müller-Pelfzer, G. Schenk, B. Stieren, and M. Hollmann, *Arzneim.-Forsch./Drug Res.*, **39**, 605 (1987).
6) M. Makita, S. Yamashita, A. Katoh, and Y. Takashita, *J. Chromatogr.*, **147**, 456 (1978).
7) M. Makita, S. Yamamoto, and Y. Takashita, *Yakugaku Zasshi*, **98**, 56 (1978).
8) L. T. F. Chan, L. H. Chhuy, and R. J. Crowley, *J. Chromatogr.*, **402**, 361 (1987).
9) D. R. Knapp, "Handbook of Analytical Derivatization Reactions," Wiley, New York, 1979, pp. 113—115.

Pre-column Fluorescence Derivatization High-Performance Liquid Chromatography of Opioid Peptides in Rat Brain and Its Use for Enzymatic Peptide Characterization

Guo-Qing ZHANG, Masaaki KAI, Mutsuko NAKANO and Yosuke OHKURA*

Faculty of Pharmaceutical Sciences, Kyushu University 62, Maidashi, Higashi-ku, Fukuoka 812, Japan. *Received July 9, 1990*

A high-performance liquid chromatographic method involving fluorescence derivatization followed by separation on a reversed-phase polymer (octadecylated polyvinylalcohol copolymer gel) column is described for the determination of opioid peptides in rat brain tissues. The peptides extracted from brain tissues were converted into fluorescent derivatives by reaction with hydroxylamine, cobalt(II) ion and borate. The derivatives were separated on an Asahipak ODP-50 column by gradient elution of acetonitrile in the mobile phase containing borate buffer (pH 9.5). The detection limits ($S/N=3$) for the peptides were 0.33—1.21 pmol per 100 μl injected. The method actually permit the determination of leucine enkephalin, methionine enkephalin, methionine enkephalin-Arg-Phe and methionine enkephalin-Arg-Gly-Leu in the tissues. The method is also applied to the characterization of the peptides in the tissues by means of enzymatic degradations with carboxypeptidase A and trypsin.

Keywords opioid peptide; brain tissue; pre-column fluorescence derivatization; high-performance liquid chromatography; octadecylated polyvinylalcohol copolymer gel column

Opioid peptides involving leucine enkephalin, (LE, Tyr–Gly–Gly–Phe–Leu) and methionine enkephalin (ME, Tyr–Gly–Gly–Phe–Met)[1] have been found to act *in vivo* as neurotransmitters *via* interaction with opiate receptors.[2] These peptides retain the sequence of either LE or ME,[3-5] which have a tyrosyl residue at the N-terminus in their molecules.

Many methods, such as bioassay,[6] radioimmunoassay (RIA),[7-9] enzyme-immunoassay,[10] radioreceptor-assay[11] and mass spectrometry,[12] either alone or in combination with high-performance liquid chromatography (HPLC), have been developed for the determination of the opioid peptides in biological samples. The bioassay, immunoassay and receptor-assay are not very selective.[13] The mass spectrometric method does not permit the simultaneous determination of opioid peptides, though the structural specificity of each peptide is sufficient.

Intact opioid peptides can be separated simultaneously by HPLC. However, spectrophotometric[14] and electrochemical[15] detections in HPLC are less selective for the opioid peptides. We previously developed a fluorescence derivatization reaction specific for N-terminal Tyr-containing peptides,[16] which uses hydroxylamine, cobalt(II) ion and borate reagents. This reaction provides a single fluorescent product for each of N-terminal Tyr-containing peptides. This reaction was utilized for a post-column fluorescence derivatization HPLC for the determination of several opioid peptides in rat brain.[17] The reaction was also applied to a pre-column fluorescence derivatization method of HPLC for N-terminal Tyr-containing peptides, where the fluorescent derivatives of the peptides were separated on an octadecylated silica gel column.[18] However, the method only allowed the assay of LE and ME in rat brain,[19] presumably due to an increased adsorption of the derivatives at the polar matrix in the support material of the column.

We have recently found that an octadecylated polyvinylalcohol copolymer gel column shows less adsorption of the fluorescent derivatives of the opioid peptides than the silica type of column and can afford an improved separation pattern. Thus, the column was subjected to the use in a pre-column fluorescence derivatization method for HPLC in the hope that endogenous opioid peptides other than LE and ME in rat brain tissues could be quantified. [D-Ala^2]LE–NH_2 was used as an internal standard for the quantification. The method was also utilized for the characterization of the peptides in the tissues by means of enzymatic degradations with carboxypeptidase A and trypsin.

Experimental

Chemicals and Solutions The following synthetic peptides were purchased from Sigma (St. Louis, MO, U.S.A.). The sequences and the abbreviations of named opioid peptides are shown in the parentheses: Tyr–Gly, Tyr–Gly–Gly, Tyr–Gly–Gly–Phe, LE, LE–NH_2, [D-Ala^2]LE–NH_2, LE–Arg, ME, ME–Arg, ME–Arg–Phe, ME–Arg–Gly–Leu, α-endorphin (α-EDP, ME–Thr–Ser–Glu–Lys–Ser–Gln–Thr–Pro–Leu–Val–Thr), γ-EDP (α-EDP–Leu), β-neoendorphin (β-NED, LE–Arg–Lys–Tyr–Pro), α-NED (β-NED–Lys), dynorphin 1-10 (DNP 1-10, LE–Arg–Arg–Ile–Arg–Pro), DNP 1-9, DNP 1-8, DNP 1-7 and DNP-B (LE–Arg–Arg–Gln–Phe–Lys–Val–Val–Thr). These peptides were dissolved in water. The solutions were stored at −80 °C and consumed within 3 weeks. Carboxypeptidase A (EC 3.4.17.1) and trypsin (EC 3.4.21.4) from bovine pancreas were purchased from Sigma. Water was deionized and then distilled before use. Other chemicals were of reagent grade.

Rat Brain Tissues Male Sprague–Dawley rats (220—280 g, 7 weeks) were anesthetized with diethyl ether and killed by dehematization. The tissues of striatum, hypothalamus, pituitary and cortex were obtained in the same manner as described previously.[19] The tissues were stored at −80 °C.

Peptide Extraction This was performed according to the previously reported solid-phase extraction method[17] with modifications. Each tissue (0.1—0.2 g) was homogenized at 0—4 °C with 3 ml of 0.1 M HCl. To the homogenate, 20 μl of 5.0 μM [D-Ala^2]LE–NH_2 as an internal standard and 20 μl of water (or synthetic peptide solution for calibration graphs) were added. The homogenate was deproteinized with 0.5 ml of 2 M $HClO_4$ and centrifuged at 2450*g* for 10 min. The supernatant was neutralized to pH 7—8 with 1 M $NaHCO_3$ (approximately 2 ml) and mixed with 2 ml of 50 mM ethylenediamine tetraacetic acid (EDTA)·2Na. The mixture was applied to a mini-cartridge packed with 0.2 g of Asahipregel T C18 (particle size, 9 μm; Asahi Chemical Ltd., Kawasaki, Japan). The cartridge was preconditioned with 2 ml of methanol, of 0.1 M borate buffer (pH 8.5) and of water. After loading the supernatant, the cartridge was washed by consecutive portions of 1 ml of water, 3 ml of 0.1 M HCl, 3 ml of water, 3 ml of 0.1 M borate buffer (pH 8.5) and 1 ml of water. A fraction containing the peptides was eluted with 1.5 ml of a mixture of methanol and 0.2 M borate buffer (pH 8.5) (4 : 1, v/v). After evaporation *in vacuo* at 30 °C, the residue was diluted with water to 300 μl and used for the subsequent fluorescence derivatization or enzymatic degradation reaction.

Fluorescence Derivatization This was performed as described previously with minor modifications.[17] To 60 μl of the sample solution were added 25 μl of a mixture of 10 mM $NH_2OH \cdot HCl$ and 0.5 mM $Co(II)(OAc)_2$, and

15 μl of water. The mixture was heated at 100 °C for 3 min and then added with 25 μl of 20 mM 2-mercaptoethanol (stabilizer of the derivatives). The reaction mixture was used for HPLC.

Enzymatic Degradation The sample solution (60 μl) was mixed with 150 mU of carboxypeptidase A or 1100 mU of trypsin in 50 mM phosphate buffer (pH 7.5). The mixture was incubated at 37 °C for 30 min and then subjected to the fluorescence derivatization.

Chromatograph and Its Operation Conditions The HPLC system consisted of Hitachi 655 chromatograph, a Rheodyne 7125 syringe-loading sample injector (100 μl loop), a Hitachi F-1100 fluorescence spectrophotometer (12 μl flow-cell) operating at 440 nm (emission wavelength) and 330 nm (excitation wavelength) and an Asahipak ODP-50 column (octadecylated polyvinylalcohol copolymer gel column; 150 × 6 mm i.d.; particle size, 5 μm, Asahi Chemical Ltd.). The column temperature was ambient (24 ± 4 °C). A gradient elution was performed by using two eluents that consisted of acetonitrile, 0.1 M borate buffer (pH 9.5) and water (1 : 10 : 39 and 5 : 2 : 3, v/v). The variation of acetonitrile concentration in the mobile phase is indicated in Fig. 1. The flow-rate of the mobile phase was 0.8 ml/min up to 25 min, thereafter 1.0 ml/min up to 55 min and again 0.8 ml/min.

Results and Discussion

Figure 1 shows a chromatogram obtained with a standard mixture of seventeen N-terminal Tyr-containing synthetic peptides including the opioid peptides. The derivatives of the peptides except for those of DNP 1-8 and β-NED (peaks coincided) were clearly separated on the reversed-phase polymer column. In addition, the synthetic peptides of Tyr–Gly, Tyr–Gly–Gly and ME-Arg were also derived. Their retention times were 3.2, 3.2 and 16.7 min, respectively, under the same HPLC conditions as for Fig. 1, though these peaks are not shown in Fig. 1. The detection limits ($S/N=3$) for the peptides were in the range 0.33—1.21 pmol on the column.

Figure 2 shows a chromatogram obtained with striatum tissue (approximately 40 mg) of rat brain according to the recommended procedure. The N-terminal Tyr-containing peptides were represented by shaded peaks. Other fluorescent peaks were also observed even if the derivation was omitted. Therefore, these peaks were caused by some fluorescent compounds present in the tissue. Similar chromatograms to Fig. 2 were obtained with other tissues of rat brain such as hypothalamus, pituitary and cortex.

The peptide derivatives fluoresce only in a borate buffer at pH 8—10[16,18]; the recommended mobile phase contains 0.1 M borate buffer of pH 9.5. The pH of the borate buffer in the mobile phase affected the retention times of the peaks. At pH 8.5, the synthetic peptide peaks were eluted slightly earlier than at pH 9.5 and are clearly separated. However, the peptide peaks of [D-Ala^2]LE–NH_2 and ME–Arg–Gly–Leu overlapped with some peaks of fluorescent substances in the biological sample eluted at retention times between 22 and 26 min in the chromatogram of Fig. 2.

The opioid peptide peaks in Fig. 2 were identified by chromatographic techniques based on retention time and co-chromatography with their synthetic peptides. For further characterization of the peptides, the enzymatic degradations utilizing carboxypeptidase A and trypsin were carried out for the tissue samples before the fluorescence derivatization. Carboxypeptidase A releases amino acid from the C-terminal end of peptides which do not contain Arg, Lys, Pro, Gly and amino acid amide residues. Trypsin

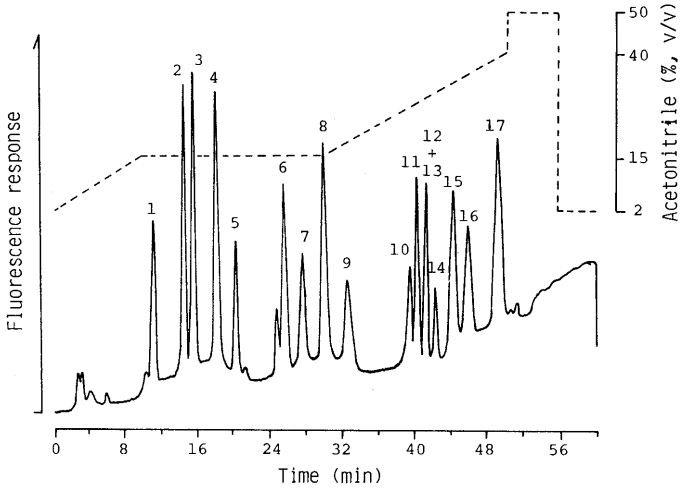

Fig. 1. Chromatogram of a Standard Mixture of Synthetic Seventeen N-Terminal Tyr-Containing Peptides

Peaks (amount injected): 1, Tyr–Gly–Gly–Phe (5 pmol); 2, ME (5 pmol); 3, LE (5 pmol); 4, LE–Arg (5 pmol); 5, α-EDP (10 pmol); 6, LE–NH_2 (10 pmol); 7, DNP 1-7 (10 pmol); 8, [D-Ala^2]LE–NH_2 (10 pmol); 9, ME–Arg–Gly–Leu (10 pmol); 10, γ-EDP (10 pmol); 11, ME–Arg–Phe (5 pmol); 12, DNP 1-8 (10 pmol); 13, β-NED (50 pmol); 14, α-NED (50 pmol); 15, DNP 1-9 (10 pmol); 16, DNP 1-10 (10 pmol); 17, DNP-B (50 pmol).

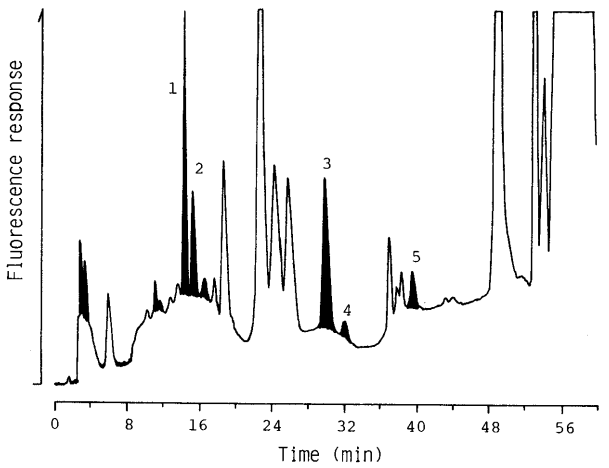

Fig. 2. Chromatogram of Striatum Tissue of Rat Brain

Shaded peaks were produced only by the fluorescence derivation. Peaks: 1, ME; 2, LE; 3, [D-Ala^2]LE–NH_2 (internal standard); 4, ME–Arg–Gly–Leu; 5, LE–Arg–Phe.

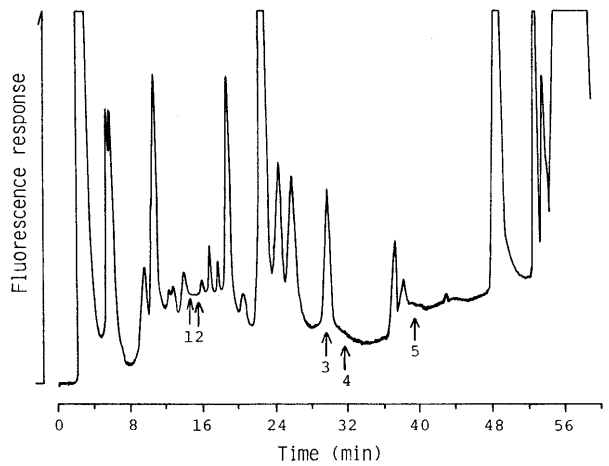

Fig. 3. Chromatogram of the Same Sample as for Fig. 2 after the Enzymatic Degradation with Carboxypeptidase A

Arrows 1—5 indicate the retention times of ME, LE, [D-Ala^2]LE–NH_2, ME–Arg–Gly–Leu and ME–Arg–Phe, respectively.

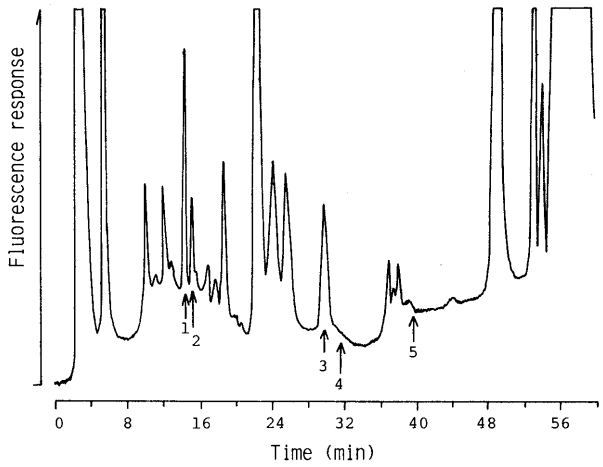

Fig. 4. Chromatogram of the Same Sample as for Fig. 2 after the Enzymatic Degradation with Trypsin

Arrows 1—5 indicate the retention times of ME, LE, [D-Ala^2]LE-NH_2, ME-Arg-Gly-Leu and ME-Arg—Phe, respectively.

mediates the hydrolysis of peptide bonds at the carboxyl sides of Arg and Lys.

As expected, the peaks corresponding to ME, LE, ME-Arg-Gly-Leu and ME-Arg-Phe disappeared, when the same sample of Fig. 2 was digested with carboxypeptidase A (Fig. 3). On the other hand, some increasing peaks were also observed. The peak at 3.2 min contains probably the peak due to Tyr-Gly-Gly, and the peak at 11.2 min was Tyr-Gly-Gly-Phe, because both peptide fragments were produced from ME and LE by the enzyme digestion. A small peak due to ME-Arg was also observed, because the fragment of ME-Arg was formed from ME-Arg-Phe.

After the degradation of the same sample with trypsin (Fig. 4), the ME-Arg-Gly-Leu and ME-Arg-Phe peaks disappeared, while the peaks due to ME, LE and [D-Ala^2]LE-NH_2 (internal standard) remained. Instead, the peak due to the fragment of ME-Arg produced from ME-Arg-Gly-Leu and ME-Arg-Phe was observed.

From these results, the shaded peaks (peaks 1, 2, 4 and 5 in Fig. 2) represent the endogenous peptides corresponding to ME, LE, ME-Arg-Gly-Leu and ME-Arg-Phe, respectively. The same results were obtained from the hypothalamus, pituitary and cortex samples. The other shaded peaks in Fig. 2 could not be characterized successfully.

The peptide extract from brain tissue was passed through a reversed phase mini-cartridge packed with AsahipregelT C18, which consists of the same material as used in the Asahipak ODP-50 column, otherwise marked interferences with biological substances were observed. Additionally the target peptides were concentrated in small volumes.

The recoveries of 100 pmol each of synthetic LE, ME, [D-Ala^2]LE-NH_2, γ-EDP, ME-Arg-Phe, ME-Arg-Gly-Leu, DNP 1-8 and DNP-B added to the homogenate of striatum, hypothalamus, pituitary or cortex were 41—45%, ($n=3$). The low recoveries for these peptides were mainly caused by the interference of other sample constituents with the derivatization reaction. Nevertheless, the constant ratio of the recovery of each peptide to that of the internal standard, [D-Ala^2]LE-NH_2 was obtained with each treatment.

Table I. Regional Concentrations of Opioid Peptides in Rat Brains

Tissue	Concentration[a] (pmol per g of tissue)			
	ME	LE	ME-Arg-Gly-Leu	ME-Arg-Phe
Striatum	541	161	118	128
Hypothalamus	350	100	85	86
Pituitary	185	114	ND[b]	159
Cortex	63	22	34	33

a) The average value of triplicate determinations. *b*) Could not be determined successfully, because of an interfering peak.

The ratio of the peak height of each of ME, LE, ME-Arg-Phe and ME-Arg-Gly-Leu to that of the internal standard added to the homogenate of striatum, hypothalamus, pituitary or cortex was linear in the range 10—800 pmol per g of the tissue. The correlation coefficients (r) of these calibration graphs were greater than 0.9964 ($n=3$ each plot).

The concentrations values of ME, LE, ME-Arg-Gly-Leu and ME-Arg-Phe in striatum, hypothalamus, pituitary and cortex of rat brain measured by the present method are shown in Table I. The values were calculated by a standard addition method for correcting the loss of recoveries of the detected peptides. The values are almost identical with those measured by the post-column method,[17] but those for ME and LE are slightly lower than those measured by the RIA methods.[7-9] The precision of the present method was established by repeated determination ($n=7$) of the same sample of striatum. The relative standard deviations were 3.3, 3.1, 4.1 and 3.7% for ME, LE, ME-Arg-Phe and ME-Arg-Gly-Leu (541, 161, 118 and 128 pmol per g of the tissue), respectively.

The sensitivity of this HPLC method is comparable with the post-column method[17] and other HPLC methods combined with mass spectrometric detection[12] and electrochemical detection,[15] though it is nearly one order of magnitude lower than the RIA method.[7-9] However, the sensitivity and reproducibility of this method are sufficient for the simultaneous quantification of the four peptides in rat brain tissue.

Acknowledgements This work was partly supported by a Grant-in-Aid for Scientific Research from the Ministry of Education, Science and Culture, Japan. Thanks should also be made due to Asahi Chemical Ltd. for the generous gifts of the HPLC columns and packing materials for the mini-cartridge.

References

1) J. Hughes, T. W. Smith, H. W. Kosterlitz, L. A. Fothergill, B. A. Morgan and H. R. Morris, *Nature* (London), **258**, 577 (1975).
2) M. Knight and W. A. Klee, *J. Biol. Chem.*, **253**, 3843 (1978).
3) S. Nakanishi, A. Inoue, T. Kita, M. Nakamura and S. Numa, *Nature* (London), **278**, 423 (1979).
4) U. Gubler, P. Seeburg, B. J. Hoffman, L. P. Gage and S. Udenfriend, *Nature* (London), **295**, 206 (1982).
5) H. Kakidani, Y. Furutani, H. Takahashi, M. Noda, Y. Morimoto, T. Hirose, M. Asai, S. Inayama, S. Nakanishi and S. Numa, *Nature* (London), **298**, 245 (1982).
6) C. Bailey and I. Kitchen, *J. Pharmacol. Methods*, **13**, 235 (1985).
7) C. Gros, P. Pradelles, C. Rouget, O. Bepoldin and F. Dray, *J. Neurochem.*, **31**, 29 (1978).
8) A. Cupo, M. Eybalin, G. Patey, J. Rossier and T. Jarry, *Neuropeptides*, **4**, 389 (1984).
9) M. W. Pittius, B. R. Seizinger, A. Pasi, P. Mehraein and A. Herz,

Brain Res., **304** 127 (1984).
10) G. Zamboni, C. A. Jones and J. Hughes, *Anal. Biochem.*, **130**, 83 (1983).
11) R. Simatov, S. R. Childers and S. H. Synder, *Brain Res.*, **135**, 358 (1977).
12) D. M. Deiderio, M. Kai, F. S. Tanzer, J. Trimble and C. Wakelyn, *J. Chromatogr.*, **297**, 245 (1984).
13) G. H. Fridland and D. M. Desiderio, *Life Sci.*, **41**, 809 (1987).
14) J. Rivier, R. McClintock, R. Galyean and H. Anderson, *J. Chromatogr.*, **288**, 303 (1984).
15) C. Kim, R. Cheng and S. R. George, *J. Chromatogr.*, **494**, 67 (1989).
16) M. Kai and Y. Ohkura, *Anal. Chim. Acta*, **182**, 177 (1986).
17) G.-Q. Zhang, M. Kai and Y. Ohkura, *Anal. Sci.*, **6**, 671 (1990).
18) M. Nakano, M. Kai, M. Ohno and Y. Ohkura, *J. Chromatogr.*, **411**, 305 (1987).
19) M. Kai, M. Nakano, G.-Q. Zhang and Y. Ohkura, *Anal. Sci.*, **5**, 289 (1989).

Biological Resolution of (2*RS*)-Tocopherol and (2*RS*)-Tocopheryl Acetate

Tetsuo SAKAMOTO,[a] Kenichi TOMITA,[a] Mitsuo YANAGI,[b] Tatsuya OZAWA,[a] and Masahiro KAJIWARA*,[c]

Shiseido Product Research Laboratories,[a] Shiseido Basic Research Laboratories,[b] 1050 Nippa-cho, Kohoku-ku, Yokohama-shi 223, Japan and Department of Medicinal Chemistry, Meiji College of Pharmacy,[c] 1–22–1, Yato-cho, Tanashi-shi, Tokyo 188, Japan. *Received July 10, 1990*

Cells of *Mycobacterium* B-142 have been shown to incorporate (2*R*,4′*R*,8′*R*)-α-tocopherol selectively from a mixture of C-2 diasteromers. (2*R*,4′*R*,8′*R*)-α-Tocopheryl acetate was isolated from the bacterial cells while the (2*S*,4′*R*,8′*R*) isomer was extracted from the culture medium. The method has been extended to other tocopherol diastereomers.

Keywords biological resolution; (2*R*,4′*R*,8′*R*)-α-tocopherol; (2*R*,4′*R*,8′*R*)-α-tocopheryl acetate; *Mycobacterium* B-142; CD

In recent years the biological activity of the tocopherols[1] has been the subject of extensive investigation. These compounds have been implicated as nutritional factors, peroxy radical scavengers and anti-oxidants. The conformation of the naturally occurring compounds has been established as (2*R*,4′*R*,8′*R*).[2] The biological activity of (2*R*,4′*R*,8′*R*)-α-tocopherol (**1a**) has been shown to be significantly greater than that of synthetically derived (2*RS*,4′*R*,8′*R*)-α-tocopherol (**1b**).[3,4]

However, the low specific rotation of these isomers (**1a** has $[\alpha]_D$ +0.32° in soybean oil) coupled with the similarity of other spectral determinants has made estimation of the concentrations of enantiomers difficult. In the course of studies on *Mycobacterium* sp., we have isolated a new mutant, *Mycobacterium* B-142, the growth of which is sensitive to administered 2-phytyl chromans.

Growth and isomer feeding studies with natural (2*R*,4′*R*,8′*R*)-α-tocopherol (**1a**) and its acetate (**2a**), which have synthetic (2*RS*,4′*R*,8′*R*) mixtures, and with analogous compounds have shown that maximum cell growth occurs only in the presence of the natural isomers and that these isomers are selectively incorporated but not fully utilized by the cells. This latter finding provides the basis for an efficient method of separating the α-tocopherol enantiomers without prior derivatization.

Experimental

Materials and Methods The synthetic tocopherols were prepared as described in an earlier paper.[3,4] Acetylation of **1a** with acetic anhydride in pyridine containing a trace of *N*,*N*-dimethylaminopyridine gave **2a**, which was identical with an authentic sample obtained from USV Pharmaceutical Corp., U.S.A. Compounds **1a**, **3a**, and **4a** were isolated from soybean oil. Natural phytol and isophytol were obtained from Wako Junyaku. Synthetic phytol was purchased from Kurare. High performance liquid chromatographic separations were carried out on a JASCO Tri Rotar II and III using a reverse phase (methanol) system. Ultraviolet (UV) spectra were determined on Hitachi 340 and JASCO UVIDEC-610C spectrometers. ^{13}C-Fourier translation nuclear magnetic resonance (^{13}C-FT NMR) spectra were measured on a JEOL GSX-400 NMR spectrometer with $(CH_3)_4Si$ as a reference. Mass spectra (MS) were measured on a Hitachi RMU-GMG spectrometer. Circular dichroism (CD) spectra were measured on a JASCO J-500 C equipped with a DP 500 data processor.

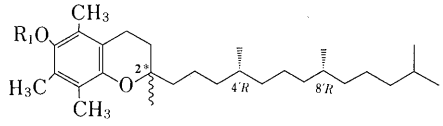

1a (2*R*, 4′*R*, 8′*R*) : R_1=H
2a (2*R*, 4′*R*, 8′*R*) : R_1=$COCH_3$
1b (2*RS*, 4′*R*, 8′*R*) : R_1=H
2b (2*RS*, 4′*R*, 8′*R*) : R_1=$COCH_3$
1c (2*RS*, 4′*RS*, 8′*RS*) : R_1=H
2c (2*RS*, 4′*RS*, 8′*RS*) : R_1=$COCH_3$

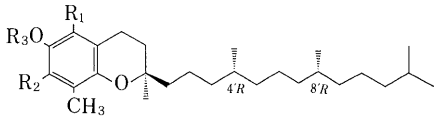

3a : R_1, R_3=H; R_2=CH_3
4a : R_1, R_2, R_3=H

Fig. 1. Structures of Tocopherols and Their Derivatives

Identification of Microorganism *Mycobacterium* B-142 was characterized by standard procedures.[5]

Culture of Microorganism The compositions of the preculture medium and culture medium are given in Table II. After growing for 7 d in preculture medium, the organisms were inoculated into a sterile Sakaguchi flask containing 100 ml of medium and 0.0036—1.0% tocopherol, and were incubated at 30 °C.

Extraction of Tocopherols After feeding of tocopherols in the above medium for 4—8 d, the cells were separated by centrifugation (19000 × *g*, for 10 min) and washed with cold EtOH. The washed cells were refluxed with a mixture of EtOH and acetone (1 : 1) for 5 min, the supernatant was

TABLE I. Identification of Mycobacterium B-142

		B-142	*Mycobacterium rhodochrous* IMF 13161
Growth	55 °C	−	−
	40 °C	+	+
	35 °C	+	+
	20 °C	+	+
MacConkey agar		−	−
Fermentation (acid)	Inositol	−	−
	Sorbitol	+	+
	Mannitol	−	−
	Maltose	−	−
	Arabinose	−	−
Gelatin liquefaction		−	−
Acid fast		+	−
Colony size		Small	Large
Colony color		Yellow-brown	White
Determination of tocopherol enantiomers		+	−

TABLE II. Culture Medium of *Mycobacterium* B-142

Preculture medium		Culture medium	
Meat extract	7.0 g	KH_2SO_4	0.35 g
Peptone	10.0 g	$(NH_4)_2SO_4$	2.0 g
Sodium chloride	3.0 g	Tocopherol	0.036—10 g
Agar	15.0 g	Dist. water	1000 ml
Dist. water	1000 ml		
Incubation	At 30 °C	Incubation	pH 7.0 at 30 °C
		Rotation	At 200 rpm

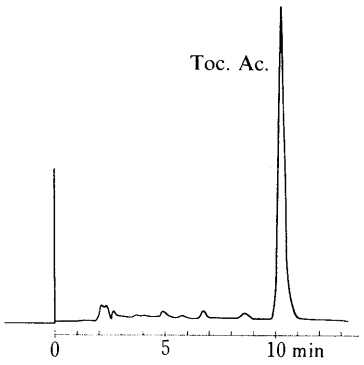

Fig. 2. HPLC of Tocopheryl Acetate from Cells

After feeding of 0.1% **2b** in the medium for 8 d, the cells were refluxed with a mixture of ethanol and acetone. The supernatant was purified by preparative HPLC.

Column, 4.6 × 250 mm TSK LS-410 (5 μ); fluent, methanol 1.5 ml/min; detection, at 280 nm (0.08AUFS); pressure, 100 kg/cm^2.

dried over anhydrous sodium sulfate and the solvents were evaporated off. Samples were purified by preparative high performance liquid chromatography (HPLC).

After HPLC, each tocopherol was identified on the bases of UV, infrared (IR), ^{1}H-NMR, ^{13}C-NMR and CD spectra.

α-Tocopherol (**1a**): UV λ_{max}^{EtOH} nm: 292. IR (film): 3450 (OH, m), 1262 (ring –O–, s), 1082 (ring –O–, s) cm^{-1}. MS *m/z*: 431 (34, $M^+ + 1$), 430 (100, M^+), 205 (8, $M^+ - C_{16}H_{33}$), 165 (97, 205−40). ^{1}H-NMR ($CDCl_3$) δ: 0.86 (12H, d, J=1.9 Hz, $CH_3 \times 4$), 0.95—1.61 (24H, m, CH_3, $CH_2 \times 9$, $CH \times 3$), 1.76 (2H, m, CH_2), 2.09 (9H, s, $CH_3 \times 3$), 2.58 (2H, t, CH_2), 4.26 (1H, s, OH). ^{13}C-NMR ($CDCl_3$) δ: 11.2 (q, CH_3), 11.7 (q, CH_3), 12.2 (q, CH_3), 19.7 (q, CH_3), 20.8 (t, CH_2), 21.1 (t, CH_2), 22.6 (q, CH_3), 22.7 (q, CH_3), 23.8 (q, CH_3), 24.5 (t, CH_2), 24.8 (t, CH_2), 28.0 (d, CH), 31.6 (t, CH_2), 32.7 (d, CH), 32.8 (d, CH), 37.3 (t, CH_2), 37.4 (t, $CH_2 \times 3$), 39.4 (t, CH_2), 39.9 (t, CH_2), 74.4 (s, C), 117.2 (s, aromatic), 118.6 (s, aromatic), 121.2 (s, aromatic), 122.4 (s, aromatic), 144.5 (s, aromatic) 145.5 (s, aromatic).

α-Tocopheryl Acetate (**2a**): IR (film): 1759 ($COOCH_3$, s), 1211 (ring –O–, s), 1080 (ring –O–, m) cm^{-1}. MS *m/z*: 472 (39, M^+), 430 (100, $M^+ - 42$), 207 (35), 205 (9, $430 - C_{16}H_{33}$), 165 (61, 205−40). ^{13}C-NMR ($CDCl_3$) δ: 11.8 (q, CH_3), 12.1 (q, CH_3), 12.9 (q, CH_3), 19.7 (q, $CH_3 \times 2$), 20.5 (q, $\underline{C}H_3CO_2$), 20.6 (t, CH_2), 21.1 (t, CH_2), 22.7 (q, $CH_3 \times 2$), 24.0 (q, CH_3), 24.5 (t, CH_2), 24.8 (t, CH_2), 28.0 (d, CH), 31.1 (t, CH_2), 32.7 (d, $CH \times 2$), 37.4 (t, $CH_2 \times 4$), 39.4 (t, CH_2), 40.1 (t, CH_2), 75.0 (s, C), 117.3 (s, aromatic), 123.0 (s, aromatic), 124.8 (s, aromatic), 126.6 (s, aromatic), 140.6 (s, aromatic), 149.4 (s, aromatic), 169.5 (s, $\underline{C}OO$).

The epimers were extracted from the feeding medium by similar methods.

Results and Discussion

Figure 3 shows the growth of *Mycobacterium* B-142 in the presence of (2*R*,4′*R*,8′*R*)- (**2a**), (2*RS*,4′*R*,8′*R*)- (**2b**) and (2*RS*,4′*RS*,8′*RS*)-α-tocopheryl acetate (**2c**). The growth rates are affected only slightly by side chain isomerism; however, the stereochemistry at C-2 of the chroman ring has a profound effect. This is shown by the results given in Table III. Of the compounds tested, only (2*R*,4′*R*,8′*R*)-α-tocopherol (**1a**) and its acetate (**2a**) showed high relative growths. The bacterial growth was influenced by the presence of methyl groups at the position, the number and stereochemistry at 2 position on the chroman ring.

The stereochemistry of the phytyl side chain appears to be of less importance, although (7*R*,11*R*)-phytol gave a much higher growth rate than its isomers. When synthetic (2*RS*,4′*R*,8′*R*)-α-tocopheryl acetate (**2b**) was added as the medium for growing bacteria, **2a** was obtained selectively as a major compound (Fig. 2) from the bacterial cells. When the bacteria were grown with (2*RS*,4*RS*,8*RS*)-α-tocopheryl acetate (**2c**), **2a** was selectively obtained from the bacteria cells. Figure 5 shows that the extracted α-tocopheryl acetate and the authentic **2a** has the same λ_{max}. Such stereospecific incorporation may occur through the bacterial cell membrane.

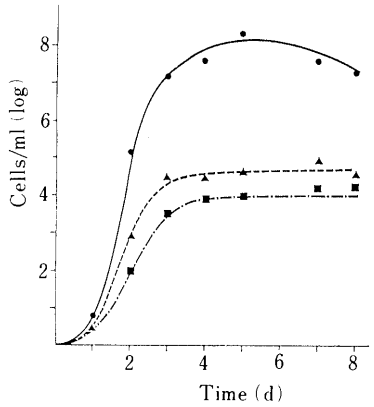

Fig. 3. Specific Growth of *Mycobacterium* B-142 with the Isomers of α-Tocopheryl Acetate

Each of the reaction systems consisted of 100 ml of the culture medium containing 0.0036 g of the material under test and 0.5 ml inoculum. The mixture was vigorously shaken and incubated at 30 °C. The number of surviving bacteria was determined by the plate count method.

—●—, **2a**; – – –▲– – –, **2b**; – · –■– · –, **2c**.

Table III. Relative Response of *Mycobacterium* B-142 to Enantiomers of α-Tocopherol

Compound	Cells/ml	Relative (%)
1a	7.04×10^7	7729
1b	1.49×10^6	164
1c	9.11×10^5	100

Each of the reaction systems consisted of 100 ml of the culture medium containing 0.0036 g of enantiomer of α-tocopherol and 0.5 ml inoculum. The mixture was vigorously shaken and incubated at 30 °C for 4 d. The number of surviving bacteria was determined by the plate count method.

Table IV. Cell Growth of *Mycobacterium* B-142 with Tocopherols

Compound	Cells/ml	Relative (%)
1c	3.87×10^7	100
1a	3.67×10^8	963
(2*R*,4′*R*,8′*R*)-γ-Tocopherol	5.47×10^7	142
(2*R*,4′*R*,8′*R*)-δ-Tocopherol	5.98×10^7	157
(2*R*,4′*R*,8′*R*)-α-Tocopherylquinone	5.18×10^7	136

Each of the reaction systems consisted of 100 ml of the culture medium containing 0.0036 g of the compound under test and 0.5 ml inoculum. The mixture was vigorously shaken and incubated at 30 °C for 6 d. The number of surviving bacteria was determined by the plate count method.

Table V. Cell Growth of *Mycobacterium* B-142 with Synthetic Precursors of Tocopherol

Compound	Cells/ml	Relative (%)
2c	5.92×10^7	100
(7*R*,11*R*)-Phytol(natural)	1.26×10^7	21
(7*R*,11*RS*)-Phytol(synthetic)	10^2	10^{-3}
(7*R*,11*RS*)-Isophytol(synthetic)	10^2	10^{-3}

Each of the reaction systems consisted of 100 ml of the culture medium containing 0.0072 g of the compound under test and 0.5 ml inoculum. The mixture was vigorously shaken and incubated at 30 °C for 10 d. The number of surviving bacteria was determined by the plate count method.

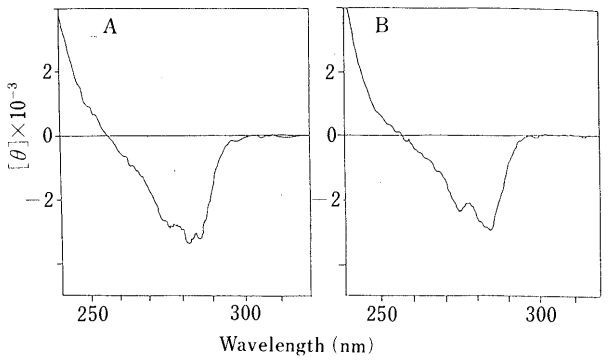

Fig. 4. CD Spectra of **2a** and Cell Extract of Cells Fed on (2*RS*,4′*RS*,8′*RS*)-α-Tocopheryl Acetate

A, **2a**; B, extract. 1 mm cell. CD, 1 m°/cm; TC, 2 s. Slit, 1 nm; scan, 50 nm/min.

Acknowledgments The authors wish to thank Ms S. Hashimoto for MS measurements, Dr. K. Iida for NMR measurements, and Mr. A. Takakuwa of JEOL for CD determination. Thanks are also due Dr. C. T. Goodhue of Eastman Kodak Company, Rochester, N.Y. 14650, U.S.A., for the generous gift of *Mycobacterium* A-7 for comparison.

References and Notes

1) *a*) L. E. Machlin, (ed.), "Vitamin E," Marcel Dekker, New York 1979; *b*) The Vitamin Society of Japan (ed.), "Vitamin Handbook," Vol. 5, Kyoto, 1989, p. 43.
2) *a*) H. Mayer, U. Gloor, O. Isler, R. Ruegg, and O. Wiss, *Helv. Chim. Acta*, **47**, 221 (1964) and references therein; *b*) H. Mayer, P. Schudel, R. Ruegg, and O. Isler, *ibid.*, **46**, 963 (1963).
3) M. Kajiwara, O. Sakamoto, and S. Ohta, *Heterocycles*, **14**, 1995 (1980).
4) *a*) H. Mayer and O. Isler, *Methods Enzymol.*, **18C**, 241 (1971): *b*) P. Schudel, H. Mayer, and O. Isler, "The Vitamins," Vol. V. ed. by W. H. Sebrell Jr. and R. S. Harris, Academic Press, New York, 1972, p. 168; *c*) M. Kajiwara, O. Sakamoto, H. Katsura, and S. Ohta, *Heterocycles*, **15**, 1209 (1981).
5) *a*) R. S. Buchanan and N. E. Gibbons, Co-Ed., "Bergey's Manual of Determinative Bacteriology," 8th ed., Baltimore Williams and Wilkins, Baltimore, 1974; *b*) C. T. Goodhue, *Biochem. J.*, **4**, 1822 (1965).

Quantitative Analysis of Sodium Valproate in Pharmaceutical Preparations by a Valproate-Selective Electrode

Hirofumi SUZUKI,* Kouichi AKIMOTO and Hiroshi NAKAGAWA

Pharmaceutical Research Center, Kanebo, Ltd., 1-5-90, Tomobuti-cho, Miyakojima-ku, Osaka 534, Japan. *Received July 23, 1990*

A simple and rapid method for the determination of sodium valproate in pharmaceutical preparations, without prior separation, has been developed using a valproate-selective electrode. A plastic liquid membrane electrode kit was used for the electrode based on the use of valproate: methyltris(tetradecyl)ammonium ion-pair complex in *n*-decanol and polyvinyl chloride matrix. The electrode showed a near-Nernstian response in the range of 10^{-2} to 2×10^{-4} M sodium valproate. Life span of the electrode was at least 1 month. The electrode was also used for the determination of the pK_a of valproic acid. Determination of 90 to 1500 μg/ml of sodium valproate in aqueous solution showed an average recovery of 100.0% (mean standard deviation 0.4%) by direct potentiometry. Pharmaceutical excipients and diluents commonly used in drug formations did not interfere with the analysis. The selectivity of the electrode to some inorganic and organic anions was described. This assay was applied to determine sodium valproate in pharmaceutical preparations and the results compared favorably with those obtained by gas chromatography.

Keywords sodium valproate; valproic acid; valproate-selective electrode; ion-selective electrode; pharmaceutical analysis

Sodium valproate (VPA-Na) is an antiepileptic agent used alone or with other anticonvulsants in the prophylactic management of simple and complex absence seizures.[1] Since VPA lacks ultraviolet (UV) absorbance at higher wavelengths (>235 nm), gas chromatography (GC) and titration in nonaqueous solutions has usually been used for the determination of VPA in pharmaceutical preparations. However, these methods have the disadvantages of requiring complicated and prior separations or non-specificity.

A potentiometric method using an ion-selective electrode has recently shown itself to be a viable means of analyzing pharmaceutical products and has been applied to the determination of active ingredients in pharmaceutical formulations.[2] These potentiometric methods can be easily used in the assay procedure without prior separations. The purpose of this study was to develop a simple and accurate assay system using a new VPA-selective electrode for the determination of VPA in pharmaceutical preparations. We used a plastic liquid membrane electrode kit[3] which has a polytetrafluoroethylene (PTFE) membrane as a carrier of a plastic matrix and VPA-methyltris(tetradecyl)ammonium as the electroactive material for the VPA-selective electrode.

Experimental

Reagents VPA-Na was purchased from Yodogawa Pharmaceutical Co., Ltd. Methyltris(tetradecyl)ammonium chloride (MTTDA-Cl), tri-*n*-octylmethylammonium chloride (Capriquat), *o*-nitrophenyl octyl ether (NPOE) and di-*n*-octylphenylphosphonate (DOPP) were obtained from Dojin Chemicals. Di-*n*-butyl phthalate (DBP), *n*-decanol and di-*n*-octyl phthalate (DOP) were from Wako Pure Chemical. Polyvinyl chloride (PVC; high relative molecular weight) was purchased from Aldrich. All other chemicals were of the best available commercial grade. Borax buffer (0.033 M, pH 9.3) was prepared from 12.6 g $Na_2B_4O_7 \cdot 10H_2O$ made up to 1 l. Pharmaceutical preparations containing VPA-Na (Hyserenin fine granules®, Hyserenin fine granules 20®, Hyserenin tablets® and Hyserenin tablets 100®) were obtained from Kanebo, Ltd.

Apparatus Potentiometry: All potentiometric measurements were carried out using an Orion expandable ion analyzer (Model EA920). The VPA-selective electrode was used with an Orion Ag–AgCl double-junction reference electrode (Model 90-02) containing saturated $Na_2B_4O_7$ solution in the outer compartment as the reference. pH and temperature measurements were performed with a Horiba glass–calomel electrode (Model 6026) and an Orion automatic temperature compensator, respectively.

GC: A Hitachi gas chromatograph (Model 163) was equipped with a flame-ionization detector and a Shimadzu integrator (Model C-R3A). The glass column, 2 m × 3 mm i.d., was packed with 5% diethyleneglycol succinate (DEGS) + 1% H_3PO_4 phase on 60—80 mesh Chromosorb W (Shimadzu). The carrier gas (nitrogen) flow-rate was 35 ml/min. The system temperatures were: column, 150 °C; injector, 220 °C; detector 220 °C.

Preparation of Electroactive Material One milliliter aliquot of *n*-decanol was mixed with 130 mg of MTTDA-Cl and shaken with an 8 ml aliquot of a 0.1 M VPA-Na aqueous solution. The organic phase was washed twice with distilled water and used for preparation of the electrode.

Electrode Preparation A liquid membrane electrode kit (Denki Kagaku Keiki Co.) was used as described previously.[3] The electroactive material (100 mg) and PVC (50 mg) were dissolved in 1.5 ml of tetrahydrofuran. A PTFE membrane filter was dipped in the mixture and placed on top of the chip of the electrode kit. Several drops of the mixture were applied to the PTFE membrane and the membrane was air dried at room temperature. The internal reference solution of the electrode was a 10^{-2} M VPA-Na solution of 0.033 M borax buffer (pH 9.3). The chip was conditioned by soaking in 10^{-2} M VPA-Na solution (pH 9.3).

Potential Measurements Cell assemblies of the following type were used: Ag–AgCl | 10^{-2} M VPA-Na solution (borax buffer, pH 9.3) || PVC membrane || test solution (borax buffer, pH 9.3) | Ag–AgCl double-junction reference electrode. The potential values were measured for the stirred solution at 25 ± 1 °C.

Selectivity Coefficients The selectivity coefficients were evaluated by the fixed interference method according to IUPAC recomendations. The potential was measured with solutions of a constant level of interference (10^{-2} M) and varying concentrations of VPA-Na from 10^{-2} to 2×10^{-4} M.

Assay by Potentiometry Standard Preparation: Two standard preparations, I and II, in 0.033 M borax buffer (pH 9.3) having known concentrations of VPA-Na 160 and 200 μg/ml, respectively, were prepared.

Assay Preparation: Pharmaceutical preparations of VPA-Na were finely powdered. An accurately weighed portion of the powder, equivalent to about 0.1 g of VPA-Na, was added to about 40 ml of borax buffer (pH 9.3) and sonicated, and borax buffer was added to make exactly 50 ml.

Procedure: The VPA-selective electrode and the Orion double-junction reference electrode were immersed successively in standard preparation I, the assay preparation and standard preparation II. The respective electron motive force (emf) values of these solutions were determined. The quantity was calculated by comparing the measured emf values of the assay preparation with the calibration line calculated from the standard preparations.

Assay by GC Pharmaceutical preparations of VPA-Na were finely powdered. An accurately weighed portion of powder, equivalent to about 0.1 g of VPA-Na, and 5 ml of standard solution (VPA-Na 10 mg/ml) were transferred to two different separators and treated identically as follows: Five milliliters of internal standard solution (diphenyl 10 mg/ml in chloroform) and 15 ml of 1 N hydrochloric acid were added and the solution was extracted with 20 ml of chloroform, centrifuged, and dehydrated by anhydrous sodium sulfate; the organic layer was then injected.

Results and Discussion

Selection of Ion-Pairing Agent Quaternary ammonium species,[4] cationic dyes and ferroin-compound cations[5] and metalloporphylines[6] have been used as ion-pairing agents for acidic drugs. In the present study, we tested quaternary ammonium species (MTTDA, Capriquat) and ethyl violet because these compounds were commercially available and ethyl violet has large extractability of an ion-pair into nonpolar solvents.[7] The membranes of the electrode contained PVC as a plastic matrix and *n*-decanol as a solvent. The response characteristics for the VPA-selective electrodes are summarized in Table I, and the effect of concentration of ion-pair in the solvent is also shown. The MTTDA-based electrode showed the lowest limit of linear range. This is probably because MTTDA forms the most hydrophobic ion-pair with VPA and extractability of the ion-pair is the best. The concentration of ion-pair in the membrane was increased, resulting in excellent performance. Based on these results, we selected the 0.2 M MTTDA–VPA ion-pair in *n*-decanol as the membrane material.

Selection of Solvent As the solvent in the membrane material, we tested *n*-decanol, DOPP, NPOE, DBP and DOP using 0.2 M MTTDA–VPA ion-pair in these solvents. The response characteristics for these electrodes revealed the one containing *n*-decanol to be excellent (Table II). The composition of around 70 : 30 percent solvent (plus sensor): polymer was shown to be most appropriate for the PVC electrodes.[8] Therefore, we selected the following membrane compositions for the VPA-selective electrode: 67% (w/w) 0.2 M VPA–MTTDA in *n*-decanol, and 33% (w/w) PVC.

Table I. Response Characteristics for Various PVC: *n*-Decanol Based VPA-Selective Electrodes (Borax Buffer, pH = 9.3)

Ion-pairing agent (M)	Slope[a] (mV/log *C*)	Correlation coefficient	Intercept (mV)	Lower limit of linear range (M)
MTTDA				
0.05[b]	-47.03 ± 1.21[c]	0.9998	144 ± 3.1	2×10^{-4}
0.1	-57.29 ± 0.33	0.9998	128 ± 1.8	2×10^{-4}
0.2	-58.26 ± 0.02	0.9999	115 ± 0.9	2×10^{-4}
Capriquot				
0.2	-56.79 ± 0.81	0.9999	119 ± 1.0	5×10^{-4}
Ethyl violet				
0.2	-54.97 ± 0.64	0.9998	128 ± 3.4	5×10^{-4}

a) Average value calculated for the range of 10^{-2} M—lower limit of linear range. *b*) Concentration of ion-pairing agent in *n*-decanol. *c*) Average value and standard deviation (S.D.) of values ($n=3$) obtained from the same electrode.

Table II. Response Characteristics for Various PVC: MTTDA Based VPA-Selective Electrodes (Borax Buffer, pH = 9.3)

Solvent	Slope[a] (mV/log *C*)	Correlation coefficient	Intercept (mV)	Lower limit of linear range (M)
n-Decanol	-58.26 ± 0.02[b]	0.9999	115 ± 0.9	2×10^{-4}
DOPP	-55.86 ± 0.84	0.9997	122 ± 3.7	2×10^{-4}
DBP	−54.7	0.998	122	5×10^{-4}
NPOE	−53.9	0.998	124	5×10^{-4}
DOP	−52.9	0.998	126	5×10^{-4}

a) Average value calculated for the range of 10^{-2} M—lower limit of linear range. *b*) Average value and S.D. of values ($n=3$) obtained from the same electrode.

The effect of quantity of membrane material mounted on the electrode to the unit's performance is shown in Table III. In this range the slope changed little but the response time of the electrode increased with increasing quantity. Therefore, we mounted 12 mg of membrane material on the electrode. Data obtained from five electrodes (Table III) indicates the high reproducibility of performance among them.

Influence of pH The influence of pH on the potential of the VPA-selective electrode was investigated. The pH was varied by adding sulfuric acid or sodium hydroxide solution dropwise to VPA-Na aqueous solution. The results are shown in Fig. 1. At lower pH (pH <6.5), the potential increases with the decrease in the pH because the protonated VPA species gradually decrease. From these potential-pH curves pK_a of VPA was evaluated. The pK_a is equal to the pH value when the electrode potential increases by $-S\times\log 2$ mV (S=electrode slope).[9] The pK_a values obtained from the curves of 10^{-3} and 5×10^{-3} M VPA-Na in the figure were 4.9 and 4.7, respectively, which were in agreement with the literature (a value of 4.8).[1] At higher pH values, the potential increases with the increase in the pH. This might be due to the increasing of ion strength with the addition of sodium hydroxide, because in the case of high ion strength like 10^{-3} M VPA-Na in 0.033 M borax solution, the potential was not changed up to pH 11.5.

Influence of Interfering Compounds The selectivity coef-

Table III. Response Characteristics for Various Quantities of Membrane Construction (Borax Buffer, pH = 9.3)

Quantity (mg)	Slope[a] (mV/log *C*)	Correlation coefficient	Intercept (mV)	Lower limit of linear range (M)
7	-54.86 ± 0.24[b]	0.9992	141 ± 0.9	2×10^{-4}
12	-58.26 ± 0.02	0.9999	115 ± 0.9	2×10^{-4}
	(-57.90 ± 1.07)[c]	(0.9996)	(117 ± 10.6)	
24	-57.00 ± 0.20	0.9996	120 ± 0.6	2×10^{-4}
36	-58.17 ± 1.05	0.9996	127 ± 4.5	2×10^{-4}

a) Average value calculated for the range 10^{-2} M—lower limit of linear range. *b*) Average value and S.D. of values ($n=3$) obtained from the same electrode. *c*) Average value and standard deviation of values obtained from five different electrodes.

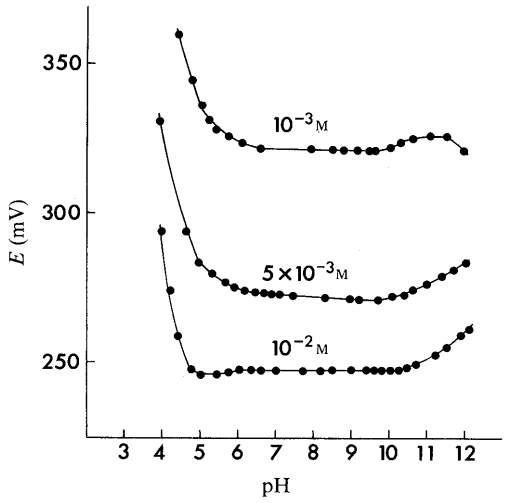

Fig. 1. Effect of pH on the Potential of the VPA-Selective Electrode for Different VPA-Na Concentrations

TABLE IV. Selectivity Coefficients for VPA-Selective Electrode

Interferent	$K_{i,j}$
NO_3^-	4.9×10^{-1}
SO_4^{2-}	6.6×10^{-2}
Cl^-	6.0×10^{-2}
CO_3^{2-}	5.4×10^{-2}
HPO_4^{2-}	3.8×10^{-2}

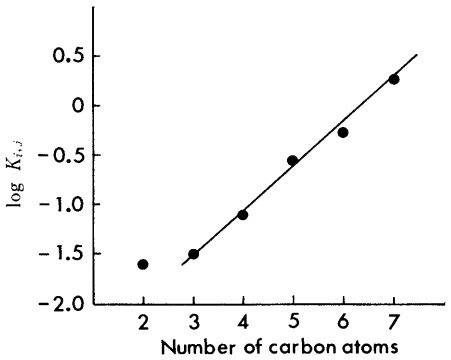

Fig. 2. Plot of log $K_{i,j}$ against the Number of Carbon Atoms of Unbranched Alkanoic Acid

TABLE V. The Allowable Limit of Excipients

Excipient	Excipient weight[a]/ VPA-Na weight[b]
Corn starch, JP	>20
Potato starch, JP	>20
Microcrystalline cellulose, JP	>20
Synthetic aluminium silicate, JP	>20
Sucrose, JP	>20
Lactose, JP	10
D-Mannitol, JP	5
Magnesium aluminometasilicate	1
Magnesium stearate, JP	>2
Hydroxypropylcellulose, JP	>2
Hydroxypropylmethylcellulose 2910, JP	>2

a) Excipient weight which gives an error of 1%. *b*) Concentration of VPA-Na is 200 μg/ml.

ficients, $K_{i,j}$ of the VPA-selective electrode determined by the fixed interference method according to IUPAC recommendations are listed in Table IV. A plot of log $K_{i,j}$ *versus* the number of carbon atoms in unbranched alkanoic acids gave a straight line as shown in Fig. 2. This indicates that selectivity of the VPA-selective electrode is governed by hydrophobicity of ions, that is, extractability of ions into the membrane in a manner similar to other electrodes based on quaternaryammoniums.[10] The influence of some excipients normally used in pharmaceutical preparations was also examined. Table V shows the quantity of excipients against VPA-Na which gives an error of 1% to the assay of VPA-Na by potentiometry. These excipients demonstrated no interference in the quantity usually used.

Assay of VPA-Na In Table VI, reproducibility and accuracy determined by the direct potential method for VPA-Na solution in the range of 90—1500 μg/ml are shown. The results show an average recovery of 100.0% and a mean standard deviation of 0.4%. The response time

TABLE VI. Determination of VPA-Na in Solution by VPA-Selective Electrode

VPA-Na (μg/ml)		Recovery (%[a])	Standard deviation
Added	Found		
89.9	89.7	99.7	0.51
149.8	150.2	100.3	0.72
299.6	199.5	100.0	0.15
599.2	599.2	100.0	0.26
898.9	895.6	99.6	0.76
1198.5	1202.2	100.3	0.36
1498.1	1498.3	100.3	0.36

a) Average of three measurements; average recovery ± mean S.D. = 100.0 ± 0.4%.

TABLE VII. Determination of VPA-Na in Pharmaceutical Preparations by VPA-Selective Electrode and GC

Sample	Electrode method		GC method	
	Recovery (%)	S.D. ($n=6$)	Recovery (%)	S.D. ($n=6$)
Hyserenin fine granules®	99.2	1.2	97.5	2.0
Hyserenin fine granules 20®	104.6	1.3	103.0	1.5
Hyserenin fine tablets®	97.7	0.5	97.5	1.4
Hyserenin fine tablets 100®	100.8	0.7	101.3	1.0

of the VPA-selective electrode in this range was short, *viz.*, within 60 s.

To check the ISE (ion-selective electrode) method recovery efficiency, we spiked VPA-Na with placebo excipients used in Hyserenin fine granules®, Hyserenin fine granules 20®, Hyserenin tablets® and Hyserenin tablets 100®. The average recoveries and mean standard deviation of VPA-Na from these mixed samples were 99.8 ± 0.2%, 100.0 ± 0.7%, 100.4 ± 0.4% and 100.3 ± 0.5%, respectively.

Commercially available preparations containing VPA-Na were determined by the ISE method and compared with GC. The results obtained by both methods (Table VII) show good agreement and high precision. The present procedure is sufficiently simple, rapid, quantitative, and reproducible for the assay of VPA-Na in pharmaceutical preparations. The ISE described is easily constructed and a potentiometric apparatus is not too costly. Furthermore, since the ISE method does not require complicated prior separation, it can be used for routine quality control.

References

1) G. K. McEvoy (ed.), "American Hospital Formulary Service Drug Information 89," American Society of Hospital Pharmacists, Bethesda, 1989, p. 1104.
2) R. K. Gilpin and L. A. Pachla, *Anal. Chem.*, **61**, 200R (1989); V. V. Cosofret and R. P. Buck, *Ion-Sel. Electrode Rev.*, **6**, 59 (1984); T. C. Pinkerton and B. L. Lawson, *Clin. Chem.*, **28**, 1946 (1982); K. Vytras, *J. Pharm. Biomed. Anal.*, **7**, 789 (1989).
3) H. Suzuki, K. Akimoto, H. Nakagawa and I. Sugimoto, *J. Pharm. Sci.*, **78**, 62 (1989).
4) C. J. Coetzee and H. Freiser, *Anal. Chem.*, **41**, 1128 (1969); H. Hara, S. Okazaki and T. Fujinaga, *Anal. Chim. Acta.*, **121**, 119 (1980); A. Mitsana-Papazoglou, E. P. Diamandis and T. P. Hadjiioannou, *ibid.*, **159**, 393 (1984); V. V. Cosofret and R. P. Buck, *J. Pharm. Biomed. Anal.*, **4**, 45 (1986); G. N. Valsami, P. E. Macheras and M. A. Koupparis, *Analyst*, **114**, 387 (1989).
5) K. Kina, N. Maekawa and N. Ishibashi, *Bull. Chem. Soc. Jpn.*, **46**, 2772 (1973).

6) N. A. Chaniotakis, S. B. Park and M. E. Meyerhoff, *Anal. Chem.*, **61**, 566 (1989).
7) S. Motomizu, S. Fujiwara, A. Fujiwara and K. Toei, *Anal. Chem.*, **54**, 392 (1982).
8) J. D. R. Thomas, *Anal. Chim. Acta*, **180**, 289 (1986).
9) T. K. Christopoulos, A. Mitsana-Papazoglou and E. P. Diamandis, *Analyst*, **110**, 1497 (1985).
10) H. J. James, G. P. Carmack and H. Freiser, *Anal. Chem.*, **44**, 853 (1972).

Effect of Aging, Castration, and Testosterone Administration on Ribonuclease and Ribonuclease-Inhibitor Activities in the Prostate of Rats

Hiroshi KUMAGAI,* Miki MATSUURA, Aki MURAKAMI and Seiyu HIROSE

Faculty of Pharmaceutical Sciences, Chiba University, 1–33 Yayoi-cho, Chiba 260, Japan. *Received June 6, 1990*

Free ribonuclease (RNase)-inhibitor activities in both ventral and dorsal prostates had their highest peaks in 4-week-old rats and smallest peaks in around 7-week-old animals. Total RNase activity in the ventral prostate decreased overall with age, while that in the dorsal prostate increased. No significant amount of free RNase activity was found in either prostate.

Weight, protein content, and free RNase-inhibitor activity in both prostates decreased after castration and increased after administration of testosterone to castrated rats. Total RNase activity in the ventral prostate was increased by castration and decreased by testosterone administration. In the dorsal prostate, total RNase activity had two peaks, 7 d after castration and 2 d after testosterone administration. A large amount of free RNase activity was found in the ventral prostate 7 d after castration and this activity was decreased by testosterone administration. In the dorsal prostate, free RNase activity was not detected after castration and testosterone administration.

These results suggest that changes in the level of RNase-inhibitor in both prostates are involved in the regulation of their RNA content through the control of free RNase activity.

Keywords RNase-inhibitor; RNase; prostate; aging; castration; testosterone; rat

Introduction

The presence of ribonuclease (RNase) inhibitors has been demonstrated in many mammalian tissues.[1,2] These inhibitors are acidic proteins with a molecular weight of about 5×10^4.[2] They inhibit bovine pancreatic RNase A noncompetitively by forming 1 : 1 complexes.[3] The inhibitors are inactivated by SH reagents, *e.g.*, *p*-chloromercuribenzoic acid and *p*-chloromercuribenzenesulfonic acid. The treatment of RNase-inhibitor complexes with SH reagents regenerates active RNases from the complexes.[1]

The precise physiological role of RNase inhibitors remains unclear. However, elevated levels of the inhibitor activity were seen in rapidly growing cells such as regenerating rat liver[4] and phytohemagglutinin-stimulated cultured human lymphocytes.[5] Therefore, RNase inhibitors have been suspected to be involved in the regulation of ribonucleic acid (RNA) and protein syntheses.[6–8] In addition, an increase in RNase-inhibitor activity was found in the rat adrenal gland stimulated by adrenocorticotropic hormone.[9] Furthermore, the inhibitor activities in rat thyroid and uterine were increased by the administration of thyroid-stimulating hormone[10] and estrogen,[11] respectively. The activity of RNase was decreased by hepatectomy,[4] phytohemagglutinin stimulation,[5] and administration of various hormones.[9–11] RNase-inhibitor in the uterus of immature rats was present in a greater amount than RNase, but free inhibitor was no longer detectable in the uterine cytoplasm after precocious treatment with estrogen[12,13] or during the course of normal development.[14] After administration of estrogen to ovariectomized rats, RNase-inhibitor activity disappeared from uterine cytosol.[15] These results appear to be contradictory to the above proposed role of the RNase-inhibitor, because the elevated RNase activity results in a decrease in RNA and protein syntheses. With respect to RNase-inhibitor in male gonads, RNase-inhibitor has been purified from rat testis and characterized,[16] but its relation to maturation or sex hormone treatment has not been examined. The relationship between androgen administration and tissue RNase activity has been studied only in mouse skeletal muscle and no significant effect of androgen was demonstrated.[17]

We found an RNase-inhibitor in rat prostate and isolated it as a protein about 4×10^4 in molecular weight (unpublished data). In the present paper, we describe the effect of aging, castration, and androgen administration following castration on this RNase-inhibitor and RNase activities in rat ventral and dorsal prostates.

Materials and Methods

Materials Testosterone propionate and *p*-chloromercuribenzenesulfonic acid were purchased from Nakarai Tesque Inc. Sesame oil was obtained from Kanto Chemical Co., Inc. Bovine pancreatic RNase A (type II-A) and yeast RNA (type VI) obtained from Sigma Chemical Co. were purified according to the methods of Hirose *et al.*[18] and Kumagai *et al.*,[19] respectively. Laboratory chow (MF) was purchased from Oriental Yeast Co., Ltd.

Animals and Their Treatments Male Wistar rats (2—7 weeks old) were purchased from Takasugi Experimental Animal Co., Ltd. They were maintained in a temperature (22±2 °C)-controlled room with 12 h light–12 h dark cycle (light on from 7.00 a.m.), and received laboratory chow and tap water *ad libitum*. The rats under the above conditions were kept for 4—10 d after purchase, and healthy rats with normal body weight gains were used in the experiment. Castration was performed by the scrotal route under ether anesthesia using 7-week-old rats. Testosterone propionate dissolved in sesame oil (20 mg/ml) was injected subcutaneously to castrated rats at 9.30 a.m.

Preparation of 100000 × *g* Supernatant (S-100) from Rat Prostate Preparation of S-100 was performed essentially as described previously.[20] Rats were exsanguinated without anesthesia. After the livers were perfused with isotonic saline, the prostates were removed quickly and rinsed in an ice-cold solution containing 20 mM Tris–HCl (pH 7.5), 200 mM sucrose, 100 mM NH_4Cl, 5 mM magnesium acetate, and 60 mM 2-mercaptoethanol. All subsequent steps were carried out at 0—4 °C. The rinsed prostates were homogenized in 2.5 vols. of the above solution using a glass homogeneizer. The homogenate was centrifuged for 20 min at 17000 × *g*. The resulting supernatant fraction was centrifuged for 90 min at 105000 × *g* to obtain S-100. The S-100, after being dialyzed against two changes of 1.5 l of a solution containing 20 mM Tris–HCl (pH 7.5), 20% glycerol, and 2 mM dithiothreitol, was used for the enzyme assay.

RNase and RNase-Inhibitor Assays Assay of free RNase activity was performed according to the procedure described previously.[21] The reaction mixture (0.2 ml) contained 50 mM Tris–HCl (pH 7.5), 20 mM ethylenediaminetetraacetic acid (EDTA), 200 μg of yeast RNA, and S-100. After incubation of the reaction mixture at 37 °C for 60 min, the reaction was terminated by the addition of 0.2 ml of 5% perchloric acid containing 0.25% uranyl acetate. The mixture was centrifuged after being cooled in

an ice-bath for 20 min, and the resulting supernatant fraction was diluted with 4 vols. of distilled water. The acid-soluble nucleotides were measured at 260 nm.

In order to measure the total RNase activity, 40 μl of 2.5 mM *p*-chloromercuribenzenesulfonic acid, which completely inactivates the RNase-inhibitor in S-100, was added to the reaction mixture for the free RNase assay. Other conditions were the same as those described above.

One unit of the free and total RNase activities was defined as the amount of enzyme which caused an increase in absorbance at 260 nm of 0.1 under the above conditions.

Assay of free RNase-inhibitor activity was performed by the method of Shortman[22] with a slight modification. The reaction mixture contained 50 mM Tris–HCl (pH 7.5), 20 mM EDTA, 200 μg of RNA, 20 μg of bovine serum albumin, 2 ng of RNase A, and S-100. Other conditions were the same as those of free RNase assay except that the incubation was carried out for 30 min.

One unit of free RNase-inhibitor activity was defined as the amount of inhibitor which produced 50% inhibition of 2 ng of RNase A activity under the above conditions.

Protein Estimation Protein determination was performed according to the method of Lowry *et al.*[23] using bovine serum albumin as standard.

Results and Discussion

Changes in Weight, Free RNase-Inhibitor Activity, and Free and Total RNase Activities of Ventral and Dorsal Prostates of Rats at Different Stages of Growth Changes in the prostate weight at different stages of growth are shown in Fig. 1. The weight of ventral and dorsal prostates increased progressively in from 3- to 8-week-old rats.

As shown in Fig. 2, free RNase-inhibitor activities in both prostates had their highest peaks in 4-week-old animals and smallest peaks at around 7-weeks. Free RNase-inhibitor activity in the ventral prostate was higher than that in the dorsal prostate. Matsuo *et al.*[24] reported that serum concentration of testosterone in rats began to increase at about 4 weeks after birth. Our results show that ventral and dorsal prostates contain the highest free RNase-inhibitor activity at 4-weeks. Therefore, it is suggested that the increase in free RNase-inhibitor activity in both prostates of 4-week-old rats may be due to the secretion of androgen.

As shown in Fig. 3, total RNase activity in the ventral prostate decreased overall with age, while that in the dorsal prostate increased. Neither the ventral nor the dorsal prostate contained any significant amount of free RNase activity. Thus, all RNases existed as complex with the RNase-inhibitor in both prostates.

When RNase–RNase inhibitor complex obtained by DEAE-Toyopearl chromatography of S-100 from ventral and dorsal prostates was analyzed on sodium dodecylsulfate polyacrylamide gels by activity staining, two bands of RNase activity with molecular weights of 14000 and 16000 were detected in the dorsal prostate. In the ventral prostate, however, only one band with molecular weight of 14000 was observed. One possible explanation for the difference in changes in total RNase activity with age between the two prostates is as follows. In the ventral prostate, the decrease in activity might be due to the decrease in RNase with a molecular weight of 14000, while in the dorsal prostate, the increase in activity might be due to the increase in RNase with a molecular weight of 16000 rather than the change in RNase with a molecular weight of 14000.

Effect of Castration and Testosterone Administration on Weight, Protein Content, Free RNase-Inhibitor Activity, and Free and Total RNase Activities of Ventral and Dorsal

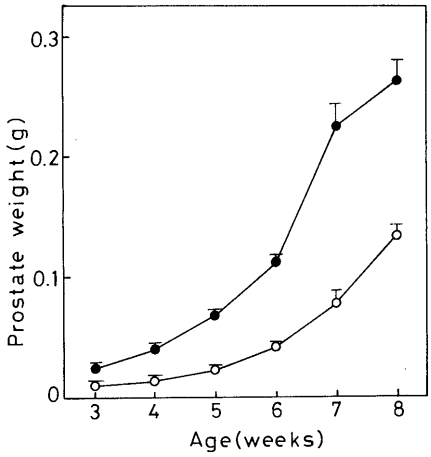

Fig. 1. Changes in Rat Prostate Weight at Different Stages of Growth

Rats used were 41.2 g (3-week-old), 81.2 g (4-week-old), 119.1 g (5-week-old), 181.2 g (6-week-old), 258.4 g (7-week-old), and 306.0 g (8-week-old) mean body-weight. Ventral (●) and dorsal (○) prostates from 1—14 rats were pooled separately for each experimental group. Each point represents mean±S.E.M. of 3—5 experiments.

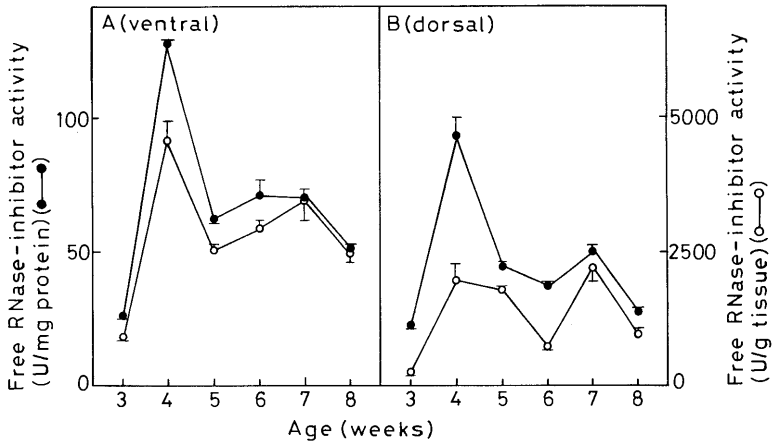

Fig. 2. Changes in Free RNase-Inhibitor Activity in Rat Prostates at Different Stages of Growth

Rats used were the same as described in the legend to Fig. 1. Ventral and dorsal prostates from 1—14 rats were pooled separately for each experimental group. S-100 was prepared from each prostate sample and assayed for free RNase-inhibitor activity as described in Materials and Methods. Each point represents mean±S.E.M. of 3—5 experiments.

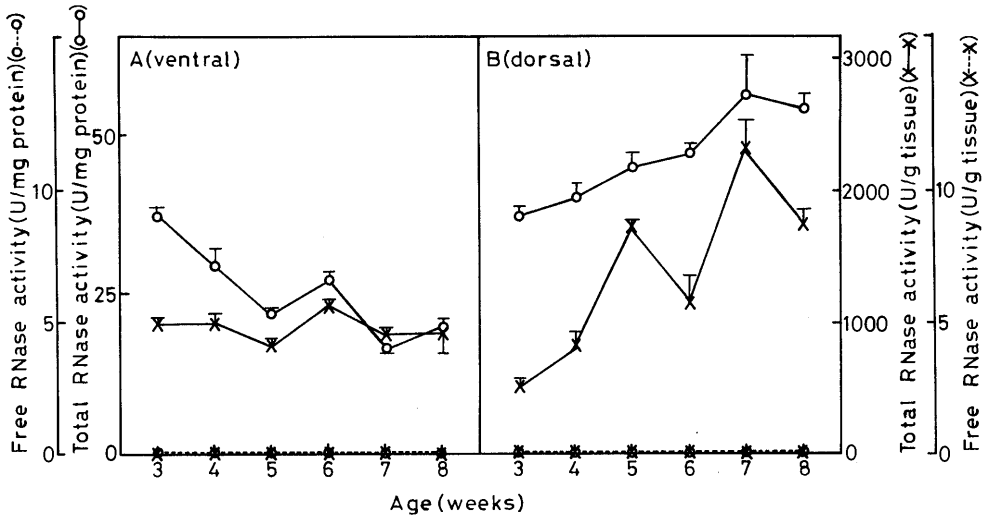

Fig. 3. Changes in Free and Total RNase Activities in Ventral (A) and Dorsal (B) Prostates from Rats at Different Stages of Growth

Rats used were the same as described in the legend to Fig. 1. S-100 was prepared from each prostate sample and assayed for free and total RNase activities as described in Materials and Methods. Each point represents mean ± S.E.M. of 3—5 experiments.

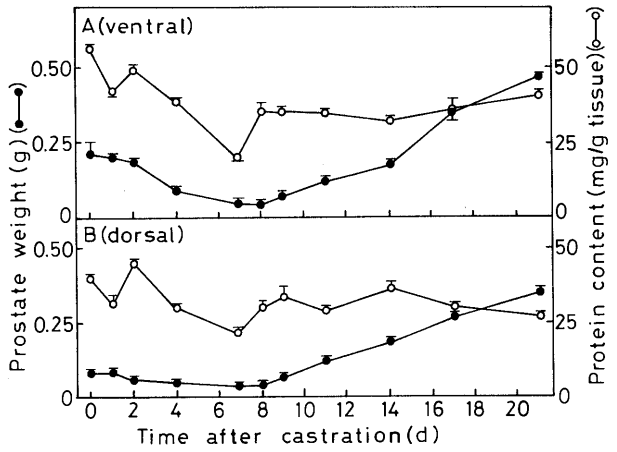

Fig. 4. Effect of Castration and Testosterone Administration on Weight and Protein Content of Rat Prostates

Seven-week-old rats (258.4 g mean body-weight) were castrated. At 1, 2, 4, and 7 d after castration, they were sacrified by exsanguination and ventral and dorsal prostates were excised from 1—5 animals for each experimental group. Each prostate sample was weighed and protein content determined as described in Materials and Methods.

Starting on the seventh day after castration, rats were injected subcutaneously with 2 mg of testosterone propionate per 100 g body weight every 24 h. They were sacrified at 1, 2, 4, 7, 10, and 14 d after the start of testosterone treatment, and ventral and dorsal prostates were excised from 1—5 animals for each experimental group. Weight of ventral and dorsal prostates and their protein content were measured. Each point represents mean ± S.E.M. of 3—5 experiments.

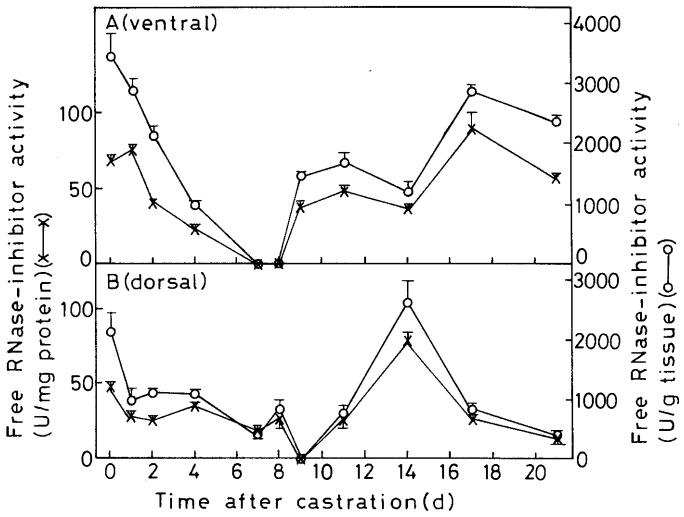

Fig. 5. Effect of Castration and Testosterone Administration on Free RNase-Inhibitor activity of Rat Prostates

Rats used and the treatment of animals were the same as described in the legend to Fig. 4. S-100 was prepared from each prostate sample and assayed for free RNase-inhibitor activity as described in Materials and Methods. Each point represents mean ± S.E.M. of 3—5 experiments.

Prostates of Rats As shown in Fig. 4, a significant decrease in weight and protein content of the two prostates was observed following castration, but the weight was increased by testosterone administration. Weight of the ventral prostate returned to control value (the value just prior castration) between 7 and 8 d after the beginning of testosterone administration, while that of the dorsal prostate returned to control value after just 2—3 d. Protein content of both prostates increased 1 or 2 d after testosterone administration and no remarkable changes were observed thereafter. As shown in Fig. 5, free RNase-inhibitor activity in both glands decreased after castration and by 7 d had disappeared from the ventral prostate. No free RNase-inhibitor activity was detected in this prostate 1 d after the beginning of testosterone administration, but activity was restored almost to control value after 10 d of daily testosterone injection. In the dorsal prostate, free RNase-inhibitor activity was not detected 2 d after the beginning of testosterone administration, but after 7 d, maximal activity was observed; this was followed by a marked fall within a few days.

As shown in Fig. 6, total RNase activity in the ventral prostate was increased by castration and decreased by testosterone administration. Free RNase activity in this prostate was not detected until 4 d after castration, but after 7 d, a large amount of the activity was found. The value of this activity was almost equal to that of total RNase activity, suggesting that RNase did not exist as complex with RNase-inhibitor 7 d after castration. The free RNase activity in the ventral prostate of castrated rats was decreased by testosterone administration. In the dorsal

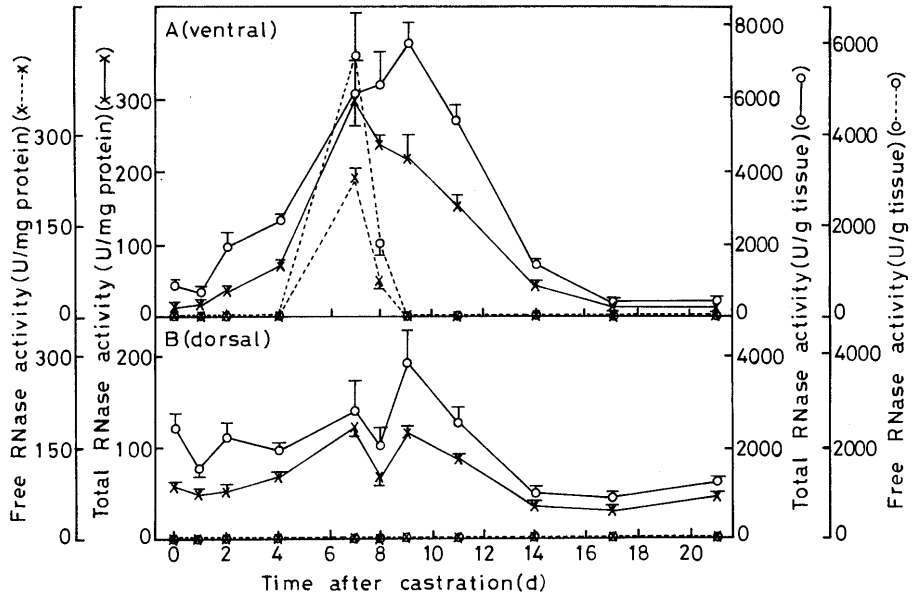

Fig. 6. Effect of Castration and Testosterone Administration on Free and Total RNase Activities of Rat Prostates

Rats used and the treatment of animals were the same as described in the legend to Fig. 4. S-100 was prepared from each prostate sample and assayed for free and total RNase activities as described in Materials and Methods. Each point represents mean ± S.E.M. of 3—5 experiments.

prostate, total RNase activity had two peaks: one was observed 7 d after castration and the other 2 d after the beginning of testosterone administration. Free RNase activity was not found in the dorsal prostate after castration and the subsequent treatment.

Our results suggest that changes in the levels of free RNase-inhibitor activity and free and total RNase activities in the ventral prostate are dependent on the amount of androgen, and that this is also true in the dorsal prostate but to a lesser degree.

Coffey *et al.*[25] reported that RNA content in the ventral prostate decreased after castration and increased after injection of testosterone to castrated rats. In the present study, castration decreased the free RNase-inhibitor activity in the animals but increased free RNase activity in this prostate. However, with the growth response to androgenic stimulation of the ventral prostate, free RNase-inhibitor activity increased and free RNase activity decreased. Our results therefore suggest that changes in the level of RNase-inhibitor in ventral and dorsal prostates are involved in the regulation of their RNA content through the control of free RNase activity.

It was reported that after injection of labeled testosterone to castrated rats, uptake of the radioactivity by the ventral prostate was 3 times higher than that by the dorsal prostate.[26] Our data show that changes in the levels of weight, protein content, free RNase-inhibitor activity, and free and total RNase activities in the dorsal prostate were all smaller than those in the ventral prostate following testosterone administration. This difference in the two glands might be due to the difference in the uptake of testosterone.

Shimazaki *et al.*[27] and Moore and Wilson[28] reported that 5α-reductase activity in the rat ventral prostate was decreased by castration and increased by testosterone administration. Mainwaring and Mangan[29] reported that the amount of dihydrotestosterone receptor protein decreased in the rat ventral prostate after castration. These results suggest that changes in the levels of 5α-reductase activity and amount of dihydrotestosterone receptor are dependent on the amount of testosterone in the rat ventral prostate. Therefore, there is another possibility that the difference in weight, protein content, free RNase-inhibitor activity, and free and total RNase activities between ventral and dorsal prostates might be due to differences in the activity of 5α-reductase and the amount of dihydrotestosterone receptor in the two glands.

References

1) J. S. Roth, *Methods Cancer Res.*, **3**, 153 (1967).
2) H. Sierakowska and D. Shugar, *Prog. Nucleic Acid Res. Mol. Biol.*, **20**, 60 (1977).
3) P. Blackburn, G. Wilson and S. Moore, *J. Biol. Chem.*, **252**, 5904 (1977).
4) K. Shortman, *Biochim. Biophys. Acta*, **61**, 50 (1962).
5) N. Kraft and K. Shortman, *Biochim. Biophys. Acta*, **217**, 164 (1970).
6) D. K. Liu, G. H. Williams and P. J. Fritz, *Biochem. J.*, **148**, 67 (1975).
7) G. A. J. goodlad and G. Y. Ma, *Biochim. Biophys. Acta*, **378**, 221 (1975).
8) D. K. Liu and P. E. Matrisian, *Biochem. J.*, **164**, 371 (1977).
9) R. C. Imarie and W. C. Hutchison, *Biochim. Biophys. Acta*, **108**, 106 (1965).
10) R. L. Greif and E. F. Eich, *Biochim. Biophys. Acta*, **286**, 350 (1972).
11) R. C. Schauer, *Horm. Metab. Res.*, **13**, 50 (1981).
12) C. W. McGregor, A. Adams and J. T. Knowler, *J. Steroid Biochem.*, **14**, 415 (1981).
13) N. A. Brockdorff and J. T. Knowler, *Mol. Cell. Endocrinology*, **44**, 117 (1986).
14) J. Munro and J. T. Knowler, *J. Steroid Biochem.*, **16**, 293 (1982).
15) M. Zan-Kowalczewska and J. S. Roth, *Biochem. Biophys. Res. Commun.*, **65**, 833 (1975).
16) J. M. Fominaya, J. M. Garcia-Sequra and J. G. Gavilanes, *Biochim. Biophys. Acta*, **954**, 216 (1988).
17) R. M. Kershner and W. L. Meyer, *Biochem. Biophys. Res. Commun.*, **70**, 513 (1976).
18) S. Hirose, H. Kumagai, M. Yoshikawa, T. Mikami and K. Igarashi, *J. Biochem.* (Tokyo), **82**, 1605 (1977).
19) H. Kumagai, K. Igarashi, M. Yoshikawa and S. Hirose, *J. Biochem.* (Tokyo), **81**, 381 (1977).
20) H. Kumagai, K. Igarashi, K. Tanaka, H. Nakao and S. Hirose,

Biochim. Biophys. Acta, **566**, 192 (1979).
21) H. Kumagai, H. Kato, K. Igarashi and S. Hirose, *J. Biochem.* (Tokyo), **94**, 71 (1983).
22) K. Shortman, *Biochim. Biophys. Acta*, **51**, 37 (1961).
23) O. H. Lowry, N. J. Rosebrough, A. L. Farr and R. J. Randall, *J. Biol. Chem.*, **191**, 265 (1951).
24) Y. Matsuo, N. Nishi and F. Wada, *Tampakushitsu Kakusan Koso*, **32**, 1126 (1987).
25) D. S. Coffey, J. Shimazaki and G. H. Williams-Ashman, *Arch. Biochem. Biophys.*, **124**, 181 (1968).
26) K. J. Tveter and A. Aakvaag, *Endocrinology*, **85**, 683 (1969).
27) J. Shimazaki, I. Matsushita, N. Furuya, H. Yamanaka and K. Shida, *Endocrinol. Jpn.*, **16**, 453 (1969).
28) R. J. Moore and J. D. Wilson, *Endocrinology*, **93**, 581 (1973).
29) W. I. P. Mainwaring and F. R. Mangan, *J. Endocrinol.*, **59**, 121 (1973).

Inhibitory Effects of Sulfur Compounds on Melanin Formation Reaction by Tyrosinase

Noriko MOTOHASHI,* Harumi NISHIKAWA and Itsuhiko MORI

Department of Radiopharmaceutical Chemistry, Kobe Women's College of Pharmacy, 4–19–1 Motoyamakita-machi, Higashinada-ku, Kobe 658, Japan. *Received June 25, 1990*

The inhibitory effects of sulfur compounds, namely cysteine and α-mercaptopropionylglycine (α-MPG) (thiol type), and *N*-methyl-2-mercaptoimidazole (MMI), 6-propylthiouracil (PTU) and ergothioneine (ESH) (thione type) on melanin formation reaction by tyrosinase, in the presence of tyrosine as a substrate, were assessed. Tyrosine oxidation was monitored both by radioassay using L-[3,5-^{3}H]tyrosine, L-[2,6-^{3}H]tyrosine and L-[carboxyl-^{14}C]tyrosine as substrates, and by spectrometry to quantitate the dopachrome formed from L-tyrosine. The rated compounds, ranked as to inhibitory effect in descending order are: cysteine ≃ α-MPG > MMI > PTU > ESH. Cysteine and α-MPG, both noncyclic thiol compounds, formed a 3,4-dihydroxyphenylalanine (dopa) conjugate to inhibit melanin formation when added at low concentrations. At high concentrations, they inactivated the enzyme by interacting with tyrosinase. In MMI, PTU and ESH of heterocyclic thione structure, dopa conjugate formation was more inhibitory than tyrosinase inactivation on melanin formation.

Keywords melanin; sulfur compound; 3,4-dihydroxyphenylalanine conjugate; tyrosinase; radioassay

Tyrosinase, a copper-containing mixed-function oxidase or monooxygenase, catalyzes phenol-*o*-hydroxylation (1) and dehydrogenation (2).

$$\text{monohydroxyphenol} + O_2 + 2H^+ \rightarrow o\text{-dihydroxyphenol} + H_2O \quad (1)$$

$$2o\text{-dihydroxyphenol} + O_2 \rightarrow 2o\text{-quinone} + 2H_2O \quad (2)$$

It catalyzes the reaction of melanin formation from tyrosine *in vivo* (Chart 1).[1] Makino *et al.*[2] showed that the two divalent copper atoms in tyrosinase have been coupled to form antiferromagnetic electron spin resonance (ESR)-undetectable copper. On the other hand, sulfur-containing amino acids of the thiol type, such as cysteine and glutathione, and other bioactive sulfur compounds of the thione type[3] used as antithyroidal drugs, such as *N*-methyl-2-mercapto-imidazole (MMI) and 6-propylthiouracil (PTU), have been reported as inhibiting the activities of copper-containing enzymes such as dopamine-β-hydroxylase and tyrosinase.[4–8] Also, cysteinyldopa, a conjugate of 3,4-dihydroxyphenylalanine (dopa) and cysteine, has been detected in urine and serum collected from malignant melanoma patients.[9,10]

With this as background, the present authors attempted to assess the inhibitory effects of thiol compounds such as cysteine and α-mercaptopropionylglycine (α-MPG), and thione compounds such as MMI, PTU and ergothioneine (ESH)[3] on melanin formation reaction catalysis by tyrosinase. α-MPG forms a stable complex with copper[11,12] and ESH occurs abundantly *in vivo*.[13] Sulfur compounds used are shown in Fig. 1.

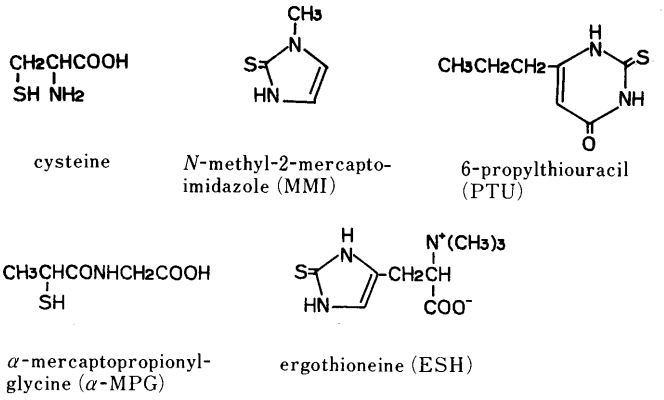

Fig. 1. Structure of Sulfur Compounds Used

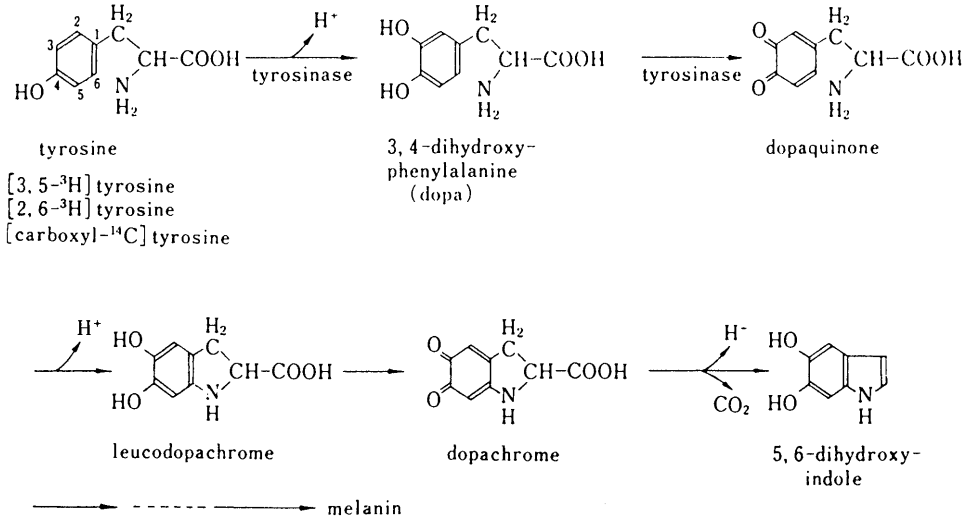

Chart 1. Scheme for the Production of Melanin by the Oxidation of Tyrosine[1]

Experimental

Materials Tyrosinase extracted and purified from mushrooms (grade III) was purchased from Sigma. L-[3,5-^{3}H]Tyrosine (1.48 MBq/μmol), L-[2,6-^{3}H]tyrosine (1.48 MBq/μmol) and L-[carboxyl-^{14}C]tyrosine (2.1 GBq/μmol), each in a 2% ethanol solution, were purchased from Amersham. The ^{3}H- and ^{14}C-tyrosine were used in a 25 mM phosphate buffer (pH 6.8) after the solvent was evaporated to dryness in nitrogen gas. α-MPG and ESH were purchased from Sigma. MMI was purchased from K & K Laboratories. Cysteine and PTU were purchased from Wako Pure Chemical. All other reagents were commercially available reagents of special grade.

Tyrosine Oxidation The starting reaction mixture was comprised of 0.4 mM L-tyrosine, 37 kBq L-^{3}H-tyrosine, 3.7 kBq L-^{14}C-tyrosine, 0 to 10 mM of a sulfur-containing compound (cysteine, α-MPG, MMI, PTU, ESH) and 100 units of tyrosinase per milliliter of 25 mM phosphate buffer (pH 6.8). The reaction was carried out at 37 °C and was terminated by adding 0.2 ml of 40% metaphosphoric acid. The progress of the reaction was monitored by radioassay using ^{3}H- and ^{14}C-tyrosine as substrates in accordance with the previous report.[14] Dopa formation and leucodopachrome formation were determined by measuring the radioactivities of 3-^{3}H released from L-[3,5-^{3}H]tyrosine and those of 6-^{3}H released from L-[2,6-^{3}H]tyrosine, respectively, both measured as ^3H_2O. 5,6-Dihydroxyindole formation was determined by measuring the residual radioactivities after $^{14}CO_2$ was released from L-[carboxyl-^{14}C]tyrosine. In these determinations, radioactivities were measured using a liquid scintillation counter. Dopachrome formation was determined by the Shimadzu recording spectrometer, Model UV 200, at a wavelength of 475 nm (ε 3700)[15] using nonradioactive tyrosine as a substrate.

Results and Discussion

Effects of Reducing Agents on Tyrosinase Tyrosinase exhibits its activities when it is in the form of oxy type monovalent copper, though its active center copper exists in divalent form when in the inactive state.[16] Taking note of this fact, comparisons were made between hydroxylamine, which reduces divalent copper to monovalent, and cysteine and α-MPG, both of which have a reductive effect due to their thiol groups. Tyrosinase and these compounds were each incubated at 37 °C for 30 min, after which their effects on the activities of tyrosinase, in the presence of L-[3,5-^{3}H]tyrosine as a substrate, were rated. The results are shown in Fig. 2. Hydroxylamine had almost no influence on tyrosinase activities, while cysteine and α-MPG markedly inhibited the activities. Aasa *et al.*[17] reported that cysteine acts on the active center copper in tyrosinase to form an enzymatically inert complex, and that α-MPG denatures the tyrosinase enzyme. Thus, the results shown in Fig. 2 suggest that tyrosinase was inactivated by pretreatment with cysteine and α-MPG.

Effects of Sulfur Compounds on Tyrosine Hydroxylation The effects of cysteine, α-MPG, MMI, PTU and ESH on tyrosine hydroxylation by tyrosinase, in the presence of L-[3,5-^{3}H]tyrosine as a substrate, were assessed. The results are shown in Table I. None of the subject thiol compounds of non-cyclic structure, *i.e.*, cysteine and α-MPG, had any inhibitory effect when added in a ratio of one-tenth the substrate tyrosine on a molar basis, *i.e.*, at a concentration of 0.04 mM. However, when added at a concentration of 0.4 mM, equivalent to the amount of the substrate, these two compounds showed a marked inhibitory effect of 97 and 91%, respectively. On the other hand, MMI, PTU and ESH, all of the thione compounds with a heterocyclic structure, showed an inhibitory effect of several % even when added at 0.04 mM. However, even when the concentration was increased to 4 mM *i.e.*, 10 times the amount of the substrate, their inhibitory rates were 76, 66 and 46%, respectively. Further investigation was then conducted using two groups, one comprising cysteine and α-MPG of thiol structure, the other MMI, PTU and ESH of thione structure.

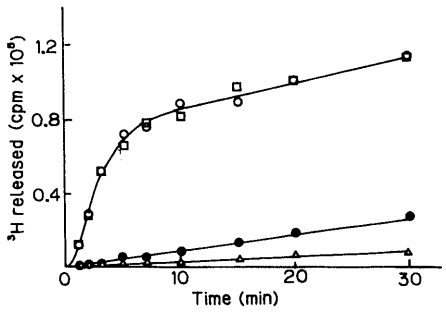

Fig. 2. Effects of Reducing Agents on Tyrosinase

The reaction mixture contained 0.4 mM L-tyrosine, 14.8 kBq of L-[3,5-^{3}H]tyrosine and 100 units of tyrosinase in 1 ml of 25 mM phosphate buffer, pH 6.8. The enzyme was preincubated with 0.4 mM reducing agent at 37 °C for 30 min. ○, control; △, added cysteine; ●, added α-MPG and □, added hydroxylamine.

Effects of Cysteine and α-MPG on Tyrosine Oxidation Figure 3 shows the effects of cysteine (I) and α-MPG (II) on tyrosine oxidation when the substrate was L-[3,5-^{3}H]-tyrosine (a), L-[2,6-^{3}H]tyrosine (b), L-tyrosine (c) or L-[carboxyl-^{14}C]tyrosine (d). When added at a concentration of 0.04 mM, cysteine and α-MPG both showed a lag time in all reaction stages (a, b, c, d). Subsequently, however, the reaction rate became nearly the same as in the control. The lag time is due to the ability of thiol compounds used to reduce dopaquinone back to dopa. In the reaction using ^{3}H-tyrosine, H release was accelerated over the control 15 to 25 min after initiation of the reaction (Fig. 3, Aa, Ba, b). It is reported that cysteine and glutathione each form a conjugate with pyrocatechol or dopa by the action of tyrosinase.[5,18] Also, Ito *et al.*[19] reported that the cysteine–dopa conjugate formed by the action of tyrosinase is essentially 5-S-cysteinyldopa, involving a bond between the 5-position of the benzene ring in dopa and the S atom in cysteine. Thus, it is thought that the H released in excess of the control when 0.04 mM cysteine was added (Fig. 3, Aa) is attributable to the release of 5-H due to the

TABLE I. Effects of Sulfur Compounds on Tyrosine Hydroxylation by Tyrosinase

Sulfur compound added	Concentration (mM)	% inhibition
Cysteine	0.04	0
	0.4	97
α-Mercaptopropionylglycine	0.04	0
	0.4	91
N-Methyl-2-mercaptoimidazole	0.04	16
	0.4	46
	4.0	76
6-Propylthiouracil	0.04	8
	0.4	30
	4.0	66
Ergothioneine	0.04	4
	0.4	17
	4.0	46

% inhibition was calculated using an equation of $(N_0-N)/N_0 \times 100$. N_0 and N represent the radioactivity of ^{3}H released from tyrosine without and with a sulfur compound, respectively. The reaction mixture contained 0.4 mM L-tyrosine, 14.8 kBq of L-(3,5-^{3}H)tyrosine, indicated amounts of sulfur compounds and 100 units of tyrosinase in 1 ml of 25 mM phosphate buffer, pH 6.8. The reaction was performed at 37 °C for 10 min.

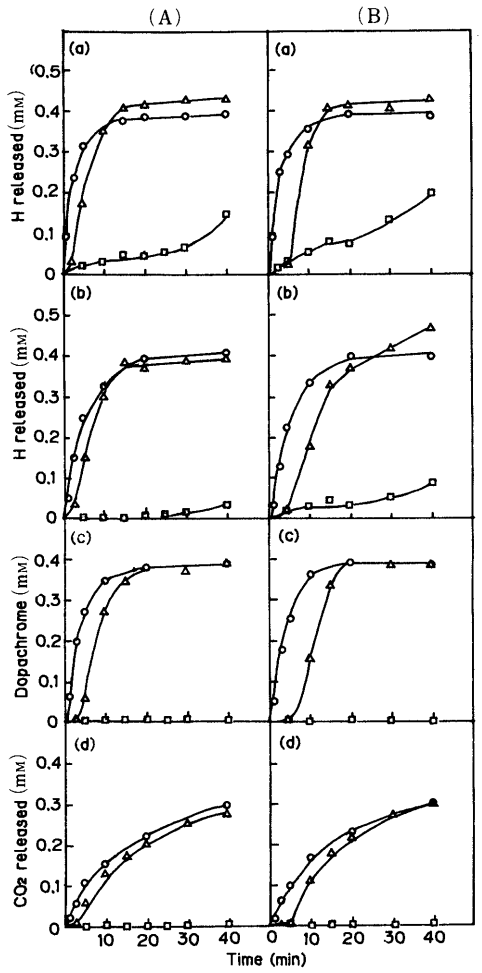

Fig. 3. Effects of Cysteine (A) and α-MPG (B) on Tyrosine Oxidation

The reaction mixture contained 0.4 mM L-tyrosine, 100 units of tyrosinase and cysteine or α-MPG in 1 ml of 25 mM phosphate buffer, pH 6.8. The radioactive substrates of 37 kBq of ^{3}H-tyrosine and 3.7 kBq of ^{14}C-tyrosine were added as indicated above. Cysteine and α-MPG were added to give the final concentration of 0 (○), 0.04 (△), and 0.4 mM (□).

(a) L-[3,5-^{3}H]tyrosine; (b) L-[2,6-^{3}H]tyrosine; (c) L-tyrosine; (d) L-[carboxyl-^{14}C]tyrosine.

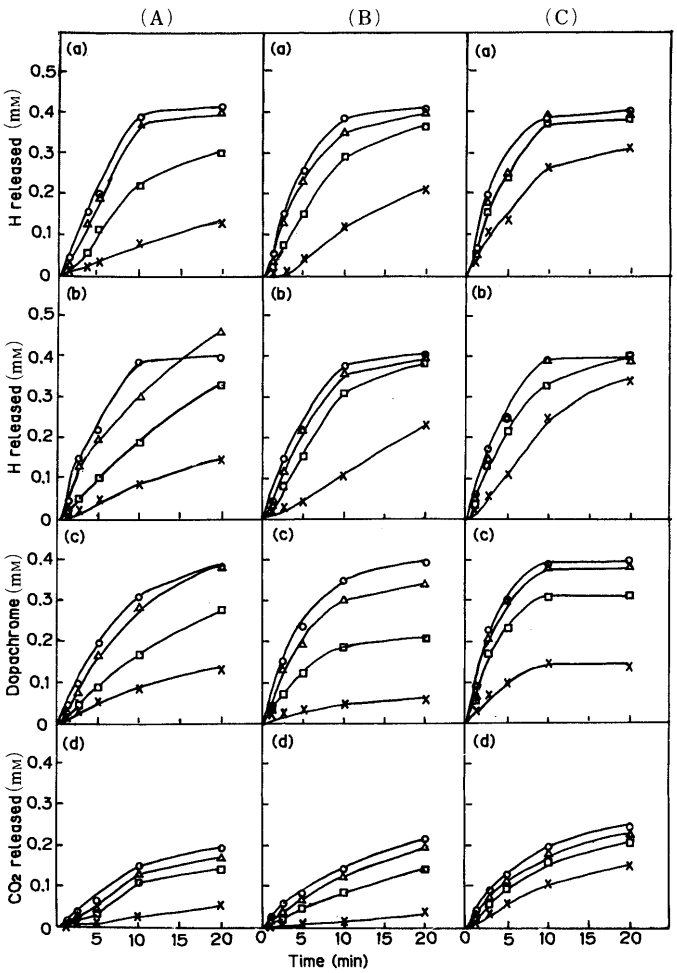

Fig. 4. Effects of MMI (A), PTU (B) and ESH (C) on Tyrosine Oxidation

The reaction mixture contained 0.4 mM L-tyrosine, 100 units of tyrosinase and MMI, PTU and ESH in 1 ml of 25 mM phosphate buffer, pH 6.8. The radioactive substrates of 37 kBq of ^{3}H-tyrosine and 3.7 kBq of ^{14}C-tyrosine were added as indicated above. MMI, PTU and ESH were added to give the final concentration of 0 (○), 0.04 (△), 0.4 (□) and 4 mM (×).

(a) L-[3,5-^{3}H]tyrosine; (b) L-[2,6-^{3}H]tyrosine; (c) L-tyrosine; (d) L-[carboxyl-^{14}C]tyrosine.

formation of 5-S-conjugate as well as to the release of 3-H. Even when α-MPG concentration was 0.04 mM, there was a tendency similar to that noted with cysteine in the reaction using L-[3,5-^{3}H]tyrosine as a substrate (Fig. 3, Ba). In addition, H release increased 25 min after, when L-[2,6-^{3}H]tyrosine was used as a substrate (Fig. 3, Bb). These findings suggest that α-MPG forms the conjugate with dopa at the 2-, 5- and 6-positions of dopa. Also, when cysteine or α-MPG was added at 0.4 mM, only a slight H release occurred (Fig. 3, a, b), but the reaction after dopachrome formation was completely inhibited (Fig. 3, c, d), suggesting the significant contribution of these compounds to tyrosinase inactivation.

Effects of MMI, PTU and ESH on Tyrosine Oxidation Figure 4 shows the effects of MMI (A), PTU (B) and ESH (C) on tyrosine oxidation. Table II shows their 50% inhibitory concentrations (I_{50}). All three, when added at 4 mM, produced a whitish-brown precipitate after several hours of reaction. Of the three, MMI most strongly inhibited the reaction using ^{3}H-tyrosine as a substrate (Table II). However, when L-[2,6-^{3}H]tyrosine was used as a substrate, 0.04 mM MMI addition caused the release of more H than with the control (Fig. 4, Ab). When the mixture with 4 mM MMI was kept standing for a long time, the whitish-brown precipitate changed gradually to black in color. Notably, MMI has been reported as forming a stable complex with divalent copper ions.[20] It has also been conjectured that MMI forms a complex with tyrosinase active center copper.[7] Also, it is known that MMI non-enzymatically binds to *o*-quinone at the 5- or 6-position of

Table II. Effects of Sulfur Compounds on Tyrosine Oxidation

Sulfur compound added	I_{50}[a] (mM)		
	L-(3,5-^{3}H)-Tyrosine[b]	L-(2,6-^{3}H)-Tyrosine[b]	L-(Carboxyl-^{14}C)-tyrosine[b]
N-Methyl-2-mercapto-imidazole	0.5	0.7	0.6
6-Propylthiouracil	1.6	0.8	0.2
Ergothioneine	8.0	1.6	0.9

a) Concentration of sulfur compounds producing 50% inhibition of initial rate of tyrosinase oxidation. *b*) Radioactive substrate used.

the latter to form an MMI-pyrocatechol conjugate.[21] It can therefore be considered that MMI inhibits melanin formation not only by the inactivating action arising from the formation of a complex with tyrosinase active center copper, but also by dopa conjugate formation *via* a reaction with dopaquinone. The melanin formation noted after the mixture was kept standing for a long time is attributable to the fact that the MMI–dopa conjugate is unstable, while the cysteine–dopa conjugate is so stable that it does not serve as a substrate for tyrosinase.[5]

In comparison with MMI, PTU had less inhibitory effect on the reaction using ^{3}H-tyrosine as a substrate, but had a greater inhibitory effect on the reaction using ^{14}C-tyrosine as a substrate (Table II). Since PTU is not likely to form a stable complex with divalent copper ions,[22] its interaction with tyrosinase active center copper is considered weak. Whittaker[23] synthesized melanin containing PTU and reported that PTU binds to an intermediate for melanin formation. In the present study, the release of H was not significantly inhibited in the reaction using ^{3}H-tyrosine as a substrate in the presence of PTU (Fig. 4, Ba, b), while dopachrome formation and CO_2 release were inhibited to increasing degrees with PTU concentration (Fig. 4, Bc, d). These findings suggest that PTU increased the release of H by binding to dopaquinone, a tyrosine oxidation product, at the 2-, 5- and 6-positions of the benzene ring of the latter, as well as inhibiting the tyrosinase activities.

ESH was less effective in comparison with MMI and PTU irrespective of the type of reaction substrate (Table II). It should be noted, however, that the I_{50} of ESH, obtained using L-[3,5-^{3}H]tyrosine as a substrate, was 16 times that of MMI, but decreased to 1.5 times that of MMI when ^{14}C-tyrosine was used as a substrate. This I_{50} value for ^{14}C-tyrosine suggests that ESH inactivated tyrosinase to almost the same extent as with MMI. It is reported that ESH in excess forms a monovalent copper complex with divalent copper ions by the weak reductive action of thiolate anions.[20] It can therefore be inferred that ESH, like MMI, inactivates tyrosinase by interaction with tyrosinase active center copper. On the other hand, the I_{50} of ESH obtained using L-[3,5-^{3}H]tyrosine as a substrate was 5 times that obtained with L-[2,6-^{3}H]tyrosine, which was considerably greater than the I_{50} ratios of MMI and PTU (MMI, 0.7; PTU, 2). Thus, it can be inferred that the H released when using L-[3,5-^{3}H]tyrosine (Fig. 4, Ca) includes, in addition to 3-H, 5-H released upon formation of the conjugate of ESH with dopaquinone at the 5-position of the benzene ring of the latter.

As stated above, the mode of inhibition of melanin formation reaction by sulfur compounds differed slightly between noncyclic thiol compounds and heterocyclic thione compounds. To summarize, in cysteine and α-MPG, the inhibitory action was due to tyrosinase inactivation by their interaction with tyrosinase active center copper when they were added at high concentrations. When added at low concentrations, their inhibitory action was due to the formation of a conjugate with dopaquinone, a tyrosine oxidation product. In MMI, PTU and ESH, it was inferred that conjugate formation was more effective than tyrosinase inactivation. The rated compounds, ranked as to inhibitory effect in the descending order, are: cysteine $\simeq$ α-MPG > MMI > PTU > ESH.

References

1) *a*) H. S. Mason, "Pigment Cell Biology," ed. by M. Gordon, Academic Press, New York, 1959, pp. 563—582; *b*) M. S. Blois, *Photochem. Photobiol. Rev.*, **3**, 115 (1978); *c*) V. J. Hesring, Jr., T. M. Ekel, P. M. Montague and J. M. Nicholson, *Biochim. Biophys. Acta*, **611**, 251 (1980).
2) N. Makino, P. McMahill, H. S. Mason and T. H. Moss, *J. Biol. Chem.*, **249**, 6062 (1974).
3) N. Motohashi, I. Mori and Y. Sugiura, *Chem. Pharm. Bull.*, **24**, 1737 (1976).
4) D. P. Hanlon, *J. Med. Chem.*, **14**, 1084 (1974).
5) H. Sanada, R. Suzue, Y. Nakashima and S. Kawada, *Biochim. Biophys. Acta*, **261**, 258 (1972).
6) M. Fujii, N. Hirano, T. Izumi and T. Furuya, *Saga Daigaku Nogaku Iho*, **36**, 95 (1974) [*Chem. Abstr.*, **81**, 102270*c* (1974)].
7) D. P. Hanlon and S. Shuman, *Experientia*, **31**, 1005 (1975).
8) H. Hidaka and A. Nagasaka, *Biochem. Pharmacol.*, **26**, 1092 (1977).
9) G. Agrup, C. Hansson, B.-M. Kennedy, K. Person, H. Rorsman, A.-M. Rosengren and E. Rosengren, *Acta Dermatovener* (Stockholm), **56**, 491 (1976).
10) G. Prota, H. Rorsman, A.-M. Rosengren and E. Rosengren, *Experientia*, **33**, 720 (1977).
11) Y. Sugiura, Y. Hirayama, H. Tanaka and K. Ishizu, *J. Am. Chem. Soc.*, **97**, 5577 (1975).
12) Y. Sugiura, *Eur. J. Biochem.*, **78**, 431 (1977).
13) P. C. Jecelyn, "Biochemistry of the SH Group," Academic Press, New York, 1972, p. 10.
14) N. Motohashi, H. Eguchi and I. Mori, *Chem. Pharm. Bull.*, **30**, 2094 (1982).
15) S. H. Pomerantz, *J. Biol. Chem.*, **238**, 2351 (1963).
16) R. L. Jolley, Jr., L. H. Evans, N. Makino and H. S. Mason, *J. Biol. Chem.*, **249**, 335 (1974).
17) R. Aasa, J. Deinum, K. Lerch and B. Reinhammer, *Biochim. Biopys. Acta*, **535**, 287 (1978).
18) H. S. Mason and E. W. Peterson, *Biochim. Biophys. Acta*, **111**, 134 (1965).
19) S. Ito and G. Prota, *Experientia*, **33**, 1118 (1977).
20) N. Motohashi, I. Mori and Y. Sugiura, *Chem. Pharm. Bull.*, **24**, 2364 (1976).
21) A. Andrawis and V. Kahn, *Biochem. J.*, **235**, 91 (1986).
22) E. R. Garrett and D. J. Weber, *J. Pharm. Sci.*, **59**, 1383 (1970); *idem ibid.*, **60**, 845 (1971).
23) J. R. Whittaker, *J. Biol. Chem.*, **246**, 6217 (1971).

A Putative Mouse Oocyte Maturation Inhibitory Protein from Urine of Pregnant Women: N-Terminal Sequence Homology with Human Nonsecretory Ribonuclease

Ryuzo SAKAKIBARA,*[,a] Kayo HASHIDA,[a] Nobuaki TOMINAGA,[a] Kazuya SAKAI,[a] Masatsune ISHIGURO,[a] Sadaomi IMAMURA,[b] Fumiko OHMATSU,[b] and Eimei SATO[c]

Department of Biochemistry, School of Pharmaceutical Sciences, Nagasaki University,[a] 1–14 Bunkyo-machi, Nagasaki 852, Japan, Imamura Women's Hospital,[b] 2–17 Ooura-machi, Nagasaki 852, Japan and Department of Animal Science, Faculty of Agriculture, Kyoto University,[c] Kyoto 606, Japan. *Received July 6, 1990*

A putative mouse oocyte maturation inhibitory protein was purified from a urine preparation from pregnant women by Sephadex G-100 gel filtration and reverse-phase chromatography on the basis of inhibitory activity of polar body formation of denuded mouse oocytes in culture. Amino terminal sequence analyses showed that residues 5 to 15 of this protein were identical to residues 1 to 11 of human nonsecretory ribonuclease. Furthermore, residues 1 to 4 of this protein were identical to residues −4 to −1, corresponding to part of a signal peptide region of eosinophil-derived neurotoxin, whose mature sequence is identical to nonsecretory ribonuclease. These results indicate that the protein purified as a putative mouse oocyte maturation inhibitory protein from the urine of pregnant women may be a product of an peculiar processing of a nonsecretory ribonuclease precursor.

Keywords oocyte maturation; inhibitory protein; urinary protein; pregnant women; N-terminal sequence; ribonuclease; nonsecretory ribonuclease; eosinophil-derived neurotoxin

Maturation of the ovarian follicle as well as the oocytes existing in the follicle is regulated by a complex interaction of stimulators and inhibitors in the hypothalamus-pituitary-ovary system. In general, it is accepted that oocyte and follicular maturation is induced by hormones, pituitary gonadotropins and ovarian estrogen. Thus, the germinal vesicle of follicle-enclosed oocytes in animals remains arrested at the dictyate state of meiosis until the occurence of a gonadotropin surge.[1,2] Upon releasing the oocytes from the follicles *in vitro*, the meiotic process resumes, leading to a germinal vesicle breakdown (GVBD) followed by the polar body formation (PBF) of the oocytes,[3,4] suggesting that factors in the folliclular constituents and/or factors secreted by other tissues sustain the meiotic arrest of oocytes. Such peptide regulators in the control of oocyte and follicular maturation,[5–7] as well as an inhibitor of follicle stimulating hormone (FSH) binding to its receptor, have been identified in follicular fluid.[8,9] However, the structures of these peptides have not been determined.

In normal pregnancy, although hormonal levels of chorionic gonadotropin (hCG) and estrogen are high, significant maturation of the oocytes and follicles do not occur for a long period during the pregnancy. This phenomenon suggests the possibility of a considerable increase in concentration of the following factors in urine during pregnancy: a factor in the follicular constituents which directly affects oocytes, and/or factors secreted by other tissues, *i.e.* a functional inhibitor of hCG and estrogen, which sustain the meiotic arrest of oocytes. For instance, Soffer *et al.* have reported that a gonadotropin-inhibitory substance has been identified in the urine of normal young children as well as of normal subjects on the basis of its inhibition of mouse uterine-ovary growth stimulated by hCG *in vivo*.[10,11] A similar gonadotropin-inhibitory substance was detected in a crude urinary preparation of pregnant women which is a partially purified pharmaceutical preparation of hCG.[12] In addition to the above studies, Blithe *et al.* reported that hCG itself at low concentrations can inhibit ovarian growth in hypophysectomized rats which have been stimulated with FSH and diethylstilbestrol.[13] On the other hand, information concerning those substances which directly affect the oocytes in the urine during pregnancy, which have possibly been leaked or excreted into the urine from follicles or other tissues, have not been available.

The purpose of the present study was to determine a factor which directly affects the oocytes and induces their meiotic arrest, if such a factor is present in urine during pregnancy. We describe here how we have identified a source of inhibitory activity on oocyte maturation in urinary extracts obtained from pregnant women using an *in vitro* bioassay based on inhibitions of spontaneously occurring maturation of mouse oocytes (GVBD and PBF) in culture. It was revealed that a purified protein which exhibits inhibitory activity on PBF of a denuded mouse oocyte in culture was a protein related to nonsecretory ribonuclease based on N-terminal amino acid sequence homology.

Experimental

Material A crude urinary preparation from pregnant women, which is a partially purified pharmaceutical preparation of hCG, was a generous gift from Organon.

Culture of Mouse Oocytes Oocytes (40 to 50) from prepubertal ICR mice (15 to 20 g body weight) were prepared by a published method.[14] Oocytes were cultured for 16 h in a 0.2 ml drop of modified Krebs Ringer medium under paraffin oil at 37 °C in humidified 5% CO_2 in air. Activities of mouse oocyte maturation inhibition were determined by inhibitory effects on GVBD and PBF of oocytes in culture, as follows. After 3 h of cultivation of the oocytes with the samples, the presence of GVBD was examined under a stereoscopic microscope. PBF was examined after 10 to 12 h of cultivation of the oocytes with the samples. The percentage of inhibition of GVBD and PBF were calculated as follows:

$$\frac{\%\text{GVBD or PBF (control)} - \%\text{GVBD of PBF (experiment)}}{\%\text{GVBD or PBF (control)}} \times 100 = \text{inhibition (\%)}$$

Sephadex G-100 Column Chromatography A crude urinary preparation from pregnant women (100 mg) was dissolved in 5 ml of 0.1% NH_4HCO_3 and the proteins were separated into tubes (7 ml) on a Sephadex G-100 column (2.5 × 100 cm). The tubes were pooled for fractions A to D and lyophilized. Each fraction was rechromatographed on a Sephadex G-100 under the same conditions and lyophilized.

Reverse-Phase High Performance Liquid Chromatography (HPLC) An

aliquot of fraction B (1 mg) from gel filtration was dissolved in purified water and applied to a column (μBondasphere C_8, 3.9 × 150 mm) of reverse-phase HPLC. The proteins were separated with a linear gradient of 0 to 60% acetonitrile in 0.1% trifluoroacetic acid (60 min) at a flow rate of 1 ml/min. Protein content was monitored by measuring the absorbance at 220 nm. Three major peaks of proteins (B1, B2, consisting of three sub-peaks, and B3) were obtained. Each peak was lyophilized and dissolved in water or a 10 mM phosphate buffered saline (pH 7.0).

N-Terminal Sequence Determination Proteins B1, B2-1, B2-2, B2-3 and B3 were analyzed on an automated Applied Biosystems model 477A protein sequencer equipped with an on-line phenylthiohydantoin (PTH) analyzer.

Miscellaneous Sodium dodecyl sulfate polyacrylamide gel electrophoresis (SDS-PAGE) was performed by Laemmli's method[15] using a 10% gel. Immunoblotting analysis of hCG was performed according to the published method.[16] Protein content was determined by the method of Bradford[17] using bovine serum albumin as the standard. All other chemicals used were standard commercial products.

Results and Discussion

To determine the nature of inhibitory activity in urine from pregnant women on mouse oocyte maturation, a commercial crude preparation of urine from pregnant women (a partially purified pharmaceutical preparation of hCG) was used. The specific activity of hCG in this preparation was 2900 IU/mg, indicating that more than 70% of the protein in this preparation includes urinary constituents other than hCG, since the specific activity of the purified hCG is >10000 IU/mg. A commercial crude preparation of urine from pregnant women, as well as its fractions B to D obtained from Sephadex G-100 chromatography (Fig. 1), was assayed for inhibitory activities to the GVBD and PBF of mouse oocytes (Fig. 2). Blithe *et al.* reported that a low concentration of hCG is a potent inhibitor of ovarian growth *in vivo* stimulated with FSH and diethylstilbestrol.[13] Our assay system was conducted *in vitro* using denuded oocytes in culture, in order to delete the effects of contamination with hCG, and fraction B was chromatographed on a Sephadex G-100 column several times until no hCG was detected immunologically using the immunoblotting method. Final yields of protein in fractions B, C and D were approximately 9, 8 and 11 mg, respectively. No further investigation was performed on fraction A since the greater part of it was hCG. When 1 mg/ml of each fraction and the original material were analyzed for mouse oocyte maturation inhibitory activity, neither the individual fractions nor the original materials showed any inhibitory effect on GVBD of mouse oocytes. On the other hand, an inhibitory effect on PBF was detected in fractions B (100%), C (32%), and D (28%), as well as in the original materials (47%). As shown in Fig. 3, the most active fraction, B, inhibited PBF dose dependently. These results suggest that some inhibitory protein to PBF of the mouse oocyte may be present in the urine of pregnant women. At the present time, it remains unknown whether fraction B inhibited only PBF, or both

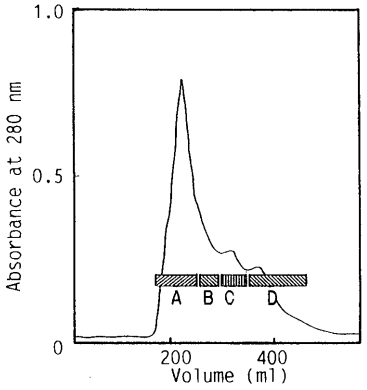

Fig. 1. Chromatographic Pattern on Sephadex G-100 of the Extracts of Urine Obtained from Pregnant Women

A crude urinary preparation from pregnant women (100 mg) was subjected to a column of Sephadex G-100 (2.5 × 100 cm), and fractions A to D were obtained under the conditions described in Experimental.

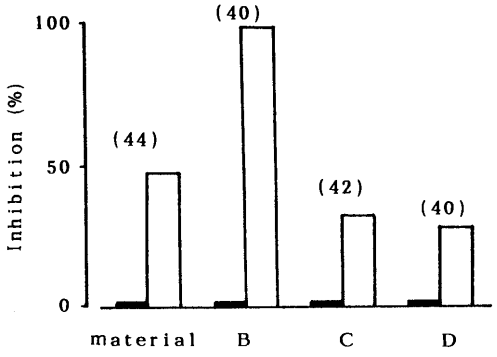

Fig. 2. Inhibition of the Material and Its Fractions (B, C and D) from Fig. 1 on GVBD (■) and PBF (□) of Mouse Oocytes at a Protein Concentration of 1 mg/ml

The numbers in parentheses are the number of oocytes analyzed.

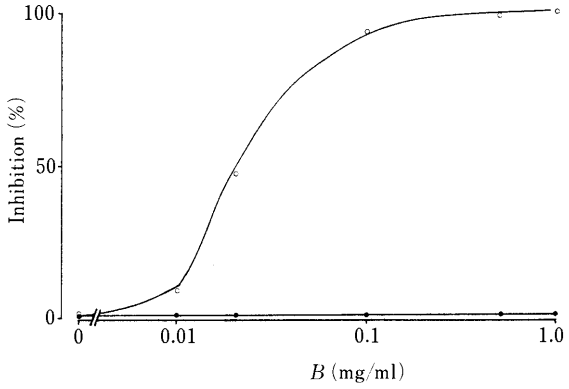

Fig. 3. Dose Dependent Inhibition of Fraction B on GVBD (●) and PBF (○) of Mouse Oocytes

The numbers in parentheses are the numbers of oocytes analyzed.

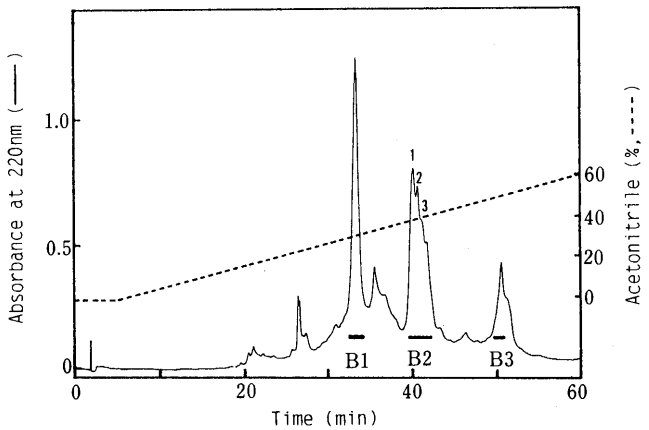

Fig. 4. Separation Profile of Proteins in Fraction B with HPLC

Fraction B (1 mg) was subjected to a column of μBondasphere C_8 (3.9 × 150 mm) and fractions B1, B2 and B3 were obtained under the conditions described in Experimental.

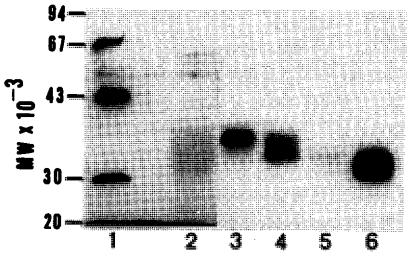

Fig. 5. SDS-PAGE of Proteins B1 (Lane 2), B2-1 (Lane 3), B2-2 (Lane 4), B2-3 (Lane 5) and B-3 (Lane 6)

Each protein corresponding to 0.1 μg protein, prepared with reduction by 5% 2-mercaptoethanol and boiling for 5 min, was electrophoresed using a 10% gel. The gel was stained with silver reagents. Lane 1 represents molecular weight marker proteins.

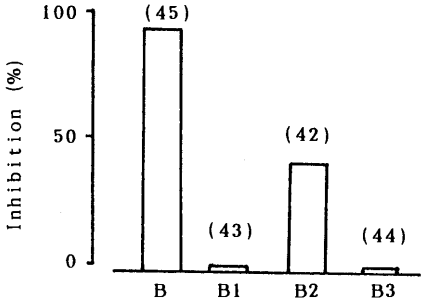

Fig. 6. Inhibition of Proteins in Fractions B, B1, B2 and B3 at a Protein Concentration of 0.3 mg/ml on the PBF of Mouse Oocytes

The numbers in parentheses are the numbers of oocytes analyzed.

GVBD and PBF. However, PBF inhibition by fraction B may not be caused by its cytotoxic effect, since fraction B did not show any cytotoxic effect on other cells tested at the concentration of 1 mg/ml (data not shown).

To purify proteins inhibiting the PBF of mouse oocytes, fraction B was subjected to reverse-phase HPLC (Fig. 4). As shown in Fig. 5, four proteins (B1, B2-1, B2-3, and B3) were purified as single bands with SDS-PAGE. Although peptide B2-2 contained two bands, it was very likely that peptide B2-2 was a mixture of peptides B2-1 and B2-3 (see below). The apparent molecular weights of these peptides were approximately 35000, 37000, 34000 and 32000 daltons (Da) for B1, B2-1, B2-3 and B3, respectively.

When 0.3 mg/ml of each protein peak (B1, B2 and B3) was analyzed for PBF inhibitory activity, only B2 revealed PBF inhibitory activity (approximately 40%) (Fig. 6). PBF inhibitory activity of B2 was not significant compared to fraction B, possibly indicating that factors involving inhibition of PBF may be lost by denaturation during HPLC, or that these effects may result from the mutual interaction of several peptide factors. At the present time, the interaction mechanism of these peptide factors remains unknown.

In this study, we have made efforts to clarify which proteins are present in the active fraction, B, by determining their amino terminal sequences. Approximately 4 μg of each peptide (B1, B2-1, B2-2, B2-3 and B3) was subjected to N-terminal sequence analysis using an automated sequencer. Each predominant N-terminal sequence except B3 was determined by 15 cycles of Edman degradation as shown in Table I. No N-terminal amino acid was detected in B3, indicating that the N-terminus of B3 may be

Table I. N-Terminal Amino Acid Sequence Analyses of Proteins

Peptide	Cycle number														
	1	2	3	4	5	6	7	8	9	10	11	12	13	14	15
B1	Lys	Glu	Ser	Arg	Ala	Lys	Lys	Phe	Gln	Arg	Gln	His	Met	Asp	Ser
	116	53	36	28	169	90	114	101	60	31	78	17	101	48	23
B2-1	Ser	Leu	His	Val	Lys	Pro	Pro	Gln	Phe	Thr	Trp	Ala	Gln	—	—
	71	103	10	115	63	133	120	76	88	33	32	57	31	—	—
B2-2	Ser	Leu	His	Val	Lys	Pro	Pro	Gln	Phe	Thr	Trp	Ala	Gln	Trp	Phe
	56	164	27	200	109	141	156	84	78	24	10	52	45	10	32
B2-3	Ser	Leu	His	Val	Lys	Pro	Pro	Gln	Phe	Thr	Trp	Ala	Gln	Trp	Phe
	94	134	14	133	135	134	122	85	96	55	15	89	55	25	47

Approximately 4 μg of each protein was subjected to an automated sequencer. Yields of PTH amino acids for cycles (pmol) are shown below each residue. Dashes indicate that the determination of PTH amino acid was not performed.

Table II. Comparison of N-Terminal Amino Acid Sequences

					1				5				10		15
B1					K	E	S	R	A	K	K	F	Q	R	Q	H	M	D	S
HPR					K	E	S	R	A	K	K	F	Q	R	Q	H	M	D	S
					1				5				10		15
B2					S	L	H	V	K	P	P	Q	F	T	W	A	Q	W	F
HNSR									K	P	P	Q	F	T	?	A	Q	W	F
EDN	M	-	-	-	-	-	-	G	S	L	H	V	K	P	P	Q	F	T	W	A	Q	W	F
	−27							−4				1			5					10			

HPR: Human pancreatic ribonuclease.[18] HNSR: Human non-secretory ribonuclease.[19] EPN: Eosinophil-derived neurotoxin.[20]

blocked. Sequences of B2-1, B2-2 and B2-3 were identical, indicating that heterogeneity of these peptides on HPLC may be due to C-terminal heterogeneity or other factors such as differences in sugar content which we are now investigating. As shown in Table II, by searching the data base of amino acid sequence (PRF-SEQDB from PRINAS), it was revealed that N-terminal 15 residues of B1 are identical to those of human pancreatic ribonuclease,[18] and residues 5—15 of B2 are identical to the N-terminal sequence of nonsecretory ribonuclease isolated from human urine.[19] Recently, Rosenberg *et al.* reported a precursor structure consisting of signal (27 residues) and mature (134 residues) polypeptide regions deduced from complementary deoxyribonucleic acid (cDNA) of eosinophil-derived neurotoxin (EDN), whose sequence of the mature form is identical to nonsecretory ribonuclease.[20] Residues 1 to 4 (S-H-V-L) of B2 were identical to residues −4 to −1 corresponding to part of a signal sequence of EDN. Although the original organ(s) of protein B2 are unknown at present, these results indicate that protein B2 may be produced by an unusual processing of a nonsecretory ribonuclease precursor form. The molecular weight of B2 (approximately 34000—37000 Da) was inconsistent with that of nonsecretory ribonuclease (approximately 16000 Da). This may be caused by differences in sugar content, since it is accepted that some ribonucleases are glycoproteins.

In conclusion, it is very likely that the protein B2, purified as a protein having putative oocyte maturation inhibitory activity based on inhibitory effects on PBF of mouse oocytes from urine during pregnancy, is a nonsecretory ribonuclease containing a precursor sequence of residues −4 to −1. Characterization of protein B2 is under investigation and may be of striking interest in understanding the significance

of ribonuclease activity as well as mouse oocyte maturation inhibitory activity.

Acknowledgements We wish to thank Miss. T. Khonoura for her skillful assistance. This work was supported by a Grant-in-Aid from the Ministry of Education, Science and Culture of Japan.

References

1) A. W. Schuetz, *Adv. Reprod. Physiol.*, **4**, 99 (1969).
2) A. Tsafriri, "The Vertebrate Ovary," ed. by R. E. Jones, Plenum Press, New York, 1969, p. 409.
3) J. D. Biggers, "The Regulation of Mammalian Reproduction," ed. by S. J. Segel, R. Crozier, P. A. Corfman, F. G. Condliffe, Charles C. Thomas, Springfield, 1973, p. 273.
4) G. Pincus and E. V. Enzmann, *J. Exp. Med.*, **62**, 665 (1935).
5) A. Tsafriri, S. H. Pomerantz, and C. P. Channing, *Biol. Reprod.*, **14**, 511 (1976).
6) T. Hillensjo, S. K. Batta, A. Schwartz-Kripner, A. C. Wentz, J. Sulewski, and C. P. Channing, *J. Clin. Endoclinol. Metab.*, **47**, 1332 (1978).
7) C. P. Channing, L. D. Anderson, D. J. Hoover, J. Kolena, K. G. Osteen, S. H. Pomerantz, and K. Tanabe, *Recent Prog. Horm. Res.*, **38**, 331 (1982).
8) N. C. Darga and L. E. Reichert, Jr., *Biol. Reprod.*, **19**, 235 (1978).
9) P. M. Sluss, P. W. Fletcher, and L. E. Reichart, Jr., *Biol. Reprod.*, **29**, 1105 (1983).
10) L. J. Soffer, W. Futterweit, and J. Salvaneschi, *J. Clin. Endocrinol. Metab.*, **21**, 1267 (1961).
11) L. J. Soffer, J. Salvaneschi, and W. Futterweit, *J. Clin. Endocrinol. Metab.*, **22**, 532 (1962).
12) M. L. Forcelledo and M. Lastra, *J. Pharm. Sci.*, **66**, 1773 (1977).
13) D. L. Blithe, P. J. Caron, J. P. Louvet, and B. C. Nisula, *Endocrinology*, **119**, 2270 (1986).
14) E. Sato, T. Ishibashi, and S. S. Koide, *Biol. Reprod.*, **37**, 371 (1987).
15) U. K. Laemmli, *Nature* (London), **227**, 680 (1970).
16) R. Sakakibara, N. Tominaga, and M. Ishiguro, *Biochem. Biophys. Res. Commun.*, **137**, 443 (1986).
17) M. Bradford, *Anal. Biochem.*, **72**, 248 (1976).
18) J. J. Beintema, P. Wietzes, J. L. Weickmann, and D. G. Glitz, *Anal. Biochem.*, **136**, 48 (1984).
19) J. J. Beintema, J. Hofsteenge, M. Iwama, T. Morita, K. Ohgi, M. Irie, R. H. Sugiyama, G. L. Schieven, C. A. Dekker, and D. G. Glitz, *Biochemistry*, **27**, 4530 (1988).
20) H. F. Rosenberg, D. G. Tenen, and S. J. Ackerman, *Proc. Natl. Acad. Sci. U.S.A.*, **86**, 4460 (1989).

Activity of Artificial Mutant Variants of Human Growth Hormone Deficient in a Disulfide Bond between Cys53 and Cys165

Eriko UCHIDA,*[,a] Haruki UEMURA,[b,1a)] Toshiki TANAKA,[b,1b)] Satoshi NISHIKAWA,[b,1c)] Seiichi UESUGI,[b] Akira TANAKA,[a] Minoru MORIKAWA,[c] Takao HAYAKAWA[a] and Morio IKEHARA[b,1b)]

Division of Biological Chemistry and Biologicals, National Institute of Hygienic Sciences,[a] 1–18–1 Kamiyoga, Setagaya-ku, Tokyo 158, Japan, Faculty of Pharmaceutical Sciences, Osaka University,[b] 1–6 Yamadaoka, Suita, Osaka 565, Japan, and Tokyo Institute for Immunopharmacology Inc.,[c] 3–41–8 Takada, Toshima-ku, Tokyo 171, Japan. *Received July 25, 1990*

In order to understand the role of Cys53 and Cys165 of human growth hormone (hGH) in receptor-binding and biological activity, artificial mutant variants of hGH were prepared in *Escherichia coli* by *in vitro* mutagenesis. Variants of hGH were constructed by replacement of Cys165 with Ala ([Ala165]hGH) or Ser ([Ser165]hGH), by replacement of Cys53 with Ala ([Ala53]hGH), by replacement of Cys53 and Cys165 with Ala ([Ala53, Ala165]hGH), or by replacement of Cys53 with Ala and Cys165 with Ser ([Ala53, Ser165]hGH). All of the variants constructed as well as reduced hGH exhibited less biological activity than that of intact hGH, and the decreases in biological activity were almost equal, as measured by a sensitive biological assay for growth hormone: adipose conversion assay using 3T3-F442A cells. These variants also showed less receptor-binding activity than that of intact hGH.

These results suggest that it is possible neither the residue Cys53 nor Cys165 is directly involved in the receptor binding, and that the disulfide bridge between Cys53 and Cys165 in hGH may not always be crucial for the biological activity, though necessary to express full hGH activity.

Keywords human growth hormone; structure–activity relationship; disulfide bridge; adipose conversion; radioreceptor assay

Growth hormone (GH) is necessary for somatic growth and development. GH is known to affect many cell types and to induce multiple biological responses not only indirectly, mediated *via* somatomedins, but also directly, by binding with its own receptor on target cells.[2)] Mouse preadipose 3T3 cells (3T3-F442A)[3)] possess somatogenic GH receptors,[4,5)] and GH promotes the conversion of preadipocytes to adipocytes in a dose dependent manner.[6,7)] Since this differentiation was observed at a low concentration of GH (10^{-10}—10^{-9} M), adipose conversion of 3T3-F442A cells can be used as a sensitive bioassay for GH.[7)] Using this GH assay method, we have studied the structure–activity relationship of human GH (hGH).[8)]

Human GH is a single polypeptide of 191 amino acid residues (MW, 22 kilodaltons (kDa)) with two disulfide bridges between Cys53 and Cys165, and between Cys182 and Cys189. The reduced-alkylated derivative of hGH retained full biological activity in rat tibia test and the pigeon crop-sac assay,[9,10)] while the derivative showed lower receptor-binding activity and immunoreactivity.[11)] Several papers have reported that the N-terminal two-thirds and the C-terminal fragment of hGH, which were isolated by plasmin- or thrombin-digestion of reduced and alkylated hGH, could recombine with each other by noncovalent interaction, and the reconstituted hormone obtained substantial biological activity.[12–15)] Tokunaga *et al.* previously reported the construction of [Ala165]hGH variant, which was genetically mutated from Cys165 to Ala in order to prevent the formation of a disulfide bond between Cys53 and Cys165.[16)] [Ala165]hGH retained similar immunological activity to intact hGH and full biological activity on rat weight gain assay. Disulfide bridges of hGH thus seem to be unnecessary for the formation of the biologically-active tertiary structure. However, the results of immunological assay do not always correlate with the biological activity,[17)] and *in vivo* assay of hGH[18)] seems to be less sensitive and less precise for determination of changes in the activity. In a previous paper, we studied the biological activities of artificial mutant variants of hGH by both *in vitro* adipose conversion assay and *in vivo* weight gain assay, and showed that the former assay was able to estimate a biological activity much more sensitively than the latter assay.[8)]

In the present paper, we report the construction of another four artificial mutant variants of hGH in which Cys53 and/or Cys165 were replaced by Ala or Ser to prevent the formation of a disulfide bond between Cys53 and Cys165: [Ser165]hGH (Cys165 to Ser), [Ala53]hGH (Cys53 to Ala), [Ala53, Ala165]hGH (Cys53 and Cys165 to Ala), and [Ala53, Ser165]hGH (Cys53 to Ala and Cys165 to Ser). Using these constructed variants and the aforementioned F442A assay systems, we investigate more precisely the role of Cys53 and Cys165 in receptor binding and biological activity, as well as the role of disulfide bond between Cys53 and Cys165 in the formation of the biologically-active tertiary structure.

Materials and Methods

Materials Various restriction enzymes, Klenow fragment of deoxyribonucleic acid (DNA) polymerase, T4 DNA ligase and polynucleotide kinase were purchased from Takara Shuzo (Kyoto, Japan). 3T3-F442A cells were kindly provided by Dr. H. Green of the Harvard Medical School. Recombinant methionyl hGH was provided by Sumitomo Pharmaceuticals Co., Ltd. (Osaka, Japan) and used as an intact hGH. Cat serum was obtained from Cololado Serum Co. (Denver, CO., U.S.A.).

Construction of Mutant Genes The mutant genes for hGH were constructed by *in vitro* mutagenesis, using single stranded M13 phage DNA, essentially as described by Zoller and Smith.[19)] The *Hpa*I-*Sal*I DNA fragment containing the hGH gene was obtained from pGH-L9[20)] and was inserted between the *Sma*I and *Sal*I sites of M13mp11 replicative-form DNA. The following deoxyoligonucleotides for the generation of mutations were synthesized by the phosphoramidite method on an automatic DNA synthesizer (Applied Biosystems, model 380A): d(CTGTAC*TCT*TTCCGT) for the mutation at Cys165 to Ser165; d(CCTCGTTG*GCA*TTCTCTG) for the mutation at Cys53 to Ala53 (italics indicate the changed codon).

Approximately 1 μg of recombinant M13mp11 single-stranded DNA was annealed to 6 pmol of a mutagenic oligonucleotide, and the single-stranded DNA was converted to double-stranded DNA by incubation with Klenow fragment and deoxynucleoside triphosphates. The

resultant reaction mixture was used directly to transfect competent JM101 cells. Positive plaques were selected by plaque hybridization using ^{32}P-labeled versions of the deoxyoligonucleotides that were used for mutation. The phage DNA was recovered by the usual method and the nucleotide sequences of the mutant genes were confirmed by Sanger's dideoxy method.[21] Each mutant gene was reinserted into the expression vector, pGH-L9,[20] after removal of the original gene for hGH and designated pGH-L9-CS3 for the Cys165→Ser165 mutant and pGH-L9-AC5 for the Cys53→Ala53 mutant, respectively. Synthesis of the gene for the mutation at Cys165 to Ala165 and construction of plasmid pHGH-165 (Cys165→Ala165) was described previously.[16] The plasmids for double mutants, [Ala53, Ala165]hGH and [Ala53, Ser165]hGH were constructed in the same way as described above and designated pGH-L9-AA6 and pGH-L9-AS7, respectively, in which the construction was started from pGH-L9-AC5 instead of pGH-L9.

Purification of Proteins Mutant genes were expressed in *E. coli* HB101 by induction of the *trp* promoter as described previously.[20] The mutant genes were expressed to generate inclusion bodies in *E. coli* cells. Variant proteins were recovered and purified as described previously.[8]

Adipose Conversion Assay Stocks of 3T3-F442A cells were maintained in the Dulbecco-Vogt modification of Eagle's medium (DMEM) supplemented with 10% calf serum. For experiments, exponentially growing 3T3-F442A cells were trypsinized and seeded into 35 mm tissue culture dishes about 1×10^4 cells in DMEM supplemented with 3% cat serum and 2% calf serum (growth medium). After 4 to 5 d, when the cells became subconfluent, the growth medium was replaced with conversion medium: DMEM supplemented with 1.5% cat serum, 1% calf serum, bovine insulin (5 μg/ml), human transferrin (5 μg/ml), triiodothyronine (2×10^{-9} M), biotin (10^{-6} M), 2-mercaptoethanol (40 μM), and mouse epidermal growth factor (30 ng/ml). Intact hGH and hGH variant proteins were diluted in medium containing 5% cat serum, sterilized by filtration through Millipore fluorocarbon filters (SLGV025LS), and then added to the culture medium. Cells were cultured a further 10—14 d causing them to undergo adipose conversion without further change of medium. Cells were then harvested in 0.3 ml of 25 mM Tris–HCl with 1 mM ethylenediaminetetraacetic acid (EDTA) (pH 7.5), disrupted by sonication (30 W, 10 s), and supernatants were obtained after centrifugation at $12000 \times g$. The activity of glycerophosphate dehydrogenase (GPDH) in the supernatant, which is a marker enzyme of adipocyte differentiation, was measured as the oxidation of reduced nicotinamide adenine dinucleotide (NADH) at 340 nm.[22] One unit of GPDH activity is defined as the oxidation of 1 nmol of NADH per minute.

Radioreceptor Assay Intact hGH was iodinated to a specific activity of 2.59—4.63 MBq/μg using the chloramine-T method.[23] Confluent monolayer cultures of 3T3-F442A cells (35 mm dishes) in the growth medium were rinsed three times with Hanks' balanced salt solution (HBSS) containing 0.1% (w/v) bovine serum albumin and 10 mM HEPES (*N*-2-hydroxyethylpiperazine-*N'*-2-ethanesulfonic acid), inoculated with [^{125}I]-labeled hGH (10^{-10} M) and unlabeled hGH variant proteins in the same buffer and incubated for 90 min at 23°C. The binding reaction was terminated by aspirating the buffer from the culture dish, and the cell layers were washed three times with the same buffer. The cells were harvested and the cell-associated radioactivity was determined with an auto gamma counter.

Results

The biological activities of intact hGH and five hGH variants, in which Cys53 and/or Cys165 were replaced by Ala or Ser and the formation of a disulfide bond between Cys53 and Cys165 was prevented, were compared with the adipose conversion assay using 3T3-F442A cells. Typical dose–response curves are shown in Fig. 1. The replacement of Cys165 with Ala or Ser caused reduction of the activity (Fig. 1A, 1C). The concentration of intact hGH that is 50% effective (ED_{50}) ranged from 0.8×10^{-10} to 2.1×10^{-10} M, whereas ED_{50} values of [Ala165]hGH and [Ser165]hGH were several times higher than that of hGH and the potency calculated from ED_{50} was 14—40% and 8—18%, respectively (Table I). The replacement of Cys53 with Ala also caused loss of the activity (Fig. 1B). [Ala53]hGH exhibited 35—63% retention of the activity of intact hGH.

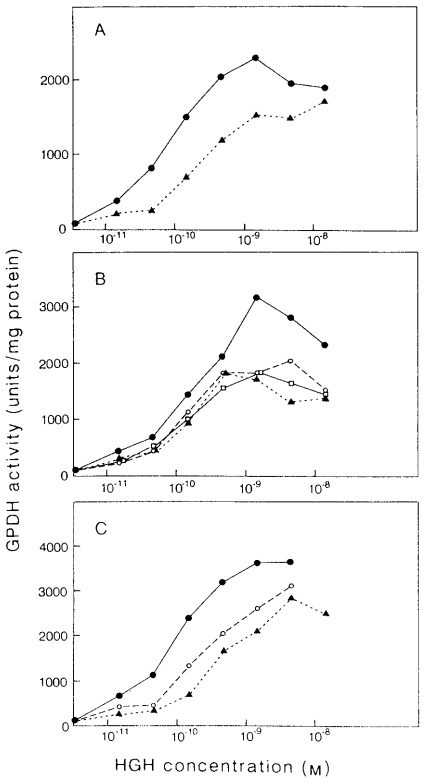

Fig. 1. Adipogenic Activity of hGH Variants in Comparison with Native hGH

(A) hGH (●) and [Ser165]hGH (▲). (B) hGH (●), [Ala53]hGH (○), [Ala53,Ala165]hGH (▲), and [Ala53,Ser165]hGH (□). (C) hGH (●), [Ala165]-hGH (▲), and fully reduced hGH by 10 mM 2-mercaptoethanol (○).

TABLE I. Comparison of Biological Activity and Binding Activity of hGH Variants

hGH variants	Biological activity[a] (adipose conversion assay) (%)	Binding activity[b] (radioreceptor assay) (%)
Intact hGH	100	100
[Ala165]hGH	28 (14—40)[c]	58
[Ser165]hGH	14 (8—18)	43
[Ala53]hGH	49 (35—63)	54
[Ala53,Ala165]hGH	44 (18—63)	53
[Ala53,Ser165]hGH	36 (30—40)	53
Reduced hGH	27	n.d.

a) Relative biological activity is calculated by comparison with ED_{50}. Values are the mean of two to four experiments. *b*) Relative receptor-binding activity is calculated by comparison with IC_{50}. Values are the mean of two experiments. *c*) Range. n.d., not determined.

However, no further reduction of the activity was observed when Cys165 of [Ala53]hGH was replaced with Ala ([Ala53, Ala165]hGH) or Ser ([Ala53, Ser165]hGH) (Fig. 1B, Table I). These five hGH variants also exhibited rather reduced activity with respect to the maximal induction of GPDH activities. Interestingly, fully reduced hGH prepared by incubation of the intact hGH in the presence of 10 mM 2-mercaptoethanol, exhibited a reduction of the activity similar to those of hGH variants, and the potency was 27% that of hGH (Fig. 1C). This suggests that the reduction of the activities of the five hGH variants may be due mainly to the deletion of the disulfide bond between Cys53 and Cys165 rather than by the replacement of Cys with Ala or

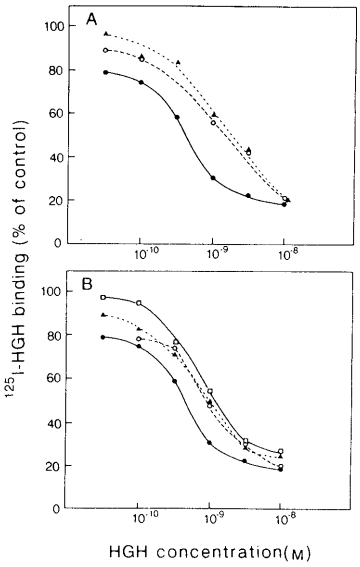

Fig. 2. Radioreceptor Assay of hGH Variants in Comparison with Native hGH

(A) hGH (●), [Ala165]hGH (○) and [Ser165]hGH (▲). (B) hGH (●), [Ala53]hGH (○), [Ala53,Ala165]hGH (▲) and [Ala53,Ser165]hGH (□).

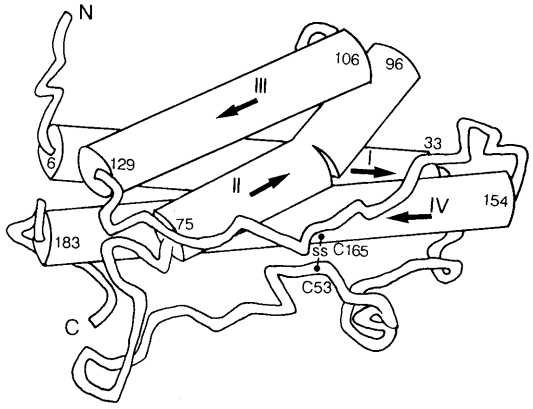

Fig. 3. Three-Dimensional Model of hGH Based on the Structure of Porcine GH[23]

Cylinder represents α-helical structure. The residues are numbered according to the hGH sequence.

Ser.

Figure 2 shows the binding activities of hGH variants to the GH receptor on 3T3-F442A cells by radioreceptor assay. All of the hGH variants are slightly less active and the relative potencies calculated from the hormone concentration required for 50% inhibition (IC_{50}) were 43 to 58% that of hGH (Table I).

Discussion

In the present study, we investigated in more detail the role of Cys53 and Cys165 of hGH as well as the role of the disulfide bridge between them in biological activity using hGH variants constructed by *in vitro* mutagenesis and a sensitive bioassay of hGH. We obtained several hGH variants in which Cys53 and/or Cys165 are replaced by Ala or Ser and the disulfide bond between Cys53 and Cys165 is completely disrupted. We were able to show that all of these variants and reduced hGH were less active than intact hGH when the biological activity was determined by adipose conversion assay using 3T3-F442A cells (Table I). These results were consistent with the previous study by Morikawa *et al.*[7] in which fully reduced hGH and reduced-alkylated hGH showed less biological activity than intact hGH on adipose conversion assay.

The three-dimensional structure of porcine GH was determined by crystal X-ray diffraction study.[24] Analysis of a folding model of hGH derived from a structural model of porcine GH showed that hGH consists of four α-helices (I: 6—33; II: 75—96; III: 106—129; IV: 153—183) which are connected antiparallel and tightly associated by hydrophobic forces (Fig. 3).[8] In this folding model, Cys53 is located in the loop between helices I and II, and Cys165 is located on the outside of the bundle in helix IV. Two possibilities are considered for the roles of Cys53 and Cys165 in receptor binding and biological activity. One is that the residue Cys53 and/or Cys165 are directly involved in receptor binding site or active site. The other possibility is that the Cys53 and Cys165 participate in conservation of the biologically-active tertiary structure by formation of a disulfide bridge. The findings that the receptor-binding and the biological activities were similar among the variants tested and reduced hGH (Table I) suggest that neither the residue Cys53 nor Cys165 might be directly involved in receptor binding. On the other hand, the deletion of the disulfide bridge between Cys53 and Cys165 of hGH is an obvious possible cause of both reduced receptor-binding and biological activity (Table I). Disulfide bridges have been considered to be unnecessary to hGH biological activity determined by traditional bioassay,[9-16] however, our results suggest that the disulfide bridge between Cys53 and Cys165 is necessary to express full biological activity on adipose conversion assay.

Attempts to identify binding and biologically active sites of hGH showed that the tertiary structure was essential for biological activity.[11] Cunningham *et al.*[25] reported that the binding determinants in hGH to the human liver receptor consist of three discontinuous segments: the NH_2-terminus of helix I, the loop from Cys53 to the start of helix II (54—74), and the COOH-terminal portion of helix IV. In the folding model of hGH (Fig. 3), the deletion of the disulfide bridge between Cys53 and Cys165 may not induce any change in the four-helices bundle structure. However, a rigid association between the four-helices bundle, which includes two binding determinants, and the loop region that connects helices I and II, which region includes the other binding determinant, may become somewhat loose. This may result in the change of the most suitable spatial arrangement of three discontinuous binding determinants, and lead to the reduction of binding activity; consequently, biological activity is also decreased. Alternatively, it may be possible to suppose that besides binding determinants, there may be certain active segment(s) in the hGH molecule which may cause the biological responses of the cells at the stage of post-receptor binding, and the most suitable spatial dispositions between such biologically active determinants and binding determinants may be lost by the disruption of the disulfide bond which rigidly connects the loop region and the four-helices bundle. This is deduced from the findings that although hGH variants can compete with intact hGH in receptor binding activity at their high

concentration (10^{-8} M), as shown in Fig. 2, these variants exhibit significantly less activity than intact hGH with respect to the induction of maximal biological activity even at their saturated concentration (Fig. 1).

In conclusion, the disulfide bond between Cys53 and Cys165 of hGH may not be crucial for the biological activity but may be necessary to express full hGH activity on adipose conversion assay.

References

1) Present address: *a) Department of Pathology, New York University, Medical Center 550 1st Ave. MSB 593, New York, NY 10016, U.S.A.*; *b) Protein Engineering Research Institute, 6–2–3 Furuedai, Suita, Osaka 565, Japan*; *c) Molecular and Cellular Biology Department, Fermentation Research Institute, AIST, Tsukuba, Ibaraki 305, Japan.*
2) O. G. P. Isaksson, S. Edén and J.-O. Jansson, *Ann. Rev. Physiol.*, **47**, 483 (1985).
3) H. Green and O. Kehinde, *Cell*, **7**, 105 (1976).
4) T. Nixon and H. Green, *J. Cell. Physiol.*, **115**, 291 (1983).
5) E. Uchida, T. Hayakawa, S. Niimi, A. Tanaka and M. Morikawa, *J. Mol. Endocrinol.*, **3**, 239 (1989).
6) M. Morikawa, T. Nixon and H. Green, *Cell*, **29**, 783 (1982).
7) M. Morikawa, H. Green and U. J. Lewis, *Mol. Cell. Biol.*, **4**, 228 (1984).
8) S. Nishikawa, Y. Nishida, H. Uemura, Y. Yamada, T. Tanaka, S. Uesugi, M. Morikawa, E. Uchida, T. Hayakawa and M. Ikehara, *Protein Engineering*, **3**, 49 (1989).
9) J. S. Dixon and C. H. Li, *Science*, **154**, 785 (1966).
10) T. A. Bewley, J. Brovetto-Cruz and C. H. Li, *Biochemistry*, **8**, 4701 (1969).
11) M. L. Aubert, T. A. Bewley, M. M. Grumbach, S. L. Kaplan and C. H. Li, *Int. J. Peptide Protein Res.*, **28**, 45 (1986).
12) C. H. Li and T. A. Bewley, *Proc. Natl. Acad. Sci. U.S.A.*, **73**, 1476 (1976).
13) C. H. Li, T. Hayashida, B. A. Doneen and A. J. Rao, *Proc. Natl. Acad. Sci. U.S.A.*, **73**, 3463 (1976).
14) C. R. Reagan, J. L. Kostyo, J. B. Mills, S. E. Gennick, J. L. Messina, S. A. Wagner and A. E. Wilhelmi, *Endocrinology*, **109**, 1663 (1981).
15) H. M. Goodman and J. L. Kostyo, *Endocrinology*, **108**, 553 (1981).
16) T. Tokunaga, T. Tanaka, M. Ikehara and E. Ohtsuka, *Eur. J. Biochem.*, **153**, 445 (1985).
17) G. W. Becker, R. R. Bowsher, W. C. Mackellar, M. L. Poor, P. M. Tackitt and R. M. Riggin, *Biotechnol. Appl. Biochem.*, **9**, 478 (1987).
18) C. H. Li, "Hormonal Proteins and Peptides," Vol. 4, ed. by C. H. Li, Academic Press, New York, 1977, pp. 1—41.
19) M. J. Zoller and M. Smith, "Methods in Enzymology," Vol. 100, ed. by R. Wu, Academic Press, New York, 1983, pp. 468—500.
20) M. Ikehara, E. Ohtsuka, T. Tokunaga, Y. Taniyama, S. Iwai, K. Kitano, S. Miyamoto, T. Ohgi, Y. Sakuragawa, K. Fujiyama, T. Ikari, M. Kobayashi, T. Miyake, S. Shibahara, A. Ono, T. Ueda, T. Tanaka, H. Baba, T. Miki, A. Sakurai, T. Ohishi, O. Chisaka and K. Matsubara, *Proc. Natl. Acad. Sci. U.S.A.*, **81**, 5956 (1984).
21) F. Sanger, S. Nicklen and A. R. Coulson, *Proc. Natl. Acad. Sci. U.S.A.*, **74**, 5463 (1977).
22) L. S. Wise and H. Green, *J. Biol. Chem.*, **254**, 273 (1979).
23) F. C. Greenwood, W. M. Hunter and J. S. Glover, *Biochem. J.*, **89**, 114 (1963).
24) S. S. Abdel-Meguid, H.-S. Shieh, W. W. Smith, H. E. Dayringer, B. N. Violand and L. A. Bentle, *Proc. Natl. Acad. Sci. U.S.A.*, **84**, 6434 (1987).
25) B. C. Cunningham, P. Jhurani, P. Ng and J. A. Wells, *Science*, **243**, 1330 (1989).

Chem. Pharm. Bull. **39**(1) 154—158 (1991) Vol. 39, No. 1

In Vitro Transport of Sodium Diclofenac across Rat Abdominal Skin: Effect of Selection of Oleaginous Component and the Addition of Alcohols to the Vehicle[1)]

Koichi TAKAHASHI,*[,a] Satoko TAMAGAWA,[a] Toyoshi KATAGI,[a] Hironori YOSHITOMI,[b] Akira KAMADA,[c] J. HOWARD RYTTING,[d] Toshiaki NISHIHATA[d] and Nobuyasu MIZUNO[a]

Faculty of Pharmaceutical Sciences, Mukogawa Women's University,[a] Hyogo, Japan, Faculty of Pharmaceutical Sciences, Fukuyama University,[b] Hiroshima, Japan, Faculty of Pharmaceutical Sciences, Osaka University,[c] Osaka, Japan, and Pharmaceutical Chemistry Department, The University of Kansas,[d] Lawrence, Kansas 66046, U.S.A. *Received March 19, 1990*

The *in vitro* percutaneous transport of sodium diclofenac from various oil vehicles was examined using rat abdominal skin as a model skin membrane. The overall transport of diclofenac through the skin from the oleaginous vehicles was very poor because of a poor solubility of sodium diclofenac in nonpolar oils. To increase the solubility and the permeability of sodium diclofenac, ethanol and *n*-octanol were added to each oil (designated as the formulated vehicles). The addition of ethanol and *n*-octanol to the nonpolar vehicles resulted in an extreme increase in drug solubility in each vehicle, with a remarkable increase in the permeation of diclofenac. The effects of oil components in the formulated vehicle on the permeation of diclofenac across the skin were in the following order: squalane ≧ squalene > liquid paraffin > middle chain triglyceride > olive oil > castor oil.

In order to clarify the reason for the differences in permeation of diclofenac from these formulated vehicles, the release of diclofenac and *n*-octanol from these vehicles *in vitro* was studied. The release rates of *n*-octanol from the formulated vehicles were in the following order: liquid paraffin > squalene ≧ squalane > middle chain triglyceride ≧ olive oil > castor oil. On the other hand, a linear correlation was observed between the initial release rate of diclofenac from the formulated vehicle and the *in vitro* permeation of diclofenac through the rat skin. Thus, the oil component in the formulated vehicle affects the release of the drug and the enhancer from the vehicle to the skin. The transport rate of diclofenac from the formulated vehicle of squalane at the steady state proportionally increased with an increase of drug concentration, and the lag times were not influenced by a change of the drug concentration in the formulated vehicles. Therefore, it may be suggested that the intrinsic permeation of diclofenac through the skin is not influenced by the concentration of sodium diclofenac in the vehicle. From these results, it is considered that the important factors in increasing the skin permeation of a drug from an oil vehicle are to select oils which have a low affinity for the drug and enhancer, and to increase the drug concentration in the oil.

Keywords percutaneous absorption; sodium diclofenac; oleaginous vehicle; solubility; drug release; primary alcohol; drug content

Introduction

Recently, percutaneous administration of nonsteroidal antiinflammatory drugs has been extensively studied as a drug delivery route promising a systemic efficacy. But the skin forms an effective barrier to the permeation of foreign material, including drugs. Thus, transdermal drug administration is generally restricted to a limited number of drugs.

Sodium diclofenac is a widely used nonsteroidal antiinflammatory drug and has generally been administered orally and rectally but not topically because of its poor absorptivity across the skin.[2)]

To improve the therapeutic efficacy of a topically applied drug, factors affecting percutaneous drug absorption should be clarified on the basis of both the physicochemical properties of the drug and the skin. In order to improve bioavailability and increase therapeutic efficacy after topical application of a drug, it is necessary to employ a percutaneous absorption enhancer and/or to use an appropriate vehicle.

Many compounds, such as pyrrolidones,[3)] *N*,*N*-diethyl-*m*-toluamide,[4)] dimethyl sulfoxide[5)] and decylmethyl sulfoxide[6)] have been suggested as penetration enhancers. Further, various surfactants[7)] and Azone[8)] have also been reported as penetration enhancers.

The other approach is to modify the formulation of the vehicle. Transdermal absorption of a drug is influenced by the physicochemical properties of both the drug and the vehicle. The selection of an appropriate vehicle is very important in increasing the efficacy of a topically applied drug.[9)] Important physicochemical factors to improve the vehicle include the solubility of the drug in the vehicle and the transfer of drug from the vehicle to the skin.

In the present study, to obtain fundamental information for transdermal permeation of diclofenac employing simplified oleaginous vehicles, nonpolar oils which have been frequently used as vehicle components in pharmaceutical and cosmetic preparations were examined. The effect of drug concentration in the vehicle on the percutaneous drug permeation was investigated.

Materials and Methods

Materials Sodium diclofenac was kindly supplied by Ciba Geigy Japan (Takarazuka, Japan). Squalene and middle chain triglyceride (MCT, Triesta-F-801R) were supplied by Nikko Chemicals Co. Ltd. (Tokyo, Japan). Squalane, olive oil, liquid paraffin and castor oil used were commercially available. An ethylene-vinyl acetate copolymer (EVA) membrane (composed with ethylene-vinyl and acetate at 90 : 10; thickness of 40 μm) was obtained from Tamapoly Co. Ltd., (Tokyo, Japan). A cellophane membrane (seamless cellulose tubing, size: 27/32) was obtained from Viskase Seles Corp. Other reagents used were of analytical grade and were used without further purification.

Preparation of Formulated Vehicles To increase the solubility and permeability of sodium diclofenac in oil, ethanol (10% w/w) and *n*-octanol (5% w/w) were added to each oil. These mixtures were designated as the formulated vehicles. Twenty-five milligrams of sodium diclofenac was mixed well with 10 g of the mixture until a clear oily fluid was obtained at 23±2 °C. The oils used to prepare the formulated vehicles are listed in Table I. These preparations were used in both the *in vitro* permeation study and in the *in vitro* release study. When oil alone was used as a single component vehicle, the drug was suspended in the vehicle.

***In Vitro* Permeation Study** After removal of abdominal hair from male Wistar rats (250 to 300 g) with electric clippers, the abdominal skin was excised under pentobarbital anesthesia immediately before the experiment. The excised skin was mounted in a Franz-type diffusion cell. In this study, 10 ml of 0.1 M sodium phosphate buffer (pH 7.2) was used as the receptor medium, and 1 g of the test vehicle was placed on the donor side. The surface area exposed for diffusion was 1.77 cm^2 (diameter = 1.5 cm). The receptor medium was kept at 37 °C and stirred with a magnetic stirrer at 600 rpm.

Aliquots (0.1 ml) of the receptor medium were withdrawn periodically for 12 h. Immediately after each collection of the medium, 0.1 ml of the fresh buffer was added. The concentration of diclofenac in the sample was determined by high performance liquid chromatography (HPLC).

***In Vitro* Release Study** The release of *n*-octanol and diclofenac from the vehicle was determined using Franz-type diffusion cells. Experiments were carried out following the same method used in the *in vitro* permeation study. An EVA membrane in *n*-octanol and a cellophane membrane in sodium diclofenac were used as separation membranes. To maintain a sink condition, 10% w/w ethanol–water in *n*-octanol and a 10% w/w ethanol–buffer solution (0.1 M sodium phosphate buffer, pH 7.2) in sodium diclofenac were employed as the receptor medium.

Solubility Study An excess amount of sodium diclofenac was added to the test vehicle. The mixture was then allowed to stand at 23 ± 2 °C for 24 h under agitation. The viscous suspension was filtrated through a membrane filter with a pore size of 0.45 μm to obtain a clear fluid, and then the concentration of sodium diclofenac was measured by HPLC.

Assay Assay of diclofenac was carried out by HPLC as described by Yaginuma *et al.*[10] Assay limitation of sodium diclofenac was 50 ng/ml. To determine the degree of presence of *n*-octanol, gas chromatography was used. The gas chromatograph (Shimadzu GC-7AG) was equipped with a flame ionization detector. The carrier gas was nitrogen at a flow rate of 40 ml/min. The column was of coiled glass, 1 m × 2 mm i.d., packed with Diasolid ZT (Nihon Chromato, Ltd.). The column temperature was set at 90 °C for 1 min and was programmed to reach 150 °C at a rate of 18 °C/min. Both the injector and the detector temperatures were maintained at 200 °C.

Results and Discussion

Effect of Vehicles on the Percutaneous Permeation of Diclofenac When each oil alone was used as a simple vehicle, diclofenac was not detected in the receptor medium during the experimental period of 12 h. For example, when 2.5 mg of sodium diclofenac was loaded in 1 g of vehicle, the detected amount of diclofenac in the receptor medium was less than 0.5 μg over a 12 h experimental period. This poor flux is considered to be responsible for the poor solubility of sodium diclofenac in the simple oil vehicles (Table I). To dissolve sodium diclofenac completely in the oil vehicle, ethanol was added to oil. But the steady state flux of diclofenac from the vehicle was below 0.5 μmol/cm^2/h. From these results, it is considered that the permeability coefficient of sodium diclofenac is low.

To enhance the permeability of sodium diclofenac, *n*-octanol was added to the vehicle containing oil and ethanol. It is well known that *n*-octanol increases the skin permeation of drugs.[11] The solubility of sodium diclofenac in the formulated vehicles containing ethanol and *n*-octanol increased remarkably compared to oil alone (Table I). The percutaneous permeation of diclofenac from each formulated vehicle yielded the results shown in Fig. 1. After a lag time, a steady state transport of diclofenac occurred in the following order for the oil used in the formulated vehicle: squalane ≧ squalene > liquid paraffin > MCT > olive oil > castor oil (Fig. 1 and Table II). The values of steady state flux, *J* (μmol/cm^2/h), and lag time were calculated and summarized in Table II.

With respect to drug permeation through the skin from the various formulated vehicles, drug molecules and/or ions should first diffuse out from the vehicle matrix to the skin surface. Then, if the drug has a low affinity for the vehicle components, it will readily diffuse out from the vehicle to the skin. From the *J* values and solubility (Tables I and II), it was revealed that high solubility of sodium diclofenac in the formulated vehicles resulted in slow permeation of diclofenac (Fig. 1). Thus, it may be concluded that a great affinity of sodium diclofenac to the vehicle inhibits the overall transport of diclofenac due to a slow release of drug and/or a poor transfer from the vehicle to the skin.

In comparison to the results of the permeation of diclofenac through rat skin after an application of sodium

TABLE I. Solubility of Sodium Diclofenac in Oils and Formulated Vehicle

	Solubility (mM)[a]	
	Vehicle	Oil
Squalane	10.1	1.0×10^{-3}
Squalene	12.4	3.7×10^{-2}
Liquid paraffin	13.7	0.7×10^{-3}
MCT	36.6	0.64
Olive oil	35.5	0.69
Castor oil	38.3	14.4

a) Solubility of sodium diclofenac in the oil and vehicle was measured at 23 ± 2 °C.

TABLE II. Permeation Parameters and Release Control Factor of Diclofenac from Formulated Vehicles

	$J^{b)}$ (nmol/cm^2/h)	$Le^{b)}$ (h)	$k^{c)}$
Squalane	112.6 ± 14.7	2.5 ± 0.5	252.8 ± 10.9
Squalene	98.7 ± 12.2	2.5 ± 0.4	233.2 ± 16.0
Liquid paraffin	65.7 ± 13.6	4.4 ± 0.8	163.9 ± 13.3
MCT	28.5 ± 7.0	3.2 ± 0.5	115.4 ± 10.8
Olive oil	4.0 ± 1.0	3.2 ± 0.5	72.4 ± 14.1
Castor oil	1.3 ± 0.3	5.5 ± 0.8	66.3 ± 10.0
Buffer[a] (pH 7.4)	0.9 ± 0.2	4.9 ± 0.9	—

a) The values were obtained from the previous study.[2] *b*) The values of steady state flux (*J*) and lag time (*Le*) were calculated from the straight line in Fig. 1. *c*) The values of release control factor (*k*) were calculated from the straight line in Fig. 4B. Each value represents the mean ± S.D. ($n = 4$ to 6).

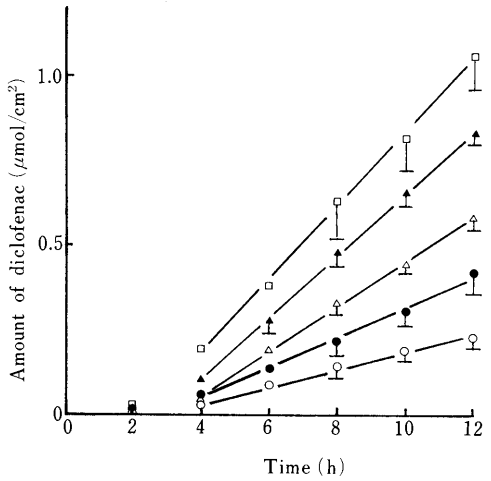

Fig. 1. Effect of the Oil Component in the Formulated Vehicles on the Permeation of Diclofenac through Rat Skin

○, squalane; □, squalene; △, liquid paraffin; ■, MCT; ●, olive oil; ▲, castor oil. Each value represents the mean ± S.D. ($n = 4$ to 6).

diclofenac in a buffer solution obtained by a preliminary experiment, the values of J obtained from the formulated vehicles, except for olive oil and castor oil, were more than 20 times larger than the value obtained from the buffer solution (Table II). From these results, it may be suggested that the lipid route in the skin barrier is mainly responsible for the permeation of diclofenac through the barrier, regardless of the ionized form of diclofenac.

Furthermore, we have already reported that the topical application of a phospholipid vehicle of sodium diclofenac increased the flux of diclofenac in rats by about 20 times in comparison to that obtained after the application of a buffer solution. And it was also suggested that the plasma levels of diclofenac in human subjects by the topical application of the phospholipid vehicles were expected to be within the clinically effective range.[12] Thus, the formulated vehicles with squalane, squalene or liquid paraffin are considered worthy of further study.

Release of Diclofenac and *n*-Octanol from Formulated Vehicles To clarify the reason for the differences in the permeation of diclofenac among the formulated vehicles, the release of *n*-octanol and diclofenac from the vehicles *in vitro* was studied. As the separation membrane, an EVA membrane as a lipoidal membrane was used in the release study of *n*-octanol. But sodium diclofenac cannot penetrate through the EVA membrane; therefore, a cellophane membrane as a porous membrane was used in sodium diclofenac.

The release rates of *n*-octanol from the formulated vehicles were in the following order: liquid paraffin > squalene ≧ squalane > MCT ≧ olive oil > castor oil (Fig. 2). It has been reported that the enhancing effect of various alcohols on transdermal drug absorption occurs by possibly increasing the permeability of the stratum corneum.[11] In this study, *n*-octanol enhanced the permeation of diclofenac across rat abdominal skin. Thus, it may be considered that a low affinity of *n*-octanol to the vehicle increases the overall transport of diclofenac due to an enhancing effect of *n*-octanol. Iwata *et al.*[13] demonstrated that the percutaneous absorption of alcohols was influenced by the coadministration of solvents. And they also suggested that, among several oils, squalane was the most effective oil for the percutaneous absorption of alcohols. Indeed, in this study, it appeared that a slow release of *n*-octanol from

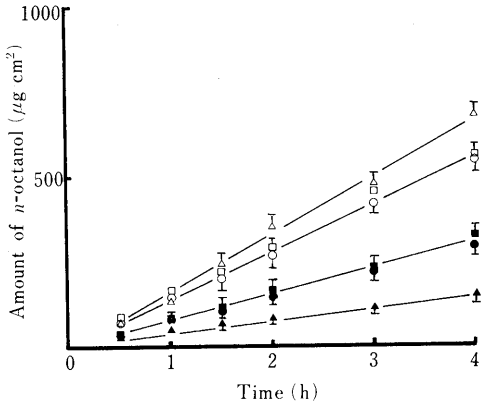

Fig. 2. Release Profiles of *n*-Octanol from the Formulated Vehicle into the Aqueous Phase through the EVA Membrane

○, squalane; □, squalene; △, liquid paraffin; ■, MCT; ●, olive oil; ▲, castor oil. Each value represents the mean ± S.D. ($n=4$).

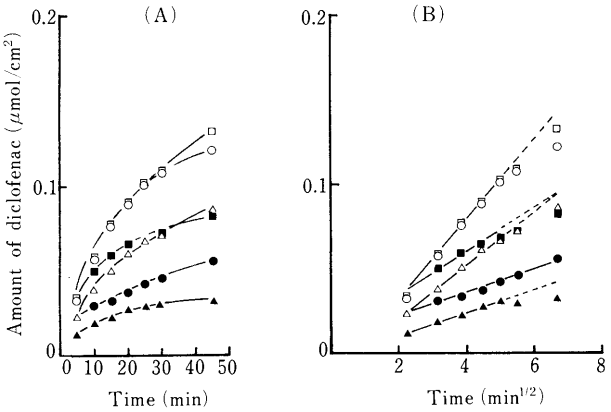

Fig. 4. Release Profiles of Diclofenac from the Formulated Vehicle into the aqueous Phase through a Cellophane Membrane

(A) Plots of the released amount of diclofenac against time; (B) Plots of the released amount of diclofenac against the square root of time. ○, squalane; □, squalene; △, liquid paraffin; ■, MCT; ●, olive oil; ▲, castor oil. Each value represents the mean ± S.D. ($n=4$).

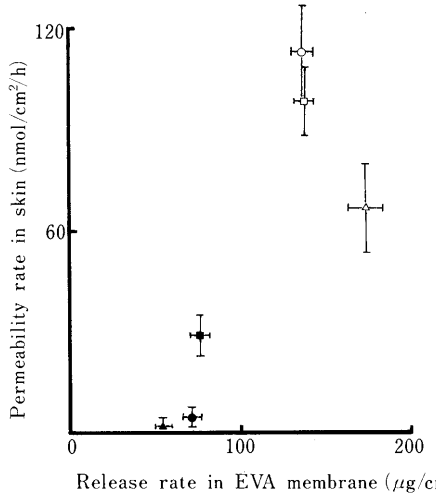

Fig. 3. Relationship between the Permeation Rate of Diclofenac through Rat Skin and the Release Rate of *n*-Octanol through the EVA Membrane

○, squalane; □, squalene; △, liquid paraffin; ■, MCT; ●, olive oil; ▲, castor oil.

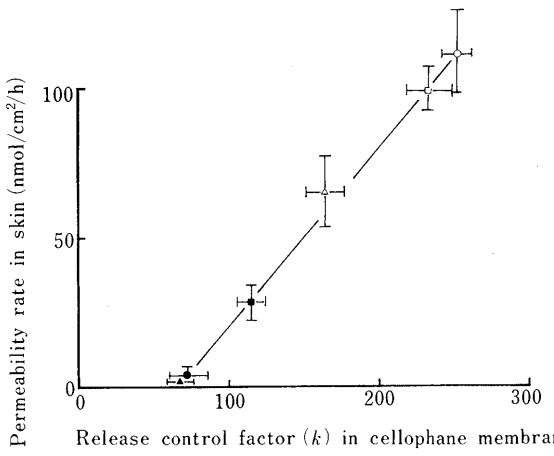

Fig. 5. Relationship between the Permeation Rate through Rat Skin and the Release Control Factor (k) through a Cellophane Membrane

○, squalane; □, squalene; △, liquid paraffin; ■, MCT; ●, olive oil; ▲, castor oil. $Y=0.598X-38.292$ ($r=0.997$).

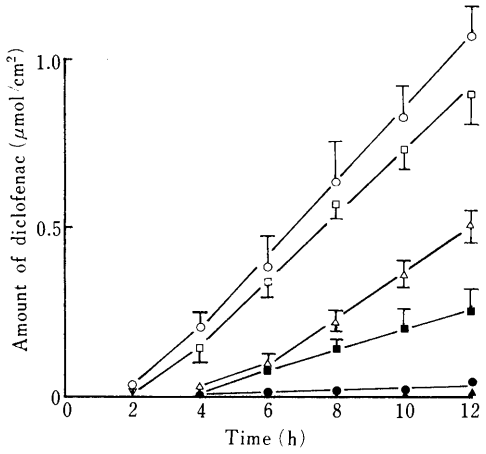

Fig. 6. Effect of the Content of Sodium Diclofenac on the Permeation of Diclofenac through Rat Skin

○, 0.5 mg/g; ●, 1.0 mg/g; △, 1.5 mg/g; ▲, 2.0 mg/g; □, 2.5 mg/g. Each value represents the mean ± S.D. ($n=4$ to 6).

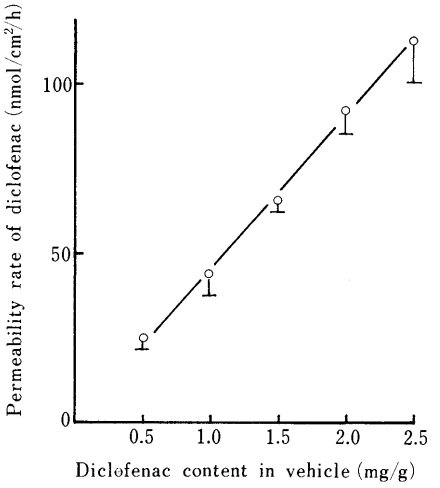

Fig. 7. Relationship between the Permeation Rate through Rat Skin and Diclofenac Content in the Formulated Vehicle

$Y=4.448X+1.165$ ($r=0.998$).

the vehicles resulted in a slow permeation of diclofenac. But a significant relationship was not observed between the release rate of *n*-octanol and the rate of diclofenac permeability (Fig. 3).

The release profiles of diclofenac from the formulated vehicles are presented in Fig. 4. When the amounts of diclofenac released were plotted against the square root of time, a linear relationship was obtained for each vehicle. From these observations, in the early stages, a leaching-type drug release process as proposed by Higuchi[14] may be applied for the release of diclofenac from the vehicles studied. The value of k in Table II was calculated from the slope of the initial straight line in Fig. 4B. This value (k) may be considered an apparent rate constant factor for the release of diclofenac from the vehicles.

A linear relationship was observed between the release rate of diclofenac from the cellophane membrane and the rate of drug permeability across rat abdominal skin (Fig. 5). This good correlation may indicate that release control factor of the drug from the vehicle is an important factor for the formulation of the vehicle to facilitate drug transport across the skin.

TABLE III. Effect of Diclofenac Content on the Permeation Parameter of Diclofenac

	Content of diclofenac (mg/g vehicle)				
	0.5	1.0	1.5	2.0	2.5
$Le^{a)}$ (h)	2.4±0.4	2.9±0.7	3.1±0.4	2.8±0.5	2.5± 0.5
$J^{a)}$ (nmol/cm²/h)	25.4±3.1	43.8±7.0	65.6±2.2	92.0±6.2	112.6±14.7
$Pe^{b)}$ ($\times 10^{-3}$ cm/h)	16.2±2.0	14.0±2.2	13.9±0.5	14.6±1.0	14.3± 1.9

a) The values of steady state flux (J) and lag time (Le) were calculated from the straight lines in Fig. 6. *b*) Permeability coefficient (Pe) was calculated from the steady state flux and the initial concentration of sodium diclofenac in the donor compartment. Each value represents the mean ± S.D. ($n=4$ to 6)

Effect of Sodium Diclofenac Content in the Formulated Vehicle Among oils used in the present study, squalane was the most appropriate oil for the formulated vehicles as well as for the simple oleaginous ones. In order to study the effects of diclofenac content in the vehicle on drug permeation through the skin, a vehicle formulated with squalane was used.

An increase in the drug concentration in the vehicle resulted in an increase in the amount of diclofenac which permeated the skin (Fig. 6). The penetration flux, J, of diclofenac at a steady state was nearly proportional to the drug concentration in the vehicle (Fig. 7). But, the values of the permeability coefficient (Pe, which was calculated from the flux and initial concentration of sodium diclofenac in the donor compartment) and lag time were not influenced by the concentration of the drug in the formulated vehicles (Table III). Similarly, the intrinsic permeability for the skin epithelium was not influenced by drug concentration in the vehicle, suggesting that the mechanism involved in the transport process is passive diffusion.

In summary, the steady-state flux of diclofenac from an oil alone or a vehicle containing ethanol and oil was low. To enhance the permeability of sodium diclofenac, *n*-octanol was added to the vehicle. The solubility and steady-state flux increased dramatically with the formulated vehicles in squalane, squalene or liquid paraffin. These results appear to be due to the low affinity (high release rate) of *n*-octanol and sodium diclofenac to these oil components. In the castor oil vehicle, however, a low release rate of *n*-octanol and sodium diclofenac and low steady-state flux were observed. This may be due to the high affinity of *n*-octanol and sodium diclofenac to the castor oil vehicle. Also, the steady-state flux of diclofenac was nearly proportional to the drug concentration in the vehicle. From these results, it is considered that the important factors for increasing skin permeation of a drug from an oil vehicle are: to select an oil which has a low affinity for the drug and enhancer; and to increase the drug concentration in the oil. And squalane, squalene or liquid paraffin may be useful oil components for the transdermal administration of sodium diclofenac.

References and Notes

1) A part of this work was presented at the 109th Annual Meeting of the Pharmaceutical Society of Japan, Nagoya, April 1989.
2) T. Nishihata, K. Kotera, Y. Nakano and M. Yamazaki, *Chem. Pharm. Bull.*, **35**, 3807 (1987).
3) D. Southwell, B. W. Barry, R. Evans and F. J. T. Fildes, *J. Pharm. Pharmacol.*, **33**, 3p (1981).

4) J. J. Windheuser, J. L. Haslam, L. Caldwell and R. D. Shaffer, *J. Pharm. Sci.*, **71**, 1211 (1982).
5) S. K. Chandrasekaran, P. S. Campbell and A. S. Michales, *AIChE J.*, **23**, 810 (1977).
6) E. Touitou and B. Fabin, *Int. J. Pharm.*, **43**, 17 (1988).
7) P. Ashton, J. Hadgraft and K. A. Walters, *Pharm. Acta Helv.*, **61**, 228 (1986).
8) R. B. Stoughton, *Arch. Dermatol.*, **118**, 474 (1982).
9) K. B. Sloan, K. G. Siver and S. A. M. Koch, *J. Pharm. Sci.*, **75**, 744 (1986).
10) H. Yaginuma, T. Nakata, H. Toya, T. Murakami, M. Yamazaki and A. Kamada, *Chem. Pharm. Bull.*, **29**, 2974 (1981).
11) N. Tsuzuki, O. Wong and T. Higuchi, *Int. J. Pharm.*, **46**, 19 (1988).
12) T. Nishihata, A. Kamada, K. Sakai, K. Takahashi and K. Matsumoto, *Int. J. Pharm.*, **46**, 1 (1988).
13) Y. Iwata, Y. Moriya and T. Kobayashi, *Cosmetics & Toiletries*, **102**, 53 (1987).
14) T. Higuchi, *J. Pharm. Sci.*, **52**, 1145 (1963).

Pressure Sensitive Adhesion and Viscoelasticity of Polyvinyl Alcohol Hydrogels. II. Simulation and Prediction of Pressure Sensitive Adhesion by Viscoelastic Data

Fumio URUSHIZAKI*,[a] and Hiroshi MIZUMACHI[b]

The Second Department of Pharmaceuticals, Research Center, Taisho Pharmaceutical Co. Ltd.,[a] Yoshino-cho 1-403, Ohmiya-shi 330, Japan and Laboratory of Chemistry of Polymer Materials, Department of Forest Products, Faculty of Agriculture, The University of Tokyo,[b] Yayoi 1–1–1, Bunkyo-ku, Tokyo 113, Japan. *Received April 23, 1990*

The control of adhesion properties such as pressure sensitive adhesion and tack (initial pressure sensitive adhesion) is important in external applications of plasters or poultices, including transdermal drug delivery systems, hospital tapes, first aid tapes and others. Excessive tack and pressure sensitive adhesion may cause skin irritation and other maladies. These problems must be overcome when developing external applied preparations.

In our previous paper, tacks expressed as rolling friction coefficients of polyvinyl alcohol (PVA) hydrogels were determined by the rolling cylinder method, and viscoelasticities were determined by dynamic viscoelastic methods.

The correlation between tacks and viscoelasticities, such as storage modulus and loss tangent, was found to be high using the statistical method of multi-regression analysis.

In the present study, the experimental results from tack and viscoelastic data of PVA hydrogels were compared with theoretical values by curve fitting.

Theoretical curves were calculated by computer simulation methods according to our equations, based on a four elements mechanical model (two Maxwell elements in parallel connection), failure criteria and viscoelastic data of PVA hydrogels.

Tack for external applied preparations formed as plasters and poultices could be predicted by these results. The prediction methods proposed in this paper are essential for establishing the ideal tack of plasters and poultices in the stage of pre-formulation.

Keywords rolling friction coefficient; pressure sensitive adhesion; tack; viscoelasticity; polyvinyl alcohol; hydrogel; adhesion; modulus; loss tangent

Introduction

Tack (initial pressure sensitive adhesion) is one of the key properties of plasters and poultices for transdermal drug deliveries, hospital tapes, and first aid tapes. This property must be determined at the pre-formulation stage so as to avoid excess pressure sensitive adhesion, since excessive tack may cause skin irritation and other maladies.[1)]

There are many methods to determine the tack of pressure sensitive adhesions (PSAs), such as the peel test, the probe tack test, the rolling ball tack test and others. These methods of expressing tack are useful in some practical cases, but the physical meaning of the values is not necessarily clear. The values determined by the tack tester are relative values under fixed conditions and do not compare with values determined by other conditions such as the determining methods, the instruments and other factors.[2)]

In our previous paper, tacks of PSAs were expressed as rolling friction coefficients, which are specific properties of PSAs and are independent of the determining methods.[3)] We discussed an excellent determining method, the pulling cylinder method, which improved on the rolling ball tack test.[4,5)] The rolling friction coefficients of PSAs can be determined by the pulling cylinder method much more easily than by the rolling ball method. Measurements obtained by the pulling cylinder method can be determined under well-defined conditions, and they require no assumption concerning the dependence of the rolling friction coefficient on velocity because the pulling velocity of the cylinder is controlled. High relationships between viscoelasticities such as the dynamic modulus, viscosity and tack were found using the rolling cylinder method.[4,5)]

The tack described by us is considered the physical and essential values of the materials, and is related to other physical properties, such as the parameters reflected by the composition of PSAs or the solubility of the tackifier in elastomers.

Tohyama *et al.* described the tack of PSAs in terms of viscosity, elasticity, solubility of ingredient materials, surface tension and surface properties of adhesive materials.[6)]

The correlation between the tack and viscoelastic data of hydrogels of polyvinyl alcohol (PVA) having high saponification values have been established.[7)] These linear relations of PVA hydrogels were made clear in a statistical manner through a multi-regression analysis. This procedure made use of the curve fitting method by means of computer simulation between theoretical values and experimental data. The experimental data of tack with PVA hydrogels was fitted to the theoretical curves of computer simulation calculated by two Maxwell elements in a parallel connection model, failure criteria, and viscoelastic data of PVA hydrogels.

From these results, the an entire range of tack of PVA hydrogels is easily handled by our method for cases of variations of PVA hydrogels. The tack of PVA hydrogel can be inferred from the viscoelastic data.

It is important to know the tack of external applications, such as those used for transdermal drug deliveries, at the pre-formulating stages. Our method is useful for establishing this.

Theoretical

The rolling friction coefficient, f, measured by the rolling cylinder tack tester is defined by the following Eq. 1:

$$f = PR/Mg \tag{1}$$

where R and Mg denote the radius and gravity of the rolling cylinder, and P corresponds to the pulling force of the

rolling cylinder at a constant speed.

When the cylinder rolls on the PSA, the rolling area of the cylinder is expressed by $bRd\theta$, where b and θ denote the length of the cylinder and rolling angle, respectively. $d\theta$ is the differentiation of θ as an expression of a small rolling distance. The cylinder makes contact with the PSA at angle $\theta=0$ and fails at $\theta=\theta_b$ in the case of constant pulling velocity, v.

Equation 1 is transformed to Eq. 2:

$$f=R^2b/Mg\cdot\int_{\theta=\theta_0}^{\theta=\theta_b}\sigma(\theta)\sin\theta\cos\theta d\theta \tag{2}$$

where σ (θ) denotes the total stress of the rolling cylinder.

Additionally, there are many mechanical models, such as the single Voigt element, Maxwell element, two Maxwell elements in parallel connection, multi Maxwell elements in parallel connection and others.

The rolling friction coefficient varied when we adopted mechanical models and failure criteria.[4)]

In this experiment, mechanical models were selected to express the tack and viscoelastic data of PVA hydrogels.

When the same mechanical models were used, the rolling friction coefficient also varied according to variations of failure criteria between PVA hydrogels and the adherend of the surface of the rolling cylinders. Theoretical curves for the rolling friction coefficients versus the peeling rate (rolling speed) were simulated with combinations of mechanical models and failure criteria.

Hata has presented a theoretical description of the peeling phenomena using a mechanical model, failure criteria and viscoelastic data.[8)]

Two Maxwell elements in a parallel connection model were used in the present analysis. The pattern of the mechanical model and the notations of the springs and dashpots relating to the elasticities and viscosities of PSAs are shown in Fig. 1.

The peeling phenomena between PSAs and adherends were explained as two patterns between the speed of the rolling cylinder and viscoelastic data of PSAs. These were considered equi-mechanically to be a kind of fracturing phenomena in two springs or dashpots of the two Maxwell elements in a parallel connection model. Two types of peeling are cohesive failure and interfacial failure. Three types of failure criteria in the mechanical model of PSAs, (A), (B) and (C) were assumed as follows: Failure of cases (A) and (B) constitute cohesive failure, and of case (C), interfacial failure.

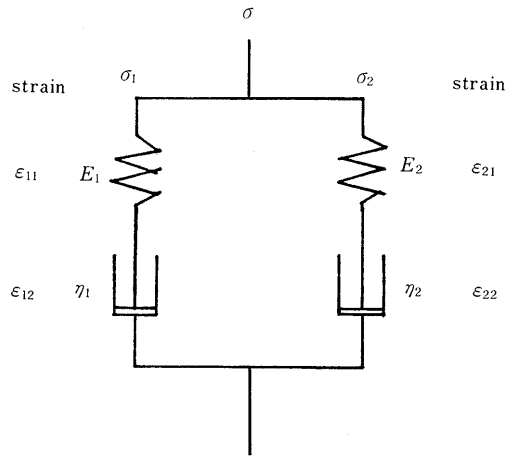

Fig. 1. Two Maxwell Elements in Parallel Connection as an Equi-mechanical Model of Pressure Sensitive Adhesives

Key: σ, σ_i=stress; ε_{i1}=strain of a spring; ε_{i2}=strain of a dashpot; E_i=modulus of a spring; η_i=viscosity of a dashpot.

These mechanical model and failure criteria were applied to the peeling phenomena of PVA hydrogels.

(A) In the region where the rate of strain is very high, failure occurs when the strain of the spring, ε_{11}, at the weak point (element 1) reaches a critical value ε_{11c}.

(B) In the region where the rate of strain is very slow, failure occurs when the strain of the dashpot, ε_{12}, at the weak point (element 1) reaches a critical value ε_{12c}.

(C) Interfacial failure happens when the storage energy W in the two springs of the two Maxwell elements in a parallel connection model exceeds the critical storage energy W_c.

The rolling friction coefficient, f, must be calculated by both the two Maxwell elements in a parallel connection model, and the failure criteria described by (A), (B) and (C).

The total stress of the two Maxwell elements in a parallel connection model is expressed as follows:

$$\sigma(\theta)=\sum_{i=1}^{2}\sigma_i(\theta)=\sum_{i=1}^{2}E_iR\{E_iR\sin\theta/v\eta_i-\cos\theta+\exp(-E_iR\theta/v\eta_i)\}/h(E_i^2R^2/v^2\eta_i^2+1) \tag{3}$$

E_i and η_i are thought of as the functions of the storage modulus and complex modulus, respectively, and h is the thickness of the PSA.

Three failure criteria were described by the following equations:

(A), spring failure in the mechanical model of two Maxwell elements in a parallel connection:

$$\varepsilon_{11}=\sigma_1(\theta)/E_1=R\{E_1R\sin\theta/v\eta_1-\cos\theta+\exp(-E_1R\theta/v\eta_1)\}/h(E_1^2R^2/v^2\eta_1^2+1)=\varepsilon_{11c} \tag{4}$$

(B), dashpot failure in the mechanical model of two Maxwell elements in parallel connection:

TABLE I. PVA for Determination of Rolling Friction and Viscoelasticity

Test sample	Saponification value (mol%)	Viscosity[a)] (cP)	Gelation[b)]	Maker's name
K-17E	97.8—98.5	28—32	○	Denka Poval
K-20	97.5—98.5	38—45	○	Denka Poval
K-24E	97.8—98.5	57—67	○	Denka Poval
NH-20	98.5—99.4	35—43	○	Nihon gohsey Gohosenol
AH-17	97.0—98.5	25—30	○	Nihon gohsey Gohosenol
AH-22	97.5—98.5	50—66	○	Nihon gohsey Gohosenol
AH-26	97.0—98.8	58—66	×	Nihon gohsey Gohosenol
CH-23	86.5—89.0	48—56	×	Nihon gohsey Gohosenol

a) Viscosity of 4% aqueous solution. b) Gelation of 15% aqueous solution on freezing at −5 °C in 20 h and defrosting at room temperature in 4 °C.

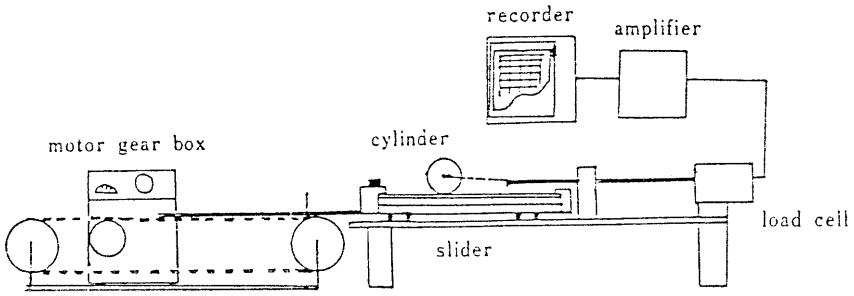

Fig. 2. Apparatus for Determining Rolling Cylinder Tack

$$\varepsilon_{12}=E_1R^2[E_1R(1-\cos\theta)/v\eta_1-\sin\theta+v\eta_1\{\exp(-E_1R\theta/v\eta_1)-1\}/E_1R]/hv\eta_1\{(E_1^2R^2/v^2\eta_1^2)+1\}=\varepsilon_{12c} \quad (5)$$

(C), interfacial failure in the mechanical model of two Maxwell elements in parallel connection:

$$W=\sum_{i=1}^{2}\varepsilon_{11}^2E_i/2=\sum_{i=1}^{2}\sigma_i(\theta)^2/2E_i=W_c \quad (6)$$

The correlation between the rolling friction coefficient and the pulling velocity of the cylinder is expressed by these equations (A), (B) and (C), which occur successively.

Experimental

Materials PVAs used in this experiment were Povals and Gohosenols of commercial grade, purchased from Denki-kagaku Kohgyo Co. Ltd., and Nihon Gosei Co., Ltd.

The saponification value, viscosity in a solution reflecting molecular size, hydrogel formation facility and other factors are listed in Table 1.

Preparation The PVA hydrogels were prepared in order to determine tack and viscoelastic data. These hydrogels had different shapes, the flat shape being used to determine of the rolling friction coefficient and the rod shape being to determine viscoelastic data. The two shapes of PVA hydrogels were presumed to have the same physical properties under the same gelating condition.

PVA hydrogels were prepared as follows: PVAs were dissolved in deionized water in a water bath at about 80°C, and PVA solutions were mixed homogeneously. Cooling down and expelling air from the PVA solutions was done at room temperature. The solutions were poured onto flat glass plates ($3.0\times19.0\,cm^2$) which were covered by anchoring papers fixed by two surface pressure sensitive adhesive tapes.

The thickness of these PVA hydrogels was controlled by the depth of the plastic frames. Polyester sheets were then overlaid on the PVA solution as liners. The gelation of PVA hydrogel was done under various conditions: freeze-thaw cycles, thawing temperature, thickness of PVA hydrogels and other factors. These PVA hydrogels were used to determine of tack.

The PVA hydrogels used to determine of viscoelastic data were 20 mm in diameter and 30 mm in length, and were shaped by using plastic tubes. Both sides of the tubes were covered by plastic sheets to prevent water loss from the hydrogels.

Gelation of PVA solutions to make up the hydrogels was carried out under freezing and thawing cycles. The freezing process consisted of standing the solution in a freezing box at -5 ± 1 °C; and the thawing process was conducted at 5, 25 and 40 °C.

Determination of Tack by the Rolling Cylinder Method The instrument used for determining the tack (initial pressure sensitive adhesion) of PVA hydrogels was the rolling cylinder tack tester, as shown in Fig. 2.

The determination of the tack of PVA hydrogels was carried out at 20 °C.

With this method, both the weight of the rolling cylinders and the rolling speed can be controlled independently, but in the proto-type rolling tack test method, such as the J. Dow method and the PST-6 method, the two factors were not able to be controlled independently.

The theoretical and logical implications of this rolling cylinder tester have been previously explained.[4,5]

Determination of Viscoelastic Data Dynamic viscoelastic data such as the storage modulus, loss modulus and loss tangent were measured by Rheolograph-gel (Tohyo-Seiki Co. Ltd.,).

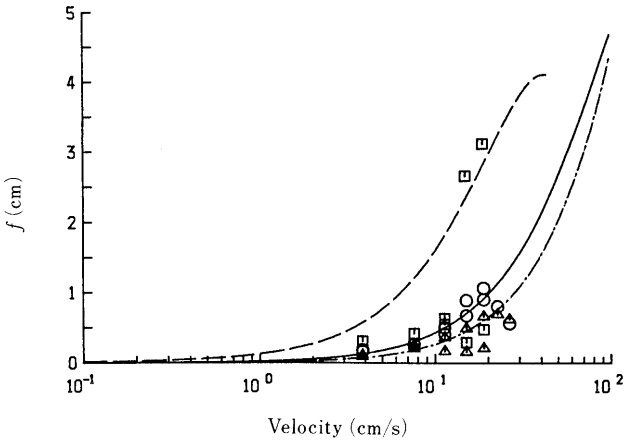

Fig. 3. Comparison between Simulated Theoretical Data and the Experimental Data of PVA Hydrogels under Variation of Carbon Chain Length

Thickness of PVA hydrogels, 0.170 cm.

carbon length	theoretical curve	exp. data	E_1 (dyn/cm²)	E_2 (dyn/cm²)	η_1 (P)	η_2 (P)	η_{1c} (P)
K-20	——	○	0.82×10^5	0.82×10^5	0.26×10^6	0.26×10^7	$0.8\times10^{+1}$
K-17E	— —	□	0.59×10^5	0.59×10^5	0.17×10^6	0.17×10^7	0.28
K-24E	—·—	△	0.19×10^5	0.19×10^5	0.13×10^6	0.13×10^7	0.10×10^{-1}

The sample size of the cylindrical-shaped PVA hydrogels was 20 mm in diameter and 30 mm in length. The amplitude of vibration was $\pm100\,\mu m$ and the frequency of vibration was 2 Hz.

Detailed conditions and results have been described in a previous article.[7]

Computer Simulation and Theoretical Curves of Pressure Sensitive Adhesion Theoretical curves of pressure sensitive adhesion about PVA hydrogels were simulated at the Computer Center of Tokyo University. Programs for the calculation were constructed using Fortran.

Results and Discussion

Comparison of Theoretical Curve with Experimental Data In our previous paper, tacks of PVA hydrogels which were determined as rolling friction coefficients by a rolling cylinder tack tester, were statistically related with viscoelastic data such as storage modulus and loss tangent.[7]

In the present paper, theoretical curves were simulated by putting the viscoelastic data of PVA hydrogels into our equations. The mechanical model and failure criteria for the tack of PVA hydrogels were determined by comparing theoretical curves with experimental data.

Variations of the tack with PVA hydrogels were affected by the chain length of PVA, the concentration of PVA in the solutions, the number of cycles of freezing and thawing, the temperature of thawing of frozen PVA solutions, the thickness of PVA hydrogels, and other factors. The effect

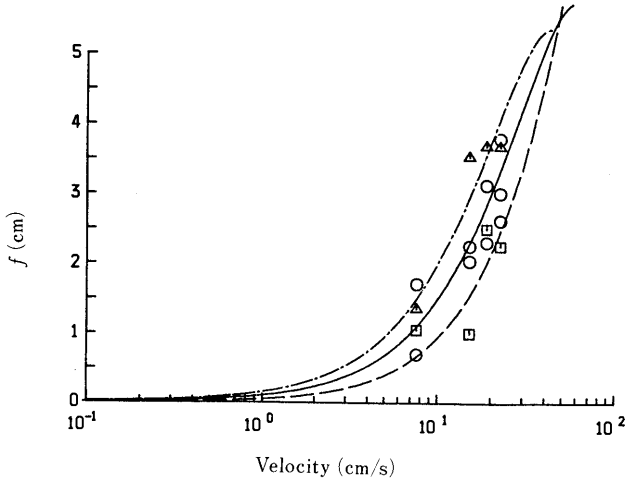

Fig. 4. Comparison between Simulated Theoretical Data and the Experimental Data of PVA Hydrogels under Variation of Thawing Temperature

Thickness of PVA hydrogels, 0.170 cm.

thawing temp.	theoretical curve	exp. data	E_1 (dyn/cm^2)	E_2 (dyn/cm^2)	η_1 (P)	η_2 (P)	η_{1c} (P)
25 °C	——	○	0.82×10^5	0.82×10^5	0.26×10^5	0.26×10^6	0.17
5 °C	— —	□	0.17×10^6	0.17×10^6	0.97×10^5	0.97×10^6	0.35×10^{-1}
40 °C	—·—	△	0.77×10^5	0.77×10^5	0.23×10^5	0.23×10^6	0.25

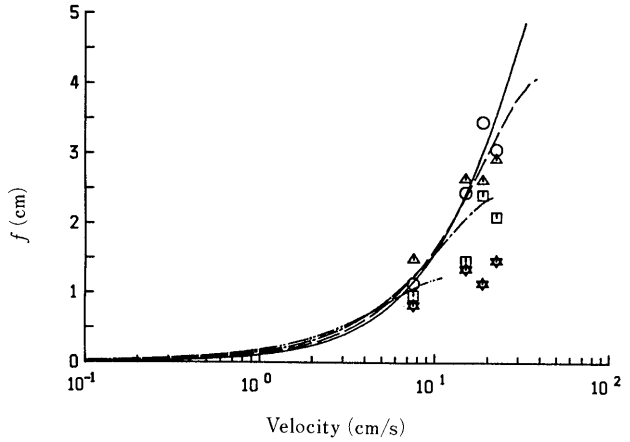

Fig. 5. Comparison between Simulated Theoretical Data and the Experimental Data of PVA Hydrogels under Variation of Thickness with Hydrogels

Thawing temperature, 25 °C; modulus, E_1 0.28×10^5 E_2 0.82×10^5 (dyn/cm^2); viscosity, η_1 0.26×10^5 η_2 0.26×10^6 (P); failure criteria, 0.18 P.

thickness of PVA hydrogels (cm)	exp. data	theoretical curve
0.149	○	——
0.237	□	— —
0.400	△	—·—
0.756	☆	—··—

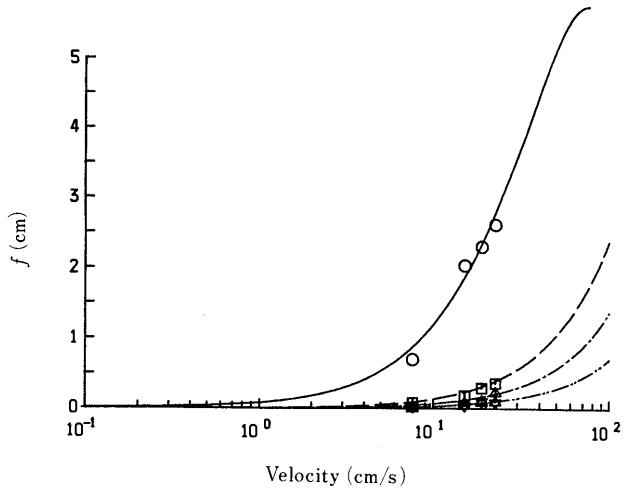

Fig. 6. Comparison between Simulated Theoretical Data and the Experimental Data of PVA Hydrogels under Variation of Freeze-Thawing Cycles

Thickness of PVA hydrogels, 0.170 cm.

freezing thawing cycles	theoretical curve	exp. data	E_1 (dyn/cm^2)	E_2 (dyn/cm^2)	η_1 (P)	η_2 (P)	μ_{1c} (P)
1	——	○	0.82×10^5	0.82×10^5	0.26×10^5	0.26×10^6	0.14
2	— —	□	0.15×10^6	0.15×10^6	0.12×10^6	0.12×10^7	0.60×10^{-2}
3	—·—	△	0.20×10^6	0.20×10^6	0.19×10^6	0.19×10^7	0.25×10^{-2}
4	—··—	☆	0.29×10^6	0.29×10^6	0.31×10^6	0.31×10^7	0.10×10^{-2}

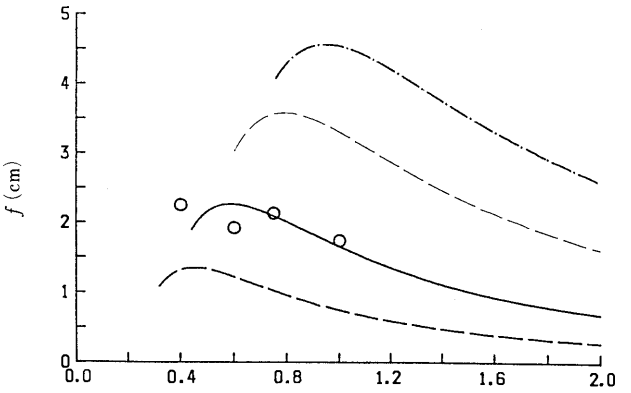

Fig. 7. Comparison between Simulated Theoretical Data and the Experimental Data of PVA Hydrogels under Variation of the Diameter of Rolling Cylinders

Thickness of PVA hydrogels, 0.170 cm; modulus, E_1 0.82×10^5 E_2 0.82×10^5 (dyn/cm^2); viscosity, η_1 0.26×10^5 η_2 0.26×10^6 (P); failure criteria, 0.10 P.

diameter of cylinder (cm)	theoretical curve
0.10	——
0.20	— —
0.30	—·—
0.05	▬▬

of diameter and weight of the rolling cylinders were also determined in preliminary experiments.[7] The theoretical curves were compared with the experimental data as shown in the following figures. Figs. 3, 4, 5 and 6 shows the effect on the tacks of the chain length, thawing temperature, thickness of PVA hydrogels and number of freeze-thaw cycles; Fig. 7 the shows relation of these figures to preliminary experiments.

Experimental data correlated well with the theoretical curves in all cases under the fixed failure criteria. But in the tack of PVA hydrogels, only failure criterion (B) was observed in the rolling friction coefficients caused by dashpot failure in mechanical models.

The failure of the dashpot in the mechanical model was affected by the relationship between the relaxation time and the determining time of PSAs. Therefore, the critical strain ε_{12c} in the mechanical models and storage modulus of PVA hydrogel were plotted, as shown in Fig. 8, for the case of

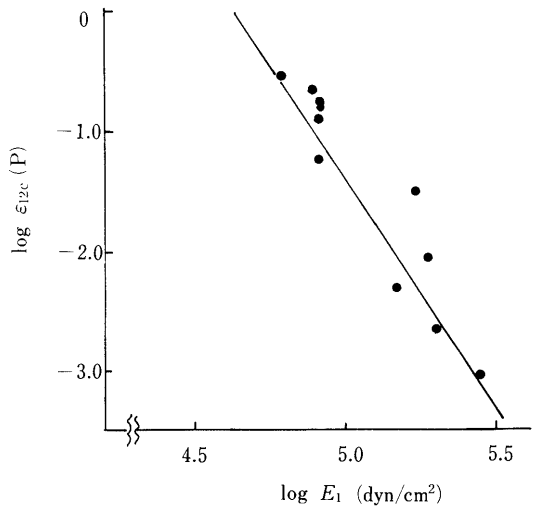

Fig. 8. Relation between the Critical Viscosities and Storage Modulus in the Case of Agreement with the Theoretical and Experimental Data

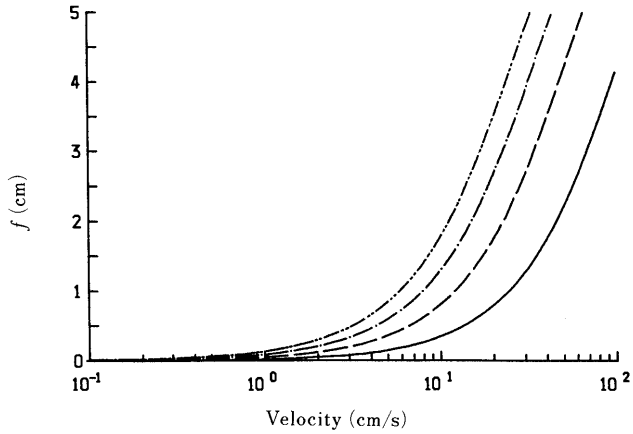

Fig. 9. Prediction of Tack under Varying Viscoelasticities of PVA Hydrogel

Thickness of PVA hydrogels, 0.170 cm; failure criteria, ε_{12c} 0.15×10^{-1}.

Prediction curve	E_1 (dyn/cm^2)	E_2 (dyn/cm^2)	η_1 (P)	η_2 (P)
——	0.1×10^5	0.1×10^5	0.7×10^4	0.7×10^5
— —	0.5×10^5	0.5×10^5	0.35×10^5	0.35×10^6
— · —	0.1×10^6	0.1×10^6	0.7×10^5	0.7×10^6
— · · —	0.5×10^6	0.5×10^6	0.35×10^6	0.35×10^7

agreement between the theoretical curves and the experimental data.

The storage modulus, E_1, of PVA hydrogels was substituted for the springs of the mechanical elements, which are on the same side of the failure dashpot of the two Maxwell elements in the parallel connection model. The logarithmic ε_{12c} and logarithmic E_1 show almost linear relationships at the critical points of the mechanical model. The following equation of regression was derived from these results:

$$\varepsilon_{12c} = 10^{17.0}/E_1^{4.0} \quad (7)$$

Prediction of Tack In the pre-formulation stages of developing externally applied preparations such as transdermal drug deliveries, it is important to predict tack and viscoelasticity. The viscoelastic data of PSAs relates to tack, which is expressed by the four elements mechanical model and failure criteria. The tack of PVA hydrogels was expressed by our equations, and the predictive tack of PVA hydrogels was simulated under variations of viscoelastic data.

These results are shown in Fig. 9. The prediction of tack with PVA hydrogels was carried out under fixed conditions without variation of viscoelasticity of the mechanical models. The fixed conditions were the thickness of the hydrogels and the failure criteria.

The patterns of tack calculated by the condition described in Fig. 9 were uniform figures, but moved to the right side, or the high rolling speed side.

Conclusion

Excessive adhesion in externally applied preparations such as transdermal drug delivery systems must be avoided to prevent skin irritation and other maladies. An ideal tack is necessary for these preparations.

The J. Dow rolling tack tester method has been generally utilized, but the values of determined results have had no well-defined logical meaning.

In our previous paper, the tack of PVA hydrogels was expressed by the rolling friction coefficient which was physically defined by the original characteristics of the materials. A strong relationship was observed between the tack and the viscoelastic data of PVA hydrogels.[3)]

In this paper, the tack of PVA hydrogels was simulated by our equations, where tack is calculated as the rolling friction coefficient from the viscoelastic data of PSAs.

The data simulated by our equation agreed with the experimental data.

The prediction of tack is possible by utilizing our equations. These methods are useful for developing ideal properties for externally applied preparations.

Acknowledgement We wish to express our thanks to Dr. Yasunori Hatano for his excellent suggestions.

References

1) F. R. Hammond Jr, "Handbook of Pressure-Sensitive Adhesive Technology," ed. by D. Satas, von Nostrand Reinhold Company, New York, 1982, pp. 32—49.
2) D. Satas, "Handbook of Pressure-Sensitive Adhesive Technology," ed. by D. Satas, von Nostrand Reinhold Company, New York, 1982 pp. 419—425.
3) F. Urushizaki, H. Yamaguchi and H. Mizumachi, *Nippon Setchaku Kyokai Shi*, **20**, 295 (1984).
4) H. Mizumachi, *Nippon Setchaku Kyokai Shi*, **20**, 522 (1984); *J. Appl. Polym. Sci.*, **30**, 2675 (1985).
5) H. Mizumachi and Y. Hatano, *J. Appl. Polym. Sci.*, **37**, 3097 (1989).
6) M. Tohyama, Y. Kitazaki and H. Watanabe, *Nippon Setchaku Kyokai Shi*, **6**, 356 (1970).
7) F. Urushizaki, H. Yamaguchi and H. Mizumachi, *Yakugaku Zasshi*, **106**, 491 (1986).
8) T. Hata, *Nippon Setchaku Kyokai Shi*, **8**, 64 (1972).

Effect of Additives on Physical Properties of Fine Ethyl Cellulose Microcapsules Prepared by the Wurster Process

Yoshinobu FUKUMORI,*[,a] Hideki ICHIKAWA,[a] Yumiko YAMAOKA,[a] Eiichi AKAHO,[a] Yoshikazu TAKEUCHI,[a] Tomoaki FUKUDA,[a] Ryuichi KANAMORI[b] and Yoshifumi OSAKO[c]

Faculty of Pharmaceutical Sciences, Kobe-Gakuin University,[a] Arise, Ikawadani-cho, Nishi-ku, Kobe 673, Japan, Pharmacy, the City of Itami Hospital,[b] Konyoike 1–100, Itami, Hyogo 664, Japan and Fuji Paudal,[c] Chuo 2–2–30, Jyoto-ku, Osaka 536, Japan. *Received April 23, 1990*

Ethyl cellulose (EC) microcapsules with fine calcium carbonate cores (32—44 μm) and drug layers were prepared. The effect of additives on the particle size distribution, the variation in drug content with particle size and the dissolution properties of the products were evaluated.

Among eight additives used, cholesterol (CH) most restrained the release of phenacetin, a model drug, which resulted in a saving of coating material and time. For sustained release of phenacetin, only 6.25% or less coating material relative to core material was sufficient. In addition, CH remarkably reduced particle agglomeration. The mean particle size of a product 25% coated with EC : CH = 2 : 1 mixture was 58 μm. However, the drug content and the phenacetin release were strongly dependent on the particle size of the product. This was the result of retardation of particle recycling in the Wurster chamber due to its adhesion to the wall by electrostatic charge. Stearyltrimethylammonium chloride, a cationic surfactant, reduced the particle adhesion when it was added to EC–CH (2 : 1) in a 1% amount on a dry basis. As a result, the particle size distribution became sharper, and there was higher homogeneity of the physical properties. This effect was not observed with polysorbate 80, a nonionic surfactant.

Keywords coating; calcium carbonate; ethyl cellulose; cholesterol; stearyltrimethylammonium chloride; microcapsule; Wurster process; fluidized bed; powder

The Wurster process[1] is a method applicable for the industrial production of microencapsulated pharmaceuticals. It can be characterized by fine powder operation. However, some techniques by which the size of the successfully processed particles can be reduced are needed.

Difficulties encountered in the coating of fine particles result from particle agglomeration and adhesion to the chamber walls and filters due to remaining solvent or electrostatic charge. The inertia of particles larger than 100 μm is high enough to overcome this cohesion and adhesion; however, with finer particle size the surface properties dominate over the inertia. This causes the production of largely agglomerated particles or imperfectly coated fine particles.

The purpose of this study was to develop a membrane formulation for the preparation of fine microcapsules. Desirable characteristics of the membrane material were as follows: (1) a low agglomeration tendency, (2) a low electrostatic charging and (3) a low membrane permeability for drugs. The third item was necessary to complete coating at a small amount of membrane material. This is of special importance in practice because fine powder has a large specific surface area.

Experimental

Materials As a core material, calcium carbonate (08 Jyutan, Maruo Calcium Co., Ltd.) was used. Ethyl cellulose (EC, 30—50 cps), cholesterol (CH, SP reagent grade), polyethylene glycol 4000 (PEG), propylene glycol (PG), palmitic acid (PA), lauric acid (LA), triacetin (TA), polysorbate 80 (PS 80) and stearyltrimethylammonium chloride (STAC) were used as purchased from Nacalai Tesque Co., Ltd. Triethyl citrate (TEC, Citroflex 2, Pfizer) and acetylated monoglyceride (AMG, Myvercet 9-40T, Koyo Mercantile Co., Ltd.) were also used as purchased. Phenacetin (Kawasaki Kagakukogyo Co., Ltd.) was used as a model drug.

Coating A Glatt GPCG-1 Wurster[1] was used. A bottom ring such as that shown in Fig. 1 was used to process a small amount of powder (calcium carbonate of 100 g).

Preparation of Microcapsules Details of the cores, the composition of spray solution and the coating conditions are listed in Table I. The coating conditions were almost similar throughout this study. Calcium carbonate was selected as a model core because of its high density (2.93 g/cm^3). Particle agglomeration of high density particles in the Wurster process was presumed to be reduced because of their high inertia. The concentration of dry lacquer (EC plus additive) in spray solution was 2.75% (w/v); EC concentration was 2.5% (w/v). Cores of 100 g were first undercoated with 100 ml of spray solution. Thereafter, 16.7 g of phenacetin (a model

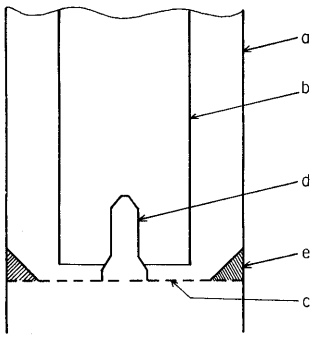

Fig. 1. Bottom Ring for Processing a Small Amount of Powder
a, chamber; b, partition; c, air distributor; d, spray gun; e, bottom ring.

TABLE I. Operating Conditions in the Preparation of EC Microcapsules

Core material	Calcium carbonate 32—44 μm	100 g
Spray solution	EC	32.5 g
	Additive	3.25 g
	Ethanol	added
	Total	1300 ml
Undercoating	Spray solution	100 ml
Fixing of drug	Phenacetin	16.7 g
	Spray solution	200 ml
Coating	Spray solution	1000 ml
Coating conditions		
Inlet air temperature (°C)		40
Outlet air temperature (°C)		30—33
Inlet air rate (m^3/min)		0.7—0.8
Spray rate (ml/min)		4.2—4.8
Spray pressure (atm)		2.3
Diameter of spray nozzle (mm)		0.8

drug), dissolved in a spray solution of 200 ml, was sprayed on the undercoated cores. Finally, 1000 ml of a spray solution was applied to overcoat 25 g of EC (25% coating level).

Particle Size Distribution A sieve analysis was performed in the range of 32—63 μm using an Alpine 200LS air jet sieve at a charged weight of 50 or 20 g and a sieving time of 5 min. Above 63 μm, a row-tap shaker (Iida Seisakusho Co., Ltd.) was used. The shaking time was 10 min and the charged weight was 50 or 20 g. A mass median diameter was used as a mean particle size.

Dissolution and Drug Content Dissolution tests were performed as previously reported.[1] JP XI disintegration 2nd fluid (pH 6.8) was used as a dissolution fluid. The prepared microcapsules were dried in vacuum at room temperature for 12 h. The sample containing 150 mg of phenacetin was tested, and concentration of the drug was spectrophotometrically determined at 245 nm. Drug content in the microcapsules was similarly determined by dissolving them in ethanol; it was also used to estimate the value of 100% release (C_∞) in dissolution tests.

As a parameter of dissolution, the constant K (apparent dissolution rate constant) defined by the following equation was determined by the least squares method.[1]

$$\ln(1 - C_t/C_\infty) = -Kt$$

where C_t was the concentration when the dissolution time was t.

Thermal Analysis The measurements of softening temperature of EC films were performed as previously reported[2]; only the heating rate was changed to 2 °C/min in this study. The test film was usually prepared by heating 5 g of ethanol solution containing 0.75 g EC and 0.075 g (10%) or 0.15 g (20%) additive on a Teflon-coated glass dish of 80 mm diameter at 60 °C for 12 h. The formed film was again dried in vacuum at room temperature for 12 h. The EC film containing CH was prepared using 3 g of ethanol solution containing 0.225 g EC and 0.0225 g CH.

EC films containing 20% or more CH did not have even surfaces; therefore, fragments of the EC–CH films were analyzed by differential scanning calorimetry (DSC). The DSC thermograms were recorded on a Shimadzu SC-30 thermal analyzer at a heating rate of 5 °C/min under a dry nitrogen flow of 30 ml/min. Samples, 8—11 mg, were crimped into aluminum cells.

Scanning Electron Microscopy (SEM) SEM was performed on a Hitachi S430.

Polarizing Microscopy An Olympus POM polarizing microscope was used with a heating stage (MHS, Union Optical Co., Ltd.).

Results and Discussion

Effect of Additives Coating was performed under the conditions shown in Table I. The additives used and the characteristics of the products are shown in Table II. An additive of 10% relative to EC was used in each case (Table

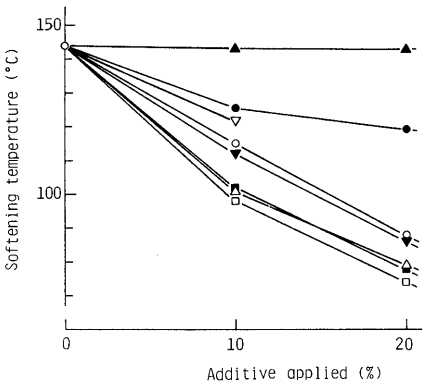

Fig. 2. Effects of Additives on Softening Temperature of EC Films
Additives: ○, TA; ●, PG; △, TEC; ▲, PEG; ▽, CH; ▼, AMG; □, LA; ■, PA.

Table II. Characteristics of EC Microcapsules Prepared by the Wurster Process

	Additives								
	None	TA	PG	TEC	PEG	CH	AMG	LA	PA
Yield (%)	89	89	87	92	91	89	90	89	91
Mean particle size (μm)	89	70	71	77	80	81	85	94	108
Drug content (%)[a]	12.2	11.9	11.8	11.5	11.7	12.2	11.9	11.8	11.7
Softening temperature (°C)	144	115	126	101	143	122	112	98	102

a) Theoretical value: 11.2% in the case of nonadditive, 11.0% in the others.

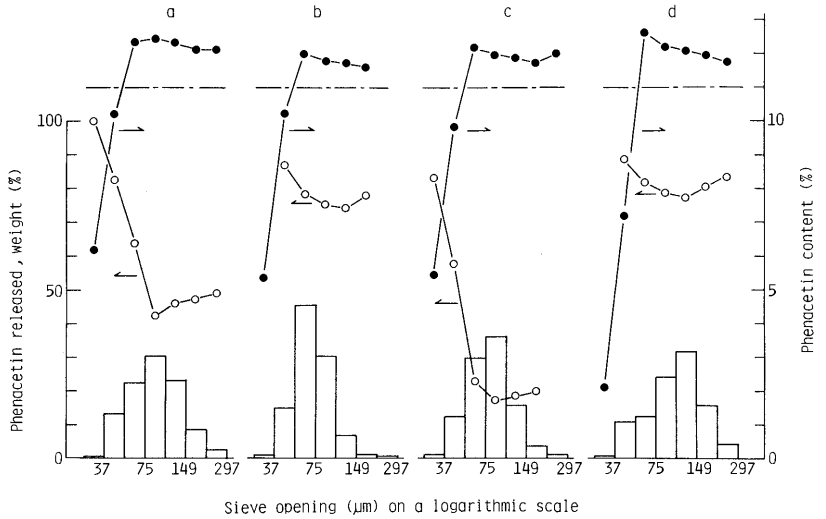

Fig. 3. Typical Particle Size Distributions of EC–Additive (10 : 1) Microcapsules and Variation of Phenacetin Content and 5 h Release with Particle Size Fractions

Additives: a, none; b, TA; c, CH; d, PA. The one-dot chain line shows the theoretical value of phenacetin content.

I). The yield was around 90%. The mean particle size of EC microcapsules without additives was 89 μm. The larger size implies more agglomeration. When compared with EC microcapsules without additives, PA and LA enhance the agglomeration, but AMG, CH, PEG, TEC, PG and TA reduce it.

The softening temperatures of EC films containing the additives are plotted against the amount of additive applied in Fig. 2. Water soluble PEG and PG exhibit only a weak plasticizing effect; PEG in particular hardly plasticized EC. The solution containing 20% or more CH exhibited a very slow evaporation of solvent, resulting in formation of an uneven film. Therefore, with EC–CH film, the softening temperature was determined only with the film containing 10% CH. Since the inlet air temperature was 40 °C (Table I), the membrane could not melt during the operation. The particle agglomeration was not related to the softening of membranes.

Typical examples of the particle size distribution of the products and the physical properties of the particles in each sieved fraction are shown in Fig. 3 for EC alone, EC–TA, EC–CH and EC–PA. EC–PA and –TA exhibited the largest and smallest mean particle size, respectively. The drug content and the percent released in 5 h show that the particles smaller than 53 μm were insufficiently coated. Clearly, this resulted from retardation in recycling within the coating chamber.

The membrane thickness was estimated to be 6 μm under the assumption that 1) the density of EC[3] and phenacetin[4] were 1.11 and 1.24 g/cm^3, respectively, 2) EC and phenacetin independently contributed to the membrane volume and 3) the membrane material was homogeneously coated on the spherical cores of 38 μm (mean of sieve openings used in preparing the cores). Theoretically, the mean particle diameter of the product without agglomeration should be 50 μm (44—56 μm). If three particles of 56 μm (the largest single core microcapsule) were agglomerated with a triangular conformation and two contact points each, the diameter of the circumscribed circle would become 121 μm. If the smallest cores of 32 μm were to be agglomerated in the same manner at the beginning stage of the process and thereafter coated to the thickness of 6 μm, the particle size would become 81 μm. Therefore, the agglomerates composed of three cores would have a size between 81 and 121 μm. Under a microscope, the fraction larger than 75 μm clearly contained agglomerates. In the

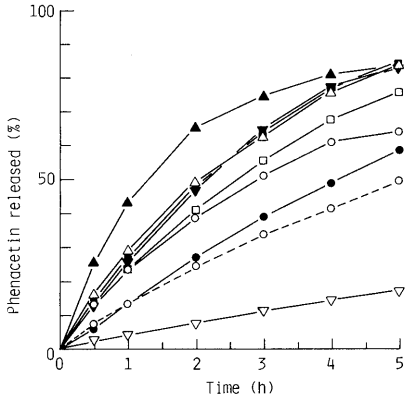

Fig. 4. Release of Phenacetin from EC–Additive (10 : 1) Microcapsules Coated by 25% as EC

Additives: ---○---, EC alone; ○, TA; ●, PG; △, TEC; ▲, PEG; ▽, CH; ▼, AMG; □, LA; ■, PA.

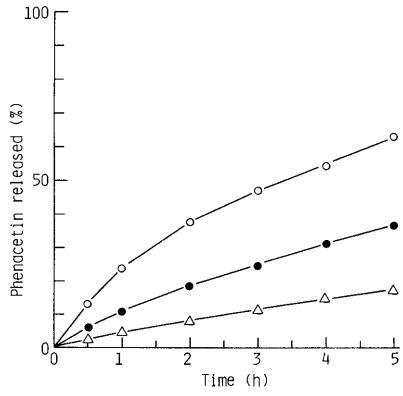

Fig. 5. Effect of the Amount of EC–CH (10 : 1) Applied on Phenacetin Release

EC applied relative to calcium carbonate core (%): ○, 6.25; ●, 12.5; △, 25.

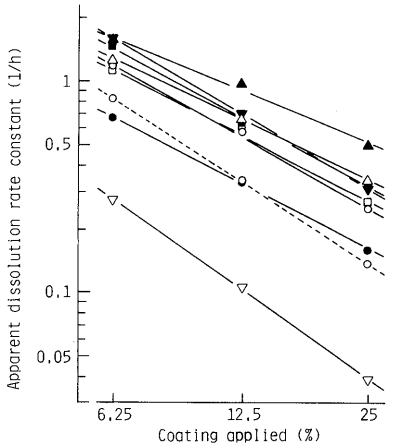

Fig. 6. Apparent Dissolution Rate Constant According to the First Order Kinetics against the Coating Level on a log–log Scale with EC-Additive (10 : 1) Microcapsules

Additives: ---○---, EC alone; ○, TA; ●, PG; △, TEC; ▲, PEG; ▽, CH; ▼, AMG; □, LA; ■, PA.

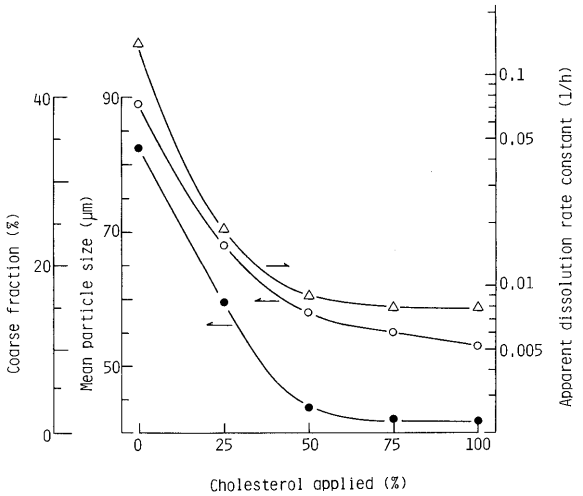

Fig. 7. Effects of CH on the Mean Particle Size (○), the Coarse Fraction (Larger than 106 μm, ●) and Apparent Dissolution Rate Constant (△) of EC–CH Microcapsules Coated by 25% as EC Plus CH

EC–CH concentration in spray solution: 2.5% (w/v).

fraction of 53 to 75 μm, agglomerates were not observed apparently, but from the above estimation this fraction might partially contain agglomerates with two cores or one core and small fragments. These results implied that the particles recycling without adhesion were agglomerates and that single core microcapsules tended to adhere to the chamber wall or filter. This is a serious problem in practical use.

The effect of additives on the dissolution of phenacetin from 25% coated microcapsules is shown in Fig. 4. Only CH reduces the release, while the other additives enhance it. In the coating of fine particles, a large amount of coating material would generally be required; therefore, additives such as CH which can restrain the release have great practical advantages.

The phenacetin release from EC–CH (10:1) microcapsules at three coating levels is shown in Fig. 5. Clearly, only 6.25 or a lesser percent coating should be sufficient for prolonged release. The apparent dissolution rate constant,[1] estimated according to the first order kinetics, is plotted against the coating level on a log–log scale in Fig. 6. The EC–CH (10:1) membrane is a permeation barrier about three times stronger than the EC membrane; PEG most enhances the release.

Effect of CH Content As shown in Table II, CH only slightly reduced particle agglomeration, though it most strongly restrained the drug release. Therefore, conditions which could produce fewer agglomerated microcapsules were sought.

Microcapsules were produced with varying CH contents at a constant EC–CH concentration of 2.5%. Coating was performed up to the level of 25% as EC plus CH. The effect of CH on mean particle size, a fraction coarser than 106 μm, a measure of agglomeration, and the apparent

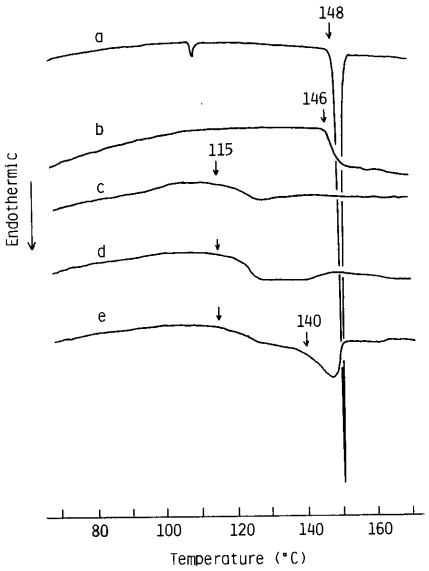

Fig. 8. DSC Thermograms of CH and EC–CH Films

(EC:CH): a, 0:1 (CH recrystallized in ethanol); b, 1:0; c, 5:1; d, 2:1; e, 1:1.

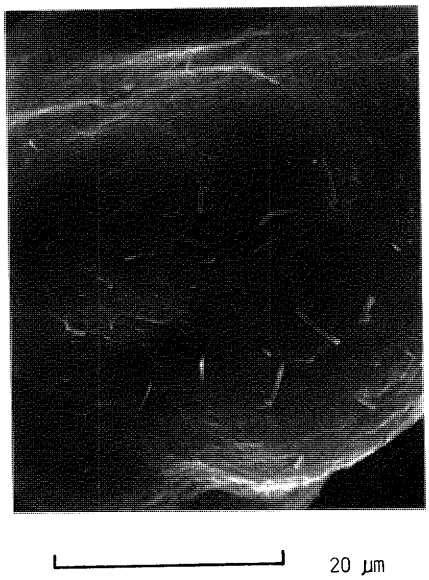

Fig. 9. SEM Photograph of EC–CH (2:1) Microcapsules Coated by 25% as EC plus CH

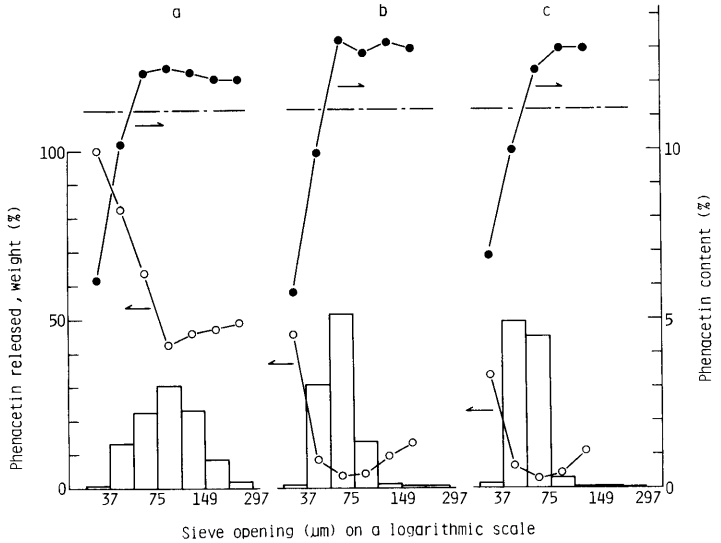

Fig. 10. Effects of CH on Variation of Phenacetin Content and 5 h Release with Particle Size Fractions of EC–CH Microcapsules Coated by 25% as EC plus CH

EC–CH concentration in spray solution: 2.5% (w/v). (EC:CH): a, 1:0; b, 2:1; c, 1:1. Mean particle size (μm): a, 89; b, 58; c, 53. The one-dot chain line shows the theoretical value of phenacetin content.

dissolution rate constant[1] are shown in Fig. 7. With increase in CH content, the agglomeration is reduced rapidly at first, and with more than a 50% addition to EC (EC : CH = 2 : 1), is almost leveled. This means that CH affords the maximum effect at the 50% addition. Figure 7 also shows that EC–CH (2 : 1) membrane was a permeation barrier about thirteen times stronger than EC membrane, offering a great advantage in fine powder coating.

The DSC thermograms of EC–CH films are shown in Fig. 8. The glass transition temperature of EC film was 146 °C, which agreed well with its softening temperature (144 °C, Fig. 2). Films containing 20% or more CH exhibited a glass transition at 115 °C. The EC–CH (1 : 1) film showed an endotherm at 140 °C. Hot-stage polarizing microscopy[5] showed the endotherm to result from melting of the crystalline material, which were probably CH crystals (Fig. 8). A very small amount of crystalline material was also observed with the EC–CH (2 : 1). These thermograms showed that the softening of EC–CH films did not occur during the coating operation. The crystallization of CH may have been related to the reduction of agglomeration. In fact, particles like crystal were observed on the surfaces of EC–CH (2 : 1 and 1 : 1) microcapsules (Fig. 9). Details of the physicochemical properties of EC–CH mixtures and their relations to particle agglomeration will be reported in the future.

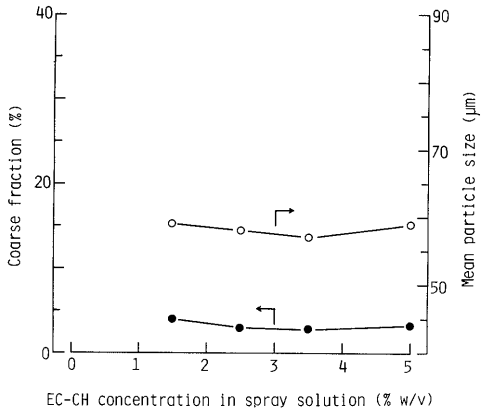

Fig. 11. Effects of EC–CH Concentration in Spray Solution on the Mean Particle Size (○) and the Coarse Fraction (Larger than 106 μm, ●) of EC–CH (2 : 1) Microcapsules Coated by 25% as EC plus CH

The effects of CH on the particle size dependency of 5 h release and drug content of products are shown in Fig. 10. The drug content is constant in the fraction larger than around 63—75 μm, but in the smaller fraction exhibits a strong dependency on particle size regardless of CH content. The 5 h release exhibits the minimum around 63—75 μm. Thus, the properties of EC–CH microcapsules remained strongly dependent on the particle size. A particular problem to be further studied was that EC–CH (1 : 1) microcapsules still exhibited a strong size dependency in spite of their narrow size distribution (Fig. 10c). This clearly resulted from retardation in recycling within the chamber. The coating was performed under a dry condition to avoid agglomeration; therefore, the retardation mainly arose from the adhesion to walls due to electrostatic charge.

Effect of the Concentration of Spray Solution Coating was performed at 1.5—5% (w/v) EC–CH concentrations up to 25% (EC plus CH) coating level; the CH content was fixed at EC : CH = 2 : 1. The mean particle size and the coarse fraction were only slightly varied, though they seemed to have the minimum value at 3.5% (w/v) (Fig. 11). The particle size dependency of drug content and 5 h release were not significantly improved.

Operating Conditions in Fine Powder Coating In the Wurster process, the inlet air rate had to be limited within a narrow range to achieve a steady recycling of particles with low ejection to the filter; therefore, the air rate could not be changed freely. Of course, one acceptable method might be to eject all particles at once and let them fall by shaking the filter. However, the core size used here was very small; therefore, such an operation would lead to a large loss due to leakage from the filter. The spray rate was also hardly changeable, because it also had to be limited within a narrow range to restrain the particle adhesion due to electrostatic charge and to keep agglomeration to

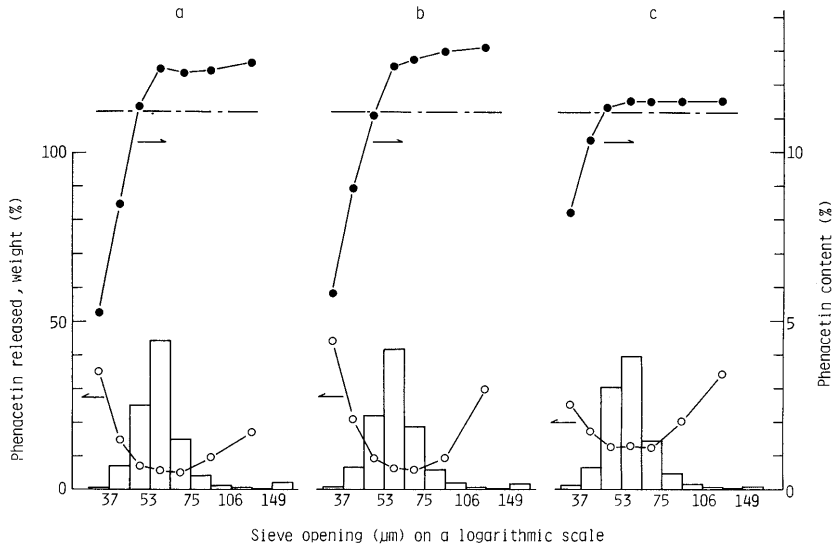

Fig. 12. Effects of Surfactant on Variation of Phenacetin Content and 5 h Release with Particle Size Fractions of EC–CH–Surfactant (2 : 1 : 0.03) Microcapsules Coated by 25% as EC plus CH

EC–CH concentration in spray solution: 3.5% (w/v). Surfactants: a, none; b, PS 80; c, STAC. Mean particle size (μm): a, 57; b, 58; c, 56.

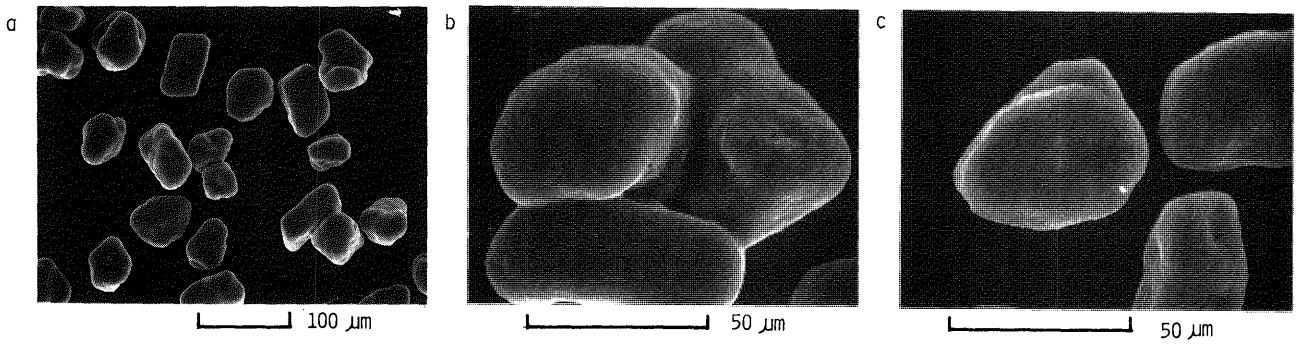

Fig. 13. SEM Photographs of EC–CH–STAC (2 : 1 : 0.03) Microcapsules Coated by 25% as EC plus CH

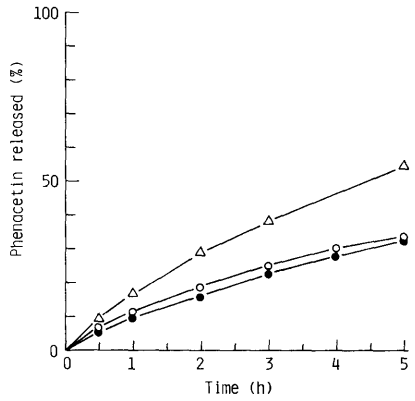

Fig. 14. Release of Phenacetin from EC–CH–Surfactant (2 : 1 : 0.03) Microcapsules Coated by 6.25% as EC plus CH

Surfactant: ○, none; ●, PS 80; △, STAC.

a low degree. The spray pressure was also unchangeable. Too high pressure caused particle ejection to the filter and too low pressure caused adhesion of wet particles within the partition. The only condition which seemed to be changeable was the inlet air temperature. However, as the temperature rose, the particle adhesion due to electrostatic charge became greater. These facts showed that improvement of properties of the product by shifting the above operating conditions was difficult.

Effect of Surfactant There thus seemed to be no way to overcome both particle agglomeration and retardation in particle recycling except to change the surface-chemical property of the membrane material so that the dry particles could not adhere to the wall.

For such a modification of coating material, surfactants were selected as additives. Figure 12 shows the effect of PS 80 and STAC. The mean particle size is not changed. While PS 80 has no significant effect, STAC decreases the size dependency of drug content. The size dependency of drug release is reduced in the fine fractions, while it is increased in the coarse fractions. However, the weight percent in coarse fractions (larger than 106 μm) significantly decreases. Thus, STAC could improve the properties of fine microcapsules.

SEM photographs of EC–CH–STAC (2 : 1 : 0.03) microcapsules are shown in Fig. 13. Some degree of agglomeration is observed. This could be the reason the mean particle size (56 μm) was larger by 6 μm than the theoretical mean diameter (50 μm). Figure 13b suggests that the interparticulate void of large agglomerates might be insufficiently covered with membrane. This may be the reason the phenacetin released was increased in the coarse particle fractions (Fig. 12c).

Figure 14 shows the phenacetin release to be increased by STAC. The dissolution profiles for EC–CH (2 : 1) microcapsules with or without surfactant are shown only for 6.25% (as EC plus CH) coating level. Although STAC enhances the phenacetin release, the membrane remains a strong permeation barrier.

Conclusion

There were two main problems in microencapsulation with the Wurster process: particle agglomeration and retardation in particle recycling. These caused variation in physical properties among size fractions of the microcapsules. In this study, EC : CH : STAC = 2 : 1 : 0.03 was proposed as a candidate for membrane formulation. This membrane material significantly reduced the agglomeration and the retardation of particles, resulting in production of microcapsules with a narrow particle size distribution. CH in the formulation remarkably restricted phenacetin release. As a result, 6.25% or less coating material was sufficient for prolonged release pharmaceuticals.

References

1) Y. Fukumori, T. Fukuda, Y. Hanyu, Y. Takeuchi and Y. Osako, *Chem. Pharm. Bull.*, **35**, 2949 (1987).
2) Y. Fukumori, Y. Yamaoka, H. Ichikawa, Y. Takeuchi, T. Fukuda and Y. Osako, *Chem. Pharm. Bull.*, **36**, 3070 (1988).
3) M. Samejima, G. Hirata and Y. Koida, *Chem. Pharm. Bull.*, **30**, 2894 (1982).
4) J. Okada and Y. Fukumori, *Chem. Pharm. Bull.*, **23**, 326 (1975).
5) Y. Fukumori, T. Fukuda, Y. Yamamoto, Y. Shigitani, Y. Hanyu, Y. Takeuchi and N. Sato, *Chem. Pharm. Bull.*, **31**, 4029 (1983).

Chem. Pharm. Bull. **39**(1) 170—176 (1991) Vol. 39, No. 1

Neocarzinostatin: Selective Tryptophan Oxidation and Neocarzinostatin-Chromophore Binding to Apo-Neocarzinostatin

Kiyoto EDO,*[a] Kunihito SAITO,[a] Yoshinobu MATSUDA,[a] Yuriko AKIYAMA-MURAI,[a] Michinao MIZUGAKI,[a] Yoshio KOIDE,[b] and Nakao ISHIDA[c]

Department of Pharmaceutical Sciences, Tohoku University Hospital,[a] 1-1 Seiryo-machi, Aoba-ku, Sendai 980, Japan, School of Fisheries Sciences, Kitasato University,[b] Sanriku, Iwate 022-01, Japan, and The Sendai Institute of Microbiology,[c] 2-5-22 Ichibancho, Aoba-ku, Sendai 980, Japan.
Received June 12, 1990

Neocarzinostatin (NCS), an antitumor protein antibiotic, is composed of apo-neocarzinostatin (apo-NCS) and neocarzinostatin-chromophore (NCS-chr), the principle of the biological activities of NCS. Apo-NCS having two tryptophan (Trp) residues at positions (39 and 83) was chemically modified by *N*-bromosuccinimide in a study on the correlation of the binding site(s) of NCS-chr. Selective oxidation of Trp residues was observed when NCS was titrated with *N*-bromosuccinimide. In contrast, non-selective oxidation of the two Trps on apo-NCS was observed and both Trp (39 and 83) of apo-NCS were titrated with *N*-bromosuccinimide. After selective oxidization, the remaining Trp residue of NCS was assigned as Trp (83). These results clearly indicate that the Trp (83) residue of apo-NCS changed from the "reactive type" to the "non-reactive type" after the binding of NCS-chr with apo-NCS. The fluorescence emission intensity of apo-NCS generated from the Trp (39) residue was quenched by NCS-chr. These data suggest that NCS-chr directly interacts with the Trp (39) residue and that a β-sheeted loop containing the Trp (83) residue of apo-NCS changes the high-order structure upon binding with NCS-chr.

Keywords neocarzinostatin; apo-neocarzinostatin; neocarzinostatin-chromophore; selective tryptophan oxidation; apoprotein-chromophore interaction

Neocarzinostatin (NCS) with an antitumor activity has been isolated from the culture filtrate of *Streptomyces carzinostaticus* var. F-41.[1] NCS consists of two components, an acidic polypeptide (apo-NCS) (Fig. 1), and a labile nonprotein chromophore (NCS-chr) (Fig. 2). Clinical studies showed that NCS is a potent anticancer reagent useful for treatment of bladder cancer[2] or, in the form of a new derivative, for the treatment of liver cancer.[3] Much evidence has suggested that NCS-chr is primarily responsible for the biological activity of NCS and its interaction with deoxyribonucleic acid (DNA) while the apo-NCS is essential for its stability and transport.[4-6] The total chemical structure and the absolute configuration of NCS-chr were elucidated.[7,8] On the other hand, the primary sequence of apo-NCS, first elucidated by Meienhofer *et al.*,[9] was revised by several groups[10-13] and the secondary structure of apo-NCS was characterized by us.[14]

It is reported that binding between apo-NCS and NCS-chr is specific and no other proteins are exchangeable for apo-NCS.[15] Recently, we suggested that carboxyl-terminal-43-peptide residue could be bound to NCS-chr.[16] This complex retains its antimicrobial activity and there is a strong hydrophobic interaction between apo-NCS and NCS-chr as well as ionic interaction.[17,18]

In this paper we studied the selective Trp oxidation of NCS and apo-NCS to further understand the mode of reversible binding between apo-NCS and NCS-chr. It is suggested that the Trp (39) residue of apo-NCS directly interacts with NCS-chr whereas a loop containing the Trp (89) residue changes the high-order structure upon binding to NCS-chr and that *N*-bromosuccinimide oxidation of the Trp residues on apo-NCS changes the high-order structure of apo-NCS to reduce the affinity with NCS-chr to apo-NCS and consequently monotryptophan-39 oxidized NCS (MTO-NCS) and ditryptophan-39 and 83 oxidized NCS (DTO-NCS) reduce those biological activities.

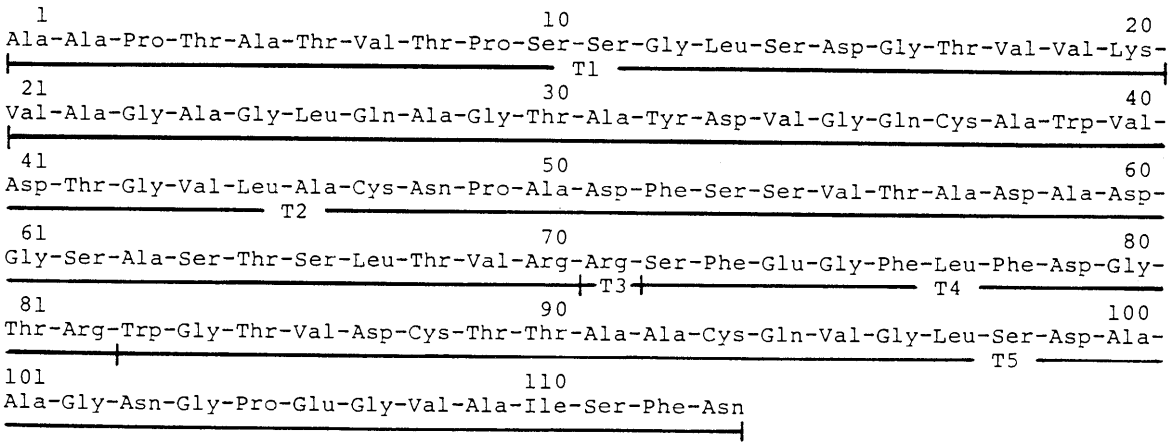

Fig. 1. Primary Structure of Neocarzinostatin Apoprotein

The tryptic peptides T1, T2, T3, T4, and T5 correspond to positions 1—20, 21—70, 71, 72—82, and 83—113, respectively.

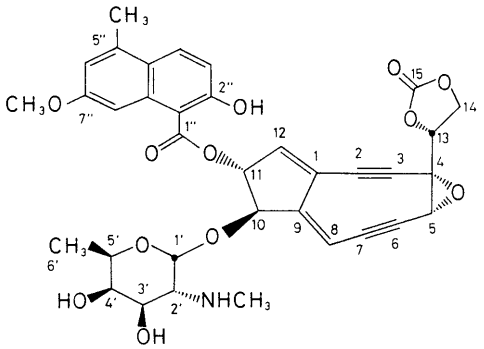

Fig. 2. The Absolute Chemical Structure of Neocarzinostatin-Chromophore

Experimental

Materials Purified NCS and apo-NCS were obtained from Kayaku Antibiotic Research Co., Ltd., Tokyo, Japan. NCS-chr was prepared by the previously reported method.[19] Other reagents were of analytically high grade and were obtained commercially. *N*-Bromosuccinimide was recrystallized from deionized warm water before use and had a mp at 173 °C. Urea was recrystallized from 50% aqueous ethanol before use.

Spectral Measurement Absorption spectra were recorded on a Hitachi 557 double wavelength double beam spectrometer at room temperature. Spectrofluorometric studies were carried out in 0.1 M acetate buffer (pH 4.0) at room temperature with a Hitachi 650-60 fluorescence spectrophotometer. The excitation wavelength was 280 nm, and the emission wavelength was between 250 and 500 nm. Circular dichroic (CD) spectra were carried out at room temperature under constant nitrogen flush, using a JASCO spectropolarimeter J-400X equipped with a data processor. The data are expressed in terms of molar ellipticity, $[\theta]$, in $\deg \cdot cm^2/dmol^{-1}$.

High Performance Liquid Chromatography (HPLC) (Pharmacia Fast Protein Liquid Chromatography (FPLC) System) The system consists of two P-500 pumps, a gradient programmer GP-250, a fixed wavelength detector UV-1 (280 nm), and a two channel recorder REC-482 for the simultaneous recording of salt gradient and optical density. A mono Q HR 5/5 anion exchange column (Pharmacia), charged $-CH_2N^+(CH_3)_3$ on the monodisperse gel particles, was used. Samples were eluted from the column at a flow rate of 2 ml/min maintaining a pressure of 20 bar (2 MPa). The separation time was 16 min. The solvent A (start buffer) was 0.1 M Tris–HCl buffer pH 7.2 and solvent B (limit buffer) was a start buffer containing 0.5 M NaCl. The gradient programmer was set as follows: a linear gradient of 0% B for 3.0 min, followed by 0—50% B for 10 min, and finally maintaining by 100% B for 3 min.

Sodium Dodecylsulfate–Polyacrylamide Gel Electrophoresis (SDS–PAGE) Ten persent SDS–PAGE was carried out as described by Laemmli.[20] The gel (1 mm thick) was fixed in 5% trichloroacetic acid for 1 h and stained with Coomassie brilliant blue. Molecular weight markers were used as the standard.

Isoelectric Focusing on Polyacrylamide Gel Polyacrylamide (5%) gel containing 2% carrier Ampholytes (LKB-producter, Bromma, Sweden) pH 2.5—4.5 was prepared as specified in the LKB manual. Riboflavin was added as a photochemical polymerizating agent. After applying the sample (1 mg/ml, 40 μl), isoelectric focusing was carried out at 4 °C. The voltage was increased from 220 to 700 V for the initial 30 min and then kept constant at 700 V for the following 3 h. The protein bands were stained with Coomassie brilliant blue R-250.

***N*-Bromosuccinimide Titration** The *N*-bromosuccinimide oxidation of NCS (M.W. 11752.7) and apo-NCS (M.W. 11093.1) was performed according to the method of Patchornik *et al.*[21] and Spande & Witkop.[22] Ultraviolet (UV) photometric titration was conducted by adding 0.01 M *N*-bromosuccinimide dropwise to NCS (0.84 mg (7.14×10^{-8} mol)/2 ml) solutions in 0.1 M acetate buffer (pH 4.0) in the presence and absence of 8 M urea. The same titration was done to apo-NCS (1.65 mg (1.49×10^{-7} mol)/2 ml). After adding each increment of *N*-Bromosuccinimide, a spectrometric reading was taken at 280 nm at room temperature.

The number of Trp residues per mole[22] is calculated by the following expression:

$$n = \mu\text{mol Trp}/\mu\text{mol protein}$$
$$= (\Delta \text{OD} \times 1.31 \times V/5.50)/(\text{OD} \times \text{a.f.} \times V \times 1000/\text{M.W.})$$
$$= (\Delta \text{OD} \times 1.31 \times \text{M.W.})/(\text{OD} \times \text{a.f.} \times 5500)$$

where n = number of Trp residues per mole of protein, OD = initial optical density at 280 nm, Δ OD = corrected optical density decrease at 280 nm, a.f. = absorptivity factor to convert optical density at 280 nm to mg/ml of protein (0.466 for NCS, 0.929 for apo-NCS), V = initial volume of titrated solution (ml), M.W. = moleclular weight of protein, 5500 = molar extinction coefficient at 280 nm for Trp.

Preparation of MTO-NCS and DTO-Apo MTO-NCS: All operations were performed in dark conditions at 4 °C. The reaction mixture of 60 mg of NCS and 0.84 mg of *N*-bromosuccinimide in 60 ml of 0.1 M acetate buffer (pH 4.0) was left at 4 °C for 30 min and then was lyophilized. Lyophilizate was applied to Bio-gel P-4 column chromatography (1.3 × 20 cm) previously equilibrated with deionized water. The optical density was monitored by absorbance at 214 nm. The main peak pooled was lyophilized (yield, 52 mg (87%)).

DTO-Apo: Thirty mg of apo-NCS in 30 ml of 0.1 M acetate buffer (pH 4.0) was added to 1.68 mg of *N*-bromosuccinimide and then the reaction mixture was left for 30 min at 4 °C. The same treatment method used for the reaction mixture was applied to the MTO-NCS preparation (yield, 23 mg (77%)).

Preparation and Purification of MTO-Apo After 25 mg of MTO-NCS in 25 ml of deionized water was left at 4 °C for 24 h in the presence of 8 M urea, this MTO-NCS solution was dialyzed overnight against deionized water and lyophilized. This crude MTO-apo solution was relyophilized and purifed with FPLC followed by desalting with a Bio-gel P-4 column (1.3 × 20 cm) and lyophilization (yield, 20 mg (85%)).

Preparation and Purification of DTO-NCS The mixture of NCS-chr (10 mg/ml, 0.5 ml) in methanol and DTO-apo (0.53 mg/ml, 9.5 ml) in 0.1 M acetate buffer (pH 4.0) was incubated at 37 °C for 12 h. The reconstituted mixture was lyophilized and purified by FPLC under the conditions previously described. Purified DTO-NCS was desalted with a Bio-gel P-4 column (1.3 × 20 cm) and then main peak monitoring at 214 nm was lyophilized (yield, 1.62 mg (31%)).

Chemical Modification of Disulfide Bonds of MTO-Apo To prepare the four-cysteines-modified derivatives of MTO-apo for proteolytic digestion, 10 mg of purifed MTO-apo was dissolved in 1.2 ml of 0.5 M Tris–HCl buffer (pH 8.0) containing 8 M urea and 0.2% ethylenediaminetetraacetic acid disodium salt (EDTA–2Na). After the addition of 300 μmol of dithiothreitol, the mixture was introduced with nitrogen gas for 10 min and heated for 3 h at 50 °C. To this mixture, 20 mg of iodoacetic acid in 0.12 ml of 1 M NaOH was added. Alkylation was conducted at pH 8.0 by adding 1 M NaOH for 30 min. The mixture was dialyzed against 0.2 M acetic acid and lyophilized. The lyophilizate was desalted by gel filtration on a Bio-Gel P-4 column (1.3 × 20 cm) eluted with deionized water and relyophilized (yield, 9 mg (90%)).

Tryptic Digestion of Tetra-*S*-carboxylmethyl MTO-Apo and Separation of Trp-Containing Peptide For proteolytic digestion of reduced MTO-apo, tetra-*S*-carboxylmethyl apo-NCS (10 mg) in 1.5 ml of 0.1 M Tris–HCl buffer (pH 7.3) was incubated with trypsin (0.13 mg) at 37 °C. The time course of the digestion was continuously monitored by FPLC at 280 nm absorbance. After the digestion was completed (about 8 h), the reaction mixture was immediately frozen and lyophilized. The separation and purification of tryptic peptide of tetra-*S*-carboxylmethyl-MTO-apo was employed by FPLC (yield, 0.5 mg (18%)).

Amino Acid Analysis Amino acid analyses were performed wit.. a JASCO model TRI-ROTAR VI instrument for *o*-phthalaldehyde detection. The samples were hydrolyzed with *p*-toluenesulfonic acid in sealed ampoules at 110 °C for 24 h. The NH_2-terminal amino acids were determined by using 5-dimethylaminonaphthalene-1-sulfonyl chloride.[23]

Reconstitution Experiment of NCSs The mixture of NCS-chr in methanol (10 mg/ml, 50 μl) and each Trp-oxidized apo-NCSs (0.53 mg/ml, 950 μl) in 0.01 M acetate buffer (pH 5.0) were incubated at 37 °C for various time intervals. Reconstitution was monitored by the isoelectric focusing technique on polyacrylamide gel using a pH gradient of 2.5 to 4.5. The protein bands were stained with Coomassie brilliant blue R-250. The reconstitution ratios were calculated by scanning at 570 nm with a densitometer (Shimadzu Model CS-920).[24]

Biological Activities Native NCS and apo-NCS and those Trp oxidized derivatives were assayed for both antibacterial and antileukemic activities. Minimum inhibitory concentrations (MIC) against *Micrococcus luteus* (*M. luteus*) (1×10^7 cells/ml) were determined using the agar plate dilution method with nutrient agar. The cytotoxic activity of purified NCS, apo-NCS and the Trp modified derivatives were assayed using an established cell line of mouse leukemic cells (L1210): Cell suspensions of

L1210 leukemia (5×10^4 cells/ml), which contained various amounts of NCS, apo-NCS and the Trp modified derivatives in RPMI 1640 medium supplemented with 5% fetal calf serum (Gibco), were incubated at 37 °C for 2 d in a CO_2 incubator. Cell numbers were counted by the dye exclusion method with trypan blue to calculate the 50% growth-inhibitory concentration (IC_{50}) values.

Results

***N*-Bromosuccinimide Titration of Trp Residues in NCS and Apo-NCS** Oxidation of NCS and apo-NCS with 0.01 M *N*-bromosuccinimide in 0.1 M acetate buffer (pH 4.0) in the presence and absence of 8 M urea were spectrometrically monitored. The addition of *N*-bromosuccinimide in small increments to the NCS solution in the presence of 8 M urea and to the apo-NCS solution in the presence or absence of 8 M urea led to a similar proportional and instantaneous decrease in Trp UV absorption at 280 nm, as shown in Fig. 3A and B. However, this decrease of NCS was halved in the absence of 8 M urea (Fig. 3A). These results showed that both Trp residues of apo-NCS in the absence of 8 M urea were oxidized in almost the same manner as in the presence of 8 M urea, and the consumption of *N*-bromosuccinimide amounted to 2.1 mol (Table I). However, NCS in the absence of 8 M urea was oxidized only at one Trp residue with 2.2 mol of *N*-bromosuccinimide. These results may indicate that one Trp residue on NCS is reactive and accessible to *N*-bromosuccinimide in the absence of 8 M urea and must be located at or near the surface of the molecule and the other Trp is resistant to oxidation by *N*-bromosuccinimide since this Trp changes from the reactive type to the non-reactive type due to the NCS-chr binding of apo-NCS.

The Preparation and Physichochemical Properties of DTO-Apo, MTO-NCS and MTO-Apo The detailed method of Trp oxidation for apo-NCS and NCS by *N*-bromosuccinimide was described in Materials and Methods. The UV spectra of NCS, MTO-NCS, apo-NCS, MTO-apo and DTO-apo in 0.1 M acetate buffer (pH 4.0) at 0.25 mg/ml concentration were shown in Fig. 4. NCS and MTO-NCS, which retain chromophore, exhibit UV absorption at around 300—400 nm but non-associated chro-

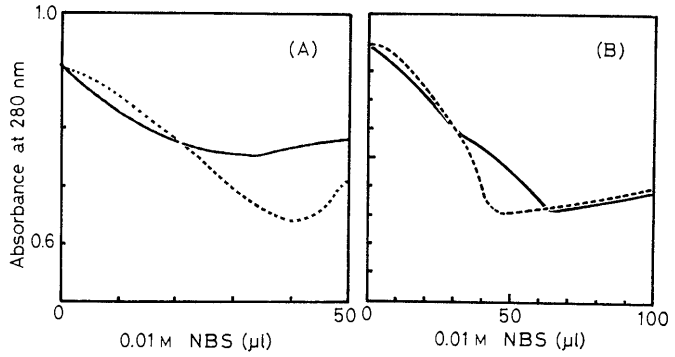

Fig. 3. Ultraviolet Spectrophotometrically Monitoring of *N*-Bromosuccinimide Oxidation of Tryptophan Residues of NCS and Apo-NCS

The oxidation of NCS (7.14×10^{-8} mol/2 ml, A) and apo-NCS (1.49×10^{-7} mol/2 ml, B) were monitored at 280 nm in 0.1 M acetate buffer (pH 4.0) in the presence (---) or in the absence (—) of 8 M urea, adding aliquots (10 μl) of 0.01 M *N*-bromosuccinimide. Plotted absorbances are corrected for dilution (< 5%).

TABLE I. Tryptophan Oxidation of NCS and Apo-NCS by NBS in the Presence and Absence of 8 M Urea

	8 M urea	Oxidized tryptophan (M)	Consumed NBS (M)/Trp
NCS	−	0.97 (1)	2.2
	+	1.74 (2)	2.8
Apo-NCS	−	1.81 (2)	2.1
	+	1.88 (2)	1.6

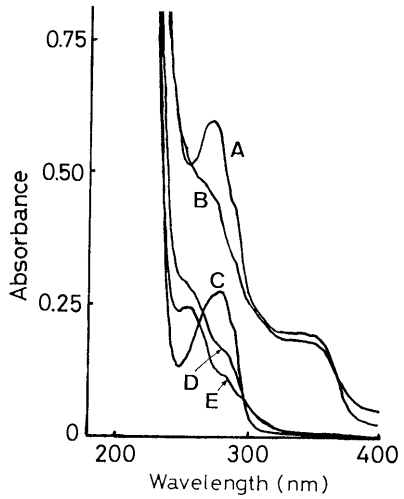

Fig. 4. UV Spectrum of NCS, MTO-NCS, Apo-NCS, MTO-Apo and DTO-Apo

The spectra were measured to 1 cm quartz cell at 0.25 mg/ml in 0.1 M acetate buffer (pH 4.0). A: NCS, B: MTO-NCS, C: apo-NCS, D: MTO-apo, E: DTO-apo.

TABLE II. Amino Acid Composition (in Residue) of NCS, MTO-NCS, MTO-Apo, DTO-Apo and Apo-NCS

Amino acid		NCS	MTO-NCS	MTO-apo	DTD-apo	Apo-NCS
Asp	12	11.80	12.66	11.55	12.33	11.86
Thr	13	12.08	12.92	11.96	13.03	12.71
Ser	11	10.20	10.50	9.23	11.39	10.25
Glu	5	5.08	5.57	5.25	5.14	5.29
Pro	4	4.33	4.61	5.02	3.93	4.20
Gly	15	14.83	14.57	15.02	15.51	15.59
Ala	18	17.93	17.74	17.14	18.60	18.80
Cys/2	4	ND	ND	ND	ND	ND
Val	12	10.33	12.06	12.66	11.47	11.54
Ile	1	1.00	1.10	1.50	0.89	1.14
Leu	6	5.79	5.39	5.74	6.00	5.88
Tyr	1	1.01	0.99	0.96	0.76	0.88
Phe	5	4.99	4.86	5.07	5.01	4.87
Lys	1	0.96	0.81	1.14	1.11	0.88
Arg	3	2.89	2.75	2.94	3.14	2.87
Trp	2	1.85	0.95	1.02	0.0	2.35

Analyses were conducted on a JASCO model TRI-ROTAR VI instrument after hydrolysis of samples in *p*-toluenesulfonic acid for 24 h at 110 °C. ND, not determined.

TABLE III. Physicochemical Properties of NCS, Apo-NCS and These Tryptophan-Oxidized Derivatives

	NCS	MTO-NCS	MTO-apo	DTO-apo	Apo-NCS
Tryptophan number	2	1	1	0	2
Isoelectric point (pI)	3.3	3.3	3.2	3.2	3.2
M.W. by SDS-PAGE	12000	12000	12000	12000	12000
N-Terminal	Ala	Ala	Ala	Ala	Ala

mophore proteins, apo-NCS, MTO-apo and DTO-apo, exhibited no UV absorption at this wavelength range. Amino acid analysis of those proteins are indicated in Table II. These data suggest that DTO-apo was oxidized at the two Trp residues, whereas MTO-NCS was oxidized only at one Trp residue under the reaction condition described above. The data of SDS–PAGE, isoelectric focusing and N-terminal analysis by the dansyl method of NCS and apo-NCS derivatives are summarized in Table III.

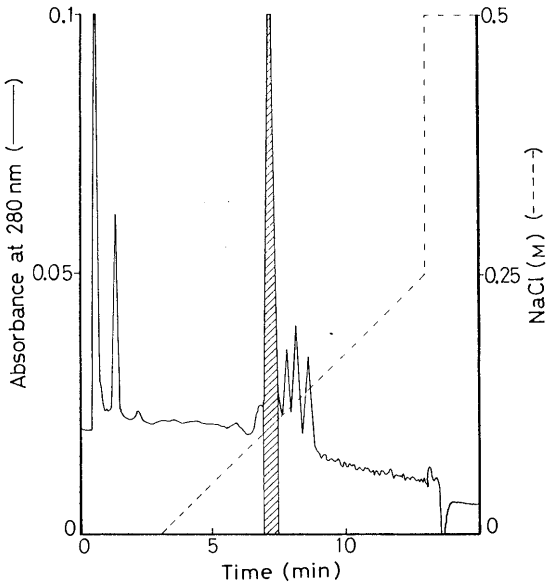

Fig. 5. Purification of Trypsin Digest of Tetra-S-carboxymethyl Mono-tryptophan-Oxidized Apo-NCS by FPLC

A 50 μl sample (10 mg/ml) was chromatographed on mono Q HR 5/5 by elution at 2 ml/min with 0.1 M Tris–HCl buffer (pH 7.2) by a NaCl gradient (- - -) as shown: pump pressure, 2 MPa; sample injection time, zero; tryptophan-contained peptide (▨).

The Elucidation of Tryptophan Residue Being Resistant against *N*-Bromosuccinimide Oxidation of NCS To elucidate the position of the Trp residue remaining after selective *N*-bromosuccinimide oxidation in NCS, MTO-apo was reduced by dithiothreitol and then alkylated by iodoacetic acid for proteolytic digestion. This tetra-*S*-carboxylmethyl MTO-apo was hydrolyzed with trypsin at 37 °C for 8 h by the method of Hirayama.[12] When this hydrolyzate was analyzed by HPLC, only one peak possessing high 280 nm absorbance was detected (Fig. 5). This isolated Trp containing fragment, which exhibited further positive reaction by *N*-bromosuccinimide oxidation (data not shown), was analyzed by an amino acid analyzer (Table IV). The amino acid compositions of this fragment were in agreement with the T5 peptide (position 83—113) designed by Kuromizu *et al.*[13] and had 0.71 mol per 1 mol of peptide. Next, the amino acid composition of a tryptic peptide corresponding to the T2 (position 21—70) was analyzed. This peptide had 0.14 mol of Trp per 1 mol of peptide. This indicates that Trp-83 was resistant to *N*-bromosuccinimide oxidation five times as much as Trp-39.

Fluorescence Analysis of Apo-NCS–NCS-chr Interaction In order to confirm the interaction of Trp on apo-NCS with NCS-chr, the fluorescence emission spectra of apo-NCS, NCS, MTO-apo, and MTO-NCS were measured (Fig. 6). When excited at 280 nm, the solution of apo-NCS in 0.1 M acetate buffer (pH 4.0) demonstrated maximum fluorescence at 352 nm. The 352 nm emission band is attributable to Trp residues. This Trp emission intensity of NCS is only 30% of that of apo-NCS. It is reported that on analysis of the molecular interaction of protein and fluorescence active compounds, fluorescence emission intensisty was generally decreased by the

TABLE IV. Amino Acid Composition of Tryptic Peptide Obtained from MTO-Apo

	Calculated[a]			Analysis			
				Tryptic peptide having tryptophan residue		Tryptic peptide corresponding to T2 residue[c]	
	NCS	T2[b]	T5	Found	Estimated	Found	Estimated
Asp	9	5	2	4.09	(4)	6.05	(6)
Asn	3	1	2				
Thr	13	5	3	2.88	(3)	5.35	(5)
Ser	11	5	2	2.14	(2)	5.03	(5)
Glu	2		1	2.03	(2)	1.82	(2)
Gln	3	2	1				
Pro	4	1	1	1.05	(1)	1.72	(1)
Gly	15	6	5	4.95	(5)	6.04	(6)
Ala	18	10	5	4.95	(5)	9.58	(10)
Cys/2	4	2	2	ND	(2)	ND	(2)
Val	12	6	3	3.44	(3)	4.87	(6)
Ile	1		1	0.95	(1)	0	(0)
Leu	6	3	1	1.10	(1)	2.76	(3)
Tyr	1	1		0	(0)	1.02	(1)
Phe	5	1	1	0.99	(1)	1.05	(1)
Lys	1			0	(0)	0	(0)
Arg	3	1		0	(0)	0.84	(1)
Trp	2	1	1	0.71	(1)	0.14	(0)
Total	113	50	31		(31)		(50)

a) The amino acid composition of apo-NCS (Kuromizu *et al.*, 1986) was used. *b*) The tryptic peptides T2 and T5 correspond to positions 21—70 and 83—113, respectively. *c*) T2 residue was prepared from MTO-apo according to Kuromizu's method.[13] ND, not determined.

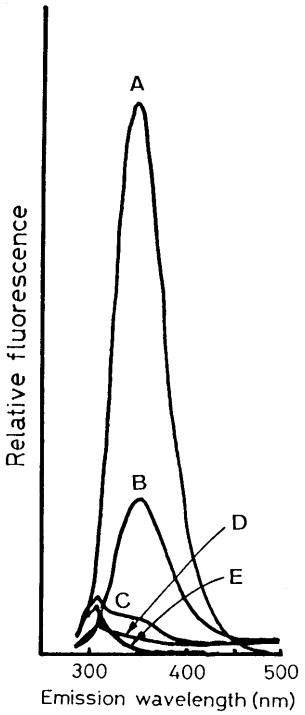

Fig. 6. Fluorescence Emission Spectra of Apo-NCS, NCS, MTO-Apo, MTO-NCS, and DTO-Apo

Uncorrected fluorescence emission spectra of protein (5×10^{-6} M) in 0.1 M acetate buffer (pH 4.0) were recorded at room temperature. Excitation wavelength was 280 nm. A: native apo-NCS, B: native NCS, C: MTO-apo, D: MTO-NCS, E: DTO-apo.

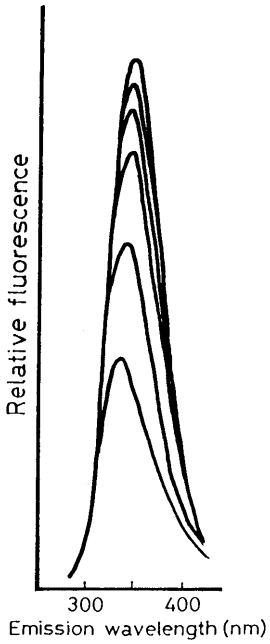

Fig. 7. Fluorescence Spectra of Apo-NCS in the Presence of NCS-chr

Fifty microliters volume of NCS-chr in methanol at various concentrations were added to 2 ml in a 0.1 M acetate buffer solution (pH 4.0) containing apo-NCS (5×10^{-6} M) and after incubation at 37°C under dark conditions for 2 h the fluorescence emission was recorded. The uncorrected fluorescence spectrum from top to bottom, correspond to varying final concentrations of NCS-chr, as follows: 0, 3.2×10^{-7}, 6.3×10^{-7}, 1.25×10^{-6}, 2.5×10^{-6}, and 5×10^{-6} M were measured at room temperature. The highest curve shows the fluorescence spectrum of free NCS-chr (5×10^{-6} M). The excitation wavelength was 280 nm.

participation of the Trp emission of protein.[25,26] This reduced emission of native NCS might be due to quenching resulting from the association of NCS-chr to apo-NCS. In

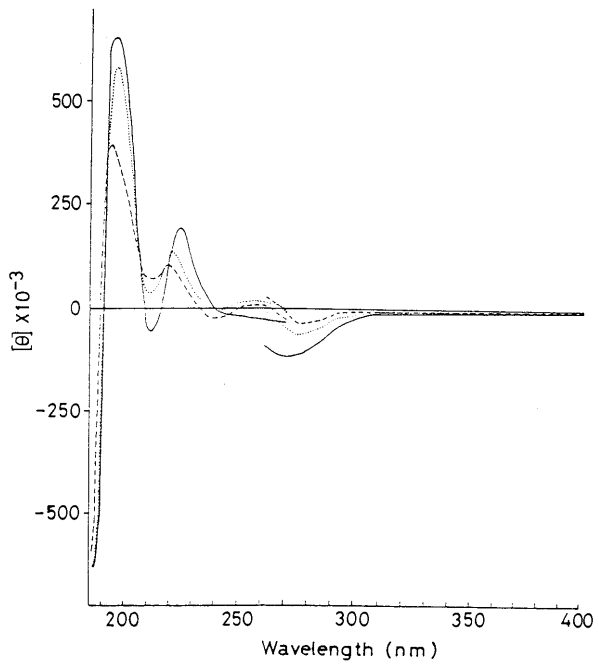

Fig. 8. CD Spectra of Apo-NCS, MTO-Apo and DTO-Apo

Spectra were recorded with apo-NCS, MTO-apo, and DTO-apo concentrations of 0.5 mg/ml (in the wavelength region of 260—400 nm) or 0.2 mg/ml (in the wavelength region of 190—270 nm) in 0.01 M phosphate buffer (pH 7.4). For measurement of near-UV and far-UV spectra, 1 and 0.1 cm cells were used, respectively. Apo-NCS (—), MTO-apo (– – –), DTO-apo (- - -).

fact, the intensity of the emission spectrum of apo-NCS at 352 nm is quenched in the presence of NCS-chr parallel with the increase of the NCS-chr concentration with blue shift. A typical example of fluorescence titration is shown in Fig. 7 for the apo-NCS–NCS-chr system. These data suggest that the interaction of NCS-chr occurred at least one of the Trp residues of apo-NCS and the environment of this Trp changed the hydrophobic circumstance. On the other hand, the fluorescence intensity of MTO-apo actually found is only 7% of that of apo-NCS, neverthless MTO-apo contains half as much Trp as apo-NCS. Furthermore, the quenching of the fluorescence emission intensity of MTO-NCS is 44% of that of MTO-apo and the fluorescence emission intensity of DTO-apo is almost negligible. The quenching of the fluorescence emission generated from apo-NCS by NCS-chr can be reasonably assumed to be due to the NCS-chr interaction with apo-NCS. This assumption is in good agreement with the X-ray and three-dementional computed graphical data discussed later.

Extensive Conformational Change during *N*-Bromosuccinimide Modification of Apo-NCS The CD spectrum of native apo-NCS was characterized by two negative peaks at about 214 and 275 nm, and two positive peaks at about 198 and 226 nm (Fig. 8). After the Trp oxidation of apo-NCS, the positive peaks at 198 and 226 nm decreased in intensity with blue shift and the negative peaks at 214 and 275 nm increased. It is assumed that the spectrum of MTO-apo contains the contribution of the intact Trp at position 89 whereas the spectrum of DTO-apo is free of the Trp contribution. According to the curve-fitting analysis (data not shown), these spectral changes suggest that the contents of α-helix and random coil decreased and those of β-sheet structure increased. These observations suggested that the *N*-bromosuccinimide modified apo-

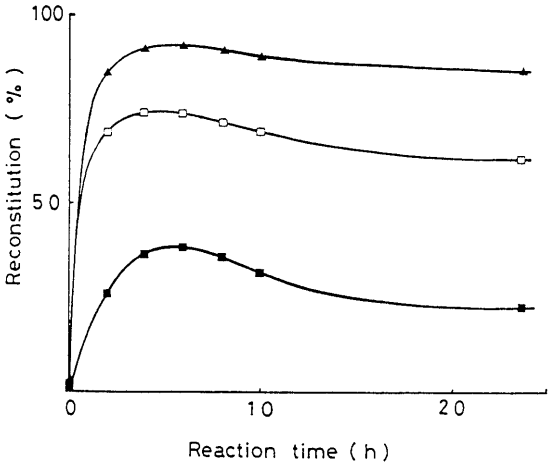

Fig. 9. The Time Course of the Reconstitution to NCS, MTO-NCS and DTO-NCS

The mixture of NCS-chr (10 mg/ml, 50 μl) in methanol with apo-NCS (▲—▲), MTO-apo (□—□), and DTO-apo (■—■) (0.53 mg/ml, 950 μl) in 0.01 M acetate buffer (pH 5.0) was incubated at 37 °C for 24 h, respectively. Reconstitution ratio (%) was calculated on the integral value of densitometry: % of NCS reconstitution = [NCS] × 100/([NCS] + [apo-NCS]).

TABLE V. Biological Activities of NCS, Apo-NCS and These Tryptophan-Oxidized Derivatives

	Number of Trp oxidized	Position of oxidized Trp	Biological activities	
			M. luteus MIC (μg/ml)[a]	L1210 cells IC_{50} (μg/ml)[b]
NCS	0		0.31	0.0088
Apo-NCS	0		>100	>5
MTO-NCS	1	39	0.78	0.038
MTO-apo	1	39	>100	>5
DTO-NCS	2	39 and 83	1.25	0.073
DTO-apo	2	39 and 83	>100	>5

a) MIC, minimum inhibitory concentration. *b*) IC_{50}, concentration which caused 50% inhibition of growth.

NCSs changed their fine high-order structure.

Reconstitution of NCS-chr and *N*-Bromosuccinimide Modified Apo-NCSs In order to show the requirement of Trp residues of apo-NCS–NCS-chr binding, apo-NCS, MTO-apo, and DTO-apo were reconstituted with NCS-chr by a previously reported method.[24] The mixture of NCS-chr and apo-NCS (MTO-apo or DTO-apo) were incubated at 37 °C (Fig. 9). The reconstitution ratio of those mixtures reached a maximum of about 90% of the theoretical value for apo-NCS, 75% for MTO-apo and 40% for DTO-apo after 5 h under identical experimental conditions.

Biological Activities of *N*-Bromosuccinimide Modified NCSs and Apo-NCS The antibacterial and antitumor activities of Trp modified NCS and apo-NCS, as well as NCS and apo-NCS, are summarized in Table V. The MICs of MTO-NCS and DTO-NCS against *M. luteus* were 40 and 25% of NCS, respectively, and the antitumor activities (IC_{50}) of MTO-NCS and DTO-NCS were 23 and 12% of NCS, respectively. On the other hand, MTO-apo and DTO-apo at several 100-fold high concentrations of NCS had none of these biological activities because these apo-NCS derivatives were not associated with NCS-chr. In this experiment, the biological activities of Trp-oxidized NCSs were reduced to 12—40% of that of the native NCS. These data suggest that MTO-apo and DTO-apo, especially DTO-apo, were not able to tightly bind with NCS-chr because of the change of the high-order structure of apo-NCS by the oxidation of Trps on apo-NCS.

Discussion

NCS has been clinically used as a cancer chemotherapeutic agent in Japan since 1977.[2] This antibiotic was the first antitumor protein in which an amino acid sequence was proposed[9] but recently its sequence has been revised by a few researchers.[10-13] We[19] and others[27,28] reported that NCS is composed of apo-NCS and NCS-chr. Many reports concerning the interactions between NCS-chr and DNA were published by Goldberg *et al.*[5] and Myers,[6,8] but there are few reports on the specific binding of NCS-chr and apo-NCS. We focused our study on the specific binding between apo-NCS and NCS-chr because NCS-chr, due to the biological activity of NCS, is very labile, and it is protected from the loss of its activities by apo-NCS.

The selective oxidation of Trp residues in NCS and its conformational effect and biological activities have been reported by Samy *et al.*[29] Namely, the two Trp residues exhibited the differential behavior of striking selectively toward oxidation by *N*-bromosuccinimide. Since Samy's paper, however, was published before the discovery of NCS-chr in the NCS molecule, there are many equivocal interpretations in this paper.

We show that the two Trp residues of NCS exhibited a differential reaction toward oxidation by *N*-bromosuccinimide while those of apo-NCS exhibited a similar effect (Fig. 3). These results are related to the selective modification of the two Trp residues by *o*-nitrophenyl sulfenyl chloride and the selective oxidation of the two Trp residues by *N*-bromosuccinimide.[30,31] Purified MTO-apo, DTO-apo and MTO-NCS were homogeneous, respectively, as shown in Table II. The NH_2-amino terminals of all the peptides were identical to Ala. These results indicate that during the oxidation process of NCS or apo-NCS by *N*-bromosuccinimide, the cleavage of the tryptophyl C-terminal was negligible. Samy *et al.* reported that when *N*-bromosuccinimide oxidation was carried out in the presence of 8 M urea, Asp and Gly were obtained as new NH_2-terminal amino acids, showing that in the denaturated state both the tryptophyl–glycyl bond (positions 79 and 80) and tryptophyl–aspartyl bond (positions 46 and 47) of NCS were cleaved (position numbers referred from Meienhofer *et al.*[9]) but in the absence of 8 M urea no new NH_2-terminal was observed.[29] Our experimental results clearly showed that Trp-39 of NCS was easily oxidized by *N*-bromosuccinimide and the Trp residue, being resistant to *N*-bromosuccinimide oxidation, was at position 83 of NCS (Table IV). These results mean that the Trp (83) residue of NCS must be located in the interior of the protein molecule while that of apo-NCS must be located in the exterior of the protein molecule. Denaturation by 8 M urea was required to make this non-reactive type Trp (83) residue accessible to *N*-bromosuccinimide. Accordingly, the high-order structure of NCS might be destroyed by 8 M urea to convert apo-NCS from NCS after the release of NCS-chr.[18]

It is reported that on analysis of the molecular interaction of protein and fluorescence active compounds, fluorescence intensity was generally decreased by the participation of the

Trp residue of the protein.[25,26] The 352 nm emission of apo-NCS was quenched in the presence of NCS-chr in a dose-response manner (Fig. 7). NCS-chr may quench the emission generated from one of the Trp on apo-NCS by competitively absorbing the excitation energy and serving as an energy acceptor as mentioned by Napier.[27] As MTO-apo exhibited only about 10% of the fluorescence emission intensity of apo-NCS, it would appear that this remaining Trp (83) residue has a relatively low quantum yield and does not contribute greatly to the total fluorescence spectrum of apo-NCS, whereas the Trp (39) residue greatly contributes. The much greater loss of fluorescence intensity (70%) of apo-NCS binding with NCS-chr must be due to the loss of fluorescence emission generated from Trp (39), suggesting the possibility that the interaction of NCS-chr directly occurred with the Trp (39) residue of apo-NCS.

The reconstitution ratio of apo-NCS, MTO-apo, and DTO-apo with NCS-chr decreased in this order (Fig. 9). As the number of oxidized Trp in apo-NCS increased, the ability of reconstitution decreased in that order and the reconstitution ratio of DTO-apo with NCS-chr was reduced to 40%. Purified MTO-NCS and purified DTO-NCS prepared by the reconstitution of NCS-chr and DTO-apo, exhibited lower activities than NCS itself. These findings mean that tryptophan oxidation on apo-NCS changes the high-order structure of peptide moiety contained tryptophan to reduce the ability of stabilization and transport of NCS-chr. In fact, it is observed that the CD spectral data of MTO-apo and DTO-apo is different from that of apo-NCS.

Sieker reported according to X-ray crystallography at 3.5 Å of resolution that NCS was composed of twisted 7-strand β-sandwich for the major portion but NCS-chr was not delineated from the course of the peptide chain at this resolution.[32] However, only an incomplete stereo diagram of NCS was indicated in this paper because it was believed that NCS consisted of 109 amino acids. It appeared that the cavity was formed by three β-sheet loops, *i.e.* position 73—90 contained hydrophobic residues (Phe–Glu–Gly–Phe–Leu–Phe (position 73—78)), position 97—112 contained hydrophobic residues (Val–Ala–Ile–Ser–Phe (position 108—112)) and position 37—50 contained hydrophobic residues (Cys–Ala–Trp–Val (position 37—40)). Recently, Ishiguro *et al.*[33] reported the modeling of the three dimensional structure of apo-NCS based on the actinoxanthin crystal structure.[34,35] These reports indicate that Trp (83) of apo-NCS locates at far from a cleft binding to NCS-chr, whereas Trp (39) locates at a cleft surface. On the basis of these reports and our experimental results we conclude that Trp (39) residue located in the exteria of apo-NCS directly interacts with NCS-chr in the binding of NCS-chr to apo-NCS, and that a β-sheeted loop structure containing Trp (83) residue may change the high-order structure and then hold NCS-chr.

A complete X-ray analysis of NCS may elucidate the structural changes of apo-NCS produced upon binding with NCS-chr.

References

1) N. Ishida, K. Miyazaki, K. Kumagai, and M. Rikimaru, *J. Antibiotics, Ser. A*, **18**, 68 (1965).
2) H. Maeda, *Anticancer Res.*, **1**, 175 (1981).
3) T. Konno, H. Maeda, K. Iwai, S. Tashiro, S. Maki, T. Morinaga, M. Mochinaga, T. Hiraoka, and I. Yokoyama, *Eur. J. Cancer Clin. Oncol.*, **19**, 1053 (1983).
4) L. S. Kappen, M. A. Napier, and I. H. Goldberg, *Proc. Natl. Acad. Sci., U.S.A.*, **77**, 1970 (1980).
5) I. H. Goldberg: Novel types of DNA-sugar damage in neocarzinostatin cytotoxicity and mutagenesis. In "Mechanisms of DNA Damage and Repair," ed. by M. G. Simic, L. Grossman, and A. C. Upton, Plenum Press, New York and London, 1986, pp. 231—244.
6) A. G. Myers, *Tetrahedron Lett.*, **28**, 4493 (1987).
7) K. Edo, M. Mizugaki, Y. Koide, H. Seto, K. Furihata, N. Ōtake, and N. Ishida, *Tetrahedron Lett.*, **26**, 331 (1985).
8) A. G. Myers, P. J. Proteau, and T. M. Handel, *J. Am. Chem. Soc.*, **110**, 7212 (1988).
9) J. Meienhofer, H. Maeda, C. B. Glaser, J. Czombos, and K. Kuromizu, *Science*, **178**, 875 (1972).
10) T. S. A. Samy, K. S. Hahm, E. J. Modest, G. W. Lampman, H. T. Keutmann, H. Umezawa, W. C. Herlihy, B. W. Gibson, S. A. Carr, and K. Biemann, *J. Biol. Chem.*, **258**, 183 (1983).
11) B. W. Gibson, W. C. Herlihy, T. S. A. Samy, K. S. Hahm, H. Maeda, J. Meienhofer, and K. Biemann, *J. Biol. Chem.*, **259**, 10801 (1984).
12) K. Hirayama, T. Ando, R. Takahashi, and A. Murai, *Bull. Chem. Soc. Jpn.*, **59**, 1371 (1986).
13) K. Kuromizu, S. Tsunasawa, H. Maeda, O. Abe, and F. Sakiyama, *Arch. Biochem. Biophys.*, **246**, 199 (1986).
14) K. Saito, Y. Sato, K. Edo, Y. Akiyama-Murai, Y. Koide, N. Ishida, and M. Mizugaki, *Chem. Pharm. Bull.*, **37**, 3078 (1989).
15) L. S. Kappen and I. H. Goldberg, *Biochemistry*, **19**, 4786 (1980).
16) K. Edo, K. Saito, Y. Akiyama, M. Mizugaki, Y. Koide, and N. Ishida, *Chem. Pharm. Bull.*, **34**, 5180 (1986).
17) K. Edo, Y. Akiyama, K. Saito, M. Mizugaki, Y. Koide, and N. Ishida, *J. Antibiotics*, **39**, 1615 (1986).
18) K. Edo, K. Saito, Y. Akiyama-Murai, M. Mizugaki, Y. Koide, and N. Ishida, *J. Antibiotics*, **41**, 554 (1988).
19) Y. Koide, F. Ishii, K. Hasuda, Y. Koyama, K. Edo, S. Katamine, F. Kitame, and N. Ishida, *J. Antibiotics*, **33**, 342 (1980).
20) U. K. Laemmli, *Nature* (London), **227**, 680 (1970).
21) A. Patchornik, W. B. Lawson, and B. Witkop, *J. Am. Chem. Soc.*, **80**, 4747 (1958).
22) T. F. Spande and B. Witkop, *Methods Enzymol.*, **11**, 498 (1967).
23) K. R. Woods and K. T. Wang, *Biochim. Biophys. Acta*, **133**, 369 (1967).
24) Y. Koide, A. Ito, F. Ishii, Y. Koyama, K. Edo, and N. Ishida, *J. Antibiotics*, **35**, 766 (1982).
25) J. Steinhardt, J. Krijn, and J. G. Leidy, *Biochemisty*, **10**, 4005 (1971).
26) Y. Ozeki, Y. Kurono, T. Yotsuyanagi, and K. Ikeda, *Chem. Pharm. Bull.*, **28**, 535 (1980).
27) M. A. Napier, B. Holmquist, D. J. Strydom, and I. H. Goldberg, *Biochem. Biophys. Res. Commun.*, **89**, 635 (1979).
28) H. Suzuki, K. Miura, Y. Kumada, T. Takeuchi, and N. Tanaka, *Biochem. Biophys. Res. Commun.*, **94**, 255 (1980).
29) T. S. A. Samy, M. Atreyi, H. Maeda, and J. Meienhofer, *Biochemistry*, **13**, 1007 (1974).
30) H. Maeda and N. Ishida, *Biochim. Biophys. Acta*, **147**, 597 (1967).
31) H. Maeda, *J. Antibiotics*, **26**, 776 (1973).
32) L. C. Sieker, Ph. D. Dissertation, University of Washington, Seattle, 1981.
33) M. Ishiguro, S. Imajo, and M. Hirama, submitted.
34) A. S. Khokhlov, P. D. Reshetov, L. A. Chupova, B. Z. Cherches, L. S. Zhigis, and I. A. Stoyachenko, *J. Antibiotics*, **29**, 1026 (1976).
35) V. Z. Pletnev, A. P. Kuzin, S. D. Trakhanov, and P. V. Kostetsky, *Biopolymers*, **21**, 287 (1982).

Reductive Metabolism of Nitro-*p*-phenylenediamine by Rat Liver

Mitsuo NAKAO,*[,a] Yukiko GOTO,[a] Akira HIRATSUKA[b] and Tadashi WATABE[b]

Hatano Research Institute, Food and Drug Safety Center,[a] 729–5 Ochiai, Hadano, Kanagawa 257, Japan and Laboratory of Drug Metabolism and Toxicology, Department of Hygienic Chemistry, Tokyo College of Pharmacy,[b] Horinouchi, Hachioji, Tokyo 192–03, Japan. *Received June 13, 1990*

Reductive metabolism of the hair dye constituent, nitro-*p*-phenylenediamine (2-nitro-1,4-diaminobenzene, NPDA), and its acetylated metabolite, NPDA N^4-acetate, was investigated with rat liver subcellular fractions, microsomes and cytosol. Under anaerobic conditions, these compounds were reduced to their corresponding amines by these fractions. The microsomal nitro-reducing activity was retarded completely by air and strongly by carbon monoxide. Reduced nicotinamide adenine dinucleotide phosphate (NADPH) functioned more effectively than reduced nicotinamide adenine dinucleotide (NADH) as an electron donor in the microsomal reduction of the nitro compounds, and flavin mononucleotide (FMN) gave rise to a marked enhancement in the microsomal activity, especially when added to an anaerobic incubation mixture containing both NADH and NADPH. The cytosolic nitro-reducing activity was attributed to xanthine oxidase, aldehyde oxidase and other unknown enzyme(s), based on the results of cofactor requirements and inhibition experiments.

Keywords hair dye; nitro-*p*-phenylenediamine; metabolism; nitroreduction; rat liver

Nitro-*p*-phenylenediamine (2-nitro-1,4-diaminobenzene, NPDA) is a dye constituent widely used in hair dyes. This dye was previously shown to induce not only bacterial mutations,[1–3] but mammalian cell mutations,[4] sister chromatid exchanges,[5–7] and unscheduled deoxyribonucleic acid (DNA) synthesis.[8,9] Moreover, its carcinogenicity has been demonstrated.[10,11] In our previous studies,[12,13] we have isolated and identified two major metabolites from the urine of rats given NPDA; one was NPDA N^4-acetate, and the other 1,2,4-triaminobenzene (TAB) N^1,N^4-diacetate. The latter was found to be excreted as a urinary metabolite in rats given TAB or TAB N^4-acetate, a possible metabolic intermediate. Based on the results of our previous studies, NPDA appears to be metabolized to NPDA N^4-acetate, TAB N^4-acetate and TAB N^1,N^4-diacetate by the following sequential steps: regioselective N^4-acetylation, nitroreduction and regioselective N^1-acetylation, respectively. NPDA may also be metabolized by an alternative pathway to TAB N^1,N^4-diacetate *via* TAB formed through its direct nitroreduction. From an *in vivo* study conducted by us, it was shown that the nitro group of NPDA and NPDA N^4-acetate were reduced in rats.[13]

The present study was undertaken to determine whether the corresponding amines are produced by nitroreduction of NPDA and its N^4-acetate in rat liver as demonstrated *in vivo*. In addition, we made an attempt using NPDA and its N^4-acetate as substrates to estimate what enzymes are involved in the reduction of the aromatic nitro compounds in the rat liver.

Materials and Methods

Chemicals NPDA and N^1-methylnicotinamide were obtained from Tokyo Chemical Industry Co., Ltd., Tokyo; flavin mononucleotide (FMN), *n*-octylamine, dicumarol and menadione from Wako Pure Chemical Industries, Ltd., Osaka; reduced nicotinamide adenine dinucleotide (NADH) and reduced nicotinamide adenine dinucleotide phosphate (NADPH) from Oriental Yeast Co., Tokyo; metyrapone and allopurinol from Aldrich Chemical Co., Inc., Milwaukee, WI.; and hypoxanthine from Sigma Chemical Co., St. Louis, MO. All other chemicals and solvents were of the highest grade available. NPDA N^4-acetate[12] and TAB N^4-acetate[13] were prepared according to published procedures. The quantitative derivatization of TAB to its N^1,N^2,N^4-tripropionate was conducted by the same method as that used to prepare TAB *N*-monoacetates.[13] The melting point and spectral data for TAB N^1,N^2,N^4-tripropionate were as follows: mp 176 °C, UV $\lambda_{max}^{ethanol}$ nm (ε): 232 (21600), 261 (18100), and MS *m/z* (relative intensity, %): 291 (M^+, 49), 235 (34), 206 (31), 179 (66), 161 (63), 123 (41), 122 (66), 57 (100).

Preparation of Rat Liver Subcellular Fractions Male Sprague-Dawley rats weighing 200 to 215 g were used. The animals were sacrificed by decapitation and their livers were rapidly excised, rinsed and homogenized in 3 volumes of 1.15% KCl with a Teflon-pestled glass homogenizer. The S9 fraction was obtained by centrifugation of the homogenate at 9000 × *g* for 20 min. Microsomes and cytosol were prepared by further centrifugation of the S9 fraction at 105000 × *g* for 60 min. The microsomal pellet obtained by this procedure was suspended in ice-cold 1.15% KCl. The protein was determined by the method of Lowry *et al.*[14]

Assay of Reduction of NPDA and Its N^4-Acetate The method of Mori *et al.*[15] was modified for incubation as follows: a standard incubation mixture for the assay of the nitro-reducing activities of S9, microsomes and cytosol consisted of 2 mM NADH, 2 mM NADPH, 0.5 mM FMN, 1.0 mM nitro compound (0.01 ml of dimethyl sulfoxide solution) and 3.6 to 7.2 mg of protein in a final volume of 1.0 ml of 20 mM Tris–HCl buffer (pH 7.4). Incubations were carried out at 37 °C for 30 min under either nitrogen or carbon monoxide in Thunberg tubes. The incubation mixture was twice alternately evacuated and flushed with nitrogen or carbon monoxide. Before the reaction was initiated by the addition of the substrate solution from the side arm into the tube, preincubation was performed for 2 min at 37 °C. The metabolites formed were determined by quantitative derivatization to their *N*-propionates as described below. After the addition of an aqueous solution (1.0 ml) of 1,4-diaminobenzene *N*,*N'*-diacetate as an internal standard to the incubation mixture, propionic anhydride (0.5 ml) was introduced, and the mixture was shaken for 15 min and then extracted three times with two volumes of ethyl acetate–*n*-butanol (1 : 1, v/v; saturated with water before use). Separated from the organic phase, the solvent was evaporated to dryness *in vacuo*. The residue was dissolved in 0.5 ml of methanol and poured onto a column of Silica gel 60 (E. Merck, Darmstadt; 10 mm × 100 mm) packed with ethyl acetate, and then eluted with ethyl acetate–ethanol (10 : 1, v/v). The eluate was evaporated until dry *in vacuo*. The residue was redissolved in ethanol and subjected to high pressure liquid chromatography (HPLC). Under the aforementioned conditions, various amounts of authentic TAB and its N^4-acetate added to the incubation media were almost quantitatively recovered. HPLC was performed with a Shimadzu model LC-6A high pressure liquid chromatograph equipped with a Shim-pack CLC-SIL column (6.0 mm × 15 cm, Shimadzu Co., Kyoto) and a SPD-6A UV absorption detector. The column was eluted with chloroform–ethanol (95 : 5, v/v) at a flow rate of 2.0 ml/min and the chromatograms were monitored by absorptiometry at 254 nm.

Mass Spectral Measurements Mass spectra (MS) were obtained with a Shimadzu model QP-1000 mass spectrometer at an ionization voltage of 70 eV and an ion source temperature of 290 °C by electron impact mode with direct insertion.

Results and Discussion

The rat liver S9 fraction had activities that reduced both nitro compounds, NPDA and NPDA N^4-acetate, to the

corresponding amines, TAB and TAB N^4-acetate, in the presence of a cofactor mixture consisting of NADH, NADPH, and FMN under anaerobic conditions. The water-soluble and unstable amines TAB and TAB N^4-acetate, formed from the nitro compounds in anaerobic incubation mixtures, were quantitatively converted to hydrophobic and stable derivatives, TAB N^1,N^2,N^4-tripropionate and 1,2-dipropionylamino-4-acetylaminobenzene, respectively. The *N*-propionates were extracted and analyzed by HPLC (Fig. 1). Under the HPLC conditions, the substrates which didn't react were eluted at retention times of less than 3 min.

The nitroreduction products were sole metabolites for these nitro compounds under the anaerobic incubation conditions used (Fig. 1). The *N*-propionates eluted from the HPLC column were further identified with the corresponding synthetic specimens by mass spectrometry; MS *m/z* (relative intensity, %) for TAB N^1,N^2,N^4-tripropionate: 291 (M^+, 53), 235 (30), 206 (26), 179 (65), 161 (60), 123 (35), 122 (66), 57 (100) and for 1,2-dipropionylamino-4-acetylaminobenzene: 277 (M^+, 72), 259 (7), 221 (51), 179 (19), 165 (100), 161 (59), 123 (64), 122 (96).

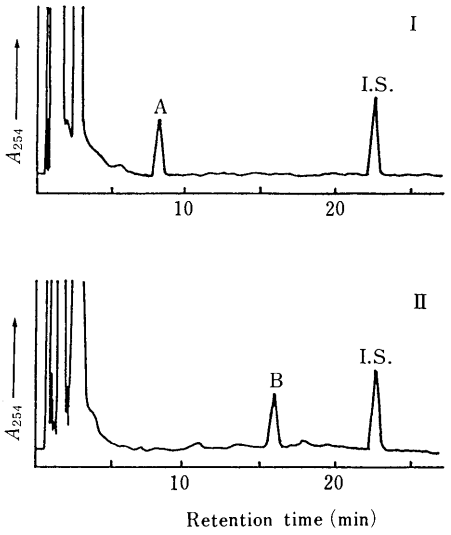

Fig. 1. High Pressure Liquid Chromatographic Separation of Anaerobic Metabolites of NPDA (I) and NPDA N^4-Acetate (II)

Mobile phase used was chloroform–ethanol (95 : 5, v/v). Other chromatographic condtions are described in Materials and Method. A: TAB N^1, N^2, N^4-tripropionate, B: 1.2-dipropionylamino-4-acetylaminobenzene, I.S.: Internal standard.

TABLE I. Anaerobic Reduction of NPDA and NPDA N^4-Acetate by Subcellular Fractions of Rat Liver

Fraction	Amines formed (nmol/mg protein/min)	
	NPDA	NPDA N^4-acetate
S9		
NADH + NADPH + FMN	0.180	0.233
Microsomes		
NADH	0.013	0.013
NADPH	0.029	0.033
NADH + NADPH	0.032	0.036
NADH + FMN	0.063	0.084
NADPH + FMN	0.090	0.162
NADH + NADPH + FMN	0.293	0.411
Cytosol		
NADH	0.027	0.039
NADPH	0.030	0.035
NADH + NADPH	0.041	0.036
NADH + FMN	0.059	0.087
NADPH + FMN	0.088	0.160
NADH + NADPH + FMN	0.080	0.153

The same metabolites as formed in the S9 fraction were isolated and identified from anaerobic incubation mixtures consisting of the rat liver microsomal or cytosolic fraction and the three cofactor mixture, either or both of the reduced pyridine nucleotides alone, or mixtures of the reduced pyridine nucleotide and FMN (Table I). However, the enzymatic nitroreduction in these incubation mixtures did not take place when the incubations were carried out under aerobic conditions.

In the presence of the three cofactor mixture, the microsomal fraction displayed apparently higher specific activity in reducing the nitro compounds than did the S9 fraction (Table I). This fact was due to the higher specific enzyme activity of the microsomes compared to cytosol. NADPH was more effective than NADH in reducing the nitro compounds when they were added as single cofactors to the microsomal incubation mixtures. However, NADH was as effective as NADPH in the cytosolic fraction.

Addition of FMN to the incubation mixtures containing the reduced pyridine nucleotide markedly increased the nitro-reducing activities of both the microsomal and cytosolic fractions (Table I). FMN had the greatest success in increasing the nitro-reducing activity when the microsomal fraction contained both of the reduced pyridine nucleotides: 9 times for NPDA and 11 times for NPDA N^4-acetate. However, in the absence of FMN, the mixture of NADPH and NADH was almost as effective as NADPH alone regarding nitroreduction by microsomes. In contrast with this, in the cytosolic incubation mixture containing both reduced pyridine nucleotides, the addition of FMN showed a rather small decreasing effect on its nitro-reducing activity, although the FMN did have a considerable increasing effect on the NADH- and NADPH-dependent nitro-reducing activities of the liver cytosol. Therefore, the data indicates that at least two different NPDA- and NPDA N^4-acetate-reducing systems are operative in the rat liver; one is localized in the microsomes, and the other in the cytosol as reported on the reduction of *p*-nitrobenzoic acid.[16]

The effect of FMN on the hepatic microsomal reduction

TABLE II. Influence of Various Inhibitors on the Anaerobic Reduction of NPDA and NPDA N^4-Acetate by Rat Liver Microsomes

Incubation system	Amines formed (nmol/mg protein/min)	
	NPDA	NPDA N^4-acetate
Complete[a]	0.261 (100)[b]	0.470 (100)
+ air	0 (0)	0.003 (1)
+ CO	0.126 (48)	0.286 (61)
+ SKF 525-A (1 mM)	0.249 (95)	0.373 (79)
+ *n*-octylamine (1 mM)	0.249 (95)	0.410 (87)
+ metyrapone (1 mM)	0.213 (82)	0.497 (106)

a) The complete incubation mixture contained microsomes (3.6 mg protein/ml), NADH (2 mM), NADPH (2 mM), and FMN (0.5 mM). *b*) Values in parentheses, percentage of activity normalized to that of complete incubation mixture.

of nitroaromatic compounds has been already demonstrated.[17-19] In the anaerobic reduction of 1-nitropyrene in the presence of flavin adenine dinucleotide (FAD) and NADPH in *E. coli*, Narai *et al.*[20] suggested that $FADH_2$, formed from FAD by enzymatic reduction, directly reduced the nitro compounds to the corresponding amines in a non-enzymatic manner. In addition, they demonstrated that FAD could be replaced by FMN or riboflavin.

The properties of the microsomal enzymes for the reduction of NPDA and NPDA N^4-acetate were studied, and the results are given in Table II. Carbon monoxide inhibited nitroreduction by 40—50%, thus indicating a possible participation of cytochromes P-450 in the microsomal nitroreduction, as had been already indicated by Gillette *et al.*[21] Metyrapone slightly enhanced the reduction of NPDA N^4-acetate, but inhibited the reduction of NPDA to a very small extent, as did SKF 525-A and *n*-octylamine. The inhibitory effect of SKF 525-A and *n*-octylamine was weak on the nitroreduction of NPDA N^4-acetate. These results are characteristic of cytochrome P-450-mediated nitroreduction.[22,23]

Generally, under anaerobic conditions, the NADPH-cytochrome P-450 reductase-catalyzed reductions of nitroaromatic compounds, nitrobenzene,[24] 5-nitrofuran derivatives,[25,26] niridazole,[27] and misonidazole[28] yield their corresponding hydroxylamines. Further reduction of the hydroxylamines to the amines is suggested to be mediated by cytochromes P-450.[29] In our present study, however, it is difficult to interpret the distinct roles of the NADPH-cytochrome P-450 reductase and cytochromes P-450 in microsomal nitroreduction of NPDA and its N^4-acetate. A further study with purified NADPH-cytochrome P-450 reductase and cytochromes P-450 will be necessary to determine the role of these microsomal enzymes in the reduction of NPDA and its N^4-acetate.

The data of many other studies demonstrate that the anaerobic activity of nitroreductase in liver cytosol consists of DT-diaphorase,[30] xanthine oxidase,[31,32] aldehyde oxidase[33,34] and other unknown enzyme(s).[35] In the liver cytosol, NADPH was a slightly better electron donor than NADH for the nitroreduction as described above (Table I). The NADPH-dependent activity was only slightly inhibited by dicumarol, which was known as a potent inhibitor for DT-diaphorase.[30] The anaerobic cytosolic nitroreduction of NPDA proceeded at a rate twice as high in the presence of hypoxanthine as in the presence of NADPH. However, hypoxanthine had little effect on the cytosolic reduction of NPDA N^4-acetate. Allopurinol, a potent inhibitor of xanthine oxidase,[31,32] strongly inhibited the cytosolic hypoxanthine-dependent nitroreduction of NPDA. A similar tendency was observed in the N^1-methylnicotinamide-dependent cytosolic reduction of NPDA and its

TABLE III. Influence of Various Cofactors and Inhibitors on the Anaerobic Reduction of NPDA and NPDA N^4-Acetate by Rat Liver Cytosol

Cofactor	Inhibitor	Amines formed (nmol/mg protein/min)	
		NPDA	NPDA N^4-acetate
NADPH (2 mM)	None	0.030 (100)[a]	0.039 (100)
	Dicumarol (0.1 mM)	0.024 (80)	0.028 (72)
Hypoxanthine (2 mM)	None	0.060 (100)	0.002 (100)
	Allopurinol (0.2 mM)	0.012 (20)	<0.002 (0)
N^1-Methylnicotinamide (1 mM)	None	0.029 (100)	0.002 (100)
	Menadione (0.5 mM)	0.011 (38)	<0.002 (0)

a) Values in parentheses, percentage of activity to that in the absence of inhibitors.

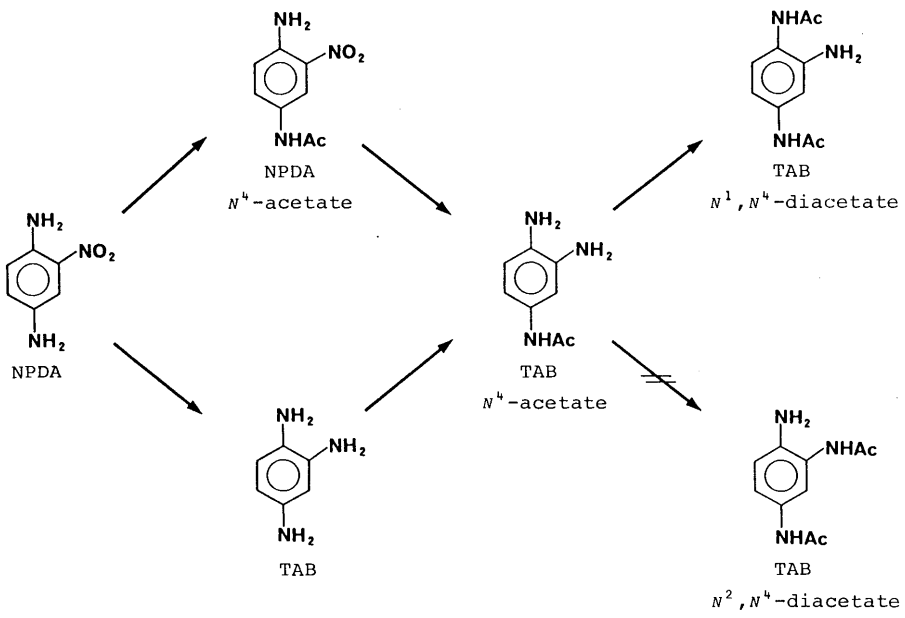

Chart 1. Proposed Pathway for the Metabolism of NPDA in Rat Liver

N^4-acetate. N^1-Methylnicotinamide, an electron donor for aldehyde oxidase,[33,34] was as effective as NADPH in the hepatic cytosolic reduction of NPDA, but had little effect on the cytosolic reduction of the N^4-acetate. Menadione, an inhibitor for aldehyde oxidase, strongly inhibited the cytosolic N^1-methylnicotinamide-dependent reduction of NPDA (Table III).

The aforementioned facts indicate that at least three enzymatic factors exist in the rat liver cytosol which affect the anaerobic reduction of NPDA to TAB, although these were less effective than the microsomal factors; they are xanthine oxidase, aldehyde oxidase, and other uncharacterized enzyme(s) requiring NADPH as a cofactor. The cytosolic factor for the anaerobic reduction of NPDA N^4-acetate to TAB N^4-acetate would differ from those for NPDA in view of its cofactor requirement. However, it is still equivocal whether the same enzymatic factor requiring NADPH should be able to reduce both NPDA and its N^4-acetate.

In our previous studies,[12,13,36] it has been considered that NPDA is successively metabolized to NPDA N^4-acetate by N^4-acetylation, to TAB N^4-acetate by nitroreduction, and further to TAB N^1,N^4-diacetate by N^1-acetylation. The present study strongly suggests that in rat liver, NPDA may be also metabolized through another possible pathway to TAB N^1,N^4-diacetate *via* TAB formed by direct nitroreduction. Accordingly, it may be concluded that there appear to be two possible pathways in the metabolism of NPDA to TAB N^1,N^4-diacetate in the rat, as summarized in Chart 1.

It may be suggested that TAB is responsible for the toxic changes induced by NPDA since the triamine, isolated and identified in the present study, has been shown to be strongly mutagenic[37-39] and myotoxic.[40]

References

1) B. N. Ames, H. O. Kammen and E. Yamasaki, *Proc. Natl. Acad. Sci. U.S.A.*, **72**, 2423 (1975).
2) Y. Takeda and R. Yoshimura, *Eisei Kagaku*, **24**, 322 (1978).
3) M. M. Shahin, C. Chopy and N. Lequesne, *Environ. Mutagen.*, **7**, 535 (1985).
4) K. A. Palmer, A. Denunzio and S. Green, *J. Environ. Pathol. Toxicol.*, **1**, 87 (1977).
5) C. E. Searle, D. G. Harnden, S. Venitt and O. H. B. Gyde, *Nature* (London), **255**, 506 (1975).
6) W. F. Benedict, *Nature* (London), **260**, 368 (1976).
7) P. E. Perry and C. E. Searle, *Mutat. Res.*, **56**, 207 (1977).
8) C. N. Martin, A. C. McDermid and R. C. Garner, *Cancer Res.*, **38**, 2621 (1978).
9) G. M. Williams, M. F. Laspin and V. C. Dunkel, *Mutat. Res.*, **97**, 359 (1982).
10) G. Reznik and J. M. Ward, *Food Cosmet. Toxicol.*, **17**, 493 (1979).
11) H. A. Milman and C. Peterson, *Environ. Health Perspect.*, **56**, 261 (1984).
12) M. Nakao and Y. Takeda, *J. Toxicol. Environ. Health*, **11**, 93 (1983).
13) M. Nakao, Y. Gotoh, Y. Matsuki, A. Hiratsuka and T. Watabe, *Chem. Pharm. Bull.*, **35**, 785 (1987).
14) O. H. Lowry, N. J. Rosebrough, A. L. Farr and R. J. Randall, *J. Biol. Chem.*, **193**, 265 (1951).
15) M. Mori, T. Matsuhashi, T. Miyahara, S. Shibata, C. Izima and H. Kozuka, *Toxicol. Appl. Pharmacol.*, **76**, 105 (1984).
16) Y. Yoshida, H. Kumaoka and M. Akagi, *Chem. Pharm. Bull.*, **16**, 2324 (1968).
17) R. Kato, T. Oshima and A. Takanaka, *Mol. Pharmacol.*, **5**, 487 (1969).
18) L. A. Poirier and J. H. Weisburger, *Biochem. Pharmacol.*, **23**, 661 (1974).
19) R. Kato, K. Iwasaki and H. Noguchi, *Mol. Pharmacol.*, **14**, 654 (1978).
20) N. Narai, S. Kitamura and K. Tatsumi, *J. Pharmacobio-Dyn.*, **7**, 407 (1984).
21) J. R. Gillette, J. J. Kamm and H. Sasame, *Mol. Pharmacol.*, **4**, 541 (1968).
22) H. A. Sasame and J. R. Gillette, *Mol. Pharmacol.*, **5**, 123 (1969).
23) K. Saito, T. Kamataki and R. Kato, *Cancer Res.*, **44**, 3169 (1984).
24) N. Harada and T. Omura, *J. Biochem.* (Tokyo), **87**, 1539 (1980).
25) M. R. Boyd, A. W. Stiko and H. A. Sasame, *Biochem. Pharmacol.*, **28**, 601 (1979).
26) J. L. Holtzman, D. L. Crankshaw, F. J. Peterson and C. F. Polnaszek, *Mol. Pharmacol.*, **20**, 669 (1981).
27) D. R. Feller, M. Morita and J. R. Gillette, *Biochem. Pharmacol.*, **20**, 203 (1971).
28) M. E. McManus, M. A. Lang, K. Stuart and J. Strong, *Biochem. Pharmacol.*, **31**, 547 (1982).
29) K. E. McLane, J. Fisher and K. Ramakrishman, *Drug Metab. Rev.*, **14**, 741 (1983).
30) R. Kato, A. Takanaka and T. Oshima, *Biochem. Pharmacol.*, **19**, 45 (1970).
31) M. Morita, D. R. Feller and J. R. Gillette, *Biochem. Pharmacol.*, **20**, 217 (1971).
32) K. Tatsumi, S. Kitamura, H. Yoshimura and Y. Kawazoe, *Chem. Pharm. Bull.*, **26**, 1713 (1978).
33) M. K. Wolpert, J. R. Althaus and D. G. Johns, *J. Pharmacol. Exp. Ther.*, **185**, 202 (1973).
34) K. Tatsumi, S. Kitamura and N. Narai, *Cancer Res.*, **46**, 1089 (1986).
35) D. S. Hewick, "Metabolic Basis of Detoxication," ed. by W. B. Jakoby, J. R. Bend and J. Caldwell, Academic Press, Inc., New York, 1982, pp. 151—166.
36) M. Nakao, Y. Goto, Y. Matsuki, A. Hiratsuka and T. Watabe, *Chem. Pharm. Bull.*, **38**, 2561 (1990).
37) R. C. Garner and C. A. Nutman, *Mutat. Res.*, **44**, 9 (1977).
38) S. Venitt and C. T. Bushell, *Mutat. Res.*, **40**, 309 (1976).
39) I. de G. Mitchell, *Mutat. Res.*, **54**, 1 (1978).
40) R. Walker, P. Grasso and I. F. Gaunt, *Food Cosmet. Toxicol.*, **8**, 539 (1970).

A New Method for Preparation of 3-Hydroxypyridines from Furfurylamines by Photooxygenation

Yueh-Hsiung KUO* and Kae-Shyang SHIH

Department of Chemistry, National Taiwan University, Taipei, Taiwan, R.O.C. *Received May 21, 1990*

Low-temperature photooxygenation (−70 °C) of furfurylamine derivatives followed by treatment with triphenylphosphine provided 3-hydroxypyridines in high yield.

Keywords furfurylamine; photooxygenation; 3-hydroxypyridine

There are many methods available for the preparation of 3-hydroxypyridines. The methods of formation of 3-hydroxypyridines by heating 2-acetylfurans[1] or 2-furoic acid derivatives[2] with ammonia give low yields. The reaction of the naturally occurring maltol glucoside with a wide variety of primary amines gives pyridiones which upon hydrolysis, yield the corresponding 3-hydroxypyridines.[3] Transformation of carbohydrates to 3-hydroxypyridines has also been reported.[4] As to the formation of 3-hydroxypyridines from aminofurans, drastic conditions are required.[5]

Photooxygenation of furans has been studied extensively from mechanistic and synthetic viewpoints.[6] Oxidative ring opening of furans leading to enediones is an important synthetic operation, since furans can be used as a masked 1,4-dicarbonyl unit.[7] Recently, Saito *et al.*[8] reported that low-temperature photooxygenation of furans followed by reduction with dimethyl sulfide stereospecifically provided *cis*-enediones, which, on subsequent treatment with trimethylsilyl cyanide, afforded 2-cyano-5-hydroxy-2,5-dihydrofurans, the latter compounds being important precursors of 4-cyanobutenolides. In the case of 2-furfuryl alcohols, the oxidation with singlet oxygen then reduction with triphenylphosphine (Ph_3P) gave the corresponding *cis*-enediones which spontaneously cyclized to afford 6-hydroxy-2*H*-pyran-3-(6*H*)-ones.[9] In this paper we wish to describe a novel and useful method to convert furfurylamines (**1**) into 3-hydroxypyridines (**2**) in high yieldes. Furfurylamine (**1**) reacted with singlet oxygen at low temperature, and the intermediate ozonides were reduced with Ph_3P to give the corresponding enediones, which underwent spontaneous condensation of the amino and carbonyl groups to yield the α-amino alcohols, which in turn afforded 3-hydroxypyridines (**2**) after dehydration and tautomerization (Chart 1).

A typical experimental procedure was as follows. A furfurylamine (**1**) and tetraphenylporphine (TPP) were dissolved in dry CH_2Cl_2. The solution was irradiated externally with a tungsten bromine lamp at −70 °C under oxygen bubbling. After 2 h, excess Ph_3P in dry CH_2Cl_2 was added to the reaction mixture, which was allowed to warm to ambient temperature after 20 min. The products were purified by neutral alumina column chromatography to afforded 3-hydroxyridines (**2**) in high yields (Table I).

TABLE I. Transformation of Furfurylamines to 3-Hydroxypyridines[a]

Entry	Furfurylamine	3-Hydroxypyridine	Yield (%)[b]
1	**1a**	**2a**	86[c]
2	**1b**	**2b**	80
3	**1c**	**2c**	83
4	**1d**	**2d**	82[c]
5	**1e**	**2e**	83
6	**1f**	**2f**	82
7	**1g**	**2g**	85
8	**1h**	**2h**	84
9	**1i**	**2i**	87

a) Experimental procedures are described in the text. *b*) Yields given are for isolated products. *c*) The product was identical with a commercial product.

Experimental

Melting points were determined on a Yanagimoto micro melting point apparatus and are uncorrected. Infrared (IR) spectra were run neat or as a KBr disc on a Perkin-Elmer 983G instrument. Proton nuclear magnetic resonance (^{1}H-NMR) spectra were run on a Varian EM-390 (90 MHz) and Bruker AM-300 (300 MHz) spectrometers in the indicated solvents. Chemical shifts and coupling constants (*J*) were measured in ppm (δ) and hertz (Hz) with respect to tetramethylsilane (TMS). The electron impact mass spectra (EI MS) were obtained on a JEOL model JMS-DX 300 double focusing mass spectrometer.

Materials Alkylfurans (R = H, Me or Et) acylated at C-5 were obtained by Vilsmeier method[10] or by reaction with acetic or propionic anhydride, with ferric chloride as a catalyst (Chart 2). The acylfurans (**3**) thus obtained reacted with hydroxyamine to give the oximes (**4**), whose reduction with Raney Ni alloy in ethanolic NaOH solution (Chart 2) afforded the furfurylamines (**1**). Details of these reactions are given below. Compounds **3b**, **3d**, **3f**, and **1a** are commercially available.

General Procedure for Photooxidation of Furfurylamine A furfurylamine (**1**) (200 mg) and TPP (3 mg) were dissolved in CH_2Cl_2 (15 ml). The solution was irradiated with a 650 W tungsten bromine lamp at −70 °C for 2 h while oxygen was passed through the solution. Then 700 mg of triphenylphosphine in 2 ml of CH_2Cl_2 was added at the same temperature. After 10 min, the reaction mixture was taken out of the dry ice–acetone

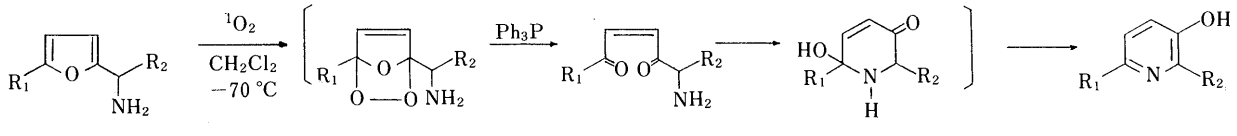

1 2

a : R_1=R_2=H **d** : R_1=Me, R_2=H **g** : R_1=Me, R_2=Et
b : R_1=H, R_2=Me **e** : R_1=Et, R_2=H **h** : R_1=Et, R_2=Me
c : R_1=H, R_2=Et **f** : R_1=R_2=Me **i** : R_1=R_2=Et

Chart 1

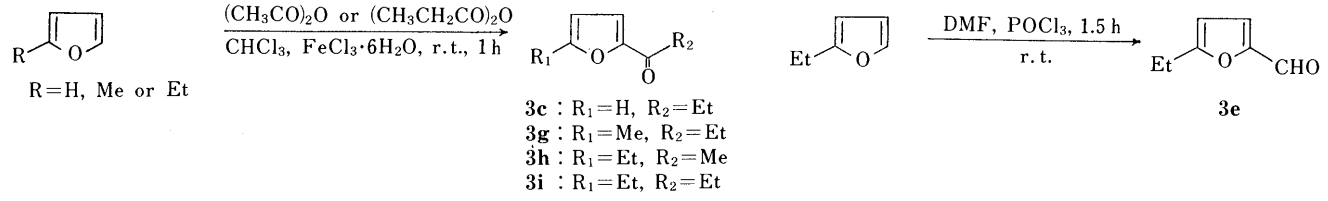

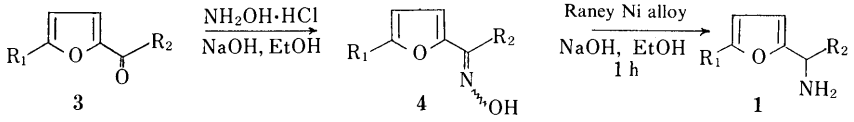

a : $R_1=R_2=H$
b : $R_1=H$, $R_2=Me$
c : $R_1=H$, $R_2=Et$
d : $R_1=Me$, $R_2=H$
e : $R_1=Et$, $R_2=H$
f : $R_1=R_2=Me$
g : $R_1=Me$, $R_2=Et$
h : $R_1=Et$, $R_2=Me$
i : $R_1=R_2=Et$

Chart 2

solution bath. The product was purified by neutral alumina chromatography to afford the corresponding 3-hydroxypyridine (**2**) in excellent yield (Table I). Physical data of products **2a**—**2i** are give below.

2a: mp 124—126 °C. IR ν_{max}^{KBr} cm^{-1}: 3000—2400, 1606, 1568, 1278, 1241, 1020, 842, 702, 639. MS *m/z* (%): 96 ($M^+ + 1$, 5), 95 (M^+, 100), 68 (12), 67 (14), 66 (6), 55 (5), 41 (22). ^{1}H-NMR (CD_3COCD_3) δ: 7.22 (2H, m), 8.08 (1H, t, $J=3.0$ Hz), 8.23 (1H, t, $J=1.5$ Hz).

2b: mp 128—130 °C. IR ν_{max}^{KBr} cm^{-1}: 3000—2400, 1600, 1574, 1285, 1182, 1130, 797, 761. MS *m/z* (%): 110 ($M^+ + 1$, 5), 109 (M^+, 100), 81 (33), 80 (77), 54 (9), 53 (16), 42 (11). ^{1}H-NMR (CD_3COCD_3) δ: 2.36 (3H, s), 6.98 (1H, dd, $J=7.5$, 4.5 Hz), 7.13 (1H, dd, $J=7.5$, 2.0 Hz), 7.95 (1H, dd, $J=4.5$, 2.0 Hz).

2c: IR ν_{max}^{neat} cm^{-1}: 3000—2400, 1574, 1449, 1285, 1167, 1119, 723, 694. MS *m/z* (%): 124 ($M^+ + 1$, 3), 123 (M^+, 59), 122 (100), 104 (8), 95 (10), 80 (12), 73 (11), 71 (14), 67 (20), 57 (19), 58 (25), 55 (32), 43 (28). ^{1}H-NMR ($CDCl_3$) δ: 1.20 (3H, t, $J=7.0$ Hz), 2.95 (2H, q, $J=7.0$ Hz), 4.50 (1H, br s, –OH), 6.96 (1H, dd, $J=7.5$, 4.5 Hz), 7.15 (1H, dd, $J=7.5$, 1.5 Hz), 8.02 (1H, dd, $J=4.5$, 1.5 Hz).

2d: mp 169—170 °C. IR ν_{max}^{KBr} cm^{-1}: 3000—2400, 1613, 1569, 1497, 1275, 1221, 827, 655. MS *m/z* (%): 110 ($M^+ + 1$, 8), 109 (M^+, 100), 108 (17), 82 (4), 81 (17), 80 (63), 54 (17), 53 (23), 51 (12), 42 (7). ^{1}H-NMR (CD_3COCD_3) δ: 2.42 (3H, br s), 7.15, 7.28 (each 1H, d, $J=8.0$ Hz), 8.22 (1H, br s), 9.05 (1H, br s, –OH).

2e: mp 102—104 °C. IR ν_{max}^{KBr} cm^{-1}: 3000—2400, 1566, 1494, 1350, 1275, 1031, 919, 827, 653. MS *m/z* (%): 124 ($M^+ + 1$, 5), 123 (M^+, 58), 122 (100), 108 (8), 95 (14), 80 (3), 67 (7), 53 (9). ^{1}H-NMR ($CDCl_3$) δ: 1.25 (3H, t, $J=7.0$ Hz), 2.78 (2H, q, $J=7.0$ Hz), 7.10 (1H, d, $J=8.0$ Hz), 7.30 (1H, dd, $J=8.0$, 2.5 Hz), 8.27 (1H, d, $J=2.5$ Hz), 9.00 (1H, br s, –OH).

2f: mp 122—124 °C. IR ν_{max}^{KBr} cm^{-1}: 3000—2400, 1575, 1494, 1380, 1282, 1126, 829, 793, 711. MS *m/z* (%): 124 ($M^+ + 1$, 35), 123 (M^+, 100), 122 (22), 108 (4), 93 (19), 94 (72), 82 (98), 81 (14), 80 (13), 53 (19), 42 (17). ^{1}H-NMR (CD_3COCD_3) δ: 2.31, 2.35 (each 3H, s), 6.83, 7.03 (each 1H, d, $J=8.0$ Hz).

2g: mp 136—138 °C. IR ν_{max}^{KBr} cm^{-1}: 3000—2400, 1574, 1492, 1369, 1268, 1162, 1129, 825, 810, 769, 705. MS *m/z* (%): 138 ($M^+ + 1$, 11), 137 (M^+, 67), 136 (100), 122 (6), 94 (5), 81 (7), 80 (8), 53 (13). ^{1}H-NMR (CD_3COCD_3) δ: 1.20 (3H, t, $J=7.0$ Hz), 2.32 (3H, s), 2.77 (2H, q, $J=7.0$ Hz), 6.86, 7.08 (each 1H, d, $J=8.0$ Hz).

2h: mp 115—117 °C. IR ν_{max}^{KBr} cm^{-1}: 3000—2400, 1573, 1499, 1338, 1279, 832, 699. MS *m/z* (%): 138 ($M^+ + 1$, 21), 137 (M^+, 78), 136 (100), 122 (14), 118 (7), 94 (6), 81 (9), 80 (10), 53 (20). ^{1}H-NMR (CD_3COCD_3) δ: 1.20 (3H, t, $J=7.0$ Hz), 2.40 (3H, s), 2.63 (2H, q, $J=7.0$ Hz), 6.84, 7.07 (each 1H, d, $J=7.0$ Hz).

2i: mp 131—133 °C. IR ν_{max}^{KBr} cm^{-1}: 3000—2400, 1600, 1568, 1491, 1430, 1352, 1283, 1128, 833, 760. MS *m/z* (%): 152 (4), 151 (M^+, 50), 150 (100), 136 (6), 135 (12), 123 (8), 108 (6), 80 (5), 67 (4), 65 (4), 55 (4), 52 (5). ^{1}H-NMR (CD_3COCD_3) δ: 1.20 (6H, t, $J=7.0$ Hz), 2.67, 2.80 (each 2H, q, $J=7.0$ Hz), 6.91, 7.15 (each 1H, d, $J=8.0$ Hz).

Preparation of 3c by Propionylation of Furan Ferric chloride hexahydrate ($FeCl_3 \cdot 6H_2O$, 0.04 g) was added to a solution of furan (1 g) in 15 ml of $CHCl_3$ and propionic anhydride (3.0 g), then the reaction mixture was stirred at room temperature for 2 h. Saturated ethylenediaminetetraacetate (EDTA) was added to the reaction mixture to remove the ferric ion, and the whole was washed with 2 N aqueous NaOH solution. The organic layer was dried with $CaCl_2$ and concentrated. Chromatography of the residue on silica gel gave compound **3c** (0.55 g).

Preparation of 3g, 3h, and 3i by Acetylation or Propionylation of 2-Methyl- or 2-Ethylfuran Acetic anhydride (or propionyl anhydride, 3.5 g) was added to a solution of 2-methyl- or 2-ethylfuran (1 g) in 30 ml of 1,2-dichloroethane. Then $FeCl_3 \cdot 6H_2O$ (0.08 g) was added, and the reaction mixture which was heated under reflux for 1 h. Work up as mentioned above gave **3g**, **3h** or **3i** (35—40% yield).

Preparation of 3e by Vilsmeier's Method $POCl_3$ (1.8 ml) was added dropwise to a mixture of 2-ethylfuran (2 g) and dimethylformamide (DMF 1.8 g) at 0—5 °C, and the reaction mixture was allowed to stand at room temperature for 1.5 h. Then the mixture was poured into ice water, neutralized with NaOAc, and extracted with ether. The extract was purified on silica gel chromatography to give **3e** (0.95 g).

3c: IR ν_{max}^{neat} cm^{-1}: 3130, 1673, 1564, 1465, 1391, 1248, 1163, 1091, 1076, 1032, 882, 762. ^{1}H-NMR ($CDCl_3$) δ: 1.20 (3H, t, $J=7.5$ Hz), 2.86 (2H, q, $J=7.5$ Hz), 6.46 (1H, dd, $J=3.5$, 1.5 Hz), 7.20 (1H, d, $J=3.5$ Hz), 7.58 (1H, d, $J=1.5$ Hz).

3e: IR ν_{max}^{neat} cm^{-1}: 3117, 1674, 1569, 1515, 1396, 1321, 1023, 961, 806, 766. ^{1}H-NMR ($CDCl_3$) δ: 1.20 (3H, t, $J=7.7$ Hz), 2.60 (2H, q, $J=7.7$ Hz), 6.16, 7.10 (1H, d, $J=3.5$ Hz), 9.40 (1H, s).

3g: IR ν_{max}^{neat} cm^{-1}: 3115, 1670, 1584, 1510, 1349, 1204, 1035, 903, 797. ^{1}H-NMR ($CDCl_3$) δ: 1.15 (3H, t, $J=7.5$ Hz), 2.39 (3H, s), 2.77 (2H, q, $J=7.5$ Hz), 6.17, 7.07 (each 1H, d, $J=3.0$ Hz).

3h: IR ν_{max}^{neat} cm^{-1}: 3117, 1670, 1584, 1511, 1355, 1297, 1206, 1109, 1015, 923, 802. ^{1}H-NMR ($CDCl_3$) δ: 1.24 (3H, t, $J=7.6$ Hz), 2.40 (3H, s), 2.70 (2H, q, $J=7.6$ Hz), 6.12, 7.07 (each 1H, d, $J=3.4$ Hz).

3i: IR ν_{max}^{neat} cm^{-1}: 3115, 1670, 1584, 1510, 1320, 1204, 1013, 903, 797. ^{1}H-NMR ($CDCl_3$) δ: 1.19, 1.30 (each 3H, t, $J=7.5$ Hz), 2.72, 2.82 (each 2H, q, $J=7.5$ Hz), 6.15, 7.10 (each 1H, $J=3.0$ Hz).

The Oximes (4b—4i) from the Acylfurans (3b—3i) An acylfuran (**3**) (1.0 g), $H_2NOH \cdot HCl$ (1.01 g), and NaOH (1.82 g) were dissolved in a mixture of 10 ml of ethanol and 2 ml of H_2O. The reaction mixture was refluxed for 20 min. The reaction mixture was acidified with 2 N HCl, and extracted with ether. The ether extract was purified to give the corresponding oxime (**4**) (75—82%).

4b: mp 41—42 °C. IR ν_{max}^{KBr} cm^{-1}: 3204, 1576, 1489, 1310, 1162, 1003, 947, 896, 826, 740. MS *m/z* (%): 126 ($M^+ + 1$, 10), 125 (M^+, 100), 108 (11), 93 (15), 84 (10), 68 (63), 65 (23), 55 (17), 53 (16). ^{1}H-NMR ($CDCl_3$) δ: 2.19 (3H, s), 6.40 (1H, dd, $J=3.4$, 1.8 Hz), 6.60 (1H, d, $J=3.4$ Hz), 7.40 (1H, d, $J=1.8$ Hz), 9.56 (1H, br s, –OH).

4c: mp 65—68 °C (*cis*+*trans*). IR ν_{max}^{KBr} cm^{-1}: 3255, 3120, 1649, 1411, 1206, 1108, 1068, 988, 952, 988, 952. MS *m/z* (%): 140 ($M^+ + 1$, 23), 139 (M^+, 100), 122 (41), 107 (27), 93 (32), 94 (78), 93 (55), 81 (40), 79 (27), 68 (35), 55 (24). ^{1}H-NMR ($CDCl_3$) δ: 1.27 (3H, t, $J=7.5$ Hz), 2.70 (2H, q, $J=7.5$ Hz), 6.55 (1H, dd, $J=3.0$, 1.5 Hz), 749 (1H, d, $J=1.5$ Hz), 7.52 (1H, d, $J=3.0$ Hz), 8.80 (1H, br s, –OH). One isomer: ^{1}H-NMR ($CDCl_3$) δ: 1.20 (3H, t, $J=7.5$ Hz), 2.80 (2H, q, $J=7.5$ Hz), 6.67 (1H, d,

J=3.0, 1.5 Hz), 7.18 (1H, d, J=3.0 Hz), 7.57 (1H, d, J=1.5 Hz), 8.80 (1H, br s, –OH).

4d: mp 81—83 °C. IR ν_{max}^{KBr} cm^{-1}: 3174, 3023, 1637, 1586, 1517, 1310, 1208, 1024, 964, 894, 802. MS m/z (%): 126 (M^++1, 7), 125 (M^+, 100), 108 (10), 82 (46), 81 (17), 79 (12), 52 (92), 51 (28), 43 (22), ^{1}H-NMR ($CDCl_3$) δ: 2.32 (3H, s), 6.14, 7.13 (each 1H, d, J=3.0 Hz), 7.44 (1H, s), 9.50 (1H, br s, –OH).

4e: mp 83—85 °C (*cis*+*trans*). IR ν_{max}^{KBr} cm^{-1}: 3201, 1641, 1583, 1521, 1327, 1185, 983, 833. MS m/z (%): 140 (M^++1, 4), 139 (M^+, 71), 124 (100), 79 (13), 69 (9), 67 (13), 65 (15), 50 (12), 51 (18). ^{1}H-NMR ($CDCl_3$) δ: 1.20 (3H, t, J=7.5 Hz), 2.63 (2H, q, J=7.5 Hz), 6.01, 6.46 (each 1H, d, J=3.0 Hz), 7.90 (1H, s), 9.50 (1H, br s, –OH). One isomer: ^{1}H-NMR ($CDCl_3$) δ: 1.20 (3H, t, J=7.5 Hz), 2.63 (2H, q, J=7.5 Hz), 6.08, 7.20 (1H, d, J=3.0 Hz), 7.40 (1H, s), 9.50 (2H, br s, –OH).

4f: mp 48—50 °C (*cis*+*trans*). IR ν_{max}^{KBr} cm^{-1}: 3254, 1623, 1592, 1543, 1374, 1221, 1208, 1018, 964, 787, 742. MS m/z (%): 140 (M^++1, 8), 139 (M^+, 88), 122 (14), 107 (8), 82 (36), 81 (13), 53 (100), 52 (21), 43 (19). ^{1}H-NMR ($CDCl_3$) δ: 2.15, 2.30 (each 3H, s), 5.99, 6.47 (each 1H, d, J=3 Hz). One isomer: ^{1}H-NMR ($CDCl_3$) δ: 2.15, 2.30 (each 3H, s), 6.10 and 7.33 (each 1H, d, J=3.3 Hz).

4g: mp 50—52 °C (*cis*+*trans*). IR ν_{max}^{KBr} cm^{-1}: 3247, 3140, 1644, 1619, 1587, 1520, 1207, 1112, 1026, 997, 948, 885, 792. MS m/z (%): 154 (M^++1, 9), 153 (M^+, 100), 136 (17), 109 (22), 108 (25), 107 (20), 96 (17), 82 (36), 53 (62), 43 (28). ^{1}H-NMR ($CDCl_3$) δ: 1.28 (3H, t, J=7.5 Hz), 2.30 (3H, s), 2.72 (2H, q, J=7.5 Hz), 6.15, 7.43 (each 1H, d, J=3.0 Hz). One isomer: ^{1}H-NMR ($CDCl_3$) δ: 1.25 (3H, t, J=7.5 Hz), 2.30 (3H, s), 2.70 (2H, q, J=7.5 Hz), 6.01, 6.55 (each 1H, d, J=3.0 Hz).

4h (*cis*+*trans*): IR ν_{max}^{neat} cm^{-1}: 3225, 3170, 1624, 1588, 1522, 1378, 1322, 1202, 1119, 1013, 982, 963, 901, 797, 742. ^{1}H-NMR ($CDCl_3$) δ: 1.24 (3H, t, J=7.0 Hz), 2.17 (3H, s), 2.68 (2H, q, J=7.0 Hz), 6.02, 6.50 (each 1H, d, J=3.5 Hz), One isomer: ^{1}H-NMR ($CDCl_3$) δ: 1.24 (3H, t, J=7.0 Hz), 2.23 (3H, s), 2.68 (2H, q, J=7.0 Hz), 6.14, 7.37 (each 1H, d, J=3.5 Hz).

4i (*cis*+*trans*): IR ν_{max}^{KBr} cm^{-1}: 3238, 1622, 1587, 1520, 1320, 1201, 1018, 983, 938, 796. MS m/z (%): 168 (M^++1, 22), 167 (M^+, 100), 152 (37), 150 (16), 135 (11), 112 (12), 106 (12), 97 (19), 96 (16), 79 (13), 67 (17), 65 (13). ^{1}H-NMR ($CDCl_3$) δ: 1.20 (6H, m), 2.65 (4H, q, J=7.8 Hz), 6.02, 6.50 (each 1H, d, J=3.0 Hz). One isomer: ^{1}H-NMR ($CDCl_3$) δ: 1.20 (6H, m), 2.65 (4H, q, J=7.8 Hz), 6.13, 7.37 (each 1H, d, J=3.0 Hz).

The Furfurylamines (1b—1i) from the Oximes (4b—4i) by Raney Ni Reduction Excess of Raney Ni alloy was added to a solution of an oxime (0.5 g) in 10 ml of ethanol and 10 ml of 2 N aqueous NaOH. The reaction mixture was stirred at ambient temperature for 1 h, then extracted with $CHCl_3$. The $CHCl_3$ extract was evaporated and the residue was purified on silica gel (saturated with Et_3N) chromatography to give the corresponding (79—85%).

1b: IR ν_{max}^{neat} cm^{-1}: 3300, 3120, 1639, 1520, 1357, 1149, 1012, 799, 734. ^{1}H-NMR ($CDCl_3$) δ: 1.37 (3H, d, J=6.7 Hz), 4.03 (1H, q, J=6.7 Hz), 4.78 (2H, br s, –NH_2), 6.04 (1H, d, J=3.1 Hz), 6.49 (1H, dd, J=3.1, 1.8 Hz), 7.28 (1H, d, J=1.8 Hz).

1c: IR ν_{max}^{neat} cm^{-1}: 3350, 3120, 1639, 1163, 1009, 945, 895, 737. ^{1}H-NMR ($CDCl_3$) δ: 0.88 (3H, d, J=7.0 Hz), 1.71 (2H, quintet, J=7.0 Hz), 3.75 (1H, t, J=7.0 Hz), 6.09 (1H, d, J=3.0 Hz), 6.27 (1H, dd, J=3.0, 1.5 Hz), 7.26 (1H, d, J=1.5 Hz).

1d: IR ν_{max}^{neat} cm^{-1}: 3344, 1574, 1442, 1129, 1021, 944, 824. ^{1}H-NMR ($CDCl_3$) δ: 2.24 (3H, s), 3.74 (2H, s), 5.86, 5.98 (each 1H, d, J=2.9 Hz).

1e: IR ν_{max}^{neat} cm^{-1}: 3350, 3120, 1639, 1163, 1009, 954, 885, 737. ^{1}H-NMR ($CDCl_3$) δ: 1.25 (3H, d, J=7.5 Hz), 1.88 (2H, br s, –NH_2), 2.65 (2H, q, J=7.5 Hz), 3.72 (2H, s), 5.87, 6.00 (each 1H, d, J=1.5 Hz).

1f: IR ν_{max}^{neat} cm^{-1}: 3286, 3130, 1600, 1562, 1310, 1163, 1018, 944, 784, 738. ^{1}H-NMR ($CDCl_3$) δ: 1.35 (3H, d, J=6.7 Hz), 2.23 (3H, s), 4.00 (1H, q, J=6.7 Hz), 5.83, 5.93 (each 1H, d, J=3.0 Hz).

1g: IR ν_{max}^{neat} cm^{-1}: 3234, 3100, 1560, 1375, 1207, 1058, 1013, 781. ^{1}H-NMR ($CDCl_3$) δ: 0.88 (3H, t, J=7.5 Hz), 1.60 (2H, quintet, J=7.5 Hz), 2.30 (3H, s), 3.72 (1H, t, J=7.5 Hz), 5.82, 5.93 (each 1H, d, J=3.0 Hz).

1h: IR ν_{max}^{neat} cm^{-1}: 3280, 3100, 1562, 1379, 1217, 1020, 785. ^{1}H-NMR ($CDCl_3$) δ: 1.19 (3H, t, J=7.5 Hz), 1.36 (3H, t, J=6.9 Hz), 2.60 (2H, q, J=7.5 Hz), 4.00 (1H, q, J=6.9 Hz), 5.84, 5.95 (each 1H, d, J=3.0 Hz).

1i: IR ν_{max}^{neat} cm^{-1}: 3290, 3101, 1556, 1374, 1323, 1057, 1011, 779. ^{1}H-NMR ($CDCl_3$) δ: 0.92 (6H, m), 1.72 (2H, m), 2.62 (2H, q, J=7.5 Hz), 3.76 (1H, t, J=7.5 Hz), 5.84, 5.96 (each 1H, d, J=3.0 Hz).

Acknowledgement The research was supported by the National Science Council of the ROC.

References

1) L. A. Walter, C. K. Springer, J. Kenney, S. K. Galen and N. Sperber, *J. Med. Chem.*, **11**, 792 (1968).
2) H. Greuter and D. Bellus, *J. Heterocycl. Chem.*, **14**, 203 (1977).
3) M. Yasue, N. Kawamura and J. Sakakibara, *Yakugaku Zasshi*, **90**, 1222 (1970).
4) *a*) H. Tsuchida, M. Komoto, H. Kato and M. Fujimaki, *Agric. Biol. Chem.*, **39**, 1143 (1975); *b*) K. Olsson, P. A. Pernemaim and O. Theander, *Acta Chem. Scand., Ser. B*, **32**, 249 (1978); *c*) H. Tsuchida, M. Komoto, H. Kato, T. Kurata and M. Fujimaki, *Agric. Biol. Chem.*, **40**, 2051 (1976).
5) *a*) J. V. S. Peterson, K. Norris, N. Clauson-Kaas and K. Svanaholt, *Acta Chem. Scand.*, **23**, 1785 (1969); *b*) J. V. B. Peterson, US. Patent 3658826 (1972) [*Chem. Abstr.*, **77**, 883341 (1972)]; *c*) I. F. Belśkii, F. I. Belśkii and V. M. Shostakovskii, *Izv. Akad. Nauk SSSR, Ser. Kim*, **1977** 1364 [*Chem. Abstr.*, **87**, 152127 (1977)].
6) *a*) I. Saito and S. S. Nittala, "The Chemistry of Peroxides," ed. by S. Patai, Wiley-Interscience, New York, 1983, p. 311; *b*) H. H. Wasserman and B. H. Lipshutz, "Singlet Oxygen," ed. by H. H. Wasserman and R. W. Murray, Academic Press, New York, 1979, p. 430; *c*) K. Gollnick and A. Griesheck, *Tetrahedron*, **41**, 2057 (1985) and references cited therein; *d*) E. L. Clennan and M. E. Mehrsheikn-Mohammadi, *J. Am. Chem. Soc.*, **106**, 7112 (1984); *e*) Y.-H. Kuo and K.-S. Shih, *J. Photochem. Photobiol. A: Chem.*, **41**, 79 (1987); *f*) Y.-H. Kuo, K.-S. Shih and S. M. Lee, *J. Photochem. Photobiol., A: Chem.*, **45**, 97 (1988); *g*) Y.-H. Kuo, K.-S. Shih, G.-H. Lee and Y. Wang, *Heterocycles*, **27**, 599 (1988).
7) *a*) G. Piancatelli, A. Scettri and M. D'Auria, *Tetrahedron*, **36**, 661 (1980); *b*) P. D. Williams and E. LeGoff, *J. Org. Chem.*, **46**, 4113 (1981); *c*) *Idem*, *Tetrahedron Lett.*, **26**, 1367 (1985); *d*) M. Petrini, R. Ballini, G. Rosini and E. Marotta, *Tetrahedron*, **42**, 151 (1986).
8) I. Saito, Y.-H. Kuo and T. Matsuura, *Tetrahedron Lett.*, **27**, 2757 (1986).
9) Y.-H. Kuo and K.-S. Shih, *Heterocycles*, in press (1990).
10) O. Achmatowicz and M. H. Burzynska, *Tetrahedron*, **38**, 3507 (1982).

Amino Acids and Peptides. XXX. Synthesis of Eglin c (41—49) and Eglin c (60—63) and Examination of Their Inhibitory Activity towards Human Leukocyte Elastase, Cathepsin G, Porcine Pancreatic Elastase and α-Chymotrypsin[1,2]

Satoshi TSUBOI,[a] Miho TAKEDA,[a] Yoshio OKADA,*,[a] Yoko NAGAMATSU[b] and Junichiro YAMAMOTO[b]

Faculty of Pharmaceutical Sciences,[a] and Faculty of Nutrition,[b] Kobe-Gakuin University, Nishi-ku, Kobe 651-21, Japan. *Received July 2, 1990*

H–Ser–Pro–Val–Thr–Leu–Asp–Leu–Arg–Tyr–OH and H–Thr–Asn–Val–Val–OH, which correspond to the sequences 41—49 and 60—63 of eglin c, respectively, were synthesized by a conventional solution approach using the newly developed 6-chloro-2-pyridyl ester method. The inhibitory activities of the above two peptides against human leukocyte elastase, cathepsin G, porcine pancreatic elastase and α-chymotrypsin were examined in comparison with those of the corresponding methyl esters.

Keywords eglin c-related peptide; chemical synthesis; inhibitory activity; human leukocyte elastase; cathepsin G; porcine pancreatic elastase; α-chymotrypsin

Eglin c, isolated from the leech *Hirudo medicinalis*,[3] consists of 70 amino acid residues[4] (Fig. 1) and effectively inhibits chymotrypsin and subtilisin as well as leukocyte elastase and cathepsin G. The latter two enzymes have attracted our interest due to their possible involvement in connective tissue turnover and diseases such as emphysema, rheumatoid arthritis and inflammation.[5,6]

Previously, we reported that a small peptide, H–Ser–Pro–Val–Thr–Leu–Asp–Leu–Arg–Tyr–OMe, which corresponds to the sequence 41—49 of eglin c, exhibited significant inhibitory activity against cathepsin G and α-chymotrypsin but not against leukocyte elastase, while the peptide H–Thr–Asn–Val–Val–OMe, which corresponds to the sequence 60—63 of eglin c, inhibited leukocyte elastase but not cathepsin G or α-chymotrypsin.[7]

This paper deals with the synthesis of H–Ser–Pro–Val–Thr–Leu–Asp–Leu–Arg–Tyr–OH and H–Thr–Asn–Val–Val–OH by using the newly developed 6-chloro-2-pyridyl active ester method and with an examination of their inhibitory activity against human leukocyte elastase, cathepsin G, α-chymotrypsin and porcine pancreatic elastase in order to study the roles of the C-terminal methyl ester groups of the above two peptides in the manifestation of the inhibitory activity.

According to the scheme shown in Fig. 2, the nonapeptide corresponding to the sequence 41—49 of eglin c was synthesized. Boc–Arg(Mts)–OH and H–Tyr–OBzl were coupled by the DPPA method[8] to avoid lactam formation,[9] to give Boc–Arg(Mts)–Tyr–OBzl. After removal of the Boc group by TFA treatment, Boc–Leu–OPyCl, Boc–Asp(OBzl)–OPyCl, Boc–Leu–OPyCl, Boc–Thr–ONSu, Boc–Val–OPyCl and Boc–Pro–OPyCl were added successively to afford Boc–Pro–Val–Thr–Leu–Asp(OBzl)–Leu–Arg(Mts)–Tyr–OBzl. After removal of the Boc group, Boc–Ser–$NHNH_2$ was coupled by the azide method[10] to give a protected nonapeptide. Boc-amino acid 6-chloro-2-pyridyl

H–Thr–Glu–Phe–Gly–Ser–Glu–Leu–Lys–Ser–Phe–Pro–Glu–Val–Val–Gly–Lys–Thr–Val–Asp–Gln–Ala–Arg–Glu–Tyr–Phe–Thr–Leu–His–Tyr–Pro–Gln–Tyr–Asp–Val–Tyr–Phe–Leu–Pro–Glu–Gly–Ser–Pro–Val–Thr–Leu–Asp–Leu–Arg–Tyr–Asn–Arg–Val–Arg–Val–Phe–Tyr–Asn–Pro–Gly–Thr–Asn–Val–Val–Asn–His–Val–Pro–His–Val–Gly–OH

Fig. 1. Structure of Eglin c

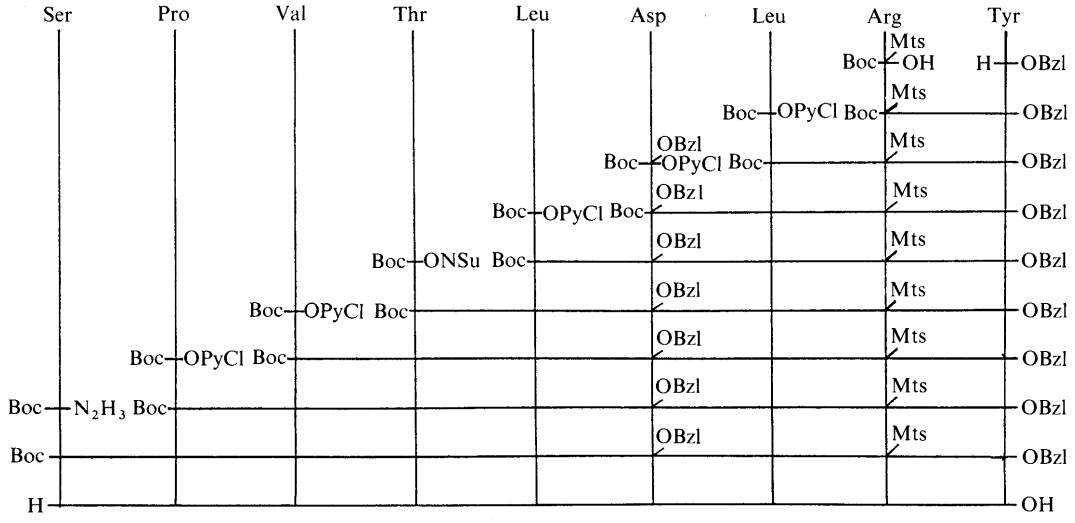

Fig. 2. Synthetic Scheme for H–(Eglin c 41—49)–OH

TABLE I. K_i Values of Eglin c (41—49) and Eglin c (60—63)

	K_i (M)			
	LE[a]	Cathepsin G[b]	α-Chymotrypsin[b]	PE[c]
H–(41—49)–OH·AcOH	ND	3.7×10^{-5}	7.2×10^{-5}	2.7×10^{-4}
H–(41—49)–OMe·2AcOH	ND	4.0×10^{-5}	2.0×10^{-5}	3.0×10^{-4}
H–(60—63)–OH	2.3×10^{-3}	ND	ND	4.8×10^{-3}
H–(60—63)–OMe·HCl	1.6×10^{-4}	ND	ND	ND

a) The substrate for LE (leukocyte elastase) was Suc–Ala–Tyr–Leu–Val–*p*NA. *b*) The substrate for cathepsin G and α-chymotrypsin was Suc–Ile–Pro–Phe–*p*NA. *c*) The substrate for PE (pancreatic elastase) was Suc–Ala–Ala–Ala–*p*NA. ND: not detectable ($K_i > 5.0\times10^{-3}$ M).

esters[11] reacted with amino groups very rapidly and the liberated pyridinol derivative was easily removed. Homogeneity of protected peptide intermediates was ascertained by thin layer chromatography (TLC), elemental analysis and amino acid analysis. The protected nonapeptide was treated with HF at 0 °C in the presence of thioanisole and *m*-cresol to give the desired peptide H–Ser–Pro–Val–Thr–Leu–Asp–Leu–Arg–Tyr–OH.

H–Thr–Asn–Val–Val–OH was synthesized as follows: Boc–Val–OPyCl and H–Val–OBzl were coupled to give Boc–Val–Val–OBzl. After removal of the Boc group, Boc–Asn–ONp and Z–Thr–OH were coupled successively by the active ester method and the DPPA method, respectively, to give Z–Thr–Asn–Val–Val–OBzl. This protected peptide was hydrogenated over a palladium catalyst to give H–Thr–Asn–Val–Val–OH. Both deprotected peptides were purified by gel-filtration on Sephadex G-25 using 3% AcOH as an eluant. The homogeneity of the peptides was ascertained by TLC, high performance liquid chromatography (HPLC) and amino acid analysis.

Next, the inhibitory activities of the above two peptides towards human leukocyte elastase, cathepsin G, α-chymotrypsin and porcine pancreatic elastase were examined and the results are summarized in Table I in comparison with those for the corresponding methyl esters.[7] Leukocyte elastase and pancreatic elastase preferentially split valyl and alanyl bonds, respectively, and therefore they have quite different substrate specificities from those of cathepsin G and α-chymotrypsin.

H–Ser–Pro–Val–Thr–Leu–Asp–Leu–Arg–Tyr–OH exhibited similar inhibitory activity to the corresponding methyl ester towards cathepsin G and α-chymotrypsin, supporting the previous conclusion that the Leu^{45}–Asp^{46} sequence of eglin c is a reactive site and important for the manifestation of the inhibitory activity.[12] It is of interest that although the above two peptides did not show inhibitory activity against leukocyte elastase, they inhibited porcine pancreatic elastase with K_i values of 2.7×10^{-4} and 3.0×10^{-4} M, respectively, suggesting differences in the structure of the active center between leukocyte elastase and pancreatic elastase.

The inhibitory activity of H–Thr–Asn–Val–Val–OH towards leukocyte elastase was decreased compared with that of the corresponding methyl ester. Both peptides exhibited weaker inhibitory activity towards pancreatic elastase than towards leukocyte elastase.

These results cast light on the enzymatic differences between leukocyte elastase and pancreatic elastase and suggest the feasibility of developing small-molecular inhibitors of leukocyte elastase for practical therapeutic use by modifying the methyl group.

Experimental

The melting points are uncorrected. Optical rotations were measured with an automatic polarimeter, model DIP-360 (Japan Spectroscopic Co.). Amino acid compositions of an acid hydrolysate (6 N HCl, 110 °C, 20 h) were determined with an amino acid analyzer, K-101 AS (Kyowa Seimitsu Co.). HPLC was conducted with a Waters M 600 instrument [columns: YMC-PACK A-312 ODS (6×150 mm) and YMC-PACK D-ODS-5 (20×250 mm)]. On TLC (Kieselgel G, Merck), Rf^1, Rf^2, Rf^3, Rf^4 and Rf^5 values refer to the systems of $CHCl_3$, MeOH and AcOH (90:8:2), $CHCl_3$, MeOH and H_2O (8:3:1, lower phase), *n*-BuOH, pyridine, AcOH and H_2O (4:1:1:2), *n*-BuOH, pyridine, AcOH and H_2O (1:1:1:1) and $CHCl_3$, respectively.

General Procedure for Synthesis of Boc-Amino Acid 6-Chloro-2-Pyridyl Esters An N^{α}-protected amino acid (8.5 mmol) and 6-chloro-2-hydroxypyridine (1.10 g, 8.5 mmol) were dissolved in DMF (30 ml) and the solution was cooled with ice-salt. DCC (2.10 g, 10.2 mmol) was added, and the reaction mixture was stirred at 4 °C overnight. After removal of dicyclohexylurea and the solvent, the residue was extracted with AcOEt. The extract was washed with 5% $NaHCO_3$ and water, dried over Na_2SO_4 and evaporated down *in vacuo* to give the title compound. Boc–Asp(OBzl)–OPyCl: yield 75.4%, oil, $[\alpha]_D^{27}$ −3.4° ($c=1.0$, benzene), Rf^1 0.81, Rf^5 0.17. Boc–Pro–OPyCl: yield 78.5%, oil, $[\alpha]_D^{27}$ −1.0° ($c=1.0$, benzene), Rf^5 0.38.

Boc–Arg(Mts)–Tyr–OBzl DPPA (1.4 ml, 5.2 mmol) and Et_3N (1.3 ml, 9.5 mmol) were added to a solution of Boc–Arg(Mts)–OH (1.98 g, 4.3 mmol) and H–Tyr–OBzl·Tos–OH (1.91 g, 4.3 mmol) in DMF (20 ml) under cooling with ice. The reaction mixture was stirred at 4 °C overnight. After removal of the solvent, the residue was extracted with AcOEt. The extract was washed with 5% Na_2CO_3, 10% citric acid and H_2O, dried over Na_2SO_4 and evaporated down. The crude material was purified by silica gel column (2.3×44 cm) chromatography to give crystals, yield 1.90 g (63.4%), mp 80—90 °C, $[\alpha]_D^{27}$ −8.5° ($c=1.0$, MeOH), Rf^1 0.6, Rf^2 0.91. *Anal.* Calcd for $C_{36}H_{47}N_5O_8S\cdot3/2H_2O$: C, 58.7; H, 6.85; N, 9.50. Found: C, 58.7; H, 6.67; N, 9.46.

Boc–Leu–Arg(Mts)–Tyr–OBzl Boc–Leu–OPyCl[11] (1.11 g, 3.2 mmol) and H–Arg(Mts)–Tyr–OBzl [prepared from Boc–Arg(Mts)–Tyr–OBzl (1.8 g, 2.5 mmol), TFA (2.0 ml, 27 mmol), anisole (0.59 ml, 5.4 mmol) and *m*-cresol (0.57 ml, 5.4 mmol) as usual] were dissolved in DMF (30 ml) containing Et_3N (0.38 ml, 2.5 mmol). The reaction mixture was stirred at room temperature overnight. After removal of the solvent, the residue was extracted with AcOEt. The extract was washed with 5% Na_2CO_3, 10% citric acid and H_2O, dried over Na_2SO_4 and evaporated down. Petroleum ether was added to the residue to afford crystals, which were collected by filtration, yield 2.03 g (99.9%), mp 51.5—65 °C, $[\alpha]_D^{27}$ −19.7° ($c=1.0$, MeOH), Rf^1 0.47. *Anal.* Calcd for $C_{42}H_{58}N_6O_9S\cdot1/2H_2O$: C, 60.0; H, 7.26; N, 10.2. Found: C, 60.1; H, 7.38; N, 10.3.

Boc–Asp(OBzl)–Leu–Arg(Mts)–Tyr–OBzl The title compound was prepared from Boc–Asp(OBzl)–OPyCl (0.95 g, 2.8 mmol) and H–Leu–Arg(Mts)–Tyr–OBzl [prepared from Boc–Leu–Arg(Mts)–Tyr–OBzl (1.81 g, 2.3 mmol) and TFA (1.8 ml, 23.0 mmol)]. The crude product was purified by silica gel column (2.5×28.7 cm) chromatography, yield 1.34 g (57.5%), mp 88.5—91 °C, $[\alpha]_D^{27}$ −26.4° ($c=1.0$, MeOH), Rf^1 0.67. *Anal.* Calcd for $C_{53}H_{69}N_7O_{12}S$: C, 61.4; H, 6.86; N, 9.64. Found: C, 61.7; H, 6.96; N, 9.44.

Boc–Leu–Asp(OBzl)–Leu–Arg(Mts)–Tyr–OBzl The title compound was prepared from Boc–Leu–OPyCl[11] (0.45 g, 1.3 mmol) and H–Asp(OBzl)–Leu–Arg(Mts)–Tyr–OBzl [prepared from Boc–Asp(OBzl)–Leu–Arg(Mts)–Tyr–OBzl (1.1 g, 1.1 mmol) and TFA (1.3 ml, 16.5 mmol)], yield

1.18 g (95.2%), mp 94.5—102.5 °C, $[\alpha]_D^{27}$ −29.0° (c=0.3, MeOH), Rf^1 0.61. *Anal.* Calcd for $C_{59}H_{80}N_8O_{13}S$: C, 61.7; H, 7.15; N, 9.92. Found: C, 61.4; H, 7.21; N, 9.74.

Boc–Thr–Leu–Asp(OBzl)–Leu–Arg(Mts)–Tyr–OBzl The title compound was prepared from Boc–Thr–ONSu (185 mg, 0.58 mmol) and H–Leu–Asp(OBzl)–Leu–Arg(Mts)–Tyr–OBzl [prepared from Boc–Leu–Asp(OBzl)–Leu–Arg(Mts)–Tyr–OBzl (549 mg, 0.486 mmol) and TFA (0.4 ml, 4.860 mmol)], yield 394 mg (65.9%), mp 114—121 °C, $[\alpha]_D^{27}$ −29.5° (c=0.5, MeOH), Rf^1 0.57, Rf^2 0.67. *Anal.* Calcd for $C_{63}H_{87}N_9O_{15}S$: C, 60.5; H, 7.14; N, 10.2. Found: C, 60.3; H, 7.07; N, 10.1.

Boc–Val–Thr–Leu–Asp(OBzl)–Leu–Arg(Mts)–Tyr–OBzl The title compound was prepared from Boc–Val–OPyCl[11] (136 mg, 0.465 mmol) and H–Thr–Leu–Asp(OBzl)–Leu–Arg(Mts)–Tyr–OBzl [prepared from Boc–Thr–Leu–Asp(OBzl)–Leu–Arg(Mts)–Tyr–OBzl (382 mg, 0.310 mmol) and TFA (0.3 ml, 3.1 mmol)], yield 213 mg (51.7%), mp 205—209 °C, $[\alpha]_D^{27}$ −21.5° (c=1.0, DMF), Rf^1 0.54. *Anal.* Calcd for $C_{68}H_{96}N_{10}O_{16}S \cdot 3/2H_2O$: C, 59.6; H, 7.44; N, 10.2. Found: C, 59.3; H, 7.22; N, 10.4.

Boc–Pro–Val–Thr–Leu–Asp(OBzl)–Leu–Arg(Mts)–Tyr–OBzl The title compound was prepared from Boc–Pro–OPyCl (55 mg, 0.16 mmol) and H–Val–Thr–Leu–Asp(OBzl)–Leu–Arg(Mts)–Tyr–OBzl [prepared from Boc–Val–Thr–Leu–Asp(OBzl)–Leu–Arg(Mts)–Tyr–OBzl (150 mg, 0.113 mmol) and TFA (0.17 ml, 2.26 mmol)], yield 27 mg (16.9%), mp 183—190 °C, $[\alpha]_D^{27}$ −24.0° (c=0.5, DMF), Rf^1 0.58, Rf^2 0.68. *Anal.* Calcd for $C_{73}H_{103}N_{11}O_{17}S$: C, 60.9; H, 7.23; N, 10.7. Found: C, 60.8; H, 7.32; N, 10.5.

Boc–Ser–Pro–Val–Thr–Leu–Asp(OBzl)–Leu–Arg(Mts)–Tyr–OBzl The title compound was prepared from Boc–Ser–N_3 [prepared from Boc–Ser–$NHNH_2$ (30 mg, 0.137 mmol) and isopentyl nitrite (0.019 ml, 0.137 mmol)] and H–Pro–Val–Thr–Leu–Asp(OBzl)–Leu–Arg(Mts)–Tyr–OBzl [prepared from Boc–Pro–Val–Thr–Leu–Asp(OBzl)–Leu–Arg(Mts)–Tyr–OBzl (163 mg, 0.114 mmol) and TFA (0.17 ml, 2.28 mmol)], yield 115 mg (54.0%), mp 130—139 °C, $[\alpha]_D^{27}$ −25.3° (c=1.0, DMF), Rf^1 0.45, Rf^2 0.67. *Anal.* Calcd for $C_{76}H_{110}N_{12}O_{19}S \cdot H_2O$: C, 59.0; H, 7.32; N, 10.9. Found: C, 58.8; H, 7.27; N, 10.8.

H–Ser–Pro–Val–Thr–Leu–Asp–Leu–Arg–Tyr–OH The protected nonapeptide (50 mg, 0.026 mmol) was treated with HF (10 ml) in the presence of thioanisole (0.30 ml) and *m*-cresol (0.1 ml) in an ice-bath for 90 min. After removal of HF, dry ether was added to the residue to afford crystals, which were collected by filtration and dissolved in H_2O. The pH of the solution was adjusted to 8 with 1 M NH_4OH and the solution was kept at 4 °C for 30 min and applied to a column of Sephadex G-25 (2.2 × 58.7 cm), which was equilibrated and eluted with 3% AcOH. The fractions (3 g each, tube Nos. 41—49) were combined and the solvent was removed by lyophilization to give a fluffy powder. The crude product was purified by preparative HPLC, yield 23 mg (83%), $[\alpha]_D^{27}$ −88.9° (c=0.1, 5% AcOH). Amino acid ratios in an acid hydrolysate: Ser (1) 0.88; Pro (1) 1.20; Val (1) 0.97; Thr (1) 0.89; Leu (2) 2.00; Asp (1) 0.84; Arg (1) 0.70; Tyr (1) 0.92 (average recovery 74.3%).

Boc–Val–Val–OBzl The title compound was prepared from Boc–Val–OPyCl[11] (1.50 g, 4.6 mmol) and H–Val–OBzl·Tos–OH (1.16 g, 3.0 mmol), yield 1.80 g (97.0%), mp 51—55 °C, $[\alpha]_D^{27}$ −46.5° (c=1.2, MeOH), Rf^1 0.77. *Anal.* Calcd for $C_{22}H_{34}N_2O_5$: C, 65.0; H, 8.45; N, 6.89. Found: C, 65.2; H, 8.67; N, 6.78. [*p*-Nitrophenyl ester method: yield 76%, oily material, $[\alpha]_D^{27}$ −44.0° (c=1.0, MeOH), Rf^1 0.77].

Boc–Asn–Val–Val–OBzl The title compound was prepared from Boc–Asn–ONp and H–Val–Val–OBzl [prepared from Boc–Val–Val–OBzl (1.1 g, 2.7 mmol) and 7.2 N HCl–dioxane (2.0 ml, 13.7 mmol)], yield 0.70 g (48.9%), mp 193—197 °C, $[\alpha]_D^{27}$ −56.3° (c=1.0, MeOH), Rf^1 0.69. *Anal.* Calcd for $C_{26}H_{40}N_4O_7$: C, 60.0; H, 7.76; N, 10.8. Found: C, 59.9; H, 7.69; N, 10.7.

Z–Thr–Asn–Val–Val–OBzl DPPA (0.48 ml, 1.7 mmol) and Et_3N (0.45 ml, 3.2 mmol) were added to a solution of Z–Thr–OH (0.36 g, 1.4 mmol) and H–Asn–Val–Val–OBzl [prepared from Boc–Asn–Val–Val–OBzl (0.50 g, 1.0 mmol) and 7.2 N HCl–dioxane (0.67 ml, 4.8 mmol)] in DMF (7 ml) under cooling with ice. The reaction mixture was stirred at 4 °C overnight. After removal of the solvent, AcOEt and H_2O were added to the residue to afford crystals, which were collected by filtration, yield 0.47 g (75.4%), mp 230—232 °C, $[\alpha]_D^{27}$ −26.0° (c=1.0, DMF), Rf^1 0.78. *Anal.* Calcd for $C_{33}H_{45}N_5O_9 \cdot 1/2H_2O$: C, 59.6; H, 6.99; N, 10.5. Found: C, 59.7; H, 6.95; N, 10.8.

H–Thr–Asn–Val–Val–OH Z–Thr–Asn–Val–Val–OBzl (0.10 g, 0.15 mmol) in DMF (3 ml) was hydrogenated over Pd catalyst. After removal of Pd and the solvent, the residue was dissolved in H_2O and lyophilized to give a fluffy powder, yield 56 mg (85.7%), $[\alpha]_D^{27}$ −50.0° (c=0.1, MeOH), Rf^3 0.47, Rf^4 0.87. Amino acid ratios in an acid hydrolysate: Thr (1) 0.90; Asp (1) 1.00; Val (2) 1.78; NH_3 (1) 1.20 (average recovery 75.3%).

Assay Procedure Human leukocyte elastase[13] and cathepsin G[14] were prepared in our laboratory according to the procedure described previously. α-Chymotrypsin was purchased from Miles Co., Ltd., Elkhart. Porcine pancreatic elastase was purchased from Sigma Chemical Co., St. Louis. Enzymatic activities of leukocyte elastase, porcine pancreatic elastase, cathepsin G and α-chymotrypsin were assayed by the method described previously using Suc–Ala–Tyr–Leu–Val–*p*NA[15] for leukocyte elastase, Suc–Ala–Ala–Ala–*p*NA for porcine pancreatic elastase and Suc–Ile–Pro–Phe–*p*NA[16] for cathepsin G and α-chymotrypsin. For determination of the effects of synthetic peptides on the enzymes, the enzymatic activity towards each substrate was assayed in the presence and in the absence of the peptide to be examined.

Acknowledgement This work was supported in part by a grant from The Science Research Promotion Fund of the Japan Private School Promotion Foundation.

References and Note

1) Part XXIX: K. Nakabayashi, S. Tsuboi, T. Fujimoto, Y. Okada, Y. Nagamatsu and J. Yamamoto, *Chem. Pharm. Bull.*, **38**, 2369 (1990).
2) The amino acids, peptides and their derivatives mentioned in this paper are of the L configuration except in the case of glycine. The abbreviations used are those recommended by the IUPAC-IUB Commission on Biochemical Nomenclature: *Biochemistry*, **5**, 3485 (1966); **6**, 362 (1967); **11**, 1726 (1972). Other abbreviations used are: Z, benzyloxycarbonyl; Boc, *tert*-butyloxycarbonyl; Suc, succinyl; OBzl, benzyl ester; ONp, *p*-nitrophenyl ester; ONSu, *N*-hydroxysuccinimide ester; OPyCl, 6-chloro-2-pyridyl ester; *p*NA, *p*-nitroanilide; DCC, *N,N'*-dicyclohexylcarbodiimide; DPPA, diphenylphosphorylazide; Et_3N, triethylamine; AcOEt, ethyl acetate; TFA, trifluoroacetic acid; DMF, dimethylformamide; AcOH, acetic acid; Tos–OH, *p*-toluenesulfonic acid.
3) U. Seemüller, M. Meier, K. Ohlsson, H. P. Mueller and H. Fritz, *Hoppe-Seyler's Z. Physiol. Chem.*, **358**, 1105 (1977).
4) U. Seemüller, M. Eulitz, H. Fritz and A. Strobl, *Hoppe-Seyler's Z. Physiol. Chem.*, **361**, 1841 (1980).
5) R. M. Senior, H. Terner, C. Kuhn, K. Ohlsson, B. C. Starcher and J. A. Pierce, *Am. Rev. Respir. Dis.*, **116**, 177 (1972).
6) A. Janoff, *Ann. Rev. Med.*, **23**, 177 (1972).
7) Y. Okada, S. Tsuboi, Y. Tsuda, K. Nakabayashi, Y. Nagamatsu and J. Yamamoto, *Biochem. Biophys. Res. Commun.*, **161**, 272 (1987).
8) T. Shioiri, K. Ninomiya and S. Yamada, *J. Am. Chem. Soc.*, **97**, 7174 (1975).
9) L. Juliano, M. A. Juliano, A. D. Miranda, S. Tsuboi and Y. Okada, *Chem. Pharm. Bull.*, **35**, 2550 (1987).
10) N. Honzle and J. Rudinger, *Coll. Chech. Chem. Commun.*, **26**, 2333 (1961).
11) S. Tsuboi and Y. Okada, *Chem. Pharm. Bull.*, **35**, 3880 (1987).
12) W. Bode, E. Papamokos, D. Musil, U. Seemüller and H. Fritz, *EMBO J.*, **5**, 813 (1986).
13) Y. Nagamatsu, U. Okamoto, Y. Tsuda and Y. Okada, *Thromb. Haemostas.*, **51**, 243 (1984).
14) Y. Nagamatsu, S. Tsuboi, K. Nakabayashi, Y. Tsuda, Y. Okada and J. Yamamoto, *Nippon Kessen Shiketsu Gakkaishi*, **1**, 203 (1990).
15) Y. Okada, Y. Tsuda, A. Hirata, Y. Nagamatsu and U. Okamoto, *Chem. Pharm. Bull.*, **30**, 4060 (1982).
16) Y. Okada, Y. Tsuda, N. Teno, Y. Nagamatsu and U. Okamoto, "Peptide Chemistry 1986," ed. by T. Miyazawa, Protein Research Foundation, Osaka, 1987, p. 261.

An Improved Method for the Synthesis of Arylacetonitriles from 3-Aryl-2-hydroxyiminopropionic Acids Using 1,1′-Oxalyldiimidazole

Tokujiro KITAGAWA,* Megumi KAWAGUCHI, and Misuzu IKIUCHI

Faculty of Pharmaceutical Sciences, Kobe Gakuin University, Ikawadani, Nishi-ku, Kobe 673, Japan. *Received July 2, 1990*

1,1′-Oxalyldiimidazole (ODI, 3) is a useful reagent for the degradation of 3-aryl-2-hydroxyiminopropionic acids (2) into the corresponding arylacetonitriles (1) under essentially neutral conditions.

Keywords 1,1′-oxalyldiimidazole; arylacetonitrile; 3-aryl-2-hydroxyiminopropionic acid; dehydration; decarboxylation

Arylacetonitriles (**1**) are very valuable intermediates for the preparations of 2-arylethylamines,[1] arylacetic acids,[2] acrylonitriles,[3] and heterocyclic compounds.[4] These compounds (**1**) have been obtained by (i) the dehydration of amides[5] or oximes[6] and the dehydrosulfurization of thioamides,[7] (ii) the reaction of metal cyanide with halogen compounds[8] or of arylzinc chloride with bromoacetonitrile,[d] (iii) the reduction of 1-cyanoalcohols[9] or thioethers,[10] and (iv) the reaction of arylaldehydes with methyl thiocyanate.[11] Another important reaction for synthesizing arylacetonitriles (**1**) is the decarboxylation and dehydration of 3-aryl-2-hydroxyiminopropionic acids (**2**) using acetic anhydride.[2a] Unfortunately, in these reactions, we have met with great difficulty in separating the desired arylacetonitriles (**1**) from the reaction mixture containing acetic anhydride, especially, in case of that **1** resembles acetic anhydride or aqueous acetic acid very closely in boiling point. For the synthesis of 2-furylacetonitrile (**1h**) from the reaction of 3-(2-furyl)-2-hydroxyiminopropionic acid (**2h**) with acetic anhydride, the previous method required a laborious procedure which involved (i) hydrolysis of unreacted acetic anhydride, and (ii) extraction of the product (**1h**) from the steam distillate.[12] In a related study, we have already demonstrated[13] that carbaldehyde oximes react easily with 1,1′-oxalyldiimidazole[14] (ODI, **3**) to give the corresponding nitriles in good yields.

In this paper, we wish to describe an improved method whereby **2** can be converted directly into arylacetonitriles (**1**) using ODI (**3**). First, we were able to prepare phenylacetonitrile (**1a**) in 85% yield directly from the reaction of 3-phenyl-2-hydroxyiminopropionic acid (**2a**) with ODI (**3**) at 70°C for 1 h in benzene with accompanying effervescence. The general applicability of this method was tested by using other 3-aryl-2-hydroxyiminopropionic acids (**2b—l**). The transformations of 3-(4-substituted phenyl)-, 3-(3,4-disubstituted phenyl)-, 3-(3,4,5-trisubstituted phenyl)-, and 3-(1-naphthyl)-2-hydroxyiminopropionic acids (**2b—g**) into the corresponding acetonitriles (**1b—g**) were also accomplished in acceptable yields as shown in Table I. Moreover, we found that the heteroaromatic compound 3-(2-furyl)-2-hydroxyiminopropionic acid (**2h**) readily reacted with ODI (**3**) to give 2-furylacetonitrile (**1h**) in 83% yield. A similar result was observed with 3-(3-indolyl)-2-hydroxyiminopropionic acid (**2l**), which was converted to 3-indolylacetonitrile (**1l**) in 84% yield. These results, which demonstrate the effectiveness of this method, are summarized in Table I.

Judging from the yields of the substituted acetonitriles (**2a—l**) in Table I, it is clear that ODI (**3**), in place of acetic anhydride, is capable of achieving arylacetonitrile forma-

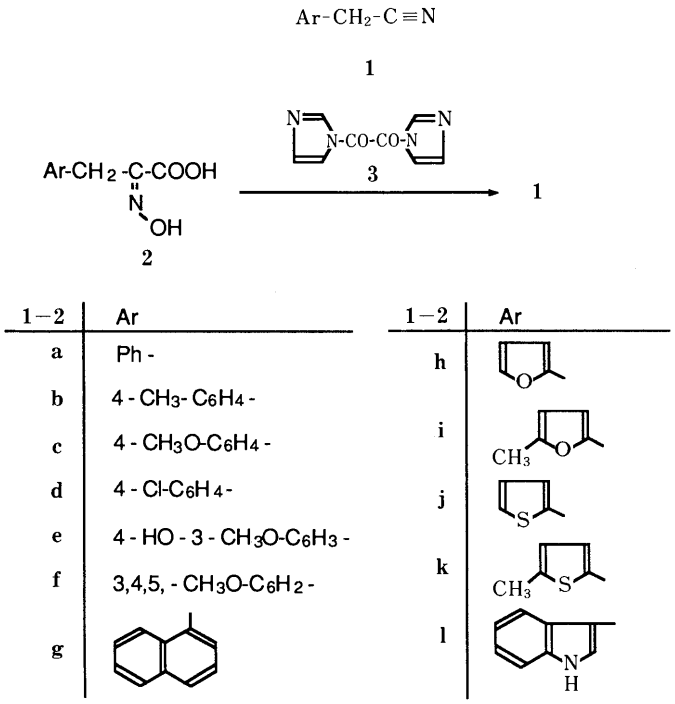

Chart 1

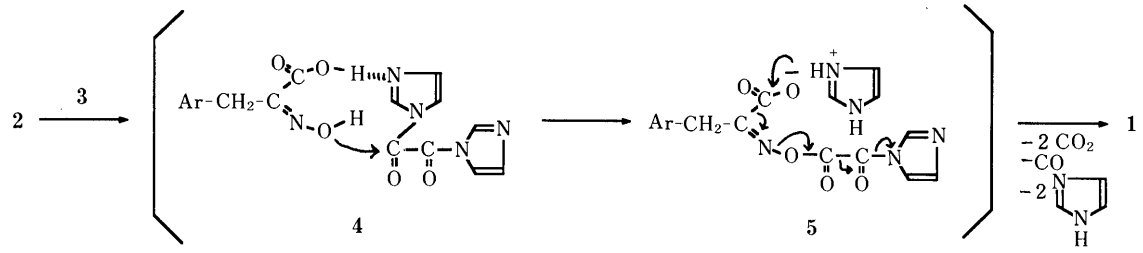

Chart 2

TABLE I. Substituted Acetonitriles (2) Prepared

Product	Yield[a] (%)	bp (°C)/Torr[b] or [mp (°C)][c] Found	Reported	IR (neat)[d] ν_{CN} (cm^{-1})	^{1}H-NMR ($CDCl_3$/TMS)[e] δ, J (Hz)
1a	85	80—82/3	98—100/9[1d]	2254	3.73 (s, 2H, $-CH_2-$), 7.33 (s, $5H_{arom.}$)
1b	95	85—87/3	107—109/9[1d]	2254	2.31 (s, 3H, $-CH_3$), 3.65 (s, 2H, $-CH_2-$), 7.17 (s, $4H_{arom.}$)
1c	90	105—107/2	74—76/0.2[1d]	2252	3.68 (s, 2H, $-CH_2-$), 3.80 (s, 3H, $-CH_3$), 6.89 (d, 2H, $J=9$, Ph-2 and 6H), 7.23 (d, 2H, $J=9$, Ph-3 and 5H)
1d	93	117—119/5	140/13[8e]	2252	3.72 (s, 2H, $-CH_2-$), 7.34 (s, $4H_{arom.}$)
1e	82	140—143/0.2	135—140/0.05[1c]	2252	3.68 (s, 2H, $-CH_2-$), 3.92 (s, 3H, $-CH_3$), 5.63 (s, 1H, –OH), 6.7—6.9 (m, $3H_{arom.}$)
1f	88	[87—88][f]	[88][21]	2244	3.69 (s, 2H, $-CH_2-$), 3.85 (s, 9H, $-CH_3\times3$), 6.52 (s, $2H_{arom.}$)
1g	90	105—107/0.2	183—187/15[22]	2252	4.10 (s, 2H, $-CH_2-$), 7.3—8.0 (m, $7H_{arom.}$)
1h	83	88—90/30	64—65/9[12]	2254	3.80 (s, 2H, $-CH_2-$), 6.2—6.5 (m, 2H, furan-3 and 4H), 7.3—7.5 (m, 1H, furan-5H)
1i	94	91—93/15	82—85/12[23]	2256	2.32 (s, 3H, $-CH_3$), 3.75 (s, 2H, $-CH_2-$), 5.97 (d, 1H, $J=3$, furan-4H), 6.23 (d, 1H, $J=3$, furan-3H)
1j	89	108—110/15	89—100/9[1d]	2254	3.88 (s, 2H, $-CH_2-$), 6.8—7.4 (m, $3H_{arom.}$)
1k	91	110—112/20		2252	2.45 (s, 3H, $-CH_3$), 3.80 (s, 2H, $-CH_2-$), 6.63 (d, 1H, $J=3$, thiophene-4H), 6.82 (d, 1H, $J=3$, thiophene-3H)
1l	84	125—128/0.03	156—158/0.2[24]	2252	3.81 (s, 2H, $-CH_2-$), 7.0—8.5 (m, $6H_{arom.}$)

a) Yield of the isolated product **2** based on **1**. *b*) Boiling points refer to the oven temperature of a Kugelrohr apparatus. *c*) Uncorrected, measured with a Yanagimoto melting point apparatus. *d*) Recorded on a Hitachi 215 spectrophotometer. *e*) Recorded on a Hitachi R-600 spectrometer (60 MHz). ^{1}H-NMR chemical shifts are reported in ppm (δ) downfield from tetramethylsilane (TMS) in $CDCl_3$ and coupling constants (J) are given in hertz. The following abbreviations are used: s, singlet; d, doublet, and m, multiplet. *f*) Recrystallized from EtOH–water.

tion through degradation of the 3-aryl- or 3-heteroaryl-2-hydroxyiminopropionic acids (**2a—l**).

As shown in Chart 2, the reaction probably proceeds *via* the formation of an intermediate (**5**) between **2** and **3**, and subsequently concerted elimination of CO_2, CO, and imidazole take place under heating to afford the corresponding arylacetonitriles (**1**).

In summary, the advantages of our method over other procedures described previously include short reaction times under essentially neutral conditions, greater ease of product isolation, higher yield, and fewer synthetic steps.

Experimental

Measurements of the physical and spectral properties were performed as indicated in the footnotes of Table I. 1,1′-Oxalyldiimidazole (ODI, **3**) was prepared as previously described.[14] Distilled benzene was subjected to successive drying over 4 Å molecular sieves. 3-Aryl-2-hydroxyiminopropionic acids (**2a—l**)[15] were prepared as previously described; **2a**,[16] **2c**,[17] **2d**,[16] **2e**,[2a] **2f**,[18] **2h**,[12] **2i**,[2b] **2j**,[2b] and **2l**.[19]

3-(1-Naphthyl)-2-hydroxyiminopropionic Acid (2g) This compound (**2g**) was prepared according to a published procedure.[2a] Hydroxylamine hydrochloride (4.3 g, 62 mmol) in water (5 ml) was allowed to react with sodium ethoxide [prepared from sodium (1.6 g, 69 mgatom) and anhydrous EtOH (40 ml)]. After removal of inorganic material by filtration, the filtrate containing free hydroxylamine was added to 1-naphthylthiopyruvic acid[20] (4.6 g, 20 mmol) and the mixture was refluxed for 1 h. After removal of the solvent under reduced pressure, the residue was dissolved in 5% NaOH (100 ml). The aqueous phase was filtered through a sintered glass filter and the filtrate was cooled to −15 °C, then acidified with 10% HCl (90 ml). The precipitate was washed with water and dried *in vacuo*; the yield was 3.5 g (90%); crystals (benzene–AcOEt), mp 169—171 °C. *Anal.* Calcd for $C_{13}H_{11}NO_3$: C, 68.11; H, 4.84; N, 6.11. Found: C, 68.38; H, 4.90; N, 6.19. IR(KBr) ν: 1707 (CO). ^{1}H-NMR (DMSO-d_6/TMS) δ: 4.27 (s, 2H, $-CH_2-$), 7.0—8.4 (m, $7H_{arom.}$).

***p*-Tolyl-2-hydroxyiminopropionic Acid (2b)** Treatment of *p*-tolylthiopyruvic acid[21] (3.9 g, 20 mmol) with hydroxylamine [prepared from hydroxylamine hydrochloride (4.3 g, 62 mmol) and Na metal (1.6 g, 69 mgatom)] as described for the preparation of **2g** gave **2b**; the yield was 3.6 g (93%); crystals (benzene–AcOEt), mp 185—186 °C. *Anal.* Calcd for $C_{10}H_{11}NO_3$: C, 62.16; H, 5.79; N, 7.26. Found: C, 61.98; H, 5.65; N, 7.24. IR(KBr) ν: 1695 (CO). ^{1}H-NMR (DMSO-d_6)/TMS) δ: 2.23 (s, 3H, $-CH_3$), 3.76 (s, 2H, $-CH_2-$), 7.06 (s, $4H_{arom.}$).

3-(5-Methyl-2-thienyl)-2-hydroxyiminopropionic Acid (2k) Treatment of 3-(5-methyl-2-thienyl)thiopyruvic acid[2b] (4.0 g, 20 mmol) with hydroxylamine [prepared from hydroxylamine hydrochloride (4.3 g, 62 mmol) and Na metal (1.6 g, 69 mgatom)] as described for the preparation of **2g** gave **2k**; the yield was 3.4 g (85%); crystals (benzene), mp 166—167 °C. *Anal.* Calcd for $C_8H_9NO_3S$: C, 48.21; H, 4.56; N, 7.03. Found: C, 48.21; H, 4.53; N, 7.12. IR(KBr) ν: 1696 (CO). ^{1}H-NMR (DMSO-d_6/TMS) δ: 2.34 (s, 3H, $-CH_3$), 3.88 (s, 2H, $-CH_2-$), 6.60 (s, $2H_{arom.}$).

Arylacetonitriles (1) General Procedure: ODI (**3**) (3.8 g, 20 mmol) was added to a solution of the appropriate 3-substituted-2-hydroxyiminopropionic acid (**2**) (20 mmol) in benzene (50 ml). The mixture was stirred at room temperature for 15 min, and then heated at 68—70 °C for 1 h. After cooling to room temperature, the resultant mixture was poured into ice water (30 ml) and the organic layer was extracted with 50 ml of benzene in several portions. The combined extracts were washed with 1% $NaHCO_3$ (15 ml), 1% HCl (15 ml), and water (15 ml), and then dried over anhydrous sodium sulfate. The organic layer was evaporated under reduced pressure to give the crude acetonitrile (**1**), which was further purified by distillation or recrystallization.

(5-Methyl-2-thienyl)acetonitrile (1k) Treatment of 3-(5-methyl-2-thienyl)-2-hydroxyiminopropionic acid (**2k**) (4.0 g, 20 mmol) with ODI (**3**) (3.8 g, 20 mmol) as described in the general procedure gave **1k**; the yield was 2.7 g (98%). *Anal.* Calcd for C_7H_7NS: C, 61.31; H, 5.15; N, 10.21. Found: C, 61.02; H, 5.23; N, 10.19. Boiling point, infrared, and nuclear magnetic resonance data for **1a—l** are shown in Table I.

References and Notes

1) *a*) P. L. Julian and B. M. Sturgis, *J. Am. Chem. Soc.*, **57**, 1126 (1935); *b*) W. Herz, *ibid.*, **75**, 483 (1953); *c*) M. A. Schwartz, M. Zoda, B. Vishnuvajjala, and I. Mami, *J. Org. Chem.*, **41**, 2502 (1976); *d*) T. Frejd and T. Klingstedt, *Synthesis*, **1987**, 40.
2) *a*) H. E. Fisher and H. Hibbert, *J. Am. Chem. Soc.*, **69**, 1208 (1947); *b*) B. F. Crowe and F. F. Nord, *J. Org. Chem.*, **15**, 81 (1950).
3) D. Shapiro, *J. Org. Chem.*, **16**, 1247 (1951).
4) I. Trummer, E. Ziegler, and O. S. Wolfbeis, *Synthesis*, **1981**, 225.
5) *a*) A. V. R. Rao, M. N. Rao, K. Garyali, and P. Kumar, *Chem. Ind.* (London), **1984**, 270; *b*) T. Kamijo, H. Harada, and K. Iizuka, *Chem. Pharm. Bull.*, **32**, 2560 (1984); *c*) A. Saednya, *Synthesis*, **1985**, 184.
6) *a*) P. Molina, M. Alajarin, and M. J. Vilaplana, *Synthesis*, **1982**, 1016; *b*) M. E. Jung and Z. Long-Mei, *Tetrahedron Lett.*, **24**, 4533 (1983); *c*) K. Mai and G. Patil, *Synthesis*, **1986**, 1037; *d*) M. M. Runde, E. W. Scott, and J. R. Johnson, *J. Am. Chem. Soc.*, **52**, 1284 (1930).
7) *a*) M.-I. Lim, W.-Y. Ren, and R. S. Klein, *J. Org. Chem.*, **47**, 4594 (1982); *b*) H. Suzuki, H. Tani, and S. Takeuchi, *Bull. Chem. Soc. Jpn.*, **58**, 2421 (1985); *c*) Y. Funakoshi, T. Takido, and K. Itabashi, *Synth. Commun.*, **15**, 1299 (1985); *d*) N. X. Hu, Y. Aso, T. Otsubo, and F. Ogura, *Bull. Chem. Soc. Jpn.*, **59**, 879 (1986); *e*) S. Kim and K. Y. Yi, *Tetrahedron Lett.*, **27**, 1925 (1986); *f*) S. Kim and K. Y.

Yi, *J. Org. Chem.*, **51**, 2613 (1986).
8) *a*) N. Furukawa, K. Kishimoto, S. Ogawa, T. Kawai, H. Fujihara, and S. Oae, *Tetrahedron Lett.*, **22**, 4409 (1981); *b*) K. Sukata, *J. Org. Chem.*, **50**, 4388 (1985); *c*) A. Kalir and R. Mualem, *Synthesis*, **1987**, 514; *d*) S. Harusawa, R. Yoneda, Y. Omori, and T. Kurihara, *Tetrahedron Lett.*, **28**, 4189 (1987); *e*) R. C. Elderfield and K. L. Burgess, *J. Am. Chem. Soc.*, **82**, 1975 (1960).
9) I. Furukawa, B. Zhou, and S. Hashimoto, *Nippon Kagaku Kaishi*, **1984**, 1208 [*Chem. Abstr.*, **101**, 191216*m* (1984)].
10) M. T. Reetz and H. Müller-Stark, *Tetrahedron Lett.*, **25**, 3301 (1984).
11) *a*) M. Kurauchi, T. Imamoto, and M. Yokoyama, *Tetrahedron Lett.*, **22**, 4985 (1981); *b*) M. Yokoyama, H. Ohteki, M. Kurauchi, K. Hoshi, E. Yanagisawa, A. Suzuki, and T. Imamoto, *J. Chem. Soc., Perkin Trans. 1*, **1984**, 2635.
12) J. Plucker, III and E. D. Amstutz, *J. Am. Chem. Soc.*, **62**, 1512 (1940).
13) T. Kitagawa, H. Sasaki, and N. Ono, *Chem. Pharm. Bull.*, **33**, 4014 (1985).
14) W. Walter and M. Radke, *Justus Liebigs Ann. Chem.*, **1979**, 1756.
15) The 3-aryl-2-hydroxyiminopropionic acids (**2**) used in this experiment are mixtures of the (*E*)- and (*Z*)-isomers.
16) N. Campbell and J. E. McKail, *J. Chem. Soc.*, **1948**, 1251.
17) R. Gaudry and R. A. Mclvor, *Can. J. Chem.*, **29**, 427 (1951).
18) L. Farkas, J. Varady, and A. Gottsegen, *Chem. Ber.*, **96**, 1865 (1963).
19) K. N. F. Shaw, A. McMillan, A. G. Gudmundson, and M. D. Armstrong, *J. Org. Chem.*, **23**, 1171 (1958).
20) S. N. Baranov and N. E. Tarnavskaya, *Ukrain. Khim. Zhur.*, **26**, 626 (1960) [*Chem. Abstr.*, **55**, 12416*c* (1961)].
21) T. Ito, T. Ishii, and M. Nishio, *Agric. Biol. Chem.*, **29**, 728 (1965).
22) M. Lamant and M. L. Moine, *Bull. Soc. Chim. Fr.*, **1961**, 1144 [*Chem. Abstr.*, **59**, 8667*h* (1963)].
23) E. L. Eliel and P. E. Peckham, *J. Am. Chem. Soc.*, **72**, 1209 (1950).
24) E. A. Markaryan and A. E. Kalaidzhyan, *Sin. Geterotsikl. Soedin., Akad. Nauk Arm. SSR, Inst. Tonkoi Org. Khim.*, No. 7, 33 (1966) [*Chem. Abstr.*, **68**, 114343*y* (1966)].

Optical Resolution of (±)-2-[4-(2-Oxocyclohexylidenemethyl)phenyl]propionic Acid

Shunji NARUTO[a] and Atsusuke TERADA*,[b]

New Lead Research Laboratories,[a] Medicinal Chemistry Research Laboratories[b], Sankyo Co., Ltd., 2–58, Hiromachi 1-chome, Shinagawa-ku, Tokyo 140, Japan. *Received July 2, 1990*

The title compound showed potent anti-inflammatory and analgesic activities. For the determination of pharmacological activity differences between the optical isomers, we resolved the title compound *via* diastereomeric separation of the (−)-phenylethyl amide derivatives and followed by amide bond cleavage with N_2O_4. The absolute configurations of the enantiomers were determined by comparison of the optical rotatory dispersion and circular dichroism spectra with those of known optically active 2-phenylpropionic acids.

Keywords anti-inflammatory; analgesic; optical rotatory dispersion; circular dichroism; optical resolution

Previously, we reported the synthesis of (±)-2-[4-(2-oxocyclopentylmethyl)phenylpropionic acid (**1**) and (±)-2-[4-(2-oxocyclohexylidenemethyl)phenyl]propionic acid (**2**), which has good anti-inflammatory and analgesic activities.[1] Among 2-arylpropionic acid derivatives having anti-inflammatory activity, considerable differences of pharmacological activities between their enantiomers are often observed.[2] Thus, it is very important to synthesize the optically active compounds in order to investigate the pharmacological activities and metabolic pathway. Compound **1**, which is on the market, has already been optically resolved and its absolute configuration determined.[3]

In this paper, we describe the optical resolution and determination of the absolute configurations of the enantiomers of **2**. In order to facilitate the separation of enantiomers, we tried to synthesize diastereomers of 1-phenylethylamide derivatives of **2** for optical resolution. Condensation of **2** with (−)-(1*S*)-1-phenylethylamine was carried out in the presence of triphenylphosphine and 2,2′-dipyridyl disulfide in dichloromethane at room temperature. High-pressure liquid chromatography (HPLC) of the reaction products showed two peaks due to two kinds of amides.

These were separated by preparative medium-pressure liquid chromatography (MPLC) (Si-60 Lobar column) to afford (−)-*N*-[(1*S*)-1-phenylmethyl]-(2*R*)-[4-(2-oxocyclohexylidenemethyl)phenyl]propionamide (**3**) ($[\alpha]_D^{20}$ −47.7°, mp 130—131 °C) and (−)-*N*-[(1*S*)-1-phenylmethyl]-(2*S*)-[4-(2-oxocyclohexylidenemethyl)phenyl]propionamide (**4**) ($[\alpha]_D^{20}$ −40.9°, mp 129—130 °C) as crystals. The structure of the amides, **3** and **4**, were assigned on the basis of the following data and elemental analysis. The infrared (IR) spectra of **3** and **4** showed an amide band at 1650 and 1635 cm^{-1} and a carbonyl absorption at 1680 and 1665 cm^{-1}, respectively. The nuclear magnetic resonance (NMR) spectrum of **3** exhibited two methyl proton peaks at 1.34 (doublet) and 1.48 ppm (doublet) and two methine proton peaks at 3.53 (quartet) and 5.09 ppm (quartet). Compound **4** had the corresponding methyl proton peaks at 1.36 and 1.50 ppm and methine proton peaks at 3.55 and 5.10 ppm. According to the literature,[4] the less polar (−)-(1*S*)-phenylethylamide of a 2-arylpropionic acid generally has *R*-configuration at the 2-position of propionic acid and the more polar amide has *S*-configuration. Consequently, the less polar amide **3** may have *R*-configuration and the more polar **4** may have *S*-configuration.

Hydrolysis of **3** with concentrated HCl and AcOH af-

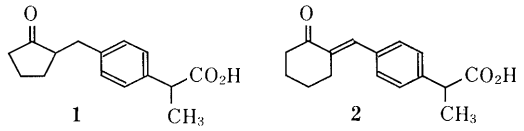

Chart 1

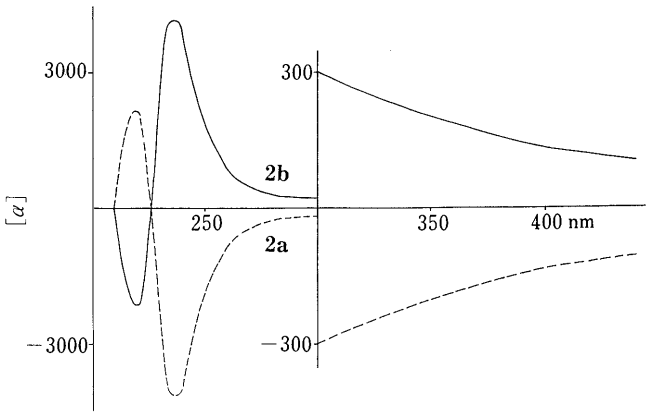

Fig. 1. ORD Spectra of **2a** and **2b**

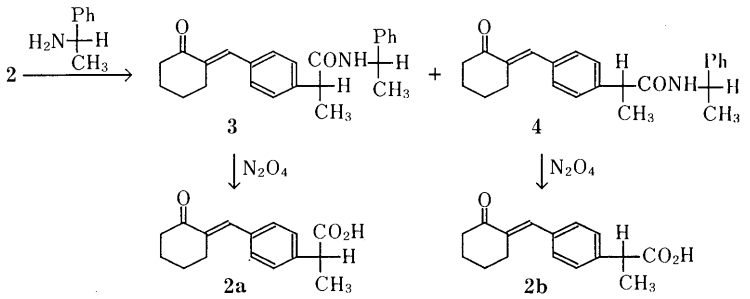

Chart 2

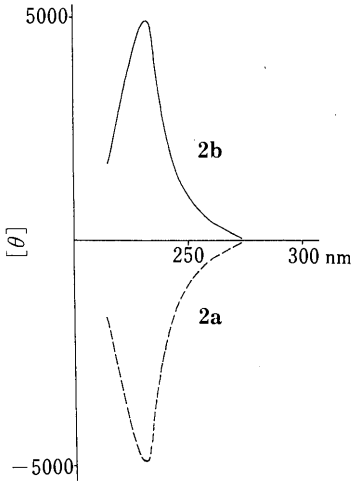

Fig. 2. CD Spectra of **2a** and **2b**

forded partially racemized compound **2a**, because the benzylic methine proton has a relatively high pK_a value. Therefore, cleavage of the amide bond of **3** and **4** was performed by diazotization with N_2O_4 followed by thermal decomposition in CCl_4[5] to afford the corresponding (−)-(1*R*)-2-[4-(2-oxocyclohexylidenemethyl)phenyl]propionic acid (**2a**) ($[\alpha]_D^{20}$ −51.4°, mp 101—103 °C) and (+)-(1*S*)-2-[4-(2-oxocyclohexylidenemethyl)phenyl]propionic acid (**2b**) ($[\alpha]_D^{20}$ 49.5°, mp 101—103 °C).

Optical rotatory dispersion (ORD) and circular dichroism (CD) spectra of **2a** and **2b** are shown in Figs. 1 and 2. As observed in the ORD spectra, **2a** showed a negative Cotton effect ([α] (nm): −4300 (238))[6] and **2b** displayed a positive Cotton effect ([α] (nm): 4300 (238)). The CD spectra of **2a** and **2b** showed a negative peak at 231 nm and positive peak at 231 nm, respectively.

From these results, the absolute configurations of the 2-position of the phenylpropionic acid moiety in **2a** and **2b** were determined to be *R* and *S*, respectively, by comparison with the spectra of (2*R*)- and (2*S*)-2-phenylpropionic acid.[7]

Thus, we obtained the optically pure compounds and determined the absolute configuration of both enantiomers. These compounds are currently being tested for biological activity and metabolic behavior, and the results will be reported elsewhere.

Experimental

Melting points were determined with a Büchi melting point apparatus and are uncorrected. IR spectra were determined on a JASCO IRA-2 grating IR spectrometer and ^{1}H-NMR spectra were measured with a Varian EM-390 or T-60 machine. HPLC was performed on a Waters ALC-401 machine with a μPorasil colum for analysis and a prep μPorasil (3/8 in. × 1 foot) or a Lobar column (Si-60, Merck Co., Ltd.) for preparation. Optical rotations were measured on a Perkin-Elmer 241 spectrometer and ORD and CD spectra were recorded on a JASCO J-20 spectrometer. All organic extracts were dried over anhydrous sodium sulfate.

(−)-*N*-[(1*S*)-1-Phenylmethyl]-(2*R*)-[4-(2-oxocyclohexylidenemethyl)-phenyl]propionamide (3) and (−)-*N*-[(1*S*)-1-Phenylmethyl]-(2*S*)-[4-(2-oxocyclohexylidenemethyl)phenyl]propionamide (4) A dichloromethane (10 ml) solution of 1.29 g of **2** was mixed with 1.1 g of 2,2′-dipyridyl disulfide, 1.31 g of triphenylphosphine and 0.6 g (−)-(1*S*)-1-phenylethylamine. The reaction mixture was kept at 0 °C for 30 min and then concentrated under reduced pressure. The residue was chromatographed on silica gel (eluted with hexane–ethyl acetate (7:3)). The amide was further purified on a Si-60 Lobar column to give 0.8 g of **3** and 0.75 g of **4**.

3: mp 130—131 °C, $[\alpha]_D^{20}$ −47.7° (*c*=0.2% EtOH). IR (Nujol): 3350, 1680, 1650 cm^{-1}. *Anal.* Calcd for $C_{24}H_{29}NO_2$: C, 79.74; H, 7.53; N, 3.88. Found: C, 79.49; H, 7.52; N, 3.73. ^{1}H-NMR ($CDCl_3$) δ: 1.34 (3H, d, *J*=7 Hz), 1.48 (3H, d, *J*=7 Hz), 1.6—2.1 (4H, m), 2.4—3.0 (4H, m), 3.53 (1H, q, *J*=7 Hz), 5.09 (1H, q, *J*=7 Hz), 6.80 (1H(NH), br d, *J*=8 Hz), 7.2—7.4 (10H, m).

4: mp 129—130 °C, $[\alpha]_D^{20}$ −40.9° (*c*=0.2% EtOH). IR (Nujol): 3300, 1665, 1635 cm^{-1}. *Anal.* Calcd for $C_{24}H_{29}NO_2$: C, 79.74; H, 7.53; N, 3.88. Found: C, 79.45; H, 7.54; N, 3.90. ^{1}H-NMR ($CDCl_3$) δ: 1.36 (3H, d, *J*=7 Hz), 1.50 (3H, d, *J*=7 Hz), 1.6—2.1 (4H, m), 2.4—3.0 (4H, m), 3.55 (1H, q, *J*=7 Hz), 5.10 (1H, q, *J*=7 Hz), 6.80 (1H(NH), br d, *J*=8 Hz), 7.2—7.4 (10H, m).

(−)-(1*R*)-2-[4-(2-Oxocyclohexylidenemethyl)phenyl]propionic Acid (2a) A stirred suspension of 2 g of sodium acetate in 12 ml of carbon tetrachloride (CCl_4) at −78 °C was treated with 4 ml of N_2O_4 (1 M CCl_4 solution). After 15 min, the stirred yellow suspension was treated dropwise with a solution of 680 mg of **3** in 1 ml of CCl_4 at 0 °C and kept for 2 h. The reaction mixture was then diluted with 20 ml of water and extracted with ether. The solvent was evaporated off under reduced pressure and the residual oil was dissolved in 3 ml of CCl_4. This solution was refluxed for 1 h. The solvent was removed under reduced pressure and the residue was chromatographed on 1 g of silica gel to afford 280 mg of the parent acid **1a**. mp 101—103 °C, $[\alpha]_D^{20}$ −51.4° (*c*=0.18% MeOH). *Anal.* Calcd for $C_{16}H_{18}O_3$: C, 74.39; H, 7.02. Found: C, 74.30; H, 7.08.

(+)-(1*S*)-2-[4-(2-Oxocyclohexylidenemethyl)phenyl]propionic Acid (2b) Compound **4** (680 mg) was treated by the same procedure as described for compound **2a** to give 270 mg of **2b**. mp 101—103 °C, $[\alpha]_D^{20}$ 49.5° (*c*=0.18% MeOH). *Anal.* Calcd for $C_{16}H_{18}NO_3$: C, 74.39; H, 7.02. Found: C, 74.21; H, 7.11.

References

1) A. Terada, S. Naruto, K. Wachi, S. Tanaka, Y. Iizuka and E. Misaka, *J. Med. Chem.*, **27**, 212 (1984).
2) T. Y. Shen, *Angew. Chem. Int. Ed. Engl.*, **11**, 460 (1972); J. S. Kaltenbronn, *J. Med. Chem.*, **16**, 490 (1973); S. Noguchi, S. Kishimoto, I. Minamida and M. Obayashi, *Chem. Pharm. Bull.*, **22**, 529 (1974); Z. H. Gaut, H. Baruth, L. O. Randall, C. Ashley and J. R. Paulsrud, *Prostaglandins*, **10**, 59 (1975); S. S. Adams, P. Bresloff and C. G. Mason, *J. Pharm. Pharmacol.*, **28**, 256 (1976).
3) S. Naruto and A. Terada, *Chem. Pharm. Bull.*, **31**, 4286 (1983).
4) G. Helmchen, H. Volter and W. Schuhle, *Tetrahedron Lett.*, **1977**, 1417.
5) G. Haas and V. Prelog, *Helv. Chem. Acta*, **52**, 1202 (1969).
6) C. L. Arcus and J. Kenyon, *J. Chem. Soc.*, **1939**, 916.
7) G. Barth, W. Voelter, H. S. Mosher, E. Bunnenberg and C. Djerassi, *J. Am. Chem. Soc.*, **95**, 532 (1970); D. Loew and O. Schuster, *Dtsch. Apoth. Ztg.*, **129**, 669 (1989); A. M. Evans, R. L. Nation, L. N. Sansom, F. Bochner and A. Somogyi, *Eur. J. Clin. Pharmacol.*, **36**, 283 (1989); G. Geisslinger, K. P. Stock, G. L. Bach, D. Loew and K. Brune, *Agents. Actions*, **27**, 455 (1989); T. A. Baillie, W. J. Adams, D. G. Kaiser, L. S. Olanoff, G. W. Halstead, H. Harpootlian and G. J. Van Giessen, *J. Pharmacol. Exp. Ther.*, **249**, 517 (1989).

Studies on the Constituents of the Seeds of *Hernandia ovigera* L. VIII.[1] Syntheses of (±)-Desoxypodophyllotoxin and (±)-β-Peltatin-A Methyl Ether

Tatsuhiko KASHIMA, Mariko TANOGUCHI, Masao ARIMOTO, and Hideo YAMAGUCHI*

Osaka University of Pharmaceutical Sciences, 2–10–65, Kawai, Matsubara, Osaka 580, Japan. *Received July 9, 1990*

(±)-Desoxypodophyllotoxin (2), a chief component of the seeds of *Hernandia ovigera* L., and (±)-β-peltatin-A methyl ether (3), an analogous phenyltetralin lignan, which have 2,3-*trans*, 3,4-*cis* configuration were synthesized according to the method developed for the synthesis of hernandin (1). The syntheses were pursued using the corresponding 4-phenyl-1,2-dihydronaphthalene lactones (9 and 10) followed by cleavage of the lactone moiety to give the unsaturated hydroxy acids (11 and 12). Subsequent hydrogenation and ring closure by means of *p*-toluenesulfonic acid afforded both 2,3-*trans*, 3,4-*cis* and 2,3-*cis*, 3,4-*cis* lignans (2 and 13 or 3 and 14), which were isolated by preparative thin layer chromatography.

Keywords *Hernandia ovigera*; hernandin; phenyltetralin lignan; desoxypodophyllotoxin; β-peltatin-A methyl ether; intramolecular Diels–Alder reaction

Hernandin (**1**) is a phenyltetralin-type lignan isolated from *Hernandia ovigera* L.[2] In the previous paper of this series,[1] the authors reported the synthesis of (±)-**1** which has 2,3-*trans*, 3,4-*cis* configuration. Most of the synthetic procedure was carried out according to the method developed by Klemm *et al.*[3a–d] and the corresponding 1,2-dihydro-3-naphthoic acid lactone was obtained by means of the intramolecular Diels–Alder reaction[4] of the cinnamyl phenylpropiolate prepared by the condensation of the two phenylpropanoid-type compounds. However, it is known that direct catalytic hydrogenation of 1,2-dihydro-3-naphthoic acid lactone affords only the 2,3-*cis* tetralin-type compound.[3] The key point of our method lies in the cleavage of the lactone moiety of 1,2-dihydro-3-naphthoic acid lactone prior to the catalytic hydrogenation leading to the tetralin-type product. The cleavage of the lactone moiety releases the restriction on the direction of attack by hydrogen in catalytic hydrogenation and makes it possible to obtain both *cis* and *trans* compounds. The unsaturated hydroxy acid obtained by the cleavage of lactone moiety afforded two kinds of hydroxy acids by catalytic hydrogenation on Pd–C, of which one had 2,3-*cis* and the other 2,3-*trans* configuration. The former was more easily lactonized than the latter by hydrochloric acid on account of the proximity of the hydroxy and carboxyl groups.

This time the authors adopted the above method for the syntheses of analogous 4-phenyltetralin-type lignans and succeeded in synthesizing (±)-desoxypodophyllotoxin (**2**) and (±)-β-peltatin-A methyl ether (**3**) (Fig. 1). The syntheses were carried out through the scheme in Chart 1.

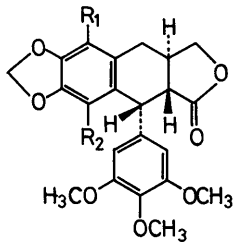

1 : R_1=H, R_2=OCH_3
2 : R_1=R_2=H
3 : R_1=OCH_3, R_2=H

Fig. 1

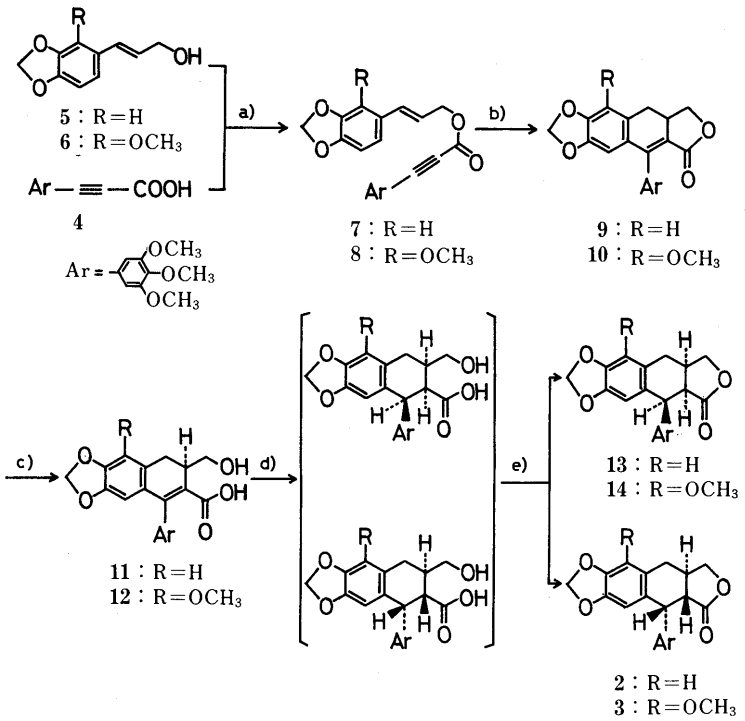

a) DCC b) DMF, Δ c) 7% KOH d) 10% Pd-C, H_2 e) *p*-TsOH, benzene

Chart 1

Concerning the starting materials, 3,4,5-trimethoxyphenylpropiolic acid[3a] (**4**) was prepared according to the method described in our previous paper.[1] *trans*-3,4-Methylenedioxycinnamyl alcohol[3a] (**5**) and *trans*-2-methoxy-3,4-methylenedioxycinnamyl alcohol[3c] (**6**) are known substances, but the method of preparation was improved in detail as described in the experimental section. The condensation of **5** or **6** with **4** gave **7** or **8**, respectively, followed by ring closure to afford **9** or **10**.[5] Compounds **9** and **10** were successively hydrolyzed to give the corresponding unsaturated hydroxy acids **11** and **12**. The next step was slightly modified from the case of the synthesis of **1**. In the former case, the experiment was done in two steps after the hydrogenation of the 1,2-dihydrohydroxy acid to distinguish the objective hydroxy acid (2,3-*trans* type) from another possible lactone (2,3-*cis* type). To improve the yield of the desired 2,3-*trans* lactone, the hydrogenated products were directly treated with *p*-toluenesulfonic acid (*p*-TsOH) without isolating the hydroxy acid and the resultant two sorts of lactones were isolated by preparative thin layer chromatography (PTLC). In the synthesis of **2**, **2** and isopicrodesoxypodophyllotoxin (**13**) were obtained in 35 and 26% yields, respectively, and in the synthesis of **3**, **3** and isopicro-*β*-peltatin methyl ether (**14**) were obtained in 48 and 27% yields, respectively. Recently Achiwa *et al.*[6] reported the synthesis of (−)-**2** from the corresponding 1,2-dihydro-(−)-**9**, which was derived from (+)-podorhizon utilizing our method followed by cyclization. These results showed that this method was advantageous for the syntheses of 4-phenyltetralin-type lignans which have the same configuration as natural products.

Experimental

All melting points were determined on a Yanaco micro melting point apparatus and are uncorrected. The instruments used in this study were as follows: infrared (IR) spectra, Jasco IR-810 spectrometer; mass spectra (MS), Hitachi M-80; nuclear magnetic resonance (NMR) spectra, Varian XL-300 and Gemini-200 instruments (with tetramethylsilane as an internal standard; chemical shifts are recorded in δ values). Column chromatography was carried out on Merck silica gel (Kieselgel 60, 70—230 mesh). Precoated silica gel plates used in PTLC were Merck Kieselgel 60 F_{254}, 0.5 mm thickness.

Starting Materials Substituted cinnamyl alcohols were prepared from the corresponding benzaldehyde *via* substituted ethyl cinnamate by means of the Wittig–Horner reaction and lithium aluminum hydride (LAH) reduction as described in the previous report.[1]

5: ^{1}H-NMR ($CDCl_3$) δ: 1.51 (1H, br s, OH), 4.29 (2H, dd, J=6.0, 1.2 Hz, CH=CHC$\underline{H}_2$O), 5.96 (2H, s, OCH_2O), 6.20 (1H, dt, J=15.6, 6.0 Hz, CH=C$\underline{H}$–CH_2), 6.52 (1H, dt, J=15.6, 1.2 Hz, C$\underline{H}$=CHCH$_2$), 6.76 (1H, d, J=7.8 Hz, C_5-H), 6.82 (1H, dd, J=7.8, 1.5 Hz, C_6-H), 6.93 (1H, d, J=1.5 Hz, C_2-H).

6: ^{1}H-NMR ($CDCl_3$) δ: 1.50 (1H, br s, OH), 3.99 (3H, s, C_2-OCH_3), 4.29 (2H, dd, J=6.0, 1.4 Hz, CH=CHC$\underline{H}_2$O), 5.94 (2H, s, OCH_2O), 6.27 (1H, dt, J=16.0, 6.0 Hz, CH=C$\underline{H}$–CH_2), 6.52 (1H, d, J=8.4 Hz, C_6-H), 6.79 (1H, d, J=16.0 Hz, C$\underline{H}$=CH), 6.95 (1H, d, J=8.4 Hz, C_5-H).

3,4-Methylenedioxycinnamyl 3′,4′,5′-Trimethoxyphenylpropiolate[3a] **(7)** A dry pyridine solution (5 ml) of **5** (0.18 g, 1.01 mmol), **4** (0.26 g, 1.1 mmol) and *p*-TsOH (9.5 mg) was treated with a dry pyridine solution (3 ml) of 1,3-dicyclohexylcarbodiimide (DCC) (0.25 g, 1.2 mmol). The mixture was stirred at room temperature for 1 h. After the addition of AcOH (2 ml), the reaction mixture was allowed to stand at 0 °C for 4 h. The precipitate was filtered off and washed with cold pyridine. The filtrate was acidified with concentrated HCl and extracted with $CHCl_3$. The extract was washed with brine and dried over anhydrous Na_2SO_4. After removal of the solvent, the resulting residue was purified by column chromatography benzene–AcOEt, 20:1) to give **7** (0.25 g, 65%). mp 135—136 °C (from hexane–AcOEt) (lit.[3a] 130—131 °C). IR $\nu_{max}^{CHCl_3}$ cm^{-1}: 2210 (C≡C), 1705 (C=O), 940 (OCH_2O). MS *m/z*: 396 (M^+). ^{1}H-NMR ($CDCl_3$) δ: 3.86 (6H, s, $C_{3',5'}$-OCH_3), 3.88 (3H, s, $C_{4'}$-OCH_3), 4.86 (2H, dd, J=6.6, 1.2 Hz, CH=CH–C$\underline{H}_2$O), 5.97 (2H, s, OCH_2O), 6.16 (1H, dt, J=15.9, 6.6 Hz, CH=C$\underline{H}$–CH_2), 6.64 (1H, d, J=15.9 Hz, C$\underline{H}$=CH), 6.77 (1H, d, J=8.1 Hz, C_5-H), 6.84 (2H, s, $C_{2',6'}$-H), 6.85 (1H, dd, J=8.1, 1.5 Hz, C_6-H), 6.95 (1H, d, J=1.5 Hz, C_2-H). *Anal.* Calcd for $C_{22}H_{20}O_7$: C, 66.66; H, 5.09. Found: C, 66.54; H, 5.08.

2-Methoxy-3,4-methylenedioxycinnamyl 3′,4′,5′-Trimethoxyphenylpropiolate[3c] **(8)** This compound was obtained in 85% yield from **6** (418 mg, 2.01 mmol) and **4** (472 mg, 2.00 mmol) by the same procedure as described in the preparation of **7**. mp 101.5—104 °C (from hexane–AcOEt). IR $\nu_{max}^{CHCl_3}$ cm^{-1}: 2210 (C≡C), 1700 (C=O), 935 (OCH_2O). MS *m/z*: 426 (M^+). ^{1}H-NMR ($CDCl_3$) δ: 3.86 (6H, s, $C_{3',5'}$-OCH_3), 3.88 (3H, s, $C_{4'}$-OCH_3), 4.01 (3H, s, C_2-OCH_3), 4.87 (2H, dd, J=6.6, 1.2 Hz, CH=CH–C$\underline{H}_2$O), 5.95 (2H, s, OCH_2O), 6.24 (1H, dt, J=16.2, 6.6 Hz, CH=C$\underline{H}$–CH_2), 6.53 (1H, d, J=8.4 Hz, C_5-H), 6.84 (2H, s, $C_{2',6'}$-H), 6.91 (1H, d, J=16.2 Hz, C$\underline{H}$=CH), 6.97 (1H, d, J=8.4 Hz, C_6-H). *Anal.* Calcd for $C_{23}H_{22}O_8$: C, 64.78; H, 5.20. Found: C, 64.70; H, 5.21.

(±)-2-Hydroxymethyl-6,7-methylenedioxy-4-(3′,4′,5′-trimethoxyphenyl)-1,2-dihydro-3-naphthoic Acid Lactone[3b] **(9)** A solution of **7** (103 mg, 0.51 mmol) in dimethylformamide (DMF) (10 ml) was heated under stirring at 145 °C for 1 h. The mixture was poured into water and extracted with $CHCl_3$. The extract was washed with brine and dried over anhydrous Na_2SO_4. The $CHCl_3$ layer was evaporated and the resulting residue was purified by column chromatography with $CHCl_3$. Repeated recrystallization of the crude product from MeOH–CH_2Cl_2 afforded **9** (77.6 mg, 39%). Colorless needles, mp 251—254 °C (lit.[3b] 252—253 °C). IR $\nu_{max}^{CHCl_3}$ cm^{-1}: 1740 (C=O), 940 (OCH_2O). ^{1}H-NMR ($CDCl_3$) δ: 2.82 (1H, d, J=16.0 Hz, one of C_1-H), 2.94 (1H, dd, J=16.0, 6.6 Hz, one of C_1-H), 3.40 (1H, m, C_2-H), 3.84 (6H, s, $C_{3',5'}$-OCH_3), 3.92 (3H, s, $C_{4'}$-OCH_3), 4.01, 4.70 (each 1H, dd, J=8.8, 8.8 Hz, lactone-CH_2), 5.97 (2H, s, OCH_2O), 6.52 (3H, br s, $C_{5,2',6'}$-H), 6.77 (1H, s, C_8-H). *Anal.* Calcd for $C_{22}H_{20}O_7$: C, 66.66; H, 5.09. Found: C, 66.58; H, 5.00.

(±)-2-Hydroxymethyl-8-methoxy-6,7-methylenedioxy-4-(3′,4′,5′-trimethoxyphenyl)-1,2-dihydro-3-naphthoic Acid Lactone[3c] **(10)** This compound (as a 9:1 mixture with dehydro-*β*-peltatin methyl ether)[5] was obtained in 46% yield from **8** (550 mg, 1.29 mmol) in DMF (30 ml) by the same procedure as described for the preparation of **9**. ^{1}H-NMR ($CDCl_3$) δ: 2.33 (1H, dd, J=16.0, 16.0 Hz, one of C_1-H), 3.29 (1H, m, C_2-H), 3.45 (1H, dd, J=16.0, 8.8 Hz, one of C_1-H), 3.83 (6H, s, $C_{3',5'}$-OCH_3), 3.92 (3H, s, $C_{4'}$-OCH_3), 4.03, 4.71 (each 1H, dd, J=8.8, 8.8 Hz, lactone-CH_2), 4.04 (3H, s, C_8-OCH_3), 5.95, 5.97 (each 1H, d, J=1.4 Hz, OCH_2O), 6.28 (1H, s, C_5-H), 6.48 (2H, br s, $C_{2',6'}$-H).

(±)-2-Hydroxymethyl-6,7-methylenedioxy-4-(3′,4′,5′-trimethoxyphenyl)-1,2-dihydro-3-naphthoic Acid (11) An MeOH solution (30 ml) of **9** (102 mg, 0.26 mmol) was stirred with KOH (2.1 g) at 50 °C for 3 h. The mixture was poured into water and extracted with $CHCl_3$ to remove neutral material. The aqueous layer was carefully neutralized with 2% HCl solution at 0 °C and extracted with Et_2O. The organic layer was washed with brine and dried over anhydrous Na_2SO_4. After removal of the solvent, **11** (104 mg, 98%) was obtained as an amorphous powder. Compound **11** was used *in situ* at the next step without purification.

(±)-Desoxypodophyllotoxin (2) and (±)-Isopicrodesoxypodophyllotoxin (13) An EtOH solution (30 ml) of **11** (95 mg, 0 23 mmol) was stirred with 10% Pd–C (95 mg) at 46 °C for 22 h in a stream of hydrogen under elevated pressure (4.7 atm). The catalyst was filtered off, and the filtrate was evaporated. The resulting residue was dissolved in dry benzene (25 ml), and the solution was refluxed with *p*-TsOH (10 mg) and 4 Å molecular sieves (80 mg) for 1 h. The molecular sieves were filtered off, then the filtrate was washed with saturated $NaHCO_3$ solution (2 ml) and brine, and dried over anhydrous Na_2SO_4. After removal of the solvent, the residue was purified by PTLC (*n*-hexane–AcOEt, 3:2) to give **2** (32 mg, 35%) and **13** (24 mg, 26%).

2: Colorless needles, mp 238—241 °C (from EtOH) (lit.[7] 234—236 °C). IR $\nu_{max}^{CHCl_3}$ cm^{-1}: 1740 (C=O), 945 (OCH_2O). MS *m/z*: 398 (M^+). ^{1}H-NMR ($CDCl_3$) δ: 2.67—2.86 (3H, m, $C_{1,2,3}$-H), 3.02—3.14 (1H, m, C_1-H), 3.76 (6H, s, $C_{3',5'}$-OCH_3), 3.81 (3H, s, $C_{4'}$-OCH_3), 3.92 (1H, dd, J=9.9, 8.7 Hz, one of lactone-CH_2), 4.46 (1H, dd, J=8.7, 6.4 Hz, one of lactone-CH_2), 4.60 (1H, d, J=1.8 Hz, C_4-H), 5.93, 5.95 (each 1H, d, J=1.5 Hz, OCH_2O), 6.35 (2H, s, $C_{2',6'}$-H), 6.53 (1H, s, C_5-H), 6.67 (1H, s, C_8-H). *Anal.* Calcd for $C_{22}H_{22}O_7$: C, 66.32; H, 5.57. Found: C, 66.30; H, 5.57.

13: Colorless needles, mp 208—210 °C (from EtOH) (lit.[3a] 203—204 °C). IR $\nu_{max}^{CHCl_3}$ cm^{-1}: 1770 (C=O), 940 (OCH_2O). MS *m/z*: 398 (M^+). ^{1}H-NMR ($CDCl_3$) δ: 2.70 (1H, dd, J=15.9, 5.0 Hz, C_3-H), 2.98 (1H, dd, J=15.9, 8.7 Hz, one of C_1-H), 3.10—3.26 (2H, m, one of C_1-H and

C_2-H), 3.50 (1H, dd, J=8.9, 7.8 Hz, one of lactone-CH_2), 3.77 (6H, s, $C_{3',5'}$-OCH_3), 3.83 (3H, s, $C_{4'}$-OCH_3), 4.32—4.50 (2H, m, C_4-H and one of lactone-CH_2), 5.96 (2H, s, OCH_2O), 6.50 (2H, s, $C_{2',6'}$-H), 6.65 (1H, s, C_5-H), 6.74 (1H, s, C_8-H). *Anal.* Calcd for $C_{22}H_{22}O_7$: C, 66.32; H, 5.57. Found: C, 66.19; H, 5.56.

(±)-2-Hydroxymethyl-8-methoxy-6,7-methylenedioxy-4-(3',4',5'-trimethoxyphenyl)-1,2-dihydro-3-naphthoic Acid (12) This compound was obtained in 99% yield from crude **10** (103 mg, 0.24 mmol) by the same procedure as described for the preparation of **11**. Compound **12** was used *in situ* at the next step without purification.

(±)-β-Peltatin-A Methyl Ether (3) and (±)-Isopicro-β-peltatin Methyl Ether (14) These compounds were prepared in 48 and 27% yields, respectively, from **12** (46 mg, 0.10 mmol) by the same procedure as used for the preparation of **2** and **13**.

3: Colorless prisms, mp 203—207 °C (from EtOH). IR $\nu_{max}^{CHCl_3}$ cm^{-1}: 1775 (C=O), 945 (OCH_2O). MS m/z: 428 (M^+). ^{1}H-NMR ($CDCl_3$) δ: 2.47 (1H, dd, J=16.5, 10.5 Hz, one of C_1-H), 2.58—2.74 (2H, m, one of C_1-H and C_2-H), 3.18 (1H, dd, J=21.3, 4.9 Hz, C_3-H), 3.76 (6H, s, $C_{3',5'}$-OCH_3), 3.81 (3H, s, $C_{4'}$-OCH_3), 3.94 (1H, dd, J=10.5, 8.7 Hz, one of lactone-CH_2), 4.07 (3H, s, C_8-OCH_3), 4.47 (1H, dd, J=8.7, 6.6 Hz, one of lactone-CH_2), 4.58 (1H, d, J=3.9 Hz, C_4-H), 5.91, 5.92 (each 1H, d, J=1.5 Hz, OCH_2O), 6.28 (1H, s, C_5-H), 6.36 (2H, s, $C_{2',6'}$-H). *Anal.* Calcd for $C_{23}H_{24}O_8$: C, 64.48; H, 5.65. Found: C, 64.60; H, 5.66.

14: Colorless needles, mp 189—190.5 °C (from EtOH). IR $\nu_{max}^{CHCl_3}$ cm^{-1}: 1765 (C=O), 940 (OCH_2O). MS m/z: 428 (M^+). ^{1}H-NMR ($CDCl_3$) δ: 2.53—2.63 (1H, m, C_1-H), 3.08—3.23 (3H, m, $C_{1,2,3}$-H), 3.52 (1H, dd, J=9.0, 7.2 Hz, one of lactone-CH_2), 3.77 (6H, s, $C_{3',5'}$-OCH_3), 3.83 (3H, s, $C_{4'}$-OCH_3), 4.03 (3H, s, C_8-OCH_3), 4.35—4.44 (2H, m, C_4-H and one of lactone-CH_2), 5.92, 5.93 (each 1H, d, J=1.5 Hz, OCH_2O), 6.38 (1H, s, C_5-H), 6.53 (2H, s, $C_{2',6'}$-H).

References and Notes

1) Part VII: M. Tanoguchi, T. Kashima, H. Saika, T. Inoue, M. Arimoto, and H. Yamaguchi, *Chem. Pharm. Bull.*, **37**, 68 (1989). Most of this work was presented at the 109th Annual Meeting of the Pharmaceutical Society of Japan, Nagoya, April 1989.
2) H. Yamaguchi, M. Arimoto, M. Tanoguchi, T. Ishida, and M. Inoue, *Chem. Pharm. Bull.*, **30**, 3212 (1982).
3) *a*) L. H. Klemm, K. W. Gopinath, G. C. Karaboyas, G. L. Capp, and D. H. Lee, *Tetrahedron*, **20**, 871 (1964); *b*) L. H. Klemm, K. W. Gopinath, D. H. Lee, F. W. Kelly, E. Trod, and T. M. Mcguire, *ibid.*, **22**, 1797 (1966); *c*) L. H. Klemm and P. S. Santhanum, *J. Org. Chem.*, **33**, 1268 (1968); *d*) L. H. Klemm, D. R. Olson, and D. V. White, *ibid.*, **36**, 3740 (1971); *e*) B. S. Joshi, N. Viswanathan, V. Balakrishnan, D. H. Gawad, and K. R. Ravindranath, *Tetrahedron*, **35**, 1665 (1979).
4) E. Ciganek, *Org. React.*, **32**, 1 (1984).
5) In the intramolecular Diels–Alder reaction of **7** and **8**, the formation of the aromatized compounds as by-products was observed in both cases. Addition to this, in the reaction of **7** to **9**, an isomer, 5,6-methylenedioxy-1,2-dihydronaphthalene lactone was also found among the products. The existence of these by-products was determined by analysis of the NMR spectra.
6) T. Morimoto, M. Chiba, and K. Achiwa, *Tetrahedron Lett.*, **31**, 261 (1990).
7) S. Takano, S. Otaki, and K. Ogasawara, *J. Chem. Soc., Chem. Commun*, **1985**, 485.

A Novel Example of Thermal Oxygenation of Aromatic Hydrocarbons with a Heterocyclic *N*-Oxide: Unusual Reactivity of Pyrimido[5,4-*g*]pteridinetetrone 10-Oxide

Magoichi SAKO, Seiji OHARA, Kosaku HIROTA, and Yoshifumi MAKI*

Gifu Pharmaceutical University, 5-6-1, Mitahora-higashi, Gifu 502, Japan. *Received July 9, 1990*

Aromatic hydrocarbons, *i.e.*, benzene, naphthalene (4), phenanthrene (6), toluene (10), *p*-xylene (14), mesitylene (18), and durene (21), were oxygenated by a member of a novel class of heterocyclic *N*-oxides, 1,3,6,8-tetrabutylpyrimido[5,4-*g*]pteridine-2,4,5,7(1*H*,3*H*,6*H*,8*H*)-tetrone 10-oxide (1), under certain thermal conditions to give the corresponding products oxygenated in either the benzene ring or the methyl group, presumably *via* a single-electron transfer process.

Keywords thermal oxygenation; aromatic hydrocarbon; heterocyclic *N*-oxide; pyrimido[5,4-*g*]pteridinetetrone 10-oxide; single-electron transfer process

Previous articles from our laboratory[1] have demonstrated that under photochemical conditions, 1,3,6,8-tetrabutylpyrimido[5,4-*g*]pteridine-2,4,5,7(1*H*,3*H*,6*H*,-8*H*)-tetrone 10-oxide (**1**) ($E^{red}_{1/2} = -0.97$ V *vs.* SCE in MeCN) functions as an electron acceptor and consequently as an agent for oxygenation or dehydrogenation, depending upon the nature of the substrates. For example, the photooxygenation of benzene, toluene, and anisole by **1** efficiently gives the corresponding phenols as major products without any photochemical intramolecular rearrangement of the *N*-oxide function. The reaction can be rationalized in terms of the involvement of an initial single-electron transfer (SET) from the benzenes to a singlet-excited **1** followed by oxygen-atom transfer, in contrast to the oxene mechanism which is generally accepted for photochemical oxygenation by heterocyclic *N*-oxides.[2]

Despite abundant examples of thermal deoxygenation of heterocyclic *N*-oxides by various reactants,[3] there is no precedent for the deoxygenation of heterocyclic *N*-oxides by aromatic hydrocarbons under thermal conditions, resulting in the oxygenation of the aromatic hydrocarbons employed.

In this paper, we wish to report that the unusual properties of the *N*-oxide **1** allow thermal oxygenation of aromatic hydrocarbons, *i.e.*, benzene, naphthalene (**4**), phenanthrene (**6**), toluene (**10**), *p*-xylene (**14**), mesitylene (**18**), and durene (**21**), presumably *via* a SET process followed by an oxygen-atom transfer process. To our knowledge, this is a first example of thermal oxygenation of aromatic hydrocarbons with a heterocyclic *N*-oxide.

When a mixture of benzene (2 M) ($E^{ox}_{1/2} = 2.68$ V *vs.* SCE)[4a] and **1** (5 mM) in dry acetonitrile was heated in a degassed tube at 135 °C in the dark for 1 d, the employed *N*-oxide **1** was recovered and no detectable amount of phenol was formed. Under similar conditions, the reaction of naphthalene (**4**) ($E^{ox}_{1/2} = 1.81$ V *vs.* SCE)[4a] with **1** gave naphthols (**5**) (as a mixture of 1- and 2-isomers in a ratio of 7:1) and 1,3,6,8-tetrabutylpyrimido[5,4-*g*]pteridine-

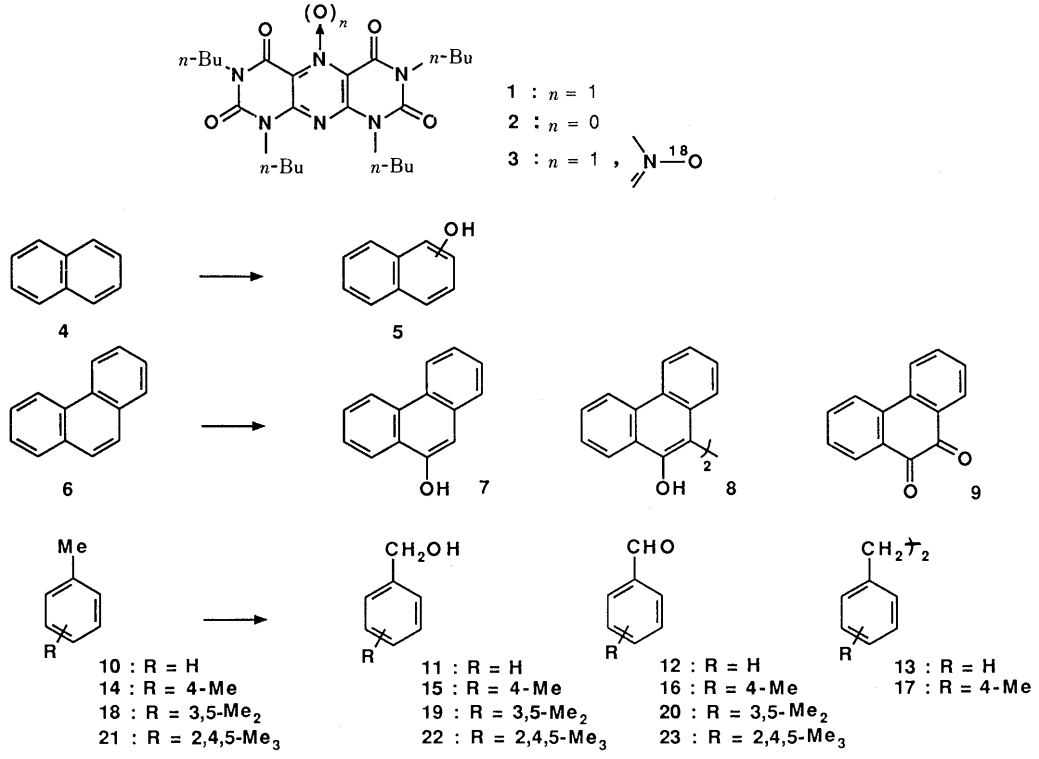

Chart 1

2,4,5,7(1*H*,3*H*,6*H*,8*H*)-tetrone (**2**) in 18 and 40% yields, respectively. Although a significant amount of **1** was recovered in this reaction, deoxygenation of **1** to **2** occurred without any other reaction. The reaction of **4** with ^{18}O-labeled *N*-oxide (**3**)[5] confirmed that the transfer of the *N*-oxide oxygen of **3** into **4** is virtually quantitative. The oxygenation of phenanthrene (**6**) ($E^{ox}_{1/2}=1.74$ V *vs.* SCE)[4a] by **1** under similar conditions resulted in the formation of 9-phenanthrol (**7**) (4%), bis(9-hydroxyphenanthren-10-yl) (**8**) (20%),[6] and 9,10-phenanthrenedione (**9**) (17%)[6] after complete consumption of **1**. When the thermal reaction of degassed benzene with **1** in a sealed tube at 135 °C was carried out without solvent, the formation of phenol in 5% yield was observed along with 13% consumption of **1**. Thus, it is evident that the thermal oxygenation of the aromatic hydrocarbons, benzene, **4**, and **6** by **1** occurs more easily as the oxidation potential decreases.

The charge-transfer (CT) interaction between **1** and **4** [405 ($\varepsilon=10$) nm] as well as between **1** and **6** [405 ($\varepsilon=16$) nm)] was evidenced by the difference ultraviolet (UV)-visible absorption spectrum of the mixture of **1** and **4** or **6** *vs.* **1**. The oxygenation of **4** and **6** by **1** was markedly accelerated by irradiation with UV-visible light, as previously demonstrated.[7]

These facts indicate that the oxygen-atom transfer from **1** to **4** or **6** probably occurs *via* SET from the substrates, **4**, and **6**, to **1** in the initially formed CT complexes.

Degassed toluene (**10**) ($E^{ox}_{1/2}=2.37$ V *vs.* SCE)[4b] was allowed to react with **1** in a sealed tube at 135°C in the dark. The *N*-oxide **1** was completely consumed after 1 d being converted into **2**. Benzyl alcohol (**11**) and benzaldehyde (**12**) were obtained in 68 and 18% yields, together with a trace amount of dibenzyl (**13**). It is noteworthy that no formation of any cresols was observed, which is in contrast to the case of the photochemical oxygenation of **10** by **1**, leading to *o*- and *p*-cresols as major products.[2] Employment of 3-methylpyridazine 2-oxide[8] in place of **1** resulted in no appreciable reaction under thermal conditions.

Under similar conditions, *p*-xylene (**14**) ($E^{ox}_{1/2}=2.06$ V *vs.* SCE)[4b] was oxidized more easily by **1** to give 4-methylbenzyl alcohol (**15**) and 4-methylbenzaldehyde (**16**) in 73 and 25% yields (after 2 h), respectively. A trace amount of 4,4'-dimethyldibenzyl (**17**) was also obtained. The oxygenation of mesitylene (**18**) ($E^{ox}_{1/2}=2.11$ V *vs.* SCE)[4b] by **1** gave 3,5-dimethylbenzyl alcohol (**19**) (69%) and 3,5-dimethylbenzaldehyde (**20**) (21%).[9]

In the case of durene (**21**) ($E^{ox}_{1/2}=1.83$ V *vs.* SCE),[4b] the corresponding oxygenated products, 2,4,5-trimethylbenzyl alcohol (**22**) (70%) and 2,4,5-trimethylbenzaldehyde (**23**) (22%),[9] were obtained.

Figure 1 shows a linear relationship between the relative consumption rates of **1** (log $k/k_{toluene}$) in the oxygenation of the methylbenzenes, **10**, **14**, **18**, and **21**, by **1** and the oxidation potentials ($E^{ox}_{1/2}$) of the methylbenzenes employed.

Weak CT bands [around 401 ($\varepsilon=3$—10) nm] between **1** and the methylbenzenes, **14**, **18**, and **21**, were observed in the difference UV-visible absorption spectra of the mixtures of **1** and the methylbenzenes *vs.* **1**.

When the reaction of **1** with **14** at 135 °C in the dark was carried out under an oxygen atmosphere for 2 h, the oxygenated products, **15** and **16**, were obtained in 116 and 224% yields based on the employed **1**, and **1** was recovered in *ca.* 99% yield. This observation implies that in the presence of oxygen the *N*-oxide **1** functions only as an electron acceptor but not as an oxygen-atom donor. Thus, the operation of the SET mechanism is also possible in the thermal oxygenation of the methylbenzenes by **1**.[10]

We propose a reaction sequence for the present thermal oxygenation of aromatic hydrocarbons by **1** as outlined in Chart 2 (a and b), by using as examples the cases of **4** and **10**.

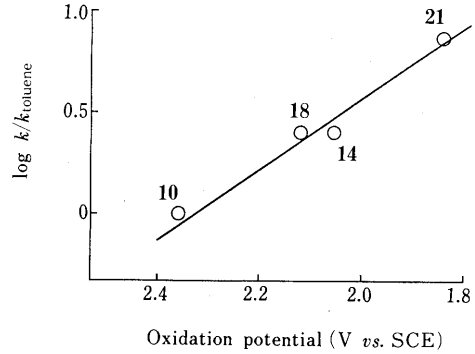

Fig. 1. Correlation between the Relative Consumption Rates of the *N*-Oxide **1** (log $k/k_{toluene}$) in the Thermal Oxygenation of the Methylbenzenes (**10**, **14**, **18**, and **21**) by **1** and the Oxidation Potentials ($E^{ox}_{1/2}$) of the Methylbenzenes Employed

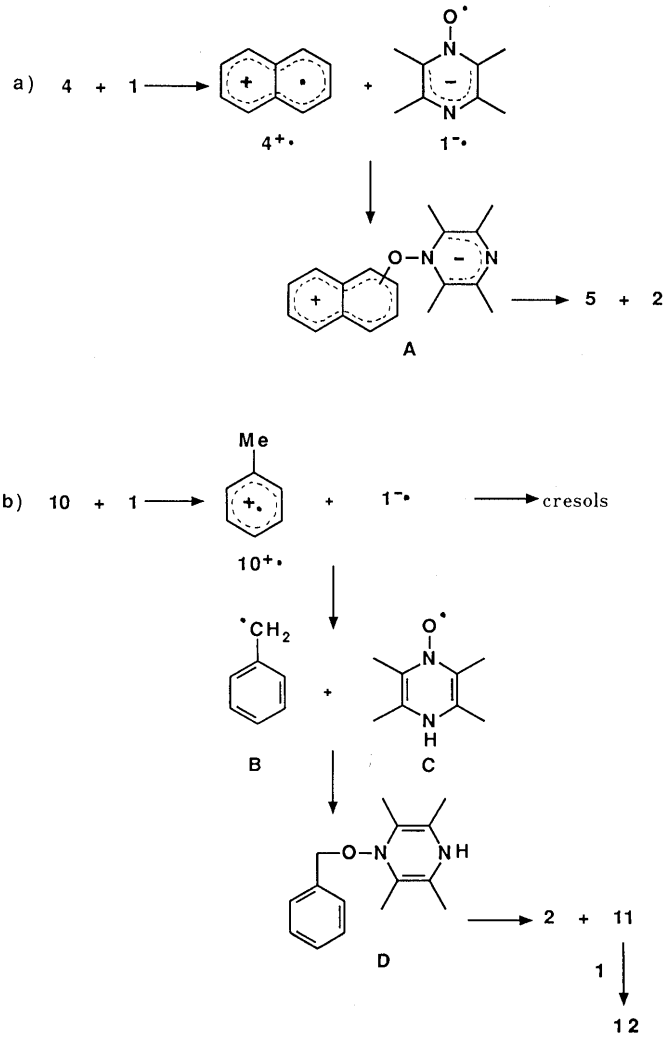

Chart 2

The SET from **4** to **1** probably occurs *via* the initial CT-complex formation to give a pair of radical ions, ($4^{+\cdot}$ and $1^{-\cdot}$). The transient zwitterionic intermediate (A) formed by coupling of $4^{+\cdot}$ with $1^{-\cdot}$ collapses to produce **5** and **2** (see a in Chart 2).[11]

In the case of **10** (see b in Chart 2), deprotonation of the cation radical $10^{+\cdot}$ generated as a result of the SET from **10** to **1** exclusively takes place under thermal conditions to give the benzyl radical (B) in preference to the coupling with $1^{-\cdot}$ leading to the formation of the cresols, which mainly occurs under photochemical conditions.[2]

Exergonic deprotonation of the methylbenzene cation-radicals to generate the corresponding benzyl radicals is frequently encountered in the thermal reactions of methylbenzenes involving the SET process.[12] The detection of **13** in the reaction of **10** with **1** provides evidence supporting the generation of B during the reaction.

Coupling of B with a nitroxyl radical (C) gives a transient intermediate (D), which leads to **11** and **2**. Further dehydrogenation of **11** by **1** proceeds *via* the analogous SET process to give **12**. Independent experiments showed that the dehydrogenation of **11** to give **12** takes place gradually in the presence of **1** or **2** under conditions analogous to those in the case of the oxygenation of **10**.

In conclusion, the present results provide the first example demonstrating that a heterocyclic *N*-oxide can behave as an electron acceptor and subsequently as an oxygen-atom donor under thermal conditions.

Experimental

Spectroscopic measurements for the structural assignment of the reaction products were performed with the following instruments: UV-visible absorption spectra with Shimadzu 260 spectrophotometer; proton nuclear magnetic resonance (^{1}H-NMR) spectra with a JEOL JNX 270 (270 MHz) spectrometer using tetramethylsilane as an internal standard; mass spectra (MS) with a JEOL JMS-D 300 machine operating at 70 eV. Gas liquid chromatography (GLC) analyses were performed with a Shimadzu GC-8APF instrument equipped with a column of 5% polyethyleneglycol (PEG) on Uniport HP (1.2 m × 3.0 mm). Thin layer chromatography analyses were carried out on Silica gel 60 plates (Merck, art. 5721) by using benzene–ethyl acetate (5 : 2) as an eluent. TLC scanning was done with a Shimadzu CS-9000 dual-wavelength flying-spot scanner for the assay of **1** and **2** (detection: 370 nm). Column chromatography was accomplished by using silica gel (Wakogel C-300).

Thermal Oxygenation of Benzene, Naphthalene (4), and Phenanthrene (6) by 1,3,6,8-Tetra-*n*-butylpyrimido[5,4-*g*]pteridine-2,4,5,7-(1*H*,3*H*,6*H*,8*H*)-tetrone 10-Oxide (1) For Benzene: A degassed solution of benzene (0.89 ml, 10 mmol) in dry acetonitrile (5.0 ml) containing **1** (12.2 mg, 0.025 mmol) was heated in a sealed tube at 135 °C in the dark for 1 d. TLC and gas chromatography (GC) analyses of the reaction mixture showed almost quantitative recovery of **1** (by TLC densitometry, *Rf* 0.27) and no detectable formation of phenol. When the reaction of benzene (5 ml) with **1** (12.2 mg, 0.025 mmol) was carried out without solvent, the formation of the expected phenol (5% yield based on the employed **1**, by GC and GC-mass) and 1,3,6,8-tetra-*n*-butylpyrimido[5,4-*g*]pteridine-2,4,5,7-(1*H*,3*H*,6*H*,8*H*)-tetrone (**2**) (*ca.* 13% yield, by TLC, *Rf* 0.35) was observed along with 87% recovery of **1**.

For **4**: A solution of **4** (1.281 g, 10 mmol) in dry acetonitrile (5.0 ml) containing **1** (12.2 mg, 0.025 mmol) was heated under conditions similar to those used in the foregoing case. TLC and GC analyses of the reaction mixture obtained after 1 d showed 40% consumption of **1** (converted into **2**) and the formation of naphthols (**5**) (as a mixture of 1- and 2-isomers with a ratio of 7 : 1, by GC and GC-mass) in 18% yield based on the employed **1**.

For **5**: A mixed solution of **5** (7.128 g, 40.0 mmol) and **1** (488 mg, 1.0 mmol) in dry acetonitrile (200 ml) was heated under conditions similar to those used in the foregoing case. The assay of the reaction mixture by TLC densitometry showed complete consumption of **1** and quantitative conversion into **2**. After removal of the solvent under reduced pressure, the resulting residue was subjected to column chromatography [eluent: *n*-hexane–benzene (5 : 2) and then benzene] to give 9-phenanthrol (**7**) (8 mg, 4% yield based on the employed **1**), bis(9-hydroxyphenanthren-10-yl) (**8**) (77 mg, 20%), and 9,10-phenanthrenedione (**9**) (35 mg, 17%). The structures of these products were confirmed by examination of the mass spectra and by comparison of their ^{1}H-NMR spectra with those of the respective authentic samples prepared from **5** by treatment with ferric chloride or by autoxidation.[6]

Thermal Oxygenation of Toluene (10), *p*-Xylene (14), Mesitylene (18), and Durene (21) by 1 A degassed solution of **1** (12.2 mg, 0.025 mmol) in **10**, **14**, **18**, or **21** (5.0 ml) was heated in a sealed tube at 135 °C in the dark. TLC and GC analyses showed smooth conversion of **1** into **2** and the formation of the corresponding benzyl alcohols, benzyl alcohol (**11**), 4-methylbenzyl alcohol (**15**), 3,5-dimethylbenzyl alcohol (**19**), or 2,4,5-trimethylbenzyl alcohol (**22**), and benzaldehydes, benzaldehyde (**12**), 4-methylbenzaldehyde (**16**), 3,5-dimethylbenzaldehyde (**20**), or 2,4,5-trimethylbenzaldehyde (**23**). The yields of these products were as follows. Products (yield based on the employed **1**): **11** (68%) and **12** (18%) from **10** (after 1 d); **15** (73%) and **16** (25%) from **14** (after 2 h); **19** (69%) and **20** (21%) from **18** (after 2 h); **22** (70%) and **23** (22%) from **21** (after 2 h). In the cases of **10** and **14**, trace amounts of the corresponding dibenzyls, dibenzyl (**13**) and 4,4′-dimethyldibenzyl (**17**), were detected in the respective reaction mixtures and their structures were confirmed by comparison of their GC retention times and GC-mass spectral data with those of authentic samples.[9]

Thermal Reaction of 4 and 10 with ^{18}O-Labeled *N*-Oxide (3) A solution of **4** (1.281 g, 10 mmol) and **3** (12.2 mg, 0.025 mmol; ^{18}O-content: 29%)[5] in dry acetonitrile (5.0 ml) was heated in a degassed sealed tube at 135 °C for 1 d. The ^{18}O-content of the product **5** was estimated to be *ca.* 30% by GC-mass spectrometry. In the reaction of **10** with **3**, the ^{18}O-content of **11** was *ca.* 30%.

Thermal Reaction of 10 with 3-Methylpyridazine 2-Oxide A solution of **10** (5.0 ml) containing 3-methylpyridazine 2-oxide (2.7 mg, 0.025 mmol) was heated under conditions similar to those used in the case of **1**. Analysis of the mixture by GC showed the recovery of the *N*-oxide employed and no formation of detectable amounts of oxidation products, **11**, **12**, and **13**.

Measurement of Relative Consumption Rates of 1 in Thermal Reaction with the Methylbenzenes, 10, 14, 18, and 21 A degassed solution of **1** (12.2 mg, 0.025 mmol) in **10**, **14**, **18**, or **21** (5 ml) was heated in a sealed tube at 135 °C in the dark. Consumption of **1** in this reaction was followed spectrophotometrically with a TLC scanner and rate constants were calculated by plotting A_t/A_0 *vs.* time (A_0 = the initial peak area of **1**; A_t = the peak area of **1** after reaction for t min). The relative consumption rates of **1** ($\log k/k_{\text{toluene}}$) based on the case of **10** are plotted in Fig. 1 as a function of the oxidation potentials ($E^{\text{ox}}_{1/2}$, V *vs.* SCE) of the methylbenzenes employed.

CT Interaction between 1 and the Aromatic Hydrocarbons, 4, 6, 14, 18, and 21 CT complex formation between **1** and the aromatic hydrocarbons was evidenced by the difference UV-visible absorption spectra of the mixtures of **1** (5 mM) and the aromatic hydrocarbons (10 mM) *vs.* **1** (5 mM) in dry acetonitrile. The observed CT bands were as follows: 405 (ε = 10) nm for **1** and **4**; 405 (ε = 16) nm for **1** and **6**; 401 (ε = 3) nm for **1** and **14**, 401 (ε = 3) nm for **1** and **18**; 401 (ε = 10) nm for **1** and **21**.

Thermal Reaction of 1 with 14 under Oxygen The solution of **1** (12.2 mg, 0.025 mmol) in **14** (5.0 ml) was heated under an oxygen atmosphere in a sealed tube at 135 °C for 2 h in the dark. TLC and GC analyses of the reaction mixture showed *ca.* 99% recovery of **1** and the formation of **15** and **16** in 116 and 224% yields, respectively, based on the employed **1**.

Thermal Reaction of 11 with 1 or 2 A degassed solution of **11** (5.4 mg, 0.05 mmol) in dry acetonitrile (5.0 ml) containing **1** (12.2 mg, 0.025 mmol) was heated in a sealed tube at 135 °C for 1 d in the dark. GC analysis of the resulting reaction mixture showed the formation of **12** in 22% yield based on the employed **1**. Employment of **2** (11.8 mg, 0.025 mmol) in place of **1** resulted in the formation of **12** in 20% yield.

References and Notes

1) M. Sako, K. Shimada, K. Hirota, and Y. Maki, *J. Am. Chem. Soc.*, **108**, 6039 (1986); Y. Maki, I. Oyabu, S. Ohara, M. Sako, Y. Kitade, and K. Hirota, *Chem. Pharm. Bull.*, **37**, 3239 (1989); Y. Maki, M. Sako, T. Murase, Y. Kitade, and K. Hirota, *Heterocycles*, **30**, 279 (1990) and preceding papers cited therein. For the preparation of the *N*-oxide **1**, see E. C. Taylor, Y. Maki, and A. McKillop, *J. Org. Chem.*, **37**, 1601 (1972).

2) M. Sako, S. Ohara, K. Shimada, K. Hirota, and Y. Maki, *J. Chem. Soc., Perkin Trans. 1*, **1990**, 863.

3) For a review, see "Chemistry of the Heterocyclic *N*-Oxides," ed. by A.

R. Katritzky and J. M. Logowski, Academic Press, New York, 1971, pp. 166—230.
4) *a*) T. Kubota, B. Uno, K. Kano, T. Kawakita, and M. Goto, *Bull. Chem. Soc. Jpn.*, **63**, 516 (1990); *b*) V. D. Parker, *J. Am. Chem. Soc.*, **98**, 98 (1976); C. J. Schlesener, C. Amatore, and J. K. Kochi, *ibid.*, **106**, 3567 (1984).
5) The ^{18}O-labeled *N*-oxide **3** was prepared by lead tetraacetate oxidation of 6-amino-5-^{18}O labeled nitroso-1,3-dibutylpyrimidine-2,4(1*H*,3*H*)-dione, which can be obtained with ease by the reaction of 6-amino-1,3-dibutylpyrimidine-2,4(1*H*,3*H*)-dione with nitrosonium tetrafluoroborate in THF containing $H_2{}^{18}O$.
6) F. Toda, K. Tanaka, and S. Iwata, *J. Org. Chem.*, **54**, 3007 (1989); T.-L. Ho, T.-W. Hall, and C. M. Wong, *Synthesis*, **1973**, 206.
7) M. Sako, S. Ohara, K. Hirota, and Y. Maki, *Chem. Pharm. Bull.*, **38**, 2676 (1990).
8) H. Igeta, T. Tsuchiya, M. Yamada, and H. Arai, *Chem. Pharm. Bull.*, **16**, 767 (1968); T. Tsuchiya, H. Arai, and H. Igeta, *Tetrahedron Lett.*, **1969**, 2747.
9) A. G. Gonzalez, L. M. Aguiar, J. D. Martin, and M. L. Rodriguez, *Tetrahedron Lett.*, **3**, 205 (1976).
10) Rastetter *et al.* have reported that 8-demethylflavin N_5-oxide oxygenates phenolates at ambient temperature in the dark to give the corresponding quinones *via* the phenoxy radical formed as a result of the initial SET from the phenolates to the *N*-oxide. [J. W. Frost and W. H. Rastetter, *J. Am. Chem. Soc.*, **103**, 5242 (1981)].
11) Recently, it has been pointed out that arene cation radicals give the corresponding arene radicals as a result of deprotonation by a base [*cf.* B. Reitstoen and V. D. Parker, *J. Am. Chem. Soc.*, **112**, 4968 (1990)]. Accordingly, there may be an alternative pathway involving the deprotonation of $\mathbf{4}^{+\cdot}$ by $\mathbf{1}^{-\cdot}$ to give 1- or 2-naphthyl radical and C which couple with each other and then collapse to produce **5** and **2**.
12) For a review, see L. Eberson, "Electron Transfer Reactions in Organic Chemistry," Springer-Verlag, 1987.

Studies on the Constituents of *Scutellaria* Species. XIV.[1] On the Constituents of the Roots and the Leaves of *Scutellaria alpina* L.[2]

Yuichi KIKUCHI,[a] Yukinori MIYAICHI,[a] Yumi YAMAGUCHI,[a] Haruhisa KIZU,[a] Tsuyoshi TOMIMORI*,[a] and Karin VETSCHERA[b]

School of Pharmacy, Hokuriku University,[a] 3 Ho, Kanagawa-machi, Kanazawa, 920-11, Japan and Institut für Pharmakognosie der Universität Wien,[b] Währinger Straße 25, A-1090 Wien, Austria. *Received August 2, 1990*

From *Scutellaria alpina* L., two new flavones (I and II) were isolated, together with eighteen known flavonoids. The structures of I and II were shown to be 5,2′,6′-trihydroxy-6,7,8-trimethoxyflavone and 5,5″,6,6″,7,7″-hexahydroxy-8,8″-biflavone (8,8″-bibaicalein) on the basis of the chemical and spectral data. Compound I has already been synthesized.

Keywords *Scutellaria alpina*; Labiatae; flavonoid; flavone; biflavone; structure elucidation

Scutellaria alpina L. is a perennial herb of the family Labiatae, which is widely distributed in mountains of central and south-central Europe and lowlands of the Ukraine and south-central Russia.[3]

As regards the constituents of the plant, no work has been reported. As part of our studies on the flavonoid constituents of *Scutellaria* species, we have now examined this plant. As described in the experimental section, two new flavones (I and II) were isolated together with eighteen known flavonoids (III—XX) from the ethanol extracts of root and/or leaves of this plant, which was cultivated in Hokuriku University. The present paper deals with their structural determination.

Compound I was obtained from the root as yellow needles, mp 246—247 °C (dec.), $C_{18}H_{16}O_8$, and was positive to the Mg–HCl test. The infrared (IR) spectrum gave absorption bands corresponding to hydroxyl and conjugated carbonyl groups and aromatic rings. Diagnostic shifts in the ultraviolet (UV) spectrum suggested the presence of a hydroxyl at the C-5 position in the flavone nucleus.[4] The proton nuclear magnetic resonance (^{1}H-NMR) spectrum of I showed the presence of three methoxyls (6H, 3.84 ppm; 3H, 4.02 ppm), two hydroxyls (2H, 9.99 ppm), one chelated hydroxyl (12.73 ppm) and one C-3 proton (6.35 ppm). In the aromatic region of the spectrum, the remaining three protons appeared as a doublet (2H, 6.46 ppm, J=8.0 Hz) and a triplet (1H, 7.16 ppm, J=8.0 Hz). These signals could be assigned to C-3′, 5′ and C-4′ protons, respectively, from their chemical shifts and coupling patterns. These findings indicated I to be a trimethyl ether of 5,6,7,8,2′,6′-hexahydroxyflavone.

The positions of the methoxyls were determined from the carbon-13 nuclear magnetic resonance (^{13}C-NMR) spectrum, in which the signals of carbons bearing the three methoxyls appeared downfield at 60.7, 61.5 and 61.8 ppm, respectively, indicating the three methoxyls to be di-*ortho* substituted by two substituents.[5] The methoxyls are, therefore, present at the C-6, C-7 and C-8 positions in the A-ring

From these results, the structure of I was determined to be 5,2′,6′-trihydroxy-6,7,8-trimethoxyflavone. Compound I has already been synthesized,[6] but this is the first report of its isolation from natural sources.

Compound II was obtained from the roots as yellow needles, mp >350 °C, Mg–HCl test (+). It gave the absorption bands of hydroxyl and conjugated carbonyl groups and benzene rings in the IR spectrum. The UV spectrum of II was characteristic of the flavone series, giving absorption maxima at 285 nm and 326 nm.[4] The fast atom bombardment mass spectrum (FAB-MS) of II showed the $[M+H]^+$ peak at m/z 539 as the base peak, although it failed to show the molecular ion peak in the electron impact (EI)-MS.

On methylation with CH_2N_2, II yielded a permethyl ether (IIa), mp 213—214 °C, $FeCl_3$ (−). The high-resolution (HR)-MS of IIa gave the molecular formula $C_{36}H_{30}O_{10}$ [m/z 622.1842 (M^+)]. Thus, the molecular formula of II was determined to be $C_{30}H_{18}O_{10}$.

The ^{1}H-NMR spectrum of II showed seven sets of signals in an integral ratio of 1 : 2 : 1 : 2 : 1 : 1 : 1. This suggests II to be a symmetric biflavone which consists of two monomeric halves of the same elemental composition, $C_{15}H_9O_5$. The ^{13}C-NMR spectra of both II and IIa showed signals which corresponded to just half the number of carbon atoms present in their respective molecular formulae. This is again in conformity with their symmetrical dimeric formulation.

The ^{1}H-NMR spectrum of II showed the presence of four hydroxyls (2H, 9.26 ppm; 2H, 10.17 ppm), two chelated hydroxyls (2H, 12.93 ppm) and two C-3/C-3″ protons (2H, 6.95 ppm). In the aromatic region of the spectrum, the remaining ten protons appeared as two triplets (4H, 7.38 ppm, J=7.3 Hz; 2H, 7.47 ppm, J=7.3 Hz) and a doublet (4H, 7.61 ppm, J=7.3 Hz) due to the B_1- and B_2-ring protons. These data suggested that all the hydroxyls were placed in the A_1- and A_2-rings. This was further supported by the ^{13}C-NMR spectrum of IIa, where the methoxyl carbon signals appeared downfield at 61.5, 61.7 and 62.4 ppm, indicating that these methoxyls were di-*ortho* substituted by two substituents.[5]

The locations of the hydroxyls were determined as follows. The presence of 5/5″-hydroxyls in II was apparent from the ^{1}H-NMR spectrum as mentioned above. In the

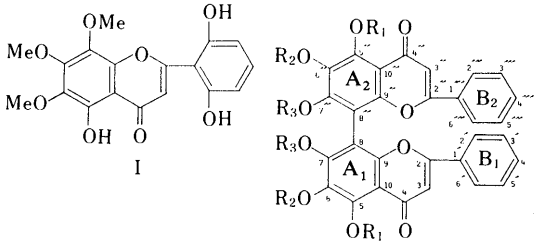

II : R_1=R_2=R_3=H
IIa : R_1=R_2=R_3=Me
IIb : R_1=R_2=Me, R_3=H

Fig. 1

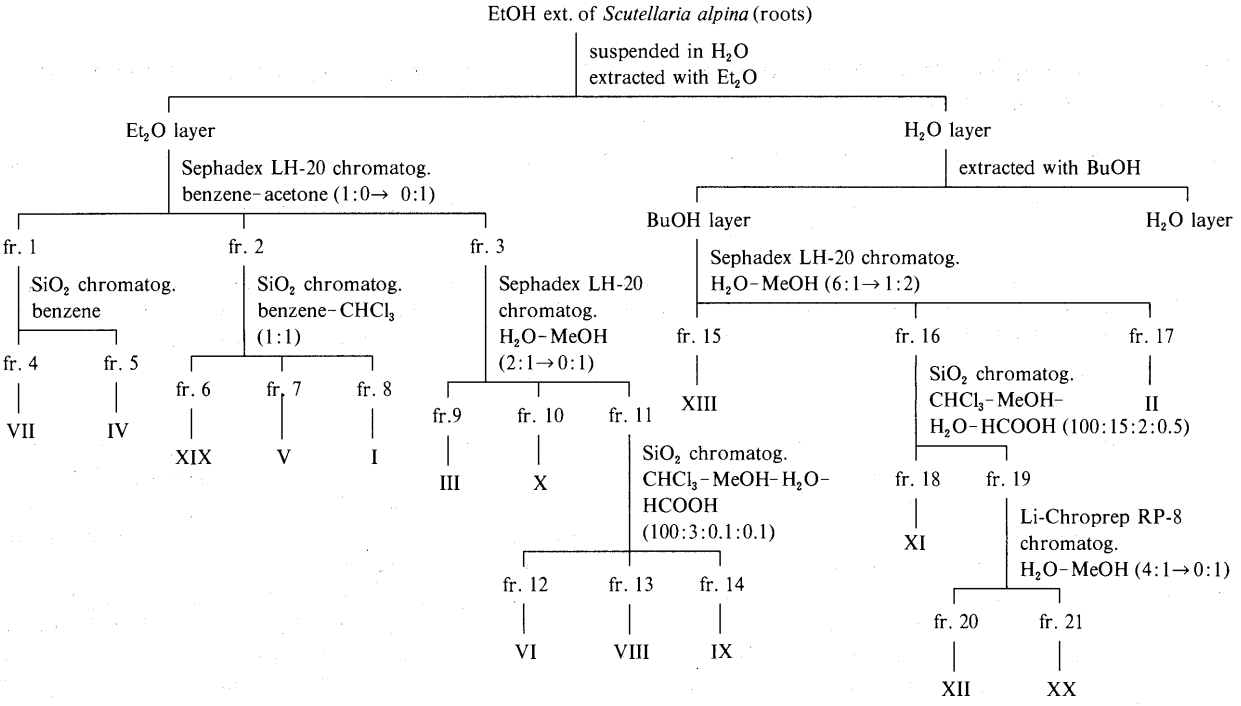

Chart 1

^{1}H-non-decoupling ^{13}C-NMR spectrum of II, the signal at 129.0 ppm was observed as a doublet (J=4.4 Hz), which was transformed into a singlet by irradiation of the chelated hydroxyl protons (12.93 ppm), indicating the presence of hydroxyls at the C-6/C-6″ positions.[7] The 7,7″-biflavone structure could be eliminated because it failed to explain the chemical shift (98.5 ppm) of C-7/C-7″, and the signal at 98.5 ppm was considered to be assigned to the C-8/C-8″ carbons having no hydroxyls. Compound II is, therefore, considered to be an 8,8″-dimer of 5,6,7-trihydroxyflavone. This was further supported by comparing the ^{13}C-NMR spectrum of II with that of 5,6,7-trihydroxyflavone (baicalein,[8] III). The C-8/C-8″, C-7/C-7″ and C-9/C-9″ signals of II were lower by 4.4 ppm, higher by 1.0 ppm and higher by 2.2 ppm, respectively, than the corresponding signals of III. Further, except for these three signals, the signals for all the carbon atoms of II appeared at essentially the same positions as those of the corresponding carbon atoms of III.

The structure of II was finally confirmed synthetically as follows. Oxidative coupling[9] of 5,6-di-*O*-methylbaicalein[10] in the presence of Ag_2O afforded a mixture of more than four compounds. The major compound, easily purified by chromatography, was the 8,8″- dimer of 5,6-di-*O*-methylbaicalein (IIb) as shown by MS, ^{1}H- and ^{13}C-NMR spectra. Compound IIb was methylated with CH_2N_2 to give IIa.

Thus, II was determined to be 5,5″,6,6″,7,7″-hexahydroxy-8,8″-biflavone(8,8″-bibaicalein). There is a pair of atropisomers in the structure II, but the circular dichroism (CD) spectrum revealed II to be a racemate.

Compounds III—XX are known flavones and were identified as baicalein (III),[8] wogonin (IV),[11] skullcapflavone II (V),[12] norwogonin (VI),[11] oroxylin A (VII),[11] scutevulin (VIII),[13] hispidulin (IX),[14] 5,7,4′-trihydroxy-8-methoxyflavone (X),[11] oroxylin A 7-*O*-glucuronide (XI),[15] wogonin 7-*O*-glucuronide (XII)[11] and baicalin (XIII)[8] (from roots);

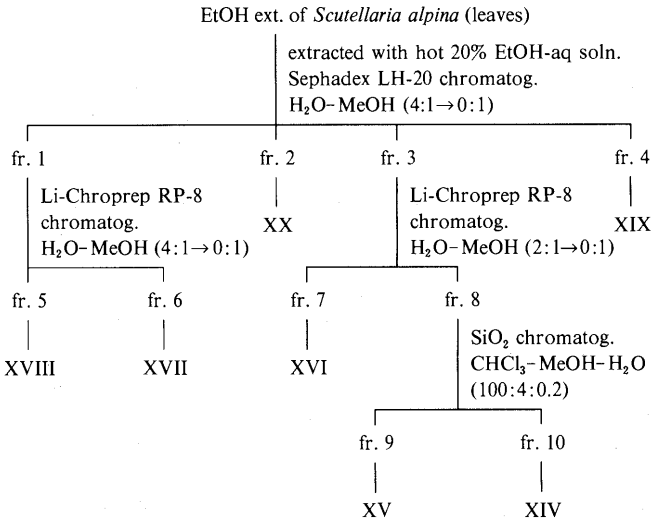

Chart 2

5,7,2′-trihydroxyflavone (XIV),[14] apigenin (XV),[16] scutellarein (XVI),[16] apigenin 7-*O*-glucuronide (XVII),[16] and scutellarin (XVIII)[16] (from leaves); chrysin (XIX),[16] and chrysin 7-*O*-glucuronide (XX)[16] (from both roots and leaves) by direct comparison with authentic samples.

Experimental

General Procedures The instruments were the same as described in the previous paper[1] except for the following. HR-MS were obtained with a JEOL JMS-DX-300 mass spectrometer. Thin layer chromatography (TLC) was carried out on Kieselgel 60F-254 (Merck) with the following solvent systems: $CHCl_3$–MeOH–H_2O–AcOH (100:5:0.2:2) (TLC-1), benzene–dioxane–AcOH (90:22:4) (TLC-2). Spots were detected by spraying dilute H_2SO_4 followed by heating.

Material *Scutellaria alpina* was cultivated in the botanical garden of Hokuriku University for two years, and harvested in September, 1987.

Extraction and Isolation As shown in Charts 1 and 2, fifteen compounds, I (15 mg), II (20 mg), III (60 mg), IV (40 mg), V (25 mg), VI

(10 mg), VII (20 mg), VIII (15 mg), IX (10 mg), X (10 mg), XI (25 mg), XII (50 mg), XIII (100 mg), XIX (30 mg) and XX (40 mg) were obtained from the roots (450 g) and seven compounds, XIV (10 mg), XV (20 mg), XVI (30 mg), XVII (20 mg), XVIII (40 mg), XIX (20 mg) and XX (30 mg), were obtained from the leaves (350 g).

I (5,2′,6′-Trihydroxy-6,7,8-trimethoxyflavone) Yellow needles (MeOH), mp 246—247 °C (dec.). EI-MS *m/z* (%): 360 (M^+, 80), 345 ($M^+ - CH_3$, 100), 211 ($C_9H_7O_6$, 40). HR-MS *m/z*: Found 360.0806, Calcd for $C_{18}H_{16}O_8$ (M^+) 360.0846; Found 345.0612, Calcd for $C_{17}H_{13}O_8$ ($M^+ - CH_3$) 345.0611. *Rf*: 0.41 (TLC-1), 0.48 (TLC-2). UV λ_{max}^{MeOH} nm (log ε): 270 (4.34), 315 (3.95), 355 sh (3.91); $\lambda_{max}^{MeOH-NaOMe}$ nm (log ε): 240 sh (4.37), 265 (4.29), 360 (4.01); $\lambda_{max}^{MeOH-AlCl_3}$ nm (log ε): 280 (4.30), 298 sh (4.20), 335 (4.03), 404 (3.69); $\lambda_{max}^{MeOH-AlCl_3-HCl}$ nm (log ε): 280 (4.30), 295 sh (4.23), 330 (3.97), 406 (3.65); $\lambda_{max}^{MeOH-NaOAc}$ nm (log ε): 269 (4.38), 315 (3.99), 355 sh (3.94). IR ν_{max}^{KBr} cm^{-1}: 3250, 3150 (OH), 1665 (conjugated CO), 1600 (arom. C=C). ^{1}H-NMR (100 MHz in DMSO-d_6): 3.84 (6H, s, $OCH_3 \times 2$), 4.02 (3H, s, OCH_3), 6.35 (1H, s, 3-H), 6.46 (2H, d, J= 8.0 Hz, 3′, 5′-H), 7.16 (1H, t, J=8.0 Hz, 4′-H), 9.99 (2H, s, 2′, 6′-OH), 12.73 (1H, s, 5-OH). ^{13}C-NMR (25 MHz in DMSO-d_6): 162.9 (C-2), 111.9 (C-3), 182.8 (C-4), 148.7 (C-5), 135.9 (C-6), 152.7 (C-7), 132.8 (C-8), 146.5 (C-9), 106.5 (C-10), 108.2 (C-1′), 157.0 (C-2′, 6′), 106.8 (C-3′, 5′), 132.3 (C-4′), 60.7, 61.5, 61.8 ($OCH_3 \times 3$).

II [5,5″,6,6″,7,7″-Hexahydroxy-8,8″-biflavone (8,8″-bibaicalein)] Yellow needles (MeOH), mp >350 °C. EI-MS *m/z* (%): 284 ($C_{16}H_{12}O_5$, 100). FAB-MS *m/z* (%): 539 (M^++H, 100). *Rf*: 0.12 (TLC-1), 0.25 (TLC-2). UV λ_{max}^{MeOH} nm (log ε): 221 (4.62), 241 (4.60), 285 (4.56), 326 (4.28); $\lambda_{max}^{MeOH-NaOMe}$ nm (log ε): 261 (4.64), 376 (4.19); $\lambda_{max}^{MeOH-AlCl_3}$ nm (log ε): 228 (4.58), 253 (4.54), 275 (4.55), 295 sh (4.41), 320 (4.23), 388 (4.37); $\lambda_{max}^{MeOH-AlCl_3-HCl}$ nm (log ε): 228 (4.58), 247 (4.62), 301 (4.47), 350 (4.35); $\lambda_{max}^{MeOH-NaOAc}$ nm (log ε): 261 (4.72), 376 (4.26); $\lambda_{max}^{MeOH-H_3BO_3-NaOAc}$ nm (log ε): 261 (4.66), 376 (4.24). IR ν_{max}^{KBr} cm^{-1}: 3450 (OH), 1650 (conjugated CO), 1610, 1580 (arom. C=C). ^{1}H-NMR (400 MHz in DMSO-d_6): 6.95 (2H, s, 3/3″-H), 7.38 (4H, t, J=7.3 Hz, 3′, 5′/3‴, 5‴-H), 7.47 (2H, t, J=7.3 Hz, 4′/4‴-H), 7.61 (4H, d, J=7.3 Hz, 2′, 6′/2‴, 6‴-H), 9.26 (2H, br s, 6/6″-OH), 10.17 (2H, br s, 7/7″-OH), 12.93 (2H, s, 5/5″-OH). ^{13}C-NMR (100 MHz in DMSO-d_6): 162.7 (C-2/C-2″), 104.3 (C-3/C-3″), 182.3 (C-4/C-4″), 146.5 (C-5/C-5″), 129.0 (d, J=4.4 Hz, C-6/C-6″), 152.8 (C-7/C-7″), 98.5 (C-8/C-8″), 147.8 (C-9/C-9″), 103.9 (C-10/C-10″), 130.8 (C-1′/C-1‴), 125.7 (C-2′, 6′/C-2‴, 6‴), 128.9 (C-3′, 5′/C-3‴, 5‴), 131.7 (C-4′/C-4‴).

Methylation of II II (15 mg) was dissolved in 0.6 ml of *N*,*N*-dimethylformamide (DMF), then CH_3I (0.4 ml) and Ag_2O (100 mg) were added to the solution, and the reaction mixture was left for 14 h with occasional shaking. Then $CHCl_3$ was added, and after removal of the resulting precipitate by filtration, the filtrate was evaporated to dryness. The residue was chromatographed on silica gel using benzene–AcOEt (4 : 1) to give crude IIa, which was recrystallized from MeOH to give IIa (15 mg) as colorless needles, mp 213—214 °C. EI-MS *m/z* (%): 622 (M^+, 45), 607 ($M^+ - CH_3$, 100), 105 (C_7H_5O, 40). HR-MS *m/z*: Found 622.1842, Calcd for $C_{36}H_{30}O_{10}$(M^+) 622.1837; Found: 607.1649, Calcd for $C_{35}H_{27}O_{10}$ ($M^+ - CH_3$) 607.1602. *Rf*: 0.67 (TLC-1), 0.62 (TLC-2). UV λ_{max}^{MeOH} nm (log ε): 218 (4.71), 270 (4.58), 306 (4.48). No change was observed in the spectrum in the presence of NaOMe, NaOAc or $AlCl_3$. IR ν_{max}^{KBr} cm^{-1}: 1648 (conjugated CO), 1582 (arom. C=C). ^{1}H-NMR (400 MHz in $CDCl_3$): 3.87, 4.02, 4.13 (each 6H, each s, $OCH_3 \times 6$), 6.70 (2H, s, 3/3″-H), 7.29 (4H, t, J=7.3 Hz, 3′, 5′/3‴, 5‴-H), 7.39 (2H, t, J=7.3 Hz, 4′/4‴-H), 7.40 (4H, d, J=7.3 Hz, 2′, 6′/2‴, 6‴-H). ^{13}C-NMR (100 MHz in $CDCl_3$): 161.1 (C-2/C-2″), 107.8 (C-3/C-3″), 177.6 (C-4/C-4″), 153.7 (C-5/C-5″), 143.9 (C-6/C-6″), 156.5 (C-7/C-7″), 111.0 (C-8/C-8″), 151.4 (C-9/C-9″), 115.1 (C-10/C-10″), 131.1 (C-1′/C-1‴), 125.6 (C-2′, 6′/C-2‴, 6‴), 128.9 (C-3′, 5′/C-3‴, 5‴), 131.5 (C-4′/C-4‴), 61.5 (C-7/7″-OCH_3), 61.7 (C-6/6″-OCH_3), 62.4 (C-5, 5″-OCH_3).

Synthesis of IIb Ag_2O (2 g) was added to a solution of 7-hydroxy-5,6-dimethoxyflavone (500 mg) in anhydrous benzene (50 ml), and the reaction mixture was heated under reflux on an oil bath for 4 h. After removal of the precipitate, the filtrate was evaporated to dryness and the residue was chromatographed on silica gel with a gradient of benzene–AcOEt (1 : 0→ 1 : 1) to give IIb as colorless needles (MeOH) (40 mg), mp 284 °C (dec.). EI-MS *m/z* (%): 594 (M^+, 45), 579 ($M^+ - CH_3$, 100), 105 (C_7H_5O, 80). HR-MS *m/z*: Found 593.9619 Calcd for $C_{34}H_{26}O_{10}$ (M^+) 594.1527; Found 579.0615, Calcd for $C_{33}H_{23}O_{10}$ ($M^+ - CH_3$) 579.1292. *Rf*: 0.42 (TLC-1), 0.17 (TLC-2). UV λ_{max}^{MeOH} nm (log ε): 218 (4.67), 235 (4.55), 268 (4.55), 317 (4.45); $\lambda_{max}^{MeOH-NaOMe}$ nm (log ε): 248 (4.66), 275 (4.65), 376 (4.27); $\lambda_{max}^{MeOH-AlCl_3}$ nm (log ε): 218 (4.71), 235 (4.63), 268 (4.57), 317 (4.51); $\lambda_{max}^{MeOH-NaOAc}$ nm (log ε): 248 (4.67), 275 (4.63), 345 (4.17); $\lambda_{max}^{MeOH-H_3BO_3-NaOAc}$ nm (log ε): 250 (4.67), 275 sh (4.63), 325 (4.30). IR ν_{max}^{KBr} cm^{-1}: 3420 (OH), 1640 (conjugated CO), 1588 (arom. C=C). ^{1}H-NMR (400 MHz in DMSO-d_6): 3.90, 3.94 (each 6H, each s, OCH_3), 6.78 (2H, s, 3/3″-H), 7.36 (4H, t, J=7.3 Hz, 3′, 5′/3‴, 5‴-H), 7.45 (2H, t, J=7.3 Hz, 4′/4‴-H), 7.56 (4H, d, J=7.3 Hz, 2′, 6′/2‴, 6‴-H), 10.45 (2H, br s, 7/7″-OH). ^{13}C-NMR (100 MHz in DMSO-d_6): 159.6 (C-2/C-2″), 107.1 (C-3/C-3″), 176.0 (C-4/C-4″), 151.7 (C-5/C-5″), 139.4 (C-6/C-6″), 155.1 (C-7/C-7″), 104.8 (C-8/C-8″), 151.7 (C-9/C-9″), 111.0 (C-10/C-10″), 131.0 (C-1′/C-1‴), 125.4 (C-2′, 6′/C-2‴, 6‴), 128.9 (C-3′, 5′/C-3‴, 5‴), 131.4 (C-4′/C-4‴), 61.4, 61.9 (C-5/5″, 6/6″-$OCH_3 \times 4$).

Methylation of IIb IIb was methylated with CH_2N_2 to give a product which was identical (UV, IR, ^{1}H- and ^{13}C-NMR, mixed fusion) with IIa.

Identification of III—XX III (mp 255 °C, dec.), IV (mp 203 °C), V (mp 181 °C, dec.), VI (mp 253 °C, dec.), VII (mp 202 °C, dec.), VIII (mp 278 °C, dec.), IX (mp 291 °C), X (mp 300—302 °C, dec.), XI (mp 173—174 °C, dec.), XII (mp 270 °C, dec.), XIII (mp 230 °C, dec.), XIV (mp 284 °C), XV (350 °C), XVI (mp 345 °C, dec.), XVII (mp 227 °C, dec.), XVIII (mp 360 °C), XIX (mp 285 °C) and XX (mp 226 °C) were identified as baicalein,[8] wogonin,[11] skullcapflavone II,[12] norwogonin,[11] oroxylin A,[11] scutevulin,[13] hispidulin,[14] 5,7,4′-trihydroxy-8-methoxyflavone,[11] oroxylin A 7-*O*-glucuronide,[15] wogonin 7-*O*-glucuronide,[11] baicalin,[8] 5,7,2′-trihydroxyflavone,[14] apigenin,[16] scutellarein,[16] apigenin 7-*O*-glucuronide,[16] scutellarin,[16] chrysin[16] and chrysin 7-*O*-glucuronide,[16] respectively, by direct comparisons with authentic specimens (UV, IR, ^{1}H- and ^{13}C-NMR, mixed fusion).

Acknowledgements We are gratefull to Miss A. Nakashima of this university for MS measurements. Thanks are also due to Mr. M. Yamamoto, botanical garden of this university, for cultivation of *Scutellaria alpina* L.

References and Notes

1) Part XIII: *Chem. Pharm. Bull.*, **38**, 3488 (1990).
2) Presented at the 108th Annual Meeting of the Pharmaceutical Society of Japan, Hiroshima, April 1988.
3) T. G. Tutin, V. H. Heywood, N. A. Burges, D. M. Moore, D. H. Valentine, S. M. Walters, and D. A. Webb, "Flora Europaea," Vol. 3, Cambridge University Press, Cambridge, 1972, p. 135.
4) T. J. Mabry, K. R. Markham and M. B. Thomas, "The Systematic Identification of Flavonoids," Springer-Verlag, New York, 1970, Chapter V.
5) K. S. Dhami and J. B. Stothers, *Can. J. Chem.*, **44**, 2855 (1966); K. Panichpol and P. G. Waterman, *Phytochemistry*, **17**, 1363 (1978).
6) S. Ryu, B. Yoo and B. Ahn, *Arch. Pharm.*, **318**, 659 (1985).
7) Y. Shirataki, I. Yokoe, M. Endo and M. Komatsu, *Chem. Pharm. Bull.*, **33**, 444 (1985); H. Komura, K. Mizukawa, H. Minakata, H. Huang, G. Qin and R. Xu, *ibid.*, **31**, 4206 (1983); H. Komura, K. Mizukawa and H. Minakata, *Bull. Chem. Soc. Jpn.*, **55**, 3053 (1982).
8) Y. Miyaichi, Y. Imoto, H. Kizu and T. Tomimori, *Shoyakugaku Zasshi*, **42**, 204 (1988).
9) E. Morishita and S. Shibata, *Chem. Pharm. Bull.*, **15**, 1772 (1967); T. Ikekawa, *ibid.*, **11**, 749 (1963).
10) C. L. Cheng and T. Y. Chao, *Acta Pharmaceutica Sinica* (薬学学報), **11**, 762 (1964).
11) Y. Miyaichi, Y. Imoto, T. Tomimori and T. Namba, *Chem. Pharm. Bull.*, **36**, 2371 (1988).
12) T. Tomimori, Y. Miyaichi, Y. Imoto, H. Kizu and Y. Tanabe, *Yakugaku Zasshi*, **104**, 524 (1983).
13) Y. Miyaichi, Y. Imoto, T. Tomimori and C. C. Lin, *Chem. Pharm. Bull.*, **35**, 3720 (1987).
14) T. Tomimori, Y. Miyaichi, Y. Imoto and H. Kizu, *Shoyakugaku Zasshi*, **40**, 432 (1986).
15) T. Tomimori, Y. Miyaichi and H. Kizu, *Yakugaku Zasshi*, **102**, 388 (1982).
16) Y. Miyaichi, H. Kizu, T. Tomimori and C. C. Lin, *Chem. Pharm. Bull.*, **37**, 794 (1989).

A Chiral Synthesis of a Unique Secodehydroabietane from Tall Oil

Kaoru FUJI,*[,a] Shang-Zhen ZHENG,[a,1)] Manabu NODE,[b] and Xiao-Jiang HAO[a]

Institute for Chemical Research, Kyoto University,[a] Uji, Kyoto 611, Japan and Kyoto Pharmaceutical University,[b] Yamashina-ku, Kyoto 607, Japan. *Received August 10, 1990*

A total synthesis of naturally occurring (+)-9,10-secoabieta-8,11,13-trien-18,10-olide (1) has been achieved from a chiral building block, (*R*)-2-methyl-2-(2-*E*-nitrovinyl)-5-pentanolide (3).

Keywords asymmetric synthesis; diterpenoid; secoabietane; abietane; total synthesis

In 1977 Conner and Rowe reported the isolation of a novel compound, 9,10-secoabieta-8,11,13-trien-18,10-olide (**1**), from the southern pine tall oil.[2)] Based on a combination of spectral analysis and biogenetic arguments, the relative stereochemistry of **1** was proposed. Unambiguous structure determination including absolute stereochemistry was provided by the conversion of levopimaric acid (**2**) into **1**.[3)]

Here, we report a total synthesis of (+)-**1**. The synthetic scheme utilized 2-(3-isopropylphenyl)ethyl bromide (**6**) prepared from 3-isopropylacetophenone (**4**). The 1,4-addition of a Grignard reagent prepared from **6** to the chiral nitroolefin **3**[4)] proceeded smoothly to afford a 1 : 1 mixture of **7a** and **7b** in 74% yield. Though it was possible to isolate each diastereomer, the mixture was directly used for further transformations. Thus, a three-step sequence involving the treatment with *p*-toluenesulfonic acid (*p*-TsOH) in methanol, mesylation, and substitution with sodium iodide in refluxing acetone provided a mixture **8** in 73% overall yield. Intramolecular alkylation of **8** was followed by the Nef reaction to give **9a** and **9b** in 11 and 51% overall yields from **8**, respectively. The undesired major ketone **9b** was equilibrated by refluxing in methanol with *p*-TsOH to yield approximately a 1.3 : 1 mixture of **9a** and **9b**, from which pure **9a** was isolated in 55% yield. The desired ketone **9a** can be obtained in high yield by recycling through this procedure. Addition of methylmagnesium bromide occurred exclusively from the α-side to afford **10**. Since cyclohexanone **9a** should exist in a chair conformation with the bulky β-arylethyl substituent disposed equatorially, the β-side of the molecule is sterically hindered by an axial methyl group (Fig. 1). Treatment of **10** with a modified polyphosphoric acid[5)] yielded 9,10-secoabieta-8,11,13-trien-18,10-olide (**1**) with inversion of the configuration at C-10. The transformation involves formation of a carbenium ion at C-10 followed by a ring flip to close the lactone ring as shown in Fig. 2.

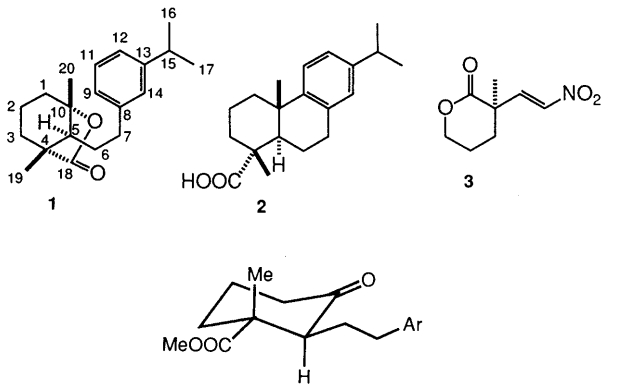

Fig. 1. Conformation of **9a**

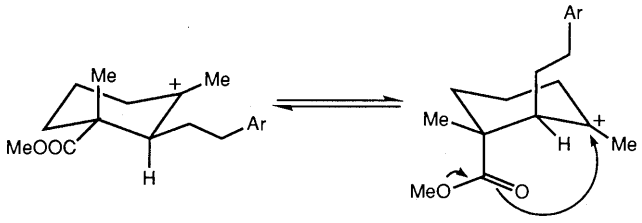

Fig. 2. Ring Flip of Intermediate Carbenium Ion

Experimental

Infrared (IR) spectra were recorded on a JASCO IR-810 spectrophotometer. Proton nuclear magnetic resonance (^{1}H-NMR) spectra were obtained with a Varian Gemini-200 spectrometer in $CDCl_3$ and signals are given in ppm using tetramethylsilane as an internal standard. High-resolution mass spectra (HRMS) were recorded on a JEOL JMS-DX

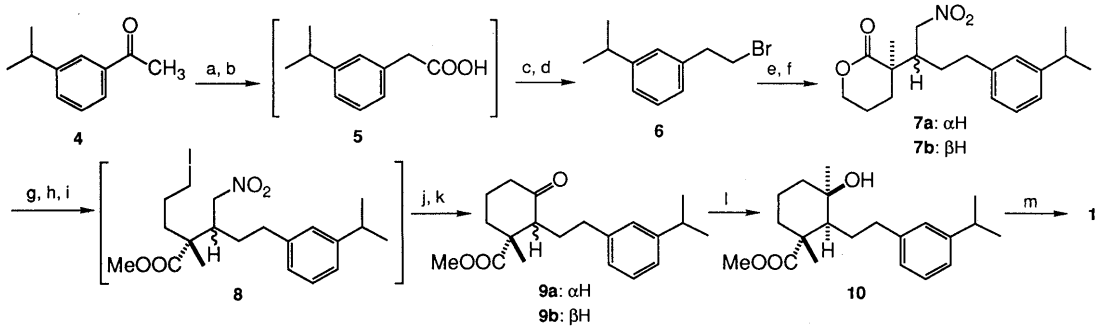

a) morpholine–sulfur b) 10% KOH c) $LiAlH_4$ d) PPh_3–NBS e) Mg f) **3** g) TsOH–MeOH h) MsCl–Et_3N i) NaI j) NaH k) NaOMe–MeOH, then $TiCl_3$ l) MeMgBr m) P_2O_5–$MeSO_3H$

Chart 1

300 mass spectrometer. Optical rotations were recorded on a JASCO DIP-181 polarimeter.

2-(3-Isopropylphenyl)ethyl Bromide (6) A mixture of 3-isopropylacetophenone (**4**)[6] (10.0 g, 62 mmol) and sulfur (4.0 g, 124 mmol) in dry morpholine (27 ml) was refluxed for 36 h, poured into ice-water, and extracted with ethyl acetate. The extract was dried (Na_2SO_4) and evaporated to give an oil that was chromatographed on silica gel (hexane–AcOEt, 5 : 1) to yield the thioamide (12.5 g). Aqueous 10% KOH (180 ml) was added to the thioamide and the mixture was heated under reflux for 36 h. After addition of 10% hydrochloric acid, the reaction mixture was extracted with ethyl acetate. The organic phase was washed twice with brine, dried (Na_2SO_4), and evaporated under reduced pressure to afford a residue, which was chromatographed over silica gel (hexane–benzene, 1 : 1) to give 3-isopropylphenylacetic acid (**5**, 7.7 g, 69% from **4**).

A solution of **5** (10.0 g, 56 mmol) in 300 ml of dry tetrahydrofuran (THF) was treated with 3.2 g (84 mmol) of $LiAlH_4$, and the solution was refluxed for 1 h. Usual extractive work-up yielded an oil (9.4 g), which was dissolved in 270 ml of THF. After addition of PPh_3 (17.7 g, 67 mmol), the mixture was stirred at room temperature for 1 h followed by the addition of *N*-bromosuccinimide (NBS) (12.0 g, 67 mmol). After being stirred for 2 h, the reaction mixture was extracted with dichloromethane. The combined organic phase was washed with brine, dried (Na_2SO_4), and evaporated under reduced pressure to give a crude product. Distillation under reduced pressure afforded 2-(3-isopropylphenyl)ethyl bromide (**6**) (11.2 g, 93%), bp 94—97 °C (3 mmHg). IR $\nu_{max}^{CHCl_3}$ cm^{-1}: 2960, 1600, 1460. ^{1}H-NMR δ: 1.25 (6H, d, J=7 Hz), 2.87 (1H, m), 3.14 (2H, m), 3.56 (2H, t, J=7 Hz), 6.89 (1H, d, J=2 Hz), 7.06 (2H, m), 7.25 (1H, t, J=8 Hz). HRMS *m/z*: Calcd for $C_{11}H_{15}Br$: 226.034. Found: 226.036.

(4*R*,5*S*)-7-(2-Isopropylphenyl)-5-nitromethyl-4,1-heptanecarbolactone (7a) and (4*R*,5*R*)-7-(2-Isopropylphenyl)-5-nitromethyl-4,1-heptanecarbolactone (7b) The Grignard reagent (0.52 M solution in THF, 16.6 ml) prepared from **6**, was added dropwise to a solution of (*R*)-2-methyl-2-(2-nitrovinyl)-5-pentanolide (**3**) (1.16 g, 6.3 mmol) in dry THF (60 ml) at −78 °C. The reaction mixture was stirred for 2 h, poured into aqueous NH_4Cl, and extracted with dichloromethane. The combined organic phase was washed with brine, dried (Na_2SO_4), and evaporated to give an oil, which was purified by passing it through a short silica gel column. Elution with hexane–AcOEt (3 : 1) gave a 1 : 1 mixture of **7a** and **7b** (1.54 g, 74%). A part of the mixture (130 mg) was separated by preparative thin layer chromatography (TLC) (hexane–Et_2O, 2 : 1) to yield **7a** (63 mg) and **7b** (55 mg).

7a: Colorless oil. $[\alpha]_D^{20}$ +17.3 (c=1.43, $CHCl_3$). IR $\nu_{max}^{CHCl_3}$ cm^{-1}: 1720, 1550, 1460, 1260. ^{1}H-NMR δ: 1.24 (6H, d, J=7 Hz), 1.33 (3H, s), 1.50—2.00 (6H, m), 2.75 (2H, m), 2.88 (1H, septet, J=7 Hz), 2.95 (1H, m), 4.15—4.45 (2H, m), 4.35 (1H, dd, J=6, 13 Hz), 4.60 (1H, dd, J=6, 13 Hz), 6.95—7.10 (3H, m), 7.20 (1H, t, J=8 Hz). *Anal.* Calcd for $C_{19}H_{27}NO_4$: C, 68.44; H, 8.16; N, 4.20. Found: C, 68.29; H, 8.33; N, 3.96.

7b: Colorless oil. $[\alpha]_D^{20}$ −8.7° (c=1.24, $CHCl_3$). IR $\nu_{max}^{CHCl_3}$ cm^{-1}: 1720, 1550, 1460, 1260. ^{1}H-NMR δ: 1.22 (6H, d, J=7 Hz), 1.31 (3H, s), 1.50—2.00 (6H, m), 2.35—2.95 (4H, m), 4.20 (1H, dt, J=3, 11 Hz), 4.36 (1H, m), 4.53 (1H, dd, J=6, 13 Hz), 4.92 (1H, dd, J=5, 13 Hz), 6.80—7.10 (3H, m), 7.20 (1H, t, J=8 Hz). *Anal.* Calcd for $C_{19}H_{27}NO_4$: C, 68.44; H, 8.16; N, 4.20. Found: C, 68.08; H, 8.21; N, 4.05.

Methyl (1*R*,2*S*)-2-[2-(2-Isopropylphenyl)ethyl]-1-methyl-4-oxo-1-cyclohexanecarboxylate (9a) and Methyl (1*R*,2*R*)-2-[2-(2-Isopropylphenyl)-ethyl]-1-methyl-4-oxo-1-cyclohexanecarboxylate (9b) Anhydrous *p*-TsOH (91 mg, 0.53 mmol) was added to a stirred solution of the 1 : 1 mixture of **7a** and **7b** (1.5 g, 4.4 mmol) in 60 ml of MeOH, and the solution was refluxed for 10 h. The solvent was removed and the residue was passed through a short column of silica gel with hexane–AcOEt (2 : 1) as an eluent to give 1.56 g of a hydroxy ester. The hydroxyester was dissolved in 80 ml of dichloromethane, and mesyl chloride (0.7 g, 6.2 mmol) was added to the stirred solution. The mixture was stirred at 0 °C for 30 min, then triethylamine (0.6 g, 6.2 mmol) was added and stirring was continued for 1 h. The reaction mixture was poured into ice water and extracted with dichloromethane. The organic phase was washed with brine, dried (Na_2SO_4), and concentrated. The crude product in dry acetone (120 ml) was treated with NaI (6.2 g, 41 mmol), and the mixture was refluxed for 10 h. The reaction mixture was poured into water and extracted with dichloromethane. The combined organic phase was washed with saturated sodium thiosulfate solution and brine, dried (Na_2SO_4), and evaporated to give a crude material, which was purified by short column chromatography over silica gel eluted with hexane–AcOEt (5 : 1) to afford a mixture **8** (1.5 g, 76%).

A solution of **8** (1.1 g, 2.3 mmol) in 20 ml of dry dimethylformamide (DMF) was added to a well-stirred solution of NaH (60%) (380 mg, 9.5 mmol) in 80 ml of dry DMF under nitrogen at 0 °C and stirring was continued for 24 h. After addition of acetic acid (1.5 ml), the solvent was removed under reduced pressure. The residue was partitioned between 2 N HCl and ether. The combined ether phase was washed, dried, and evaporated to give a crude oil, which was passed through a short column of silica gel. Elution with hexane–AcOEt (5 : 1) gave an oil, which was dissolved in dry methanol (20 ml). Sodium methoxide (1 M in MeOH, 2.3 ml) was added and the mixture was stirred for 1 h followed by addition of 20% aqueous $TiCl_3$ (5.4 ml) and ammonium acetate (2.8 g) in water (12 ml) under nitrogen at 0 °C. The reaction mixture was stirred at room temperature for 2 h. After addition of 2 N hydrochloric acid (50 ml), the mixture was extracted with dichloromethane. The organic layer was washed with brine, dried (Na_2SO_4), and evaporated to give a crude product, which was purified by short column chromatography (hexane–AcOEt, 7 : 1), affording 373 mg (81%) of **9b** as a colorless oil. $[\alpha]_D^{20}$ −2.2° (c=2.0, $CHCl_3$). IR $\nu_{max}^{CHCl_3}$ cm^{-1}: 1725, 1230. ^{1}H-NMR δ: 1.21 (6H, d, J=7 Hz), 1.22 (3H, s), 1.50 (1H, m), 1.60—1.90 (4H, m), 2.00—2.50 (5H, m), 2.70 (1H, m), 2.85 (1H, septet, J=7 Hz), 3.60 (3H, s), 6.90—7.04 (3H, m), 7.18 (1H, t, J=8 Hz). HRMS (FAB) *m/z*: Calcd for $C_{20}H_{28}O_3$+H: 317.213. Found: 317.212. Further elution with the same solvent gave 78 mg (17%) of **9a** as a colorless oil. $[\alpha]_D^{20}$ +9.8° (c=1.56, $CHCl_3$). IR $\nu_{max}^{CHCl_3}$ cm^{-1}: 1730, 1720, 1240. ^{1}H-NMR δ: 1.03 (3H, s), 1.15 (1H, m), 1.24 (6H, d, J=7 Hz), 1.68—2.45 (8H, m), 2.70 (1H, m), 2.90 (2H, m), 3.65 (3H, s), 6.90—7.10 (3H, m), 7.21 (1H, t, J=8 Hz). HRMS (FAB) *m/z*: Calcd for $C_{20}H_{28}O_3$+H: 317.214. Found: 317.212.

Conversion of 9b into 9a Anhydrous *p*-TsOH (41 mg, 0.24 mmol) was added to a stirred solution of **9a** (75 mg, 0.24 mmol) in dry MeOH, and the reaction mixture was refluxed for 3.5 h. After removal of the solvent, the residue was purified by preparative TLC with Et_2O–hexane (1 : 1) to give 41 mg (55%) of **9a** together with 32 mg (43%) of recovered **9b**.

Methyl (1*R*,2*S*,3*R*)-1,3-Dimethyl-1-hydroxy-2[2-(2-isopropylphenyl)-ethyl]cyclohexanecarboxylate (10) A stirred solution of **9a** (78 mg, 0.25 mmol) in 20 ml of dry THF was treated with MeMgBr in THF (0.94 M, 0.54 ml) at 0 °C, and the reaction mixture was stirred for 2 h. After addition of 20 ml of saturated NH_4Cl, the mixture was extracted with dichloromethane. The organic layer was washed with brine, dried, and evaporated to give **10** (82 mg, 100%), which was purified by short column chromatography on silica gel eluted with Et_2O. Colorless oil: $[\alpha]_D^{20}$ −12.2° (c=1.64, $CHCl_3$). IR $\nu_{max}^{CHCl_3}$ cm^{-1}: 3600, 1720, 1260. ^{1}H-NMR δ: 1.13 (1H, br s), 1.24 (6H, d, J=7 Hz), 1.26 (3H, s), 1.34 (3H, s), 1.40—1.95 (8H, m), 1.95 (1H, t, J=5 Hz), 2.57 (2H, m), 2.87 (1H, septet, J=7 Hz), 3.67 (3H, s), 6.96—7.07 (3H, m), 7.22 (1H, t, J=7 Hz). HRMS (FAB) *m/z*: Calcd for $C_{21}H_{31}O_2$ $(M-H_2O+H)^+$: 315.233. Found: 315.232.

9,10-Secoabieta-8,11,1-trien-18,10-olide (1) A mixture of P_2O_5 (200 mg), $MeSO_3H$ (1.36 ml), and **10** (74 mg, 0.2 mmol) was stirred for 30 min, then poured into ice-water and extracted with dichloromethane. The combined organic layer was washed with brine, dried (Na_2SO_4), and evaporated to give a residue, which was purified by preparative TLC on silica gel developed with Et_2O–hexane (1 : 3) to give **1** (43 mg, 65%) as a colorless oil. $[\alpha]_D^{20}$ +9.2° (c=1.85, $CHCl_3$) (lit.[3] $[\alpha]_D^{25}$ +9.5° (c=0.11), $CHCl_3$). *Anal.* Calcd for $C_{20}H_{28}O_2$: C, 79.95; H, 9.39. Found: C, 79.92; H, 9.46. Spectroscopic data were identical with the reported data.[3]

References and Notes

1) Visiting researcher from Northwest Normal University, Lanzhou, Gansu, China.
2) A. H. Conner and J. W. Rowe, *Phytochemistry*, **16**, 1777 (1977).
3) W. Herz and S. Mohanraj, *J. Org. Chem.*, **45**, 5417 (1980).
4) *a*) K. Fuji, M. Node, H. Nagasawa, Y. Naniwa, and S. Terade, *J. Am. Chem. Soc.*, **108**, 3855 (1986); *b*) K. Fuji, M. Node, H. Nagasawa, Y. Naniwa, T. Taga, K. Machida, and G. Snatzke, *ibid.*, **111**, 7921 (1989).
5) P. E. Eaton, G. R. Carlson, and J. T. Lee, *J. Org. Chem.*, **38**, 4071 (1973).
6) B. N. Campbell and E. C. Spaeth, *J. Am. Chem. Soc.*, **81**, 5933 (1959).

Clonal Micropropagation of *Gentiana scabra* BUNGE var. *buergeri* MAXIM. and Examination of the Homogeneity Concerning the Gentiopicroside Content

Yoichi YAMADA,[a] Yukihiro SHOYAMA,*[,a] Itsuo NISHIOKA,[a] Hiroshi KOHDA,[b] Akira NAMERA,[b] and Takamitsu OKAMOTO[b]

Faculty of Pharmaceutical Sciences, Kyushu University,[a] Higashiku Fukuoka, Japan and Institute of Pharmaceutical Sciences, Hiroshima University,[b] School of Medicine, 1-2-3 Kasumi, Minami-ku, Hiroshima 734, Japan. *Received June 5, 1990*

When the axillary buds of *Gentiana scabra* BUNGE var. *buergeri* MAXIM. were cultured on Murashige–Skoog (MS) medium supplemented with a combination of gibberellin A_3 (GA) and 6-benzylaminopurine (BAP) (1 mg/l each) at 25 °C under 16 h light conditions for 60 d, the direct multiple shoot formation (18.5 shoots per axillary bud) occurred. The MS medium containing GA–BAP (2.5 mg/l each) mostly stimulated the multiple shoot formation having approximately 71 shoots per tissue in the second subculture of the regenerated shoot. The hormone free MS medium stimulated root formation. These clonally propagated plants were transplanted to vermiculite. Quantitative analysis of gentiopicroside contained in the root of plantlets was carried out by high performance liquid chromatography using *p*-anisic acid as an internal standard. Obviously, the variation of the clonally propagated plants was smaller than that of the cultivated plants bred by morphological selection. From this system, 4.7×10^8 clonally propagated plants can be theoretically obtained from an axillary bud in a year.

Keywords *Gentiana scabra* var. *buergeri*; axillary bud culture; clonal propagation; quantitative analysis; gentiopicroside

It is well-known that *Gentiana* spp. contain a bitter principle, gentiopicroside, and that these roots have been widely used as a stomachic. *Gentiana scabra* var. *buergeri* is a perennial herb of the family Gentianaceae indigenous to Japan. Some differences in the content of gentiopicroside depend on the strain as well as the growth place.[1,2] However, since there has been no survey of the homogeneity of gentiopicroside content in wild strains and in the seasonal variation of gentiopicroside content in individuals, it is still obscure as to whether the difference in content of gentiopicroside depends on individuals or on their ages. Therefore, the breeding of a homogeneous strain with respect to gentiopicroside content is necessary. The homogeneous characteristics of secondary metabolites in the clonally propagated plants have been determined in several species, *e.g. Stevia rebaudiana*,[3] *Bupleurum falcatum*,[4] *Angelica acutiloba*,[5] *Aconitum carmichaeli*,[6] *Rehmannia glutinosa*[7] and *Atractylodes* spp.[8]

In this investigation, the clonal micropropagation of *G. scabra* var. *buergeri* by axillary bud culture will be presented. Furthermore, in order to estimate the homogeneity of the populations, the quantitative analysis of gentiopicroside in the root of clonally propagated plantlets will also be investigated.

Materials and Methods

Plant Materials The cultivated *G. scabra* var. *buergeri* were collected from a field in Iizuka City, Fukuoka Prefecture in March, 1989. The roots of clonally propagated plants were collected from plantlets cultured on hormone free Murashige and Skoog (MS)[9] medium for 3 months. These roots were stored at 0 °C until analysis. The axillary buds for tissue culture were obtained from a cultivated strain in the herbal garden of the Faculty of Pharmaceutical Sciences, Kyushu University in May, 1987 and from cultivated plants in a field in Sakugi, Futamigun, Hiroshima Prefecture in July, 1987.

Tissue Culture Portions of a node (1 cm in length) having axillary buds were removed from one plant, sterilized with 3% sodium hypochlorite solution containing 0.1% Tween 80 for 10 min, then with 70% ethanol for 30 s and finally were thoroughly washed twice with sterilized water. The axillary buds were dissected from the nodes under a binocular microscope. Sections (1.0—2.0 mm in length) had two leaf primordia. The basal medium consisted of MS, and Gamborg B5 (B5)[10] salts supplemented with indoleacetic acid (IAA), indolebutylic acid (IBA), 1-naphthaleneacetic acid (NAA), 6-benzylaminopurine (BAP) and gibberellin A_3 (GA) in the concentrations and combinations indicated in the Tables. Culture conditions were indicated in individual tables. In the initiation stage, 4—5 axillary buds as indicated in Table I were individually cultured for 60 d. In the subculture of shoots propagated in the initial stage, 6—8 shoots, as indicated in Table II, were cultured. In the root forming media, various strengths of IAA, NAA or IBA were used at 25 ± 1 °C under 16 h of light for 60 d.

Quantitative Analysis of Gentiopicroside Gentiopicroside was isolated from the roots of *G. scabra* var. *buergeri* and identified by field-desorption mass (FD-MS) spectrum, and proton nuclear magnetic resonance (^{1}H-NMR) and carbon-13 nuclear magnetic resonance (^{13}C-NMR) spectra of its tetraacetate. These data were as follows. FD-MS *m/z*: 356 $(M)^+$. ^{1}H-NMR (CD_3Cl) δ: 5.44 (d, $J=2$ Hz, C_1-H), 7.40 (d, $J=1$ Hz, C_3-H), 5.66 (ddd, $J=7$, 10, 17 Hz, C_6-H), 5.25 (bd, $J=6$ Hz, C_7-H), 5.57 (brs, C_8-H), 3.30 (d, $J=7$ Hz, C_9-H), 5.19 (brs, C_{10}-H), 5.20 (d, $J=9$ Hz, $C_{1'}$-H), 4.86 (d, $J=8$ Hz, $C_{2'}$-H), 4.96 (t, $J=9$ Hz, $C_{3'}$-H), 5.08 (t, $J=9$ Hz, $C_{4'}$-H), 3.74 (ddd, $J=2$, 5, 11 Hz, $C_{5'}$-H), 4.16 (dd, $J=2$, 12 Hz, $C_{6'}$-H), 4.28 (dd, $J=4$, 12 Hz, $C_{6'}$-H), 2.1, 2.0, 1.9 (CH_3CO). ^{13}C-NMR (CD_3Cl) δ: 116.9 (C-1), 147.7 (C-3), 125.2 (C-4), 132.7 (C-5), 96.1 (C-6), 69.4 (C-7), 96.5 (C-8), 45.1 (C-9), 118.7 (C-10), 104.4 (C-1′), 68.1 (C-2′), 70.4 (C-3′), 72.3 (C-4′), 72.3 (C-5′), 61.7 (C-6′), 163.0 (C=O), 170.6, 170.1, 169.4, 169.1 ($CH_3\underline{C}O$), 20.7, 20.6, 20.5 ($\underline{C}H_3CO$). Quantitative analysis was carried out by high performance liquid chromatography (HPLC) as in the following. The dried root powder (50 mg) was extracted 3 times with MeOH (5 ml) for 15 min under sonication. The solvent was removed *in vacuo*. The residue was dissolved in H_2O (0.5 ml) and injected into SEP-PAK C18 (waters), and washed with H_2O (15 ml), and then eluted with 50% MeOH (15 ml). The eluate was evaporated *in vacuo*. The residue was dissolved in the mobile phase, and an internal standard (*p*-anisic acid; 0.25 mg/ml) solution (2 ml) was added and injected into HPLC. Analyses were performed on a Gasukuro Kogyo Model 576 HPLC which was connected with an Inatosil ODS (4.6 × 250 mm, Toso) and equipped with a variable wave length detector (detection set at 265 nm). The mobile phase was the mixture of 0.01 M AcONa (pH 4.6)–MeOH (1 : 1). Gentiopicroside (2.10 mg) was dissolved in the mobile phase solution, diluted stepwise, and *p*-anisic acid solution (0.25 mg/ml) (1 ml) was added, and the 10 μl portions were injected into HPLC twice. The calibration plots were obtained from the ratio of peak heights of *p*-anisic acid and gentiopicroside as indicated in Fig. 3. In this procedure, the recovery of gentiopicroside was found to be 96.7%.

Results and Discussion

The effect of GA–BAP on shoot formation from axillary buds is shown in Table I. All combinations of GA and BAP stimulated shoot formation, especially 1 mg/l GA and 1 mg/l BAP gave direct multiple shoot complexes having an average of 18.5 shoots per tip during a 60-day-culture. The addition of IAA and BAP to the medium gave shoot

TABLE I. Multiple Shoot Formation from Axillary Bud

Hormone (mg/l)		Shoot No. per culture	Multiple shoot forming culture	Fresh weight (mg)
GA	BAP			
0.1	0.1	8.8	4/5	224
0.1	0.5	8.0	3/5	282
0.1	1.0	11.8	4/5	388
0.5	0.1	9.0	3/4	346
0.5	0.5	6.5	3/4	332
0.5	1.0	8.0	3/4	225
1.0	0.1	13.3	3/4	456
1.0	1.0	18.5	4/4	509

Culture condition: MS medium, 25±1 °C, 16 h light, 60 d.

TABLE II. Multiple Shoot Formation from Axillary Bud

Hormone (mg/l)		Shoot No. per culture	Hormone (mg/l)		Shoot No. per culture
IAA	BAP		NAA	BAP	
0.1	0.1	3.2	0.1	0.1	4.3
0.1	1.0	3.0	0.1	1.0	6.0
0.5	0.1	2.8	0.5	0.1	3.3[a]
0.5	1.0	2.8	0.5	1.0	9.5
1.0	0.1	2.8	1.0	0.1	1.3[a]
1.0	1.0	2.5	1.0	1.0	11.0

Culture condition: MS medium, 25±1 °C, 16 h light, 60 d. *a*) Callus forming segment.

TABLE III. Multiple Shoot Formation from Regenerated Shoot

Hormone (mg/l)		Multiple shoot forming culture	Shoot No. per culture	Fresh weight (mg)
GA	BAP			
0.5	2.5	6/6	54.5	1128
0.5	5.0	7/7	38.6	973
1.0	2.5	8/8	63.8	1105
1.0	5.0	8/8	42.3	966
2.5	2.5	7/7	70.7	2097
2.5	5.0	6/6	44.0	1323

Culture condition: MS medium, 25±1 °C, 16 h light, 60 d.

TABLE IV. Root Formation of Shoot Propagated

Hormone (mg/l)		Root No. per culture	Root forming culture	Fresh weight (mg)
NAA	0.1	4.3	4/6[a]	487
	1.0	9.1	6/7[a]	263
IAA	0.5	6.4	8/10	841
	1.0	4.2	7/10	315
IBA	0.5	3.4	4/8	470
	1.0	3.6	4/8	445
FH[b]		10.7	19/20	895

Culture condition: MS medium, 25±1 °C, 16 h light, 60 d. *a*) Callus formation. *b*) Hormone free medium.

formation, however, the multiplication ratio was low (Table II). The supplement of NAA and BAP was much better than the combination of IAA and BAP (Table II), although callus formation occurred at the base of a shoot.

In order to accelerate multiple shoot formation, in the second stage the shoots propagated were transferred to a new medium supplemented with higher concentrations of

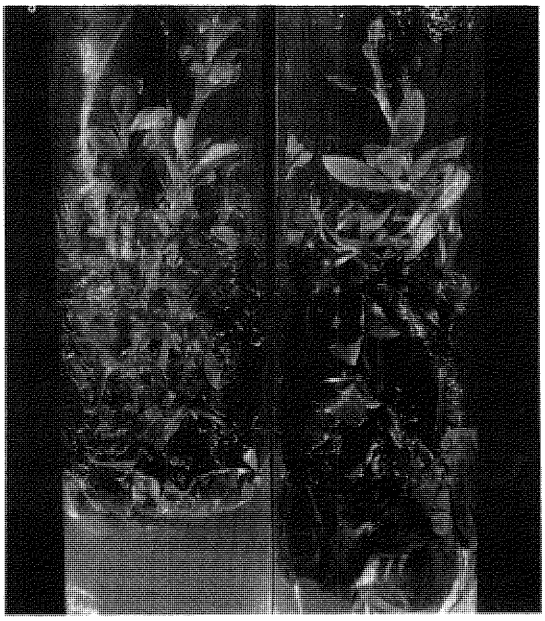

Fig. 1. Multiple Shoot Formation from Regenerated Shoot

Fig. 2. Root Formation of Shoot Propagated

GA and BAP as shown in Table III, since the addition of 1 mg/l GA and 1 mg/l BAP stimulated the multiple shoot formation in the first stage. During a 60-day-culture the base of shoot growth manifested multiple complexes and finally produced multiple shoots. The medium containing GA–BAP (2.5 mg/l each) mostly stimulated the multiple shoot formation having approximately 71 shoots per culture as shown in Fig. 1. This multiplication rate was constantly obtained for several generations. On the other hand, abnormal shoot formation occasionally occurred during culture on the medium supplemented with concentrations of GA higher than 2.5 mg/l and BAP. Therefore, the medium containing GA–BAP (2.5 mg/l each) can be routinely used for the micropropagation system.

In order to determine the suitable basal medium and effective hormone for rooting, the MS media containing

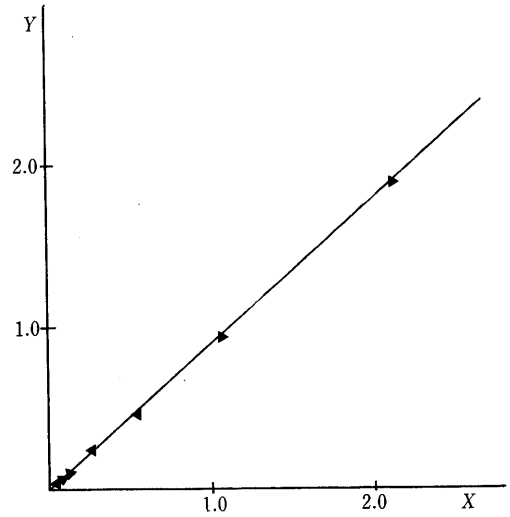

Fig. 3. Calibration Curve of Gentiopicroside

$Y=0.8966x-0.0011$ ($\gamma=0.9999$). X: content ratio (gentiopicroside/*p*-anisic acid). Y: peak height ratio.

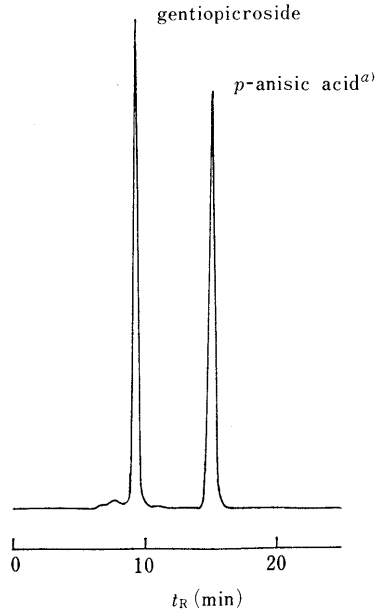

Fig. 4. Chromatogram of HPLC for Quantitative Analysis of Gentiopicroside and *p*-Anisic Acid

HPLC conditions: Column, Inertosil ODS (4.6×250 mm). Mobile phase, 0.1 M AcONa (pH 4.6): MeOH = 1.1. Flow rate, 0.5 ml/min. Detection, 265 nm. *a*) Internal standard.

IAA, NAA and IBA or without hormone were tested on shoots propagated at 25 °C under 16 h of light for 60 d (Table IV). It was found that the MS medium supplemented with 0.5 mg/l IAA promoted root formation (80%). On the other hand, the addition of NAA to the medium stimulated callus formation. The hormone free medium also stimulated rooting. The ratio was 95% and the growth of plant was good as indicated by the fresh weight in Table IV and in Fig. 2. Therefore, this medium can be used as a root-forming medium. These clonally propagated plants were completely transplanted to vermiculite.

Quantitative analysis of gentiopicroside was carried out by HPLC using *p*-anisic acid as an internal standard. The calibration curve was quite linear (Fig. 3), showing that the recovery was complete. The chromatogram for quantitative analysis of gentiopicroside is also shown in Fig. 4.

TABLE V. Gentiopicroside Contents of Clonally Propagated Plantlets (1) and Cultivated Strain (2) of *Gentiana scabra* var. *buergeri*

Material	*N*	% of dry weight	% of C.V.[a)]
1[b)]	30	8.07±0.91[c)]	11.3
2	25	11.72±2.21	18.8

a) Coefficient of variation. *b*) Cultured on the hormone free MS medium for 90 d. *c*) Significantly different from the cultivated strain, $p<0.01$.

Table V shows the content of gentiopicroside and the coefficient of variation in the roots of clonally propagated plantlets derived from a single original plant and of the cultivated strains which were sexually propagated from seeds. A homogeneous tendency was observed in the clonally propagated plants with respect to the gentiopicroside content when compared on the basis of the coefficient of variation although differences in the coefficient of variation were not statistically significant. The cultivated strain has been bred by sexual selections concerning flower color, flower shape, flower period and/or plant height. Therefore, the breeding of a homogeneous strain of *G. scabra* var. *buergeri* concerning the gentiopicroside content may be difficult by morphological selection.

Regeneration from the tip tissue culture of *G. scabra* var. *buergeri* has been previously presented.[11,12] Maruta *et al.*[11] reported that the supplement of 0.1 mg/l NAA and 7.5 mg/l BAP to the MS medium mostly stimulated multiplication of tip tissue at a rate of 7 shoots per culture. The authors have succeeded in improving approximately 10 times the multiplication rate when shoots were cultured on a medium containing 2.5 mg/l GA and 2.5 mg/l BAP as already discussed. Significant differences in the multiplication rate may occur depending on the synergistic effect of GA and BAP supplemented in the medium. In this micropropagation system, 4.7×10^8 clonally propagated plants can be theoretically gained from an axillary bud in a year. This procedure could be utilized to facilitate a large-scale cultivation of homogeneous plant of *G. scabra* var. *buergeri*.

Acknowledgements The authors wish to thank Mr. T. Yokoyama for the donation of roots of *G. scabra* var. *buergeri* cultivated.

References and Notes

1) T. Hayashi, *Yakugaku Zasshi*, **96**, 356 (1976).
2) T. Saito, N. Kikuchi, O. Itsukaichi, A. Kumagai, and T. Sugawara, Abstracts of Papers, The 17th Shoyaku Bunseki Toronkai, 1988, p. 43.
3) Y. Tamura, S. Nakamura, H. Fukui, and M. Tabata, *Plant Cell Rep.*, **3**, 180 (1984).
4) N. Hiraoka, T. Kodama, M. Oyanagi, S. Nakano, Y. Tomita, N. Yamada, O. Iida, and M. Satake, *Plant Cell Rep.*, **5**, 319 (1986).
5) Y. Miura, H. Fukui, and M. Tabata, *Planta Medica*, **54**, 79 (1988).
6) K. Hatano, Y. Shoyama, and I. Nishioka, *Planta Medica*, **54**, 152 (1988).
7) M. Matsumoto, Y. Shoyama, I. Nishioka, H. Iwai, and S. Wakimoto, *Plant Cell Rep.*, **7**, 636 (1989).
8) K. Hatano, Y. Shoyama, and I. Nishioka, *Planta Medica*, **56**, 131 (1990).
9) T. Murashige and F. Skoog, *Physiol. Plant*, **15**, 437 (1962).
10) O. L. Gamborg, R. A. Miller, and K. Ojima, *Exp. Cell. Res.*, **50**, 151 (1968).
11) I. Maruta, S. Kiyone, and E. Matsumoto, *Bull. Nagano Veg. Ornam. Crops Exp. Sta. Jpn.*, **5**, 57 (1989).
12) I. Tazawa, T. Abe, and T. Sasagara, *Ikushugaku Zasshi*, **39**, Suppl. (1), 72 (1989).

Studies on Agalwood (Jinkō). X. Structures of 2-(2-Phenylethyl)chromone Derivatives

Tenji KONISHI,[a] Kiyoshi IWAGOE,[a] Akira SUGIMOTO,[a] Shiu KIYOSAWA,*[,a] Yasuhiro FUJIWARA,[a] and Yasuo SHIMADA[b]

Kyoto Pharmaceutical University,[a] Nakauchi-cho, Misasagi, Yamashina-ku, Kyoto 607, Japan and Mitsuboshi Seiyaku Company,[b] 153, Gose-shi, Nara 639–22, Japan. *Received July 6, 1990*

Three new kinds of phenylethylchromone derivatives, called AH_{17}, AH_{20} and AH_{23}, were isolated from acetone and pyridine extracts of agalwood (Jinkō) from Kalimantan. The structures of AH_{17} and AH_{23} were characterized as 5α,6β,7β-trihydroxy-8α-methoxy-2-(2-phenylethyl)-5,6,7,8-tetrahydrochromone and 5α,6β,7β,8α-tetrahydroxy-2-[2-(2-hydroxyphenyl)ethyl]5,6,7,8-tetrahydrochromone, respectively. AH_{20} was found to be a trimer formed by the ether-linkage made of 2-(2-phenylethyl)chromone and 2 mol of agarotetrol at $C_{5,8'}$ and $C_{6,5'}$.

Keywords 2-(2-phenylethyl)chromone; agalwood; Aquilariaceae; ^{1}H-NMR; ^{13}C-NMR; NOE

In previous papers of this series[1] it was reported that acetone and pyridine extracts of agalwood (Jinkō) from Kalimantan contained various 2-(2-phenylethyl)chromone derivatives such as hydroxylates, methoxylates and hydrogenates, and the dimers and trimers of a 2-(2-phenylethyl)-chromone unit, formed by C–C or ether-linkage.

This paper deals with the isolation and characterization of three new additional minor constituents from the acetone and pyridine extracts, tentatively called H_{17}, AH_{20} and AH_{23}. The procedure of isolation is described in the experimental section.

AH_{17} (**1**), a white powder, $C_{18}H_{20}O_6$, $[\alpha]_D$ +1.94°, exhibited absorption bands due to a phenylethyl group and a trisubstituted γ-pyrone ring in the infrared (IR) and ultraviolet (UV) spectra. The proton nuclear magnetic resonance (^{1}H-NMR) spectrum of **1** showed four methine proton signals due to the cyclohexenyl moiety together with those of a methoxy and three hydroxy protons. These protons were assigned based on comparison with the data for agarotetrol as shown in Table I. Acetylation of **1** afforded a triacetate (**3**), the ^{1}H-NMR spectrum of which showed acetylation shifts of C_5, C_6 and C_7-H, but no shift of C_8. Therefore, the methoxy group was assigned to be linked at C_8. This was also supported by the C_8 signal at δ 70.17 which showed a low field shift of about 3 ppm, compared with that of agarotetrol in the carbon-13 nuclear magnetic resonance (^{13}C-NMR) spectrum of **1**.

Accordingly, AH_{17} was suggested to be 5α,6β,7β-trihydroxy-8α-methoxy-2-(2-phenylethyl)chromone, **1**.

AH_{23} (**4**), colorless needles, $C_{17}H_{18}O_7$, mp 143—145 °C, was also thought to be a 2-(2-phenylethyl)-5,6,7,8-tetrahydrochromone derivative based on the UV and IR spectra. The ^{1}H-NMR spectrum of **4** showed that the signal pattern of the four methine protons attached to the cyclohexenyl ring was analogous to that of agalotetrol, and their chemical shifts and coupling constants were in fairly good accord with those of **2**, as shown in Table I. The peracetate (**5**) derived from **4** by treatment with acetic anhydride and pyridine showed the presence of five acetoxy groups at δ 2.06, 2.09, 2.09, 2.17 and 2.34 ppm. The signal at δ 2.34

TABLE I. ^{1}H-NMR Spectral Data for AH_{17}, AH_{23} and AH_{20} (δ in DMSO-d_6)

	AH_{17} (**1**)	AH_{23} (**4**)	AH_{20} (**6**)		
			Unit A	Unit B	Unit C
5-H	4.32 dd (J=8.1, 6.6)	4.31 d (J=7.3)	5.31 d (J=8.3)	4.87 d (J=7.7)	
6-H	3.74 ddd (J=8.1, 5.9, 2.1)	3.84 dd (J=7.3, 2.0)	4.36 dd (J=8.3, 2.1)	4.96 dd (J=7.7, 1.9)	7.46 d (6′-H) (J=9.3)
7-H	3.93 ddd (J=3.8, 3.7, 2.1)	3.75 dd (J=3.8, 2.0)	3.91 dd (J=3.2, 2.1)	3.98 dd (J=3.7, 1.9)	7.88 d (7′-H) (J=9.3)
8-H	4.14 d (J=3.7)	4.49 d (J=3.8)	4.58 d (J=3.2)	4.60 d (J=3.7)	
5-OH	5.83 d (J=6.6)				
6-OH	5.18 d (J=5.9)				
7-OH	5.09 d (J=3.8)				
3-H	6.10 s	6.09 s	6.12 s, 6.16 s, 6.20 s[a]		
CH_2CH_2	2.87 m ($C_{7''}$) 2.96 m ($C_{8''}$)	2.81 m ($C_{7''}$) 2.88 m ($C_{8''}$)	2.62, 2.68, 2.86, 2.94[a] (each m, 2H), 3.00 (m, 4H)		
C_6H_5	7.24 m (1H) 7.26 m (4H)	6.71 dt (4″-H) 6.80 dd (3″-H) 7.02 dt (5″-H) 7.08 dd (6″-H) (each J=7.5, 1.5)	7.02 (m, 2H), 7.20, 7.27 (m, 13H)[a]		
CH_3O	3.36 s				

a) Individual assignments of units A, B and C are difficult.

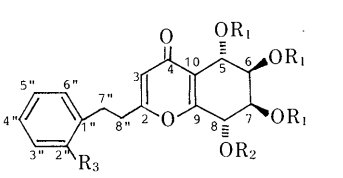

1 : $R_1=R_3=H$, $R_2=CH_3$
2 : $R_1=R_2=R_3=H$
3 : $R_1=CH_3CO$, $R_2=CH_3$, $R_3=H$
4 : $R_1=R_2=H$, $R_3=OH$
5 : $R_1=R_2=CH_3CO$, $R_3=CH_3COO$

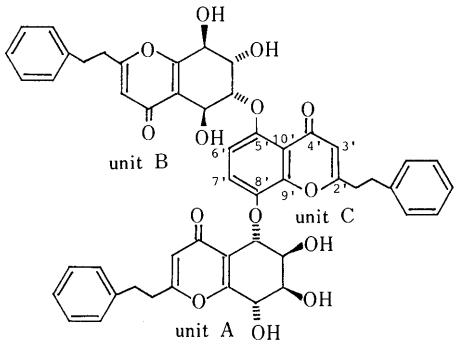

6

Chart 1

TABLE II. ^{13}C-NMR Spectral Data for AH_{17}, AH_{23} and AH_{20}[a]

Carbon	AH_{17}	AH_{23}	AH_{20}		
			Unit A	Unit B	Unit C
2,2′	168.20	168.30	167.82, 167.82, 167.97[b]		
3,3′	113.54	112.34	112.75, 112.95, 110.17[b]		
4,4′	179.60	178.38	177.94, 177.96, 178.31[b]		
5,5′	71.37	68.32	77.87	66.97	151.77
6,6′	72.91	70.59	68.62	82.88	113.63
7,7′	75.47	72.59	72.86	70.33	123.02
8,8′	70.17	64.61	64.35	63.39	144.47
9,9′	169.29	163.00	159.58, 161.75[b]		149.51
10,10′	120.53	120.64	120.34, 121.69[b]		117.98
1″	140.43	125.96	139.76, 139.88, 139.96[b]		
2″	128.83	155.00	128.31	128.31	128.31
3″	128.56	114.79	128.21	128.21	128.21
4″	126.63	127.23	126.01, 126.10, 126.17[b]		
5″	128.56	118.81	128.21	128.21	128.21
6″	128.83	129.60	128.31	128.31	128.31
7″	35.15	26.72	34.02, 34.08, 34.21[b]		
8″	32.74	32.24	31.62, 31.62, 31.76[b]		
CH_3O	58.93				

a) Assignments were based on the results of ^{1}H-^{13}C-COSY. b) Individual assignments of units A, B and C are difficult.

was assigned to the acetoxyl function linked to the phenyl group because it is further downfield than the other acetoxy groups. The observed values of the phenylethyl carbon signals in the ^{13}C-NMR spectrum were in close agreement with those values of AH_{2b}, the 1′-hydroxyl derivative of isoagarotetrol taking the solution effect into account.[1c]

Accordingly, AH_{23} was characterized as 5α,6β,7β,8α-tetrahydroxy-2-[2-(2-hydroxyphenyl)ethyl]5,6,7,8-tetrahydrochromone, **4**.

AH_{20} (**6**), a white powder, $[\alpha]_D$ −27.83°, showed a molecular ion at *m/z* 882 in the field desorption-mass spectrum (FD-MS) giving the molecular formula $C_{51}H_{46}O_{14}$. The IR and UV spectra of **6** exhibited strong absorption maxima due to a γ-pyrone ring. The ^{1}H-NMR spectrum showed the presence of three proton signals at δ 6.12, 6.16 and 6.20, and three sets of phenylethyl groups, indicating the tri-2-(2-phenylethyl)-chromone derivative for **6**, considering molecular weight. Two units of the trimer, units A and B, appeared to be 5,6,7,8-tetrahydroxyphenylethylchromone derivatives based on the presence of two sets of four methine proton signals which were assigned by ^{1}H selective irradiation. Unit A was characterized as agarotetrol linked at C_5 by the ether bond to another monomeric unit (unit C), based on the four vicinal methine protons which showed analogous chemical shifts and coupling systems to those of AH_{10}, AH_{15} and AH_{18}.[1d,e] Likewise, unit B was suggested to be agarotetrol formed an ether-linkage at C_6 to unit C because of the low field displacement of 6-H, about 0.6 ppm compared with that of unit A (Table I). It appears that the structure of unit C is 5,8-dialkoxy-2-(2-phenylethyl)chromone, based on the two doublet proton signals assumed to be located at the C_6 and C_7 positions of the chromone ring. The structure was supported by the ^{13}C-NMR spectrum, indicating a similar sequence of the carbon signals in the chromone ring to those of AH_7, 5,8-dihydroxy-2-(2-phenylethyl)chromone (Table II).[1f] Their assignments were confirmed by the analyses of ^{1}H–^{13}C correlation spectroscopy (COSY). In order to determine the positions of two ether-linkages among units A, B and C, **6** was subjected to measurement of the nuclear Overhauser effect (NOE) difference values. Irradiation of 5-H at δ 5.31 resulted in an appreciable NOE increase of the 7′-H at δ 7.88, and NOE was detected between the 7-H at δ 3.98 and 6′-H at δ 7.46. Therefore, it was found that units A and B were linked to unit C by ether bonds at $C_{5,8'}$ and $C_{6,5'}$ positions, respectively.

Accordingly, AH_{20} was characterized as the trimer **6**.

AH_{17} is the first example of the methoxy function in the hexenyl ring of the polyoxy 2-(2-phenylethyl)chromone derivatives, agarotetrol and isoagarotetrol.[1b] It is said that the cyclohexenyl moiety of agarotetrol has 5e′-OH group in contrast to its 5-O-acetate, in which the 5-OH group is a′ configuration because of the intramolecular hydrogen bonding and the steric and electrostatic repulsions between the pyrone carbonyl and the 5-OAc function.[2] But the interconversion of 5e′-OH and 5a′-OAc did not accompany in the cyclohexenyl moiety of **1** and **3** as shown in the ^{1}H-NMR spectra. Therefore, the conformational change in the cyclohexenyl moiety of 2-(2-phenylethyl)-5,6,7,8-tetrahydrochromones is thought to depend delicately on the other substituent groups at C_6, C_7 and C_8 positions together with the relationship between the γ-pyrone carbonyl and the 5-OH function. The hydroxylation at C_2 position of the phenylethyl group as shown in AH_{23} has also been found in the structures of AH_9[1f] and AH_{2b}.[1c] AH_{20} is specific for the ether-linkage at $C_{6,5'}$ and $C_{5,8'}$ between each unit of the two agarotetrols and 2-(2-phenylethyl)-chromone.

Experimental

Melting points were determined on a micro melting point apparatus (Yanagimoto) and are uncorrected. The UV spectra were obtained in MeOH with a Shimadzu UV-200s spectrometer, and IR spectra (in KBr disks and $CHCl_3$) with a Shimadzu IR 27G spectrometer. The ^1H (300.0 MHz) and ^{13}C (75.4 MHz) NMR spectra were taken on a Varian XL-300 spectrometer in dimethyl sulfoxide-d_6 (DMSO-d_6) and $CDCl_3$ solutions. Chemical shifts are given in δ (ppm) with tetramethylsilane as an internal standard (s, singlet; d, doublet; t, triplet; dd, double doublet; ddd, double double doublet; m, multiplet; br, broad).

Column chromatographies were performed on Kieselgel 60 (70—230 mesh, Merck), Kiesel 60 silanisiert (70—230 mesh, Merck), Sephadex LH-20 (Pharmacia Fine Chemicals), and LiChroprep Rp-8 (40—63 mesh) pre-packed column (Merck).

Isolation of AH_{17}, AH_{20} and AH_{23} The fraction $B^{1g)}$ (650 mg) was subjected to column chromatography ($CHCl_3$–MeOH, 9 : 1 v/v) to give crude AH_{16} (65 mg), AH_{17} (62 mg) and a residue. AH_{17} (40 mg) was obtained as colorless needles from the crude fraction which was further chromatographed on a column of Sephadex LH-20 (MeOH). A pyridine extract (300 g) from residue-$2^{1a)}$ was refluxed with MeOH to obtain a viscous extract (56.5 g) which on silica gel column chromatography ($CHCl_3$–MeOH–H_2O, 90 : 10 : 1 v/v) gave four fractions, fr_1 (8.6 g), fr_2 (11.1 g), fr_3 (7.7 g) and fr_4 (18.5 g). Fr_4 (18.5 g) was chromatographed on Sephadex LH-20 (MeOH) followed by LiChroprep Rp-8 (MeOH–H_2O, 7 : 3 v/v) to yield AH_{23} fraction (211 mg). AH_{23} (18 mg) was obtained as colorless needles by repeated column chromatography on silica gel ($CHCl_3$–MeOH–H_2O, 8 : 2 : 0.2 v/v).

AH_{17} (1) A white powder, (mp 130—135 °C), $[\alpha]_D$ +1.94 (c = 1.03, MeOH). UV λ_{max}^{MeOH} nm (ε): 207 (18216), 252 (13678). IR (KBr, cm^{-1}): 3360 (OH), 1658, 1600 (γ-pyrone ring). ^1H- and ^{13}C-NMR: Tables I and II. FD-MS m/z: 332 (M^+), 302 ($M^+ - H_2O$). *Anal.* Calcd for $C_{18}H_{20}O_6 \cdot 2/3H_2O$: C, 62.78; H, 6.24. Found: C, 62.72; H, 6.07.

Acetylation of 1 A mixture of Ac_2O–pyridine (1 : 1 v/v, 2 ml) and **1** (10.3 mg) was allowed to stand for a day at room temperature, and evaporated to dryness under reduced pressure. The residue was purified by column chromatography (hexane–AcOEt, 2 : 1 v/v) to give **3** (9.5 mg) as a white powder. $[\alpha]_D$ −104.8° (c = 1.03, $CHCl_3$). UV λ_{max}^{MeOH} nm (ε): 202 (21984), 243 (11816). IR ($CHCl_3$) cm^{-1}: 1752 (ester), 1665, 1625 (γ-pyrone ring). ^1H-NMR ($CDCl_3$, 80 MHz): 2.04 (s, 6H, $CH_3CO \times 2$), 2.16 (s, 3H, CH_3CO), 2.86 (m, 4H, CH_2CH_2), 3.59 (s, 3H, CH_3O), 4.45 (d, J = 3.3 Hz, 8-H), 5.58 (dd, J = 3.3, 2.5 Hz, 7-H), 5.61 (dd, J = 8.5, 2.5 Hz, 6-H), 6.11 (d, J = 8.5 Hz, 5-H), 6.13 (s, 3-H), 7.25 (m, 5H, aromatic H). Atmospherie pressure ionization-mass spectrum (API-MS) m/z: 459 $[M+H]^+$ (100%).

AH_{23} (4) Colorless needles, mp 143—145 °C. UV λ_{max}^{MeOH} nm (ε): 210 (12846), 246 (9653). IR (KBr) cm^{-1}: 3355 (OH), 1645, 1560 (γ-pyrone ring), 1222, 1095, 1010, 982, 740 (1,2-disubstituted benzene). ^1H- and ^{13}C-NMR: Tables I and II. API-MS m/z: 335.2 $[M+H]^+$ (100%).

Acetylation of 4 **4** (11 mg) was acetylated in the same manner as described for **1** to give an acetate (**5**, 9 mg) as a white powder. (mp 72—74 °C), $[\alpha]_D$ −17.4° (c = 1.09, MeOH). UV λ_{max}^{MeOH} nm (ε): 243 (14416). IR ($CHCl_3$) cm^{-1}: 1755 (ester), 1670, 1632 (γ-pyrone ring). ^1H-NMR ($CDCl_3$, 80 MHz): 2.06, 2.09, 2.09, 2.17, 2.34 (each s, CH_3CO), 2.80 (m, 4H, CH_2CH_2), 5.49 (dd, J = 7.9, 2.5 Hz, 7-H), 5.50 (dd, J = 3.3, 2.5 Hz, 6-H), 5.99 (s, 3-H), 6.11 (d, J = 3.3 Hz, 5-H), 6.18 (d, J = 7.9 Hz, 8-H), 7.26 (m, 4H, aromatic H). API-MS m/z: 545.2 $[M+H]^+$.

AH_{20} (6) A white powder (mp 143—145 °C), $[\alpha]_D$ −27.83° (c = 0.97, MeOH). UV λ_{max}^{MeOH} nm (ε): 212 (50063), 247 (48242). IR (KBr) cm^{-1}: 3320 (OH), 1652, 1595 (γ-pyrone ring). ^1H- and ^{13}C-NMR: Tables I and II. FD-MS m/z: 883 $[M+H]^+$.

Acknowledgements The authors are grateful to the staff of the Central Analysis Room of Kyoto University for elemental analysis and to Dr. Keiji Hashimoto of Kyoto Pharmaceutical University for FD- and API-MS.

References

1) *a*) Y. Shimada, T. Tominaga, T. Konishi, and S. Kiyosawa, *Chem. Pharm. Bull.*, **30**, 3791 (1982); *b*) Y. Shimada, T. Konishi, S. Kiyosawa, M. Nishi, K. Miyahara, and T. Kawasaki, *ibid.*, **34**, 2766 (1986); *c*) Y. Shimada, T. Konishi, and S. Kiyosawa, *ibid.*, **34**, 3033 (1986); *d*) K. Iwagoe, T. Konishi, S. Kiyosawa, Y. Shimada, K. Miyahara, and T. Kawasaki, *ibid.*, **34**, 4889 (1986); *e*) K. Iwagoe, S. Kodama, T. Konishi, S. Kiyosawa, Y. Fujiwara, and Y. Shimada, *ibid.*, **35**, 4680 (1987); *f*) K. Iwagoe, T. Konishi, S. Kiyosawa, Y. Shimada, K. Miyahara, and T. Kawasaki, *ibid.*, **36**, 2417 (1988); *g*) T. Konishi, S. Kiyosawa, Y. Shimada, K. Miyahara, and T. Kawasaki, *ibid.*, **37**, 1428 (1989); *h*) T. Konishi, K. Iwagoe, S. Kiyosawa, and Y. Fujiwara, *Phytochemistry*, **28**, 3548 (1989).

2) E. Yoshii, T. Koizumi, and T. Oribe, *Tetrahedron Lett.*, **1978**, 3921.

Direct Monitoring by Carbon-13 Nuclear Magnetic Resonance Spectroscopy of the Metabolism and Metabolic Rate of ^{13}C-Labeled Compounds *in Vivo*

Katsumi IIDA,[a] Osamu HIDOH,[b] Junichi FUKAMI,[b] and Masahiro KAJIWARA*,[a]

Department of Medicinal Chemistry, Meiji College of Pharmacy, 1–22–1 Yato-cho, Tanashi-shi, Tokyo 188, Japan[a] and 1–35–23 Nozawa, Setagaya-ku, Tokyo 154, Japan.[b] *Received July 2, 1990*

Carbon-13 nuclear magnetic resonance spectroscopy has been used to observe the transformations of [1-^{13}C]-D-glucose to [1,1′-$^{13}C_2$]-D-trehalose, and [3-^{13}C]-L-alanine to [2-^{13}C]-L-glutamic acid in the living body of *Gryllodes sigillatus*. [3-^{13}C]-D-Alanine was not metabolized.

The metabolic rate of [1-^{13}C]-D-glucose was found to be altered by prior injection of boric acid.

Keywords ^{13}C-NMR *in vivo*; ^{13}C-glucose; ^{13}C-trehalose; ^{13}C-alanine; ^{13}C-glutamic acid; metabolism; metabolic rate; boric acid

Introduction

The stable isotope carbon-13 (^{13}C), which is in nature at 1.1%, is useful in biochemical research[1] because labeled positions can be easily identified by carbon-13 nuclear magnetic resonance spectroscopy (^{13}C-NMR) of extensive chemical shift without chemical degradation. It is very important in a wide area that the metabolic pathways in living body is directly investigated. Therefore we are interested in developing this method to monitor *in vivo* systems. The use of superconducting magnets provides extremely stable magnetic fields which can be adjusted with high sensitivity, so that it is possible to measure ^{13}C-NMR signals without a deuterium lock system and without spinning the nuclear magnetic resonance (NMR) tube. The pulse sequence of NMR is also a matter of great importance to avoid tissue damage to living organisms.

Glucose is an energy source, and trehalose, which is produced from glucose, is an important blood sugar of insects.[2] Further, alanine is metabolized to glutamic acid, a neurotransmitter. Therefore, [1-^{13}C]-D-glucose (**1**), [3-^{13}C]-L-alanine (**3**), and [3-^{13}C]-D-alanine (**4**) were each injected into *Gryllodes* (*G.*) *sigillatus*, and their transformation in all a living body was directly monitored by ^{13}C-NMR. The effect of boric acid on the metabolic rate of [1-^{13}C]-D-glucose (**1**) was also examined.

Results and Discussion

[1-^{13}C]-D-Glucose (**1**) was intraabdominally injected into *G. sigillatus*. After 30 min, the C-1 signals of injected [1-^{13}C]-D-glucose (**1**) were observed at 92.8 ppm (α-form) and 96.7 ppm (β-form) by ^{13}C-NMR *in vivo*.[3] After 1 h, a new signal due to [1,1′-$^{13}C_2$]-D-trehalose (**2**) appeared at 93.9 ppm[4] and increased there after in parallel with the decrease of the signals at 92.8 and 96.7 ppm. After 4 h, [1-^{13}C]-D-glucose (**1**) had been completely metabolized in the body of *G. sigillatus* (Fig. 1). Thus, [1-^{13}C]-D-glucose (**1**) was not subjected to glycolysis, but was predominantly metabolized to [1,1′-$^{13}C_2$]-D-trehalose (**2**) (Fig. 2). The metabolite was isolated from *G. sigillatus* in 27% yield, and identified as [1,1′-$^{13}C_2$]-D-trehalose (**2**) by ^{13}C-NMR, and fast atom bombardment mass spectrometry (FAB-MS).[5]

Boric acid, which is said to be toxic to the digestive

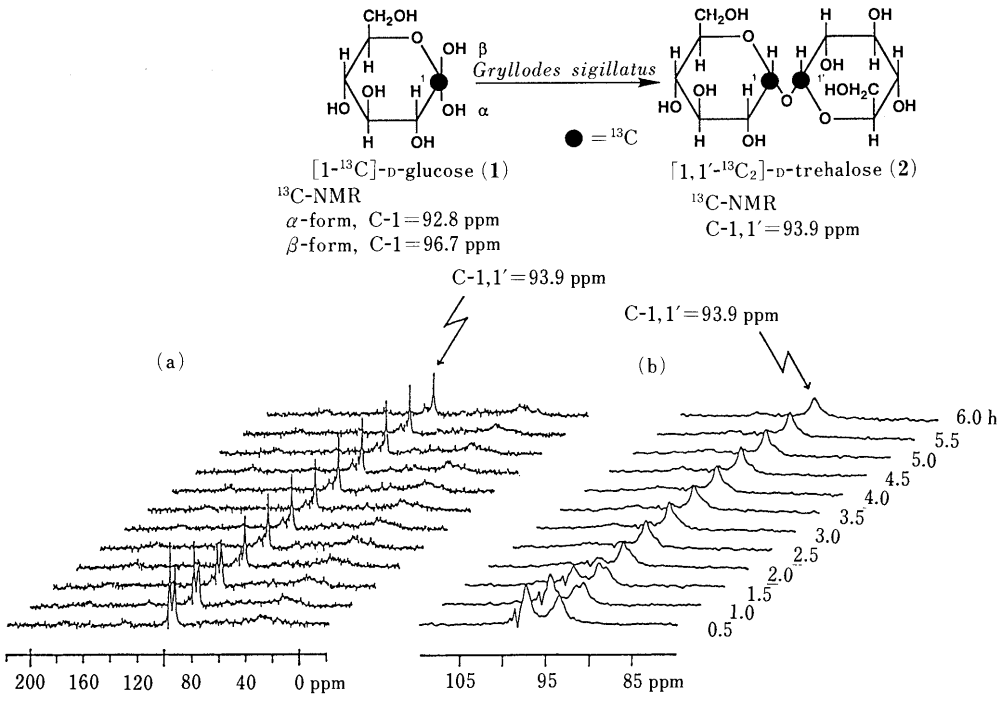

Fig. 1. ^{13}C-NMR Spectra of the *in Vivo* Transformation of [1-^{13}C]-D-Glucose (**1**) in *G. sigillatus* (a) and Expanded ^{13}C-NMR Spectra from 80 to 110 ppm (b)

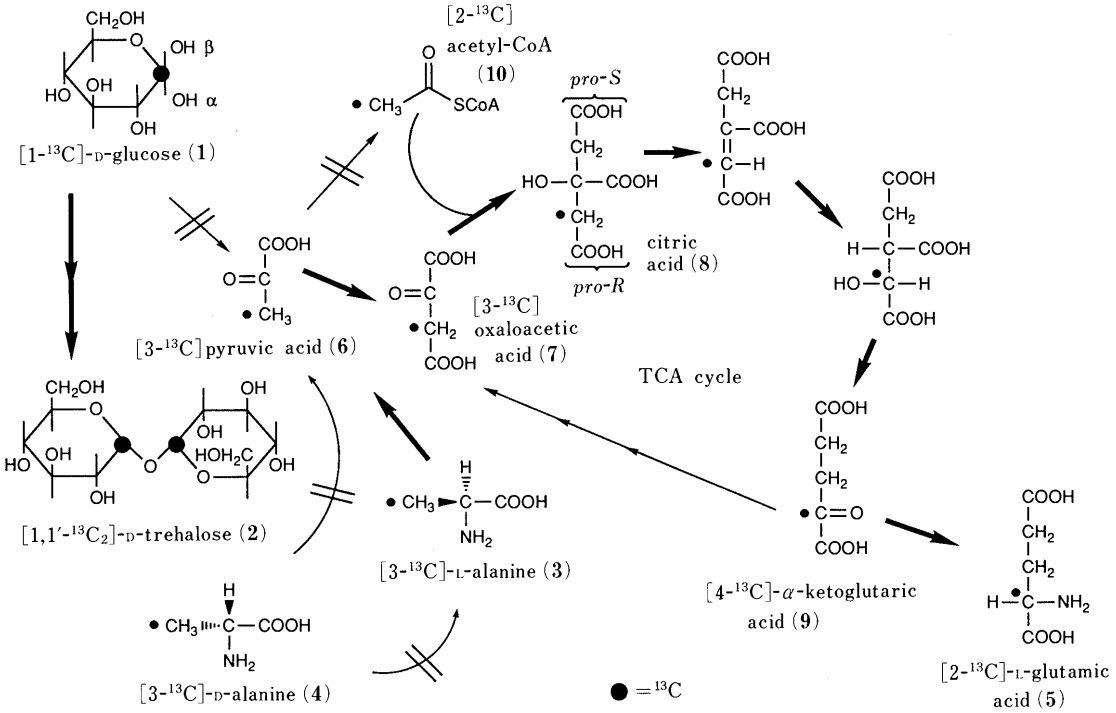

Fig. 2. The Metabolic Pathways of ^{13}C-Labeled Compounds in *G. sigillatus*

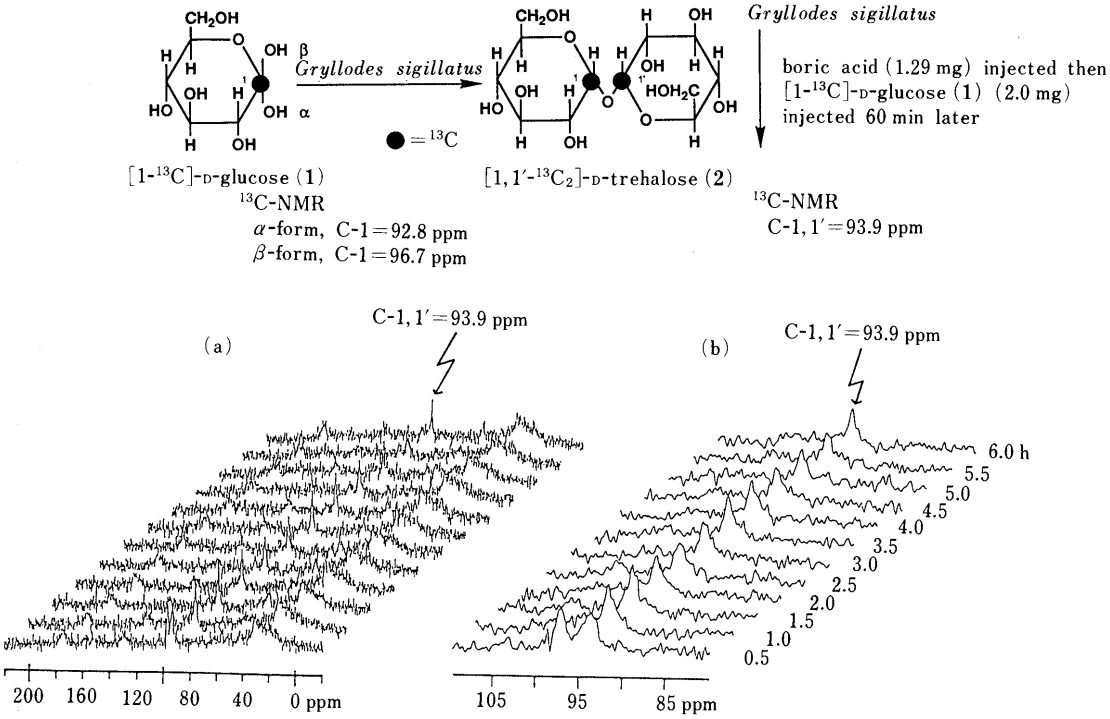

Fig. 3. ^{13}C-NMR Spectra Showing the *in Vivo* Transformation of [1-^{13}C]-D-Glucose (**1**) in the Presence of Boric Acid in *G. sigillatus* (a) and Expanded ^{13}C-NMR Spectra from 80 to 110 ppm (b)

processes and to decrease metabolism, usually is used as a antihelmintic for the cockroach. We investigated boric acid have effects upon the metabolism of D-glucose. When [1-^{13}C]-D-glucose (**1**) was intraabdominally injected into *G. sigillatus* 30 min after boric acid, the transformation of [1-^{13}C]-D-glucose (**1**) to [1,1'-$^{13}C_2$]-D-trehalose (**2**) was completed within 1 h (Fig. 3). Thus the metabolism of [1-^{13}C]-D-glucose (**1**) to [1,1'-$^{13}C_2$]-D-trehalose (**2**) unexpectedly was speeded up by boric acid.

Next, [3-^{13}C]-L-alanine (**3**) was intraabdominally injected into *G. sigillatus*. After 1 h, the C-3 signal of injected [3-^{13}C]-L-alanine (**3**) was observed at 17.9 ppm by ^{13}C-NMR *in vivo*.[3b-e,6] After 2.5 h, a new signal appeared at 55.8 ppm, and this was assignable to C-2 of L-glutamic acid (**5**) formed from L-alanine *via* the Tricarboxylic acid (TCA) cycle (Fig. 4).[3b,c,6] The signal of [3-^{13}C]-L-alanine (**3**) finally disappeared. However, when [3-^{13}C]-D-alanine (**4**) was injected into *G. sigillatus*, it was not transformed

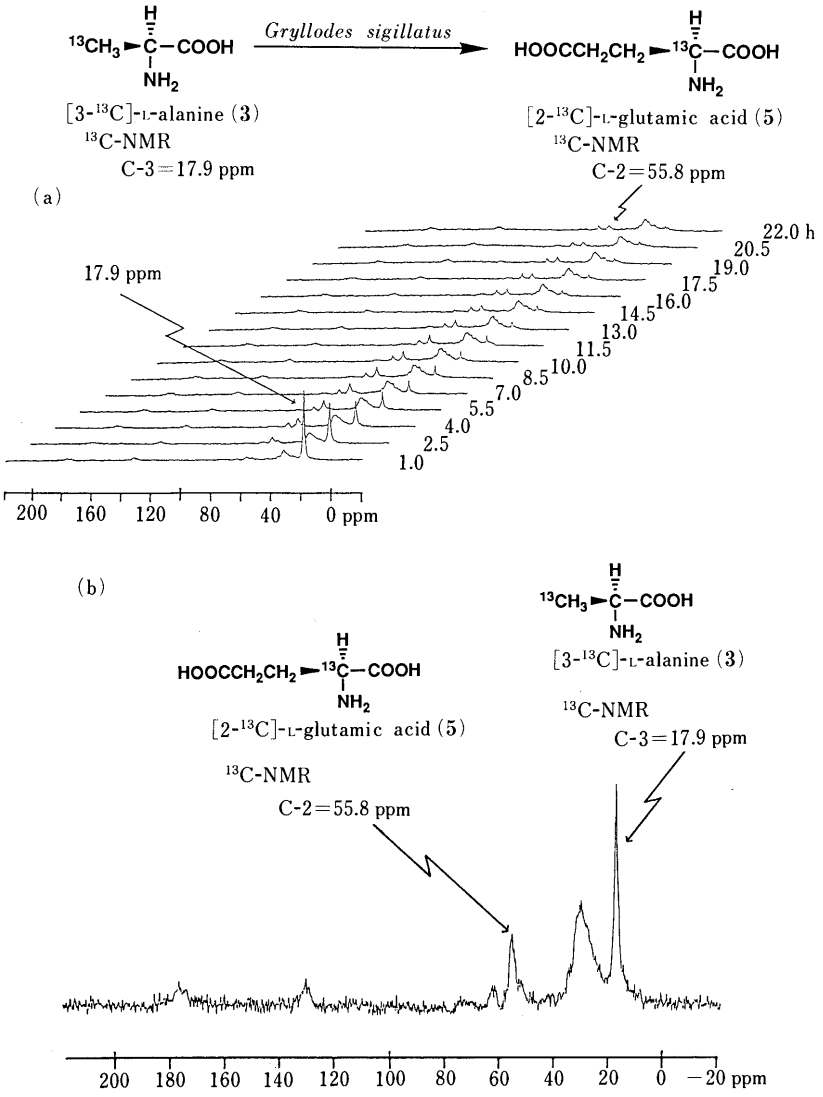

Fig. 4. ^{13}C-NMR Spectra Showing the *in Vivo* Transformation of [3-^{13}C]-L-Alanine (**3**) in *G. sigillatus* (a) and Expanded ^{13}C-NMR Spectrum at 4 h (b)

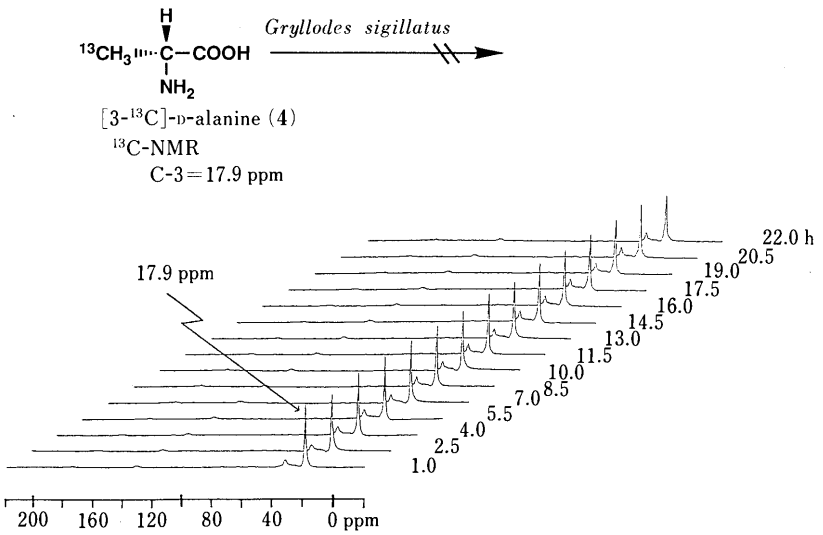

Fig. 5. ^{13}C-NMR Spectra Showing the Absence of *in Vivo* Transformation of [3-^{13}C]-D-Alanine (**4**) in *G. sigillatus*

(Fig. 5). [3-^{13}C]-L-Alanine (**3**) was presumably metabolized to [3-^{13}C]pyruvic acid (**6**). [3-^{13}C]Pyruvic acid (**6**) would then be converted into [3-^{13}C]oxaloacetic acid (**7**) in the TCA cycle, and successively to *pro-R* methylene ^{13}C-labeled citric acid (**8**), [4-^{13}C]-α-ketoglutaric acid (**9**), and [2-^{13}C]-L-glutamic acid (**5**). The [3-^{13}C]pyruvic acid (**6**) was not

significantly metabolized to [2-^{13}C]acetyl-Coenzyme A (**10**), which would lead successively to *pro-S* methylene ^{13}C-labeled citric acid, [2-^{13}C]-α-ketoglutaric acid, and finally [4-^{13}C]-L-glutamic acid (Fig. 2).

Experimental

Instruments ^{13}C-NMR spectra *in vivo* were recorded 100 MHz on a JEOL GSX-400 spectrometer with 10 mm multinuclear probes, referenced to $CDCl_3$ as an external standard. The spectral width was 24 kHz with 32 k data points, which corresponds to a resolution of 1.47 Hz per point. The determined 90° pulse width was 8.0 μs, the acquisition time was 0.021 s, the pulse delay time was 1.0 s, and the probe temperature was 27 °C. The pulse sequence of proton irradiation involved gate decoupling without nuclear Overhauser effect (NOE). The spectra of samples were measured at an organism without deuterium lock and without samples spinning.

Materials The insects used were adult male *G. sigillatus*. [1-^{13}C]-D-Glucose (99 atom% ^{13}C) was supplied by Cambridge Isotope Laboratories. [3-^{13}C]-D-Alanine[7] and [3-^{13}C]-L-alanine[7] (100% ee, 99 atom% ^{13}C) were prepared from ^{13}C-iodomethane (99 atom% ^{13}C), which was obtained from Cambridge Isotope Laboratories.

Measurement of Metabolism of [1-^{13}C]-D-Glucose, and [3-^{13}C]-D- and L-Alanine by NMR *in Vivo* A solution of [1-^{13}C]-D-glucose, [3-^{13}C]-D-alanine or [3-^{13}C]-L-alanine (2.0 mg) in water (20 μl) was intraabdominally injected into an insect, which was put into an NMR tube, and the time course of signals was observed by ^{13}C-NMR.

Measurement of Metabolism of [1-^{13}C]-D-Glucose in the Presence of Boric Acid by NMR *in Vivo* A solution of boric acid (1.29 mg) in water (10 μl) was intraabdominally injected into *G. sigillatus*. After 30 min, a solution of [1-^{13}C]-D-glucose (2.0 mg) in water (10 μl) was intraabdominally injected, and the insect was put into an NMR tube. The time course of signals was observed by ^{13}C-NMR as above.

Conclusion

The transformation of ^{13}C-labeled compounds was successfully monitored by *in vivo* ^{13}C-NMR. The effect of an added drug on the metabolic rate was also observed to determine as the time proceeds. And the difference of metabolism between D-amino acid and L-amino acid was first observed, the metabolic pathways were confirmed for ^{13}C-labeled position of metabolite. This technique could be applicable to the studies of the metabolism of various drugs and agricultural chemicals.

Acknowledgement We wish to thank Mr. Kazuhiro Matsusita of JEOL Co. and Dr. Katsuyuki Kurumaya for many helpful suggestions during the course of this work.

References and Notes

1) *a*) K. Kurumaya, T. Okazaki, N. Seido, Y. Akasaka, Y. Kawajiri, M. Kajiwara, and M. Kondo, *J. Labelled Comp. Radiopharm.*, **27**, 217 (1989); *b*) K. Kurumaya, T. Okazaki, and M. Kajiwara, *Chem. Pharm. Bull.*, **37**, 1151 (1989); *c*) K. Kurumaya, T. Okazaki, and M. Kajiwara, *Chem. Pharm. Bull.*, **38**, 1058 (1990).
2) *a*) G. R. Wyatt and G. F. Kalf, *J. Gen. Physiol.*, **40**, 833 (1957); *b*) D. J. Candy and B. A. Kilby, *Nature* (London), **183**, 1594 (1959); *c*) D. J. Candy and B. A. Kilby, *Biochem. J.*, **78**, 531 (1961).
3) *a*) E. Breitmaier and W. Voelter, "Carbon-13 NMR Spectroscopy," VCH Verlagsgesellschaft, Weinheim 1987, pp. 27, 380; *b*) K. Ugurbil, T. R. Brown, J. A. den Hollander, P. Glynn, and R. G. Shulman, *Proc. Natl. Acad. Sci. U.S.A.*, **75**, 3742 (1978); *c*) K. L. Behar, O. A. C. Petroff, J. W. Prichard, J. R. Alger, and R. G. Shulman, *Magnetic Resonance in Medicine*, **3**, 911 (1986); *d*) B. J. Blackburn, H. M. Hutton, M. Novak, and W. S. Evans, *Exp. Parasitol.*, **62**, 381 (1986); *e*) C. A. Behm, C. Bryant, and A. J. Jones, *Int. J. Parasitol.*, **17**, 133 (1987).
4) T. Usui, N. Yamaoka, K. Matsuda, K. Tuzimura, H. Sugiyama, and S. Seto, *J. Chem. Soc., Perkin Trans. 1*, **1973**, 2425.
5) K. Iida and M. Kajiwara, *J. Chromatogr.*, **515**, 573 (1990). $^{12}C_{10}{}^{13}C_2H_{22}O_{11}$: molecular weight = 344.31. FAB-MS: $m/z = 343$ ($M^+ - 1$, 3%).
6) M. Barany, C. Arus, and Y-C. Chang, *Magnetic Resonance in Medicine*, **2**, 289 (1985).
7) K. Iida and M. Kajiwara, *J. Labelled Comp. Radiopharm.*, in press.

Effect of Intraperitoneally Administered β-1,3-Glucan, SSG, Obtained from *Sclerotinia sclerotiorum* IFO 9395 on the Functions of Murine Alveolar Macrophages

Teruaki SAKURAI,[a] Iwao SUZUKI,[a] Akira KINOSHITA,[a] Shozo OIKAWA,[b] Akiyoshi MASUDA,[b] Masumi OHSAWA[b] and Toshiro YADOMAE*,[a]

Tokyo College of Pharmacy,[a] Horinouchi 1432-1, Hachioji, Tokyo 192-03, Japan and Nippon Beet Sugar Mfg., Co., Ltd.,[b] Chuo-ku, Tokyo 104, Japan. *Received May 7, 1990*

The effect of intraperitoneally (i.p.) administered SSG, a β-1,3-glucan obtained from the culture filtrate of the fungus *Sclerotinia sclerotiorum* IFO 9395, on the functions of alveolar macrophages (AM) in CDF_1 mice was examined. SSG administered i.p. increased the number of AM and enhanced several functions of murine AM (lysosomal enzyme activity, phagocytic activity, candidacidal activity, H_2O_2 production and interleukin 1 (IL-1) production) at a dose of 250 μg/mouse on days 1 and 8, especially on day 8. Furthermore, SSG (250 μg/mouse) administered i.p. for 10 consecutive days significantly inhibited the experimental pulmonary metastasis of Lewis Lung Carcinoma (3LL) on BDF_1 mice.

Keywords alveolar macrophage; SSG; β-1,3-glucan; lysosomal enzyme activity; phagocytic activity; candidacidal activity; H_2O_2 production; IL-1 production; pulmonary metastasis

Introduction

The lungs are always exposed to various antigens in ambient air. Alveolar macrophages (AM) are known to play an important role in removing antigens from the lungs by nonspecific phagocytosis and to play a regulatory role in antigen presentation in lung tissue.[1] AM are also important in inhibiting the pulmonary metastasis of cancer cells in lung tissue.[2] It has been known that AM differ from other local macrophages in many respects, such as their lysosomal enzymes, metabolic activity for energy requirement, morphology, functions and their antigen markers on the cell surface, since AM situate at the air-tissue interface on the anatomical position.[3-6]

Recently, considerable attention has been focused on biological response modifiers (BRMs). BRMs are very useful in defending against repullulation and metastasis of cancer when they are used in therapy combining surgery, radiation and chemotherapy.[7] It has been often reported that administration of BRMs enhances the peritoneal macrophages (PM) function in mice. However, there have been few reports about BRMs which can enhance the functions of AM. Therefore, we decided that to investigate the modulation of AM functions by BRMs would be of value in enhancing our understanding of their potential use.

Several kinds of polysaccharides are well known to possess immunomodulating effects and exhibit significant antitumor activities.[8] Two kinds of glucans, lentinan and schizophyllan, have been applied clinically in Japan.[9] We have examined the antitumor and immunomodulating activities of SSG, a highly branched β-1,3-glucan obtained from the liquid-cultured broth of a fungus *Sclerotinia sclerotiorum*.[10,11]

SSG administered intraperitoneally (i.p.) was effective in augmenting PM functions.[10]

In this study, the effects of SSG administered i.p. on murine AM functions (increment of AM number, lysosomal enzyme activity, phagocytic activity, candidacidal activity, H_2O_2 production and interleukin 1 (IL-1) production) and on inhibition of experimental pulmonary metastasis of 3LL were examined.

Materials and Methods

Animals Specific-pathogen-free male CDF_1 (BALB/c × DBA/2), BDF_1 (C57BL/6 × DBA/2) and C3H/HeJ mice were purchased from Japan SLC, Inc. (Shizuoka). CDF_1 and BDF_1 mice were used at 6—8 weeks of age. C3H/HeJ mice were used at 4 weeks of age. These animals were bred under specific-pathogen-free conditions.

Preparation of SSG A preparation method of SSG was previously described.[11] The SSG was made up of less than 1% protein and >98% carbohydrates. Lipopolysaccharide (LPS) contamination of this preparation was less than 0.00014% (1.4 pg/μg of test sample).

Preparation of AM Alveolar cells (AC) were harvested from CDF_1 mice by bronchial lavage.[6] The mice were anesthetized by i.p. injection of 150 mg/kg of sodium pentobarbital (Nembutal®, Dainabot Co., Ltd., IL.) and exanguinated by cutting the arteria renalis. The thoracic cavity was opened and the lung with trachea was removed. The lavage fluid (Ca^{2+} and Mg^{2+}-free phosphate-buffered saline containing 0.05% ethylenediaminetetraacetic acid (EDTA)) was introduced in 1.0 ml amounts from a 1.5 ml of medium, the lung was gently massaged, and the lavage fluid was withdrawn from the lungs. A total of 6.0 ml of lavage fluid per mouse was used. AC were resuspended in an ice-cold RPMI-1640 medium (Nissui Seiyaku Co., Ltd., Tokyo) supplemented with 5 mM Hepes, penicillin (100 U/ml) and streptomycin (100 μg/ml) containing 10% heat-inactivated fetal calf serum (FCS) (Boehringer Mannheim, GmbH). At least 97% of AC were AM as judged by using cell smears of either a Diff-Quik Stain kit (Kokusai Shiyaku Co., Ltd., Hyogo) or a nonspecific esterase stain. AC were incubated for 2 h at 37 °C in a CO_2 incubator and were washed twice with a warmed RPMI-1640 medium to remove any nonadherent cells.

Preparation of PM Peritoneal cells (PC) were collected from the peritoneal cavity of CDF_1 mice by washing twice with 5 ml of Hank's balanced salt solution (Nissui) containing heparin (5 U/ml). The PC were resuspended in an ice-cold PRMI-1640 medium. The total cell number was counted with a hemocytometer, and cells were differentiated by using a Diff-Quik Stain Kit. The PC were incubated for 2 h at 37 °C in a CO_2 incubator and were washed twice with a warmed RPMI-1640 medium to remove any nonadherent cells. The resultant cells were used as PM.

Experimental Protocols SSG was dissolved in physiological saline, and aliquots (250 μg/0.2 ml) of the solution were used for administration into CDF_1 mice. As a positive control for the activation of AM, the suspension of 1 KE of OK-432 (Picibanil®, a group of streptococcal preparation, kindly provided by Chugai Pharmaceutical Co., Ltd., Tokyo) was injected i.p. into mice, and PM were collected 4 d after the injection.[12] Acid phosphatase activity was measured using Triton X-100 lysates of macrophages with *p*-nitrophenyl phosphate (Sigma Chemical Co., St. Louis, MO.) as a substrate.[13] Phagocytic activity was assayed by a method described previously,[14] using fluorescein-conjugated zymosan particles (prepared from Zymosan A; Sigma) opsonized with a complement (guinea pig serum). Candidacidal activity was assayed by the method of Sasada and Johnston[15] with minor modifications[13] using *Candida albicans* IFO 1269. H_2O_2 production was assayed using scopoletin in the presence of phorbol myristate acetate (sigma) as described previously.[13] IL-1 production was assessed by measuring lymphocyte-activating factor (LAF) activity[16] using thymocytes of C3H/HeJ mice in the presence of a submitogenic concentration of concanavalin A (Con A).[13]

Assay of Experimental Pulmonary Metastasis of 3LL Experimental metastasis assay was according to a method described previously.[17] The cells of Lewis Lung Carcinoma (3LL) maintained by subcutaneous passage in C57BL/6 mice (1×10^5) were injected into the tail vein of BDF_1 mice (semisyngeneic to 3LL). Three weeks after the implantation, the mice were anesthesized and autopsied. Pulmonary metastasis was estimated by counting the numbers of metastatic nodules on the pulmonary surface after washing the lungs in a physiological saline.

Statistics All results are expressed as the mean ± standard deviation (S.D.). Statistical evaluations in all experiments were performed by the Student's *t*-test. A value of $p<0.05$ was considered significant.

Results

Changes in the Numbers of AM by i.p. Administration of SSG In a previous study, we have shown that SSG administered i.p. possessed an optimal dose (250 μg/mouse) for exhibiting antitumor and immunomodulating activities, including enhancement of the functions of PM.[10] On the basis of this finding, a single i.p. administration of 250 μg/mouse of SSG was used in this series of experiments.

First, we examined the number of AM by i.p. administration of SSG (250 μg/mouse) until day 12. As shown in Fig. 1, SSG increased the number of AM at two phases. In the early phase, a significant increment in the number of AM was observed from 6 h (Fig. 1-A) and a peak appeared at 12 h. The effect was maintained until 24 h, then dropped to the control level at 48 h. In the late phase, a significant increment in the number of AM appeared from day 8 to 10 and dropped to the control level on day 12 (Fig. 1-B).

Changes in Lysosomal Enzyme Activity of AM by i.p. Administration of SSG Figure 2 shows the effect of SSG administered i.p. on the lysosomal enzyme activity of AM. As a result, SSG enhanced the acid phosphatase activity at two phases. As shown in Fig. 2-A, significant enhancement of acid phosphatase activity of AM was observed at 24 h. The effect was maintained until 48 h. The other peak of acid phosphatase activity of AM appeared on day 8 (Fig. 2-B). The activity was dropped to the control level on day 10.

Based on these results, the following experiments were designed to measure several functions of AM on days 1 (24 h) and 8.

Effect of SSG on Various Functions of AM All the activities measured are summarized in Table I. Phagocytic activity was significantly enhanced on day 8 by i.p. injection of SSG, though it was not enhanced on day 1. The level of

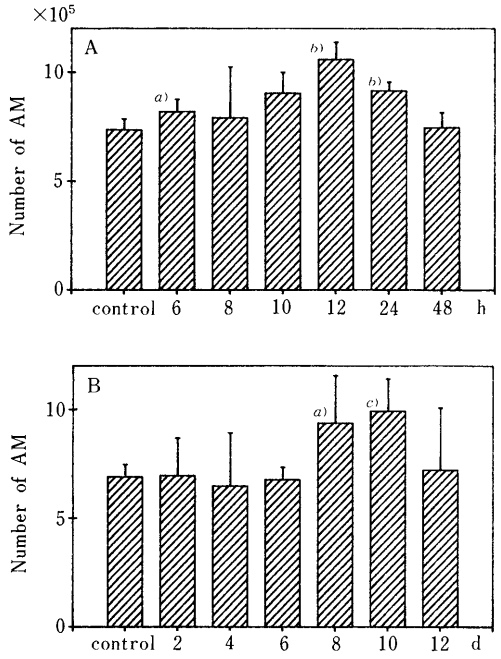

Fig. 1. Changes in the Numbers of AM by i.p. Administration of SSG

SSG (250 μg/mouse) was administered i.p. into CDF_1 mice. Changes in the number of AM were observed until 48 h (A) or 12 d (B) after the administration of SSG. Results are expressed as the arithmetic mean + S.D. of six mice. *a*) $p<0.05$. *b*) $p<0.001$. *c*) $p<0.01$.

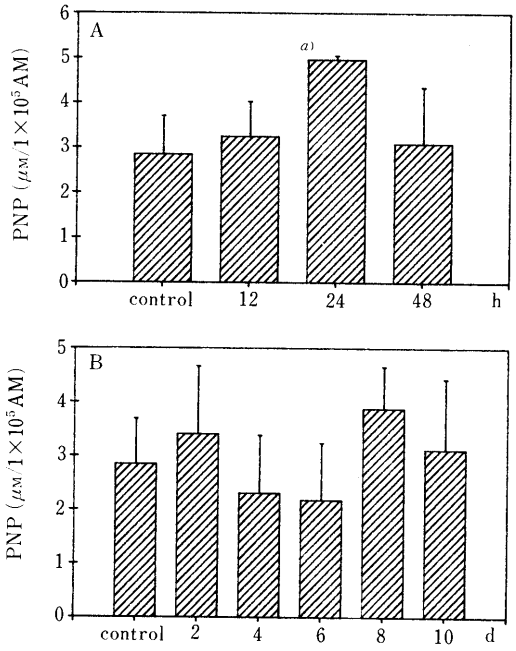

Fig. 2. Changes in Lysosomal Enzyme Activity of AM by i.p. Administration of SSG

SSG (250 μg/mouse) was administered i.p. into CDF_1 mice. Changes in acid phosphatase activity of AM were observed until 48 h (A) or 10 d (B) after the administration of SSG. Results are expressed as the arithmetic mean + S.D. of six mice. *a*) $p<0.01$.

TABLE I. Effect of SSG on the Various Functions of AM

Sample[a]	Dose	Macrophages	Day[b]	Phagocytic activity (%)[c]	Candidacidal activity (%)[c]	H_2O_2 production[c,d]	IL-1 production[e,f]
	Control	AM		27.0 ± 6.0	61.6 ± 13.3	183.4 ± 55.4	249.3 ± 104.9
SSG	250 μg	AM	1	22.6 ± 6.4	70.4 ± 10.3	213.8 ± 98.0	229.4 ± 123.9
SSG	250 μg	AM	8	38.0 ± 2.8[g]	76.5 ± 8.3[h]	326.0 ± 89.5[g]	436.8 ± 79.0
	Control	PM		25.4 ± 2.4	61.2 ± 0.6	371.0 ± 122.0	251.1 ± 108.2
OK-432	1 KE	PM	4	47.4 ± 15.5[h]	69.0 ± 2.8[g]	2215.9 ± 497.9[i]	804.9 ± 446.2[h]

a) Samples were administered i.p. into CDF_1 mice on day 0. *b*) Days after the administration of samples. *c*) Results are expressed as the arithmetic mean ± S.D. of six mice. *d*) pmol of H_2O_2/2 h per 2×10^5 AM. *e*) Results are expressed as the arithmetic mean ± S.D. of three mice. *f*) Uptake of ^{3}H-TdR (cpm). *g*) $p<0.01$. *h*) $p<0.05$. *i*) $p<0.001$.

TABLE II. Inhibition of Experimental Pulmonary Metastasis of 3LL by i.p. Administration of SSG[a]

	No. of mice	Number of metastatic nodules[b]	Growth inhibition (%)
Control	8	14.1±5.0	—
SSG	7	4.6±1.8[c]	67.4

a) SSG (250 μg/mouse) was administered i.p. for 10 consecutive days (days-10—-1) and 1×10^5 3LL cells were implanted *via* the tail vein of BDF_1 mice on day 0. Metastatic nodules of 3LL were counted on day 21. *b*) Results are expressed as the arithmetic mean±S.D. *c*) $p<0.01$.

activity observed on day 8 was lower than that of the PM obtained from mice given an i.p. injection of OK-432.

SSG (250 μg/mouse) administered i.p. significantly enhanced the candidacidal activity of AM on day 8. The level of activity observed in the group of mice in which SSG was administered i.p. was comparable to that of PM obtained from mice given an i.p. injection of OK-432.

H_2O_2 production of AM was significantly increased by injection of SSG on both days 1 and 8. The level of activity was lower than that of PM from mice given an i.p. injection of OK-432.

Intraperitoneal administration of SSG (250 μg/mouse) slightly augmented the production of IL-1 from AM on day 8. The level of activity was lower than that of PM from mice given an i.p. injection of OK-432. On day 1, SSG administered i.p. did not affect the IL-1 production of AM.

Inhibition of Experimental Pulmonary Metastasis of 3LL by i.p. Administration of SSG SSG (250 μg/mouse) was administered i.p. for 10 consecutive days (days-10—-1) and 1×10^5 3LL cells were implanted on day 0. Metastatic nodules of 3LL were counted on day 21. As a result, the number of nodules of the control group of mice was 14.1±5.0, compared to only 4.6±1.8 ($p<0.01$) nodules counted on the lung surface of the SSG-treated group of mice.

Discussion

In the lungs, AM are the first host defense cells to interact with infections by microorganisms and to modulate the ensuing inflammation.[18] AM also play the main role in the lungs in inhibiting the pulmonary metastasis of tumor cells.[2]

In this study, we showed that a single i.p. administration of 250 μg/mouse of SSG enhanced the functions of murine AM. The effect of SSG appeared in two phases, on days 1 and 8. On day 8, SSG increased the number of AM and affected the functions of AM, including lysosomal enzyme activity, phagocytic activity, candidacidal activity, H_2O_2 production and IL-1 production. On the other hand, on day 1, SSG increased the number of AM but affected only the lysosomal enzyme activity of AM. Based on these results, we presumed that various functions of AM were enhanced systematically by SSG on day 8, while a few functions of AM—an increase in number and lysosomal enzyme activity, which were augmented on day 1—may be evanescent primary changes which occurred from an acute phase inflammation-like response to the i.p. injection of SSG.

SSG administered i.p. increased the number of AM (Fig. 1). A concept that AM originate from a precursor in the bone marrow and belong to the cells of the mononuclear phagocyte system has been generally accepted.[19] However, recent studies showed a possibility that AM proliferate and differentiate through stimulation by colony stimulating factors (CSFs).[20-22] Previously, we reported that SSG (250 μg/mouse) administered i.p. enhanced the colony-stimulating activity in serum and in the supernatant of peritoneal cells in mice.[23] Thus, we assume that an increase in the number of AM by SSG administered i.p. may be due to the release of CSFs. On the other hand, IL-1 has been shown to induce the secretion of CSFs from mononuclear phagocytes.[24] In this study, we also showed that SSG administered i.p. augmented IL-1 production of AM on day 8 (Table I). This result supported the conception that an increased amount of IL-1 by SSG augmented CSF production which in turn caused the proliferation of AM.

It is known that AM release reactive oxygen intermediates during phagocytosis,[25,26] and considerable evidence exists that these metabolites play a significant role in the antimicrobial activity of these cells.[27] Lysosomal enzymes also play an important role in the antimicrobial activity in AM.[28] Therefore, the enhanced candidacidal activity of AM after i.p. administration of SSG may be due to the augmented functions, including phagocytosis, lysosomal enzyme and the release of oxygen metabolites. Candidasis is a fungal infection. Therefore, SSG should be effective against infectious diseases.

The importance of activated AM in inhibiting pulmonary metastasis of experimental tumors is reported.[29] In this work, we also demonstrated that SSG administered i.p. inhibited the experimental pulmonary metastasis of Lewis lung carcinoma. The effect may be strongly related to the augmented functions of AM by SSG administered i.p.

The present study demonstrates that SSG activates functions of AM following the i.p. administration. The effectiveness of SSG is characteristic among antitumor polysaccharides. The administration of polysaccharides, including glucans, may be effective in the therapy for microbial infections in lung tissue and pulmonary metastasis of cancer cells.

Acknowledgment This work was supported by a Grant-in-Aid from the Uehara Memorial Foundation. We are grateful to Mr. T. Hayashi and Miss N. Hirokami for their technical assistance.

References

1) T. Thepen, N. van Rooijen and G. Kraal, *J. Exp. Med.*, **170**, 499 (1989).
2) I. J. Fidler, W. E. Fogler, A. F. Brownbill and G. Schumann, *J. Immunol.*, **138**, 4509 (1987).
3) W. S. Walker, "Immunobiology of the Macrophages," ed. by D. S. Nelson, Academic Press, Inc., New York, 1976, pp. 91—110.
4) J. E. Hearst, G. A. Warr and G. J. Jakab, *J. Reticuloendothel. Soc.*, **27**, 443 (1980).
5) S. E. Ullrich and H. B. Herscowitz, *J. Reticuloendothel. Soc.*, **28**, 111 (1980).
6) K. S. Akagawa and T. Tokunaga, *J. Exp. Med.*, **162**, 1444 (1985).
7) K. Ishihara, *Biotherapy*, **1**, 19 (1987), (in Japanese).
8) N. R. Di Luizo, *Springer Sem. Immunopath.*, **8**, 387 (1985).
9) I. Azuma, "Immunostimulants Now and Tommorow," ed. by I. Azuma and G. Jolles, Japan Scientific Societies Press, Tokyo, 1987, pp. 41—56.
10) I. Suzuki, K. Hashimoto and T. Yadomae, *J. Pharmacobio-Dyn.*, **11**, 527 (1988).
11) I. Suzuki, K. Hashimoto, N. Ohno, H. Tanaka and T. Yadomae,

Int. J. Immunopharmac., **11**, 761 (1989).
12) T. Kawaguchi, M. Suematsu, H. M. Koizumi, H. Mitsui, S. Suzuki, T. Matsuno, H. Ogawa and K. Nomoto, *Immunopharmacology*, **6**, 177 (1983).
13) I. Suzuki, H. Tanaka, A. Kinoshita, S. Oikawa, M. Osawa and T. Yadomae, *Int. J. Immunopharmac.*, **12**, 675 (1990).
14) I. Suzuki, H. Tanaka, Y. Adachi and T. Yadomae, *Chem. Pharm. Bull.*, **36**, 4871 (1988).
15) M. Sasada and R. B. Johnston, *J. Exp. Med.*, **152**, 85, (1980).
16) M. S. Meltzer and J. J. Oppenheim, *J. Immunol.*, **118**, 77 (1977).
17) R. M. Abdallah, J. R. Starkey and G. G. Meadows, *J. Natu. Cancer Inst.*, **78**, 759 (1987).
18) S. Becker, R. B. Devlin and J. S. Haskill, *J. Leuk. Biol.*, **45**, 353 (1989).
19) R. van Furth, Z. Cohn, J. G. Hirscsh, J. H. Humphrey, W. G. Spector and H. L. Langevoot, *Bull. WHO*, **46**, 845 (1972).
20) B. D.-M. Chen, M. Mueller and T.-H. Chou, *J. Immunol.*, **141**, 139 (1988).
21) K. S. Akagawa, K. Kamoshita and T. Tokunaga, *J. Immunol.*, **141**, 3383 (1988).
22) H.-S. Lin, B. L. Lokeshwar and S. Hsu, *J. Immunol.*, **142**, 515 (1989).
23) K. Hashimoto, I. Suzuki, M. Ohsawa, S. Oikawa and T. Yadomae, *J. Pharmacobio-Dyn.*, **13**, 512 (1990).
24) W. E. Fibbe, J. van Damme, A. Billiau, P. J. Voogt, N. Duinkerken, P. M. C. Kluck and J. H. F. Falkenburg, *Blood*, **68**, 1316 (1986).
25) L. R. DeChatelet, D. Mullikin and C. E. McCall, *J. Infect. Dis.*, **131**, 1443 (1975).
26) T. D. Sweeney, V. Castranova, L. Bowman and P. R. Miles, *Exp. Lung Res.*, **2**, 85 (1981).
27) R. B. Johnston, *Fed. Proc.*, **37**, 2759 (1978).
28) M. Suga, *Rinsho Meneki*, **22**, 1 (1990).
29) I. J. Fidler, *Cancer Res.*, **34**, 1074 (1974).

Phytogrowth-Inhibitory and Antimicrobial Activities of 3,4′-Dihydroxy-α,β-diethylstilbene, the Isomer of Diethylstilbestrol

Yoshihiko INAMORI,*[,a] Masafumi OGAWA,[a] Kazuki NISHIGUCHI,[a] Satoko KOYAMA,[a] Hiroshi TSUJIBO,[a] Yasuyoshi MIKI[b] and Shoji TAKEMURA[b]

Osaka University of Pharmaceutical Sciences,[a] Kawai, Matsubara-shi, Osaka 580, Japan and Faculty of Pharmaceutical Sciences, Kinki University,[b] Kowakae, Higashiosaka-shi, Osaka 577, Japan. *Received June 13, 1990*

3,4′-Dihydroxy-α,β-diethylstilbene (I), like diethylstilbestrol (II), showed phytogrowth-inhibitory and antimicrobial activities. First, compound I showed strong growth-inhibitory activity against the roots of two kinds of plants. The inhibitory activity of I was almost equal to that of sodium 2,4-dichlorophenoxyacetate used as a positive control. The phytogrowth-inhibitory activity of I was much higher than that of II. Next, unlike II, I had broad antifungal spectrum against pathogenic fungi. Compound I showed antifungal activity against six kinds of *Fusarium oxysporum* sp. This compound also had antibacterial activity against pathogenic and plant-pathogenic bacteria. These antibacterial activities of I were as high as those of II, the isomer of I. It should be emphasized that by shifting one of the phenolic hydroxyl groups of II to *meta*-position, phytogrowth-inhibitory activity was largely increased, while antimicrobial activity was unchanged.

Keywords 3,4′-dihydroxy-α,β-diethylstilbene; diethylstilbestrol; oxystilbene-related compound; antifungal activity; antimicrobial activity; phytogrowth-inhibitory activity; plant-pathogenic fungus; *Fusarium oxysporum*; pathogenic fungus

It has already been reported by the authors that nonsteroidal estrogen, diethylstilbestrol (II, Chart 1) and hexestrol (III) showed antifungal activity,[1-3] phytogrowth-inhibitory activity,[2,3] coronary vasodilator action on the isolated guinea pig heart[1,4] and hypotensive effect on rats.[1,3] 3,3′-Dihydroxy-α,β-diethylstilbene (IV) and 3,3′-dihydroxy-α,β-diethyldiphenylethane (V) which are isomers of II and III, respectively, were also found to have the same biological activities.[2,5-9] Among them, diphosphate of II is used in treatment of prostatic cancer.[10] Compound V has also been reported to show antitumor activity on human mammary carcinoma implanted in nude mice.[11] Compounds IV and V, unlike II and III, were found to have no hormonal side effect.[12-14] These reports indicate the importance of the biological activity of diethylstilbestrol-related compounds. However, no work has been done on the above-mentioned activities of 3,4′-dihydroxy-α,β-diethylstilbene (I, Chart 1).

In this work, the phytogrowth-inhibitory and antimicrobial activities of I were examined in comparison with those of II, an isomer of I.

Materials and Methods

Chemicals 3,4′-Dihydroxy-α,β-diethylstilbene (I) and diethylstilbestrol (II) were used for the phytogrowth-inhibitory and antimicrobial activity tests. Compound I was synthesized by Miki *et al.*[15] Diethylstilbestrol (II) was obtained from Aldrich Chemical Co., Inc. Sodium 2,4-dichlorophenoxyacetate (Tokyo Kasei Co., Ltd.) was used as a positive control for the phytogrowth-inhibitory activity test.

Organisms The plants used were Komatsuna (*Brassica rapa* L.) and Kaiwaredaikon (*Raphanus sativus* L. var. *raphanistroides* MAKINO). Microorganisms used for the antimicrobial activity tests are listed in Tables II and III.

Antimicrobial Activity Tests Antimicrobial testing was carried out under the following four conditions: 1) assay method: agar dilution method, 2) incubation temperature: fungi and plant-pathogenic bacteria, 27 °C; pathogenic bacteria, 37 °C, 3) incubation time: fungi, 7 d; *Fusarium oxysporum* sp., 5 d; pathogenic bacteria, 18 h; plant-pathogenic bacteria, 48 h and 4) medium: fungi, potato sucrose agar; *Fusarium oxysporum* sp., potato dextrose agar; plant-pathogenic bacteria, heart infusion agar; pathogenic bacteria, nutrient agar.

Phytogrowth-Inhibitory Activity Test[16] Aliquots (1 ml) of dimethyl sulfoxide (DMSO) of I and sodium 2,4-dichlorophenoxyacetate were each diluted in 100 ml of sterilized agar (0.8%, Difco) to the concentration of 50 ppm. The agar containing chemicals or DMSO alone (control) was poured into a 500 ml sterilized biopot. Then, 20 seeds of each plant sterilized with 70% EtOH and 1% NaClO were put on the agar and left for 7 d under 9000 lux illumination. The lengths of the roots were measured and averaged. The phytogrowth-inhibitory activity was expressed as the ratio of the length of roots treated with the chemicals to that of the control (1.00).

Results and Discussion

Phytogrowth-Inhibitory Activity of 3,4′-Dihydroxy-α,β-diethylstilbene (I) As shown in Table I, 3,4′-dihydroxy-α,β-diethylstilbene (I) showed strong inhibitory activity against the elongation of roots of two kinds of plants. The inhibitory activity of I was almost equal to that of sodium 2,4-dichlorophenoxyacetate used as a positive control. The inhibitory activity of I was much higher than that of II,[2] the isomer of I.

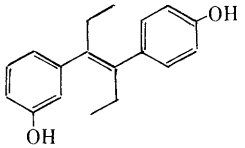

3,4′-dihydroxy-α,β-diethylstilbene (I)

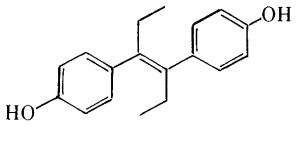

diethylstilbestrol (II)

Chart 1

TABLE I. Phytogrowth-Inhibitory Activity of 3,4′-Dihydroxy-α,β-diethylstilbene (I)

Plant	Growth (Ratio)[a]		
	I	II[b]	2,4-D[c]
Brassica rapa L.	0.10	0.43	0.07
Raphanus sativus L. var. *raphanistroides* MAKINO	0.13	0.65	0.11

a) Growth in control experiments after 7 d was taken as 1.00. Concentration: 50 ppm. Quantity of light: 9000 lux. Experimental size: 20 seeds/group, 2 groups. *b*) Diethylstilbestrol, ref. 2. *c*) Sodium 2,4-dichlorophenoxyacetate.

TABLE II. Antimicrobial Activity of 3,4′-Dihydroxy-α,β-diethylstilbene (I)

Microorganism	Antimicrobial activity (MIC[a]: μg/ml)	
	I	II[b]
Fungi		
Trichophyton mentagrophytes IFO-5811	8.0	40.0[c]
Trichophyton rubrum IFO-5467	20.0	70.0[c]
Aspergillus niger IFO-4414	15.0	>1000.0[c]
Penicillium citrinum IFO-6026	30.0	>1000.0[c]
Penicillium notatum IFO-4046	15.0	>1000.0[c]
Penicillium thomii IFO-7002	12.0	>1000.0[c]
Mucor racemosus IFO-4581	15.0	>1000.0[c]
Candida albicans IAM-4966	50.0	>1000.0[c]
Bacteria		
Bacillus subtilis PCI-219	8.0	7.0
Staphylococcus aureus 209-P	12.0	6.0
Sarcina lutea IAM-1099	12.0	7.0
Proteus mirabilis IFO-3849	50.0	7.0
Escherichia coli IFO-12734	8.0	>1000.0

Culture conditions: fungi: 27 °C, 7 d, bacteria: 37 °C, 18 h. Medium: fungi: potato sucrose agar, bacteria: nutrient agar. Assay method: agar dilution method. *a*) Minimum inhibiory concentration. *b*) Diethylstilbestrol. *c*) Ref. 1.

TABLE III. Antimicrobial Activity of 3,4′-Dihydroxy-α,β-diethylstilbene (I) on Plant-Pathogenic Microorganisms

Microorganism	Antimicrobial activity (MIC[a]: μg/ml)	
	I	II[b]
Fusarium oxysporum sp.		
Fusarium oxysporum f. sp. *raphani* IFO-9972	4.0	1.0[c]
Fusarium oxysporum f. sp. *lycopersici* IFO-6531	7.0	5.0[c]
Fusarium oxysporum f. sp. *niveum* IFO-4471	7.0	5.0[c]
Fusarium oxysporum f. sp. *cucumerinum* IFO-6384	5.0	4.0[c]
Fusarium oxysporum f. sp. *conglutians* IFO-6383	5.0	3.0[c]
Fusarium oxysporum f. sp. *melonis* IFO-6385	5.0	6.0[c]
Bacteria		
Agrobacterium tumefaciens IFO-3058	9.0	9.0
Pseudomonas syringae pv. phaseoicola IFO-12656	9.0	9.0
Pseudomonas syringae pv. tabaci IFO-3508	9.0	10.0
Pseudomonas stutzeri IFO-12510	9.0	9.0
Corynebacterium michiganense IFO-12471	1000.0	1000.0

Culture conditions: *Fusarium oxysporum* sp., 27 °C, 5 d; bacteria, 27 °C, 48 h. Medium: *Fusarium oxysporum* sp., potato dextrose agar; bacteria, heart infusion agar. Assay method: agar dilution method. *a*) Minimum inhibitory concentration. *b*) Diethylstilbestrol. *c*) Ref. 8.

In addition to I and II,[2] it was reported previously that hexestrol (III),[3] 3,3′-dihydroxy-α,β-diethylstilbene (IV)[2] and 3,3′-dihydroxy-α,β-diethyldiphenylethane (V)[6] showed phytogrowth-inhibitory activity, with the latter having the most potent inhibitory activity against both plants.[6] Compound I showed the same inhibitory activity as V against both plants. The phytogrowth-inhibitory activities of I in this work II—V[2,3,6] were supported by our previous paper[17] which reported that 3,3′,4,5′-tetrahydroxystilbene and 3,3′,4,5′-tetrahydroxybibenzyl isolated from *Cassia garrettiana* (Leguminosae) showed the same activities. Batatasin III[18] and lunularin,[19] having the same skeleton as I were also found to have phytogrowth-inhibitory activity. These reports indicate that such biological activity might be common in oxystilbene-related compounds. We are now investigating the phytogrowth-inhibitory activities of many oxystilbene-related compounds.

Antimicrobial Activity of 3,4′-Dihydroxy-α,β-diethylstilbene (I) As shown in Table II, compound I, unlike II, showed broad antifungal spectrum on pathogenic fungi, while the antibacterial activity of I was slightly lower than that of II. To date, II,[1,3] 3,3′-dihydroxy-α,β-diethylstilbene (IV)[2] and 2,2′-dihydroxy-α,β-diethylstilbene[12] have also been reported to show antifungal activity against pathogenic fungi. However, the antifungal activity of I against pathogenic fungi is being reported here for the first time.

As shown in Table III, compound I also showed antimicrobial activity against six kinds of *Fusarium oxysporum* sp. and other plant-pathogenic bacteria. The antibacterial activity of I was as high as that of II, while the former's antifungal activity against *Fusarium oxysporum* sp. was slightly lower than those of II.

In addition to I and II, hexestrol (III), 3,3′-dihydroxy-α,β-diethylstilbene (IV)[2] and 3,3′-dihydroxy-α,β-diethyldiphenylethane (V)[8] were reported to have antifungal activity against *Fusarium oxysporum* f. sp. *lycopersici* IFO-6531 and other *Fusarium oxysporum* sp. The antifungal activities of these oxystilbene-related compounds in this work were also supported by our reports that 3,3′,4,5′-tetrahydroxystilbene,[20] the constituent of *Cassia garrettiana* and its derivative, 3,4-*O*-isopropylidene-3,3′,4,5′-tetrahydroxystilbene[21] showed antifungal activities against *Fusarium oxysporum* sp. *Fusarium oxysporum* sp. are well known not only as plant-pathogenic fungi but also as causative organisms of keratomycosis. However, no low-toxicity antifungal substances have been discovered as yet. In this respect, it is noteworthy that all of the oxystilbene-related compounds tested inhibited the growth of *Fusarium oxysporum* sp. Further studies on antifungal activity of many oxystilbene derivatives against *Fusarium oxysporum* sp. are required.

It was found that by shifting one of the phenolic hydroxy groups of II to the *meta*-position, phytogrowth-inhibitory effect and antifungal activity on pathogenic fungi were greatly increased. Among the diethylstilbestrol-related compounds tested, 3,3′-dihydroxy-α,β-diethylstilbene[12] and 3,3′-dihydroxy-α,β-diethyldiphenylethane[13] have been reported to have no hormonal side effect. However, the hormonal effect of I has not been examined as yet. Further studies on the hormonal side effect of I are in progress.

References

1) Y. Inamori, M. Kubo, M. Ogawa, M. Moriwaki, H. Tsujibo, K. Baba and M. Kozawa, *Chem. Pharm. Bull.*, **33**, 4478 (1985).
2) Y. Inamori, M. Kubo, M. Ogawa, H. Tsujibo, Y. Miki and S. Takemura, *Chem. Pharm. Bull.*, **35**, 3502 (1987).
3) Y. Inamori, T. Kobayashi, M. Ogawa and H. Tsujibo, *Chem. Pharm. Bull.*, **36**, 815 (1988).
4) Y. Inamori, M. Kubo, M. Ogawa, M. Moriwaki, H. Tsujibo, K. Baba and S. Takemura, *Chem. Pharm. Bull.*, **33**, 420 (1985).
5) Y. Inamori, M. Kubo, H. Tsujibo, M. Ogawa, Y. Saito, Y. Miki and S. Takemura, *Chem. Pharm. Bull.*, **35**, 887 (1987).
6) Y. Inamori, H. Tsujibo, M. Ogawa, Y. Miki and S. Takemura, *Chem. Pharm. Bull.*, **36**, 3137 (1988).
7) Y. Inamori, H. Tsujibo, H. Hachiken, Y. Miki and S. Takemura, *Chem. Pharm. Bull.*, **36**, 1252 (1988).
8) Y. Inamori, M. Ogawa, H. Amino, M. Tsuboi, S. Yamaguchi, H. Tsujibo and S. Takemura, *Chem. Pharm. Bull.*, **38**, 2045 (1990).
9) Y. Inamori, M. Ogawa, Y. Ohno, S. Nishihata, H. Tsujibo, Y. Miki and S. Takemura, *Chem. Pharm. Bull.*, **37**, 3137 (1989).
10) K. Shida, J. Shimazaki, E. Urano, H. Kurihara, H. Takahashi, N.

Furuya and M. Taya, *Nippon Hinyokika Gakkai Zasshi*, **63**, 27 (1972).
11) M. R. Schneider, G. Kranzfelder, E. von Angerer, H. Schonenberger, M. Metzler, R. Th. Michel, H. P. Fortmeyer and G. Ruckdeschel, *J. Cancer Res. Clin. Oncol.*, **100**, 247 (1981).
12) D. Adam and H. Schonenberger, *Arzneim.-Forsch.*, **16**, 738 (1966).
13) R. W. Hartmann, G. Kranzfelder, E. V. Angerer and H. Schonenberger, *J. Med. Chem.*, **23**, 841 (1980).
14) R. W. Hartmann, H. Buchborn, G. Kranzfelder, H. Schonenberger and A. Bogden, *J. Med. Chem.*, **24**, 1192 (1981).
15) Y. Miki, H. Hachiken, Y. Saito, K. Okada, S. Takemura and Y. Inamori, *Chem. Pharm. Bull.*, in preparation.
16) Y. Inamori, M. Kubo, H. Tsujibo, M. Ogawa, K. Baba, M. Kozawa and E. Fujita, *Chem. Pharm. Bull.*, **34**, 3928 (1986).
17) Y. Inamori, Y. Kato, M. Kubo, M. Yasuda, K. Baba and M. Kozawa, *Chem. Pharm. Bull.*, **32**, 213 (1984).
18) Y. Hashimoto, K. Hasegawa and A. Kawarada, *Planta*, **108**, 369 (1972).
19) J. Gorham, *Phytochemistry*, **16**, 249 (1977).
20) The antifungal activity of 3,3′,4,5′-tetrahydroxystilbene on *Fusarium oxysporum* sp. will be reported elsewhere.
21) Y. Inamori, M. Kubo, Y. Kato, M. Yasuda, H. Tsujibo, K. Baba and M. Kozawa, *Chem. Pharm. Bull.*, **33**, 2904 (1985).

Isolation and Characterization of α-Mercaptopropionylglycine–2,4-Dihydroxyphenylalanine Conjugates Produced through Mushroom Tyrosinase Reaction

Noriko MOTOHASHI,* Harumi NISHIKAWA and Itsuhiko MORI

Department of Radiopharmaceutical Chemistry, Kobe Women's College of Pharmacy, 4–19–1 Motoyamakita-machi, Higashinada-ku, Kobe 658, Japan.
Received June 25, 1990

Several kinds of α-mercaptopropionylglycine (α-MPG)–2,4-dihydroxyphenylalanine (dopa) conjugates produced through a mushroom tyrosinase reaction from tyrosine as a substrate in the presence of α-MPG were separated by high-performance liquid chromatography. The two main peaks were analyzed by coloring reactions, ultraviolet spectrometry and proton magnetic resonance determination. 5-S-α-MPG–dopa conjugate and 6-S-α-MPG–dopa conjugate were formed in a ratio of nearly 1 to 1. These conjugates shortened the lag time in tyrosine hydroxylation by tyrosinase and reduced the inhibition of tyrosine hydroxylation by α-MPG.

Keywords 2,4-dihydroxyphenylalanine conjugate; α-mercaptopropionylglycine; cysteine; tyrosinase; high performance liquid chromatography

It is a well-known fact that a thiol compound forms a stable conjugate with *o*-quinone produced during melanin formation reaction, inhibiting tyrosinase reaction.[1–6] It has recently been suggested that cysteine and glutathione may inhibit mammalian melanogenesis by the formation of a conjugate with a reaction intermediate and by direct action on the active site of tyrosinase.[7] Meanwhile, the action of cysteine and α-mercaptopropionylglycine (α-MPG) on *Neurospora* tyrosinase has been substantiated; *i.e.*, the former forms a mixed valence $Cu^{2+} \cdot Cu^{+}$ complex with the active center copper of tyrosinase, inactivating the tyrosinase; the latter denatures the tyrosinase.[8] We demonstrated that these two compounds inhibit melanin formation reaction by mushroom tyrosinase in two action modes, conjugate formation and enzyme inactivation.[9] Notably, the cysteine-2,4-dihydroxyphenylalanine (dopa) conjugate produced through tyrosinase reaction proved to comprise mainly 5-S-cysteinyldopa.[10] In the present study, the α-MPG–dopa conjugate was separated to determine its structure, which was compared with that of the cysteine-dopa conjugate.

Experimental

Materials Tyrosinase. as extracted and purified from mushrooms (grade III), was purchased from Sigma. L-[3,5-^{3}H]tyrosine (1.48 MBq/mol) in 2% ethanol solution was purchased from Amersham. This preparation was used in 25 mM phosphate buffer (pH 6.8) after the solvent was evaporated to dryness in nitrogen gas. Cysteine, ninhydrin, 2,6-dichloroquinone chloroimide (Gibbs reagent), 5,5′-dithiobis(2-nitrobenzoic acid) (DTNB) and ammonium phosphomolybdate were purchased from Wako Pure Chemical. α-MPG was purchased from Sigma. All other reagents were commercially available and of special grade.

Conjugate Formation and Separation 10 μmol L-dopa, 12 μmol cysteine or α-MPG and 4500 units of mushroom tyrosinase were dissolved in 25 ml of 25 mM phosphate buffer (pH 6.8), followed by shaking at 25 °C for 60 min. The reaction was terminated by the addition of 6 N HCl to reach a pH value of 1. This reaction mixture was concentrated to dryness under reduced pressure below 30 °C and then dissolved in a small quantity of 0.2 M acetic acid.

The resulting conjugates were separated by high performance liquid chromatography (HPLC) using a Shimadzu liquid chromatograph, Model LC-3A, and an ultraviolet (UV)/visible light spectrophotometer, Model SPD-1, at 290 nm. The column was Nucleosil C_{18} (5 μm) (Macherey), 25 cm × 4.6 mm i.d., through which 0.2 M acetic acid, as mobile phase, was passed at a flow rate of 0.8 ml/min. The effluent was collected and concentrated to dryness under reduced pressure below 30 °C. The UV spectrum was taken in the wavelength range of 220 to 340 nm using a Shimadzu recording spectrometer, Model UV 200, in the presence of 1 N HCl as solvent. Proton magnetic resonance (^{1}H-NMR) spectrum was taken using a Varian XL-200 spectrometer in the presence of 1 N DCl as the solvent and *tert*-buthanol as the internal standard ($\delta = 1.28$).

Tyrosine Hydroxylation The starting reaction mixture comprised 0.4 mM L-tyrosine, 14.8 kBq L-[3,5-^{3}H]tyrosine and 10 units of mushroom tyrosinase in 1 ml of 25 mM phosphate buffer (pH 6.8). The reaction was carried out in the presence of 0.48 mM cysteine or α-MPG alone or in combination with 0.2 mM of their conjugate at 37 °C. The reaction was terminated by the addition of 0.2 ml of 40% metaphosphoric acid. The ^{3}H released was measured as ^3H_2O by radioassay, as reported previously,[11] using a liquid scintillation counter.

Results

Separation of Cysteine–Dopa Conjugates Figure 1 shows the HPLC patterns of the resulting cysteine–dopa conjugates. Peak D was identified as dopa. Peaks A, B, C and E were separated and subjected to UV spectrometry. ^{1}H-NMR was also measured for peak E, obtained in the greatest amount. The results were compared with the UV spectral and ^{1}H-NMR data of cysteine–dopa conjugates separated by ion exchange chromatography by Ito *et al.*[10] Peaks A, B, C and E were assigned to 2-S-cysteinyldopa, 2,5-S,S-cysteinyldopa, 6-S-cysteinyldopa and 5-S-cysteinyldopa, respectively, the latter being dominant (about 70%).

Separation of α-MPG–Dopa Conjugates Figure 2 shows

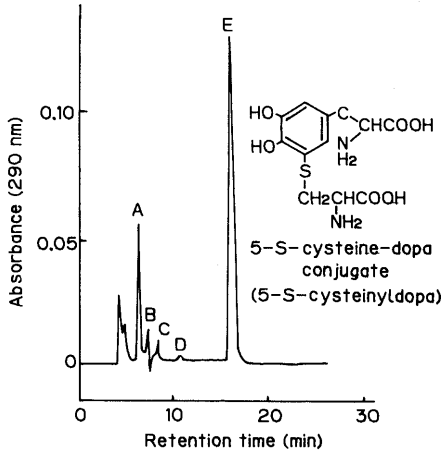

Fig. 1. Chromatogram of Cysteine–Dopa Conjugate Induced by Tyrosinase

Column, Nucleosil C_{18} (5 μm) 25 cm × 4.6 mm i.d.; eluent, 0.2 M acetic acid; flow rate, 0.8 ml/min. Peaks: A = 2-S-conjugate, B = 2,5-S,S-conjugate, C = 6-S-conjugate, D = dopa, E = 5-S-conjugate.

TABLE I. The Data of Chromatography, Coloring Reaction and Spectrometry of α-MPG–Dopa Conjugates

Peak	Compound	Retention volume[a] (ml)	Coloring reaction			UV[c] λ_{max} (nm)	^{1}H-NMR[d] δ (ppm)
			Gibbs	DTNB[b]	Ninhydrin		
D	5-S-Conjugate	42.6	+	−	+	294	6.93, 6.96 (centered) (ABq, J=2 Hz)
E	6-S-Conjugate	46.0	−	−	+	293	6.92 (s like) 6.95 (s like)

a) Analytical condition: column, Nucleosil C_{18} (5 μm) 25 cm × 4.6 mm i.d.; eluent, 0.2 M acetic acid; flow rate, 0.8 ml/min. *b*) 5,5′-Dithiobis(2-nitrobenzoic acid). *c*) Measured in 0.1 N HCl. *d*) Measured in 0.1 N DCl using *tert*-buthanol (δ=1.28) as an internal standard. The data indicated only the aromatic signals.

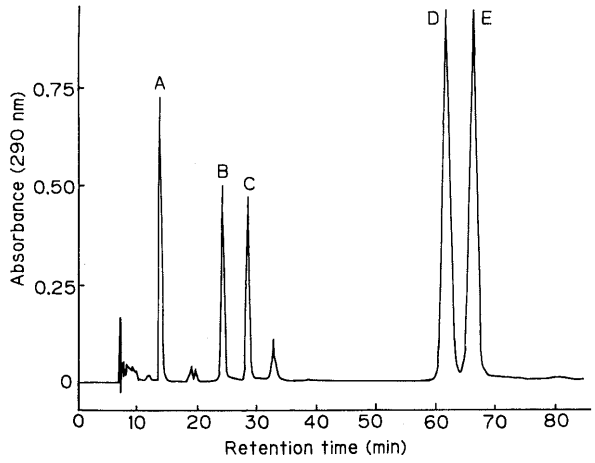

Fig. 2. Chromatogram of α-MPG–Dopa Conjugates Induced by Tyrosinase

Column, Nucleosil C_{18} (5 μm) 25 cm × 4.6 mm i.d.; eluent, 0.2 M acetic acid; flow rate, 0.8 ml/min. Peaks: A=dopa, B and C=unidentified, D=5-S-conjugate, E=6-S-conjugate.

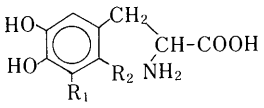

5-S-α-MPG–dopa conjugate: R_1=–S–CH(CH$_3$)–CONHCH$_2$COOH, R_2=H

6-S-α-MPG–dopa conjugate: R_1=H, R_2=–S–CH(CH$_3$)–CONHCH$_2$COOH

Fig. 3. Structure of α-MPG–Dopa Conjugates

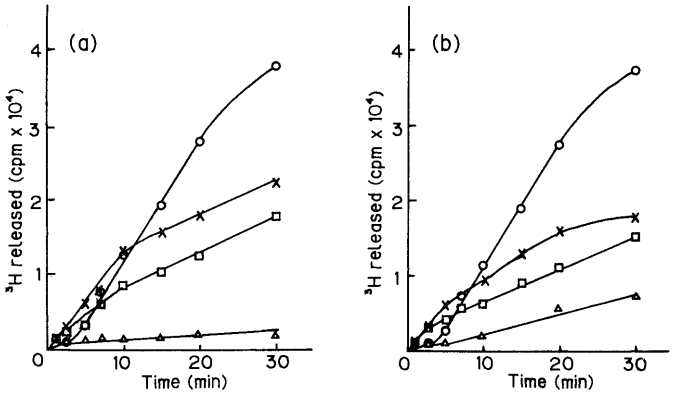

Fig. 4. Effects of Cysteine and α-MPG–Dopa Conjugates on Tyrosine Hydroxylation by Tyrosinase

The control solution contained 0.4 mM L-tyrosine, 14.8 kBq of L-[3,5-^{3}H]tyrosine and 10 units of tyrosinase in 1 ml of 25 mM phosphate buffer, pH 6.8. (a) ○, control; △, added 0.48 mM cysteine; ×, added 0.48 mM cysteine and 0.2 mM cysteine–dopa conjugate; □, added 0.2 mM cysteine–dopa conjugate. (b) ○, control; △, added 0.48 mM α-MPG; ×, added 0.48 mM α-MPG and 0.2 mM α-MPG–dopa conjugate; □, added 0.2 mM α-MPG–dopa conjugate.

the HPLC patterns of the resulting α-MPG–dopa conjugates. Dopa eluted in peak A. Peaks B through E were separated to determine their structure, but peaks B and C were produced in such small amounts that their structure could not be determined. Peaks D and E, produced in large amounts, were subjected to coloring reactions, UV spectrometry and ^{1}H-NMR measurement. The results are shown in Table I. Ninhydrin coloring reaction revealed the presence of an amine in both peaks. Also substantiated was the presence of a phenolic hydroxyl group in both peaks in the ammonium phosphomolybdate test. These findings suggest the presence of dopa in both peaks. Gibbs's reaction revealed that peak D does not involve hydrogen substitution at the *para*-position to an aromatic hydroxyl group, while peak E is a substitution product. Both peaks were negative for thiol group reaction by DTNB. It was therefore, inferred that α-MPG, like cysteine, is bound to the benzene ring of dopa *via* its S atom.

Integration of the ^{1}H-NMR curves of peaks D and E revealed a dopa–α-MPG compositional ratio of 1 to 1. Also, peak D was found to involve cleavage of the benzene ring protons to the ABq type with J=2 Hz. To explain this finding, two protons were presumed to exist in the *meta*-position with respect to each other. As for peak E, the two protons were presumed to exist in the *para*-position with respect to each other, since two slightly broader singlets appeared at 6.92 and 6.95 ppm. Based on these findings, peak D was identified as 5-S-α-MPG–dopa conjugate, and peak E as 6-S-α-MPG–dopa conjugate (Fig. 3). These two were produced in a ratio of almost 1 to 1.

Effects of Conjugates on Tyrosine Hydroxylation Figure 4 shows the effects of conjugates on tyrosine hydroxylation by tyrosinase when L-[3,5-^{3}H]tyrosine was used as a substrate. Tyrosine hydroxylation showed a slight lag time in the control. Cysteine and α-MPG both inhibited tyrosine hydroxylation, but the lag time was eliminated by the addition of cysteine or α-MPG conjugate. In addition, the inhibition of tyrosine hydroxylation by cysteine and α-MPG was reduced by the addition of these conjugates.

Discussion

The α-MPG–dopa conjugates induced from the substrate tyrosine by mushroom tyrosinase mainly comprised 5-S- and 6-S-dopa conjugates in a ratio of almost 1 to 1, showing a distinct contrast with the fact that the 5-S-conjugate accounted for about 70% of the cysteine–dopa conjugates, the contribution of the 6-S-conjugate comprising several

percent at most (Fig. 1). Meanwhile, the dopa conjugate formed by the reaction of methionine with dopaquinone was essentially 6-S conjugate.[6] In α-MPG, the 5-S- and 6-S-conjugates respectively induced by cysteine and methionine were both main products. This may be attributable to the common properties of α-MPG and cysteine/methionine, *i.e.*, α-MPG and cysteine both have a thiol group, and α-MPG and methionine both have a methyl group at the terminal adjoining the thiol group or sulfide.

The addition of conjugates shortened the lag time in tyrosine hydroxylation, and reduced the inhibitory effects of cysteine and α-MPG. This agrees well with the effects of cysteine–pyrocatechol conjugate addition reported by Sanada *et al.*[12] They explained these effects by the following hypothesis: 1) The chelation of tyrosinase active center cuprous ions and thiol was replaced by the chelation of cuprous ions and conjugate. 2) Binding of the conjugate to tyrosinase resulted in a change in the enzyme's conformation, thus showing resistance to the thiol compound. This hypothesis may apply to the effects of cysteine– and α-MPG–dopa conjugates noted in the present study.

References

1) S. Roston, *J. Biol. Chem.*, **235**, 1002 (1960).
2) W. S. Pierpoint, *Biochem. J.*, **98**, 567 (1966).
3) M. Seiji, T. Yoshida, H. Itakura and T. Irimajiri, *J. Invest. Dermatol.*, **52**, 280 (1969).
4) H. Sanada, R. Suzue, T. Nakashima and S. Kawada, *Biochim. Biophys. Acta*, **261**, 258 (1972).
5) R. C. Cowley and J. M. Palmer, *Phytochemistry*, **18**, 729 (1979).
6) M. N. Gupta and P. J. Vithayathil, *Bio-Org. Chem.*, **11**, 101 (1982).
7) J. R. Jara, P. Aroca, F. Solano, J. M. Martinez and J. A. Lozano, *Biochim. Biophys. Acta*, **967**, 296 (1988).
8) R. Aasa, J. Deinum, K. Lerch and B. Reinhammer, *Biochim. Biophys. Acta*, **535**, 287 (1978).
9) N. Motohashi, H. Nishikawa and I. Mori, *Chem. Phrm. Bull.*, **39**, 142 (1991).
10) S. Ito and G. Prota, *Experientia*, **33**, 1118 (1977).
11) N. Motohashi, H. Eguchi and I. Mori, *Chem Pharm. Bull.*, **30**, 2094 (1982).
12) H. Sanada, Y. Nakashima, R. Suzue and S. Kawada, *J. Nutr. Sci. Vitaminol.*, **22**, 389 (1976).

Calcium-Binding Protein Regucalcin Stimulates the Uptake of Ca^{2+} by Rat Liver Mitochondria

Seiichi MORI and Masayoshi YAMAGUCHI*

Department of Environmental Biochemistry, School of Pharmaceutical Sciences, University of Shizuoka, 395 Yada, Shizuoka City 422, Japan.
Received August 2, 1990

The effect of the calcium-binding protein regucalcin on the Ca^{2+} transport system in rat liver mitochondria was investigated. Ca^{2+} transport was assayed by the method of Millipore filtration to estimate mitochondrial $^{45}Ca^{2+}$ accumulation. $^{45}Ca^{2+}$ uptake was stimulated by the presence of regucalcin (1.0 and 2.0 μM). This stimulation was remarkable during 1.0 min after $^{45}Ca^{2+}$ addition, while appreciable stimulation was no longer seen at 3 min. Regucalcin (2.0 μM)-induced stimulation of $^{45}Ca^{2+}$ uptake was prevented by the presence of ruthenium red (1.0 μM) and lanthanum chloride (0.1 mM). Regucalcin (2.0 μM) did not increase the mitochondrial adenosine triphosphatase (ATPase) activity during 3.0 min after Ca^{2+} addition. Meanwhile, $^{45}Ca^{2+}$, which accumulated in the mitochondria during 5.0 min after $^{45}Ca^{2+}$ addition, was not released by the addition of regucalcin. Regucalcin may stimulate Ca^{2+} uptake in rat liver mitochondria independently of the energy.

Keywords calcium; regucalcin; calcium-binding protein; calcium transport; rat liver mitochondria

Ca^{2+} plays an important role in the regulation of many cell functions. Liver metabolism is regulated by increase of Ca^{2+} in the cytosol of liver cells due to hormonal stimulation.[1,2] The Ca^{2+} effect is modulated in liver cells through calmodulin, a calcium-binding protein.[3,4] We recently reported that a calcium-binding protein (regucalcin), which differs from calmodulin, is distributed in the hepatic cytosol of rats.[5,6] The molecular weight of regucalcin was estimated to be 288000, and the Ca^{2+} binding constant was found to be $4.19 \times 10^5\ M^{-1}$ by equilibrium dialysis.[6] This novel protein has a reversible effect on the activation of various enzymes by Ca^{2+} in liver cells.[7-10]

On the other hand, the low cytoplasmic Ca^{2+} concentration of living cells is maintained by energy-requiring pumps. These pumps either remove Ca^{2+} to the extracellular space by transport across the plasma membrane or accumulate it inside intracellular organelles such as the mitochondria and endoplasmic reticulum.[11,12] More recently, it has been found that regucalcin can directly activate (Ca^{2+}–Mg^{2+})-adenosine triphosphatase (ATPase), which functions as a Ca^{2+} pump in rat liver plasma membranes,[13] suggesting that regucalcin may play a role in the stimulation of the homeostasis of increased cytosolic Ca^{2+} in liver cells.[14] Moreover, liver mitochondria can transport the cytoplasmic Ca^{2+} using the energy of respiration or of adenosine triphosphate (ATP) hydrolysis.[12] The present investigation was therefore undertaken to clarify the effect of regucalcin on the Ca^{2+} transport system in rat liver mitochondria. It was found that regucalcin stimulates Ca^{2+} uptake by the mitochondria.

Materials and Methods

Chemicals $^{45}Ca^{2+}$ (specific activity 32.89 mCi/mg) used was obtained from New England Nuclear (Boston, Mass., U.S.A.). ATP was purchased from Sigma Chemical Co. (St. Louis, MO, U.S.A.). Calcium chloride, ruthenium red, lanthanum chloride and all other reagents were obtained from Wako Pure Chemical Co. (Osaka, Japan). The chemicals were dissolved in distilled water and then passed through ion-exchange resin to remove metal ions.

Animals Male Wistar rats, weighing 100—120 g, were used. They were obtained commercially from Japan SLC, Inc., Hamamatsu, Japan. The animals were fed commercial laboratory chow (solid) containing 57.5% carbohydrate, 1.1% Ca, and 1.1% P at a room temperature of 25 °C, and were allowed distilled water freely. After 1 week on this diet animals were killed by bleeding.

Isolation of Regucalcin Liver was perfused with Tris–HCl buffer (pH 7.4, containing 100 mM Tris, 120 mM NaCl, 4 mM KCl, cooled to 4 °C). Liver was removed, cut into small pieces, suspended 1:4 in Tris–HCl buffer (pH 7.4) and homogenized in a Potter-Elvehjem homogenizer with a Teflon pestle. The homogenate was spun at 5500*g* in a refrigerated centrifuge for 10 min and the supernatant was spun at 105000*g* for 60 min. Regucalcin in the 105000*g* supernatant (cytosol fraction) was purified to electrophoretic homogeneity by gel filtration on Sephadex G-75 and G-50 followed by ion exchange chromatography on diethylaminoethyl (DEAE)-cellulose, as reported previously.[5]

Preparation of Hepatic Mitochondria Liver was perfused with ice-cold 0.25 M sucrose solution, immediately cut into small pieces, suspended 1:9 in the homogenization medium containing 0.25 M sucrose, 0.5 mM ethyleneglycol bis(2-aminoethylether)-*N*,*N*,*N*′,*N*′-tetraacetic acid (EGTA) and 10 mM 4-(2-hydroxyethyl)-1-piperazineethanesulfonic acid (Hepes), pH 7.4 and homogenized in a Potter-Elvehjem homogenizer with a Teflon pestle. The homogenate was centrifuged at 3000*g* for 10 min to remove nuclei, unbroken cells and cell debris. The resultant supernate was centrifuged at 22500*g* for 15 min to sediment the mitochondrial fraction.[15] The mitochondrial fraction was resuspended in 0.25 M sucrose, 10 mM Hepes, pH 7.4, to a final protein concentration of 6—7 mg/ml.

$^{45}Ca^{2+}$ Uptake $^{45}Ca^{2+}$ uptake was measured by the Millipore filtration technique, which modified the method of Whiting and Barritt.[16] The mitochondria (1.2—1.4 mg of protein/ml) was preincubated for 1 min at 37 °C in 2.0 ml of medium containing 150 mM KCl, 10 mM Hepes, 2 mM K-phosphate, 2 mM K-succinate, 2 mM $MgCl_2$, 4 μM rotenone, 2 mM ATP (adjusted to pH 7.4 with KOH) and other additions (regucalcin and/or inhibitors) as indicated. The final pH was 7.4. At a designated time after addition of 25 μM $CaCl_2$ (containing 5.0 mCi $^{45}Ca^{2+}$/l) as a final concentration, a 0.5 ml sample was filtered through a 0.22 μm prewetted Millipore filter. The precipitate was washed with 150 mM KCl/10 mM Hepes (pH 7.4), transferred to a scintillation vial and counted for radioactivity. $^{45}Ca^{2+}$ uptake is expressed as nmol of $^{45}Ca^{2+}$ accumulated per mg protein of the mitochondria. Protein concentration was determined by the method of Lowry *et al.*[17]

$^{45}Ca^{2+}$ Release Isolated rat liver mitochondria was incubated in the presence of 25 μM Ca^{2+} (5.0 μCi $^{45}Ca^{2+}$) and 2 mM ATP for 5 min at 37 °C in the Ca^{2+} uptake assay buffer, and then regucalcin (0.5—2.0 μM) was added to the incubation mixture. At a designated time after the addition of regucalcin, a 0.5 ml sample was filtered through a 0.22 μm pre-wetted Millipore filter to determine the amount of $^{45}Ca^{2+}$ remaining in the vesicles. The precipitate on the filter after filtration was washed with 150 mM KCl/10 mM Hepes (pH 7.4), and transferred to a scintillation vial. $^{45}Ca^{2+}$ remaining in the mitochondria is expressed as nmol of $^{45}Ca^{2+}$ per mg protein of the mitochondria.

ATPase Activity The mitochondrial ATPase activity was determined in the medium described above for the analysis of Ca^{2+} uptake.[18] The mitochondria was incubated for 10 min in the presence or absence of 2.0 μM regucalcin before Ca^{2+} addition. The reaction was started by adding 25 μM Ca^{2+} as a final concentration, and at a designated time it was stopped by addition of ice-cold trichloroacetic acid to a final concentration of 5.0%. After centrifugation for 10 min at 6000*g*, inorganic phosphate

was measured according to the method of Nakamura and Mori.[19] ATPase activity was expressed as nmol of inorganic phosphate released per mg protein.

Statistical Methods The significance of differences between values was estimated by Student's t-test. A p value of less than 0.01 was considered to indicate a statistically significant difference.

Results

The mitochondria isolated from rat liver was incubated for 1 min in medium containing 2 mM ATP and 2.0 μM regucalcin, and then $^{45}Ca^{2+}$ was added. $^{45}Ca^{2+}$ uptake by the mitochondria increased rapidly during 1 min after the addition, and it was saturated at 3 min (Fig. 1). The presence of regucalcin (2.0 μM) caused a significant increase of $^{45}Ca^{2+}$ uptake by the mitochondria (Fig. 1). This increase was seen at 15 s after the addition.

The effect of increasing concentrations of regucalcin (0.5, 1.0, and 2.0 μM) on $^{45}Ca^{2+}$ uptake by the mitochondria is shown in Fig. 2. The mitochondria was incubated for 15 and 60 s after the addition of $^{45}Ca^{2+}$. Mitochondrial $^{45}Ca^{2+}$ uptake at 15 s after the addition was significantly increased by the presence of 1.0 μM regucalcin, and with 2.0 μM regucalcin an appreciable effect was seen at 60 s after the addition.

The effect of ruthenium red or lanthanum chloride, which is a potent inhibitor of mitochondrial calcium uptake,[1,12] on $^{45}Ca^{2+}$ uptake by the mitochondria is shown in Fig. 3. The mitochondria was incubated for 1.0 min in the presence of the inhibitors with or without regucalcin (2.0 μM), and the uptake was measured 30 s after $^{45}Ca^{2+}$ addition. The presence of ruthenium red (1.0 μM) or lanthanum chloride (0.1 mM) caused an inhibition of mitochondrial $^{45}Ca^{2+}$ uptake. Also, regucalcin-induced increase in mitochondrial $^{45}Ca^{2+}$ uptake was completely inhibited by those inhibitors.

ATPase activity in the mitochondria increased during 1.0 min after Ca^{2+} addition (Fig. 4). This increase was not enhanced by the presence of regucalcin (2.0 μM). Also, in the absence of Ca^{2+}, regucalcin (2.0 μM) had no effect on the mitochondrial ATPase activity (data not shown).

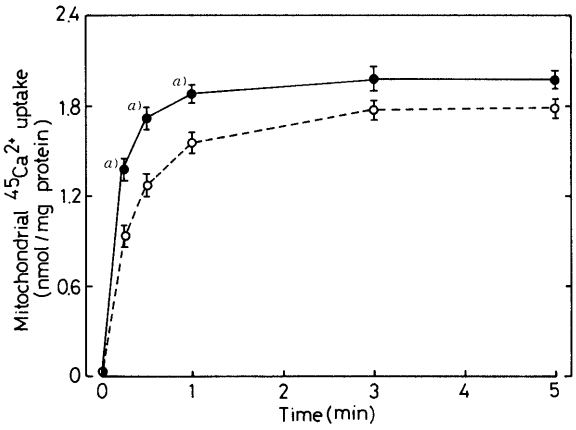

Fig. 1. Effect of Regucalcin on $^{45}Ca^{2+}$ Uptake by the Mitochondria of Rat Liver

$^{45}Ca^{2+}$ uptake was measured as described in the experimental section. The mitochondria was incubated for 1.0 min in the presence of 2 mM ATP and 2.0 μM regucalcin. At zero time $^{45}Ca^{2+}$ was added and the mixture was incubated for 5 min. Each value represent the mean ± SEM of five experiments. *a)* $p<0.01$, as compared with the control value without regucalcin. ○---○; control, ●---●; regucalcin.

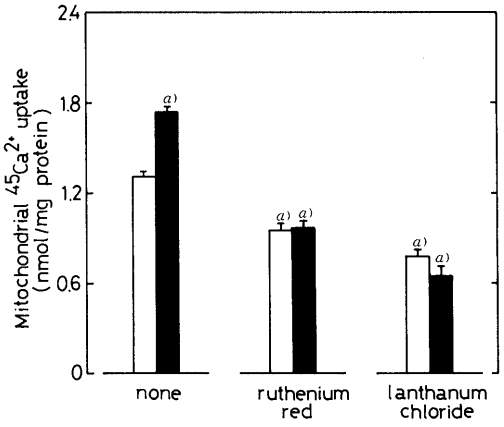

Fig. 3. Effect of Inhibitors on $^{45}Ca^{2+}$ Uptake by the Mitochondria of Rat Liver

$^{45}Ca^{2+}$ uptake was measured as described in the experimental section. The mitochondria was incubated for 1.0 min in the presence of 1.0 μM ruthenium red or 0.1 mM lanthanum chloride with or without 2.0 μM regucalcin, and it was further incubated for 30 s after $^{45}Ca^{2+}$ addition. Each value represents the mean ± SEM of five experiments. *a)* $p<0.01$, as compared with the control value without regucalcin. □; none, ■; regucalcin.

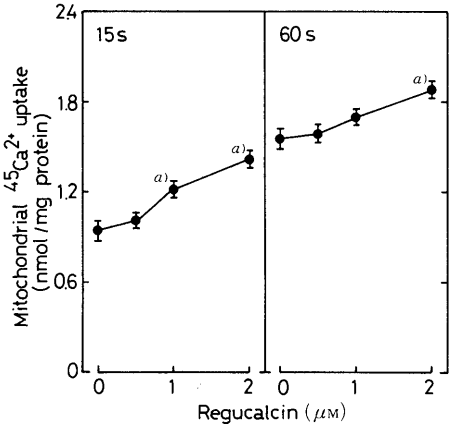

Fig. 2. Effect of Increasing Concentrations of Regucalcin on $^{45}Ca^{2+}$ Uptake by the Mitochondria of Rat Liver

$^{45}Ca^{2+}$ uptake was measured as described in the experimental section. Regucalcin was included in the incubation medium at a concentration of 0.5, 1.0 or 2.0 μM. The mitochondria was incubated for 15 and 60 s after $^{45}Ca^{2+}$ addition. Each value represents the mean ± SEM of five experiments. *a)* $p<0.01$, as compared with the control value without regucalcin.

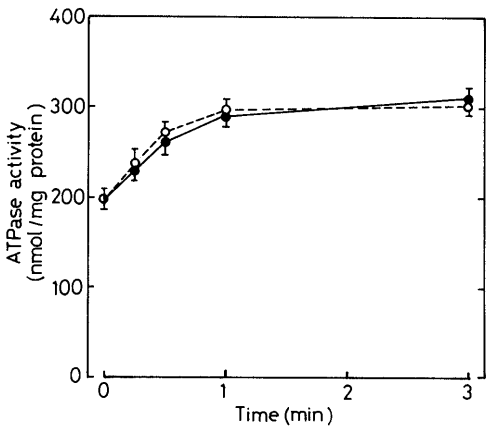

Fig. 4. Change of ATPase Activity in the Mitochondria of Rat Liver

The mitochondria was incubated for 1.0 min in the presence of 2.0 mM ATP and 2.0 μM regucalcin before the addition of Ca^{2+}. At zero time Ca^{2+} was added to give a final concentration of 25 μM. The mitochondria was further incubated for 3.0 min. At a designated time after Ca^{2+} addition, the mitochondrial ATPase activity was measured as described in the experimental section. Each value represents the mean ± SEM of five experiments. ○---○; control, ●---●; regucalcin.

On the other hand, isolated liver mitochondria was incubated for 5 min in medium containing 2.0 mM ATP and $^{45}Ca^{2+}$. The mitochondrial $^{45}Ca^{2+}$ uptake was saturated by incubation for 5 min. Regucalcin was then added to the incubation mixture. This addition (2.0 μM) resulted in no significant release of $^{45}Ca^{2+}$ from the mitochondria during 10 min after the addition of the protein; the mitochondrial $^{45}Ca^{2+}$ of control or regucalcin group was 1.79 ± 0.12 or 1.83 ± 0.14 nmol $^{45}Ca^{2+}$/mg protein (mean $\pm$ S.E.M. of five experiments), respectively.

Discussion

It was reported previously that $^{45}Ca^{2+}$ bound to regucalcin, which is a calcium-binding protein isolated from rat liver cytosol, is transported into the mitochondria dependent on ATP.[20] The present study was undertaken to clarify whether regucalcin can directly stimulate Ca^{2+} uptake by liver mitochondria, and it was found that regucalcin does stimulate $^{45}Ca^{2+}$ uptake by the mitochondria. This stimulatory effect was seen at 15 s after the addition of $^{45}Ca^{2+}$, and it continued for 1.0 min. Thus, regucalcin increased the initial rate of $^{45}Ca^{2+}$ uptake by the mitochondria; this effect was clear at 2.0 μM. The potent inhibitors (ruthenium red and lanthanum chloride) clearly inhibited the regucalcin (2.0 μM)-stimulated $^{45}Ca^{2+}$ uptake by the mitochondria, and regucalcin had no effect on $^{45}Ca^{2+}$ release. These results suggest that regucalcin is directly involved in $^{45}Ca^{2+}$ uptake in the mitochondria.

At present, we do not know the mechanism of regucalcin action which stimulates hepatic mitochondrial Ca^{2+} uptake. A Ca^{2+} carrier of the mitochondria has been reported to be a glycoprotein,[21] but the energy of respiration or of ATP hydrolysis is utilized to generate a membrane potential (and a proton gradient) that is responsible for driving Ca^{2+} electrophoretically.[22] However, regucalcin (2.0 μM) did not cause a significant alteration of Ca^{2+}-dependent ATPase activity in the mitochondria, nor did it have any effect on the mitochondrial ATPase activity in the absence of Ca^{2+}. From these results, it is assumed that regucalcin had no effect on the ATP-dependent or the respiration-dependent Ca^{2+} uptake by the mitochondria. Meanwhile, radioiodinated regucalcin can bind to isolated rat liver mitochondria.[14] Liver mitochondria transports the metal from $^{45}Ca^{2+}$-binding regucalcin using the energy of ATP hydrolysis.[20] Presumably, regucalcin binds the mitochondria, and the bound protein may easily bind extramitochondrial $^{45}Ca^{2+}$. The metal may be transported through the mechanism of Ca^{2+} uptake by liver mitochondria. The mechanism of regucalcin action on mitochndrial Ca^{2+} uptake, however, remains to be elucidated.

The physiological significance of regucalcin in stimulating Ca^{2+} uptake by liver mitochondria has not been clarified. The low cytoplasmic Ca^{2+} concentration of living cells is maintained by energy-requiring pumps. These pumps either remove Ca^{2+} to the extracellular space by transport across the plasma membrane or accumulate it inside intracellular organelles such as the mitochondria and endoplasmic reticulum.[1,11,12] Regucalcin may be partly involved in cytoplasmic Ca^{2+} homeostasis by stimulating mitochondrial Ca^{2+} uptake in liver cells.

Acknowledgement This work was supported in part by a Grant-in-Aid for Scientific Research (C) (No. 63571053) from the Ministry of Education.

References

1) J. R. Williamson, R. H. Cooper and J. B. Hoek, *Biochim. Biophys. Acta*, **639**, 243 (1981).
2) P. H. Reinhart, W. N. Taylor and F. L. Bygrave, *Biochem. J.*, **223**, 1 (1984).
3) W. Y. Cheung, *Science*, **207**, 19 (1980).
4) A. R. Means and J. R. Dedman, *Nature* (London), **285** 73 (1980).
5) M. Yamaguchi and T. Yamamoto, *Chem. Pharm. Bull.*, **26**, 1915 (1978).
6) M. Yamaguchi and K. Sugii, *Chem. Pharm. Bull.*, **29**, 567 (1981).
7) M. Yamaguchi and H. Yoshida, *Chem. Pharm. Bull.*, **33**, 4489 (1985).
8) M. Yamaguchi and H. Shibano, *Chem. Pharm. Bull.*, **35**, 2025 (1987).
9) M. Yamaguchi, S. Mori and Y. Suketa, *Che. Pharm. Bull.*, **37**, 388 (1989).
10) M. Yamaguchi and S. Mori, *Biochem. Med. Metab. Biol.*, **43**, 140 (1990).
11) E. Carafoli and M. Zurini, *Biochim. Biophys. Acta*, **683**, 279 (1982).
12) D. Nichols and K. Åkerman, *Biochim. Biophys. Acta*, **683**, 57 (1982).
13) C. Pavoine, S. Lotersztajn, A. Mallat and F. Pecker, *J. Biol. Chem.*, **262**, 5113 (1987).
14) M. Yamaguchi, S. Mori and S. Kato, *Chem. Pharm. Bull.*, **36**, 3532 (1988).
15) V. Prpić, T. L. Spencer and F. L. Bygrave, *Biochem. J.*, **176**, 705 (1978).
16) J. A. Whiting and G. J. Barritt, *Biochem. J.*, **206**, 121 (1982).
17) O. H. Lowry, N. J. Rosebrough, A. L. Farr and R. J. Randall, *J. Biol. Chem.*, **193**, 265 (1951).
18) M. G. P. Vale, A. J. M. Moreno and A. P. Carvalho, *Biochem. J.*, **214**, 929 (1983).
19) M. Nakamura and K. Mori, *Nature* (London), **182**, 1141 (1958).
20) M. Yamaguchi, *Chem. Pharm. Bull.*, **33**, 3390 (1985).
21) E. Panfili, G. Sandri, G. L. Sottocasa, G. Lunazzi, G. Lint and G. Graziosi, *Nature* (London), **264**, 185 (1976).
22) H. Rottenberg and A. Scarpa, *Biochemistry*, **13**, 4811 (1974).

Double Fluorescent Labeling Method Used for a Study on Liposomes

Hideyuki SAWAHARA,*[,a,1)] Shigeru GOTO,[a] and Nadao KINOSHITA[b]

Faculty of Pharmaceutical Sciences[a] and School of Health Sciences,[b] Kyushu University, 3–1–1 Maidashi, Higashi-ku, Fukuoka 812, Japan.
Received May 23, 1990

Carboxyfluorescein (CF) and Calcein (CAL) have almost the same fluorescent spectrum. However, only CAL forms a nonfluorescent chelate with the Co^{2+} ion. It was proven that this phenomenon can be used for the fractional determination of CF and CAL. And this fractional determination method was available for a study on liposomes.

Keywords drug delivery system; liposome; double fluorescent labeling method; carboxyfluorescein; calcein; cobalt ion; ethylenediaminetetraacetic acid

Liposomes formed by a bilayer membrane of phospholipids can contain or entrap various agents. Since the liposome is biodegradable and considered scarcely poisonous,[2)] it is potentially useful as a so-called drug delivery system (DDS) that would deliver desired agents to a specific site.[3–5)]

Several methods of evaluating the distribution of liposomes are well known, and the labeling method of using radioactive isotopes is also widely applied[4)]. However, this method has some defects in terms of simplicity and safety in experimental operation. In addition, in the case of using liposomes containing radioactive substances, it is difficult to distinguish between the radioactivity in the liposomes and that leaked out of the liposome during storage as well as in experiments. Therefore, we carried out this investigation with the intention of simplifying the operation without losing measurement sensitivity by using of two kinds of fluorescent substances which permit fractional determinations.

In 1977, Weinstein *et al.* chose a water soluble fluorescent substance, carboxyfluorescein (CF) to be contained in liposomes, and ingeniously applied the self-quenching phenomenon characteristic of the fluorescent substance to study the liposomes.[6)] In 1980, Allen *et al.* also chose calcein (CAL) for the same purpose, and reported that CAL is superior to CF in terms of stability of fluorescent intensity in physiological pH range.[7)] Figure 1 shows the chemical structure of CF and CAL.

While both CF and CAL have the skeletal structure of fluorescein as well as very similar fluorescent spectra, only CAL forms a nonfluorescent chelate with the Co^{2+} ion. We noted that fractional determination might be possible using CF and CAL. First, optimum conditions were examined for fractional determination of CF and CAL *in vitro*. Then, two kinds of liposomes which contained CF or CAL were prepared. Thus, the disappearance of these liposomes from the circulation *in vivo* was examined in mice, and establishment of a double fluorescent labeling method to study liposomes was attempted.

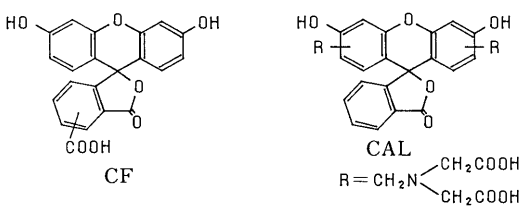

Fig. 1. Chemical Structures of CF and CAL

Experimental

Reagents CF was purchased from Eastman Kodak Inc., and purified by the method of Ralston *et al.*[8)] CAL was purchased from Wako Pure Chemical Industries, Ltd., and used as it was. Cholesterol (Chol) and all other reagents used were of the highest grade commercially available. Egg phosphatidylcholine (PC) was extracted from the yolk and purified by the modification of the methods of Rhodes *et al.*[9)] and Bangham *et al.*[10)] The purity of purified PC was confirmed by the thin layer chromatography (TLC) method of Abramson *et al.*[11)] The PC was then dissolved into chloroform and kept at −20 °C on a nitrogen substitution.

Preparation of Solutions of CF and CAL to be Contained in Liposomes Purified CF was dissolved with a minimal volume of 1 N NaOH and the solution was finally adjusted to pH 7.4 and 100 mM with *ca.* 0.1 N NaOH, as well as distilled water. CAL was dissolved with a minimal volume of 2 N NaOH and the solution was finally adjusted to pH 7.4 and 86 mM with *ca.* 0.1 N NaOH, as well as distilled water. These solutions of 100 mM CF and 86 mM CAL were confirmed isotonic with blood by a cryoscopic method.

Quenching of Fluorescence of CF and CAL by the Co^{2+} Ion Fluorescent intensities of CF and CAL were measured at excitation 470 nm (slit 4.0 nm) and emission 520 nm (slit 7.5 nm) by a self-recording fluorescent spectrophotometer (Shimadzu Seisakusho Ltd., Model RF-502). 0.1 M Tris–HCl buffer (pH 8.5) was used for a quenching experiment of the fluorescence of CF and CAL, according to the method of Wallach *et al.*[12)] Further, considering the association of plasma with the fluorescent quenching of CF and CAL, the following experiments were carried out. Namely, 0.5 ml of rabbit plasma and 0.5 ml of $CoSO_4$ solution were added to 4 ml of 1.25 μM CF, and agitated. Then the sample was left at room temperature for more than 30 min and the fluorescent intensity of CF was measured. The final concentrations of CF and plasma were 1 μM and 10% (v/v), respectively. Concentrations of the Co^{2+} ion used were nine kinds of 2, 5, 10, 15, 20, 25, 30, 40, and 50 μM. A similar examination was carried out by adding 0.5 ml of ethylenediaminetetraacetic acid (EDTA) solution (EDTA was dissolved with a minimal volume of 1 N NaOH, and the pH was adjusted to 8.5 with 0.1 N NaOH and distilled water) instead of the Co^{2+} ion solution. The final concentrations of EDTA were 0.25, 1, 2.5, 5, 10, 15, 20, and 25 mM, respectively. The same experiment was carried out separately by using 1.25 μM CAL solution instead of 1.25 μM CF.

Preparation of CF-Containing Liposomes and CAL-Containing Liposomes A chloroform solution of PC (20 μmol) and Chol (20 μmol) was poured into a pear type flask, and the chloroform was distilled under reduced pressure by using a rotary evaporator. Next it was poured into a desiccator and dried for more than 1 h under decreasing pressure created by using a vacuum pump. Then, 2 ml of 100 mM CF solution was added into the dried flask, and hydrated at 37 °C for 10 min. By vortexing it, multilamellar vasicles (MLV) were prepared. Small unilamellar vesicles (SUV) were also prepared through processing MLV at 37 °C for 40 min by using a probe-type sonicator (Heatsystems-ultrasonics, Inc., Model W-220) equipped with a microchip. CF which was not enclosed in the liposomes was adsorbed on the diethylaminoethyl (DEAE) Sephadex A-25 column (1.4 × 3.7 cm), while CF-containing liposomes were obtained by elution with a phosphate buffered saline (PBS; 137 mM NaCl, 2.6 mM KCl, 6.4 mM Na_2HPO_4, 1.4 mM KH_2PO_4, pH 7.4). To remove residual MLV, 3 ml of the eluted sample was slowly layered on 2 ml of a 10% sucrose phosphate buffer (10% sucrose, 6.4 mM Na_2HPO_4, 1.4 mM KH_2PO_4, pH 7.4) previously placed in a tube (Hitachi Koki Co., Ltd., 5CN tube) and centrifuged at 105000 *g* for 60 min by an ultracentrifuge (Hitachi Koki Co., Ltd., Model 65P) and swing rotor (RPS-50 Type). To remove the smaller

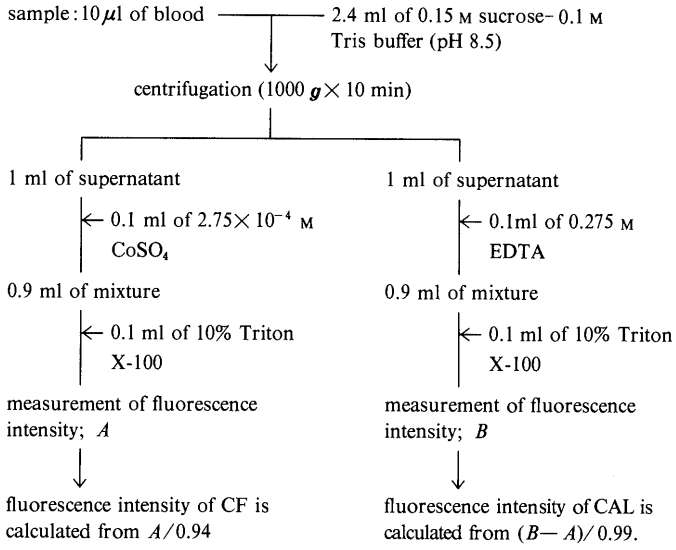

Chart 1. Flow Chart for Determination of Fluorescent Intensities of CF and CAL in 10 μl of Blood Collected from the Tail Vein of Mice after Intravenous Injection

vesicles, the supernatant layer was recentrifuged at 159000 *g* for 180 min according to the modified method of Barenholz *et al.*[13] The resulting pellet placed on 2 ml of a 10% sucrose phosphate buffer was recovered. The pellet was resuspended with PBS and used for examination *in vivo*. All experiments were carried out at 4 °C. Likewise, CAL-containing liposomes were prepared according to the same method, except for using the 86 mM CAL solution (pH 7.4) instead of a 100 mM CF solution (pH 7.4).

Measurement of Size Distribution by Using an Electron Microscope Liposome samples were negative-stained with 2% uranyl acetate. The geometric properties of the vesicles were observed under a transmission-type electron microscope (Model-1200EX) of Jeol Inc. From the electron microscope photographs, Green diameters of the vesicles were measured and a size distribution graph was made. The size distribution of vesicles containing CF or CAL was determined by counting 503 and 335 vesicles, respectively.

Transition of Liposome Concentration within the Circulation of Mice A dosage solution, a mixture of CF-containing SUV (CF-SUV) and CAL-containing SUV (CAL-SUV) which was mingled so that CAL attained the equivalent fluorescence intensity of 100 μM of CF concentration, was injected into the tail vein of female mice with a weight of 30.1 g and 31.4 g (slc: ICR strain) by 5 ml/kg weight. At 5, 10, 15, 20, 30, 60, 120, 180, 240 and 300 min after the injection, 10 μl of blood was sampled from the tail vein (10 μl each of 10 times). The samples were immediately poured into 2.4 ml of 0.15 M sucrose–0.1 M Tris–HCl buffer (pH 8.5) and well agitated, then centrifuged at 1000 *g* for 10 min, and the supernatant without hemolysis was divided into two parts by 1 ml, and kept at 4 °C until measurement. The transition of concentrations of CF-SUV and CAL-SUV within the blood was then measured according to the method of Chart 1. The fluorescent recoveries of CF and CAL as measured were 94 and 99%, respectively.

Results and Discussion

CF and CAL have a favorable linear relationship between concentration and fluorescent intensity in the solutions of 1 nM to 1 μM. Figure 2 shows the influence of the Co^{2+} ion on fluorescence by use of a 1 μM solution, which is the highest concentration in the above experiment. Based upon the above results, the concentration of the Co^{2+} ion necessary to quench the fluorescence of CAL was determined as 25 μM. There was no influence on the fluorescence of CF by the Co^{2+} ion. On the other hand, when a total amount of CF and CAL in the buffer containing 10% plasma was measured, it was found that the fluorescence of CAL was influenced by divalent metallic ions[12] such as Ca^{2+} or Mg^{2+} in blood, and therefore,

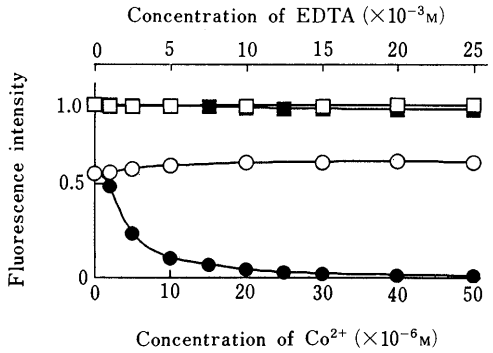

Fig. 2. Effect of $CoSO_4$ and EDTA Concentrations on Fluorescent Intensities of CF (1 μM) and CAL (1 μM) in Tris–HCl Buffer (pH 8.5) Containing Rabbit Plasma (10%)

(■) CF + $CoSO_4$; (□) CF + EDTA; (●) CAL + $CoSO_4$; (○) CAL + EDTA.

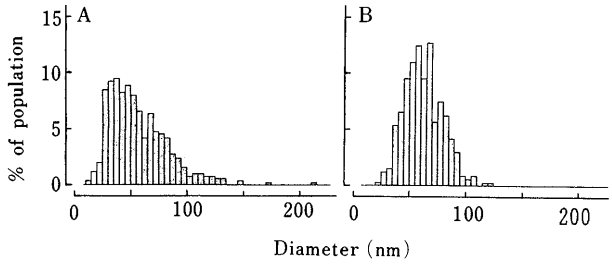

Fig. 3. Size Distribution of Liposomes Containing CF (A) or CAL (B)

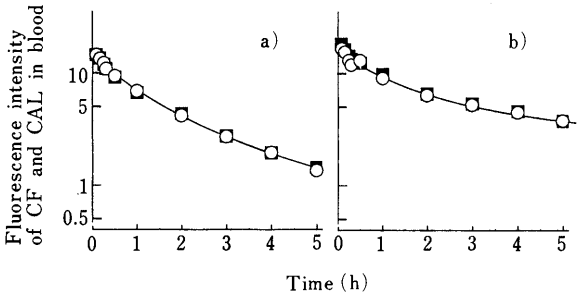

Fig. 4. Decreasing Fluorescent Intensities of CF (■) and CAL (○) in Blood after Intravenous Injection in Female slc: ICR Mice

EDTA was used to eliminate them. Figure 2 shows also the influence of EDTA on 1 μM of either CF or CAL. On the basis on Fig. 2, the concentration of EDTA was determined as 25 mM when a total amount of CF and CAL in the blood was measured. In this measurement, the ratio of molar fluorescent intensities of CF to CAL was 1 to 0.67.

Figure 3 shows the size distribution of two kinds of SUV. The mean diameter of CF-SUV was 56.8 nm and that of CAL-SUV was 62.5 nm. An fluorescently equivalent mixed solution of CF-SUV and CAL-SUV was injected into the mouse vein. Figure 4 shows the elimination profile of CF-SUV and CAL-SUV from the circulation after intravenous injection in mice. This investigation was carried out on two mice. The mouse of figure a) eliminated liposomes slightly faster from its blood compared to mouse b). However, it became clear that the elimination rate of CF was completely in accordance with that of CAL within a single body. This fact has proven that this measurement method can simultaneously compare the transition of two kinds of liposomes within the same circulation.

We chose CF and CAL for a combination of two kinds of fluorescent substances, both of which possess the skeleton structure of fluorescein and can be determined under identical fluorescence measurement conditions (excitation wave length of 470 nm and fluorescent wave length of 520 nm). Fractional determination of both CF and CAL can be performed with such simple laboratory manipulation as adding a solution of the Co^{2+} ion to each sample containing CF and CAL, quenching the fluorescence of CAL, measuring the fluorescence of CF only, and further evaluating the fluorescent intensity of both CF and CAL based upon an EDTA-added sample.

Liposomes with a PC and Chol mole ratio of 1 and 1 composition were used in this experiment. It was confirmed by Kirby *et al.*[14] that CF which had been enclosed in liposomes similar to those mentioned above did not leak into the circulating blood. Therefore, we employed this leak-free composition to develop a fractional determination method. As the particle size of liposomes is known to have an effect on their distribution,[15-21] the size was homogenized as much as possible by a centrifugal method.[13] Thus CF-SUV and CAL-SUV with identical lipid-composition and similar particle size were injected into mice, and highly accurate results were obtained showing that the elimination rates of CF and CAL from the circulation were entirely identical to each other, as shown in Fig. 4. The results proved that this double fluorescent labeling method would allow the prompt and accurate comparison of the distribution of two kinds liposomes with a minimum number of animals, thus eliminating complicated variations due to individual differences among animals.

References and Notes

1) Present address: *Development Research Laboratories, Banyu Pharmaceutical Co., Ltd., 810- Nishijo, Menuma-machi, Osatogun, Saitama 360-02, Japan.*
2) Y. M. Rustum, C. Dave, E. Mayhew, and D. Papahadjopoulos, *Cancer Res.*, **39**, 1390 (1979).
3) H, Kikuchi and K. Inoue, *Saiboukogaku*, **2**, 1136 (1983).
4) G. Gregoriadis: "Liposome Technology," Vol. 3, ed. by G. Gregoriadis, CRC Press, Florida, 1984, pp. 1—282.
5) H. Kikuchi and K. Inoue, *Yukagaku*, **34**, 784 (1985).
6) J. N. Weinstein, S. Yoshikami, P. Henkart, R. Blumenthal, and W. A. Hagins, *Science*, **195**, 489 (1977).
7) T. M. Allen and L. G. Cleland, *Biochim. Biophys. Acta*, **597**, 418 (1980).
8) E. Ralston, L. M. Hjelmeland, R. D. Klausner, J. N. Weinstein, and R. Blumenthal, *Biochim. Biophys. Acta*, **649**, 133 (1981).
9) D. N. Rhodes and C. H. Lea, *Biochem. J.*, **65**, 526 (1957).
10) A. D. Bangham, M. W. Hill, and N. G. A. Miller, *Methods Membr. Biol.*, **1**, 1 (1974).
11) D. Abramson and M. Blecher, *J. Lipid Res.*, **5**, 628 (1964).
12) D. F. H. Wallach and T. L. Steck, *Anal. Chem.*, **35**, 1035 (1963).
13) Y. Barenholz, D. Gibbes, B. J. Litman, J. Goll, T. E. Thompson, and F. D. Carlson, *Biochemistry*, **16**, 2806 (1977).
14) C. Kirby, J. Clarke, and G. Gregoriadis, *Biochem. J.*, **186**, 591 (1980).
15) R. L. Juliano and D. Stamp, *Biochem. Biophys. Res. Commun.*, **63**, 651 (1975).
16) C. A. Hunt, Y. M. Rustum, E. Mayhew, and D. Papahadjopoulos, *Drug Metab. Dispos.*, **7**, 124 (1979).
17) R. M. Abra and C. A. Hunt, *Biochim. Biophys. Acta*, **666**, 493 (1981).
18) Y. Sato, H. Kiwada, and Y. Kato, *Chem. Pharm. Bull.*, **34**, 4244 (1986).
19) Y. E. Rahman, E. A. Cerny, K. R. Patel, E. H. Lau, and B. J. Wright, *Life Sci.*, **31**, 2061 (1982).
20) T. M. Allen and J. M. Everest, *J. Pharmacol. Exp. Ther.*, **226** 539 (1983).
21) H. Kiwada, S. Obara, H. Nishiwaki, and Y. Kato, *Chem. Pharm. Bull.*, **34**, 1249 (1986).

Effect of Reticuloendothelial Blockade on Tissue Distribution of ^{99m}Tc-Labeled Synthetic Liposomes in Ehrlich Solid Tumor-Bearing Mice

Rensuke GOTO,* Hiroyuki KUBO and Shoji OKADA

Department of Radiobiochemistry, School of Pharmaceutical Sciences, University of Shizuoka, 395 Yada, Shizuoka-shi 422, Japan.
Received June 19, 1990

The effect of a reticuloendothelial blockade was examined on the tissue distribution of ^{99m}Tc-labeled synthetic liposomes prepared from *N,N*-didodecyl-N^{α}-[6-(trimethylammonio)hexanoyl]-L-alaninamide bromide ($N^+C_5Ala2C_{12}$) in Ehrlich solid tumor-bearing mice.

While a pre-dose of unlabeled phosphatidyl choline liposomes (natural liposomes) hardly influenced the tissue distribution of $N^+C_5Ala2C_{12}$ liposomes, the pretreatment of dextran sulfate depressed the uptake in liver accompanied by increasing that in tumor and other tissues except the stomach. However, the extent of liver depression of $N^+C_5Ala2C_{12}$ liposomes by dextran sulfate was lower than that of natural liposomes and the pre-dose of unlabeled natural liposomes had a minor effect on the tissue distribution of $N^+C_5Ala2C_{12}$ liposomes compared with that of natural liposomes. In the liver uptake of $N^+C_5Ala2C_{12}$ liposomes, it was suggested that Kupffer cell phagocytosis was not the main mechanism.

Keywords synthetic liposome; amphiphile; reticuloendothelial blockade; dextran sulfate; tissue distribution

Introduction

In order to apply liposomes prepared from amphiphiles containing amino acid residues (synthetic liposomes) to radiopharmaceuticals, we labeled the liposomes with ^{99m}Tc by embedding stearylamine-diethylenetriamine pentaacetic acid (SA-DTPA) as ^{99m}Tc-ligand, where the amphiphiles used were *N,N*-didodecyl-N^{α}-[6-(trimethylammonio)hexanoyl]-L-alaninamide bromide ($N^+C_5Ala2C_{12}$),[1] *N,N*-didodecyl-N^{α}-{6-[dimethyl(2-carboxyethyl)ammonio]hexanoyl}-L-alaninamide bromide ($CAC_2N^+C_5Ala2C_{12}$)[1] and *S*-{1-carboxy-2-[(2,3-bishexadecyloxy propoxy)carbonyl]ethyl}homocysteine ($HcyM^-G2C_{16}$).[2] The radioactivities of these liposomes, as well as the liposomes prepared from phosphatidylcholine and cholesterol (natural liposomes), were taken up highly in the liver and spleen of Ehrlich solid tumor-bearing mice while they accumulated to a lesser extent in tumor.[3] However, among the three synthetic liposomes tested, $N^+C_5Ala2C_{12}$ liposomes were found to bind firmly to Ehrlich ascites tumor cells *in vitro*.[3]

It is, therefore, of interest to study the tissue distribution of synthetic liposomes under depression of their accumulation in the liver by the use of agents masking reticuloendothelial uptake. Actually, some attempts have been made to reduce the liver uptake of radioactive liposomes by pretreatment with a high dose of multilamellar vesicles (MLV) or small unilamellar vesicles (SUV)[4-7] and with dextran sulfate.[8,9] Here we report the effect of the pretreatment of unlabeled natural liposomes or dextran sulfate on the tissue distribution of ^{99m}Tc-labeled synthetic liposomes because both of the preinjections were expected to bring about the blockade.

Materials and Methods

Materials Dextran sulfate (MW. 500000) was purchased from Sigma Chemical Co., St. Louis, Mo. Phosphatidylcholine (Phospholipid-PCE; from egg yolk) was the product of Nippon Fine Chemical Co., Hyogo. Reagents for synthetic liposomes were described previously.[10] Other chemicals used were of guaranteed grade. Male mice (dd/Y, 20—25 g) were obtained from Japan SLC, Inc., Hamamatsu.

Preparation of ^{99m}Tc-Labeled Synthetic and Natural Liposomes Containing SA-DTPA *N,N*-Didodecyl-N^{α}-[6-(trimethylammonio)hexanoyl]-L-alaninamide bromide ($N^+C_5Ala2C_{12}$) and *N,N*-didodecyl-N^{α}-{6-[dimethyl(2-carboxyethyl)ammonio]hexanoyl}-L-alaninamide bromide ($CAC_2N^+C_5Ala2C_{12}$) were synthesized by the procedure of Murakami *et al.*,[1] *S*-{1-carboxy-2-[(2,3-bishexadecyloxypropoxy)carbonyl]ethyl}-homocysteine ($HcyM^-G2C_{16}$) by the procedure of Neumann and Ringsdorf[2] and SA-DTPA as a ligand of ^{99m}Tc by the procedure of Hnatowich *et al.*[11] Preparation of unlabeled and ^{99m}Tc-labeled liposomes was previously reported.[10]

Ehrlich Solid Tumor-Bearing Mice Mice (dd/Y, 20—25 g) bearing Ehrlich solid tumor were obtained by subcutaneous injection of 0.2 ml of Ehrlich ascites tumor cell suspension (1×10^8 cells/ml saline) 7 d before use.

Tissue Distribution of ^{99m}Tc-Labeled Liposomes in Ehrlich Solid Tumor-Bearing Mice after Preinjection of Unlabeled Natural Liposomes or Dextran Sulfate Into tumor-bearing mice ($n=5$) unlabeled natural liposomes (800 mg phosphatidylcholne/kg body weight) were injected intravenously at 1 h and dextran sulfate (75 mg/kg body weight) intraperitoneally at 17 h before the intravenous injection of 0.2 ml of ^{99m}Tc-labeled liposomes (5×10^7 cpm/ml saline, 50 μg/ml). After collecting blood from the carotid artery under etherization at a given time after injection, solid tumor and other organs were excised and weighed. The radioactivity was counted in a gamma counter (Beckman Gamma 5500).

Results and Discussion

Effect of Preinjection of Natural Liposomes on Tissue Distribution of Labeled $N^+C_5Ala2C_{12}$ and Natural Liposomes ^{99m}Tc-Labeled $N^+C_5Ala2C_{12}$ or natural liposomes were injected in Ehrlich solid tumor-bearing mice 1 h after preinjection of unlabeled natural liposomes of SUV. As shown in Table I, the preinjection of unlabeled natural liposomes resulted in about a 17% reduction in the liver uptake of the labeled natural liposomes 1 h after injection. Abra *et al.*[4] reported that, by the pretreatment of a high intravenous dose of MLV, the distribution in liver of similar liposomes encapsulating ^{14}C-insulin was depressed to 1/6 and those in blood rose 29-fold in comparison with the case of no pretreatment. The degree of reduction of natural liposomes shown in Table I was low compared with the result of Abra *et al.*[4] Such a moderate reduction might be due to the small size of preinjected liposomes belonging to SUV.

On the other hand, with respect to ^{99m}Tc-labeled $N^+C_5Ala2C_{12}$ liposomes, this approach showed no effect on the liver uptake. This suggests that other sites different from that of natural liposomes participate in the liver uptake of $N^+C_5Ala2C_{12}$ liposomes.

Effect of Preinjection of Dextran Sulfate on Tissue Distribution of Labeled $N^+C_5Ala2C_{12}$ and Natural Liposomes Since dextran sulfate is known to be toxic to hepatic

TABLE I. Effect of Pre-dose of Natural Liposomes on Tissue Distribution of ^{99m}Tc-Labeled Liposomes in Ehrlich Solid Tumor-Bearing Mice

	Natural liposomes % dose/g of tissue				$N^+C_5Ala2C_{12}$ liposomes % dose/g of tissue			
	Time after i.v. injection (h)				Time after i.v. injection (h)			
	1 (Control)[c]	1	3	6	1 (Control)[c]	1	3	6
Tumor	0.71±0.12	0.63±0.17	0.77±0.02	0.74±0.03	1.41±0.09	1.39±0.15	1.29±0.18	1.56±0.16
Brain	0.06±0.01	0.11±0.02[b]	0.07±0.01	0.05±0.03	0.68±0.03	0.64±0.04	0.55±0.02	0.52±0.06
Pancreas	0.35±0.08	0.41±0.16	0.31±0.05	0.33±0.04	2.27±0.22	1.88±0.26	1.52±0.05	1.61±0.39
Liver	34.2 ±1.3	28.4 ±0.94[a]	28.0 ±2.7	23.1 ±2.8	30.5 ±4.1	29.9 ±4.5	24.4 ±0.58	21.8 ±0.6
Spleen	11.0 ±3.0	24.1 ±3.5[a]	20.9 ±2.2	13.0 ±1.1	7.69±0.70	9.54±1.39	10.5 ±1.3	9.15±1.05
Kidney	3.37±0.44	4.01±0.32	3.60±0.20	3.26±0.28	3.57±0.27	4.27±0.47	4.27±0.47	4.18±0.38
Stomach	1.04±0.29	1.00±0.30	0.98±0.12	0.89±0.14	0.63±0.06	0.74±0.15	1.07±0.08	0.79±0.11
Muscle	0.13±0.01	0.17±0.22	0.72±0.06	0.51±0.07	2.13±0.24	2.13±0.18	2.31±0.16	1.63±0.06
Lung	1.09±0.15	3.25±0.78[a]	1.63±0.29	1.18±0.10	2.76±0.19	2.38±0.30	1.84±0.18	1.50±0.23
Testis	0.09±0.01	0.12±0.02	0.09±0.01	0.08±0.02	1.53±0.11	1.49±0.17	1.27±0.11	1.17±0.11
Blood	3.03±0.16	4.95±0.38[a]	2.90±0.28	2.13±0.1	2.45±0.30	3.20±0.05[a]	1.40±0.12	0.90±0.08

Each value represents the mean±S.D. for five mice and is normalized to body weight of 25 g. *a*) $p<0.001$, *b*) $p<0.01$ (The values at 1 h were compared with the control). *c*) Saline was injected in place of dextran sulfate solution.

TABLE II. Effect of Pre-dose of Dextran Sulfate on Tissue Distribution of ^{99m}Tc-Labeled Liposomes in Ehrlich Solid Tumor-Bearing Mice

	Natural liposomes % dose/g of tissue				$N^+C_5Ala2C_{12}$ liposomes % dose/g of tissue			
	Time after i.v. injection (h)				Time after i.v. injection (h)			
	1 (Control)[c]	1	3	6	1 (Control)[c]	1	3	6
Tumor	1.44±0.76	2.24± 0.72	2.28± 0.95	2.50± 0.97	1.13±0.19	2.51±0.30[a]	2.61±0.79	2.83±0.06
Brain	0.04±0.01	0.18± 0.09[b]	0.10± 0.05	0.15± 0.07	0.10±0.02	0.32±0.07[a]	0.13±0.03	0.11±0.02
Pancreas	0.33±0.07	0.93± 0.26[b]	0.73± 0.22	0.99± 0.29	0.37±0.04	0.98±0.19[a]	0.69±0.18	0.77±0.29
Liver	38.7 ±4.3	17.8 ± 2.8[a]	16.4 ± 4.3	16.9 ± 1.6	26.0 ±1.1	20.9 ±2.6[b]	20.2 ±1.4	22.2 ±3.3
Spleen	24.8 ±5.6	57.7 ±18.5[b]	84.3 ±21.1	56.2 ±30.5	7.37±1.64	21.8 ±1.7[a]	28.8 ±2.8	23.9 ±6.9
Kidney	3.85±0.52	8.75± 2.52[b]	6.46± 1.81	5.20± 1.63	3.64±0.26	5.69±0.60[a]	4.47±0.65	4.42±0.84
Stomach	3.05±0.74	1.33± 0.34[b]	1.09± 0.16	1.13± 0.22	0.67±0.06	0.55±0.18	0.60±0.13	0.95±0.42
Muscle	0.19±0.04	0.34± 0.07[b]	0.19± 0.05	0.35± 0.03	0.20±0.05	0.45±0.09[a]	0.38±0.05	0.31±0.07
Lung	1.54±0.17	14.4 ± 4.5[a]	19.1 ± 8.6	4.15± 3.41	2.96±0.35	13.3 ±1.2[a]	6.13±1.71	5.93±2.25
Testis	0.16±0.03	0.34± 0.12	0.21± 0.05	0.57± 0.30	0.35±0.07	0.66±0.12[b]	0.68±0.19	0.74±0.11
Blood	1.87±0.24	12.1 ± 6.5[b]	2.71± 0.18	1.55± 0.71	4.20±0.67	12.4 ±1.6[a]	4.37±0.95	2.11±0.46

Each value represents the mean±S.D. for five mice and is normalized to body weight of 25 g. *a*) $p<0.001$, *b*) $p<0.01$ (The values at 1 h were compared with the control). *c*) Saline was injected in place of dextran sulfate solution.

macrophages, attempts have been made to use it as a reagent for reticuloendothelial blockade to alter tissue distribution of liposomes.[8,9] Here, we investigated the effect of dextran sulfate (75 mg/kg body weight) on the tissue distribution of ^{99m}Tc-labeled $N^+C_5Ala2C_{12}$ liposomes, where ^{99m}Tc-labeled natural liposomes were also tested.

Souhami *et al.*[8] found that, in the animals thus blockaded 2 h after injection of dextran sulfate, there was a rapid disappearance of cationic liposomes from the blood without concomitant organ uptake, suggesting that an interaction occurred between the highly negative-charged dextran sulfate and the positive liposomes. Patel *et al.*[9] reported that maximal liver suppression was reached at 12 h after dextran sulfate injection. Since the $N^+C_5Ala2C_{12}$ liposomes tested have cationic charges, mice were treated with dextran sulfate during sufficient time (17 h) before the injection of $N^+C_5Ala2C_{12}$ liposomes. Table II shows the effect of dextran sulfate on the distribution (% dose per gram of tissue) of ^{99m}Tc-labeled $N^+C_5Ala2C_{12}$ and natural liposomes in mice bearing Ehrlich solid tumor. The preinjection of dextran sulfate reduced the liver uptake of the natural liposomes to 46% at 1 h after injection, and the liver blockade caused an increase in uptake in the tumor and other tissues except the stomach. This increase may be due to a remarkable increase in the concentration of radioactivity in the blood. Regarding the $N^+C_5Ala2C_{12}$ liposomes, the injection of dextran sulfate reduced the liver uptake to 77% at 1 h after injection, indicating that the degree of depression was low compared with the natural liposomes. The liver blockade produced an increase in uptake in the tumor and other tissues, except the stomach, similar to natural liposomes. The high uptake of liposomes in the spleen and lung might be because these organs belong to the reticoloendothelial system which preferentially took up the liposomes in the blood which were increased by the liver blockade.

Such a lower depression in the liver uptake of $N^+C_5Ala2C_{12}$ liposomes as mentioned above might be due to their positive charges, in agreement with the result that no effect of a carbon-induced blockade on the liver uptake was seen with positively charged SUV.[8] Therefore, we further tested weakly positive $CAC_2N^+C_5Ala2C_{12}$ liposomes and negative $HcyM^-G2C_{16}$ liposomes similarly. Table III shows the effect of dextran sulfate preinjection on the tissue distribution of the two synthetic liposomes in Ehrlich solid tumor-bearing mice. The injection of dextran sulfate reduced the

TABLE III. Effect of Pre-dose of Dextran Sulfate on Tissue Distribution of ^{99m}Tc-Labeled Synthetic Liposomes in Ehrlich Solid Tumor-Bearing Mice

	$CAC_2N^+C_5Ala2C_{12}$ liposomes % dose/g of tissue				$HcyM^-G2C_{16}$ liposomes % dose/g of tissue			
	Time after i.v. injection (h)				Time after i.v. injection (h)			
	1 (Control)[c]	1	3	6	1 (Control)[c]	1	3	6
Tumor	0.45±0.05	0.90±0.30	1.09±0.17	0.75±0.10	0.62±0.12	2.90± 0.13[a]	1.92± 0.19	1.68± 0.35
Brain	0.04±0.00	0.17±0.02[a]	0.08±0.02	0.05±0.01	0.05±0.01	0.29± 0.13[b]	0.18± 0.12	0.12± 0.07
Pancreas	0.23±0.00	1.00±0.39[b]	0.50±0.23	0.39±0.02	0.28±0.04	1.63± 0.71[b]	0.77± 0.25	0.72± 0.46
Liver	35.8 ±1.4	27.8 ±3.4[b]	25.9 ±3.2	21.9 ±2.5	42.4 ±4.3	32.2 ± 4.5[b]	33.9 ± 3.9	24.6 ± 3.1
Spleen	11.8 ±2.1	48.9 ±3.1[a]	25.7 ±3.5	33.4 ±8.6	13.5 ±1.8	60.5 ±15.5[a]	35.5 ±11.0	43.1 ±13.0
Kidney	2.47±0.19	3.57±0.95	3.30±0.44	4.27±0.30	3.23±0.50	5.32± 1.52	4.94± 1.31	5.11± 0.18
Stomach	0.77±0.17	0.60±0.29	0.71±0.18	0.52±0.20	3.50±0.33	1.69± 0.18[a]	2.26± 0.37	0.70± 0.34
Muscle	0.16±0.07	0.27±0.10	0.23±0.05	0.22±0.13	0.15±0.03	0.52± 0.23[b]	0.44± 0.20	0.29± 0.17
Lung	2.40±0.44	23.7 ±8.8[a]	7.29±4.24	4.63±1.49	1.71±0.31	33.7 ± 5.1[a]	10.5 ± 3.0	4.85± 4.31
Testis	0.11±0.01	0.33±0.08[a]	0.23±0.06	0.23±0.03	0.18±0.03	0.96± 0.21[a]	0.55± 0.22	0.41± 0.15
Blood	0.90±0.07	2.63±0.69[a]	1.13±0.08	0.83±0.08	1.10±0.10	5.92± 2.67[b]	1.79± 0.40	0.70± 0.38

Each value represents the mean±S.D. for five mice and is normalized to body weight of 25 g. *a*) $p<0.001$, *b*) $p<0.01$ (The values at 1 h were compared with the control). *c*) Saline was injected in place of dextran sulfate solution.

liver uptake of $CAC_2N^+C_52C_{12}$ liposomes to 78% and of $HcyM^-G2C_{16}$ liposomes to 76% 1 h after injection. The extents of reduction were similar to that of $N^+C_5Ala2C_{12}$ liposomes. The liver blockade had similar effects on the distribution in other tissues to those of $N^+C_5Ala2C_{12}$ liposomes. Accordingly, the moderate reduction by dextran sulfate might not be due to the charge, but to the structure of these synthetic liposomes.

The behavior of $N^+C_5Ala2C_{12}$ liposomes in the liver was somewhat different from that of natural liposomes; the extent of the liver depression due to dextran sulfate was lower than that of natural liposomes and the pre-dose of natural liposomes (SUV) had no effect on the uptake of $N^+C_5Ala2C_{12}$ liposomes. Roerdink *et al.*[12] reported that, on a per cell base, the uptake of SUV consisting of sphingomyelin, cholesterol and phosphatidylserine by Kupffer cells far exceeded the uptake by parenchymal cells. On the other hand, in our preliminary experiment, no significant difference was found between Kupffer cells and parenchymal cells in the uptake of synthetic liposomes. In the liver uptake of the synthetic liposomes tested, it was suggested that Kupffer cell phagocytosis was not the main mechanism.

References

1) Y. Murakami, A. Nakano and H. Ikeda, *J. Org. Chem.*, **47**, 2137 (1982).
2) R. Newmann and H. Ringsdorf, *J. Am. Chem. Soc.*, **108**, 487 (1986).
3) R. Goto, H. Kubo, Y. Daicho and S. Okada, *Chem. Pharm. Bull.*, **38**, 2805 (1990).
4) R. M. Abra, M. E. Bosworth and C. A. Hunt, *Res. Commun. Chem. Pathol. Pharmacol.*, **29**, 349 (1980).
5) Y. J. Kao and R. L. Juliano, *Biochim. Biophys. Acta*, **677** 453 (1981).
6) M. E. Bosworth and C. A. Hunt, *J. Pharm. Sci.*, **71**, 100 (1982).
7) Chu-Hua Kang, W. Voigt and D. H. Haynes, *JRCS Med. Sci.*, **11**, 420 (1983).
8) R. L. Souhami, H. M. Patel and B. E. Ryman, *Biochim. Biophys. Acta*, **674**, 354 (1981).
9) K. R. Patel, M. P. Li and J. D. Baldeschwieler, *Proc. Natl. Acad. Sci. U.S.A.*, **80**, 6518 (1983).
10) R. Goto, H. Kubo and S. Okada, *Chem. Pharm. Bull.*, **37**, 1351 (1989).
11) D. J. Hnatowich, B. Friedman, B. Clancy and M. Novak, *J. Nucl. Med.*, **22**, 810 (1981).
12) F. Roerdink, J. Regts, B. V. Leeuwen and G. Scherphof, *Biochim. Biophys. Acta*, **770**, 195 (1984).

THE STERIC EFFECT OF A TRIFLUOROMETHYL GROUP

Takabumi NAGAI, Goro NISHIOKA, Mayumi KOYAMA, Akira ANDO, Takuichi MIKI, and Itsumaro KUMADAKI*
Faculty of Pharmaceutical Sciences, Setsunan University, 45-1, Nagaotoge-cho, Hirakata, 573-01, Japan

In the study of ene reaction of trifluoromethyl ketones, a trifluoromethyl group was found to behave as a much larger substituent than commonly believed. Similar results were obtained in the dehydration of trifluoromethyl homoallyl alcohols.

KEYWORDS trifluoromethyl; ketone; steric effect; ene reaction; dehydration; alcohol; cyclohexene; transition state

There are many biologically active organofluorine compounds[1] and their activities are attributed to the fact that the steric requirement of a fluorine atom is nearly as small as a hydrogen atom, while a carbon-fluorine bond is much stronger than a carbon-hydrogen bond.[2] Therefore, an organism cannot distinguish a fluorine derivative of a biologically active compound from the unfluorinated one and the fluorine compound is taken up in the metabolic path of the original compound. This is called the "mimic effect" of fluorine compounds. Similar examples are known where a methyl group is replaced by a trifluoromethyl group. Thus, trifluoromethyldeoxyuridine derivatives show antiviral activity, since they are taken up in the place of thymidine due to the similarity of the shapes of the two compounds.

In the course of our study of the ene reaction of trifluoromethyl ketones,[3] we noticed that a trifluoromethyl group behaves as a much larger substituent than the above generalization indicates. Thus, the reaction of trifluoroacetone with 2-octene gave an l-isomer regio- and stereoselectively,[3b] based on Prelog-Seebach's notation.[4] This result is explained by comparison of the transition states (**A**) and (**B**). Namely, the steric repulsion between the trifluoromethyl group and the alkenyl part of 2-octene in **B** is much larger than that between the methyl and the alkenyl part in **A** and the l-isomer is formed through **A**.

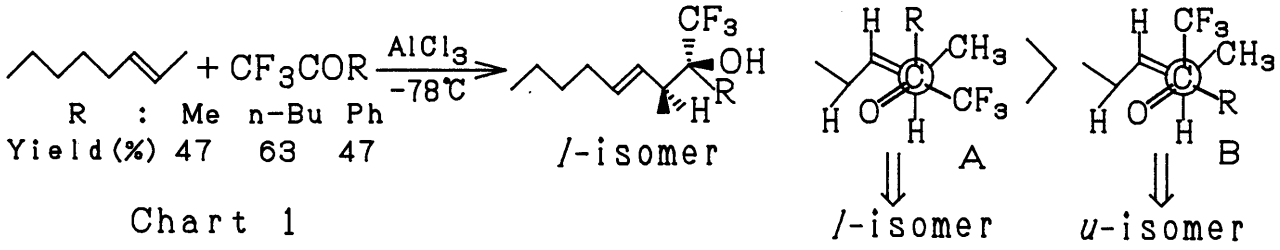

Chart 1

Interestingly, other trifluoromethyl ketones, 1,1,1-trifluoro-2-hexanone and α,α,α-trifluoroacetophenone, gave products of the same stereochemistry as trifluoroacetone did.[5] (Chart 1) These results suggest that a trifluoromethyl group behaves as a larger substituent than an n-butyl or a phenyl group in this reaction. This is far from the above idea concerning the steric effect of a trifluoromethyl group.

On the other hand, concerning the steric effect of a trifluoromethyl group, there have been a few reports. Taft has proposed a scale of the steric effect, Es.[6] Dubois' Group critically revised the Es and proposed Es' scale.[7] The Es value of a phenyl group is not mentioned, but Es' value of a phenyl group is much larger than that of a trifluoromethyl group. This is far from our results. Sternhell et al. reported effective van der Waals' radii based on the rotational barrier of biphenyl derivatives.[8] Here, a trifluoromethyl group shows a value, 2.2 Å, similar to a sec-butyl group does. This seems to be consistent with our results. However, unbelievably, in their scale a trimethylsilyl group is smaller than a tert-butyl group and an amino group is larger than a dimethylamino group. Therefore, we studied the steric effect of a trifluoromethyl group more extensively. We synthesized a number of trifluoromethyl ketones and reinvestigated their ene reaction with cyclohexene, 1,2-disubstituted alkene of the

least steric requirement. The results are summarized in Chart 2.[9]

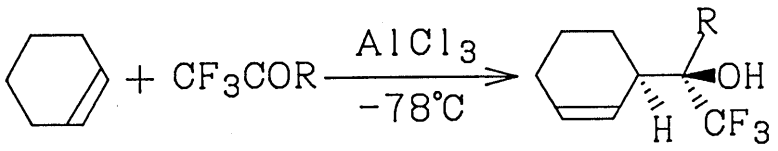

R :	H	Me	n-Bu	Ph	iso-Bu	c-Hex	sec-Bu	CF_3	thexyl
Yield(%)	43	53	41	21	9	6	6.7	7	0

Chart 2

Trifluoroacetaldehyde and the ketones to cyclohexyl trifluoromethyl ketone reacted with an equimolar amount of cyclohexene at -78°C to give ene reaction products of the same stereochemistry. Only when the four equivalents of cyclohexene were used did sec-butyl trifluoromethyl ketone give a small amount of the product. The thexyl ketone did not react at all, even when ten equivalents of cyclohexene was used. Hexafluoroacetone reacted without a catalyst at 150°C to afford a small amount of the product. Therefore, a thexyl group is much larger than a trifluoromethyl group. The fact that sec-butyl trifluoromethyl ketone gave the product of the same stereochemistry as trifluoroacetone did shows that a sec-butyl group is slightly smaller than a trifluoromethyl group.

If the steric effect of the alkyl groups could be estimated from the yields of the ene reaction,[10] the order of the steric effect is as shown in Chart 2 and a trifluoromethyl group has slightly larger steric effect than a sec-butyl group in the transition state of this reaction. This suggests that not the total volume, but the shape of a substituent near the reaction center affects the reaction. Thus, a thin n-butyl group had a smaller steric effect than a β-branched isobutyl group, the steric effect of which was smaller in turn than that of an α-branched sec-butyl group. A flat phenyl group had a smaller effect than an isobutyl group. A sec-butyl group acts as a slightly smaller substituent than a trifluoromethyl group, if the C-H part of the former is directed to the reaction center in the transition state of the slow reaction.

Next, dehydration of the homoallyl alcohols was investigated to compare the steric effect of a trifluoromethyl group with those of other alkyl groups. This dehydration was established to proceed through an anti-elimination mechanism.[11] Thus, if an alkyl group (R) is smaller than a trifluoromethyl group, this reaction will give an E-isomer preferably. If larger, a Z-isomer will be formed. The results of dehydration summarized in Chart 3 show that the E/Z ratio decreases with the increase of the steric effect of the alkyl groups.[12]

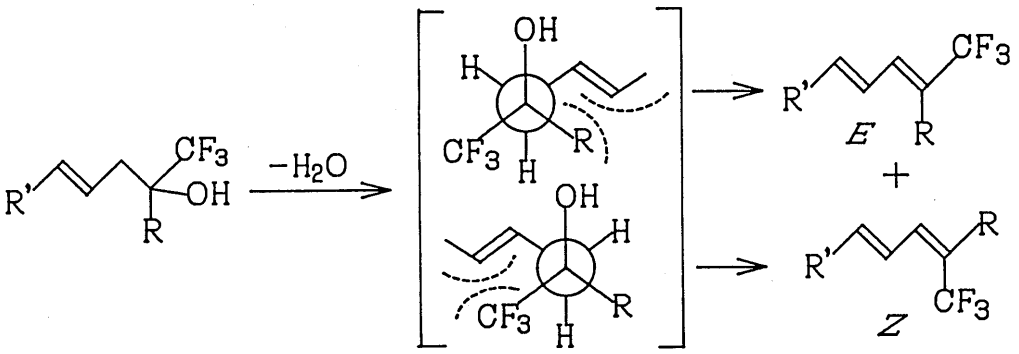

R =	H	Me	Ph	n-Bu	iso-Bu	c-Hex	sec-Bu	thexyl
E/Z =	13/2	9/2	3/1	2/1	5/2	7/8	2/3	1/10[12]

Chart 3

This order is slightly different from that observed in the ene reaction. A cyclohexyl group is about the same as a trifluoromethyl group, a sec-butyl group is a little larger than a trifluoromethyl

group. This difference may be due to the difference in the reaction temperatures, -78°C in the ene reaction and 110°C in the dehydration. Thus, a rapid rotation around the C-C bond at 110°C makes the difference between the n-butyl and isobutyl groups much smaller than at -78°C. The C-H part of the sec-butyl group is nearly fixed to the reaction center at -78°C and it behaves as a smaller substituent than a trifluoromethyl group, but at 110°C, rotation around the C-C bond becomes faster and the sec-butyl group behaves as a larger substituent than a trifluoromethyl group.

In conclusion, a trifluoromethyl group behaves as a much larger substituent in the transition states of some reactions than formerly believed, even though the total volume of a trifluoromethyl group may be similar to that of a methyl group in an interaction mimicking a methyl analog of a biologically active compound. Therefore, a round and hard trifluoromethyl group has a larger steric effect than a thin and flexible n-butyl group or a flat phenyl group, even though its total volume is much smaller than the latter.

REFERENCES AND NOTES

1) a) E. J. Ariens, "Drug Design," Vol. 5, Academic Press (1975);
b) R. Filler and Y. Kobayashi, "Biomedical Aspects of Fluorine Chemistry," Kodansha, Ltd. (1982).
2) R. D. Chambers, "Fluorine in Organic Chemistry," P.5, John Wily & Sons (1973).
3) a) Y. Kobayashi, T. Nagai, and I. Kumadaki, Chem. Pharm. Bull., **32**, 5031 (1984);
b) T. Nagai, I. Kumadaki, T. Miki, Y. Kobayashi, and G. Tomizawa, Chem. Pharm. Bull., **34**, 1546 (1986)
c) T. Nagai, T. Miki, and I. Kumadaki, Chem. Pharm. Bull., **34**, 4782 (1986).
4) "l" is based on "like-unlike" notation by D. Seebach and V. Prelog, Angew. Chem. Int. Ed. Engl., **21**, 654 (1982). "Syn-anti" or "threo-erythro" notations are ambiguous for our compounds.
5) The reaction of 1,1,1-trifluoro-2-hexanone gave 6-methyl-5-(trifluoromethyl)-7-dodecen-5-ol (**1**), colorless oil, 63 %, ^{19}F-NMR: 11.97 ppm (from BTF) with two cyclized products 10 % yield (in total), but any stereo isomer of **1** was not observed. This was dehydrated to (5Z,7E)-6-methyl-5-(trifluoromethyl)-5,7-dodecadiene with smaller amounts of (4Z,7E)- and (4E,7E)-4,7-dienes, but (5E,7E)-diene was not obtained.[11] The structure of the ene product from trifluoroacetophenone was similarly determined.
6) R. W. Taft, Jr., "Steric Effects in Organic Chemistry," edited by M. S. Newman, P. 556, Wiley, New York, (1956).
7) J. A. MacPhee, A. Panaye, and J.-E. Dubois, Tetrahedron, **34**, 3553 (1978).
8) G. Bott, L. D. Field, and S. Sternhell, J. Am. Chem. Soc., **102**, 5618 (1980).
9) A typical experiment is as follows. Reaction of equimolar amounts of cyclohexene, isobutyl trifluoromethyl ketone and $AlCl_3$ in anhydrous CH_2Cl_2 at -78°C for 2.5 h gave l-3-[1-hydroxy-3-methyl-1-(trifluoromethyl)butyl]cyclohexene (9 %). Colorless oil. HRMS Calcd. for $C_{12}H_{19}F_3O$: 236.139. Found: 236.139. ^{1}H-NMR ($CDCl_3$) : 0.97 (3H, d, J=6.7 Hz), 1.00 (3H, d, J=6.7 Hz), 1.31-1.43 (1H, m), 1.45-1.64 (3H, m), 1.78-2.03 (5H, m), 2.09 (1H, bs), 2.58-2.66 (1H, m), 5.74 (1H, bd, J=10.4 Hz), 5.84-5.90 (1H, m). ^{19}F-NMR ($CDCl_3$) ppm: 12.89 (s). No other products were isolated bedsides the starting materials. A mixture of the l and the u-isomers (4:1) was obtained by the Grignard reaction of 3-bromocyclohexene and CF_3CO-iso-Bu with Mg. The isomers were separated by a preparative glc and showed well separated ^{19}F-NMR. The l-isomer was dehydrated by pyridine and phosphoryl chloride to 3-[2-methylpropyl(trifluoromethyl)methylene]cyclohexene: colorless oil. There was no correlation observed between the 2-H and methylene-H of the isobutyl group in 2D-NOE. The low chemical shift on ^{19}F-NMR (-7.78 ppm, s) shows that the trifluoromethyl group is cis to the double bond. The other reaction products gave satisfactory spectral data. Their structures were determined by similar Grignard reaction and dehydration. Details will be published elsewhere in the near future.
10) Trifluoroacetaldehyde polymerizes in the reaction condition. The yield, based on the used cyclohexene was quantitative.
11) T. Nagai, M. Hama, M. Yoshioka. M. Yuda, N. Yoshida, A. Ando, M. Koyama, T. Miki, and I. Kumadaki, Chem. Pharm. Bull., **37**, 177 (1989).
12) The dehydration reactions were carried out as in ref. 11 and the structures of dienes were determined similarly. The relative ratios are estimated from the ^{19}F-NMR (90MHz), ^{1}H-NMR (400MHz), and peak area on GLC.

(Received October 3, 1990)

MALE-SPECIFIC METABOLISM OF SIMVASTATIN BY RAT LIVER MICROSOMES

Naotaka UCHIYAMA,* Yayoi KAGAMI, Yuko SAITOH and Masakatsu OHTAWA
Central Research Laboratories, Banyu Pharmaceutical Co., Ltd., Shimomeguro, Meguro, Tokyo 153, Japan

Simvastatin was more effectively metabolized by the liver microsomes of male rats than females. The sex difference appeared in the composition of the metabolites. Two male-specific metabolites were identified by NMR and mass spectrometry as 3"-hydroxy and 3',3"-dihydroxy-$\Delta^{4',5'}$ derivatives of simvastatin.

KEYWORDS simvastatin; metabolite; identification; rat; liver microsome; sex difference

Simvastatin (SV) is a lactone prodrug, whose hydroxy-acid (SVA) is a potent competitive inhibitor of 3-hydroxy-3-methylglutarylcoenzyme A reductase,[1] a rate limiting enzyme in cholesterol biosynthesis. Simvastatin is effective in lowering plasma cholesterol in humans.[2] The metabolic disposition of SV has been reported.[3,4] Vyas[3a] and Vickers[3b] reported that simvastatin was metabolized by male rat hepatic microsomes to generate 6'-hydroxy, 3"-hydroxy and 6'-exomethylene derivatives of SV and SVA as major metabolites. Here we describe the isolation of male specific metabolites of SV by rat liver microsomes and their structural identification by NMR and mass spectrometry.

[Butanoate-1"-^{14}C]SV (specific activity 5.0 μCi/mg; radiochemical purity 92%), non-radiolabeled SV, SVA, 6'-CH_2OH-SV, 6'-COOH-SV and the hydroxy-acid form of 3'-OH-SV, i.e. 3'-OH-SVA were obtained from Merck Sharp & Dohme Research Laboratories (Rahway, NJ). 6'-Exomethylene-SV was prepared in our laboratory. The chemical structures of these metabolites are shown below.

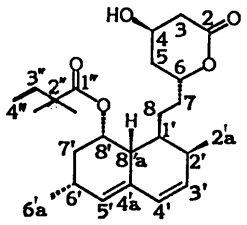

simvastatin (SV)

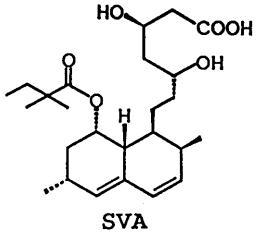

SVA

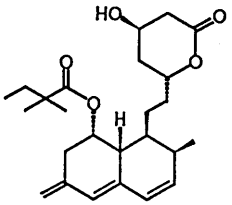

6'-exomethylene-SV

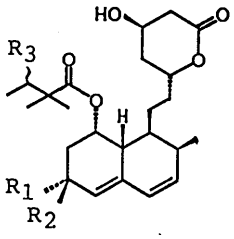

6'-OH-SV (R_1=CH_3, R_2=OH, R_3=H)

3"-OH-SV (R_1=CH_3, R_2=H, R_3=OH)

6'-CH_2OH-SV (R_1=H, R_2=CH_2OH, R_3=H)

6'-COOH-SV (R_1=H, R_2=COOH, R_3=H)

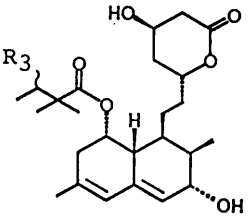

3'-OH-SV (R_3=H)

3',3"-di-OH-SV (R_3=OH)

The liver of male and female Sprague-Dawley rats (aged 7 weeks) was removed and homogenized with 1.15% KCl in 0.01 M phosphate buffer (pH 7.4). A microsomal pellet was prepared from the homogenate by differential centrifugation. A 1-ml reaction mixture containing 1-4 mg of protein equivalent of liver microsomes, 1 mM NADP, 1 mM NADPH, 10 mM glucose-6-phosphate, 1 unit of glucose-6-phosphate dehydrogenase, 3 mM $MgCl_2$ and 100 mM phosphate buffer (pH 7.4) was preincubated at 37°C for 5 min under air atmosphere. Then [^{14}C]SV (100 nmol in 10 μl of acetone) was added and the incubation was continued for 15 min. The reaction was terminated by adding 1 ml of acetone. The residual substrate and metabolites were extracted with 2 ml of ethyl acetate. The organic layer was evaporated to dryness. The residue was reconstituted in a mobile phase for HPLC analysis. In a scale up experiment, the metabolites were isolated by reversed-phase HPLC (column; Senshu-Pak (ODS-4251-N, 250 mm x 10 mm i.d.) and Wako Pak (Nucleosil 5C18, 250 mm x 4.6 mm i.d.), mobile

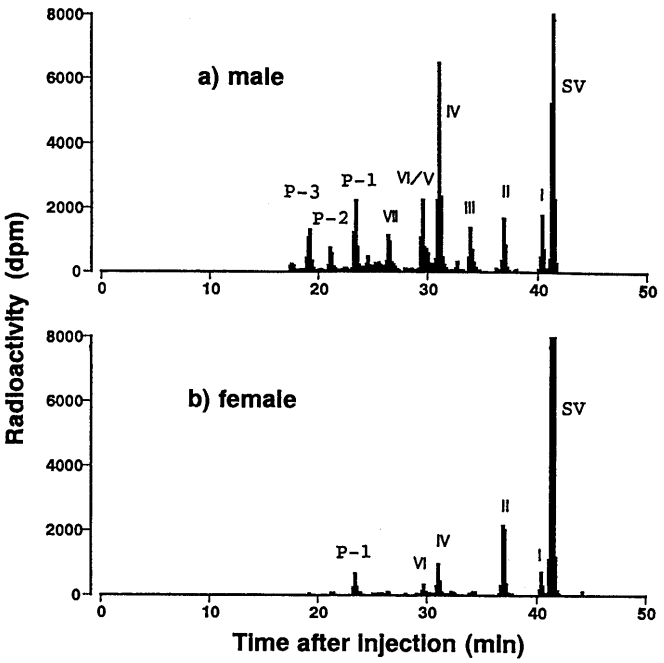

Fig. 1. Radiochromatograms of [^{14}C]SV and Its Metabolites Formed by Hepatic Microsomes from Male and Female Rats

HPLC analysis was done on a Wako Pak column (Nucleosil 5C18, 250 mm x 4.6 mm i.d.). Linear gradient elution was employed: the initial mobile phase composition was 20% phosphate buffer and 80% acetonitrile. The flow rate was 1.0 ml/min and the column oven was meintained at 35°C. The HPLC effluent was collected at 10-s intervals. The radioactivity of each fraction was measured by liquid scintillation spectrometry.

Table I. Proton NMR of SV and Its Metabolites

Proton	Chemical shifts (ppm)		
	SV	3"-OH-SV	3',3"-di-OH-SV
1'-CH	1.7	1.6	1.8
2'-CH	2.38	2.37	2.00
3'-CH	5.79	5.79	3.94
4'-CH	6.00	6.00	5.64
5'-CH	5.51	5.52	5.93
6'-CH	2.47	2.46	
7'-CH_2	1.97	1.98	2.13, 2.46
8'-CH	5.38	5.42	5.60
8'a-CH	2.27	2.28	2.0
3-CH_2	2.63, 2.75	2.60, 2.75	2.62, 2.78
4-CH	4.38	4.36	4.35
5-CH	1.7, 2.0	1.73, 1.93	1.8, 2.0
6-CH	4.62	4.62	4.67
7-CH_2	1.3, 1.9	1.33, 1.87	1.5, 2.0
8-CH_2	1.4, 1.5	X	X
3"-CH		3.81	3.89
3"-CH_2	1.6		
4"-CH_3	0.84	1.16	1.09
2'a-CH_3	0.90	0.85	0.74
6'a-CH_3	1.11	1.09	1.77
2"a-CH_3	1.13	1.14, 1.15	1.05, 1.08
4-OH	X	X	X
3"-OH		2.90	X

X; The spectrum was not intense enough to identify the protons. Chemical shifts were recorded in parts per million (ppm) relative to tetramethylsilane as an internal standard.

phase; acetonitrile/0.025 M ammonium phosphate buffer (pH 3.0) and acetonitrile/water). The fast atom bombardment mass spectra were measured with a Jeol DX-300. The proton NMR spectra in $CDCl_3$ were measured using a Varian VRX-300.

The radiochromatograms of organic solvent extracts from the incubation mixtures are shown in Fig. 1. After incubation with the male liver microsomes, ten radioactive peaks appeared in addition to unchanged [^{14}C]SV, but only five radioactive metabolites were formed by the female liver microsomes. Peaks III and VII appeared in male rats but not in the females. The identities of radioactive peaks by comparing their retention times (t_R) with those of authentic standard compounds were: I, 6'-exomethylene-SV; II, SVA; V, 6'-CH_2OH-SV; VI, 6'-COOH-SV. After the peak IV was treated with dilute KOH at room temperature, the t_R produced was identical with that of 3'-OH-SVA. This indicates that the lactone moiety of IV was hydrolyzed to generate the corresponding hydroxy-acid. Therefore, IV was identified as the lactone form of 3'-OH-SVA, i.e., 3'-OH-SV. As reported by Vickers[3b], 3'-OH-SV is the acid rearrangement product of 6'-OH-SV. Thus, peak IV represents the formation of 6'-OH-SV by the microsomes.

Peaks III and VII, which are formed from male rat liver microsomes, were isolated and their structures were analyzed. The FAB mass spectrum of III showed a protonated molecular ion at m/z 435 indicating the incorporation of one oxygen atom into SV. The proton NMR of III revealed a hydroxy-bearing 3"-methyne proton (δ 3.81 ppm, m) coupled to 4"-methyl protons (δ 1.16 ppm, d, J=6 Hz) and to a 3"-hydroxy proton (δ 2.90 ppm, brd, J=6 Hz). The configuration of the 3"-hydroxy group was not determined. There were essentially no changes in any other signals compared with those of SV. Table I shows the assignments of the protons of SV and its metabolites using ^{1}H-^{1}H shift correlation spectroscopy. From these results, III was identified as

the 3"-hydroxylated metabolite of SV (3"-OH-SV). These spectral data agreed with those of one of the male rat microsomal metabolites reported by Vickers et al..[3b]

The FAB mass spectrum of VII showed a protonated molecular ion peak at m/z 451 and a Na adduct ion at m/z 473, which indicate incorporation of two oxygen atoms into SV. The proton NMR spectrum of VII showed a hydroxy-bearing 3'-methyne proton (δ 3.94 ppm, m) coupled to an olefinic 4'-methyne proton (δ 5.64 ppm, brd, J=6 Hz). There was also an olefinic 5'-methyne proton (δ 5.93 ppm, brs) and 6'a-methyl protons (δ 1.77 ppm, brs). Irradiation of the 3'-methyne proton (δ 3.94 ppm) enhanced the signal intensity of the proton at **0.74 ppm (2'a-methyl)**. Irradiation of 2'a-methyl protons (δ 0.74 ppm) increased the signal intensity of the proton at 3.94 ppm (3'-methyne). These data indicate that 3' α-position was hydroxylated and the diene of SV was rearranged to $\Delta^{4',4'a}$ and $\Delta^{5',6'}$. Also, the NMR spectrum revealed that hydroxylation occurred at the 3"-position because of the presence of hydroxy-bearing 3"-methyne proton at 3.89 ppm (q, J=5 Hz) coupled to 4"-methyl protons at 1.09 ppm (d, J=5 Hz). From these spectral data, peak VII was identified as the 3',3"-dihydroxy-$\Delta^{4',5'}$ derivative of SV (3',3"-di-OH-SV).

Table II. Specific Activities for the Metabolism of Simvastatin and Formation of Metabolites by Hepatic Microsomes from Male and Female Rats

Substrate/ Metabolite	Specific activity (nmol/mg protein/min) Male	Female	Ratio Male/Female
SV	3.97±0.33	0.44±0.11	9
6'-CH_2-SV	0.24±0.04	0.03±0.01	8
SVA	0.20±0.03	0.15±0.03	1.3
3"-OH-SV	0.23±0.04	-	-
6'-OH-SV	0.92±0.18	0.05±0.01	18
6'-CH_2OH-SV	0.08±0.04	-	-
6'-COOH-SV	0.23±0.13	0.01±0.01	23
3',3"-di-OH-SV	0.22±0.06	-	-

- ; not detected
Each value represents the mean±S.D. of five (male) or three (female) experiments. [^{14}C]SV (0.1mM) was incubated at 37°C for 15 min with hepatic microsomes from male and female rats.

As shown in Table II, the specific activity for the metabolism of SV by the male microsomes was 9-fold higher than that by the females, and those for the formation of 6'-COOH-SV, 6'-OH-SV and 6'-CH_2-SV were 8-23 times higher by the male microsomes.

In this study, a sex difference was found in the metabolism of SV by rat liver microsomes. SV was more effectively metabolized by the male microsomes than females. In addition, male specific metabolites, i.e., 3"-OH-SV and 3',3"-di-OH-SV, were present. As an acid-catalyzed rearrangement from 6'-OH-SV to 3'-OH-SV had been shown,[3b] the putative 6',3"-dihydroxy metabolite may be formed as the microsomal metabolite, which was rearranged to 3',3"-di-OH-SV in a similar manner. Indeed, when 3"-OH-SV was incubated with male rat liver microsomes, a metabolite which converted into 3',3"-di-OH-SV under acidic condition was shown by HPLC. This labile metabolite showed a quasi-molecular ion peak at m/z 473 ($[M+Na]^+$) on FAB mass spectrometry and the UV spectrum characteristic of modified heteroannular diene. Both 6'-OH-SV and 3"-OH-SV were formed as male rat microsomal metabolites, so that 3',3"-di-OH-SV could be formed from either or both of these metabolites. Because 3"-OH-SV and 3',3"-di-OH-SV were found in the male rats but not in the females, it is revealed that 3"-hydroxylation of SV is catalyzed by male-specific microsomal enzymes.

REFERENCES

1) W.F.Hoffman, A.W.Alberts, P.S.Anderson, J.S.Chen, R.L.Smith and A.K.Willard, J. Med. Chem., **29**, 849 (1986).
2) L.A.Simons, P.J.Nestel, G.D.Calvert and G.L.Jennings, Med. J. Aust., **147**, 65 (1987); J.F.Walker and J.A.Tobert, Eur. Heart J., **8**, 93 (1987); M.J.T.M.Mol, D.W.Erkelens, J.A.G.Leuven, J.A.Schouten and A.F.H.Stalenhoef, Atherosclerosis, **69**, 131 (1988); V.Lecliercq and C.Harvengt, Int. J. Clin. Pharmacol. Ther. Toxicol., **27**, 76 (1989); D.A.Pietro, G.Mantell, J.E.Staggers, T.J.Cook, Am. J. Cardiol., **63**, 682 (1989); N.Nakaya and Y.Goto, J. Clinical Therapeutics & Medicines, **5**, 1097 (1989).
3) a) K.P.Vyas, Abstracts of Papers, 8th International Symposium on Atherosclerosis, Rome, October 1988, p1068; b) S.Vickers, C.A.Duncan, K.P.Vyas, P.H.Kari, B.Arison, S.R. Prakash, H.G.Ramjit, S.M. Pitzenberger, G.Stokker and D.E.Duggan, Drug Metab. Dispos., **18**, 476 (1990).
4) J.I.Germershausen, V.M.Hunt, R.G.Bostedor, P.J.Bailey, J.D.Karkas and A.W.Alberts, Biochem. Biophys. Res. Commun., **158**, 667 (1989); N.Uchiyama, Y.Saitoh, Y.Kagami, K.Hara, K.Saitoh, Y.Sawasaki and M.Ohtawa, Xenobio. Metabol. Dispos., **5**, 133 (1990); M.Ohtawa, N.Uchiyama, K.Saitoh, Y.Esumi and Y.Jin, Xenobio. Metabol.Dispos., **5**, 151 (1990); S.Vickers, C.A.Duncan, I-Wu Chen, A.Rosegay and D.E.Duggan, Drug Metab. Dispos., **18**, 138 (1990); M.Ohtawa, N.Uchiyama, Y.Saitoh, A.Suzuki, C.Tanno, N.Nakaya and Y.Gotoh, J. Clinical Therapeutics & Medicines, **5**, 1123 (1989).

(Received October 11, 1990)

PURIFICATION AND SOME PROPERTIES OF SQUALENE-2,3-EPOXIDE:LANOSTEROL CYCLASE FROM RAT LIVER

Masayuki KUSANO, Ikuro ABE, Ushio SANKAWA and Yutaka EBIZUKA*

Faculty of Pharmaceutical Sciences, The University of Tokyo, 7-3-1 Hongo, Bunkyo-ku, Tokyo 113, Japan

Squalene-2,3-epoxide:lanosterol cyclase was purified from rat liver in five steps as a soluble and homogeneous protein. The purified enzyme showed a single band on SDS-polyacrylamide gel electrophoresis with a molecular weight of 75 kD. In its native state it behaved as a homo-dimer. The isoelectric point of 5.5 and the apparent Km value for (3S)-squalene-epoxide of 55 μM were estimated for the cyclase.

KEYWORDS squalene-2,3-epoxide; lanosterol; cyclase; rat liver

Squalene-2,3-epoxide is a versatile intermediate in the biosynthesis of sterols and cyclic triterpenoids since it cyclizes into lanosterol in animals, yeast and fungi and in higher plants it undergoes cyclization into cycloartenol and various skeletal types of cyclic triterpenoids. The mechanisms of these cyclizations have been the subject of many chemical investigations since Ruzicka et al. proposed the so called "biogenetic isoprene rule".[1] Enzymes that mediate the cyclization of squalene-2,3-epoxide have been found in many organisms.[2,3] In mammalian systems, squalene-2,3-epoxide:lanosterol cyclase is associated with the endoplasmic reticulum,[4,5] while in yeast it is a soluble protein.[6] Previous attempts to purify mammalian cyclases have met with difficulties[4,5,7] and no complete purification of cyclase giving lanosterol as the product has been reported from any source. In previous papers we have reported the complete purification of four cyclases from two different plants.[8-10] In continuing our studies on the mechanistic and evolutionary aspects of these cyclases, we report here the purification of squalene-2,3-epoxide:lanosterol cyclase from rat liver by applying a procedure similar to the one which was successful in the purification of plant cyclases.

The cyclase from rat liver was purified as a soluble and homogeneous protein in four steps starting from the solubilized protein fraction. Among the chromatographic separations employed, hydroxylapatite was the most efficient: the cyclase was recovered quantitatively in a non-adsorbed fraction leaving most of the other proteins on the column. About a 20-fold increase of specific activity was achieved by this single step. Isoelectric focusing, a successful step in the purification of cyclases from plant origin, was also applicable to the rat liver cyclase and an isoelectric point of 5.5 was estimated. No increase of specific activity was obtained with a Q-sepharose column, but contaminant proteins were efficiently removed. The last purification step by HPLC gel filtration resulted in a 1860-fold overall increase of specific activity with 28% recovery (Table). The final cyclase preparation gave a single band on SDS-PAGE and the molecular mass was estimated to be 75 kD (Fig.).

Hog liver cyclase required detergent for solubilization as well as for activation.[4,5,7] With the microsomal fraction, the presence of lower concentrations (0.1-0.2%) of deoxycholate greatly activated the rat cyclase but significantly inhibited it at more than 0.3%. On the other hand, Triton X-100 activated the cyclase, not as much as deoxycholate but there was no significant inhibition within the range tested (0-0.5%). The Triton X-100 activation was much more prominent with the solubilized enzyme, as the presence of 0.05-0.15% Triton X-100 in the assay mixuture activated upto more than 500%.

Table. Purification of Squalene-2,3-epoxide:lanosterol Cyclase from Rat Liver

Purification step	Total volume (ml)	Total protein (mg)*	Total activity (pkat)	Specific activity (μkat/kg)	Purification (fold)	Yield (%)
(1) Microsomes	28.2	603.5	141	0.234	1.0	100
(2) Solubilized enzyme	23.3	135.1	167	1.24	5.3	118
(3) Hydroxylapatite	38.2	6.08	153	25.2	108	109
(4) Isoelectric focusing	4.74	0.36	75.2	209	893	53
(5) Q-sepharose	7.20	0.21	41.1	196	838	29
(6) Gel filtration (G3000SW)	12.6	0.09	39.2	436	1863	28

*) Starting from 25 g of liver.

The effect of salt (KCl) concentration on the cyclase was then tested, since the hog liver cyclase required not only detergent but also a high ionic strength (0.4 M KCl) in the buffer for its optimal activity.[5,6] But the solubilized rat liver cyclase activity decreased with the increasing concentration of KCl (0-1.0 M) in the presence of optimal concentration of Triton X-100. In this respect, hog liver cyclase seems exceptional since all other cyclases from yeast and higher plants were susceptible to high ionic strength.[6,8-10] The cyclase showed a broad pH optimum within a pH range of 6.5-8.0 under the standard assay condition. The apparant Km value for (3S)-squalene-2,3-epoxide was 55 μM assuming that only 3S enantiomer was accepted as the substrate,[11] the reported value for hog liver cyclase being 25 μM.[5] There was no significant inhibition by cholesterol, the end product of this pathway in rat.

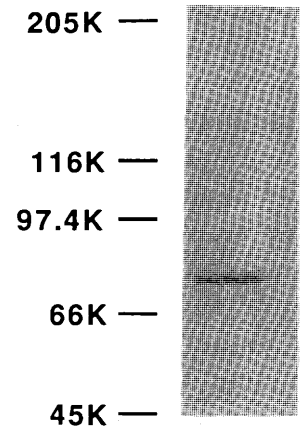

Fig. SDS-PAGE (7.5 %) of Purified Rat Liver Cyclase

Native rat liver enzyme has a homo-dimer structure, since the MW estimated from SDS-PAGE is about one half of that obtained by elution volume on gel filtration. This is in sharp contrast to the cyclases of hog liver and yeast since they exist as a monomer of 90 kD and 40-55 kD, respectively.[5,7,12] Cyclases of higher plant origin form a tetramer or a dimer in two different plant species.[8-10] These features may be a reflection of phylogenetic significance.

The availability of purified cyclase proteins and/or cloned genes encoding these enzymes will facilitate further studies on the detailed mechanism of cyclization reactions. Recently cloning of the cyclase-coding gene of Candida albicans has appeared.[13] To date, we have purified three types of cyclases. One is described in this report and the other two from higher plants produce cycloartenol and β-amyrin as the cyclization products. Now we are studying the relationship between the structures of these enzymes and their catalytic properties.

MATERIALS AND METHODS

General (RS)-[3-^{3}H]-Squalene-2,3-epoxide (spec.act.8.9x10^{10}dpm/mmole) was prepared by the reported method.[14] Q-sepharose and Sephadex G-25 were purchased from Pharmacia. Centricon-10 from Amicon. Hydroxylapatite was Biogel HT of BioRad. The HPLC column for gel filtration was TSK-G3000SW (7.5x600 mm) of TOSOH; it was pre-calibrated with a molecular weight marker kit from Oriental. Ampholytes pH 4-6 and 3.5-10 were Ampholines of LKB and mixed in a 4 to 1 ratio before use. SDS-polyacrylamide gel electrophoresis was carried out by the method of Laemmli.[15] Protein concentration was

estimated by a modified Lowry's method[16] with bovine serum albumin as a standard.

Preparation of Soluble Enzyme Male rats (Wistar) weighing about 200 g, fasted overnight, were anesthetized with sodium thiopental, and the livers were perfused with 0.1 M potassium phosphate buffer (pH 7.5) containing nicotinamide (30 mM) and $MgCl_2$ (5 mM). Livers were then removed and homogenized with two and a half volumes of the same buffer using a Teflon-glass homogenizer. After centrifugation at 10,000 x g for 30 min, the supernatant was further centrigufed at 105,000 x g for 60 min to give microsomal pellets, which were suspended in 0.1 M potassium phosphate buffer (pH 7.4) containing glycerol (20%, v/v), EDTA (1 mM) and DTT (1 mM). The microsomal fraction was then treated with 0.2%(w/v) Triton X-100. Centifugation at 105,000 x g for 60 min yielded solubilized enzyme in the supernatant. Phosphate buffers in the following purification procedure contained Triton X-100 (0.2%, w/v), glycerol (10%, v/v), EDTA (1 mM) and DTT (1 mM) for enzyme stabilization.

Enzyme Assay The standard assay mixture contained 0.1 M potassium phosphate buffer (pH 7.4), Triton X-100 (0.1%, w/v), 50 nmol of (RS)-[3-^{3}H]-squalene-2,3-epoxide (3.0×10^6 dpm) and an enzyme preparation in a total volume of 1.0 ml. The reaction mixture was incubated for 60 min at 35°C and the reaction was terminated by adding 1.0 ml of 6% (w/v) ethanolic potassium hydoxide. The reaction products were then extracted with 2.0 ml of cyclohexane and the solvent was removed *in vacuo*. The extract was spotted on a silicagel TLC plate (Merck, Art.11798) and developed with CH_2Cl_2. The zone corresponding to lanosterol (Rf:0.25) was visualized by spraying methanolic solution of berberine chloride,[17] scraped off, and submitted to radioactivity counting.

Enzyme Purification Solubilized proteins were first chromatographed on a hydoxylapatite column (50x70 mm), pre-equilibrated with 5 mM phosphate buffer. A non-adsorbed fraction from this column was then separated by isoelectric focusing (pH gradient supported by 0-50% glycerol density gradient in a 110 ml column) in a 1% carrier ampholyte solution. Cyclase activity appeared in the fraction of pH 5.5. After the buffer exchange, the active fraction was applied on a Q-sepharose column (15x70 mm) and eluted with a linear gradient of 4-40 mM phosphate buffer. The active fraction was concentrated by Centricon-10 and finally purified by HPLC gel filtration on a TSK-G3000SW column using 50 mM phosphate buffer (pH 6.8) containing Triton X-100 (0.1%, w/v), glycerol (10%, v/v), KCl (0.2 M), EDTA (1 mM) and DTT (1 mM) as an eluent at a flow rate of 0.7 ml/min.

ACKNOWLEDGEMENT The authors are deeply indebted to Dr. N. Watanabe and Dr. A. Kawashima of Research Center, Taisho Pharmaceutical Co. Ltd. for a generous supply of rat liver. Part of this work was supported by a research grant from Futaba Electronics Memorial Foundation for which we are grateful.

REFERENCES

1) A.Eschenmoser, L.Ruzicka, O.Leger and D.Arigoni, Helv.Chim.Acta, **38**, 1890 (1955).
2) T.W.Goodwin in "Biosynthesis of Isoprenoid Compounds vol.1", ed. by J.W. Porter and S.L.Spurgeon, Wiley, New York, pp.443-480 (1980).
3) J.L.Gaylor, pp.495-497 of ref.1.
4) P.D.G.Dean, P.R.Ortiz de Montellano, K.Bloch and E.J.Corey, J.Biol.Chem., **242**, 3014 (1967).
5) S.Yamamoto, K.Lin and K.Bloch, Proc.Natl.Acad.Sci.USA, **63**, 110 (1969).
6) I.Schechter, F.W.Sweat and K.Bloch, Biochim.Biophys.Acta, **220**, 463 (1970).
7) A.Duriatti and F.Schuber, Biochem.Biophys.Res.Commun., **151**, 1378 (1988).
8) I.Abe, Y.Ebizuka and U.Sankawa, Chem.Pharm.Bull., **36**, 5031 (1988).
9) I.Abe, U.Sankawa and Y.Ebizuka, Chem.Pharm.Bull., **37**, 536 (1989).
10) I.Abe, Y.Ebizuka, S.Seo and U.Sankawa, FEBS Lett., **249**, 100 (1989).
11) D.H.R.Barton, T.R.Jarman, K.C.Watson, D.A.Widdowson, R.B.Boar and K.Damps, J.Chem.Soc. Perkin Trans. 1, 1134 (1975).
12) A.I.Scott, Texas A&M University, personal communication.
13) R.Kelly, S.M.Miller, M.H.Lai and D.R.Kirsch, Gene, **87**, 177 (1990).
14) M.Rohmer, C.Anding and G.Ourisson, Eur.J.Biochem., **112**, 541 (1980).
15) U.K.Laemmli, Nature, **227**, 680 (1970).
16) A.Bensadoun and D.Weinstein, Anal.Biochem., **70**, 241 (1976).
17) A.Duriatti, P.Bouvier-Nave, P.Benveniste, F.Schuber, L.Delprino, G.Balliano and L. Cattle, Biochem.Pharmacol., **34**, 2765 (1985).

(Received October 29, 1990)

A FIRST TOTAL SYNTHESIS OF (±)-AMBININE

Miyoji HANAOKA,* Won Jea CHO, Yoko SUGIURA, and Chisato MUKAI
Faculty of Pharmaceutical Sciences, Kanazawa University, Takara-machi, Kanazawa 920, Japan

A first total synthesis of (±)-ambinine (**1**) was completed using the 13-methylprotoberberine (**10**), a plausible biogenetic precursor, which could be prepared *via* the isoquinolone derivative (**8**).

KEYWORDS ambinine; *cis*-hexahydrobenzo[*c*]phenanthridine; first total synthesis; protoberberine; 2,3,7,8,9-pentaoxygenated benzo[*c*]phenanthridine; isoquinolone

Ambinine (**1**),[1] isolated from *Corydalis ambigua* Cham. in 1984, has a *cis*-10b-methylhexahydrobenzo[*c*]-phenanthridine skeleton with a 2,3,7,8,9-pentaoxygenated substitution pattern on two aromatic rings, as shown by its spectral data. This alkaloid is the first benzo[*c*]phenanthridine alkaloid having a penta oxy functionality at 2,3,7,8, and 9 positions on its two aromatic rings, although several 2,3,7,8,10-pentaoxygenated alkaloids[2] have been isolated.

Recently we completed a biomimetic synthesis[3] of corynoline (**2**), a *cis*-10b-methylhexahydrobenzo[*c*]-phenanthridine alkaloid from a protoberberine alkaloid, corysamine (**3**). The unusual substitution pattern of **1** strongly prompted us to apply our biomimetic procedure to a synthesis of **1** even though its structure has recently been established by an X-ray analysis[4] during our synthesis. In this communication we describe a first total synthesis of (±)-ambinine (**1**).

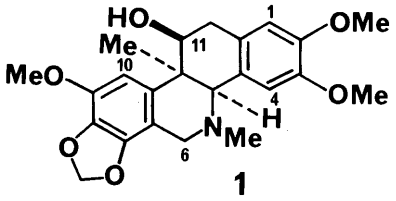

1

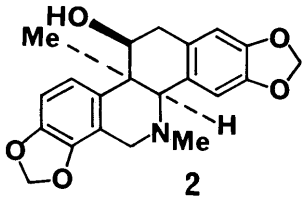

2

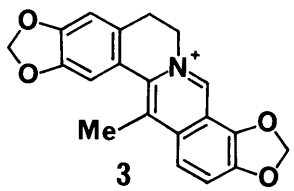

3

Condensation of the bromo-amine (**4**)[5] with the aldehyde (**5**),[6] followed by reduction with sodium borohydride ($NaBH_4$) afforded the amine (**6**: 95%), which was converted into the isoquinoline (**7**) in 90% yield by treatment with α-chloro-α-methylthioacetyl chloride.[7,8] Introduction of the methyl group at the C-4 position in **7** was realized by consecutive exposure to lithium diisopropylamide and methyl iodide to give **8** in 75% yield. Desulfurization of **8** with Raney-Ni easily occurred with concomitant removal of the bromine atom to provide **9** (90%). The Bischler-Napieralski reaction of **9** with $POCl_3$ in toluene gave, after reduction with $NaBH_4$, the 13-methyltetrahydroprotoberberine (**10**)[9] in 59% yield. The 13-methyl derivative (**10**) was then dehydrogenated with iodine to furnish the corresponding quarternary salt (**11**: 87%). Thus, the significant precursor (**11**) for our synthesis of **1** was prepared through α-chloro-α-methylthioacetyl chloride-mediated isoquinolone formation,[8] followed by methylation at the C-4 position as key steps. This provides a new general synthesis of 13-methylprotoberberine alkaloids.

The protoberberine (**11**) was reduced with lithium aluminum hydride and then N-methylated with dimethyl sulfate to give the methosulfate (**12**: 95%). The final and most crucial stage in our synthesis[3] was carried out as follows. A successful transformation of **12** into (±)-**1** was initiated by the selective C_6-N bond cleavage with 25% potassium hydroxide-methanol at refluxing temperature, followed by oxy functionalization at the styrene moiety with thallium trinitrate in methanol to form the isoquinolinium compound (**13**) with dimethoxyethyl functionality. Successive exposure of this plausible intermediate to $NaBH_4$, 15% hydrochloric acid, and sodium cyanoborohydride effected reduction of the iminium moiety, cyclization, and reduction of the resulting iminium salt to yield (±)-ambinine (**1**) in 53% overall yield from **12**, along with (±)-11-

Dedicated to the memory of Professor Zen-ichi Horii.

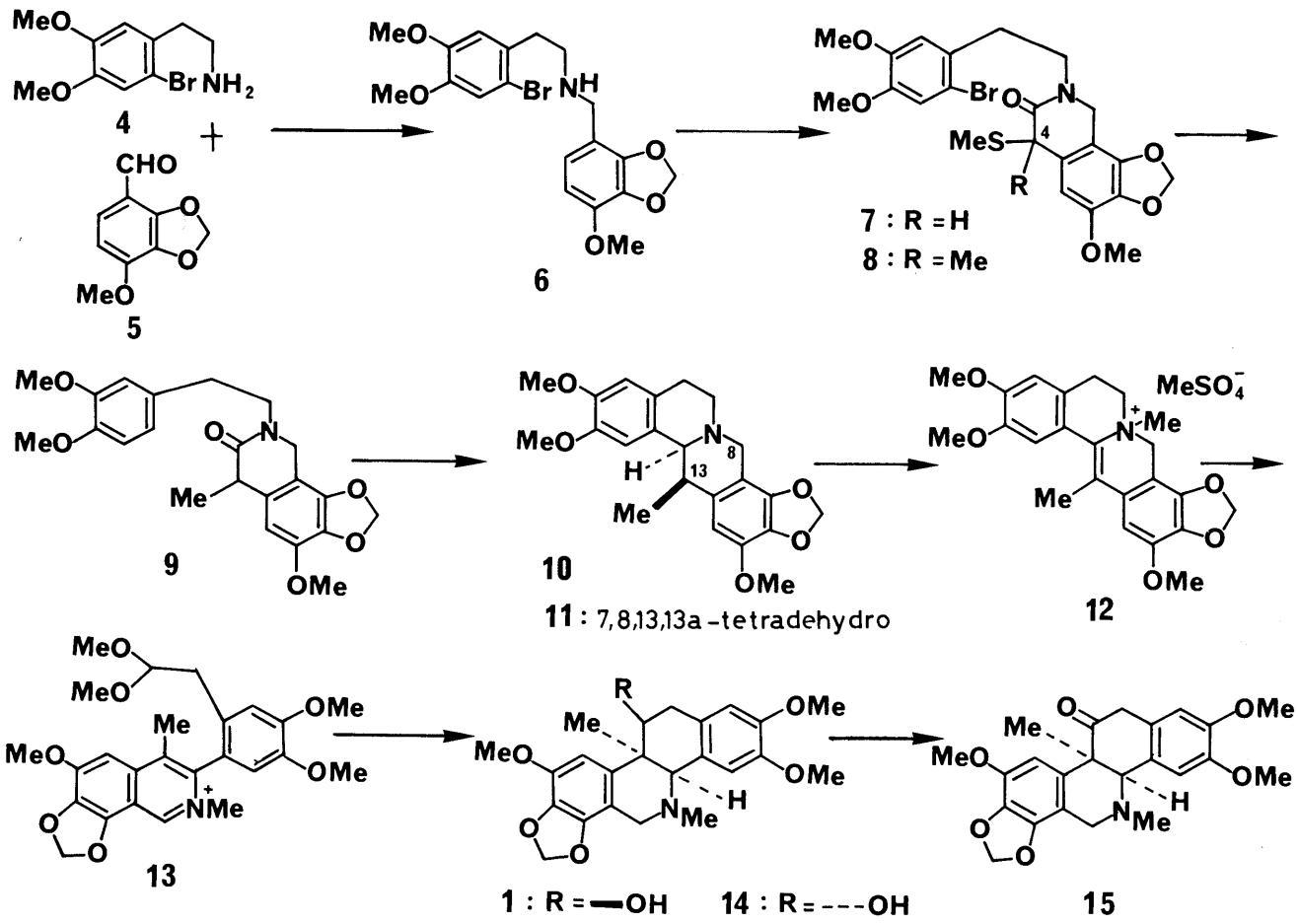

epiambinine (**14**: 16%). The synthetic ambinine was identical with the natural one as shown by spectral comparison and thin layer chromatography. Therefore, we could unambiguously confirm the structure of **1**[4] by its synthesis. The structure of **14** was established by conversion into the corresponding 11-keto derivative (**15**), which was identified with the authentic sample derived from ambinine (**1**).

Thus, we could succeed not only in a first synthesis of (±)-ambinine , but also in demonstrating the generality of our biomimetic procedure for cis-10b-methylhexahydrobenzo[c]phenanthridine alkaloids.

ACKNOWLEDGEMENT We are grateful to Prof. Y. Harigaya, School of Pharmaceutical Sciences, Kitasato University, for a generous supply of natural ambinine and its spectra.

REFERENCES AND NOTES

1) Z. Cui, M. Qi, L. Lim, and D. Yu, Acta Pharm. Sin., **19**, 904 (1984).
2) V. Simanek,"The Alkaloids," vol. 26, ed. by A. Brossi, Academic Press, New York, 1985, p185.
3) M. Hanaoka, S. Yoshida, and C. Mukai, Tetrahedron Lett., **29**, 6621 (1988).
4) Z. Cui, P. Zhu, M. Onda, Y. Harigaya, M. Iguchi, Y. Konda, H. Takayanagi, and H. Ogura, J. Nat. Prod., **53**, 1182 (1990).
5) J. Harley-Mason, J. Chem Soc., **1953**, 200.
6) B. A. McKittrick and R. Stevenson, J. Chem. Soc. Perkin Trans. 1, **1984**, 709.
7) Y. Tamura, J. Uenishi, H. Maeda, H. D. Choi, and H. Ishibashi, Synthesis, **1981**, 534.
8) S. Yasuda, T. Hirasawa, and M. Hanaoka, Tetrahedron Lett., **28**, 2399 (1987).
9) The stereochemistry of **10** was determined by its spectrum.

(Received November 15, 1990)

LICORICE-SAPONINS F3, G2, H2, J2, AND K2, FIVE NEW OLEANENE-TRITERPENE OLIGOGLYCOSIDES FROM THE ROOT OF GLYCYRRHIZA URALENSIS

Isao KITAGAWA,* Jun Liang ZHOU, Masahiro SAKAGAMI, Emiko UCHIDA, and Masayuki YOSHIKAWA

Faculty of Pharmaceutical Sciences, Osaka University, 1-6 Yamada-oka, Suita, Osaka 565, Japan

Following the structure elucidation of licorice-saponins A3, B2, C2, D3, and E2, the structures of five more new oleanene-triterpene oligoglycosides named licorice-saponins F3 (1), G2 (5), H2 (7), J2 (10), and K2 (12), concomitantly isolated from the root of Glycyrrhiza uralensis Fischer (Tohoku-kanzo in Japanese), have been determined on the basis of chemical and physicochemical evidence. During the process, a facile chemical conversion method from olean-12-ene or olean-12-en-11-one oligoglycosides to an olean-11,13-diene oligoglycoside, has been found.

KEYWORDS Glycyrrhiza uralensis; Glycyrrhizae Radix; licorice-saponin F3; licorice-saponin G2; licorice-saponin H2; licorice-saponin J2; licorice-saponin K2; olean-11,13-diene oligoglycoside

In our continuing chemical characterization studies of crude drug processing,[1] we have initiated a chemical study of botanically identified licorice roots of various origins. Recently, we isolated ten oleanene-triterpene oligoglycosides and glycyrrhizin (4) from the root of Glycyrrhiza uralensis Fischer (Leguminosae)[Tohoku-kanzo (東北甘草) in Japanese] and elucidated the chemical structures of five of them named licorice-saponins A3, B2 (9), C2 (11), D3 (3), and E2.[2] Afterwards, we found two sweet oligoglycosides, apioglycyrrhizin and araboglycyrrhizin, from the root of G. inflata [Shinkyo-kanzo (新疆甘草) in Japanese].[3] In this paper, we describe the structure elucidation of licorice-saponins F3 (1), G2 (5), H2 (7), J2 (10),[4] and K2 (12),[4] which were isolated together with licorice-saponins A3, B2, C2, D3, and E2 from the root of G. uralensis previously.[2,5] This paper also presents a facile chemical conversion method from an olean-12-ene or an olean-12-en-11-one oligoglycoside to an olean-11,13-diene oligoglycoside (i.e. 11 or 12).

Licorice-saponin F3 (1), mp 215-217 °C, $[\alpha]_D^{20}$ -20 °(MeOH), $C_{48}H_{72}O_{19}$,[6] IR (KBr, cm^{-1}) : 3400, 1760, 1720, ^1H NMR (500 MHz, pyridine-d_5, δ) : 5.36 (d, J = 7.6 Hz, 1'-H), 5.68 (d, J = 6.9 Hz, 1"-H), 6.10 (br.s, 1'"-H), gave deoxoglabrolide (2),[7] methyl glucuronide, and methyl rhamnoside, upon methanolysis. Ethereal CH_2N_2 treatment of 1 provided dimethyl ester 1a, mp 207-209 °C, $C_{50}H_{76}O_{19}$, IR (cm^{-1}) : 3420, 1745, ^1H NMR (δ) : 4.92 (d, J = 7.2 Hz, 1'-H), 5.67 (d, J = 7.3 Hz, 1"-H), 6.20 (br.s, 1'"-H), positive FAB MS (m/z) : 1003 $(M+Na)^+$.

Methylation (CH_3I-DMSO-NaH) and subsequent $NaBH_4$ reduction of 1a followed by methanolysis, liberated methyl 3,4-di-O-methylglucopyranoside (a) and methyl 2,3,4-tri-O-methylrhamnopyranoside (b) in a 2:1 ratio. Comparison of ^{13}C NMR data for 1a (Table I) with those for D3 trimethyl ester (3a), led us to expect that licorice-saponins F3 (1) and D3 (3) have an identical trisaccharide moiety while F3 has a 30,22-lactone moiety in place of the 22β-OAc and 20β-COOH residues in D3. The expectation was verified by deacetylation (5% aq. KOH) of 3 and subsequent treatment with Dowex 50W x 8 (H^+) to furnish 1. Thus, the structure of licorice-saponin F3 (1) has been clarified as shown.

On ethereal CH_2N_2 treatment, licorice-saponin G2 (5), mp 229-230 °C, $[\alpha]_D^{20}$ +34 °(MeOH), $C_{42}H_{62}O_{17}$, UV (MeOH, nm, ε) : 249 (10600), IR (cm^{-1}) : 3350, 1720, 1648, ^1H NMR (δ) : 5.34 (d, J = 7.7 Hz, 1'-H), 5.59 (d, J = 6.7 Hz, 1"-H), ^{13}C NMR (125 MHz, pyridine-d_5, δc) : 63.1 (24-C), 104.4, 104.9 (1', 1"-C), positive FAB MS (m/z) : 877 $(M+K)^+$, 861 $(M+Na)^+$, 839 $(M+H)^+$, gave trimethyl ester 5a, mp 176-178 °C, $C_{45}H_{68}O_{17}$, IR (cm^{-1}) : 3367, 1720, 1648, ^1H NMR (δ) : 4.94 (d, J = 7.9 Hz, 1'-H), 5.56 (d, J = 7.6 Hz, 1"-H).

Methanolysis of 5a provided methyl 24-hydroxyglycyrrhetinate (6a)[8] and methyl glucuronide, while methanolysis, after $NaBH_4$ reduction and subsequent complete methylation of 5a, liberated methyl 2,3,4,6-tetra-O-methylglucopyranoside (c) and methyl 3,4,6-tri-O-methylglucopyranoside (d) in a 1:1 ratio. Based on these findings and examination of ^{13}C NMR data for 5a (Table I), the structure of licorice-saponin G2 has

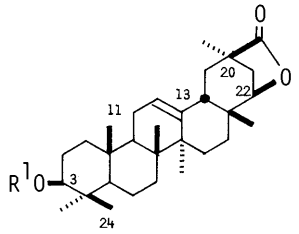

1 : R^1= Sr (licorice-saponin F3)
1a : R^1= SrMe
2 : R^1= H (deoxoglabrolide)

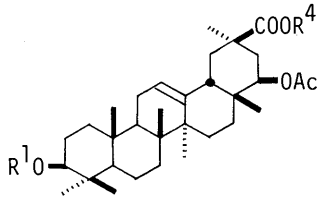

3 : R^1= Sr, R^4= H (licorice-saponin D3)
3a : R^1= SrMe, R^4= CH_3

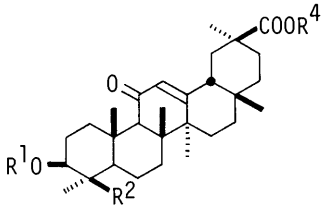

4 : R^1= S, R^2= CH_3, R^4= H (glycyrrhizin)
5 : R^1= S, R^2= CH_2OH, R^4= H (licorice-saponin G2)
5a : R^1= SMe, R^2= CH_2OH, R^4= CH_3
6a : R^1= H, R^2= CH_2OH, R^4= CH_3

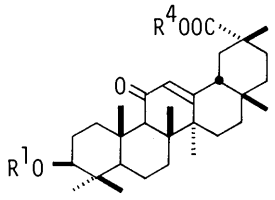

7 : R^1= S, R^4= H (licorice-saponin H2)
7a : R^1= SMe, R^4= CH_3
8 : R^1= R^4= H (liquiritic acid)

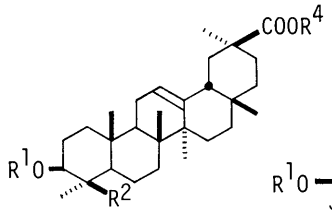

9 : R^1= S, R^2= CH_3, R^4= H (licorice-saponin B2)
9a : R^1= SMe, R^2= R^4= CH_3
10 : R^1= S, R^2= CH_2OH, R^4= H (licorice-saponin J2)
10a : R^1= SMe, R^2= CH_2OH, R^4= CH_3

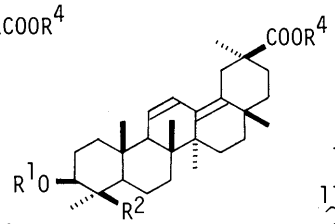

11 : R^1= S, R^2= CH_3, R^4= H (licorice-saponin C2)
11a : R^1= SMe, R^2= R^4= CH_3
12 : R^1= S, R^2= CH_2OH, R^4= H (licorice-saponin K2)
12a : R^1= SMe, R^2= CH_2OH, R^4= CH_3

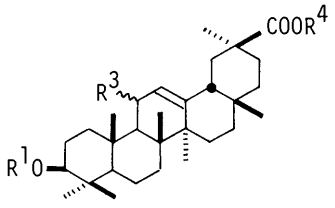

13 : R^1= SMe, R^3= α-OAc & α-OCH_3, R^4= CH_3
14 : R^1= S, R^3= β-OH, R^4= H

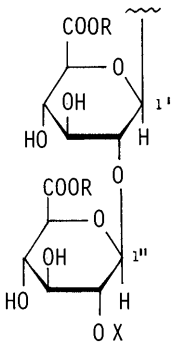

S : R = X = H
SMe : R = CH_3, X = H
Sr : R = H, X = α-L-rham(py).
SrMe : R = CH_3, X = α-L-rham(py).

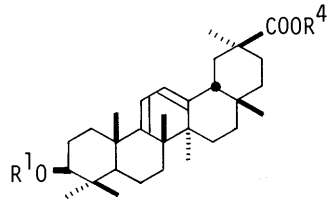

15 : R^1= S, R^4= H
15a : R^1= SMe, R^4= CH_3

Table I. ^{13}C NMR Data for 1a, 5a, 7a, 10a, and 12a (at 22.5 MHz in pyridine d_5, δc)

		1a	5a	7a	10a	12a
Sapogenol moiety	C-3	89.9	89.9	89.2	89.8	89.8
	C-11	47.5	198.9	199.0	47.5	125.3
	C-12	124.8	128.6	128.6	122.2	126.4
	C-13	140.6	168.7	168.4	144.3	135.2
	C-18	47.5	48.6	46.3	48.2	135.2
	C-22	84.3	38.2	37.1	36.2	36.2
	C-24	16.3	16.3	16.2	62.8	62.4
	C-29	28.0	28.0	178.1	28.1	28.1
	C-30	180.1	176.5	19.3	177.0	178.2
3-O-β-D-Glucurono-pyranosyl moiety	C-1'	104.7	104.1	104.9	104.0	104.0
	C-2'	79.1	81.9	84.3	81.1	80.8
	C-3'	76.3[a]	75.2	76.4[a]	76.3[a]	76.6
	C-4'	72.2[b]	72.2	72.5[b]	72.1	72.1
	C-5'	77.9[c]	77.2	77.3[c]	77.4[b]	77.7[a]
	C-6'	170.1[d]	169.6	170.1[d]	169.6	169.8
2'-O-β-D-Glucurono-pyranosyl moiety	C-1"	102.4	105.5	106.8	104.7	104.5
	C-2"	78.2	76.5[a]	76.6[a]	76.6[a]	76.6
	C-3"	76.6[a]	76.8[a]	77.4[c]	77.0[b]	77.0[a]
	C-4"	72.8[b]	72.2	72.9[b]	72.1	72.1
	C-5"	77.6[c]	77.2	77.6[c]	77.4[b]	77.4[a]
	C-6"	169.8[d]	169.6	170.2[d]	169.6	169.8
2"-O-α-D-Rhamno-pyranosyl moiety	C-1‴	101.6				
	C-2‴	71.8				
	C-3‴	72.8				
	C-4‴	73.9				
	C-5‴	69.1				
	C-6‴	18.5				

a), b), c), d) Assignments may be interchangeable within the same column.

been determined as 5.

Licorice-saponin H2 (7), mp 209-210 °C, $[\alpha]_D^{25}$ +31 °(MeOH), $C_{42}H_{62}O_{16}$, UV (MeOH, nm, ε) : 248 (10700), IR (cm^{-1}) : 3400, 1725, 1650, ^1H NMR (δ) : 4.97 (d, J = 7.6 Hz, 1'-H), 5.35 (d, J = 7.6 Hz, 1"-H), ^{13}C NMR (δc) : 105.0 (1'-C), 106.8 (1"-C), 128.8 (12-C), 169.0 (13-C), 180.6 (29-C), 199.4 (11-C), positive FAB MS (m/z) : 861 $(M+K)^+$, 845 $(M+Na)^+$, liberated liquiritic acid (8) [9] and methyl glucuronide upon methanolysis.

Ethereal CH_2N_2 treatment of 7 afforded trimethyl ester 7a, mp 169 °C, $C_{45}H_{68}O_{16}$, IR (cm^{-1}) : 3362, 1722, 1654, ^1H NMR (δ) : 4.95 (d, J = 7.3 Hz, 1'-H), 5.33 (d, J = 7.7 Hz, 1"-H), positive FAB MS (m/z) : 887 $(M+Na)^+$,

which, upon methanolysis after $NaBH_4$ reduction and subsequent methylation, liberated methyl glycosides (c and d) as it did from 5a. These findings together with ^{13}C NMR data for 7a (Table I) led us to formulate licorice-saponin H2 as 7.

Licorice-saponin J2 (10), mp 263-265 °C, $[\alpha]_D^{25}$ +21 °(MeOH), $C_{42}H_{64}O_{16}$, IR (cm^{-1}) : 3405, 1729, 1615, ^1H NMR (δ) : 5.00 (d, J = 7.6 Hz, 1'-H), 5.65 (d, J = 7.0 Hz, 1"-H), was converted to trimethyl ester 10a, mp 198-199 °C, $C_{45}H_{70}O_{16}$, IR (cm^{-1}) : 3445, 1730, by CH_2N_2 methylation. These findings together with the examination of ^{13}C NMR data for 10a (Table I) led us to expect that J2 (10) was an 11-deoxo analog of licorice-saponin G2 (5). The expectation was verified by converting 5 in high yield to J2 (10) by reduction with zinc amalgam and HCl.

Methylation with CH_2N_2 of licorice-saponin K2 (12), mp 207-209 °C, $[\alpha]_D^{25}$ +28 °(MeOH), $C_{42}H_{62}O_{16}$, UV (MeOH, nm, ε) : 241 (13000), 249 (15000), 259 (9200), IR (cm^{-1}) : 3460, 1690, 1629, ^1H NMR (δ) : 5.04 (d, J = 7.6 Hz, 1'-H), 5.64 (d, J = 6.1 Hz, 1"-H), 5.54 (br.d, 11-H), 6.52 (br.d, 12-H), positive FAB MS (m/z) : 845 $(M+Na)^+$ afforded trimethyl ester 12a, mp 179-181 °C, $C_{45}H_{68}O_{16}$, IR (cm^{-1}) : 3424, 1731, 1621, positive FAB MS (m/z) : 903 $(M+K)^+$. These physicochemical properties and the examination of ^{13}C NMR data for 12a led us to presume the structure of licorice-saponin K2 (12) with a heteroannular 11,13-diene structure.[10]

To prove the structure 12, we carried out a conversion from known oligoglycoside. Thus, licorice-saponin B2 trimethyl ester (9a) was subjected to constant-current electrolysis (Pt, 40 mA/cm^2, MeOH-AcONa)[11] to provide a mixture of 11α-OAc and 11α-OMe derivatives (13). Treatment of 13 with 1% aq. HCl furnished licorice-saponin C2 trimethyl ester (11a) in 61% yield from 9a. On the other hand, $NaBH_4$ reduction of glycyrrhizin (4) in EtOH-H_2O (1:1) at 90 °C yielded an 11β-hydroxy derivative 14, mp 208-210 °C, $C_{42}H_{64}O_{16}$, ^1H NMR (δ) : 4.45 (dd, J = 6.5, 6.5 Hz, 11α-H),[12] in 95% yield. Treatment of 14 with 2% aq. HCl-dioxane (1:1) yielded a mixture of a 9,12-homoannular diene analog 15 and licorice-saponin C2 (11),[13] whereas treatment of 14 in dioxane-H_2O (1:1) with heating provided 11 in an excellent yield (82% from 4). Finally, $NaBH_4$ reduction of licorice-saponin G2 (5) and subsequent treatment of the product with dioxane-H_2O as above furnished licorice-saponin K2 (12) in 76% yield, thus the structure 12 was substantiated.

ACKNOWLEDGEMENT The authors are grateful to the Ministry of Education, Science, and Culture of Japan for financial support (Grant No. 02403027).

REFERENCES AND NOTES

1) a) I.Kitagawa and M.Yoshikawa, J.Traditional Sino-Japanese Medicine, Vol.6, No.4, 101 (1985); b) Idem, ibid., Vol.7, No.3, 55 (1986); c) I.Kitagawa, T.Taniyama, M.Yoshikawa, Y.Ikenishi, and Y.Nakagawa, Chem. Pharm.Bull., 37, 2961 (1989), and previous papers cited therein.
2) I.Kitagawa, J.L.Zhou, M.Sakagami, T.Taniyama, and M.Yoshikawa, Chem.Pharm.Bull., 36, 3710 (1988).
3) I.Kitagawa, M.Sakagami, F.Hashiuchi, J.L.Zhou, M.Yoshikawa, and J.Ren, Chem.Pharm.Bull., 37, 551 (1989).
4) The trivial names licorice-saponins I2 and J2 (obtained in 0.002% respectively from the root) in previous paper2)were changed to licorice-saponins J2 and K2, respectively in this paper.
5) M.Yoshikawa, J.L.Zhou, M.Sakagami, F.Hashiuchi, and I.Kitagawa, presented at the 108th Annual Meeting of the Pharmaceutical Society of Japan, held in Hiroshima, Apr.4-6, 1988, Abstract Papers p.316.
6) The molecular composition of the compound given with the chemical formula was determined by elemental analysis and(or) high resolution mass-spectrometry.
7) L.Canonica, G.Russo, and A.Bonati, Gazz.Chim.Ital., 96, 772 (1966).
8) L.Canonica, B.Danieli, P.Manitto, G.Russo, and A.Bonati, Gazz.Chim.Ital., 97, 1359 (1967).
9) L.Canonica, G.Russo, and E.Bombardelli, Gazz.Chim.Ital., 96, 833 (1966).
10) a) S.Shibata, I.Kitagawa, and H.Fujimoto, Chem.Pharm.Bull., 14, 1023 (1966); b) M.Nose, S.Amagaya, T.Takeda, and Y.Ogihara, ibid., 37, 1293 (1989).
11) a) I.Kitagawa, T.Kamigauchi, H.Ohmori, and M.Yoshikawa, Chem.Pharm.Bull., 28, 3078 (1980); b) M. Yoshikawa, H.K.Wang, V.Tosirisuk, and I.Kitagawa, Chem.Pharm.Bull., 30, 3057 (1982).
12) S.Shibata, K.Takahashi, S.Yano, M.Harada, H,Saito, Y.Tamura, A.Kumagai, K.Hirabayashi, M.Yamamoto, and N.Nagata, Chem.Pharm.Bull., 35, 1910 (1987).
13) The separation of 11 and 15 was effected after CH_2N_2 methylation to provide 11a and 15a, mp 180 °C, $C_{45}H_{68}O_{15}$, IR (cm^{-1}) : 3440, 1727, 1660, ^1H NMR (pyridine-d_5 + D_2O, δ) : 5.30, 5.31 (both d, J = 7.3 Hz, 11,12-H), ^{13}C NMR (22.5 MHz, pyridine-d_5, δc) : 154.9, 115.7, 125.5, 146.0 (9,11,12,13-C).

(Received November 22, 1990)